
IMWA2021
CYMRU WALES

IMWA2021
CYMRU ► WALES

Proceedings of the 14th IMWA Congress – "Mine Water Management for Future Generations"

12–15 July 2021

eventbocs – Virtual Congress Venue

Editors

Peter Stanley

Christian Wolkersdorfer

Karoline Wolkersdorfer

International Mine Water Association

Mine Water Management for Future Generations
2021, Cardiff, Wales, United Kingdom

ISBN 978-3-00-069673-2

Editors
Peter Stanley, Christian Wolkersdorfer, Karoline Wolkersdorfer

Cover Design
Karoline Wolkersdorfer

Layout and Typesetting
Jigsaw Graphic Design

All abstracts were reviewed by 2 – 3 experts of the International Scientific Committee.
All full papers were reviewed by 1 – 2 experts of the International Scientific Committee.

www.IMWA.info

Organizers

Natural Resources Wales (NRW)

Cyfoeth Naturiol Cymru
Natural Resources Wales

Welsh Government

Llywodraeth Cymru
Welsh Government

The Coal Authority

The Coal Authority

Cardiff University

CARDIFF UNIVERSITY
PRIFYSGOL CAERDYDD

International Mine Water Association

IMWA2021
CYMRU ► WALES

International Scientific Committee (ISC)

Bert Allard, Sweden
John George Annandale, South Africa
Margarida Horta Antunes, Portugal
Carlos Felipe Aravena, Chile
Tim Aubel, Germany
Mattias Bäckström, Sweden
Jeff Bain, Canada
Selina Mary Bamforth, United Kingdom
Andre Banning, Ireland
Maria Dolores Basallote, Spain
Sod-Erdene Bazardorj, Mongolia
Melanie Lise Blanchette, Australia
Andrey Bogomolov, Russia
Anna Bogush, United Kingdom
Rob Bowell, United Kingdom
Jo Burgess, South Africa
Manuel Antonio Caraballo Monge, Chile
Jo Cavanagh, New Zealand
Rosa Cidu, Italy
Henk Coetzee, South Africa
Andy Davs, United States
Camilo Raul de los Hoyos, Argentina
Gareth Digges La Touche, United Kingdom
Wenfeng Du, China
Lee Evans, Australia
Marlese Fairgray, Australia
Nuria Fernandez Castro, Brazil
Adriano Fiorucci, Italy
Elvis Fosso-Kankeu, South Africa
Silvia Cristina Alves França, Brazil
Rudy Sayoga Gautama, Indonesia
Cleber Jose Baldoni Gomes, Brazil
William Mario Goodman, United States
Jabulani Gumbo, South Africa
Robert S. Hedin, United States
Altus Huisamen, South Africa
Andrei Ivanets, Belarus
Ryan Thomas Jakubowski, United States
Sajjad Jannesar Malakooti, Iran
Lucinda Johnson, United States
Raymond H. Johnson, United States
Andrew Clifford Johnstone, South Africa
David Richard Jones, Australia
Margarete Maria Kalin, Switzerland
Päivi M. Kauppila, Finland
Anu Kettunen, Finland
Elena Khayrulina, Russia
Lisa Bithell Kirk, United States
Robert Lawrence Kleinmann, United States
Frans Knops, Netherlands
Konstantinos Kollias, Greece
Natalie A. Kruse Daniels, United States
Morten Birch Larsen, Denmark
Ulla Lassi, Finland
Anthony Le Beux, France
Simon Antony Lorentz, South Africa
Michael Losavio, United States
Paul Joel Lourens, South Africa
Mark Lund, Australia
Rudzani Lusunzi, South Africa
Tatyana Lyubimova, Russia
Justin Kambale Maganga, Kenya
Maria Mamelkina, Finland
Malibongwe Shadrach Manono, South Africa
Cherie McCullough, Australia
Matthew P. McGann, Peru
Broder Merkel, Germany
Thomas Metschies, Germany
Michael Arthur Milczarek, United States
Jacek Motyka, Poland
Kevin Myers, United States
Robert W. Nairn, United States
Carmen Mihaela Neculita, Canada
Darrell Kirk Nordstrom, United States
Iuliia Ozarian, Russia
Michael Paul, Germany
Steven Richard Pearce, United Kingdom
James Pope, New Zealand
Xunchi Pu, China
Nada Rapantova, Czech Republic
Mark Thomas Roberts, United Kingdom
Pierre Rousseau, Australia
Carlos Ruiz Cánovas, Spain
Lotta Sartz, Sweden
Christopher James Satterley, United Kingdom
Ivo André Homrich Schneider, Brazil

Ralph Schöpke, Germany
Martin Schultze, Germany
Alison Sinclair, Australia
Abhay Soni, India
Peter Clive Stanley, United Kingdom
Wanghua Sui, China
Jacek Szczepiński, Poland
Esther Takaluoma, Finland
Teresa Maria Valente, Portugal
Danie Vermeulen, South Africa
Denys Villa Gomez, Australia
Changshen Wang, China
John Douglass Waterhouse, Australia
Anne Weber, Germany
Paul Weber, New Zealand
Holger Weiß, Germany
Phil Whittle, Australia
Tom Williams, United Kingdom
Christian Wolkersdorfer, South Africa
Peter Woods, Australia
Sergey Zhdanov, Russia

Local Organizing Committee (LOC)

Champion

Peter Stanley	*Natural Resources Wales*

Members

Trystan James	*Natural Resources Wales*
Catherine E Rees	*Natural Resources Wales*
Devin Sapsford	*Cardiff University*
Peter Brabham	*Cardiff University*
Rhys Savage	*Cardiff University*
Chris Satterley	*The Coal Authority*
Carl Banton	*The Coal Authority*
Eifiona Williams	*Welsh Government*

Professional Conference Organizers (PCO)

James Parsons	*Cazbah*
Karoline Wolkersdorfer	*wolke events*

IMWA 2021
Sponsors & Partners

wsp

MEM
The Science Behind Success

Cyfoeth Naturiol Cymru
Natural Resources Wales

Llywodraeth Cymru
Welsh Government

Cardiff University
Prifysgol Caerdydd

The Coal Authority

IMWA2021
CYMRU ► WALES

Cyfarchiadau annwyl anfonog, Welcome dear delegate to the 14th annual IMWA Congress

Croeso, welcome to IMWA 2021, the first virtual IMWA congress brought to you from a platform in Wales. We had wanted to greet you in person at ICCWales in Newport with a smile and a "cwtch" (a friendly Welsh hug), however we still can't even share a cautious "cwtch" with extended family and close friends. The year has been difficult for all of us and we found that during preparation we focused more on the pandemic than on anything else. Hope however, is on the horizon. We will all know loved ones whom have either caught or succumbed to the virus and hence we realised that a live event was not possible. Having lost the IMWA 2020 congress, we wished to avoid losing a second event and having already expended much effort, we considered this virtual event was achievable.

The Chair of the Local Organising Committee (LOC) asked the IMWA Executive Committee about an option to postpone the live event as the organisers remain contracted with ICCWales. The LOC is very grateful that the Executive has been supportive in allowing them and ICCWales to host a live event as IMWA 2023, inviting you back so that you will have opportunity of visiting, sharing our hospitality and enjoying our countryside that has provided rich mineral rewards since the Bronze Age. Exploitation of reserves here has generated wealth, industry and since the mining renaissance revenues that helped provide the governance, landscapes, education and innovation we enjoy so much today; like flotation discovered and patented at Glasdir Copper Mill near Dolgellau in Snowdonia, North West Wales. As we continue seeking these advances in science, innovation and sustainable management of natural resources our ambition remains to successfully transform to a sustainable society. We'd like to think this event is a helpful stone in achieving this.

We hope that you enjoy this virtual congress, that it provides insight and networking opportunities that reward, and you feel stimulated to return to IMWA safely in future years. In Wales we want you to see our wonderful countryside, our mines, mining heritage, our abbeys, castles and of course feel the strength of our passion for family, rugby and song. We hope to see and meet with you once again, though we appreciate that matters will take time to return to a position where we can travel safely and gather, free from Covid-19.

In delivering this virtual IMWA 2021 congress, we thank all our reviewers from the International Scientific Committee (ISC); the people behind the scenes who helped in organising; our collaborators at Welsh Government, The Coal Authority and Cardiff University; our corporate sponsor WSP that includes Golder Associates, and Mine Environment Management Ltd as sponsor of the topic themes Legacy Mine Impacts, Prediction of Acid Mine Drainage & Metal Leaching (AMD-ML) and Clean Up & Rehabilitation. We extend our thanks to all contributors and the volunteer session chairs that have made this event possible. It has been rewarding working together with you to enable hosting this event and we look forward to working together again in delivering IMWA 2023.

Dear friends all around the world, let's strive on helping make IMWA 2022 in Christchurch, New Zealand and IMWA 2023 back here at ICCWales in Newport as live events the successes that our mine water family have experienced previously.

Keep well, stay safe, love your families and neighbours and with the German miner's greeting "Glückauf" we are wishing you all the best!

Peter Stanley – IMWA 2021 Chair
Christian Wolkersdorfer – IMWA President

Contents

Efficient Methodologies in the Treatment of Acid Water from Mines with Recovery of Byproducts

Osvaldo Aduvire[1,2], Mayra Montesinos[2,3], Nereyda Loza[1,2]

[1]*SRK Consulting, Peru*

[2]*Pontifical Catholic University of Peru (PUCP), Peru*

[3]*Hudbay S.A.C., Peru*

Abstract

In general, the treatment of acid mine water is done via a one-stage process, at a determined pH level (Direct Treatment). In this article, a staged treatment methodology is presented (Staged Treatment), that makes the recovery of byproducts with economic value possible, as well as benefiting the environment by reducing contamination. This is achieved because we diminish the amount of non-usable slurry. For this reason, we will present the obtained results in Direct Treatment compared to those the Staged Treatment had, plus which byproducts were collected at different pH levels in the Staged Treatment. Finally, we will show a flow sheet explaining the Staged Treatment.

Mining activity generates a large volume of mining residues and exposed surfaces with the presence of sulphides that in contact with the atmosphere and water in rainy seasons initiate complex processes of physical, chemical and biological transformations, which give rise to the generation of acidic mine drains that require a treatment before unloading them to a receiving body.

Lately, the population is demanding the development of sustainable mining projects with greater environmental control, lower water consumption, which include methodologies that consider solid or liquid mining waste as second generation resources with possibilities of use and recovery to obtain by-products with economic value.

To incorporate these expectations into mining projects, have the potential to use mining waste and reduce discharges to the environment, we have developed acid water treatment systems that allow to recover by-products sequentially to certain pH ranges and obtain sludge with specific metal load values that we have called Stage-divided Treatment ou Staged Process.

In the sizing of acid water treatment systems, it is essential to have a good geochemical characterization of the effluent, ranging from field monitoring, using portable equipment to perform in situ measurements of flow, pH, eh, dissolved oxygen, conductivity, temperature, flow, turbidity, acidity, alkalinity, to water sampling for chemical analysis in total and dissolved concentrations.

To choose the sequence in the treatment system, experimental neutralization and precipition tests are carried out on equipment such as imhoff jug and cone tests where various reagents are tested for treatment and at various pH values, with which we obtain the dosing of reagents and the sequencing of the treatment. Based on the results obtained in the hydrogeochemical characterization of the effluents and the results of the tests, the processes and stages to be considered are chosen in the design of the processing facility.

These methodologies will reduce the costs of treating minewater, extend the life of waste deposits and reduce the discharge of solid and liquid waste into the environment, in addition to the recovering and collecting of by-products with possibilities of economic use.

Keywords: Treatment, Acid Water, Staged, Recovering, By-products

Methodology

Prior to experimental tests, field measurement were carried out with portable equipment for pH, Eh, disolved oxigen, elctrical conductivity and flow.

Sample-taking was performed pursuant to standardized procedures in 250 and 500 ml HDPE flasks, which were first washed with 10% nitric acid and rinsed water from the sampling point. In the laboratory, metals were analized in total and dissolved concentrations, they were filtered al 0.45 microns, preserved with HNO_3 to pH<2 and chilled to 4C° for transportation purposes.

Experimental neutralization and sedimentation tests were carried out seeking to obtain doses of reagents to be used in treatment processes by means of curves in which hydrolysis zones were identified.

Experimentation and Results

In the experimental tests, the flow rates to be treated and the concentrations present in the effluents are also taken into account, the latter determining whether only treatment will be carried out or treatment will be carried out along with metal recovery. If only treatment is chosen, the process will be in a single stage (Direct Process), but, if we opt for the recovery of byproducts with economic value, the treatment will be staged with separation of solid phases (Staged Process). The equipment used in the laboratory includes pH meter, beaker, magnetic stirrer, precision balance, redox potential meter, jar test, imhoff cones, etc.

Direct experimental tests and trials included the monitoring of specific parameters for indirect tracking of neutralization reactions and the construction of experimental reagent consumption curves required to reduce mine drainage acidity. The reagent used was lime and the various neutralization curves constructed evidenced hydrolysis and/or buffer zones, where solid phases are for the case under study.

A. Direct and Stages process comparison. Case 1.

Table 1 shows the quality of a mine drainage whose pH<3 with Fe, Mn, Zn and other contents. To treat this water, a series of experimental trials have been carried out aimed at obtaining final concentrations that comply with the LMP of the current legislation for the mining-metallurgical sector. The estimation of the lime consumption for the treatments is presented below by means of a direct and staged test.

The first alternative is to perform neutralization tests by direct process, where the pH of 2.3 is increased until reaching pH 10, in Table 2 we can see the concentrations at the

Table 1 *Characteristics of mine drainage before treatment.*

pH	Fe	Al	Mn	Mg	Pb	Zn
	mg/L	mg/L	mg/L	mg/L	mg/L	mg/L
	Total Concentrations					
2.3	259	18.1	353	98	2.8	50

Table 2 *Characteristics of acid drainage after direct neutralization.*

Parameter	Unit	Final Concentrations	
		Totals	Dissolved
pH	u.e	10	
Fe	mg/L	1.5	0.9
Al	mg/L	1.02	0.8
Mg	mg/L	6.5	4.3
Mn	mg/L	180	166
Pb	mg/L	0.09	0.02
Zn	mg/L	1.1	0.72

Table 3 *Characteristics of acid drainage after each stage of neutralization.*

Parameter	Unit	Concent. Stage 1		Concent. Stage 2	
		Tot.	Dis.	Tot.	Tot.
pH		4.5-5.0		5.5-10	
Fe	mg/L	0.29	0.1	0.08	0.06
Al	mg/L	1.07	1.08	0.06	0.03
Mg	mg/L	59	51.5	3.9	3.56
Mn	mg/L	305	266	0.963	0.153
Pb	mg/L	1.03	0.98	<0.01	<0.01
Zn	mg/L	49.3	17.8	0.13	0.035

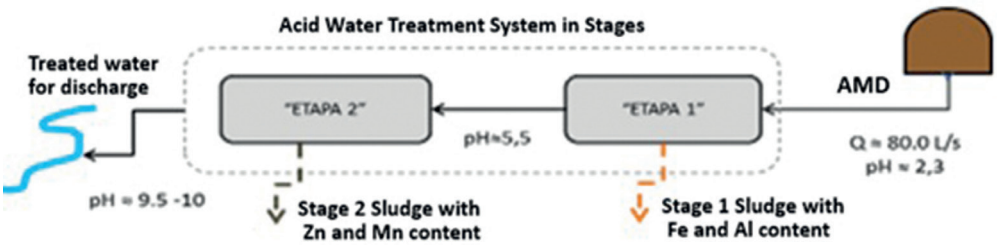

Diagram 1 *Design of a staged acid water treatment plant.*

end of the neutralization process, where Mn contents are still evident. This would indicate that to continue withdrawing Mn of water, the process should be continued and flocculants or other reagents added to make the Mn pass to the solid phase. The consumption of lime in the alternative of Case 1 (Direct Test) to obtain the results of Table 2 reached 620 mg/L.

The second alternative of treatment of mine water and taking into account the concentrations present in the sample (Table 1) has been to design a treatment in two (2) stages, in the first stage pH 5.5 was reached and the slurry was mainly removed from Fe and in less quantity of Al, in the second stage the treatment reached the pH 10 where a sediment was obtained with an important content of Zn and Mn with possibilities of recovery of the first one.

Unlike direct treatment where only one slurry is obtained, in the staged treatment two more slurries are obtained, therefore, once the first stage is finished, the slurry is removed, then the process is continued with the addition of neutralizing reagent until reaching the final pH where the second neutralization stage ends, after which the formed solids will also be required.

The results obtained in the staged test are clear, in terms of the effectiveness of removing metallic load from water. Table 3 shows the concentrations of metals in the water after the 2 stages of treatment, achieving effective removal of Zn and Mn, a result not achieved with the direct test.

The mass balance performed as part of the monitoring of the reactions involved in the process, as shown in Fig. 1, also highlights the removal of metals of interest at each stage of the test.

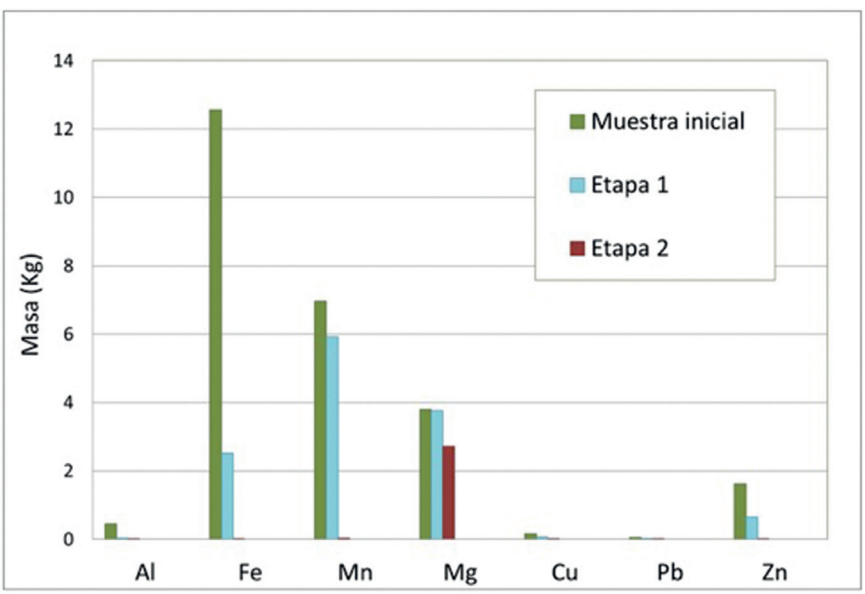

Figure 1 *Variation of the mass content of Fe, Zn and Mn among other minors in the staged-type test.*

Table 4 Mine effluent for experimental tests.

Sampling Point	pH	STS	As	Cr	Cu	Fe	Pb	Zn	Al	Mn
Parameters		mg/L	mg/L	mg/L	mg/L	mg/L	mg/L	mg/L	mg/L	mg/L
Nv 2C (Total Conc.)	3.5	382	0.94	0.108	10.67	210.3	7.06	936.8	72.14	14
Nv 2B (Dissolved Conc.)	3.5	382	0.01	0.067	10.38	51.24	1.96	891.6	64.61	14
LMP	6-9	50	0.1	-	0.5	2	0.2	1.5	-	-

The lime consumption in the alternative of the case 1 (Staged Test) to obtain the results of table 4, is as follows: 260 mg/L in the first stage and 240 mg/L in the second stage, reaching a total lime consumption of 500 mg/L. Diagram 1 shows the sequence corresponding to the acid water treatment system by means of stage neutralization.

As a result of the comparison of the direct and staged treatments, in the latter, better results are achieved in the removal of metallic load, in addition to consuming 120 mg/L less of lime.

B. Direct and Staged processes comparison. Case 2.

For this comparison we have chosen a mine effluent called Nv 2 that has a pH of 3.5, the electrical conductivity exceeds 4170 µS/cm and some values of the majority elements measured in total and dissolved concentrations (mg / l) exceed the LMP of reference according to current Peruvian legislation (DS N° 010-2010-MINAM) for the discharge of liquid effluents from mining-metallurgical facilities.

The results obtained in the tests to determine the consumption of neutralization reagent give the following results: in the case of direct testing or direct neutralization, a lime consumption of 1080 mg/L was estimated to reach a pH of 8.5 (Fig. 2), while for the staged test the consumption of lime to reach a pH = 8.5 was 820 mg/L (Fig. 3).

Comparing the lime consumption obtained in the process of direct neutralization and staged neutralization, it can be deduced that for effluents with a significant metallic load, the staged neutralization consumes 260 mg/L less of reagent, which represents an appreciable saving in the lime consumption, when it comes to important volumes of mine water to be treated. For instance, if we consider implementing a staged neutralization plant of 500 l/s and that the lime cost is 0.5 US$/kg, a saving of 4'043,520 kg of lime is obtained per year, equivalent to a saving of 2'021,760 US$/year.

This will result in a process of lower cost of mine water treatment, but in addition there are added improvements such as obtaining byproducts with possibilities of economic

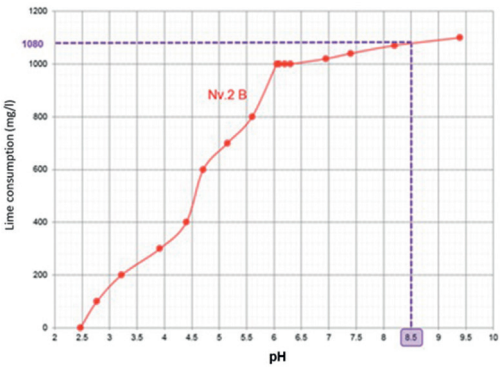

Figure 2 Lime consumption in the direct test.

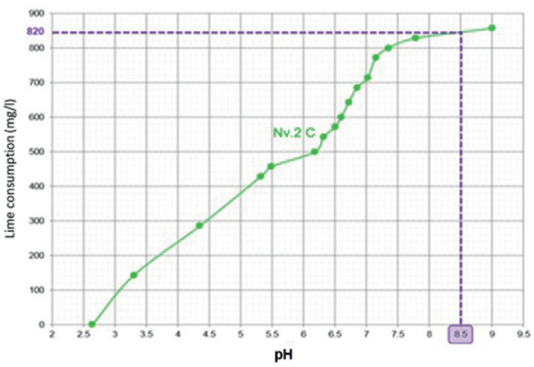

Figure 3 Lime consumption in the staged test.

Table 5 Characteristics of a mine drainage before neutralization.

pH	Fe	Al	Mn	Mg	Pb	Zn
	mg/L	mg/L	mg/L	mg/L	mg/L	mg/L
	Total Concentrations					
2.9	180	90	95	70	5	1200

use, lower requirement in the handling of slurry, among other secondary advantages.

C. Neutralization and recovery tests in three stages.

Table 5 shows the majority of metallic load and the pH of a mine drain, which has been carried out neutralization tests in three stages to obtain three byproducts with high contents of Fe, Al, and Zn.

The zone of buffering and hydrolysis can be observed in the curves of lime consumption both in terms of pH and redox potential. Figure 4 shows the evolution of the redox during the neutralization process, where the values of Eh descend to values of 50 mV that correspond to natural waters without affection.

Picture 1 shows the slurry obtained in a three stage neutralization test: in the first stage the pH 4 was reached and orange ocher colored sludge (M-1) that would correspond to Fe hydroxides was removed, in the Second stage the neutralization process was continued until reaching pH 5.5, where white-colored slurries (M-2) corresponding mainly to the hydroxides of Al, and finally in the third stage of treatment the pH reached higher values to 8.5 where a dark brown to black slurry (M-3) was recovered and it would correspond to the solid phases of Zn as a major compound and in a smaller proportion to the rest of elements such as Mn, Mg, Pb present in the mine water that passed to the solid phase at pH above neutral.

If the slurry of Fe and Al of the treatment process, at pH higher than the range of mobilization of these 4 and 5.5 elements respectively, these formed solid phases are redissolved and go again to water, so it would require adding as many of alkaline material (lime) to form again solid phases (pH 8) and to remove them from the water, which increases the lime consumption in the process, as well as requiring in some cases flocculants, coagulants and scavengers additions, therefore, the cost of the acidic mine water treatment is higher.

The slurries obtained in the treatment of mine water by means of a 3-stage system could have the following applications: the slurry with Fe content (M-1) could be used as a ceramic pigment, the slurry with aluminum (M-2) would be used in the blasting work to improve the explosives, and the slurry at the high Zn (M-3) content would be used to obtain a zinc concentrate.

When the concentrations of metals (Al, Cu and Zn) present in the mine water have

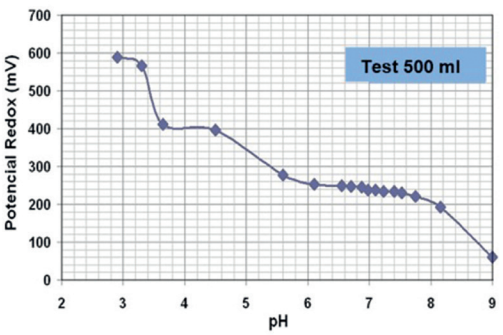

Figure 4 Evolution of Eh in the treatment.

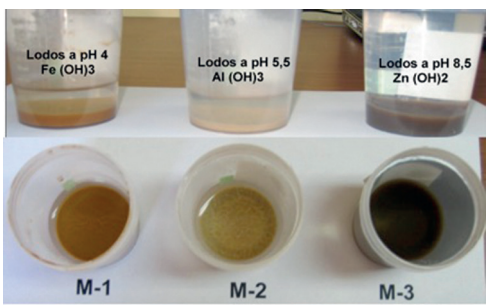

***Picture 1** Solid phases obtained in a sequential staged test by removing solid phases.*

significant values (higher than 300 or 500 mg/L), it is feasible to study the recovery of these elements as byproducts, the experimental tests must be staged in order to obtain at each stage a slurry with a high metallic content, which could be sent to the concentrator plant or a similar process for its recovery, and in some cases to be reused as the slurry with high aluminum content that can be sent to mine for the improvement of Anfo as an explosive and to obtain Anfo aluminized.

D. Unit operations that constitute a staged treatment system.

The main Unitary Operations involved in a staged treatment system are: Dissolution (of process reagents), Agitation and Decantation (Fig. 5) in each stage and they are complemented by secondary operations that allow controlling the process.

Implementing staged acidic water treatment system allows obtaining slurry with well-defined characteristics and the same peculiarities, with chances of recovering metals from slurry process.

The water from the treatment process can be discharged to a local natural watercourse (receiving body), after controlling its quality in order to cause minimum environmental impact, while the slurries that do not have a recovery interest will be stored in adequate containers for it or generally sent to the tailings deposit or another deposit prepared for this purpose. After the experimental stage, a pilot must be carried out to allow measuring adequately the treatment system for each type of mine water.

Conclusions

The sizing of the acid water treatment system based on the content of acidity and staged, on one side, it allows to take better advantage of the resources by spending less lime in the neutralization process, and on the other side, it allows to recover metals from the slurries of the process. This makes acidic water treatments more efficient, less expensive and with greater environmental control.

Obtaining byproducts with economic value can have a direct economic advantage by consuming less quantity of lime, but it also

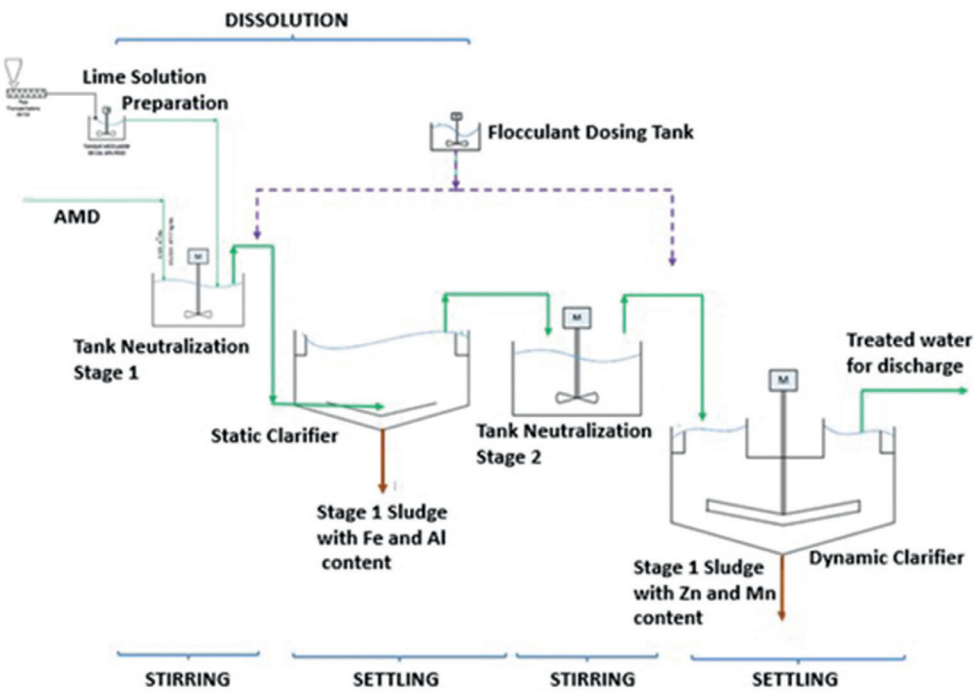

Figure 5 *Unitary operations that constitute a staged treatment system.*

entails other added benefits such as: reducing the volume of slurries to be transferred to the storage deposits, thus increasing life of these deposits and operating costs are reduced, among others.

References

Aduvire, O. and Aduvire, H. (2005) Aguas ácidas de mina: caracterización, mineralogía y microbiología. Ingeopres 141, pp. 52-62.

Aduvire, O. 2006. Drenaje Acido de Mina: Generación y Tratamiento. Madrid: Instituto Geológico y Minero de España. Edición IGME. Código: SID-63187. Publicación Electrónica 136p.

Bigham, J.M., Schwertmann, U., Carlson, L. y Murad, E. (1990). A poorly crystalized oxyhydroxysulfate of iron formed by bacterial oxidation of Fe(II) in AMD. Geochimica Cosmochimica Acta, 54, 2743-2754.

Bigham, J.M. y Nordstrom, D.K. 2000. Iron and aluminum hydroxysulfates from acid sulfate waters. En: Alpers, C.N., Jambor, J.L. y Nordstrom, D.K. (eds), Sulfate minerals: crystallography, geochemistry and environmental significance. Reviews in Mineralogy & Geochemistry, MSA, Virginia. USA. (40), 350-403.

Buamah, R. 2009. Adsorptive Removal of Manganese, Arsenic and Iron from Groundwater. UNESCO-IHE, Institute for Water Education, Delft, The Netherlands.

Jönsson, J., Jönsson, J. and Lövgren, L. (2006) Precipitation of secondary Fe(III) minerals from acid mine drainage. Applied Geochemistry 21, pp. 437-445.

Nordstrom, K. 1985. The rate of ferrous iron oxidation in a stream receiving acid mine effluent. Hydrologic Sciences, 1, 113-119.

Nordstrom, K. 2000. Aqueous redox chemistry and the behavior of iron acid mine waters. En: Wilking, R., Ludwig, R, y Ford, R. Proceeding of the Workshop on Monitoring Oxidation-Reduction Processes for Ground-water Restoration. Cincinnate, OH, USA. 43-47.

Rose, A., Means, B. y Shah, P. 2003. Methods for passive removal of manganese from acid mine drainage. Annual West Virginia Surface Mine Drainage Task Force Symposium. Morgantown, WV, USA. 12pp.

Sánchez, J., López, E., Santofimia, E., Aduvire, O., Reyes, J. Barettino. D. 2005. Acid mine drainage in the Iberian Pyrite Belt (Odiel river, Spain): geochemistry, mineralogy and environmental implications. Applied Geochemistry, 20, pp. 1320-1356.

Stumm, W. and Morgan, J.J. 1996. Aquatic Chemistry, chemical equilibria and rates in 3rd; Wiley; New York.

Developing Integrated Water Management Models to Address Water Related Risks and Provide Resilience in the Mining Industry

Scott Anderson[1], Tyler Tinkler[2]

[1]*GHD, 999 Hay Street Perth WA 6000, Australia, scott.anderson@ghd.com*

[2]*GHD, 23 Honeysuckle Drive Newcastle NSW 2300, Australia, tyler.tinkler@ghd.com*

Abstract

Integrated Water Management models comprises a spatially lumped representation of the components of a mine water management system and their interactivity including water supply and conveyance infrastructure, hydrological and hydrogeological processes, ore processing, water treatment and waste disposal. The model can be used to assess different operational and/or expansion scenarios and their evolution over a mine's life to provide probabilistic outputs of impacts to the water system and identify areas where capacity is constrained and optimisation opportunities exist. We examine the potential benefits and limitations through case studies in both underground and open cut operations, throughout the mine life cycle.

Keywords: IMWA2021, Full Paper, Integrated Water Management, Water Supply, Environmental Containment, Underground Mining, Open Cut Mining, Mine Closure

Introduction

An Integrated Water Management model comprises a spatially lumped representation of the components of a mine water management system (MWMS) and their interactivity including water supply and conveyance infrastructure, hydrological and hydrogeological processes, ore processing, water treatment, waste disposal and tailings storage facilities. The model can be used to assess different operational and/or expansion scenarios and their evolution over a mine's life to determine the impacts to the water system and identify areas where capacity is constrained and optimisation opportunities exist. The model can provide answers to the following water related issues:

- **What** – what type of capacity constraint exists (water surplus/deficit or inadequate quality)?
- **Where** – where does the capacity constraint exist (tanks/dams/pumps/pipelines)?
- **When** – when does the issue manifest (immediately or in several years)?
- **Likelihood** – what is the likelihood that the issue will manifest (under climate change)?
- **Impact** – which mine performance measures are impacted (ore production, safety or environment)?
- **Magnitude** – how big is the impact and what will the cost be (financial/environmental/social)?

Methods

Our approach to water and contaminant balance models incorporates all components of a MWMS, as well as the interdependencies between them to provide probabilistic outputs of the magnitude of impacts. We employ a multidisciplinary approach that includes inputs from hydrological, hydraulic, hydrogeological, chemical and tailings practitioners. The modelling incorporates these inputs and the probabilities surrounding them to provide improved predictions of a MWMS behaviour and then assigns a likelihood to a certain impact occurring. The most basic form is a semi-distributed spatially lumped catchment mass balance approach (Ladson 2004), expressed as ordinary differential equation that is typically solved in minutes or hours with an explicit numerical scheme. Catchment runoff is often an important component, typically

estimated using the Australian Water Balance Model (Boughton 2003) for which regional parameters are available (Boughton and Chiew 2003), but site specific calibration is preferred, especially for land uses unique to mine sites (Kunz *et al* 2013).

Rainfall inputs are typically sourced from a synthetic historical record (DSITI 2019). These records are limited to the availability of nearby rain gauges, orographic effects and the daily time scale limits the temporal resolution of the models.

Groundwater inputs are typically estimate separately, with varying degrees of coupling employed depending on the complexity of the interaction (Rassam and Werner 2008). Tailings storage facilities are commonly present and often represent the single largest water flux within the system (Watson 2000).

Traditional water and contaminant balance models may consider each component in isolation (e.g. tailings storage facility) and only assess a static design scenario rather than changes over the mine life. Impacts on other components of the system are often ignored or based on simplistic assumptions that may not adequately reflect the system complexity. This is especially true under rare combinations of events where MWMS are pushed to their limits and can behave in unexpected ways that are not anticipated from a traditional deterministic design approach.

The concept and advantages of integrated MWMS models is widely documented (Gosling 2010, Younger 2006), and such models are successfully implemented across most mine operations in Australia for regulatory and operational reasons. This paper focuses on contrasting estimates from "simpler" design methods and MWMS models. Through two case studies successfully implemented in lithium and gold mines, we demonstrate situations where simplistic "worst case" design assumptions may lead to under or over design.

Case study 1: Environmental containment design for small underground gold mine

Underground mines are not afforded the luxury possessed by established open cut operations of large mining voids for water storage. Many operations are expected by decision makers and regulators to be 'zero discharge' which is often poorly defined and understood. Simplistic design approaches may be adopted to demonstrate compliance with this expectation that underestimates the actual likelihood and leads to unexpected outcomes during the operation of the mine. A simplified schematic of a proposed new underground mine in Central West NSW is

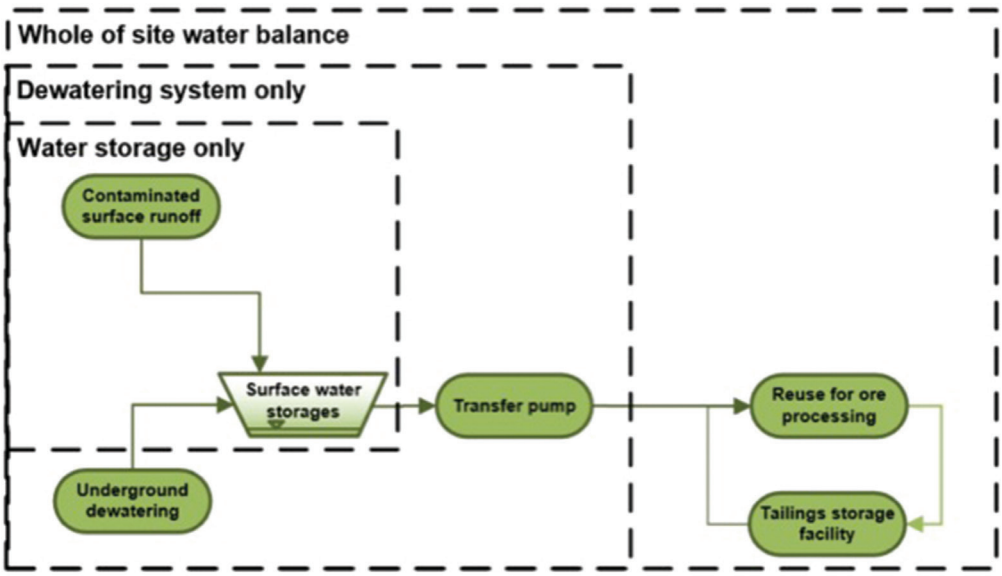

Figure 1 *Conceptual MWMS schematic.*

shown in Figure 1. The project proposed to transfer ore and water to another existing mine for processing.

Figure 1 shows the varying levels of scope of the assessment of the performance of the environmental containment of the MWMS. Throughout the design of the project, as more information was available, the scope of the assessment was expanded and the performance reassessed, as shown in Table 1.

Table 1 shows that considering the surface water storage only for containing runoff from the catchment (a traditional hydrologic design) does not represent the actual performance of the system because the initial water volume of the storage depends on the operation of the remainder of the system. Considering only the dewatering system captures the limitations of the transfer pump and variability with predicted groundwater inflows over time. During the peak of groundwater inflows, that typically occurs as the decline reaches final depth in the first half of the mine life, the dewatering capacity of contaminated runoff is reduced by the need to continually dewater the underground mine for its safe operation.

However, Table 1 shows that ultimately, the performance of the system was limited by the net losses from the processing and tailings emplacement operations. Improving the performance would require additional contaminated water storage, however the integrated modelling can demonstrate that this can be located at either the new or existing mine site, potentially reducing costs.

Consideration of cumulative risks of the of the full mine life (with varying groundwater inflows and ore processing rates) which is relatively short compared to traditional public infrastructure, can also better inform decision makers.

In summary Case Study 1 has demonstrated how an Integrated Water Management model coupled with probabilistic inputs delivers can be used to answer the following:

- **What** – potential downstream surface water impacts
- **Where** – at either the main or satellite site
- **When** – the early part of mine life as the decline reaches full depth
- **Likelihood** – 86% chance of exceedance during life of mine of requirement for off-site discharge
- **Impact** – actual and perceived downstream water quality impacts

Through the understanding of all these issues, a solution that was optimised for both cost and risk to the miner was able to be achieved. This would not have been the case if simpler modelling techniques were used. This limitation of this approach is the availability of information to inform design and feasibility budgets, which is not also possible in the permitting and design schedule.

Case study 2: Operational water surplus and deficits for an open cut lithium mine

Preconceived ideas about specific issues within a MWMS can often limit the scope of water balance assessments leading to a form of confirmation bias in the outcomes. In this situation, a mine operator may only want to examine a few narrow scenarios such as wettest or driest year in recent history and only for the ensuing year or two. This can have the impact of over or under design and also misses the opportunity to identify potential other MWMS constraints or opportunities with reasonable planning and implementation timeframes to affect outcomes.

Table 1 *Environmental containment system performance.*

Design basis	Environmental containment performance - initial	Environmental containment performance – under peak groundwater inflows	Environmental containment performance – life of mine
Water storage	1% AEP 72 hour duration	1% AEP 72 hour duration	1% AEP 72 hour duration
Water storage capacity and dewatering system	1% AEP	4% AEP	16% chance of exceedance during life of mine
Whole of site water balance	7% AEP	14% AEP	86% chance of exceedance during life of mine

Case Study 2 examines an open cut lithium mine in Western Australia to demonstrate the advantages of Integrated Water Management models coupled with probabilistic climate inputs. The mine is located in one of the wettest parts of the state and therefore the conventional wisdom had been that surplus contaminated water leading to offsite discharge was the primary concern of the MWMS. This was not unfounded as it had been the major MWMS issue observed by the mine operator over the preceding decade. A comprehensive water balance model was developed for the MWMS that utilised the previous 50 years of observed climate data applied sequentially in a "semi-Monte Carlo" approach over the ensuing 15 years of the mine's life. The model accounted for changes to the MWMS over that timeframe including dewatering rates, ore processing volumes and development of additional tailings storage facilities. The advantage of this method is that it subjects the MWMS to a large range of the historically observed climate patterns over the remaining mine life and therefore provides results that are probabilistic instead of deterministic.

Figure 2 shows the outcomes of water surplus or deficit risks as determined by the water balance model of the mine. From Figure 2, it can be observed (as the mine operator suspected) that surplus water leading to offsite discharge was indeed a significant risk over the remaining mine life. However, what was not expected was the significant risks of processing water shortages. The risk of process water shortages was not expected to manifest until 2024 but grows significantly to approximately 50% by 2027 before falling away for the remainder of the mine life. Had a model been developed that just examined a wet climate scenario and only for the ensuing 1 to 3 years (as was initially proposed) then the water deficit risk would not have been identified as early as it had. This has provided the miner with sufficient time to examine and implement mitigation measures which significantly reduces the risk of processing water shortages and the impacts to mine revenue and profitability associated with it.

Following identification of the water deficit risks from the initial water balance modelling work, the operator wished to explore strategies to mitigate these risks. The only feasible options identified included a combination of both additional storage volume and additional water sources. This could be in the form of increasing the storage capacity of existing onsite storages coupled with a new locally acquired offsite water

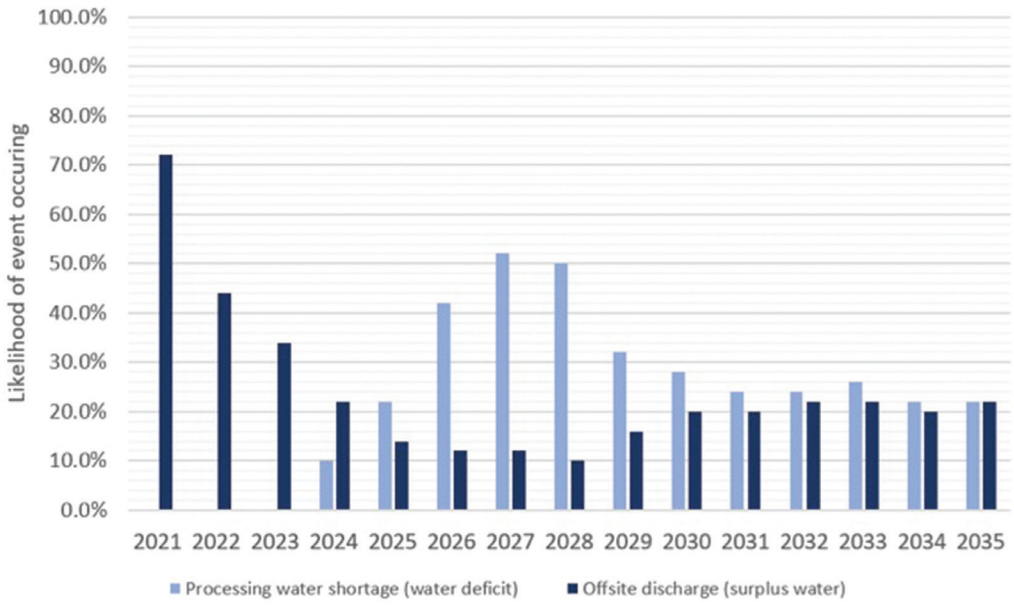

Figure 2 *Modelled water surplus or deficit risk.*

supply or a completely new offsite dam and associated catchment.

The water balance developed previously was used to assess combinations of additional storage and water supply required to mitigate the risk of process water shortages. The outcomes of this modelling are summarised in Table 2. It demonstrates the difference between using a model that only assesses outcomes against a "worst case" scenario versus models that provide probabilistic results and therefore allow for a risk based approach. Under a "worst case" scenario model, the recommendation would be for additional storage in the order of 12 to 20 GL. This is a large storage relative to the mining operations and potential cost prohibitive. Under a probabilistic model, the cost of the additional storage was traded off against the costs of reduced processing due to the water shortages. In this case, a 2 percent annual exceedance probability was determined to provide an optimal balance and lead to the recommendation of additional storage in the order of 6 to 12 GL. This option still exposed the mine operation to approximately 30% likelihood of a year with processing water shortages up to 40% over the remaining mine life but allowed for a significantly smaller storage than that recommended by the "worst case" scenario and avoided unnecessary overdesign and the associated costs for the mine operator.

In summary, Case Study 2 has demonstrated how an Integrated Water Management model coupled with probabilistic climate inputs delivers critical and actionable information on the mine's MWMS including:

- **What** – significant water surplus and deficit risks
- **Where** – storage capacity constraint
- **When** – immediately for water surplus and in 3-4 years for water deficits
- **Likelihood** – 10% to 70% for water surplus events and 0% to 50% for water deficit events
- **Impact** –ore processing capacity (and therefore mine revenue)
- **Magnitude** – up to 40% of ore processing capacity lost

Through the understanding of all these issues, a solution that was optimised for both cost and risk to the miner was able to be achieved. This would not have been the case if simpler modelling techniques were used. It should be noted that this method only provides an estimate for the magnitude of the additional storage volume required and that outcomes can vary significantly depending on the quality and reliability of the inputs and assumptions the model is based on. These models also tend to become less reliable the further one attempts to forecast into the future. These factors should not be discounted when interpreting results.

Conclusions

Through the two case studies covering a range of production scales in both underground and open cut operations and throughout the mine life cycle, the authors of this paper have demonstrated how an Integrated Water Management model approach provides an improved mine resilience tool for identifying MWMS risks and then providing solutions that are timing, cost and impact optimised. The complexity of the multidisciplinary inputs to the these models is there main limitation compared to simpler techniques, which requires an integrated systems thinking in planning and development.

Acknowledgements

The authors are grateful for contributions from Caroline Holmes, Mark Shaw, Bas Wijers, Paul Phillips, Doug Edgar and Nathan Malcolm for their contributions.

Table 2 *Additional storage volumes and water supply required to mitigate process water shortages.*

Average annual additional water supply provided	Size of additional storage required – under "worst case" conditions	Size of additional storage required – under 2 percent exceedance conditions	Size of additional storage required – under 5 percent exceedance conditions
500 ML/year	≈20.0 GL	≈12.0 GL	≈6.5 GL
1000 ML/year	≈12.0 GL	≈6.0 GL	≈4.5 GL

References

Boughton, W (2003) The Australian water balance model. Environmental Modelling & Software 19 (2004) 943–956.

Boughton, W and Chiew, F (2003) Calibration of the AWBM for use on ungauged catchments. Technical Report 03/15 CRC for catchment hydrology.

Department of Science, Information Technology and Innovation (DSITI) (2019) SILO Data Drill. Queensland Government. Retrieved from http://www.longpaddock.qld.gov.au/silo/ on 2 August 2019.

Gosling, S (2010) Developing water balance models as an operational tool for sustainable mine water management. Water in Mining, Chile.

Kunz, Nadja & Woodley, Alan (2013) Improving the accuracy of mine site water balances through improved estimation of runoff volumes. In Moran, Chris (Ed.) Water in Mining 2013 Proceedings, The Australasian Institute of Mining and Metallurgy, AusIMM, Brisbane, QLD.

Ladson (2008) Hydrology: An Australian Introduction. Oxford University Press, Melbourne, Australia.

Rassam, D. And Werner, A. (2008) Review of groundwater–surfacewater interaction modelling approaches and their suitability for Australian conditions. eWater Technical Report eWater Cooperative Research Centre, Canberra.

Watson, S. J. (2000) The development of water balance models for tailings management. Australian Geomechanics.

Younger, P. L (2006) The water footprint of mining operations in space and time - a new paradigm for sustainability assessments?, Parkville Victoria, Australasian Inst Mining & Metallurgy.

Should Irrigation With Mine-Affected Water Be Considered Part Of The Long-Term Strategy To Manage Acid Mine Drainage In The Witwatersrand Goldfields?

John George Annandale, Meiring du Plessis, Phil Tanner, Sarah Heuer

Department of Plant and Soil Sciences, University of Pretoria, South Africa

Abstract

Due to South Africa's mining legacy, large volumes of acid mine drainage (AMD) threaten the quality of water resources. Treatment technologies exist, but are expensive and energy intensive. In the Witwatersrand Goldfields, three High Density Sludge water treatment facilities were established as emergency measure to neutralise large volumes of AMD in the Eastern, Central and Western Basins. These have been effective short-term measures, but sustainable long-term solutions are sought. Productive, cost-effective use can be made of these mine-affected waters if used for irrigation, and livelihoods will be created. It is worthwhile to attempt to address any potential concerns with this option.

Keywords: irrigation, AMD, DSS, Goldfields, Mine-closure

Introduction

Many deep underground mines in the Witwatersrand Goldfields closed in the late 1990s and early 2000s and began to flood. Pyrite exposed to air and water generates acid mine drainage (AMD). When mines close, active pumping and water treatment ceases, and this water starts to decant with potentially serious downstream consequences.

Specifically, the salt load to Vaal River System was highlighted by the Department of Water and Sanitation (DWS). Target salinities of 600 mg/L have proved difficult to meet, necessitating the unsustainable release of 5-11 units of expensive Lesotho Highlands water for dilution, for each unit of AMD entering the system. This could lead to a surplus of water in the lower catchment where it is not needed. The decant risk was identified for the whole of the Witwatersrand Goldfields which is divided into the Eastern Basin, Central Basin and the Western Basin.

Short-term solution

When mine water decanted from the Western Basin and spilled into a nearby nature reserve, a sense of urgency was created. This, together with the risk of flooding infrastructure, motivated the introduction of the "short-term" solution. Decisions had to be made on pumping water from the basins and keeping levels below "Environmental Critical Levels" to protect the environment and infrastructure. High Density Sludge (HDS) plants were built in the Eastern Basin (80 Ml/d), Central Basin (72 Ml/d) and Western Basin (33 Ml/d).

HDS is a relatively cheap water treatment option that addresses the acidity of water and reduces trace element levels. However, the salt load to the Vaal River System is still unacceptable, and longer-term solutions are sought. Reverse Osmosis (RO) was mooted as the preferred technology for the long-term solution, as it is a proven technology that has been successfully demonstrated. However, it has high capital and running costs and is energy intensive.

Long-term solutions

The volume of AMD is relatively small compared to that required by local water utility, Rand Water. Treating this mine-affected water to potable standards with RO, therefore, will not make a big contribution to the fresh water supply of Gauteng. It will also be expensive and energy intensive to treat, and there may be resistance to domestic consumption of purified mine water. Due to the prevalence of abandoned and ownerless mines, this is a taxpayer liability.

The key water management requirement is to keep as much salt as possible out of the Vaal River. This makes irrigation, a consumptive use of water with the

opportunity to precipitate gypsum in the soil, worth considering (Annandale *et al*, 1999). Apart from creating livelihoods, irrigation should be a cost-effective option. In addition, commercial irrigation with water from the Vaal System was curtailed several years ago, as it was not considered a priority water use. Hence, there is clear motivation for other water sources (grey water, sewage, industry and mine water) to be used for irrigation.

Irrigation with mine-affected waters

A number of concerns arose when irrigation with mine water was suggested as a potential long-term option. These were:

- Are the waters suitable for sustained irrigation?
- What is the environmental impact?
- Is land available in the built up Witwatersrand region?
- Will farmers be willing to irrigate with these waters?
- What are costs/benefits of this option?

This paper attempts to respond to these concerns, with some covered in more detail than others.

Are waters suitable for irrigation?

Data for untreated and treated mine impacted waters from the Goldfields' was supplied by DWS. This data was collated to determine the 95th percentile of constituents, and the 5th percentile for pH, in order to provide a "worse case" assessment of the suitability of these waters for irrigation. These water qualities are given in Table 1.

Although these treated and untreated waters contain fair amounts of Na and Cl and a high total salt concentration (EC), they are primarily gypsiferous waters from which gypsum precipitation can be expected, when irrigating to achieve a low leaching fraction. Consequently, the negative effect of the high EC can expected to be less pronounced than when irrigating with a water of similar salinity, but that is non-gypsiferous.

A site-specific, risk-based irrigation water quality Decision Support System (DSS), developed by du Plessis *et al* (2017), was used to ascertain under what conditions these waters may be suitable for irrigation. In a nutshell, the DSS is able to assess the implications of irrigating with a range of waters, including mining-impacted waters, on soil and crop resources, as well as on irrigation equipment. This is done through the assessment of Suitability Indicators, with each divided into one of four Fitness-For-Use (FFU) classes, which are colour coded to make output intuitive, and are presented as being 'ideal', 'acceptable', 'tolerable' or 'unacceptable.

Table 1 *Water qualities used to assess suitability for irrigation. EB (Eastern Basin), CB (Central Basin) and WB (Western Basin). AMD denotes untreated water, and HDS is treated water.*

Constituent	EB AMD	EB HDS	CB AMD	CB HDS	WB AMD	WB HDS
pH	6.2	7.2	5.8	8.4	5.8	8.6
EC mS/m	300	260	490	403	350	385
Ca mg/l	370	340	517	668	520	650
Mg mg/l	120	95	251	178	130	90
Na mg/l	200	206	207	192	110	170
SO4 mg/l	1600	1660	3760	2710	2200	2400
Cl mg/l	120	120	96	97	80	85
HCO_3 mg/l		166				50
SAR	2.3	2.6	1.9	1.7	1.1	1.6
Fe mg/l	100	0.2	610	0.13	120	1.3
Mn mg/l	0.4	0.1	25	1.5	30	3.1
Al mg/l			144	0.05		
Ni mg/l				0.02	3	0.05
B mg/l					1.3	1.6
F mg/l					1.3	1.4
U µg/l				5	86	29

Table 2 Salinity response of selected crops after Maas and Hoffmann (1977).

Crop	Threshold ECe (mS/m)	Slope (% per dS/m)
Maize	170	12
Soybean	500	20
Wheat	600	7.1

The DSS was used for several site-specific, 45 year simulations, using the water quality of the specific basins, before and after treatment. A representative weather station close to each basin was selected, with sprinkler irrigation so foliage is wetted to assess scorching, and for irrigation to field capacity after 30 mm soil water depletion with 10 mm room for rain. Therefore, any leaching would occur through rainfall. Maize mono-cropping in summer, or a crop rotation of soybean in summer and a small grain in winter (wheat or stooling rye), were selected as the cropping systems. Crops vary greatly in their tolerance to salinity, and the thresholds above which yields decline, and the rate at which they decline for these crops, are presented in Table 2 (Maas and Hoffman, 1977).

The results of the DSS simulations are presented briefly below:

Root Zone Salinity

Except for untreated Central Basin water, root zone salinity is predicted to fall mostly in the ideal or acceptable suitability categories. Of more importance is that the effect of salinity on yield of the selected crops (maize, soybean and wheat). This is discussed below.

Soil Permeability

Having lower SAR values, the Western Basin waters are assessed to present less soil permeability problems than the Eastern Basin waters. They fall predominantly within the ideal/acceptable categories. Soil infiltration was identified as a tolerable problem for irrigation with treated Eastern Basin water. However, by adopting appropriate management practices, it should be possible to overcome any soil physical problems.

Trace Element Accumulation

Several trace element concentrations were reported as below detection limits (BDL). In such cases, the detection limit was taken to conservatively assess the waters for irrigation. Where such trace elements come up as potentially problematic, more careful analyses with lower detection limits are indicated. Specifically for these simulations, Se and Hg are highlighted. Table 3 presents DSS output for trace elements of potential concern, before and after water treatment.

On face value, the concentrations of several trace elements in untreated waters will accumulate to unacceptable levels within an unacceptably short period of time. Treatment clearly addresses any concerns around Fe, Al and Ni, as well as for Mn in the Eastern

Table 3 Years to reach international soil threshold values of selected trace elements of potential concern. Colours indicate fitness-for–use classes. EB (Eastern Basin), CB (Central Basin) and WB (Western Basin). AMD denotes untreated water, and HDS is treated water.

Mine Water	EB AMD	EB HDS	CB AMD	CB HDS	WB AMD	WB HDS
Fe	7	>1000	1	>1000	5	463
Mn	65	260	1	17	1	8
Al	-	-	5	>1000	-	-
F	-	-	-	-	185	172
Ni	-	-	-	>1000	8	482
U	-	-	-	260	14	42

Basin. Mn is still assessed to be potentially Unacceptable after treatment in the Central and Western Basins.

In view of the fact that Fe, Al and Mn are present in high concentrations in natural soils, it is debateable to what extent their concentrations pose a real problem as far as trace element accumulation is concerned. If necessary, their concentrations in the soil solution can probably also be managed by liming the soil and maintaining a suitable redox potential, conditions essential for successful irrigated crop production. The high Fe and Mn concentrations can, however, also present problems with deposits forming on produce irrigated with overhead application systems (an aspect that is not assessed by the DSS).

Uranium is obviously an element of concern to the general public, and the Western Basin waters should be more carefully analysed to ascertain if levels are indeed problematic, and if so, potential solutions should be sought.

Root Zone Effects on Crop Yield

There appear to be no concerns about salinity effects on yields of maize, soybean and wheat using waters from the Eastern and Western Basin, whether treated or not. The poorest water quality is for the Central Basin. In summer, moderate yield depression is expected for maize, and only a slight yield depression for more salt tolerant soybeans, if we irrigate with untreated mine water. Although wheat is quite salt tolerant, moderate yield loss is also expected in winter, as there is little to no rainfall to dilute salinity in the root-zone. Once the water is treated, none of our crops should show any meaningful yield depression due to salinity.

Problems with Irrigation Equipment

All of the untreated waters are predicted to present corrosion problems, while the treated Eastern Basin waters are predicted to be ideal, treated Central Basin water presents a tolerable level of corrosiveness, and the treated Western Basin water is predicted to be scaling to a tolerable degree. The Western Basin waters are predicted to present various degrees of problems if used with drip irrigation, while it is only the Fe content of the untreated Eastern Basin waters that is expected to present clogging problems. Untreated Central Basin water has high levels of Fe and Mn that would cause problems with micro irrigation systems, and after treatment, it is the pH and to a lesser extent Mn that would need to be considered. These effects are not important if overhead sprinkler irrigation is used.

Environmental impact – the fate of solutes

Irrigation is a consumptive use of water, and with calcium and sulphate dominated mine waters, there is an opportunity to precipitate a large amount of gypsum in the soil profile, thereby removing these salts from the water system. Such gypsum precipitation is not harmful to the soil, and the capacity for such precipitation is not limited. A large fraction of the salt applied to fields with these waters is predicted to precipitate in the soil profile as gypsum. For the Eastern Basin waters, just under 40% of the salt is expected to precipitate after HDS treatment, and just over 40% for untreated water. For the Western Basin, in excess of 60% of the salt should precipitate post treatment, and just over 50% pre-treatment. Predictions for the Central Basin are that around 35% of salts will be immobilised with irrigation using untreated water, rising dramatically to around 55% immobilisation irrigating with treated water.

Salts not precipitating must be leached from the root-zone for irrigation to be sustainable. It is likely that salt plume concentrations leaching from irrigated fields will be greatly attenuated by rainfall, and the ultimate fate of these salts will depend heavily on the irrigated field's position in the hydrologic landscape, but lags between irrigation application and salts surfacing in water bodies are likely to be decades or even much longer (Annandale *et al*, 2006). Should irrigation be considered, a geohydrological modelling exercise will be useful to best site irrigated fields. It may also be possible to site fields in order to be able to intercept percolation for possible re-use or treatment, but the salt load in this water will be considerably lower than the salt load applied to fields through irrigation. This will obviously have cost implications for the irrigation water use option of managing mine water.

Availability of land and willingness of farmers to irrigate with mine water

Dryland farming is a risky business, and margins are currently under pressure. It is expected that commercial farmers would welcome the availability of mine water for irrigation, as long as there is surety of supply at low cost, if reasonable crop yields are attainable, and if their soils and ground water resources will not be polluted. Irrigation should reduce their production risk substantially. The capital costs for irrigated farming are high, as are the input costs for seasonal production, but these can be carried by the growers in exchange for a commitment to productively utilise the mine water supplied to them. Irrigation is not only likely to be a cost effective way of dealing with the mine water problem, but increased production will create employment.

Table 4 indicates the area needed to utilise the mine water. Area required depends on cropping system and the availability of storage for times when little or no water can be used for irrigation.

There has been concern expressed over the availability of irrigable land near the mine water sources. A report by van der Laan *et al* (2014) indicates that land is available, especially if piped out of heavily built up areas. If water is conveyed to regions of lower elevation, it can be supplied to farmers under pressure, which will save greatly on electricity costs to pump water, making the irrigation option even more financially feasible and sustainable for growers. If water is allowed to decant, this may result in several smaller streams that may be easier to utilise through irrigation, but detailed studies will be required to determine the opportunities and risks of this option.

Economic aspects of mine water irrigation

The Goldfields waters are not very acidic, and it appears feasible to utilise untreated mine waters (except for the Central Basin), especially if growers commit to the application of limestone to their fields. The HDS treated waters are more suitable for irrigation than the untreated waters, but it is unlikely that growers will be able to bear these pre-treatment costs, should this be required.

The cost to the taxpayer of the irrigation option will depend on whether water is pumped or allowed to decant, as well as the cost of any necessary conveyance infrastructure. In addition, the cost of current pre-treatment with the HDS process will remain if irrigation with untreated water is deemed undesirable. There will also be the cost of interception and treatment of water percolating beyond the root-zone, if this is required.

Because there are so many potential irrigation options available, and their economic analyses are scale and cropping system dependent, it is essential to undertake detailed economic analyses of any specific proposed irrigation schemes. However, if the irrigated crop production system is set up to deliver yields close to those obtained with good quality water, an income should be generated from mine water, instead of a treatment cost. The economic activity and job creation associated with the irrigation option will also be of great benefit to the country.

Conclusions

It seems clear that with careful planning, irrigation with mine-impacted waters are an option worthy of serious consideration in the Goldfields of South Africa. The potential financial and energy savings compared to

Table 4 *Irrigated areas required for two cropping systems in the three basins.*

Mine Water	Eastern Basin 80 Ml/d		Central Basin 72 Ml/d		Western Basin 33 Ml/d	
Cropping	Maize	Soy-wheat	Maize	Soy-wheat	Maize	Soy-wheat
system	221 mm	767 mm	222 mm	771 mm	244 mm	831 mm
Area	13200 ha	3800 ha	11800 ha	3400 ha	4900 ha	1500 ha

other treatment options, combined with the job creation and productive use of these waters, certainly make this a potentially attractive option. It would be prudent to control or regulate the process if considered. Assessments made here rely on the accuracy of the water quality data supplied. It is imperative that decisions are made based on reliable data.

References

Annandale, J.G., Jovanovic, N.Z., Benadé, N & Tanner, P.D., 1999. Modelling the long term effect of irrigation with gypsiferous water on soil and water resources. Agric. Ecosyst. Environ. 76: 109-119.

Annandale, J.G., Jovanovic, N.Z., Hodgson, F.D.I., Usher, B., Aken, M.E., Van Der Westhuizen, A.M., Bristow, K.L. & Steyn, J.M., 2006. Prediction of the environmental impact and sustainability of large-scale irrigation with gypsiferous mine-water on groundwater resources. Water SA, 32 (1), 21-28.

Du Plessis, H.M., Annandale, J.G., Benade, N., van der Laan, M., Jooste, S., du Preez, C.C., Barnard, J., Rodda, N., Dabrowski, J., Genthe, B. & Nell, P. 2017 Risk based, site-specific, irrigation water quality guidelines. Vol1. Description of Decision Support System WRC Report TT727/17

Maas, E.V. & Hoffman, G.J. 1977. Crop salt tolerance–current assessment. Journal of the Irrigation and Drainage Division 103: 115-134.

Van der Laan, M., Fey, M.V., van der Burgh, G., de Jager, P.C., Annandale, J.G. & du Plessis, H.M. 2014. Feasibility study on the use of irrigation as part of a long-term acid mine water management strategy in the Vaal Basin. WRC Report No. 2233/1/14

Mobility of Uranium in Groundwater-Surface Water Systems in a Post-Mining Context (Central Portugal)

I.M.H.R. Antunes[1], P.C.S. Carvalho[2], M.T.D. Albuquerque[3], A.C.T. Santos[4]

[1]*ICT | University of Minho, Campus de Gualtar, 4710 - 057 Braga, Portugal, imantunes@dct.uminho.pt*

[2]*University of Coimbra, MARE – Marine and Environmental Science Centre, Department of Life Sciences, Coimbra, Portugal, paulacscarvalho@gmail.com*

[3]*Instituto Politécnico de Castelo Branco | CERNAS | QRural and ICT | Universidade de Évora; Portugal, teresal@ipcb.pt*

[4]*GeoBioTec, Department of Geosciences, University of Aveiro, Aveiro, Portugal, uc41232@uc.pt*

Abstract

In uranium abandoned mine areas, particularly with mine tailings and open-pit lakes, the mobility of potentially toxic elements still acts as a source of surface and groundwater contamination. The water of open-pit lakes from Ribeira de Bôco mine and associated groundwater and surface water from the area is neutral and with low metal contents. However, some water samples are contaminated with Cd, Cr, Cu, Fe, Mn, As, and U and should not be used for human consumption or in agricultural activities. The baseline uranium threshold is considerably high for groundwater, which is supported by geogenic features and mining activities.

Keywords: Geogenic Contents, Uranium mines, Surface and Groundwater, Contamination

Introduction

Water resources has become a serious environmental problem on a global scale. Nowadays, the global concern is to ensure sufficiency in water quantity for public health, food security, and water access demand (UNESCO, 2019). However, this natural resource is becoming scarce because of increased consumption, extended droughts, and water quality degradation, mainly associated to anthropogenic activities (Satapathy *et al*., 2009; Val *et al*., 2019; Mello *et al*., 2020). Future scenarios for water resources are predicting water scarcity, with a decrease in the amount of precipitation and limitation on groundwater recharge for the next five decades.

The impact from mine waste on socio-economically disadvantaged communities worldwide continues to be documented on surface-groundwater systems (e.g., Dambacher *et al*., 2007; Jiang *et al*., 2015; Babayan *et al*., 2019; Pal and Mandal, 2019; Flett *et al*., 2021). Pollution studies associated with uranium mines are commonly carried out within the context of watersheds (e.g., Fernandes and Franklin, 2001; Winde, 2010).

In Portugal, for 80 years ago, uranium mining activities ceased leaving as a legacy over 61 radioactive ore deposits involving uranium and radium production. These mining activities have been abandoned into the environment, without recovery processes, and the resulted areas contain tailings and rejected materials deposited and exposed to the air and water since those years. Consequently, uranium and potentially toxic elements (PTE) are leaching on these areas, which act as a source of surface and groundwater contamination (e.g., Antunes *et al*., 2020; Neiva *et al*., 2019).

Uranium and arsenic contamination pose a concern for the protection of the environment and for water quality (Skierszkan *et al.* 2020). Geochemical environment, groundwater provenance and hydrogeochemistry will affect the mobility of selected metals and As (e.g., Bird *et al.* 2020), particularly in post-mining contexts. Growing worldwide concern over uranium contamination of groundwater resources has placed an emphasis on understanding uranium mobility and potential toxicity in groundwater-surface water systems (Byrne *et al*., 2021).

The purpose of this study is to identify the geochemical characteristics of surface and groundwater with a particular focus on uranium and other trace elements mobility in an abandoned uranium mine from Portugal, where water resources are scarce and consequently a regularly monitoring and quality is needed for integrated water management.

Study area

In Portugal, between 1908 and 2001, different deposits of radioactive ore were extracted from the production of radium and uranium (north and central Portugal). The old uranium mine of Ribeira do Bôco (40°31′17′′N; 7°38′26′′W) is located about 2.5 km SW from Arcozelo village (Gouveia, central Portugal). The area is in the Central Iberian Zone of the Iberian Massif (e.g., Farias *et al.*, 1987), which is one of the many mines from the uranium-bearing Beiras area. The ore deposit is mainly of supergenic nature with dominant mineralization in autunite and torbernite. The regional geology is characterized by smoky and zoned quartz veins and basic rocks with pitchblende, sulphides, and secondary uranium minerals (Cameron, 1982). Underground exploitation resulted in waste rock dumps with high concentration of radionuclides. High levels of radiation have been reported in the surrounding water and soil (Carvalho, 2014).

The mine was exploited in two open-pit mines, located on the east of the Ribeira de Bôco stream, between 1986 and 1988. A total of 32.5 tons of ore were exploited with an average content of 0.97% U_3O_8 and containing 31.7 kg of U_3O_8. The pit lake contains approximately 108,000 m^3 of water, with 20 meters deeper (Fig. 1a). Two dumps containing tailings, waste rocks, and rejected material from the mine exploration (total of 39,580 m^3) are located close to the open pit lake and are slightly covered by vegetation but was not yet restored (Fig. 1b). Surface runoff and mine water are discharged into a small creek, which displays typical features of mine contamination, such as deposition of yellow-reddish precipitates (Fig. 1c, d).

The area has rural characteristics with vegetation that is dense and mainly with herbaceous species (Fig. 1e). Around the abandoned mine, small agricultural areas occur with potato crops, vineyards, and pastures (Fig. 1f), which are irrigated by the Ribeira de Bôco stream and wells located in the stream margins.

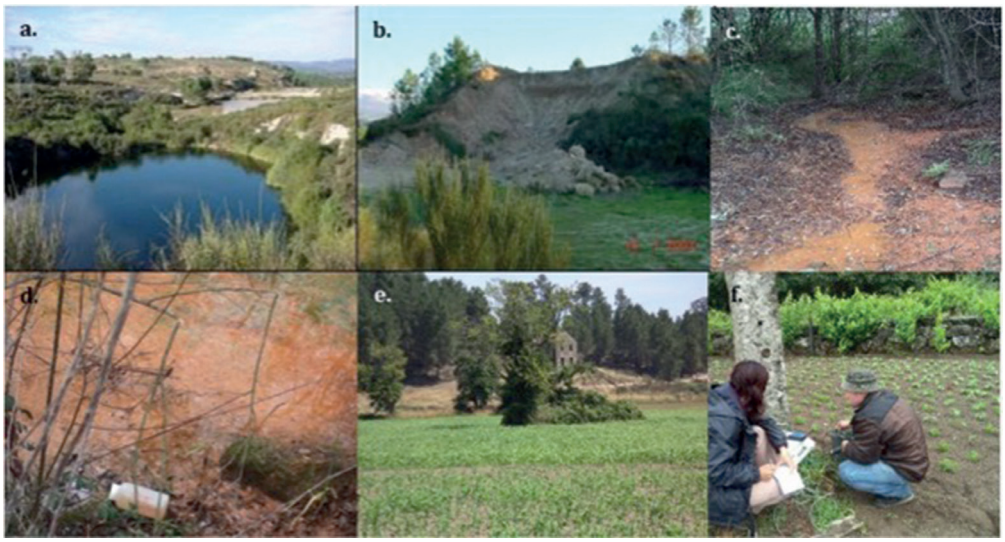

Figure 1 *Field images illustrating the old abandoned mine area of Ribeira do Bôco (Central Portugal): a. open pit lake; b. mine dumps; c, d. water mine with ochre-precipitates; e. vegetation and crops; f. well in an agricultural area.*

Methods

A total of twenty-one water samples, corresponding to open pit water (Rb2, 6, 16, 24), water mine drainage (Rb5), surface water (Rb1, 3, 7, 9, 11, 13, 15, 19, 22), and groundwater (Rb4, 8, 10, 12, 14, 17, 18, 23), were selected on the study area (Fig. 2). The temporal variability of water was represented by two sampling campaigns, during a hydrological year, and representing the raining and dried seasons. All water samples were collected, and analysed for physico-chemical properties, as well as selected potentially toxic elements. The water points located outside mine influence area (Rb18, 19, 22, 23; Fig. 2) have been selected to characterize the natural geochemistry of the area. The distribution of water sampling points was not uniform due to the nonuniformity of well distribution and water stream availability. The main purpose of the wells is for water supply to residents, and domestic animals and agricultural irrigation.

Temperature, pH, Eh, and electrical conductivity (EC) were measured in situ using a multiparameter HANNA HI929828 model. The water samples were filtered through 0.45 µm pore size membrane filters. Those for the determinations of major and trace elements (e.g., Ca, Mg, Fe, U, Th, As, Co, Cd, Pb, Cu, Zn, and Mn) were acidified with suprapur HNO3 at pH 2 and analysed by Inductively Coupled Plasma Optical Emission Spectrometry (ICPOES), using a Horiba Jovin Yvon JV2000 2 spectrometer. Anions were determined in non-acidified samples by ion chromatography with a Dionex ICS 3000 Model. Duplicate blanks and laboratory water standards were analysed to assess quality control of the obtained results. The accuracy of the methods was verified using certified patterns and the measurement precision was greater than 5%. The laboratory water analyses were obtained at the Department of Earth Sciences, University of Coimbra, Portugal.

Figure 2 *Geographical setting of studied area (Central Portugal) and location of water sampling points (Rb): x – open pit,* o *– surface water,* • *– well.*

Results

The Piper diagram shows the main geochemical characteristics of the water from Ribeira de Bôco area, considering the water samples collected upstream and downstream mine influence (Fig. 3a, b). The dominant hydrochemical facies of most water samples is undefined type or locally (Na+K)-SO_4^{2-} while the water collected on the influence of mine area, shows a (Na+K)-Cl^- water type to undefined one, according to Piper's classification. There is no significant variation between the water collected on the raining and dried period (Fig. 3).

The hydrochemical processes that control chemistry in the study area could be expressed by the contribution of major ions to the water mineralization (expressed through the EC). However, the water has lower mineralization and the correlation found between EC and major ions are lower (R2: EC-SO_4^{2-} = 0.2182; EC-Mg = 0.0311; EC-Cl- = 0.0732; Na-Cl = 0.0732), otherwise the bicarbonate ion appears with a better correlation (R2: EC-HCO3 = 0.7001; EC-Ca = 0.8893; EC-Na = 0.7652), suggesting the influence of water-rock interaction processes, including weathering of minerals, with release of alkaline metals and production of alkalinity. Particularly on surface water, these correlations seem to corroborate higher geological and agricultural activity contributions.

Most water samples are neutral (pH ranges from 5.5 to 7.4) and showing low metal content (EC = 22-264 µS/cm; TDS = 4-157 mg/L). The spatial geochemical variability indicates that the water collected under the influence of mine activities tend to present the highest EC and TDS values, and HCO3-, K, Ca, Mg, Cd, Co, Cu, Fe, Mn, Ni, Pb, Sr, and As contents. However, there is no significant variation on water composition between raining and dry period.

The water sample Rb5, receiving water mine drainage, is the most mineralized water and contains the highest contents of Fe, Mn, Cd, Sr and As (Table 1). The highest Fe (up to 20.1 mg/L) and Mn (2.9 mg/L) contents are supported by the occurrence of yellow-reddish precipitates (Fig. 1c, d).

The maximum contents of As, Th and U in groundwater are higher than water from the open pit (Table 1), probably due to pH-Eh conditions. In the area, there is an elevated U and As baseline in groundwater and surface water. Regional uranium mobilization is sufficient to produce water U-enrichment, which is promoted by the weathering of sulphide-ore deposits and consequent U concentration into fractures around ore deposits that might act as preferential conduits for groundwater flow and chemical weathering.

Some water samples are contaminated with Cd, Cr, Cu, Fe, Mn, As and U and

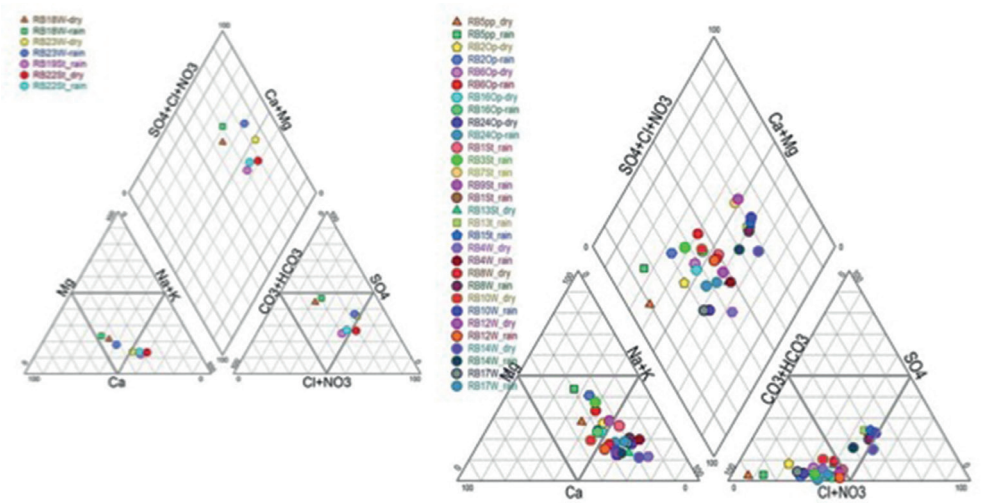

Figure 3 *Hydrochemistry classification (Piper diagram) of the water from the Ribeira de Bôco area: a. water samples located outside mine influence; b. water samples in the mine influence.*

Table 1 Minimum and maximum values obtained in the water from Ribeira do Bôco area.

	EC	Fe	Mn	Cd	Co	Cr	Cu	Ni	Pb	Sr	Zn	As	Th	U
	(µS/cm)	mg/L		µg/L										
Open pit	35-103	0.01-0.22	0.01-0.08	2.7-26.0	nd - 11.8	14.9-47.3	nd - 13.1	nd - 13.0	3.3-14.8	15.3-27.0	nd - 23.3	28.5-48.6	11.2-31.5	nd - 60.0
Rb5 (mine drainage)	248-264	15.4-20.1	1.5-2.9	44.3-79.6	4.7-11.4	21.8-37.5	nd - 10.5	nd - 10.5	6.8-17.4	79.2-80.2	nd - 22.8	74.7-76.6	30.7-23.9	31.2-54.2
Surface water	23-103	nd -0.21	0.01-0.08	6.6-28.8	nd - 11.8	22.2-54.0	nd - 13.5	nd - 16.2	9.5-16.6	13.3-40.9	nd - 178.0	29.2-54.4	14.1-31.7	23.3-89.2
Groundwater	22-162	nd - 1.16	0.01-0.22	6.3-37.2	nd - 12.2	21.9-51.9	nd - 12.3	nd - 13.5	5.7-18.3	5.9-52.8	nd - 41.6	24.9-54.5	11.1-32.4	nd - 83.3

should not be used for human consumption or in agricultural activities, considering water framework referenced values (Portuguese Decree, 1998; 2017; World Human Organization, 2011).

Conclusions

Mining regions constitute an important challenge in the management of water resources since its impacts could be an environmental risk and human health concern.

Portugal has important resources of groundwater that may be strategic to face the expected dry years to come. Furthermore, regularly monitoring and evaluating groundwater quality is needed for integrated management and policy making.

In the surveyed area, the baseline threshold of some potentially toxic elements is considerably high, in which concerns to groundwater and surface water. The natural geogenic conditions (geological setting and local geology) and mining activities are the main control on the mobility of potentially toxic elements in the groundwater-surface water systems, particularly in this post-mining affected area.

Development of methods to establish the location of contaminated groundwater entry to surface water environments, and the potential effects on ecosystems, is crucial to develop both site-specific and general conceptual models of uranium behaviour and potential toxicity in affected surface and groundwater environments, which will be a support to the application of adequate preventive and monitoring methodologies in post-mining contexts.

Acknowledgements

The authors thank FCT – Fundação para a Ciência e a Tecnologia, I.P., through the project's reference UIDB/04683/2020, UIDP/04683/2020.

References

Antunes IMHR, Santos ACT, Valente TMF, Albuquerque MTD (2020). Spatial mobility of U and Th in a U-enriched area (Central Portugal). Appl Sci 10, 7866.

Babayan G, Sakoyan A, Sahakyan G (2019) Drinking water quality and health risk analysis in the mining impact zone, Armenia. Sust Wat Res Manag 5, 1877-1886.

Bird KS, Navarre-Sitchler A, Singha K (2020) Hydrogeological controls of arsenic and uranium dissolution into groundwater of the Pine Ridge Reservation, South Dakota. Appl Geoch 114, 104522

Byrne P, Fuller CC, Naftz DL, Runkel RL, Lehto NJ, Dam WL (2021) Transport and speciation of uranium in groundwater-surface water systems impacted by legacy milling operations. Sci Tot Environ 751, 143314

Cameron J (1982) Mineralogical Aspects and origin of the uranium in the vein Deposits of Portugal, IAEA, Vienna, Austria.

Carvalho FP (2014) The National Radioactivity Monitoring Program for the Regions of Uranium Mines and Uranium Legacy Sites in Portugal. Proc. Ear. Planet. Sci. 8, 33-37.

Dambacher JM, Brewer DT, Dennis DM, Macintyre M, Foale S (2007) Quantitative modelling of goldmine impacts on Lihir Island´s socioeconomic system and reef edge community. Environ Sci Technol 41, 555-562.

Farias P, Gallastehui G, Lodeiro FG, Marquinez J, Parra LLM, Catalán JRM, Macia GP, Fernandez LR (1987) Appontaciones al conocimiento de la lito.estratigrafia y estrutura de Galicia Central. IX Reunion de Geologia do Oeste Peninsular. Publ Mus Mineral Geol, Porto, Abs 1, 411-413.

Fernandes HM, Franklin MR (2001) Assessment of acid rock drainage pollutants release in the uranium mining site of Poços de Caldas – Brazil. J Environ Radioact 54, 5-25.

Flett L, McLeod CL, McCarthy JL, Shaulis BJ, Fain JJ, Krekeler MPS (2021) Monitoring uranium mine pollution on Native American Lands: Insights from tree bark particulate matter on

the Spokane Reservation, Washington, USA. Environ Res 194, 110619.

Jiang X, Lu WZ, Zhao HQ, Chen M (2015) Quantitative evaluation of mining geo-environmental quality in Northeast China: comprehensive index method and support vector machine models. Eart Sci 73, 7945-7965.

Mello K, Taniwaki RH, Paula FR, Valente RA, Randhir TO, Macedo DR, Leal CG, Rodrigues CB, Hughes RM (2020) Multiscale land use impacts on water quality: Assessment, planning, and future perspectives in Brazil. J Environ Man 270: 110879. https://doi.org/10.1016/j.jenvman.2020.110879.

Neiva AMR, Carvalho PCS, Antunes IMHR, Albuquerque MTD, Santos ACT, Cunha PP, Henriques SBA (2019). Assessment of metal and metalloid contamination in the waters and stream sediments around the abandoned uranium mine area from Mortórios; central Portugal. J Geoch Explor https://doi.org/10.1016/j.gexplo.2019.03.020

Pal S, Mandal I (2019) Impact of aggregate quarrying and crushing on socio-ecological components of Chottanagpur plateau fringe area of India. Enviorn Eart Sci 78, 661.

Portuguese Decree (1998). Decreto-Lei 236/98 – Legislação Portuguesa de Qualidade da água. Diário da República I-A, 1998, 3676-3722.

Portuguese Decree (2017). Legislação Portuguesa de Qualidade da água. Diário da República I-A, 2017, 5747-5765.

Satapathy DR, Salve PR, Kapatal YB (2009) Spatial distribution of metals in ground/surface waters in the Chandrapur district (Central India) and their plausible sources. Environ Geol 56: 1323-135.

Skierszkan EK, Dockrey JW, Mayer KU, Beckie RD (2020) Release of geogenic uranium and arsenic results in water-quality impacts in a subarctic permafrost region of granitic and metamorphic geology. J Geoch Explor 217, 106607

UNESCO (2019) The United Nations World Water Development Report 2019: Leaving No One behind. UNESCO, Paris. Available in: https://www.unwater.org/publication/world-water-development-report -2019/

Val AL, Bicudo EM, Bicudo DC, Pujoni DGF, Spilki FR, Nogueira IS, Hespanhol I, Cirilo JÁ, Tundisi JG, Val P, Hirata R, Feliciano SM, Azevedo SMFO, Crestana S, Ciminelli VST (2019) Water quality in Brazil. Water Quality in the Americas: Risk and opportunities. IANAS-IAP, Mexico City.

Winde F (2010) Uranium pollution of the Wonderfonteinspruit: uranium toxicity, regional background and mining-related sources of uranium pollution, SA. J Radiol 36, 239-256

World Human Organization (2011). Guidelines for drinking water quality. 4th Ed (Geneva). Available at http://Whqlibdoc.Who.int/publications/2011/9789241548151_eng.pdf

Refurbishment of Water Treatment Plant Borna-West – From Lab Over Pilot Scale to Operation Plant Modification

Tim Aubel[1], Falk Thürigen[1], Roland Mayer[1], Andre Hertzsch[2]

[1]*G.E.O.S. Ingenieurgesellschaft mbH, Schwarze Kiefern 2, 09633 Halsbrücke, Germany, t.aubel@geosfreiberg.de*

[2]*Lausitzer und Mitteldeutsche Bergbau-Verwaltungsgesellschaft mbH, Walter-Koehn-Straße 2, 04356 Leipzig, Germany*

Abstract

In this paper the refurbishment of the water treatment plant Borna-West in Germany is presented.

Experimental resulting from lab tests and onsite pilot testing over a period of several months combined with the consideration for other necessary changes in plant operation. While ongoing plant operation the integration of an additional process step and a refurbishment of the plant was achieved.

Keywords: Iron Removal, Removal of Hydrogen Carbonate, Active Water Treatment, Refurbishment, Lab Test, Pilot Test, Full Scale Plant

Introduction

In the lignite mining areas of Central Germany and Lusatia the regional water balance is heavily changed by the past and present mining industry. Through the groundwater rerise significant amounts of iron and sulfate enter the receiving water bodies. For the protection of the environment several water treatment plants are in operation to remove the iron.

Initial position

The water treatment plant Borna-West, which is in operation since 2007, is a replacement of a simple pumping station. The operation of the pumping station was necessary to prevent a national road from being flooded. As the iron contamination in the receiving water bodies was and is rising a water treatment plant had to be installed to protect the river Pleiße.

Borna West has a capacity of 65 m^3/h and is processing a classical Low-Density-Sludge (LDS)-treatment-scheme; by pH-adjustment with lime, parallel aeration, flocculation, and sedimentation. The water to be treated is a mix of rebounding groundwater, dump seepage water and surface water with an iron concentration between 100 and 300 mg/L (mainly iron(II)) and a total inorganic carbon concentration (TIC) between 80 and 90 mg/L.

This high level of TIC, which derives from hydrogen carbonate, leads to an unnecessary consumption of lime and to an increased production of sludge, which has to be disposed.

Lab tests

Analysis of the original sludge composition of the treatment plant led to the conclusion, that the large volume as well as the low iron content of the sludge is caused by high amounts of total inorganic carbon (mainly free carbonic acid) in the raw water.

As shown in Table 1, most iron is present as iron(II) and requires an oxidation step to be removed as iron hydroxide.

Therefore, several laboratory tests with and without aeration step were carried out before adjusting the pH-value with lime and aeration for iron oxidation.

The introduction of the aeration stage resulted in a significant change in the lime content of the precipitated sludge, as shown in Table 2.

Table 1 exemplary raw water composition (excerpts).

Parameter	Dimension	Value
pH		5.7
conductivity	µS/cm	3250
sulfate	mg/L	2200
iron (total)	mg/L	250
ferrous iron	mg/L	246
ferric iron (calculated)	mg/L	4
total inorganic carbon (TIC)	mg/L	69

Table 2 sludge composition (lab tests/excerpts).

Parameter		Sludge from water without additional pre-aeration step	Sludge from water with additional pre-aeration step
iron	%	20.1	36.1
calcite	%	32.2	7.2
dolomite	%	9.7	1.6
lime total	%	**41.9**	**8.8**

Based on the results of sludge composition, sludge volume and dewatering behaviour, calculations were made that predicted a 20% reduction of the annual sludge mass (for disposal) and a 40% reduction in annual lime consumption.

The joint conclusion from laboratory scale experiments and calculations were the basis for an on-site pilot test and the integration into ongoing plant operation.

Pilot test

For the pilot test several variants were reviewed and one preferred option was elaborated. It consisted of a separate concrete tank (volume 45 m^3) with an installed surface aerator. This additional treatment step was installed between the water collecting basin and the pH-adjustment/aeration step of the original treatment scheme. The integration was achieved through a bypass pipe in the treatment scheme and could handle the full flow of the treatment plant (60 – 70 m^3/h).

Figure 1 shows the tank for the additional pre-treatment step and the surface aerator in operation.

The pre-treatment step was running over a period of several months and was carefully monitored by periodic sampling routines and measuring campaigns.

In figure 2 a typical drop in the TIC-concentration after starting the surface aerator is presented.

Figure 1 View on the pre-aeration tank (left side) and the surface aerator in operation (right side).

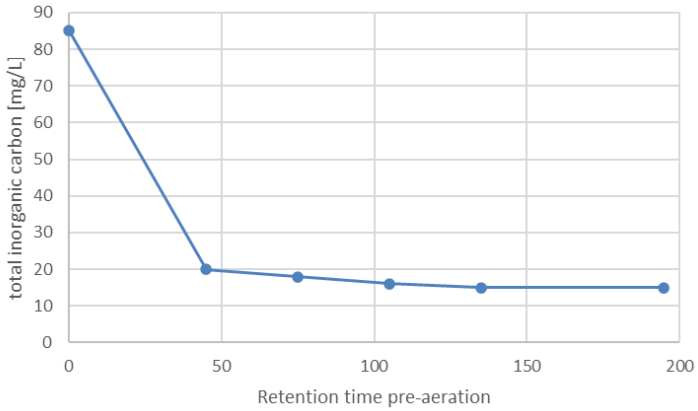

Figure 2 TIC-concentration depending on retention time pre-aeration.

The graph showed that a retention time of 40 minutes in the pre-aeration step is sufficient to reduce the TIC-concentration by 75%.

Before and after the pilot period the sludge composition in the sludge storage tank was analysed and showed substantial differences (Table 3).

Again, the pre-aeration led to a substantial composition change of the sludge (higher iron concentration, substantial lower lime concentration). Sulfate removal is not a target parameter of the water treatment plant. Depending on the fluctuating composition of the raw water, the sulfate concentration is at the limit of the gypsum equilibrium, therefore sulfate is sometimes precipitated as gypsum.

Compared to table 2 the lime concentration of both pilot test sludges was higher than in the lab tests. This is due to the fact that the adjustment of the pH-value in the water treatment plant is not working in an optimised way.

The lime dosing prior to the currently ongoing refurbishment of the plant is regulated by measuring the pH in the pH adjustment stage and in the discharge pumping station. These two values are combined and regulate the speed of the solid lime dosing.

If the operating parameters (flow rate of 65 m^3/h) are put in relation to the residence time in the sedimentation tank (10 h in continuous operation), there is an enormous time delay, reinforced by the fact that the plant does not run in continuous operation for lack of water. Therefore, the lime dosing mainly works in overdosing mode.

The predictions of the laboratory tests - a 20% reduction in the annual sludge mass to be disposed as well as a 40% reduction in the annual lime consumption - could be confirmed.

As the concrete tank of the pilot test was not winter proof, the to-be-treated water amount is increasingly reduced, the problems

Table 3 sludge composition (pilot test/excerpts).

Parameter		Produced sludge without additional pre-aeration step	Produced Sludge with additional pre-aeration step
iron	%	21.0	34.8
sulfate	%	2.0	1.53
calcite	%	58.93	20.78
dolomite	%	4.13	4.85
lime total	%	**63.06**	**25.63**

of the pH adjustment and several other needed modifications led to the decision, that a refurbishment of the water treatment plant is necessary.

Necessary changes in plant operation mode

During the planning process a variant consideration was done, taking into account the following specifications:

- flexibilization of plant flow rate → adapted to incidental water volume
- avoidance of discontinuous operation
- permanent integration of the pre-aeration step
- optimisation of pH-adjustment/lime dosing
- optimisation of flocculation
- modernisation of the process control system
- possibility of dealing with heavy rain fall events
- continued use of components where possible

Refurbishment

The results of the variant consideration and the planning process of the preferred option are summarized in table 4.

The heart of the refurbished water treatment plant is the new 3-chamber-concrete basin, in which the pre-aeration, the pH-adjustment/lime dosing with parallel aeration for iron oxidation and the flocculation are combined in three sub-basins in sequence (figure 3).

The challenge of the refurbishment is that all construction work has to be carried out in a very limited space while the plant is in operation.

The new 3-chamber basin is constructed between lime silo, old pH-adjustment and pumping station 2. All new piping is constructed until the final meter and all new control circuits will be prepared.

Finally, on day x, all new piping is connected, the new process control system is installed, and the new process has to start up. All this work has to be carried out within a very tight time frame, as it depends on weather conditions and there is only a limited time window of one to a maximum of five days of plant shutdown due to the limited water storage capacity in the retention basin.

Conclusions

The water treatment plant Borna-West is a very good example of how a theoretical data evaluation followed by intensive laboratory tests and verification in a pilot test on site can lead to a planning process that is very well validated with real process data.

The refurbished water treatment plant will provide significant cost savings due to reduced lime consumption and sludge

Table 4 *Results of planning process.*

Original status water treatment plant Borna-West	Refurbished water treatment plant Borna-West
fixed flow rate (65 m^3/h)	adjustable flow rate (10-65 m^3/h)
no TIC removal	TIC removal
lime dosing regulated by two pH probes (one with > 10h delay)	lime dosing regulated by two pH probes in two subsequent reaction tanks
dosing of flocculant directly in pipe to sedimentation tank	separate flocculation tank with slow stirrer
only 5-6 h operation time per day (start-stop, start-stop)	adjustable flow rate for a quasi-continuous operation
process control system with limited fault/alarm messages	modern process control system
one raw water pipe for normal operation/heavy rain fall event	separated raw water pipes for normal operation/heavy rain fall event (different pipe diameters)

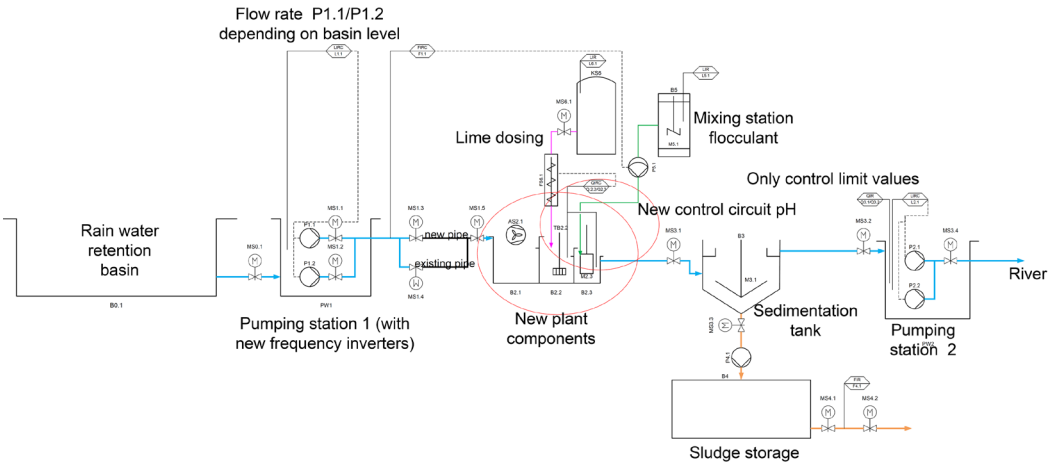

Figure 3 New flow sheet of water treatment plant Borna-West.

volume, will discharge better water quality into the river, and will be much more flexible to handle different volumes of water generated.

Acknowledgements

The authors thank Dr. Janneck, Dr. Glombitza and all other involved persons at G.E.O.S. for their contributions especially during lab/pilot tests, LMBV for the readiness to use financial resources and their support through all phases and the operators of the plant for their permanent willingness to implement ideas on site and support the experiments.

References

Janneck, Eberhard; Glombitza, Franz; Rolland, Wolfgang: "Reduction in lime hydrate consumption for pit water purification by physical removal of free carbonic acid.", World of Mining – Surface & Underground 60 (2008) No. 6

Looking Deeper: Key Considerations for Planning Mining Hydrogeology Investigations using Deep Boreholes

Ed Austin[1], Grace Yungwirth[2], Michal Dobr[3], Sofia Nazaruk[4]

[1]*Golder Associates, Citibase Edinburgh Gyleview, Gyleview House, 3 Redheughs Rigg, Edinburgh West Office Park, South Gyle, Edinburgh, EH12 9DQ, UK, Ed_Austin@golder.com*

[2]*Golder Associates, 20 Eastbourne Terrace London W2 6LG, UK, GYungwirth@golder.com*

[3]*Golder Associates, 2920 Virtual Way #200, Vancouver, BC V5M 0C4, Canada, MDobr@golder.com*

[4]*Golder Associates, Attenborough House, Browns Lane Business Park, Stanton-on-the-Wolds, Nottinghamshire, NG12 5BL, UK, SNazaruk@golder.com*

Abstract

Hydrogeological investigations of the deep subsurface are becoming an integral part of mine design and development alongside the geological, geophysical, and geotechnical investigation programmes. Data obtained from these site and depth specific investigations improve hydrogeological characterisation, resulting in reduced project risk and uncertainty.

Deep hydrogeological investigations using deep boreholes (>500 m depth) require specialised planning, services and equipment, and testing procedures. This paper aims to present key considerations when planning and executing deep borehole-based hydrogeology investigations, drawing on experience across three different continents, to aid practitioners planning for similar programmes on mining projects.

Keywords: Deep Mining, Hydrogeology Testing, Packer Testing

Introduction

The majority of underground mining developments are positioned below the water table and require hydrogeological characterisation to support studies of feasibility, mine design planning and assess impacts of the mine development on the environment. In most cases, the hydrogeological characterisation below 500 m depth will be aided by investigations using small diameter drillholes. Given the cost of drilling, hydrogeological investigations are often conducted in multi-purpose boreholes which are drilled for the primary purpose of collecting geological and geotechnical data. The borehole depth, diameter, and selected testing method poses challenges that require specialised resources. This paper highlights some of the key considerations in relation to hydrogeological investigations in deep boreholes.

Transmissivity and Beyond

The primary aim of most deep mining hydrogeological investigation is characterisation of hydraulic properties of the hydrostratigraphic units present in the area of the mine development. Improving the quality of the available data allows better understanding of potential mine inflows and hydraulic gradients and reduces the risk and uncertainty associated with the basis of mine design. Information on the nature of the flow regime and groundwater chemistry also provides support to the construction design including grouting, stability of the underground workings, and trade-off studies.

The data collected as part of these investigations are also required for costing studies, baseline definitions and environmental assessments, and water disposal and water treatment studies. Improving the data

quality in mining hydrogeology investigations in deep boreholes should allow improved confidence and a wider application to studies in support of the mining development.

Perils of the Deep –Downhole Environment and Equipment Selection

Challenges of deep borehole testing are generally similar to those that can occur with shallower testing, but the risks are magnified by the depth. Common challenges are related to the potential variability of conditions along the depth of the borehole so an array of test stages should be considered.

Technical challenges stem from the selection of the suitable equipment to allow collection of defensible data from the deep intervals. At deeper depths, hydraulic testing equipment becomes more feasible (and safer) to use over pneumatic equipment because it does not have to overcome the hydrostatic pressure at depth prior to inflation. This approach however means that the methods to apply and deliver the inflation pressure and to create a pressure differential for testing are often shared and requires more complicated equipment that employs a series of mechanical and or pressure actuated valves to allow and maintain packer inflation. Equipment for deep hydrogeological testing can therefore be quite different in their design and operation compared to typical gas operated borehole testing systems generally used for shallow hydrogeological testing with which operators may be more familiar.

For most mine hydrogeology investigations real-time data monitoring from the test interval is not feasible, and autonomous pressure data collection is utilised instead. Inability to directly observe the pressure response during the test introduces risks around the test progression (e.g., the test may not be progressed long enough to observe static conditions), as well as potential for loss of data in the event of logger failure. To mitigate these risks, real-time data are often collected, simultaneously with the downhole memory gauge, from the upper part of the water column inside the test tubing (above the test interval), however the utility of this approach is limited by the equipment and testing methodology used. This secondary shallower real-time data monitoring cannot be easily implemented within a sealed or pressurised system and will not reflect the formation response if the test interval is isolated using a down hole shut-in valve. Testing using a downhole shut-in valve that isolates the test interval from the test tubing is of particular value in low permeability formations which are commonly encountered in deep investigations.

Planning - the Key Stage of Investigation

Detailed planning of the hydrogeological investigation can and should occur during all stages of the ground investigation programme. Input to planning prior to the programme commencing is of key importance. The planning stage should include input from specialists to ensure that proper testing methodology and equipment is selected. This will avoid informal design based on existing familiarity with a general technique or type of equipment used previously which may not be fully appropriate for the current planned investigation.

The application of generic testing designs can be inappropriate for all types of investigations, however deep investigations in hard rock mining developments tend to be viewed generically as low flow, with a low risk of fracture flow/ enhanced zones of permeability and therefore planning activities may not consider potential variability in downhole conditions.

Investigations for mine development in deep sedimentary environments like coal and salt or in "high flow" environments like karst, fault zones or zones of enhanced permeability inherently have water placed higher in the risk view of project stakeholders. These projects may engage larger drilling rigs, and well control and mud engineers, with an expectation to demonstrate and quantify higher flow conditions and challenges may arise with constraints around fluids and stability. The stakeholders on these projects generally have background that reflects experience based on hydrocarbon exploration, not groundwater. These experiences can be very helpful and knowledge exchange between the disciplines

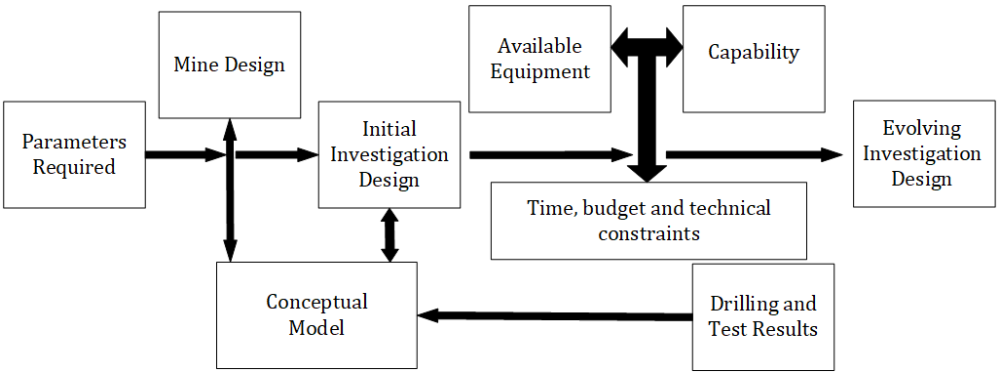

Figure 1 *Considerations at planning stage.*

should be encouraged, however there are some unique considerations related to test work in deep multi-purpose mining boreholes and oil and gas investigations. It should be noted that although some equipment manufacturers supply both sectors there is less crossover within professional practitioners. Some mining practitioners have experience in the nuclear repository sector; these experiences are also very valuable.

The considerations at the first phase of planning are inter-related and can be summarised in a flow chart (fig. 1).

Designing and Planning Deep Hydrogeologic Investigations with Constraints

The design of ground investigations will naturally consider the hydrogeological conceptual model, known ground conditions, the proposed mine design, and the design parameters that the investigation is required to obtain. It is rare for a mining hydrogeological investigation to be considered the primary aim of a deep drilling programme. Hydrogeological investigations will be in most cases viewed as an add-on to the geological and geotechnical investigations. Time required for hydrogeological tests during drilling is seen as drilling downtime because the borehole is not being advanced during these periods so hydrogeological testing activities are often constrained by the need to minimise drill rig down time and to avoid borehole destabilisation or collapse during testing activities.

Testing challenges can be considered in two broad categories: budgetary and time related; and technical and capability related.

An example of budgetary constraints may be a limit to the amount of time the exploration program can set aside for hydrogeological data collection or similarly the amount of time that is available to meet a project milestone. An example of a technical constraint may be the permitted volume of water that can be discharged or a limit to the local workforce capability. Hydrogeological investigations in deep boreholes uses complex equipment and should be supervised by an experienced testing engineer and supported by a drilling crew to convey the tool and support the testing. Complex programmes may require simplification, supervision and training. Ultimately the majority of ways to address issues related to technical or capability constraints have budgetary and time implications. A summary of key testing considerations are listed here:

Budgetary or time related considerations:

1. Equipment outlay and level of expense afforded to specialised testing and monitoring equipment including narrow diameter equipment suitable for use at the pressures expected in the deep subsurface and automated data collection equipment. The nature of deep drilling and conveying specialised equipment to depth also increases the risk of tool loss which can add cost to the programme.
2. The cost of drill rig down time needed to conduct the hydrogeological testing

may be constrained. Drilling contracts often included charges related to testing time and time for testing also means the advancement will be delayed. There are often set associated costs related to length of drilling programmes, e.g., personnel fees, camp charges, fuel.

3. Hydrogeological testing adds time to a geological/geotechnical drilling programme. Extension of the drilling programme to accommodate hydrogeological testing activities may have to be balanced with the effect on project milestones.
4. Scheduled time for hydrogeological tests may be constrained by factors such as the need to circulate fluid to stabilise the unsupported borehole (or control gas in the case of deep coal deposits). When estimating the duration of the individual tests, it is important to consider all of the following: time to flush the drilling fluids from the borehole prior to testing; time to pull rods and convey the equipment to position in the borehole (time increases with depth); time required to observe the test response (this may be long in low permeability formations or may have to include an allowance if real time instrumentation is not available); time for proper test preparation and potential repeat stages or extensions. Inadequate borehole preparation and tests being terminated too early due to time pressures are factors that can have a direct effect on test reliability and data quality.

Technical or capability related:

1. Consideration of drilling fluids: Drilling fluids containing muds, other additives, or brine may be required during drilling to maintain borehole stability, control gasses or to avoid dissolution of the formation around the borehole (in the case of salts/evaporites). These fluids can have an effect on observed hydraulic response of the formation if they clog the pores and features in the vicinity of the borehole. Dense fluids can also have an effect on interpretation of the test results if the analysis is done assuming the pressure responses were those of pure water. Ideally drilling fluids should be flushed from the borehole prior to testing activities however this may not be practical.
2. Drilling grease and rod vibration: Large amounts of drilling grease are often used to reduce drill rod vibration in areas where there is a deep water table. This should be noted during drilling activities as it can have an effect on hydrogeologic testing.
3. Test design: If it is suspected that drilling fluids or drilling grease have locally lowered the permeability around the borehole or clogged the borehole wall, a testing methodology that allows fluid to move into the borehole from the formation (i.e., rising head or constant rate pumping test versus falling head or injection testing) should be selected. Fluid moving from the formation into the borehole could be expected to be less influenced by these effects. This type of testing is challenging in narrow diameter drillholes and where groundwater levels are deep and specialised equipment (and capacity to operate it) may be required. Additionally, there may be practical or permitted limits on the volume of fluids that can be abstracted or discharged.
4. Need for high pressure equipment: Some inflatable packer systems for deep well testing require higher pressures to be delivered to the system to operate it and an associated higher degree of control and measurement. These systems require high pressure pumps, gauges, and controls and therefore additional training in the use of this equipment. There may be a desire for wireline deployed (versus tubing conveyed) investigation equipment to speed up the testing time; but this can limit the equipment selection and maximum depth of deployment.
5. Low permeability conditions: Testing in low permeability conditions can be complicated as formation responses take longer to observe. The use of a down hole shut-in valve is recommended when testing in lower permeability formations to accelerate the observed response. Downhole valves can be difficult to operate successfully, and leakage of equipment valves can be misinterpreted as formation response.

6. Support and direction of inexperienced mine site staff and contractors: Most hydrogeological investigations involve the use of drilling contractors and inexperienced site staff to support the investigation therefore direction, supervision, and training will be required. Most contractors will have previous experience, sometimes this experience will be based on a standard method and/or operation guided by the manufacturer. Whilst this is useful, adherence to the investigation design will need to be checked as it is common for a habit to be developed of going through the motions of a test without paying attention to the test data being collected resulting in poor investigation outcomes.

Additional Challenges and Considerations

The above discussion confirms that collecting hydrogeological data from deep boreholes is challenging. The challenges vary with each specific investigation but there are some common aspects to most deep investigations; these include the following: borehole preparation requirements; advantages of planning testing activities over day shift; focusing on local/relevant variations to hydrogeologic condition over longer borehole lengths; test stages and optimisation; and test analysis.

Borehole Preparation

Borehole preparation prior to hydrogeologic testing is key to the success of the testing activities. Flushing of the borehole to reduce the influence of drilling muds, fluids and additives is required. This must be done in conjunction and discussed in advance with the drilling contractor, mud engineer and client representative. In some cases, there may be a trade-off between borehole cleaning and borehole stability. Also, the flushing is often inadequate, being shortened to save time and may unduly influence the test results. The risk can be managed by good record keeping and monitoring of volumes, density and viscosity of drilling and testing fluids. In a similar manner, static water levels corresponding to each test interval are required, but the period of time required to obtain the static levels is neglected.

The Day Shift Advantage

Most drilling investigations will make use of day and night shift work. The quality of work is often best during the day shift. As such there are benefits to timing the more active stages of the hydrogeological test to be carried out during the day shift and using night shift for less active parts of the test sequence like recovery stages.

Focus on Local/Relevant Hydrogeologic Variations

Many underground mine developments can involve boreholes of more than 1,000 m and some of these will intercept long sections of formation that would appear to be homogenous. As such there can be tendency to use test intervals at the scale of hundreds of metres, but this approach can overlook and mask local variations in hydraulic properties.

Test Stages and Optimisations

Testing should be progressed through several individual test stages to be flexible and adaptable to conditions encountered and to optimise data collection. An example of adaptation is to observe the response to initial test stages and extend the recovery time so that equilibrium or pressure recovery is achieved and recorded during testing. As described earlier, the hydrogeological investigation is often planned to be "piggybacking" on the main drilling investigation resulting in a pressure to reduce the testing time. However, it is important to run each test to completion as the ability to repeat test work is often limited. Each test stage should be considered carefully to inform the next stage and justify the approach and time spent on the test. For instance, a response from an initial falling head test (FHT) indicative of a low permeability would suggest that a further stage of injection or production to/from the formation is unlikely to be sustainable and would not produce an analysable pressure response. In this case, re-apportioning testing time to allow full recovery of the FHT to determine static levels and/or a test repeat to confirm the response may be more valuable use of testing time.

Test progression decisions should assess each test stage response prior to progression to the next stage. Whilst following a rulebook

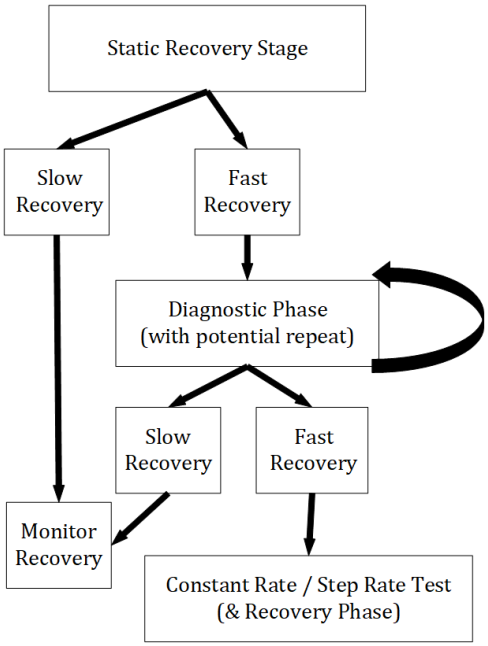

Figure 2 *Example of Flow Sheet Guidance for Test Stages.*

can be counter-productive, the use of decision flow sheets (a simplified example is shown in fig. 2) can provide a useful basis of support as well as a communication tool between designers, practitioners, and operators.

Test Analysis

The use of specialised software for hydrogeological test analyses in hydrogeology investigations that have been well designed and correctly executed can provide more information than just transmissivity and pore pressures. Additional information on the nature of flow and boundary effects can also be obtained. Diagnosis of the flow condition is based on diagnostic curves (Gringarten, 2008), similar to pumping test diagnostic curves (Kruseman & de Ridder. 2000). Diagnostic tools can use "skins" (Pickens *et al.*, 1987), the deconvolution of pressure data and the pressure derivative to interpret all types of test which can be considered individually or as multiples via superposition. An example of a software for hydrogeological data analysis is Golder's proprietary curve fitting Hydrobench software that allows comparison of results from different test stages.

Conclusions

Hydrogeological investigations using deep boreholes involve substantial challenges. These are primarily the result of complexities that occur due to the unique borehole drilling methods, presence of low permeability formations, and the specialised testing equipment that is required for testing at depth. The challenges can be overcome using specialist resource to support test planning and supervision, provide training and guidance, and carry out data analysis. This paper has discussed some of the key factors for consideration by mining hydrogeology practitioners when designing hydrogeologic investigations in deep, multi-purpose mining boreholes.

References

Gringarten AC (2008) From Straight Lines to Deconvolution: The Evolution of the State of the Art in Well Test Analysis. February 2008 SPE Reservoir Evaluation & Engineering 11 (1):41-62

Kruseman GP, de Ridder NA (2000) Analysis and Evaluation of Pumping Test Data 2nd Edition. Publication 47, ILRI, The Netherlands

Pickens JF, Grisak GE, Avis JD, Belanger DW, Thury M (1987) Analysis and Interpretation of Borehole Hydraulic Tests in Deep Boreholes: Principles, Model Development, and Applications. Water Resources Research Vol 23 No 7 Pages 1341-1375 July 1987

Methods of Environmental Bioindication of Rivers Prone to Technogenic Salinization

M.A. Baklanov[1], P.B. Mikheev[1,2], O.I. Mikheeva[3], T.A. Sheina[1], E.A. Khayrulina[1]

[1]*Federal State Autonomous Educational Institution of Higher Education "Perm State National Research University", Perm;*

[2]*Khabarovsk Branch of the Federal State Budget Scientific Institution "Russian Federal Research Institute of Fisheries and Oceanography" ("KhabarovskNIRO"), Khabarovsk;*

[3]*Perm Branch of the Federal State Budget Scientific Institution "Russian Federal Research Institute of Fisheries and Oceanography" ("PermNIRO"), Perm*

Abstract

Indication of technogenic salinization in freshwater water bodies is an important tool for the detection of environmental degradation. Studies of the chemical composition of rivers of the Kama River basin prone to salinization were supplemented by an analysis of cyanobacterial-algal cenoses and communities of zooplankton macrozoobenthos and fish. In the most saline sections of the rivers, halophilic and euryhaline species of diatoms, zooplankton and zoobenthos dominate; fish are not found. Moreover, we have tested the parasitological and haematological analysis of fish for the possibility of using it in bioindication of lower and intermediate levels of salinization. The results show the possibility of using new markers of salinity found by means of parasitological and haematological analyses. The development and application of new methods of bioindication of technogenic salinization of rivers, along with the traditional chemical and biological techniques, are important for the assessment of the impact of anthropogenic stress factors on the biota.

Keywords: Bioindication, Technogenic Salinization, Fish Parasites, Fish Blood.

Introduction

Salinization of boreal freshwater water bodies is a serious problem due to the significant transformation of ecosystems in places of formation of contrasting technogenic geochemical anomalies with an increased content of water-soluble salts, as well as at a considerable distance from salinization sources. In various parts of the world, river ecosystems prone to anthropogenic salinization are characterized by degradation of biodiversity at all trophic levels, which leads to biotic imbalances and negative socio-economic consequences (Cañedo-Argüelles et al., 2013). Compared with other pollutants, salt is one of the least studied technogenic stress factors affecting boreal freshwater ecosystems (Vörösmarty et al., 2010; Bernhardt et al., 2017). At the same time, methods for environmental assessment of rivers using biological markers are an important tool in the indication of anthropogenic salinization. There are several systems for bioindication of salinization in freshwater ecosystems based on the assessment of structure of diatoms, zooplankton, and macrozoobenthos communities. Under technogenic salinization of rivers, the species composition of biotic components changes from freshwater type to salt-tolerant type with a decrease in the overall level of biodiversity.

Findings

Russia is one of the world leaders in the production of potash and magnesium salts (Potash facts 2021). Extraction takes place within the Verkhnekamskoe Deposit of Potassium and Magnesium Salts (VDPMS, Perm Krai), the side effect of which is technogenic salinization of the environment. VDPMS contains about 30% of the world reserves of potash salts. Mining began in the 1930s, and during the period of the deposit's operation, about 270 million tons

of halite waste and 30 million m^3 of clay-salt sludge have be stored on the surface (Khayrulina et al., 2018). In the areas affected by salt tailings piles, mineralization of natural water bodies reaches 50 g/L, the content of chlorides increases to 9.0 g/L, sodium - up to 3.0 g/L, potassium - up to 1 g/L; the content of calcium, magnesium, sulphates, as well as trace elements such as Mn, Pb, Sr, Rb, and Co increases (Liu, Lekhov, 2012). On the territory of the VDPMS, many rivers are prone to technogenic salinization, the indication of which was carried out on the basis of the chemical composition analysis of the rivers.

Studies of the chemical composition of the rivers of the Kama River basin prone to salinization were supplemented by the analysis of algal flora, zooplankton, macrozoobenthos, and fish. The changes in algal flora, zooplankton, macrozoobenthos and ichthyofauna were revealed. Thus, within river sections with the highest salt load, the green alga *Enteromorpha intestinalis* appears, indicating chloride pollution, along with the diatom *Actinocyclus normanii*, a representative species of the algal flora of the Caspian Sea (Martynenko et al., 2017). We observed significant changes in zooplankton: during salinization, the disappearance of cladocerans and a decrease in the species diversity of rotifers and copepods were noted. The basis of planktonic zoocenoses of rivers prone to salinization is made up of halophilic species, in particular *Brachionus plicatilis*, typical of shallow brackish water bodies (Krainev, 2014). An indicator of negative reaction of macrozoobenthos to salinity was also found: in areas with salt load, its biodiversity decreased by 1.5-3.0 times (Baklanov et al., 2019). Bentocenoses in saline zones significantly differed in Shannon's index, Balushkina chironomid index, as well as in the position of halophilic and euryhaline species in the structure of dominance of benthic invertebrate communities. Ichthyological studies showed that water salinization radically affects fish population structure. There are no fish in the area of intense salinization. Short-term visits of eurybiontic fish species from the Kama Reservoir were recorded in different years in the lower reaches of rivers (Site 3 at Table 1), where they are attracted by the presence of food items (Baklanov et al., 2019).

Along with traditional methods of bioindication based on the analysis of species composition of algae and invertebrates, such methods of bioindication as parasitological and haematological analyses of fish were tested for the first time. Quantitative and qualitative characteristics of blood elements

Table 1 *Average values of various parameters of algal cenoses, zooplankton and zoobenthos communities, as well as ichthyofauna of three sections of the Volim River drainage basin (Perm Krai, Russia), differing in the degree of anthropogenic salinization.*

Ecosystem's element	Parameter	Site 1	Site 2	Site 3
Potamophytoplankton (Martynenko et al., 2017)	N, K cells / L	719	452	684
	B, mg/L	1.592	0.555	3.310
	Shannon index	4.15	2.59	3.47
Zooplankton (Krainev, 2014)	N, ind. / m^3	9380	200	2020
	B, mg / m^3	29.83	0.23	0.69
	Species number	32	4	12
Macrozoobenthos (Baklanov et al., 2019)	N, ind. / m^2	1856	30663	12541
	B, mg / m^2	7.73	44.15	15.34
	Shannon index	1.21	0.31	0.53
Fish (Baklanov et al., 2019)	Species number	1	No fish	7
Total dissolved solids, g/L		0.57	41.99	8.68

reflect the physiological state of the fish organism. Analysis of the parasitic load makes it possible to assess the state of many ecosystem components since parasites' life cycle linking to various biotic elements. It was found that fish living under conditions of technogenic salinization showed a high degree of parasitic infections and a number of haematological parameters, potentially indicating a decrease in immunity. Thus, according to the results of the pilot project carried out in 2020, the ruffe *Gymnocephalus cernua* of the Volim River, exposed to the influence of the BKRU-3 waste disposal facility of Uralkali PJSC, had high level of helminth infection and a high proportion of erythrocyte morphological abnormalities. We identified values of infection extensity and intensity and determined the number of parasite species, which is more than double the background values in fish inhabiting unpolluted environment, in the Gaiva River in particular (Mikheeva, Mikheev, 2014) (Table 2). Erythropenia and significant morphological changes in erythrocyte series were also found in fish, which indicates an environmental hazard (Fig.). We also noted an increase in the rate of erythropoiesis (a greater number of young forms of erythrocytes) and an increase in the content of progenitor cells and monocytes in white blood (Table 3). It appears to be an active adaptive reaction of the ruffe to a stress factor.

According to literary sources, in most cases, fish living in polluted conditions have high helminths infection rate and morphological abnormalities of blood elements (Khan and Thulin, 1991; Kuperman, 1992; Katalay and Parlak, 2004; Marcogliese, 2005). The main mechanism that determines the increase in the number of helminthiases and structural abnormalities of blood elements in fish under conditions of pollution is immunosuppression, which manifests itself under negative influence of stress factors (Dunier, 1996). On the other hand, a number of studies describe a decrease in the parasitic load on fish under pollution compared with

Table 2 *Parasite infection of various organs of the ruffe of the Volim and Gaiva Rivers.*

Localization	Volim River	Gaiva River
	Parasite (IE; PA; II)	
stomach	*Bunodera luciopercae* 23%; 1,3; 1-2	
	Camallanus truncatus 12%; 1; 1-1	
	Triaenophorus nodulosus 35%; 2.5; 1-4	
intestine	*Ichthyocotylurus platycephalus* 12%; 8.3; 2-18	
	Bunodera luciopercae 15%; 2.3; 2-3	
	Camallanus truncatus 4%; 2; 2-2	
	Triaenophorus nodulosus 27%; 4; 4-4	
urinary bladder	*I. platycephalus* 8%; 6; 1-11	
ureters	*I. platycephalus* 100%; 12.9; 2-26	*I. platycephalus* 65%; 18.1; 7-74
kidneys	*I. platycephalus* 77%; 7.6; 2-18	
eye vitreous body	*Diplostomum spathaceum* 12%; 1.7; 1-2	
	Tylodelphys clavata 38%; 1.9; 1-2	*T. clavata* 4%; 1,0; 1
	Posthodiplostomum clavata 35%; 1.8; 1-4	
	P. brevicaudatum 8%; 1.0; 1	*Rhipidocotyle campanula* 11%; 1; 1
eye lens	*Diplostomum spathaceum* 88%; 2.3; 1-6	*D. spathaceum* 50%; 2.3;2-3
	Tylodelphys clavata 23%; 2; 2-2	

Note: IE – infection extensity; PA - parasite abundance; II - infection intensity.

Table 3 Average values of the peripheral blood leukocytes ratio of the ruffe of the Volim and Gaiva Rivers.

Indicator		Volim River	Gaiva River
Progenitor cells	Relative value, %	9,7	5,9
	Absolute value, thousand/1 μL	9,56	7,62
Neutrophils	Relative value, %	2,4	2,4
	Absolute value, thousand/1 μL	2,43	3,05
Eosinophils	Relative value, %	1,0	0,2
	Absolute value, thousand/1 μL	0,95	0,31
Monocytes	Relative value, %	5,9	2,7
	Absolute value, thousand/1 μL	5,86	3,34
Lymphocytes	Relative value, %	81,0	88,8
	Absolute value, thousand/1 mcL	79,67	113,08

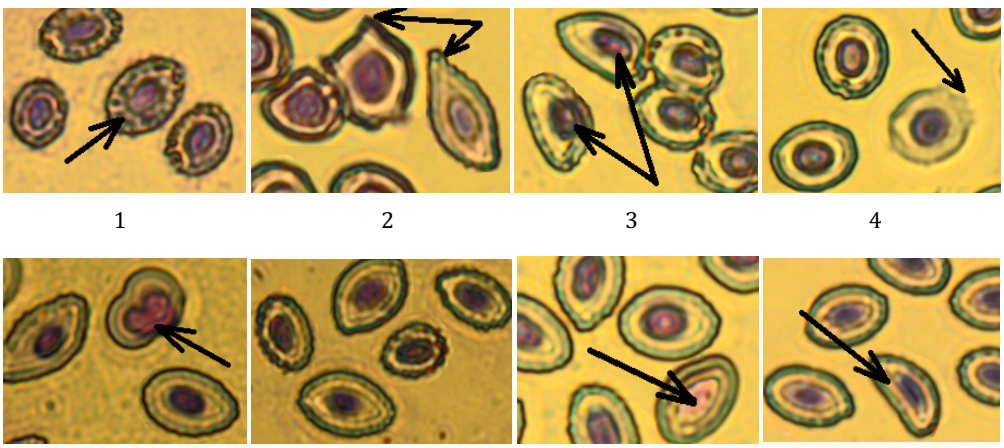

Fig. *Aberrant erythrocytes in ruffe of the Volim River prone to anthropogenic salinization: 1) cytoplasmic vacuolization, 2) poikilocytosis, 3) acentric location of the nucleus, 4) scalloped contour, 5) duplication of the nucleus, 6) anisocytosis, 7) chromatinolysis, 8) deformation of the nucleus.*

background data, which was determined by differentiated effect of pollutants on various types of parasites and by elimination of taxon-specific intermediate hosts sensitive to pollution (Blanar, 2009; Hanzelová et al., 2011). Since parasites are a connecting element of many components of biota, it is preferable to use an integrated approach to the study of the parasitological situation in water bodies prone to technogenic salinization. This requires an analysis of seasonal dynamics of the pollutant ions concentration in combination with studies of an abundance of intermediate hosts of fish parasites (Poulin, 1999; Marcogliese, 2005).

Conclusions

Examinations of the composition of algal flora, zooplankton, macrozoobenthos, ichthyofauna, indicators of infection and localization of parasites, as well as the characteristics of fish blood make it possible to indicate the level of salinity in rivers. Our results show the possibility of using new markers discovered by parasitological and hematological analyses. The development and application of new methods of bioindication along with the traditional analysis of the chemical composition of rivers is an important element in the analysis of the impact of anthropogenic stress factors on biota.

Acknowledgments

The studies were partly funded by the RF Ministry of Education, project # 2019-0858 Biogeochemical and geochemical studies of the landscapes against mineral deposits exploitation, development of new monitoring and forecasting methods for the environment.

References

Baklanov MA et al. (2019) Assessment of anthropogenic salinisation impact on the benthic invertebrates and fish in a small river – a tributary of the Kama Reservoir IOP Conf. Ser.: Earth Environ. Sci. 321 012060

Bernhardt ES, Rosi EJ, Gessner MO (2017) Synthetic chemicals as agents of global change. Front. Ecol. Environ. 15, 84–90. (doi:10.1002/fee.1450)

Blanar CA, Munkittrick KR, Houlahan J, Maclatchy DL, Marcogliese DJ (2009) Pollution and parasitism in aquatic animals: a meta-analysis of effect size. Aquatic toxicology (Amsterdam, Netherlands), 93(1), 18–28. https://doi.org/10.1016/j.aquatox.2009.03.002

Cañedo-Argüelles M, Kefford BJ, Piscart C, Prat N, Schäfer RB, Schulz CJ (2013) Salinisation of rivers: an urgent ecological issue. Environ Pollut.;173:157-67. doi: 10.1016/j.envpol.2012.10.011. Epub 2012 Nov 29. PMID: 23202646.

Dunier M (1996) Water pollution and immunosuppression of freshwater fish, Italian Journal of Zoology, 63:4, 303-309, DOI: 10.1080/11250009609356150

Hanzelová V, Oros M, Scholz T (2011) Pollution and diversity of fish parasites: Impact of pollution on the diversity of fish parasites in the Tisa River in Slovakia. Species Diversity and Extinction. 265-296.

Katalay S, Parlak H (2004) The effects of pollution on haematological parameters of black goby (Gobius niger L., 1758) in Foça and Aliağa Bays. EU J Fish Aquat Sci 21: 113–117

Khan RA, Thulin J (1991) Influence of pollution on parasites of aquatic animals. Adv Parasitol.;30:201-38. doi: 10.1016/s0065-308x(08)60309-7. PMID: 2069073.

Khayrulina EA, Khomich VS, Liskova MYu (2018) Environmental issues of potash deposit development. Bulletin of the Tula State University. Geosciences, (2), pp. 112-126. (In Russ.)

Krainev EYu (2014) Raspredelenie zooplanktona reki Yaivy i nekotorykh eyo pritokov [Zooplankton distribution in the river Yaiva and some of its tributaries] Rybokhozyaistvennye vodoyomy Rossii: fundamental'nye i prikladnye issledovaniya [Fishery reservoirs of Russia: fundamental and applied research] (Saint-Petersberg: GosNOIRH Publ) pp. 459–469

Kuperman BI (1992) Parasites as bioindicators of the pollution of water bodies. Parasitology. No.6, pp. 479-482. (In Russ.)

Liu Y, Lekhov AV (2012) Modeling the change in the filtration parameters of gypsum rocks during the filtration of brines // Geoecology. Engineering geology. Hydrogeology. Geocryology. No. 6. P. 551 - 559.

Marcogliese DJ (2005) Parasites of the superorganism: are they indicators of ecosystem health? Int. J. Parasitol. 35, 705–716.

Martynenko NA, Pozdeev IV, Baklanov MA (2017) Struktura al'gocenosov rek Permskogo kraya v usloviyakh antropogennogo zacoleniya otkhodami kalii'nogo proizvodstva [Algaecenoses structure of the Permskiy krai rivers under anthropogenic salinization of potassium production wastes] Vestnik Permskogo universiteta. Seriya: Biologia [*Bulletin of Perm University. Biology*] 3 pp. 347–354

Mikheeva, O. I., Mikheev, P. B. (2014) Preliminary data on the parasitofauna of fish in the Kama reservoir basin. Part 1, 2. Proceedings of the Samara Scientific Center of the Russian Academy of Sciences, 16 (5-1), 575-587.

Potash facts (2021, Jan 15) Retrieved from https://www.nrcan.gc.ca/science-data/science-research/earth-sciences/earth-sciences-resources/earth-sciences-federal-programs/potash-facts/20521.

Poulin R (1999) The functional importance of parasites in animal communities: Many roles at many levels? Int J Parasitol.;29:903–14.

Vörösmarty CJ, McIntyre PB, Gessner MO, Dudgeon D, Prusevich A, Green P, Glidden S, Bunn SE, Sullivan CA, Liermann CR, Davies PM (2010) Global threats to human water security and river biodiversity. Nature 467, 555–561. https://doi.org/10.1038/nature09440

Justification For Modification Of The NAG Test Method To Suit Varied Mining Waste Geochemical Characteristics On A Site-Specific Basis

Andrew Barnes[1], Steven Pearce[2], Diana Brookshaw[2], Mark Roberts[1], Seth Mueller[3]

[1]*Geochemic Ltd, Lower Race, Pontypool, NP4 5UH, Wales, United Kingdom, abarnes@geochemic.co.uk, mroberts@geochemic.co.uk*

[2]*Mine Environmental Management Ltd, Vale Street, Denbigh, Denbighshire, LL16 3AD, Wales, United Kingdom, spearce@memconsultants.co.uk, dbrookshaw@memconsultants.co.uk*

[5]*Boliden AB, Sweden, seth.mueller@boliden.com*

Abstract

The Net Acid Generation (NAG) test is generally carried out using a consistent method, irrespective of the site or the geochemical properties of material being tested. There are significant risks posed by utilising standard methods to assess processes which are inherently site specific like AMD. This can lead to misleading interpretations of results which is particularly true where the NAG liquor is being used to give an indication of elemental mobility during sulfide oxidative weathering. Examples include an average 3 pH unit increase between pre and post boiling, and greater than 60% reduction in nickel release to the NAG liquor.

Keywords: Net Acid Generation (NAG) Test, Hydrogen Peroxide Leach, Acid Mine Drainage

Introduction

Net acid generation (NAG) testing has been widely used by mine waste geochemists globally to aid in prediction of acid rock drainage and metals leaching (ARDML) since the mid 1990's. The test method allows the rapid determination of the acid generation potential through the use of hydrogen peroxide (H2O2) to rapidly oxidise sulfide minerals and release associated acidity. The oxidation process occurs in the same manner as would occur with oxygen as the primary oxidising agent albeit much more rapidly. The generated acidity in turn reacts with any rapidly available neutralising potential (carbonates and some silicates) allowing the determination of Net acidity through back titration. In combination with Acid Base Accounting (ABA) methods and other ARDML prediction techniques, the test can be a very effective tool to aid mine waste characterisation.

The concept, and ultimately the NAG method used today has been developed by a number of pioneer researchers over the past 40 years. These include; Sobek *et al* (1978), Finkelman & Giffin (1986), O'Shay *et al* (1990) and Miller *et al* (1997). The work culminated in the currently accepted 'quasi' standard as published by Smart *et al* (2002) in the AMIRA ARD test handbook.

The leachate generated during NAG testing can be analysed to give an indication of the potential mobility of contaminates from a waste material during weathering. Several authors have also suggested the use of NAG test leachate data as an aid to prediction of mine water discharge chemistry (Miller *et al*, 1997; Stewart *et al*, 2006; Sapsford *et al*, 2010; Barnes *et al* 2015). However, a number of recent studies have observed that the standard NAG testing methodology can greatly under or over predict the leachate pH (see Stewart *et al*, 2006; Charles *et al* 2015; Karlsson *et al* 2018) influencing the concentrations of dissolved trace elements (noting that the solubility of many key metal species is highly pH dependant).

Karlsson *et al* (2018) undertook NAG testing on waste rock from a number of

Scandinavian mine sites and compared the results to actual site seepage data. The study found that the standard NAG testing method often over predicted pH from circum-neutral deposits (i.e. was overly optimistic) and under predicted pH from mine wastes which themselves were generating acidic seepage. Previous work by Charles *et al* (2015) following similar observations of high pH values (in excess of pH 10) from post boiling stage NAG test data (i.e. NAG pH) showed that the high pH conditions were potentially attributed to CO2 disequilibria following degassing of the sample during the 2 hour boiling step.

The generation of elevated pH may not be a concern when the tests are solely used to give an indication of potential acid forming and non-acid forming behaviour. However, the large deviation in pH from that which would be expected in the field can result in very large error when using NAG leachate data to assess mobility risk of key toxic metal or metalloid species. This is due in part to the sensitivity of the mobility of these species to pH.

This paper presents the justification for modification of the NAG test on a site-by-site basis as demonstrated through particular experience at the Kevitsa mine site in northern Finland.

Kevitsa Case Study

Kevitsa ore deposit is a Ni-Cu-PGE mineralisation hosted in a mafic / ultra-mafic cumulate. The waste rock from the deposit comprises largely of amphibole 'tremolite' ≈30%, and diopside 'augite' ≈35%. With minor amounts of Mg olivine 'forsterite' ≈5%, orthopyroxene 'enstatite' ≈7.5% with relatively low concentrations of serpentine. Carbonates are present as calcite and dolomite, but concentrations are generally less than 1% (total inorganic carbon content = 0.8% equivalent as calcite). Sulfide minerals are present in the waste typically at concentrations less than 1% mainly as pyrrhotite, chalcopyrite and pentlandite. Nickel is recognised as a key element potentially mobilised under circum neutral conditions as a result of sulfide oxidation.

Due to the presence of calcite and dolomite, and generally low sulfide content, the majority of the waste rock at Kevitsa is Non-Acid Forming (NAF) having and excess of acid neutralising capacity to acid generating capacity.

Between 2013 and 2017 in the region of 400 NAG tests were undertaken on samples of waste rock and tailings from the Kevitsa deposit using the Smart *et al* (2002) method. Associated NAG liquor analysis was undertaken on a small sub-set of 17 of these samples. As is conventional the NAG liquor was collected following the boiling step and prior to the NAG back titration. The NAG pH and electrical conductivity (EC) was also measured following the boiling step. The results of the standard NAG testing showed nickel release less than 1 mg/kg for the waste rock samples with an average pH of 8.85.

with an average pH of 8.85.

On review of the data with respect to observations made by Charles *et al* (2015), it was thought likely that the high NAG pH and low Ni mobility may be attributed to the boiling step used in the standard NAG method. This can have the effect of increasing the leachate pH due to degassing of dissolved CO_2 in the sample and forming a CO_2 disequilibrium between the solution and the atmosphere.

Based on the above, during the most recent waste characterisation study undertaken on the Kevitsa waste rock during 2017 / 2018, it was decided to utilise a modified NAG method. This method included a pre-boil NAG pH and EC measurement together with pre-boil sample of NAG liquor.

Results of revised testing

To understand the effect of the boiling step on leachate quality, NAG testing with pre-boil and post-boil pH measurements were undertaken on six samples (See Figure 2). All samples showed a post-boil pH increase ranging from 0.79 pH units (GCL0046-058) and up to 2.7 pH units (GCL0046-052) with an average increase of 1.47 pH units. To determine the impact of pH on the leach samples, the concentration of dissolved constituents sampled prior to boiling were

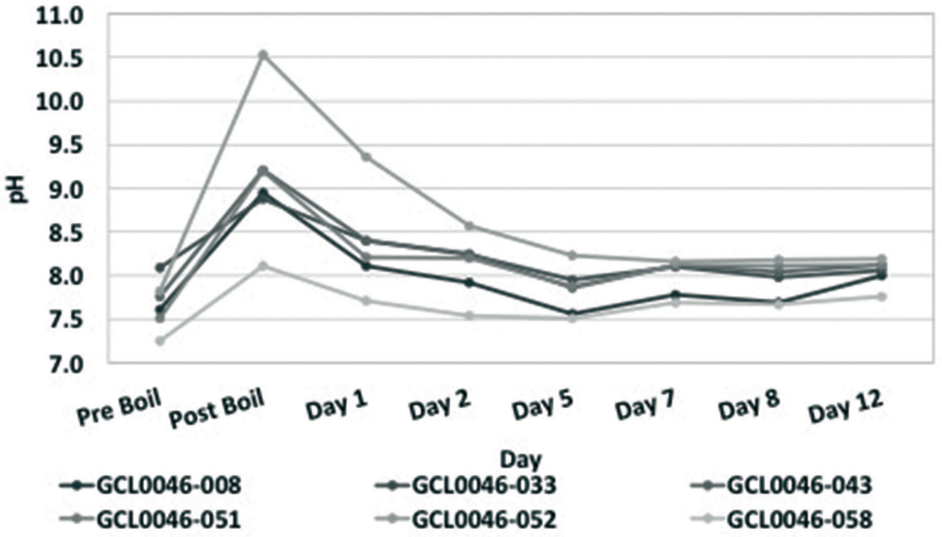

Figure 1 *Evolution of pH following boiling of NAG solution.*

compared to those sampled at the end of the 12 day equilibration period. The results of boiling support the findings of Charles *et al* (2015) showing that the initial post boil pH increase recovers to near the pre-boiling pH given roughly 5 days which is attributed to equilibrium with atmospheric CO_2 as indicated in Charles *et al* (2015). It is clear however, that if NAG liquor samples are taken for analysis immediately following the post boiling stage, that the leachate pH will be out of equilibrium which is likely to affect the solubility of many elements that are of interest in a geochemical characterisation study.

In the above analysis, and also in all NAG tests undertaken for the current stage of work in the project, leachates were routinely sub-sampled for elemental analysis prior to the heating stage. In the case of the NAG pH equilibrium tests shown above, samples were also taken after the 12-day equilibration period for GCL0046-058 and 052. The results of nickel release for the pre-boil and post 12-day re-equilibration period analysis are shown in Figure 3. The graph demonstrates that the nickel release in the NAG leachates post-boil equilibration are roughly 60% lower than the pre-boil concentrations despite the solution pH largely recovering to pre boil levels.

The lower concentrations of metals in the NAG liquor following boiling can be attributed to reduced mobility of nickel at elevated pH through such processes as precipitation of hydroxides and adsorption on to mineral surfaces however, the failure of concentrations to recover to pre-boil levels indicates that the processes that are responsible for reducing the mobility are not completely reversible.

Comparison of Historic NAG Data

In order to test the theory, modified NAG tests were undertaken on 64 of the samples from the 2013 to 2017 sampling which had previously been run with the Smart *et al* (2002) method. This allowed the pre-boil NAG pH from the NAG re-runs to be compared to the post-boil NAG pH values from the historic testing (see Figure 4). There is a clear difference in the overall NAG pH distribution, with no samples having a pre-boil NAG pH exceeding pH 8, while three quarters of the post-boil NAG pH for the same samples exceeding pH 8.5. The maximum post boil pH values were pH 11.5 with the average pH increase between pre and post boil NAG pH of 3 pH units.

Historical NAG liquor data was also compared to new data obtained at the pre-boiling stage of the standard NAG test (expressed as a ratio of nickel release relative to sulfur on a logarithmic scale, as above). The resultant graph resembles a pH

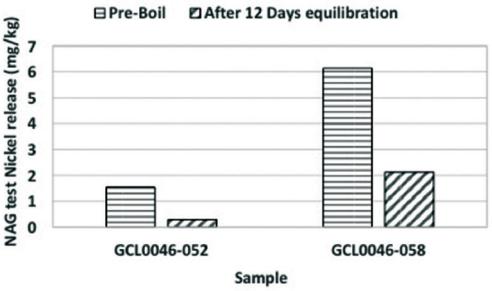

Figure 2 Difference in nickel release Pre-boil and post equilibration for sample GCL0046-052 and GCL0046-058.

dependant leach curve which demonstrates the importance of pH to nickel mobility (Figure 5). It is clear that the historical NAG data plots in the pH range >8.5 and relative nickel:sulfur ratios are significantly lower. Because the relative change in nickel mobility was found to be in the orders of magnitude between the pH range of 7-9. It is clear that estimation of nickel mobility using the NAG test is very sensitive to testing method, and that by using liquor data from the standard method to make initial assessment of nickel mobility will result in an large underestimation of nickel concentrations.

Key Observations

NAG liquor / hydrogen peroxide leach analysis is an important tool for initial assessment of metal mobility from mining waste. This is especially true on un-weathered sulfidic material such as drill core where water leaching tests would yield little usable information.

Observations made in the current study broadly agree with the findings of Charles *et al* (2015) and Karlsson *et al* (2018). The current study shows that even following an extended re-equilibration period, the metals concentrations and in some cases the pH does not fully recover to their pre-boil levels. The current study is limited as the elemental analysis was only undertaken at the end of the equilibration period. It would aid the study to understand the behaviour of dissolved metals over the full equilibration period including the period immediately following boiling.

The results of this study and the work of previous authors clearly demonstrate that NAG liquor data obtained from the standard NAG test, should be used with caution and that the standard NAG method, although reliable as an indicator of ARD properties (i.e. NAF or PAF), especially when used in conjunction with acid base accounting and mineralogical assessment, may be misleading when used to assess potential leachate pH and elemental mobility. This is especially true when assessing circum neutral and alkaline drainage situations, and when dealing with NAF samples, as the standard method can lead to a large over-estimation in pH. This in turn can lead to significant decrease in metals concentrations in the leachate, and therefore an under-estimation of concentrations if then inferred to the deposit.

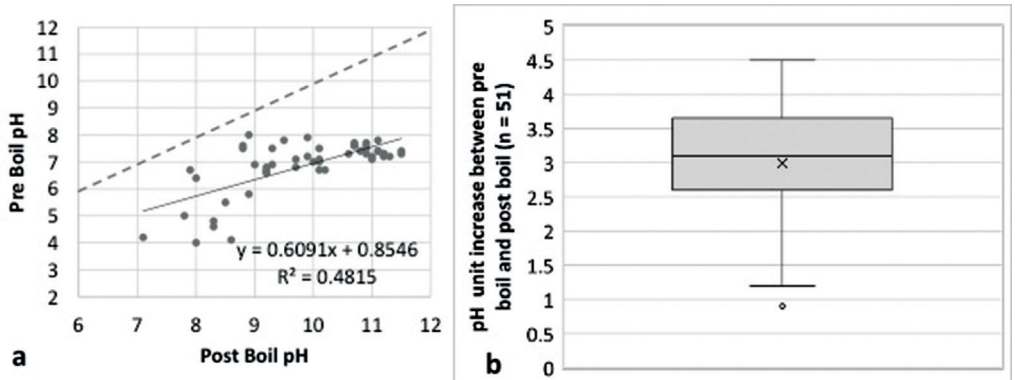

Figure 3 Comparison of the distribution of pH values obtained for the same 51 samples at a post-boil stage and pre-boil stage (a) and box and whisker plot showing the pH unit difference between pre and post boil NAG pH values for the same samples (b).

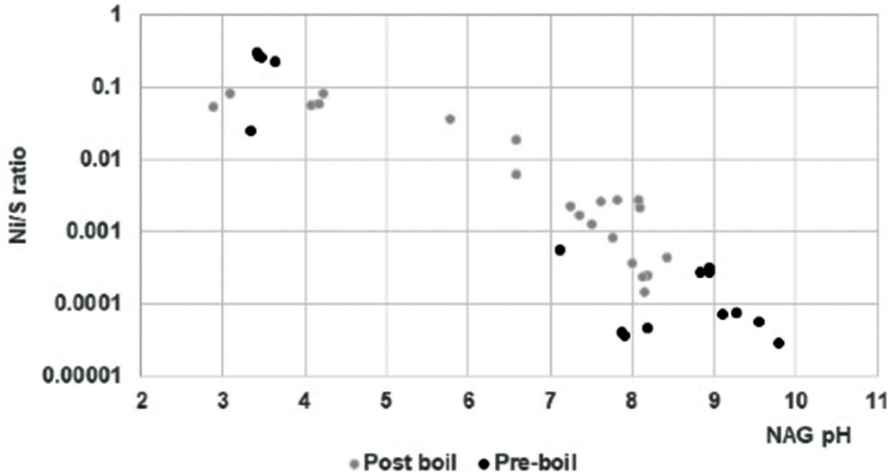

Figure 4 *Comparison between Ni/S ratio determined in pre-boil and post-boil NAG leachates.*

We would recommend that pre and post boil NAG pH is determined for all NAG testing as a matter of routine. The authors believe that this can give important information on the materials behaviour. In addition, if leachate samples are to be collected, the authors recommend that, when NAF material is being tested, that this is done prior to the boiling step to avoid limitations in element mobility due to the pH increase that can occur during the boiling step.

References

Barnes, A., Sapsford, D.J., Bowell, R.J., Dey, B.M. (2013). An assessment of Rapid-Turnaround Tests for ARD Prediction. Presentation given at the 23rd World Mining Congress. August 11th to 15th 2013, Montreal, Canada.

Charles, J.C., Barnes, A., Declerq, J., Warrender, R., Brough, C., Bowell, R.J. (2015). Difficulties of interpretation of NAG test results on net neutralizing mine wastes: initial observations of elevated pH conditions and theory of CO2 disequilibrium. In: Proceedings of the 10th International Conference on Acid Rock Drainage and IMWA Annual Conference. April 21 – 24, 2015. Santiago, Chile. ppTBC

Finkelman, R.B. and Giffin, D.E. (1986). Hydrogen Peroxide Oxidation: An Improved Method for Rapidly Assessing Acid-Generating Potential of Sediments and Sedimentary Rocks.

Karlsson, T., Räisänen, M. L., Lehtonen, M., Alakangas, L. (2018). Comparison of static and mineralogical ARD prediction methods in the Nordic environment. Environmental Monitoring and Assessment 190. 719

Miller, S., Robertson, A., & Donahue, T. (1997). Advances in acid drainage prediction using the net acid generating (NAG) test. In Proceedings fourth international conference on acid rock drainage, (pp. 533–547). Vancouver, B. C. Canada May 31 – June 6, 1997, volume II.

O'Shay, T.A., Hossner, L.R., Dixon, J.B. (1990) A modified hydrogen peroxide oxidation method for determination of potential acidity in pyritic overburden. Journal of Environmental Quality 19. 778-782.

Sapsford, D. Bowell, R., Dey, M., Williams, C. and Williams, K. 2010. A Comparison of Kinetic NAG tests with Static and Humidity Cell Tests for the Prediction of ARD

Smart, R., Skinner, W. M., Levay, G., Gerson, A. R., Thomas, J. E., Sobieraj, H., Schumann, R., Weisener, C. G., Weber, P. A., Miller, S. D., & Stewart, W. A. (2002). ARD test handbook: Project P387A, A Prediction and Kinetic Control of Acid Mine Drainage. Melbourne: AMIRA international Ltd 42 p.

Sobek, A.A., Schuller, W.A, Freemen, J.R. and Smith R.M. (1978). Field and Laboratory Methods Applicable to Overburdens and Mine soils. Report EPA-600/2-78-054, US National Technical information Report. PB-280495.

Stewart, W.A., Miller, S.D., Smart, R. (2006). Advances in Acid Rock Drainage (ARD) Characterisation of Mine Wastes. Paper Presented at the 7th International Conference on Acid Rock Drainage (ICARD), March 26-30, 2006, St Louis MO. R.I. Barnhisel (ed.) Published by the American Society of Mining and Reclamation (ASMR), 3134 Montavesta Road, Lexington, KY 40502. Pp 2098 - 2119

Employment Of A Double Continuum Model To Characterize Groundwater Flow In Underground Post-Mining Setups: Case Study Of The Ibbenbüren Westfield

Diego Bedoya-Gonzalez[1,2], Timo Kessler[2], Maria-Theresia Schafmeister[2]

[1]*Department of Geography and Geology, University of Salzburg, Hellbrunner Str. 34, 5020, Salzburg, Austria, diegoalexander.bedoyagonzalez@sbg.ac.at*

[2]*Institute for Geography and Geology, University of Greifswald, Friedrich-Ludwig-Jahn Str. 17a, 17487 Greifswald, Germany, timo.kessler@uni-greifswald.de; Schaf@uni-greifswald.de*

Abstract

Underground hard coal mining usually disrupt the mechanical equilibrium of the geological media, creating fractured zones in the bedrock. The present study employs a Double-Continuum model to assess the influence of the fractured and porous media on the percolation process at the Ibbenbüren Westfield. Model results displayed good agreement with measured mine water discharges. While fractured continuum reacts readily to heavy precipitations, water is released slowly from the matrix. This behavior generates a gradual decrease in the discharge over the dry season. Findings obtained from this approach can be integrated into reactive transport models to predict long-term evolution of mine drainages.

Keywords: Hard Coal Mining, Double-Continuum Model, Mine Water Discharge, Ibbenbüren Westfield

Introduction

Underground coal mining operations tend to modify the nature of the subsurface rock structure (Kim *et al*. 1997; Newman *et al*. 2017). The employment of high-recovery methods redistribute, concentrate and/or reorientate the stress field of the rocks, generating strains (i.e., deformations) along the sequence (David *et al*. 2017). Large vertical deformations create fracture networks that provoke duality on the fundamental hydraulic processes (Qu *et al*. 2015; Zhang *et al*. 2018; Liu *et al*. 2019). This behavior is evidenced, for example, in "diffuse" or slow infiltration in pristine rocks coupled with concentrated or "rapid" fluid flow along the fracture networks (Király 1994). The contrast is even more considerable if coal mines are developed into fairly impermeable rock sequences (Morin and Hutt 2001; Wolkersdorfer 2006).

The representation of dual systems is usually complicated by requiring extensive assignment of physical and chemical properties for both media. Many of these properties are even impossible to obtain for fracture networks. It is from this dilemma where double-continuum models (DC) arose as an appropriate approach (Pruess and Narasimhan 1985). The way how fractures are treated as a network of mean characteristics solves the difficulties of obtaining detailed info for constructing discrete fractured models and the inability of equivalent porous models (EPM) for considering strong heterogeneities. DC models simulate fractured porous media as two overlapping and interacting continua, with different flow, transport and storage parameters. The interaction between both is achieved through a mass transfer function determined by the size and shape of the blocks, as well as their local difference in pressure and/or temperature potentials (Beyer and Mohrlok 2006). Over time these models have been applied to numerous subsurface geochemical processes, such as oil recovery, geothermal energy, nuclear waste repositories, and CO2 sequestration (e.g., see Azom and Javadpour 2012; Hao *et al*. 2013). For coal mining areas, this approach can potentially be extended to simulating the quantity and quality of mine drainage, including contaminant migration,

characterizing the rebound process at post-mining sites, and predicting water inflows within mining-disrupted sequences.

The present study uses recent progress in the characterization of water-conducting fracture zones to set up a double-continuum model of a coal mining zone. Our purpose is to emulate the infiltration process within the disturbed shallow overburden of the Ibbenbüren Westfield. Compared to other coal mining districts in Germany, this area is sharply delineated by the topography and local geology, resulting in an easily controllable area for testing the approach. Modeling intends to determine the influence of each flow element within the time-dependent water discharge of the mining area (i.e., the temporal distribution of the rapid (fracture) and slow (matrix) flow components).

The Ibbenbüren Westfield

Mining in the Ibbenbüren Westfield was founded on the exploitation of anthracitic coal seams encountered in a shallow Carboniferous crustal block. Here, operations stopped in June 1979, with excavations as deep as 600 m below the ground level (DMT GmbH & Co. KG 2019). After its closure, the area was flooded under control up to an elevation of around 65 m above the sea level (a.s.l.). At this height, groundwater reached the Dickenberg adit, which still maintains the same phreatic level by discharging exceedance of water out of the area (Rinder *et al*. 2020).

Due to the phreatic level of the former coalfield is above the foreland surface (< 55 m a.s.l.), precipitation turns into the only source of groundwater recharge. The development of a water-conducting fracture zone together with a sparse Quaternary offer neither storage capacity nor great resistance for meteoric water to percolate(Lotze *et al*. 1962; Bässler 1970). Consequently, the volume and temporal distribution of the discharged mine water is directly dependent on the water dynamics through the siliciclastic overburden. This is true for the area enclosed by the Northern and Southern Carboniferous Marginal faults, Mieke Fault and Pommer-Esche Fault, which represent effective hydrogeological boundaries for the field (Figure 1) (Prof. Dr. Coldewey GmbH 2018). Furthermore, groundwater can only be extracted in areas higher than the Dickenberg

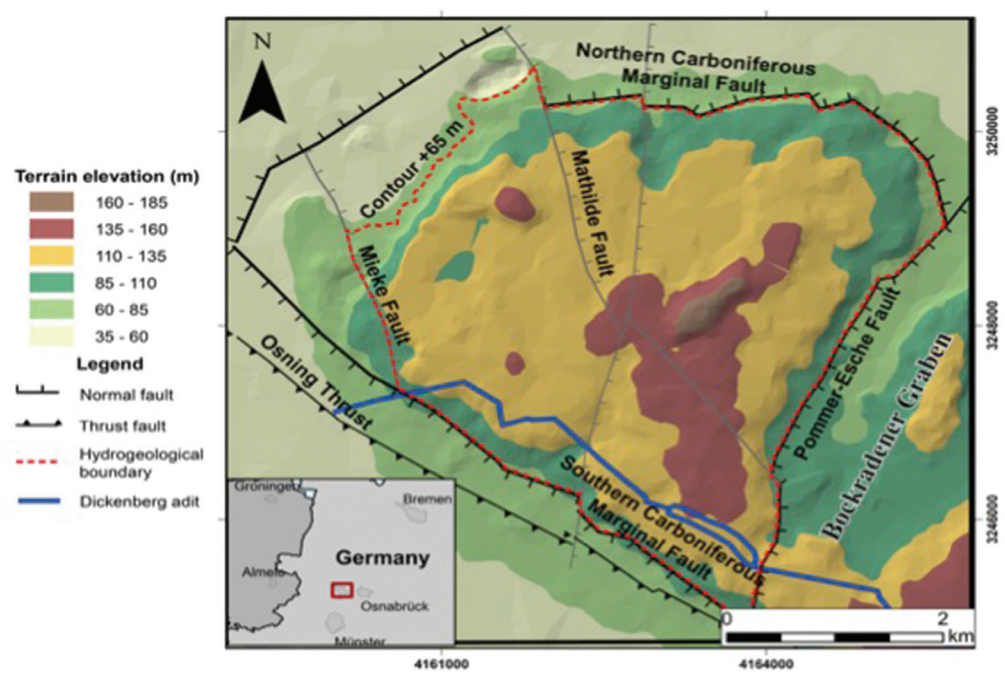

Figure 1 *Location map of the Ibbenbüren Westfield. The Carboniferous blocks present some faults that turn into effective hydrogeological boundaries for the coalfield (modified after Bedoya-Gonzalez et al. 2021).*

adit, turning the terrain contour +65 m into an additional hydrogeological limit

Methods

TOUGH2 (Pruess *et al.* 2012) is used to simulate the unsaturated overburden of the Ibbenbüren Westfield. The software employs Richards' equation to describe Darcy-type fluid flow in the variably saturated porous media. Space discretization is done by means of integral finite differences and fully implicit first-order finite differences in time (Xu *et al.* 2000). Modeling scenarios include isothermal flow conditions, with 2-phase and one water component

Geometry and grid construction

Conceptualization of the study area is depicted in Figure 2. The design and dimensions of the numerical model is made according to the hydrogeological limits previously described and illustrated in Figure 1. The 3D system is discretized into a number of vertical columns of 1 ha base and variable height to represent the concave shape of the area. The height difference between columns is selected equal to 5 m after considering the average thickness of the layers. The total number of columns for each height interval is, then, calculated by intersecting the DEM of the Westfield with the base boundary (65 m a.s.l.).

Horizontal layers in each column were assigned maintaining the lithological proportions and stritigraphical position as described in Bedoya-Gonzalez *et al.* (2021). Exceptions are the zones above 140 meters, which are assigned to anthropogenic waste rock deposits, and the first 5 meters of each column that correspond to highly weathered intervals. The depth at which the model splits into two continua is set at 45 meters above the deepest mined coal seam within the unsaturated zone (i.e., the nearest seam above the adit). This height was determined from empirical relationships after taking into account the thickness of the mined coal seam as well as the thickness and composition of the overburden (e.g., see Palchik 2003) However, fracture zone heights of 30 to 40 meters are also considered. Finally, fracture density per grid block is assumed to be equal to 10, resulting in a total exchange area of 10000 m^2 between the fracture continuum and the matrix.

Parameterization

Parameters used in this model are listed in Table 1. These values were extensively searched in the literature and assigned according to their correspondence with the lithological units. The calculation of relative permeability and capillary pressure values is performed according to the Van Genuchthen parametric model. However, since the Van Genuchthen parameters have been developed for porous media, their use in the fracture continuum is purely for model calibration and do not have physical meaning (e.g., see Kordilla *et al.* 2012). For the model calibration, parameters are only varied within

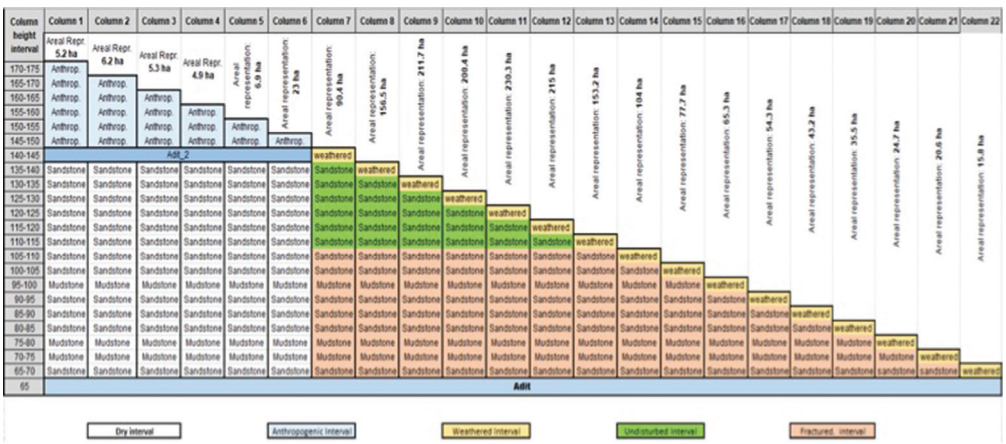

Figure 2 *Graphical representation of the 2D-grid discretization of the model.*

reasonable ranges consistent with the actual field conditions (values in parenthesis in Table 1).

Boundary conditions and initial conditions

The lateral sides of the matrix continuum, as well as the top of the model, are defined as no flow boundaries. The lower boundary is set to allow free drainage under gravity force. Lastly, a specified flux boundary is set at the top of the columns to account for diffuse recharge.

As initial conditions, Tough2 only needs the water saturations for each element. In our case, initial saturations were computed with a steady state simulation. The applied total recharge for this computation is 240 mm/y, which corresponds to the average recharge across Germany. Once the sequence reaches steady state, daily infiltration values are applied to the first element of the columns (see Figure 2). This amount varies temporarily and is estimated based on both daily precipitation and monthly average recharge for Ibbenbüren.

Model application

Fluid flow is simulated only in the vertical component of each column, only allowing lateral exchanges between fractures and matrix continua. The total discharge of the studied area is thus obtained by summing the discharge of all columns at the base (i.e., at 65 m a.s.l.). In the case of columns covered by waste rock deposits, discharge measurements are made around 145 m a.s.l., where an additional adit directs the water from these deposits to the Dickenberg adit.

Measuring the vertical flow of the system is valid if one considers that the overall fluid flow under unsaturated conditions is mainly driven by gravity and capillary forces in the vertical component. Also, a fairly homogeneous distribution in the horizontal plane of the zone allows this approach. Potentially, a horizontal fracture zone exists throughout the Westfield, as the Dickenberg and Buchholz coal seams were extensively mined. Also, core samples analyzed by Bedoya-Gonzalez *et al.* (2021) suggest that the proportions between sandstones and mudstones are similar throughout the shallow overburden.

Results and discussion

Figure 3 shows the actual and simulated discharge volumes of the Dickenberg adit for the year 2008. The simulated curve in the graph corresponds to the best match obtained from using the values listed outside the parentheses in Table 1. In overall, a good agreement between the two lines is observed. The greatest differences of up to 20% are associated with a small lag between the two signals from January to March. However, an advance of the simulated signal was expected because the rapid flow from the time the water reaches the adit to the point of discharge measurement was not taken into account.

According to the simulation, the system would be dominated by a high permeability

Table 1 *Hydraulic parameters used in the model. Values outside the parentheses indicate the values that showed the best agreement in our model (from *Prof. Dr. Coldewey GmbH and DMT GmbH & Co. KG 2018; ** Freeze and Cherry 1979; [¥]Bedoya-Gonzalez et al. 2021; [ŦΦ]Kordilla et al. 2012; [Φ]Parajuli et al. 2017.*

Lithology	Permeability	Effec. Porosity	Van genuchten parameters		
	(m^2)	(-)	θr (-) [ŦΦ]	Alpha (m-1) [ŦΦ]	M [ŦΦ]
Sandstone	1e-12	0,15	0,15	0,1	0,35
	(1e-12-1e-14)*	(0,1-0,16)[¥]	(0,15–0,45)	(0,5–0,01)	
Mudstone	1e-17**	0,05 **	0,65	0,04	0,22
			(0.6–0.7)		
Weathered interval	1e-12	0.35	0,1	2,6	0,65
	(5e-11-1e-13)*	(0,15–0,4)*	(0,04–0,4)		(0,5–0,7)
Antropogenic deposit	1.0e-11	0.35*	0.05	3,5	0,7
	(1e-10 – 5e-12)*				
Fractured continuum	1.0e-8	0,99[¥]	0,05	2	0,7
	(1e-7 – 1e-10)			(0,01- 5)	(0,4–0,75)

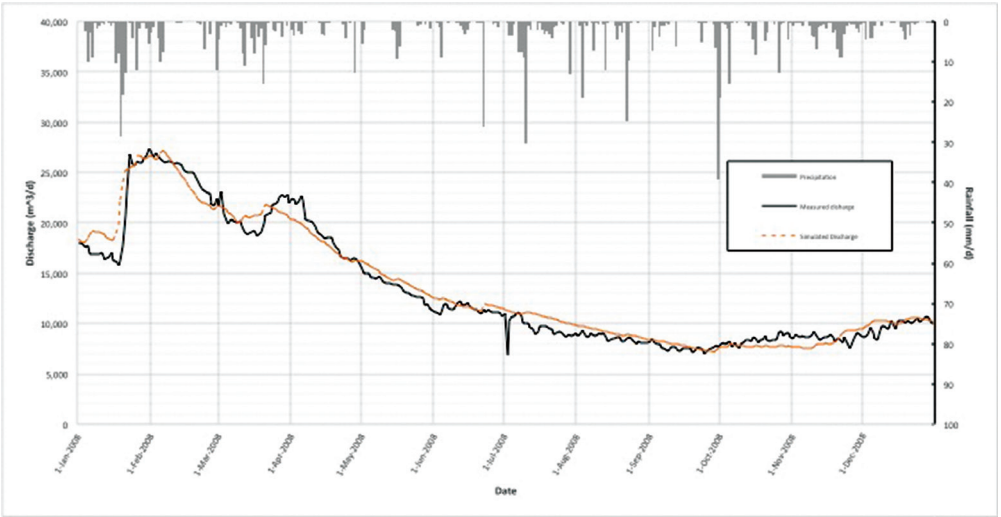

Figure 3 *Comparison between the measured and simulated discharge of the Dickenberg adit.*

media. The fractured continuum cause the system to react quickly during the months of higher precipitation generating the peaks of the discharge, while the recession of the signal is dominated by the matrix. Then, it is likely that during the summer months the saturation will slowly drop, meaning that the fractures are desaturated and the matrix has a much lower capillary pressure than the fractures (essentially holding water and slowly releasing). New water that may precipitate during summer may enter the fractures when the matrix capacity is shortly exceeded, but will mostly enter the matrix. This behavior causes that the system does not readily respond to heavy precipitation events in drier seasons, as potentially could show other types of models (e.g., see Rudakov *et al*. 2014).

Despite of the good agreement, results of the present paper should be considered as preliminary and be taken with caution. It is expected that a more extensive calibration process will bring better fits to some discrepancies, especially for the periods preceding the abundant discharges in January. Additionally, the parameters that presented the best curve adjustment corresponded to the end-members identified in the literature (e.g., the highest extension of the fracture zone and the greatest permeability for the sandstones). This could be due to the no identification, evaluation or calibration of sensitive parameters such as model geometry or conduit spacing. This latter would be, in fact, an influential parameter for the extension of the approach to modeling contaminant transport through the sequence.

Conclusions

The application of a double-continuum model positively fitted the transient discharge of the Dickenberg adit in the Ibbenbüren Westfield. The good agreement between the calculated and measured discharge for the year 2008 was possible by coupling a high permeability fracture continuum with a low permeability matrix continuum. Flow from the fractured media would derive in heavy and short discharges during the higher precipitation months, while the matrix would be responsible for a smoothed transition to the summer months, not being affected by strong precipitation events during this period. Consequently, the application of this approach to coal mining areas would add important aspects to mine water models, as they could estimate the relevance of each geological media with respect to mine drainage quality (e.g., Acid Mine Drainage generation). However, the results presented in this paper should be considered as preliminary due to the lack of study of other potentially sensitive factors, such as conduit spacing.

References

Azom PN, Javadpour F (2012) Dual-Continuum Modeling of Shale and Tight Gas Reservoirs. Soc Pet Eng. https://doi.org/doi:10.2118/159584-MS

Bässler R (1970) Hydrogeologische, chemische und Isotopen – Untersuchungen der Grubenwässer im Ibbenbürener Steinkohlenrevier. Z deutsch geol Ges 209–286

Bedoya-Gonzalez D, Hilberg S, Redhammer G, Rinder T (2021) A Petrographic Investigation of the Carboniferous Sequence from the Ibbenbüren Mine : Tracing the Origin of the Coal Mine Drainage. Minerals 11:1–19. https://doi.org/https:// doi.org/10.3390/min11050483

Beyer M, Mohrlok U (2006) Parameter estimation for a double continuum transport model for fractured porous media. In: Proceedings of ModelCARE'. IAHS Publ. 304, 2006., The Hague, The Netherlands, June 2005, pp 80–86

David K, Timms WA, Barbour SL, Mitra R (2017) .Tracking changes in the specific storage of overburden rock during longwall coal mining. J Hydrol 553:304–320. https://doi.org/10.1016/j.jhydrol.2017.07.057

DMT GmbH & Co. KG (2019) Abschluss-betriebsplan des Steinkohlen-bergwerks Ibbenbüren Anlage 17 – Prognose zur optimierten Wasserannahme nach Stilllegung des Steinkohlenbergwerkes Ibbenbüren (Ostfeld). RAG Anthrazit Ibbenbüren GmbH, Essen, Germany

Freeze R, Cherry JA (1979) Physical Properties and Principles. In: Brenn C, McNeily K (eds) Groundwater, 1st edn. Prentice-Hall Inc., Englewood Cliffs, New Jersey 07632, p 624

Hao Y, Fu P, Carrigan CR (2013) Application of a dual-continuum model for simulation of fluid flow and heat transfer in fractured geothermal reservoirs. Proceedings, 38th Work Geotherm Reserv Eng vol SGP-TR-198 Stanford Univ Stanford, Calif 462–469

Kim JM, Parizek RR, Elsworth D (1997) Evaluation of fully-coupled strata deformation and groundwater flow in response to longwall mining. Int J Rock Mech Min Sci 34:1187–1199. https://doi.org/10.1016/S1365-1609(97)80070-6

Király L (1994) Groundwater flow in fractures rocks: models and reality. In: 14th Mintrop Seminar über Interpretationsstrategien in Exploration und Produktion. Ruhr Universität Bochum, pp 1–21

Kordilla J, Sauter M, Reimann T, Geyer T (2012) Simulation of saturated and unsaturated flow in karst systems at catchment scale using a double continuum approach. Hydrol Earth Syst Sci 16:3909–3923. https://doi.org/10.5194/hess-16-3909-2012

Liu Y, Liu Q meng, Li W ping, *et al* (2019) Height of water-conducting fractured zone in coal mining in the soil–rock composite structure overburdens. Environ Earth Sci 78:242–255. https://doi.org/10.1007/s12665-019-8239-7

Lotze F, Semmler W, Kötter K, Mausolf F (1962) Hydrogeologie des Westteils der Ibbenbürener Karbonscholle. Springer Fachmedien Wiesbaden GmbH., Wiesbaden, Germany

Morin K a, Hutt NM (2001) Environmental geochemistry of minesite drainage: practical theory and case studies. MDAG Publishing, Vancouver, British Columbia, Canada Cover

Newman C, Agioutantis Z, Boede Jimenez Leon G (2017) Assessment of potential impacts to surface and subsurface water bodies due to longwall mining. Int J Min Sci Technol 27:57–64. https://doi.org/10.1016/j.ijmst.2016.11.016

Palchik V (2003) Formation of fractured zones in overburden due to longwall mining. Environ Geol 44:28–38. https://doi.org/10.1007/s00254-002-0732-7

Parajuli K, Sadeghi M, Jones S (2017) A binary mixing model for characterizing stony-soil water retention. Agric For Meteorol 244–245:1–8

Prof. Dr. Coldewey GmbH (2018) Abschlussbetriebsplan des Steinkohlen-bergwerks Ibbenbüren Anlage 16 – Auswirkungen des Grubenwasseranstiegs im Ostfeld des Bergwerkes Ibbenbüren der RAG Anthrazit Ibbenbüren GmbH. Münster, Germany

Pruess K, Narasimhan TN (1985) A practical method for modeling fluid and heat flow in fractured porous media. Soc Pet Eng J 25:14–26. https://doi.org/doi:10.2118/10509-PA

Pruess K, Oldenburg C, Moridis G (2012) TOUGH2 user's guide , version 2. 210

Qu Q, Xu J, Wu R, *et al* (2015) Three-zone characterisation of coupled strata and gas behaviour in multi-seam mining. Int J Rock Mech Min Sci 78:91–98. https://doi.org/10.1016/j.ijrmms.2015.04.018

Rinder T, Dietzel M, Stammeier JA, *et al* (2020) Geochemistry of coal mine drainage,

groundwater, and brines from the Ibbenbüren mine, Germany: A coupled elemental-isotopic approach. Appl Geochemistry 121:104693. https://doi.org/10.1016/j.apgeochem.2020.104693

Rudakov D V., Coldewey WG, Goerke-Mallet P (2014) Modeling the Inflow and Discharge from Underground Structures within the Abandoned Hardcoal Mining Area of West Field (Ibbenbüren). –. In: Sui, Wanghua; Sun, Yajun; Wang C (ed) An Interdisciplinary Response to Mine Water Challenges. 12th International Mine Water Association Congress (IMWA 2014). Xuzhou, China, 18-22 August 2014;, pp 699 – 705

Wolkersdorfer C (2006) Water Management at Abandoned Flooded Underground Mines. Springer, Freiberg, Sachsen

Xu T, White SP, Pruess K, Brimhall GH (2000) Modeling of pyrite oxidation in saturated and unsaturated subsurface flow systems. Transp Porous Media 39:25–56. https://doi.org/10.1023/A:1006518725360

Zhang Y, Cao S, Wan T, Wang J (2018) Field Measurement and Mechanical Analysis of Height of the Water Flowing Fracture Zone in Short-Wall Block Backfill Mining beneath the Aquifer: A case study in China. Geofluids 2018:. https://doi.org/10.1155/2018/7873682

Evaluation of Preferential Pathways for an Effective Dewatering and Depressurization of the Aitik Open-Pit, Norrbotten, Sweden

Boddaert Florent[1], Mwagalanyi Hannington[2], Sholl Simon[1], Beale Geoff[1]

[1]*Piteau Associates, Canon Court, West Abbey Lawn, Shrewsbury, UK SY2 5DE, United-Kingdom, fboddaert@piteau.com, ssholl@piteau.com, gbeale@piteau.com*

[2]*Boliden Mineral AB, Aitik, Sakajärvi 1, 982 21 Gällivare, Sweden, Hannington.Mwagalanyi@boliden.com*

Abstract

Boliden's Aitik mine in northern Sweden has a mine plan which will deepen the pit to 850 mbgl by the end of mine life. The control on pit slope pore pressures becomes critical to ensure stable slopes and a safe operation. This often requires numerical groundwater modelling to support the geotechnical analysis. Following industry best practice, a multi-disciplinary approach has been adopted over different campaigns of characterisation to improve the understanding of source zones, pathways and magnitudes of water reaching the pit wall and floor. This enabled the construction of a detailed conceptual model, with a high level of confidence, that served as a basis for the construction of a 3D numerical groundwater flow model.

Keywords: Pore-Pressure, Depressurisation, Dewatering

Introduction

The Aitik Main pit is excavated in metamorphosed Cu-Au-Ag porphyry rocks of the Kiruna-Ladoga shear zone. Mining has been ongoing at the site since 1968. The Life of Mine plan (LoM) has been revised to underpin continued ore production from the Main pit. The depth and geometry of the pit walls will evolve significantly over the projected mine life until 2043. The operating pit floor sump is currently at a depth of -470 mbgl (fig. 1). At the end of the LoM, the footprint of the Main pit will extend on both sides of the existing limit to reach a length of 3.6 km by 1.5 km of width. The pit floor in the Main pit is expected to reach a depth of -850 mbgl.

The conditions to ensure the stability of the pit wall will be increasingly challenging with a deeper pit. Existing pit walls are already subject to a close monitoring of slope movements and pore-pressure behind the pit walls from the pit crest to the pit floor. In addition, slope stability analysis is carried out on a regular basis to verify the conformity of the current and future slope design with local hydrogeological and geomechanical conditions. Slope stability analysis suggests that deepening the open pit results in a lower Factor of Safety (FoS). Although these results are highly sensitive to hydrogeological assumptions used. The analysis demonstrates that undrained conditions will produce a FoS of less than 1. Conversely, a drained condition, where the phreatic surface is greater than 100 m behind the pit wall, would produce a FoS that exceeds 1.5. Therefore, the effective depressurization of the pit walls is a central component of the pit slope stability.

Aitik has proactively installed horizontal drains in the pit walls and pumping wells in the pit floor to depressurize and dewater the current Main pit. To reach the depressurization objectives (to ensure that acceptance criteria are met) associated with the LOM pit expansion, this strategy must be further adapted and optimised. The evaluation of preferential groundwater pathways enables the efforts to be focused on sectors of the Main pit witnessing an excess of inflow from the pit wall and crest.

General context

The mine topography is typically a low-gradient terrain. Pre-mining surface water comprised of small, shallow streams associated with, and connected to, numerous peat bogs with standing water and small lakes. The Sakajoki river flows from the south of the mine where its course changes to the northeast, cutting between the Main and Salmijärvi pits. An analysis of the pre-mining

topography indicates that some tributaries of the Sakajoki river were covered by the Waste Rock Storage Facility (WRSF) and intercepted by the Main pit and Salmijärvi. (fig. 2). The drainage area upgradient of the hangingwall of the Main pit is about 7.8 km^2.

Aitik has a sub-arctic climate without dry seasons. Months of November to March have an average temperature below to -10°C. Over the period 1996-2020, the Mean Annual Precipitation (MAP) is equivalent to 610 mm/yr. There is an accumulation of snow over the freezing period, and it can reach 0.7 m depth at the end of the period of snow accumulation in March.

The geology at Aitik is divided into footwall, ore zone, and hangingwall, according to the structural contact and copper grades (fig. 3). The ore zone consists of biotite and muscovite schists and gneisses. Feldspar-biotite-amphibole gneiss with sub-economic Cu-grades occur in the footwall area. The hangingwall mainly comprises un-mineralised feldspar-biotite-amphibole gneiss, which is separated from the ore zone by a thrust fault. The dominant foliation within the ore zone dips 40–60° west and strikes approximately N–S, which is parallel to the footwall and hangingwall contacts. The major thrusting striking N–S and dipping 35–40°W (generated in the hangingwall) is highlighted by a zone of ductile deformation within the hangingwall of several hundreds of metres wide.

Quaternary deposits form an unconsolidated sediment cover of moraines and fluvio-glacial sediments. More recent sediments (Holocene) correspond to fluvial deposits and peats and are associated to phenomenon of continental erosion and accumulation of organic matter which leads to the surface accumulation of clay and which acts as barrier of the groundwater flow due to its low permeability. A refined analysis carried with an interpolation of available drill data and outcrops defined an average thickness of Quaternary deposits of 15 m around the Aitik mine.

Pit hydrogeology

The development of the mine modified the groundwater regime locally around the Main pit, with the development of a zone of drawdown. To the east of the Main pit

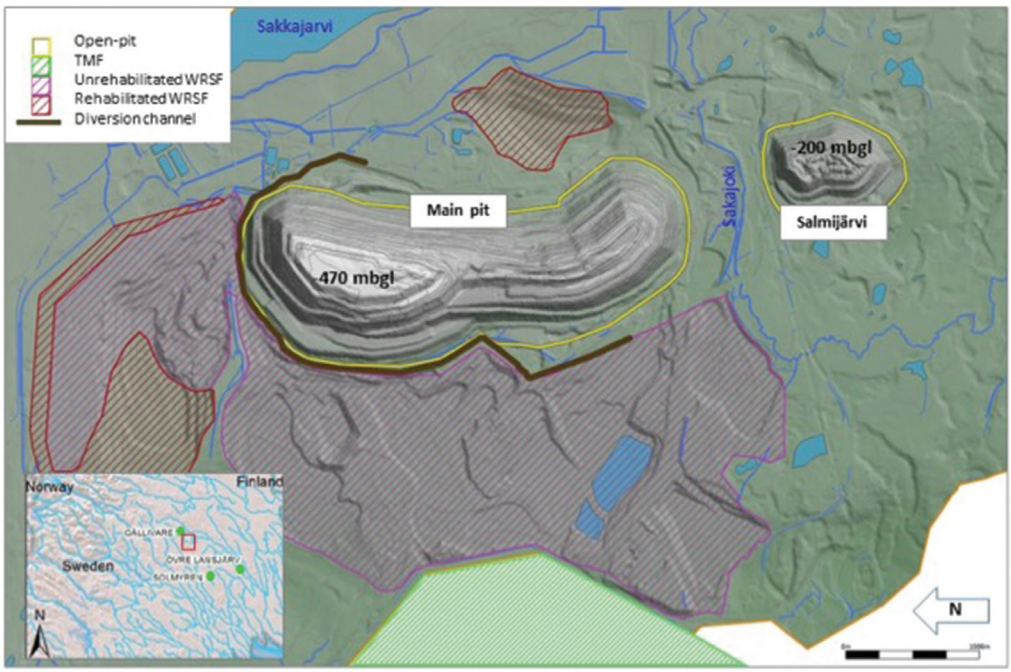

Figure 1 *Principal mine facilities and surface water hydrology (note that the mine coordinate system includes a rotation of ≈90°anticlockwise from north).*

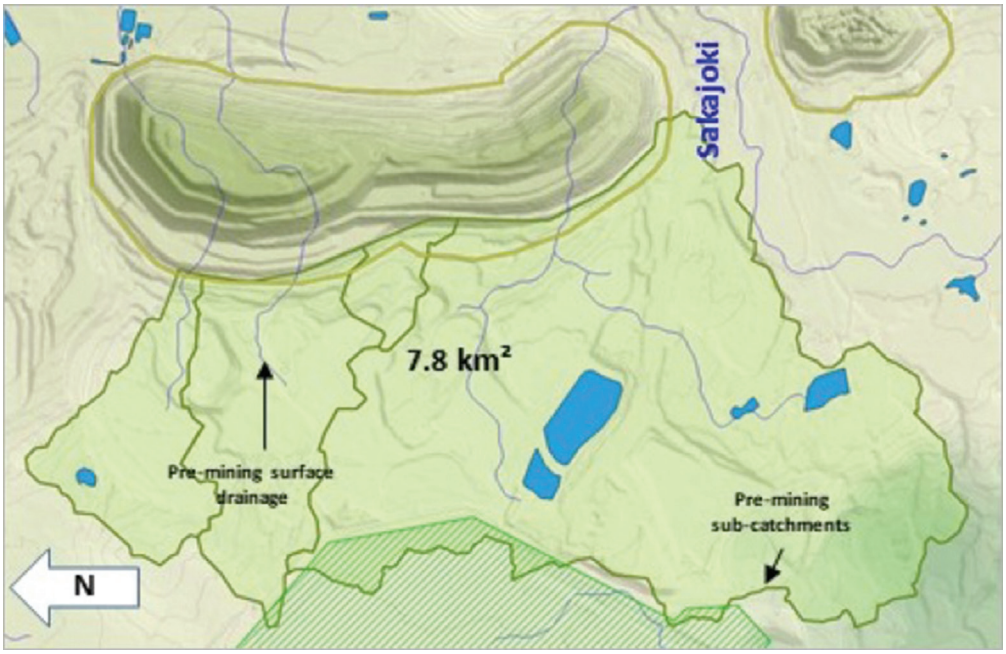

Figure 2 Pre-mining drainage system near the Main pit.

in the footwall, groundwater levels show a clear seasonal fluctuation in monitoring boreholes. There is also an overlying trend of groundwater level decrease over the period 2005–2020.

The seasonal recharge fluctuation is not perceived at the crest of the hangingwall. This suggests that the WRSFs and natural superficial deposits to the west of Main pit (hangingwall side) have a significant storage capacity which subdues the seasonal recharge signature resulting from snowmelt. Bedrock groundwater levels in the area of the WRSF also remain relatively constant. The difference of seasonal fluctuation between the footwall and hangingwall is also observed in the Vibrating Wire Piezometers (VWPs) behind the pit wall (fig. 4).

A detailed review of pore-pressures measured along the lower hangingwall indicate that VWPs mostly record a water level similar to the pit floor. Mid-slope piezometers show a downward head gradient. This is a balance between: (i) downward drainage to the pit floor and to horizontal drain holes, and (ii) continuous recharge along the crest of the wall. Piezometers in the upper wall also show a downward head gradient, but pressures are higher. This reflects on-going recharge along the crest of the hangingwall. The piezometers are mostly in steady state which reflects the sustained and on-going

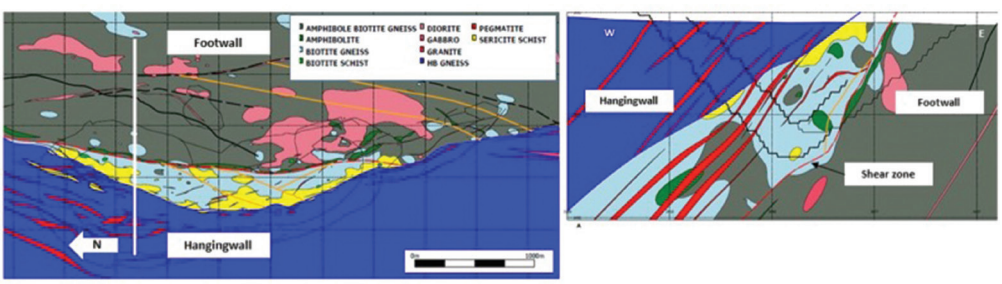

Figure 3 East-West section with the hangingwall and footwall separated by the shear zone. a) Picture taken from the south looking to the north. b) Geological model (Karlsson Peter).

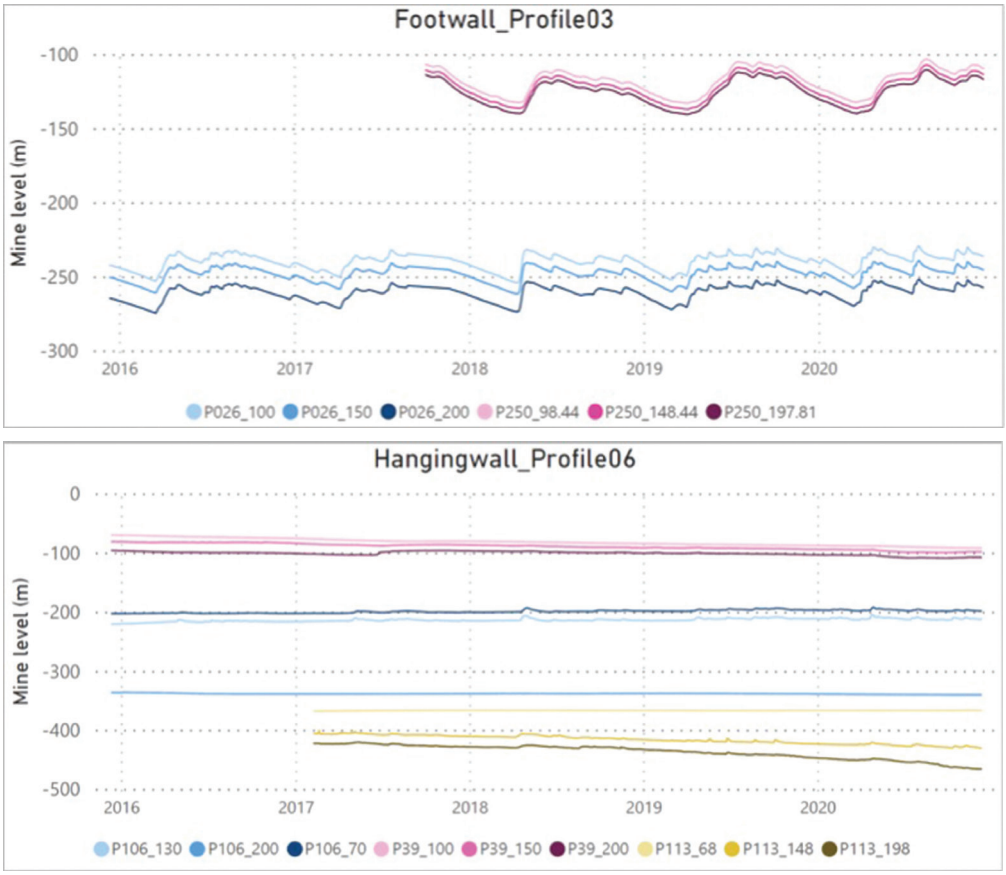

Figure 4 *Comparative response of footwall and hangingwall VWPs to seasonal recharge.*

nature of the recharge. There has been little change in pressure during the past 4 years, which reflects the relatively stable depth and areal extent of the pit over this time period.

A detailed analysis of the water balance components has been carried out to estimate groundwater inflows contributions to the Main pit. Groundwater inflows are estimated from pumping rate during the winter months, assuming that there is no surface water inflow during winter because of the low temperatures, which means the only source of inflow is groundwater. Estimated groundwater inflows range from 4,500 to 6,500 m^3/d from historical observations.

Artificial recharge and connectivity

Several campaigns of groundwater characterisation have been carried out to understand the interaction of the Main pit with the surrounding groundwater system and identify the predominant recharge components to the Main pit. A special focus has been given to the sector to the west of the Main pit with the diversion channel.

The ongoing artificial recharge from the Tailing Management Facility (TMF) and WRSFs to the west of the Main pit prevents the expansion of the area of drawdown from the pit to the west. The consulting company O'Kane (2018) estimated average annual percolation on the WRSFs (un-reclaimed, reclaimed top and reclaimed slope surfaces) through unsaturated flow modelling. It has been evaluated that WRSFs directly to the west of the main pit could receive between 55 and 60% of the mean annual precipitation (compared to 8.5% estimated from natural recharge above). The TMF is also likely to provide a substantial flow towards the Main pit. Literature review, flow rates in the collection channel, chemistry in the

groundwater around the WRSF and TMF catchments indicate that an estimated 13,825 m^3/d infiltrates from the TMF and flows towards the Main pit via the original drainage system which is a preferential pathway for the groundwater from the southwest of the mine area.

The runoff and groundwater flow in the moraine and is intercepted by a diversion channel along the pit crest of the hangingwall. The diversion channel has been constructed around the rim of the hangingwall and northern end wall. It is designed to collect seepage and runoff from the WRSF and TMF sector. However, it is identified as a feature potentially creating recharge to the underlying bedrock and to the pit crest. The flow rate gradually increases along its flow path although specific sectors lead to a local decrease in the surface flow rate, suggesting infiltration.

A detailed review of the water chemistry in different sectors of the Main pit and diversion channel has been carried (Amézquita Rico, 2019), and results are summarised as follow:

- The water quality of seepages in the upper hangingwall is very similar to water quality of the diversion channel water and the main tributary coming from beneath the dumps. Waters from the diversion channel and the seepages are acidic (pH 3.5 to 4.2). The dissolved elemental concentrations in drill holes near the pit wall and in seepages in the upper pit wall (particularly trace metal concentrations) indicate that the water in the hangingwall slope has a strong influence from the TMF.
- Samples from horizontal drains located in the lower pit wall of the western hangingwall have near-neutral pH (6.2 to 7.9) and a high alkalinity. The water quality does not indicate an influence of the diversion channel and TMF.
- A similar conclusion is obtained to the north of the Main pit in the shear zone and footwall where chemistry of seepages from horizontal drains in the lower pit wall differs significantly from the diversion channel.

The chemistry of seepages in the upper western hangingwall corresponds to a mixture of diversion channel water and waters are believed to be runoff from the dumps or infiltrated waters from the tailings.

Implications on the dewatering and depressurisation strategy

The volume of water reaching the Main pit is essentially coming from the crest of

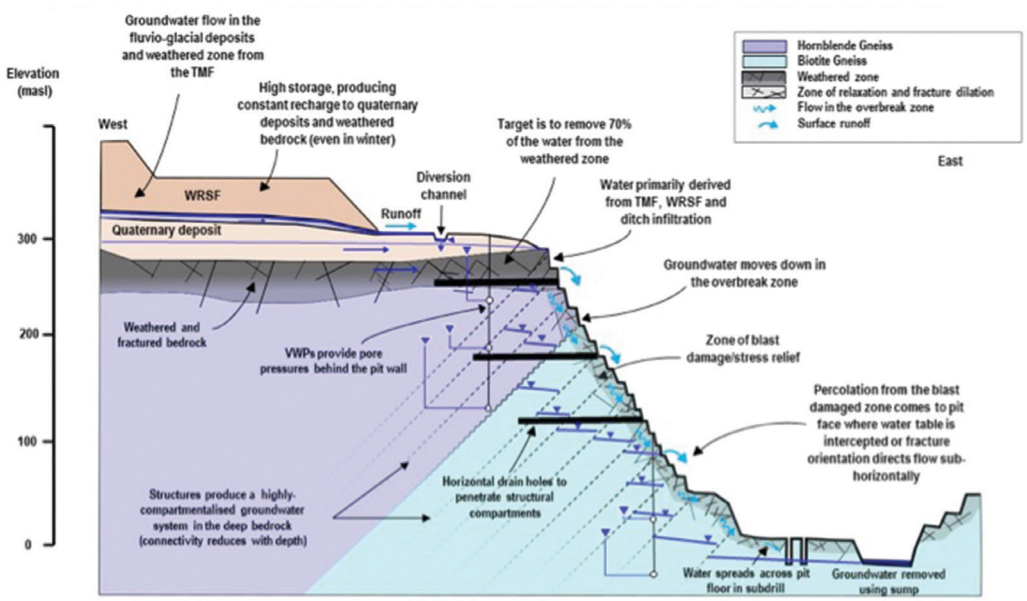

Figure 5 Conceptual section for the hangingwall.

the hangingwall. Groundwater inflow to the open-pit is not expected to increase significantly over time because the LoM plan considers mainly the excavation in a hydrogeological unit associated to a very low hydraulic conductivity.

The lower fractured and compartmentalized bedrock has shown an effective depressurisation with horizontal drains. Nevertheless, the partial interception of sub-superficial flows in the quaternary deposits and weathered bedrock by the diversion channel creates a constant recharge to the underlying units and overbreak zone at the level of the pit crest (fig. 5). The location of this recharge component at the top of the pit wall impacts the ability to achieve depressurization objectives.

A numerical model has been developed as a tool to evaluate the pore pressure distribution, and alternative dewatering and depressurisation strategies. It is used to optimize the configuration and number of horizontal drains. One of the modelling objectives is also to assess water management above the pit crest to help develop alternate strategies to intercept water before it ingresses to the open-pit. Going forward, dewatering of the pit crest and control of recharge sources to the west of the Main pit should form a key part of the future dewatering strategy.

Conclusions

The pore-pressure distribution has a major effect on the slope stability of open-pit walls. An evaluation and control of the pore-pressure distribution is only possible with a precise characterization of the groundwater system. Consequently, any field program involving water level and quality monitoring can be used to quantify source zones, pathways behind the pit-wall and magnitudes of water reaching the pit wall and floor. At Aitik, it has been found that fluvio-glacial deposits play a major role in the conveyance of water to the pit and streams have been diverted around the crest of the hangingwall and end walls and these provide on-going (year round) recharge to glacial sands and gravels around the pit area, together with seepage losses from water storage ponds, waste rock areas and other mine facilities. Water from the glacial deposits infiltrates into the bedrock particularly in areas of faulted rock and where the zone of weathering of the underlying bedrock is thinner. Much of the water moves into the overbreak (blast damaged) zone within the pit, and then allows movement of water behind the pit wall to reach the pit floor and increase the total dewatering requirements and pore pressures behind some of the slopes. Horizontal drains are installed to reduce pore pressure in the pit slopes. The effectiveness of the drains is partially reduced by the on-going flow down the over-break zone. Strategies to capture the fluvio-glacial groundwater outside of the pit, or before it can migrate through the overbreak zone, are seen to produce more tangible benefits regarding both dewatering and depressurisation objectives.

References

Amézquita Rico William Giovanny, 2019 Detailed Understanding of Water Flow Systems in the South to Western Side of Aitik Mine

Bergab, 2008. Utökad studie av hydrogeologiska konsekvenser av planerad brytning

Bergab, 2012. Hydrogeologisk utredning för två nya dagbrott

Csicsek Akos, 2016. Visualisation of structures in Aitik using Leapfrog

Golder, 1993. Efterbehandling av sandmagasin i Aitik - Hydrogeologiska förutsättningar för åtgärdsplan

Hagerdon David, 2015. Water handling in Aitik mine

Hatch, 2016. Draft Aitik Groundwater Model Report, H349861-00000-22A-066-000X

Hydrosense, 2020. Hydrogeologi Aitik – Förhållanden och förutsättningar

Karlsson Peter, 2020. Boliden Summary Report – Resources and Reserves for 2019

Obregón Castro Cynthia Lorena, 2019. Detailed Understanding of Groundwater Systems of the Northern Side of Aitik Mine – Geological/ Structural Setting and Inflow System

O'Kane, 2018. Forecasting long term water quality after closure: Boliden Aitik Cu mine

Wanhainen Christina, 2005. On the Origin and Evolution of the Palaeoproterozoic Aitik Cu-Au-Ag

Numerical Groundwater Flow Modelling in Support of Mine Water Supply in an Endoreic Groundwater System, Tasiast Mine, Mauritania

Martin Boland[1], Florent Boddaert[1], Geoff Beale[1], Glen Hein[2], Pieter Labuschagne[3], Ryan Cox[4]

[1]*Piteau Associates, Abbey Lawns, Shrewsbury, SY2 5DE, UK, mboland@pitteau.com*

[2]*Kinross Gold Corporation, Tasiast Mine, Mauritania, Glen.Hein@Kinross.com*

[3]*GCS, Kwazulu-Natal, South Africa, Pieterl@gcs-sa.biz*

[4]*Global Environmental Monitoring (GEM) Ltd., UK, rcox.gem@gmail.com*

Abstract

Tasiast Mine is located on the western margin of the Sahara Desert. Water for mine operations is supplied from a wellfield located 60 km west of the mine site and 25 km from the Atlantic coast. The wellfield abstracts highly saline water from depths of >80m. The key regulatory requirement is to show that abstraction will not impact either water supply for local communities or baseflow to ecosystems. Since 2012 a 3D numerical groundwater flow model has been used, and updated annually, as part of regulatory compliance. Unlike most groundwater systems, natural groundwater elevations at the wellfield are below mean sea level, and simulating the interaction between abstraction at the wellfield and the groundwater system at the coast is challenging, requiring the ocean to act as a recharge boundary rather than a discharge zone. Extreme evaporation rates (>4m/year), driven by constant dry offshore winds and the fine-grained nature of surface materials, means that significant amounts of groundwater are removed from depth inland due to wind-induced negative soil pressures. A 1D SEEP-W model was developed to quantify the recharge deficit developed over time in the coastal plain, together with determining the depth below which evaporation stops. These outputs were incorporated into a 2D numerical model transect, representing 5km of the coastal plain, which determined the interaction between sea water intrusion and evaporation. The 2D model shows that evaporation efficiently removes water from the system, with pseudo steady-state conditions being achieved after 1,200 years of simulation. Evaporation from the coastal plain becomes the dominant driver within the local water balance, with the upward flux from the coastal flats balancing the inflow rate from the ocean. From the initial head distribution, groundwater levels quickly drop below sea water level due to evaporation. Deeper groundwater levels occur at greater distances from the coast, where the influence of sea water intrusion decreases. Modelled groundwater levels reached equilibrium after ≈2,000 years which is consistent with the period (<2.5k BP) since hyper arid conditions are considered to have developed in the wellfield area. The modelling demonstrates that natural below sea level piezometric levels result from high vertical flow (evaporation) which is not compensated by horizontal flow either from the ocean, or aquifer units to the east. The modelling approach has had regulator acceptance and maintained confidence in the ability of the 3D groundwater model to simulate the complex groundwater system and underpin predictive simulations of wellfield operation

Keywords: Endoreic Basins, Evapotranspiration, SEEP-W Modelling

Introduction

The Tasiast Mine is an open pit gold mine operation located in the Inchiri Wilaya region of Mauritania, approximately 280 km to the northeast of the capital city of Nouakchott. Water for mine operations is supplied from the Sondage wellfield which is located 60 km to the west of the mine site and 25 km to the east of the Atlantic coast. The wellfield lies 5 km from the western boundary of the Parc National du Banc d'Arguin (PNBA), a national park designated by UNESCO as a World Heritage site for its marine and coastal environments. Although the wellfield is located at a considerable distance from the mine site, it was selected as the mine water supply due to the fact that it is a highly saline water body present at depths of >80m below ground level, and was therefore neither of use as a potential water supply for local communities nor provides baseflow to any surface drainages or ecosystems.

The wellfield currently comprises 44 operational abstraction wells, oriented approximately north-south over a distance of about ≈20km, with the saline water transmitted the 60km to the mine site via three pipelines. Approximately 15 wells are operated at any one time, with the location of these wells being moved around the wellfield according to an operational plan, which is reviewed every 3 months. The aim of varying the location of operating wells is to ensure that abstraction is evenly distributed across the full area of aquifer covered by the wellfield. The Sondage is currently licensed to abstract a daily volume of 30,000 m^3 to the end of December 2034. To date, the daily abstraction rate has averaged between 8,000 and 13,500 m^3, with a maximum daily rate of about 24,500 m^3/d being recorded in 2012. The average abstraction rate during Q4 2020 was 13,279 m^3/d.

Groundwater is abstracted from a 5-10 m thick semi-confined sand layer, further details of which are provided below. Mean annual rainfall in the region averages about 100 mm, while the mean annual potential evaporation is 1-2 orders of magnitude greater at about 4000 mm.

A numeric groundwater flow model has been developed in order to assess the potential extent of drawdown related to wellfield operation that may develop over the period of the license (through to 2034). The model is used to assess both potential impacts to fresh water aquifers located to the north and south of the wellfield, as well as potential impacts to important ecological receptors in the Parc National du Banc d'Arguin (PNBA) west of the wellfield.

In order to replicate the baseline condition that pre-Sondage water levels were below sea level, the model was originally set up with a constant head boundary (CHB) set at -6 masl at a distance of approximately 6km inland from the coast. As part of a subsequent third party review of wellfield operation it was requested that the regional numerical model be modified so that the CHB was set at 0 masl along the coast. This change was aimed at allowing the model to simulate drawdown to the coast, and therefore predict whether any impact may occur within the PNBA, including to the coastal elements of the park. This paper details how these changes have been incorporated within the groundwater modelling approach.

Hydrogeology

Amended NAG test

The Sondage wellfield abstracts saline groundwater from a series of sand layers that occur near the base of the Continental Terminal sedimentary sequence. The sand layers form an aquifer unit which is about 5-10 m in thickness, and occurs at a depth of about 80 m below ground surface in the area of the wellfield. The sand unit is overlain by a series of interbedded low permeability sands, silts and clays, also assigned to the Continental Terminal sequence, and which form a semi-confining layer to the aquifer unit. These overlying sediments produce little water during drilling of boreholes, however downward leakage is expected to provide recharge to the underlying aquifer.

The entire sedimentary sequence dips to the west and is present at a progressively greater depth westwards under the Banc

d'Arguin national park (PNBA). The sedimentary sequence is underlain by crystalline basement rocks.

Figure 1 shows a west-east section that illustrates the conceptual hydrogeological model.

The depth of the water table in the area of the Sondage is approximately 36-46 m below ground level, which is approximately 4 to 6 meters below mean sea level. This is consistent with the below mean sea level groundwater levels reported from other areas of the Coastal Terminal sequence in northwest Mauritania (IWACO 1995).

The origins of these coastal depressions in piezometric elevation (referred to as endoreic basins) which are present in Saharan Northern Africa have been described in a number of scientific papers since the 1960s (Achambault 1960). Models for the development of these basins, which are found from the Atlantic coasts of Mauritania and Senegal to inland regions of Mali and Chad, include sea level change, evapotranspiration, over abstraction, geological subsidence and drainage to deeper aquifers.

In coastal zones, the development of these inland hydraulic gradients promotes the intrusion of saline marine waters and the potential for salinization of potable water. This potential impact has led to considerable research being undertaken on the Trarza aquifer (part of the Continental Terminal Aquifer) in Mauritania, which supplies drinking water to Nouakchott from the Idini wellfield (Aranyossy and Ndiaye 1992, Lacroix and Semega 2005 and Mohamed *et al* 2014). Studies of water levels, isotopes and mathematical modelling all confirm the importance of evaporation in the maintenance of these depressions, with Lacroix and Semega (op cit) proposing that the endoreic conditions in the Trarza aquifer developed subsequent to the sea level rise which began 18k years BP and which reflect the fact that steady state conditions relative to current sea level may have still not developed.

Under natural conditions in these basins groundwater is removed through evaporation, with this process operating most effectively along the coastal area where saturated groundwater occurs close to the ground surface. The very high average evaporation rate (>4m/year) found inland, and which is driven by the constant dry offshore winds and the fine-grained nature of the shallow materials, means that significant amounts of groundwater may be removed from depth further inland as a result of wind-induced negative soil pressures and upward unsaturated groundwater gradients.

TDS concentrations reported from wells located in the coastal plain west of the Sondage range from about 100,000 to 140,000 mg/L. These data illustrate the effect of the evapo-concentration that occurs within the coastal plain (sabkha) zones, resulting in salinity values that are significantly higher than both seawater (≈ 25,000 mg/L) and TDS values measured at the Sondage (16,000 to 50,000 mg/L).

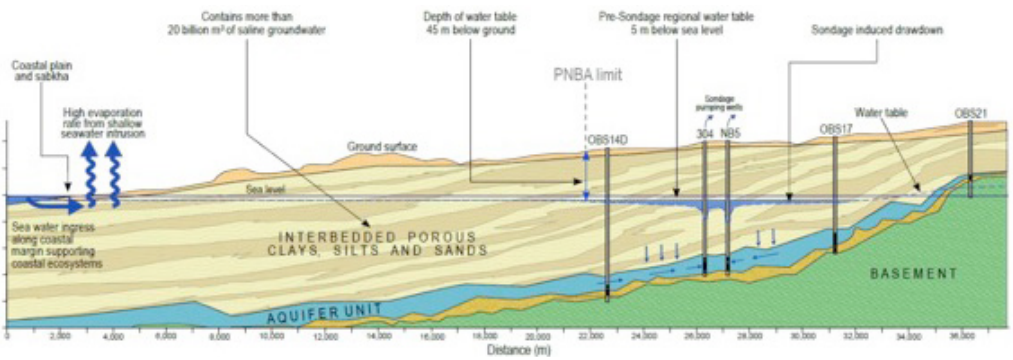

Figure 1 *Conceptual cross section of the hydrostratigraphic units and flow mechanisms controlling groundwater elevations in the Sondage and PNBA area.*

The sabkhas developed in the coastal plain are sustained by periodic flooding by extreme high tides, with the infiltrated sea water being evaporated from shallow depths and resulting in deposition of concentrated salt deposits (Figure A2). This groundwater near the coast, containing TDS concentrations significantly higher than sea water, will act as a recharge boundary to the inland basin where regional groundwater elevations sit below sea level.

Numerical modelling of the sabkha groundwater system

A variably saturated flow model was developed to simulate the impact of evaporative losses on groundwater levels in the coastal flats and sabkhas present the coastal margin of the PNBA. The numerical modelling allows the influence on groundwater elevation of each component of the water balance (sea water intrusion, evapotranspiration, recharge, groundwater flow) to be evaluated, and the development of natural below sea level groundwater elevations, as seen in the monitoring network associated with the Sondage, to be assessed. This detailed modelling was then used as the basis for updating how the coastal plain is simulated in the regional groundwater model.

The conceptual model of processes controlling the formation and maintenance of the coastal sabkha groundwater system was combined with meteorological data derived from the Mauritanian national weather station network to undertake 1D SEEP-W modelling of the recharge deficit that will accumulate over time in the coastal plain, together with the determination of the extinction depth that will develop within the coastal plain deposits. The outputs from the 1D modelling study were then incorporated into a 2D model section across the coastal plain, which was used to evaluate lateral and vertical flows; in particular the influence of sea level as a constant head boundary to the groundwater system. The results of this coastal modelling study were then used to underpin how both evaporation and the presence of the ocean was incorporated into the regional 3D groundwater flow model.

The model outputs show that evaporation removes water efficiently from the system in the first 50 years of simulation. Pseudo steady-state conditions are subsequently achieved after 1200 years of simulation. Contours of total pressure head simulated in the model after 2000 years are shown in Figure 6-7 and demonstrate that evaporation from the coastal plain becomes the dominant driver within the local water balance, with the upward flux from the sabkha/coastal flats eventually balancing the inflow rate from the constant head boundary.

The numerical modelling of the coastal plain hydrogeological system demonstrated that groundwater elevations decrease to greater than -5 (masl) at a distance of 5 km inland from the coast, as evaporation exceeds

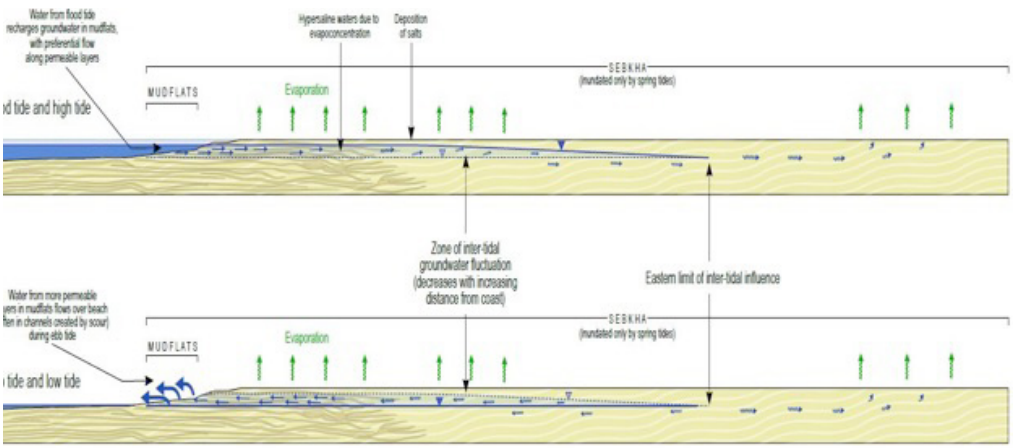

Figure 2 *Schematic cross section of the interaction of tidal flooding and sea water intrusion in the coastal plain of the PNBA.*

the rate of sea water ingress to the system. This is consistent with observed conditions in the region, as well as the extinction depth of 6-10 m which the 1-D numerical modelling predicted for evaporation in the tight soils in the area. This range of values is in accordance with literature values (Shah *et al*). Figure A2 also illustrates the self-buffering nature of the groundwater system. Any fall in groundwater levels inland of the coast would result in reduced evaporation which, in turn, would naturally mitigate the drawdown.

Based on the results of the coastal model and the review of antecedents, it is demonstrated that the natural distribution of piezometric levels below sea level is the result of high vertical flow (evaporation) which is not compensated by horizontal flow, either from the sea to the west or ny inflow from aquifer units along the other boundaries of the model. The boundary condition is assigned with a potential evapotranspiration equivalent to 2.500 mm/yr in the entire area of the regional flow model. A review of regional meteorological station data shows this value to be equivalent to the potential evaporation (PE) value at the coast (where humidity may be high) and to be considerably less than inland values which are measured at >4,500 mm/yr. Based on the results of the coastal model, the extinction depth in the regional model (below which evaporation is effectively zero) is fixed to 7.5 m.

Calibration of the regional numerical flow model

The extent of the regional impact assessment groundwater flow model was defined so that it covers the Sondage wellfield and its potential wider area of influence, and ensures that the edges of the model do not influence the results of the model during the simulation. The model area is equivalent to 15,819 km² and the entire inland area of the PNBA is included in the model domain. The model domain includes the Boulanouar and Benichab wellfields, which provide potable water supply to the cities of Nouakchott and Nouadhibou. Extending the model to include these areas allows regional groundwater level data provided by the Centre National de Resource d'Eau (CNRE) to be incorporated in the model.

A steady state calibration was established using data from both the Sondage and the regional data obtained from the CNRE. A transient calibration of the model, covering the period 2007 through Q1 2019, was then carried out using the measured abstraction rates from both the Sondage wellfield, and the local community abstractions at Chami and Wad Chebka.

Residuals indicate a highly successful calibration, with all but a few locations exhibiting residual errors in the +5 to -5% range.

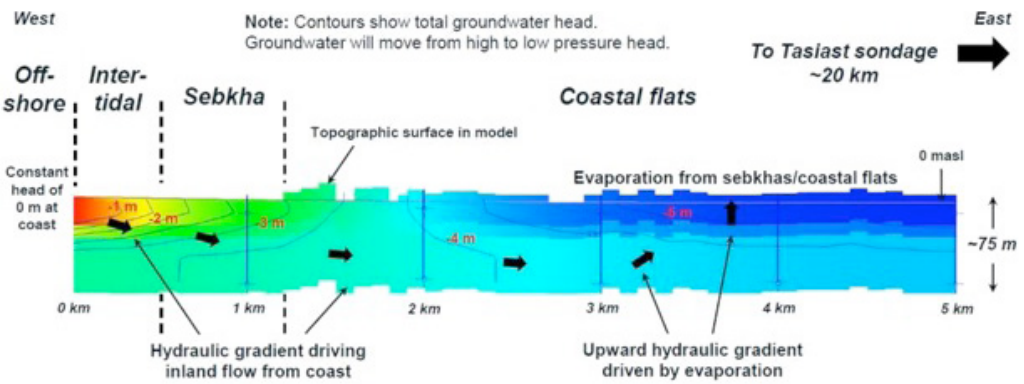

Figure 3 *Modelled groundwater pressure head beneath coastal plain in PNBA.*

The calibrated transient model was then used to run a series of predictive future simulations, including a conservative simulation based on the Sondage wellfield abstracting at the maximum permitted rate of 30,000 m^3/d through to the end of 2034. The model simultaneously simulated an increasing abstraction from the community wells at both Chami and Wad Chebka, to reflect the potential for population growth in both communities, coupled with a period of no groundwater recharge occurring during the entire simulation period.

Along the eastern boundary of the PNBA the most conservative model predicts that the water table will fall from 38.5 mbgl at present to 42.6 mbgl (in 2034). The simulated drop in the water table decreases going to the west (beneath the PNBA) and does not extend within 12 km of the coastal plain. The potential amount of evaporation along the coast is about 50 times greater than the permitted abstraction of the Sondage and therefore abstraction at the Sondage wellfield will not influence groundwater levels along the coast. In addition the updated model predicted, for all simulated cases, that Sondage abstraction would have no potential impacts on the "fresh" water zones to the north and south of the Sondage.

Conclusions

The model shows good calibration to the extensive database of well levels and pumping volumes to date. The model also replicates the condition, observed in the field, whereby groundwater levels in the area are naturally 4-6 m below sea water level. The model scenarios were run based on the highly conservative assumption that future abstraction would immediately occur at the maximum licensed rate of 30000 m3/d, and which is in fact more than twice the current abstraction rate. Even under this conservative approach the predictive model shows that drawdown will not affect water levels in community wells located to the north and south of the wellfield; and would therefore also not impact on the urban wellfields of Boulanouar and Benichab which are located further afield, and neither will the drawdown affect groundwater levels at the coast inside the PNBA. The current Life of Mine for the Tasiast operations is 2035. Given this relatively short timeframe for ongoing operation of the wellfield the groundwater flow model has not been run to date to simulate potential impacts associated with climate change. However the increased frequency of flooding of the coastal plain that should occur in response to rising sea levels should result in a shallower groundwater table inland from the coast, with the result that the area of drawdown associated with the wellfield will be reduced even further.

Acknowledgements

The authors thank all Tasiast staff for their support in the monitoring and management of the Sondage wellfield, and provision of the data which supported this study.

References

Aranyossy, J.F. and Ndiaye, B. 1992 Etude et modelisation de la des depressions piezometriques en Afrique sahelienne Revue des Sciences de l'eau 6, 81-96.

Archambault, J. 1960 Les eaux souterraines de l'Afrique occidentale. Berger-Levrault pp139 IWACO 1995 Etude des ressources en eau de la zone Nouakchott-Nouadhibou.

Lacroix, M. and Semega, B. 2005 Genesis of an endoriec piezometric coastal depression in sub-Sahelian West Africa: the Continental Terminal Aquifer of Trarza (Mauritania) Geodinamica Acta 18/5 389-400.

Mohamed, A.S., Marlin, C., Leduc, C. and Jiddou, M. 2014 Modalites de recharge d'un aquifer en zone semi-aride:cas de la nappe du Trarza (Sud-Ouest Mauritanie) Journal des Sciences Hydrologiques 59 (5) 1046-1062.

Shah, N, Nachabe, M. and Ross, M. 2007 Groundwater 45 (3) 329-338.

Numerical Modelling of Mine Pollution to Inform Remediation Decision-making in Watersheds

Patrick Byrne[1], Patrizia Onnis[1,2], Robert L. Runkel[3], Ilaria Frau[1], Sarah F. L. Lynch[4], Aaron M. L. Brown[5], Iain Robertson[5], Paul Edwards[6]

[1]*Liverpool John Moores University, School of Biological and Environmental Sciences, Liverpool L3 3AF, UK, p.a.byrne@ljmu.ac.uk*

[2]*Environment & Sustainability Institute and Camborne School of Mines, University of Exeter, Penryn TR10 9FE, UK*

[3]*U.S. Geological Survey, Denver Federal Center, P.O. Box 25046, Mail Stop 415, Denver, Colorado 80225, United States*

[4]*AECOM, Ground, Energy and Transactions Solutions (GETS), New York Street, Manchester M1 4HD, UK*

[5]*Department of Geography, Swansea University, Swansea SA2 8PP, UK*

[6]*Natural Resources Wales, Swansea University, Singleton Park, Swansea SA2 8PP, UK*

Abstract

Prioritisation of mine pollution sources for remediation is a key challenge facing environmental managers. This paper presents a numerical modelling methodology to evaluate potential improvements in stream water quality from remediation of important mine pollution sources. High spatial resolution synoptic sampling data from a Welsh watershed were used to calibrate the OTIS solute transport model. Simulation of mine pollution remediation scenarios using OTIS revealed decreases in stream Zn concentrations between 9% and 62% under mean streamflow conditions. Remediation scenarios under low streamflow conditions were less effective (<1% to 17% decrease in Zn concentrations), due to diffuse and metal-rich groundwater inflows.

Keywords: OTIS, Mine Pollution, Remediation, Water Quality, Synoptic Sampling

Introduction

In the United Kingdom (UK), millennia of metal mining have produced substantial quantities of mine wastes that contaminate approximately 2800 km of watercourses (Johnston *et al.* 2008). Pollution from abandoned metal mines is recognised as a major cause of failure to achieve environmental objectives set out in statutory River Basin Management Plans (RBMPs) (Jarvis and Mayes 2012). As such, identification and prioritisation of mine pollution sources for remediation is one of the major challenges facing environmental managers.

In UK watersheds, potential improvements in stream water quality from remediation or treatment of mine pollution sources are evaluated using a mass balance approach (Jarvis and Mayes 2012). Under the approach, metal loads from point sources of pollution (e.g. drainage adits or tributary inflows) are subtracted from a total watershed metal load (calculated downstream from all known mine workings) to simulate the remediation of the point sources. However, there are two key limitations to this approach that may affect the efficacy of remediation and compliance with the mine pollution reduction targets set out in RBMPs. First, metal loading data from diffuse pollution sources are generally not available, therefore mass balance modelling of water quality improvements are limited to evaluation of point source remediation only. Second, the mass balance approach does not consider natural attenuation of metal pollutants by instream chemical reactions (e.g. first order decay processes such as sorption and precipitation). As mine pollutants in UK watersheds (Zn, Pb, Cd) generally behave in a non-conservative manner (Jarvis *et al.* 2019, Byrne *et al.* 2020), neglecting chemical reactions may over- or underestimate the effects of remediation on stream water quality.

The primary aim of this research was to demonstrate a modelling methodology that overcomes these limitations and allows environmental managers to evaluate potential water quality improvements from different remediation strategies in mined watersheds. Further details on the methodology and results are described in Byrne *et al.* (2020).

Methods

Synoptic Sampling

Working in the heavily mined (primarily Pb and Zn) Nant Cwmnewyddion watershed in central Wales, we conducted tracer dilution and synoptic sampling (multiple water quality samples collected across a watershed under steady-state flow conditions) experiments under mean (Q45) and extremely low (Q99) streamflow conditions in July 2016 and July 2018, respectively. A concentrated sodium bromide (NaBr) solution was injected into the stream during both experiments and allowed to reach plateau concentrations over the 2.5 km study reach. Synoptic sampling was then carried out at 25 stream sites and 18 inflow sites in 2016, and at 31 stream sites and 6 inflow sites in 2018. Bromide concentrations (filtered at 0.45 μm) were determined by ion chromatography, and Zn concentrations (filtered at 0.45 μm, acidified) were determined by inductively coupled plasma mass spectroscopy. As Br is considered to behave in a conservative manner in circum-neutral streams like the Nant Cwmnewyddion (Dzombak and Morel 1990), the observed dilution of Br was used to estimate streamflow at all stream sample sites using the tracer-dilution method (Runkel *et al.* 2013). Further details on the methodological approach can be found in Byrne *et al.* (2020).

Numerical Modelling

Zinc concentration and streamflow data from the synoptic sampling campaigns were used to calibrate the OTIS (One-dimensional Transport with Inflow and Storage) solute transport model (Runkel 1998). The OTIS model has been widely used to simulate hydrologic and geochemical processes in streams (Runkle 2007); however, application of the steady-state model to simulate watershed processes is rare.

There are four steps involved in the OTIS modelling process (Walton-Day *et al.* 2007). Physical transport parameters (dispersion coefficient (D); stream cross-sectional area (A); storage zone cross-sectional area (AS); storage zone exchange coefficient (α)) were determined from Br breakthrough curves at three 'transport sites' and from field measurements at a fourth transport site (**STEP 1**). OTIS models for filtered Zn in 2016 (Q45) and 2018 (Q99) were then calibrated assuming conservative transport. In this study, conservative transport assumes no removal of metal species from solution by sorption or precipitation processes. The study reach was first subdivided into twenty-four (2016) and thirty (2018) sub-reaches to bracket the location of synoptic samples. Then, lateral inflow concentrations (the difference in streamflow between the downstream ends of adjacent model reaches divided by the distance between the downstream ends of the model reaches) were estimated for each model sub-reach by using either sampled inflow concentrations or effective inflow concentrations. Effective inflow concentrations represent the mean dissolved Zn concentration entering a stream segment under the assumption of conservative transport, and may be developed using simple mass balance calculations on individual stream segments (Kimball *et al.* 2002). If the simulated Zn concentration profiles (assuming conservative transport) plotted above the observed Zn concentration profiles, reactive (non-conservative) transport was assumed (**STEP 2**). Simulation of non-conservative transport was then conducted by estimating first-order removal coefficients (λ) using non-linear least squares regression in OTIS-P (Runkel 1998) (**STEP 3**). Once calibrated, simulation of remedial alternatives was achieved by changing the lateral inflow concentrations of different mine pollution source areas to mimic potential remediation scenarios (**STEP 4**).

Remediation scenarios assumed a 94% reduction in inflow or source area filtered Zn concentrations, which is comparable with other mine pollution treatment schemes in the UK (Stanley 2020). The remediation

scenarios simulated in this study, and based on consultation with the environmental regulator (Natural Resources Wales), included reductions in Zn from Wemyss Mine and Frongoch Adit and an aggregate of both sources.

Results and Discussion

Stream Chemistry and Streamflow

Zinc exceeded regulatory standards (15 µg L^{-1}) along the entire study reach and under both streamflow conditions (fig. 1). Stream Zn concentrations varied between 40 µg L^{-1} and 2901 µg L^{-1} under Q45 flow conditions (fig. 1a). Inflow concentrations from Mill Race Stream (4997 µg L^{-1}), which drains Wemyss Mine, and Frongoch Adit (3907 µg L^{-1}) appeared to be the main drivers of increased stream Zn concentrations. However, high Zn concentrations (maximum = 8514 µg L^{-1}) were also observed in several narrow diameter pipes draining the left bank of the stream opposite Graig Goch Mine. Stream Zn concentrations were substantially higher under Q99 flow conditions, varying between 18 µg L^{-1} and 8146 µg L^{-1} (fig. 1b). Increases in stream concentrations again appeared to be related to surface inflows from Mill Race Stream (5825 µg L^{-1}) and Frongoch Adit (9000 µg L^{-1}). A substantial increase in stream Zn concentrations was observed opposite Graig Goch Mine. However, only one of the drainage pipes (7358 µg L^{-1}) adjacent to Graig Goch Mine was flowing under Q99 flow conditions, and the negligible loading from this pipe cannot account for the observed increase in stream concentrations.

Streamflow at the end of the study reach was 27.5^{-1} s^{-1} under Q99 flow conditions compared to 203 L s^{-1} under Q45 flow conditions (see Byrne *et al.* 2020). Frongoch Adit (mine water) was the largest contributor to overall streamflow under Q45 (12%) and Q99 (35%) flow conditions. However, streamflow increases in the reach next to Graig Goch Mine accounted for 12% and 29% of total streamflow under Q45 and Q99 flow conditions, respectively (Byrne *et al.* 2020). In the absence of surface tributary inflows in this reach (flow from the narrow diameter pipes was negligible), these data indicate

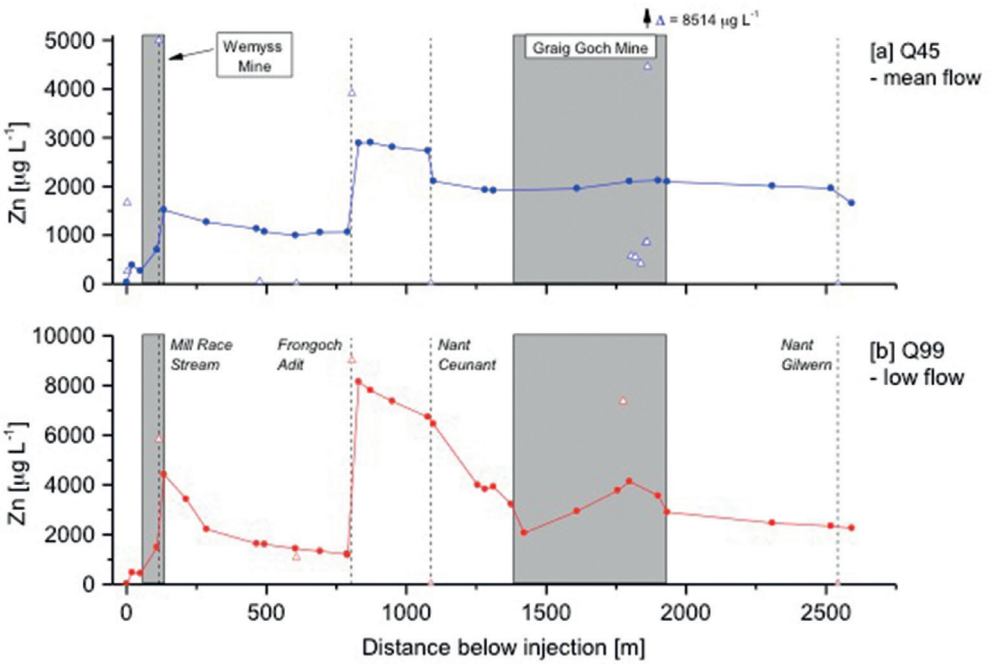

Figure 1 *Filtered Zn concentrations (circle = stream, triangle = inflow) under Q45 (mean flow) (a) and Q99 (low flow) (b) streamflow conditions in the Nant Cwmnewyddion. The locations of streamside mine wastes are indicated by grey boxes and labelled in (a). Major inflows (mine water and tributary) are indicated as dashed vertical lines and labelled in (b).*

diffuse groundwater was contributing to the increased streamflow in this reach. Zinc loads from this reach accounted for 20% and 31% of the total stream Zn load under Q45 and Q99 flow conditions, respectively.

OTIS Modelling

Initial conservative model simulations under Q45 streamflow conditions showed close correspondence between the simulated and observed Zn concentration data (fig. 2a). This indicates chemical (non-conservative) attenuation processes (e.g. sorption and precipitation) were relatively unimportant, and Zn was transported largely as a conservative solute. However, conservative model simulations under Q99 streamflow conditions showed the simulated data plotted above the observed Zn concentration data (fig. 2b), indicating removal of Zn by chemical reactions was important under extreme low flow conditions. Subsequent reactive (first-order decay) modelling demonstrated good fits with the observed Zn concentration data under both streamflow conditions.

Simulation of three mine site remediation scenarios (1. Wemyss Mine; 2. Frongoch Adit; 3. Wemyss Mine and Frongoch Adit) indicated variable improvements in stream water quality under different streamflows, and under different remediation scenarios (fig. 3). Under both streamflow conditions, the optimal scenario was remediation of both Wemyss Mine and Frongoch Adit, which achieved a 62% and 17% reduction in filtered Zn concentrations under Q45 and Q99 streamflows, respectively. However, it must be noted that remediation of Frongoch Adit alone could achieve similar improvements in stream water quality (52% and 16% reduction in filtered Zn under Q45 and Q99 conditions, respectively), primarily due to the large Zn loading from Frongoch Adit and that much of the filtered Zn originating from Wemyss Mine is removed by instream chemical reactions upstream from Frongoch

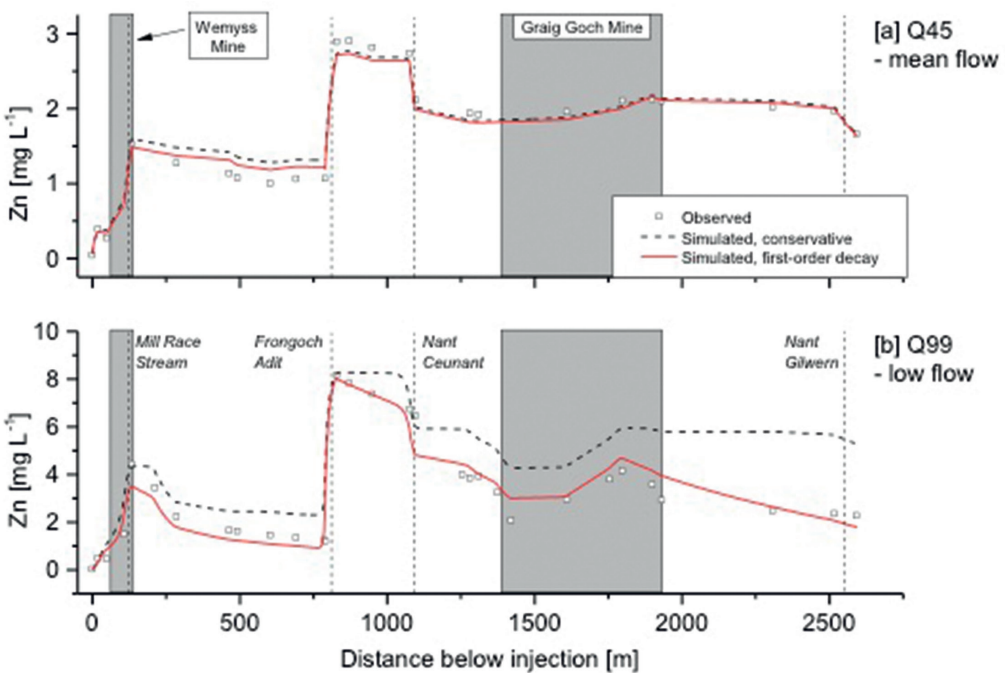

Figure 2 *Observed filtered Zn concentrations (squares), and simulated conservative (dashed line) and reactive (first-order decay)(red line) Zn concentrations under Q45 (mean flow) (a) and Q99 (low flow) (b) streamflow conditions in the Nant Cwmnewyddion. The locations of streamside mine wastes are indicated by grey boxes and labelled in (a). Major inflows (mine water and tributary) are indicated as dashed vertical lines and labelled in (b).*

Adit. It is noticeable also that the simulated reductions in filtered Zn concentrations were substantially lower under Q99 flow conditions. This is most likely due to high Zn concentration water entering the stream along an approximately 600 m length of the channel adjacent to Graig Goch Mine. Under Q99 flow conditions, this Zn-rich water is not diluted to the same extent as under Q45 flow conditions; and therefore, the effect on stream water quality and remediation efficacy is more severe.

Conclusions

This study demonstrates how numerical modelling of solute transport in mined watersheds can be used to simulate potential stream water quality improvements from different hypothetical mine site remediation alternatives. The OTIS model, calibrated with hydrological and Zn concentration data from synoptic sampling campaigns, simulated stream Zn reductions ranging from <1% to 62%, depending on the streamflow and the remediation scenario. Once calibrated, the OTIS model can easily simulate remediation of multiple sources of mine contamination across a watershed.

This study also demonstrates the importance of considering diffuse sources of mine contamination and reactive transport of solutes when simulating potential water quality improvements from different remediation approaches. OTIS simulations revealed how remediation of a single mine contamination source (Frongoch Adit) could yield similar water quality improvements to remediation of more than one source (Frongoch Adit and Wemyss Mine), due to in-stream attenuation of much of the Zn loading from one of the sources (Wemyss Mine). Furthermore, simulations of Zn concentrations under Q99 low flow conditions revealed remediation could be less effective than under Q45 mean flow conditions, largely due to untreated Zn-rich

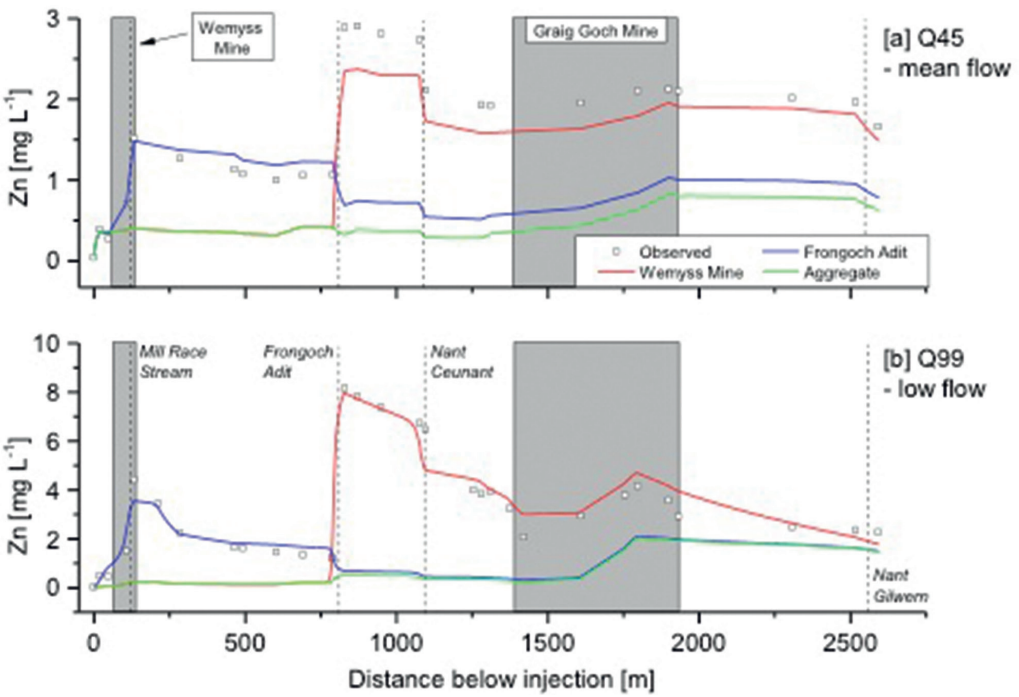

Figure 3 *Observed (squares) and simulated filtered Zn concentrations under Q45 (mean flow) (a) and Q99 (low flow) (b) streamflow conditions in the Nant Cwmnewyddion. Three different remediation scenarios are considered: Wemyss Mine (red line), Frongoch Adit (blue line), and an aggregate of Wemyss Mine and Frongoch Adit (green line). The locations of streamside mine wastes are indicated by grey boxes and labelled in (a). Major inflow (mine water and tributary) are indicated as dashed vertical lines and labelled in (b).*

water entering the system via diffuse subsurface pathways adjacent to Graig Goch Mine.

In many global regions, climate change is expected to increase the frequency and magnitude of flow extremes (low and high) in watersheds (Arnell *et al*. 2013). In temperate regions like the UK, this shift in hydrological regime is likely to increase the importance of diffuse contamination sources (Arnell *et al*. 2015), which may include runoff and erosion of surface mine wastes during high flows and contaminated groundwater efflux during low flows. Therefore, monitoring and modelling methodologies that consider diffuse sources of mine contamination will be needed by environmental managers to mitigate mine contamination in the future. Ongoing research in UK watersheds is focussed on simulation of solute transport and remediation effectiveness over a greater range of streamflows, and in particular during Q10 (high flow) events.

Acknowledgements

The authors thank the organisers and hosts of the IMWA2021 Conference, in addition to the anonymous reviewers of this manuscript, whose comments have been valuable during the peer-review process. This research was funded by the UK Natural Environment Research Council (grant NE/S009507/1). Funding for R.L.R. was provided by the U.S. Geological Survey, Toxic Substances Hydrology Program. Any use of trade, firm, or product names is for descriptive purposes only and does not imply endorsement by the U.S. Government.

References

Arnell NW, Gosling SN (2013) The impacts of climate change on river flow regimes at the global scale. J Hydrol 486:351-364

Arnell NW, Halliday SJ, Battarbee RW (2015) The implications of climate change for the water environment in England. Prog Phys Geogr 39:93-120

Byrne P, Onnis P, Runkel RL, Frau I, Lynch SFL, Edwards P (2020) Critical shifts in trace metal transport and remediation performance under future low river flows. Environ Sci Technol 54:15742-15750

Dzombak DA, Morel FMM (1990) Surface complexation modelling: Hydrous ferric oxide. John Wiley & Sons, New York

Jarvis AP, Davis JE, Orme PHA, Potter HAB, Gandy CJ (2019) Predicting the benefits of mine water treatment under varying hydrological conditions using a synoptic mass balance approach. Environ Sci Technol 53:702-709

Jarvis AP, Mayes WM (2012) Prioritisation of abandoned non-coal mine impacts on the environment: Future management of abandoned non-coal mine water discharges. Science Project SC030136/R2. Environment Agency, Bristol

Johnston D, Potter H, Jones C, Rolley S, Watson I, Pritchard J (2008) Abandoned mines and the water environment. Science Project SC030136-41. Environment Agency, Bristol.

Kimball BA, Runkel RL, Walton-Day K, Bencala KE (2002) Assessment of metal loads in watersheds affected by acid mine drainage by using tracer injection and synoptic sampling: Cement Creek, Colorado, USA Appl Geochem 17:1183-1207

Runkel RL (1998) One-dimensional transport with inflow and storage (OTIS): A solute transport model for streams and rivers. U.S. Geological Survey, Denver, Colorado

Runkel RL (2007) Towards a transport-based analysis of nutrient spiralling and uptake in streams. Limnol Oceanogr Methods 5:50.62

Runkel RL, Walton-Day K, Kimball BA, Verplanck PL, Nimick DA (2013) Estimating instream constituent loads using replicate synoptic sampling, Peru Creek, Colorado. J Hydrol 489:26-41

Stanley P (2020) Personal communication, 18 May

Walton-Day K, Paschke SS, Runkel RL, Kimball BA (2007) Using the OTIS solute-transport model to evaluate remediation scenarios in Cement Creek and the Upper Animas River. In: Church SE, Von Guerard P, Finger SE (eds) Integrated Investigations of Environmental Effects of Historical Mining in the Animas River Watershed, San Juan County, Colorado. U.S. Geological Survey, Denver, Colorado

Using Coal Combustion Residues for Abandoned Coal Mine Reclamation

Chin-Min Cheng[1], Tarunjit Butalia[1], Robert Baker[1], Justin Jent[2], William Wolfe[1]

[1]*Department of Civil, Environmental and Geodetic Engineering, The Ohio State University, 470 Hitchcock Hall, 2070 Neil Ave., Columbus, OH 43210, U.S.A.*

cheng.160@osu.edu; butalia.1@osu.edu; baker.1549@osu.edu; Wolfe.55@osu.edu

[2]*American Electric Power, 1 Riverside Plaza, Columbus, Ohio 43215, U.S.A, Jent@aep.com*

Abstract

Two full-scale demonstration projects using coal combustion residues (CCRs) to reclaim abandoned mines were carried out near the Conesville and Cardinal coal-fired power plants located in eastern Ohio. Water quality data collected over a ten-year period from 2010 to 2020 were analysed to assess the environmental impacts associated with this mine reclamation approach. Statistically significant water quality changes were observed at both sites after reclamations began. By using linear discriminant analysis on the hydrogeochemcial characteristics of the water samples, we identified if the backfilled CCRs have observable influences on the water quality of the underlying shallow aquifers. CRs have observable influences on the water quality of the underlying shallow aquifers.

Keywords: Coal Mine Reclamation, Coal Combustion Residues, Flue Gas Desulfurization, Groundwater, Hydrochemical Property, Multivariate Statistical Analysis

Introduction

In the state of Ohio, there are over 800 km^2 of un-reclaimed strip-mined lands (AMLs) left behind after the mining operations were ceased, which pose risks to the public and the environment. These AMLs discharge highly acidic and mineralized mine drainages (AMD), disrupt the flows of surface water streams and lakes, create dangerous highwalls, and degrade the ecosystems and habitats of the impacted watersheds. Limited public funds and natural resources are available to reclaim these AMLs.

In a previous study (Wolfe *et al*. 2009), we identified hundreds of miles of potentially dangerous AML highwalls in close proximity of coal-fired power plants. Finding an environmentally benign and technically feasible approach using coal combustion residues (CCRs), including bottom ash, coal ash, flue gas desulfurization (FGD) gypsum, and stabilized FGD material (sFGD), to reclaim AMLs can reduce costs and consumptions of natural resources. sFGD is a mixture of lime, coal ash, and calcium sulphite FGD by-product. FGD is a wet scrubber used in a coal-fired power plant to remove sulfur dioxide from the flue gas. We carried out the first stage study investigating the chemical/leaching characteristics of CCRs, characterizing potential project sites, and gathering inputs from public and industrial stake holders. In the second stage, two full-scale demonstration projects were carried out at the highwall pit complexes near the Conesville and Cardinal coal-fired power plants located in eastern Ohio.

To demonstrate the potential of using high-volume CCRs in abandoned coal mine reclamation, the associated environmental impacts were evaluated by regularly characterizing the leaching properties of the backfilling CCRs and monitoring the water quality of the uppermost aquifers underlying the reclamation sites. The water quality monitoring started approximately 15 months prior to the beginning of the reclamation. In this study, we detected if there are any significant water quality changes as a result of the reclamation practice, differentiated the causes of occurring water quality changes, and discussed the environmental implications of this reclamation practice.

Reclamation Sites

Conesville Five Points

The Middle Kittanning No.6 coal seam underlying the Conesville Five Points site was extensively surface mined prior to the 1977 Surface Mining Control and Reclamation Act (SMCRA), resulting in exposed highwalls, open pits, and adjacent mine spoil deposits. This site comprises three phases. The reclamations at Phases 1 and 2 were completed in 2016. Approximately 1.5 million metric tons of bottom ash, fly ash, sFGD and FGD gypsum were placed. Over 7 km of highwall are eliminated and about 0.44 km^2 of abandoned mined lands were reclaimed (Figure 1(a)). Phase 3 is currently on going, which is expected to use ca. 2.0 million metric tons of sFGD and FGD gypsum to reclaim a total of approximately 1.7 km of highwalls.

Cardinal Star Ridge

The Cardinal site consists of a highwall complex created from previous pre-law mining and an active mining permit. The total length of the highwall was approximately 150 m. The reclamation involved placing a thick layer of calcareous mine spoil material at the bottom of the highwall pit to a height of five to eight feet above the high-water mark of the groundwater level. The highwall was reclaimed back to its original contour using approximately 410,000 metric tons of FGD gypsum produced from the nearby Cardinal power plant. The fill was encapsulated with alkaline mine overburden and revegetated. The reclamation was completed in 2015 (Figure 1(b)).

Groundwater Monitoring

Conesville Five Points

Because Phase 3 is still on going, the discussion focuses only on Phases 1 and 2. In Phases 1 and 2, the water quality monitoring network comprises eight groundwater monitoring wells and four surface water locations. MW-0901 serves as a hydraulically up-gradient well. MW-0902, MW-1001, and MW-0904 are installed at the edge of the backfilling area to capture the water quality change in the down-gradient shallow aquifer. MW-0905, MW-0906, and MW-1101s are at further down-gradient locations representing

Figure 1 *Reclamations at (a) Conesville Five Points and (b) Cardinal Star Ridge sites. Pictures on the left are the landscapes before reclamation began. Pictures on the right are the conditions approximately five years after reclamations were completed.*

approximately 5-year groundwater travel time from the backfilling area.

Cardinal Star Ridge

A total six monitoring wells were installed. OAE-1001A and OAE-1002 are hydraulically down-gradient wells, located at the south and east sides, respectively, of the reclamation area. The screens of both wells were set in the mine spoil layer. OAE-1003 and OAE-1005 are located on the edge of the west and north highwalls, respectively, which were completed within the Pittsburg No. 8 coal seam. Two clustered wells, OAE-1504S and OAE-1504C, were installed in the reclaimed highwall/pit after the backfilling of FGD gypsum was completed. The shallow well (OAE-1504s) screens at the fractured bedrock at the base of the underlying mine spoil bench. The deeper monitoring well (OAE-1504C) screens within the limestone and sandstone stratigraphic layers.

At a given site, water quality monitoring started approximately 15 months before reclamation began to establish background levels. Monthly water samples were collected before and during reclamation. After the reclamation was completed, sampling frequency was reduced to quarterly and/or semi-annually. The water monitoring is still on going at the Conesville site. The last set of water samples from the Cardinal site was collected in July 2020.

Water Quality Change

For a given groundwater monitoring well, we compared the field observations recorded after the reclamation began to upper (UPL) and lower (LPL) prediction limits. These two-sided prediction intervals were established from the background data. Any observations that either exceed the UPLs or below the LPLs are considered statistically significant with 99% confidence. At both sites, after reclamations began, we observed statistically significant water quality changes. There is at least one monitored constituent in one or more of the sampling locations exceeds either a UPL or a LPL. The significance of the water quality changes has been discussed elsewhere (Cheng *et al*. 2016).

Impacts from Backfilled CCRs

To identify if the backfilled CCRs are the sources of the observed water quality changes, we used a linear discriminant analysis (LDA) method (Lambrakis et. al. 2004, Lautz *et al*. 2014) to differentiate two hydrogeochemical signatures of the water samples. "Sulfate signature", combining the equivalent ratios of major cations (i.e., Ca, Mg, and Sr) to sulfate, distinguishes the dominance of sulfate minerals, e.g., gypsum, in each water group. "Boron signature", a combination of the equivalent ratios of Ca, Mg, and Na to boron, is used to differentiate the background groundwater and leachates from CCRs. LDA detects the patterns of hydrogeochemical signatures implicit in different water groups, i.e., background data and leachates of CCRs, by generating discriminate functions using a set of "training" data (i.e., training dataset). In order to overcome the statistical constraints (Efron, 1979) associated with the limited numbers of available background and CCR leachate data, we used a multivariate bootstrapping method to increase the sample size of each water group to 1000.

Conesville Five Point Site

We compared the sulfate and boron hydrogeochemical signatures of the MW-0902 and MW-0904 groundwater samples collected after the reclamation began to that of the background samples and the leachates from laboratory leaching tests. With two linear discriminate functions (DFs), LDA is able to accurately identify the differences of the sulfate (99.97%) and boron (96.90%) signatures in the training dataset among different water groups. By using the LDA results, we created a sulfate-boron score biplot (Figure 2) to observe the changes of the hydrogeochemical characteristics at MW-0902 and MW-0904 after the reclamation began.

As demonstrated in Figure 2 (a) and (b), the data points of water samples collected during site construction (black hollow circles) are close to (MW-0902) or within (MW-0904) the clusters of the background samples (grey hollow circles). It is also true

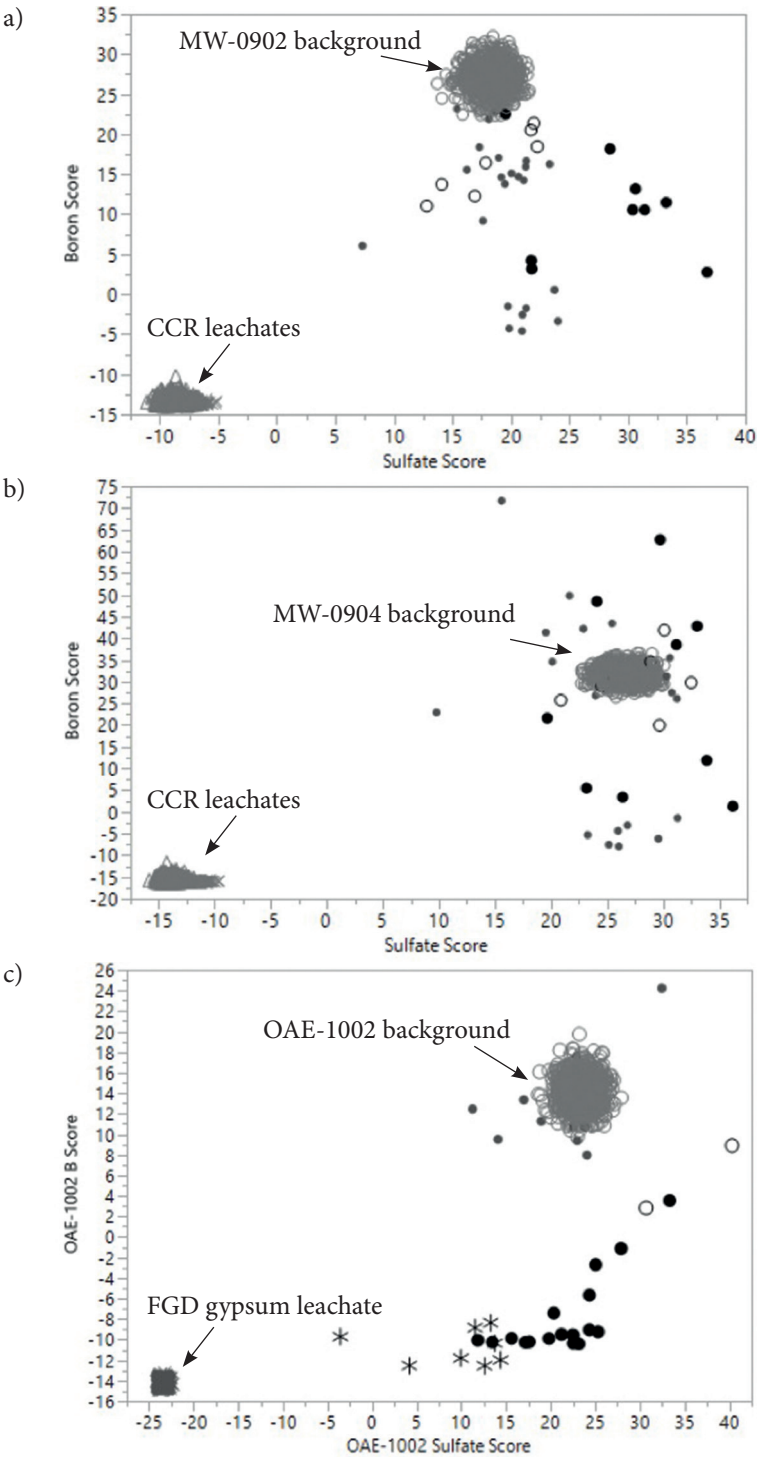

Figure 2 *Sulfate-Boron signature biplots of (a) MW-0902, (b) MW-0904, and (c) OAE-1002. Grey hollow circles, grey hollow triangle, and grey crosses progresses are the training data points of background, sFGD, and FGD gypsum leachates, respectively. Black hollow circles represent water samples collected during site construction. Grey dots are water samples collected during backfilling. Black dots are water samples collected after reclamation was completed.*

during the early stage of the backfilling period. As the backfilling of CCRs continued, boron scores (grey dots) started deviating from the background clusters. After the reclamation at Phases 1 and 2 was completed, both boron and sulfate scores of the water samples at both wells (black dots) were no longer within the ranges of the background samples. However, the changes do not move toward to the hydrogeochemical signatures of the CCR leachates.

It suggests the impacts from the backfilled CCRs on the water quality of the shallow aquifer underlying the Phases 1 and 2 area is currently not apparent. Instead, the water quality changes are likely associated with the Appalachian Regional Reforestation Initiative (ARRI) approach used to reclaim the area. This approach is characterized by the use of local end dumped spoil piles placed in an interlocking manner to encourage saturation and limit offsite erosion to promote tree survival and growth. With higher infiltration of rainfalls and runoffs, increasing concentrations of sodium and chloride are observed in the underlying aquifer (data not shown).

Cardinal Star Ridge Site

The resulting DFs accurately (100%) identified the differences between OAE-1002 and FGD gypsum leachate in both sulfate and boron signatures. The Sulfate-Boron signature biplot is shown in Figure 2 (c). Also included in the figure are the data points representing the OAE-1002 water samples collected during and post reclamation.

As shown in Figure 2 (c), the sulfate and boron signatures of OAE-1002 all deviated from the background (grey circles) after the backfilling began (grey and black dots). For the samples collected after the reclamation was completed (black dots), the signatures became similar to the signatures of the porewater in the FGD gypsum fill (OAE-1504S). The observation indicates the water quality of the underlying shallow aquifer has been affected by the leachate from the backfilled FGD gypsum.

Among all monitoring wells, OAE-1504S has the highest concentrations of Ca, sulfate, and B, which is attributable to the weathering of the backfilled FGD gypsum. After reclamation was completed, not only the concentrations of these constituents at OAE-1002 started increasing, the equivalent ratios of Ca to sulfate (Ca/SO_4^{-2}) also increased and became similar to the ratio observed in the fill (MW-1504S) (data not shown).

Environmental Implication

The water quality data were compared to the primary drinking water standards, i.e., maximum contaminant levels (MCLs) or action levels. A statistical summary of the data is shown in **Table 1**. As shown in the table, at both Conesville and Cardinal sites, As and Sb in at least one of the water samples collected after the reclamation was completed exceeded the respective drinking water standards. Five out of the total 95 water samples showed F exceeding the MCL at the Cardinal site. None of the water samples exceeded the drinking water standards for Ba, Be, Cd, Cr, Cu, Hg, Pb, and Se.

Both As and Sb are within the naturally occurring background levels. After the reclamation was completed, the water samples collected from the porewater of the FGD gypsum fill (OAE-1504s) contained the highest fluoride concentration among the ones collected from other wells, ranging from 1 to 6 mg/L. The concentration range is slightly higher or similar to the ones observed in the background levels (Figure 3). No fluoride exceedance was observed in the downgradient underlying aquifer (OAE-1001 and OAE-1002) after reclamation was completed.

Conclusion

At both demonstration sites, the change of local hydrogeological condition from reclamation activities, such as logging, grading, dewatering, and backfilling, likely caused temporary and some permanent water quality changes. However, at the Cardinal site, the effect of CCR leachate from the reclaimed highwall pit on the water quality of a hydraulically downgradient well was later detected. Higher concentrations of B, sulfate, and calcium were observed. Currently, no constitutes have exceeded the regulatory leaching limits set by the state agency for utilizing CCRs in mined land reclamation. In addition, the concentrations

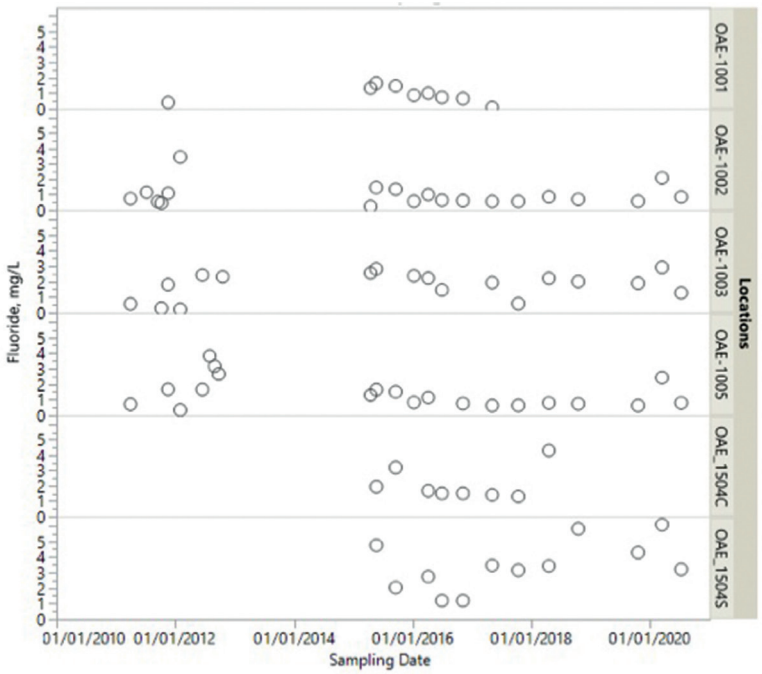

Figure 3 *Temporal trends of fluoride at Cardinal Star Ridge site.*

Table 1 *Statistical summary of constituents of concern in water Samples collected after reclamation was completed.*

		As	Ba	Be	Cr	Cd	Cu	Hg	Pb	Se	F	Sb
		µg/L	mg/L	µg/L	µg/L	µg/L	µg/L	ng/L	µg/L	µg/L	mg/L	µg/L
100.0%	maximum	19.6	1.630	0.390	9.70	4.50	1.10	17.6	4.70	15.60	0.93	80.0
75.0%	quartile	4.3	0.117	0.200	0.63	1.40	0.20	3.4	0.06	2.40	0.40	23.1
50.0%	median	2.0	0.043	0.106	0.10	0.08	0.10	2.3	0.03	0.09	0.22	16.9
25.0%	quartile	1.3	0.019	0.010	0.08	0.02	0.06	1.6	0.02	0.05	0.10	0.05
0.0%	minimum	0.4	0.007	0.004	0.03	0.01	0.03	0.7	0.01	0.03	0.04	0.02
Total N of Samples		94	94	94	94	94	94	94	94	94	94	94
N of detectable		62	94	26	74	70	44	17	31	28	77	48
MCL		10	2.00	4	100	5	1300*	2000	15*	50	4	6
% higher than MCL		8.5	0	0	0	0	0	0	0	0	0	83.0
						Cardinal Star Ridge						
100.0%	maximum	14.0	0.400	0.058	7.00	1.00	3.20	28.2	4.60	11.00	6.07	38.0
75.0%	quartile	2.7	0.066	0.045	2.00	0.60	1.51	4.3	0.56	8.60	2.22	25.0
50.0%	median	1.9	0.047	0.030	2.00	0.50	0.62	1.7	0.06	1.00	1.41	19.0
25.0%	quartile	0.9	0.022	0.010	1.00	0.02	0.14	0.9	0.02	0.20	0.76	17.0
0.0%	minimum	0.6	0.011	0.010	0.11	0.01	0.03	0.2	0.01	0.07	0.10	8.0
Total N of Samples		95	95	95	95	95	95	95	95	95	95	74
N of detectable		20	95	6	42	19	23	46	20	15	67	62
% higher than MCL		1.1	0	0	0	0	0	0	0	0	5.3	83.8

Unit: mg/L except for Hg (ng/L); * Action Level

of eleven selected constituents of concerned in all of the water samples remained at comparable levels with the local aquifers. The water quality monitoring is still ongoing at both sites to evaluate long-term effect. This study helps validate and improve current safeguards in permits authorizing CCRs placement in coal mines. The placement of virgin CCR materials under the permitting and performance standard requirements at mine sites, can result in a positive impact to human health and the environment when it is used to mitigate pre-existing mining hazards. With the passage of the CCR regulations, greater emphasis has been placed upon utilizing CCRs within mine reclamation practices to ensure that water quality is not impaired.

Acknowledgements

The authors thank the Ohio Coal Develop-ment Office of the Ohio Development Service Agency and The Ohio State University for funding support.

References

Cheng CM, Amaya M, Butalia, TS, Baker R, Walker H, Massey-Norton J, Wolfe W (2016) Short-term Influence of Coal Mine Reclamation using Coal Combustion By-Products on Groundwater Quality. Sci. Tot. Environ. 571: 834-854, doi:10.1016/j.scitotenv.2016.07.061

Efron B (1979) Boorstrap methods: Another look at the Jackknife, The Ananals of Statistics, 7:1-26.

Lambrakis N. Antonakos A, Panagopoulos G. (2004) The use of multicomponent statistical analysis in hydrogeological environmental research, Wat. Res. 38: 1862-1872

Lautz LK, Hoge GD, Lu Z, Siegel D, Christian K, Kessler JD, Teale NG (2014) Using discriminate analysis to determine sources of salinity in shallow groundwater prior to hydraulic fracturing, Environ. Sci. Technol. 48: 9601-9069

Wolfe W, Butalia T, Walker H, Baker R (2009) FGD By-product Utilization at Ohio Coal Mine Sites: Past, Present, & Future, CDO/D-07-06, Final Report, 2009. Columbus, OH.

Recovering Rare Earth Elements from Acid Mine Drainage with Mine Land Reclamation

Chin-Min Cheng, Tarunjit Butalia, John J. Lenhart, Jeffrey Bielicki

Department of Civil, Environmental and Geodetic Engineering, The Ohio State University, 470 Hitchcock Hall, 2070 Neil Ave., Columbus, OH 43210, U.S.A.

cheng.160@osu.edu, butalia.1@osu.edu, lenhart.49@osu.edu, bielicki.2@osu.edu

Abstract

In this study, we demonstrated a trap-extract-precipitate (TEP) process that effectively recovers rare earth elements (REEs) from coal mine drainage (CMD). This three-stage process uses environmentally benign industrial by-products to retain CMD REEs from CMD. It then applies an extraction/precipitation procedure to produce a concentrate feedstock (>7.5 wt.% of total REEs) that can be economically processed to produce marketable rare earth oxides. We envision the TEP process can be integrated with abandoned mine land reclamation to create a commercially viable approach to mitigate CMD and restore lands that are adversely impacted by historical mining.

Keywords: Rare Earth Elements, Acid Mine Drainage, Coal Mine Reclamation, Beneficial Use Of Coal Combustion Residues, Flue Gas Desulfurization By-products

Introduction

Rare earth elements (REEs) (including scandium, yttrium and a group of 15 lanthanides) are often considered to be critical components in the productions of renewable energy hardware, electric vehicles, health care and military equipment, and consumer electronic products. The demand of REEs has been projected to be growing at an annual rate of 5-9% in the next 25 years (Alonso *et al.* 2012). China overwhelmingly dominates the current worldwide rare earth productions (over 95%) (Hatch 2012), causing significant instability for the global market. Finding alternative sources has become a critical issue for the US and other countries.

Recovering REEs from the sludge of coal mine drainage (CMD) remediation system has been suggested as an environmentally beneficial and economically feasible alternative (Ayora *et al.* 2016). CMD remediation systems are normally operated at active mine sites. In the United States, CMD discharging from an active mine is mitigated to meet federal effluent limits based on the quality of the receiving water bodies by the coal mining operator. However, there are many CMDs discharging from abandoned mines, where mining activities occurred prior to current state and federal mining regulations, and therefore, remain untreated. In the state of Ohio, approximately 2000 kilometres streams are currently impaired by CMD. Implementing adequate treatment systems for these abandoned CMDs is limited by funds available for the state and federal reclamation agencies, local conservation organizers, and watershed associates.

In this study, we tested a three-stage process that first retains REEs from CMD using alkaline industrial by-products and then concentrates the retained REEs using a non-acid based organic ligand extraction procedure. The lixiviant is then oxidized to form REE precipitates. This trap-extract-precipitate (TEP) process can be integrated with abandoned mine land (AML) reclamation to create an approach that provides economic incentives to AML reclamation and remediates CMD discharges. It provides a long-term, high-volume beneficial use for coal combustion residuals, which otherwise needs to be disposed of in a landfill and eliminates public safety hazards and threats to local environment and ecological systems posed by AMLs.

Experimental

Materials

The alkaline industrial by-products used in this study to retain CMD REEs include two stabilized flue gas desulfurization materials (sFGDs) and a lime sludge produced from the softening process of a drinking water treatment plant. sFGD is a mixture of lime (CaO), coal ash, and calcium sulfite FGD by-product, which is produced from the wet scrubber for removing sulfur dioxide (SO2) from the coal flue gas. We obtained the sFGDs from two pulverized-coal power generating facilities burning bituminous coal located in east and southeast Ohio. sFGD 1 was obtained from the wet scrubbers at Plant C that used limestone slurry as the desulfurization reagent. sFGD 2 was produced from the lime slurry used at Plant G. Magnesium hydroxide was added to the lime slurry to enhance SO2 removal. Both wet scrubber systems are natural oxidation systems. All materials were dried in an oven at 60 °C before being crushed and sieved using a No.60 sieve.

The CMD used in this study was periodically collected from the Flint Run, a perennial CMD stream from the seepage discharge of a reclaimed abandoned surface mine, located at 36.06170–82.51139. Each batch of CMD was preserved at 4 °C before use and purged with nitrogen to minimize oxidation during test.

Retaining REEs

A series of column tests were carried out to simulate the percolation condition that occurs when using a passive treatment unit for CMD mitigation and REE recovery. The tests were carried out under various percolation rates ranging from 0.5 to 2 liquid-to-solid per day ($L{\cdot}S\text{-}1{\cdot}day^{-1}$). In addition, the retention of REEs was also investigated by a series of batch experiments, which simulates the retention of REEs under a completely mixed condition. These tests were carried out by adding predetermined amounts of sFGD 1 or WTP sludge (DRWP) to bottles. CMD was then added to each bottle to achieve a specific liquid-to-solid (L/S) ratio, which ranged from 5 to 1000.

Extraction

The spent solids obtained from the column and batch tests were air dried before extraction. The spent solids were mixed with an extraction solution prepared from sodium citrate at a ratio ranging from 1:10 to 1:40. The mixture was then heated in a hot block at 80 °C under different doses of sodium dithionite, a strong reductant. After heating for 15 minutes, the extract was separated from the suspension by filtering through a 0.45-μm filter and collected for chemical analysis. The extraction residues were then air dried for chemical analysis.

Precipitation

After extraction, we separated REEs from the lixiviants by promoting the formation of Na-REE-double sulfate precipitates (REE concentrate) through an oxidation process.

Results and Discussion

Retaining CMD REEs

Results obtained from the column tests (Figure 1 (a)) demonstrate that all three tested solids were able to recover over 98% of REEs under a wide range of percolation conditions before the materials exhausted neutralization capacities. In one of the tests (Column D with sFGD 1), only approximately 90% of REEs passing through the column was retained, which was due to a breakthrough.

The recovery of CMD REEs was also evaluated under a completely mixed condition. As shown in Figure 1 (b), when sFGD 1 was used, the retaining efficiency remained above 95% at an L/S ratio 50 or lower. At a higher L/S ratio of 100, although the retaining efficiency decreased to 83.8%, the concentration of total REEs (T-REEe) in the spent solids reached 94.2 μg/g (dry basis), which is the highest among the sFGD1 batches.

In the batches using the WTP sludge, over 98% of the total REEs mass in CMD partitioned to the solids under an L/S ratio less than 250. The retaining efficiency decreased at higher L/S ratios. The highest concentration of T-REEe in the spent solid after the reaction reached approximately 230 μg/g.

Extracting Retained REEs from Spent Solids

To optimize the extraction process, different sodium dithionite doses, pH buffering conditions, and liquid-to-solid ratios were tested. Results obtained from the extraction tests are shown in Figure 2. The extraction efficiency shown in the figure was calculated using the following equation.

$$\text{Extraction Efficiency},\% = \frac{C_{lx,i} \times V_{lx}}{C_{ss,i} \times m_{ss}} \times 100 \quad \text{eq.1}$$

where $C_{ss,i}$ and $C_{lx,i}$ are the concentrations of REE, i, in the spent solids and lixiviant, respectively; m_{ss} is the amount of spent solids used in the extraction process; and V_{lx} is the volume of lixiviant.

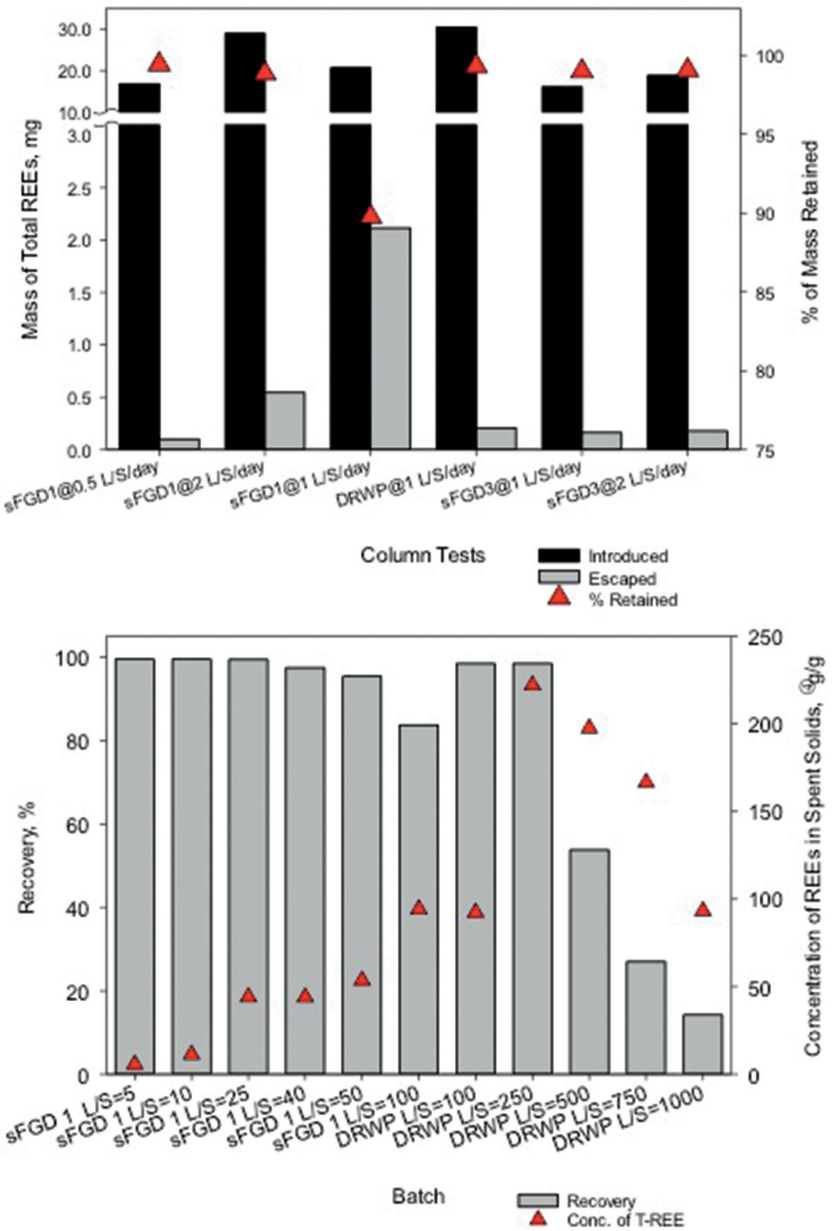

Figure 1 *Retaining AMD REEs under (a) percolation and (b) completely mixed conditions.*

As shown in Figure 2, the extraction efficiency was not affected when we decreased the dose strength to ⅓ of the original strength (columns shaded in light grey in Figure 2). To test the effect of buffering, we carried out the extraction process with and without a buffering solution and obtained slightly better extraction efficiency (columns shaded in light red in Figure 2). It was demonstrated that the effect of pH change during the extraction process is insignificant.

To optimize the use of the extraction solution, we conducted a series of extraction process using different solid-to-extractant (S/L) ratios ranging from (1/40 to 1/10) and evaluated the extraction efficiency (columns shaded in dark grey in Figure 2). It was found that no observable change in extraction efficiency when the S/L ratio was increased from 1/40 to 1/30. The extraction efficiency significantly decreased with higher ratios.

Producing REE Concentrate

The extracts produced from two of the selected extraction procedures of E1 and E8 were purged with air under various flow rates and duration to observe the effects on the formation of REE concentrates. Formation of precipitates was observed during purging (Figure 3). After purging, precipitate was recovered by filtrating the extract using a 0.45μm filter and dried in an oven at 105°C. The amounts of precipitates formed during the purging process were determined gravimetrically and the results are shown in Figure 4 (a). Also shown in the figure are the amounts of REEs in the extract before and after purging.

Since the amounts of precipitate formed during the purging process are limited, the concentration of T-REEs in the solids was determined based on the principal of mass balance. As shown in Figure 4(b), we are able to precipitate over 90% of the extracted REEs and form a REE concentrate with the T-REEe concentration of approximately 7.5%wt.

Full-Scale Application

The TEP process can be integrated with AML reclamation to create an AML reclamation approach, which is illustrated in Figure 5. In a full-scale application, sFGD (fresh

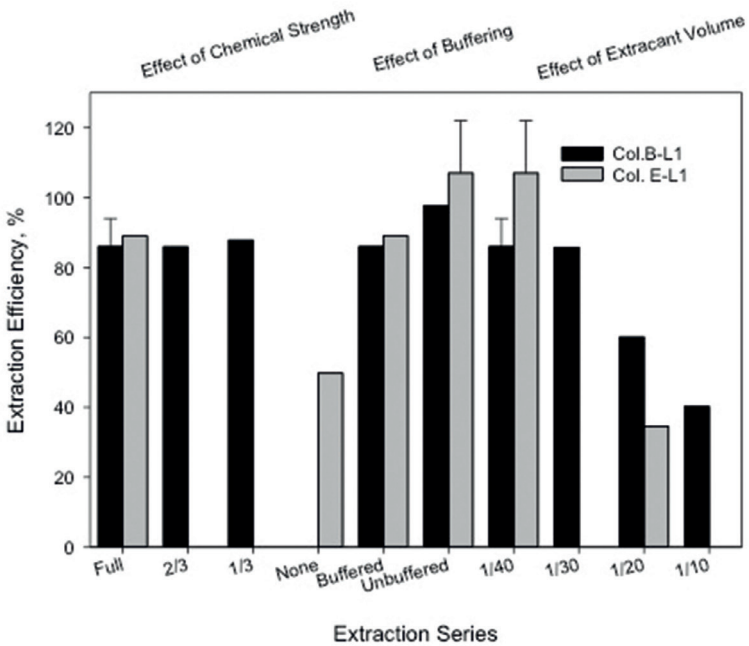

Figure 2 *Efficiency of entrapped REEs in sFGD1 (Col. B-L1) and WTP sludge (Col. E-L1) extracted by different extraction condictions. Full strength of sodium dithionite is 3 grams per 1 gram of spent solid. The ratio of spent solid to the volume of citrate extractant ranged from 1/40 to 1/10.*

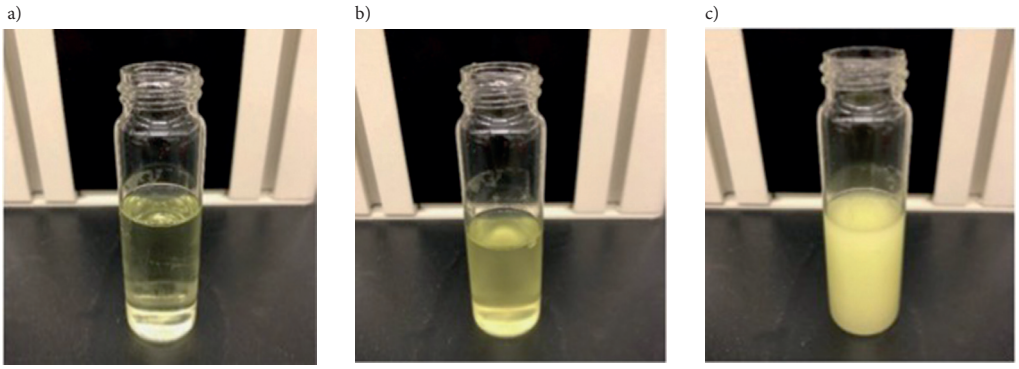

Figure 3 Formation of precipitates during purging. (a) Lixiviant before purging; (b) Lixiviant during purging; (c) Lixiviant after purging.

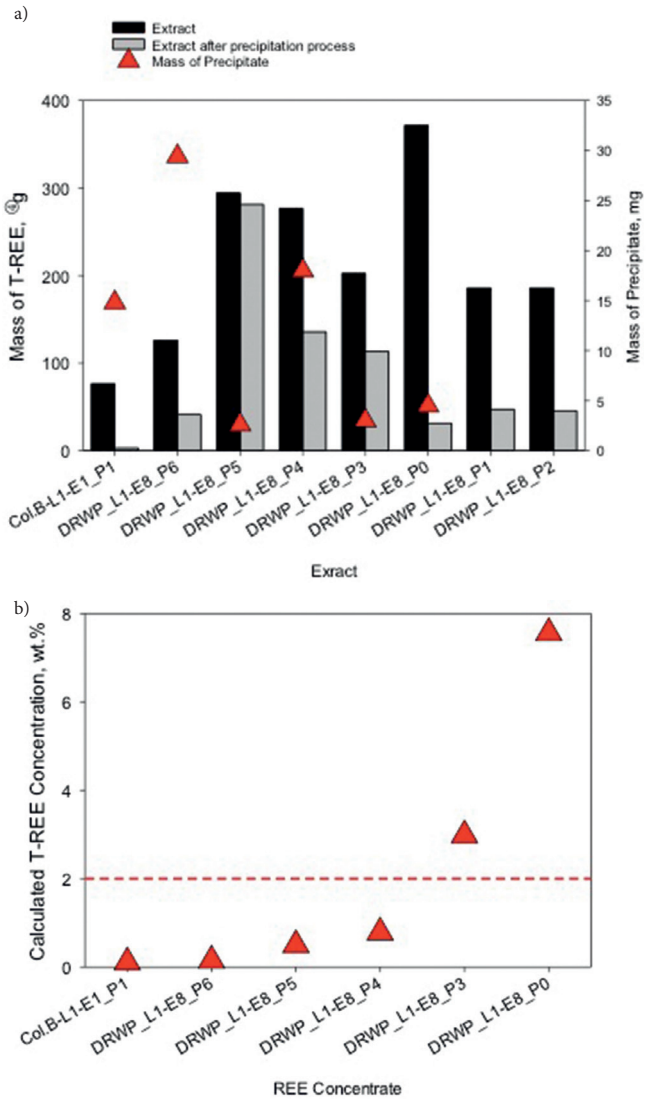

Figure 4 (a) Precipitation of REE concentrate and (b) calculated T-REEe concentration in REE concentrates from selected aeration batches.

or landfilled), WTP sludge, and/or other environmentally benign alkaline industrial by-products are used to backfill and reclaim the AML (Figure 5(a)). With proper engineering design, CMD seeping out of the abandoned mine is collected by a drainage system and directed to nearby treatment cells (Figure 5(b)).

In the remediation cells, filled with suitable alkaline materials (e.g., sFGD and WTP sludge), a CMD dispensing system (e.g., geotextile material) is placed within the fill to facilitate the percolation of CMD, and consequently accelerate the mitigation process (Figure 5(c)). After the material exhausts its neutralization capacity, the spent solids are removed from the treatment cells for the following extraction and precipitation processes (Figure 5(d)). The operation is renewable by placing another batch of the alkaline material in the treatment cells.

Acknowledgements

The authors thank the U.S. Department of Energy, Ohio Coal Development Office of the Ohio Development Service Agency, and The Ohio State University for funding support. We also thank the technical supports from Ohio Department of Natural Resources and National Energy Technology Laboratory.

References

Alonso, E., Sherman, A. M., Wallington, T. J., Everson, M. P., Field, F. R., Roth, R., & Kirchain, R. E. (2012). Evaluating rare earth element availability: A case with revolutionary demand from clean technologies. Environ. Sci. Technol. 46:3406-3414.

Hatch, G. P. (2012). Dynamics in the global market for rare earths. Elements, 8, Retrieved from http://elements.geoscienceworld.org/content/8/5/341

Ayora, C., Macias, F., Torres, E., Lozano, A., Carrero, S., Nieto, J.-M., Perez-Lopz, R., Fernandez-Martines, A., Castillo-Michel, H., 2016, Recovery of rate earth elements and yttrium from passive remediation

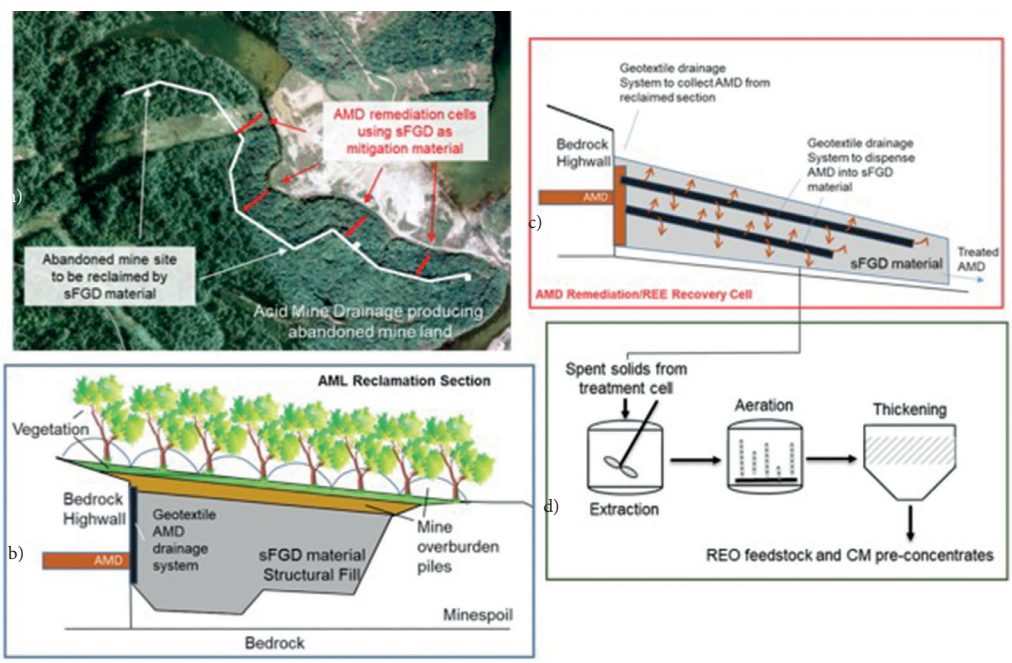

Figure 5 *Schematic description of concept that integrates TEP process and AML reclamation.*

Distributions of Rare Earth Elements in Coal Mine Drainages

Chin-Min Cheng, Tarunjit Butalia, John J. Lenhart, Jeffrey Bielicki

Department of Civil, Environmental and Geodetic Engineering, The Ohio State University, 470 Hitchcock Hall, 2070 Neil Ave., Columbus, OH 43210, U.S.A.

cheng.160@osu.edu; butalia.1@osu.edu; lenhart.49@osu.edu; bielicki.2@osu.edu

Abstract

In the U.S., rare earth elements (REEs) are reported to be closely associated with coal deposits, especially in the Appalachian Basins. Historical coal mining in the Northern Appalachian Coal field of the United States has produced significant amount of coal drainage (CMD). In this study, we investigated 29 abandoned CMDs in eastern Ohio, USA. The main objective of this study is to understand the geochemical behaviour of REEs in CMD. Results obtained from this study provide the knowledge that will form the basis of a reactive transport model, which can be used to predict REE retention and recovery.

Keywords: Coal Mine Drainage, Rare Earth Elements, Abandoned Coal Mine, Mine Drainage Chemistry

Introduction

In response to increasing global demand and supply dominance of China, finding alternative sources of rare earth elements (REEs) has become a critical national security issue for other countries, including the United States. Coal and coal ash are considered as important alternative sources for REEs. In the U.S., high concentrations of rare earths have been reported to be closely associated with coal deposits (Hatch 2012), especially in the Appalachian Basins. In addition to coal and coal ash, another potential important alternative REE source is coal mine drainage (CMD). CMD occurs during and after coal mining. When surface and/or groundwater comes in contact with geologic strata and ore bodies containing sulfide minerals, such as pyrite (FeS2), exposed by coal mining, the accelerated oxidation of sulfide minerals in the presence of natural oxidants (e.g., ferric iron and oxygen) or induced by certain micro-organisms can produce sulfuric acid (Evangelou 1998, Johnson 2003). It promotes the weathering of REE-bearing rocks and minerals in the host geologic strata (Jennings *et al*. 2000, Lottermoser 2007).

Historical coal mining in the Northern Appalachian Coal field produces significant amount of mine drainage, which causes widespread degradation of water resources. According to Ohio Department of Natural Resources, CMD have degraded more than 2000 km of streams in Ohio. Currently, state, and federal funds for abandoned mine land reclamation are raised through taxes on coal extraction in the region, but these funding sources are limited.

In this study, we investigated CMD discharges from abandoned coal mines and refuse piles in eastern Ohio. The main objective of this study is to understand the geochemical behavior of REEs in CMD. A multivariate statistical analysis technique, principal component analysis, was used to correlate the hydrogeochemical characteristics of CMD and the concentrations of REEs.

Study and Methods

A total of 29 CMD discharges were studied. These CMD discharges are from historic underground mines at different coal seams, abandoned surface mines, and minespoil/ refuse piles. Refuse/slurry piles disposed from mines and coal preparation plants are also major sources of acid drainage.

We used PHREEQC, an aqueous geochemical modeling code developed by the United States Geological Survey (USGS) (Charlton and Parkurst 2002), to calculate the speciation distribution of REEs in CMD. The thermodynamic dataset compiled by the Lawrence Livermore National Laboratory is used, which includes stability constants of the

REE sulfate, chloride, phosphate, hydroxide, and carbonate complexes.

To simplify the analysis of complex chemical correlations between REEs and other monitoring parameters, we used a principal components analysis (PCA) to extract information from the water quality dataset. PCA is a statistical technique that quantifies the relationship among water quality parameters, such as pH, acidity, and concentrations of major and rare earth elements, and finds a new set of independent and uncorrelated variables, i.e., principal components (PCs), to represent the original water quality data. Each PC is a linear combination of the original water quality parameters. No pre-treatment of the original data was performed as the PCA was carried out on a correlation matrix. Left-censored data were replaced by the values equal one-half of the detection limits. A commercially available statistical program, JMP, developed by SAS Institute was used to carry out PCA.

Results and discussion

General Hydrochemical Property of CMDs

All water samples are highly mineralized with total dissolved solids (TDS) concentration ranging from 247 to 7364 mg/L. The pH value ranged from acidic (2.3) to circumneutral (6.89). The major ions in the CMD samples include sulfate, Ca, Mg, Fe, Al, Na, Si, Mn, Cl, and K (Figure 1(a)). By comparing the relative concentrations of major cations and anions in the CMD samples, the waters are categorized as $Ca\text{-}SO_4$ and $Mg\text{-}SO_4$ type. In addition to these aforementioned major elements, the waters also contain a number of trace constituents (Figure 1(b)), such as Tl, Co, P, Cr, and V. However, not all of the samples contain detectable levels of trace constituents. As shown in Figure 1(c), the concentration levels of REEs vary significantly among these CMD discharges. The concentration of total REEs (ΣREEs) ranges from 2212 to 5 µg/L. Y, Nd, and Ce are the most abundant REEs. The heavy (Y, Tb, Dy, Ho, Er, Tm, Yb, and Lu) and critical REEs (i.e., Y, Dy, Eu, Dy, and Tb) account for approximately 34% and 48% of total REEs, respectively (Figure 1(c)).

Geochemical Property of REEs in CMDs

It has been suggested that the concentrations of rare earth elements in CMD are strongly correlated with pH (Grawunder *et al*. 2018). However, this correlation was not observed in this study. As shown in Figure 2, the pH of four CMD discharges with the highest total and critical REEs concentrations are less than 4.0. However, not all CMD discharges with low pH values contain high REE concentrations. No significant correlation between the pH and concentration of total (r=-0.366) was observed. Similar ΣREEs-pH correlation was also reported by Stewart *et al*. (2017).

The correlations among ΣREEs, critical REEs, and other hydrochemical parameters in CMDs were analyzed using a principal component analysis (PCA). The loadings of the considered parameters for the first three principal components (PCs), which explain 70.9% of the observed variance in the hydrochemical properties, are shown in the table embedded in Figure 3. In addition, the eigenvalue for each component and cumulative percent of variance explained by these three PCs are shown. The first PC (PC1) explaining approximately 34.7% of the variance shows that the CMD samples with high acidity also contain relatively higher ΣREEs, critical REEs, and a number of major constituents, i.e., Al, Ca, Fe, Mg, and Mn. It demonstrates the significance of the oxidation process by the acidity forming minerals. PC2 explaining 23.5% the variances has relatively strong loadings from B, K, and Na suggests some of the CMD samples were affected by fresh streams or surface runoff. As shown in Figure 3, CMD samples with higher pH normally contain higher concentrations of Na, Cl, and B. PC3, explaining approximately 12.7% of the variance, suggests acidity was mostly contributed from Fe for these CMD samples. Acidity was measured using the standard "hot peroxide treatment" method, mainly results from the potential for hydrolysis of dissolve ferric iron (Fe^{3+}), ferrous iron (Fe^{2+}), Al, and Mn^{2+}, as well as the precipitation of associated hydroxide solids.

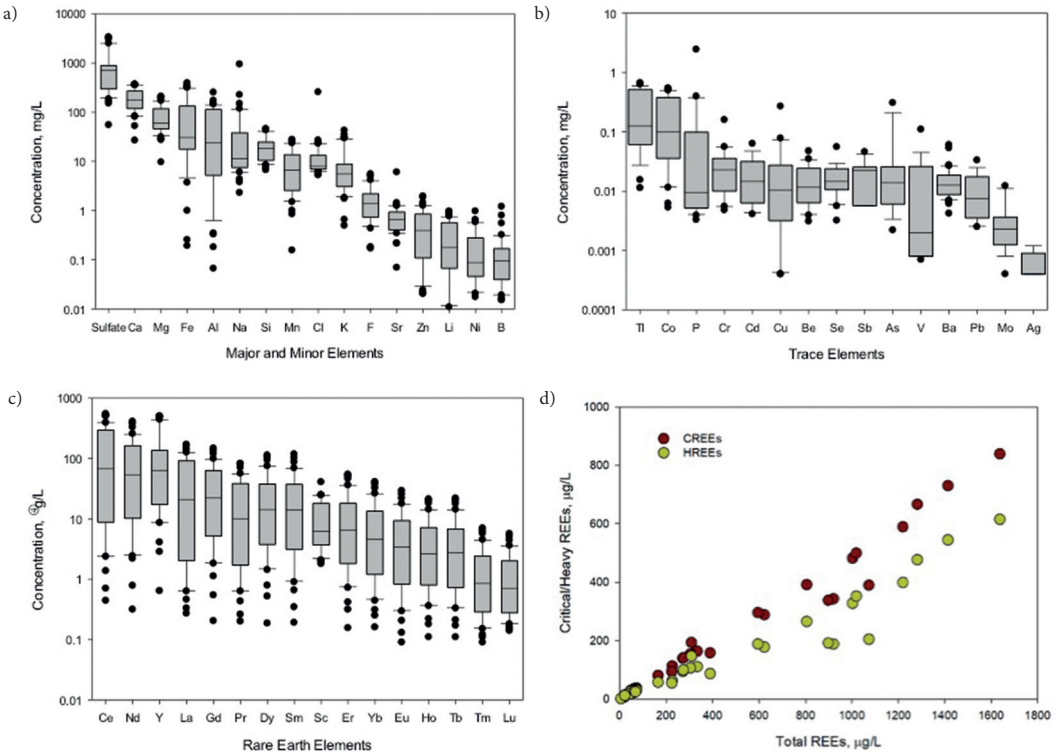

Figure 1 *Concentrations of (a) major and minor, (b) trace, and (c) rare earth elements in CMD discharges. Only detectable data are included in the plots. (d) Concentrations of total heavy (Y, Tb, Dy, Ho, Er, Tm, Yb, and Lu) and total critical REEs (i.e., Y, Dy, Eu, Dy, and Tb) as a function of total REEs.*

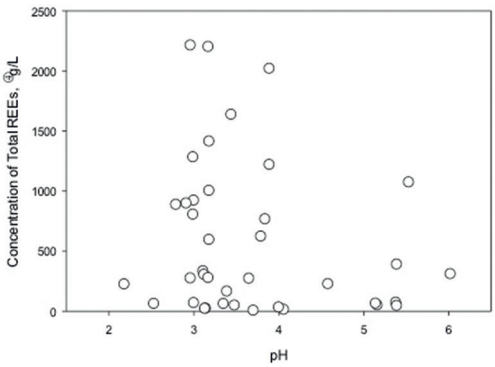

Figure 2 *Correlations between pH and concentrations of total REEs.*

As demonstrated in Figure 3, instead of pH, ΣREEs and critical REEs showed better correlations with acidity. In fact, among the three acidity-related cations, Mn has the strongest correlation with ΣREEs and critical REEs, followed by Al (Table 1). In addition to Mn and Al, Mg also shows high correlation.

Enrichment of REEs

The concentrations of REEs were normalized with North American Shale Composite (NASC, Taylor and McLennan, 1985) to detect REE enrichment. The REE enrichment patterns are described using [La/Gd]N, [La/Sm]N, and [La/Yb]N to compare relative levels of light REEs (LREEs) (i.e., La, Ce, Pr, Nd, and Sm) to middle REEs (MREEs) (i.e., Eu, Gd, Tb, Dy) and heavy REEs (HREEs) (i.e., Ho, Er, Tm, Yb, and Lu). As shown in Figure 4, the CMD samples showed a clear MREE enrichment compared with LREEs and HREEs, which has been a typical feature of REEs in acidic environments (Johannesson and Lyons 1995).

In addition, mostly positive Ce anomalies were shown in the studied CMDs, indicating the immobilization of $Ce3^{+}$ by oxidation to $Ce4^{+}$ played an insignificant role in the migration of Ce. The strong correlation between Mn and REEs indicates the

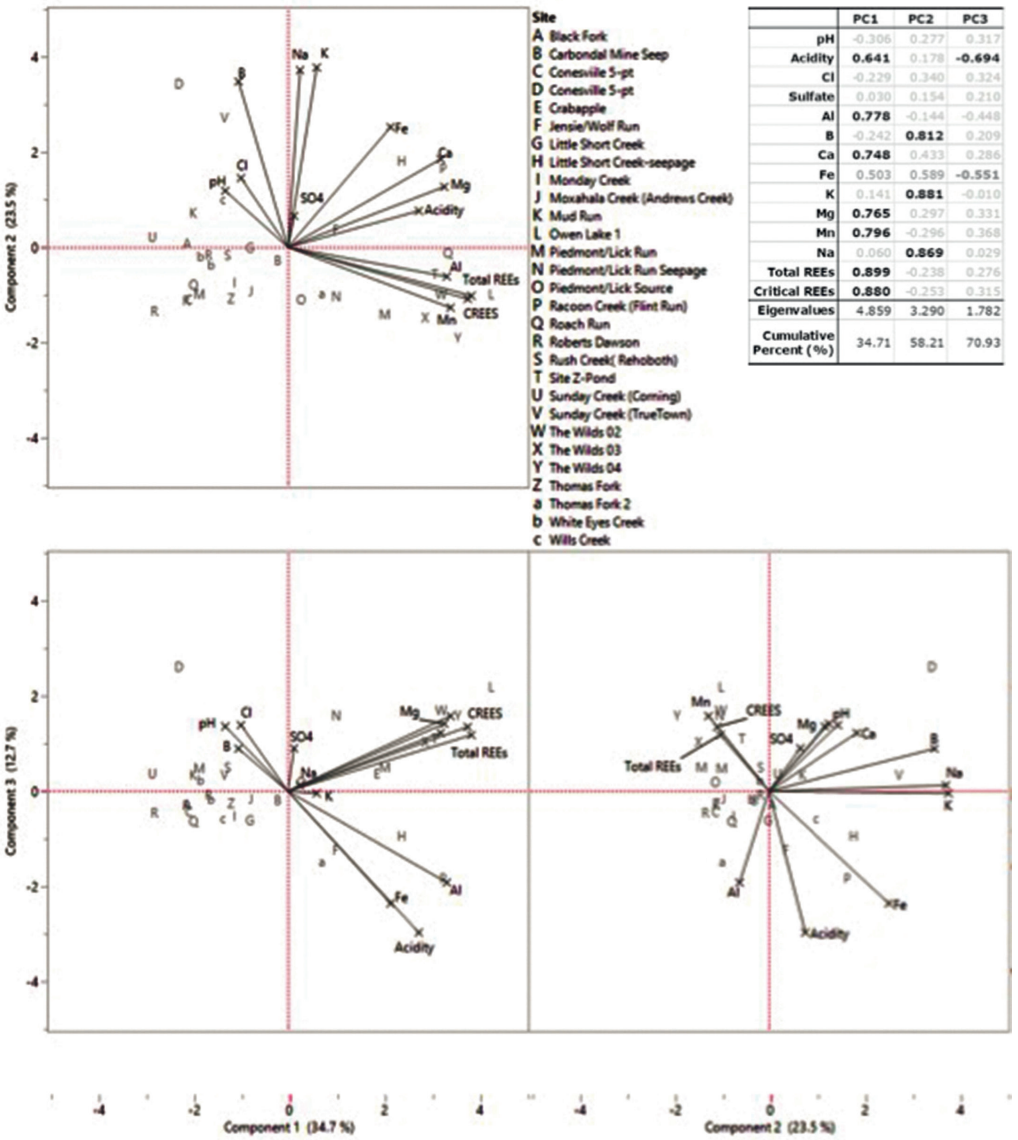

	PC1	PC2	PC3
pH	-0.306	0.277	0.317
Acidity	**0.641**	0.178	**-0.694**
Cl	-0.229	0.340	0.324
Sulfate	0.030	0.154	0.210
Al	**0.778**	-0.144	-0.448
B	-0.242	**0.812**	0.209
Ca	**0.748**	0.433	0.286
Fe	0.503	0.589	**-0.551**
K	0.141	**0.881**	-0.010
Mg	**0.765**	0.297	0.331
Mn	**0.796**	-0.296	0.368
Na	0.060	**0.869**	0.029
Total REEs	**0.899**	-0.238	0.276
Critical REEs	**0.880**	-0.253	0.315
Eigenvalues	4.859	3.290	1.782
Cumulative Percent (%)	34.71	58.21	70.93

Figure 3 *The score and loading plots of REEs and major constituents from principal component analysis.*

Table 1 *Correlation coefficients between critical REEs and four constituents of interest (Al, Mg, Mn, and Fe).*

	Y	Nd	Eu	Tb	Dy
Al	0.6776	0.7692	0.6756	0.6715	0.6841
Mg	0.6845	0.6243	0.628	0.6606	0.6745
Mn	0.8391	0.8331	0.8281	0.8399	0.8452
Fe	0.0252	0.2283	0.1386	0.1093	0.1126

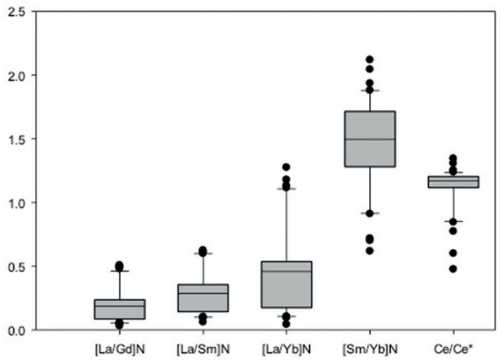

Figure 4 *NASC-normalized patterns of the REE concentrations.*

dissolution of Mn-bearing minerals led to an enrichment of associated Ce, which resulted in a positive Ce anomaly in the CMDs.

Speciation of REEs in CMD

Aqueous speciation of REEs in water plays an important role in the migration of REEs in CMD (Grawunder *et al.* 2015). Results from the speciation calculation are summarized in Figure 5. As demonstrated, $Ln(SO^4)^+$ is the most dominant species, except for Sc, Gd, and Ce. Free trivalent ion species are the primary forms for Sc, Ce, and Gd. Except for naturally occurring Ce^{4+} and Eu^{2+}, REE are usually trivalent. Both Eu^{2+} and Ce^{4+} are negligible. $Gd(SO_4)^{2-}$ is more abundant than the mono-sulfate complex. The observation, in general, agrees with other studies (Zhao *et al.* 2007)

Conclusions

The concentrations of total REEs (ΣREEs) in the 29 CMDs discharging from abandoned coal mines and refuse piles in eastern Ohio varied significantly, ranging from 2212 to 5 µg/L. Y, Nd, and Ce are the most abundant REEs. Instead of pH, ΣREEs and critical REEs show better correlations with acidity. Based on results from the multivariate statistical analysis of the geochemical parameters, among the three acidity-related cations (i.e., Fe, Al, and Mn), Mn has the strongest correlation followed by Al. Mg also shows high correlation. The NASC-normalized REEs patterns suggest there is an obvious enrichment of MREEs than the LREEs and HREEs in the CMD. Calculation of REEs speciation demonstrates that sulfate complexes ($Ln(SO_4)^+$) are predominate species. However, for Ce and Gd, trivalent free ions are the major forms. Results obtained from this study provide the knowledge that will form the basis of a reactive transport model that can be used for REE retention and recovery.

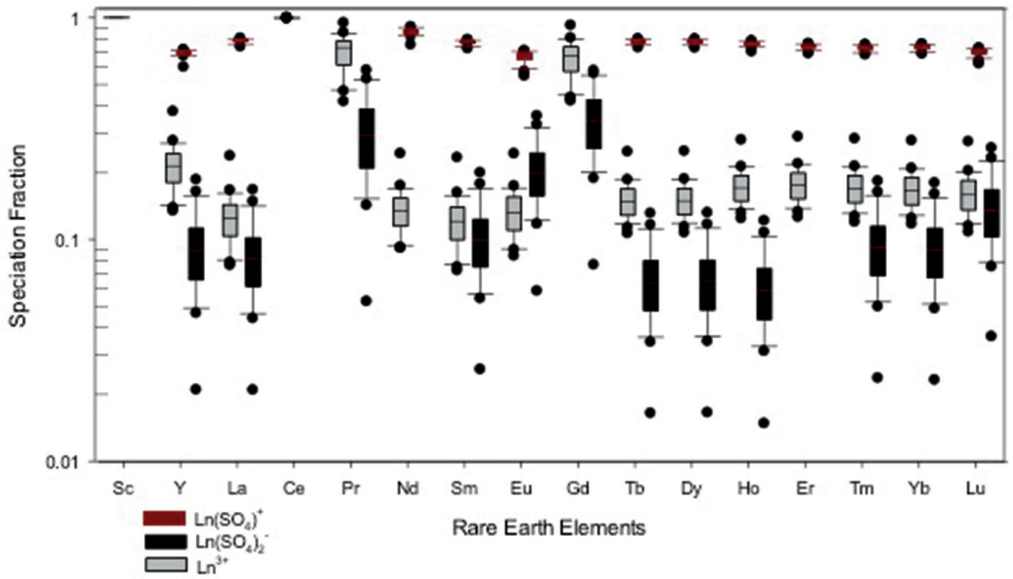

Figure 5 *Speciation fractions of REEs in CMDs.*

Acknowledgements

The authors thank the U.S. Department of Energy, Ohio Coal Development Office of the Ohio Development Service Agency, and The Ohio State University for funding support. We also thank the technical supports provided by Ohio Department of Natural Resources and National Energy Technology Laboratory.

References

Evangelou , V.P., 1998, Pyrite chemistry: the key for abatment of acid mine drainiage. In: Geller A, Klapper H, Salomons, W., editors. Acidic Mining Lakes: Acid Mine Drainage, Limnology and Reclamation. Berlin: Springer, P.197-222.

Grawunder A, Lonschinski M, Merten D, Büchel G (2015) Rare earth elements as a tool for studying the formation of cemented layers in an area affected by acid mine drainage. Appl Geochem 54:100–110

Grawunder A, Lonschinski M, Handel M, Wagner S, Merten, D, Mirorodsky D, Buchel G (2018) Rare earth element patterns as process indicators a the water-solid interface of post mining area, Appl Geochem 96:138-154

Hatch, G. P. (2012). Dynamics in the global market for rare earths. Elements, 8, Retrieved from http://elements.geoscienceworld.org/content/8/5/341

Jennings. S. Dollhopf D. Inskeep W. 2000, Acid production from sulfi de minerals using hydrogen peroxide weathering. Appl Geochem 15:235–243.

Johannesson, K.H., Lyons, W.B., 1995. Rare-earth element geochemistry of Color Lake, an acidic freshwater lake on Axel-Heiberg-Island, Northwest-Territories, Canada. Chem Geol 119:209–223.

Johnson D., 2003, C2003, Hemical and microbiological characteristics of mineral spoils and drainage waters at abandoned coal and metal mines. Water Air Soil Pollut 3:47 – 66

Lottermoser, B., 2007, Mine Wastes Characterization, Treatment and Environmental Impacts, 2nd edn. Springer Publisher, Heidelberg

Rudisell, M.T., Stuart, B.J., Novak, G., Payne, H., Togni, C.S., 2001, Use of flue gas desulfurization by-product for mine sealing and abatement of acid mine drainage, Fuel 80: 837-843

Zhao F, Cong Z, Sun H, Ren D (2007) The geochemistry of rare earth elements (REEs) in acid mine drainage from the Sitai coal mine, Shanxi Province, North China, Coal Geol. 70:184-192.

A 3D Feflow Hydrogeological Uranium Underground Mine Model, France

Fabrice Compère[1], Guillaume Kern[2], Gaël Bellenfant[1]

[1]*BRGM, 3 av. Claude Guillemin, 45100 Orléans, France, f.compere@brgm.fr, g.bellenfant@brgm.fr*

[2]*ORANO, 2 rte Lavaugrasse, 87250 Bessines-sur-Gartempe, France, guillaume.kern@orano.group*

Abstract

A groundwater flow model was implemented to reproduce the complex hydrosystem behaviour of a remediated uranium mine to better control its environmental footprint. The geology was represented using a layered approach. The open pit, the underground galleries and the tailing storage area were integrated into the model through 3D unstructured finite elements. The model is based on unsaturated Richard's equations and includes interaction between groundwater and rivers. After an inversion procedure, the calibrated model successfully reproduces the observed water level fluctuations (piezometers and open pit).

Keywords: Mine, Hydrogeology, Model, 3D, Geometry

Introduction

During the mining operations, dewatering modifies hydrogeological conditions by lowering groundwater levels which consequently increases infiltration and seepage from the surface water network (Adams and Younger, 1997). When the pumping stops, the hydrogeological system rebalances itself but the remaining mining infrastructures can potentially alter definitely natural groundwater flow, leading to an aquifer with triple porosity (primary porosity of the rock and secondary porosity caused by mining-induced fracturing and mining voids), which can be called a 'mine aquifer' according to Wolkersdorfer (2008).

The main objective of this work is to improve the knowledge of the hydro system of a remediated uranium mine located in France to better control its environmental footprint. More specifically, the local effect on groundwater flow of an open pit mine and flooded underground galleries has been studied using a 3D groundwater model. Considering the necessity to include in a larger system detailed features as an open-pit, underground galleries and a storage area, the finite element method (Rapantova *et al.*, 2007) was selected as a numerical method. On the base of classical layered model, complex geometries were integrated inserting 3D unstructured mesh.

Description of the site

The former mining site (mean altitude of 250 m ASL) is located near the interfluve between two main rivers flooding at the North and the South. The source of two minor rivers is located next to the site, whose upstream part presents intermittent flow (fig. 1).

According to the stratiform conceptual model of hard rock aquifers (Lachassagne,

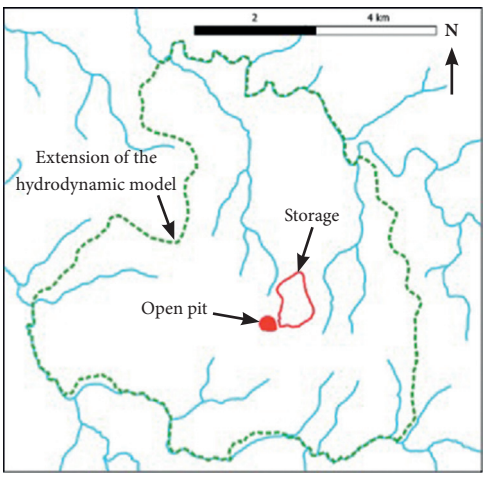

Figure 1 *Extension of the modelized area and rivers network.*

2014), the main geological unit consists of alterites (weathered cover with clay-rich material, with a local thickness from 4 m to 12 m) overlaying horizontally fissured granite (local thickness of 30 m) and a non-altered granite substratum.

The studied area hosts disseminated uranium deposits. Uranium orebodies occur as vertical episyenitic pipes: vuggy granites that resulted from quartz leaching. Nine main ore bodies were identified inclined from 45° to 90° of variable size, with circular horizontal sections ranging from 100 m^2 to 1500 m^2 with a vertical extension from tens of meters to more than 700 m.

Extraction began by open pit method (115 m deep), followed by underground works (maximal depth of 400 m) composed of galleries surrounding extraction zones. Tailings were managed in a dedicated tailing storage facility (TSF) built directly on alterites. The TSF (370 000 m2) includes peripheral and internal dams (made of mine tailings, waste rocks and alterites) which split the storage into 4 different cells (fig. 2).

Following the ending of the mine activity and therefore stopping pumping operations in 2001, the open pit and underground mine cavities are currently entirely flooded. Storage area was covered by a compacted waste rocks layer overlaid with an earth soil layer in 2001 to reduce, amongst other aims, direct infiltration of rainfall. Surface runoff, water percolating laterally through the peripheral dams (collected with surrounding trenches) and water collected from two drains located at the bottom of the storage (North limit), are directed towards various basins.

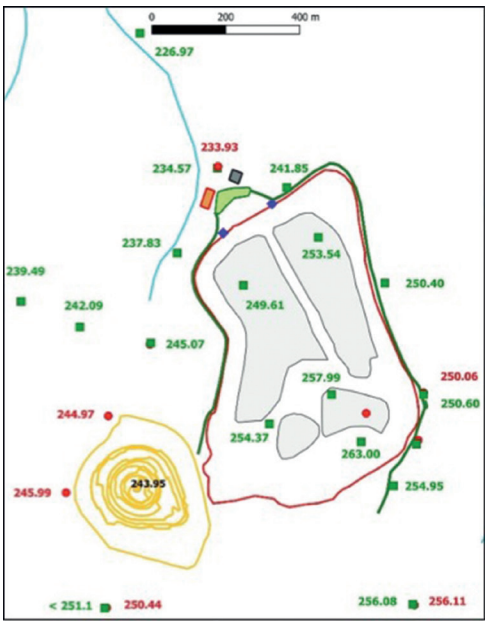

***Figure 2** Map of the site with open pit, storage area, piezometers and piezometric levels (march 2018).*

Hydrogeological context

Aquifers' hydrodynamical properties

Porosity of alterites and fissured granite is generally in the range between 2% and 8%; both formations present very different hydraulic conductivities, with low values for alterites (between 10^{-7} m/s and 5.10^{-6} m/s) and higher values for fissured granite (from 10^{-6} m/s to 5.10^{-3} m/s). Non-altered granite substratum presents very low hydraulic conductivity and storage capacity. Various pumping tests conducted at low flow-rate (about 1.5 m^3/h) on piezometers, allowed to estimate transmissivities from 10-7 m^2/s to a maximum of 2.10^{-5} m^2/s.

Piezometry

Twenty-two piezometers were implemented to monitor groundwater levels and six have been installed in the storage area to measure the water level in the dams and cells filled with tailings. Short piezometers intersect the base of alterites and the upper parts of the fissured granite while long piezometers intersect the lower part of the fissured granite and the top of the non-altered granite substratum.

Figure 2 illustrates piezometric levels measured in March of 2018. Except for the influence of the open-pit and the storage area, the main hydraulic gradient is oriented from the South to the North, following the topography. Highest groundwater levels at the south are close to the topographical limit separating two watersheds. Since 1993, water level series show very low amplitude for most of the piezometers, except those close to the open pit, influenced by the regular rise of the water table.

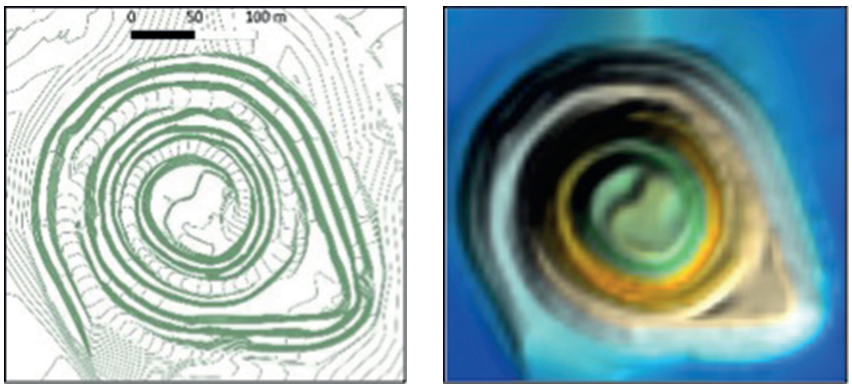

Figure 3 *Vectorial topographical map (left) of the open pit and its numerical grid representation (right).*

Analysis of the water table rising in the open pit

A deep well, very close to the open pit, has been used to follow the water level rising since the end of dewatering operations. The rising was slower when the water started to fill the open pit. A water balance of the open pit was obtained by estimating 1) direct inflow due to direct precipitation and 2) the evaporation loss (calculated using local meteorological data). A 3D geometry of the open pit was obtained from a digital elevation map (fig. 3), allowing to estimate the surface and volume of the water body in function of the water level in the open pit. Daily evolution of water volume was calculated, and an average value of 14 m^3/h was found. Considering the periods including at least 5 consecutive days without rainfall and constant water level, the groundwater contribution (mean value of 8,5 m^3/h) was supposed equal to the estimated evaporation process.

Model elaboration

Feflow (Diersch, 2014) allows to simulate groundwater flow using Finite Element Method (FEM) technique in discretization of the continuous domain modelling area into set of discrete sub-domains or elements. Division to smaller elements allows accurate representation of complex geometry, specifically using 3D unstructured mesh.

Model extension and FEM meshing

Main rivers were used to delimitate the North and South extension of the model (area of 27 km^2). Null flux boundaries were set on west and east sides to represent the watershed limits (in granitic domain, groundwater flow mainly follows topography). Rivers, open pit,

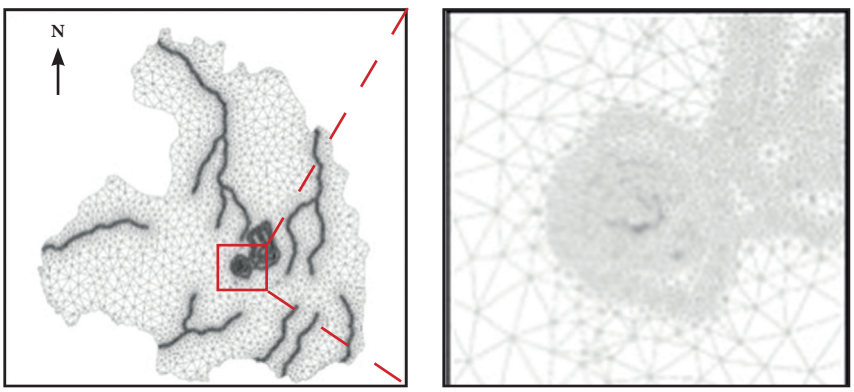

Figure 4 *Finite elements meshing of the whole model (left) and zoom centered on the open-pit (right).*

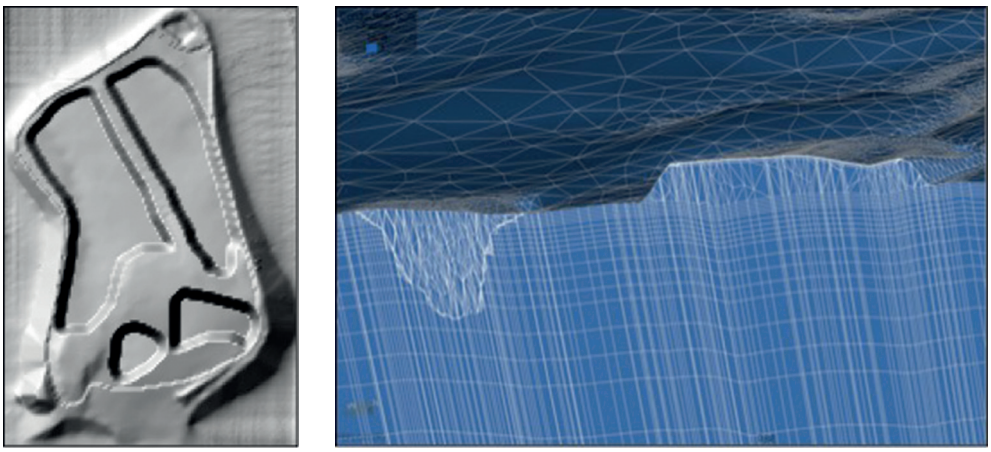

Figure 5 *Storage area with the peripheral and internal dams (left) and vertical slice view into the model displaying the open pit and the storage area filled with unstructured elements (right).*

storage zone geometry and piezometers were inserted as nodes and lines to be integrated in the meshing process. FEM meshing was performed using the "Triangle" algorithm provided by Feflow, ensuring its regularity using "2D mesh smoothing" and respecting the Delaunay criterion (fig. 4).

3D model structure (except galleries network)

Surface topography was obtained merging a large Digital Elevation Model (DEM grid of 25 m × 25 m with meter accuracy in Z) with a more precise one (grid of 5 m × 5 m with centimeter accuracy in Z). Using Golden Software Surfer®, the Radial Basis Function (multi quadratic option and null R^2 parameter) was applied to estimate the Z altitude on each node of the model.

Geometry of the four cells within the residual's storage area was obtained combining various paper maps (particularly the original topography corresponding to the storage basement) and sketches describing the dimensions and shape of the external dam and the internal dams separating the cells. Final geometries grid files (top of the storage, dams, layers of recovering materials, storage cells) were generated using interpolation processes with Surfer® (fig. 5).

A classical layered approach was used for the geological model (470 m thick) including, from top to bottom: alterites (5 × 1 m thick layers), fissured granite (5 × 2 m thick layers and 4 × 5 m thick layers) and non alterated granite substratum (3 × 10 m thick layer, 3 × 20 m thick layer, and 11 layers with thickness increasing from 26 m to 37 m).

Once the layered structure created, the volumes corresponding to the open pit, the tailings and the storage area dams were discretized in 3D unstructured elements (tetrahedrons) using the Feflow TetGen meshing tool (fig. 5).

Generation of underground galleries

Geometry of the central axis of each gallery was available as a georeferenced shapefile (ArcGis format). This skeleton was imported into Blender software (www.blender.org) using Blender GIS (hgithub.com/domlysz/BlenderGIS), an add-on allowing to import and export most common GIS data format.

Once imported in Blender, each continuous segment (3D line) has been treated individually. Using the Bevel data's segments properties, 3D polygons were automatically generated joining square cross sectional shape regularly placed along the line (square side size of 4.5 m for main galleries and 3.74 m for secondary galleries, fig. 6). A special attention has been given to obtain a coherent geometry, limiting the number of faces and avoiding any self-intersection between polygons (i.e. perfect fit at galleries intersections), with manual adjustment if necessary.

Using Blender's Bevel tool, an accurate representation with 3D polygons was

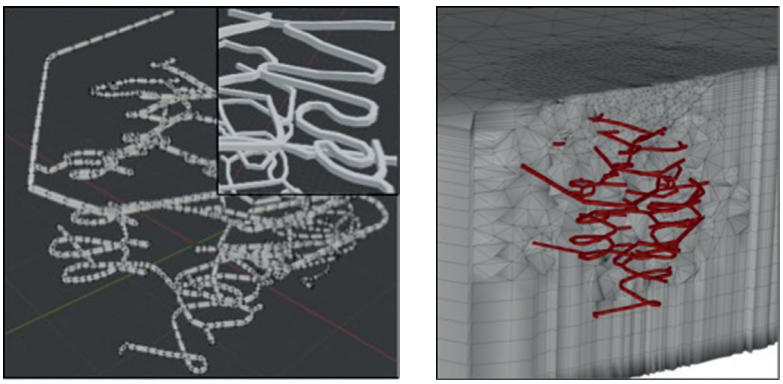

Figure 6 *3D polygonal modeling of underground galleries with Blender (left) and integration into the Feflow model using unstructured elements (right).*

obtained for the whole galleries network, and exported as a 3D shapefile with Blender GIS.

With Feflow's TetGen meshing tool, the full 3D polygonal representation of the underground structures was integrated into the layered geological model using unstructured mesh (fig. 6). As for the open-pit void, a pseudo-porous material ("air layer" approach; Diersch, 2014) was used to simulate the open-pit void with a reasonably high conductivity (several orders of magnitude higher than surrounding rock) and a porosity of one.

River's network

For the main rivers at the north and south of the domain limit and the downstream part of their tributaries, hydraulic head boundary condition has been imposed (first-order limit condition with constant hydraulic head). Upstream part of the tributaries were treated as fluid-transfer boundary condition (Cauchy-type limit with an associated out-transfer coefficient).

Recharge

Since 1979, the daily mean flow-rate is measured in the river flowing at the north limit of the model. To evaluate the part of efficient rainfall distributed between runoff and infiltration into underlying aquifer, Gardenia software (Thiery, 2010) was used. Gardenia is an application for lumped hydrologic modelling, simulating the main water cycle mechanisms in a catchment basin by applying simplified physical laws for flow through successive reservoirs. Fitting the model to the observed flow-rate data, the efficient rainfall is distributed between runoff and infiltration.

Following the analysis of the water table evolution into the open pit, a daily balance series was calculated integrating the loss by direct evaporation, the influxes of rainfall and runoff. An average flowrate over 5-day time step was computed from the water balance and applied as well boundary condition at the bottom of the open pit. The transient simulation started when the open pit was already partially filled (water level at an altitude of about 168 m).

Recharge applied on the storage area was determined, based on the analysis of monthly volumes passing through the collecting basins installed on the site.

Hydrodynamic model configuration

The hydrodynamic model, based on unsaturated Richard's equations (Van-Genuchten model), and including interaction between groundwater and rivers, runs in transient state over 16 years, with a recharge calculated at a time step of 5 days. Calculation time-step is automatically controlled and limited to a maximum of 10 days.

Calibration of the model

Using an inversion process (FePest tool integrated in Feflow – Doherty, 2007), the hydrodynamics properties (hydraulic conductivities, specific storage, parameters specific to the unsaturated flow) of the

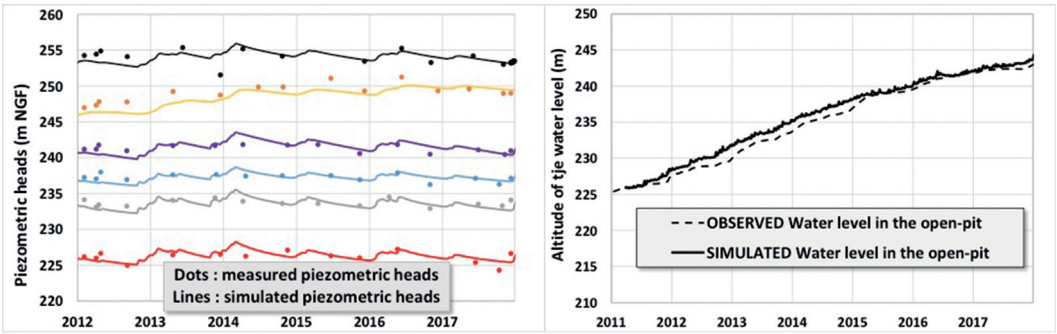

Figure 7 Comparison of observed and simulated series (piezometers and open pit).

geological formations and the material constituting the storage area, have been fitted to reproduce the evolution of piezometric heads measured on multiples piezometers and the observed raise of the water table into the open pit. Pilot point method was used to calibrate the model considering the spatial variation of the parameters. Comparison between observed and simulated data is presented in figure 7.

Conclusion

3D unstructured elements meshing allowed to insert in an large hydrodynamic model very detailed features as an open pit, a network of underground galleries and a storage area (including dams, storage cells containing residuals, covering layer).

Tedious integration of high-resolution structures into a 3D model, requires a coherent software chain (ArcMap, ArcScene, Surfer®, Blender, Feflow), with strong effort dedicated to the mesh quality. Workflow induces time consuming phases as digitalization, georeferencing, numerical interpolation and adjustment of 3D automatically generated polygons.

The general hydrodynamic configuration of the site is well reproduced, with a strong effort focused on the modelling of the water level rising in the open pit.

Future works will focus on transport simulation to characterize the migration of solutes within the various components of the site and particularly the behavior of the water flowing through the residuals of the storage area.

References

Adams R, Younger P.L. (1997). Simulation of ground water rebound in abandoned mines using physically based modelling approach. In: Proceedings of the 6th international mine water association congress, Bled, pp 353–362.

Diersch, H.-J.G. (2014). "FEFLOW: Finite Element Modeling of Flow, Mass and Heat Transport in Porous and Fractured Media." Springer, Verlag Berlin Heidelberg.

Doherty, J. (2007). PEST® surface water modeling utilities: Numerical Computing, Watermark, Brisbane, Australia; 2007.

Lachassagne P. Dewandel B., Wyns R. (2014). The conceptual model of weathered hard rock aquifers and its practical applications. In "Fractured Rock Hydrogeology". N°20. pp.13-46. International Association of Hydrogeologists Selected Papers. Sharp J.M. (Ed.) – CRC Press, Taylor and Francis Group.

Rapantova N., Grmela A., Vojtek D., Halir J., Michalek B. (2007). Ground water flow modelling applications in mining hydrogeology. Mine Water Environ 26:264–270.

Thiéry D. (2010). Reservoir Models in Hydrogeology. in "Mathematical Models Volume 2, chapter 13, pp. 409-418 - Environmental Hydraulics Series". Tanguy J.M. (Ed.) – Editions Wiley/ISTE London. ISBN: 978-1-84821-154-4.

van Genuchten, M.Th. (1980). A closed-form equation for predicting the hydraulic conductivity of unsaturated soils. Soil Sci. Soc. Am. J. 44:892– 898.

Wolkersdorfer C. (2008). Water management at abandoned flooded underground mines: fundamentals, tracer test, modelling, water treatment. Springer, Heidelberg.

Younger P.L., Banwart S.A., Hedin S.H. (2002). Mine water: hydrology, pollution, remediation. Kluwer, London, p 464.

Surface Water on the Influence of the Carajás Mineral Province (Brazil) – Consequences to an Indigenous Community

H. Correa, I.M.H.R. Antunes, A.P.M. Reis

ICT, University of Minho, Campus de Gualtar, 4710 - 057 Braga, Portugal,
helenamedleg@hotmail.com, imantunes@dct.uminho.pt, pmarinho@dct.uminho.pt

Abstract

The Cateté River belongs to the Itacaiúnas River watershed, including the most prominent mining area of Brazil with active mines of Fe, Cu, Ni, and Mn. This river has a high vulnerability associated with the drainage of mining effluents and crosses the "Xikrin-Cateté Indigenous Land".

Most water samples from Cateté river are neutral and poorly mineralized, but with high concentrations of Fe, Mn, Ni, Cu, Cr, Zn, and Pb. Some waters are contaminated and unsuitable for human consumption and agricultural activities. The water contamination is mainly associated with mine activities; however, Fe is also related to geological setting and lithologies.

Keywords: Potentially Toxic Elements, Mines, Itacaiúnas River, Contamination, Indigenous Communities

Introduction

The global concern is to ensure sufficiency in water quantity for public health, food security, and water access demand (UNESCO, 2019). Brazil contains the largest volume of freshwater of any nation in the world, with extensive rivers and containing about 12% of the availability of fresh water in planet (ANA, 2020). However, this natural resource is becoming scarce because of increased consumption, extended droughts, precarious distribution, inadequate treatment infrastructures, and water quality degradation, mainly associated to anthropogenic pressures (Val *et al*., 2019; Mello *et al*., 2020). Water resources are threatened not only by climate change scenarios but also by increasing levels of pollution, which has become a serious environmental problem on a global scale (Satapathy *et al*., 2009).

The diversity of geological environments gives Brazil one of the biggest mineral potential (Santana *et al*., 2020) and the second-largest producer of mineral ores in the world (National Minerals Information Center/US Geological Survey, 2017), with important reserves of iron, manganese, niobium, and nickel. Several Brazilian states, particularly Minas Gerais and Pará, are economically dependent on mining activities (Reis and Silva, 2015; Milanez *et al*., 2019). Mining activities, although relevant and indispensable for human socioeconomic development, accelerates natural processes and increases the likelihood of releasing toxic elements at higher rates in adjacent areas (Satapathy *et al*., 2009; Paraguassú *et al*., 2019; Alves *et al*., 2020). Mining regions constitute an important challenge in the management of water resources since its impacts could be an environmental risk and human health concern.

The generation of large amounts of solid waste and effluents, derived from mining activities, represents a potential source of contamination since potentially toxic elements (PTE) can be dispersed by the action of natural factors or accidentally leading to water by mine drainage (e.g., Lottermoser, 2007; Kipp *et al*. 2009; García-Lorenzo *et al*., 2012; Antunes *et al*., 2018).

Growing global concern about the protection of water quality has led to increasing attention to monitoring and risk assessment of PTE in water bodies (Sahoo *et al*. 2019). The main subject of this research is the evaluation of the water quality of the Cateté River, located in the south-eastern

region of the State of Pará - northern region of Brazil, and extensively used by an indigenous community.

Study area

The Itacaiúnas River watershed (05˚10´ to 07˚15´S latitude, 48˚37´ to 51˚25´longitude) is located in the Brazilian Amazonia, Carajás region, Pará State, Northern Brazil (Fig. 1). Amazonia contains most of the country's surface water (ANA, 2019). The population of Itacaiúnas River watershed is approx. 700,000 persons in an area of approx. 41,500 km^2.

Geologically, the area is in the southern portion of the Amazonian Craton, southwest region of the Carajás Mineral Province, one of the most important metallogenic provinces in the world, containing world-class Fe (iron) and Cu (copper) mines, as well as Mn (manganes) and Ni (niquel) ones (Vasquez *et al*., 2008; Sahoo *et al*., 2019). The Mineral Province of Carajás is divided into two geological domains: Carajás, specifically where the Xikrin TI of the Cateté River is located and Rio Maria domain (Vasquez *et al*., 2008).

Two of the main tributaries of Itacaiúnas River are the Cateté (western side) and Parauapebas (eastern side). The Cateté River has an extension of about 168.3 km and crosses the "Xikrin-Cateté Indigenous Land (XIL)" (Fig. 1). The Cateté and Itacaiúnas rivers supply the Indigenous Land, and water is considered by the indigenous community as a cultural and human belongs. However, the Cateté River has a high vulnerability associated with the drainage of effluents from mining activities and water contamination will promote a severe influence on the culture, leisure, and health problems of the indigenous community.

The XIL of the Cateté River corresponds to a national reserve area, which is traditionally occupied by indigenous communities, in an extension up to 438,000 ha, with a perimeter of approximately 360 km and a population of 1183 inhabitants, called "Caiapó-Xikrin population" (ISA, 2020). This reserve's territory is surrounded by agricultural activities and a contrasting between pasture vegetation and dense forest, with an abundance of species, especially chestnut (Costa, 2019). Rivers are the main determining factor on the human occupation and on the practice of indigenous culture, such as the natural human bathing, fishing activities and water management

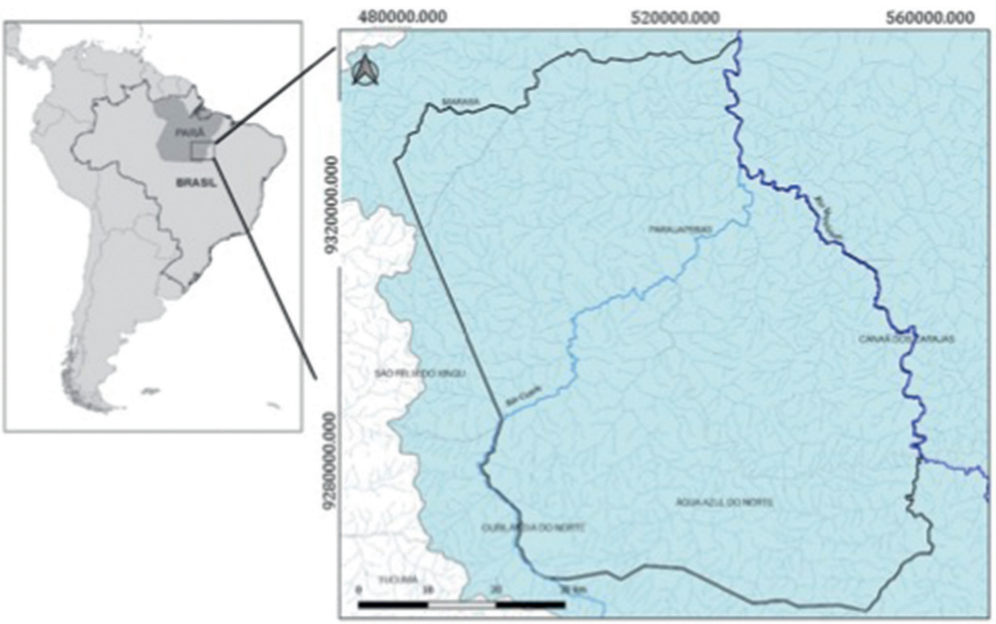

Figure 1 *Geographic setting of study area and delimitation of Xikrin-Cateté Indigenous Land area crossed by Cateté river.*

on indigenous food local production (e.g., manioc), as well as, on recreational activities (Corrêa, 2021). The indigenous community has been suffering severe impacts on cultural activities and health, because of the contamination of the water river.

Methods

A total of fourteen water samples were collected on the Cateté River around the area of Xikrin indigenous village (Fig. 2). The sampling water points were selected to characterize the water from Cateté River upstream and downstream the influence of mine drainage. The two villages - Cateté and Djudjekô – are located on the main influence of Cateté River and the river ports are represented by water samples PT06 and PT07, respectively (Fig. 2).

The physico-chemical properties - colour, turbidity, pH, Total Dissolved Solids (TDS), Biological Oxygen Demand (CBO5) and Dissolved Oxygen (DO) - and selected PTE – Copper, Chromium, Iron, Manganese, Nickel, Zinc, Lead, Mercury, and Aluminium from water were determined. To obtain a space-time water characterization, the water sampling was obtained twice in a year, to represent the raining season (January) and the wet season (June). The water parameters were determined in a certified laboratory, the Multi-Analysis Laboratory (Belém do Pará, Brazil) and according to Brazilian water frameworks and Standard Methods for the Examination of Water and Wastewater (CONAMA, 2005; Carvalho, 2015).

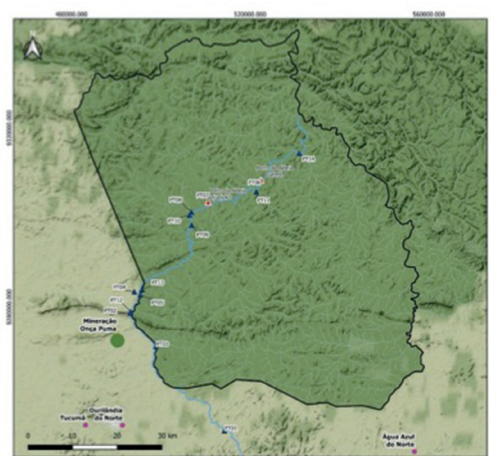

Figure 2 *Xikrin-Cateté Indigenous Land area and location of Cateté river sampling points (▲ – water sampling point; ▲ – river ports; ● – mine area).*

Results

Most water samples have pH values ranging from 6.0 to 8.0, are moderately oxygenated (Dissolved Oxygen = 5.4–10.4 mg/L) and poorly mineralized (TDS = 18–72 mg/L). The waters are slightly alkaline and are classified as mixed Ca-Na-HCO_3- type, indicating that they are mainly influenced by silicate rock weathering (Sahoo *et al.*, 2019). The variation of pH values from the water will be able to promote the increase in PTE contents absorbed into particulate matter (sediments). The relation between TDS and major ions suggest that rock weathering is the dominant process controlling water composition (Sahoo *et al.*, 2019).

Almost major ions and TDS water contents from Cateté river are higher in the rainy season than in the dry season like as been found in other surface waters from the Itacaiúnas River watershed (Sahoo *et al.*, 2019). The water of the Cateté River shows high concentrations of chemical elements, such as Cr (up to 0.09 mg/L), Fe (up to 13.3 mg/L), Mn (up to 1.78 mg/L), Ni (up to 0.04 mg/L), Zn (up to 0.5 mg/L), Cu (up to 0.13 mg/L), Al (up to 0.39 mg/L) and Pb (up to 0.05 mg/L).

In general, in the rainy period, there are higher Cr, Mn, Ni, Zn and Cu than in the dried period (Fig. 3), which could be associated to the increase of surface water flow and the mobility of these elements from sediments to water. Otherwise, Fe water contents tend to have higher values in the dry season probably due to a concentration effect. The Fe concentration in the water from Itacaiúnas river watershed and its tributaries, such as the Cateté river, is mainly associated to the natural geology of the area (Salomão *et al.*, 2020). However, the highest Fe content on the Cateté river water were found downstream the influence of mining activities (sample points PT08 and PT09; Fig. 3). So, the presence of Fe in the waters of the Cateté River is related with the geological setting and local lithology but is also influenced by the mining activities.

Some water points are contaminated with Fe, Mn, Ni, Cu, Cr, and Zn, and unsuitable for human consumption and agricultural activities (Fig. 3), according to CONAMA (2005). The water contamination of the Cateté river is mainly associated with mine activities developed in the area.

Conclusions

The Itacaiúnas river basin is located in one of the most important mining areas in Brazil, which includes mining activities with the exploration of lateritic nickel deposits. The Cateté River belongs to the Itacaiúnas River basin and has been the main receptor of effluents from these mining activities. These rivers supply the villages of the Indigenous Land, crossing the Xikrin Indigenous Community of the Cateté River. Rivers are determining factors in the positioning of indigenous communities, and their culture is heavily dependent on water, from daily activities that include the practice of fishing and the production of food products, as well as their use in recreational and fun activities.

The results of this study provided valuable information on PTE contamination in water resources located in an area from Itacaiúnas watershed occupied by an indigenous community. The characterization of surface water from Cateté river indicate that Fe, Mn, Ni, Cu, Cr, and Zn are potential contaminants, and exhibited higher concentrations that the reference values established by Brazilian national frameworks.

Although Fe and Ni mines are active in the region, high enrichment of Fe and Mn is not only related to mining, but rather to geological conditions ineherent to the Amazonian region, that where reinforced by land use changes (Salomão *et al.*, 2018). Very high concentration of Fe and Mn is the common geochemical signature of surface water in the Itacaiúnas river watershed (Sahoo *et al.*, 2019). The occurence and spatial distribution of PTE reflect different local geological and antropogenic factors active in the Itacaiúnas river watershed (Sahoo *et al.*, 2019). The main contamination source in the region is associated to mining activities, but also to natural geological background.

The obtained results in surface water reinforce the evidence of environmental and human health risks associated with mine activities and the relevant application of adequate preventive and monitoring methodologies. The mining sector has produced water quality degradation and environmental disasters in recent years. Enforcement of environmental laws, inspection and control from environmental agencies, application of measures and pressure from society are strongly needed to avoid water quality contamination from mining and continued disasters.

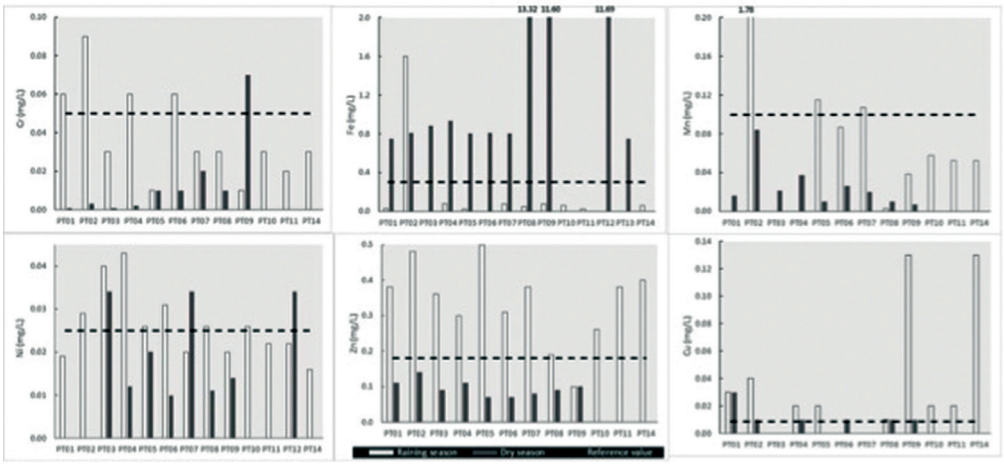

Figure 3 *Seasonal chemical variation in waters from the Cateté river. Reference value (CONAMA, 2005).*

This study will be a useful tool for the authorities responsible for environmental management, especially when assessing the impact of economic activities, such as mining and agriculture, on water resources in this climate region. Further studies that continue to monitor and assess the level of contamination of water resources in the watershed are crucial to preserving access to safe freshwater sources. The main motivation for this study comes for the recognition of the importance of the mining sector in Brazil and the significant environmental, social, and economic impacts attributed to the mining extraction processes. To the future is necessary more specific frameworks and tools for sustainability performance evaluation especially suited to the mining sector.

Acknowledgements

The authors acknowledge to Eran Paulo Rodrigues and Prof. Reginaldo Sabóia de Paiva from GTEMA/CNPQ/UFPA (Brazil) for the information and data provided and to FCT – Fundação para a Ciência e a Tecnologia, I.P., through the project's reference UIDB/04683/2020, UIDP/04683/2020.

References

Alves W, Ferreira P, Araújo M (2020) Challenges and pathways for Brazilian mining sustainability. Res Pol. https://doi.org/10.1016/j.resourpol.2020.101648

ANA (2019) Qualidade de rios em nove estados está ruim ou regular, aponta estudo. Acessível em https://www.ana.gov.br/noticias-antigas/qualidade-de-rios-em-nove-estados-esta-ruim-ou.2019-03-15.6696430832 [accessed on the 20th April 2021].

ANA (2020) Enquadramento – Bases Conceituais. Acessível em http://pnqa.ana.gov.br/enquadramento-bases-conceituais.aspx [accessed on the 20th April 2021].

Antunes IMHR, Neiva AMR, Albuquerque MTD, Carvalho PCS, Santos ACT, Cunha PP (2018) Potential toxic elements in stream sediments, soils and waters in an abandoned radium mine (central Portugal). Environ Geochem Health 40(1):521-542, doi:10.1007/s10653-017-9945-2

Carvalho CGP de (2015) Análise da acumulação de metais pesados oriundos de atividades de mineração na terra indígena Kikrin Cateté. Trabalho de Conclusão de Curso de Graduação em Engenharia de Minas e Meio Ambiente. Universidade Federal do Pará (UFPA). 49 pp.

CONAMA – Ministério do Meio Ambiente (2005) Resolução nº 357, de 17 de março de 2005. Disponível em https://www.mma.gov.br./port/conama/res/res05/res35705.pdf

Corrêa HS (2021) Avaliação da Qualidade da Água na Influência de Atividades Mineiras e seus Efeitos na Comunidade Indígena dos Xikrins do Rio Cateté (Pará, Brasil). Unpublished Ms Thesis em Ciências e Tecnologias do Ambiente, Universidade do Minho (Braga, Portugal), 97 pp.

Costa RNL (2019) BAKRUKREN: o difícil exercício de soberania alimentar pelos Xikrin do Cateté, da aldeia DJu-djekô, no município de Parauapebas, Pará. Dissertação de Mestrado em Dinâmicas Territoriais e Sociedade na Amazônia, Universidade Federal do Sul e Sudeste do Pará. Marabá – Pará – Brasil.

García-Lorenzo ML, Pérez-Sirvent C, Martínez-Sánchez MJ, Molina-Ruiz J (2012) Trace elements contamination in an abandoned mining site in a semi-arid zone. J Geochem Explor 113: 23-35. https://doi.org/10.1016/j.gexplo.2011.07.001

ISA (2020) Terra Indígena Xikrin do Cateté. https://terrasindigenas.org.br/pt-br/terras-indigenas/3646 [accessed on the 21st July 2020].

Kipp GG, Stone JJ, Stetler LD (2009) Arsenic and uranium transport in sediments near abandoned uranium mines in Harding County, South Dakota. Appl Geochem 24(12):2246-2255, doi: 10.1016/j.apgeochem.2009.09.017

Lottermoser BG (2007) Mine Wastes Characterization, Treatment, Environmental Impacts. Springer, Berlin. 2ed.

Mello K, Taniwaki RH, Paula FR, Valente RA, Randhir TO, Macedo DR, Leal CG, Rodrigues CB, Hughes RM (2020) Multiscale land use impacts on water quality: Assessment, planning, and future perspectives in Brazil. J Environ Man 270: 110879. https://doi.org/10.1016/j.jenvman.2020.110879

Milanez B, Magno L, Pinto RG (2019) Da política fraca à política privada: o papel do setor mineral nas mudanças da política ambiental em Minas Gerais. Brasil. Cad Saú Publ 35: e00051219. https://dx.doi.org/10.1590/0102-311X00051219.

National Minerals Information Center/US Geological Survey (2017) Global iron-ore production data: clarification of reporting from the USGS. Min Eng 69: 20-23.

Paraguassú L, Leite MGP, Moreira FWA, Mendonça FPC, Eskinazi-Sant´Anna EM (2019) Impacts of mining in artificial lake of Iron Quadrangle-MG: past marks and changes of the present. Environm Ear Sci 167(78): 1-10. https://doi.org/10.1007/s12665-019-8158-7.

Reis JC, Silva H (2015) Mineração e desenvolvimento em Minas Gerais na década 2000-2010. Novos Cad NAEA 18: 73-100.

Sahoo PK, Dall`Agnol R, Salomão GN, Junior JSF, Silva MS, Souza Filho PWM, Powell MA, Angélica RS, Pontes PR, Costa MF, Sequeira JO (2019). High resolution hydrogeochemical survey and estimation of baseline concentrations of trace elements in surface water of the Itacaiúnas River Basin, southeastern Amazonia: implication for environmental studies. J Geochem Explor 205: 106321.

Salomão GN, Agnol RD, Sahoo PK, Júnior JSF, Silva MS, Souza Filho PW, Júnior WRN, Costa MF (2018) Geochemical distribution and thresholds values determination of heavy metals in stream water in the sub-basins of Vermelho and Sororó rivers, Itacaiúnas River watershed, Eastern Amazon, Brazil. Geochim Bras 32: 179-197.

Salomão GN, Agnol RD, Sahoo PK, Angélica RS, Medeiros Filho CA, Ferreira Júnior JS, Silva MS, Souza Filho PWM, Nascimento Júnior WR, Costa MF, Guilherme LRG, Siqueira JO (2020) Geochemical mapping in stream sediments of the Carajás Mineral Province: Background values for the Itacaiúnas River watershed, Brazil. App Geochem 118.

Santana CS, Olivares DMM, Silva VHC, Luzardo FHM, Velasco FG, Jesus RM (2020). Assessment of water resources pollution associated with mining activity in a semi-arid region. J Environ Manag 273: 111148

Satapathy DR, Salve PR, Kapatal YB (2009) Spatial distribution of metals in ground/surface waters in the Chandrapur district (Central India) and their plausible sources. Environ Geol 56: 1323-135. https://doi.org/10.1007/s00254-008-1230-3

UNESCO (2019) The United Nations World Water Development Report 2019: Leaving No One behind. UNESCO, Paris. Available in: https://www.unwater.org/publication/world-water-development-report -2019/

Val AL, Bicudo EM, Bicudo DC, Pujoni DGF, Spilki FR, Nogueira IS, Hespanhol I, Cirilo JÁ, Tundisi JG, Val P, Hirata R, Feliciano SM, Azevedo SMFO, Crestana S, Ciminelli VST (2019) Water quality in Brazil. Water Quality in the Americas: Risk and opportunities. IANAS-IAP, Mexico City.

Vasquez ML, Rosa-Costa LT, Silva CG, Ricci PF, Barbosa JO, Klein EL, Lopes ES, Macambira EB, Chaves CL, Carvalho JM, Oliveira JG, Anjos GC, Silva HR (2008) Geologia e Recursos Minerais do Estado do Pará: Sistema de Informações Geográficas – SIG: texto explicativo dos mapas Geológico e Tectônico e de Recursos Minerais do Estado do Pará. Escala 1:1.000.000. Belém: CPRM, 328pp.

In-Situ Hydrogen Peroxide Dosing Trials to Design Semi-Passive Treatment Schemes

Michael Cox, Christopher Satterley, Waqas Ahmed, Benjamin Cordier

The Coal Authority, 200 Lichfield Lane, Mansfield, Nottinghamshire, NG18 4RG, UK, mikecox@coal.gov.uk, christophersatterley@coal.gov.uk, waqasahmed@coal.gov.uk

Abstract

The oxidation kinetics of ferrous iron in coal mine water can be increased using hydrogen peroxide solution. To determine hydrogen peroxide demand the Coal Authority used desktop modelling based on a presumption that all mine waters had a similar behaviour for iron oxidation kinetics.

During the early stages of project design trials of hydrogen peroxide dosing were undertaken to study the behaviour in-situ of real mine water rather than in a laboratory with synthetic water. Both trials demonstrated the benefits of using actual mine water because it allowed for efficient and cost effective, semi-passive treatment schemes to be designed.

Keywords: Iron Oxidation, Hydrogen Peroxide

Introduction

Sometimes a passive coal mine water treatment scheme requires the addition of chemicals to increase the removal rate of iron, due either to a lack of available treatment area or a change in mine water quality or discharge requirements. This can be achieved using either hydrogen peroxide to increase the kinetics of the oxidation of ferrous to ferric ions (Leavitt 2010),

$$Fe^{2+} + H^{+} + \tfrac{1}{2}H_2O_2 \rightarrow Fe^{3+} + H_2O \qquad (1)$$

or sodium hydroxide solution to increase the solution pH. The rate of ferrous oxidation can be described by the rate equation (Stumm and Lee 1961),

$$-\frac{d[Fe^{2+}]}{dt} = k[Fe^{2+}][O_2]\,[OH^-]^2 \qquad (2)$$

The Coal Authority incorporated trials of hydrogen peroxide dosing of the coal mine water during the early stages of two projects which allowed for efficient and cost effective, semi-passive treatment schemes to be designed. These trials were undertaken at the Lynemouth treatment scheme (Northumberland, UK) and at the Polkemmet treatment scheme (West Lothian, UK).

Lynemouth Trial

Lynemouth treatment scheme, located on the site of the former Lynemouth Colliery, controls the water levels in the disused mine workings to prevent both pollution of the Morpeth aquifer, which supplies both drinking water and industrial supplies and uncontrolled discharges to surface. It consists of two treatment areas. Phase 1, built in 2013, consists of two 5,000 m^2 lagoons, in series, each preceded by a cascade. This could not pump sufficient water from the coalfield to prevent water levels rising in it. Consequently, Phase 2 was built in 2019, which consists of a cascade before three 4,000 m^2 lagoons in parallel; these collectively discharge into a second cascade that feeds two 5,500 m2 lagoons in parallel. The combined treated water from Phase 1 and Phase 2 is discharged to the local beach outfall. The scheme has a discharge permit of 150 kg/d of iron.

Phase 2 substantially increased the water flow and the iron concentration at the scheme. During its design stage the Coal Authority became aware that there was insufficient land available for a passive treatment scheme so it was planned to implement hydrogen peroxide dosing at the site to improve the ferrous ion oxidation during high mine

water flows. An initial assessment of the 35%w/w hydrogen peroxide required was calculated. Firstly, from the equation, 0.35 ml of 35%w/w hydrogen peroxide per gramme of dissolved ferrous ions (Younger *et al.* 2002) which indicated that 330 L/d could be required. Secondly, Coal Authority data from similar schemes was used as a model, which indicated that 525 – 1140 L/day could be needed depending on raw water flows and iron concentrations. Both calculations gave a wide variation in the volumes for the hydrogen peroxide consumption, which made the selection of the correct treatment process difficult.

To enable the design of the hydrogen peroxide dosing system and improve the estimate for hydrogen peroxide consumption a series of trials were conducted. These on-site trials used Phase 1 aerated mine water which was pumped from its outlet channel into the test tank. A 1,000 L IBC was used for this because it was recognised that its 1 m^2 surface area and 1m depth would represent the active water column of a lagoon. Hydrogen peroxide (3%w/w) was continually dosed in-line between the channel and the IBC via a dosing rig. Water filled the IBC in upward flow mode and it was allowed to overflow from the IBC until the contents achieved a "steady state". At this time both flows of water and hydrogen peroxide were stopped, the IBC isolated and the test began. This was a 48 hour period of batch reaction to simulate precipitation and settling in a lagoon. Samples were taken from near the water's surface every three hours and analysed for total iron, ferrous ion and ferric ion concentrations. Six trials were carried out and the concentrations and dosing pump rates of hydrogen peroxide dosing are described in Table 1.

Those trials in which no dosing occurred corresponded to a passive treatment scheme. The results did not fit Eq. (2) proposed by Stumm and Lee (1961) since the curve for iron removal against time was sigmoidal (Fig 1) and fitted the logistic equation,

$$\eta = \frac{[Fe]_{out}}{[Fe]_{in}} = \frac{L}{1+e^{-k(t-t_0)}} \quad (3)$$

where η is % removed, L is the maximum efficiency for the tests, t0 is the midpoint of the S-shaped curve, k is the slope of the curve at the mid-point. Sigmoidal graphs are associated with autocatalytic mechanisms (Moore and Pearson 1981), a characteristic of which is that the reaction is catalysed by one of its products. No attempt was made to confirm this for this particular mine water and further research is required to explain these results.

For the trials that were dosed the results followed a second order rate reaction (Fig 2),

$$\frac{1}{[Fe]_{out}} = \frac{1}{[Fe]_{in}} + At_{res}\text{, where } A = B[H_2O_2]^c \quad (4)$$

and t_{res} is residence time, B and c are empirical curve fitting parameters ($B = 9.2527 \times 10^{-5}$ and $c = 1.9702$) and $[H_2O_2]$ expressed as µL of 100 %w/w hydrogen peroxide per L of mine water treated.

From Eq. (4), it was calculated that 220 L/d 35%w/w hydrogen peroxide could be required to dose Phase 2. An estimate 35-80% lower than the previous calculations for volume used.

During the building of Phase 2, 35%w/w hydrogen peroxide was dosed into Phase 1 to allow it to treat higher water flows. Dosing was transferred to Phase 2 for commissioning to minimise the risk of an environmental incident whilst its flows were established. Initially dosing was at 187 L/d (130 ml/min). The average total iron load in the Phase 2 discharge was 26.3 kg/day and the average total iron load for the scheme was 67.6 kg/day or 45.1% of the 150 kg/day permitted discharge. Encouraged by this, the dosing was decreased step wise to determine the minimum for the scheme. The doses used, water flows and its iron contents are in Table 2 and the corresponding iron loadings achieved for Phases 1 and 2 and the scheme are in Table 3.

Table 1 *Hydrogen peroxide concentrations and dosing rates used in Lynemouth trials.*

Test	1	2	3	4	5	6
100 %w/w H_2O_2, (µL/L)	0	5	10	0	15	20
H_2O_2 Pump rate, (mL/min)	0	36	72	0	109	145

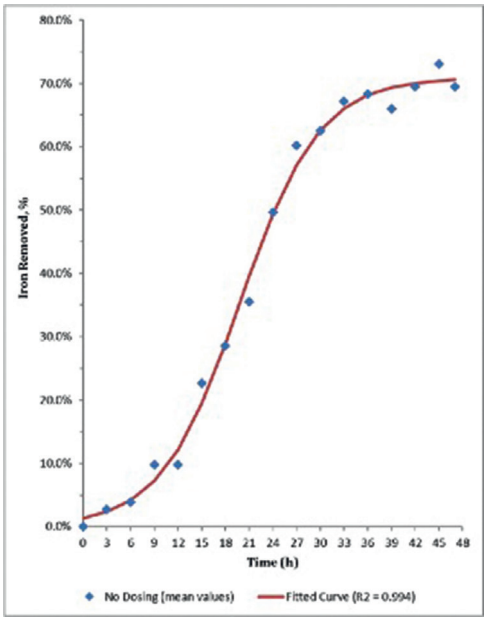

Figure 1 *Lynemouth - Iron removed without dosing.*

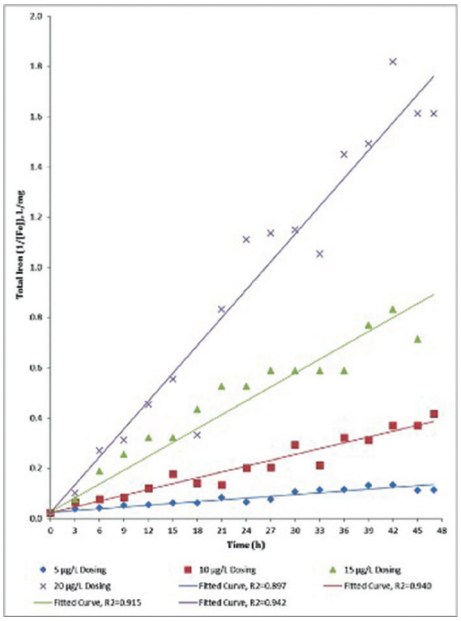

Figure 2 *Change in total iron with time, with dosing.*

Table 2 *Trial parameters employed during Phase 2 commissioning (mean values).*

Trial	35 %w/w H_2O_2 Dosed to Phase 2 only	Mine Water Total Iron	Water Flow Phase 1	Water Flow Phase 2	Discharge Total Iron Phase 1	Discharge Total Iron Phase 2
	L/d	mg/L	L/s	L/s	mg/L	mg/L
Trial 1	187	51.2	71.8	107.9	6.6	2.8
Trial 2	151	45.1	61.1	103.1	5.2	2.8
Trial 3	118	42.6	64.0	108.0	5.9	2.0
Trial 4	89	49.5	70.0	110.6	5.9	2.6
Trial 5	54	51.9	71.0	99.8	5.8	2.7
Trial 6	22	48.5	69.4	110.3	5.2	3.2
Trial 7	0	48.2	70.2	111.0	5.3	3.5

Table 3 *Trial results achieved during Phase 2 commissioning (mean values).*

Trial	35 %w/w H_2O_2 Phase 2 only	Discharge Iron Load Phase 1	Discharge Iron Load Phase 2	Discharge Iron Load Total
	L/d	kg/d	kg/d	kg/d
Trial 1	187	41.3	26.3	67.6
Trial 2	151	28.3	24.6	52.7
Trial 3	118	32.9	18.9	51.8
Trial 4	89	35.8	25.1	60.8
Trial 5	54	35.8	24.0	59.8
Trial 6	22	31.0	30.2	61.2
Trial 7	0	32.1	33.6	65.7

For all the trials, the daily iron load in the discharge ranged from 34.5-45.1% of the permitted discharge of 150 kg/d total iron. Indeed with no dosing to the scheme the iron load was 43.8% of the permitted discharge which provided a margin of safety should either an increase in iron concentration or an increase in flow occur.

Polkemmet Trial

Polkemmet treatment scheme, located near Whitburn, West Lothian, is a semi-passive treatment scheme that has no cascade. Oxidation of ferrous iron is achieved with 35%w/w hydrogen peroxide solution injected into the mine water transfer pipe at the headwork. The mine water is transferred about 230 m to three lagoons. Two lagoons (1160 m^2 and 1344 m^2) operate in parallel and the combined discharges feed a third lagoon (1485 m^2). The discharge from the third lagoon feeds a single reed bed (3200 m^2). The Coal Authority decided to refurbish the scheme for several reasons. Firstly, it cannot abstract sufficient mine water to maintain the below ground level, which historically has led to several uncontrolled discharges at surface. Secondly, its reed bed is severely overgrown and is not working correctly; furthermore, it cannot be isolated or easily maintained. Thirdly, the current lagoons have low residence times and experience short-circuiting. Fourthly, it has a high operating cost because it uses 35 %w/w hydrogen peroxide to oxidise the ferrous iron and bring about the precipitation of ferric hydroxide. Currently, it uses 429 L/d 35%w/w hydrogen peroxide equivalent to 157 t/y.a

The refurbishment, planned for 2021–2023, will include constructing a cascade and two new reed beds, re-piping the existing lagoons so that they operate in parallel and constructing two new primary lagoons. There is insufficient land available for a fully passive scheme and although a cascade has been included to decrease both the reliance on hydrogen peroxide use and operating cost, it is anticipated that some dosing will be required.

Trials were conducted to inform the design of the dosing system and estimate hydrogen peroxide consumption. For these, mine water was taken from the riser main to pass down a cascade. It was calculated that the mine water delivered, at 3m height, a 0.5 L/s flow that decreased sharply so it was unlikely that this flow could be attained if a fully representative 4m high cascade was used. A two-stage cascade (stage 1, 2.5 m high; stage 2, 1.5 m high), Fig 3, with intermediate pumping was used. If sized for 0.5 L/s (Younger *et al*. 2002) the cascade would be narrow and unstable therefore it had a larger width to flow ratio of 150. Hydrogen peroxide (7.71%w/w) addition was to the aerated mine water in the buffer tank whilst a pipe mixer provided additional mixing. The water filled a 1000 L IBC in upward flow mode and overflowed from the IBC until the contents achieved a "steady state". At this time both flows of water and hydrogen peroxide were stopped, the IBC isolated and the 48 hour test period began. Samples were taken from near the water's surface every three hours and analysed for total iron, ferrous ion and ferric ion concentrations. Hydrogen peroxide concentrations and dosing pump rates used in the twelve trials are collated in Table 4.

A cascade was beneficial because the first stage increased the dissolved oxygen from 5.1% to 84.7%. Stage 2 did not increase the dissolved oxygen further because the water was nearly saturated with oxygen, which restricted its ability to absorb more oxygen. Aeration increased the raw mine water from pH 6.33 (mean) to pH 6.77 (mean) due to carbon dioxide degassing.

Unlike Lynemouth, those results for the non-dosing trials did not show a sigmoidal curve which suggested that no autocatalytic mechanism was promoting the ferrous oxidation (Fig 4). Polkemmet mine water is partially oxidised and contains about 10-15% ferric iron. It's aerated, undosed, water oxidised much faster than Lynemouth's, after

Table 4 *Hydrogen peroxide concentrations (µL/L) and dosing rates (mL/min) for Polkemmet trials.*

Test	1	2	3	4	5	6	7	8	9	10	11	12
100 %w/w H_2O_2,	0.0	2.5	12.5	17.5	20.0	1.0	7.5	0.0	10.0	15.0	5.0	0.0
H_2O_2 Pump rate,	0	44	221	310	354	18	133	0	177	265	88	0

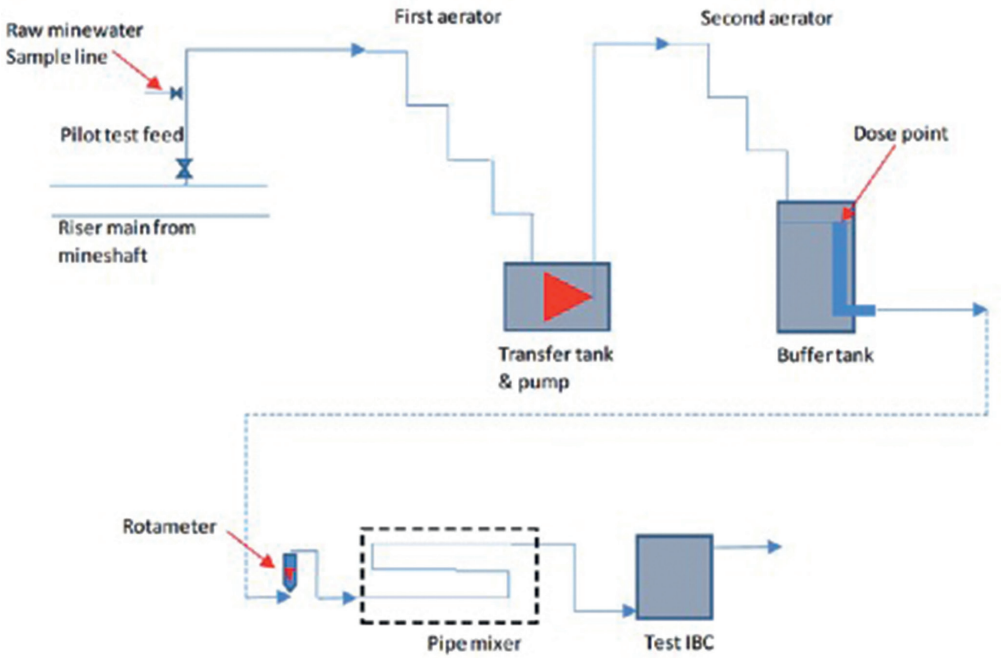

Figure 3 *Layout of Equipment for Polkemmet Test Work.*

15 hours iron removal was 79.4% compared to the 22.7% iron removal of Lynemouth. Laboratory and field studies have shown that precipitated hydrous ferric oxides can catalyse the oxidation of ferrous ions adsorbed on their surfaces (Tamura 1980, Dempsey 2002, Geroni 2011). The presence of ferric iron, and associated hydrous ferric oxides, may be promoting a much faster oxidation of the ferrous iron than the suggested autocatalytic mechanism.

Analysis of the results from the dosed trials identified that that they followed a second order reaction, Eq. (4), similar to Lynemouth,

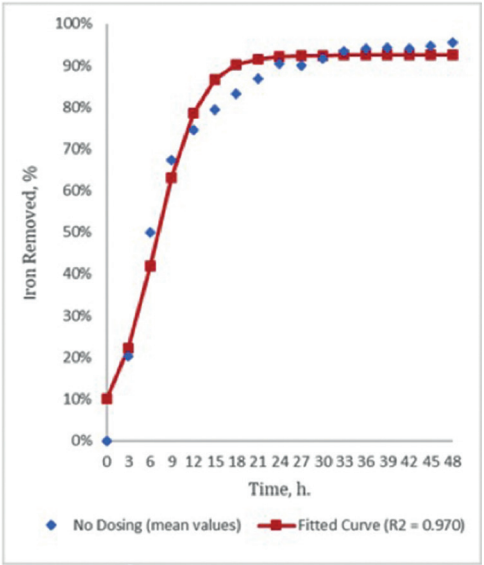

Figure 4 *Polkemmet - Iron removed without dosing.*

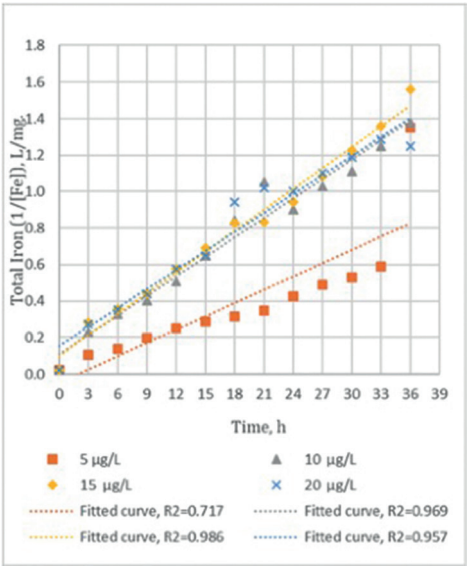

Figure 5 *Change in total iron with time, with dosing.*

where the empirical curve fitting parameters were B = 8.480 × 10^{-3} and c = 0.4989 and [H_2O_2] expressed as µL of 100 %w/w hydrogen peroxide per L of mine water treated. The observed faster rate of iron removal without dosing suggests that the need for hydrogen peroxide could be much decreased compared with the 429 L/d currently used but this would depend on the cascade's efficiency to aerate the abstracted mine water. It was calculated that 100-200 L/d 35%w/w hydrogen peroxide could be required.

Conclusions

Previously the Coal Authority's approach to designing dosing systems applied desktop modelling and a prior knowledge that assumed that mine waters had a similar behaviour for iron oxidation kinetics during dosing. This work demonstrated that desk top models can calculate a higher volume of hydrogen peroxide needed to be dosed compared with the results obtained from trials on real mine water. In addition, the mine waters in these trials demonstrated markedly different behaviours that were specific to each site. Results from Lynemouth suggested that an autocatalytic mechanism contributed to the oxidation of ferrous iron in the undosed trials and further research is needed to confirm this.

Desktop modelling suggested that Lynemouth needed to be dosed with 330 L/d 35%w/w hydrogen peroxide. A second order rate equation derived from the on-site test results calculated 220 L/day was needed. A saving of 110 L/d or 45 t/y in chemical used. Dosing continued during Phase 2 commissioning to minimise the risk of an environmental incident whilst scheme flows were established. It was progressively decreased such that when it was stopped the iron load of the discharge remained substantially less than its 150 kg/d maximum discharge limit. This result suggested that the model from the trial did not accurately reflect the scheme's true performance. Indeed, the model does not take into account the actual residence times in the lagoons, which may have to be included as an empirical factor to improve it. Work is underway to determine the actual residence times.

The results for the Polkemmet trials confirmed that a cascade would be substantially beneficial to provide aeration and some carbon dioxide degassing and one has been included into the new scheme's design. Provision has also been made for dosing equipment in it, as the mine water is considered marginal in terms of treatment through passive oxidation alone.

This work demonstrated the benefits of undertaking hydrogen peroxide dosing test work on site using actual mine water because it allowed for efficient and cost effective, semi-passive treatment schemes to be designed. Furthermore, it provided an equation that the Coal Authority will be able to use in the future to model hydrogen peroxide dosing at treatment schemes.

References

Dempsey BA, Dietz J, Jeon BH, Roscoe HC, Ames R (2002) Heterogeneous oxidation of ferrous iron for treatment of mine drainage. In Barnhisel RI and Collins M (Eds), Proceedings American Society of Mining and Reclamation 2002: 487-495,

Geroni JN, Sapsford DJ (2011) Kinetics of iron (II) oxidation determined in the field. Appl Geochem 26: 1452-1457

Leavitt BR (2010) In-situ iron oxidation using hydrogen peroxide. In Barnhisel RI (Ed), Proceedings American Society of Mining and Reclamation 2010: 551-569

Moore JW, Pearson RG (1981) Kinetics and Mechanism, 3rd edition, Wiley, Chichester, p26.

Summ W, Lee GF (1961) Oxygenation of ferrous iron. Ind Eng Chem 53: 143-146, https://doi.org/10.1021/ie50614a030

Tamura H, Kawamura S, Hagayama M (1980) Acceleration of the oxidation of Fe2+ ions by Fe(III)-oxyhydroxides. Corros Sci 20: 923-971. https://doi.org/10.1016/0010-938X(80)90077-3

Younger PL, Banwart SA and Hedin RS (2002) Mine Water: Hydrology, Pollution, Remediation. Kluwer, Dordrecht, p278, https://doi.org/10.1007/978-94-010-0610-1.

Alternative Reagents for the Treatment of Pb-Zn Mine Drainage in Wales

J. Dean, B. Alkhazraji, D.J. Sapsford

Cardiff School of Engineering, Cardiff University, Cardiff, CF24 3AA; sapsforddj@cardiff.ac.uk

Abstract

This paper presents the results of a laboratory-scale dosing experiment to test the efficacy of four low-cost / alternative reagents to removed dissolved Zn, Cd, and Pb from contaminated mine water. Hydrogen phosphate (Na_2HPO_4) achieved >95% Pb removal, but lower Zn and Cd removal. Sodium metasilicate (Na_2SiO_3) and sodium bicarbonate ($NaHCO_3$) did not achieve suitable metal removal. A 99-244 mg/L dose of sodium carbonate (Na_2CO_3) removed high levels of Zn (99% ±0.2), Cd (95% ±3), and Pb (88% ±3). Sodium carbonate dosing of Zn-Cd-Pb-contaminated mine water could form the basis of a new, low cost, and low input treatment process.

Keywords: Zinc, Lead, Mine Water, Alternative Reagents

Introduction

Over 1300 abandoned non-ferrous metal mines are known to exist in Wales. These sites contribute towards approximately 100 km of river reaches in Wales failing to meet Environmental Quality Standards (EQS) for Zn, Cd, and Pb (Jarvis *et al*. 2007). Contaminated mine water must be treated to avoid wide-spread pollution of surface water bodies, however treating water from these sites is both challenging and costly (Jarvis *et al*. 2012). Passive treatment of circumneutral Zn-contaminated mine water often requires systems with a large footprint (e.g. Nairn *et al*. 2010), which can be inappropriate for remote upland mine sites. Alternatively, adsorption-based treatment systems may achieve high metal-removal efficiencies, but they can be high-cost and may quickly become saturated with respect to contaminants (e.g. Warrender *et al*. 2010). Active treatment systems can be costly to operate (URS 2014) and typically use reagents such as lime (CaO) and sodium hydroxide (NaOH). These strong bases present operational challenges in relation to control of dosing, reagent dispensing and health and safety, especially when lone operators are maintaining systems in remote locations. Previous work conducted by this research group has identified that a carbonate-based system may be appropriate to treat circumneutral Pb-Zn mine drainage in Wales (Williams *et al*. 2020). This paper seeks to build on this existing work by investigating the effect of dosing two real mine waters with Na_2CO_3, a relatively safe-to-handle and low-cost reagent, alongside three more low cost and/or relatively safe alternative mine water treatment reagents. It is envisaged that this work will be expanded in the future and will lead to the development and implementation of a 'semi-passive' mine water treatment system whereby circumneutral metal mine drainage in Wales will be treated in a low cost, low input system.

Methods

Mine water was collected from two abandoned Pb-Zn mines in mid Wales. The first mine site, Abbey Consols, is located 1 km east of the village Pontrhydfendigaid in Ceredigion. Water draining Abbey Consols mine water is circumneutral and contains elevated levels of Zn (>15 mg/L), Cd (>40 µg/L) and Pb (>130 µg/L). Mine water (3 L/s) drains into the River Teifi, a Special Area of Conservation, which contributes towards the river failing to meet its Water Framework Directive (WFD) target for Zn for 29 km (NRW, 2016). Water was also sampled from Nant y Mwyn Pb

mine, Rhandirmwyn, Carmarthenshire. Nant y Mwyn water is also circumneutral and it is similarly contaminated with Zn, Pb, and Cd. This mine is an important source of Zn to the River Tywi, which fails to meet its WFD target for Zn for approximately 65 km downstream (NRW, 2014). Treating mine water discharges from these sites has the potential to prevent a combined total of 14 tonnes of Zn, Cd, and Pb from entering local surface water courses.

Mine water was treated using four low cost/alternative reagents: sodium carbonate (Na_2CO_3), sodium bicarbonate ($NaHCO_3$), sodium hydrogen phosphate (Na_2HPO_4), and sodium metasilicate (Na_2SiO_3). These reagents are summarised in Table 1.

A 10 g/L stock solution was made-up for each reagent. Between 0 and 2.5 mL stock was mixed with 100 mL of mine water in magnetically stirred borosilicate glass beakers. Experiments were run for between 1 and 120 minutes to test the effect of variable reaction time on metal removal. Following the predefined reaction time, samples were filtered through 0.45 µm filter membranes, acidified using 0.1 mL of 10% (v/v) HNO_3, and analysed by ICP-MS. Sample pH was recorded before and after each treatment using a Mettler Toledo Seven Multi S40 m along with an InLab Expert Pro ISM pH probe. All experiments and pH measurements were completed in triplicate.

Table 1 *A summary of water treatment reagents used in this study.*

Reagent	Common application(s)
Na_2CO_3	pH adjustment and softener in water treatment
$NaHCO_3$	Acid neutralisation
Na_2HPO_4	Water treatment to prevent plumbosolvency
Na_2SiO_3	Coagulant in water treatment

Results and Discussion

A summary of the unamended mine waters is provided in Table 2. This data is presented alongside a target value for each metal, defined here as 3-times the approximate Environmental Quality Standard for the respective metal. This is the desired concentration of each metal following treatment. Over 99% removal is required to meet the target value for Zn and Cd, and >97% removal is required to meet the target value for Pb. Evidently, for any of these dosing strategies to be considered for future research, they must be shown to achieve very high (>97%) metal removal rates.

All four of the reagents tested have the potential to raise the pH of mine water. The effect of dose on water pH is presented in Figure 1.

Following 120-minute reaction time, the pH of Abbey Consols and Nant y Mwyn water containing 244 mg/L Na_2CO_3 was almost identical (pH 8.75 and pH 8.76, respectively). Indeed, the pH of the two mine waters responded to being dosed with Na_2CO_3 in a very similar fashion, as indicated by a strong positive correlation between dose and pH (r = 0.93). Under the same conditions, $NaHCO_3$ increased the pH of these waters to between 7.59 and 7.81. Na_2HPO_4 increased the Abbey Consols water from pH 5.50 to 6.44 and the Nant y Mwyn water from pH 6.60 to 6.95. Interestingly, Na_2SiO_3 was found to be quite insoluble in Nant y Mwyn water, hence the dose was adjusted to a maximum of 24.4 mg/L which resulted in a final pH of 8.78, whereas a 244 mg/L dose of Na_2SiO_3 in Abbey Consols water resulted in a lower final pH of 8.11.

Table 2 *Summary of unamended mine water. Target values refer to an appropriate effluent concentration for a mine water treatment system, as suggested by URS (2014).*

	pH	Zn (mg/L)	Zn target (mg/L)	Cd (µg/L)	Cd target (µg/L)	Pb (µg/L)	Pb target (µg/L)
Nant Y Mwyn	6.6	13.0	0.036	50.7	0.3	138.7	6
Abbey Consols	5.5	15.9		41.7		132.7	

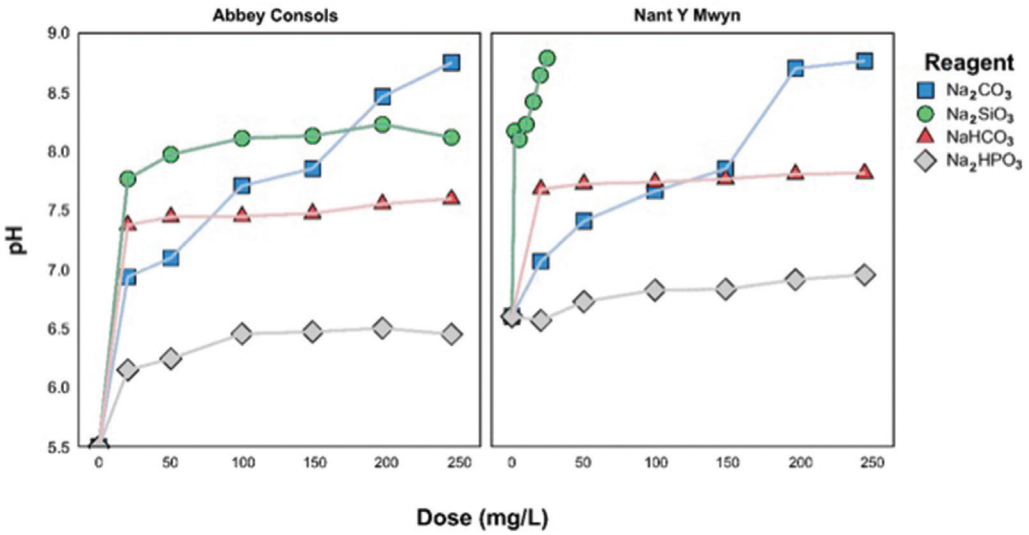

Figure 1 *pH of two mine water samples with a variable dose of the four reagents.*

A Comparison of Reagent Efficacy in the Removal of Dissolved Metals

The removal of dissolved metals from Abbey Consols and Nant y Mwyn mine water following 120 minutes reaction time is presented in Figure 2. Sodium carbonate was highly effective at removing Zn (maximum 99.3% removal), Cd (maximum 98.0% removal), and Pb (maximum 92.2% removal) from solution. Between 0 and 99 mg/L dosage, metal removal from both waters increased sharply (Figure 2). The maximum removal of dissolved metals from mine water by Na_2CO_3 did not necessarily correspond to the maximum reagent dose (244 mg/L), but always occurred at >99 mg/L. Above 99 mg/L dosage, metal removal plateaued at 99% ±0.2 (Zn), 95% ±3 (Cd), and 88% ±3(Pb). These removal rates result in a final Zn, Cd, and Pb concentration within one order of magnitude of the target values presented in Table 2. Sodium carbonate dosing appears to be a viable method to treat mildly acidic to circumneutral Pb-Zn mine drainage.

Sodium hydrogen phosphate (Na_2HPO_4) was more effective at removing Pb from Nant y Mwyn water (maximum 95.4% removal) than sodium carbonate, although this was not true for Abbey Consols water where Na_2CO_3 outperformed Na_2HPO_4: maximum removal by Na_2HPO_4 and Na_2CO_3 was 48% and 92%, respectively. The maximum Zn and Cd removal by Na_2HPO_4 was 50.5% and 50.1%, respectively This demonstrates that although it performed well for Pb removal from the Nant y Mwyn water, Na_2HPO_4 is not suitable for the treatment of Zn and Cd in these waters and would, without removal of residual phosphate, potential cause further pollution.

Neither $NaHCO_3$ or Na_2SiO_3 performed particularly well in this set of experiments for any of the elements studied. The maximum removal of dissolved Zn by $NaHCO_3$ (32%) was much lower than by Na_2SiO_3 (69%), and both were outperformed by Na_2CO_3 (maximum 99.3% removal). Similar results are observed for Pb and Cd, although maximum removal for these elements was lower than for Zn. Based on the comparatively low metal removal rates by these reagents, $NaHCO_3$ or Na_2SiO_3 should not be considered further for Pb-Zn removal from these mine waters.

A geochemical equilibrium model was run in PHREEQC, using the wateq4f thermodynamic database, to predict the saturation state of relevant Zn-based minerals in mine water containing 99 mg/L of the various reagents. All reagents caused the mine water pH to increase (Figure 1). Despite this pH increase, $Zn(OH)_2$ was never predicted to be oversaturated. Zinc carbonate, silicate, and phosphate minerals were all predicted to be oversaturated in

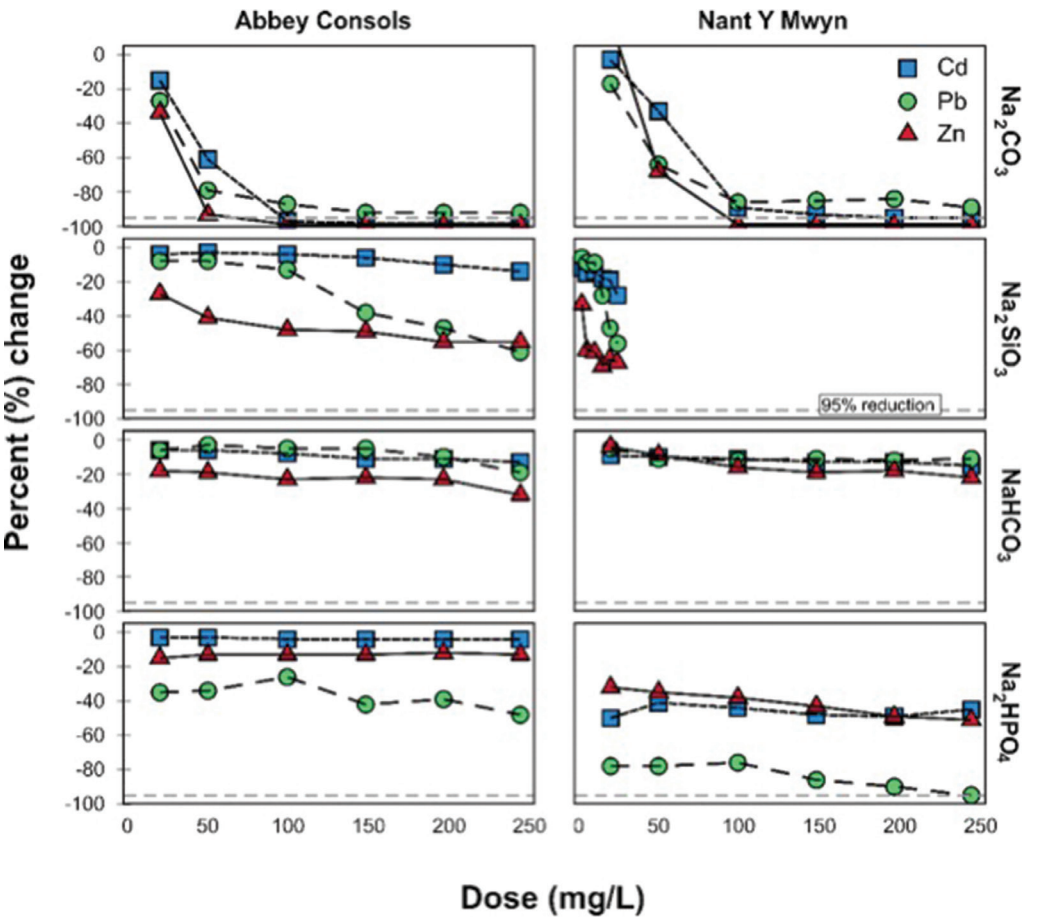

Figure 2 *Percent change in dissolved (<0.45 µm) metal concentration following dosing with Na_2CO_3 (top row), Na_2SiO_3 (second row), $NaHCO_3$ (third row), and Na2HPO4 (bottom row). Grey, dashed horizontal line represents 95% reduction in metal concentration.*

response to dosing with their respective salts under the abovementioned conditions. Based on the high efficacy of the Na_2CO_3 treatment for Zn removal, multiple Zn carbonate-based minerals were considered in this modelling exercise. Smithsonite, $ZnCO_3$, is predicted to be oversaturated and may therefore form in these waters and remove Zn from solution. Other Zn hydroxycarbonate minerals, namely hydrozincite ($Zn_5[OH]_6[CO_3]_2$), are known to form in place of pure Zn carbonates under similar conditions (Zachara *et al.* 1989). As such, the thermodynamic database was amended with the solubility constant for hydrozincite (6.41) taken from Apps and Wilkin (2015). Hydrozincite was also found to be oversaturated in the Na_2CO_3-dosed water. Based on the Pourbaix diagram constructed for a Zn-H_2O-CO_2 system presented by Meda *et al.* (2014) and the experimental work by Zachara *et al.* (1989), it would be expected that hydrozincite will form from these CO_3-amended waters. This is an important point because it has implications for designing a field-scale water treatment system. Hydrozincite typically forms small (10's of µm) flake-like crystals which can be slow to settle. It will be important to properly characterise the Zn-based precipitate to design a suitable Na_2CO_3 dosing system.

The effect of reaction time

Sodium carbonate was found to be the most effective reagent for Zn, Cd, and Pb removal from solution. Metal removal by Na_2CO_3 was not greatly affected by the range of reaction

Table 3 Metal removal from two mine water samples dosed with 99 mg/L and 244 mg/L Na_2CO_3 after 1 minute and 120-minute reaction time.

Site	Dose (mg/L)	Reaction Time (min)	Zn	Cd	Pb
			Percent removal (%)		
Abbey Consols	99	1	98.0	95.7	82.6
Abbey Consols	99	120	99.2	97.2	87.5
Nant Y Mwyn	99	1	98.4	87.3	81.7
Nant Y Mwyn	99	120	98.6	89.4	85.9
Abbey Consols	244	1	98.7	97.4	89.2
Abbey Consols	244	120	99.2	98.0	92.0
Nant Y Mwyn	244	1	98.7	94.5	84.9
Nant Y Mwyn	244	120	99.2	95.0	89.3

times employed in this work (Table 3). For example, Zn removal from Abbey Consols water was 1.2% higher after 120 minutes following a 99 mg/L Na_2CO_3 dose than after 1 minute reaction time. Similar results can be observed for Zn, Cd, and Pb following a 99 mg/L and 244 mg/L dose in both Abbey Consols and Nant y Mwyn water.

A longer reaction time (120 minutes) resulted in there being 0.19 mg/L (Abbey Consols) and 0.03 mg/L (Nant y Mwyn) less Zn in the final solution than after 1 minute reaction time. Similar results are observed for Cd and Pb. Although the majority of Zn (>98%), and other metals, was removed from solution after just 1 minute, the comparatively small decrease in concentration between 1 and 120 minutes is important when considering the target value of 0.036 mg/L for Zn presented in Table 2. Following 1 minute reaction time, Abbey Consols water contained 0.32 mg/L Zn, approximately 10-times more than the target value. After 120 minutes, however, the Abbey Consols water contained 0.12 mg/L Zn, only 3.8-times greater than the target value. The same general trend holds true for Cd and Pb.

The typically high metal removal rates irrespective of time are of interest because it may be possible to design a water treatment system which is able to handle water with variable residence time. For example, it may be desirable to treat water using a 120 minute reaction time under 'normal' operating conditions, but then at times of higher flow treat a much greater volume of water using the same sized treatment plant by allowing for a shorter reaction time. This could offer a pragmatic solution to treating high volumes of contaminated mine water during infrequent times of heavy rainfall without the cost or space requirements of building a larger treatment facility, both of which are important considerations when treating water from abandoned mines in remote upland areas.

Conclusions

This work tested the efficacy of four commonly used water treatment reagents in removing dissolved Zn, Cd, and Pb from two mine water samples. Na_2HPO_4 achieved high Pb removal (>95%) in one of these waters but failed to remove sufficient Zn and Cd. Na_2SiO_3 and $NaHCO_3$ both performed poorly in comparison with Na_2HPO_4 for Pb, and Na_2CO_3 for Zn, Cd, and Pb. Na_2CO_3 clearly outperformed all other reagents tested. A 99 mg/L dose of Na_2CO_3 resulted in a final water pH of 7.66-7.70 and achieved over 99% (Zn), 95% (Cd), and 88% (Pb) metal removal. The bulk of dissolved metals were removed from solution after just 1 minute reaction time, although increasing the reaction time pushed the final metal concentration down towards the target value following treatment. Assuming that the cost of Na_2CO_3 is approximately £200/tonne (UPS 2014) and a 99 mg/L dose is used, 1 m3 of mine water could be treated for <£0.02. Sodium carbonate dosing offers an effective and low cost means of treating Zn-Cd-Pb-contaminated circumneutral mine water in Wales.

Acknowledgements

The work was supported and undertaken under the auspices of the EPSRC (EP/R51150X/1) and the METAL-SoLVER project (#82347 Welsh European Funding Office).

References

Apps J, Wilkin R (2015) Thermodynamic Properties of Aqueous Carbonate Species and Solid Carbonate Phases of Selected Trace Elements pertinent to Drinking Water Standards of the US. Environmental Protection Agency Report

Jarvis A, Fox A, Gozzard E, Hill S, Mayes W, Potter H (2007) Prospects for effective national management of abandoned metal mine water pollution in the UK. In: Proceedings of the international mine water association symposium, pp.27-31.

Jarvis A, Mayes W, Coulon P, Fox A, Hill S, Johnston D, Potter HAB, Thorn P, Watson I (2012) Prioritisation of abandoned non-coal mine impacts on the environment. SC030136/R12

URS (2014) Metal Mine Water Treatment review. URS Infrastructure and Environment UK Ltd, Manchester.

Medas D, De Giudici G, Podda F, Meneghini C, Lattanzi P (2014) Apparent energy of hydrated biomineral surface and apparent solubility constant: an investigation of hydrozincite. Geochimica et Cosmochimica Acta 140, pp 349-364

Nairn R, LaBar J, Strevett K, Strosnider W, Morris D, Garrido A, Neely C, Kauk K (2010) Initial evaluation of a large multi-cell passive treatment system for net-alkaline ferruginous lead-zinc mine waters. Proceedings America Society of Mining and Reclamation, pp 635-649

NRW (2014) Abandoned Mine Case Study: Nant y Mwyn Lead Mine. Natural Resources Wales

NRW (2016) Abandoned Mine Case Study: Abbey Consols Lead & Zinc Mine. Natural Resources Wales

Warrender R, Pearce N, Perkins W, Brown A, Sapsford D, Bowell R, Dey M (2010) Field Trials of Low-Cost Permeable Reactive Media for the Passive Treatment of Circum-Neutral Metal Mine Drainage in mid-Wales, UK. Proceedings of the international mine water association symposium, pp 291-294

Williams T, Dent J, Eckhardt T, Riding M, Sapsford, D (2020) Treatability trials to remove zinc from Abbey Consols mine water, Wales, UK. Proceedings of the international mine water association symposium, pp 255-230.

Zachara J, Kittrick J, Dake L, Harsh J (1989) Solubility and surface spectroscopy of zinc precipitates on calcite. Geochimica et Cosmochimica Acta 53(1), pp 9-19

Laboratory Testing to Determine the Effectiveness of Capping and Risk of Long-Term Metal Release from Mine Waste at the Abandoned Abbey Consols Lead-Zinc Mine, Wales, UK

Julia Dent[1], Andrew Barnes[2], Ben Gersten[2], Mark Roberts[2], Tom Williams[3], Thomas Eckhardt[4]

[1]*Mine Environment Management, Vale Street, Denbigh, Denbighshire, UK, LL16 3AD, jdent@memconsultants.co.uk*

[2]*Geochemic Ltd, Lower Race, Pontypool, Wales UK, NP4 5UH, abarnes@geochemic.co.uk, bgersten@geochemic.co.uk, mroberts@geochemic.co.uk*

[3]*Natural Resources Wales, Swansea University Singleton Campus, Tom.Williams@cyfoethnaturiolcymru.gov.uk*

[4]*WSP UK Ltd, Kings Orchard, 1 Queen Street, Bristol, BS2 0HQ, UK, Thomas.Eckhardt@wsp.com*

Abstract

The effectiveness of a proposed low permeability cover system for historical mining waste at the abandoned Abbey Consols lead-zinc mine, Wales, UK, was tested using laboratory columns. A reduced infiltration rate could still result in release of metals reducing the benefits of the cover system. Two column scenarios simulated average infiltration conditions and a reduced infiltration rate (the low permeability cover). Results showed the reduced infiltration column produced higher concentrations of key solutes (cadmium, lead and zinc) but a lower load. Zinc and cadmium loads narrowed between the two columns over time suggesting the low permeability cover benefit diminishes.

Keywords: Lead-zinc, Abandoned Mine, Column Tests, Remediation

Introduction

Abbey Consols mine is located near Pontrhydfendigaid, Mid-Wales, and derives its name from the nearby Strata Florida Abbey. A total recorded output of 1,236 tons of lead ore and 1,765 tons of zinc ore were mined between 1848-1909 (Jones 1922). The former lead and zinc mine has been abandoned since operations ceased in 1909 (Conflein 2019), and approximately 32,000 tonnes of spoil material remains on site (BGS 2012). An extensive ground investigation (GI) was undertaken in early 2019 to delineate the extent and composition of contaminated material, as well as understand how remediation options such as waste capping could improve waste stabilisation and seepage and runoff water quality from the site. As part of the GI samples of both mine waste and soil were gathered at the site.

Column leaching experiments on mine waste were set-up by Geochemic Ltd, contracted by WSP on behalf of Natural Resources Wales (NRW). The primary focus of this study was to determine the contaminate contribution (mainly cadmium, lead and zinc) from leaching of spoil from the waste tips and to determine the potential benefits and risks of capping the spoil with a low permeability cover system. The tests were also intended to determine the potential for flushing-out of the stored soluble salts that may be released due to a rising ground water table during a storm event.

Methodology

Sampling

The column tests used a bulk waste composite from a mix of individual samples of waste material collected during the GI (tab. 1). The seven samples of spoil incorporated in the composite sample had a range of sulfur, lead and zinc contents and was classified as gravelly mine spoil.

Table 1 Individual waste sample depths, composition and location.

Geochemic Sample ID	Weight received (kg)	Depth	Sulfur total (%)	Pb (mg/kg)	Zn (mg/kg)	Location within the waste tip area (N / S / Mid)
GCL0076-002	5.55	2.50-3.50	0.119	5700	1290	Mid
GCL0076-003	7.04	1.20-2.50	0.107	5340	3480	N
GCL0076-004	32.5	1.00-	1.59	4820	34200	N
GCL0076-005	6.7	0.10-	0.145	697	5320	Mid
GCL0076-007	18.86	0.80-	0.518	26100	4920	Mid
GCL0076-012	17.54	1.00-1.00	0.229	8030	4990	S
GCL0076-014	17.12	0.40-	0.0508	1230	1420	S

Sample Preparation

The samples were screened at 25 mm and any oversized material was removed. The screened samples were blended together to make a single composite sample of roughly 90 kg. A representative 10 kg sub sample was obtained through cone and quartering and the remainder was further split into four separate 20 kg portions.

The 10 kg sub sample was weighed and then dried at 60 °C for 48 hours prior to being re-weighed then crushed to 90% passing 6.5 mm with a jaw crusher. This was then riffle split to obtain two test portions. The 100 g test portion was further dried at 105 °C to determine the residual moisture content and then pulverised to >80% passing 75 µm. This test portion was sent to ALS Hawarden for elemental characterisation including sulfur and carbon speciation, elemental abundance and mineral composition.

Column preparation and operation

Two 200 mm internal diameter columns were constructed from clear Perspex® acrylic (Fig. 1). The columns were 1 m in height and featured a suspended floor at the base to facilitate draining. The false floor was drilled to allow draining of collected leachate on to which a layer of polypropylene felt filter material was placed to prevent fines from being washed out of the column. Each column was loaded with two of the 20 kg test portion splits. The samples were loaded at field moisture content to prevent changes to the material characteristics that may occur during drying. The columns were covered with opaque foam material to prevent light ingress and minimize temperature fluctuations at the edge of the column. A standard laboratory temperature of 20 °C (+/-5 °C) was maintained throughout experimentation.

The columns were flushed weekly with ultra-pure 18.2 MΩ deionised water using an automated spray irrigation system. This allowed for a uniform dose to the columns at precise time intervals. As the primary objective of the columns was to identify the difference between application of a low permeability cover system and an uncovered system, the irrigation rate was varied with Column 1 receiving the equivalent of 1560 mm of infiltration per year and the Column 2 receiving the equivalent of 156 mm of infiltration per year. Leachate was collected at the base of the column in Tedlar® gas sampling bags to limit atmospheric interaction.

The columns were operated for 8 months with samples being collected on a weekly basis. Analysis of parameters pH, electrical conductivity, oxidation / reduction potential, alkalinity and acidity were determined immediately upon collection at Geochemic's Laboratory using a Metrohm® automated system. In addition, sulfate was determined turbimetrically using HACH SulfaVer4® method.

Every four weeks, a composite sample of leachates was sent to ALS Hawarden for a detailed elemental analysis suite including major cations and anions and trace elements by ICP-MS. The composite sample was made from equal volumes of the weekly leachates

Figure 1 *Laboratory columns and set-up (image: Geochemic Ltd).*

from each of the weeks within the four-week period. A final flushing event was introduced to the column test methodology following the normal month 8 method. A volume of around 7.5 L was added to each column to fully saturate the columns (from the base, to simulate a groundwater flush). The water added sat above the height of the waste in each column by around 20 mm. The water was left for 24 hours, and then both columns were drained down. Following column draindown the volume of water was recorded, a slightly higher volume of water was retained in Column 2 low infiltration (1.04 L) than in Column 1 high infiltration (0.46 L).

Results

Composite characteristics

Analysis of the composite waste sample shows elevated concentrations of trace metals with lead and zinc concentrations at 1.58% and 0.67% by weight respectively. Cadmium which is often associated with zinc ores is also shown to be elevated at 15 mg/kg. The sulfur content of the composite was determined to be 0.19% of which 0.02% of which was shown to be water soluble sulfate.

Leaching test results

The low infiltration column (Column 2) was found to generate the lowest pH and highest concentrations of zinc (up to 1,400 mg/L), lead (up to 12 mg/L) and cadmium (up to 3.25 mg/L) (Fig. 2 to 7). In the case of zinc and cadmium, the concentrations were shown to be around 5 to 10 times higher than in the high flushing column (Column 1) whereas concentrations of lead were of a similar magnitude in both columns. Calculation of mass release from the columns (considering the lower leachate generation rate) shows that the concentrations are much higher for the low flushing columns, the release rate for each metal (measured in mg release per kg of spoil) is initially four to five times lower due to the lower volume of leachate generated. Mass loads were normalised using sample mass size.

Lead release in the columns appears to be solubility controlled by anglesite, based on the leachate saturation indices indicated using the thermodynamic modelling code PHREEQC. The load released narrowed over time between the two columns for zinc and cadmium. This increase in load is likely a combination of variation in flow paths

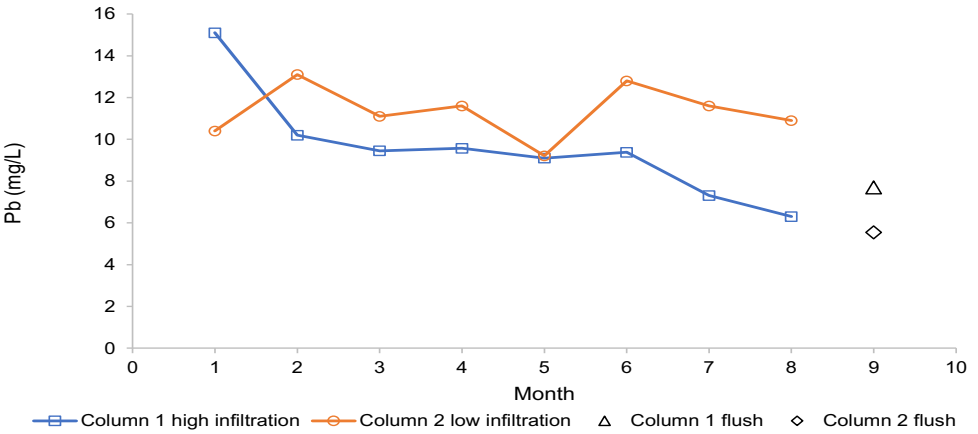

Figure 2 Dissolved lead in monthly column leachates and final flush event.

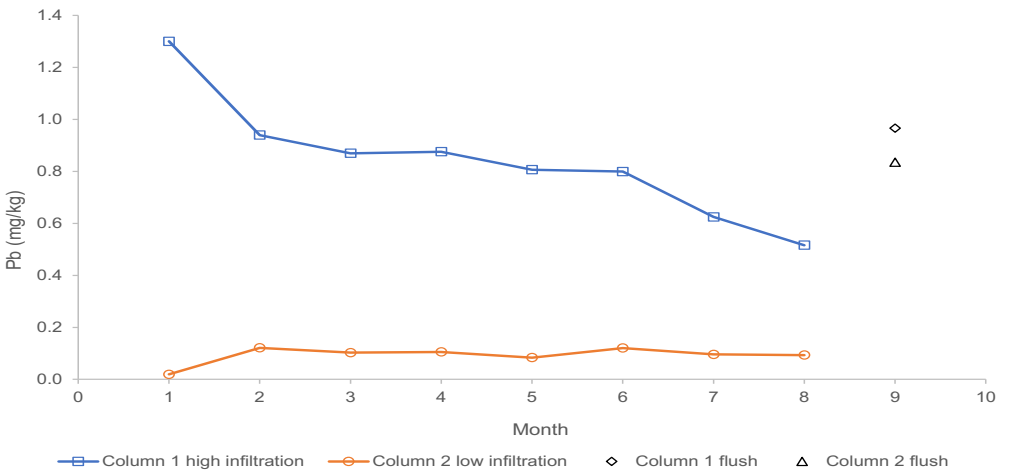

Figure 3 Lead mass loads by month.

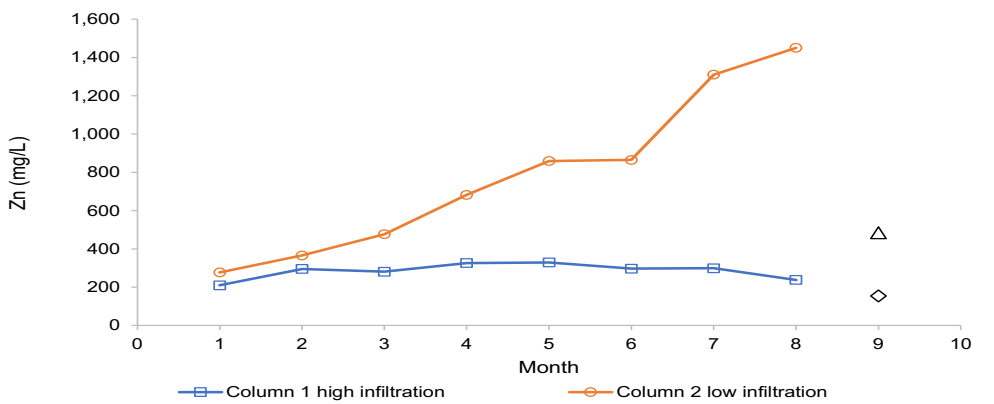

Figure 4 Dissolved zinc in monthly column leachates and final flush event.

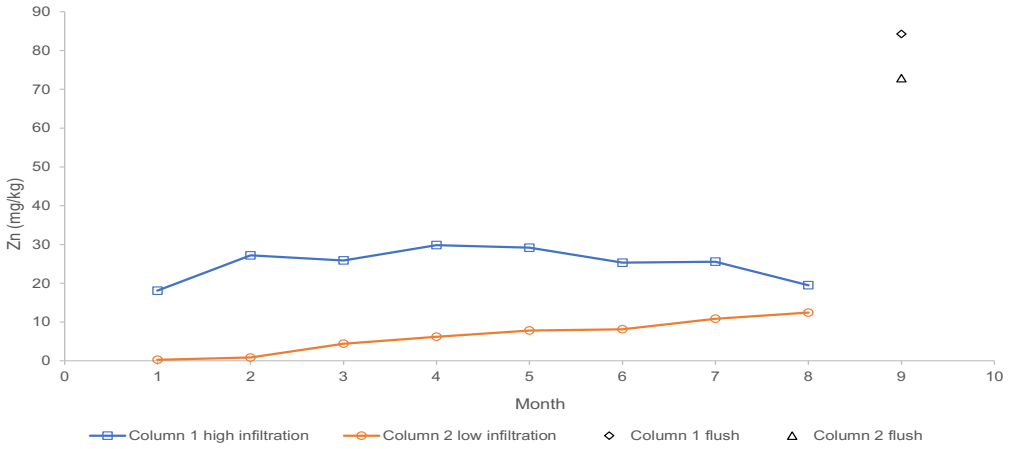

Figure 5 *Zinc mass loads by month.*

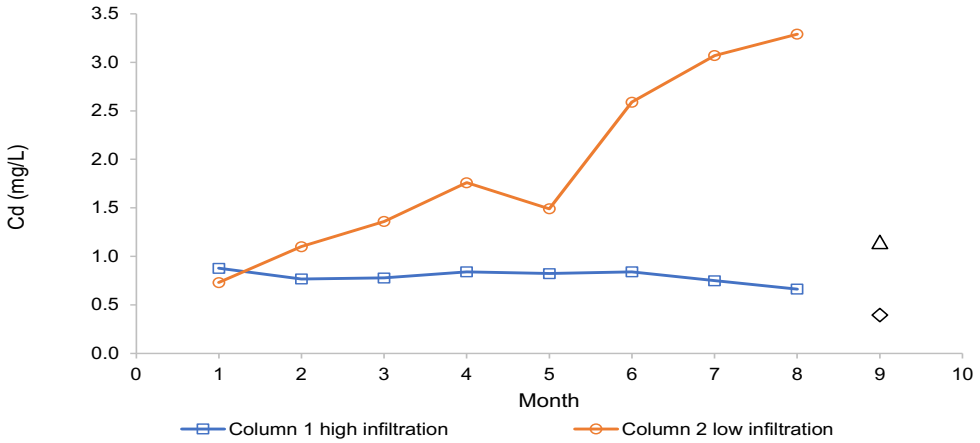

Figure 6 *Dissolved cadmium in monthly column leachates and final flush event.*

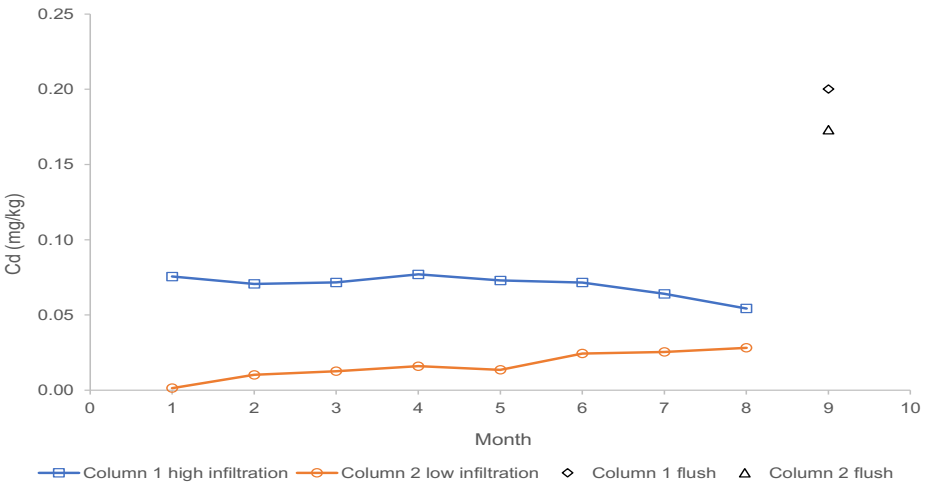

Figure 7 *Cadmium mass loads by month.*

and metal release pathways, an increased moisture content, saturation and potentially increasing load from finer material in the columns (whereas coarser material is flushed quicker). Zinc may also have some solubility constraints, as saturation indices for the leachate suggest some zinc minerals (particularly carbonates) are close to zero.

Zinc concentrations released in the average infiltration column remained relatively similar, around 200 mg/L across the weekly leachates and the flushing event. Zinc concentrations in the lower infiltration column increased through the test to 1400 mg/L, although around 500 mg/L in the flush event (diluted following the higher flow rate). The flood event leachate produced higher concentrations of key solutes (cadmium and zinc) in the reduced infiltration column, but the mass load of solutes from both columns was greater. The higher concentrations released in the flood flush are assumed to be a build-up of secondary minerals within the waste rock. The total solute mass released from the average infiltration column was greater than the lower infiltration column even when including the final flush event. The overall test mass loads released as a proportion of initial concentrations (tab. 2) shows that the higher infiltration rates (Column 1) releases higher metal loads than the lower rate, even after a flushing event.

Conclusions

The test results show that reducing the infiltration to the Abbey Consols spoil may effectively reduce the overall metals load being discharged from the waste material but increasing zinc and cadmium concentrations in the low infiltration column discharge suggest that released loadings could end up being substantial, diminishing the remediation effect. Therefore, placing a low permeability cover on the surface of the waste may be a suitable option for reducing the load but is likely to be insufficient to meet the remediation targets for this site, which is dependent on a long-term, reliable minimisation of trace metal release.

The potential retention of trace metals within the spoil material under reduced flushing does raise questions on the possibility of a build-up of secondary minerals within the waste material that may be available to be flushed in the case where the groundwater table may temporarily rise and flood the tailings as may occur in a flooding event. Following a flush event remobilisation of cadmium and zinc was seen at greater concentrations in the lower infiltration column, suggesting a build-up of the secondary minerals within the waste.

The results were used to influence the remediation design, justifying the need for impermeable lining and specific groundwater drainage to further reduce or eliminate the contact between water and the waste. Leaking caps have the potential to cause substantial metal release, in the worst case providing similar results to an uncapped condition. The tests highlight the potential risk from stored solutes in mining waste located in an area liable to flooding or fluctuating groundwater levels, potentially driven by changing climates.

Table 2 *Percentage released of initial concentrations.*

Parameter	Percentage released of total (no flush) (%)		Percentage released of total (with flush) (%)	
	Column 1 (high infiltration)	Column 2 (low infiltration)	Column 1 (high infiltration)	Column 2 (low infiltration)
Zn	2.98	0.75	4.24	1.88
Cd	3.72	0.82	5.05	2.03
Pb	0.043	0.004	0.05	0.01

References

Coflein (2019) Florida Lead and Zinc Mine; Abbey Consols Mine, Nr. Strata Florida Abbey; Bronberllan, Coflein. [online] Coflein.gov.uk. Available at: https://coflein.gov.uk/en/site/33843/details/florida-lead-zinc-mineabbey-consols-mine-nr-strata-florida-abbeybronberllan [Accessed 17 Nov. 2019].

Jones OT (1922) Lead and Zinc: The mining district of North Cardiganshire and West Montgomeryshire. Special reports on the mineral resources of Great Britain, Memoirs of the Geological Society.

Palumbo-Roe B, Banks VJ, Colman TC (2012) Notes on a site visit to the abandoned Abbey Consols Mine, Mid Wales, British Geological Survey Open Report, OR/12/047, 23pp

Performances of a Semi-Passive Field-Pilot for Bioremediation of AS-rich Acid Mine Drainage at the Carnoules Mine (France)

C Diaz-Vanegas[1,2], C Casiot[1], L Lin[3], L De Windt[4], A Djibrine[2,3], A Malcles[3], M Héry[1], A Desoeuvre[1], O Bruneel[1], F Battaglia-Brunet[2], J Jacob[2]

[1]*HydroSciences Montpellier, University of Montpellier, CNRS, IRD, Montpellier, France*

[2]*French Geological Survey (BRGM), Water, Environment, Process and Analyses Division, Orléans, France*

[3]*France LGEI (Laboratoire de Génie de l'Environnement Industriel), Institut Mines-Télécom Alès, Alès, France*

[4]*MINES ParisTech, PSL University, Centre de Géosciences, Fontainebleau, France*

Abstract

Passive and semi-passive treatment systems show great potential to treat AMD originating from abandoned mines. However, these methods still have operational shortcomings that limit their use at field scale, particularly dealing with arsenic rich effluents. The aim of this study was to determine iron and arsenic removal yields of two field treatment devices, which were designed to optimize the natural process of bio-oxidation and co-precipitation to clean-up the mine waste water from the ancient Carnoulès mine. Almost one year of monitoring showed the efficiency and the stability of the treatment under environmental and operational variations. Using assisted aeration and bacterial support in the devices, average arsenic (As) and iron (Fe) removals of 67% and 43% were achieved from an effluent containing up to 111 mg/L As and 1067 mg/L Fe. Additional steps will be considered to reach water quality and sludge disposal requirements.

Keywords: Mine Wastes, Arsenic Removal, Bio-Oxidation, Field-Pilot

Introduction

Arsenic is very common in Acid Mine Drainage (AMD) and represents a threat for aquatic ecosystems and human health. The development of passive or semi-passive effective, sustainable and affordable process for the treatment of As-rich AMD is essential. However, most of these processes are still running at laboratory scale only. The present study focused on the evaluation in field conditions of two semi-passive treatment devices for arsenic (As) and iron (Fe) removal from high-As AMD, at the abandoned Carnoulès mine in Southern France. These devices exploit bacterial Fe and As oxidation followed by As co-precipitation with ferric(hydroxy)sulfates. The present study is in continuity with previous laboratory and field scale trials carried out since 2014, within the framework of the projects "IngECOST-DMA" (Fernandez-Rojo *et al.* 2017, 2018, 2019; Laroche *et al.* 2018) and "COMPAs" (ongoing project) From this previous .

Methods

Two devices of 1 m^3 each were installed next to the source of the AMD stream, at the base of the Carnoulès tailing dam. The devices were both directly fed with AMD water by a pump. Devices worked in down-flow conditions and were equipped with two-air diffusers at their bottom to ensure sufficient oxygen supply (Fig. 1). The outlet effluent was discharged in the AMD downstream. Two support media were compared. One device was filled with plastic support Biofill® (device "PS") and the other with a mixture 80/20 (mass ratio) of wood and pozzolana (device "WP"). Plastic support had a porosity of 98% and a specific surface area of 160 m^2/m^3. The wood and pozzolana mixture had a porosity of 62% and an estimated specific surface area of 333 m^2/m^3. The working volumes were 263 L for PS and 290 L for WP. The treatment was carried out under controlled flow rates (15 L/h or 30 L/h) in discontinuous operation during seven periods (A-G) from

Table 1 Duration of each working period, flow rate and corresponding theoretical hydraulic retention time.

Period	Duration (days)	Start and end date for each period	Flow rate (L/h)	HRT (h) PS device	HRT (h) WP device
A	33	July 25 to August 28	15	17.5	19.3
B	13	December 6 to December 19	15	17.5	19.3
C	36	January 16 to February 21	15	17.5	19.3
D	19	February 21 to Mars 12	30	8.8	9.7
E	29	May 20 to June 18	30	8.8	9.7
F*	27	July 9 to August 5	30	8.8	9.7
G*†	43	August 5 to September 18	15	17.5	19.3

* Accumulation of the sludge in the bottom of the devices caused clogging of the aeration systems during period F and beginning of period G; † Cleaning of the air diffusers was done in mid-period G.

August 2019 to September 2020. Periods were defined based on changes in the inflow rate and/or undesired interruptions.

The physico-chemistry of inlet and outlet waters were monitored at least once a week. Analysis included pH, temperature, dissolved oxygen concentration (DO), conductivity and redox potential (converted to standard hydrogen electrode (SHE)). These parameters were measured in-situ by a portable multi meter. Analysis of total dissolved Fe, As and S were carried out by ICP-MS. Redox Fe species (Fe(II), Fe(III)) were analyzed by colorimetry. Redox As species (As(III), As(V)) were analyzed using HPLC-ICP-MS. The methods are detailed in Fernandez-Rojo *et al.* (2017). The results were used to calculate the saturation index of As and Fe solid phases using the geochemical modeling software CHESS (van der Lee *et al.* 2003). Additional water samples were occasionally taken for Total Organic Carbon (TOC) analysis by catalytic oxidation (method NF EN 1484).

A sludge sampling campaign was conducted in period F (July 27). The sludge that had accumulated onto the support media was recovered from two sections of each device. The first section corresponded to the first 50 cm from the top of the device. The second section corresponded to the remaining 50 cm until the bottom of the device. The composition of the sludge (mineralogy, As/Fe molar ratio, As redox speciation) was determined using X-Ray Diffraction and ICP-MS or HPLC-ICP-MS after appropriate dissolution (Fernandez-Rojo *et al.* 2017). A leaching test (ISO 17294-2:2016) was carried out on a subsample of the mixture of upper and lower section of the sludge from the PS device, it was evaluated the sludge of PS due to the similarity of the sludge composition between the devices. We applied a solid to liquid ratio of 1:10. The analysis was run by the external laboratory WESSLING (France).

Data were analyzed by non-parametric test Mann-Whitney; the p-values were obtained at the level of $p < 0.05$. The statistical analyses and graphs were performed with the R free software.

Figure 1 AMD stream and treatment device in-situ (polyethylene container).

Results and discussion

Inlet water

The knowledge of the variability of the physico-chemistry of the AMD is important in the perspective of future sizing of a real-scale treatment. During the one-year monitoring period, the water temperature varied from 7 to 31 °C (Table 2). The Fe and As concentrations during the coldest and rainiest months (430 and 42 mg/L, respectively, from December to April) were almost half of the concentration measured during the driest and hottest months (1000 and 102 mg/L, respectively, from July to August). Both elements were mostly in reduced forms Fe(II) and As(III). In general, pH and redox potential variation reflected the dissolved Fe concentration variation. The pH ranged from 3.2 to 5, with the lowest values during periods of highest concentration of Fe and As. The redox potential ranged from 224 to 628 mV SHE, with lowest values during periods of lowest concentration of Fe and As. This was related to the common origin of Fe, As and protons in the Carnoulès AMD (dissolution of As-rich pyrite) and the control of AMD redox status by the Fe(III)/Fe(II) couple as generally observed (España *et al.* 2005). The DO of the inlet water ranged from 1 to 11 mg/L, the lowest values being observed during the hottest periods. The average TOC value in the inlet water was 3.65 ± 1.5 mg/L, indicator of a low organic content effluent. These results confirmed some variability of the Carnoulès AMD physico-chemistry (Casiot *et al.* 2006; Elbaz-Poulichet *et al.* 2006; Egal *et al.* 2010). However, the continuous supply of high concentration of Fe(II) ensures the sustainability of the treatment based on biological Fe(II) oxidation.

General performances

The concentrations of dissolved Fe(II), total dissolved Fe and total dissolved As in the inlet and outlet waters allowed to calculate the oxidation and removal yields in each device. The theoretical hydraulic retention time (HRT) and devices performances are presented in Fig. 1 and Fig. 2. The oxidation and removal percentages were slightly higher (Mann-Whitney, p-value < 0.05) for the WP device than for the PS device (Fig. 2). However, no significant differences were evidenced for Fe and As removal rates (Mann-Whitney, p-value > 0.05) considering the one hour residence time difference between the two devices (WP had a bigger working volume).

Variation of the performances along the different periods differed substantially between the two devices. The average Fe(II) oxidation efficiency remained at a maximum from period A to period E with the WP device, while the PS device showed a progressive increase of the average Fe(II) oxidation efficiency among these periods. This reflected a faster adaptability and stability of the WP device illustrated by the smaller standard deviation of the oxidation yields within each period (Fig. 2A).

No significant performances variation (Mann-Whitney, p-value > 0.05) was observed between the two HRT (≈9 h and ≈18 h) evaluated among the Fe oxidation, Fe removal and As removal for each device. For both devices, the highest performances obtained during the monitoring period reached 92 ± 6% for iron oxidation, 43 ± 11% for iron removal and 67 ± 10% for arsenic removal for a HRT of 9h.

The lowest performances for iron oxidation and iron removal in both systems were observed during periods F and G (Fig. 2A and Fig. 2B), which corresponded to

Table 2 *General characterization of the inlet water physico-chemistry, the values were estimated with all the data obtained during the seven monitoring periods (n=58).*

	pH	T (°C)	DO (mg/L	Eh (mV)	Fe(II) (mg/L)	Fe (mg/L)	S (mg/L)	As (mg/L)	As(III) (%)	As(V) (%)	TOC (mg/L)
Minimum	3.2	7.1	1	224	326	427	587	42	50	14	2.8
Maximum	5.1	32.0	11	628	1079	1067	1109	111	86	50	7.1
Median	4.2	20.7	6	443	705	768	889	86	74	26	2.4

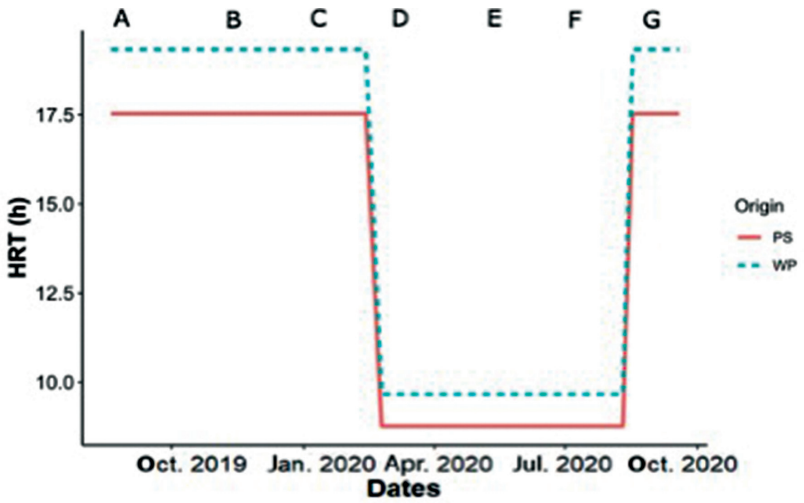

Figure 2 *Variation of the hydraulic retention time (HRT) across the monitoring periods.*

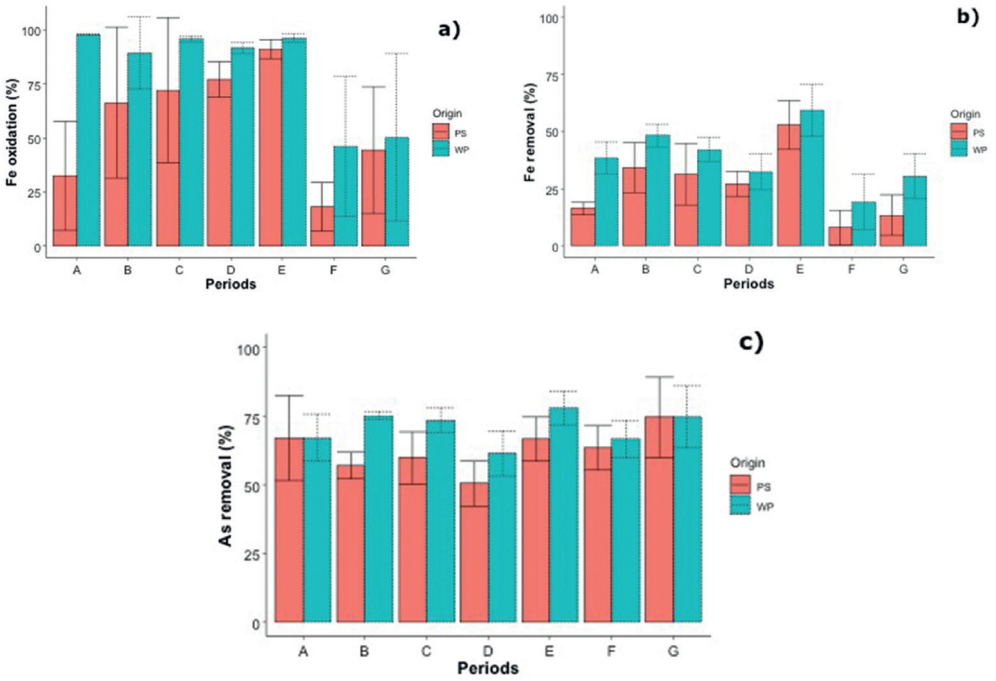

Figure 3 *Performance of PS and WP devices (a) percentage of iron oxidation, (b) percentage of iron removal and c) percentage of arsenic removal.*

periods of poor oxygen supply caused by the clogging of the aeration systems. However, the decrease of iron removal did not impact the arsenic removal, which reached 60 to 75% during periods F and G (Fig. 2.C). This may be related to the sorption of arsenic onto Fe-As solid phases that had already accumulated in the devices during the previous periods and/or to the co-precipitation of As with the low amount of newly formed Fe(III). In this respect, arsenic removal reaching 5-97% had been observed in the previous field pilot that only oxidized 20% of Fe(II) (Fernandez-Rojo *et al*. 2019)

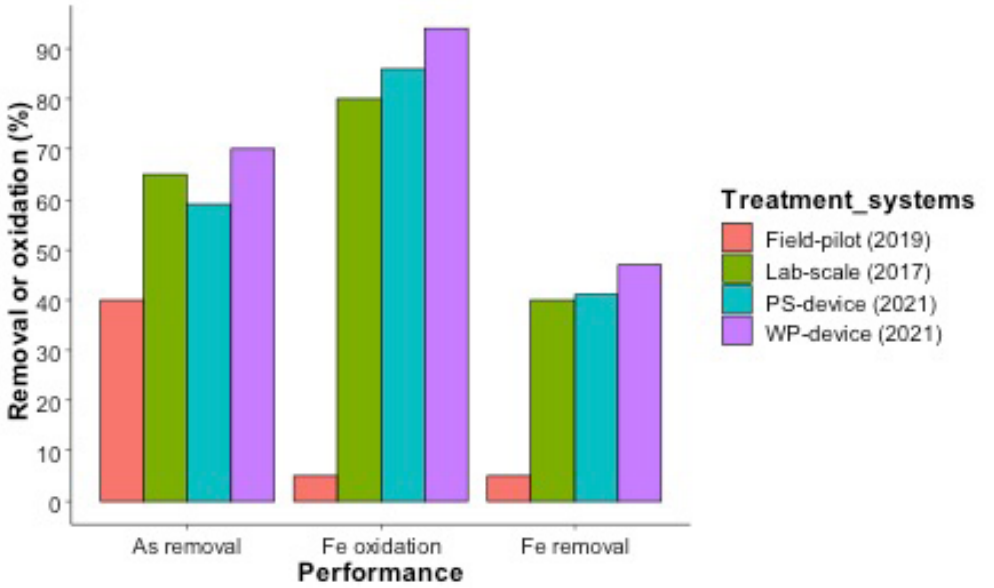

Figure 4 *Performances (in term of Fe(II) oxidation, Fe removal and As removal) obtained for the WP and PS devices (present study), previous field-scale pilot (Fernandez-Rojo* et al. *2019) and laboratory-scale reactor (Fernandez-Rojo* et al. *2017) with hydraulic retention times of 10±1h, 9±1h, 9±1 and 8±1h, respectively.*

Comparison with previous laboratory and field pilot experiments

In our previous field pilot (Fernandez-Rojo *et al*. 2019), the clogging of the sand bed and insufficient oxygen supply using simple diffusion at the air/water interface were important limitations. In the present study, forced aeration and the use of a support of higher porosity (> 60% versus < 40% for the sand) improved the performances compared to our previous passive field-scale experiment. Indeed, the present devices exhibited higher Fe oxidation and removal and higher As removal than our previous field pilot at similar HRT values, these performances were close to the yields of our laboratory bioreactor (Fig. 3).

Sludge characterization

Sludge recovery and characterization in the upper and lower sections inside each device (Table 3) provided an evaluation of the homogeneity of the biological treatment inside the devices. During the dismantling of the devices, we observed that the PS sludge was more compacted and strongly attached to the filling material contrary to the WP sludge that was waterier and thus easily transported to the bottom of the system. Consequently, the PS precipitates were more homogenously distributed inside the device than the WP precipitates. The average Fe, As and S contents of the sludge were similar for the PS and WP devices. However, the As/Fe molar ratio of the PS sludge was slightly higher than the one of the WP sludge.

Table 3 *Characterization of the sludge accumulated at the PS and WP supports, sampled from the upper and lower section.*

Device		As (g/kg dry wt.)	Fe (g/kg dry wt.)	S (g/kg dry wt.)	As/Fe (molar)	As(III) (%)	As(V) (%)
PS	top	82.5	306.4	45.4	0.36	17	83
	bottom	68.2	275.9	39.8	0.33	19	81
	average	75 ± 10	291 ± 22	43 ± 4	0.35 ± 0.02	18 ± 1	82 ± 1
WP	top	49.9	254.2	45.5	0.26	17	83
	bottom	67.2	316.0	55.2	0.28	17	83
	average	58 ± 12	285 ± 43	50 ± 7	0.27 ± 0.01	17 ± 0	83 ± 0

Table 4 *Amount of element leached from the sludge of the PS device (in mg per kg of dried material) and pH of the leachate during leaching test.*

Parameters	As	Cd	Cr	Cu	Ni	Pb	Zn	SO_4^{2-}	COT	pH
Class 1[1]	25	5	70	100	40	50	200	--	1000	4 <pH< 13
PS sludge[2]	4.7	0.09	0.26	0.23	0.97	0.14	23	5500	20	2.7

[1]Classification of the European Council Directive 1999/31/ EC of April 26. 1999 on the landfill of waste; class 1: reserved for special industrial. [2]Sludge sample from July 27of 2020.

Only one crystallized Fe phase jarosite was identified by XRD, in both the PS and WP devices. This was in agreement with the positive value of jarosite saturation index calculated from outlet water chemistry. The sludge contained up to 83 g/kg (dry wt.) of arsenic mainly under As(V) form (81-83%) whatever the section and the device, which is advantageous for sludge management since As(V)-bearing solid phases are more stable than As(III)-bearing ones.

Perspectives for the sludge disposal

Leaching tests provide guidance on the compatibility of the sludge with storage in landfill waste facilities. The leachate from the PS sludge showed values below most thresholds for storage in Class 1 (hazardous industrial waste). The pH was the only parameter that exceeded the standard (Table 4). Therefore, addition of a neutralization agent to increase the pH would be necessary in the perspective of long-term storage. This should deserve additional trial.

Conclusions

These results demonstrated that our semi-passive devices achieving biological iron oxidation can function in real field conditions and exhibit stable performances with low maintenance during several months, under variable AMD physico-chemistry. The present devices combined the forced aeration and high porosity filling material, which appeared to be key factors to increase the performances compared to our previous field pilot. The wood and pozzolana mixture showed a better stability of Fe(II) oxidation yield than the plastic support. Our study provided fundamental and technical advances for a full-scale treatment facility adapted for an As-rich AMD. Additional stages are in progress to improve the quality of the treated water.

Acknowledgements

The authors thank the Agence de l'Environnement et de la Maîtrise de l'Energie (ADEME) [APR-GESIPOL-2017-COMPAs] for the financial support, the Occitanie region and BRGM for co-funding of the PhD grant of Camila Diaz-Vanegas, and OSU-OREME for co-funding of the long-term monitoring of Carnoulès AMD physico-chemistry. The authors gratefully acknowledge IMWA for their time in reviewing this paper.

References

Casiot C, Pedron V, Bruneel O, *et al* (2006) A new bacterial strain mediating As oxidation in the Fe-rich biofilm naturally growing in a groundwater Fe treatment pilot unit. Chemosphere 64:492–496. https://doi.org/10.1016/j.chemosphere.2005.11.072

Egal M, Casiot C, Morin G, *et al* (2010) An updated insight into the natural attenuation of As concentrations in Reigous Creek (southern France). Appl Geochemistry 25:1949–1957. https://doi.org/10.1016/j.apgeochem.2010.10.012

Elbaz-Poulichet F, Bruneel O, Casiot C (2006) The Carnoules mine. Generation of As-rich acid mine drainage, natural attenuation processes and solutions for passive in-situ remediation. Difpolmine (Diffuse Pollut From Min Act

España JS, Pamo EL, Santofimia E, *et al* (2005) Acid mine drainage in the Iberian Pyrite Belt (Odiel river watershed, Huelva, SW Spain): Geochemistry, mineralogy and environmental implications. Appl Geochemistry 20:1320–1356. https://doi.org/10.1016/j.apgeochem.2005.01.011

Fernandez-Rojo L, Casiot C, Laroche E, *et al* (2019) A field-pilot for passive bioremediation of As-rich acid mine drainage. J Environ Manage 232:910–918. https://doi.org/10.1016/j.jenvman.2018.11.116

Fernandez-Rojo L, Casiot C, Tardy V, *et al* (2018) Hydraulic retention time affects bacterial community structure in an As-rich acid mine drainage (AMD) biotreatment process. Appl Microbiol Biotechnol 102:9803–9813. https://doi.org/10.1007/s00253-018-9290-0

Fernandez-Rojo L, Héry M, Le Pape P, *et al* (2017) Biological attenuation of arsenic and iron in a continuous flow bioreactor treating acid mine drainage (AMD). Water Res 123:594–606. https://doi.org/10.1016/j.watres.2017.06.059

Laroche E, Casiot C, Fernandez-Rojo L, *et al* (2018) Dynamics of Bacterial Communities Mediating the Treatment of an As-Rich Acid Mine Drainage in a Field Pilot. Front. Microbiol. 9

Méndez-García C, Peláez AI, Mesa V, *et al* (2015) Microbial diversity and metabolic networks in acid mine drainage habitats. Front Microbiol 6:1–17. https://doi.org/10.3389/fmicb.2015.00475

van der Lee J, De Windt L, Lagneau V, Goblet P (2003) Module-oriented modeling of reactive transport with HYTEC. Comput Geosci 29:265–275. https://doi.org/10.1016/S0098-3004(03)00004-9

Mintek's Integrated cloSURE™ Technology for Treatment of Acid Mine Drainage

Kerri du Preez

Biometallurgy, Mintek, Private Bag X3015, Randburg 2125, South Africa, kerrihud@gmail.com

Abstract

Mintek has developed cloSURE™ for treatment of AMD. The process consists of two stages, biological sulfate reduction followed by oxidation for sulfide removal and biosulphur production. The process was demonstrated at laboratory scale and achieved sulfate reduction rates of 196 g/m^3/d with 87% sulfate removal, and up to 98% sulphide removal. The pH level increased to 7.5 and metals were found to be within South African target water quality limits for irrigation. The results of the research show that cloSURE™ is a potential solution for sustainable treatment of point sources of AMD.

Keywords: Biological Sulfate Reduction, Mine Water Treatment, Acid Mine Drainage, Water Re-use

Introduction

The legacy of acid mine drainage (AMD) in South Africa has caused widespread contamination of river catchments. The AMD is typically characterised by high sulfate concentrations, in excess of 3 g/L, with relatively low concentrations of metals. Currently there is no sustainable solution for point sources of AMD discharge in remote locations in South Africa.

Mintek has developed cloSURE™, a technology which employs biological processes to treat mine impacted water. The aim is to produce water that is fit for re-use in irrigated agriculture. cloSURE™ is suitable for small point sources in remote locations that lack services and infrastructure, such as legacy mines and mines after closure. The process consists of two stages, namely a biological sulfate reduction (BSR) step followed by an oxidation step for sulfide removal and biosulphur production.

Stage 1 employs biological sulfate reduction to remove sulfate, increase alkalinity and pH, and remove metals. Biological sulfate reduction employs anaerobic, sulfate reducing bacteria (SRB) which are present in natural environments such as the sediment of lakes and wetlands, cattle rumen and subsequent manure. SRB use sulfate as the terminal electron acceptor for cellular respiration, and consume simple organic substrates such as lactate and acetate for energy (Hansen 1993). These organic substrates are converted to bicarbonates which raise the alkalinity and pH of the treated water. The biological reduction of sulfate produces sulfide that bind to the metals in solution to form metal sulfides, which are stable at neutral pH, reducing metal concentrations in the effluent to trace amounts (van Hille *et al*. 2019). There is also potential for selective recovery of the retained metal sulfides.

The primary reactions are as follows:

$$2CH_2O(aq) + SO_4^{2-} + H+ \rightarrow H_2S+2HCO_3^- \quad [1]$$

$$H_2S + Me^{2+} \rightarrow MeS + 2H^+ \quad [2]$$

Reduction of sulfate results in the production of sulfide which can be corrosive to irrigation equipment and may pose a safety risk to plant operators. In the second stage of the process, the focus is on the biological removal of sulfide and residual metals, and the recovery of biosulphur, in order to produce treated water that is fit for use in irrigated agriculture. Sulfide oxidising bacteria are found in aquatic systems in floating bacterial mats, and oxidise sulfide to sulphur and sulfate with increasing concentrations of oxygen. Sulfide is partially

oxidised to sulphur under conditions where the stoichiometric ratio of sulfide to oxygen is greater than 2:1 (Buisman *et al.* 1990; van Hille and Mooruth 2011):

$$2HS^- + O_2 \rightarrow 2S^0 + 2OH^- \quad [3]$$

When more oxygen is available, sulfide oxidisers readily produce sulfate:

$$2HS^- + 4O_2 \rightarrow 2\,SO_4^{2-} + 2H^+ \quad [4]$$

For the purposes of cloSURE™'s stage 2 treatment, partial oxidation of sulfide to sulphur is preferred to minimise the production of sulfate, which would nullify the effects of the biological sulfate reduction treatment step. Sulphur oxidisers are cultivated in a floating biofilm in an oxidation tank. This biofilm prevents escape of any hydrogen sulfide to the atmosphere and minimises diffusion of oxygen into the tank, ensuring maximum sulfide concentrations and minimum oxygen concentrations.

Development of Stage 1 culminated in an 18 month pilot study at a mine site (Neale *et al.* 2018), treating 250 L/d, and removing 95% of the sulfate from the mine water. At the time of piloting Stage 1, the Stage 2 concept was being developed in the laboratory.

The cloSURE™ process produces significantly less solid waste, with decreased toxicity and increased stability, compared to conventional chemical precipitation methods. It requires relatively low capital costs, and operating costs can be greatly reduced when using inexpensive carbon sources and/or passive or semi-passive treatment designs.

The aim of this study was to demonstrate the integrated treatment process at small scale and assess the quality of the treated water as fit-for-use. The objectives were to:

1. Run an integrated cloSURE™ treatment process at laboratory scale and obtain sufficient data assess the quality of the water.
2. Assess the suitability of the water for irrigation purposes against the irriga tion target water quality guidelines (DWAF 1996)
3. Analyse the components of the biofilm formed.

Method

cloSURE™ Process Setup

An integrated process was set up at Mintek, to treat 5.2 L of AMD per day and is shown in Figure 1:

1. Stage 1: Biological sulfate reduction column
2. Stage 2: Sulfide oxidation tank

Figure 1 *Photograph of Mintek's laboratory setup, the BSR columns are in the background and the sulfide oxidation tanks are in the foreground.*

The Stage 1 BSR column consisted of a packed bed of woodchips, and had a working volume of 50 L. The column was inoculated with an effluent sample from Mintek's pilot plant, containing a representative consortium of microbes including SRB. The temperature was maintained at 35 °C. Raw mine water was obtained from a coal mine site in Mpumalanga Province, South Africa, with sulfate concentrations between 2.5 g/L and 4.0 g/L, and a pH level of 3. Table 1 gives the parameters of the neutralised feed water. The water was neutralised with lime to pH 6. The carbon source was cow manure, which was removed and replaced with fresh manure at weekly intervals. The column was continuously operated with a hydraulic retention time (HRT) of 10 d and a flow rate of 5.2 L/d.

The Stage 2 sulfide oxidation tank had a horizontal flow configuration and a working volume of 14 L. The tank consisted of a packed bed of polypropylene biofilter material, one third the depth of the tank, the surface of the water was inoculated with dried biofilm from prior Mintek laboratory work, to encourage the development of a floating sulphur biofilm. Nutrients were added the form of ammonium sulfate, di-potassium hydrogen phosphate and glycerol. The tank was continuously operated with a flow rate of 1.4 L/day to achieve a HRT of 10 days.

Target Water Quality Limits for Irrigation

The South African Water Quality Guidelines for Irrigation Water Use (DWAF 1996) is a specification of the required water qualities for various irrigation uses. The guideline provides limits in order to assess the fitness of the water to be used for irrigation activities, primarily crop production. It gives three concentrations ranges for water qualities:

1. Target Water Quality Range (TWQR) which is considered a satisfactory concentration for continuous application with no impact on soil or crop yield.
2. The maximum acceptable concentration for fine textured neutral to alkaline soils
3. Acceptable for irrigation only over the short term on a site-specific basis

This study compared metals concentrations to the more stringent TWQR only.

Analyses

Both the BSR column and sulfide oxidation tank were sampled twice weekly for pH, redox potential, temperature, electrical conductivity, and sulfide and sulfate concentrations

Redox potential and pH were measured directly using pH and ORP electrodes (Knick Partavo 904(X) meter with Metrohm pH probe, 6.0220.100 Hamilton Liq Glass ORP probe). Electrical conductivity (EC) was determined using an EC probe (WTW Cond 330 meter and WTW TetraCon325 probe).

Sulfate was determined using Merck sulfate cell tests (100-1000 mg/L and 0.5-50 mg/L) and Prove 300 spectroquant. Sulfide was determined by the potentiometric method, using a Metrohm Tiamo autotitrator and AgS titrode, titrated against silver nitrate. Sulfide samples were preserved with NaOH and analysed immediately.

Once stable results were obtained in both stages, water samples were collected and sent for metals analysis at Waterlab. Pretoria. Metals samples were filtered and preserved with HNO_3, and metals were analysed with ICP-MS.

The biofilm was harvested every 14 days. A sample was dried and weighed, and analysed at Mintek using ICP, Leco sulphur analysis and X-Ray Diffraction (XRD) Analysis

Table 1 *Average parameters for the neutralised feed water over the study period.*

Parameter	Average Value
Sulphate Concentration (mg/L)	2 775
Sulphate Loading Rate (g/m3/d)	237
Flow Rate (L/d)	5.2
pH	6.5
Substrate: Cow Manure (kg/wk)	1.5

Results

Sulfate and Sulfide Removal

The cloSURE™ treatment vessels had been running for approximately one year, but had to be stopped for four month during the Covid-19 Lockdown. Day 0 in this paper refers to the restart date after the lockdown period. After startup, the column had elevated levels of sulfate, which decreased from Day 35. Between Day 35 and Day 80, an average volumetric sulfate reduction rate of 173 g/m^3/d (1.48 mol/m^3/d) and 57% sulfate removal was attained. From Day 90 the volumetric sulfate reduction rate increased and stabilised at an average of 196 g/m^3/d (2.05 mol/m^3/d), with 87% sulfate removal. Sulfate concentrations and salfate reduction rates over the study period are shown in Figure 2.

Typical values for sulfate reduction in passive treatment processes range between 28 g/m^3/d (0.3 mol/m^3/d) and 76 g/m^3/d (0.8 mol/m^3/d) (Gusek 1998; Pulles *et al.* 2016). While the laboratory cloSURE™ process is not strictly a passive process due to the addition of substrate on a regular basis, the sulfate reduction rates achieved were much higher than expected for a process fed with a complex substrate, and indicate promising potential as a treatment technology.

In Stage 2, the sulfate initially increased as the sulfide was oxidised to sulfate. Once the biofilm was established, sulfate was no longer produced in the oxidation stage from Day 35, indicating that sulfide removed was converted to sulphur in the biofilm. The sulfide graph in Figure 3 illustrates that from Day 80, increased sulfate reduction rates produced high concentrations of sulfide in the Stage 1 treated water. Once the biofilm had established in Stage 2, partial sulfide oxidation occurred and sulfide concentrations in the treated water remained low, with 78–98% of the sulfide removed.

pH levels increased through the process, with a pH of 7.5 from Day 80, during stable operation, indicated in Figure 3. The pH remained constant irrespective of the fluctuating feed pH, indicating alkalinity production and a stable Stage 1 (BSR) reactor.

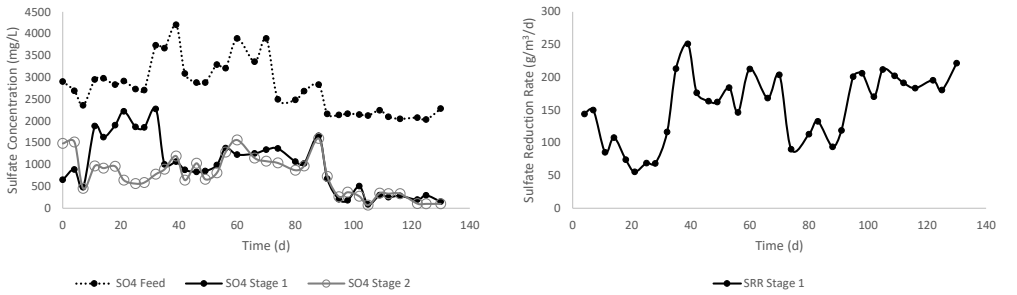

Figure 2 *Sulfate concentrations (left) in the neutralised feed and each Stage of the process, and volumetric sulfate reduction rates (SRR) (left) for Stage 1.*

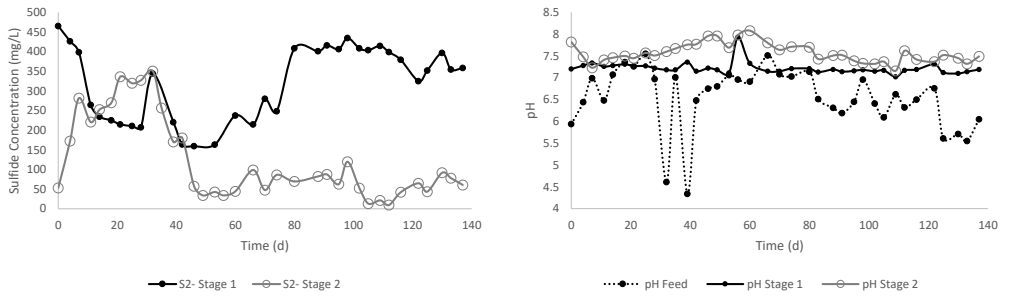

Figure 3 *Sulfide concentrations (left) and pH (right) of the neutralised feed and each Stage of the process.*

Table 2 Metals concentrations in the neutralised feed and each Stage of the process.

	AMD Feed	Neutralised Feed	Stage 1	Stage 2	TWQR
			mg/L		
Cl	13	12	-	-	100
F	<0.2	<0.2	<0.2	<0.2	2
Na	65	65	172	330	-
Ca	516	622	367	117	-
Mg	136	131	283	344	-
Al	111	2.59	0.525	0.551	5
As	0.001	<0.001	0.001	<0.001	0.1
Be	0.053	0.001	<0.001	<0.001	0.1
B	0.729	0.587	0.531	0.712	0.5
Cd	<0.001	<0.001	<0.001	<0.001	100
Cr^{6+}	0.06	<0.01	<0.01	<0.01	0.1
Co	0.015	0.011	<0.001	<0.001	0.05
Cu	0.05	0.034	0.034	0.029	0.2
Fe	43	0.92	0.208	0.238	5
Pb	0.0008	0.002	0.002	0.002	0.2
Li	0.287	0.26	0.132	0.267	2.5
Mn	1.4	1.18	0.199	0.015	0.02
Mo	<0.001	<0.001	<0.001	<0.001	0.01
Ni	0.543	0.257	0.092	0.105	0.2
Se	<0.001	<0.001	<0.001	<0.001	0.02
V	<0.025	0.049	<0.025	<0.025	0.1
Zn	2.1	0.741	0.071	0.499	1

Biofilm

Sulphur results indicated that 24% of the biofilm consisted of total sulphur and 20% elemental sulphur by mass. The biofilm yield was 234 g/m^2 for a single harvest. Research at the University of Cape Town indicates that hydraulic retention times of 2-3 days increase sulphur accumulation in the film up to 90% by mass (Personal Communication, Rob van Hille, 2019). Long retention times of more than 4 days yielded 25-40% sulphur by mass in the biofilm with a large organic and inorganic component. This suggests that higher yields can be achieved with optimisation of residence time in the integrated treatment system.

Results from ICP analysis (and confirmed by XRD) of the biofilm indicate the presence of magnesium (7.11%) and calcium (2.91%), as well as small amounts of manganese (0.11%) and iron (0.05%). XRD analysis indicated the magnesium is present in the form of struvite ($(NH_4)MgPO_4 \bullet 6(H_2O)$), and makes up 74% of the biofilm by mass. Calcium, iron and manganese are present in much lower levels in the forms of bixbyite ($(Mn,Fe)_2O_3$), graftonite ($(Fe,Mn,Ca)_3(PO_4)_2$) and ankerite ($Ca(Fe,Mg,Mn)(CO_3)_2$).

It is likely that the presence of magnesium phosphate compounds in the biofilm is also due to the high quantities of nutrients delivered to the Stage 2 system. Optimisation of nutrients and residence times may minimise the presence of inorganic compounds. There is potential for the oxidation stage to produce enough biofilm to be harvested and used as a valuable biosulphur fertiliser product, offsetting some of the treatment cost.

Target Water Quality Ranges

Table 2 gives the concentration of metals in the mine water, the neutralised mine water feed and the treated water. The TWQR (DWAF 1996) for each compound is given.

The parameters that exceed the TWQR are shaded in Table 1. These results confirm that the mine water consists of low concentrations of metals, and the majority of these fall within the TWQR without treatment. Aluminium, boron, iron, manganese, nickel and zinc are the exceptions. After neutralisation with lime, the concentrations of metals decrease to varying extents, but boron, manganese and nickel still exceed the TWQR. After treatment in both stages of the cloSURE™ process, all metals meet TWQR.

Other elements that remain in high concentrations in the effluent are magnesium, calcium and sodium. There are no individual water quality targets for these ions, however, they are used to calculate the sodium adsorption ration (SAR), which is a measure of the ratio of sodium to calcium and magnesium. The SAR for the treated water is 3.5 (calculated based on DWAF 1996). The impact of the SAR on soil quality is also dependent on the electrical conductivity, but generally the higher the ratio (>20), the greater the impact on soil permeability and infiltration (DWAF 1996).

Conclusion

With the number of coal mines due to close in the near future, cost effective technologies suited to remote locations are urgently required. The laboratory scale demonstration of the cloSURE™ process successfully removed sulfate in Stage 1, and removed sulphide in Stage 2, as well as increased the pH in the treated water. The biofilm in Stage 2 was able to successfully recover sulphur from the mine water, and based on its composition, could potentially be a value by-product from the water treatment process. The metals and SAR results show that the treated water is potentially fit for re-use in irrigated agriculture, however, this needs to be confirmed in irrigation trials and soil studies. The results of the research show that cloSURE™ is a potential solution for sustainable treatment of point sources of AMD, which will produce water that is fit for re-use in irrigated agriculture, in turn promoting economic hubs and food security in post-mining regions.

Future Work

The success of this study, led to a second piloting phase to test the integrated cloSURE™ process at scale. Funding has been granted to Mintek to demonstrate the process at scale at a mine site in Mpumalanga. Part of the scope of these projects is to evaluate the economics and logistical requirements for a field scale cloSURE™ process, as well as complete field irrigation trials using the treated water.

Acknowledgements

The author would like to thank the following organisations for the funding of laboratory and pilot studies and for their ongoing support: Mintek for funding and laboratory support, Anglo American for funding, access to mine water and a site location for piloting, Coaltech for funding.

References

Buisman CJ, Geraats BG, Ijspeert P, Lettinga G (1990) Optimization of sulphur production in a biotechnological sulphide-removing reactor. Biotechnology and Bioengineering 35: 50-56

Department of Water Affairs (1996) South African Water Quality Guidelines Volume 4: Agricultural Use – Irrigation. Second edition.

Gusek JJ (1998) Three case histories of passive treatment of metal mine drainage, in Proceedings of the 19th Annual West Virginia Surface Mine Drainage Task Force Symposium, West Virginia University, Morgantown, West Virginia

Hansen TA (1993) Carbon metabolism of sulfate-reducing bacteria. In: The Sulfate-Reducing Bacteria: Contemporary Perspectives. Odom, J.M., Singleton, J.R. (Editors.) Springer New York, New York, NY, pp. 21–40. doi:10.1007/978-1-4613-9263-7

Neale JW, Gericke M, Mühlbauer R. (2018) On-Site Pilot-Scale Demonstration of a Low-Cost Biological Process for the Treatment of High-Sulphate Mine Waters. In: Wolkersdorfer Ch; Sartz L; Weber A; Burgess J; Tremblay G: Mine Water – Risk to Opportunity (Vol I). – p. 164-171; Pretoria, South Africa

Pulles W, Coetser L, Heath R, Mühlbauer, R. (2004): Development of high-rate passive sulphate reduction technology for mine waters. – In: Jarvis A P, Dudgeon B A, Younger PL: mine water 2004 – Proceedings International

Mine Water Association Symposium 1. – p. 253-262, 8 Fig.; Newcastle upon Tyne (University of Newcastle)

Pulles W, Lodewijks HM, Toerien A, Muhlbauer R, van Niekerk JA, Richardt A (2016) Passive treatment of acid mine drainage at Vryheid Coronation Colliery, South Africa. In AB Fourie & M Tibbett: Proceedings of the 11th International Conference on Mine Closure, Australian Centre for Geomechanics, Perth, pp. 425-438

van Hille R, and Mooruth N (2011) Investigation of sulphide oxidation kinetics and impact of reactor design during passive treatment of mine water. WRC report KV268/11

van Hille R, Marais T, Huddy R, Johnson-Robertson M, Smart M, Couperthwaite J, Horn E, Pott E, Naidoo N, Burke M, Jian J and Harrison S (2019) An integrated bioprocess for ARD remediation and renewable energy generation. WRC Report No. K5-2392

Algae Bioaccumulation Capacity for Metals in Acid Mine Drainage (AMD) – A Case Study in Frongoch Mine, UK

Tianhao Du[1], Anna Bogush[2], Paul Edwards[3], Peter Stanley[3], Luiza C. Campos[1]

[1]*Department of Civil, Environmental & Geomatic Engineering, Faculty of Engineering, University College London, London, WC1E 6BT, United Kingdom*

[2]*Centre for Agroecology, Water and Resilience, Coventry University, Coventry, CV8 3LG, United Kingdom*

[3]*Natural Resources Wales, 29 Newport Road, Cardiff CF24 0TP, United Kingdom*

Abstract

Algae living in the AMD water around the Frongoch Mine, the UK, were collected and identified by microscope. Metals' concentration was evaluated in AMD water and algae in two seasons (June and October) in 2019 to assess the bioaccumulation capacity of algae. Two types of algae, *Ulothrix sp*. and *Oedogonium sp*., were found to be the main species at the Frongoch mine, and they revealed a high capacity of metals bioaccumulation. Concentrations of metals in AMD water from higher to lower were Zn>>Pb>Cd>Fe>Cu. Study results identified the bioaccumulated metals concentrations in algae from higher to lower were Fe>Pb>Cu>Cd>Zn.

Keywords: Bioaccumulation, Green Algae, Bioindicator, Metals

Introduction

Acid mine drainage (AMD) refers to the deposits and tailings generated by mine site exploitation and exposure to the natural environment (water, air and bacteria) which can produce acidic conditions and leach metals (Favas *et al*. 2016; Bogush *et al*. 2016). Algae have an essential role in the AMD environment because photosynthesis can provide nutrients for other microorganisms to keep the environment stable. Meanwhile, algae can accumulate some metals (Orandi and Lewis 2013). This is the first reported study that investigates the metal accumulation by algae with accurate chemical methods from AMD of Frongoch Mine (in West Wales, UK). Also, the results can help to determine the magnitude of metal contamination in the Frongoch Mine area and provide information and recommendation for AMD remediation by algae in Frongoch Mine.

Methods

Study site and sample collection

This project's study site is Frongoch Mine (Figure 1), which was one of the largest mines in North Ceredigion (Murphy 2015).

Physical and chemical analysis

All the algae samples were stored in the original AMD water and characterised by microscope (Zeiss) and then compared with literature (Canter-Lund and Lund 1998). Sequential metal extraction from algae was carried out by two steps of water-leaching and acid digestion. A microwave acid digestion procedure was applied for the residue of algae. Metals' concentrations in two steps water-leachates and digests were determined by ICP-OES analysis.

Result and discussion

Microphotograph's identification results show there are only two types of algae *Ulothrix sp*. and *Oedogonium sp*. Table 1 shows the metal concentrations of AMDs from the Frongoch Mine. The highest Zn concentration was observed on site G that exceeded the GSDEP (1993) 70 times and followed by Pb, Cd and Fe. Metal's concentration was slightly higher in the autumn sampling (S2, C2, G2 and M2) period than in summer (S1, C1and G1). This seasonal change of metal concentration in AMD was also mentioned by Oh and Yoon (2013), who found that the metal concentration in AMD in summer samples was higher than that in spring samples.

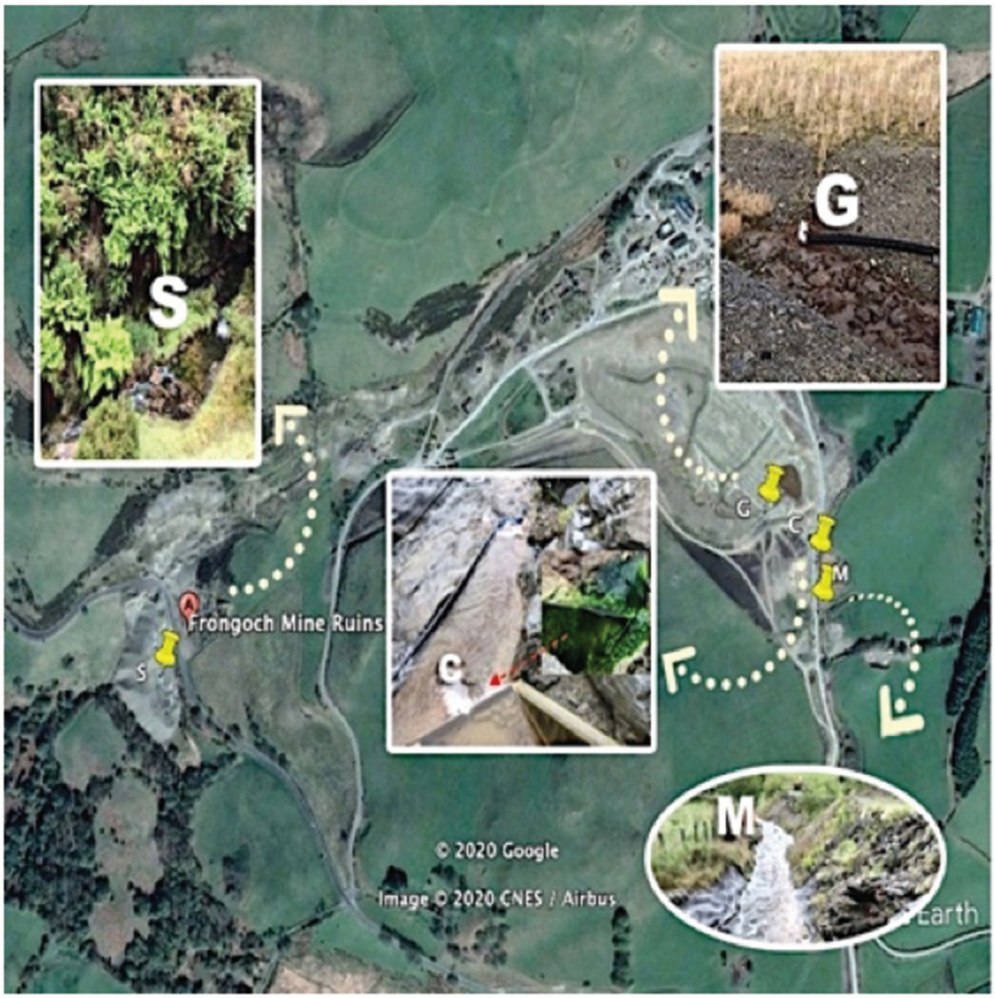

Figure 1 *The four water sample collection sites in Frongoch Mine. © Google and Digital Globe (2020).*

Accumulation of metals in algae decreased in the following order: Fe>Pb>Zn>Cd>Cu. High concentrations of Zn (79.4-90.6%) in algae were found in the algae acid digest fraction, which indicates that Zn mainly accumulated inside algae. A significant Zn ratio can also be adsorbed on the surface of algae (6.4-20.6%). Pb is however mainly accumulated inside the algae, as shown by the high Pb content measured in the algae acid digest fraction (>97.5%).

Conclusions

Zn and Pb are the primary metals in the AMDs from the Frongoch Mine. Two species of algae *Ulothrix sp*. and *Oedogonium sp*., were identified can survive and accumulate metals in AMD. The results from this study identify that algae could be used as a bioindicator for the assessment of water pollution at Frongoch Mine. Based on the above results, further study may focus on examining the statistical relationship between different metals accumulation and background water from different sites to establish the pattern of metal accumulation by algae in this area. Also, factors that caused seasonal changes should be identified by more sampling and analysis.

Acknowledgements

The authors thank Judith Zhou and Utku Solpuker from Environmental Engineering Laboratory, University College London, for providing techniques support. The authors also thank

Table 1 Metal concentration of acid mine drainage from Frongoch Mine.

Metals Sample	pH	Zn (mg/L)	Pb (mg/L)	Cd (mg/L)	Cu (mg/L)	Fe (mg/L)
S1	6.19	13.8 ± 0.25	<DL*	0.03 ± 0.01	<DL*	0.01 ± 0.01
C1	4.81	84.1 ± 0.93	4.22 ± 0.16	0.23 ± 0.04	0.08 ± 0	<DL
G1	3.57	314 ± 3.01	2.93 ± 0.13	0.44 ± 0.01	0.01± 0	0.29 ± 0.01
S2	6.85	15.7 ± 0.32	0.64 ± 0.14	0.03 ± 0.01	0.05 ± 0.01	<DL
C2	4.89	139 ± 1.85	1.74 ± 0.14	0.38 ± 0.01	0.18 ± 0.02	<DL
G2	3.46	351 ± 3.18	3.8 ± 0.174	0.5 ± 0.02	<DL*	1.42 ± 0.01
M2	6.59	7.32 ± 0.52	<DL*	<DL*	0.2 ± 0.01	<DL
GSDEP**	5.5-9	5.0	0.1	2.0	3.0	3.0

* DL: Detection Limit, Zn: 0.0079 mg/L, Pb: 0.074 mg/L, Cd: 0.0044 mg/L, Cu: 0.0039 mg/L, Fe: 0.0044 mg/L. **GSDEP - General standards for discharge of environmental pollutants (1993).

Natural Resource Wales for providing study site access and sampling help.

References

Bogush AA, Voronin VG, Tikhova VD, Anoshin GN (2016) Acid Rock Drainage Remediation and Element Removal Using a Peat-Humic Agent with Subsequent Thermal Treatment of the Metal–Organic Residue. Mine Water Environ 35:536–546.

Canter-Lund H, Lund JWG (1998) Freshwater algae: their microscopic world explored, Reprinted. Biopress Ltd, Bristol

Favas PJC, Sarkar SK, Rakshit D, *et al* (2016) Acid Mine Drainages From Abandoned Mines. In: Environmental Materials and Waste. Elsevier, pp 413–462

GSDEP (1993) (1986) General Standards For Discharge Of Environmental Pollutants (Part A: effluents). Environmental Standards GSR 801 (E):

Murphy F (2015) Frongoch metal mine, Ceredigion. Dyfed Archaeological Trust 104.

Oh S-Y, Yoon M-K (2013) Biochar for Treating Acid Mine Drainage. Environmental Engineering Science 30:589–593. https://doi.org/10.1089/ees.2013.0063

The Relationships Between Negative Pore-Water Potential, Water Content, Relative Humidity and Sulfide Oxidation in Waste Rock – A Case Study

Eben Dy[1], Kidus Tufa[1], Eizabeth Fisher[1], Zhong-Sheng (Simon) Liu[1], Kevin Morin[2], Michael O'Kane[3], Tim O'Hearn[4], Cheng Huang[1], Wei Qu[1]

[1]*National Research Council Canada, 4250 Wesbrook Mall, Vancouver, BC V6T1W5, Canada*

[2]*Minesite Drainage Assessment Group (MDAG.com), Surrey, BC, Canada*

[3]*O'Kane Conultants Inc., 112-112 Research Drive, Saskatoon, SK S7N3R3, Canada*

[4]*Bureau Veritas, 4606 Canada Way, Burnaby, BC V5G 1K5, Canada*

Abstract

Acid rock drainage from mine waste is caused by the oxidation of sulfide minerals in moisture and air. In a test column filled with waste rock, oxidation was measured by oxygen consumption, moisture by weight, and negative pore-water potential indirectly by relative humidity. The results show an interesting correlation between the three.

In waste rock piles, moisture can reach areas not accessed by seepage of meteoric or ground water through vapour transport. Rocks retain/release moisture based on their water retention characteristics. This will in turn influence the relative humidity of the surrounding air space and sulfide oxidation rate.

Keywords: Sulfide Oxidation, Oxygen Consumption Test, Water (Moisture) Content, Humidity, Waste Rock

Introduction

Acid rock drainage and metal leaching (ARD-ML) is the outflow of acidic water from mine waste that often contains elevated metal(loid)s. ARD-ML is an environmental issue with potentially detrimental effects on the biota of receiving water bodies (Jennings 2008). The main source of acidity in ARD-ML is the oxidation of sulfide-containing minerals, such as pyrite (FeS_2). The overall chemical reaction for ARD-ML production from pyrite oxidation can be expressed as:

$$FeS_2 + {}^7/_2\, O_2 + H_2O \rightarrow Fe^{2+} + 2SO_4^{2-} + 2H^+ + \text{heat} \qquad \text{[eq. 1]}$$

It can be seen from the equation above, that for sulfide oxidation and acid production to occur, both water and oxygen must be present. In fact, a common way to prevent sulfide oxidation of mine tailings is to submerge them under water to prevent oxygen exposure. Conversely, given the right combination of sulfide surface exposure to air and water, the ARD-ML generating reaction rate is expected to escalate.

When a waste rock pile is wetted by meteoric water (snowmelt and/or rain), or groundwater, the rocks retain some of the water based on its water retention characteristics even as the excess water drains away. Understandably, the resulting negative pore-water pressure (PWP) condition of the rocks will influence how much of the active sulfide surface area will actually be exposed to both water and air.

Oxygen consumption (OxyCon) tests, first published by Elberling *et al.* (1994), have been used to measure the kinetic rate of sulfide oxidation. In this test, an oxygen sensor monitors the drop in the oxygen level within a closed container filled with waste rocks. As sulfide oxidation occurs, the oxygen content inside the container will decrease. In the case of rocks with relatively high levels of exposed sulfides, the oxygen level inside the container will decrease more sharply. Recently, much work on OxyCon

tests has been published by Earth Systems (Schmieder *et al*. 2012). OxyCon tests have been used to investigate the effect of many rock parameters, including sulfide content, particle size and moisture content.

This study explores one aspect of ARD-ML generation by OxyCon test that is often overlooked: the role of the pore-water pressure, or suction of waste rock, as shown by Salmon *et al*. (2018). The oxygen consumption rates of relatively dry rocks (with moisture contents of ≈2.0 wt.% and lower) were measured to study the role of PWP (suction) on the sulfide oxidation rate. Measuring suction of waste rock is challenging due to their large sizes and irregular shapes, and most commercial analysers are designed for soil. Headspace relative humidity (RH) was used as a direct indication of the suction of waste rocks.

Methods

Rock samples from a mine site were crushed passed through a 0.64-cm sieve. The samples were homogenized and split into three representative portions: one portion for characterization by acid base accounting (ABA), one portion for Rietveld XRD analysis and one portion for OxyCon testing.

A 10.2 cm (d) × 20.3 cm (h) column was filled with 2.854 kg of rocks to a height of 17.8 cm as shown in fig. 1 below. The column was equipped with a water distributor at the top and a drain at the bottom for collecting water effluents. The column also has an air input line at the bottom and a corresponding output line at the top.

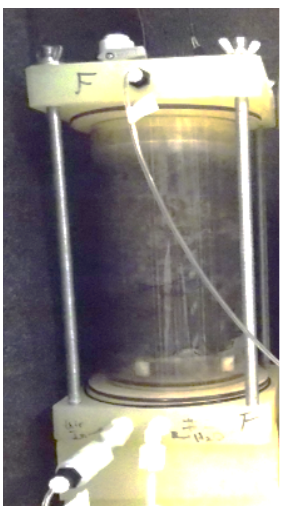

Figure 1 *Photograph of the experimental setup, including custom-made columns with connections for water and gas flow.*

Fig. 2 shows schematic representations of the OxyCon test procedures. Before beginning of the OxyCon test, the columns were wetted with deionized water at 16 mL/min, as shown in Fig. 2a, until 600 mL of effluents were collected. After the leaching process, the column was purged with dry air for two weeks as shown in Fig. 2b. The direction of air flow was from the bottom up—opposite to the direction of water flow and consistent with the belief that air mostly enters covered waste rock dumps from the toe (Pearce *et al*. 2016). This leaching process was repeated three times to condition the sample. The pH of the effluent was close to neutral as expected from ABA analysis.

Oxygen consumption test was performed as shown in Fig. 2c. In our version of the OxyCon test, air was circulated from the columns to external sensors, which measured the concentrations of O_2 and RH. After each OxyCon test cycle, the column was again purged with dry air (Fig. 2b) to remove moisture from the waste rocks. The weight of the column was then recorded, and moisture content for the next round of OxyCon test was calculated. While rocks in the column were being dried, sensor lines were isolated from the columns for calibration and performance validation. Seven OxyCon-drying cycles were performed until the oxygen consumption slowed down appreciably. As a final quality control procedure, the rocks were humidified again with water-saturated air using the same configuration as in fig. 2b. The OxyCon rate was measured to ensure that retardation of oxygen consumption did not arise simply from of the depletion of active sulfide surfaces. This is reported as the 8^{th} cycle in the results below.

Results and Discussion

Representative portions of the rock sample underwent ABA analysis and Rietveld analyses. The results are shown in tab. 1 and 2, respectively. As can be seen in tab. 2, this waste rock sample contains a substantial

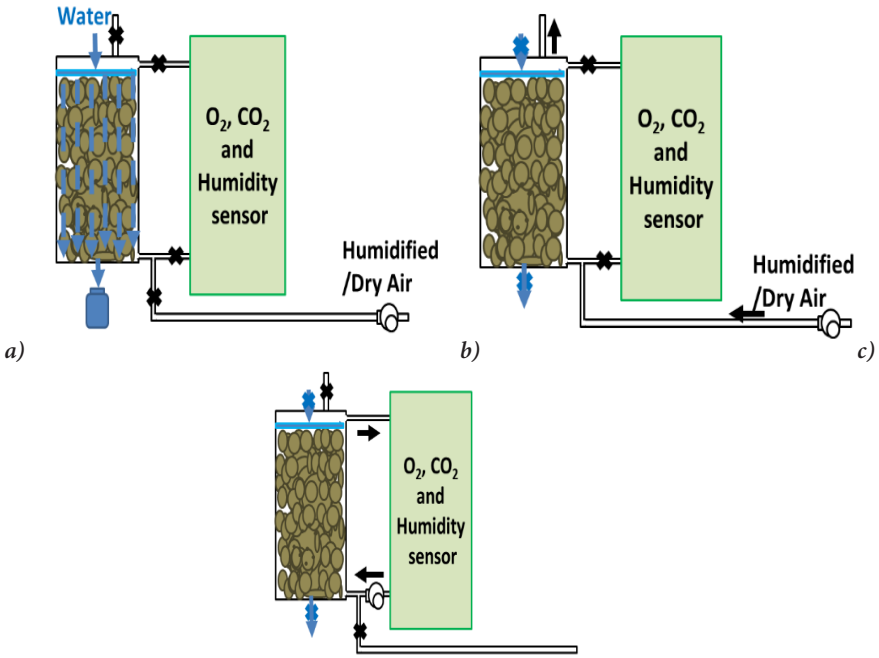

Figure 2 *Experimental processes: a) column wetting, b) column drying or humidification and c) oxygen consumption, carbon dioxide generation and humidity monitoring. "X" indicates where valves were closed. Black arrows indicate the direction of air flow while blue arrows indicate the direction of water flow.*

Table 1 *Results of acid base accounting analysis.*

Parameter	Unit	Result	Parameter	Unit	Result
Paste pH		7.0	Non-Extractible S	wt.%	0.31
CO_2	wt.%	2.7	Acid generation potential	kg $CaCO_3$ /t	51.9
$CaCO_3$ equiv.	kg $CaCO_3$ /t	61.4	Mod. ABA neutralization potential	kg $CaCO_3$ /t	50.5
Total S	wt.%	2.02	Fizz rating		SLIGHT
HCl Extractible S	wt.%	0.05	Net neutralization potential	kg $CaCO_3$ /t	-1.4
HNO_3 Extractible S	wt.%	1.66	Neutralization potential ratio		1.0

Table 2 *Results of Rietveld XRD quantitative phase analysis.*

Mineral	Ideal Formula	Wt.%			
Quartz	SiO_2	68.1	Clinochlore	$(Mg,Fe^{2+})_5Al(Si_3Al)O_{10}(OH)_8$	1.5
Illite/ Muscovite 2M1	$K_{0.65}Al_{2.0}Al_{0.65}Si_{3.35}O_{10}(OH)_2$ / $KAl_2AlSi_3O_{10}(OH)_2$	15.8	Calcite	$CaCO_3$	0.5
Ankerite-Dolomite	$Ca(Fe^{2+},Mg,Mn)(CO_3)_2$. $CaMg(CO_3)_2$	7.0	Siderite	$Fe^{2+}CO_3$	0.4
Pyrite	FeS_2	3.8	Rutile	TiO_2	0.2
Kaolinite	$Al_2Si_2O_5(OH)_4$	2.5	Jarosite	$K_2Fe_6^{3+}(SO_4)_4(OH)_{12}$	0.2

Table 3 Summary of experimental results for the OxyCon tests.

Cycle #	Wt.% H_2O	RH, +/- 0.02	PWP (kPa)	OxyCon rate (%O_2/min)
1	1.97	.99	-1.4	1.25E-03
2	1.52	.92	-11	1.04E-03
3	0.77	.65	-59	8.72E-04
4	0.69	.58	-74	5.73E-04
5	0.69	.50	-94	2.86E-04
6	0.69	.48	-1.0 x10^2	2.06E-04
7	0.62	.44	-1.1 x 10^2	7.18E-05
8	0.69	.58	-74	2.15E-04

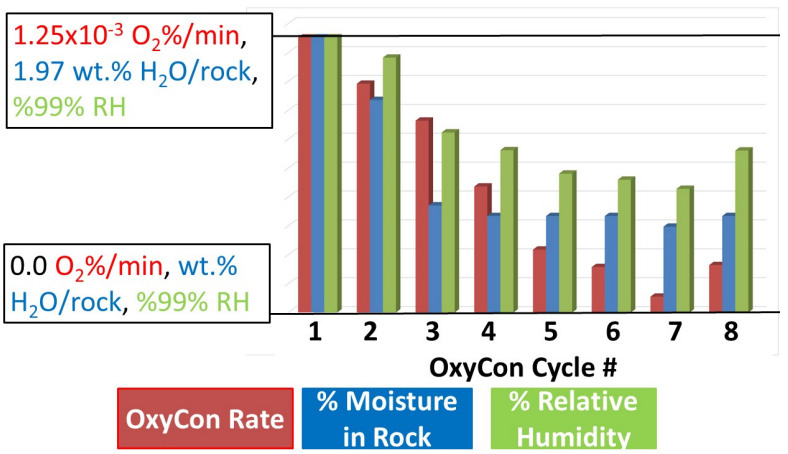

Figure 3 *A comparison of oxygen consumption rate (O_2%/min), RH and wt.%H_2O of rock column.*

amount of sulfide in the form of pyrite. The oxygen consumption was therefore expected to be easily measurable. Calcite was also present, which explains the neutralization potential measured during the ABA analysis.

OxyCon tests were subsequently performed at different levels of moisture content for a total of eight cycles, the results of which are shown in tab. 3. Between each OxyCon test cycle, dry air was used to gradually remove moisture from the rocks, and the weight of the column was recorded in order to calculate for the remaining moisture content. After seven OxyCon test cycles with progressively drier rocks, humid air was pumped through the rocks for cycle 8 to restore some moisture to the column before the eighth and final OxyCon measurement.

Fig. 3 shows the measured oxygen consumption rate versus the moisture content of the rocks and the headspace humidity. The rate of oxygen consumption is fastest in the first cycle. Beginning at cycle four, the moisture content of the rocks no longer changes significantly, and it was observed that the rate of oxygen consumption is more correlated to the headspace humidity, which in turn is related to the suction condition of the waste rocks. RH was lowest at cycle 7 and, as expected, the rate of oxygen consumption was at its minimum. When RH was raised at cycle 8, the rate of oxygen consumption increased proportionately.

Steger published a series of paper on the oxidation of sulfide minerals, such as pyrite, chalcopyrite and pyrrhotite. In the seventh paper of the series, Steger (1982) reported the results of oxidation experiments on pyrrhotite under controlled environmental conditions of 50 °C and various RH: 37%, 50%, 55%, 62% and 75%. He found that, at 37% RH, sulfate formation occurred but

oxide formation did not. This is possible because sulfate formation does not require water while hydroxides and oxides do. As RH increases, ferric oxides begin to form and the formation rate continuously increase with RH with the slope maximizing at 57-59%. The SO_4^{2-} formation also peaked at RH of 57-59%. This can be explained by further oxidation and hydrolysis reactions, and migration of species that can only occur with water molecules. Rosenbaum *et al.* (2015) observed that dried pentlandite-pyrrhotite nickel concentrate pre-weathered for 21 day at 40 °C and 30-50% RH, did not demonstrate self-heating (sulfur oxidation) capacity in a subsequent test. On the other hand, dried samples that were pre-weathered at 70 and 80% RH and otherwise similar conditions showed proportionately increasing self-heating capacity. Both studies demonstrates the importance of environmental humidity for sulfide oxidation in dry rocks. While both studies were done at elevated temperature to accelerate reaction kinetics, our study shows that such sulfide oxidation can still be observed even at room temperature (23 °C) and low % RH.

During the experiments, an interesting observation made was that dry air can be moistened when flowed through relatively dry waste rocks. Fig. 4 shows the change in the RH of the column headspace before and after flowing through a column containing waste rocks with a water content of 0.62%. The initial RH of the air was between 0.05-0.10 but its RH became 0.44 afterward purging through the column.

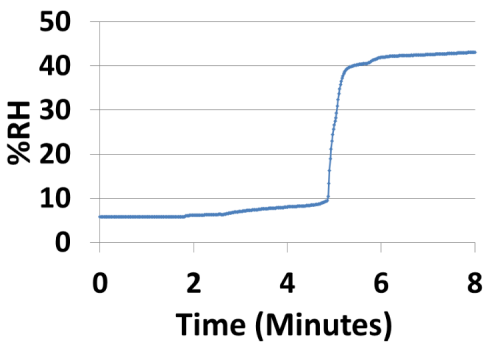

Figure 4 *%RH of the headspace as a function of time during cycle seven of the OxyCon test.*

Headspace relative humidity (RH) can be used as a direct indication of the suction of waste rocks, as high suction will reduce the number of water molecules (and therefore the RH) in the headspace above the sample. This relationship is given by the Kelvin equation:

$$Total\ suction = \frac{R(T+273.15)}{V_w} \ln\left(\frac{p}{p_0}\right) \quad \text{[eq. 2]}$$

Where R is the gas constant (8.3143 J/mol-K), T is temperature (C), V_W is the molar volume of water (1.8×10^{-5} m^3mol^{-1}), p_0 is the saturation vapor pressure at the sample temperature, and p is the equilibrium vapor pressure in the headspace. The term p/p_0 is the equilibrium RH of the sample (Warrick 2002).

An observation during experiments further demonstrated the relationship between rock moisture content and suction. When the lid of a test column was opened to accelerate drying, the top surface of the column appeared quite drier (bone dry) than the bottom of the column. After air recirculated throughout the column at the start of OxyCon testing, however, the top layer appeared as wet as the rest of the waste rocks in the column. This demonstrates the ability of air to redistribute moisture throughout the waste rocks. Such internal redistribution of moisture within full-scale waste rock piles and mine walls has been reported in the past (Morin and Hutt 1997 and 2001) but rarely documented in detail.

Depending on their PWP, waste rocks can act as a humidifier when the atmosphere is very dry and vice versa. In a waste rock pile, this means that moisture can reach waste rock through water vapour transport, to areas not influenced by seepage of liquid water.

Conclusion

Our study demonstrates that the suction condition of waste rock can play an important role in the sulfide oxidation process. In this case study (<2.0% moisture), it was observed that consumption of oxygen by pyrite oxidation did not slow appreciably until the moisture content of the rock was around 0.6%wt. and the RH was 0.44. There are strong positive correlations between oxygen

consumption rate, the moisture content of the waste rock and RH of the surrounding air when RH is <0.99 and the moisture content is <2.0%. Our measurements also show that waste rocks can effectively draw water from the pore-air space to drive the oxidation of pyrite. In a waste rock pile, it means that moisture can reach waste rocks through water vapour transport, to areas not influenced by seepage of liquid water. This implies that pore-air humidity may be sufficient for sustaining ARD-ML in mine waste dumps even without a fresh supply of meteoric or ground water. Since waste rocks can retain water in general, it is unlikely that rocks in commercial scale dumps can reach the level of dryness needed to stop sulfide oxidation completely.

These results are important to our understanding of ARD-ML, especially as it supports assumptions regarding water transport and acid generation in ARD-ML modeling work (Morth 1972; Liu 2017, 2018, 2019) used to design and evaluate mine waste storage facilities.

Acknowledgements

This project was funded by the National Research Council Canada Energy, Mining and Environment Research Centre, and the Environmental Advances in Mining Program. The NRC authors wish to acknowledge the contributions of collaborators from O'Kane Consultants, MDAG and Bureau Veritas.

References

Elberling B, Nicholson RV, Reardon EJ, Tibble P (1994) Evaluation of sulphide oxidation rates: a laboratory study comparing oxygen fluxes and rates of oxidation product release. Can Geotech J, 31(3), 375-383.

Jennings SR, Neuman, DR, Blicker PS (2008) Acid mine drainage and effects on fish health and ecology: a review. Reclamation Research Group Publication, Bozeman, MT.

Liu Z-S, Huang C, Ma L, Dy E, Xie Z, O'Kane M, Pearce S (2017) Experimental models of metal leaching for scaling-up to the field, 9th Australian Acid and Metalliferous Drainage Workshop Proceedings, 44-50.

Liu Z-S, Huang C, Ma L, Dy E, Xie Z, Tufa K, Fisher E, Zhou J, Morin k, Aziz M, Meints C, O'Kane M, Tallon L (2018) Rate-control quotient of mineral dissolution from waste rock dumps, 41st BC Mine Reclamation Symposium, https://open.library.ubc.ca/cIRcle/collections/59367/items/1.0374928.

Liu Z-S, Huang C, Ma L, Dy E, Xie Z, Tufa K, Fisher EA, Zhou J, Morin K, Aziz M, Meints C, O'Kane M, and Tallon L (2019), The characteristic properties of waste rock piles in terms of metal leaching, J Contaminant Hydrology, 226, 103540.

Morin KA, Hutt NM (1997) Environmental geochemistry of minesite drainage: practical theory and case studies, MDAG Publishing (MDAG.com), ISBN 0-9682039-0-6

Morth AH, Smith and Shumate KS. 1972. Pyrite systems: a mathematical model, Contract Report for the U.S. Environmental Protection Agency, EPA-R2-72-002.

Pearce S, Dobchuk B, Shurniak R, Song J, Christensen D (2016) Linking waste rock dump construction and design with seepage geochemistry: an integrated approach using quantitative tools, Proceedings IMWA 2016, Freiberg Germany, Drebenstedt, Carsten, Paul, Michael (eds.)

Rosenblum F, Finch JA, Waters KE, Nesset JE, A test apparatus for studying the effects of weathering on self-heating of sulphides, The Conference of Metallurgist 2015, Can Inst of Mining, Metallurgy and Petroleum, www.metsoc.org , IBSN: 978-1-926872-32-2

Salmon U, Marton R, O'Kane M (2018) Evolving kinetic test methods for reactive mine waste rock, Proceedings of the 11th International Conference on Acid Rock Drainage, Pretoria, South Africa.

Schmieder PJ, Taylor JR and Bourgeot N (2012), Oxygen consumption techniques to quantify acidity generation rates, 1st International Acid and Metalliferous Drainage Workshop in China, Beijing. http://earthsystemseurope.com/wp-content/uploads/2013/05/Schmieder-et-al-2012_OxCon.pdf

Steger HF, Oxidation of sulfide materials, VII: effect of temperature and relative humidity on the oxidation of Pyrrhotite, Chemical Geology, 35(1982), 281-215.

Warrick AW (2002), Soil Physics Companion, CRC Press.

Assessment of the Chemical and Ecological Recovery of the Frongoch Stream Following Remediation at Frongoch Lead and Zinc Mine, Mid Wales

Paul Edwards[1], John F. Murphy[2], J. Iwan Jones[2], Chloe Morgan[1], Rory P.D. Walsh[3], Julie Gething[1]

[1]*Natural Resources Wales, 29 Newport Road, Cardiff CF24 0TP, UK, paul.edwards@cyfoethnaturiolcymru.gov.uk, chloe.morgan@cyfoethnaturiolcymru.gov.uk, julie.gething@cyfoethnaturiolcymru.gov.uk*

[2]*Queen Mary University of London, School of Biological and Chemical Sciences, Mile End Road, London, E1 4NS, UK, j.i.jones@qmul.ac.uk, j.f.murphy@qmul.ac.uk*

[3]*Swansea University, Singleton Park, Swansea, SA2 8PP, UK, r.p.d.walsh@swansea.ac.uk*

Abstract

Diversion of Frongoch Stream in 2011 reduced inflows to Frongoch Mine, increasing streamflow and diluting contaminants. This, together with subsequent surface water management, capping, hydroseeding and revegetation from 2013-2018, led to overall decreases of 87%, 93% and 87% for dissolved Zn, Pb and Cd respectively. Residual discharges, however, still cause the stream to fail to comply with Water Framework Directive standards and there is only modest evidence of biological recovery to date. Sediment metal concentrations in 2020 indicate that ecological recovery may be impaired by enduring bed-sediment contamination, even where erosion and sediment transport of mine waste is successfully managed.

Keywords: Metal Mine Remediation, Sediment Contamination, MetTol, Macroinvertebrates, Water Quality

Introduction

Treatment of coal mine discharges has protected and improved over 350 km of rivers in the UK in recent decades. Ecological recovery downstream of treated coal mine discharges can be rapid, due to natural washing of ochre from riverbeds (Wiseman *et al*. 2002). In contrast, metal mines remain a major cause of failure to achieve Water Framework Directive (WFD) standards with 1,300 mines adversely affecting over 700 km of rivers in Wales alone. Due to technical challenges and funding limitations, relatively few full-scale remediation schemes have been completed for UK metal mines and, to date, there is limited evidence of ecological recovery following these schemes.

Frongoch Mine, in the upper Ystwyth catchment in Mid Wales, UK (fig.1), was one of the most productive metal mines in Wales, producing over 100,000 tonnes of lead and zinc ore from 1798 until its closure in 1904 (Bick 1996). Large waste dumps were reprocessed to extract metals between 1917 and 1930, but these remained a source of metals pollution to Frongoch Stream thereafter. The mine is in the Silurian, Devil's Bridge Formation, largely composed of interbedded sandstone and mudstone. Annual rainfall is ≈2,000 mm and the surrounding land is mainly rough pasture/moorland. Prior to remediation, pollutant pathways to Frongoch Stream included surface runoff and shallow groundwater discharges, including a discharge from a culvert of unknown origin. Deeper groundwater from the mine drains via Frongoch Adit to the Nant Cwmnewydion in a neighbouring valley (Edwards *et al*. 2016). Frongoch ranked as Wales' second most polluting mine (Mullinger 2004), contributing to failures to achieve WFD standards for Zn, Pb and Cd in Frongoch Stream, Nant Cell, Nant Cwmnewydion, Nant Magwr and Afon Ystwyth (Stokes 2012). Annual metal discharges to Frongoch Stream were 6.5 and 0.5 tonnes of dissolved Zn and Pb

respectively, while Frongoch Adit discharged approximately twice those amounts (Edwards *et al*. 2016).

Remediation at Frongoch Mine was completed in four phases from 2011 to 2018. In February 2011, Environment Agency Wales (EAW) stopped Frongoch Stream overflowing from Mill Pond into an open stope at the northeast of the mine by diverting it back into its original watercourse via a culvert from the pond. This reduced the flow to Frongoch Adit and increased dilution of metals in Frongoch Stream downstream of the mine. From January to May 2013, EAW (Natural Resources Wales (NRW) from April 2013) constructed a drainage channel around the northern and western perimeter of the site to intercept clean surface water and divert it away from the mine waste. A flood attenuation pond was built to receive this channeled water and discharge it immediately upstream of the old culvert discharge. From January to June 2015, NRW relocated mine waste to the north of the site where it was re-profiled to enhance runoff. A series of ponds was created to convey the drainage to the flood attenuation pond and provide a habitat for wildlife. A continuous section of imperforated pipe was placed in the perimeter channel to carry relatively clean water through an area of lead-rich tailings lagoon deposits highlighted by a geochemical assessment (Mustard 2013). The ponds and drainage channels were lined with geosynthetic clay liner (GCL) and most of the reprofiled area was covered with a minimum of 300 mm of compacted clay plus 100 mm of restoration soils, seeded with common bent grass. In total, over 23,000 m^2 of the site was capped in 2015, covering approximately 65% of the contaminated mine waste. From May to July 2018, 7,600 m^2 of the previously reprofiled but uncapped area was covered with GCL under a minimum of 350 mm confining layer and restoration soils. In September 2018, a further 5,000 m^2 was sprayed with experimental mixtures including commercial hydroseeding products with biochar, mycorrhizae and plant nutrients.

Monitoring methods

Monthly water quality spot sampling was carried out on surface and groundwater discharges and their receiving watercourses from 2011 to 2020. Sampling stations relevant to this study are shown in fig.1. Water quality data were also available for these sites from investigations prior to 2011, but there were gaps in the time series, notably in 2010. Water quality upstream of the discharges to Frongoch Stream was fully compliant with WFD standards, so monitoring stopped here in 2014. Spot samples of water were collected

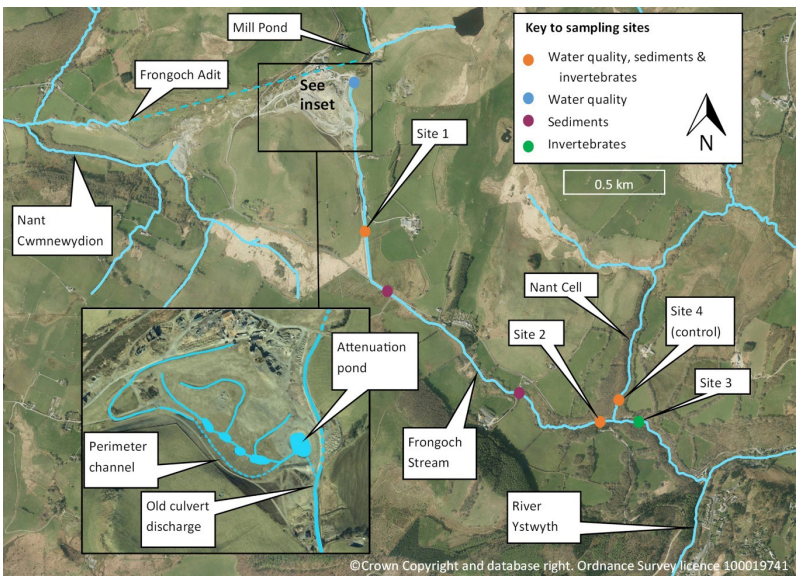

Figure 1 *Map of sampling sites and mine features in Nant Cell and Nant Cwmnewydion catchments.*

using standard NRW protocols and analysed in NRW's laboratory. Simultaneous flow gauging was carried out on the mine discharges and at Site 1, which was gauged by using a hand-held flow meter to measure velocity and multiplying this by cross-sectional area.

Samples of the macroinvertebrate community were collected from four sites on Frongoch Stream and Nant Cell on three occasions: August 2009, October 2019 and August 2020. These included three sites successively downstream of Frongoch Mine and a control site on Nant Cell (fig.1). All samples were collected using standard NRW protocols and the number of individuals of each taxa captured were calculated for each sample. A newly-developed biotic index to metal pollution (MetTol; Jones *et al.* 2016) was applied to the macroinvertebrate community data to assess any reduction in stress after the remediation. MetTol assigns a score (0-100) to each taxon present in a sample based on its tolerance to metal pollution. The final index value is the average of the scores for the sample, giving a measure of the average metal tolerance of taxa found at the site. MetTol index values typically vary between 25-55, with higher MetTol index values indicating a community under less metal stress. The 90th percentile of assigned MetTol scores was also calculated for each sample to provide a more focussed indication of the prevalence of metal-sensitive taxa. This latter approach is particularly appropriate when seeking evidence of recolonisation of stream sites by metal-sensitive taxa following management interventions.

Bed-sediment metals data for Frongoch Stream and Nant Cell (fig.1) were available from three M.Sc. studies linked to the remediation programme (Morgan 2013, Foggin 2016 and Lort 2017) and from NRW sampling in 2020 using standard NRW protocols for sample collection and analysis. Unfortunately, these surveys used disparate sample collection and analysis methods, which complicates comparisons of sediment metal concentrations over time. In particular, different size fractions of the fine sediment were considered by different surveys and information on the relative weight or volume of different fractions in each sample was not always available.

Results

Diversion of Frongoch Stream in 2011 reduced inflows to underground mine workings, increasing streamflow at Site 1 by ≈300%, providing more dilution of runoff and groundwater discharges from the southeast corner of the mine site. Compared with 2007-2009 data, dissolved Zn, Pb and Cd at Site 1 all reduced by >80% in the period from February 2011 to December 2012 (fig.2).

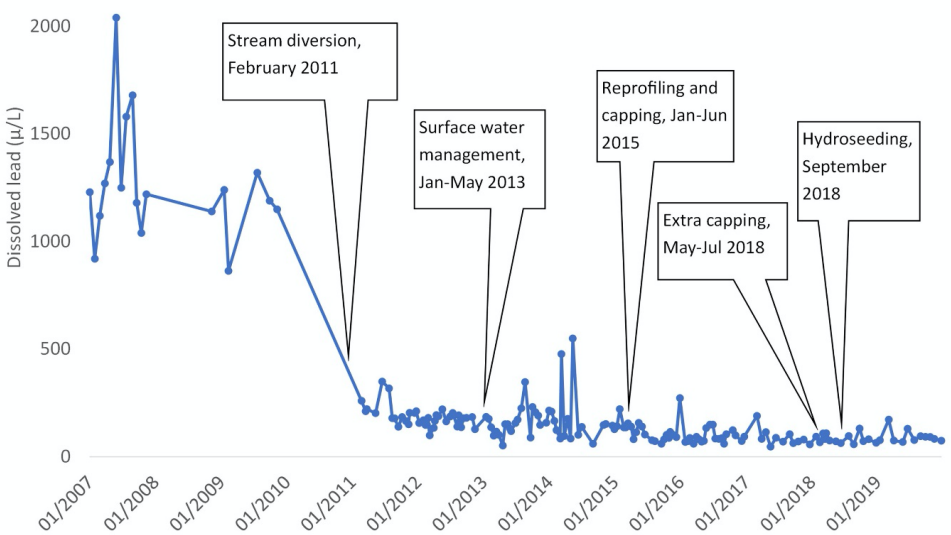

Figure 2 *Dissolved lead concentrations at Site 1 on Frongoch Stream.*

Frongoch Adit flow reduced by ≈80% following the diversion and although metal concentrations in the residual flow increased, the Zn, Pb and Cd loads reduced by 44%, 63% and 58% respectively. Reprofiling works in 2013 may have caused spikes in concentrations of metals in Frongoch Stream in 2013-14, but there was an overall reduction in metal concentrations over the period from March 2011, after the stream diversion, to January 2020, when monitoring stopped due to Covid-19 restrictions. A non-parametric Mann-Kendall test combined with a Theil-Sen estimator detected significant ($P<0.05$) downward trends over this period for Zn, Cd and especially Pb. There were, however, no obvious step reductions following the remediation phases after March 2011.

Based on a comparison of mean data from 2007-2009 and 2017-19, the combined remediation measures reduced dissolved Zn, Pb and Cd concentrations in Frongoch Stream by 87%, 93% and 87% respectively. Residual sources of these metals, however, still cause the stream to fail to comply with WFD standards. Bioavailable fractions of Zn and Pb at Site 1 in 2017-19 were 160 and 74 times higher than WFD standards respectively, while dissolved Cd was 63 times higher than the WFD standard based on hardness band. Zn, Pb and Cd concentrations were only ≈25% lower at Site 2 than at Site 1, so they also greatly exceeded WFD standards at this site. The Nant Cell control site (Site 4) is compliant with WFD standards for Zn and Cd, but marginally fails the standard for Pb, based on 2017-19 data.

The number of macroinvertebrate individuals and taxa captured in samples from sites 1-3 increased substantially between summer 2009 and autumn 2019, either side of the remediation, but a similar pattern was seen in the Nant Cell control site (tab. 1). Further sampling in summer 2020 found a consistent decrease in the number of individuals and taxa captured relative to the previous autumn, suggesting that seasonal and inter-annual variation may be important confounding factors to be considered when interpreting the data. Applying the MetTol index to the community data enables better identification of the unconfounded metal stress signal over the three sampling occasions. At sites 2 and 3 there have been distinct improvements with the macroinvertebrate community beginning to include more metal-sensitive taxa, such as the caddis flies *Silo pallipes*, *Sericostoma personatum*, the mayfly *Ecdyonurus*, and the stonefly *Perla bipunctata*. Considering 90%ile MetTol, there appears to be a sustained increasing trend at both these sites. At Site 1, just below the mine, there is less conclusive evidence for sustained improvements; MetTol values have decreased slightly but 90%ile MetTol has increased over the sampling period suggesting the first tentative steps

Table 1 *Community indices calculated for sites in Frongoch Stream/Nant Cell catchment.*

Site name	Date	Number of individuals	Taxon richness	MetTol	90%ile MetTol
Site 1	Aug 2009	20	8	43	52
	Oct 2019	753	25	38	50
	Aug 2020	308	23	36	57
Site 2	Aug 2009	61	11	29	40
	Oct 2019	645	28	36	50
	Aug 2020	240	14	35	54
Site 3	Aug 2009	244	20	31	41
	Oct 2019	579	34	40	52
	Aug 2020	107	24	38	58
Site 4	Aug 2009	53	15	38	53
(control)	Oct 2019	247	28	41	53
	Aug 2020	81	23	41	50

towards recovery may be occurring. The metal-sensitive taxa *S. pallipes*, *S. personatum*, and the non-biting midge *Chironomini* have been recorded intermittently at the site. At the Nant Cell control site, MetTol (38-41) and 90%ile MetTol (50-53) values varied less between surveys, but were not consistently greater than at sites 1 and 2 in the impacted Frongoch Stream.

Concentrations of Zn, Cd and Pb in bed-sediment at all sites on Frongoch Stream sampled in 2020 continue to far exceed the thresholds recommended by Jones *et al.* (2016) for fine sediments (<2000 µm) based on species sensitivity distributions derived from ecological field data (tab. 2). In particular, Pb concentrations are still over 50-100 times higher than the threshold values. Concentrations at the control site on Nant Cell in 2020 were below these thresholds. A time-series of consistently analysed sediment data from sites 1-4 is not available, but the data collected do not suggest a consistent reduction in sediment metal concentrations in Frongoch Stream over the 2013-2020 period.

Conclusions

Remediation at Frongoch Mine has controlled the release of contaminated mine waste and reduced metal concentrations in Frongoch Stream, but only modest biological recovery has been observed to date. Continuing impacts on the macroinvertebrate fauna can be attributed to enduring high concentrations of Zn, Cd and Pb in both the water column and streambed sediments.

Analysis of water quality and flow data for sampling sites at Frongoch Mine by Morgan (2020) concluded that the old culvert discharge is the largest remaining source of metals to Frongoch Stream. Other remaining sources include a separate groundwater discharge, which enters Frongoch Stream via the flood attenuation pond, and surface runoff, most of which also discharges via the pond outfall. With the exception of the 2011 stream diversion, reductions in metal concentrations in the Frongoch Stream have occurred progressively rather than in step changes following remediation phases. Morgan (2020) found that capping in 2015 and 2018 improved the quality of surface runoff from the mine site, but effects on groundwater sources were less evident.

Metal concentrations have continued to far exceed WFD standards even during periods where there was no visible discharge to Frongoch Stream via the old culvert or the flood attenuation pond, e.g. during the drought of summer 2018. This suggests that metal concentrations are augmented by diffuse groundwater inputs during periods of low flow, as observed by Byrne et al. (2020) in the neighbouring Nant Cwmnewydion

Table 2 *Sediment metal concentrations at sites in Frongoch Stream/Nant Cell catchment.*

Site name	Date	Zn mg/kg		Cd mg/kg		Pb mg/kg	
		<2000 µm	<63 µm	<2000 µm	<63 µm	<2000 µm	<63 µm
Site 1	2013 - 2017	Range 3034 - 36171*		Range 0.31 - 33*		Range 1318 - 12100*	
	Aug-20	9480	12700	48.1	34.1	1620	15300
	Sep-20	1660	5360	3.74	13.3	2970	14400
Site 2	2013 - 2017	Range 45 - 9156*		Range 0.77 - 11*		Range 2150 - 5221*	
	Aug-20	3900	9330	8.29	22.8	4530	8150
	Sep-20	2870	6930	6.79	20.3	2230	8450
Site 4 (Control)	2013 - 2017	Range 119 - 316*		Range 0.02 - 0.7*		Range 50 - 1100*	
	Aug-20	144	428	0.183	0.883	30	212
	Sep-20	136	298	0.185	0.664	32	222
Threshold concentration**		447	N/A	4.7	N/A	133	N/A

*Range includes variable size fractions <2000 µm, **Jones *et al.* (2016)

catchment. These diffuse sources may reduce the benefits of future treatment of the point source discharges.

The biological signal from sites on the Frongoch Stream suggests that the first tentative steps towards recovery are taking place, but the sediment data tempers hope that recovery will be rapid, even if groundwater sources of dissolved metals are treated. This is supported by Clements *et al*. (2010), who found a significant delay in macroinvertebrate recovery following stream restoration, partly due to residual sediment metal contamination. The macroinvertebrate community in Frongoch Stream will remain under stress for as long as the fine streambed sediment that many of the animals consume is contaminated to this extent. If the remediation has sufficiently reduced inputs of metal-laden water and sediment to the stream, much of the entrained and adsorbed metal should eventually be flushed downstream, allowing more metal-sensitive taxa in Nant Cell and the catchment upstream of Frongoch Mine to colonise and persist.

Acknowledgements

The Frongoch Mine Remediation Project was partly funded by the European Regional Development Fund, provided through Welsh Government and delivered by NRW with technical support from the Coal Authority.

References

Bick D (1996) Frongoch Lead & Zinc Mine, British Mining No 30. A monograph of the Northern Mine Research Society, July 1996.

Byrne P, Onnis P, Runkel R, Frau I, Lynch S and Edwards P (2020) Critical Shifts in Trace Metal Transport and Remediation Performance under Future Low River Flows. Environ. Sci. Technol. 2020, 54, 24, 15742–15750.

Clements W, Vieira N and Church S (2010) Quantifying restoration success and recovery in a metal-polluted stream: a 17-year assessment of physicochemical and biological responses. Journal of Applied Ecology 2010, 47, 899–910.

Edwards P, Williams T & Stanley P (2016) Surface water management and encapsulation of mine waste to reduce water pollution from Frongoch Mine, Mid Wales. In Proceedings IMWA 2016, Leipzig/Germany. Drebenstedt, Carsten, Paul, Michael (Eds.). Mining Meets Water, Conflicts and Solutions. pp546-553.

Foggin H (2016) Hydrogeochemical observations and evaluation of the effects of remediation upon stream sediment quality at Frongoch Mine mid-Wales. MSc dissertation, Aberystwyth University.

Jones J, Spencer K, Rainbow P, Collins A, Murphy J, Arnold A, Duerdoth C, Pretty J, Smith B, Fitzherbert M, O'Shea F, Day M, Groves S, Zhang Y, Clarke A, Stopp, J, McMillan S (2016) The Ecological impacts of contaminated sediment from abandoned metal mines. Department for Environment, Food and Rural Affairs, London, p. 359.

Lort J (2017) Assessment of stream sediment quality and the Fe/Mn oxide coatings of stream pebbles in the watercourses of Frongoch Mine, mid-Wales. MSc dissertation, Aberystwyth University.

Morgan C (2020) Effectiveness of abandoned mine remediation measures in reducing metal pollution, Ystwyth catchment, Wales. MSc dissertation, Swansea University.

Morgan T (2013) The impact and extent of metal contamination on the river Ystwyth as a result of discharge from Frongoch Mine, near Pont Rhyd y Groes. MSc dissertation, Aberystwyth University.

Mullinger N (2004) Review of Environmental and Ecological Impacts of Drainage from Abandoned Metal Mines in Wales. Environment Agency Wales Report Ref: EATW/04/02.

Mustard G (2013) Geochemical characterisation and assessment of remediation works at Frongoch Metal Mine, Mid-Wales. MSc dissertation, Swansea University.

Stokes M (2012) WFD Abandoned Mines Investigation Project: Afon Ystwyth catchment. Environment Agency Wales Tech Report No: AR_SW_12_06.

Wiseman I, Rutt G, Edwards P (2004) Constructed wetlands for minewater treatment: environmental benefits and ecological recovery. Journal of the Chartered Institution of Water and Environmental Management, 18, 133–138.

Osmodialysis – The Future of Oil Production Water Treatment

Matthias Fuhrland, Thomas Grießler

Fluvicon GmbH, Peter Tunner-Straße 19, 8700 Leoben, fluvicon@fluvicon.com

Abstract

With Osmodialysis, the Austrian company fluvicon GmbH has developed a continuously operating, extremely robust membrane process based on forward osmosis that is capable of cleanly separating oil and salt water. Fouling and scaling - the two major problems of membrane separation technology - play no role. That enables extremely long membrane service lives despite high oil loads and water hardness. The range of applications extends from the treatment of produced waters, condensate and seepage water in the oil and gas industry, to the purification of contaminated seawater after tanker accidents, shipwrecks and well disasters.

Keywords: Forward Osmosis, Oil Separation, Produced Waters, Leachate, Condensate

Introduction

Produced waters from the oil and gas industry are among the most difficult to treat of all industries due to their high salinity and residual oil content of usually > 300 mg/L. To date, many expensive treatment steps are required to purify the saline water to less than 30 mg/L residual oil content. For reinjection into the reservoir, the oil content should ideally be < 5 mg/L. Also, for subsurface or marine disposal of such waters, the residual oil content should be separated as completely as possible. Both as the water-to-oil ratio of production increases and as international environmental standards rise, the problem worsens and also becomes a cost factor. Until now, no technology seemed capable of achieving complete separation in a continuous process at a reasonable cost. But that is now changing.

The Austrian company fluvicon is developing membrane separation processes based on forward osmosis. Forward osmosis is the direct biomimetic replication of the natural process of osmosis and, like reverse osmosis, is one of the molecular separation processes used in water treatment. Here, the naturally existing osmotic pressure is utilized as the driving force. In contrast to reverse osmosis, the raw water flows past the membrane without pressure in forward osmosis. On the other side of the membrane is a draw solution, which with its high salt content draws the water molecules from the raw water through the membrane (fluvicon 2021). The hitherto unsolved problem of the technical use of forward osmosis was that the absorbed water must be removed again from the draw solution in order to enable a continuous process, because this is the only way in which the principle can be applied economically. While earlier approaches to the technical use of forward osmosis worked with thermal recycling of the draw solution or partial disposal of the diluted draw solution and subsequent dosing of salt, fluvicon had the idea of combining the osmotic principle as in nature with other principles or process steps to generate continuous processes working at room temperature. The resulting innovative and patented processes include Ionosmosis (Fuhrland/Grießler 2021) and Osmodialysis. While the product of Ionosmosis is pure water, the product of Osmodialysis is pure salt water.

Principle

Osmodialysis is a newly developed process for purifying contaminated salt water (e.g., reservoir water or seawater) in a highly energy-efficient continuous process. The salt water may be loaded with oil, dirt, aromatics, organics and/or solutes. Oil and salt water are separated by an innovative combination of different membrane separation steps including forward osmosis. Pure salt water and a pure oil fraction are obtained as products.

The Osmodialysis process (Fig.1) proceeds as follows:

1. In the dialysis stage, the loaded salt water is divided into two or optionally three partial streams. The first partial stream contains clean water and the salt load. It subsequently serves as the draw solution. The second partial stream contains water, oil and other freight. It is subsequently used as raw water. Optionally, the first partial stream can be separated into a stream with predominantly monovalent ions and a stream with predominantly divalent ions containing the hardness components such as lime. This allows the hardness of the product water to be adjusted.
2. Clean water is drawn in the forward osmosis (FO) module from the dirty raw water side to the saline draw solution side, thereby diluting the draw solution. The oil and other load end up in the concentrate. The diluted draw solution leaves the forward osmosis module as purified salt water. If the hardeners were separated as a partial stream, they can be fed back in here (proportionally, if necessary). Depending on the requirements, the partial flow of the hardness components can also be fed into the concentrate (proportionally, if necessary) or used in some other way.

In very simplified terms, the unique charm of the approach developed is that, after a very short run-in phase to generate an initial draw solution, the overall process can ideally be kept running with minimum effort to compensate for energy losses, because the draw solution is continuously regenerated from the raw water. The concentrate is an oil-containing fraction from which a pure oil fraction is recovered by continuous skimming.

Development status

The Osmodialysis process was successfully developed in the laboratory and then scaled up to the size of a fully automated demonstration plant (Fig. 2) with the support of the German partner MionTec. Depending on the oil content of the raw water, the demonstration plant produces about 100 liters of pure salt water per hour with a residual oil content of < 2 mg/L. Based on this plant, feasibility studies were conducted for various pilot customers. Among others, pure saline water has been successfully extracted from produced waters of oil production and from seepage waters of gas production on a ton scale. Of particular interest to the pilot customers was the fact that the hardness level of the product water is adjustable. Oil contents between 300 mg/L and 50000 mg/L did not cause fouling of the membranes for months. Extremely high lime contents (54° German hardness) in the feed water did not lead to fouling of the membranes for months. With fluvicon's Osmodialysis, these extreme waters can not only be treated economically, but a real recycling of the oil fraction is also conceivable, since the tests with crude oil emulsions have shown that the separated oil has a water content < 1%.

Advantages compared to the state of the art

a) *Separation efficiency and treatability:* The worldwide standard for continuous treatment of produced water is density separation, e.g. by means of parallel plate separators. The separation efficiency achievable on an industrial scale is

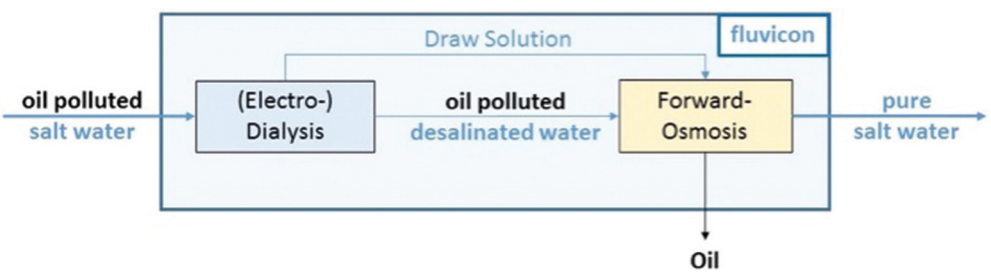

Figure 1 Osmodialysis process.

Figure 2 *Demonstration plant for Osmodialysis.*

approx. 300 mg/L residual oil content. The resulting product water thus still meets the criteria for hazardous waste but still contains a lot of valuable oil. Treatment of this product water or even of the original produced water with pressure-driven membrane separation technology (Reverse Osmosis, Nanofiltration) is out of the question, since the membranes would be blocked by the oil within a very short time. In this respect, Osmodialysis has a clear unique selling point in terms of separation efficiency.

b) *Simplification of the process:* According to the published state of the art, an extremely high level of technical and physical effort is required to achieve a separation of oil and salt water on an industrial scale that is even remotely comparable to that of Osmodialysis. Known for this purpose is a complex large-scale process chain consisting of density separation by means of parallel plate separators, coagulation with polymers, flotation, adsorption filters (e.g. nutshell filters) and a downstream multi-stage treatment of process water and flotation sludge (OMV 2018). Osmodialysis promises extreme simplification here, not only by substituting several separation steps at once, but also because no flotate sludge is produced at all. In addition, the offshore suitability of such a process chain (e.g. use on ships of the disaster command) is questionable, whereas Osmodialysis as a membrane process will have no problems here.

c) *Oil recycling:* While chemical-physical treatment produces a sludge as a result of coagulation and flotation that must go into incineration as hazardous waste, Osmodialysis ultimately produces only an oil fraction that can be recycled (see Fig. 3).

d) *Resource requirements:* Osmodialysis has no material resource requirements except for very small amounts of cheap chemicals for occasional cleaning routines. This gives it a clear advantage over material-intensive adsorption processes, such as activated carbon or nutshell filters, cleavage systems with bentonite-based separating agents, or the chemical-physical separation mentioned under b) with its high demand for polymer additives and flotation agents. The cost advantages of Osmodialysis are evident both in the procurement of consumables and in their disposal with the bound oil. Only electrodialysis requires significant energy, while forward osmosis operates without pressure.

All in all, Osmodialysis promises both technologically justified, international compliance with high environmental standards and massive cost advantages compared with the state of the art, thanks to its unprecedented selectivity, simplicity and robustness.

Application potential of Osmodialysis

The major application potential of Osmodialysis is in the field of extraction and processing of crude oil and natural gas on the one hand, and in maritime or offshore transportation of oil on the other. The main applications of the clean separation of oil and salt water are expected to be

1. Treatment of produced waters, from which the oil or aromatics and other hydrocarbons must be separated as completely as possible

Figure 3 Oil and salt containing produced water before (left side) resp. after (center) Osmodialysis and oil fraction separated from it (right side).

2. Treatment of process waters, e.g. seawater used for cooling or rinsing in offshore production, or seepage or condensation waters contaminated with aromatics
3. Cleaning of contaminated seawater after tanker accidents, shipwrecks, pipeline leaks and well blowouts
4. Purification of bilge water of arriving ships in ports and purification of port water

Saline produced waters from deep wells for oil and gas production are a huge environmental and economic challenge internationally. Statistics showed a water-to-oil ratio (WOR) of 10:1 as early as 2012 (Produced Waters Society 2012). For the U.S. alone, which has a market share of approximately 13%, this translates to over 21 billion barrels of oil drilling wastewater per year. Most produced waters have higher salinity than seawater. With increasingly depleted and drying reservoirs, WOR will continue to rise, making treatment technologies increasingly urgent. Water online and Transparency Market Research projected the global volume of produced waters to increase to 340 billion barrels by 2020 (Transparency Market Research 2016). Many of these oily saline waters are not economically treatable today. Independent of the problem of residual oil content, the usually high water hardness leads to massive scaling of the plants. A large proportion of the water has to be sunk into depleted reservoirs at great logistical expense, which is becoming increasingly difficult as environmental standards rise. At the same time, however, the wells need water to stimulate the reservoirs and to cool and flush the drills. Fresh water here would lead to further leaching of the reservoir. So recycling the saline produced waters here has a huge economic impact, but requires technologies to remove oil and lime. The Colorado School of Mines estimates that treatment and handling of produced waters can account for more than 10% of the total oil price, depending on the reservoir. The two largest cost drivers for produced water treatment are energy consumption as the clear number 1, and in the number 2 position, the chemical costs of the chemical-physical treatment steps. These two points in particular, along with robustness and selectivity, represent the level of innovation and the unique selling point of Osmodialysis.

The clean separation of oil from seawater is also a standard problem worldwide, for which there is hardly any suitable technology. The chemical-physical processes that can be used onshore are hardly ever used for seawater because it is very complex and expensive. In addition, huge quantities of the above-mentioned process-relevant consumables would be needed in the event of an oil spill. In the past, therefore, an immediate but controversial measure was the use of chemical dispersants, which were spread on the oil spills by airplane and break down the oil into small droplets so that they are pressed under water and become more easily biodegradable. BP used 7 million liters of Corexit for this purpose after the Deepwater Horizon spill. In total, Deepwater Horizon spilled more than 500 million liters of oil into the sea. In 2018, BP put the total cost of the disaster at $65 billion for "cleanup and legal costs" (Reuters 2018). This equates to a cost of $130 per liter of crude oil in the sea. Since the disaster, there has been global awareness of the need for appropriate environmental technology. However, despite various research approaches, a robust separation technology still does not exist. Despite the lack of available offshore technology for large-volume, clean separation of oil from seawater, the requirements for re-injection of depleted

mixtures are strictly regulated. According to international environmental guidelines, a purity level of 99.9985 % would be required, i.e. a maximum residual oil content of 15 mg/L – a value that is unlikely to be achieved offshore with the state of the art (Spiegel 2010). Here, a pressureless membrane-based separation technology can finally provide a remedy. With Osmodialysis technology, seawater can be treated cleanly offshore in the future without the use of chemicals.

Conclusions

Fluvicon's Osmodialysis and Ionosmosis technologies open up the possibility of broad technical application of forward osmosis after decades of research. Osmodialysis as a simple process for the clean separation of oil and saltwater that can be applied on a large scale opens up great potential for economically viable solutions to ecological challenges in the oil and gas industry as well as in the oil transportation sector. fluvicon has laid the foundations for this through successful research and development and is now looking for pilot customers and cooperation partners for all types of application fields.

References

https://fluvicon.com/english/#video (April 2021)

Fuhrland, M., Griessler, T.: Ionosmose: Neue Grundlagentechnologie mit breitem Anwendungsspektrum, gwf Wasser/Abwasser issue 2/2021

OMV 2018: youtube.com/watch?v=MxWriQHSK04

Produced Water Society 2012: http://www.producedwatersociety.com

Transparency Market Research 2016: https://www.wateronline.com/doc/produced-water-treatment-systems-share-growth-trends-and-forecast-tmr-0001

Reuters 2016: https://www.reuters.com/article/us-bp-deepwaterhorizon-idUSKBN1F50NL

Spiegel 2010: https://www.spiegel.de/wissenschaft/natur/us-umweltkatastrophe-riesentanker-soll-oel-aus-dem-golf-saugen-a-704232.html

Challenges of Watershed Mine Drainage Characterisation and Remediation at Scale: Force Crag Base Metal Mine, Cumbria, UK

Catherine J. Gandy[1], Adam P. Jarvis[1], Nick Cox[2], Stephen Lofts[3], John Malley[4], Arabella M.L. Moorhouse-Parry[2], Katherine S. Neate[1], Barbara Palumbo-Roe[5], Hugh A.B. Potter[6]

[1]*School of Engineering, Devonshire Building, Newcastle University, Newcastle upon Tyne NE1 7RU, United Kingdom, catherine.gandy@newcastle.ac.uk, adam.jarvis@newcastle.ac.uk, k.neate2@newcastle.ac.uk*

[2]*The Coal Authority, 200 Lichfield Lane, Mansfield, Nottinghamshire NG18 4RG, United Kingdom, Nick-Cox@coal.gov.uk, AbbyMoorhouse@coal.gov.uk*

[3]*UK Centre for Ecology & Hydrology, Lancaster Environment Centre, Library Avenue, Bailrigg, Lancaster LA1 4AP, United Kingdom, stlo@ceh.ac.uk*

[4]*National Trust, Bowe Barn, Borrowdale Road, Keswick CA12 5UP, United Kingdom, john.malley@nationaltrust.org.uk*

[5]*British Geological Survey, Nicker Hill, Keyworth, Nottingham NG12 5GG, United Kingdom, bpal@bgs.ac.uk*

[6]*Environment Agency, Horizon House, Bristol BS1 5AH, United Kingdom, hugh.potter@environment-agency.gov.uk*

Abstract

The challenges of watershed mine drainage characterisation and remediation are reported. Whilst the substantial benefits of point source remediation under low flow conditions are demonstrated, the dominance of diffuse sources on instream zinc flux at higher flows limits the overall improvement in downstream water quality. A watershed approach to remediation is therefore required with consideration given to remediation of diffuse, as well as point, sources. The design and installation of infrastructure, such as flow-monitoring devices and boreholes, throughout the Force Crag mine watershed has enabled a comprehensive investigation of the nature and importance of the various pollution sources.

Keywords: Mine Drainage Characterisation, Remediation, Diffuse Sources, Zinc, Bacterial Sulfate Reduction

Introduction

Abandoned base metal mines are a major source of aquatic pollution in the UK contributing more than half of the mass flux of zinc and cadmium to freshwaters in England and Wales (Mayes *et al*. 2010). The majority of these mines are located in upland areas with steep topography which adds to the practical difficulties of executing mine water management at scale. Remediation efforts are typically targeted at point sources of pollution, such as abandoned mine entrances. However, diffuse inputs, such as runoff from mine waste heaps, remobilisation of metals from streambed sediment and the direct influx of groundwater, also contribute to the overall metal burden in receiving watercourses and have proven to be particularly important during higher flow conditions (Gozzard *et al*. 2011; Jarvis *et al*. 2019; Mighanetara *et al*. 2009). A watershed approach to remediation is therefore required to encompass both point and diffuse sources of pollution.

The UK's first full-scale passive treatment system for metal mine drainage was commissioned in 2014 at Force Crag, Cumbria, following 10 years of watershed mine drainage characterisation and system design. A synoptic mass balance approach to assessing point and diffuse sources of pollution (Runkel *et al.* 2016) identified the main point source of pollution to be remediated. The treatment system harnesses bacterial sulfate reduction to immobilise the main contaminant metals, zinc, lead and cadmium, within the compost substrate of two identical vertical flow ponds. The final discharge enters a nutrient-sensitive

upland river, the Coledale Beck. Appropriate infrastructure was designed and installed to allow close control and monitoring of flow-rate and water quality within the treatment system, including in the receiving watercourse to enable the benefits of treatment to be quantified. Additional infrastructure, such as boreholes, has recently been installed to enable an assessment of groundwater-surface water interactions and gain an understanding of the influence of riparian subsurface flows on metal flux.

This paper outlines the approach taken to characterise mine drainage within this watershed to enable design of an appropriate remediation system and evaluates the performance of the system in terms of its benefits to the receiving watercourse under varying hydrological conditions. Ongoing research to identify important diffuse sources of pollution is also discussed.

Methods

The synoptic mass balance approach to assessing point and diffuse sources of pollution involves synchronous measurements of flow-rate and water quality at both point sources and instream locations. Such monitoring was carried out on 14 occasions prior to treatment system commissioning and encompassed the full range of hydrological conditions. Instream locations were chosen upstream and downstream of both point sources and suspected diffuse sources. A suite of flow monitoring infrastructure, including flat V-weirs and sharp crested V-notch weirs, has been installed in the Coledale Beck catchment. Flow monitoring was undertaken at additional locations using salt gulp-injection dilution gauging. Further synoptic monitoring has been undertaken on 7 occasions since treatment system commissioning in addition to approximately fortnightly monitoring of the treatment system. This included measuring influent and effluent concentrations and flow-rates together with water quality and flow-rate of the Coledale Beck downstream of the treatment system.

Water samples were collected in 30 mL polypropylene bottles with those for subsequent metals analysis acidified with 1% v/v concentrated nitric acid. Samples for filtered metals analysis were filtered through a 0.45 µm cellulose nitrate filter. All samples were stored at 4 °C prior to analysis. Total and filtered metals analysis was undertaken using a Varian Vista-MPX ICP-OES or Agilent 770 Series ICP-MS. Anions analysis was conducted using a Dionex DX320 ion chromatograph. Field measurements of pH, temperature, ORP and electrical conductivity were made on site using a pre-calibrated Myron L 6P Ultrameter. Total alkalinity was determined at the time of sample collection using a Hach Digital Titrator with 1.6N sulphuric acid or 0.16N sulphuric acid with a Bromcresol-Green Methyl-Red indicator.

Results and Discussion

Synoptic monitoring identified the Level 1 discharge as the main point source of pollution to the Coledale Beck. Zinc is the principal contaminant metal of concern (mean total 3,129 µg/L) but lead (mean total 38.3 µg/L) and cadmium (mean total 15.1 µg/L) are also present at elevated concentrations. During low flow conditions, Level 1 accounts for the majority of the zinc in the Coledale Beck downstream of the mine site (fig. 1). However, as the Coledale Beck flow-rate increases, the instream zinc flux also increases sharply (fig. 1) and this increase is not accounted for by the Level 1 point source alone. Under the highest flow conditions monitored (670 L/s), total zinc flux in the Coledale Beck reached 14 kg/day, with Level 1 representing only 26% of this total (3.65 kg/day). Although other, minor, point sources contribute to the increased zinc flux it is diffuse sources of zinc that dominate the instream zinc flux in the Coledale Beck as flow-rate increases (Jarvis *et al*. 2019).

Despite the increased contribution of other point and diffuse sources of zinc with increasing flow in the Coledale Beck, the Level 1 discharge remains the single greatest point source contributor to instream zinc flux under all flow conditions and was therefore selected for remediation. In a combined initiative between the Coal Authority, Environment Agency, National Trust (the landowner) and Newcastle University, the UK's first full-scale passive treatment system for metal mine

drainage was commissioned in 2014 to treat the Level 1 discharge. Passive systems are the preferred option in the UK due to the remote upland settings in which abandoned metal mine discharges are typically located, which make active treatment logistically difficult. Another key requirement is to keep treatment system size to a minimum due to land constraints. The treatment system at Force Crag comprises two downwards flow Vertical Flow Ponds (VFPs) which operate in parallel. The design flow rate of the system is 6 L/s, with each VFP receiving 3 L/s from the Level 1 discharge. At the base of each VFP is a perforated pipe network which is overlain by a 200 mm layer of carboniferous limestone to maintain permeability. Overlying the limestone is a 450 mm layer of compost substrate comprising 45% v/v PAS100 compost, 45% v/v woodchips, and 10% v/v dried activated sewage sludge. The compost provides a long-term source of carbon and encourages the development of anoxic conditions, essential for survival of the sulphate reducing bacteria. The woodchips, meanwhile, assist with provision of porosity while the activated sewage sludge acts as an initial source of available carbon for metabolism of the sulphate reducing bacteria. The effluent waters from each VFP pass through a small aerobic wetland before discharging into the Coledale Beck. The remaining Level 1 water discharges, untreated, directly into the Coledale Beck. Whilst most compost bioreactors reported in literature have hydraulic residence times on the order of days, based on laboratory-scale (Mayes *et al.* 2011) and pilot-scale (Gandy *et al.* 2016) investigations the treatment system at Force Crag was designed to have a hydraulic residence time of 15 to 20 hours.

The treatment system has been successful in reducing the influent total zinc concentration from a mean of 3,129 µg/L to a mean of 279 µg/L (mean zinc removal of 90.4%) (Table 1). Other metals, such as lead and cadmium, are also successfully removed with mean treatment efficiencies in excess of 90% (Table 1). Variations in system performance, resulting in low treatment efficiencies at times, were due to operational changes. Similarly, a decrease in sulfate concentration observed between the influent (mean 26.6 mg/L) and effluent (mean 16.5 mg/L) indicates that bacterial sulfate reduction is an important removal mechanism within the treatment system.

Simultaneous monitoring of the treatment system and the Coledale Beck downstream of Force Crag mine over a wide range of hydrological conditions has enabled an assessment of the overall benefits of the treatment system to the Coledale Beck. A substantial improvement in downstream

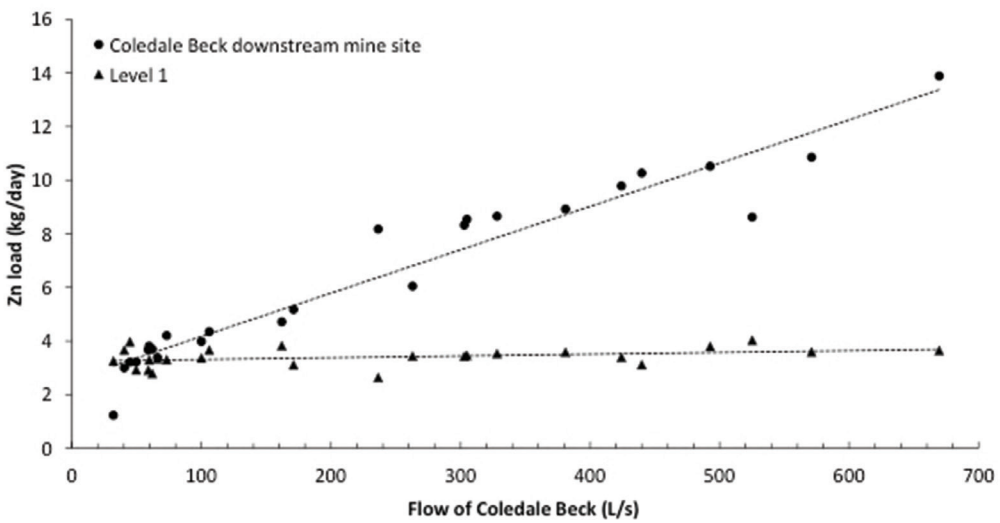

Figure 1 *Zinc flux in the Level 1 discharge and the Coledale Beck downstream of the mine site prior to remediation.*

Table 1 Mean influent and effluent total concentrations, and treatment efficiency, of zinc, lead and cadmium in the Force Crag treatment system. The range of values is given in parentheses.

Parameter	Zn	Pb	Cd
Influent concentration (µg/L)	3,129 (1,253-4,490)	38.3 (10.6-151.9)	15.1 (6.3-21.5)
Effluent concentration (µg/L)	279.2 (17.0-1,460.9)	3.67 (0.31-15.0)	1.25 (0.10-5.20)
Treatment efficiency (%)	90.4 (43.6-99.5)	91.0 (57.4-99.6)	90.6 (55.2-99.4)

water quality has been observed under low flow conditions (< 270 L/s) with total zinc concentration reduced from a pre-treatment system maximum of 860 µg/L to below 600 µg/L (Fig. 2). At higher flows, however, the benefits are limited. This is partly due to additional Level 1 water entering the Coledale Beck under such flow conditions since the treatment system only treats 6 L/s of Level 1 water with the remaining Level 1 water (up to 25 L/s) entering the Coledale Beck untreated. Consequently, at higher flows, the contribution of the Level 1 discharge to the instream zinc concentration increases. However, as demonstrated by Jarvis *et al.* (2019), and shown in Fig. 1, additional, diffuse, sources of zinc dominate the instream zinc flux under higher flow conditions. These findings have serious implications for watershed management since, despite the substantial environmental benefits of remediating the Level 1 discharge under low flow conditions, diffuse inputs of zinc limit the benefits of remediation at higher flows. To reduce the absolute flux of metals downstream, therefore, remedial efforts must also focus on diffuse sources.

Current research, in partnership with the British Geological Survey and UK Centre for Ecology and Hydrology, is investigating the influence and nature of groundwater-surface water interaction to the overall metal flux in the Coledale Beck. Further synoptic mass balance monitoring has been undertaken with a more intensive focus on an approximately 400 m reach to investigate the influence of riparian and hyporheic flows. Previous catchment-scale synoptic monitoring identified significant discrepancies between the sum of the point source zinc inputs and the

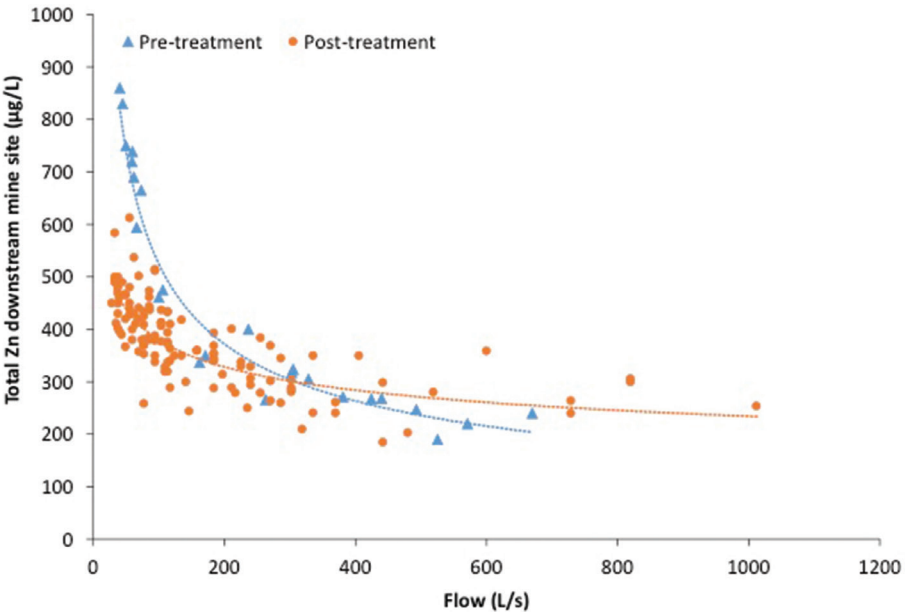

Figure 2 Zinc concentration in the Coledale Beck downstream of the mine site before and after remediation. The Environmental Quality Standard (EQS) for filtered zinc downstream of the mine is 12.3 ug/L and so the Coledale Beck is significantly polluted.

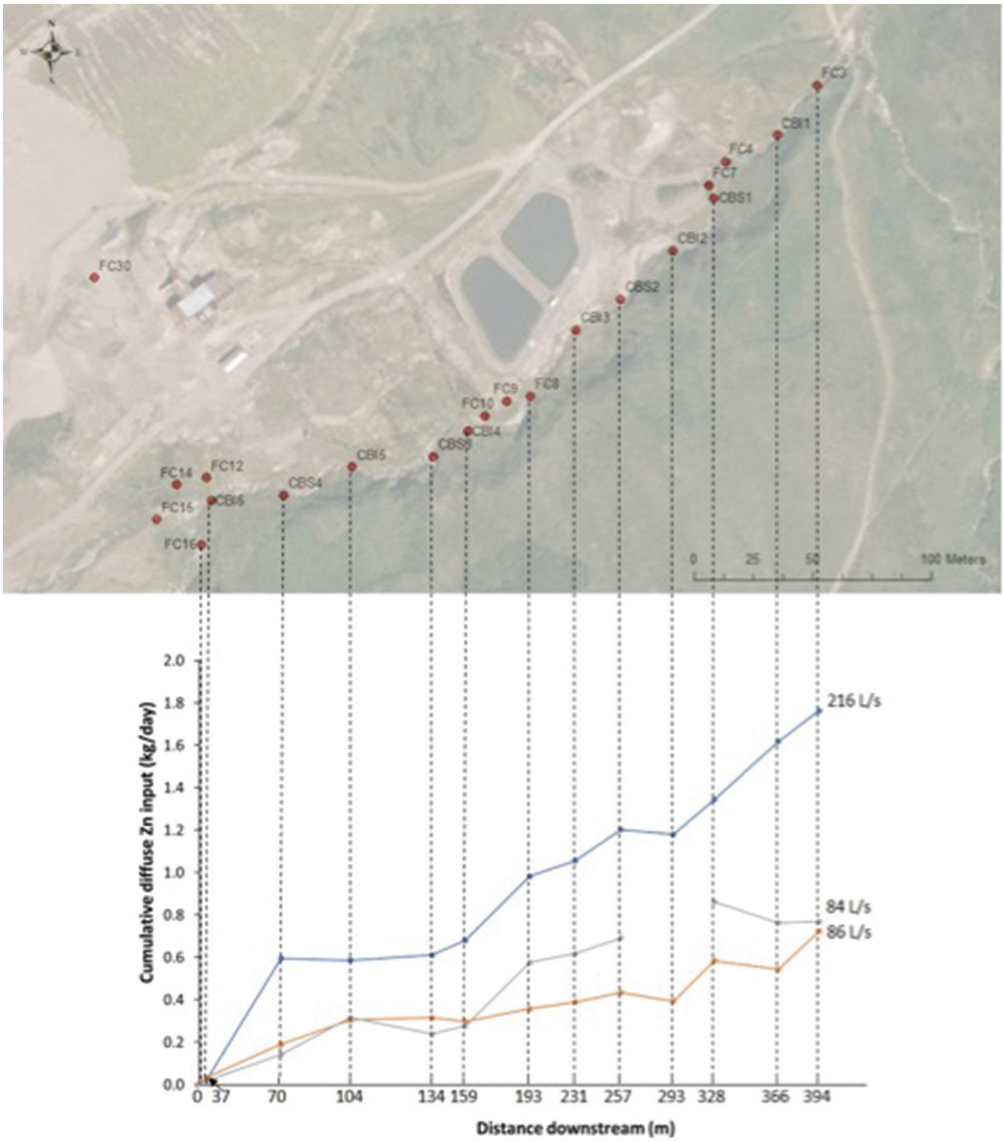

Figure 3 *Cumulative diffuse zinc input to the Coledale Beck over a 400 m reach during intensive synoptic mass balance monitoring. The flow-rates shown are for the most downstream monitoring point on the Coledale Beck.*

overall zinc flux within this reach, particularly under higher flow conditions. Intensive synoptic monitoring, encompassing a total of 13 instream locations, 6 point source inputs and a tributary, has been undertaken on 3 occasions. Diffuse zinc input is defined as the difference between (1) the sum of the upstream zinc flux plus any point source zinc fluxes within each stream reach and (2) the instream zinc flux at the downstream location of that reach. The cumulative diffuse zinc input is the sum of these reach-scale diffuse inputs from upstream to downstream. As shown in Fig. 3, the cumulative diffuse zinc input increases downstream under both flow conditions monitored but the rate of increase is greater at higher flows. Under low flow conditions (86 L/s,) the total diffuse zinc flux over the 400 m reach was 0.7 kg/day whilst under higher flow conditions (216 L/s) it

Figure 4 *Location of boreholes installed in riparian zones and mine spoil.*

was 1.8 kg/day. Such intensive monitoring enabled the identification of several stream reaches over which a marked increase in diffuse zinc flux occurred, under both flow conditions, and this informed site selection for the installation of boreholes in the riparian zones (Fig. 4).

Conclusions

This work demonstrates the need for a watershed approach to mine water management. The Coledale Beck catchment is one of the best instrumented catchments in the UK with the installation of flow-gauging infrastructure enabling accurate monitoring of flow-rates in the main river channel, tributaries and point sources. Synoptic mass balance monitoring using this infrastructure identified the main point source of pollution and informed design of the UK's first full-scale passive treatment system for metal mine drainage. Whilst the benefits of remediating point sources are clearly evident at low flow, diffuse sources of pollution limit the overall benefits at higher flows. Ongoing research aims to identify these diffuse sources with further infrastructure such as boreholes recently installed to assess groundwater-surface water interactions and gain an understanding of the influence of riparian subsurface flows on metal flux. The techniques employed at Force Crag are applicable to other base metal mines in the UK and internationally.

Acknowledgements

The research was funded by the UK Government Department for Environment, Food & Rural Affairs and Environment Agency (Project No. SC090024/1) and the UK Coal Authority. We are grateful for the assistance of Mr Patrick Orme and Ms Jane Davis with fieldwork and laboratory work and to the National Trust for site access. The views expressed are those of the authors and not necessarily those of the Coal Authority, Environment Agency or National Trust.

References

Gandy CJ, Davis JE, Orme PHA, Potter HAB, Jarvis AP (2016) Metal removal mechanisms in a short hydraulic residence time subsurface flow compost wetland for mine drainage treatment. Ecological Engineering 97:179-185

Gozzard E, Mayes WM, Potter HAB, Jarvis AP (2011) Seasonal and spatial variation of diffuse (non-point) source zinc pollution in a historically metal mined river catchment, UK. Environ. Pollut. 159:3113-3122

Jarvis AP, Davis JE, Orme PHA, Potter HAB, Gandy CJ (2019) Predicting the benefits of mine water treatment under varying hydrological conditions using a synoptic mass balance approach. Environ. Sci. Technol. 53(2):702-709

Mayes WM, Davis JE, Silva V, Jarvis AP (2011) Treatment of zinc-rich acid mine water in low residence time bioreactors incorporating waste shells and methanol dosing. Journal of Hazardous Materials 193:279-287

Mayes WM, Potter HAB, Jarvis AP (2010) Inventory of aquatic contaminant flux arising from historical metal mining in England and Wales. Science of the Total Environment 408(17):3576-3583

Mighanetara K, Braungardt CB, Rieuwerts JS, Azizi F (2009) Contaminant fluxes from point and diffuse sources from abandoned mines in the River Tamar catchment, UK. J. Geochem. Explor. 100(2-3):116-124

Runkel RL, Kimball BA, Nimick DA, Walton-Day K (2016) Effects of flow regime on metal concentrations and the attainment of water quality standards in a remediated stream reach, Butte, Montana. Environ. Sci. Technol. 50:12641-12649

Shear Behaviour of Compacted Gold Mine Tailings and Gold Mine Tailings Composite for Possible Use in Mine Backfilling

S.P. Gcasamba[1], K. Ramasenya[1], V.R.K. Vadapalli[1], S. Ekolu[1], S.M. Nyale[2]

[1]*Council for Geoscience, PVT Bag 112, Pretoria, 0001, sgcasamba@geoscience.org.za*

[2]*Department of Civil Engineering Science, University of Johannesburg, Auckland Park, South Africa, 2006*

Abstract

Utilisation of gold mine tailings (GMT) in mine reclamation requires a thorough understanding of its geotechnical characteristics. In this paper, a detailed experimental study carried on compacted gold mine tailings and gold mine tailings composite of varying curing ages is presented. Strength characteristics were investigated using consolidated drained (CD) and consolidated undrained (CU) triaxial tests under different confining pressures. The results obtained from the test showed that GMT composites exhibited higher strengths compared to untreated tailings. CD shear test revealed that GMT has a moderate capacity to withstand shear stress while the CU test showed an occurrence of static liquefaction.

Keywords: Gold Mine Tailings, Shear Strength, Box Shear Test, Triaxial Test

Introduction

For more than a century, South Africa's mining sector has played a pivotal role in the economic development of the country. Like many other mining jurisdictions, it is faced with a legacy of negative environmental and societal impacts. The severity of mining impacts on the environment and society has been observed in most areas where there are abandoned mines, with the most severe impacts noted in the eMalahleni coalfields and the Witwatersrand goldfields.

The Witwatersrand goldfields has over 270 gold mine tailings (GMT) covering an estimated area of 400 km^2 (AngloGold Ashanti 2004; Oelefse *et al.* 2009). A fraction of the tailings is beneficially utilised in mine backfilling, albeit in small quantities (Mashifana 2018; Van der Merwe *et al.* 2011). In the Witwatersrand goldfields, gold mining although not the only mineral resource mined is associated with several environmental issues, such as subsidence caused by underground voids, contamination of soils and water resources due to seepages from mine residue stockpiles and deposits (Sanmiquel *et al*. 2018). Given the prevailing environmental degradation in the Witwatersrand Basin, underground mine backfilling using mine waste was proposed as the most suitable rehabilitation method (Kleinhans and Van Rooy 2016).

Underground mine backfilling provides ground support and regional stability, thus reducing subsidence (Der Verleihung 2009; Potgieter 2003). Backfills can be classified as uncemented or cemented. Uncemented backfill materials include hydraulic fills, sand fills, aggregate fills and rock fills, whereas the most common cemented backfills are cemented paste fills, cemented hydraulic fills, and cemented rock fills (Sheshpari 2015; Sivakugan *et al.* 2015). Typically, backfills are prepared using waste rock, mill tailings, quarried rock, sand, and gravel. The most commonly used material is the waste rock and mill tailings due to their abundance in mining regions. Cemented backfills use low concentrations of cement (Lokhande 2005; Belem and Benzaazoua 2008), usually 3% to 7% in dry weight, which represents 50 to 75% of the backfill cost (Grice 2001).

The physical and chemical characteristics of the backfill are crucial in the selection of filling material and may influence the mechanical properties of a backfill (Hefni and Hassani 2020). Research into backfills has shown that cemented paste fills are the best option for backfilling due to their competitiveness and strength development.

In this study, the shear behaviour of GMT under laboratory conditions was assessed for use in cemented paste backfilling. The use of GMT in mine backfilling provides effective means of waste storage, resulting in the minimisation of environmental degradation.

Materials and experimental investigations

Representative GMT samples in a wet state were collected from a tailings storage facility on a gold mine in the Witwatersrand goldfields. The samples were obtained using an auger from a depth of 0.5 m to 5 m to ensure that the non-oxidised layer was represented. Representative samples of the GMT were prepared to form a homogenous sample. As part of sample preparation, the homogeneous sample was air dried at room temperature for 48 hours and a composite sample (GMT and cement) was generated to determine the shear strength characteristics.

Lafarge CEM II 52.5N (at 3%) and tap water were used in all mixes in the test series during the geotechnical testing protocol. The samples investigated were remoulded to 95% maximum dry density (MDD) and cured in moisture obtained during moulding over a 7, 28 and 56 days curing period at a room temperature of about 23 °C. The static strength characteristics of the sample were thoroughly studied using consolidated drained (CD) and consolidated undrained (CU) triaxial test with pore water measurements to determine strength characteristics. During the test series, all samples were tested under different confining pressures of 50, 100 and 200 kPa. The influence of various parameters on the shear strength characteristics was also noted.

Results and discussions

Strength characteristics are crucial for materials used for engineering construction. The strength properties of the materials are affected by variations in the density, particle size distribution and confining pressure. Consolidated drained (CD) and undrained triaxial tests were carried out under confining pressures of 50, 100 and 200 kPa on GMT. The test was performed as per ASTM D3080 to determine the shear strength characteristics of GMT. The samples were tested at a relative density of 2.209 to study their compaction behaviour. Mohr-Coulomb total strength parameters, namely, cohesion (c) and angle of shear resistance (φ) were determined.

Material characterisation

Important geotechnical properties like particle size distribution, atterberg limits, compaction characteristics, permeability and compression characteristics of the tailings were previously determined and are tabulated in Table 1 (Gcasamba *et al.* 2019). From the test results, it can be observed that the particle size of the tailings is medium to course size which is ideal for paste fills (Landriault 2001). Atterberg limits revealed that the tailings are non-plastic, which is an indication of soils with inherent shear resistance to sliding in fluvial conditions (Bartle 2000). The compaction characteristics of the tailings provide an opportunity to be used in mine backfilling. The coefficient of permeability showed permeability in a range of silt to sand soils. The tailings have a compressive strength within the recommended range between 200 kPa to 5000 kPa (Fall and Benzaazoua 2003).

Consolidated drained and consolidated undrained triaxial test results

Consolidated drained and undrained triaxial test results for GMT under different confining pressures are presented in Figures 1 and 2 respectively. During the test series, consolidation at all confining pressures took place rapidly and was completed in 5 minutes. The development of pore water pressure in the

Table 1 *Geotechnical properties of GMT and GMT composites (Gcasamba et al. 2019).*

	Particle size (mm)	Atterberg limits	Compaction (kg/m³)	Permeability (m/s)	Compression (kPa)
GMT	Sand to silt	Non plastic	1588	3.8E-07	129
GMT composites (7 days)	Silt to sand	Non plastic	1555	2.9E-07	315
GMT composites (28 days)	-	-	-	2.9E-07	386
GMT composites (56 days)	-	-	-	9.0E-07	412

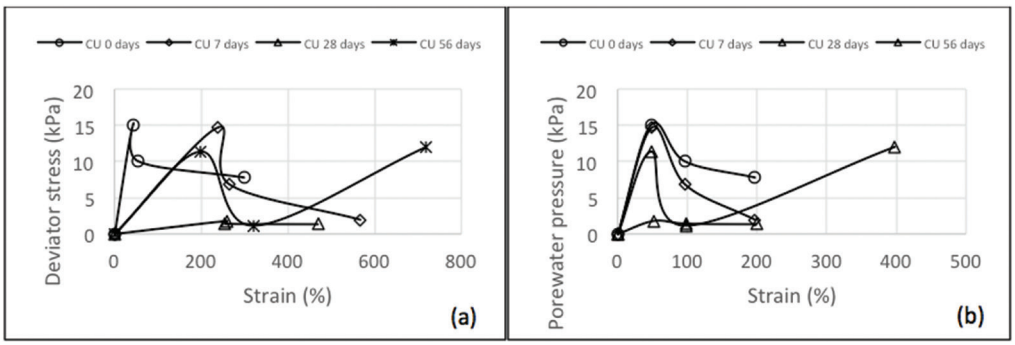

Figure 1 *Results of CD test: (a) Deviator stress vs. axial strain, (b) Pore water pressure vs. axial strain.*

tests shows a correlation with volume changes of the sample. Samples exhibiting contraction in the CD test series were observed to develop positive pore water pressures in the CU test series. Whereas samples exhibiting dilation in the CD test developed negative pore water pressure. The degree of negative pore water pressure was noted to decrease with increasing confining pressures, similarly, dilation decreased with increasing confining pressure. An increase in contraction was observed in CD tests with the increase in confining pressure and developments in pore water pressure increased with increasing confining pressure in the CU test. The development of liquefaction in CU tests was noted corresponding to the development of high pore water pressure and increased confining pressure.

It was observed that the axial strain at failure increases with an increase in confining pressure. It was also observed that the peak value for pore water pressure rise increases with an increase in confining pressure. The deviator stress attained peak value at an axial strain of 11.39, 4.57, 4.78 and 4.13 following a 0, 7, 28 and 56 days of curing for the CD test (figure 1a). At the axial strains of 15.5, 14.67, 1.8 and 12.03 a peak in deviator stress was obtained during the CU test following the different ages of curing; followed by a sharp decline due to static failure (Figure 2a).

The liquefaction behaviour noted during the CU test may be due to high variabilities of effective stress. Hakam (2016) noted the liquefaction susceptibility of soils. The author noted that soils under high effective stress, are easier to liquefy than soils under low effective stress. The same effect was noted during the CU test, liquefaction corresponded with the high effective stress.

Shear strength parameters in response to varying curing ages are presented in table 2. It was observed that the strength parameters corresponding to CD tests are comparable with the strength parameters from the CU tests except for cases where static liquefaction was observed.

At the initial stage (no cement and zero days of curing) of the shear test, the results

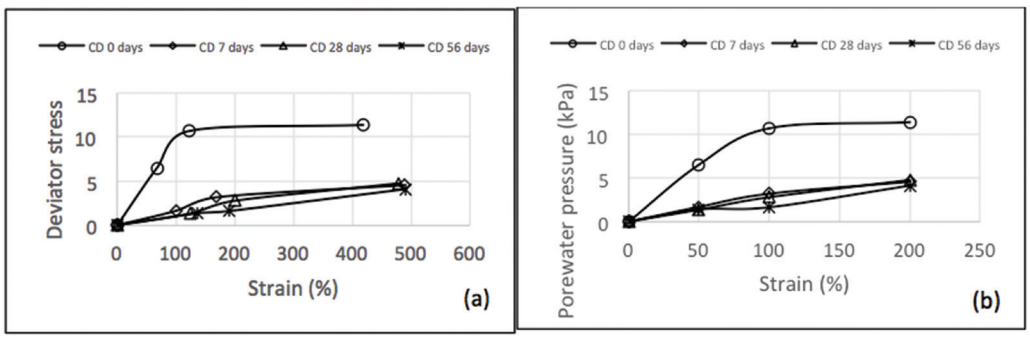

Figure 2 *Results of CU test: (a) Deviator stress vs. axial strain, (b) Pore water pressure vs. axial strain.*

revealed minimum values of the angle of internal friction (φ), recorded at 27° and 30° respectively for CD and CU tests. An increase in the angle of internal friction was noted until the 28 days of curing for CD tests followed by a slight decrease by the 56 days of curing. During the CU test, an increase in φ was noted until the seventh day. After the 28 and 56 days of curing, the angle of internal friction was recorded at 0° due to static failure. Based on the results, the effect of curing on the φ of the tailings was observed during the CD test whereas the effects of curing during CU tests was negligible.

Similarly to the angle of internal friction, values of cohesion were minimal at zero cement addition and curing and improved with increasing curing periods and cement addition for CD while the opposite was observed for CU tests, as noted by Uchaipichat and Limsiri (2011). An increase in cohesion was noted until the 56 days for the CD tests while an increase in cohesion during CU tests was observed until the 7 days of curing. Studies conducted by Moayed *et al.* (2011) corroborate the significance of cement on cohesion and the angle of internal friction. The authors noted the significant increase in these shear properties of soils with cement addition.

Conclusions

The results obtained from the consolidated drained shear test indicate that the tailings have a moderate capability to withstand shear stress and could be suitable for civil works. The CU test, however, showed an occurrence of static liquefaction indicating the possibility of liquefaction when used in civil works. Similarities in shear strength characteristics were observed during the previous shear tests conducted using box shear (Gcasamba *et al.* 2019) and the CD test. The shear box results showed improved shear strength characteristics with the age of curing and cement addition. The values of cohesion ranged from 8 to 42 and 12 to 107 respectively for the box shear test and CD test. Similarly, the angle of internal friction during both tests improved with the age of curing and cement addition. The shear strength results for both tests are an indication of a highly cohesive material. Contrary, the CU test showed minor effect of curing and cement addition, at 28 days of curing, static liquefaction was observed during the CU test series. These results are an indication that in a loose state, the undrained stress path will result in liquefaction, although in a dense state, liquefaction may be prevented due to the tendency of materials to dilate during drainage as a result of pore water pressure. Further studies on the liquefaction resistance of the tailings before utilisation, especially in earthquake-prone areas is necessary.

Acknowledgement

The authors would like to thank Council for Geoscience for funding the project.

Reference

AngloGold Ashanti (2004). Case studies: South Africa, Woodlands Project — Good progress being made with phytoremediation project. Environment – AngloGold Ashanti Report to Society: Johannesburg, South Africa.

Bartle H. (2000). What is soil plasticity? How does it allow you to prevent soil failures? B.C's Watershed Technical Bulletin.

Belem, T.; Benzaazoua, M. (2008). Design and Application of Underground Mine Paste Backfill Technology. Geotech. Geolog. Eng., 26, 147–174. DOI: 10.1007/s10706-007-9154-3.

Der Verleihung Tag (2009). Systematic selection and application of backfill in underground

Table 2 *Consolidated drained and undrained triaxial shear strength parameters.*

	State	CD test		CU test	
		Cohesion (kPa)	Angle of internal friction (°)	Cohesion (kPa)	Angle of internal friction (°)
GMT	Compacted	12	27	8	30
GMT composites (7 days)	Compacted	91	33	11	33
GMT composites (28 days)	Compacted	89	37	0	0
GMT composites (56 days)	Compacted	107	29	0	0

mines. Der Fakultät für Geowissenschaften, Geotechnik und Bergbau der Technischen Universität Bergakademie Freiberggenehmigte.

Fall, M.; Benzaazoua, M. (2003). A Model for Predicting the Performance of Underground Paste Backfill. Proceedings of Intern Conf. Was. Tech. and Man, 969–980.

Gcasamba. Sisanda Prudence; Ramasenya. Koena; Diop. Souleymane; Vadapalli, Viswanath Ravi Kumar; Ekolu, Stephen. (2019). Comparative study of two biggest mineral wastes in South Africa for mine reclamation: A geotechnical study. In Mine Water – Technological and Ecological Challenges; Khayrulina, E.; Wolkersdorfer, Ch.; Polyakova, S.; Bogush, A., Eds.; Perm State University: Perm, Russia; pp 77 – 83.

Grice, T. (2001). Recent mine fill developments in Australia. Proceedings of the 7th international symposium on mining with Backfill: Minefill'01, Seattle, USA, 351–357.

Hakam Abdul. (2016). Laboratory liquefaction test of sand based on grain size and relative density. J. Eng. Technol. Sci., Vol. 48, No. 3, 334-344.

Hefni, M.; Hassani, F. (2020). Experimental development of a novel mine backfill material: Foam mine fill. Minerals, 10, 1–16, doi:10.3390/min10060564.

Kleinhans, I.; Van Rooy, J.L. (2016). Guidelines for sinkhole and subsidence rehabilitation based on generic geological models of a dolomite environment on the East Rand, South Africa. J. African Earth Sci. 117, 86–101, doi:10.1016/j.jafrearsci.

Landriault, D. (2001). Backfill in Underground Mining. In Underground Mining Methods Engineering Fundamentals and International Case Studies, Hustrulid, W. A. Eds.; SME: Littleton, Colorado, 608–609.

Lokhnde R.D. and Singh K.B. (2005). Subsidence control measure in coal mines. Journal of Scientific & Industrial Research, 64, pp. 323–332.

Mashifana T.P. (2018). Beneficiation of Barberton gold mine tailings: the effect of fly ash on the mineralogy and micrograph. University of Johannesburg, Department of Chemical Engineering, South Africa.

Moayed, R. Z.; Samimifar, M.; Kamalzare, M. (2011). Improvement of Shear Strength Characteristics of Saline Soils Using Cement and Polymer. Int. J. Geotech. Eng. 5, 317–327. DOI: 10.3328/IJGE.2011.05.03.307-314.

Oelefse, O. H. H.; Hobbs, P. J.; Rascher, J.; Cobbing, J. E. (2009).The pollution and destruction threat of gold mining waste on the Witwatersrand – a West Rand case study, CSIR, Natural Resources and the Environment, Pretoria, South Africa.

Potgieter J.H. (2003). Fly ash research at Technikon of Pretoria, South Africa. Technikon of Pretoria.

Sanmiquel, L.; Bascompta, M.; Vintró, C.; Yubero, T. (2018). Subsidence management system for underground mining. Minerals; 8, doi:10.3390/min8060243.

Shespari M. (2015). A review of underground mine backfilling methods with emphasis on cemented paste backfill. Department of Civil Engineering, University of Ottawa, Ottawa ON, Canada, 20.

Sivakugan N., Veenstra R. and Naguleswaran N. (2015). Underground mine backfilling in Australia using paste fills and hydraulic fills. International Journal of Geosynthetics and Ground Engineering, 1(18).

Uchaipichat, A.; Limsiri, C. (2011). Shear Strength Characteristics of Cemented Loose Sands. Austr. J. Basic Appl. Sci. 5, 771–776.

Van de Merwe Elizabeth M., Prinsloo Linda C., Kruger Richard A. and Mathebula Lethabo C. (2011). Characterization of coal fly ash modified by sodium lauryl sulphate. World of Coal Ash (WOCA) Conference, Denver, USA.

Integrated Dynamic Mine Water Balance Modelling with EcoBalance Model Libraries

Kirsi-Marja Haanpää[1], Jacobus J. Van Blerk[2], Jacobus J.P. Vivier[3], Eric K. Howell[4], Rodolfo Avila[4]

[1]*AFRY, Elektroniikkatie 13, FI-90590 Oulu, Finland, kirsi-marja.haanpaa@afry.com*

[2]*AquiSim Consulting Pty Ltd, 109 Bosduif Crescent, Wierda Park, Centurion, South Africa, aquisim@netactive.co.za*

[3]*Artesium Consulting Services (Pty) Ltd, 249 Draaihals Street, Leeuwfontein Estates, South Africa, koosvivier@gmail.com*

[4]*AFRY, Frösundaleden 2A, SE-169 99 Stockholm, Sweden, eric.howell@afry.com, rodolfo.avila@afry.com*

Abstract

Integrated water balance modelling is a tool that assists in the critical mining industry task of water management planning. The process starts with conceptualisation, which includes identification and description of all relevant site water management structures and usually involves the introduction of simple water balance modelling spreadsheets. Irrespective of their complexity, these models are usually analytical and utilise a deterministic approach. For more flexible modelling and a better understanding of the water management scenarios, dynamic water balance models are applied. This paper presents how the Ecolego® software tool is used for integrated dynamic mine water balance modelling.

Keywords: Water Balance Modelling, Water Management, Dynamic Modelling, Ecobalance, Ecolego

Introduction

The diversity of mining projects has increased substantially over the past three decades. At the same time, there has been an emphasis on environmental issues, decontamination of former industrial sites, a recognition of global warming issues, and a focus on the ability of project developers to initiate, operate, and close transient projects without compromising the land and water resource values that underpin existing and future land uses (Hancock & Wolkersdorfer 2012). For mine sites, water balance modelling is the primary tool for water management planning. Water management challenges vary depending on mine geographical location, local environs, and mine operations. Notwithstanding, mine water management can be considered as a global challenge for the industry.

The probabilistic site water balance modelling approach has become increasingly common during the past fifteen years. Dynamic and probabilistic modelling approaches were introduced by Nalecki & Gowan in 2008. Today, the probabilistic site water balance modelling approach is generally accepted in the mining industry. The use of a solely probabilistic approach has, however, been disputed (Swanson *et al.* 2018) due to risk of over-engineering and a hybrid deterministic water balance modelling approach has been introduced.

Despite the modelling approach, a model is always an appendage of an expert on the field. As stated by Swanson *et al.* (2018), the modeller must understand the model's dynamics, including when and where the project is most vulnerable to extreme events, and why the vulnerability exists. To provide an advanced tool for deterministic, hybrid deterministic, or solely probabilistic site water balance modelling, this paper describes how the Ecolego® software tool could work as an appendage of a site water management modelling professional.

Ecolego® Software Tool

Ecolego® (https://www.ecolego.se/) is a powerful and flexible software tool for creating dynamic and complex process models and performing deterministic or probabilistic simulations. Ecolego® has primarily been used for conducting risk assessments of complex dynamic systems evolving over time, with specialised databases and other add-ons designed for the field of radiological risk assessment. However, Ecolego® is easily adapted to various other applications, e.g., transport of chemicals and elements from emission to biota uptake, water balance simulation in mining industry (EcoBalance), or contaminated land simulation, using its compartmental modelling approach. Ecolego® is designed with re-usability and quality assurance as a primary focus, which leads to better models and less work for the user. Libraries of model components are easily created and modified. Ecolego® includes a parameter database with an integrated system for data tracking and quality assurance. Ecolego Player allows a reviewer to browse the model, inspect equations, and re-run simulations.

Ecolego® interface is comprised of an interaction matrix view that makes complex models easier to organize and view, a model graph view that presents the model conceptually, and a relationship graph view where interactions between objects can be established and manipulated. Ecolego® possesses all requirements for advanced probabilistic analysis, including probability density functions, Monte Carlo and Latin Hypercube sampling, and parameter correlation settings. In addition, Ecolego® features a powerful and simple-to-use library of models where specific model components can be stored and later inserted into other analyses.

The EcoBalance Model

Introduction

The objective of the integrated dynamic mine water balance systems model is to inform the planning, design and management of mine water and mass load throughout the mining life cycle. Of specific importance is to identify the water demand in the different sections of the mine, as well as the containment reservoir requirements for contaminated mine water storage and re-use. The integrated system approach allows for environmental value engineering by means of risk-cost-benefit optimisation.

EcoBalance

EcoBalance is a dynamic and integrated mine water balance system-level model within Ecolego® that is used to analyse mine water systems for the purposes of mine planning, design, optimization and value engineering throughout the mining life cycle. Some

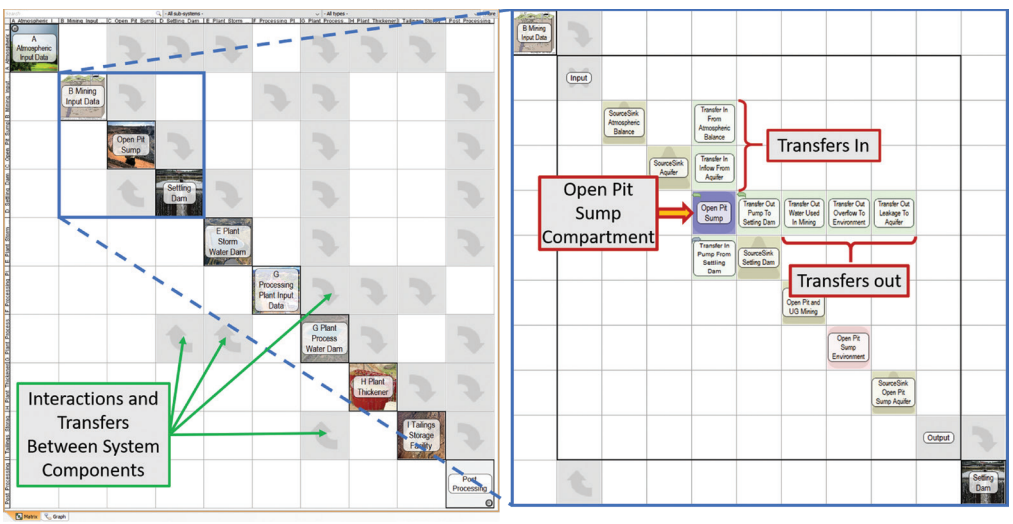

Figure 1 *EcoBalance Compartmental Systems Modelling Approach.*

of the inherent Ecolego® features makes it particularly attractive for integrated dynamic mine water balance modelling. EcoBalance adopted the interaction matrix together with the compartmental systems modelling approach embedded in Ecolego® to represent the transient transfer of water through the natural and mining environment, as well as within each compartment (fig. 1).

The possibility to develop and incorporate predefined libraries of typical mining components that are easily adaptable for the water fluxes and balances for the mining environment, is of particular advantage. As illustrated below, this means that typical mining components (e.g., open pit, settling dam, storm water dam, or tailings storage facility) can be defined as an available Block in the Library Folder. Each of these Blocks contain typical features and parameter values that can be altered to the project specific conditions (fig. 2).

By combining these predefined and validated libraries, it is possible to create integrated mine water balance models that can be used for performing deterministic and probabilistic simulations. The optimisation routine embedded to Ecolego® can be used to optimise the design of system features and operational conditions (e.g., pumping rates). A specific advantage of EcoBalance is that the component libraries automatically link inputs and outputs and check the component and total system balances. Using the library collection, EcoBalance allows for easy construction of a site-specific and integrated dynamic mine water balance. This feature allows for a considerable time-, and subsequently, cost-saving factor while managing balance errors in complex systems.

The user interface visualisation utilises an interaction matrix approach that makes complicated models with many interconnections easier to view and manage

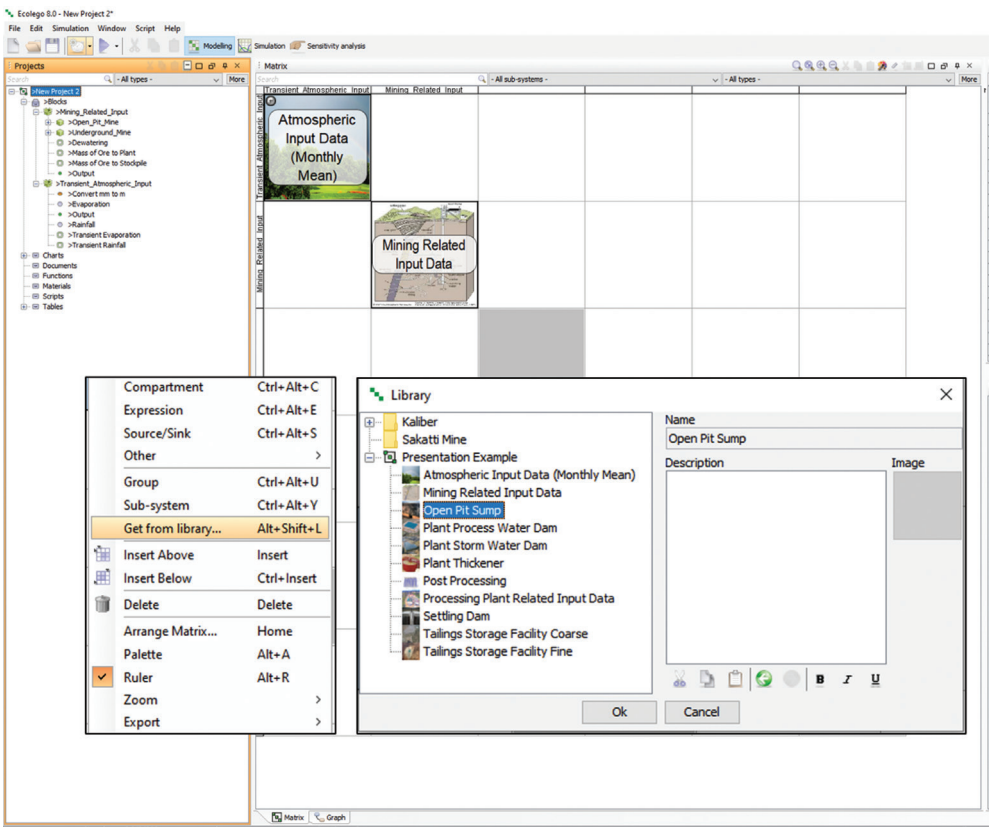

Figure 2 *Predefined Blocks of Typical Mining Features Can Be Imported into a New Project from the Library Folder.*

(fig. 3). Combined with hierarchical sub-systems, the user interface facilitates the ease of construction and documentation of large complex models. A model graph option as an alternative to the interaction matrix presents the system in a conceptually intuitive way. Salt and chemical constituent mass load and transport modelling are also allowed as an integrated and dynamic linked option.

EcoBalance Implementation to A Real-Life Mining Environment

EcoBalance has been applied to diverse mining environments, including the Keliber mine (Keliber Technology Oy) in Finland for a site wide water and loading balance modelling. As a further example, below is visual representation of the mine water balance flow main components and interactions diagram for a mine in Southern Africa where EcoBalance was implemented and applied for site wide water balance modelling (fig. 4). The model could be applied to an integrated open pit and underground linked project. The modelling scenarios were used to inform storm water design criteria and quantify surplus water volumes and the life of mine water quality as chemical constituent concentrations. Based on both flow and mass modelling, mine water containment reservoirs and transfer pumping capacities could be informed to identify value engineering opportunities as potentials of capital expenditure reduction and postponement.

For illustrative purposes, examples of important life of mine dynamic modelling outcomes produced from EcoBalance, amongst many other informative transient analyses, include e.g. mine external make-up water demand curve (fig. 5) and overflows to the environment as timing of events and volumes (fig. 6).

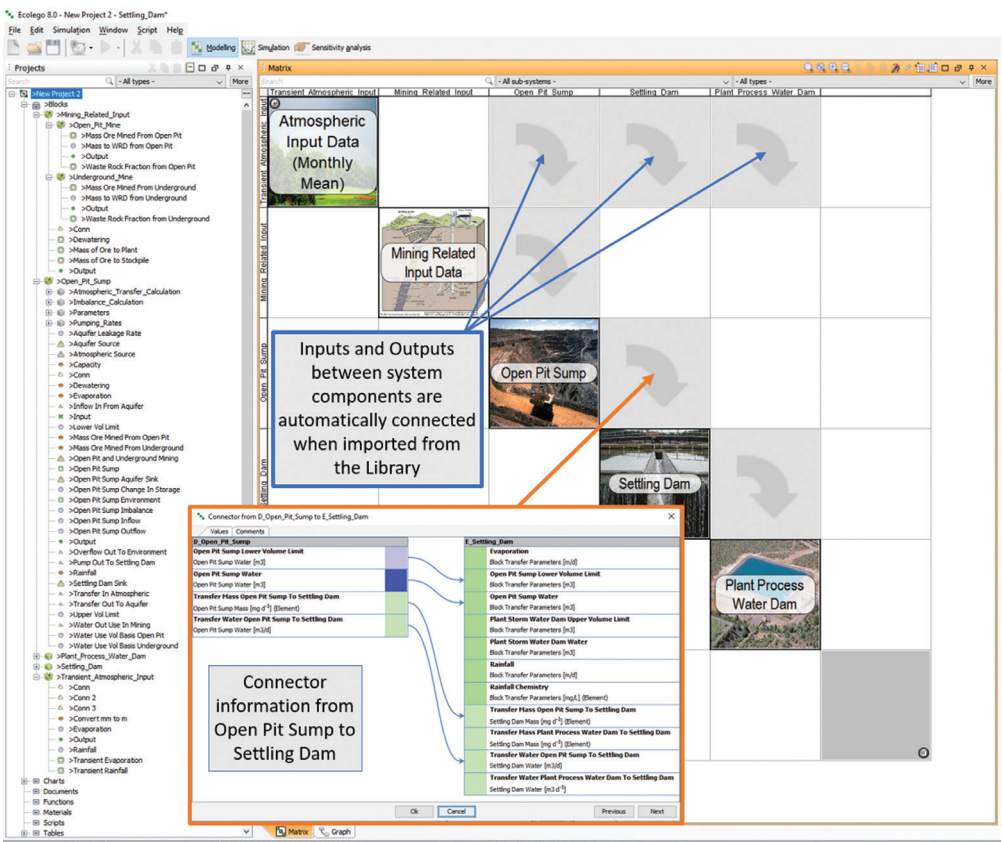

Figure 3 *EcoBalance Visualization of an Interaction Matrix.*

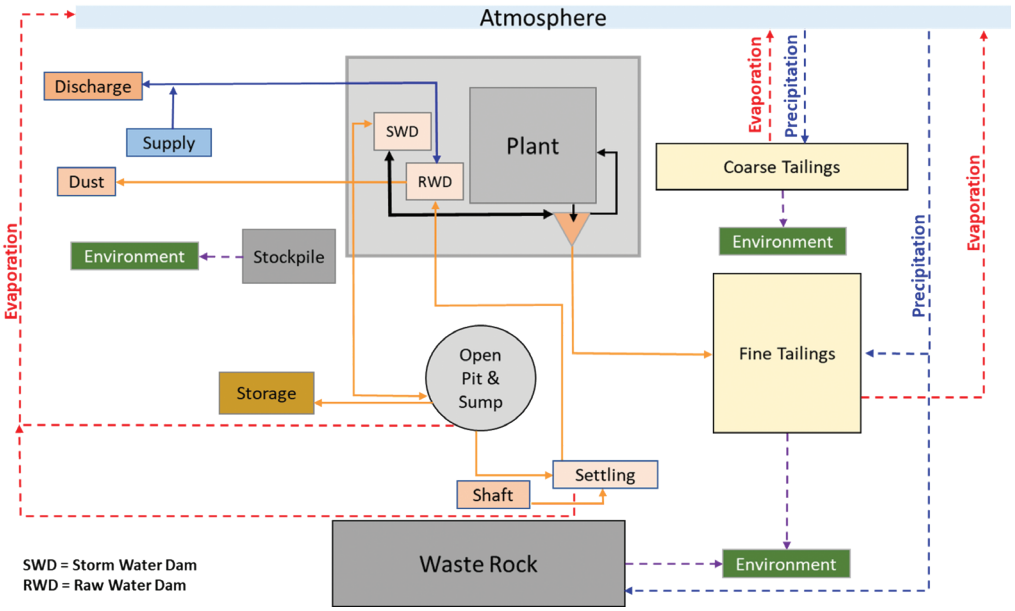

Figure 4 EcoBalance Case Example Water Flow Main Components.

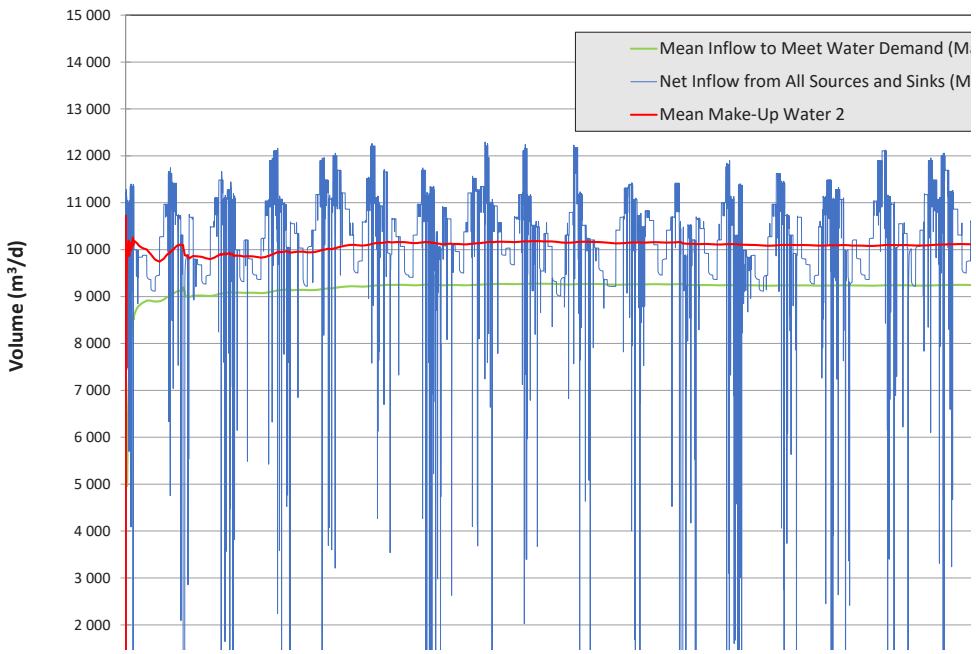

Figure 5 EcoBalance Example: Mine External Make-Up Water Demand Curve.

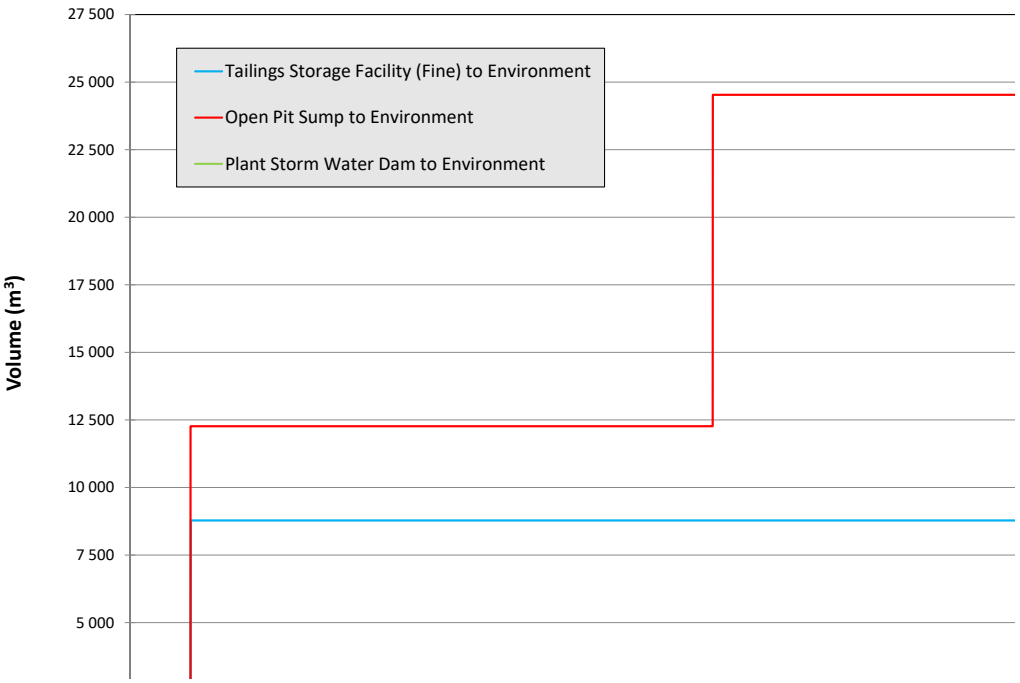

Figure 6 *EcoBalance Example: Overflows to the Environment, Timing of Events and Volumes.*

Conclusions

Integrated water balance modelling is a tool that assists in the critical mining industry task of water management planning. EcoBalance is a dynamic and integrated mine water balance system-level model within Ecolego® that is used to analyse mine water systems for the purposes of mine planning, design, optimisation and value engineering throughout the mining life cycle. Some of the inherent Ecolego® features makes it particularly attractive for integrated dynamic mine water balance modelling. Using the library collection, EcoBalance allows for easy construction of a site-specific and integrated dynamic mine water balance. This feature allows for considerable time-saving, and subsequently, cost-saving factor while managing balance errors in complex systems. A specific advantage is that the component libraries automatically link inputs and outputs and check the component and total system balances. Salt and metal transport modelling are also allowed as an integrated possibility. The user interface visualisation utilises an interaction matrix that makes complicated models with many interconnections easier to view and manage, whereas the model graph presents the system in a conceptually intuitive way. Combined with hierarchical sub-systems, the user interface and large library of models facilitates the ease of construction and documentation of large complex model systems.

Acknowledgements

The authors thank co-workers and collaborators who have given input to this work.

References

Hancock S, Wolkersdorfer C (2012) Renewed Demands for Mine Water Management. In: Mine Water and the Environment, June 2012, DOI: 10.1007/s10230-012-0176-6

Nalecki P, Gowan M (2008) Mine Water Management – Dynamic, Probabilistic Modelling Approach. In: Rapatnova N, Hrkal Z, 2008 Mine Water and the Environment, Ostrava (VSB – Technical University of Ostrava), p 469-472

Swanson S, Breckenridge L, Leduc M (2018) Mine Water Balances – A New Proposed Approach. In: Drebenstedt C, Paul M, IMWA 2016 – Mining Meets Water – Conflicts and Solutions, Freiberg/Germany (TU Bergakademie Freiberg), p 528 – 534

A Comparison of Be and W in Mine Drainage Downstream Two Different Repositories Storing Tailings from a Skarn Ore

Re-mining as an alternative remediation method

Lina Hällström, Lena Alakangas

Applied Geochemistry, Luleå University of Technology, 97187 Lulea, Sweden, lina.hallstrom@ltu.se

Abstract

The geochemical behaviour of beryllium (Be) and tungsten (W) in neutral mine drainage (NMD) downstream of two skarn tailings repositories (Smaltjärnen and Morkulltjärnen) was studied. Surface water was sampled monthly during 2018, with epilithic water diatoms used as bioindicators. Smaltjärnen (1918–1963) has been open to the atmosphere for over 30 years, while Morkulltjärnen (1969–1989) was covered and water-saturated directly after closure. NMD with high concentrations of dissolved Be from Smaltjärnen and dissolved W from Morkulltjärnen had negative environmental impacts as far as 5 km from the Yxsjöberg mine site. Re-mining could be a potential remediation method.

Keywords: Neutral Mine Drainage, Tungsten, Beryllium, Tailings, Re-mining, Remediation

Introduction

To ensure a sustainable mine waste and water management in the future, further geochemical knowledge regarding several high-tech critical elements is needed (Filella and Rodriquez-Murillo, 2017). Thus, the demand of beryllium (Be) and tungsten (W) in society are expected to increase due to their incorporation in green technology (European Comission, 2020). Consequently, there is a risk that the geochemical cycles of these elements in the environment will change as mining increases to meet industrial demand (Nuss and Blengini, 2018). At present, the speciation, mobility, transport and fate of Be and W from mine waste to the terrestrial environment is poorly studied although both are considered potentially harmful elements (Strigul *et al*., 2009; Taylor *et al*., 2003). Research regarding environmental problems related to mine drainage has mainly focused on acid mine drainage (AMD). As such, there is insufficient knowledge about the mobility and ecotoxicity of metals, including Be and W, in Neutral Mine Drainage (NMD). Understanding the geochemical behaviour of Be and W is important since a lack of knowledge can result in the implementation of inappropriate preventative measures for mineral weathering during the commissioning phase of mine closure, potentially increasing the extent to which these elements are released to the environment.

Skarn ores can be enriched in both Be and W, which may end up in the tailings due to inefficient extraction techniques. Furthermore, skarn tailings can contain high concentrations of carbonates and generate neutral mine drainage (NMD) (Kwak, 2012). This makes historical skarn tailings enriched in Be and W an ideal setting to study, to increase the knowledge regarding the geochemical behaviour and impact of mine drainage on the downstream water quality and ecosystems. In this study, mine drainage downstream of two tailings repositories (Smaltjärnen and Morkulltjärnen) from the same skarn ore were compared with respect to: 1) Be and W concentrations; 2) Be and W distribution between dissolved and particulate fractions; and 3) the mine drainage impact on epilithic water diatoms. Epilithic water diatoms can be used as a first bioindicator for discerning negative environmental impacts downstream of mine tailings (CEN, 2004b).

Furthermore, the feasibility of using re-mining as a potential remediation method was investigated for the Smaltjärnen tailings. Thus,

re-mining historical and environmentally hazardous tailings enriched in Be and W could be used as a remediation method for decreasing adverse impacts to the surrounding environment, as well as supporting the domestic production of these critical metals (Hällström *et al.*, 2018).

Study site

The skarn tailings stored in the Smaltjärnen and Morkulltjärnen repositories originate from the former W, Cu and CaF_2 mine in Yxsjöberg, Sweden (Fig. 1). The Smaltjärnen repository was used between 1918–1963, and the tailings have been stored open to the atmosphere for more than 30 years. Previous studies have shown that the Smaltjärnen tailings are enriched in Be (284 mg/kg) and W (960 kg/mg), together with pyrrhotite (2 wt%), calcite (6 wt%), and fluorite (4%) (Hällström *et al.*, 2018). Beryllium is mainly hosted by the unusual mineral danalite ($Fe_4Be_3(SiO_4)_3S$) (Hällström *et al.*, 2020b), while W is found in scheelite ($CaWO_4$) (Hällström *et al.*, 2020a,b). Tailings generated between 1969–1989 were stored in Morkulltjärnens repository. The Morkulltjärnen impoundment was covered and water-saturated directly after closure. Mine water from Smaltjärnen drains into the Pumpbäcken stream, while the Morkulltjärnen tailings drain into the Nittälven River. The Pumpbäcken and Nittälven merge south of the Yxsjöberg mine site (Fig.1).

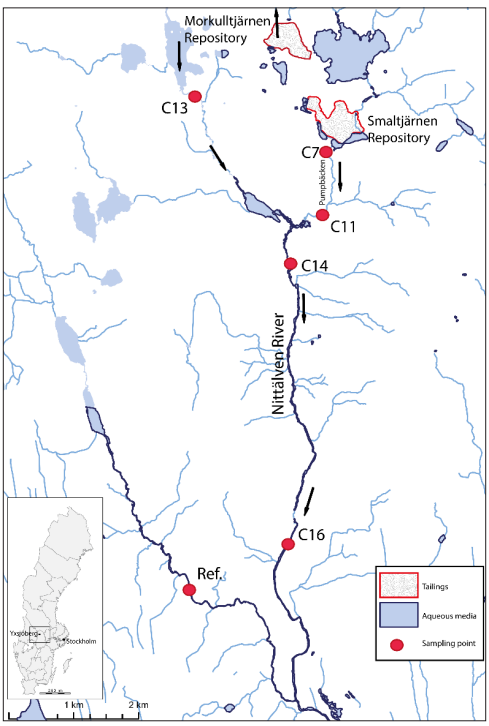

Figure 1 Catchment areas of the Morkulltjärnen (1) and Smaltjärnen (2) repositories, along with sampling locations downstream of the Yxsjöberg mining area.

Methods

Surface water was sampled at five sampling points downstream of the Smaltjärnen and Morkulltjärnen repositories, as well as at one reference point (Ref) (Fig. 1).

The pH, electrical conductivity (EC) and temperature were measured in the surface water. A pHenomenal MU 6100H multi-parameter meter equipped with a pHenomenal 111 electrode (662–1157; VWR International, Radnor, PA) was used for the pH measurements. The surface water was pumped through Geotech polycarbonate and acrylic filter holders (Geotech Environmental Equipment Inc., Denver, CO) with a diameter of 142 mm. The filters (0.22 µm cellulose acetate membrane filters) were pre-washed with 5% acetic acid for 72 h and rinsed with MilliQ water for 24 h. Screening analyses (71 elements) of the filtered surface water (dissolved phase) were carried out by ALS Scandinavia (ALS Scandinavia, Luleå, Sweden) using an inductively coupled plasma sector field mass spectrometer (ICP-SFMS). The utilised method was validated with the certified reference materials SLEW-2, CASS- 2 and NASS-4 for all elements analysed by ALS Scandinavia (Rodushkin & Ruth, 1997). Total and dissolved F, SO_4 and Cl were analysed by ion chromatography (CSN ISO 10304-1, CSN EN 16192). Duplicates of each sampling batch were carried out to control the reproducibility of the screening analysis. Blanks and standards were used for quality control. The filters used for surface water filtration were analysed for the particulate phase according to the same procedure as the dissolved phase at ALS Scandinavia after lithium metaborate and HNO_3/HF/HCl digestion.

Epilithic water diatoms were sampled from the Nittälven and Pumpbäcken at sampling points C7, C11, C13, C14 and Ref. in October 2018. The sampling procedure was carried out according to the European/Swedish standard protocol (CEN, 2014a). The samples were sent to SLU Uppsala for analysis and were analysed according to the European/Swedish standard protocol SS-EN 14407 (CEN, 2014b). A total of 400 diatom valves were counted under an optical microscope, and the species of each valve was identified to determine taxonomic richness and evenness (Kahlert, 2012).

Results & Discussion

Total concentrations in surface water

The water quality at the outlet of Smaltjärnen lake (C7) was negatively affected by ongoing sulfide oxidation at the Smaltjärnen repository. The average pH in C7 was lower than in the Ref (pH: 5.7 and 6.2, respectively), and the average EC was higher (350 and 34 µS/cm, respectively), Tab 1. Furthermore, at the outlet of Smaltjärnen, the total concentrations of Be, Ca, F, and S (average values of 42 µg/L and 52, 1.7, and 51 mg/L, respectively) were strongly enriched compared to the Ref (Tab. 1). The release of Ca and S originates from secondary gypsum dissolution and F from fluorite weathering. Thus, the open storage of tailings in the Smaltjärnen repository has resulted in pyrrhotite oxidation, calcite depletion, fluorite weathering, and the secondary formation of hydrous ferric oxides (HFO) and gypsum in the upper-parts of the tailings (Hällström *et al.*, 2020a). The pH in the upper parts of the tailings has been lowered from 8 to 4, but calcite have had the potential to partly buffer the mine drainage, resulting in a release of NMD to the groundwater (Hällström *et al.*, 2020a) and the surface water in C7. The elevated concentrations of Be at C7 can be traced to ongoing oxidation at the Smaltjärnen repository. Thus, danalite ($Fe_4Be_3(SiO_4)_3S$) has oxidised down to a depth of 1.5 m, with Be mobilisation intensifying due to the acid produced from pyrrhotite oxidation (Hällström *et al.*, 2020b). Sampling site C7 also showed slightly enriched total concentrations of Fe and W (average values of 4.9 mg/L and 0.7 µg/L, respectively) relative to the reference site. Previous studies have provided evidence for W mobilisation at the Smaltjärnen repository, with the release of W as an indirect consequence of sulfide oxidation (Hällström *et al.*, 2020a). Thus, the acid produced has released CO_3^{2-}, which in turn has moved downwards and weathered scheelite (CaWO4) by anion exchange. Tungstate partly adsorbed to hydrous ferric oxides (HFOs) and remained immobilised within the Smaltjärnen repository (Hällström *et al.*, 2020a).

Downstream Morkulltjärnen repository (C13), neutral pH (average 6.7), low EC (29 µS/cm) and low concentrations of Be, Ca, F, and S were present (Tab. 1). These results indicate that the preventative measures of physical cover and water saturation have decreased sulfide and danalite oxidation at the Morkulltjärnen repository, as well as indirectly affected calcite depletion, fluorite weathering and the secondary

Table 1 *Average total concentrations of the major elements (Al, Ca, F, Fe, Mn, S; mg/L) and trace elements (Be and W; µg/L) in surface water collected from Ref, C7, C11, C13, C14 and C16. N represents the number of samples taken.*

		pH	EC	Al	Ca	F	Fe	Mn	S	Be	W
	N		µS/cm			mg/L				µg/L	
Ref	6	6.2	34	0.1	3.8	<0.2	1.7	0.1	0.9	0.3	0.2
C7	6	5.7	350	0.3	52	1.7	4.9	1.4	51	42	0.7
C11	6	5.9	270	0.3	40	1.2	2.4	0.9	39	31	0.5
C13	6	6.7	29	0.1	3.0	<0.2	1.1	0.3	1.2	0.1	1.8
C14	4	6.4	61	0.1	9.9	0.3	1.1	0.5	7.5	3.9	1.4
C16	1	6.5	37	0.1	4.1	0.2	1.1	0.2	2.1	1.1	1.5

formation of HFO. C13 samples showed high concentrations of total W (average 1.8 µg/L), with concentrations up to seven times higher than what was measured in Ref. In C14, water from Smaltjärnen and Morkulltjärnen has co-mingled. There, total concentrations of Be, W and S (average 3.9 and 1.4 µg/L, and 7.5 mg/L, respectively) relative to Ref, while F concentrations were also above the detection limit (0.2 mg/L). At C16, 5 km downstream of the Yxsjöberg mine site, Be, Bi, S and W concentrations were still 2-6 times higher than what was measured in the reference sample. This shows that Be released from Smaltjärnen, along with W released from Morkulltjärnen, were transported more than 5 km from the Yxsjöberg mine site and contradicts previous claims that Be and W are immobile elements.

Element distribution between dissolved and particulate fractions

At C7 and C11, more than 90% of Be and F was transported in the dissolved phase (Fig. 3). As mentioned in the introduction, Be should precipitate as insoluble hydroxides in the absence of complexing ligands. A strong correlation between dissolved Be and F was observed in the surface waters downstream of the Smaltjärnen repository. The high affinity at which Be complexes with F in aqueous solutions at pH < 8 has also been reported in other studies (e.g., Nordstrom, 2008). Furthermore, Be-fluorocomplexes can transport Be long distances and are small enough to pass through 0.2 µm filters (Veselý *et al.*, 1989). Based on the measured pH values (5.2-6.6), BeF^+ should be the dominant species downstream of Smaltjärnen.

Iron was present in similar proportions (40-50%) in the dissolved and particulate fractions at all sampling locations. The Fe concentrations decreased between C7 and C11, ultimately reaching values similar to what was measured in Ref. Iron is known to form HFO under oxidising conditions, and – in this way – has most likely settled into the sediments of the Pumpbäcken. In the surface water downstream of Smaltjärnen, W showed a similar pattern as Fe, i.e., it was mainly transported in the particulate fraction (70%). Furthermore, W concentrations also decreased between C7 and C11, with adsorption or co-precipitation with HFO the most likely mechanism underlying this observation. Tungsten is known to have a high affinity for HFO when the pH is below 8 (Gustafsson, 2003), and subjecting the

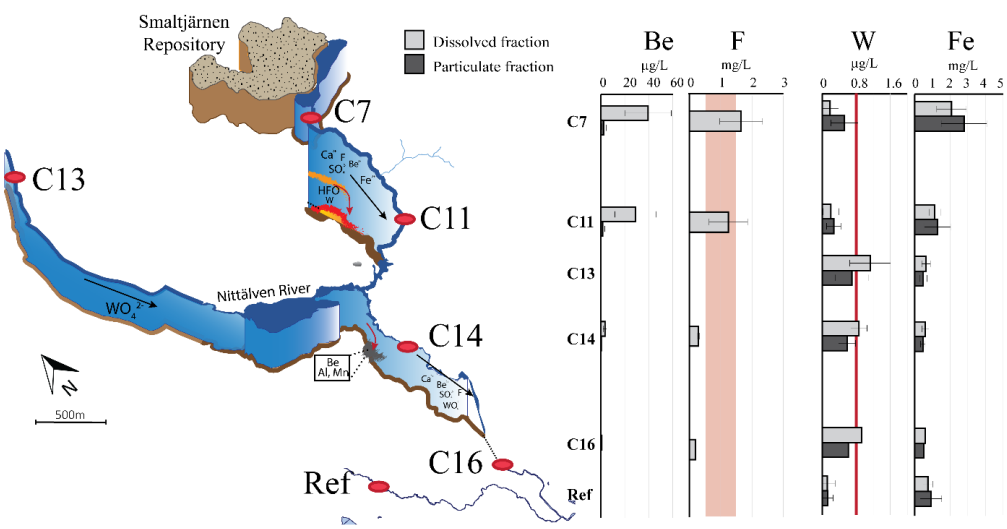

Figure 3 *Dissolved and particulate concentrations of Be, F, W and Fe in surface waters downstream of the Smaltjärnen (C9, C11) and Morkulltjärnen repositories (C13), as well as the Nittälven River (C14, C16). The red lines in the concentration illustrations represents the guideline values for W (0.8 µg/L) and F (0.5-1.5 mg/L).*

Smaltjärnen tailing to a seven-step sequential extraction indicated that W co-precipitates with Fe (Hällström *et al*., 2020a). However, W demonstrated different geochemical behaviour downstream of Morkulltjärnen. There, W was mainly transported in the dissolved phase, and at concentrations that exceeded the suggested guideline value for fish in aqueous media (0.8 mg/L) (Strigul *et al*., 2009). High concentrations of dissolved W were also observed from C14 and C16 samples. It is likely that the high concentrations of dissolved W are due to the lack of HFO, which means that the lack of sulfide oxidation in the tailings of the Morkulltjärnen repository has indirectly increased the mobility of W. The higher release of W from Morkulltjärnen compared to Smaltjärnen needs to be studied further.

Mine drainage impacts epilithic water diatom community structure

The diatoms *Achnanthidium minutssiumum*, *Aulacoseira*, *Brachysira neoexilis*, *Fragilaria gracilis* and *Tabellaria flocculosa* are all considered to be metal-tolerant species that can adapt to surface waters with high concentrations of metals (Kahlert, 2012). Cases in which these species have a joint relative abundance over 50% indicate that metal pollution has negatively impacted the surrounding ecosystem. Downstream of both Smaltjärnen and Morkulltjärnen, the metal-tolerant species of diatoms showed a relative abundance more than 50%. At C7 and C11, *Braschysira neoexilis* was the dominant species. The strong growth of *Braschysira neoexilis* at these sites can most likely be explained by low pH values and enriched concentrations of dissolved Be, Ca, F, Fe, and S. Based on the presented results, it is impossible to determine which of the elements had the strongest impact on the diatom community. However, It should be noted that the Be and F concentrations were above the threshold limits for aquatic organisms, while Ca and S concentrations did not exceed drinking water standards (WHO, 2004).

At C13, *Achnanthidium minutssiumum* showed a relative abundance of 58%. *Achnanthidium minutissimum* is classified as a circumneutral, metal-tolerant diatom (Dixit *et al*., 1991) that is often found at high levels in streams and lakes under oligotrophic conditions and that contain elevated concentrations of trace metals (Cattaneo *et al*., 2004;). At C13, only dissolved W was present at elevated concentrations and is likely the cause of the *Achnanthidium minutssiumum* dominance.

Conclusion

This study shows the importance of studying the mobility of critical metals in neutral mine drainage (NMD). Beryllium and W have previously been considered immobile elements. However, analyses of the NMD from the Smaltjärnen and Morkulltjärnen repositories showed that both dissolved Be and W can be transported more than 5 km under favourable conditions, as well as exert negative impacts on the surrounding ecosystem. Furthermore, the results have revealed that neither open storage nor storage with cover and water-saturation is an optimal mine waste strategy for the skarn tailings of Yxsjöberg.

Table 2 *The relative abudances of metal-tolerant diatom species (Achnanthidium minutssiumum, Aulacoseira, Brachysira neoexilis, Fragilaria gracilis and Tabellaria flocculosa) in Ref, C7, C13 and C14.*

Taxonomy	Ref	C7	C13	C14
Achnanthidium minutissimum group II	6%	0%	58%	22%
Aulacoseira	0%	0%	0%	6%
Brachysira neoexilis	4%	46%	7%	31%
Fragilaria gracilis	1%	0%	1%	1%
Tabellaria flocculosa	22%	4%	2%	5%
Sum:	33%	50%	68%	64%

The water quality downstream of the Smaltjärnen repository was strongly affected by a decrease in pH and high concentrations of Be, Ca, F and S in the mine drainage. Consequently, the metal-tolerant species *Brachysira neoexilis* has become dominant in the downstream ecosystem, and serves as a bioindicator of the negative impact of mine drainage on the surrounding environment. The noticeable decrease in water quality can be explained by pyrrhotite and danalite oxidation, calcite depletion and fluorite weathering in the exposed tailings. The Smaltjärnen tailings can be expected to weather for hundreds of years since only a small part has weathered during 50-100 years of storage.

The near-neutral pH and low concentrations of Be, Ca, F and S measured downstream of the Morkulltjärnen repository showed that cover and water saturation have limited the geochemical weathering in those tailings. However, high dissolved W concentrations and a strong abundance of the metal tolerant diatom *Achnanthidium minutssiumum* in the surface waters downstream of this repository are indicative of the negative environmental impacts of Morkulltjärnen.

Both the noticeable decrease in water quality and substantial changes in diatom community structure emphasise the need to find a more effective remediation approach. Re-mining could be a beneficial remediation method for the Smaltjärnen tailings since most W was found in intact scheelite grains. If re-mining were to be implemented as a remediation method, the residues produced by the process must be environmentally safe. This means that both primary and secondary minerals hosting Be, F and W need to be extracted. More research regarding mineral processing and metallurgy is needed to ensure that a sustainable extraction process is applied at this site.

Acknowledgements

This work was supported by SGU (dnr 36-1932/2019), Vinnova (Grant numbers 215 06 631), and J. Gust. Richert foundation (dnr 2018-00420), as well as co-funded by the Center of Advanced Mining and Metallurgy (CAMM2) at LTU.

References

CEN (2014a) Water quality – Guidance for the routine sampling and pretreatment of benthic diatoms from rivers and lakes. EN 13946: 2014. European Committee for Standardization: Brussels, Belgium.

CEN (2014b) SS-EN 14407. Water quality – Guidance for the identification and enumeration of benthic diatom samples from rivers and lakes. EN 13946: 2014. European Committee for standardization: Brussles, Belgium.

Dixit S. S., Dixit A. S., & Smol J. P. (1991) Multivariable environmental interences based on diatom assemblages from Sudbury (Canada) lakes. Freshwater Biology, 26(2), 251-266.

European Commission (2020) Critical raw materials. https://ec.europa.eu/growth/sectors/raw-materials/specific-interest/critical_en. Date: 2021-05-09

Filella M. & Rodríguez-Murillo J. C. (2017) Less-studied TCE: are their environmental concentrations increasing due to their use in new technologies? Chemosphere 182, 605-616.

Gustafsson, J. P. (2003) Modelling molybdate and tungstate adsorption to ferrihydrite. Chemical Geology 200, 105-115.

Hällström L. P., Alakangas L., & Martinsson O. (2018) Geochemical characterization of W, Cu and F skarn tailings at Yxsjöberg, Sweden. Journal of Geochemical Exploration 194, 266-279

Hällström L. P., Alakangas L., & Martinsson O. (2020a) Scheelite weathering and tungsten (W) mobility in historical oxidic-sulfidic skarn tailings at Yxsjöberg, Sweden. Env. Sci. & Pol. Res. 27, 6180-6192

Hällström L. P., Salifu M., Alakangas L., & Martinsson O. (2020b) The geochemical behaviour of Be and F in historical mine tailings of Yxsjöberg, Sweden. Journal of Geochemical Exploration 218, 106610.

Kahlert M. (2012) Utveckling av en miljögiftsindikator – kiselalger i rinnande vatten. ISSN: 1651–8527

Kwak T.A. (2012) W-Sn skarn deposits: and related metamorphic skarns and granitoids. Elsevier: Berlin, Germany.

Nordstrom D.K. (2008) Questa baseline and pre-mining ground-water quality investigation 25. Summary of results and baseline and pre-mining ground-water geochemistry, Red River

Valley, Taos County, New Mexico, 2001-2005 US Geological Survey. United States Geological Survey: Reston, VA.

Nuss P., & Blengini G. A. (2018). Towards better monitoring of technology critical elements in Europe: Coupling of natural and anthropogenic cycles. Science of the Total Environment 613, 569-578.

Strigul N., Koutsospyros A., & Christodoulatos C. (2009) Tungsten in the former Soviet Union: review of environmental regulations and related research. Land Contamination and Reclamation 17, 189.

Taylor T. P., Ding M., Ehler D. S., Foreman T. M., Kaszuba J. P., & Sauer N. N. (2003) Beryllium in the environment: a review. Journal of Environmental Science and Health 38, 439-469.

Veselý J., Beneš P., & Ševčí K. (1989) Occurrence and speciation of beryllium in acidified freshwaters. Water Research 23, 711-717.

World Health Organization (2004) Sulfate in Drinking-water, background document for development of WHO Guidelines for Drinking-water Quality. WHO/SDE/03.04/114. WHO: Geneva, Switzerland.

Variability in Mine Waste Mineralogy and Water Environment Risks: a Case Study on the River Almond Catchment, Scotland

Simon Haunch[1], Alan MacDonald[2], Christopher McDermott[3]

[1]*Scottish Environment Protection Agency, 231 Corstorphine Road, Edinburgh, simon.haunch@sepa.org.uk*

[2]*British Geological Survey, Research Avenue South, Edinburgh, amm@bgs.ac.uk*

[3]*School of Geoscience, Grant Institute, James Hutton Road, Edinburgh, christopher.mcdermott@ed.ac.uk*

Abstract

The River Almond catchment contains coal, oil shale and ironstone mine waste and displays widespread surface water metals pollution. Mineralogical investigations and geochemical modelling at four mine waste sites identified pyrite oxidation and jarosite, siderite and aluminosilicate dissolution reactions as the primary sources of metal pollutants (Fe, Mn, Al). Carbonate dissolution reactions control drainage pH. Pyrite is absent in burnt oil shale waste, however, trace content in unburnt shale horizons is implicated as a source of Fe in drainage waters. Site specific water quality and load assessments indicate pyrite bearing coal and ironstone sites present the greatest water environment risks.

Keywords: Coal, Oil Shale, Ironstone, PHREEQC

Introduction

Mine waste is a common visual reminder in many formerly mined river catchments and the associated drainage waters often present serious risks to surface water quality (Rees *et al*. 2002, Younger 2004) Oxidation of sulphide minerals, particularly pyrite (FeS_2), and the associated pollutant release may be more severe in surface deposited mine waste than in subsurface mines due to the continued availability of atmospheric oxygen and limited availability of carbonate minerals to buffer acidity (Rees *et al*. 2002, Younger 2004). Diffuse mining pollutant sources, such as mine waste drainage, can be the dominant source of surface water metals and can account for up to 98% of in-stream Fe load during high flow events (Mayes *et al*. 2008). National scale treatment programs exist for mine water discharges from underground coal mines however no similar program is currently available for coal mine waste or other mining waste drainage in Scotland.

The River Almond catchment, west of Edinburgh, has been mined for the last five centuries; limited silver deposits at Hilderston were targeted in the 1600s, coal and ironstone mining began in the 1700s and 1800s and oil shale was mined from the 1860s to the 1960s. Underground coal mining ended in the 1980s, however, surface mining for coal and fireclay continued until 2012. Mine wastes from coal, oil shale and ironstone are widespread and many surface water bodies in the catchment display elevated pollutant concentrations (Haunch *et al*. 2013). Most mine waste is overburden, interburden or other rock discarded at surface during mine development. Oil shale waste is unusual as it consists of a small percentage of mine development waste, but the majority is a burnt, friable, orange industrial waste produced when the mined oil shale was heated to derive various hydrocarbon chemicals in the now closed Scottish Shale Oil Industry (Louw & Addison 1985). This history of mining and associated legacy of mine wastes and poor water quality makes the River Almond an ideal catchment to undertake a case study to assess variability in the mineralogy of mine wastes and associated water environment risks.

Site Selection & Investigation Methods

Four mine waste sites were selected, their locations are shown on Figure 1 and are described below.

S1–Fauldhouse ironstone mine waste is 58,000 m^2 in size and consists predominantly

of grey argillaceous waste with a notable proportion of siderite ironstone nodules and fragments of finely banded coal and shale. The site is associated with the Fauldhouse iron industries of the 1800s.

S2–Whitburn coal mine waste is 540,000 m^2 in size and is partially restored with vegetation cover and public access. The site is adjacent to the former Whitrigg Colliery (1900-1972). A small pilot mine water treatment scheme is in place, drainage samples were recovered from the main site drainage at the effluent end of a limestone trench installed as part of the treatment scheme.

S3–Benhar coal mine waste is 25,000 m^2 in size and consists of a low-lying area of waste and a central conical area with a diffuse drainage displaying orange precipitates. Historic maps indicate the waste is sourced from both the former East Benhar (coal) mine and Fallahill Colliery.

S4–Hermand oil shale mine waste 14,000 m^2 in size (small compared to most oil shale sites but this allowed easier access and characterisation) and consists of a burnt orange-red waste, with some darker unburnt horizons of black oil shale. The waste was deposited by the adjacent historic Hermand Oil works (1883–1894) which received oil shale from the Hermand No.6 mine.

Mine waste samples were recovered from each site and Quantitative X-Ray Diffraction (QXRD) analysis was undertaken at the University of Edinburgh. Mine waste drainage samples were recovered and analysed at the British Geological Survey (BGS) laboratories Keyworth, UK. PHREEQC inverse modelling was used to assess mineralogical controls on water chemistry from rainfall to mine waste drainage. A GIS was constructed using information from West Lothian Council, BGS, Scottish Environment Protection Agency (SEPA) and National Library of Scotland (NLS) (Haunch 2013).

Mine Waste Mineralogy

The results of the QXRD mineralogical analysis are summarised in Table 1. The Fauldhouse ironstone mine waste (S1) and coal mine waste sites (S2 & S3) each display similar mineralogical assemblages consistent with shale and mudstone source lithologies. However, a number of key features warrant further consideration; *1)* Pyrite (FeS_2) is identified above 1 wt% at S1 in a quarter of samples, at S2 pyrite was identified above 1wt% in two of 23 samples while at S3 no pyrite was identified, *2)* Jarosite ($KFe_3(OH)_6(SO_4)_2$), essentially a hydrated form of pyrite, is identified above 1 wt% in every sample at S1, while at S2 jarosite is identified above 1 wt% in only two samples and at S3 no jarosite is identified, *3)* Siderite ($FeCO_3$) is identified at S3 in four of 17 samples with contents ranging between 1.42 and 4.2 wt%.

Oil shale mine waste (S4) mineralogy consists mainly of quartz, feldspars, clay minerals, hematite, cordierite and mullite.

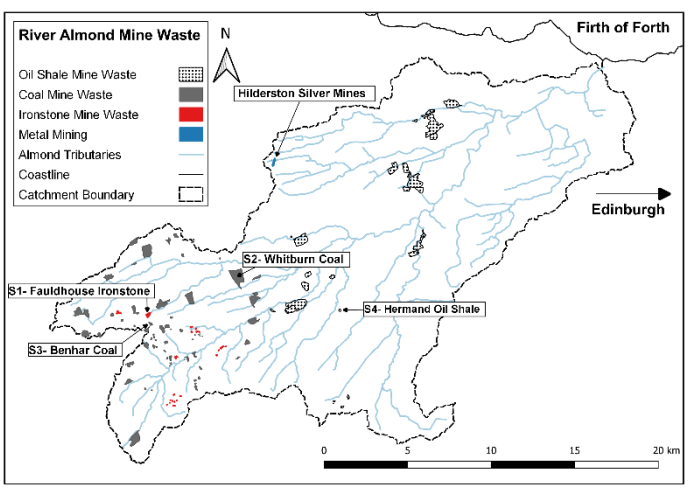

Figure 1 *Mine waste distribution in the River Almond Catchment.*

This assemblage is consistent with thermal industrial processing of the waste in the historic Scottish Shale Oil Industry (Haunch 2013). Two samples were analysed from black horizons in the waste, and these revealed a mineralogy consistent with raw unprocessed oil shale (Louw & Addison 1985) and contain trace (0.7 & 0.3 wt%) pyrite content.

In summary, mineralogical analysis indicates that the Fauldhouse ironstone mine waste (S1) contains notable proportions of acid generating minerals pyrite and jarosite, the Whitburn coal mine waste (S2) contains notable but lower abundance of these acid generating minerals, the Benhar coal mine waste (S3) contains siderite but no pyrite or

Table 1 *Mineralogical analysis results determined using Quantitative X-Ray Diffraction on waste rock samples recovered at four mine waste sites in the River Almond Catchment.*

Phase	Formula	Site 1 Fauldhouse				Site 2 Whitburn				Site 3 Benhar				Site 4 Hermand			
		n	Max	Median	Min	*n*	Max	Median	Min	*n*	Max	Median	Min	*n*	Max	Median	Min
Quartz	SiO_2	*24*	4.3	<1	<1	*23*	2.2	1.4	<1	*17*	6	3.9	<1	*19*	47.1	30.3	13.8
Microcline	$KAlSi_3O_8$	*24*	7.4	4.5	<1	*23*	7.3	3.1	<1	*7*	11.2	7.0	3.3	*2*	4.3	3.6	2.9
Albite	$NaAlSi_3O_8$	*24*	1.8	<1	<1	*1*	1.1	-	1.1	*7*	11.3	6.0	4.3	*19*	4.9	2.4	<1
Orthoclase	$KAlSi_3O_8$	*24*	1.2	<1	<1	*21*	4.9	2.3	<1	*7*	16.4	4.8	1.9				
Anorthite	$CaAl_2Si2O_3$													*18*	12.4	7.9	<1
Dickite	$Al_2Si_2O_5(OH)_4$	*24*	62.9	44	28.4					*10*	30.5	22.4	10.1				
Illite	$K_{1.5\text{-}1.0}Al_4[Si_{6.5\text{-}7.0}Al_{1.5\text{-}1.0}O_{20}](OH)_4$	*22*	21.9	10.1	5.1	*23*	55.2	40.0	12.3	*8*	48.6	29.1	24.7				
Kaolinite	$Al_2Si_2O_5(OH)_4$	*24*	22.4	15.6	1.4	*23*	52.2	22.6	11.7	*17*	52.0	34.0	13.7	*16*	10.9	1.0	<1
Muscovite	$KAl_2(AlSi_3O_{10})(OH)_2$	*24*	18.8	13.8	8.2	*23*	36.4	22.4	17.0	*5*	47.7	40.7	35.8	*19*	53.9	18.6	2.7
Calcite	$CaCO_3$	*23*	1.1	<1	<1	*23*	3.9	<1	<1	*2*	1.9	1.1	<1	*4*	1.12	<1	<1
Dolomite	$(CaMg)(CO_3)_2$	*23*	1.0	<1	<1	*23*	1.0	<1	<1					*16*	3.4	<1	<1
Siderite	$FeCO_3$	*20*	5.0	<1	<1	*1*	2.2	-	2.21	*4*	4.2	2.4	1.4	*2*	<1	-	<1
Pyrite	FeS_2	*24*	7.5	<1	<1	*23*	1.5	<1	<1					*2*	<1	-	<1
Jarosite	$KFe_3(SO_4)_2(OH)_6$	*24*	3.5	2.1	1	*23*	1.7	<1	<1								
Goethite	$FeOOH$	*24*	12.2	1.9	<1	*23*	1.2	<1	<1	*10*	1.6	1.2	<1				
Lepidocrocite	$y\text{-}FeO(OH)$	*1*	1.5	-	1.5												
Hematite	Fe_2O_3					*1*	1.3	-	1.3					*19*	13.2	8.3	1.4
Cordierite	$(Mg,Fe)_2[Si_5Al_4O_{18}].nH_2O$													*13*	16.9	4.4	<1
Mullite	$3Al_2O_{3.2}SiO_2$													*12*	35.6	28.1	20.7

Table 2 *Drainage water quality analysis results from samples recovered at four mine waste sites in the River Almond Catchment. Note: Mn EQS is based on the bioavailable fraction.*

Site	Temp	Eh	pH	EC	Ca	Mg	Na	K	HCO_3	Cl	SO_4	Fe_{tot}	Fe^{2+}	Fe^{3+}	Mn	Al
	°C	mV		µS/cm	mg/L	mg/L	mg/L	mg/L	mg/L	mg/L	mg/L	mg/L	mg/L	mg/L	mg/L	µg/L
EQS											400		1	1	0.123	15
S1	19.0	582	3.5	1041	97.2	10.9	9.9	0.5	<5	12.0	569.5	127.9	70.4	88.3	11.9	7347
S2	8.9	227	6.2	1697	217.3	52.4	6.9	10.7	188.0	6.0	669.1	78.6	67.3	11.3	12.1	61
S3	12.2	282	6.7	243	23.8	18.0	4.6	2.7	136.7	5.1	20.8	1.0	1.0	0.1	0.05	74
S4	13.0	386	6.5	353	51.4	8.5	14.3	23.8	155.0	15.4	26.2	2.4	0.9	1.5	0.5	154

Table 3 Mine waste drainage characteristics at four sites in the River Almond Catchment.

Site	Mine Waste	pH	Pollutants > EQS	MW Classification (Rees 2002)	Saturation Indices	MAMDI (Kuma *et al*. 2011)	Comments
S1	Ironstone	Acidic 3.5	Fe, Mn, Al, SO4	Net acidic, sulphate dominant	Goethite 5.15 Jarosite 2.75	49.0	Jarosite precipitates identified by QXRD in drainage channel close to waste. Orange Fe precipitates extend 2+ km downstream.
S2	Coal	Circum-neutral 6.2	Fe, Mn, Al, SO4	Net alkaline, sulphate dominant	Goethite 9.18 Jarosite 8.37	62.4	Treatment scheme in place and limestone trench increases Ca, Mg, HCO content. Ocherous impacts persist 1 km downstream.
S3	Coal	Circum-neutral 6.7	Fe, Al	Net alkaline, sulphate dominant	Goethite 7.32 Jarosite -2.23	96.0	Orange precipitates in drainage immediately adjacent to site.
S4	Oil shale	Circum-neutral 6.5	Fe, Mn, Al	Net alkaline, sulphate dominant	Goethite 8.71 Jarosite 1.74	90.3	Orange precipitates in drainage immediately adjacent to site.

jarosite and the Hermand oil shale waste (S4) is mainly a hematite bearing waste but with discrete horizons of unprocessed oil shale which contain trace pyrite content.

Mine Waste Drainage Characteristics

Mine waste drainage water quality analysis results are summarised in Table 2. The key characteristics of the drainage, using several assessment and classification schemes, are summarised in Table 3. Comparison is made to Scottish Environmental Quality Standards (EQS) for Fe, Mn, Al and SO_4 (SEPA 2020); above EQS concentrations indicates potential risks to surface water quality and ecology. The Rees *et al*. (2002) mine water classification scheme has been used to assess the net alkalinity and sulphate dominance of waters. A full trace metals suite was also undertaken and is summarised within the Modified Acidic Mine Drainage Index (MAMDI) score (Kuma *et al*. 2011); lower MAMDI values (ranging 0-100) indicate higher concentrations of pollutants of concern. In general, the results indicate the Fauldhouse ironstone site (S1) is potentially the most polluting, followed by the Whitburn coal mine waste (S2) and the Hermand oil shale (S4). The Benhar coal mine waste (S3) drainage displays the least pollution potential.

Mine Waste Drainage Evolution

PHREEQC inverse modelling has been used to identify the main hydrochemical processes controlling mine waste drainage at each of the sites. Each model returned a number of solutions, those displayed in Figure 2 were selected based on the prevailing geochemical conditions at each site.

Fauldhouse ironstone mine waste (S1) modelling results indicate pyrite oxidation (2.5-3.1 mmol/kg(H_2O)) is the main control on Fe and SO_4 release. Jarosite dissolution (0.54 mmol/kg(H_2O)) was identified as a secondary control on Fe and SO_4 release in two of the model solutions. Calcite and/or dolomite dissolution (i.e., carbonate buffering) control Ca & Mg in drainage waters, but this buffering is not sufficient to consume all proton acidity (H^+) released from pyrite oxidation and prevent low pH drainage (pH 3.5). Goethite precipitation in all three solutions is consistent with observations of orange precipitates both on waste rock surfaces in recovered cores and within the drainage channel. Dissolution of aluminosilicate minerals such as feldspars and micas and the corresponding precipitation of the hydrated clay mineral illite are likely associated with Al releases.

Whitburn coal mine waste (S2) modelling results are similar to S1 with pyrite oxidation (3.66 mmol/kg (H_2O)), carbonate buffering and aluminosilicate reactions being the primary control on drainage water chemistry. As drainage samples were recovered following the limestone trench it is likely that some of the calcite (2.58-2.99 mmol/kg(H_2O)) and dolomite (2.16-2.56 mmol/kg(H_2O)) dissolution in the model solutions is representative of the limestone trench and not the mine waste water rock interactions. This is supported by additional sampling from two shallow boreholes installed into the waste pile which indicated perched groundwater with a pH of 5.5-5.8 and lower calcium (60 &148 mg/L) and magnesium (18.5 & 31.5 mg/L) concentrations than the sampled discharge (Ca - 217 mg/L & Mg - 52.3 mg/L).

Benhar coal mine waste (S3) solutions also indicate pyrite oxidation, carbonate buffering and aluminosilicate dissolution and precipitation reactions but notably at much lower values than S1 and S2. It should be noted that pyrite and dolomite were not identified in the mineralogical analysis but were included in the model as the most like source of SO_4 and Mg in the discharge. Model solution 1 indicates siderite dissolution is the main source of Fe in the drainage. This is considered the most credible solution based on the QXRD identified siderite and goethite contents (up to 4.2 & 1.6 wt% respectively), absent or very low pyrite content and observed Fe precipitates in the main drainage area.

The Hermand oil shale waste (S4) model solutions indicate carbonate and aluminosilicate reactions are of primary control on drainage chemistry. Pyrite oxidation was identified as a contributor in all four solutions, but in practice at the site this must be limited to the identified discrete horizons of unburnt oil shale which contain trace contents of pyrite. Two of the model solutions also suggest hematite dissolution may be involved in Fe release. This would require an excess of proton acidity; possible sources of acidity could include pyrite oxidation or infiltrating rainfall. However, it is unclear whether the

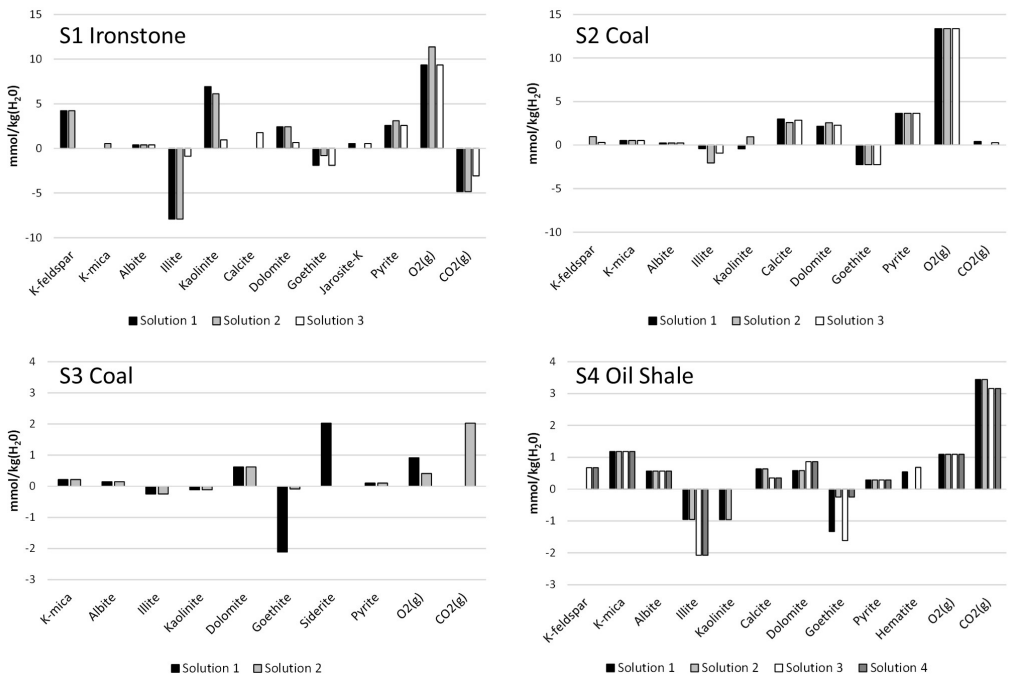

Figure 2 *PHREEQC inverse modelling results for four mine waste sites in the River Almond Catchment based on mineralogy and drainage water chemistry, +ve=dissolution, -ve= precipitation.*

hematite dissolution could result in Fe release at neutral pH and ambient temperature conditions.

Mineral phases containing Mn were not identified in the QXRD analysis at any of the sites. Manganese is commonly present in soils and rocks as a minor substitution within minerals, particularly Fe bearing minerals, and on clay mineral surfaces (Gilkes & McKenzie 1988). Mineral dissolution reactions, particularly where pH is low, are likely to liberate Mn and account for the concentrations in the drainage at each site.

Water Environment Risk Assessment and Catchment Waste Abundance

The risks posed by mine waste drainage depends on the concentrations of pollutants (measured via MAMDI scores) and the pollutant load. Drainage streams at mine waste sites are often diffuse making direct field measurement difficult. Instead, an estimate of the average flow can be gained by estimating effective rainfall from climate data. In Table 4 drainage volumes have been calculated by multiplying the site area by the average annual rainfall (1998–2019) measured at SEPA's Whitburn rainfall station (968 mm/yr) in the catchment minus the potential evaporation (501 mm/yr). These drainage volumes have then been multiplied by pollutant concentrations to calculate average annual metal loads.

The risk assessment indicates the coal site, S2, poses the greatest overall risk to water quality due to the size of the source (540,000 m^2), associated drainage volumes and quality (MAMDI-62.4). The S1 ironstone drainage quality (MAMDI-49) is potentially more polluting than S2 but the source size (58,000 m^2) is much smaller resulting in lower pollutant loads and lower overall risk ranking. The second coal site S3 and the oil shale site S4 are broadly similar and present a low risk to water quality.

Further work is required to assess how drainage quality and risk varies between different coal, ironstone and oil shale sites across the whole catchment. Indeed, it is evident from the difference in risk between sites S2 and S3 that there is likely to be variability within each waste type, and that this is ultimately the result of waste mineralogy. At oil shale sites the risk will be dependent on the proportion of unburnt black shale. Nevertheless, the overall abundance of waste (Table 5) in the catchment suggests coal mine waste is likely to be of greatest concern followed by ironstone and oil shale.

Conclusions

This study indicates the importance of mine waste mineralogy in assessment of metal release, drainage evolution and water environment risks. In the River Almond catchment, mine wastes derived from

Table 4 *Mine waste drainage volumes, pollutant loading estimation and risk ranking.*

	S1 Ironstone	S2 Coal	S3 Coal	S4 Oil Shale
Area (m^2)	58,000	540,000	25,000	14,000
Drainage Estimate (L/s)	0.86	8.01	0.37	0.21
Fe (kg/yr)	3471	19,863	11.7	15.7
Mn (kg/yr)	325	3057	0.6	3.2
Al (kg/yr)	200	154	8.6	1.0
MAMDI	49	62.4	96	90
Risk Rank	2- Medium/High	1- High	4- Low	3-Low

Table 5 *Mine waste abundance in the Almond River Catchment.*

	Oil Shale	Coal	Ironstone
Area (km^2)	4.15	3.91	0.274
Catchment %	1.05	0.98	0.07

historic coal, oil shale and ironstone mining industries are confirmed as sources of Fe, Mn, Al and SO_4. Pyrite oxidation reactions in ironstone and coal mine wastes are identified as the main control on elevated Fe concentrations in drainage waters. Jarosite dissolution plays a secondary role although it is likely PHREEQC inverse modelling does not fully represent the movement of pollutants from pyrite to jarosite and into drainage waters. Siderite dissolution is implicated as a source of Fe at a coal mine waste site with low abundance of pyrite.

The oil shale waste site investigated consisted mainly of burnt orange waste containing hematite and little to no pyrite. However, discrete horizons of unburnt black oil shale with trace pyrite content were identified and modelling suggested pyrite oxidation reactions in these horizons as a source of Fe in drainage waters. Some model solutions also implicated hematite dissolution in Fe release. Carbonate buffering was shown to influence drainage pH, Ca and Mg content in drainage at all sites. Al in drainage waters is likely to be associated with the dissolution of aluminosilicate minerals.

Site specific risk assessments indicate pyrite bearing coal and ironstone sites present the greatest water environment risks. Notably while ironstone mine waste drainage quality is extremely poor, ironstone mine waste abundance is low suggesting a lower overall risk, than coal mine waste, at the catchment scale.

Mine waste drainage is currently excluded from national scale mine water remediation programs and in many mined catchments continues to be a source of elevated metals and regulatory classification downgrades. This study demonstrates that further work is required to incorporate mine waste mineralogy and drainage monitoring into catchment water quality assessments and water body improvement objectives.

References

Gilkes R.J., McKenzie R.M., 1988. Geochemistry and Mineralogy of Manganese in Soils. In: Graham R.D., Hannam R.J., Uren N.C. (eds) Manganese in Soils and Plants. Developments in Plant and Soil Sciences, vol 33.

Haunch, S., MacDonald, A.M., Brown, N., McDermott, C.I., 2013. Flow Dependent Water Quality Impacts of Historic Coal and Oil Shale Mining in the Almond River Catchment, Scotland, Applied Geochemistry 39, 156-168.

Haunch, S. 2013. The Legacy of Historic Mining and Water Quality in a Heavily Mined Scottish River Catchment. PhD Thesis, University of Edinburgh.

Kuma, J.S., Younger, P.L. & Buah, W.K., 2011. Numerical Indices of the Severity of Acidic Mine Drainage: Broadening the Applicability of the Gray Acid Mine Drainage Index. Mine Water Environ 30, 67–74.

Louw S. J., Addison J. 1985. Studies of the Scottish Oil Shale Industry, Volume1, History and Mineralogy, Institute of Occupational Medicine, historical research report, TM/85/02; 1985.

Mayes, W. M., Gozzard, E., Potter, H. A. B., Jarvis, A. P. 2008. Quantifying the Importance of Diffuse Minewater Pollution in a Historically Heavily Coal Mined Catchment, Environmental Pollution 151, 165-175

Rees, S. B., Bowell, R. J., Wiseman, I., 2002. Influence of Mine Hydrogeology on Mine Water Discharge Chemistry, In: Younger PL, Robins NS, Mine Water Hydrogeology and Geochemistry, Geological Society, London, Special Publications 198, 379-390.

SEPA, 2020. WAT-SG-53, Environmental Quality Standards and Standards for Discharges to Surface Waters.

Younger, P. L., 2004. Environmental Impacts of Coal Mining and Associated Wastes: a Geochemical Perspective: In. Geological Society, London, Special Publications 2004, 234, 169-209.

UNEXMIN and UNEXUP Projects: Development of Submersible Robots for Survey of Flooded Underground Mines

S. Henley

Resources Computing International Ltd, Matlock, Derbyshire, UK

Abstract

A series of submersible robots have been developed in the EU-funded UNEXMIN (Horizon2020, 2016–2019) and UNEXUP (EIT Raw Materials, 2020–2022) projects, for surveying and exploration of flooded underground mines. the robots carry cameras and a range of different instrumentation to determine physical and chemical properties of wall rocks and water; there are also water samplers to allow further laboratory analysis of the water.

The first generation of robots (UX1) is designed for dives to a maximum of 500m depth, and no contact with wall rock, though they include a water sampling unit. In UNEXMIN the prototype design included a 60 cm diameter spherical pressure-hull with instrument and camera ports, and thruster manifolds on either side. A number of problems with the design were identified during trials, so in UNEXUP a complete re-design produced a modular robot (UX1-NEO) of similar shape, exterior dimensions, and instrumentation capabilities, but with considerable weight reduction as well as a new thruster configuration for improved manoeuvrability. This is the version currently being tested.

The second generation currently under development (UX2-DEEP) will be similar in appearance but is designed to dive to 1500–2000 m maximum depth and will include also a device for sampling the wall rock. Both generations include pH, conductivity, temperature and pressure sensors, gamma-ray detector, and magnetometer. Six cameras (to give all-round vision) use white light and ultraviolet sources (the latter to identify fluorescent minerals). In the first generation there was also a multi-spectral unit, but this was found difficult to use because of problems in registration of the time-sliced images when the robot was moving. This is now being replaced by a hyperspectral unit, which not only gives much more spectrometric data but also avoids the image-matching problem.

A series of trials have been carried out at mines around Europe. These include the open-pit Kaatiala mine in Finland, and undergound mines: Idrija mercury mine (Slovenia), Urgeiria uranium mine (Portugal), and Deep Ecton copper mine (Staffordshire, UK). Currently a new set of trials are under way in Hungary and Ukraine. Examples are shown from Urgeirica and Ecton. In particular, extensive dives in May 2019 at Ecton yielded much new data on geology and archaeology, as well as the water which had been almost undisturbed since the mine flooded to river level in the late 1850s.

Keywords: Underground Mines, Submersible Robots

Numerical Modelling of Transient Groundwater Flow and Contaminant Transport at the Myra Falls Mine Site

Mahmoud Hussein[1], Paul Ferguson[1], Christoph Wels[1]
Nicole Pesonen[2]

[1]*Robertson GeoConsultants Inc., Vancouver, Canada, mhussein@rgc.ca*
[2]*Myra Falls Mine Site, Campbell River, Canada*

Abstract

The Myra Falls mine is an underground lead-zinc mine on Vancouver Island, British Columbia, Canada. The mine site has been operated since the 1970s and is affected by Acid Rock Drainage (ARD) generated by sulphide-bearing waste rock in the historic waste rock dumps. A numerical groundwater flow and transport model was developed using the software MODFLOW/MT3D to simulate the movement of groundwater and the transport of zinc in the Myra Valley Aquifer (MVA) and to predict Zn loads to Myra Creek during an emergency shutdown of the site-wide SIS.

Keywords: ARD, MODFLOW/MT3D, Groundwater Model, MVA, Myra Creek

Modelling Objectives

The main objectives of the numerical modeling are to simulate "current conditions" for groundwater in the MVA from 2012 to 2019, including six years when the site-wide SIS consisted of the system of Old TDF underdrains in the Lower Old TDF Reach and two full years (since October 2017) when the Phase I Lynx SIS was also operating and to predict Zn loads to Myra Creek during an emergency shutdown of the site-wide SIS due to a power loss on site.

Model Overview

A transient groundwater flow model using the finite difference code MODFLOW and a solute transport model using the MT3D code were developed as part of updating the Site-Wide WLBM for the Myra Falls Mine Site. Together, these are often referred to as the "groundwater model" throughout this paper, unless the flow or transport model is specified.

The groundwater model is calibrated to eight years of monitoring data, including recent performance monitoring data collected during the operation of a fence of pumping wells that are intended to capture ARD-affected groundwater before it reaches Myra Creek. The model is a numerical representation of a conceptual hydrogeological model that has been developed iteratively since 2013. The model is incorporated into a site-wide Water and Load Balance Model (WLBM) that predicts loads and concentrations in Myra Creek due to contaminant loads from unimpacted areas and the water treatment system and groundwater affected by ARD.

The model domain and boundary conditions are shown in Figure 1. The groundwater model simulates groundwater flows and Zn concentrations in the MVA and Zn loading to Pumphouse No.4, the Lynx SIS and Myra Creek from January 1st, 2012, to December 31st, 2019. Simulated flows and loads are shown in Figure 2 and simulated Zn plumes are shown in Figure 3.

Sources of Seepage

Seepage (ARD) from the Lynx TDF berm and WRD#1 and WRD#6 are the major sources of Zn and other constituents to groundwater in the MVA. Secondary sources include PAG waste rock in the Mill and ETA/Cookhouse areas, sulphidic surface waste near the Superpond and in the HW office area and the former Myra Pit, and seepage from the Seismic Upgrade Berm.

Discussion – Current Conditions

The overall spatial extent of the simulated Zn plume is reasonably consistent with observed Zn concentrations in the MVA. For instance,

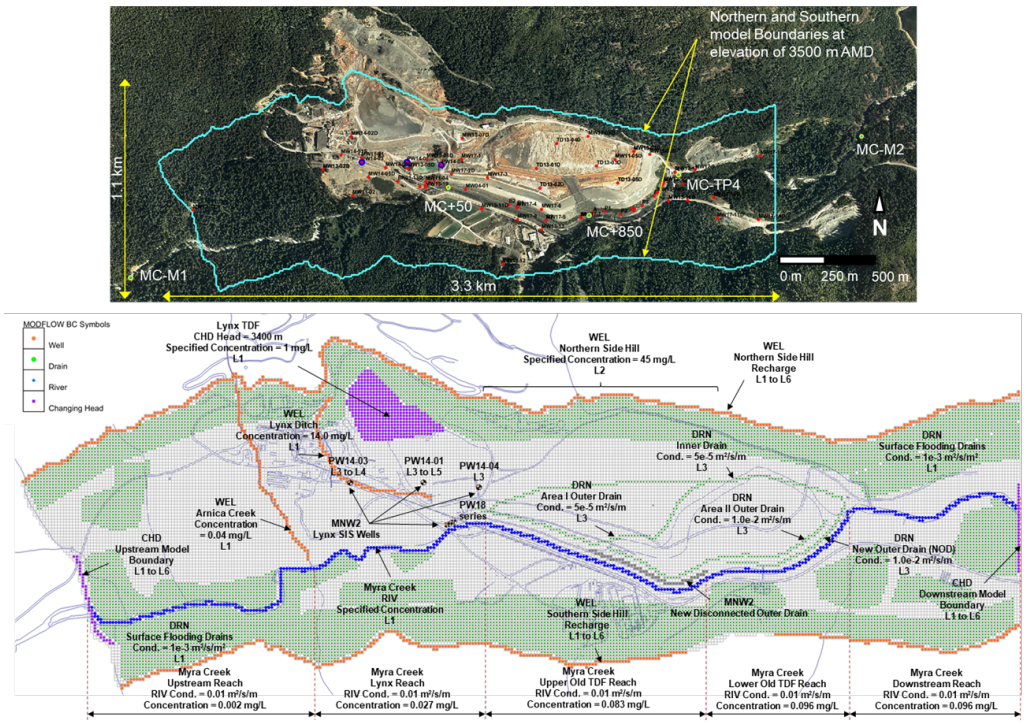

Figure 1 *Model Domain (top) Boundary Conditions and Internal Sources and Sinks (Bottom).*

the elevated Zn concentrations, observed in wells screened beneath the Old TDF (and within the main plume that migrates towards the Old TDF under-drains) are well reproduced by the model. Simulating these wells was a priority during model calibration to ensure Zn loads to the Old TDF under-drains could be represented.

Zn concentrations in key wells in the Mill area are also simulated reasonably, e.g. ≈15 to 20 mg/L Zn at MW13-05D (near PW14-01), and up to 50 mg/L Zn at MW13-06D (north of the Superpond near the toe of the Lynx berm).

The groundwater model simulates decreased Zn concentrations in groundwater in the Upper Old TDF Reach that are attributed to operating the Phase I Lynx SIS, where observed Zn concentrations have decreased from more than 20 mg/L in 2017 to less than 5 mg/L in late 2019 (and 2020). The model slightly overestimates the overall effectiveness of the Old TDF under-drain system as the system is simulated to capture nearly all of the Zn plume with no appreciable simulated bypass. Conceptually, approximately 10% of the Zn load in Myra Creek is related to groundwater bypass in the Lower Old TDF Reach. However, the fit between observed and simulated Zn loads to Pumphouse No. 4 in 2019 was very good, and the model reproduces the observed decrease in captured Zn loads in 2019 during operation of the Lynx SIS.

Discussion – Predictive Runs (SIS Shutdown)

The groundwater model was modified to predict Zn loads to Myra Creek during an emergency shutdown of the site-wide SIS due to a power loss on site for the following three scenarios: Scenario 1; Site-Wide SIS Shutdown, Scenario 2; Old TDF Under-Drain Shutdown and Scenario 3; Phase I Lynx SIS Shutdown. SIS shutdown was assumed during low flow conditions for groundwater in August 2018.

For Scenario 1, the groundwater model predicts increased Zn loads to Myra Creek at MC-TP4 from groundwater within days to a few weeks of the site-wide SIS shutdown

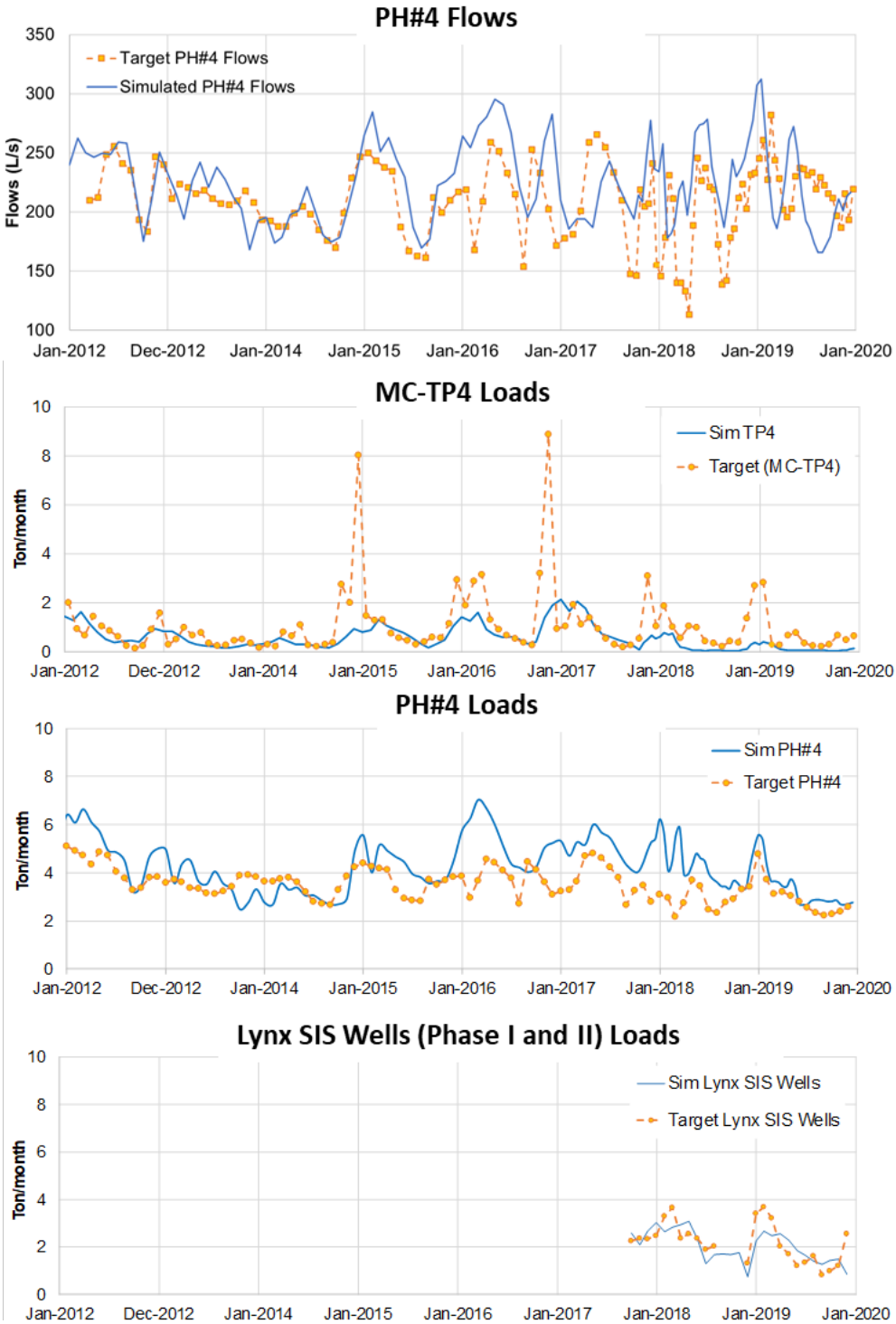

Figure 2 *Simulated Monthly Flows to PH#4 and Zn Loads to Myra Creek, PH#4 and SIS wells 2012 to 2019.*

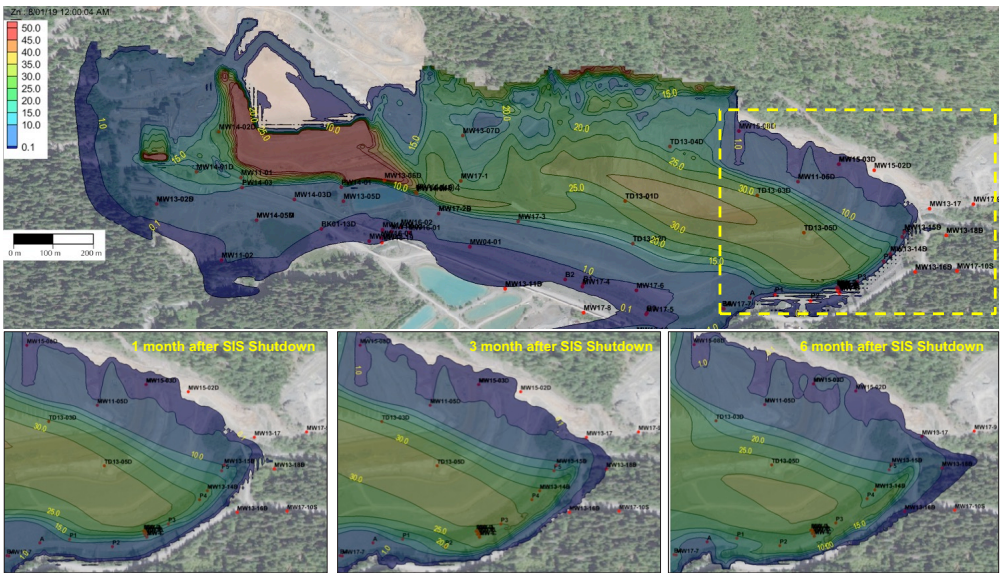

Figure 3 *(Top) Simulated Zn Plume (Layer 3) – Lynx SIS Operating (August 2019). (Bottom) Simulated Zn plume in the Lower TDF reach 1, 3 and 6 months after SIS shutdown, Scenario 1.*

(Figure 4). Zn loads are predicted to be about one order-of-magnitude higher than the simulated Zn loads to Myra Creek during summer low flow conditions prior to SIS shutdown within this period. The model predicts monthly Zn loads to Myra Creek will increase to approximately 5.8 t/month within six months.

The groundwater model predicts that the majority of the Zn load in groundwater in the shallow MVA will report to Myra Creek within close distance to the Old TDF. Nevertheless, the model also predicts some bypass of impacted groundwater in the shallow MVA. The model predicts that the leading edge of this developing "off-site" Zn plume will have advanced approximately 250 m east of the Old TDF at the end of the 16-month prediction period. This implies an average Zn transport velocity in groundwater of approximately 16 m/month towards the downstream model boundary. It should be noted that the model conservatively assumes that Zn transport in groundwater is not retarded due to the adsorption of Zn to MVA formation materials in the Downstream Reach. Experience at other sites with similar water quality and geology suggests that zinc shows some affinity for sorption resulting in retardation in the order of 30 – 50%. This implies the Zn plume in groundwater of the MVA could also be retarded, possibly migrating less than 200 m in one year. However, Zn retardation would only delay increased Zn loading to the creek in the Old TDF Reach by a few days, given the short distance (≈15 m) between the NOD and Myra Creek in the Lower Old TDF Reach (near MC-TP4).

For Scenario 2, the groundwater model predicts that effectively 100% of the increased Zn load to Myra Creek during the first two months following a shutdown of the site-wide SIS is related to the shutdown of the Old TDF under-drains. The high Zn load during this period is related to the migration of the main Zn plume that is captured by the Old TDF under-drains to Myra Creek. Following this period, the shutdown of the Old TDF under-drains accounts for 85 – 90% of the predicted Zn load to Myra Creek for Site-wide SIS shutdown (Scenario 1). For Scenario 3, the groundwater model predicts an increase in Zn loading about two months following the shutdown of the Phase I Lynx SIS. This Zn load is related to the Zn plume in the Lynx Reach and Upper Old TDF Reaches reaching Myra Creek near the car bridge and in the Upper Old TDF Reach.

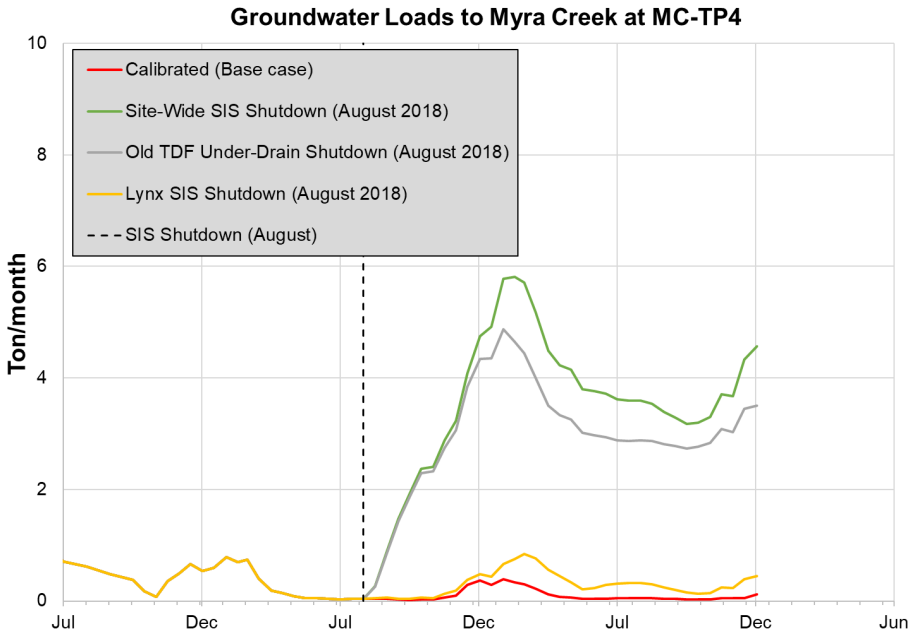

Figure 4 Predicted Zn Loads to Myra Creek at MC-TP4 from Groundwater, SIS Shutdown Scenarios, Shutdown in August.

Key Findings

Operating the Lynx SIS (since October 2017) has reduced loads of Zn and other constituents related to ARD in Myra Creek. This is particularly evident at stations MC+50 (in the Lynx Reach near the car bridge) and MC+800 in the Old TDF Reach. Operating the Lynx SIS also appears to have decreased Zn loads in groundwater captured by the Old TDF under-drains and delivered to the Superpond via Pumphouse No. 4.

The groundwater model provides a reasonable numerical representation of groundwater conditions in the MVA, as a good match between observed heads and the groundwater flow field and the flows captured by the Old TDF under-drains and the Lynx SIS is achieved. Moreover, the inferred Zn plume in groundwater and Zn loads captured by the Old TDF under-drains and the Phase I Lynx SIS are well reproduced. The development of a transient groundwater flow model has significantly improved RGC's understanding of the seasonal behaviour of the groundwater system and has identified aspects of the conceptual model that require improvement.

While the Phase I Lynx SIS has been operating, groundwater captured by the Old TDF under-drains via Pumphouse No. 4 has remained the largest contributor of flow and Zn loads to the Superpond. Groundwater captured by the Phase I Lynx SIS represents the primary contributor of acidity, Al, and Cu loads to the Superpond and are the second largest contributor of SO4 and Zn loads. Process water represents a substantial source of alkalinity to the Superpond that will increase if the milling rate increases.

Zn concentrations in Myra Creek at MC-TP4 and MC-M2 are predicted to increase within days to a few weeks of the site-wide SIS being shut down. Approximately 1 mg/L Zn is predicted initially which is approximately 30 times higher than the 0.033 mg/L Zn-t provincial WQG. Higher Zn concentrations are predicted (≈2 mg/L Zn) about six months after SIS shutdown (or about 60 times higher than WQG), as Zn loads to groundwater (and Myra Creek) increase due to increased recharge by rainfall during the wetter months of the year. Zn concentrations are predicted to remain in the range of 0.5 to 1.5 mg/L Zn

until the end of the prediction period.

Approximately 90% of the predicted Zn load during shut down of the site-wide SIS is related to the shutdown of the Old TDF underdrains. The predicted Zn load to Myra Creek due to shut down of the Phase I Lynx SIS is relatively small and represents only a small proportion of the predicted Zn load to the creek during a shutdown of the site-wide SIS. Moreover, the groundwater model predicts it will take several months for Zn loads in Myra Creek to increase due to shut down of this system, due to the longer travel for the plume in the Lynx Reach to Myra Creek.

Investigating the Radiological Safety of Uranium Ore Deposits from a Uranium Mine in Namibia

Vaino Indongo[1,2], Vera Uushona[1,3], Manny Mathuthu[1], Zivayi Chiguvare[2]

[1]*Center for Applied Radiation Science and Technology (CARST), North-West University (Mafikeng), Cnr Albert Luthuli Road and University Drive, 2735, Mmabatho, South Africa, vainoindongo@gmail.com, nvuushona@yahoo.com, Manny.Mathuthu@nwu.ac.za*

[2]*Namibia University of Science and Technology (NUST), 13 Jackson Kaujeua Street, P/Bag 13388, Windhoek, Namibia, zchiguvare@unam.na*

[3]*National Radiation Protection Authority of Namibia, Ministry of Health and Social Services, Harvey Street, Namibia*

*nvuushona@yahoo.com; *vainoindongo@gmail.com; Manny.Mathuthu@nwu.ac.za; zchiguvare@unam.na*

Abstract

Namibia is one of the four leading countries in Uranium mining which results in huge tailing deposits. The main aim of this study was to assess radiological hazards posed to employees by uranium ores deposits from a uranium mine in the Erongo Region. Gamma spectrometry was used to determine the radiological health indices of primordial radionuclides of ^{238}U, ^{232}Th and ^{40}K in samples. The weighted mean of activity concentrations of ^{226}Ra, ^{232}Th and ^{40}K and their Indices were all above the WHO stipulated limits. The findings of this research indicate that uranium mining activities pose a high risk of radiation hazards to employees.

Keywords: NORM, Radiological Health Indices, Gamma Spectrometry

Introduction

The increasing rate of electricity demand has resulted on more uranium mining and milling activities in the world. In Namibia, uranium was first discovered in Rossing Mountains, Namib Desert of Erongo Region. The region has a deposit containing high grade of uranium in a type of granite called alaskites. Uranium ore deposits occur in sedimentary basins deposited on top of very old basement metamorphic rocks, either from the basin (sedimentary) or basement (metamorphic) rocks.

Mining activities have also began to contribute to human exposures to radiations, which have now became an increasingly concern in the world. Background radiation is increasing continuously due to mining and milling activities in the environment. Natural occurring radioactive materials (NORM) contribute to the increase in background and protection measures need to be put in place for health and safety. Nowadays radiation protection has become one major and crucial role for the betterment of human health. Exposures to radiations on living organisms, including humans, from natural radioactivity at different levels depends on natural radioactive elements present in each area (Alzubaidi *et al*., 2016). Erongo Region is one diminutive area, in comparison to the whole world, which requires scientific approach to determine radiation exposure levels to humans, in order to scientifically report to the Policy makers on radiation level if it is in agreement with international basic safety standards (WHO, 1994). The main aim of this study was to assess radiological hazards posed to employees by uranium ores deposits from a uranium mine in the Erongo Region.

Methods

Sampling technique

Random sampling technique was employed to select the sampling sites around and within the mines. The GPS values and name of the mine under study will not be published

in this work because of the confidentiality agreements signed with the mines.

Collection and preparation of samples

The uranium ore deposits have been collected from randomly selected points around a mine crusher in Erongo Region. The samples were transported to the Analytical; laboratory, at the Centre of Applied Radiation, Science and Technology (CARST), North-West University (NWU), South Africa. During preparation, the samples were dried for 30 days, crushed for homogeneity (ISO18589–2, 2007). All samples were packed and sealed in Vaseline geometry (VasGeo) plastic containers. The mass for each sample was measured for use during computing to determine radioactivity concentration analyses. Each sample was sealed in a container for more than 23 days to allow radon and its progeny to reach secular equilibrium (ISO18589–3, 2007). Also, standard samples were used for calibrations of energy and efficiency of the gamma detector before counting of samples.

Results and Discussion

Analysis

The gamma spectrometry techniques, which allow identification and quantification of radionuclides, was utilized to determine the gamma-emitting radionuclides present in the samples based on energies and the peak areas of the full-energy peaks of the gamma lines (ISO18589–3, 2007). The analyses where performed in the Centre for Applied Radiation Science and Technology (CARST), NWU, Mafikeng campus. A High-Purity Germanium (HPGe) detector manufactured by Canberra Industries (Meriden, CT, USA) with detector model GCW2021 and relative efficiency of ≥ 20% and a resolution of ≤ 2.100 keV for 1332 keV gamma ray emission of ^{60}Co, was used for contng the activity of each sample. The sample data was acquired using Genie 2000 vs 3.3 Gamma Acquisition software. Counting for each sample took 12 hours (43200 s). The gamma energy 1460.63 keV was utilized to determine activity concentration for ^{40}K (Ademola *et al*., 2014). Both ^{238}U and ^{232}Th are alpha emitters, hence their activities were measured based on the daughter products, which are gamma emitters. Therefore, the activity concentrations of the ^{238}U and ^{232}Th radionuclides were determined using the energy of their daughter products that occurred during their decay series (Durusoy and Yildirim, 2017). After radioactive secular equilibrium between ^{226}Ra, ^{222}Rn, ^{214}Pb and ^{214}Bi has been established, the short-lived decay radionuclides ^{226}Ra, ^{214}Pb and ^{214}Bi of ^{222}Rn were measured (ISO18589–3, 2007). Therefore, energy lines (285.22 keV and 351.93 keV) for ^{214}Pb and (609.31 keV, 1120.29 keV and 1764.49 keV) ^{214}Bi was used to determine the activity concentration for ^{226}Ra, a daughterof ^{238}U, as shown in Table 1. It is also assumed that ^{232}Th and its decay radionuclides ^{228}Ac and ^{212}Pb are in radioactive equilibrium (ISO18589–3, 2007). Hence, energy lines (238.63keV) for ^{212}Pb, and (338.32 keV, 911.20 keV) for ^{228}Ac were utilized for determining activity concentration of ^{232}Th, shown in Table 1–2.

The Genie 2000 Gamma Analysis Software was then used to determine the specific activities (bq/kg) of the radionuclides (Chhangte *et al*., 2018). It calculates using the above equation.

The activity concentrations obtained at the respective energies of their radionuclides under considerations were tabulated as indicated in Tables 1–3. All activity concentrations for daughter nuclides of ^{226}Ra were detected. Some activity concentrations for daughter nuclides for ^{232}Th were not detected, therefore indicated as ND – non-detectable in Table 2.

Activity concentrations for ^{226}Ra, ^{232}Th and ^{40}K calculated in the ore deposits range as 2808.00 ± 27.33 Bq.kg^{-1} to 7289.00 ± 56.90 Bq.kg^{-1}, 129.80 ± 12.62 Bq.kg^{-1} to 306.90 ± 13.93 Bq.kg^{-1} and 561.90 ± 8.49 Bq.kg^{-1} to 984.10 ± 23.62 Bq.kg^{-1}, respectively. The maximum activity concentration determined here is 7289.00 ± 56.90 Bq.kg^{-1} for ^{226}Ra and minimum is 129.80 ± 12.62 Bq.kg^{-1} for ^{232}Th. Tables 1 shows the results obtained.

The weighted mean of activity concentrations (with their uncertainties) of ^{226}Ra, ^{232}Th and ^{40}K calculated using equation (1) are in the range of 2855.84 ± 11.02 Bq.kg^{-1} to 6700.44 ± 24.02 Bq.kg^{-1}, 136.62 ± 3.23 Bq.kg^{-1} to 258.72 ± 3.19 Bq.kg^{-1} and 261.90 ± 8.49 Bq.kg^{-1} to 984.10 ± 23.62 Bq.kg^{-1},

Table 1 The summarized activity concentrations (weighted means) for ^{226}Ra, ^{232}Th and ^{40}K.

Sample no	Weighted means of Activity concentrations [Bq.kg^{-1}]		
	^{226}Ra	^{232}Th	^{40}K
ORE1	5593.88 ± 20.48	255.85 ± 3.83	889.30 ± 20.65
ORE2	6004.68 ± 22.20	232.20 ± 2.05	858.60 ± 24.69
ORE3	3682.19 ± 13.89	192.89 ± 3.30	881.30 ± 24.81
ORE4	2855.84 ± 11.02	136.62 ± 3.23	845.60 ± 23.50
ORE5	4281.26 ± 15.68	189.09 ± 1.69	874.60 ± 24.47
ORE6	3648.43 ± 13.89	146.35 ± 3.74	561.90 ± 8.49
ORE7	6508.41 ± 23.87	258.72 ± 3.19	984.10 ± 23.62
ORE8	6700.44 ± 24.02	248.35 ± 10.44	897.30 ± 35.40

respectively. These results shows that the weighted mean of ^{226}Ra is high and ^{232}Th is low in activity concentrations of the uranium ore deposits. The worldwide values of 35, 30 and 400 Bq.kg^{-1} (UNSCEAR, 2000) were significantly lower than the average activity concentration values for ^{238}U, ^{232}Th and ^{40}K, respectively, in this study.

Dose Rate

Absorbed dose

The absorbed dose rate in air is based on the activity concentration of natural radionuclides in uranium ore samples. Dose conversion factors for radionuclides present in samples are used to assess the dose rate. The United Nations Scientific Committee on the Effects of Atomic Radiation (UNSCEAR) defined these conversion factors, and the gamma absorbed dose rates were calculated using the following Equation (2) (UNSCEAR, 2000):

$$D(\frac{nGy}{h}) = 0.462A_U + 0.604A_{Th} + 0.0417A_K \quad (2)$$

Where A_U, A_{Th} and A_K are activity concentrations for ^{238}U, ^{232}Th and ^{40}K, respectively. It is also crucial to know that the activity concentration for ^{238}U is approximated by that of ^{226}Ra daughters because of radioactive equilibrium that has been set.

Annual Effective Dose Rate (AEDR)

It is also best to estimate the annual effective dose rate absorbed by humans as a result of natural radionuclides present in the uranium ore samples. UNSCEAR (2000) has stipulated dose conversion coefficient that convert the absorbed dose rate in air to the effective dose of 0.7 Sv Gy^{-1} and the outdoor occupancy of 0.2. The estimated average time spent on the mining site everyday of a year is 4.8 h (UNSCEAR, 2000).

$$AEDR(\mu Sv\ y^{-1}) = D(nGy\ h^{-1}) \times 8760\ (h\ y^{-1}) \times 0.2 \times 0.7\ (Sv\ Gy^{-1}) \times 10^{-3} \quad (3)$$

Radium Equivalent

The gamma radiation hazards which may arise from uranium ore deposits if by any chance used in construction materials of offices and buildings within the mine by contractors needs to be assessed as well. For this reason radium equivalent should

Table 2 The computed values of dose rates, annual effective dose rates, radium equivalents and external hazard indexes of uranium ores.

Sample no.	D(nGy.h^{-1})	AEDR(μSv.y^{-1})	Raeq (Bq.kg^{-1})	H_{ex}
ORE1	2512.31 ± 23.00	3081.10 ± 28.21	5457.48 ± 49.83	14.75 ± 0.13
ORE2	2496.75 ± 25.35	3062.01 ± 31.09	5421.31 ± 54.86	14.65 ± 0.15
ORE3	2641.56 ± 16.36	3239.61 ± 20.07	5729.63 ± 35.45	15.48 ± 0.10
ORE4	1647.31 ± 13.21	2020.27 ± 16.20	3571.16 ± 28.63	9.65 ± 0.08
ORE5	1349.73 ± 17.80	1655.30 ± 21.83	2933.08 ± 38.53	7.93 ± 0.10
ORE6	1811.06 ± 18.32	2221.08 ± 22.46	3930.53 ± 39.70	10.62 ± 0.11
ORE7	1792.62 ± 28.97	2198.47 ± 35.53	3898.81 ± 62.72	10.54 ± 0.17
ORE8	3168.85 ± 34.74	3886.28 ± 42.61	6877.55 ± 75.42	18.59 ± 0.20

be computed which details more about the gamma output for ^{238}U, ^{232}Th and ^{40}K. The expression to calculate radium equivalent activity in the uranium ore deposits is shown in the equation (UNSCEAR, 2000):

$$Ra_{eq} = A_{Ra} + 1.43A_{Th} + 0.077A_{K} \quad (4)$$

where A_{Ra}, A_{Th} and A_{K} are average activity concentrations for ^{226}Ra, ^{232}Th and ^{40}K, respectively. Also here, the activity concentration for ^{238}U is replaced by that of ^{226}Ra. Note that the half-life of ^{226}Ra is very high (1600 years) and may be in disequilibrium with ^{238}U (UNSCEAR, 2000). The highest value of this concentration (Ra_{eq}) should not exceed 370 Bq.kg^{-1} (Amanjeet *et al*., 2017).

The radium equivalent concentrations calculated for the samples of uranium ore analysed with the high-purity germanium detector were very high. The lowest value calculated is for ORE 5 sample which is 2933.08 ± 38.53 and the maximum was for ORE 8 which 6877.55 ± 75.42 Bq.kg^{-1}. These values are way too large compared to the safely defined 370 Bq.kg^{-1}. The management of mine should at no time allow a small fraction or portion of uranium ores to get contact with building materials used for construction in the mine. Therefore, preventative measures should be taken to avoid any contact of uranium ores with construction materials.

External Hazard Index

The External Hazard Index (H_{ex}) due to gamma rays emitted from the three primordial radionuclides was introduced as a result of external exposures from these materials. These exposures are estimated by emission of photons (gamma rays) from ^{222}Rn (radon) and ^{220}Rn (thoron) together with their short-lived products (UNSCEAR, 1988, Amanjeet *et al*., 2017). The aim was to have maximum permissible limit of 1 mSv y^{-1} due to natural radioactive materials (Kamunda *et al*., 2016). The approximation of external radiation doses as measured by gamma spectrometry from building materials is known as external hazard index (UNSCEAR, 1988).

$$H_{ex} = \frac{Au}{370} + \frac{ATh}{259} + \frac{Ak}{4810} \leq 1 \quad (5)$$

where A_{Ra}, A_{Th} and A_{K} are activity concentrations of ^{226}Ra, ^{232}Th and ^{40}K radionuclides as calculated from uranium ore samples. The maximum external hazard index calculated is for ORE 8 and minimum for ORE 5, which are 18.09 ± 0.20 and 7.93 ± 0.10, respectively.

Discussions and conclusion

The **absorbed dose rate (D)**, both weighted mean and average errors, were determined with a minimum of 1349.73 ± 17.80 *nGy.h*$^{-1}$ and a maximum of 3168.85 ± 34.74 *nGy.h*$^{-1}$. These results indicate that absorbed dose to workers due to all three primordial radionuclides of ^{238}U, ^{232}Th and ^{40}K in uranium ore deposits is very higher than the recommended value of 35, 420 and 45 Bq.kg^{-1} (UNSCEAR, 2000), on the earth's crust. Also, the absorbed dose rates were significantly higher than the world average of 60 *nGy.h*$^{-1}$ recommended by UNSCEAR (2000). The **annual effective dose rate (AEDR)** shows a weighted mean and average errors with minimum of 1655.30 ± 21.83 *μSv.h*$^{-1}$ and maximum of 3886.28 ± 42.61 *μSv.y*$^{-1}$. The annual effective dose rate values are significantly higher than the world permissible value of 70 *μSv.y*$^{-1}$ (UNSCEAR, 1988).

Radium equivalent (***Ra***$_{eq}$) shows values between 2933.08 ± 38.53 *Bq.kg*$^{-1}$ and 6877.55 ± 75.42 *Bq.kg*$^{-1}$. All ore samples presented that the calculated radium equivalent values are higher than the maximal permissible value of 370 Bq.kg^{-1} for building materials (UNSCEAR, 2000). This means that uranium ore deposits should not in any way allowed to be in close contact or used in material to be used for building of dwellings or offices. The **external exposures** (external hazard index, H_{ex}) was calculated with a minimum of 7.93 ± 0.10 and maximum of 18.59 ± 0.20. The external hazard index of uranium ore samples were higher than the maximum permissible limit of 1 mSv.y^{-1} due to natural radioactive materials in the mine (Kamunda *et al*., 2016).

To conclude, the radioactivity level of uranium ore sediments calculated from a uranium mine in Erongo Region, Namibia, indicates that uranium mining activities pose a high radiological health risk to employees. Therefore, there is a high risk of possible cancer cases that may arise as a result of

continued exposure to radioactivity from primordial nuclides of ^{238}U, ^{232}Th and ^{40}K.

Recommendations

In addition to all protocols and radiation safety measures that are already put in place by uranium mines in collaboration with the National Radiation Protection Authority (NRPA) and in compliance with IAEA, close check-ups and examinations for employees must be put in place and implemented on a regular basis.

References

Ademola, A. K., Bello, A. K. & Adejumobi, A. C. 2014. Determination of natural radioactivity and hazard in soil samples in and around gold mining area in Itagunmodi, south-western, Nigeria. Journal of Radiation research and applied sciences, 7, 249-255.

Alzubaidi, G., Hamid, F. & Abdul Rahman, I. 2016. Assessment of natural radioactivity levels and radiation hazards in agricultural and virgin soil in the state of Kedah, North of Malaysia. The Scientific World Journal, 2016.

Amanjeet, Kumar, A., Kumar, S., Singh, J., Singh, P. & Bajwa, B. 2017. Assessment of natural radioactivity levels and associated dose rates in soil samples from historical city Panipat, India. Journal of Radiation Research and Applied Sciences, 10, 283-288.

Chhangte, L., Rohmingliana, P., Sahoo, B., Sapra, B., Zoliana, B. & Pachuau, Z. Measurement of primordial radionuclides in soils and building materials from Mizoram, India. Mizoram Science Congress 2018 (MSC 2018), 2018. Atlantis Press.

Durusoy, A. & Yildirim, M. 2017. Determination of radioactivity concentrations in soil samples and dose assessment for Rize Province, Turkey. Journal of Radiation Research and Applied Sciences, 10, 348-352.

ISO18589–2 2007. Measurement of Radioactivity in the Environment - Soil - Guidance for the Selection of the Sampling Strategy, Sampling and Pre-treatment of Samples.

ISO18589–3 2007. Measurement of Radioactivity in the Environment - Soil - Measurement of Gamma-emitting Radionuclides.

Kamunda, C., Mathuthu, M. & Madhuku, M. 2016. An Assessment of Radiological Hazards from Gold Mine Tailings in the Province of Gauteng in South Africa. International Journal of Environmental Research and Public Health, 13, 138.

Unscear 1988. Sources, Effects and Risks of Ionizing Radiation: United Nations Scientific Committee on the Effects of Atomic Radiation UN.

UNSCEAR 2000. Effects of Ionizing Radiation. United Nations, New York, 453-487.

WHO 1994. International basic safety standards for protection against ionizing radiation and for the safety of radiation sources.

Prediction of Water Quality Parameters Using Unmanned Aerial Vehicle Multispectral Imagery in Acidic Water Bodies in the Iberian Pyrite Belt (Tharsis, SW Spain)

Melisa Alejandra Isgró[1,2], María Dolores Basallote[1], Luis Barbero[2]

[1]*Department of Earth Sciences, Research Center on Natural Resources, Health and the Environment (RENSMA), University of Huelva, Campus El Carmen s/n, 21071 Huelva, Spain; meli.isgro@gmail.com, maria.basallote@dct.uhu.es*

[2]*Department of Earth Sciences, University of Cádiz, Campus Universitario de Puerto Real, 11510 Puerto Real, Cádiz, Spain, luis.barbero@uca.es*

Abstract

This study presents a novel approach of using high-resolution multispectral data acquired by an unmanned aerial system (UAS) combined with in situ chemical data to assess water quality parameters at 12 relatively small water bodies located in the Tharsis complex, an abandoned mining area highly affected by acid mine drainage (AMD) pollution. The spectral data jointly with water physicochemical data were used to estimate water quality parameters using regression analysis. Parameters including pH, ORP, EC, Al, Cu, Fe, Mn, S, Si, and Zn were estimated with high accuracy levels while Ba, Ca, and Mg showed low accuracy.

Keywords: Acid Mine Drainage, Abandoned Mine, Water Monitoring, Drone, Low Altitude Remote Sensing, Multispectral Sensor

Introduction

AMD is the main environmental pollution problem associated with coal and metal-bearing mineral mining. It is of international concern due to the difficulty in avoiding its formation and its long-lasting nature; it can occur indefinitely even after mining operations have ceased (Qian and Li 2019). Thus, there is a need to develop monitoring tools that can be used by the competent environmental agency and companies in charge of the mining concessions. Traditional procedures for water quality monitoring in reservoirs involve in-situ measurements, sampling, and laboratory analysis. Remote sensing provides a powerful alternative tool that is less time-consuming and provides spatial and temporal information to monitor water quality changes. However, this approach has been scarcely used to report the water quality status in mining areas. Water bodies associated with AMD have a complex composition that requires quantifying a wide range of parameters and few studies have addressed this issue by applying quantitative modeling of hydrochemical concentrations (Tesfamichael and Ndlovu 2018; Modiegi *et al*. 2020). Most recently, UAS-based hyperspectral data have been successfully used to monitor acidic water, generating high-resolution hydrogeochemical maps (Flores *et al*. 2021). Indeed, UAS is becoming increasingly popular in environmental monitoring due to its acquisition flexibility, high spatial and temporal resolution achieved, and the possibility of acquiring data not affected by cloud cover.

In this context, the calibration of empirical models is proposed through regression analysis to predict water quality parameters using in situ physicochemical parameters and spectral reflectance values obtained by a commercial sensor, the Micasense RedEdge-MX Dual. This sensor has already been tested for many purposes such as crop mapping, forestry, minerals mapping and land cover analysis. The Iberian Pyrite Belt (IPB), which hosts one of the largest concentrations of massive sulfides on Earth and is well-known for its mining tradition and extensive AMD environmental impacts, was selected as the study area. This work is

intended to implement an easily reproducible tool that can be used to monitor water bodies with different complex compositions in mine-affected zones.

Methods

Field campaigns were carried out during July and October 2020, consisting of simultaneous flight surveys with the Micasense RedEdge-MX Dual sensor onboard a UAS and in situ physicochemical data acquisition. The sampling sites involved 12 different water bodies containing acid and non-acid waters located in two abandoned mining sites in the Tharsis complex, in the IPB (fig. 1), the Tharsis Mine (fig. 1 A) and the Lagunazo Mine (fig. 1 B).

Field physicochemical parameters such as pH, electrical conductivity (EC), and oxidation-reduction potential (ORP) were measured at each sampling point (yellow circles, fig. 1) with a CrisonMM40 þ multimeter, previously calibrated with certified solutions. Water samples were collected in high-density polyethylene (HDPE) bottles previously washed with a solution of 10% HNO^3, filtered immediately after sampling through a 0.45 mm pore size cellulose nitrate membrane, and acidified to pH < 2 with HNO^3. The samples were analyzed by inductively coupled plasma-atomic emission spectroscopy (ICP-AES; Perkin-Elmer® Optima 3200 RL) for major elements determination (Al, Ba, Ca, Cu, Fe, K, Mg, Mn, Na, P, S, Si, Sr, and Zn) at the Institute of Environment Assessment and Water Research (IDAEA-CSIC, Barcelona). Sierra Bullones (SB, fig. 1A) was not water sampled due to its inaccessibility. However, as it is connected underground to Filón Norte, and since their chemical properties have been shown to be similar (González *et al.* 2018), they were considered the same for this study.

The flight surveys were performed with the multispectral sensor Micasense RedEdge-MX Dual Camera onboard a DJI Matrice 210 V2 RTK. For all the missions, the height was set at 120 m AGL (above ground level) altitude to ensure a ground sample distance (GSD) of 8 cm/pixel, the overlapping was set at 80% frontal and 75% side image overlap, the grid was simple, and the speed was set at 10 m/s. It is assumed that all the multispectral imagery is in the nadir position due to the location of the camera. The Downwelling light sensor (DLS 2) and MicaSense's calibrated reflectance panel (CRP) were used in all the flights. The multispectral images were processed using the Pix4D mapper Structure from Motion (SfM) software. To perform the extraction of the spectral signature of each of the water bodies from the multispectral imagery, the centroid of the water body shape was extracted and the mean reflectance value of all the pixel values included in a circular buffer of 3 m around each centroid point was estimated using the zonal statistics plugin of QGIS 3.10.7.

The collected data were divided into two subsets, the model calibration dataset (70%) and the validation dataset (30%). The waterbodies flights from July (EP) and from October (FC, FN, EG, EL, ML, SB, LLA, and LLB) were used for the model calibration, while the validation dataset consisted of the Th18, EG, and FS from July and LLC from

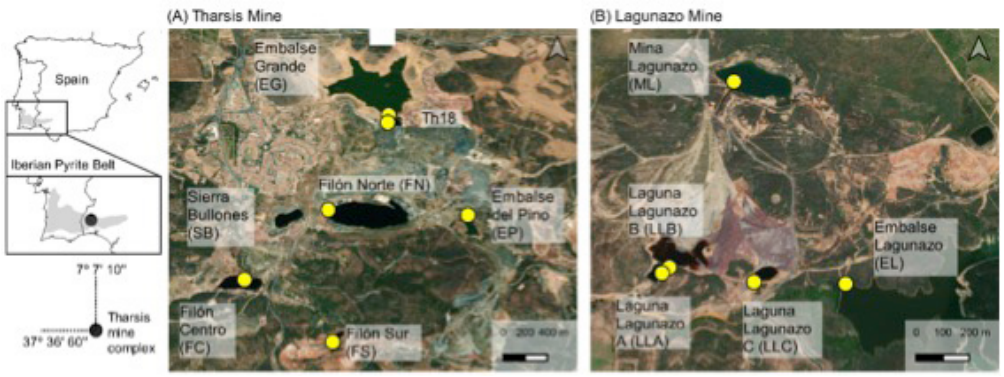

Figure 1 *Location map of the sampling sites. Yellow circles indicate the water samples collection.*

Table 1 List of Spectral Band Combinations (SBCs) tested in this study.

Algorithm	Band math	Reference
A1 (NDVI)[1]	(NIR-R650)/(NIR+R650)	(Rouse and Space 1978)
A2 (NDWI)[2]	(g560-NIR)/(g560+NIR)	(McFeeters 1996)
A3	r650/re705	Simple ratio
A4	re705/nir	Simple ratio
A5	(g531/g560)*r650	Three-band algorithm
A6	(re705/re717)*r668	Three-band algorithm
A7	(g560*g531)/b475	Three-band algorithm
A8	(g560-g531)/b475	Three-band algorithm
A9	(g560/g531)*b475	Three-band algorithm
A10	(re705/r650)*g531	Three-band algorithm

[1]Normalized difference vegetation index (NDVI); [2]Normalized difference water index (NDWI)

October (the only data for LLC presented). To determine which spectral bands and/or spectral band combinations (SBCs) were the best predictor for each chemical parameter, a correlation analysis was carried out between the raw and the ln-transformed chemical data versus the mean reflectance values of the spectral bands and the tested SBCs. Then, using the model calibration dataset, empirical models were constructed relating the mean reflectance values of the significant bands and/or the SBCs as the predictable variable with the chemical data and ln-transformed chemical data as the dependent variable. A total of 17 water quality parameters (pH, ORP, EC, Al, Ba, Ca, Cu, Fe, K, Mg, Mg, Na, P, S, Si, Sr, and Zn), the 10 sensor's spectral bands and 10 SBCs (table 1) were considered in this study. To ensure reliable models, simple linear regression (SLR) and multiple linear regression (MLR) using a stepwise selection method were tested. The prediction quality of the models was assessed on the validation dataset and the performance metric statistics calculated were: normalized root mean square error (RMSE%), mean absolute percentage error (MAPE), Mean absolute error (MAE), bias, and coefficient of determination (R^2). The best-fitted models were used to generate spatial distribution maps.

Results

According to the in situ and laboratory measurements of the water quality parameters, which are representative of the water surface layer's composition at the time of sampling, the waterbodies selected showed a wide range of water compositions, from circumneutral to extremely acidic pH (0.01 - 7.76) and from low to high metal-enriched solutions (e.g., 0.04 - 4795.70 mg L^{-1} of Al, 0.04 - 318.67 mg L^{-1} of Mn, 0.06 - 2011.35 mg L^{-1} of Zn). Concerning the pH value, EP, FC, FN, FS, SB, ML, TH18, LLA, LLB, LLC correspond to acid waters (pH 0.01 - 3.81) while EG and EL are non-acid water (pH 6.62 - 7.76).

Apart from the physicochemical composition, the water bodies can be grouped based on their colors, which mainly depends on the contents of organic matter, algae, suspended particulates, and nutrients. Thus, while EG and ML have shades of brown or green, EP and ML present greenish-blue color, and the rest of the acid water bodies have a dark reddish-brown color. The Fe^{+2} ions give water a greenish color and when Fe^{+3} ions are more abundant, they are responsible for giving the water the intense red color (Schroeter and GläÄer 2011; Riaza *et al.* 2014; Davies and Calvin 2017; Flores *et al.* 2021). Although in this study, the Fe speciation was not quantified, the ORP values of about 500 mV found in all the dark reddish-brown acid waters indicate oxidized aqueous environments and the prevalence of ferric iron (Flores *et al.* 2021). In contrast, the redox potential in the greenish-blue acidic water bodies (i.e. EP and ML) was about 300 mV, suggesting that Fe^{+2} ions prevail over Fe^{+3}. The dissolved iron composition in the dark reddish-brown acid waters was between 352.37 (TH18) and 68940.00 (LLB) mg L^{-1}, while for the rest of the water bodies it ranged between 0.05 (EL) - 0.99 (ML) mg L^{-1}.

The elements K, P, Na, and Sr did not show a significant correlation with any spectral band or SBC, and they were discarded from the model calibration. The parameters correlated to a band or SBC with a Pearson coefficient exceeding 0.8 were used to construct different SLR and MLR models. Among the various regression representations with the validation dataset, the models having the best performance metric statistics were selected as the final model to predict the spatial distribution of water parameters (table 2). The lowest values of RMSE% registered by the selected models (RMSE% = 4 for ln(ORP) and RMSE% = 12 for ln(Ca) reflected the good prediction capability of the models. Ln(Al), ln(Ca), and ln(Mn) showed a tendency to underestimate the observed values (bias ranging from -0.11 to -0.73), while the rest of the models tended to overestimate the real values, giving a positive bias (from 0.0 to 0.75). Even though ln(Ca) showed good results in the model calibration and the validation metrics were better than other models, the R^2 showed poor correlation between the observed and modeled values (R^2 = 0.56). Due to the low accuracy in the prediction, ln(Ca), Ba, and ln(Mg) were dismissed ($0.42<R^2<0.70$) (table 2). The rest of the models presented good fitness between modeled and observed values with R^2 values between 0.81 and 0.99, showing the robust relationships found between the spectral and physicochemical data. Ln(Si) had the best correlation between modeled and observed values of all, confirming the high R^2 (0.99) and low RMSE% value (18%, table 2).

Few studies have quantitatively analyzed water bodies in mining environments applying remotely-sensed spectra to compare with the above findings. Recently Flores *et al.* (2021) applied UAS-hyperspectral imaging to map pH, redox, Al, and Fe concentration in the confluence between the Odiel River and the Tintillo River (Iberian Pyrite Belt, Huelva province). They applied a supervised random forest regression approach, obtaining R^2 values of 0.73, 0.82, 0.68, and 0.66, respectively, with the pixels only used as the validation set. Instead, our study found R^2 values of 0.98 (pH), 0.85 (ORP), 0.98 (Al), and 0.94 (Fe). Although our values are higher, the prediction of water quality parameters in a rapidly changing environment, such as a river, is a more challenging task since the spectral response of water can be affected by the water depth and dynamics. By contrast, the spectral response of a deep and steady water body is expected to be homogeneous, giving higher performance metrics. Schroeter and GläÄer (2011) characterized some water quality parameters in lignite mining lakes, among them pH and Fe. They used a bivariate correlation between Landsat TM satellite data and the chemical analysis, but no models were developed. The highest correlation was found between the red band and Fe (r=0.645), while pH and the red band were poorly correlated (r

Table 2 *Performance metric statistics for the best-fitted water quality parameters.*

WQP	Regression	Candidate model	RMSE%	MAPE	bias	R^2
pH	MLR	2.046-5.674*A1+56.413*A7	15%	0.19	0.31	0.98
ln(ORP)	SLR	6.397-25.657*A7	4%	0.03	0.16	0.85
ln(EC)	SLR	3.633-138.510*g531	32%	0.04	0.09	0.87
ln(Al)	MLR	6.230-142.199*A7+6.751*A1	14%	-0.04	-0.17	0.98
Ba	SLR	0.003+0.818*g560	57%	0.97	0.00	0.42
ln(Ca)	SLR	6.223-81.167*g531	12%	0.10	-0.11	0.56
ln(Cu)	SLR	4.957-170.154*A7	57%	0.17	1.09	0.92
ln(Fe)	SLR	9.489-275.345*A7	25%	0.01	0.75	0.94
ln(Mg)	SLR	6.606-114.772*g531	14%	0.10	0.13	0.7
ln(Mn)	SLR	4.865-135.763*A7	75%	0.056	-0.73	0.95
ln(S)	SLR	9.874-181.692*g560	14%	0.09	0.33	0.81
ln(Si)	SLR	4.336-99.318*A7	18%	-0.19	0.19	0.99
ln(Zn)	SLR	6.259-184.166*A7	40%	0.11	0.22	0.83

SLR: Simple linear regression; MLR: Multiple linear regression

= −0.378). However, in the present study, the correlations found were stronger for both parameters. The pH was correlated with r650 (r = 0.765) but had the highest correlation with A1 (r = −0.92, table 1). The Fe concentration was also correlated with r650 (r = −0.66) having the best correlation with A7 (r = −0.93, tab.). Tesfamichael and Ndlovu (2018) estimated physicochemical parameters from ASTER and Landsat imagery in a gold mining area. Both satellites performed similarly in estimating Eh and Ca ($0.25 < R^2 < 0.36$ and $19 < RMSE\% < 56$). Redox potential was estimated using the blue band (Landsat) and SWIR 6 (ASTER), while Ca was estimated using short-wave infrared band (Landsat) and NIR (ASTER). In this study, ORP was best estimated using A7 ($R^2 = 0.85$ and RMSE% = 4 and ln(Ca) using g531 (R^2 0.56 and RMSE% = 12). In light of this, the models generated with UAS-multispectral imagery were different in the selected bands than in the previous studies but the accuracy of the obtained models was higher, enhancing the value of low altitude remote sensing at a local scale.

Finally, to show the real potential of UAS for monitoring acidic water and predicting water quality parameters, the empirical relationships obtained were extended to the LLC validation dataset, producing spatial distribution maps for each studied parameter (fig. 2). LLC (fig. 1B) is a small waterbody highly affected by AMD, originated by surficial waters flowing through the waste dump and pyritic waste. The water is stagnant and its composition is expected to be homogeneous throughout the water surface. Nevertheless, fig. 2 shows the surface water intake at the right edge, which has a different composition from the rest of the water body. This water intake was analyzed and presented a pH value of 3.12, EC of 0.415 mS/cm (ln EC=0.415 mS/cm), and ORP of 415 mV (ln ORP=6.028 Mv). These values are coincident with the ones observed in fig. 2.

Conclusion

The current study demonstrates that the application of empirical models to generate spatial distribution maps can be an effective and easily applicable monitoring tool in AMD-affected sites. Moreover, the Micasense RedEdge-MX Dual commercial sensor performed well, predicting several water quality parameters, which is especially valuable for small water bodies that cannot be monitored by satellites due to their low spatial resolution. The results obtained here are intended to contribute to the water

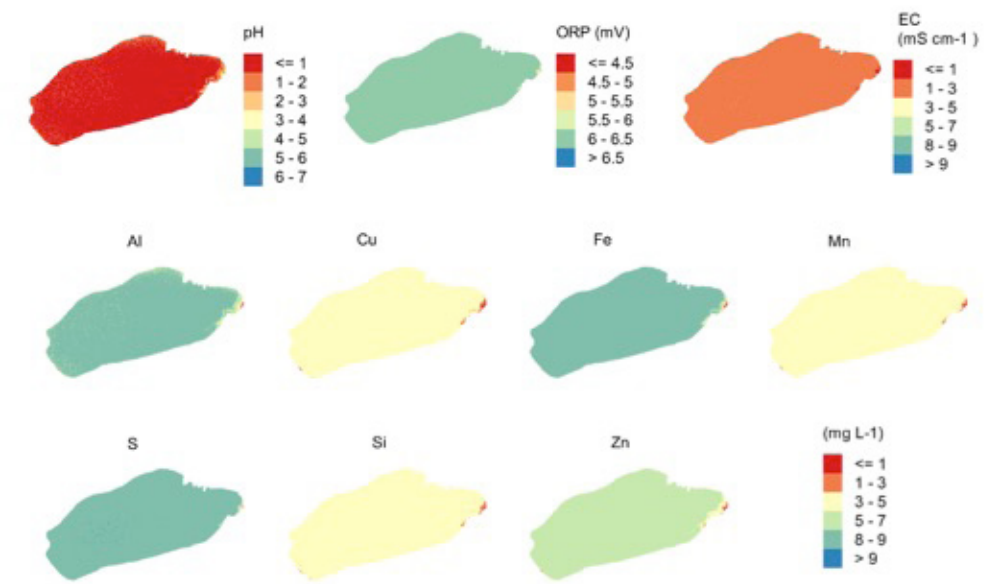

Figure 2 *Spatial distribution maps for the estimated water quality parameters in Laguna Lagunazo C (LLC). All the models were performed with ln-transformed data, except pH.*

resources management and decision-making process during the exploitation and closure phase of mining sites. It is noteworthy that the empirical models are data-driven and are based on in situ water quality measurements. Thus, the models found in this study should be calibrated for application in other locations, water type, and/or season. For instance, if in a mining area is neutral and alkaline metalliferous drainage rather than just AMD, this must be considered during the calibration phase. Further studies should be done to investigate the influence of seasonal variability on the reflectance values of the water bodies due to changes in the dissolved concentrations of pollutants.

Acknowledgements

This study was supported in part by the Erasmus Mundus Joint Master Degree (EMJMD) in Water and Coastal Management (WACOMA) with the contribution of the Erasmus+ Programme of the European Union. This work is also supported by Plan Andaluz de Investigación RNM 166 Environmental radioactivity research group (LB). UAS equipment from University of Cádiz Drone Service supported by MINECO infrastructure projects (EQC2018-00446-P and UNCA-2013-1969). M.D. Basallote thanks the Spanish Ministry of Science and Innovation for the Postdoctoral Fellowships granted under application reference IJC2018-035056-I.

References

Davies GE, Calvin WM (2017) Quantifying Iron Concentration in Local and Synthetic Acid Mine Drainage: A New Technique Using Handheld Field Spectrometers. Mine Water Environ 36:299–309. https://doi.org/10.1007/s10230-016-0399-z

Flores H, Lorenz S, Jackisch R, *et al* (2021) UAS-Based Hyperspectral Environmental Monitoring of Acid Mine Drainage Affected Waters. 1–25

González RM, Olías M, Macías F, *et al* (2018) Hydrological characterization and prediction of flood levels of acidic pit lakes in the Tharsis mines, Iberian Pyrite Belt. J Hydrol 566:807–817. https://doi.org/10.1016/j.jhydrol.2018.09.046

McFeeters SK (1996) The use of the Normalized Difference Water Index (NDWI) in the delineation of open water features. Remote Sens Environ 25:687–711

Modiegi M, Rampedi IT, Tesfamichael SG (2020) Comparison of multi-source satellite data for quantifying water quality parameters in a mining environment. J Hydrol 591:125322. https://doi.org/10.1016/j.jhydrol.2020.125322

Qian G, Li Y (2019) Acid and Metalliferous Drainage – A Global Environmental Issue. J Min Mech Eng 1–4

Riaza A, Buzzi J, García-Meléndez E, *et al* (2014) Monitoring acidic water in a polluted river with hyperspectral remote sensing (HyMap). Hydrol Sci J 60:1064–1077. https://doi.org/10.1080/02626667.2014.899704

Rouse JW, Space G (1978) Monitoring the vernal advancement of retrogradation of natural vegetation. Third ERTS Symp 1:48–62

Schroeter L, GläÄer C (2011) Analyses and monitoring of lignite mining lakes in Eastern Germany with spectral signatures of Landsat TM satellite data. Int J Coal Geol 86:27–39. https://doi.org/10.1016/j.coal.2011.01.005

Tesfamichael SGU of A and L for quantifying hydrochemical concentrations in abandoned gold mining, Ndlovu A (2018) Utility of ASTER and Landsat for quantifying hydrochemical concentrations in abandoned gold mining. Sci Total Environ 618:1560–1571. https://doi.org/10.1016/j.scitotenv.2017.09.335

Biodiversity Benefits of Coal Mine Water Remediation Schemes for Bird Life

Rosie O. Jaques[1], Arabella M.L. Moorhouse-Parry[2], Richard Carline[2], William M. Mayes[1], Susan L. Hull[3]

[1]*Department of Geography, Geology and Environment, University of Hull, Hull, HU6 7RX, UK, w.mayes@hull.ac.uk*

[2]*The Coal Authority, Mansfield, Nottinghamshire, NG18 4RG, UK*

[3]*Department of Biological and Marine Sciences, University of Hull, Hull, HU6 7RX, UK*

Abstract

Lagoons and reedbeds are established components of mine water treatment systems for iron-rich coal mine drainage. This study coupled modified British Trust for Ornithology (BTO) Breeding Bird Survey monitoring with habitat survey to assess the presence and usage of two UK coal mine water treatment systems by bird species. Over thirty species were documented at the two sites including four red listed, eight amber listed and eighteen green listed species (under the BTO Birds of Conservation Concern designation). There were statistically significant associations of bird group with specific habitat types suggesting that a mosaic of habitats at coal mine treatment systems benefits bird diversity and that these sites may have conservation potential at the landscape level.

Keywords: Mine Water, Remediation, Bird Survey, Ecology, Constructed Wetlands

Introduction

The legacy of coal mine water pollution in the United Kingdom has led to an extensive management programme run by the UK Government's Coal Authority addressing predominantly iron (Fe)-rich coal mine waters (Johnston *et al*. 2008). This programme consists of over 80 schemes which protect ≈350 km of streams from mine drainage (Coal Authority, 2021). A large proportion of these treatment systems incorporate lagoons and aerobic reedbeds to aid settlement of Fe as the chief pollutant of concern. These systems are engineered to maximise Fe removal within the available land area (e.g., Sapsford and Watson, 2011). However, the creation of a mosaic of open water, marginal and reedbed habitats associated with the treatment may provide benefits for local biodiversity.

Reedbed habitats have seen severe global declines in the last 150 years (Mitsch and Gosselink, 2015) and are considered a priority habitat type in the UK under biodiversity action plans and in the European Union. There is extensive literature on the importance of such habitats for bird life, notably declining passerine (perching bird) species such as Bearded Tit (*Panurus biarmicus*) as well as the Eurasian Bittern (*Botaurus stellaris*) for which considerable conservation efforts have been developed in the EU in recent decades (RSPB, 2013). Indeed, there have been major efforts in modern extractive industries to incorporate reedbed habitats as part of site restoration (Jarvis and Walton, 2010).

Across the treatment schemes within the current portfolio, the Coal Authority manage over 35 hectares of reedbed across the UK coalfields. The potential biodiversity benefits of these mine treatment wetlands have, however, received relatively little attention. Batty *et al*. (2005) demonstrated that although macroinvertebrate diversity and abundance was lower in coal mine water treatment systems than natural wetlands, the communities present were sufficient to potentially support higher organisms. More recent research which looked at a variety of constructed wetlands, including some used for mine water treatment, suggested that artificial reedbeds are just as diverse as natural systems for a number of different taxa, however, such as small mammals, moths and stem-dwelling invertebrates (Athorn, 2017)

This preliminary study aimed to undertake a baseline survey of bird species and their associated habitat usage at two coal mine water treatment systems in South Yorkshire, UK.

Methods

The study sites at Woolley and Strafford (South Yorkshire, UK) both treat circumneutral pH, ferruginous pumped coal mine water from Carboniferous Coal Measures strata. Treatment systems at both sites comprise aeration cascades, lagoons, and polishing reedbed cells. Reedbed cells are dominated by common reed (*Phragmites australis*) with marginal vegetation consisting of sedges and rushes with additional planting along the banks in some areas. These are typical in configuration of treatment systems adopted in the UK for coal mine water (and ironstone mine water) remediation (Coal Authority, 2021).

Habitat surveys at each site were undertaken during initial site visits using the Joint Nature Conservation Committee Phase 1 Survey procedure (JNCC, 2010). Bird surveys were undertaken using a modified British Trust for Ornithology (BTO) Breeding Bird Survey (BTO, 2021a), which is a long-established technique for the monitoring of bird populations during the UK breeding season (April-June). Early morning surveys in late Spring and early Summer were undertaken at each site following a timed (two and a half hour) transect route around each site, with stops at key vantage points. Repeat surveys were undertaken eight times at Strafford and six times at Woolley during 2019.

Birds were identified based on visual observation and vocalisations with abundance counted in each habitat unit present at the sites. Species present were compared to established lists of conservation concern (BTO, 2021b; IUCN, 2021) to consider the relative conservation importance of birds observed. Overall bird density (bird abundance per hectare) was compared across the sites using a T-test to test the null hypothesis that there was no significant difference in average bird density between the sites. A Chi-Squared test was undertaken to test if there was a significant association between bird group and Phase 1 habitat type.

Results and Discussion

Bird species and abundance

Over three hundred and fifty birds across thirty species were documented at the two sites during the surveys. These include a number of birds of conservation concern under the British Trust for Ornithology (BTO) Birds of Conservation Concern designation (BoCC4) including four red listed species, eight amber listed and eighteen green listed species (Tab. 1).

There were also 16 species rated on the amber or red list of the International Union for the Conservation of Nature (IUCN, 2021). Of particular note were the reedbed specialist species such as Reed Bunting (*Emberiza schoeniclus*), Sedge and Reed Warblers (*Acrocephalus schoenonaenus* and *Acrocephalus scirpaceus* respectively) and species that are considered indicators of healthy aquatic environments such as the Grey Heron (*Ardea cinerea*) and Kingfisher (*Alcedo atthis*: Furness and Greenwood, 2013). Two red list species more commonly associated with agricultural habitats, Linnet (*Linaria cannabina*) and Yellowhammer (*Emberiza citrinella*), were observed around the margins of the Woolley site (Tab. 1).

There was no significant difference in average bird density at the two sites (T-test: t: 0.66; degrees of freedom: 12; $P>0.05$) despite the slight differences in species encountered at the two sites (Tab. 1; Fig. 1). Woolley had a mean bird density of 7.8 birds/ha (standard deviation: 1.99) with Strafford showing on average 9.1 birds/ha (standard deviation: 1.97). It is worth noting that these densities are of a similar range to published densities for bird populations from natural or modified wetland systems. For example, Báldi and Kisbenedek (1999) observed bird densities of 10.2-11.4 birds/ha across both margins and the interior of mature reedbed in central Hungary, while Paracuellos (2006) reports densities ranging from 0.9 to 25.9 birds/ha in fragmented reedbed in the Netherlands.

Bird species habitat preference

As would be anticipated given the range of species observed, there were strong and significant associations between bird species and Phase 1 habitat (Chi-squared: 386; degrees

Table 1 *Examples of bird species of conservation importance observed at the Woolley and Strafford coal mine water treatment systems and their UK and international conservation status. Only bird species of amber or red status on either scheme included. Sites: S: Strafford; W: Woolley.*

Common name	Scientific name	Site	BTO BoCC4 rating	IUCN rating
Buzzard	*Buteo buteo*	W	Green	Amber (least concern)
Carrion Crow	*Corvus corone*	W	Green	Amber (least concern)
Grey Heron	*Ardea cinerea*	SW	Green	Red (least concern)
Grey Wagtail	*Motacilla cinerea*	W	Red	Unknown
House Martin	*Delichon urbicum*	SW	Amber	Red (least concern)
Kestrel	*Falco tinnunculus*	W	Amber	Red (least concern)
Kingfisher	*Alcedo atthis*	W	Amber	Unknown
Linnet	*Linaria cannabina*	W	Red	Red (least concern)
Long-tailed Tit	*Aegithalos caudatus*	W	Green	Amber (least concern)
Moorhen	*Gallinula chloropus*	SW	Green	Amber (least concern)
Reed Bunting	*Emberiza schoeniclus*	SW	Amber	Red (least concern)
Reed Warbler	*Acrocephalus scirpaceus*	SW	Green	Amber (least concern)
Sedge Warbler	*Acrocephalus schoenobaenus*	W	Green	Amber (least concern)
House Sparrow	*Passer domesticus*	SW	Red	Red (least concern)
Swallow	*Hirundo rustica*	SW	Green	Red (least concern)
Swift	*Apus apus*	SW	Amber	Amber (least concern)
Willow Warbler	*Phylloscopus trochilus*	SW	Amber	Red (least concern)
Yellowhammer	*Emberiza citrinella*	W	Red	Red (least concern)

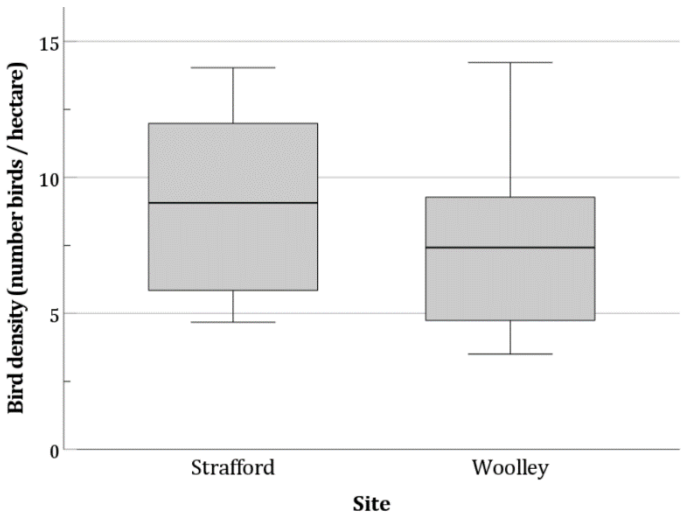

Figure 1 *Bird density (number of birds per hectare) observed at the two study sites. Data show mean, interquartile range and range (n: 8 for Strafford; n: 6 for Woolley)*

of freedom: 21; P<0.001; Tab. 2). Reedbeds were favoured by passerine (perching bird) species including the amber listed Reed Bunting (*Emberiza schoeniclus*) and green listed Sedge and Reed Warblers (*Acrocephalus schoenonaenus* and *Acrocephalus scirpaceus* respectively). Swifts (*Apus apus*) were also commonly found feeding above reedbed areas.

Open water areas of lagoons and margins of wetlands were beneficial for waterfowl, herons and kingfisher, while marginal grassland and scrub habitat was used by a range of passerines including the red-listed Yellowhammer (*Emberiza citrinella*) and Linnet (*Linaria cannabina*). Field observations showed kingfishers actively preying on small fish in open water areas of wetland cells at the Woolley site, which offers a useful indication of a healthy aquatic ecosystem at distal parts of the treatment system.

Management implications

The data highlight the potential importance of coal mine water treatment sites for bird life, including some species of conservation concern. The presence of species associated with open water and reedbed habitat (e.g., Sedge and Reed Warbler: *Acrocephalus schoenonaenus* and *Acrocephalus scirpaceus*) during the breeding season is encouraging given many mine treatment systems in the UK are located in valleys that would have historically contained floodplain wetlands prior to agricultural and industrial modification (Davidson, 2014).

Habitat variability within and around the margins of treatment systems appears key in driving a greater diversity of species (Tab. 2). Such patterns are widely documented in other settings around heavily modified wetland systems, where greater habitat heterogeneity and complexity can positively influence the diversity of prey species for birds (e.g., Day *et al.*, 2017). This is an area that is being actively considered in coal mine water treatment system design for future schemes where land availability allows.

The design and engineering of coal mine water remediation schemes will continue to be driven by water quality targets (e.g., Sapsford and Watson, 2011) and maintenance requirements, but there is scope for complementary management interventions that enhance bird diversity. For example, reedbed designs now include areas of open water at both cell inlets and outlets to help control the spread of the reeds and to improve access to the wetland cells when reed cutting is required.

Furthermore, trials by the Coal Authority are underway at sites where reedbeds are now being refurbished, to help improve the recovery of the reedbeds through transplantation of plants (and associated sediments and potential invertebrate populations) from acclimatised populations and established seedlings. This should allow the reeds to establish more quickly, which will likely assist iron removal, but also help re-establish the wetland habitat more rapidly. From a habitat

Table 2 *Aggregate number of observations across both sites of species presence (grouped by bird class) in different habitats across the coal mine water treatment systems.*

Bird class	Open water	Reedbed	Grassland / scrub	Woodland
Anatidae (water birds)	87	3	1	0
Galliformes (landfowl)	0	0	1	0
Ciconiformes (herons)	1	3	0	0
Accipitriformes (diurnal birds of prey)	0	1	0	1
Columbiformes (pigeons and doves)	0	2	4	4
Apodiformes (swifts)	0	20	0	0
Passeriformes (perching birds)	0	140	7	32
Coraciiformes (kingfishers)	2	1	0	0

management perspective, this is particularly important for older treatment systems where the reedbeds may be supporting isolated bird communities reliant on the treatment system. It is worth noting that at treatment sites where multiple reedbeds are present, maintenance activities are often staggered to minimise any impact on treatment capacity; this has the added benefit of ensuring that local reedbed habitat is retained.

Routine reed cutting is an essential maintenance activity at coal mine water treatment systems. In natural wetlands, this assists in maintaining the reedbed by slowing the build up of organic debris in the treatment cells (Valkama *et al*., 2008). In mine water reedbeds a build up of organic detritus can reduce treatment performance by causing the water to short circuit, thereby reducing residence times and consequently iron removal rates. Another advantage of reed cutting, however, is that it can also help maximise the extent of reedbed edges, which in other studies have been shown to be preferred by numerous species (e.g., Reed Warbler: *Acrocephalus scirpaceus*) above reedbed interior habitats (Baldi and Kisbenedek, 1999).

Many of the species observed at the sites are not typically associated with aquatic or wetland habitats. Site margins (open grassland, grass banks, hedgerows and woodland) were particularly important for a range of predominantly passerine species which included some of conservation concern (Tab. 1). Maximising site margins for potential bird food resources and breeding sites through a reduced mowing regime (i.e., once per year) and the planting of a diverse mix of native herbaceous and flowering plants to encourage insect prey could be of benefit in these areas of treatment systems. Interestingly, Yellowhammers and Linnets, both Red listed by BTO, (2021b) are farmland birds, suggesting that the careful management of industrial sites across a broader area may have potential for the conservation of these species.

Conclusions

The baseline survey of birds undertaken at two coal mine water treatment systems in the UK shows the presence of a range of bird species of conservation interest during the breeding season. Both sites showed similar bird species density with strong associations apparent between bird type and their habitat usage. Efforts to ensure greater habitat variability within coal mine water treatment systems are likely to benefit bird diversity.

Assessment of bird communities at other mine water treatment systems would help add to this preliminary study as would usage over the entire year to determine if such sites are also used by winter visitors as well as summer breeding species. Comparisons with natural systems would also be useful in assessing the relative contribution of mine water treatment systems to changes in bird biodiversity. Such information could not only assist in helping formulate habitat management plans at established treatment systems, but potentially assist in integrating mine water treatment with landscape scale conservation measures during planning phases.

Acknowledgements

The authors thank the organisers and hosts of the IMWA2021 Conference, in addition to the anonymous reviewers of this manuscript, whose comments have been valuable during the peer-review process. This work formed part of the Bachelor of Science degree in Geography for ROJ and thanks are extended to Sean Box (Severn Trent Services) for facilitating site access.

References

Athorn. M. (2017) *Conservation value of Constructed Wetlands*, Nottingham University PhD Thesis p162

Báldi A, Kisbenedek, T, (1999) Species-specific distribution of reed-nesting passerine birds across reed-bed edges: effects of spatial scale and edge type. Acta Zoologica Academiae Scientiarum Hungaricae, 45:97-114.

Batty LC, Atkin L, Manning, DAC, (2005) Assessment of the ecological potential of mine-water treatment wetlands using a baseline survey of macroinvertebrate communities. Environ Pollut, 138:412-419.

British Trust for Ornithology (2021a) Breeding Bird Survey. Available at: https://www.bto.org/our-science/projects/bbs [last accessed 20/4/21]

British Trust for Ornithology (2021b) Birds of Conservation Concern 4: the red list for birds. Available at: https://www.bto.org/our-science/publications/psob [last accessed: 20/4/21]

Coal Authority (2021) Coal Mine Water Treatment. Available at https://www.gov.uk/government/collections/coal-mine-water-treatment [last accessed: 20/4/21]

Davidson NC, (2014). How much wetland has the world lost? Long-term and recent trends in global wetland area. Marine and Freshwater Research, 65: 34-941.

Day G, Mayes WM, Wheeler PM, Hull SL (2017). Can aggregate quarry silt lagoons provide resources for wading birds?. Ecol Eng, 105:189-197.

Furness RW, Greenwood JJ. eds., (2013). Birds as monitors of environmental change. Springer Science & Business Media.

IUCN (2021) International Union for the Conservation of Nature: Red List. Available at: https://www.iucnredlist.org/ [last accessed 20/4/21]

JNCC (2010) Handbook for Phase 1 habitat survey: a technique for environmental audit. Nature Conservancy Council. UK

Jarvis D. Walton G. (2010) Restoration of aggregate quarry lagoons for biodiversity. UK: DEFRA Aggregate Levy Sustainability, 14.

Johnston D, Potter H, Jones C, Rolley S, Watson I, Pritchard J (2008) Abandoned mines and the water environment. Science Project SC030136-41. Environment Agency, Bristol.

Mitsch WJ. Gosselink JG, (2015). *Wetlands*. John Wiley & Sons.

Paracuellos M., (2006). Relationships of songbird occupation with habitat configuration and bird abundance in patchy reed beds. Ardea Wageningen, 94:87.

RSPB (2013) Bringing Reedbeds to Life: Creating and Managing Reedbeds for Wildlife. Royal Society for the Protection of Birds, Peterborough, UK.

Sapsford DJ, Watson I. (2011). A process-orientated design and performance assessment methodology for passive mine water treatment systems. Ecol Eng, 37:970-975.

Valkama, E., Lyytinen, S., & Koricheva, J. (2008) The impact of reed management on wildlife: a meta-analytical review of European studies. Bio Cons. 141, 364-374

Natural Tracers for Mine Water Fingerprinting – A First Step to a Hydrogeochemical Monitoring Plan for Risk Assessment During Mine Water Rebound in the Ruhr District Area, Germany

Henning Jasnowski-Peters, Christian Melchers

Research Center of Post Mining, Technische Hochschule Georg Agricola University, Herner Str. 45, 44787 Bochum, Germany, henning.peters@thga.de

Abstract

Bromide as natural tracer in combination with hydrochemistry and isotope geochemistry has been applied to distinguish regional aquifers from mine water derived from Upper Carboniferous hosted former hard coal mining area in the Ruhr District, Germany. The hydrogeochemical dataset successfully identified different origins of salinity, i.e. halite dissolution vs. seawater evaporation. Cl/Br ratios and molar Na/Cl ratios of mine water differ significantly compared to groundwater in Upper Cretaceous host rocks consisting of Coniacian-Santonian and Cenomanian-Turonian fractured aquifers. The bromide tracer has the potential to be used for risk management purposes during mine water rebound in order to verify containment.

Keywords: Tracers, Hydrochemistry, Mine Water Rebound, Monitoring, Hard Coal

Introduction

Mine water rebound in the former Upper Carboniferous hard coal mining region of the Ruhr Valley is a long-term billion Euro project operated by the former coal mining company Ruhrkohle AG. Since hard coal mining ceased at the end of 2018, the region is on transition to the post mining stage (Melchers *et al*. 2020). In order to manage risk of contamination and accurately forecast mine water rebound water levels, conformance and containment of mine water needs to be frequently monitored. This study aims to provide and develop a hydrogeochemical monitoring toolset using preferentially natural tracers to mitigate any unwanted loss of containment, besides being an ecological feasible and cost effective solution. Upper Carboniferous hosted mine waters, hence, groundwater which came into contact with underground mine workings, are characterized by high salinity and high levels of sulfate and iron species resulting from (di)sulfide oxidation processes within the mine. One of the major tasks in characterizing deep, saline fluid inventories is to identify the origin of salinity. Brine-type, Na-Cl dominated basinal waters can have different origins (Hanor 1994; Kharaka and Hanor 2014). Two major processes are (a) evaporative pathways of formerly trapped or infiltrated seawater and (b) subsurface dissolution of salt minerals, preferentially halite. Initial seawater composition, i.e., sensu strictu connate waters, can be subsequently modified after entrapment by diagenesis, water-rock interaction, microbial interactions and mixing with groundwater in the subsurface.

Geology & Hydrogeological framework

The former coalfield of the Ruhr Valley is situated in folded and weakly metamorphosed Paleozoic basement rock of Upper Carboniferous age referred to as the Rhenish Massif (Kukuk 1938). Upper Carboniferous siliciclastics intercalated with coal measures (Namurian to Westphalian A-C) forms the host rock of the former mining area. The folded Upper Carboniferous strata is gently dipping towards the North. It is unconformably overlain by Mesozoic sediments of the Muensterland Basin, which are dominated by Upper Cretaceous marls and carbonates (Hiss and Mutterlose 2010). These two geological provinces contain both Na-Cl type basinal groundwaters with electric conductivities exceeding 200.000 µS/ cm. In the Muensterland Basin, the brine infiltrates

Cenomanian-Turonian strata and builds a regional aquifer extending from the northern edge of the basin, towards the southern border to the Paleozoic basement known as the Haarstrang ridge (Struckmeier 1990). Numerous spas and former saltworks are located in the region and making use of this saline aquifer since mediaeval times. Up to 1500 meters thick, marly sediments of the Emscher Formation, Middle Coniacian to Upper Santonian, were deposited on top of the Cenomanian-Turonian carbonate sequence. The Emscher Formation consists of homogeneous grey to dark grey coloured sediments of finely laminated to thick layered and in parts organic rich (Type II) marls. Hydrogeologically, the Emscher Formation is a thick aquitard whereas its uppermost part includes a local fractured aquifer in the Ruhr District. Enclosed by aquitards, the Cenomanian-Turonian aquifer is confined. Evaporite deposits in the area are represented by Permian (Zechstein) and Triassic (Upper Bunter, Roet Fm.) salt sequences. They were deposited on the northern rim of the Muensterland Basin and along the western margin down to the Lower Rhine region. The Upper Santonian Haltern Formation incl. Recklinghausen Formation overlying the Emscher Formation represents an important drinking water reservoir for the region. Currently, it is necessary for baseline requirements to identify certain waterbodies exhibiting hydrogeochemical fingerprints inherited from different host rocks, i.e. Upper Carboniferous basement, Cenomanian-Turonian or Coniacian-Santonian signatures. It is anticipated that during the main rebound phase mine water will infiltrate the overburden and potentially mix with Cenomanian-Turonian saline aquifer, and subsequently, will rise within the pore network and fault pathways of the Emscher Formation. As prerequisite, Haltern Formation strata as drinking water reservoir must be kept free from mine waters.

Halogen Geochemistry

Halogens, especially bromide (Br^-), have been used frequently to decipher the origin of brines, but also to distinguish organic matter types with organobromide content (ten Haven *et al.* 1988). Especially Type II marine organic matter is prone to contain up to 1000 mg/L bromine (Vassilev 2000). Chloride vs. sodium species have been evaluated to further distinguish halite dissolution vs. a general seawater evaporation trend (Kharaka and Hanor 2014). General seawater contains 65 to 67 mg/L bromide, which increases subsequently in the solution during evaporation up to a value of 6000 mg/L (Hanor 1994). During crystallization of halite, bromide is preferentially retained in solution (Braitsch and Herrmann 1963). This fact enables the linkage between bromide concentration to track halite dissolution and evaporation paths of saline fluids.

Methods

Over 200 samples have been collected for hydrogeochemical analyses from 2017 to 2020. Available literature data was reviewed, and quality controlled using general ion balance assessment. Hydrogeochemical analyses of major cations and anions were conducted by certified lab analyses according to DIN ISO 11885 and DIN 10304- 1 protocols. As trace elements strontium, barium, boron and bromide species were analysed. Monitored on-site parameters are electric conductivity, pH, ORP, temperature and oxygen content of the water using WTW Multi 3320. Oxygen and hydrogen stable isotope measurements were obtained with an optical analyser (Picarro 2130i, Picarro,Inc., Santa Clara, CA, USA) using the laser-based principle of cavity ringdown spectroscopy. The standard deviation per sample was on average 0.06‰ for $\delta^{18}O$ and 0.48‰ for $\delta^{2}H$.

Results and Discussion

Upper Carboniferous host rock, Upper Cretaceous Cenomanian-Turonian aquifer and Upper Cretaceous overburden section containing mainly Coniacian-Santonian Emscher Formation groundwater have been defined as potential hydrochemical end members. For risk assessment purposes, these three groups need to be characterized using baseline thresholds. In the Piper plot (Fig. 1), most of the analysed samples of Upper Carboniferous mine waters and Cretaceous Cenomanian-Turonian aquifer samples plot

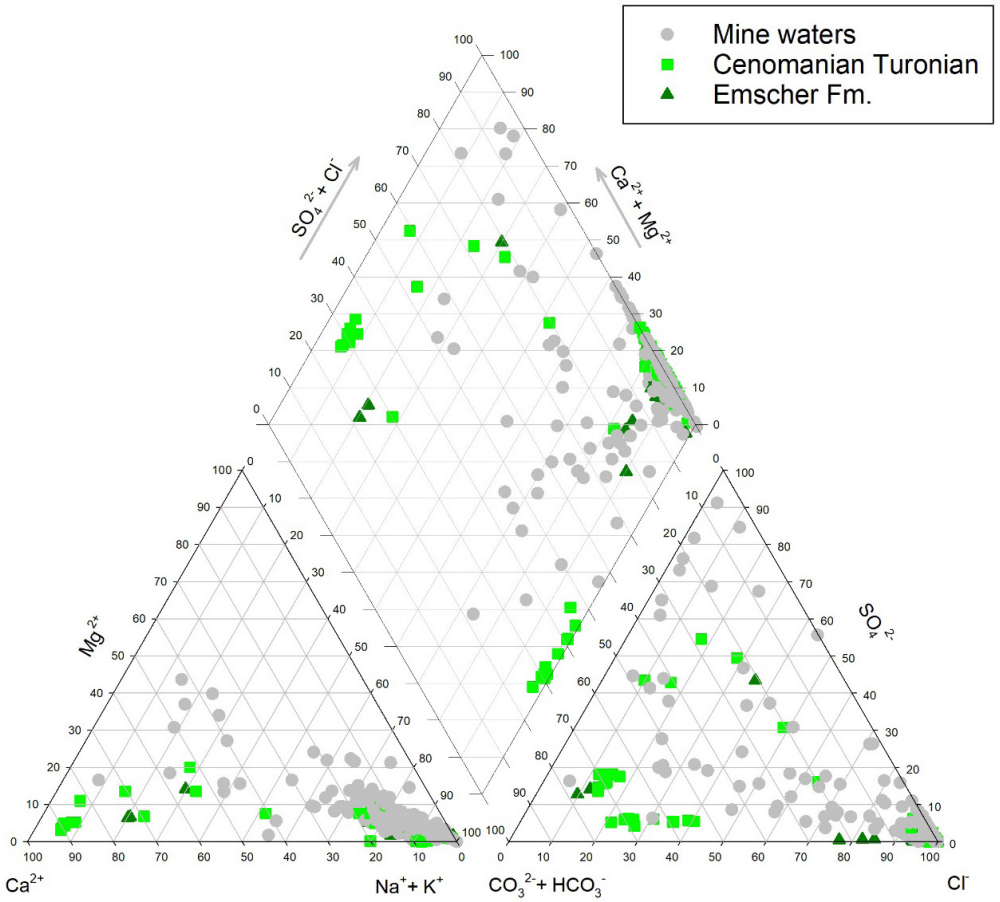

Figure 1 *Piper Plot: hydrochemical facies of mine water samples vs. Upper Cretaceous groundwater.*

within the diamond plot in the right quadrant being identified as Na-Cl dominant waters. Using major cations and anions distributions of the data yield no clear distinction between the saline aquifers of Upper Cretaceous and Upper Carboniferous hosted mine waters.

Hydrogen and oxygen stable isotopes

The compilation of oxygen and hydrogen isotopes helps to decipher the salinity of groundwater and its origin, because of isotope fractionation processes during evaporation or mixing of various isotope reservoirs (Fig. 2). For comparison, a global (GWML) and local meteoric waterline (LWML) representation (IAEA- GNIP data from the city of Bad Salzuflen, Germany) as well as the reference standard V-SMOW and the local Ruhr District meteoric water signature are included. Grobe & Machel (2002) concluded a mixing trend of present day meteoric water and seawater (SMOW) at that time. However, having compiled n=213 samples revealed a trend which levelled off at δ^2H = -20‰ towards more positive $\delta^{18}O$-values ranging in between $\delta^{18}O$ = -4 to -1‰ for most of the deeper mine waters in the Upper Carboniferous host rocks. Such trend is in agreement with either oxygen exchange reactions or evaporation-recharge. Oxygen exchange reactions result in more positive oxygen isotope uptake, common at elevated temperatures, and respectively for a constant shift towards more positive $\delta^{18}O$-values. A freshwater evaporation prior to recharge trend is indicative for affecting both, oxygen and hydrogen isotopes to increase. Upper Cretaceous situated samples and data from

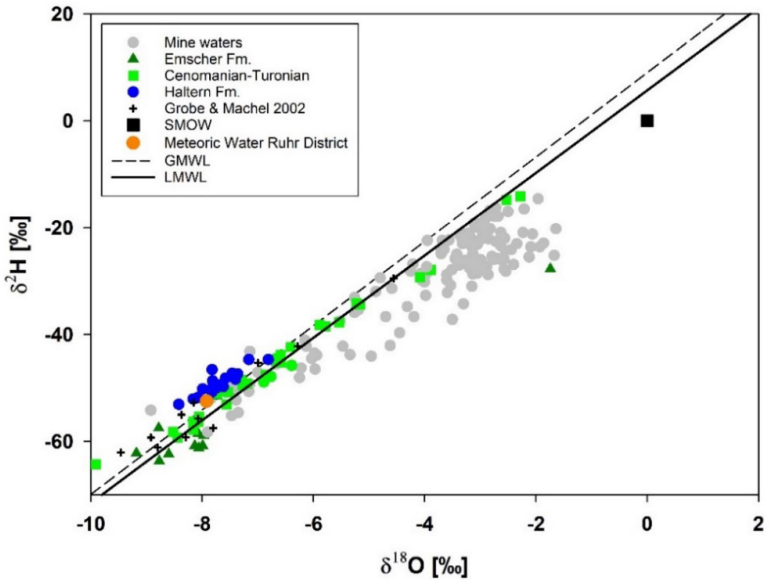

Figure 2 *Oxygen and hydrogen stable isotope analysis of mine water samples vs. Upper Cretaceous groundwater; LMWL=Local meteoric water line; GMWL= Global meteoric water line; SMOW=Standard Mean Ocean Water.*

spas and springs of the Muensterland Basin plot along the predefined slopes of GWML and LWML. This data is consistent with data points from Grobe & Machel (2002) and is recognised as modified meteoric waters infiltrating from the North. Lowest values of δ^2H = -58 to -65‰ and δ^{18}O = -9.9 to -8‰ are reported preferentially from formation waters of the Emscher Formation.

For comparison, data from the Haltern Formation as major drinking water reservoir exhibit excess deuterium and plots left of the GWML. Excess deuterium values and more negative δ^{18}O values compared to the GWML are characteristic for low temperature water-rock interaction and microbial processes. All samples plot significantly below the SMOW reference value and hence are not associated with an evaporative seawater path.

Halogen geochemistry

In Figure 3 molar concentrations of sodium vs. chloride ions are plotted. The data trend indicates either halite dissolution having a linear correlation with an ideal slope of mNa/mCl = 1 compared to a linear trend of seawater evaporation which corresponds to a slope value of mNa/mCl = 0.86.

As already suggested by Wedewardt (1995) and Grobe & Machel (2002), saline groundwater from Cenomanian Turonian aquifer system plot on the Na/Cl slope = 1 line as well as samples from the western part of the Ruhr District. Upper Carboniferous mine waters as well as formation waters from the Emscher Formation instead plot on the classical seawater evaporation trajectory (SET). Their formation waters are related to ancient evaporated and modified seawater trapped as porewater. Halite dissolution initiated by meteoric water infiltration is the obvious scenario for the saline waters of the Cenomanian-Turonian aquifer system and has been confirmed with the larger data trend.

Figure 4 illustrates a log-log cross plot of bromide vs. chloride mass concentration ratios. Modern seawater ratio which exhibits a value of Cl/Br=288 has been implemented as reference and starting point of SET. Wedewardt (1995)'s subset of mine waters range from Cl/Br=350 to Cl/Br=1450 values with a mean of Cl/Br=789. Cl/Br values >1500 were sampled within the mine workings by the authors but are often associated with Upper Cretaceous sourced groundwater. Especially samples from easternmost collie-

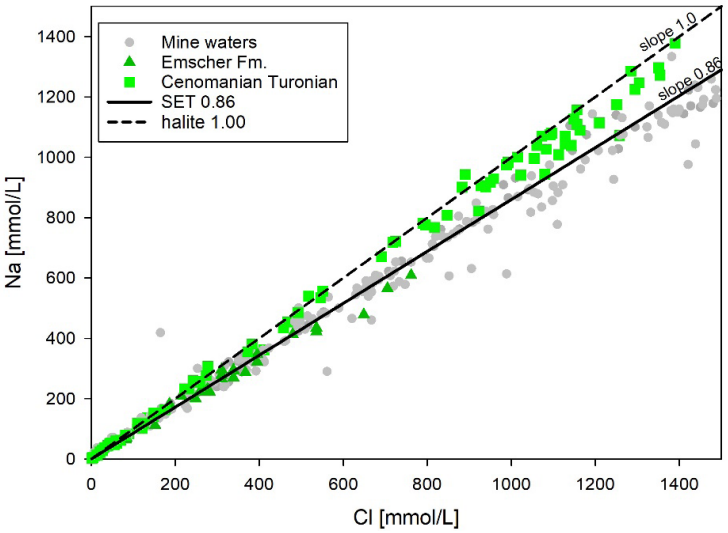

Figure 3 *Molar concentrations of chloride and sodium of mine water samples vs. Upper Cretaceous groundwater; SET 0.86=seawater evaporation trajectory; halite 1.00= halite dissolution line.*

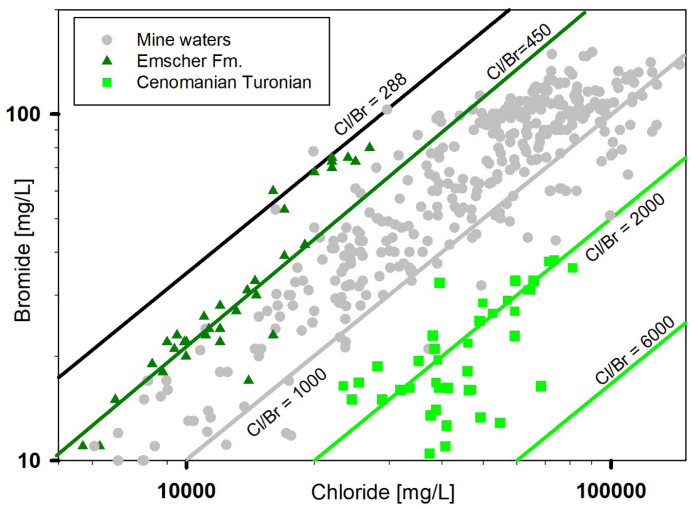

Figure 4 *Log-Log-plot of bromide vs. chloride mass concentrations of mine water vs. Upper Cretaceous groundwater.*

ries exhibit such high Cl/Br data within the mine. On the other hand, mine water in collieries from the western border of the Ruhr District show anomalously high Cl/Br values, which correspond to halite dissolution from Zechstein formations in the vicinity. Emscher Formation strata hosted groundwater generally has Cl/Br <450 values. Two samples report even higher Cl/Br ratios than seawater. The Cenomanian-Turonian aquifer system including various samples from spas and springs in the Muensterland Basin which were preferentially sourced by this water consistently corresponds to Br/Cl ratios >2000. Br/Cl ratios with values in between 1500 to 2000 are closely associated with mines and indicate mixing of the two prominent saline aquifers.

Conclusions

The dataset reveals that the hydrochemistry of the Cenomanian-Turonian regional aquifer in the Muensterland Basin stems from modified meteoric water due to halite dissolution – as has been suggested by former researchers (Grobe and Machel 2002; Wedewardt 1995). Mine waters have their own distinctive Cl/Br pattern derived from Upper Carboniferous formation water modified due to water rock interaction and coal maturation. Emscher Formation hosted groundwater exhibit anomalous high bromide concentrations most likely due to organobromide contribution from organic matter type II. The dataset identifies water bodies modified by halite dissolution from Zechstein in the western part and is able to differentiate groundwater from Emscher Formation, Cenomanian-Turonian aquifer and mine water in the eastern part of the Ruhr District. As follow-up project, we will compare the hydrochemical data with additional trace element data including lithium and strontium.

Acknowledgements

The authors would like to thank Forum Bergbau und Wasser for financial support, Ruhrkohle AG for their support in providing access to samples and data. Laura Cebula is thanked for extensive fieldwork support.

References

Babel M., Schreiber B. C. (2014) Geochemistry of Evaporites and Evolution of Seawater. In: Holland HD (ed) Treatise on geochemistry, 2nd edn., vol 9. Elsevier, Amsterdam, pp 483–560

Braitsch O, Herrmann AG (1963) Zur Geochemie des Broms in salinaren Sedimenten: Teil 1: Experimentelle Bestimmung der Br-Verteilung in verschiedenen natürlichen Salzsystemen. Geochimica et Cosmochimica Acta 27:361–391.

Fontes J, Matray JM (1993) Geochemistry and origin of formation brines from the Paris Basin, France. Chemical Geology 109:177–200.

Grobe M, Machel HG (2002) Saline groundwater in the Muensterland Cretaceous Basin, Germany: clues to its origin and evolution. Marine and Petroleum Geology 19:307–322.

Hanor JS (1994) Origin of saline fluids in sedimentary basins. Geological Society, London, Special Publications 78:151–174.

Hiss M, Mutterlose J (2010) Field trip E6: Cretaceous geosites of the eastern Ruhr Area and the southern Muensterland. sdgg 66:168–183.

Kharaka YK, Hanor JS (2014) 7.14 - Deep Fluids in Sedimentary Basins. In: Holland HD (ed) Treatise on geochemistry, 2nd edn. Elsevier, Amsterdam, pp 471–515

Kukuk P (1938) Geologie des Niederrheinisch-Westfälischen Steinkohlengebietes: Textband. Springer Berlin Heidelberg, Berlin, Heidelberg

McCaffrey MA, Lazar B, Holland HD (1987) The evaporation path of seawater and the coprecipitation of Br- and K+ with halite. J Sediment Petrol 57:928–938.

Melchers C, Westermann S, Reker B (2020) Evaluation of mine water rebound processes in the German Coalfields of Ruhr, Saar, Ibbenbüren, and the adjacent European countries. Berichte zum Nachbergbau, vol 1. Selbstverlag des Deutschen Bergbau-Museums Bochum, Bochum

Struckmeier W (1990) Wasserhaushalt und hydrologische Systemanalyse des Münsterländer Beckens. Wasser und Abfall, vol 45. Landesamt für Wasser und Abfall Nordrhein-Westfalen, Düsseldorf

ten Haven HL, de Leeuw JW, Schenck PA, Klaver GT (1988) Geochemistry of Mediterranean sediments. Bromine/organic carbon and uranium/organic carbon ratios as indicators for different sources of input and post-depositional oxidation, respectively. Organic Geochemistry 13:255–261.

Vassilev S (2000) Contents, modes of occurrence and origin of chlorine and bromine in coal. Fuel 79:903–921.

Wedewardt M (1995) Hydrochemie und Genese der Tiefenwässer im Ruhr-Revier. DMT-Berichte aus Forschung und Entwicklung, vol 39. DMT, Bochum

Enhancing Biological Nitrogen Removal from Mine Site Water in Cold Climate

Piia Juholin[1], Kirsi-Marja Haanpää[1], Elena Torresi[2], Fernando Morgan-Sagastume[2]

[1]*AFRY Finland Oy, Elektroniikkatie 13, FIN-90590 Oulu, Finland, piia.juholin@afry.com, kirsi-marja.haanpaa@afry.com*

[2]*AnoxKaldnes - Veolia Water Technologies AB, Klosterängsvägen 11A, 226 47 Lund, Sweden, elena.torresi@anoxkaldnes.com, fernando.morgan@anoxkaldnes.com*

Abstract

Biological nitrogen removal from cold mine water can be challenging due to low biological activity of the biomass, which may increase the size of the treatment unit and lead to increased costs. This paper introduces some design solutions that may improve the usability of biological nitrogen removal in cold climate. These solutions include taking advantage of warmer seasons and the thermal energy of underground mine water, heating and reuse of waste heat produced in concentration plants, treating a specific water stream with a considerable nitrogen load, and pretreating the influent.

Keywords: Moving Bed Biofilm Reactor, Biological Nitrogen Removal, Nitrogen Compound, Cold Climate, Waste Heat

Introduction

Nitrogen compounds, such as ammonium (NH_4^+), nitrite (NO_2^-), and nitrate (NO_3^-), in mine site discharge water can cause eutrophication in barren Northern environments, since natural background concentrations are generally low. In some mines in Nordic countries, current environmental permit regulations limit the total nitrogen concentration discharge water to 14 mg/L. In addition, authorities have been paying more attention to nitrogen loading of mine sites than before, which indicates that environmental permits are tightening.

Careful detonation or passive removal techniques are not always sufficient, or even possible, actions to reduce the nitrogen loading to the environment. In some cases, active treatment techniques are needed to keep under the environmental permit limits. A proven technology for the biological removal of nitrogen from cold mine site waters is the moving bed biofilm reactor (MBBR), which has been demonstrated to sustain long-term nitrogen removal even at temperatures around 4 °C.

Sources of Nitrogen

Nitrogen compounds reach mine site water streams from the detonation of nitrogen-based explosives. Other possible nitrogen sources are nitric acid (HNO_3), used in pH adjustment and in metal recovery processes, and cyanide (CN^-) from gold extraction. Since nitrogen discharges to water streams cannot be fully avoided, active or passive water treatment of mine site discharge water may be required to remain within environmental permit limits and to reduce environmental impacts.

The main sources of nitrogen compounds in the mining industry are explosives. The amount of nitrogen ending up in mining waters varies from mine to mine. From 0.2 to 28% of nitrogen from ANFO (ammonium nitrate/fuel oil) explosives can get into drainage water (Sjölund 1997; Morin and Hutt 2009; Jermakka *et al*. 2015). Explosive usage in underground mines can be higher compared to open-pit mines, due to overloading of some areas and incomplete detonation of loaded boreholes (Jermakka *et al*. 2015). From 5 to 20% of the loaded explosives' nitrogen in underground mining

operations and 1% in open-pit operations can remain in blasted material from which it may dissolve in water. Proper mine water management can reduce the contact between blasted material and water, thus reducing the nitrogen load to water streams. This is possible especially in underground mines.

Due to the usage of explosives, mine dewatering water can be a substantial source of nitrogen discharged into the environment. Depending on the nitrogen balance of a mine, treating mine dewatering water may reduce nitrogen loading significantly, which makes its treatment beneficial. In mine dewatering water, nitrogen compounds are often in a more reduced form compared with leachates from dumping areas. This is due to the nitrification processes taking place at dumps (Nilsson 2013). In a study by Morin and Hutt, dissolved nitrogen concentrations in underground mine dewatering water were studied after blasting. It was noticed that 51–56% of the total nitrogen was present as NO_3^- while 40–46% was NH_4^+ and 2.9–4%, NO_2^-. (Morin and Hutt 2009)

Nitrogen compounds dissolve at waste rock dumps where rainfall and melted snow infiltrate through the deposits. The deposits can release nitrate and ammonia long-term. However, the ammonium and nitrate release can also be rapid when the waste rock material comes into contact with water (Jermakka *et al.* 2015). Spring flooding can cause considerable nitrogen release from the deposits due to low microbiological activity in cold water and extensive runoff volume (Mattila *et al.* 2007). Oxidation of nitrogen species in the waste rock dumps has been identified mainly during summer. At the same time, the low organic matter proportion in the deposits may limit denitrification. (Jermakka *et al.* 2015)

Another possible nitrogen source is the excess water of processing plants. In the process unit operations, blasted rock material comes into contact with water, and ammonium and nitrate may leach into the process water (Jermakka *et al.* 2015). Process water pH tends to be low. Acidic and reducing conditions lead to denitrification when the concentrations of ammonium, ammonia (NH_3), or nitrogen gas are increased. Due to the reducing environment, the main nitrogen components of processing plant effluents are ammonium and ammonia. Besides the nitrogen species originating from explosives, the use of nitric acid, ammonium chloride or ammonium hydroxide in the process may increase nitrogen discharges. (Bosman 2009)

Processing plant effluent discharges are usually led to a tailings pond with tailings material. Possible acidic pH of the effluent and tailings can cause reducing conditions at the tailings pond as well, if ammonia and ammonium concentrations are elevated.

Contrary to the tailings pond, conditions at water ponds are often oxidizing. In water ponds, the fraction of nitrate has been observed to increase up to 70–95% while ammonium and nitrite fractions are 0–10% and 2–30%, respectively. Oxidation is increased during the summer season due to increased biological activity. Water ponds can remove nitrogen especially when retention time is long and a carbon source, such as some plants that may release carbon compounds, is available. (Mattila *et al.* 2007; Jermakka *et al.* 2015)

Choosing the water stream to be treated with an active nitrogen removal process depends on the nitrogen balance. It is often beneficial to target the water treatment to certain water streams with the highest nitrogen loads. The load depends on the nitrogen concentration and water flow rate. This kind of **targeted water treatment** reduces the required treatment capacity and thus decreases the investment and operating costs. Often, major nitrogen loads result from mine dewatering, and thus mine dewatering water treatment can be most beneficial. Also, waste rock dumps, with their long-term nitrogen release characteristics, generate runoff suitable for targeted water treatment.

Effect of Temperature on Biological Treatment Processes

Biological processes are strongly dependent upon temperature. As an example, nitrification rates double with a 10 °C increase, while denitrification rates double with 4 °C increase. In general, the optimal nitrification temperature ranges from 8 to 30 °C (Given and Meyer 1998).

The impact of cold temperatures on decreased microbial activity in biological treatment can be addressed and overcome with the application of moving bed biofilm reactors (MBBRs). In an MBBR, the microbial biomass grows as a biofilm on a protected surface area provided by plastic carrier elements that are freely moving within the whole reactor volume. This allows for long biomass retention times (i.e., high biomass concentrations in the reactor), and the process can be operated at low temperatures without relying on sludge age as a design parameter. As an example, treatment of mine site waters even at 4 °C has resulted in complete nitrification and denitrification (Dale *et al.* 2015). The MBBR process can be designed for even lower temperatures. However, size of the treatment unit needs adjustment based on the effect of temperature on the microbial kinetics. MBBRs are also known for compactness and for being able to handle variations in load, temperature and toxic shocks better than biological processes relying on biomass in suspension rather than on biofilm attached to carriers. Therefore, the design is a trade-off between the operating temperature and size of the process. The process could further benefit from warmer seasons, external heating, relocating the treatment facility close to a heat source, or pretreatment (Fig. 1).

Benefits from Warmer Seasons

In Northern areas, seasonal temperature variations are substantial and affect the temperature of mine site waters. In Nordic countries, mine water temperature is above 5 °C approximately five months a year depending on the site location. During summertime, referring to a three-month period from June to August, the water temperature can range from 15 to 20 °C. Most of the year, the water temperature stays below 5 °C, mostly around 1 to 2 °C, or even close to 0 °C.

Approximately 50–80% of total site runoff, caused by snow melting, occurs during the three-month summer period, depending strongly on site location and typical climatic conditions of the area. This season can be considered warm season, and the water temperature is over 5 °C. However, the main runoff peak usually occurs in late spring or early summer when the water temperature is still below 5 °C. During the snowmelt peak flow, concentrations of nitrogen and other compounds are relatively low. However, due

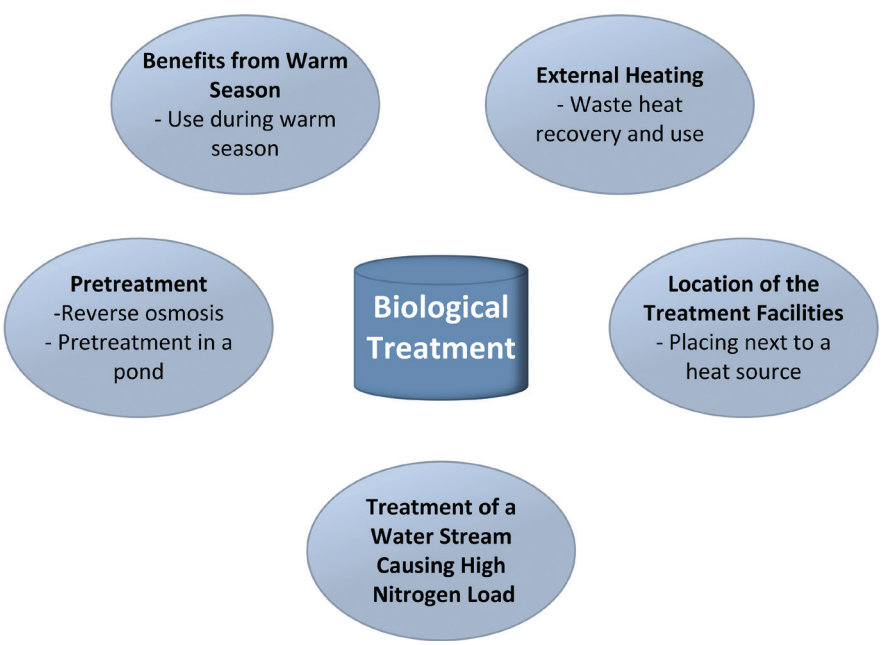

Figure 1 *Enhancing Biological Nitrogen Removal Processes in Cold Climate.*

to high flow rates, environmental loading can become high. The runoff peak period may be a challenge for biological nitrogen treatment due to high flow rate and low temperature.

Part of the runoff peak is usually retained on the mine site and stored in water ponds. To enable nitrogen removal, it might be beneficial to store the nitrogen-containing water streams until the summer period to take advantage of the natural temperature increase. Such operations, however, require careful site water management.

External Heating

In biological processes, heating is most beneficial during start-up to improve biomass activity. When the biological process is working, external heating becomes less important. Also, during the coldest season, heating may be required to increase biological activity.

In Nordic mines, the heat source for buildings and domestic hot water production is often a fuel, such as wood chips burnt in a boiler. The produced heat is distributed with a district heating system. During peak consumption, more expensive fuels, such as oil, natural gas, or liquefied petroleum gas, can be burnt in the boilers. Heating nitrogen-containing water with external heating sources can similarly be done. However, heating large volumes of water increases operating costs of biological treatment considerably and causes environmental impacts, although it is one of the most effective ways to enhance biological nitrogen removal.

Mines consume a lot of energy, for example, in extraction, processing, and mineral transportation, as well as to sustain operations and to avoid environmental risks (Patsa *et al*. 2015). Use of energy causes waste heat generation, which, until now, has been relatively poorly recovered in the mining industry. Waste heat usage can reduce environmental impacts by reducing the use of required energy sources. A possible waste heat source of mine sites are concentration plants where, for example, compressors and grinding circuits generate waste heat and need cooling. The compressors generate remarkable amounts of heat since 100% of energy fed into the compressors turns into heat. Most of the heat can be recovered from the cooling system by using heat exchangers and transferring the energy, for example, to a water circuit. In a case study, available water-heating power of screw compressors was estimated to be 100–150 kW. (Holopainen *et al*. 2013)

High temperature processes, such as autoclaves and digesters, are also possible waste heat sources. Recovered heat is already consumed, for example, in the preheating of incoming materials. However, heat recovery potential still exists. As an example, recovery from calcination exhaust gases has been identified in aluminium production. (Brough and Jouhara 2020) Mine exhaust air has also been described as having potential for waste heat recovery. In a case study, the exhaust air temperature was 15 °C and its energy content was estimated to be substantial (Holopainen *et al*. 2013).

In addition, renewable energy sources such as geothermal energy have substantial potential. Until recent years, geothermal energy had rarely been used in the mining industry (Boynton *et al*. 2018). Mine dewatering water is often described as a heat resource from which geothermal energy can be recovered (Obracaj and Sas 2018). However, if mine dewatering water requires biological or other treatment which benefits from elevated temperatures, heat recovery from dewatering water is not advisable. In such a case, geothermal energy should be recovered from another source.

Location of the Treatment Facilities

In treatment of underground mine dewatering water, the biological water treatment unit can be located in an underground mine to prevent on-surface heat losses. In general, mine water temperature is approximately 10 °C at 100 m below the ground surface, and it increases by 1 °C when depth increases 100 m; however, temperature is location dependent. (Holopainen *et al*. 2013).

Mine water temperature and dewatering flow rate are affected by surface water flow into the mine. Surface water inflow causes substantial monthly flow rate and temperature variations. The amount of surface water inflow to underground mines varies from mine to mine.

Space availability may limit locating a water treatment unit underground, as biological treatment can require large treatment units. Alternatively, the treatment unit could be located on ground-surface level close to the mine portal where on-surface heat losses from the mine water would still be minimized.

Similarly, the biological process could be located next to its potential external heat source. If external heating is done with the energy of the heat plant or waste heat of the concentration plant, locating the treatment close to the heat source, if mine site layout allows, is beneficial.

Pretreatment

RO

Reverse osmosis has been studied as a concentration method prior to biological processes. In a study, actual mine water having relatively low ammonium concentration, 9.48 mg/L, was concentrated up to 104 mg/L NH_4-N. It was observed that the permeate quality did not deteriorate considerably in the concentration of feed above a volumetric reduction factor of 20. RO produces purified water to be used in other processes or to be let into the environment. However, besides nitrogen compounds, salt and metals may concentrate in the process, which can cause metal toxicity to microorganisms. (Häyrynen *et al*. 2008) Ammonium concentration can become a limiting factor in the concentration process. If ammonium concentration increases above 1 gN/L, ammonia may be generated at high pH levels, which may inhibit biological activity.

The concentrated stream produced in RO can be treated biologically. The concentration process considerably decreases the volume of basins required in the biological process. Also, concentrated water volume reduces heating costs and may reduce the use of fresh water if the permeate can be used instead. However, pretreatment increases investment and operating costs, estimated to be 0.31–0.34 €/m³ in a study by Häyrynen *et al*. and 0.488 US$ in a study by Grossi *et al*. (Häyrynen *et al*. 2008; Grossi *et al*. 2021).

Pretreatment in a Pond

Nitrogen removal requires nitrification, where nitrogen in reduced form is oxidized. In the second phase, nitrate can be reduced in anoxic conditions to nitrogen gas. As a pretreatment method, nitrogen compounds can be pre-oxidized in ponds through biological processes. The phenomenon occurs in relatively low temperatures, although cold temperature slows down the process and increases the formation of nitrite and ammonia. Vegetation can also take up a fraction of nitrogen. The process can be enhanced with aeration when contact with air is improved or with the implementation of MBBRs downstream of lagoons (LagoonGuard™ MBBRs; AnoxKaldnes_VWT).

In gold-processing plants, cyanide (CN^-), and cyanide-derived compounds thiocyanate (SCN^-) and cyanate (CNO^-) can be present in effluents. Prior to biological treatment, their oxidation can be enhanced with the addition of oxidizing chemicals, such as H_2O_2 or Caro's acid (Kratochvil *et al*. 2017), but also biologically using specially designed MBBRs for this effect (Tracer™Cyanides – MBBR; AnoxKaldnes-VWT).

Conclusion

Biological processes are commonly used methods for nitrogen treatment of waters from the mining industry. Nevertheless, biological activity decreases in low temperatures typical of cold-climate regions.

One possibility to enhance biological treatment processes is to implement biological treatment technologies that are able to cope with colder temperatures and process variations, such as MBBRs, and/or to preferentially treat biologically during warmer seasons when water temperature naturally increases. This requires water storage during winter and peak runoff seasons. Water heating with an external source is also possible, although it adds to the operating costs and increases environmental air emissions. Recovery of waste heat and its use in water heating is an interesting topic and could have potential in biological water treatment.

Depending on the feed water quality, pretreatment can also enhance the biological treatment process. For example, oxidation of nitrogen compounds with aeration or with chemicals can improve and simplify the actual biological treatment process. Another pretreatment process is reverse osmosis, which can be used as a concentration method to reduce the size of biological treatment basins and thus decrease the investment costs.

Acknowledgements

The authors thank co-workers and collaborators who have given input on this work.

References

Bosman C (2009) The hidden dragon: nitrate pollution from open-pit mines - a case study from the Limpopo province, South Africa. In: Abstracts of the International Mine Water Conference. pp 849–857

Boynton K, Berkley M, Perkins S, Albert-Green S (2018) Geothermal energy in mining-a renewable and reliable energy solution. GRC Transactions 42

Brough D, Jouhara H (2020) The aluminium industry: A review on state-of-the-art technologies, environmental impacts and possibilities for waste heat recovery. International Journal of Thermofluids 1–2

Dale C, Laliberte M, Oliphant D, Ekenberg M (2015) Wastewater treatment using MBBR in cold climates. In: Proceedings of Mine Water Solutions in Extreme Environments. Proceedings of the second International Conference on Mine Water Solutions in Extreme Environments, Vancouver, pp 1–17

Given B, Meyer S (1998) Biological treatment of tailings solution at the nickel plate mine. In: Proceedings of the 22nd Annual British Columbia Mine Reclamation Symposium in Penticton, BC, 1998. The Technical and Research Committee on Reclamation. pp 157–171

Grossi LB, Magalhães NC, Araújo BM, de Carvalho F, Andrade LH, Amaral MCS (2021) Water conservation in mining industry by integrating pressure-oriented membrane processes for nitrogen-contaminated wastewater treatment: Bench and pilot-scale studies. Journal of Environmental Chemical Engineering 9. doi.org/10.1016/j.jece.2020.104779

Häyrynen K, Langwaldt J, Pongrácz E, Väisänen V, Mänttäri M, Keiski RL (2008) Separation of nutrients from mine water by reverse osmosis for subsequent biological treatment. Minerals Engineering 21:2–9. doi.org/10.1016/j.mineng.2007.06.003

Holopainen R, Huusko A, Heikkinen J, Korhonen K, Ritola J (2013) Kaivokset uusiutuvan energian tuottajina ja hyödyntäjinä VTT-R-04082-13

Jermakka J, Wendling L, Sohlberg E, Heinonen H, Merta E, Laine-Ylijoki J, Kaartinen T, Mroueh UM (2015) Nitrogen compounds at mines and quarries: Sources, behaviour and removal from mine and quarry waters-Literature study

Kratochvil D, Mohamm F, Xiao C, Borsoi A, Littlejohn P (2017) Management of nitrogen compounds in mine wastewater: comparing selective adsorption and electro-oxidation to other treatment methods. In: Conference of Metallurgists

Mattila K, Zaitsev G, Langwaldt J (2007) Biological removal of nutrients from mine waters Biologinen ravinteiden poisto kaivosvedestä Kaira-hankkeen loppuraportti

Morin KA, Hutt NM (2009) Mine-water leaching of nitrogen species from explosive residues. In: GeoHalifax. pp 1549–1553

Nilsson L (2013) Nitrogen transformations at the Kiruna mine - The use of stable nitrogen isotopes to trace nitrogen-transforming processes

Obracaj D, Sas S (2018) Possibilities of using energy recovery in underground mines. In: E3S Web of Conferences. EDP Sciences

Patsa L, Zyl D van, Zarrouk SJ, Patsa E, van Zyl D, Arianpoo N (2015) Geothermal Energy in Mining Developments: Synergies and Opportunities Throughout a Mine's Operational Life Cycle

Sjölund G (1997) Kväveläckage från sprängstensmassor

The Importance of Adequate Waste Rock Characterization: A Case Study of Unsuccessful Drainage Quality Prediction

Teemu Karlsson[1,2], Muhammad Muniruzzaman[3,4], Päivi M. Kauppila[1], Lena Alakangas[2], Marja Lehtonen[5]

[1]*Circular Economy Solutions, Geological Survey of Finland, Neulaniementie 5, 70211 Kuopio, Finland, teemu.karlsson@gtk.fi*

[2]*Department of Civil, Environmental and Natural Resources Engineering, Division of Geosciences and Environmental Engineering, Luleå University of Technology, 97187 Luleå, Sweden*

[3]*Water Management Solutions, Geological Survey of Finland, Vuorimiehentie 5, 02151 Espoo, Finland*

[4]*Department of Environmental Engineering, Technical University of Denmark, Miljøvej, Building 115, 2800 Kgs. Lyngby, Denmark*

[5]*Circular Economy Solutions, Geological Survey of Finland, 02151 Espoo, Finland*

Abstract

Current Finnish practices in waste rock characterization may result in improper drainage quality prediction. In this paper, we present a case study involving such inadequate predictions. Our results demonstrated that the waste rock materials with relatively low contents of harmful elements and S can still produce poor-quality drainage, and the waste rock characterization approach developed by the government should be re-evaluated. Special attention should be paid to low carbon content, low neutralization potential, and geochemical properties of single rock types rather than average concentrations of the whole rock mass.

Keywords: Aqua Regia Extraction, Geochemical Modelling, AMD-PHREEQC, Acid Mine Drainage, Waste Rock Mineralogy

Introduction

Poor-quality drainage originating from mine waste weathering is a severe environmental issue for mining industry. To design the waste disposal facilities and water management, the waste material should be characterized in an early stage of a mining project. The appropriate characterization methods should be systematically and carefully chosen, as improper characterization of mine waste might result in unexpected costs at later stages.

In Finland, it is a legislative requirement to evaluate if extractive waste is inert or not using aqua regia (AR) leachable element concentrations and S-content of the waste. According to the Finnish Government (2013), mine waste can be classified as inert if, among other criteria, the AR-extractable concentrations of As, Cd, Co, Cr, Cu, Hg, Mo, Ni, Pb, V, and Zn do not exceed the threshold values, i.e. the so-called "PIMA values" defined in the Government Decree on Assessment of Soil Contamination and Remediation Needs (Finnish Government 2007). Furthermore, the sulfidic S concentration should be ≤0.1%, or the NPR determined by the standard method EN 15875, should be >3 when the sulfidic S concentration is 0.1-1%.

We present a case study, where the waste rock materials of a small gold mine in Finland (Mine A) were inadequately characterized, and the drainage quality prediction was unsuccessful. The objective of this study is to investigate how to avoid similar situations in the future. We evaluated the use of PIMA values for mine waste characterization and demonstrate that relatively low concentrations of harmful elements within waste rock materials can still lead to poor-quality drainage if the mineralogical composition of the waste rock is unfavorable. We revised the original characterization scheme and compared the results with a similar waste rock site in Finland (Mine B). Furthermore,

reactive transport modelling with AMD-PHREEQC was applied to investigate how modelling could be used to support the quantitative prediction of the ultimate drainage quality.

Materials and methods

The Mine site A represents a small-scale open pit gold mine in Finland. It was active in 2013–2016, and during the operation, around 169 000 t of waste rock was excavated and piled to an area of around 6.5 ha at the mine site. The base of the waste rock area is rather impermeable. The quality of the drainage has been monitored, and the drainage waters have been collected for treatment. The waste rock materials were originally characterized in 2012, utilizing composite split drill core samples, and were mainly composed of meta-greywacke, feldspar porphyry rock, and vulcanite (ISAVI 2018). The characterization methods included AR extraction (ISO-11466), ABA-test with the determination of the acid production potential (AP) by total S content and the neutralization potential (NP) by the Sobek method (EN-15875), and mineralogical investigation by light microscope. Based on these analyses, the rock materials were not completely inert, but the concentrations of the harmful elements in the rock mass were below the PIMA lower guideline values. Therefore, no major element mobilization as well as generation of poor-quality drainage were expected. To supplement the earlier characterization, further similar geochemical analyses were conducted in 2014 and 2015 for 15-20 kg composite waste rock samples collected from the pile surface.

The Mine A case was compared with that of the Mine B, which is a similar-scale nickel-copper mine in Finland. The latter involves both open pit and underground mine. It was active in 2007–2008, during which around 165 000 t of waste rock was excavated. Some of the waste rock material, which consists mainly of mica gneiss, gabbro, and amphibole rock, has been piled to a waste rock area of around 1.1 ha at the mine site. The Mine B waste rock site has been investigated by Karlsson *et al.* (2018) in 2016. The investigations included a waste rock drainage sample, and three 15-20 kg composite waste rock samples collected at the mine site, which were analyzed by AR extraction, ABA-test, and FE-SEM-EDS-method. Further investigations of the waste rock pile drainage have been conducted by Leskinen (2020).

In addition to the existing published data, more detailed mineralogical investigations by FE-SEM-EDS and XRD methods were conducted at the Research laboratory of the Geological Survey of Finland for the mixed composite samples collected from the Mine A in 2015 and Mine B in 2016. Furthermore, the AMD-PHREEQC code (Muniruzzaman *et al.*, 2020) was applied to the Mine A case to model the evolution of the drainage quality. The simulations involve reactive transport processes by explicitly taking into account the partially saturated water flow, multiphase and multicomponent transport of aqueous and gaseous species, aqueous speciation, and kinetic mineral/dissolution reactions.

Results and discussion

The results show that the drainage concentrations of Al, Co and Ni have been three to tens of times higher at the Mine A compared with the Mine B, even though the drainage of the Mine B waste rock pile has been slightly more acidic (pH 3.3-4.3) than the drainage from the Mine A waste rock pile (3.5-5.0) (Table 1). The drainage of Mine A waste rock pile contained high concentrations of Al (16-215 mg/L), Co (3-9 mg/L), Ni (7-38 mg/L) and SO_4 (1100-4400 mg/L), while the Cu concentrations were low (0.02 mg/L). The drainage of the Mine B waste rock pile contained more Cu (0.1-0.3 mg/L) than the Mine A drainage, but the concentrations of Al (11 mg/L), Co (0.6 mg/L), Ni (7-12 mg/L) and SO_4 (610-990 mg/L) were lower compared with the Mine A drainage.

Based on the geochemical analyses, the environmental management of Mine B waste rock is however expected to be more challenging than that of waste rock from mine A, since the waste rock contains higher contents of harmful elements and acid production potential than the waste rock at the Mine A. The waste rock at the Mine A contained sulfur 0.1-0.7%, carbon <0.05-0.1%, Co 7-37 mg/kg, Cu 57-160 mg/

kg and Ni 19-122 mg/kg, whereas the waste rock at Mine B contained more sulfur (1.7-1.9%) and carbon (0.2-0.3%), and the concentrations of Co (68-80 mg/kg), Cu (198-471 mg/kg) and Ni (648-818 mg/kg) were clearly higher than at Mine A (Table 2). The measured acid production potentials were relatively low (5-21 kg $CaCO_3$/t) at Mine A, but so were also the neutralization potentials (5-14 kg $CaCO_3$/t), which resulted in potentially acid producing rock material (NPR 0.5-1.2). At the Mine B, both the AP (53-58 kg $CaCO_3$/t) and NP (13-22 kg $CaCO_3$/t) were higher compared with the Mine A waste rock material and resulted in lower NPR than at Mine A (0.2-0.4).

Mineralogically the Mine A and Mine B waste rock materials were quite similar, the main difference being the presence of carbonates and hornblende and somewhat

Table 1 *The waste rock pile drainage qualities at the mines A and B. The pH was measured in the field. The metals as dissolved concentrations, SO_4 as total concentration.*

Waste rock pile drainage	pH	Al	Co	Cu	Ni	SO_4
		mg/L	mg/L	mg/L	mg/L	mg/L
Mine A						
October 2014[1)]	4.4	40			14	1200
September 2015[1)]	5.0	16	3	0.02	7	1100
October 2016[1)]	4.1	63			20	1200
August 2017[1)]	3.5	215	9	0.02	38	4400
Mine B						
August 2014[2)]	3.4			0.3	12	990
June 2016[3)]	3.3	11	0.6	0.2	7	610
August 2017[2)]	4.3			0.1	11	830

[1)]ISAVI (2018), [2)]Leskinen (2020), [3)]Karlsson *et al.* (2021)

Table 2 *Waste rock geochemistry of the surface composite samples collected from the mines A and B. AP, NP and NPR determined as instructed in EN-15875.*

Waste rock geochemistry	tot S	tot C	Co	Cu	Ni	AP	NP	NPR
	%	%	mg/kg	mg/kg	mg/kg	kg $CaCO_3$/t	kg $CaCO_3$/t	
PIMA threshold value			20	100	50			
PIMA lower guideline value			100	150	100			
PIMA upper guideline value			250	200	150			
Mine A								
Meta greywacke[1)]	0.2-0.7	<0.05-0.05	16-25	57-102	33-37	6-21	7-14	0.7-1.2
Feldspar porfyr[1)]	0.1	0.1	7	160	19	5	5	1.2
Int. Volcanite[1)]	0.2-0.3	<0.05	28-37	60-77	105-122	7-10	7-9	0.9-1.0
Mixed surface sample[1)]	0.4	<0.05	24	95	88	13	7	0.5
Mine B								
Mixed surface samples[2)]	1.7-1.9	0.2-0.3	68-80	198-471	648-818	53-58	13-22	0.2-0.4

[1)]ISAVI (2018) [2)]Karlsson *et al.* (2018)

higher amount of sulfides in the Mine B samples. The main minerals in the mixed composite sample of the Mine A were quartz (32 wt.%), plagioclase (27 wt.%), biotite (26 wt.%), and chlorite (5 wt.%), whereas the Mine B samples were mainly composed of biotite (26-34 wt.%), plagioclase (17-21 wt.%), quartz (10-19 wt.%), hornblende (3-9 wt.%), and chlorite (1-9 wt.%). The detected sulfides at Mine A rock sample included pyrrhotite (0.5 wt.%), chalcopyrite (0.04 wt.%) and traces of Co-pentlandite, while the Mine B sample included pyrrhotite (1.0-1.5 wt.%), pyrite (0.02-0.7 wt.%), chalcopyrite (0.0-0.03 wt.%) and pentlandite (0.0-0.03 wt.%). In addition, high proportion of unclassified sulfides occurred in Mine B sample as a fine-grained mixture with silicates (2.3-3.1 wt.%), with a ratio of around 1:1. Carbonate minerals were not detected in the Mine A sample, whereas the Mine B samples included 0.0-0.05 wt.% dolomite. The SEM images showed that in Mine A waste rock material the Co-pentlandite existed as small inclusions inside the pyrrhotite grains (Fig. 1). Similar co-existence of pyrrhotite and pentlandite was not detected in the Mine B sample. Inclusions of sulfides inside each other are known to provoke galvanic effects, that enhance the weathering processes (Chopard *et al*., 2017). In the cases of Mine A and Mine B, the total S represents the sulfidic S, as besides sulfides no other S-minerals were detected.

AMD-PHREEQC was applied to test the use of modelling in supporting the prediction of drainage quality. Figure 2 shows the simulated drainage quality profiles at the outlet of the Mine A waste rock pile compared to the measured data. The release of acidity, Fe, Ni and Co are due to sulfide mineral oxidation under the presence of atmospheric conditions (a-e). The low pH resulting from the sulfidic reactions leads to the dissolution of aluminosilicates as reflected in the elevated concentrations of Al, Mg and K (f-h). The drainage pH appears to stabilize around 4, which might be a result of gibbsite and/or ferrihydrite buffering. The retention of Ni and Co in the waste rock pile appears to be low, as reflected in their high effluent concentrations. The reactive transport simulation performed with AMD-PHREEQC was able to capture the concentration ranges for different elements relatively well, especially when considering the conceptual simplifications and various assumptions that had to be made about the waste rock pile properties. Nevertheless, this exercise clearly demonstrate that the utilization of a model-based approach, (as used with AMD-PHREEQC in this study) involving even a simple conceptual model, is adequate for more quantitative interpretation

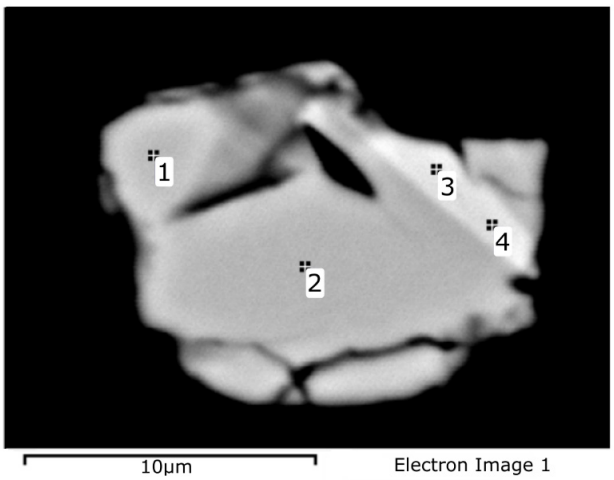

Figure 1 *Co-pentlandite inclusion in pyrrhotite in Mine A waste rock. According to the spectrum data; 1: pyrrhotite (S 40.50, Fe 59.50), 2: pyrrhotite (S 40.20, Fe 59.80), 3: Co-pentlandite (S 36.14, Fe 31.86, Co 7.52, Ni 24.48), 3: Co-pentlandite (S 35.93, Fe 34.70, Co 6.37, Ni 23.00). Results in weight%.*

of the monitoring data and for the ultimate waste rock management purposes.

High-Ni drainage has also been reported at the Diavik waste rock project by Bailey *et al.* (2015). At the Diavik type III waste rock test pile, which was constructed in 2006, the rock material was mostly granitic. The average concentration for sulfur was 0.05 wt.%, for carbon 0.03 wt.%, and for Ni 27 mg/kg (measured by the XRF method). The main sulfide mineral was pyrrhotite, which also hosted most of the Ni and Co. Despite the low S, Ni and Co content, basal drainage with pH of <4.5, and high dissolved metal concentrations e.g. for Ni (maximum of 20 mg/L) and Co (maximum of 3.8 mg/L) were measured in 2010, after four years from the construction of the pile.

Based on our results, the main causes for the drainage quality, which is lower than expected at the Mine A site compared with Mine B, were related to low carbon and carbonate content and neutralization potential of the rock material together with the occurrence type of sulfides at waste rock of the Mine A. The main metals detected in the drainage, i.e. Ni and Co, often co-precipitate with and adsorb to secondary minerals in waste piles (e.g. Ribeta *et al.*, 1995), which typically decreases their content in mine site drainage. In addition to affecting the weathering processes of the sulfides and drainage pH, the lower neutralization potential may result in decreased precipitation of secondary minerals, and reduced attenuation of metals in the waste rock pile. Furthermore, the galvanic processes might have enhanced the weathering rates of sulfides in Mine A case, but this should be more thoroughly investigated.

The case study underlines that the Finnish practice, which follows current regulations, to compare waste rock analysis results to the PIMA-threshold values, which are originally meant for soil contaminant assessment, and having a limit value of 0.1 wt.% of sulfidic S for inert waste rock, requires further consideration. For example, according to the Finnish legislation the waste rock from the Diavik test pile would have been classified as inert, which is not a correct classification based on the drainage quality. However, in the case of the Mine A waste rock material, the classification based on the regulations seems to be correct as it was not classified as inert. But as the Ni and Co concentrations of the combined rock mass exceeded only the PIMA threshold values, but not the lower guideline

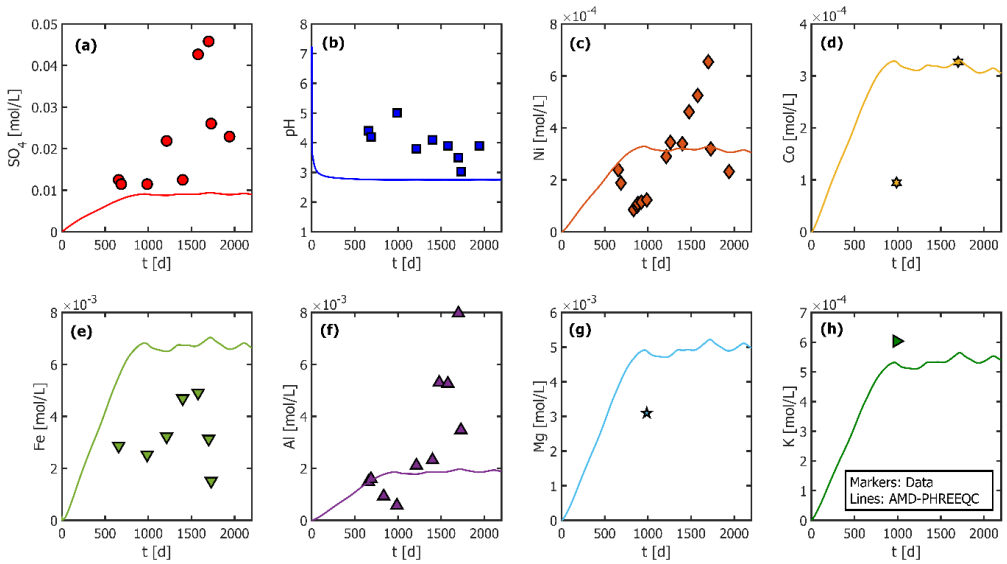

Figure 2 *Temporal evolution of the Mine A waste rock pile drainage quality: breakthrough curves of SO_4 (a), pH (b), Ni (c), Co (d), Fe €, Al (f), Mg (g), and K (h).*

values, only minor amounts of Ni and Co mobilization were expected. It should also be noted, that relying on average concentrations of a waste rock pile material might not result in accurate drainage quality prediction. According to Vriens *et al.* (2019), waste rock cells consisting of 10% of the total waste rock mass may dominate the drainage quality.

To improve the waste rock characterization in the future, and to avoid the underestimation of the harmful element mobilities, special attention should be paid to the neutralization potential and carbon content, and to the single rock types rather than average properties of the rock mass. Our results suggest that rock materials with a low (e.g. <0.1 wt.%) carbon concentration have a high risk to generate poor-quality drainage with high metal concentrations, even though the harmful element concentrations in the rock material are relatively low. However, further investigations are needed to confirm the effect of C content in harmful mobility assessment. Furthermore, detailed investigations including kinetic testing and geochemical modelling are highly recommended to be combined with the basic static tests and geochemical characterization. It should be noted that also several other factors affect the ARD generation, e.g. rock texture, climate, and microbiological activity.

Conclusions

When comparing the geochemistry of the Mine A and Mine B cases, the Mine B waste rock material is expected to have more potential to produce drainage with higher harmful element concentrations. However, the concentrations of Al, Co and Ni were clearly higher in the Mine A drainage. This discrepancy can be explained by the mineralogical differences of the inspected waste rock materials. Especially the lack of carbon and neutralizing minerals in the Mine A rock material may result in reduced attenuation of harmful elements by precipitation and co-precipitation as secondary phases.

This study demonstrates that waste rock material with relative low amounts of harmful elements and S can produce poor-quality drainage. The characterization procedure in the Mine A case should have been more thorough, including detailed mineralogy, kinetic testing, and geochemical modelling, to provide a better prediction of future drainage scenarios. Based on our results, the rock materials with a low (<0.1 wt.%) carbon concentration appear to have a high risk to generate poor-quality drainage with high metal concentrations, which should be taken into account in future waste rock characterization. This indicates that the basis for the Finnish legislative requirements to utilize the PIMA element values and 0.1 wt.% sulfidic S content for inert rock material should be further evaluated. Furthermore, it should be investigated if the C content could have more weight in the evaluation.

References

Bailey BL, Blowes DW, Smith L, Sego DC (2015) The Diavik Waste Rock Project: Geochemical and microbiological characterization of low sulfide content large-scale waste rock test piles. Applied Geochemistry 65, 54-72, doi:10.1016/j.apgeochem.2015.10.010

Chopard A, Plante B, Benzaazoua M, Bouzahzah H, Mario P (2017) Geochemical investigation of the galvanic effects during oxidation of pyrite and base-metals sulfides. Chemosphere 166(2), 281-291, doi: 10.1016/j.chemosphere.2016.09.129

Finnish Government (2013) Government Decree on Mining Wastes 14.3.2013. Finnish Government Decree 190/2013 (in Finnish and Swedish)

Finnish Government (2007) Government Decree on the Assessment of Soil Contamination and Remediation Needs. Finnish Government Decree 214/2007 (in Finnish and Swedish)

ISAVI (2018) Documents of the Issue: Rämepuron kaivoksen toiminnan lopettamiseen liittyvien jälkihoitotoimenpiteiden loppuun saattaminen ja ympäristöluvan muuttaminen, Ilomantsi (in Finnish). Regional State Administrative Agency for Eastern Finland, ISAVI/4358/2018. https://ylupa.avi.fi/fi-FI/asia/1533527, accessed April 12, 2021

Karlsson T, Alakangas L, Kauppila P, Räisänen ML (2021) A Test of Two Methods for Waste Rock Drainage Quality Prediction: Aqua Regia Extraction and Single-addition Net-acid Generation Test Leachate Analysis. Mine Water and the Environment, published online 21 May 2021, doi: 10.1007/s10230-021-00784-0

Karlsson T, Kauppila PM, Lehtonen M (2018) Prediction of the long-term behaviour of extractive wastes based on environmental characterization: correspondence of laboratory prediction tests with field data. Bulletin of the Geological Survey of Finland 408, 11-25, doi:10.30440/bt408

Leskinen J (2020) Water quality of the old Särkiniemi open-pit mine and water treatment testing with industrial by-products (in Finnish). Thesis, Technology, Communication and Transport, Savonia University of Applied Sciences, 64 pp

Muniruzzaman M, Karlsson T, Ahmadi N, Rolle M (2020) Multiphase and multicomponent simulation of acid mine drainage in unsaturated mine waste: Modeling approach, benchmarks and application examples. Applied Geochemistry 120 (6):104677, doi:10.1016/j.apgeochem.2020.104677

Ribeta I, Ptacek CJ, Blowes DW, Jambor JL (1995) The potential for metal release by reductive dissolution of weathered mine tailings. Journal of Contaminant Hydrology 17, 239-273, doi:10.1016/0169-7722(94)00010-F

Vriens B, Peterson H, Laurenzi L, Smith L, Aranda C, Mayer KU, Beckie RD (2019) Long-term monitoring of waste-rock weathering at the Antamina mine, Peru. Chemosphere 215, 858-869, doi:10.1016/j.chemosphere.2018.10.105

Finite-Element Modelling Approach to Study Flow Processes During Groundwater Rebound in Abandoned Underground Hard Coal Mines

Timo Kessler, Maria-Theresia Schafmeister

University of Greifswald, Institute for Applied Geology and Hydrogeology, Friedr.-Ludwig-Jahn-Str. 17A, D-17487 Greifswald

Abstract

Groundwater rebound is one of the key challenges for the renaturation of underground mines. Numerical models can support the computation of rebound curves and the identification of long-term groundwater levels after steady-state conditions are reached. The present finite-element model case was to test the combination of different flow types and parameter configurations inside mine workings in order to optimally represent the flow patterns in cavity volumes and fractured rock masses. The approach may be an alternative to common pond-and-pipe models, particularly, if estimated cavity volumes of mine workings are uncertain or if groundwater levels in the surroundings are precarious.

Keywords: Groundwater Rebound, Finite-element Modelling, Flooding, Underground Mine, Hard Coal

Introduction

After the abandonment of underground hard coal mines, groundwater rebound constitutes a challenge for post-mining management of collieries. While mine water is constantly removed during active mine operation, water inflows from overlying aquifers and regional groundwater flow steadily flood mine workings once pumping is stopped. Targeting an environmentally compatible renaturation of collieries the prediction of rebound curves and steady-state groundwater levels in the surroundings of the mine are essential information.

In practice, pond-and-pipe models are typically employed to calculate the internal groundwater rebound. They use a finite-volume approach to balance the entire void space (including mine workings, mined coal seams, cavities and pore space) and the inflow of groundwater. Such models define flow functions at known water transfer points between two hydraulically disconnected volumes (Kortas and Younger 2007; Kessler *et al.* 2020). This is advantageous regarding the fragmented data basis, as mining reveals the geology and rock constitution only point-by-point relative to the entire aquifer volume mining has an effect on. On the other hand, groundwater heads in the contiguous rock matrix are not calculated and thus, cannot resolve the potentiometric rebound in the surroundings of the mine.

Fully-meshed finite-element models discretize the entire modeling space including rock matrix, geological structures and, if needed, single cavities and mine workings. That means that the model domain needs to be parameterized in its entire extent. The approach is thus costly in computation time and data requirements. The advantages are the depiction of physically-based flow and transport processes and spatially differentiated rebound curves that can be computed for any point within the modelling space (Kessler *et al.* 2020).

Model outline

The former hard-coal mining site Westfalen in Germany was selected for modelling groundwater rebound using a finite-element approach. The colliery has hydraulically an "island position" and is thus isolated from other mining sites or any neighbouring mine water management systems (Rüterkamp *et al.* 2000). It can be considered a closed system and is as such suitable for the present modeling approach. The colliery was finally closed in the year 2000 and since then infiltrating water is expected to flood the

mine. Due to backfilling of the shafts, the ongoing groundwater rebound is neither measured nor documented. As a result, a classical model calibration along measured groundwater heads is impossible. The baseline of the model is a detailed representation of the "empty" mine workings embedded in large-scale model space. The mine workings constitute the bulk of the floodable cavity volume in the mine. Unlike pond-and-pipe models both free flow in the cavities and porous medium flow are combined. The hydraulic parameterization is iteratively adjusted and analysed on its sensitivity regarding the modeled rebound curve.

Despite the backfilling of the winding shafts, the focus of the model is laid on the design of a discretized model that is able to reproduce the water level rise inside the mine. Backfilled shafts are yet considered as preferential flow paths with hydraulic conductivities higher than the adjacent rock matrix (Rüterkamp *et al.* 2000). At the same time, the model should be able to show the consequences on groundwater potentials in the contiguous rock matrix. Such an approach requires knowledge about the geometry and the hydraulic circumstances of the mine workings, a profound database of material properties and fracture characteristics in the collapsed overburden, and an quantitative idea of water inflows from extraneous and geogenic sources. Most of that information is available or can be estimated for the Westfalen site.

Location and hydrogeology

The Westfalen mine is located near the city of Ahlen in North Rhine-Westphalia at the Eastern edge of the Ruhr coal mining area. The mined coal seams are part of a 650 m thick stratigraphic sequence of the Upper Carboniferous period (Angrick 1999). It consists of alternating strata of sandstones, silt- and mudstones and interposed coal seams (Rüterkamp *et al.* 2000). The thickness of the overburden varies between 730 m in the Southwest and 1060 m in the Northeast (Angrick 1999). It consists of massive Upper Cretaceous sediments forming two major aquifers. The lower aquifer is fractured and consists of 165-185 m of carbon-rich marlstones of the Cenoman and Turon stage (Rüterkamp *et al.* 2000). Overlying is a hydraulic barrier, the "Emscher Mergel", which is built of clayey marlstones with a thickness of 475-525 m. Above follows an upper aquifer which is, in the lower Campanian marlstones fractured, and covered by some quaternary sediments that form a porous aquifer (Rüterkamp *et al.* 2000). Regarding the groundwater rebound primarily water from the lower confined aquifer is expected to infiltrate into the mine workings, besides some deep groundwater that flows through the mining area.

The carboniferous layers are subject to NE-SW striking folding and NW-SE trending normal faults dividing the mining district into a set of horst and graben structures (Hahne and Schmidt 1982; Grabert 1998). From a hydrogeological point of view, the fault structures are relevant as they transfer water from the lower aquifer into the mine workings below. Secondary fracture networks evolve above the mined seams due to mining activities and collapse of the overburden. The movement and disruption of rock masses increases the fracture void space and the hydraulic conductivity (Bahls 1963). They are less important for water inflow into the mine, but in reverse may facilitate the intrusion of mine water into the overburden (Rüterkamp *et al.* 2000). These mining induced fractures are time-dependent as subsidence and the high overburden pressure slowly close the fractures and void spaces.

Methods

Model setup

The numerical flow model is setup and run with the finite-element code FEFLOW (Diersch 2014). The modelling area of the Westfalen site covers an area of 500 km² with the colliery situated in the centre of the area. The boundaries of the model are constant-head limited and set in a far enough distance from the mine to allow large depression cones without influencing the regional groundwater flow too much. Due to hydraulic barrier of the "Emscher Mergel", no meteoric inflow or groundwater recharge is defined. Instead, the entire model is considered confined aquifers with varying hydraulic potentials.

The core of the model is the representation of the mine working itself including shafts, adits, banks and longwalls. All of those mining cavities are depicted at the appropriate scale and located correctly within the three-dimensional modelling space. The colliery has seven shafts and four main levels between 850 and 1200 m below the surface. The model is discretized with a structured meshing algorithm, facilitating a layered mesh design at all depths. Each mining level is represented as one separate modelling layer (Figure 1). Around the mine workings the mesh is refined to match the dimension of the cavities. Main adits and winding shafts are represented as one-dimensional discrete structures inside the model space that are not discretized separately. They are understood as embedded cylindrical objects that facilitate pipe flow and that are computed with the Hagen-Poiseuille equation (Sutera and Skalak 1993). Similarly, tectonic faults are treated as two-dimensional, subvertical planes with a Darcy flow type.

The rock matrix honours the hydrogeological units as well as the mining induced heterogeneities in the overburden of the min workings. According to Ma *et al.* (2016) a collapsed overburden of mined seams can be classified into three zones, the cavity, fissure and bending zone. Following this scheme, the matrix is divided into a set of model subspaces (undisturbed rock matrix, broken rock matrix, fissure zone and cavity zone).

Water inflows from the overlying Turon aquifer are considered with infiltration wells inside the discrete adits. In total 8 water inflow points are defined at the two lowest mining levels summing up to 5.3 m^3 per minute. Further boundary conditions such as leakage coefficients between the lower and the deeper aquifer or between matrix and the discrete structures are not defined. The transfer rates are unknown and vertical water transfer is accounted for at the inflow points.

Parameterization

The layered model structure allows to define hydraulic conductivities and specific storage values for all geological units in the overburden separately (Table 1). The same is done for the model subspaces in the hanging wall of the mine workings. Worked areas like gobs, longwalls and collapsed hanging walls, for example, are handled as highly conductive matrix bodies relating to the level of resolution and disorder (see cavity or fissure zone in Table 1). Most of the used parameter values are taken from the literature (e.g. Bahls 1963; Baltes *et al.* 1998; Denneborg and Müller 2017; König *et al.* 2017). Adits

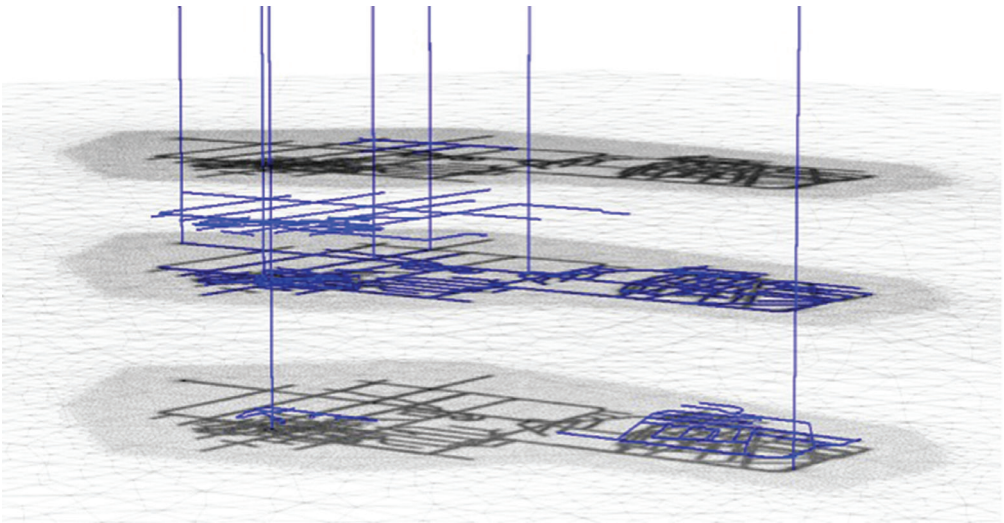

Figure 1 *Discretization of the mining layers including the winding shafts and main adits implemented as one-dimensional discrete features.*

Table 1 *Hydraulic parameterization of geological units and model subspaces within the mine workings (values adapted from e.g. Baltes* et al. *(1998); Denneborg and Müller (2017); König* et al. *(2017).*

	Hydraulic cond. horiz. [m/s]	Hydraulic cond. vert. [m/s]	Hydraulic aperture [m]	Specific storage [1/m]	Diameter / Thickness [m]
			overburden		
Campan (upper aquifer)	1e-07	3e-07	0.001	1e-04	
"Emscher Mergel" (hydraulic barrier	1e-10	1e-10	< 0.0001	1e-05	
Turon (lower aquifer)	2e-07	5e-07	0.001-0.003	1e-04	
"Essener Grünsand" (hydraulic barrier)	3e-08	5e-08	< 0.0001	1e-05	
			mining unit (carbonic deep aquifer)		
undisturbed rock matrix	8e-09	5e-09	< 0.0001	1e-07	
broken rock matrix	4e-08	1e-08	0.002	1e-06	9-24
fissure zone	4e-06	1e-05	0.005-0.05	5e-04	3-6
cavity zone	1e-02	1e-02	0.01-0.2	1e-04	1-2
			mine workings		
mine adits			0.002	0.95	5.5
mine shafts			0.002	0.95	4.0
			geological structures		
tectonic faults	1e-04	1e-04	0.001	1e-04	3.0

and shafts are defined as of tube geometry, specific storage and hydraulic aperture within the cavity volume. They determine how the structures internally facilitate water flow.

Groundwater rebound calculation

In order to model groundwater rebound, the entire colliery needs to be in a drained condition in the initial state. To achieve this, a constant-head boundary condition is set at the bottom of the deepest winding shafts. Once steady-state conditions are reached, the boundary conditions were removed and the model was converted into a transient model. Based on the steady inflow on the two lowest mining levels the model calculates the potentiometric heads inside the cavity volumes and in the adjacent rock matrix.

Unlike pond-and-pipe models for sites with an active mine water management, the present model cannot be calibrated with measured rebound curves, as the shafts of the Westfalen colliery became backfilled when the mine was closed. Instead, parameter variations are used to analyse the sensitivity of how the implementation of mining cavities or collapsed hanging walls affect the groundwater rebound. Starting point is a reference model that calculates a complete rebound in a time frame of 30 years.

Results and Discussion

The finite-element approach models the groundwater rebound as a combination of pipe and matrix flow. Mining adits and shafts are represented as one-dimensional discrete structures that are parameterized separately. Alternatively, mine workings can be discretized, too, but it is important to note that complete drainage of specific parts within the saturated zone is not feasible with internal boundary conditions.

The specific storage of cavity volumes needs to be set nearly 1, where values between 1e-04 to 1e-06 are commonly used for the rock matrix. An sensitive parameter for the cavity volumes is the hydraulic aperture inside the structures. Low values cause high storage captures inside the mine workings and keep the hydraulic gradient at a low level. Inflow water rapidly moves inside the adits and the water level increases almost simultaneously. In reverse, large apertures reduce the storage capacity and extend the

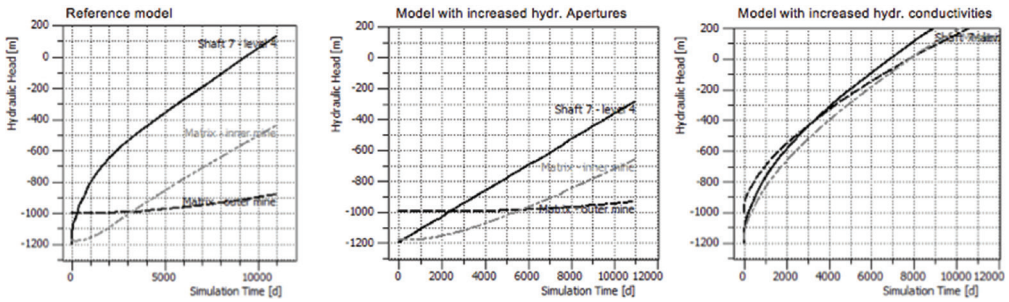

Figure 2 *Groundwater rebound curves for: a) the bottom of the shaft No.7 (black solid line), b) in the unworked rock matrix within the mining area on the third mining level (grey dashed line), and c) in the rock matrix outside the mining area on mining level 4 (black dashed line). The left graph shows the reference case, the middle graph increased hydraulic apertures and the graph on the right illustrates the rebound with increased hydraulic conductivities.*

flooding period. It also requires a remarkably higher computation effort. The effect of this parameter is shown in Figure 2. The left picture shows the reference model and the graph in the middle illustrates the rebound if large hydraulic apertures are used. The initial stage of the rebound in the shaft and inside the mined area is much slower and shows a linear increase.

The second important aspect of finite-element models is the parameterization of the gobs and the collapsed overburden. A vertical division of model subspaces was applied using hydraulic conductivities that decline with vertical distance from the mining level. The caving zone near the worked seams with void spaces of several decimetres in diameter have conductivities several orders of magnitude higher compared to the broken or fractured rock 20-50 m above. The fractured or disordered overburden may not be important for the downward movement of groundwater from upper aquifers. It is rather relevant for the upward infiltration during the flooding of the mine workings. The effect of an increased hydraulic conductivity of the rock matrix (two orders of magnitude) is shown in the left picture of Figure 2. The potentiometric rebound in the shaft and in the rock matrix is almost simultaneous, but also much faster compared to the reference case.

Finite-element have proven to be a good alternative for rebound modelling if the geometry and location of the main cavities are known and hydraulic properties of the adjacent rock matrix and the collapsed overburden can be estimated. The primary limitation of the approach is the numerical effort, as fine meshes as well as discrete structures require, depending on the parameterization, a lot more computational power as pond-and-pipe models would do.

References

Angrick J (1999) Bergwerk Westfalen - Geologie und Lagerstätte

Bahls R (1963) Überlegungen über die vermutliche Sohleführung im westlichen Baufeld der Zeche Westfalen als Vorbereitung für die Aufstellung eines Abbauplanes. Bochum, Germany

Baltes B, Fischer-Appelt K, Larue PJ, Javeri V (1998) Entwicklung und Anwendung analytischer Methoden zur Eignungsuntersuchung der Verbringung bergbaufremder Rückstände in dauerhaft offene Grubenräume im Festgestein

Denneborg M, Müller F (2017) Hydrogeologische Systembeschreibung und Auffälligkeiten an der Tagesoberfläche. NRW, Germany

Diersch H-JG (2014) FEFLOW. Springer Berlin Heidelberg, Berlin, Heidelberg

Grabert H (1998) Abriß der Geologie von Nordrhein-Westfalen. Schweizerbart, Stuttgart

Hahne C, Schmidt R (1982) Die Geologie des Niederrheinisch-Westfälischen Steinkohlengebietes. Verlag Glückauf GmbH, Essen, Germany

Kessler T, Mugova E, Jasnowski-Peters H, *et al* (2020) Grundwasser in ehemaligen deutschen Steinkohlenrevieren – ein wissenschaftlicher

Blickwinkel auf Grubenflutungen. Grundwasser 25:259–272. https://doi.org/10.1007/s00767-020-00460-0

König CM, Rosen B, Rüber O, Tielker J (2017) Modellierung des Stofffreisetzungspotentials und der Stoffausbreitung über die Grundwasserströmung. NRW, Germany

Kortas L, Younger PL (2007) Using the GRAM Model to Reconstruct the Important Factors in Historic Groundwater Rebound in Part of the Durham Coalfield, UK. Mine Water Environ 26:60–69. https://doi.org/10.1007/s10230-007-0152-8

Ma L, Wang G-C, Shi Z-M, *et al* (2016) Simulation of groundwater level recovery in abandoned mines, Fengfeng coalfield, China. J Groundw Sci Eng 4:344–353

Rüterkamp P, Hewig R, Domrös M, *et al* (2000) Hydrogeologisches Gutachten zu möglichen Auswirkungen des Grubenwasseranstiegs nach Einstellung der bergbaulichen Wasserhaltung des Steinkohlenbergwerks Westfalen. Essen, Germany

Sutera SP, Skalak R (1993) The History of Poiseuille's Law. Annu Rev Fluid Mech 25:1–20. https://doi.org/10.1146/annurev.fl.25.010193.000245

Long-Time Effect of Ancient Salt Production (Perm Krai, Russia)

Elena Khayrulina, Natalya Mitrakova

Perm State National Research University, Bukireva, 15, 614990, Perm, Russia
elenakhay@gmail.com, mitrakovanatalya@mail.ru

Abstract

On the territory of the outflow of ancient brine wells in the valley of the Usolka River, soils and vegetation, transformed under the long-term impact of highly mineralized waters on the soil pore, were studied. Brines from ancient brine-lifting wells flow in streams along the soil surface and flow into the Usolka River determining its Na-Cl composition. The study area is characterized by the presence of salt-tolerant plants. Long-term influence of sodium-chloride waters on alluvial soils of the Usolka River led to the formation of a secondary gley sulfate-chloride solonchak (Gleyic Fluvic Solonchak (Loam, Salic)).

Keywords: Salinity, Gleyic Fluvic Solonchak, Brine Wells, Halophyte, Terrestrial and Aquatic Ecosystems

Introduction

In Perm Krai (Russia) salt has been mined for about 500 years. For 400 years salt had been extracted from brine wells. Some of these wells exist to this day. Activization of karst processes leads to entry of saline ground water through the wells onto the earth surface (Kharitonov 2015). Verkhnekamskoe Potash Deposit opened only 90 years ago. Potash ores are extracted mainly by underground mining methods. The territory of the Verkhnekamskoe Potash Deposit territory has the current anthropogenic impact of potash mining is combined. Research of environmental consequences of ancient brine production allows determining long time influence of salinization on terrestrial and aquatic ecosystems.

The impact of highly mineralized waters on the ecosystem leads to a change in the chemical composition of surface water and groundwater, which affects the soil cover in their physical and chemical properties (Hulisz *et al*. 2013; Salama *et al*. 1999), the composition of vegetation with the change of native plant species to salt-tolerant ones, to the extent of halophytes emergence (Lavrinenko *et al*. 2012; Piernik *et al*. 2015; Sommer *et al*. 2020).

Ancient brine wells have retained their influence for a long time and determined salt-tolerant terrestrial and aquatic ecosystems. This research can help to forecast anthropogenic impact of potash mining.

The purpose of this work is to study properties of alluvial soils of the Usolka River valley in the area of influence of brine wells and to investigate the soil-forming process and the vegetation cover.

Study area

The studies were conducted in the north-east of the central part of Perm Krai in the Aleksandrovsky District on the territory of one of the first Russian settlements with the production of salt, Yaivinsky ostrozhok, founded in 1570, where a group of five historical wells in the Usolka River valley persist to this day (Khayrulina *et al*. 2017). Salt mining was carried out on the south-eastern periphery of the salt deposit and outside the potash deposit outline of the Verkhnekamskoe salt deposit (Fig. 1). Geologically, the study area is located in the Cis–Ural foredeep, in the southern part of the Solikamsk depression, within the Ust–Igumsky salt swell.

Natural outlets of saline waters in the Usolka River valley contributed to the active development of salt industry. Brine mining was carried out from a depth of 30–40 m with brine pipes. Salt production in the Usolka

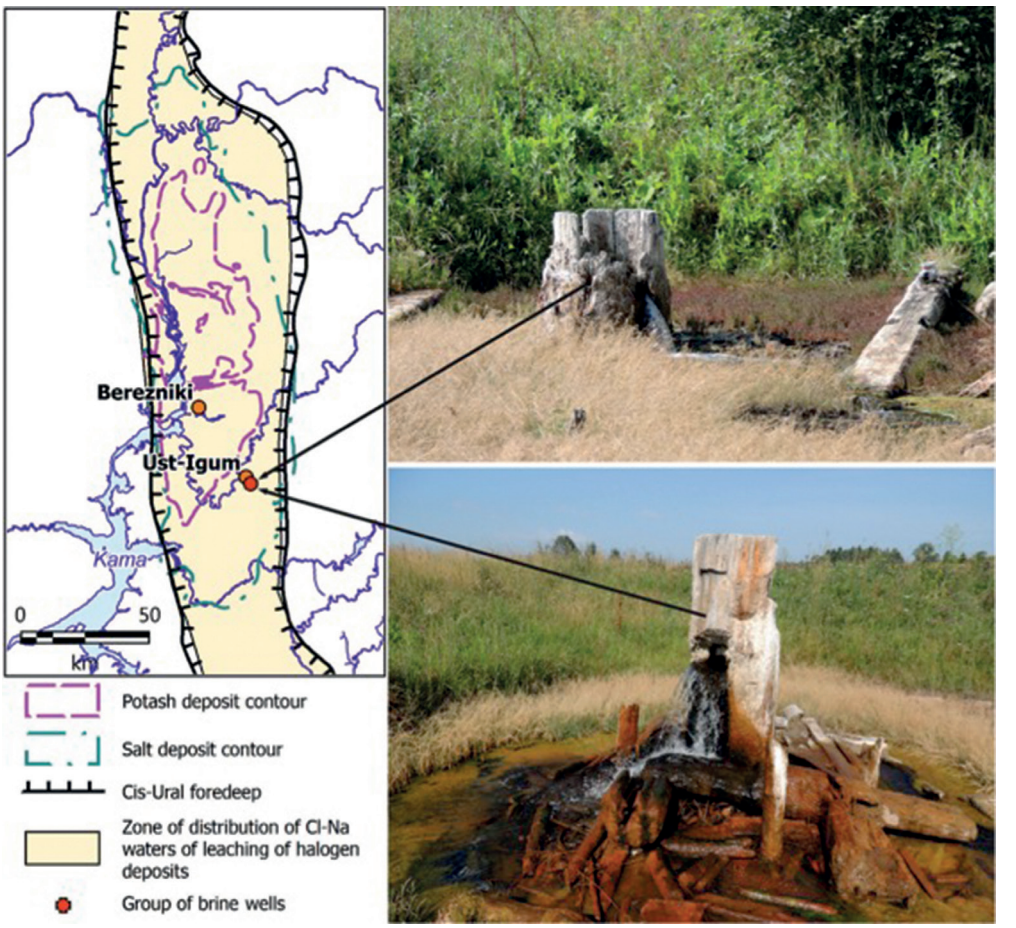

Figure 1 *Distribution of potash and salt deposits of the Verkhnekamskoe salts deposit and location of objects of observation (images: E.A. Khayrulina).*

River valley was stopped in the 18th century. The study area is significantly remoted from industrial enterprises and settlements that excludes modern anthropogenic influence.

Methods

Five wells are located on a floodplain terrace 80–120 m from the Usolka River. Sampling of water from brine-lifting wells, streams and rivers was carried out in 2015, 2016 and 2017. In water, the following criteria are determined: pH – by potentiometric method, HCO_3^- – by titration method according to GOST 31957-2012; Fe_{total} – by photometric method; Cl^-, K^+, SO_4^{2-}, Ca^{2+}, Na^+, Mg^{2+}, NO_3^-, NO_2^- – by capillary electrophoresis using Kapel-104 (Russia); dry residue – by gravimetric method according to PND F 14.1: 2: 4.261-10; mineralization – by calculation method; specific electrical conductivity – using conductometer Hanna HI 8733 (Germany).

Soil samples were taken in the floodplain of the Usolka River in 2016 at a distance of 15–20 cm from the channel of a salty stream pouring out from brine-lifting wells. The soil types were determined according to World Reference Base for Soil Resources (World reference base 2015). Physicochemical research of soils included (Theory and practice 2006; Mineev 2001): determination of organic matter according to Tyurin; determination of pH_{H_2O} and pH_{KCl} using potentiometric method according to GOST 26483-85; determination of hydrolytic acidity using Kappen method; determination of exchangeable cations using Kappen-Gilkowitz method; determination

of the cation exchange capacity (CEC) in carbonate samples using the barium chloride method; determination of mobile potassium using flame photometry; the quantity and quality of soluble salts was determined in water extractions: Na^+ and K^+ – using flame photometry; Cl^- – titration with silver nitrate; Ca^{2+}, Mg^{2+} – by trilonometric method; the amount of sulfate ions was calculated as a difference between the amounts of cations and anions; the amount of toxic salts – using the calculation method. The sodium adsorption ratio (SAR) was used to isolate sodium soils; SAR is the ratio of the concentration of Na^+ to the square root of the sum of Ca^{2+} and Mg^{2+}. Agrochemical properties are determined only in the surface layers. The content of water-soluble ions was determined throughout the soil profile.

Result and Discussion

At the present stage, mineralization of the waters pouring out from the wells is 30–34 g/L for the brine-lifting wells of the Yaivinsky ostrozhok; chloride and sodium ions prevail; the flow rate of the wells is 0.009–0.011 m^3/s. The chemical composition of the waters of the brine wells was stable. The content of Cl^- in brines exceeded the MPC (Maximum allowable concentration) by 49 times and reached 14700 mg/L, while the content of Na exceeded the MAC by 82 times and amounted to 9800 mg/L (Table 1). Outflows of wells form hydromorphic conditions in the area of the floodplain terrace and flow into the Usolka River in the form of two streams.

The inflow of brines into natural waters transforms the Ca^-HCO_3 composition of rivers into Na^-Cl composition. Mineralization of water in rivers, into which saline underground springs are discharged, is much lower due to dilution with fresh waters and amounts to 1.2–1.3 g/L. The predominance of Na and Cl in the chemical composition of the Usolka River waters above the influx of well outflows indicates the presence of salt sources that we have not yet discovered.

As a result of long–lasting inflow of highly mineralized groundwater onto the surface from brine wells of the Yaivinsky ostrozhok, in the floodplain of the Usolka River, a secondary gley humus solonchak with a sulfate-chloride sodium type of salinity (Gleyic Fluvic Solonchak (Loam, Salic)) was formed. The examined secondary solonchak was formed from the alluvial humus gley soil typical of floodplains of taiga landscapes, the upper horizon of which is characterized by heavy granulometric composition, a weakly acidic or acidic reaction of the soil medium, and a low adsorption capacity (Vasiliev *et al*. 2014).

In the profile of the studied secondary solonchak, we identified three horizons: solonchak, gleyed, and alluvial rock. S[AYg] – solonchak horizon, 0–45/45 cm, with signs of gleying; Gs – gleyed horizon, 45–95/52 cm, dark-gray-glaucous, with an emerging prismatic structure; at a depth of 80–90 cm, we found decaying wood and stones. Cgs – alluvial gley rock, occurring from a depth of 95 cm, light gray-glaucous; moist, structureless with a smell of hydrogen sulfide.

In the surface soil layers (thickness of layer 10 cm) of three different pits of the solonchak, the content of organic carbon varied from 0.9 to 2.9%, the neutral and slightly alkaline reaction of the soil is explained by the influx of sodium chloride water from the brine wells. The studied solonchaks are characterized by an average adsorption capacity of 25.2–36.3 mmol/100 g (Table 2), which is typical for alluvial soils and, seemingly, is associated with low values of organic matter. The amount of mobile potassium compounds varied from

Table 1 *Chemical composition of surface waters in the area of outflowing brine wells.*

Sampling site	pH	Content, mg/L								
		HCO_3^-	SO_4^{2-}	Cl^-	Ca^{2+}	Mg^{2+}	Na^+	K^+	Fe_{total}	TDS
MAC	6,5–8,5	–	100	300	180	40	120	50	0,1	–
Wells	7,08	285	3176	14732	1179	12	9886	26	1.4	29417
The Usolka River	8,1	222	161	492	94	17	352	1.4	–	1342

Table 2 Agrochemical properties of solonchak.

Soil name	№	Layer, cm	C_{org}, %	pH_{H2O}	pH_{KCl}	CEC mmol/100 g	K_{HCl} mg/100 g	SAR
Gleyic Fluvic Solonchak (Salic, Loam)	1	0–10	2.88	7.15	7.06	36.3	12.5	13.8
	2	2–12	2.9	7.72	7.16	25.2	50	19.8
	3	2–12	0.9	8.2	7.59	29.6	50	17.9

12.5 to 50 mg/100 g; it appears that this is due to the supply of potassium from the waters of brine wells.

The maximum content of toxic salts – 1.1% – was noted in the 0–10 cm layer and 1.2% – in the 100–115 cm layer; the minimum amount of toxic salts – 0.55% – was noted in the 27–40 cm layer. The amount of toxic salts indicates a high degree of soil salinity; the surface soil layer was characterized by chloride sodium type of salinity, from a depth of 11 cm – by sulfate-chloride sodium type; from a depth of 60 cm, sulfate ions and sodium cations prevailed (Fig. 2), which is associated with a change in the prevailing anions in the water extract from soil. The waters of the brine wells with chloride type of salinization determined the chemical properties of the soil profile.

We noted the highest content of Cl^- and Na^+ in the 0–10 cm layer – 613 and 425 mg/100 g of soil, respectively; the content of Cl^- decreased by 1.5–2.3 times with the depth of the soil profile; the content of Na^+ also decreased with depth by 1,4–2 times, but at a depth of 100–115 cm it increased to the surface horizon values (Fig. 2). We observed the highest content of Ca^{2+}, Mg^{2+} and SO_4^{2-} in the solonchak in 100–115 cm layer; it amounted to 91, 10 and 609 mg/100 g, respectively. We found gypsum at a depth of 60 cm. The formation of gypsum can be associated with exchange reactions in soil as a result of the interaction between calcium of the soil adsorption complex and sulfate–sodium solutions (Yamnova *et al.* 2013). As a result of the impact of salt water on the surface layer of the soil, at a depth of 27–40 cm, we observed a minimum content of almost all ions.

The sodium adsorption ratio (SAR) for the surface layer of sample 1 (0–10 cm) is 13.2, the highest value of the ratio – 17.1 – was observed in the 11–21 cm layer, the lowest SAR value – 12.8–11.2 – at a depth of 60–115 cm. In the surface layers of samples 2 and 3, SAR values were 19.8 and 17.9, respectively. SAR values over 13 indicate a significant

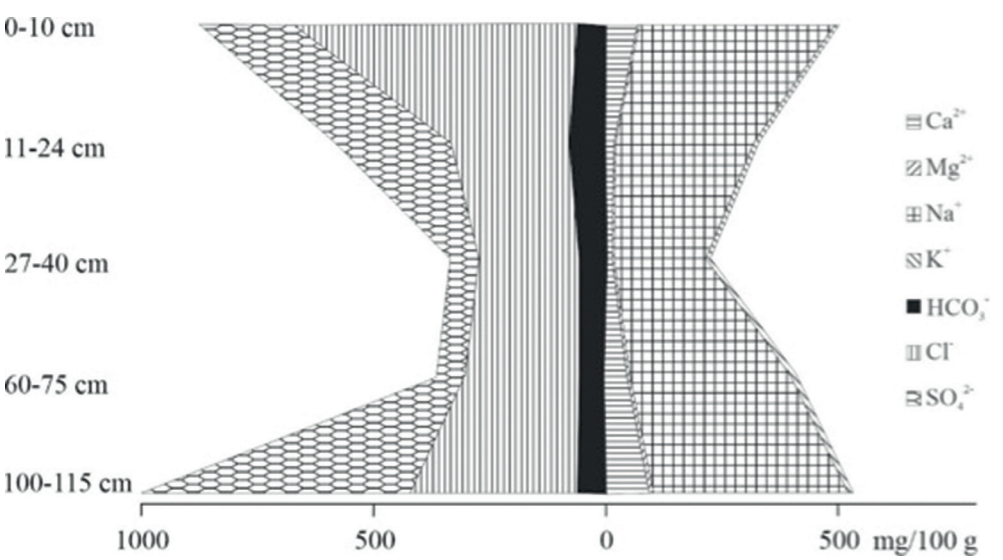

Figure 2 Salt profile of solonchak.

proportion of sodium in the soil adsorption complex and a soil alkalinization.

The content of water-soluble sodium and the sodium adsorption ratio (SAR) in solonchak indicated the transition of sodium into the soil adsorption complex; sodium, displacing other cations, mainly calcium and magnesium, from the soil adsorption complex, contributed to the deterioration of the physicomechanical properties of the soil, which caused its viscosity, stickiness, lack of structure in the wet state and firmness in the dry state.

The secondary solonchak is formed from alluvial soil that is quite mature. The main soil-forming factors in solonchak formation in the valley of the Usolka River in the brine outlet area were saline waters, relief, climate and the duration of the brine impact on the soil cover. Despite the fact that saline waters are classified as eventual soil-forming factors, in our study they were the main cause of the emergence of solonchaks. However, in spite of the genetic and chemical changes in the soil, with the limitation or complete absence of the influence of brines, the soil evolution can go the opposite way, desalinization of saline soils will occur, the soil will again become alluvial humic.

The vegetation cover of the study area is represented by species associated with floodplain meadow landscapes. The floodplain tallgrass of the study area includes meadow fescue *Festuca pratense* Huds., alsike clover *Trifolium hybridum* L., common yarrow *Achillea millefolium* L., meadow vetchling *Lathyrus pratensis* L., cock's-foot *Dáctylis glomerata* L., timothy-grass *Phleum pratense* L. meadow buttercup *Ranunculus acris* L., autumn hawkbit *Leontodon autumnalis* L., smooth meadow-grass *Poa pratensis* L., garden angelica *Angelica officinalis Hoffm*., meadowsweet *Filipendula ulmaria* (L.) Maxim, parsnip *Pastinaca sylvestris* Mill. The plant community is represented mainly by salt tolerant plant species.

High salinity of soils along the salty stream led to the appearance of glasswort *Salicornia perennans* **WILLD**. It belongs to the group of obligate halophytes with the highest resistance to salts that grow well and develop on saline soils, absorb a large amount of salts from the soil.

Usually, halophytes grow on highly saline soils on the sea coasts, along the shores of salt lakes. Halophytes form red "glades" and "paths" in places where highly mineralized waters are discharged; in this case, they grow along the banks of a stream formed by the waters of ancient brine wells. In a humid climate with a leaching water regime, the appearance of halophytes is possible with a long-term impact of saline waters on soils; most often this process has anthropogenic origin.

The distribution area of the obligate halophyte Salicornia perennans Willd in Perm Krai is local. Currently, we are working on creating a natural monument to protect this ecosystem, which comprises brine wells, soils and vegetation.

Conclusions

As a result of long-term unloading of ancient brine wells in the floodplain of the Usolka River, in the area of alluvial gley humus soils, secondary solonchak with sulfate-chloride sodium type of salinization was formed. In Perm Krai, due to the humid type of climate and leaching water regime, the formation of saline soils is associated only with the natural discharge of saline springs in floodplains of rivers in areas of salt mass bedding, as well as with the consequences of the industrial extraction of potash salts.

In addition to transformation of the soil cover of the Usolka River valley, there was a change in the ionic composition of natural waters of the Usolka River, a change in plant species to more salinization resistant: in the immediate vicinity of the streams flowing from the wells, the obligate halophyte Salicornia perennans Willd appeared, which is a plant unique for Perm Krai.

Ancient brine wells have retained their influence for a long time and determined transformation of terrestrial and aquatic ecosystems. This research can help to forecast ecosystem changes due to potash mining influence.

Acknowledgements

This work was supported by the Ministry of Science and Higher Education of the Russian Federation

(No 2019–0858) and The program of activities of the world-class research and education center.

References

Hulisz P, Piernik A (2013) Soil affected by soda industry in Inowrocław. Technogenic soils of Poland; Charzyński P, Hulisz P, Bednarek RM, Eds.; Polish Society of Soil Science, Toruń, pp. 125–140. ISBN 978–83–934096–1–7

Kharitonov TV (2015) Alternative underground leaching salts of BSZ. Problemy mineralogii, petrografii i metallogenii. Nauchnye chtenija pamjati P.N. Chirvinskogo. P. 375–382. In Russian

Khayrulina EA, Novoselova LV, Poroshina NV (2017) Natural and anthropogenic sources of soluble salts on the territory of the upper Kama potash deposit. Geographical bulletin 1(40): 93–101. doi 10.17072/2079–7877–2017–1–93–101 In Russian

Lavrinenko IA, Lavrinenko OV, Dobrynin DV (2012) Long–term dynamics and destruction of marsh vegetation in the Kolokolkova Bay of the Barents Sea. Vegetation of Russia 21: 66–77. https://doi.org/10.31111/vegrus/2012.21.66 In Russian

Mineev VG (2001) Practicum in Agricultural Chemistry. Moscow State University Publ. 689 p.

Piernik A, Hulisz P, Rokicka A (2015) Micropattern of halophytic vegetation on technogenic soils affected by the soda industry. Soil Science and Plant Nutrition, 61 (1): 98–112. DOI: 10.1080/00380768.2015.1028874

Salama RB, Otto CJ, Fitzpatrick RW (1999) Contributions of groundwater conditions to soil and water salinization. J. Hydrogeology, 7: 46–64. https://doi.org/10.1007/s100400050179

Sommer V, Karsten U, Glaser K (2020) Halophilic Algal Communities in Biological Soil Crusts Isolated From Potash Tailings Pile Areas. Frontiers in Ecology and Evolution, 8 (46). https://doi.org/10.3389/fevo.2020.00046

Theory and practice chemical analysis of soils (Edd. Vorobyova LF). M.: GEOS, 2006. 400 p.

Vasiliev AA, Romanova AV Iron and Heavy Metals in Alluvial Soils of the Middle Pre Ural Region. Publishing Printing Center "Prokrost": Perm, Russia, 2014; ISBN 978–5–94279–210–7. (In Russian).

World reference base for soil resources 2014 (2015) Food and agriculture organization of the United Nations, Rome. 192 p.

Yamnova IA, Pankova EI (2013) Gypsic pedofeatures and elementary pedogenetic processes of their formation. Eurasian Soil Science 46 (12): 1117–1129. DOI: 10.1134/S1064229313120089

Steel Slag-Limestone Reactor with Resistance to Fe: Laboratory and Pilot Scale Evaluations of Mn Treatment Efficiency

Duk-Min Kim[1], Youn-Soo Oh[2], Hyun-Sung Park[2], Dae-Gyu Im[1], Woong-Lim Lim[1], Hye-Rim Kwon[1], Joon-Hak Lee[2]

[1]*Department of New Energy and Mining Engineering, Sangji University, Wonju 26339, South Korea, kdukmin8@sangji.ac.kr, ORCID 0000-0002-1537-6866, daegull1995@naver.com, dndfla08@naver.com, ossgpfla@naver.com*

[2]*Korea Mine Reclamation Corporation (MIRECO), Wonju 26464, South Korea, oys1223@mireco.or.kr, hspark@mireco.or.kr, jun292@mireco.or.kr*

Abstract

Mixed substrate of steel slag and limestone were applied in reactors to evaluate resistibility to Fe. Steel slag mixed with limestone could decrease Mn from 32–46 mg L^{-1} to <3 mg L^{-1} with addition of 4.5–24.4 mg L^{-1} of Fe in the bench-scale experiment. In the pilot-scale experiments in five mines in South Korea, 95–99% of Mn was removed during the maximum test period of 4 years. Precipitation as Fe and Mn carbonates may have contributed to the Mn removal and resistibility to Fe.

Keywords: Manganese, Passive Treatment, Mine Drainage, Mn Carbonates, Fe Resistibility

Introduction

Mn is one of the common contaminants in mine drainage. Mn in drinking water has been found to affect the nervous system (USEPA 2004; Rodríguez-Barranco *et al.* 2013), and it has been associated with intellectual impairment in school-aged children (Bouchard *et al.* 2011; Rodríguez-Barranco *et al.* 2013). To remove Mn in mine drainage, pH higher than 9.5 is often required, so active treatment has been generally applied.

Slag leach beds (SLBs) have been applied in pilot- and full-scale passive treatment systems of Mn in the last 25 years (Ziemkiewicz 1998; Hamilton *et al.* 2007; Skousen *et al.* 2017 and references therein). In this method, freshwater reacts with steel slag to generate alkaline water to treat Mn-bearing water at downstream. However, it is generally difficult to meet environmental standards for Mn and pH at the effluent due to the changing flow rate of the alkaline water and contaminated water (Goetz and Riefler 2014). As an alternative of SLBs, a slag reactor containing steel slag to directly react with contaminated water can be used. Two issues need to be overcome to apply a slag reactor. One is clogging of the substrate, which can induce overflow; this can be improved by applying a stop-log to decrease the outflow water level and induce a sufficient hydraulic gradient. The other one is that Fe^{2+} of the influent inhibits Mn removal due to the prior oxidation of Fe^{2+} (Nairn and Hedin 1993; Gouzinis *et al.* 1998) and/or reductive dissolution of Mn oxides by Fe^{2+} (Burdige *et al.* 1992; INAP 2012).

Development and assessment of passive Mn treatment system with tolerance of Fe is limited. The objective of this study is to evaluate Fe-tolerance in some kinds of slag reactor, to assess the mechanism, and to assess Mn treatment efficiencies of several pilot-scale slag reactors.

Materials and methods

In the bench-scale experiment, S, SL, and SG reactors were filled with steel slag, steel slag (40 vol.%) + limestone (60%), and steel slag (40%) + Mn-coated gravel (60%), respectively. Steel-making slag from a basic oxygen furnace of a steelmaking factory in South Korea was used. It had CaO, SiO_2, Fe oxides, MgO, Al_2O_3, MnO, and P_2O_5 contents of 29.4%, 15.0%, 27.8%, 6.9%, 3.5%, 3.4%, and 2.1%, respectively. The diameters of the steel

slag, limestone and Mn-coated gravel were 2–6 mm, 2–5 cm, and 2–5 cm, respectively. The manufacturing procedure of the Mn-coated gravel is described in Kim *et al.* (2017). A layer of 4–5 cm diameter gravel was installed at the bottom of each reactor to create uniform upward flow.

The three reactors were operated for 366 days. Initial inflow Mn concentrations were 30–50 mg L^{-1}, and residence times were 0.6–1.8 d. After the reactions with Mn alone, both Fe and Mn were added to the inflow for 41 additional days. Fe, Fe^{2+}, and Mn concentrations were 4.5–24.4 mg L^{-1}, 3.1–12.0 mg L^{-1}, and 32–46 mg L^{-1}, respectively, and residence times were 0.8–1.5 d at that time.

Pilot-scale treatment systems were installed and operated in Ilwol, Dalseong, Dadeok, Sambong, Taehwa, and Sindong mines in various regions in South Korea. Inflow Mn concentrations ranged between 2 and 45 mg L^{-1} and operation periods ranged between 0.5 and 4 years.

The pH values were measured using a portable meter (model Orion 3 Star). Dissolved Fe^{2+} concentrations in the water samples were determined using a portable colorimeter (model Hach DR-890) following the phenanthroline method (APHA 2017). Alkalinity was determined in the field via volumetric titration using a digital titrator (model Hach AL-DT, Hach). Water samples were filtered through a 0.45-μm membrane and then transferred into 50-mL PE tubes. Samples for cation analysis were preserved by adding ≈10 drops of concentrated nitric acid to maintain the pH <2, and then stored at 4 °C until analysis. Concentrations of dissolved cations were analyzed by Inductively Coupled Plasma Optical Emission Spectroscopy (ICP-OES, Varian 720-ES) at the Institute of Mine Reclamation Technology (IMRT), Korea Mine Reclamation Corporation. Relative standard deviations were less than 5% of the measured values for ICP-OES. Precipitates in the SL reactor were analyzed via scanning electron microscopy (SEM) with energy dispersive spectroscopy (EDS), Carl Zeiss Supra40) at IMRT.

Results and discussion

Mn treatment efficiency and resistibility to Fe in bench-scale experiment

Tolerance to Fe was evaluated in all reactors in the bench-scale experiment. The operation period and discussions were added from the previous study (Kim *et al.*, 2017). Outflow pH from the reactors increased to 6.9–7.8 from 3.1–5.0. The Fe concentrations at 4.5–24.4 mg L^{-1} in the inflow were almost exhausted to <0.05 mg L^{-1} in the outflow. The S (slag) and SG reactors had outflow with Mn at 2.7– 12.4 mg L^{-1} and 1.2–29.0 mg L^{-1}, respectively (Fig. 1). Mn exceeded 2 mg L^{-1} even with Fe at <5 mg L^{-1} for both the S and SG reactors. In contrast, the SL reactor showed Mn consistently less

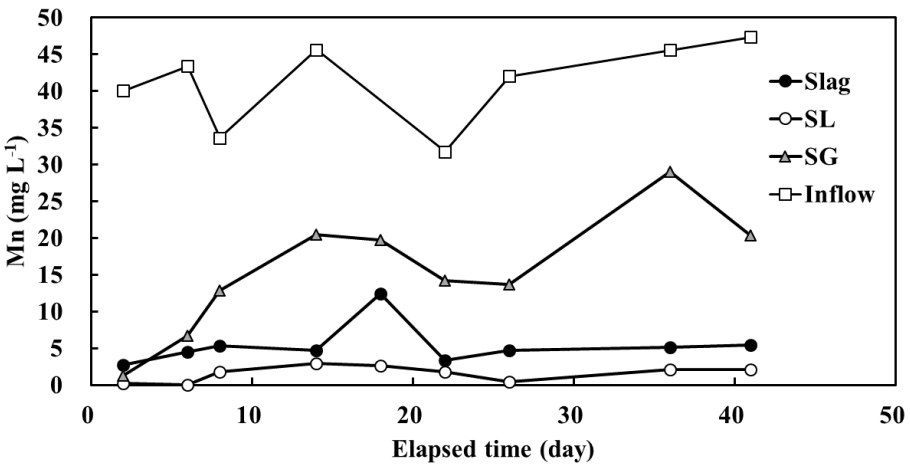

Figure 1 *Variation in Mn concentrations as a function of elapsed time since Fe addition for the S, SL, and SG reactors.*

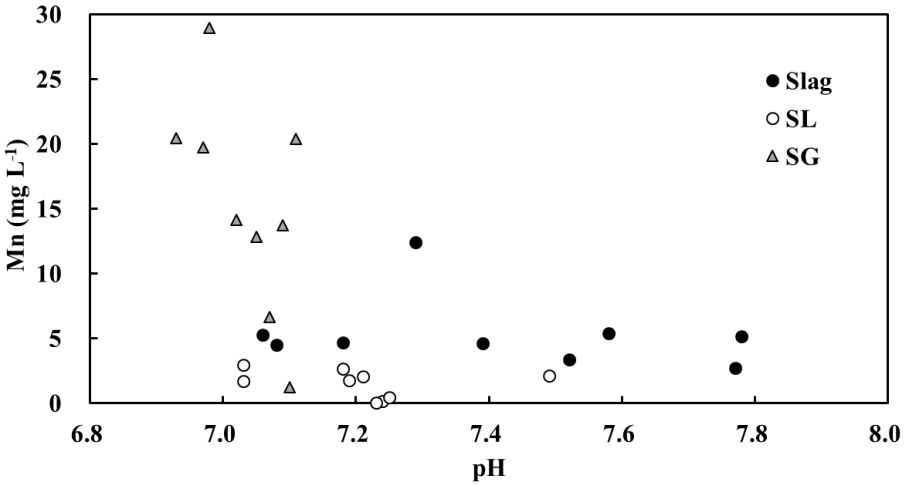

Figure 2 Plot of Mn concentrations against pH after the Fe addition for the S, SL, and SG reactors.

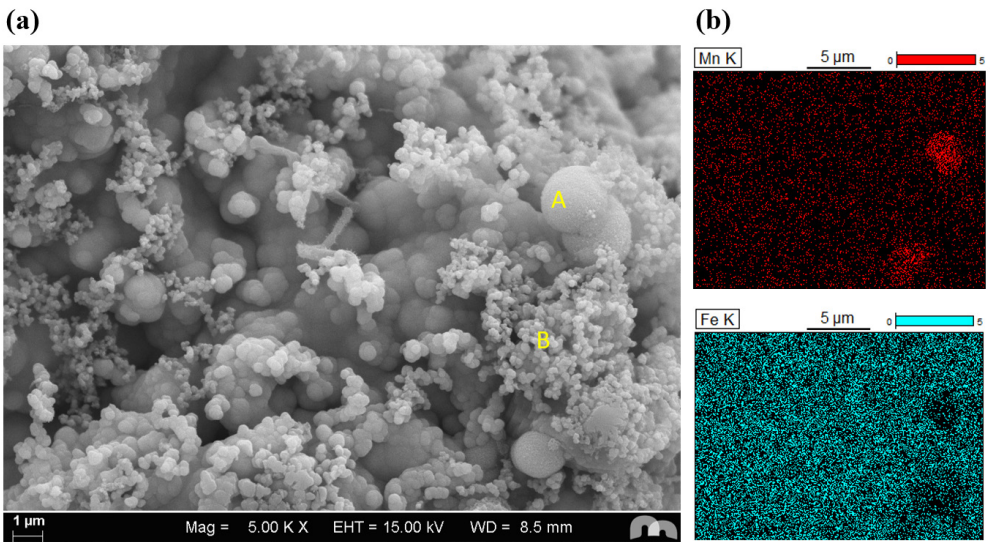

Figure 3 (a) An SEM image of Mn and Fe compounds on the surface of the limestone in the SL reactor (5000x) and (b) EDS mapping results for Mn and Fe.

than 3.0 mg L^{-1}, even with Fe concentration at 24.4 mg L^{-1}. In the plot of Mn concentrations against pH (Fig. 2), SL reactor also showed lower Mn concentrations than S and SG reactors in similar pH condition.

Precipitates on the surface of limestone were collected from the SL reactor and analyzed by using SEM and EDS (Fig. 3 and Table 1). There were several spheres and aggregates which were enriched in Mn and Fe, respectively (Fig. 3a and b). Analysis results from EDS showed that carbon was also enriched in both A and B positions (Table 1), which indicates Mn and Fe carbonates. Therefore, Mn and Fe could be also present as carbonates in the SL reactor, which will be oxidized eventually to Mn oxides such as MnOOH and MnO_2. Thus, carbonates may help the effective removal of Mn even in the presence of Fe. Luan (2012) also reported precipitation of Mn as carbonate in treatment facilities using limestone.

Table 1 EDS analysis results for precipitates at the surface of the limestone in the SL reactor. Positions A and B are indicated in Fig. 3a.

Element	Proportion (atomic %)	
	Position A	Position B
Mn	21.05±0.22	1.77±0.13
Fe	1.67±0.18	12.36±0.20
C	11.38±0.21	9.49±0.62
O	57.37±0.53	61.18±0.45

Table 2 Mn treatment data from laboratory (bench) and pilot scale systems including slag reactor which consists of steel slag and limestone.

Mine	Lab.	Dadeok	Ilwol	Sambong	Sindong	Taehwa
Province	-	Gyeongsang-buk-do	Gyeongsang-buk-do	Gyeongsang-nam-do	Gangwon-do	Chungcheong-nam-do
Steel slag : Limestone (vol. ratio)	4:6, slag 100%	1:1	1:1	4:6	4:6	4:6
Avg. Mn removal efficiency	96%	95%	98%	98%	98%	99%
Avg. inflow Mn (mg L^{-1})	44	2	7	2	8	4
Avg. inflow pH	6.4 (3.2–8.2)	7.3	7.1 (6.1–7.9)	7.0 (6.8–7.7)	7.8 (6.6–8.5)	6.6 (6.5–6.7)
Avg. outflow pH	8.5 (6.9–9.4)	9.0	8.7 (7.9–10.2)	9.2 (8.8–9.7)	11.1 (9.7–11.8)	10.9 (10.6–11.1)
Test period (yr)	2	0.5	4	0.5	0.5	0.5

Accordingly, limestone could have enhanced Mn removal by carbonate formation on the surface (Franklin and Morse, 1983; Aziz and Smith, 1992; Hem and Lind, 1994; Bamforth *et al*., 2006; Aguiar *et al*., 2010; Silva *et al*., 2012a, b). Moreover, presence of limestone may prevent localized pH decrease during Fe^{2+} oxidation to Fe hydroxides, which can help to maintain Mn removal efficiency and to prevent redissolution of Mn oxides.

Mn treatment efficiency in pilot-scale experiments

Pilot-scale passive treatment facilities including slag reactor which consists of steel slag and limestone were operated in five abandoned mines in South Korea (Table 2), which included three coal mines (Ilwol, Sindong, and Taehwa) and two metalliferous mines (Dadeok and Sambong). Especially, the slag reactor at the Ilwol mine removed 98% of the inflow Mn of 12 mg L^{-1} in average for four years (Fig. 4; Kim *et al*., 2021). Although Mn oxides accumulated in the slag reactor, the increase in water level of the reactor could not be observed. The slag reactors at the other four mines (Dadeok, Sambong, Sindong, and Taehwa) also showed Mn removal efficiencies of 95–99% from the inflow of 2–8 mg L^{-1} during the operation period of 0.5 yr. Additionally, the slag reactor at the Sambong mine also removed Zn of 9 mg L^{-1} at the inflow due to the pH increase.

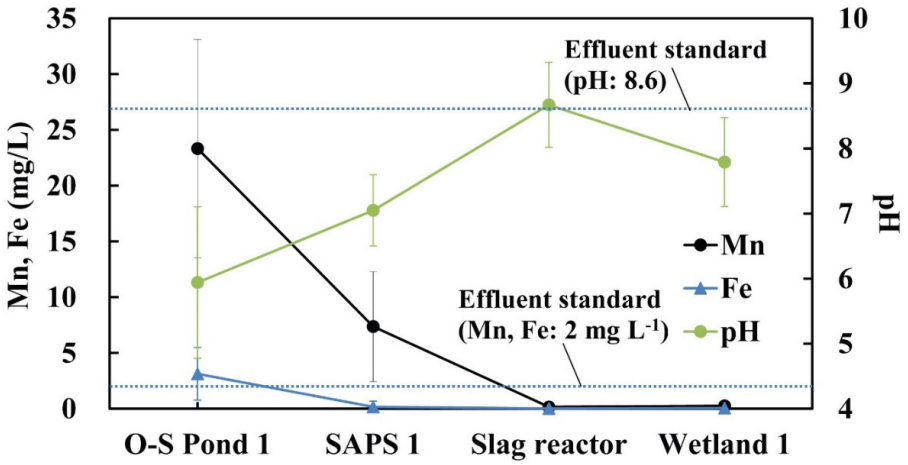

Figure 4 Average Mn and Fe concentrations and pH in the outflow from the pilot-scale treatment facilities for 281 days in the Ilwol mine. The error bars indicate standard deviations. The South Korean standards (for "clean" areas) for Mn (2 mg L^{-1}) and pH (8.6) are also indicated (Kim et al., 2021).

Conclusions

The reactor with mixed substrate of steel slag and limestone removed Mn from 32–46 mg L^{-1} to <3 mg L^{-1} even with the addition of 4.5–24.4 mg L^{-1} of Fe during the bench-scale experiment. Presence of limestone could maintain stable Mn removal efficiency possibly owing to carbonate formation on the surface and/or prevention of localized pH decrease during Fe^{2+} oxidation to Fe hydroxides. Pilot-scale slag-limestone reactors were recently operated in five mines in South Korea and 95–99% of Mn was removed during the maximum test period of 4 years.

Acknowledgements

This work was supported by R&D project of the Mine Reclamation Corporation, Korea in 2013–2020. The authors gratefully acknowledge the help of Mr. Dong-Kwan Kim at MIRECO during the experiments.

References

Aguiar A, Xavier G, Ladeira A (2010) The use of limestone, lime and MnO2 in the removal of soluble manganese from acid mine drainage. WIT Trans Ecol Environ 135:267–276. https://doi.org/10.2495/WP100231

APHA (2017) Standard Methods for the Examination of Water and Wastewater, 23rd edn. American Public Health Association, American Water Works Association and Water Environmental Federation, Washington DC

Aziz HA, Smith PG (1992) The influence of pH and coarse media on manganese precipitation from water. Water Res 26:853–855. https://doi.org/10.1016/0043-1354(92)90017-X

Bamforth SM, Manning DAC, Singleton I, *et al* (2006) Manganese removal from mine waters – investigating the occurrence and importance of manganese carbonates. Appl Geochem 21:1274–1287. https://doi.org/10.1016/J.APGEOCHEM.2006.06.004

Bouchard MF, Sauvé S, Barbeau B, *et al* (2011) Intellectual Impairment in School-Age Children Exposed to Manganese from Drinking Water. Public Health Services, US Dept of Health and Human Services, Washington, D.C.

Burdige DJ, Dhakar SP, Nealson KH (1992) Effects of manganese oxide mineralogy on microbial and chemical manganese reduction. Geomicrobiol J 10:27–48

Franklin ML, Morse JW (1983) The interaction of manganese(II) with the surface of calcite in dilute solutions and seawater. Mar Chem 12:241–254. https://doi.org/10.1016/0304-4203(83)90055-5

Goetz ER, Riefler RG (2014) Performance of steel slag leach beds in acid mine drainage treatment. Chem Eng J 240:579–588

Gouzinis A, Kosmidis N, Vayenas D., Lyberatos G (1998) Removal of Mn and simultaneous removal of NH3, Fe and Mn from potable water using a trickling filter. Water Res 32:2442–2450. https://doi.org/10.1016/S0043-1354(97)00471-5

Hamilton J, Gue J, Socotch C (2007) The use of steel slag in passive treatment design for AMD discharge in the Huff Run watershed restoration. In: Proceedings of the 24th ASMR. pp 272–282

Hem JD, Lind CJ (1994) Chemistry of manganese precipitation in Pinal Creek, Arizona, USA: A laboratory study. Geochim Cosmochim Acta 58:1601–1613. https://doi.org/10.1016/0016-7037(94)90562-2

INAP (2012) The GARD Guide. The Global Acid Rock Drainage Guide. The International Network for Acid Prevention (INAP)

Kim DM, Park HS, Kim DK, Lee, JH (2017) Enhanced Mn treatment in mine drainage using autocatalysis in a steel slag-limestone reactor. In: Wolkersdorfer C, Sartz L, Sillanpää M, Häkkinen A (ed). Proceedings of IMWA 2017, International Mine Water Association, 1063–1069.

Kim DM, Park HS, Hong JH, Lee, JH (2021) Assessing pilot-scale treatment facilities with steel slag-limestone reactors to remove Mn from mine drainage. Mine Water Environ (submitted).

Nairn RW, Hedin RS (1993) Contaminant removal capabilities of wetlands constructed to treat coal mine drainage. In: Moshiri GA (ed). Lewis publishers, Boca Raton, FL, USA, pp 187–195

Rodríguez-Barranco M, Lacasaña M, Aguilar-Garduño C, *et al* (2013) Association of arsenic, cadmium and manganese exposure with neurodevelopment and behavioural disorders in children: A systematic review and meta-analysis. Sci Total Environ. 454–455:562–577

Silva AM, Cunha EC, Silva FDR, Leão VA (2012a) Treatment of high-manganese mine water with limestone and sodium carbonate. J Clean Prod 29–30:11–19. https://doi.org/https://doi.org/10.1016/j.jclepro.2012.01.032

Silva AM, Cordeiro FCM, Cunha EC, Leão VA (2012b) Fixed-bed and stirred-tank studies of manganese sorption by calcite limestone. Ind Eng Chem Res 51:120913092229000. https://doi.org/10.1021/ie301752q

Skousen J, Zipper CE, Rose A, *et al* (2017) Review of passive systems for acid mine drainage treatment. Mine Water Environ 36:133–153. https://doi.org/10.1007/s10230-016-0417-1

USEPA (2004) Drinking Water Health Advisory for Manganese. EPA-822-R-04-003. U.S. Environmental Protection Agency, Washington, D.C.

Ziemkiewicz PF (1998) Steel slag: applications for AMD control. In: Proceedings of the 1998 conference on hazardous waste research. pp 44–62

Distribution of Metals and Toxic Elements Between Carbonate, Sulfate, and Oxide Mineral Precipitates

Julie J. Kim[1], Satish C.B. Myneni[2], Catherine A. Peters[1]

[1]*Department of Civil & Environmental Engineering, Princeton University, Princeton, NJ, 08544, juliejk@princeton.edu*

[2]*Department of Geosciences, Princeton University, Princeton, NJ, 08544*

Abstract

Immobilization of toxic elements from pH adjusted sulfidic mine waters via coprecipitation in carbonate minerals was studied. To design toxic metal mitigation efforts and to assess permanence, it is important to know how trace elements distribute between mineral precipitates of different reactivity and stability under environmental conditions. Experiments using synthetic mine waters were conducted and various imaging and analytical approaches were coupled to image and quantify trace element uptake in precipitated mineral phases. In the copresence of carbonate and oxide minerals, or carbonate and sulfate minerals, cadmium and zinc concentrations were consistently higher in calcium carbonate phases and demonstrated patterns of coprecipitation.

Keywords: Toxic Metals, Mine Waste, Mine Drainage, Mineral Coprecipitation, Solid Solution

Introduction

Sulfide-based mines are ubiquitous in the U.S. and worldwide, yet beneficial reuse or carbonation of these mine wastes is limited. Motivated by the successful pilot and full-scale carbon mineralization projects in ultramafic or alkaline mines (Kelemen *et al.* 2020), we consider carbonation scenarios in sulfidic mines. The evident drawback of the low pH conditions can be overcome by considering low-cost or recycled alkaline additives. To date, many different alkaline materials, and wastes such as fly ash, red mud, steel slag, have been chemically and mineralogically characterized and quantified in terms of their carbonation potential (Renforth 2019; Catalano *et al.* 2012). With carbonate precipitation, toxic metals and metalloids (e.g., lead, cadmium, arsenic, zinc, etc.) may also be coprecipitated out in the form of solid solutions, for the dual benefit of carbon mineralization and toxic metal mitigation. Relevant observations were reported in the case of carbonation of fly ash leachates, which led to trace metal-bearing calcium carbonate precipitates (Hunter *et al.* 2021). With the formation of metal-bearing carbonates, achieving permanency of the treatment is critical and any risks associated with carbonate redissolution, such as new acidity generation from the oxidation and dissolution of sulfides, must be minimized. New acidity generation is expected to be offset by co-disposed or blended alkaline additives, yet this needs to be carefully engineered.

Recent literature has shown that by coprecipitation, metals and metalloids can be precipitated out even at concentrations below saturation of the respective end members, by scavenging their way into the dominant end-member phase. Prieto *et al.* (2016) demonstrated that in the case of solid solution ($(Ca,Cd)CO_3$) precipitation, cadmium concentrations remaining in solution were nearly 2 orders of magnitude lower than in the case of only otavite ($CdCO_3$) precipitation. Hunter *et al.* (2021) also found that thermodynamic models of solid solution precipitation significantly underestimated the extent of trace metal incorporation. For As, Cr, Zn, and Cu, it was found that the ratio of observed concentrations (in the solid) to thermodynamically predicted concentrations (in the solid) ranged anywhere between 5 and 3000 (Hunter *et al.*, 2021). With this, it is likely that coprecipitation reactions serve a much bigger role in toxic component uptake from solution than previously predicted.

In this work, we tested various carbonation scenarios in batch experiments involving synthetic mine waters to test if toxic metal concentrations can be minimized and fall below acceptable water concentrations (as set by the U.S. EPA). The metals and metalloids we selected as trace elements were Pb, Zn, As and Cd, and we designed the experiment to involve oxidized forms of sulfur (VI) and iron (III), and calcium and carbon to enable simultaneous precipitation of sulfate, iron oxide and/or carbonate minerals. To comment on the stability and permanency of the element uptake, we mapped out how the four elements distributed between carbonate, sulfate, or (oxy)hydroxide phases, since these are minerals that exhibit different degrees of reactivity and stability. We also showed which phase(s) are most effective at element uptake and whether they formed binary or ternary solid solutions.

Methods

A series of batch experiments were set up at room temperature using salts of the desired cations and anions. Oxidized forms of As (V), Fe (III) and SO_4 salts were added, and reactions were carried out in vials open to the atmosphere. Geochemical modeling software, PHREEQC (Parkhurst and Appelo 2013), was used to determine the ratio of major cations (calcium and iron) and anions (carbonate, sulfate) as well as the pH that would lead to specific mineral phases or a set of phases to study the extent of uptake as well as the distribution of elements among the phases formed. The phases of interest are three polymorphs of Ca-carbonates (calcite, vaterite, or aragonite which are the expected products of carbonation, Fe- and Ca-sulfate phases (natrojarosite and gypsum), which are two of the most common oxidized sulfur-bearing phases in mining environments, and iron-oxyhydroxide phases. Mine water composition data from gold, copper, coal, silver, uranium, or sulfur mines were compiled from the literature, and initial concentrations of the minor elements in our experiments (As, Cd, Pb, and Zn) were selected to fall within reported ranges. The initial concentrations of the trace elements are summarized in Table 1. These concentrations (with the exception of zinc) exceed the U.S.EPA's maximum allowable concentrations according to drinking water regulations of the Safe Drinking Water Act. Treated solutions were collected after 1-week, and solution samples were acidified with nitric acid for Inductively Coupled Plasma - Mass Spectrometry (ICP-MS) analysis. Solid precipitates were three times DI-washed and twice ethanol-washed and dried for

Table 1 *Summary of initial conditions and final solution ICP-MS data for select batches.*

Case		pH_{init}	Initial (mol/L)	Final (mol/L)	% decrease	U.S.EPA standards (mol/L)
Carbonate & Sulfate (C1)	As	7	0.002	6.83E-05	> 95	0.0001
	Cd		0.001	5.19E-06	> 99	0.00007
	Zn		0.002	1.96E-06	> 99	0.08
	Pb		0.001	6.70E-08	> 99	0.00004
Carbonate & Oxide (C2)	As	7		5.07E-07	> 99	
	Cd			3.07E-06	> 99	
	Zn			1.99E-06	> 99	
	Pb			9.35E-08	> 99	
Sulfate only (C3)	As	4		3.95E-04	> 74	
	Cd			7.15E-04	> 32	
	Zn			1.01E-03	> 38	
	Pb			5.00E-04	> 5	
Sulfate & Oxide (C4)	As	4		6.66E-07	> 99	
	Cd			9.23E-04	> 14	
	Zn			1.10E-03	> 33	
	Pb			2.65E-04	> 53	

X-ray Diffraction (XRD) and Scanning or Transmission Electron Microscopy (S(T)EM) analyses.

Results and Discussion

After a 1-week period, all metal and metalloid concentrations in the two carbonated batches (C1 and C2), were decreased by >99% for all cases, except As in case C1, which decreased by approximately 95% (Table 1). Carbonation led to carbonate precipitates that effectively reduced metal(loid) concentrations from the solution, leading to treated solutions that fell well below the maximum limit set by the U.S.EPA. Non-carbonated, or sulfate and oxide precipitated batches (C3 and C4) showed variable decreases in concentrations. The data most prominently captures reduced effectiveness of Pb, Cd, and Zn uptake from the solution without carbonate precipitation. In terms of the solid phases, XRD analyses showed presence of vaterite (C1), calcite (C2), gypsum (C1 and C4), Fe (III)-oxide (C2 and C4), and Natrojarosite (C3).

In case C1 of simultaneous calcium carbonate and gypsum precipitation, vaterite was the dominant polymorph of calcium carbonate that was observed. Spherical vaterites were found in the solution and many were found attached to the needle structures of the gypsum as seen in Figure 1a. It is unknown whether the vaterite precipitated on the gypsum needles (using it as a substrate) or formed in solution and later attached to the gypsum. The TEM image (Figure 1b) and element distribution maps of As, Zn, and Cd (Figure 1c-e) highlight the distinct spherical morphology of vaterite and the spatial distribution of three elements in the crystal. Lead is not mapped because it was detected at very low concentrations. Zinc and cadmium maps show homogeneous distribution of the elements throughout the spherical particle, indicating coprecipitation as the mechanism of uptake in the solid. Other possible mechanisms of uptake include adsorption of ions on the surface, or precipitation of a new, secondary phase on the surface. Arsenic shows both a spotty and a homogeneous distribution within the particle, and this trend suggests simultaneous distribution of arsenic in the crystal and on the surface, coming from either precipitation of new phases or adsorption. Figure 1f of quantitative solid phase EDS data highlights the apparent metal(loid) distribution between vaterite and gypsum. The affinity of As, Cd, and Zn to associate with vaterite over gypsum is clearly observed, while for Pb, this trend is not so clear. Pb incorporation into vaterite may be less favorable because Pb forms an aragonite group end member phase, cerussite ($PbCO_3$), and this phase is also the least soluble phase of the three carbonate endmembers (Zn, Cd, and Pb-carbonates).

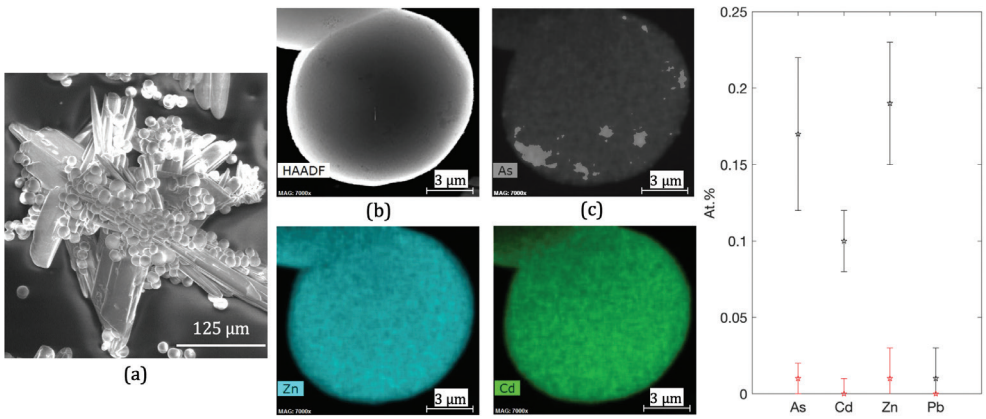

Figure 1 *(a) SEM image of precipitated gypsum and spherical vaterite crystals from C1. (b) STEM image, and single particle EDS element map of (c) arsenic, (d) zinc, and (e) cadmium. Lead map is not shown because it was detected at very low concentrations. (f) Plot of atomic % vs. elements, highlighting the extent of metal incorporation in calcium carbonate (black) and gypsum (red).*

SEM-EDS analysis of the solids formed in case C2 of simultaneous carbonate and oxide precipitation shows a clear division of elements between the two phases (Table 2). The calcite phase shows higher concentrations of Cd and Zn, while the Fe (III) phase shows higher concentrations of As and Pb. While EDS mapping of iron and oxygen (Figure 2) show numerous hotspots of the two elements supporting the probable formation of iron (oxy)hydroxide, we could not identify the specific crystalline Fe (III) phase from our XRD analyses. This may due to the formation of amorphous iron phases or thin iron-(oxy) hydroxide coatings that did not produce identifiable peaks in our XRD patterns.

In the calcite phase, we analyzed both the outer surface and a fractured surface for the elemental presence, and we found significantly higher atomic % of Zn and Cd on the fractured surface than the outer surface. This serves as good evidence for coprecipitated Cd and Zn in the calcite phase. The similarity in the crystal group of otavite ($CdCO_3$), Smithsonite ($ZnCO_3$), and calcite is one likely explanation for the strong affinity of Cd and Zn to associate with calcite. Cerussite forms an aragonite group crystal structure (orthorhombic), and arsenate forms a calcium arsenate phase, where the crystal structure differs significantly from the calcite group, thus reducing ease or likelihood of coprecipitation. For the iron (III) phase, we can predict that there may be some competition between coprecipitation and adsorption, as iron oxides are well known for their effective adsorption capacities. Residual As and Pb concentrations in the solution may be adsorbing to the oxide phase after precipitation. Another notable feature from this batch is the codetection of Ca and C in the Fe (III) phase spots (see EDS data box in Figure 2a). This could be indicative of calcite crystals coated with an iron oxide layer, an observation that is quite desirable for these carbonation scenarios, as iron oxides could serve as a protective layer for the calcium carbonates.

Table 2 Summary of element incorporation in Fe (III) phase and calcite from C2.

Element	Fe (III) Phase: At. % ± Stdev	Calcite: At. % ± Stdev
As	0.33±0.05	0.02±0.04
Cd	0.11±0.02	0.32±0.09
Zn	0.22±0.07	0.44±0.11
Pb	0.13±0.03	0.02±0.03

Two different sulfate phases were observed in cases C3 and C4, and these phases were identified by XRD as natrojarosite and gypsum, respectively (Figure 3). Solid phase analyses showed strong arsenic association with the natrojarosite phase in case C3, and this is also supported by the largest percentage decrease in arsenic concentration in the solution after 1 week (Table 1). Arsenic associations with jarosite group minerals have also been observed and reported in the literature. Hudson-Edwards (2019) found that arsenate oxyanions can substitute for sulfate groups in the T-site of the jarosite structure, leading to arsenojarosite phases of varying arsenate to sulfate ratios.

For the gypsum observed in case C4, formation of an iron oxide coating is clear from SEM-EDS analyses of some select spots (Figure

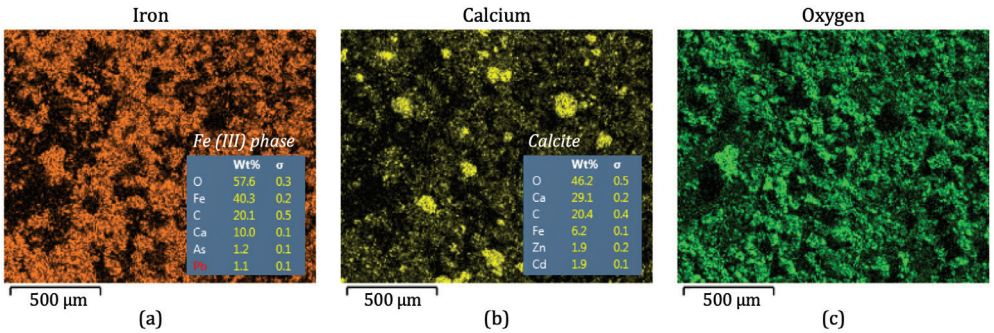

Figure 2 *EDS element maps of (a) iron, (b) calcium, and (c) oxygen from C2 solids. Blue boxes summarize the elemental composition from one point in the map.*

3b and 3c), and there is some preliminary evidence that minor element (Pb and As) concentrations are locally higher in these Fe rich regions. (Figure 3c). This observation of Fe (III) phase and Pb and As association agrees well with results presented for case C2 and is also supported by the solution data for C4 presented in Table 1.

From the proposed in-situ carbonation in mine waste sites, it is expected that there will be large volumes of precipitates generated, further motivating us to consider reutilization of the precipitated carbonates. However, the products created will be classified as high-volume, low-end, as defined by Sanna *et al.* (2015), due to the incorporated toxic components. This could limit direct application of the precipitates in the field (e.g., use as liming agents or soil additives) because there is risk of re-release of the toxic components into the environment. However, if analysis of the metal(loid) concentration shows to be low enough, mixing with other pure liming agents for diluted application in soils or other acidic settings may be appropriate. Alternatively, we can consider applications in concrete production or use as paint additives. The different morphologies and polymorphs of calcium carbonates observed in these systems can be taken advantage of in terms of serving different functions in paint such as dispersion, brightness, transparency, etc. (Li *et al.* 2013).

Conclusions

Carbonation in sulfidic mine waters will induce new sets of reactions, including carbonate coprecipitation reactions, and we showed through our experimental results that toxic components in synthetic mine waters were effectively minimized under these carbonation scenarios via the formation of metal and metalloid bearing carbonates. Carbonates were the most effective phase in uptake of Cd and Zn, and we observed formation of ternary solid solutions. In the copresence of oxide and calcium carbonate, we observed Cd and Zn in the carbonate phase, and As and Pb in the oxide phase. Efficacy of carbonation for simultaneous CO_2 mineralization and metal uptake in Zn or Cd mines is expected to be high, while other treatment methods may be favorable for mines rich in Pb or As. Additional analyses on the overall stability of the system or the reactivities of the coprecipitated crystals remain to be analyzed in greater depths in future works. Finding the conditions that would minimize, if not mitigate, the potential for redissolution of the precipitated carbonates is a major consideration in the context of sulfidic mines, and achievement of shielded carbonate precipitation may be a solution for this.

Acknowledgements

This material is based upon work supported by the High Meadows Environmental Institute (HMEI) at Princeton University. The authors also acknowledge the use of Princeton's Imaging and Analysis Center, which is partially supported through the Princeton Center for Complex Materials (PCCM), a National Science Foundation

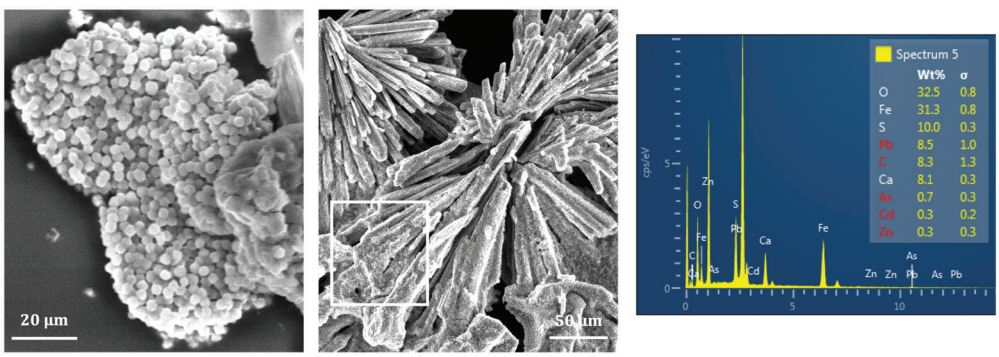

(a) (b) (c)

Figure 3 *SEM image of (a) precipitated Na-jarosite from C3 and (b) Fe-coated gypsum from C4, with the iron-rich region marked by the white box. (c) Point EDS spectra from the white boxed region.*

(NSF)-MRSEC program (DMR-2011750).

References

Hunter HA, Ling FT, Peters CA (2021) Coprecipitation of Heavy Metals in Calcium Carbonate from Coal Fly Ash Leachate. ACS ES&T Water 1:339–345. https://doi.org/10.1021/acsestwater.0c00109

Prieto M, Heberling F, Rodríguez-Galán RM, Brandt F (2016) Crystallization behavior of solid solutions from aqueous solutions: An environmental perspective. Prog Cryst Growth Charact Mater 62:29–68. https://doi.org/10.1016/j.pcrysgrow.2016.05.001

Kelemen PB, McQueen N, Wilcox J, *et al* (2020) Engineered carbon mineralization in ultramafic rocks for CO2 removal from air: Review and new insights. Chem Geol 550:119628. https://doi.org/10.1016/j.chemgeo.2020.119628

Catalano JG, Huhmann BL, Luo Y, *et al* (2012) Metal release and speciation changes during wet aging of coal fly ashes. Environ Sci Technol 46:11804–11812. https://doi.org/10.1021/es302807b

Renforth P (2019) The negative emission potential of alkaline materials. Nat Commun 10:1401. https://doi.org/10.1038/s41467-019-09475-5

Sanna A, Uibu M, Caramanna G, Kuusik R, Maroto-Valer M.M (2014) A review of mineral carbonation technologies to sequester CO2. Chem Soc Rev 43:8049–8080. https://doi.org/10.1039/c4cs00035h

Li G, Li Z, Ma H (2013) Synthesis of aragonite by carbonization from dolomite without any additives. Int J Miner Process 123:25–31. https://doi.org/10.1016/j.minpro.2013.03.006

Hudson-Edwards, KA (2019). Uptake and release of arsenic and antimony in alunite-jarosite and beudantite group minerals. American Mineralogist, 104(5), 633–640. https://doi.org/10.2138/am-2019-6591

Parkhurst DL, Appelo CA (2013). Description of input and examples for PHREEQC version 3–A computer program for speciation, batch-reaction, one-dimensional transport, and inverse geochemical calculations, volume book 6 series Techniques and Methods. https://pubs.usgs.gov/tm/06/a43.

Mobilization Of Environmentally Hazardous Elements Dressing Tailings Of Loparite Ores Under Atmospheric Precipitation

Eugenia Krasavtseva[1,2], Dmitry Makarov[2], Vladimir Masloboev[2], Victoria Maksimova[1,2], Anton Svetlov[2]

[1]*Laboratory of Nature-Inspired Technologies and Environmental Safety of the Arctic of the Federal Research Centre "Kola Science Centre of the Russian Academy of Sciences", Fersmana 14, 184209 Apatity, Russia; e.krasavtseva@ksc.ru, v.maksimova@ksc.ru*

[2]*Institute of North Industrial Ecology Problems – Subdivision of the Federal Research Centre "Kola Science Centre of the Russian Academy of Sciences", Fersmana 14a, 184209 Apatity, Russia; makarov@inep.ksc.ru, masloboev@mail.ru, a.svetlov@ksc.ru*

Abstract

The paper investigates the mobilization of environmentally hazardous elements from loparite ore concentration tailings when exposed to atmospheric precipitation. A sulfuric acid solution simulating acid rain and distilled water were used as model solutions. When exposed to a weak sulfuric acid solution, a manifold increase in the decomposition rate of the tailings was observed. The concentrations of non-ferrous metals in the resulting solutions, when the test material was moistened with an acid solution, many times exceeded the maximum permissible concentrations for fishery water bodies. An intense transfer to the solution of rare earth elements was observed.

Keywords: Loparite Ores, Acid Rain, Environmental Hazard, Pollutants, Rare Earths

Introduction

The operation of mineral deposits involves the formation of a large amount of waste – overburden and tunneling rock, tailings, etc. In Russia's Murmansk Region, where a number of major mining project are located, over 200 million tons of mining waste is generated and stockpiled annually (2019 Report). Russia's only loparite mine is located on the Kola Peninsula in Murmansk Region. Over many years of operation, its tailing storage facilities (TSF) have accumulated a huge amount of waste that remains when loparite is recovered — approx. 6.5 million tons held in the decommissioned TSF section and over 11 million tons in the operating TSF (Goryachev 2020, Ratkin 2008). The annual increment in the tailings quantity is 440 000 t tons.

Outdoor storage of finely ground rare-metal ore concentration tailings involves the risk of interaction with atmospheric oxygen, precipitation, and soil water. Air pollution with acid anhydrides (SO_2, SO_3, NO, NO_2) due to anthropogenic emissions results in acid precipitation (Mesyats 2013). Further, the effects of acid rain are felt both in the areas adjacent to non-ferrous smelters and at a considerable distance from those. Major sources of atmospheric pollution with sulfur dioxide, nickel, and copper include the Severonickel and Pechenganickel smelters (Kryuchkov 1989). In Ratkin (2008) it was shown that the average long-term local sulfate pollution zone of both snow cover and liquid precipitation is located at a distance of up to 70 km from the center point of the industrial site in Monchegorsk.

In a number of papers examining the interaction of mining waste with acid rain, dissolved organic matter, etc., it was shown that the introduction of an aggressive agent leads to an intensification of the conversion of environmentally hazardous elements into mobile forms (Lugovskaya 2003, Smolyakov 1996, Dehaye 1988, Nazreen 2017). Studies also exist on the interaction of a number of minerals and rocks with dilute solutions of sulfuric acid and acidified river water (Sokolova 2013, Savenko 2018). Modeling of chemical weathering and hypergene transformation processes of apatite-nepheline and

copper-nickel ores is thoroughly discussed in (Masloboev 2014, Maksimova 2013).

The study goal was to examine environmentally hazardous elements migration from the concentration tailings of loparite ores when exposed to acid atmospheric precipitation under model conditions.

Methods

Fresh concentration tailings from a loparite ore mine were studied. Since the differentiation of the tailings material in terms of grain size and material composition was noted as early as at the storage stage (Goryachev 2020), tailings collected in February 2020 from a sump at the concentrator plant, before these were sent to the TSF, were studied.

The concentration tailings are fine-grained sand with the mineral particles sized 0.01–0.5 mm.

Chemical composition of the fresh concentration tailings of loparite ore, wt.%: SiO_2 – 48.53, TiO_2 – 1.35, Al_2O_3 – 22.40, Fe_2O_3 – 5.12, FeO – 0.66, MnO – 0.25, CaO – 1.42, MgO – 0.38, K_2O – 4.24, Na_2O – 13.43, P_2O_5 – 0.68, SrO – 0.35, F – 0.08, SO_3 – 0.11.

Mineral composition analysis was conducted by PJSC Kola Geological Information Analytical Center. The mineral composition of the fresh loparite ore concentration tailings is dominated by nepheline (62.22%), aegirine (18.71%), feldspar (16.51%). Impurities of apatite, sodalite, loparite were found.

Samples of the loparite ore concentration tailings underwent open acid unlocking and subsequent analysis for trace element content by inductively coupled plasma mass spectrometry at the Shared Use Center, Institute of North Industrial Ecology Problems – Subdivision of the Federal Research Centre "Kola Research Center of the Russian Academy of Sciences" (INEP KSC RAS) (using ELAN 9000 DRC-e mass spectrometer by Perkin Elmer, USA). Chemical analysis results are shown in Table 1.

The laboratory study of the chemical weathering of minerals when exposed to atmospheric precipitation was carried out as described in (Maksimova 2013). Considering the time span of the natural hypergene processes in minerals, the experiment was carried out in accelerated conditions. Tailings samples weighing 70 g were placed in temperature-controlled cells at 50 °C; the samples were periodically moistened with 0.002 N sulfuric acid solution or distilled water (control samples) at 25 ml/day for 20, 40, and 60 days. After 60 days, the samples treated with distilled water at a S:L ratio of 1:10, the resulting solutions were filtered through an MFAS OS-2 membrane filter (pore size 0.47 μm). Filtrate pH was measured and the filtrates were sent for quantitative chemical analysis (ICP-MS, ion exchange chromatography, direct potentiometry, atomic adsorption spectrometry).

Results and discussion

The initial pH values and element concentrations were measured in a solution obtained after treating the loparite ore concentration tailings with distilled water at the same S:L ratio and exposure time (t = 1 day).

When interacting with water, the pH value slightly increases from 8.2 to 8.8 in the time interval from 20 to 40 days, and then returns to close to the initial value. After the interaction of the tailings with a 0.002 N

Table 1 *Element composition of the fresh loparite ore concentration tailings.*

Element	Contain, mg/kg	Element	Contain, mg/kg	Element	Contain, mg/kg
Ni	7.51	Ce	1031	U	17.4
Cu	6.44	Pr	38.8	Ta	123
Cr	2.3	Nd	121	Nb	1459
Sr	1289	Sm	14.7	Mn	1580
Zn	240	Ba	179	Al	75800
Pb	16	V	34.9	Fe	26300
La	202	Th	26.3	Zr	2630

Table 2 Concentrations of aluminum, silicon, sodium, and potassium in the resulting solutions when interacting with water and sulfuric acid.

Contain, µg/L	Distilled water				0.002 N H_2SO_4			
	1 day	20 days	40 days	60 days	1 days	20 days	40 days	60 days
Al	0.95	0.54	0.45	0.50	0.95	4.00	8.60	14.30
Si	5.3	5.12	6.29	5.22	5.3	4.11	7.63	10.04
K	1.57	1.63	1.93	2.10	1.57	24	56.4	103
Na	48.4	54.0	47.40	83.20	48.4	336	617	900

Figure 1 *Appearance of the loparite ore concentration tailings at the end of the experiment. From left to right: moisturizing agent – distilled water, sulfuric acid solution.*

solution of sulfuric acid, the pH of the leach solution decreases with increasing time of the experiment and reaches 4.68 by the end of the experiment. The largest decrease in the pH value — from 8.2 to 5.1 — was observed in the first twenty days.

The dissolution of the mineral matrix under the action of leaching agents was assessed by the results of filtrate analysis for potassium, sodium, aluminum, and silicon, which are some of the elements found in the main minerals of the tailings material (Table 2). Compared to the control series of experiments, where the leaching agent was distilled water, after the interaction of the tailings particles with sulfuric acid, the concentration of basic cations in the resulting solutions increased by a factor of 2 to 10. At the same time, uneven transfer of elements into solution was observed. In particular, the release of sodium ions: its concentration exceeded that of potassium by a factor of almost 20 at the end of the experiment, which indicates incongruent dissolution of nepheline.

Figure 1 shows the tailings at the end of the experiment (after 60 days). X-ray phase analysis identified the composition of the salt bloom formed on the surface of the tailings material – a mixture of thenardite and 12-hydrate aluminum-potassium sulfate.

Possible reaction equations for the formation of the newly identified phases are as follows:

$$K_2SO_4+Al_2(SO_4)_3+24H_2O \rightarrow 2KAl(SO_4)_2\cdot 12H_2O;$$

$$2NaCl + H_2SO_4 \rightarrow Na_2SO_4 + 2HCl.$$

The change in the concentrations of Zn, Sr, and Mn is shown in Figure 2. As one

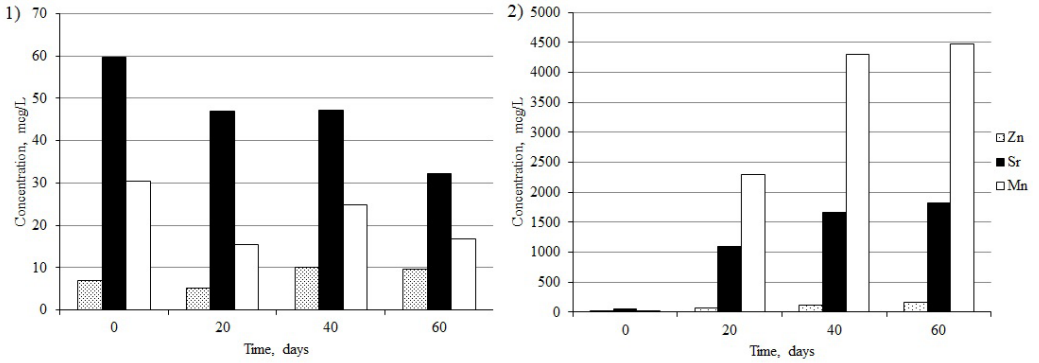

Figure 2 *Concentrations of non-ferrous metals in the resulting solutions when interacting with water (1) and sulfuric acid (2).*

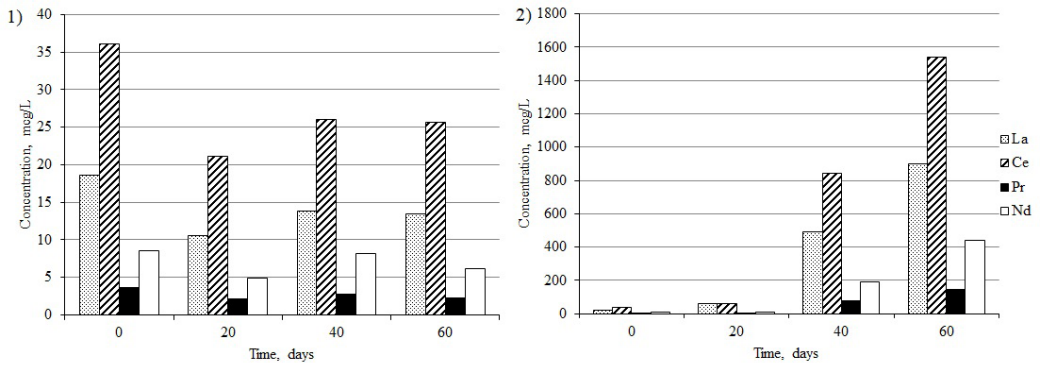

Figure 3 *Concentrations of REEs in the resulting solutions when interacting with water (1) and sulfuric acid (2).*

can see, after the interaction of the tailings material with distilled water, a slight excess of the MPC is observed already on the first day for Mn (10 μg/L) (Fig. 2.1) (Order 2016).

After the interaction of the tailings particles with a sulfuric acid solution, the transfer rate of Zn, Sr, and Mn into the solution increased sharply (Fig. 2.2). At the end of the experiment, the MPC was exceeded as follows: by a factor of 5, 17, and 448 for Sr, Zn, and Mn, respectively.

The change in the concentrations of rare earth elements (REEs) contained in the loparite ore tailings, in the leaching solutions after the interaction of the tailings with water and dilute sulfuric acid depending on the duration of the experiment is shown in Figure 3. Note that neither MPCs nor maximum and approximate permissible concentrations of REEs in soils are established.

Once in the soil, REEs, due to the different stability of the bond with humic substances, can both be adsorbed and desorbed when exposed to the dissolved organic matter (Xiangke 2000, Savenko 2019). In general, the behavior of REEs in soils is similar to that of non-ferrous metals; however, their phytotoxicity has not yet been sufficiently studied (Thomas 2013). It is known that the concentration of light REEs in the roots of vascular plants is usually higher than in other plant organs, including shoots (Carpenter 2015, Grosjean 2019, Mikołajczak 2017, Nazreen 2017, Thomas 2013). However, the accumulation of these in leaves and stems, being the main organs of photosynthesis, can have major consequences for plant development (Thomas 2013).

The transition of REEs into solution is also intensified when dilute sulfuric acid is

added as a leaching agent instead of distilled water. Compared to the control series of experiments, the concentration of La and Ce in the solution increased by a factor of 45 and 60, respectively.

It can be concluded that the interaction of the tailings material with sulfuric acid solution intensifies the process of metal transition, in particular, Zn, Mn, Sr, La, Ce, Pr, Nd, into a soluble, i.e. more bioavailable, form.

Conclusions

Mobilization of environmentally hazardous elements from fresh loparite ore concentration tailings when exposed to atmospheric precipitation was studied in laboratory conditions.

A significant acceleration of chemical weathering is noted under model conditions that simulate the effects of acid rain.

The concentrations of Zn, Mn, Sr in the resulting solutions at the end of the experiment, when the tailings material was moistened with a dilute solution of sulfuric acid, were many times above the applicable MPCs. Intense transition of light REEs, in particular, La, Ce, Pr, Nd, into a dissolved, more bioavailable form was observed.

The probability and intensity of acid precipitation should be taken into account in the geoenvironmental assessment of the risk of the negative environmental impact of loparite ore concentration tailings.

Acknowledgements

This study was carried out as part of the research project 0226-2019-0011 and partially funded by the RFBR grant 19-05-50065 Microcosm, project № KO1030 Supporting Environmental, Economic and Social Impacts of Mining Operations Program Kolarctic CBC 2014–2020.

References

2017 Order N 552 "On approval of water quality standards for fishery water bodies, including standards for maximum permissible concentrations of harmful substances in the waters of fishery water bodies." (Ministry of Agriculture of Russia). Retrived from http://publication.pravo.gov.ru/Document/View/0001201701160006

2019 State report "On the State and Environmental Protection of the Murmansk Region in 2018" (Ministry of Natural Resources and Ecology of the Murmansk Region). Retrived from https://gov-murman.ru/region/environmentstate/

Carpenter D, Boutin C, Allison J, Parsons J, Ellis D (2015) Uptake and Effects of Six Rare Earth Elements (REEs) on Selected Native and Crop Species Growing in Contaminated Soils. PloS one 10.e0129936, doi:10.1371/journal.pone.0129936

Dehaye J, Badillo M, Zikovsky L (1988) A laboratory study of the effects of acid rain on industrial waste and its impact on the physicochemical properties of groundwater. Radioanal. Nucl. Chem. 127(3):209-217

Goryachev AA, Krasavtseva EA, Laschuk VV, Ikkonen PV, Smirnov AA, Maksimova VV and Makarov DV (2020) Assessment of the environmental hazard and the possibility of processing the tailings of the dressing of loparite ores. Ecology and Industry of Russia 24(12):46-51

Grosjean N, Le Jean M, Berthelot C *et al.* (2019) Accumulation and fractionation of rare earth elements are conserved traits in the Phytolacca genus. Sci Rep 9:18458, doi:10.1038/s41598-019-54238-3

Kryuchkov VV, Makarova TD (1989) Aerotechnogenic impact on ecosystems of the Kola North. Apatity: Ed. Kola Scientific Center of the Academy of Sciences of the USSR, 96 p

Lugovskaya AS, Nesterov DP, Vasilyeva TN, Makarov DV, Makarov VN (2003) Mineral formation in the interaction of mining waste with acid rain and acidic pore solutions. Mineralogy Technogenesis 4:85-98

Maksimova VV, Krasavtseva EA, Makarov DV, Masloboev VA (2013) Modeling the chemical weathering of apatite-nepheline ore dressing tailings under the influence of atmospheric precipitation. Mineralogy Technogenesis 14:203-209

Masloboev VA, Seleznev SG, Makarov DV, Svetlov AV (2014) Evaluation of the environmental hazard of storage of wastes from mining and processing of copper-nickel ores. Physics and Technology Problems of Mineral Development 3:138-153

Mesyats SP, Ostapenko SP (2013) Methodical approach to assessing the intensity of chemical weathering of mineral raw materials from

technogenic deposits. Bulletin of the Murmansk State Technical University 16(3):566-572

Mikołajczak P, Borowiak K, Niedzielski P (2017) Phytoextraction of rare earth elements in herbaceous plant species growing close to roads. Environmental Science and Pollution Research 24:1-13., doi:10.1007/s11356-017-8944-2

Nazreen M, Amalina A, Omar M (2017) Bioaccumulation of Rare Earth Element by Water Lettuce (Pistia stratiotes). Oriental Journal of Chemistry 33:1097-1102, doi:10.13005/ojc/330305

Ratkin NE, Shablova AV (2008) Quantitative assessment of airborne industrial pollution of the territory of the Murmansk region (part 1). Theoretical and Applied Ecology 1:38-44

Savenko AV, Savenko VS (2019) Influence of natural organic acids on the mobilization of macro- and microelements from rocks. Reports of the Academy of Sciences 485(3):351-355

Savenko AV, Savenko VS, Dubinin AV (2018) Mobilization of macro- and microelements from rocks during their interaction with water. In: Zamana LV, Shvartsev SL (Eds) Geological evolution of the interaction of water with rocks. Materials of the third All-Russian scientific conference with international participation, p. 165-169

Smolyakov BS, Pavlyuk LA, Nemirovsky AM (1996) Acidity and ionic composition of atmospheric precipitation and aerosols in the Novosibirsk region. Optics of the atmosphere and ocean 9(6):773-779

Sokolova TA (2013) Mineralogy and micromorphology of soils, the processes of destruction of quartz, amorphous minerals of silica and feldspars in model experiments and in soils: possible mechanisms, rate, diagnostics (analysis of the literature). Pochvovedenie 1:98–112

Thomas Ph, Carpenter D, Boutin C, Allison J (2013) Rare earth elements (REEs): Effects on germination and growth of selected crop and native plant species. Chemosphere 96. doi:10.1016/j.chemosphere.2013.07.020

Xiangke W *et al.* (2000) Sorption and desorption of Eu and Yb on alumina: mechanisms and effect of fulvic acid. Appl Radiat Isot. 52:165–73

The Effects of Storm Events on Sediment, Nutrient, and Biofilm Dynamics in a Stream Recovering from Acid Mine Drainage

Natalie Kruse Daniels[1], Jennie Brancho[1], Morgan L. Vis[2]

[1]*Environmental Studies Program, Voinovich School of Leadership and Public Affairs, Ohio University, Athens, Ohio 45701, USA, krusen@ohio.edu, ORCID 0000-0002-8684-1315*

[2]*Environmental and Plant Biology Department, Ohio University, Athens, Ohio 45701, USA, vis-chia@ohio.edu*

Abstract

This study quantified changes in nutrients, sediment transport, and algal biomass during normal and storm conditions in a treated acid mine drainage stream. Nitrate, sulfate, total reactive phosphorous (TRP), sediment deposition and total suspended solids (TSS) were measured during each sampling event. Biological response was measured by comparing algal biofilm biomass. Antecedent precipitation index (API) was an indicator of runoff potential. As API increased TSS increased, while chlorophyll a, conductivity, and sulfate decreased. TSS, nitrate, and sediment deposition were higher overall during storm events. TRP remained low at all sites during the sample period, suggesting phosphorous limitation.

Keywords: Phosphorus Limitation, Climate Change, Algae Biomass, Sediment Deposition, Antecedent Precipitation Index

Introduction

Although the effects of climate change on acid mine drainage (AMD) streams is an emerging area of research, several studies have investigated the effects of warming temperatures and changing precipitation regimes on metal toxicity, pyrite oxidation, and seasonal fluctuations in AMD generation and composition (Anawar 2013, Nordstrom 2009). Depending on the site and duration of the storm, AMD discharges from mines display one of three behaviors that affect acidity and contaminant concentrations in the stream. During high flow, reaction sites may be cut off from oxygen required to form AMD due to flooding. This phenomenon is known as sparing (Kruse *et al*. 2014). Sparing causes contaminant concentrations to increase at a slower rate than discharge due to dilution and slower rates of AMD formation (Kruse *et al*. 2014, Mack *et al*. 2014). Alternatively, AMD discharges may exhibit flushing behavior. Flushing occurs when contaminant concentrations increase at a faster rate than discharge (Kruse *et al*. 2014), and this phenomenon may occur for several different reasons. Following heavy precipitation or snowmelt, water can overfill the most accessible mine pools and spill over into disconnected pools that are only accessible during high flow events. This increased connection to mine pools results in greater generation of AMD and higher contaminant loads (Mack *et al*. 2014). Flushing may also be caused by the faster dissolution of soluble salts during heavy storms (Nordstrom 2009). If neither flushing nor sparing occurs, AMD contaminant concentrations will increase at the same rate as discharge (Kruse *et al*. 2014). Systems may display different behaviors relative to the duration of the storm, with flushing more likely to occur at the beginning and sparing later during prolonged storms (Kruse *et al*. 2014, Nordstrom 2009). The rates of AMD generation during storms are likely to be site-specific (Kruse *et al*. 2014). AMD contaminant concentrations following storm events are hysteretic, depending on the duration and frequency of storm events (Nordstrom 2009).

Storm events can also impact contaminant concentrations by scouring sediments from the streambed. In AMD systems, the majority of these sediments are metal hydroxides. By

scouring sediments, storms uncover new sediments onto which heavy metals and nutrients can sorb (Chapman *et al.* 1983). Depending on the behavior of AMD generation during storm events, such scouring can reduce heavy metal and/or nutrient loads or prevent drastic spikes in concentrations that may have toxic or otherwise harmful effects. However, scouring of sediments and subsequent generation of new metal hydroxides may further limit biofilms by smothering communities and decreasing light availability (Smucker and Vis 2011).

Increased storm frequencies and intensities may also alter nutrient retention and transport on a catchment level. Precipitation events restore connections between terrestrial landscapes and the aquatic ecosystems, allowing transport of pollutants from other land uses within the watershed into the stream via runoff. Once in the stream, nutrients are either stored in biomass, soil, or groundwater, transported back to the atmosphere as a gas (e.g. nitrogen), or carried downstream (Welter and Fisher 2016). Nutrients typically associated with sediment include ammonium, particulate organic nitrogen, and phosphorous (Lloyd *et al.* 2016). Substantial proportions of the annual sediment (Inamdar *et al.* 2017) and total phosphorous (Lloyd *et al.* 2016) export load have been attributed to the most intense storm events of that year. Storm events may contribute to higher nutrient concentrations via nitrogen and phosphorous loading from runoff or lower nutrient concentrations via greater export of sediments and nutrients.

Study Site

The fourth largest tributary to Raccoon Creek (Kruse *et al.* 2013), Hewett Fork is located within the headwaters of Raccoon Creek (Kruse *et al.* 2012). Hewett Fork is approximately 24.8 km long, and the subwatershed drains 104.9 km^2. The confluence of Hewett Fork and Raccoon Creek occurs at river kilometer (RKM) 144.2 on Raccoon Creek (Kruse *et al.* 2013). Sediment dynamics, nutrient concentrations, and biofilm abundance were measured at six sampling sites within Hewett Fork: HF137, HF095, HF090, HF060, HF045, and HF039. HF137 is upstream of the Carbondale Doser and the confluence of Carbondale Creek and Trace Run with Hewett Fork. This site is not currently impacted by AMD. Therefore, HF137 was used as the reference site for this study. The remaining five sites were used as the experimental group. HF095 and HF090 are located within the impaired zone, HF060 and HF045 within the transition zone, and HF039 within the improved zone.

Field Methods

Sediment transport, nutrient concentrations, and biofilm communities were measured at all six sites during normal and storm conditions. Sampling began May 28, 2018 and ended November 1, 2018 to capture three important annual hydrologic events: heaviest storms in spring, lowest flow in summer, and poorest water quality in fall. Prior to each sampling event, a Myron Ultrameter II datasonde was calibrated. The pH probe was calibrated using standard solutions with pH values of 7, 4, and 10 in that order. The conductivity probe was calibrated using a standard solution of 1413 µS/cm. At each site, several field parameters were collected using the Myron Ultrameter II datasonde. Water temperature was immediately recorded in degrees Celsius. Then, the Myron Ultrameter II datasonde was set aside to allow the meter to settle before measuring pH and conductivity.

Nutrient Concentrations

Three nutrient concentrations were measured at each site during each sampling event: nitrate (NO_3^-), sulfate (SO_4^{2-}), and total reactive phosphorous. At each site, one 1 L water sample was collected in an HPDE bottle, filtered at the lab, and partitioned into subsamples for each measurement. Total reactive phosphorous subsamples were kept frozen at -20 °C until analysis. To prevent interference from iron in phosphate measurements, total reactive phosphorous samples were prepared using the ascorbic acid/colorimeter method (Stainton *et al.* 1976). Total reactive phosphorous concentrations were measured using a Genesys™ 20 Visible Spectrophotometer (Thermo Fisher Scientific Inc. Waltham, MA). Nitrate and sulfate concentrations were measured within

48 hours of sample collection using a HACH DR/890™ colorimeter (Hach Company, Loveland, CO) with HACH powder pillow reagents (Hach Company 2009). Nitrate concentrations were measured using the cadmium reduction method (method 8192) (Hach Company 2015), while sulfate concentrations were measured using the US EPA SulfaVer 4 Method (method 8051) (Hach Company 2018).

Sediment Deposition

Sediment traps were constructed and deployed in the streambed on April 30 at each site to measure deposition, consisting of 36 plastic containers (3 in. by 3 in. by 2 in.) nested in a plastic rack. A pre-weighed amount of dry river rock was placed into each sampling container prior to deployment to weigh the trap down. The sediment traps were dug into the bed to ensure the tops of each container were flush with the bed to maximize sediment capture. During each sampling event, three containers were removed at random from the sediment traps at each site as replicates. At the lab, sediment deposition samples were emptied into pre-weighed aluminum trays. These samples were then placed into the oven until dry and weighed. Grain size analysis was conducted every fourth sampling event. Once the sediment deposition samples were fully dried, they were passed through a series of two sieves, one with a mesh size of 2 mm and the other 425 μm. The amount of sediment in each sieve was weighed, and the total weight from both sieves was subtracted from the total deposition sample weight.

Sediment Transport

Sediment transport through the water column was quantified by measuring total suspended solids (TSS) according to method 2540 (American Public Health Association *et al.* 2005). Prior to sample collection, 22 filters (0.45 μm) were rinsed and dried for one hour. These filters were then placed in a desiccator until analysis. During each sampling event, a 1 L water sample was collected in an HDPE bottle at each site and placed on ice for transport back to the lab. These samples were placed in the refrigerator and analyzed within 48 hours of collection. The 1 L water sample was shaken to homogenize and then divided into three 300 mL replicate subsamples per site. Each subsample was filtered onto the pre-weighed filter paper using a MultiVac 310-MS-T Vacuum Filtration System (New Star Environmental, Roswell, GA). For quality control, two blank samples were filtered per sampling event. These samples were placed into the laboratory oven and allowed to dry for 1 hour at 100 °C. After drying, the samples were put into the dessicator to cool to room temperature and the mass of sediment measured. The resulting TSS values for each subsample were averaged to generate one TSS value per site per sampling event.

Biofilm Abundance

At each site, ten cobbles were randomly selected to analyze the biofilm communities on the substrate. Using a soft brush, biofilm was scrubbed from a 25 cm^2 area on each rock into a single sample; this sample was placed in a labeled and preweighed 20 mL scintillation vial. These vials were kept on ice for transport to the laboratory and then kept frozen. At the lab, each sample was freeze-dried for a minimum of 48 hours. The scintillation vials were weighed again once dry. Chlorophyll a Analysis – Chlorophyll a concentrations were analyzed according to EPA method 445.0 (Arar and Collins 1997). The weight of each of the borosilicate tubes was recorded prior to and following the addition of 2-4 mg of sample. Three borosilicate tubes were used for each sample as replicates. To each tube, 10 mL of 90% acetone was added. Tubes were covered in plastic wrap and aluminum foil and placed in the freezer for 24 hours. After 24 hours, chlorophyll a concentrations were measured using a Turner TD-700 fluorometer (Turner Designs, Sunnyvale, CA). An amount of 0.1 M HCl was added to each sample to account for phaeophytin-a.

Results

Measured using total annual precipitation (cm), 2018 has been the wettest year on record since the Carbondale doser was installed in 2004. Antecedent Precipitation Index (API) values were calculated for each day in 2018 and correlated with other variables. In Figures 1 and 2, trends in normal and storm conditions.

Conductivity decreased as water quality improved with distance from the doser. The highest conductivity value was measured as 1100 µS/cm at HF039 on July 19. All other values ranged from 198.1 µS/cm to 673.0 µS/cm. Each site followed relatively the same pattern as the reference site, though downstream sites experienced less variation during fall sampling events (HF060, HF045, and HF039 in September and October). Conductivity was significantly negatively correlated with API ($p = 0.0003$, $r2 = -0.8009$). In normal and storm conditions, the conductivity decreased as API increased. The correlation between pH and API was not significant ($p = 0.0735$, $r2 = 0.4751$). The pH did not show any clear differences between normal and storm conditions when plotted against API. Like conductivity, sulfate concentrations decreased as water quality improved further downstream from the doser. Sulfate concentrations were highest between July and September. All sites showed the same pattern of changes in sulfate over the sample period. Median sulfate concentrations were significantly correlated with API ($p = 0.0000$, $r2 = -0.8886$). In both normal and storm conditions, sulfate decreased as API increased.

Nitrate concentrations varied greatly at each site over the sample period. Nitrate concentrations were not significantly correlated with API ($p = 0.9607$, $r2 = -0.0139$). No pattern was discerned between API and nitrate. Nitrate concentrations were overall higher in storm events than normal events, though storm concentrations also varied greatly. Total reactive phosphorous concentrations peaked during the first sampling event on May 28. However, all concentrations measured during the sample period were between 0 mg/L (below detection) and 0.0018 mg/L. Most concentrations measured after the initial sampling event were below detection. As a result, the correlation between phosphorous and API was not significant ($p = 0.5575$, $r2 = -0.1647$), and no pattern between phosphorous and API or weather was detected.

Over the course of the sampling period, sediment deposition followed the same pattern as the reference site for all sites except HF045. HF045 experienced much less deposition and resuspension than the rest of the sites. At all sites, the highest sediment deposition values occurred between June and mid-July and again at the end of October, while the greatest resuspension values also occurred in mid-July (July 19). No significant correlation was found between median sediment deposited per day and API ($p = 0.2653$, $r2 = 0.3073$). Additionally, no clear pattern between sites or API values was observed. Sediment deposition was more likely to be higher during storm events, though high variation was found in both weather conditions. Compared to the reference site, TSS varied more in all sites, with sites further downstream deviating more from the pattern seen at HF137 than the upstream sites. TSS at HF095 and HF090 peaked during June, HF060 and HF045 peaked during July, and TSS at HF039 peaked in September. HF045 experienced the greatest variation in TSS values during the sample period. Median TSS was significantly positively correlated with API ($p = 0.0141$, $r2 = 0.6380$). However, TSS values showed different patterns in normal and storm conditions. During normal conditions, TSS did not show a clear trend with API. TSS increased with increasing API during storm conditions.

At the reference site, chlorophyll a peaked during the final sampling event on October 22. At all other sites, however, chlorophyll a peaked during August. Chlorophyll a was consistently low at all sites during June and began to increase in mid-July. In September, chlorophyll a values decreased again at all sites, followed by another increase in October. The highest peaks in chlorophyll a were measured at HF045 and HF137, the reference site. Median chlorophyll a was significantly negatively correlated with API ($p = 0.0156$, $r2 = -0.6107$). Chlorophyll a decreased as API increased in both normal and storm conditions. This trend was slightly clearer in storm than normal conditions.

Discussion

The hypotheses tested in this study are partially supported by the data. While downstream sediment transport increased during storm events, this increase did not coincide with a

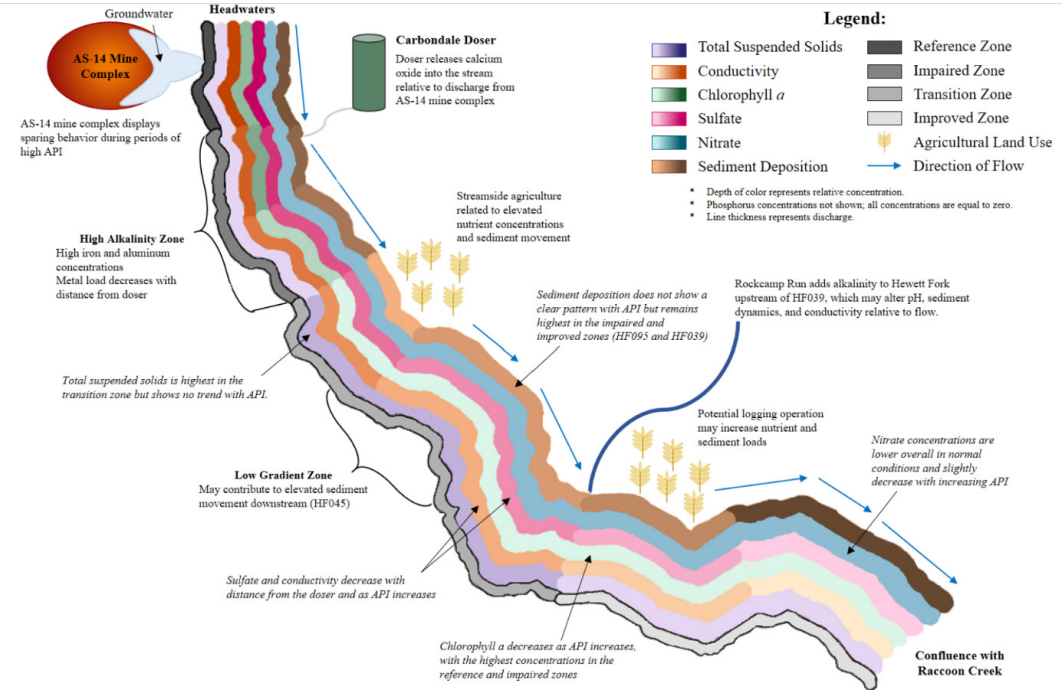

Figure 1 *Conceptual model of sediment, nutrient, and biofilm dynamics in normal flow conditions.*

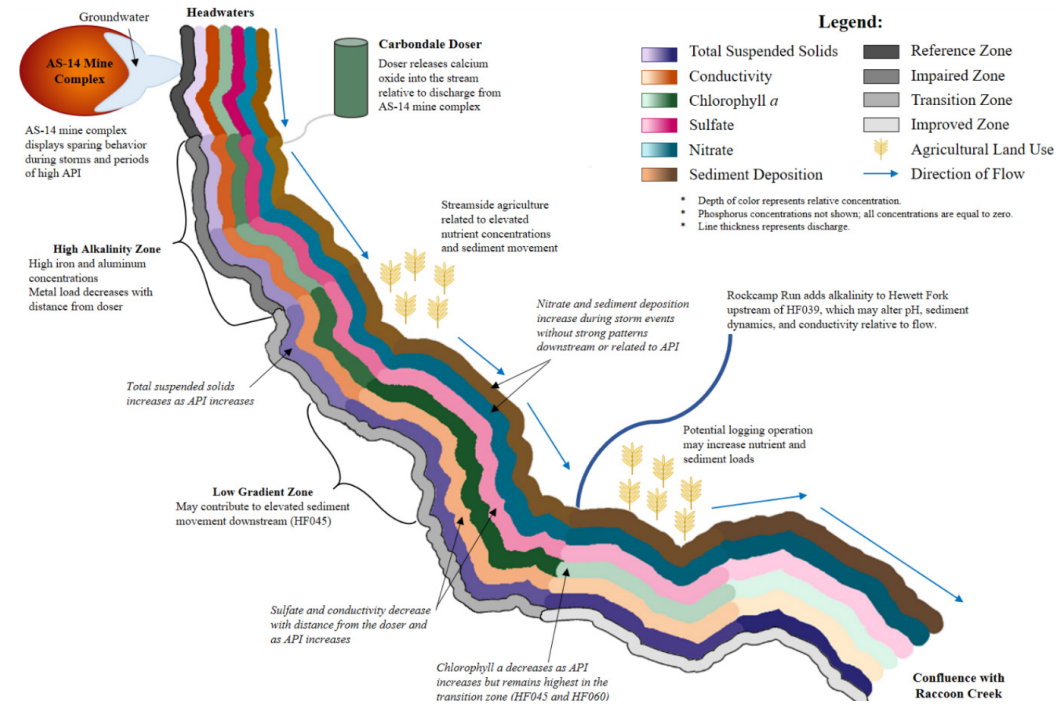

Figure 2 *Conceptual model of sediment, nutrient, and biofilm dynamics in storm conditions.*

decrease in nutrient concentrations. Instead, phosphorous concentrations remained low in all weather conditions, and nitrate showed only a slight increase during storms. The relationship between sediment transport and chlorophyll a was more complicated than hypothesized. High chlorophyll a values coincided with periods of low sediment deposition at most sites, but peaks in TSS values occurred at the same time as peaks in chlorophyll a at HF045 and HF039.

The parameters measured in this study may be affected by a variety of factors, including the Carbondale doser treatment system, AS-14 mine complex, and surrounding land use. During normal weather conditions, sulfate, conductivity, and chlorophyll a decreased with increases in API. Nitrate, TSS, and sediment deposition did not show any trend with API during normal weather conditions. TSS, nitrate concentrations, and sediment deposition showed high variation in normal weather conditions, but nitrate did show a slight increase in concentration as water quality improved downstream. Sediment deposition did not show a clear trend related to water quality with highest deposition rates in the impaired and improved zones. Sulfate and conductivity each decreased as water quality improved downstream. TSS, on the other hand, was highest in the transition zone. In storm conditions, TSS increased and sulfate, conductivity, and chlorophyll a decreased with increasing API. Sediment deposition and nitrate were each slightly higher in storm conditions, though both parameters showed high variability and no clear pattern related to API or water quality. Sulfate and conductivity decreased downstream as water quality improved. TSS increased downstream with the highest concentrations in the improved zone. Chlorophyll a was highest in the transition zone during storm events.

Conclusions

Climate change may affect AMD streams by altering geochemical processes and sediment and nutrient transport patterns. These changes may in turn have negative impacts on the biological communities living in the stream. Overall, API seemed to exert strong controls on stream characteristics, altering biofilm communities and concentrations of both AMD pollutants and suspended sediments. Nutrient patterns were not as strongly linked to API, though nitrate concentrations were higher during storm events. This study also found very low concentrations of phosphorous. Like previous studies, these low concentrations indicate that AMD streams are likely phosphorous limited.

References

Anawar HM (2013) Impact of climate change on acid mine drainage generation and contaminant transport in water ecosystems of semi-arid and arid mining areas. Phys Chem Earth 58-60: 13-21

Arar E, Collins GB (1997) In vitro determination of chlorophyll a and phaeophytin a in marine and freshwater algae by fluorescence. 1st ed. USEPA. Office of Research and Development. Cincinnati, Ohio

Chapman BM, Jones DR, Jung RF (1983) Processes controlling metal ion attenuation in acid mine drainage streams. Geochimica et Cosmochimica Acia 47: 1957-1973

Hach Company. 2015. Nitrate cadmium reduction method 8192. Loveland, CO

Hach Company. 2018. Sulfate US EPA SulfaVer 4 Method 8051. Loveland, CO

Hach. 2009. DR/820, DR/850, DR/890 Portable datalogging colorimeter instrument manual. 2nd ed. Hach Company 68 pp

Inamdar S, Johnson E, Rowland R, Warner D, Walter R, Merritts D (2017) Freeze-thaw processes and intense rainfall: the one-two punch for high sediment and nutrient loads from mid-Atlantic watersheds. Biogeochem 1-17

Kruse NA, Bowman JR, Mackey AL, McCament B, Johnson KS (2012) The lasting impacts of offline periods in lime dosed streams: a case study in Raccoon Creek, Ohio. Mine Water Environ 31(4): 266-272

Kruse NA, DeRose L, Korenowsky R, Bowman JR, Lopez D, Johnson KS, Rankin E (2013) The role of remediation, natural alkalinity sources, and physical stream parameters in stream recovery. J Environ Manag 128: 1000-1011

Kruse NA, Stoertz MW, Green DH, Bowman JR, Lopez DL (2014) Acidity loading behavior in coal-mined watersheds. Mine Water Environ 33(2): 177-186

Lloyd CEM, Freer JE, Johnes PJ, Collins AL (2016) Using hysteresis analysis of high-resolution water quality monitoring data, including uncertainty, to infer controls on nutrient and sediment transfer in catchments. Sci Tot Environ 543(A): 388-404

Mack, B., J. Skousen, and L. M. McDonald. 2014. Effect of flow rate on acidity concentrations from above-drainage underground mines. Mine Water Environ 34(1): 50-58

Nordstrom DK (2009) Acid rock drainage and climate change. J Geochemical Exploration 100: 97-104

Smucker NJ, Vis ML (2011) Acid mine drainage affects the development and function of epilithic biofilms in streams. J N Am Benthological Soc 30(3): 728-738

Stainton MP, Capel MJ, Armstrong FAJ (1977) The Chemical Analysis of Freshwater. 2nd ed. Fisheries and Environ Canada. Fisheries and Marine Service. Winnipeg, Manitoba, Canada

Welter JR, Fisher SG (2016) The influence of storm characteristics on hydrological connectivity in intermittent channel networks: implications for nitrogen transport and denitrification. Freshwater Bio 61: 1214-1227

Mobilization of Bound Arsenic and Antimony from Peat used for the Treatment of Mining-Affected Waters

Uzair Akbar Khan[1], Vera Luostarinen[1], Aileen Ziegelhöfer[1,2], Katharina Kujala[1]

[1]*University of Oulu, PO Box 4300, 90014 University of Oulu, Finland, katharina.kujala@oulu.fi*

[2]*University of Applied Sciences FH Aachen, Germany*

Abstract

Mining-affected waters need to be purified for their safe discharge into water bodies. In Finland, peatlands are frequently used in the polishing phase of water treatment. Changes to inflow water quality to the treatment peatlands can trigger release of previously bound contaminants from the peat. A laboratory column experiment was designed to simulate leaching of arsenic and antimony from peat by transition from highly contaminated wastewater to less contaminated water. Inflow water composition change led to leaching and redistribution of bound arsenic and antimony in the peat column. Peak of bound arsenic/antimony shifted towards the outlet during the leaching phase.

Keywords: Mining-affected Water, Peatlands, Arsenic, Antimony, Mobilization

Introduction

Peatlands used for passive treatment of mining-affected waters are common in Finland. As a final treatment step, they are employed to remove various contaminants such as sulphate, nitrogen, phosphorous, metals, and metalloids before the water is discharged into the environment. It has been demonstrated that even in a cold climate, they can provide effective removal of many contaminants (Khan *et al*., 2020; Kujala *et al*., 2019) as the adsorption and retention capacity of peat for many of the contaminants commonly found in mining-affected waters is well established (Brown *et al*., 2000; Liu *et al*., 2008). In recent years, attention has been diverted to risks associated with using natural peatlands for mining-affected water treatment in the long-term. Over the course of their service life, contaminants removed in treatment peatlands can accumulate in very high concentration in the peatland media and can subsequently leach out under favourable conditions (Khan *et al*., 2019; Palmer *et al*., 2015). Such leaching events can happen as a result of changes in biogeochemistry of the peatlands brought about by changes in inflow water composition. Inflow water composition can change due to mine closure or as a result of dilution during snowmelt season and storm events. Arsenic and antimony are two of the most common contaminants in mining affected waters, which co-occur in mines extracting sulphide ores e.g., pyrite (Arai *et al*., 2010). Both metalloids have very similar chemical properties despite having some characteristic differences and are efficiently removed in treatment peatlands (Palmer *et al*., 2015). However, there is a possibility of their mobilization as they are mostly removed by adsorption on peat (Besold *et al*., 2018; 2019) and precipitation with sulfide (Gammon & Frandsen, 2001). Arsenic and antimony are hazardous for human health, and their elevated concentration in the environment can have detrimental effects for the ecosystem (Abernathy *et al*., 1999; Cooper & Harrison, 2009; Dovick *et al*., 2016).

In this study, we simulated the effect of changes in inflow mining-affected water composition on outflow water quality in treatment peatlands by employing flow-through peat columns. The objective was to ascertain whether a substantial decline in arsenic and antimony concentration in the inflow can lead to leaching from peat columns loaded with these contaminants. Thus, this study provides a unique opportunity to see changes in contaminant concentration in peat and water simultaneously while peat

undergoes leaching, hence providing a rare insight into contaminant redistribution characteristics of peatlands heavily polluted with mining-affected water.

Methods

Site description and sampling

Peat for the column experiment was obtained from a treatment peatland polishing pre-treated mine process water at a gold mine in Northern Finland. The mean annual temperature at the site is -0.5 °C and mean annual precipitation 500-600 mm. The site is typically snow covered from October to May. The peatland has been in operation since 2010 and receives 3100 m^3 d^{-1} water. A more detailed description of the sampling site can be found in Khan *et al.* (2020). The peat was collected outside the main flow area of the process wastewater to minimize background concentrations of arsenic and antimony. Peat was sampled from the upper 20 cm in autumn 2019 and stored at 4 °C prior to column construction. Arsenic and antimony concentrations in the peat were 43.5 mg kg_{DW}^{-1} and 7.8 mg kg_{DW}^{-1}, respectively.

Column construction and experimental set-up

The experiment consisted of eight flow through columns: four to study loading and leaching of arsenic and antimony each (Figure 1). Each column comprised a 30 cm long and 5.2 cm diameter plastic column. A perforated plastic disc was used on both sides for even flow distribution across the entire cross section. In addition, a 2.5 cm layer of inert quartz sand (particle size 2-3 mm) was provided on both ends of the column between peat and the circular plastic disc. The columns were filled with peat. Three porewater samplers (Rhizon samplers, Rhizosphere Research Products B.V.) were installed in each column at 7.5 cm, 15 cm, and 22.5 cm from the bottom. Rhizon samplers have a pore size of 0.15 µm and are a convenient way to collect porewater in a non-destructive way for determination of dissolved constituents. Columns were incubated at 5 °C throughout the experiment which corresponds to the average *in situ* temperature measured in 10 cm depth. Inflow at the bottom of each column was provided at an average rate of 5 mL d^{-1} using a peristaltic pump (MINIPULS 3, Gilson Inc.). Columns were loaded with artificial mining-affected water containing high concentrations of arsenic (four columns) or antimony (four columns) for 35 days. The artificial mining-affected water contained 6 mg L^{-1} arsenic or antimony (supplied as arsenate or antimonate, respectively), 6 g L^{-1}sodium sulfate, 25 mg L^{-1} ammonium chloride and 60 mg L^{-1} sodium nitrate. The pH was adjusted to 7. After 20 days of loading, the arsenic and antimony concentrations were lowered to 2 mg L^{-1} and one column loaded with antimony containing water was sacrificed. After 35 days, one column per set was sacrificed and the inflow water changed to low arsenic/antimony water (0.2 mg L^{-1} arsenic/antimony, 2 g L^{-1} sodium sulfate, 25 mg L^{-1} ammonium chloride, 60 mg L^{-1} sodium nitrate, pH 7) to induce leaching. The remaining columns were sacrificed after 8 days (arsenic, antimony), 16 days (arsenic) and 40 days (arsenic, antimony) under leaching conditions.

Determination of arsenic and antimony concentrations in inflow water, outflow water and peat

Arsenic and antimony concentrations in column inflow and outflow water were determined using colorimetric assays in 96-well plates based on Dhar *et al.* (2004) and Tighe *et al.* (2018). Briefly, for determination of arsenic concentrations, arsenic in samples and standards was oxidized with potassium iodate to arsenate which was subsequently

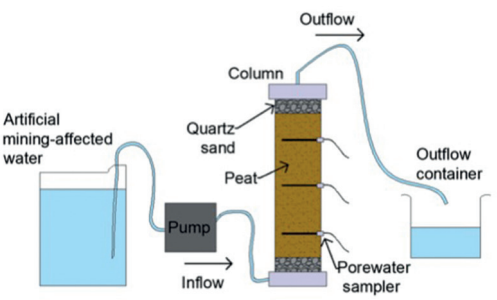

Figure 1 *Schematic diagram of the flow-through column experiment.*

reacted with a colour reagent containing ascorbic acid, ammonium molybdate, antimony potassium tartrate and sulfuric acid to form arseno-molybdate complexes with absorbance at 880 nm. Phosphate forms phosphor-molybdate complexes when reacting with the colour reagent which likewise absorb at 880 nm, and any phosphate contained in the samples will thus increase the total absorbance. To correct for potential colour formation due to phosphate, in a second set of reactions all arsenic was reduced to arsenite (which does not form arseno-molybdate complexes) with a reducing agent containing sodium metabisulfite, sodium thiosulfate and sulfuric acid prior to the addition of the colour reagent. Arsenic concentrations were calculated from the corrected absorbance using calibration curves in a concentration range from 0 to 10,000 µg arsenic L^{-1}.

For determination of antimony concentration, antimony in the samples was acidified with sulfuric acid and reacted with potassium iodide reagent (20 g L^{-1} ascorbic acid, 112 g L^{-1} potassium iodide) to form potassium iodoantimonite complexes with absorbance at 425 nm. Concentrations were calculated using calibration curves in a concentration range from 0 to 10,000 µg antimony L^{-1}.

Sacrificed peat columns were divided into 3 to 4 cm thick segments. Arsenic, antimony, iron, and manganese concentrations in peat were determined by a certified laboratory (Eurofins oy) using ICP-MS after aqua regia microwave digestion.

Results

The peat flow-through columns were loaded with artificial process and mine dewatering water containing high concentrations of arsenic and antimony, respectively, for approximately 1 month. During the late loading phase, the columns removed both arsenic and antimony with removal efficiencies ranging from 50-85% (arsenic) and 65-95% (antimony) (Fig. 2). There were two sampling timepoint during loading stage where leaching of antimony was observed (day -15). It may be attributed to a sampling error or the inherent heterogeneity of peat. When the inflow was changed to water with lower arsenic/antimony concentration, leaching was induced (Fig. 2). Arsenic concentrations in the outflow increased rapidly and reached a maximum 6 to 16 days after the onset of leaching conditions (Fig. 2A). After that, arsenic concentrations in the column outflow slowly declined again, but were higher than inflow concentrations until day 40 when the last of the columns was sacrificed.

Antimony concentrations in the outflow likewise increased after the onset of leaching (Fig. 2B). However, unlike with arsenic, no peak in outflow concentration was observed but concentrations increased slowly until day 40. Contrary to the results seen here, it has

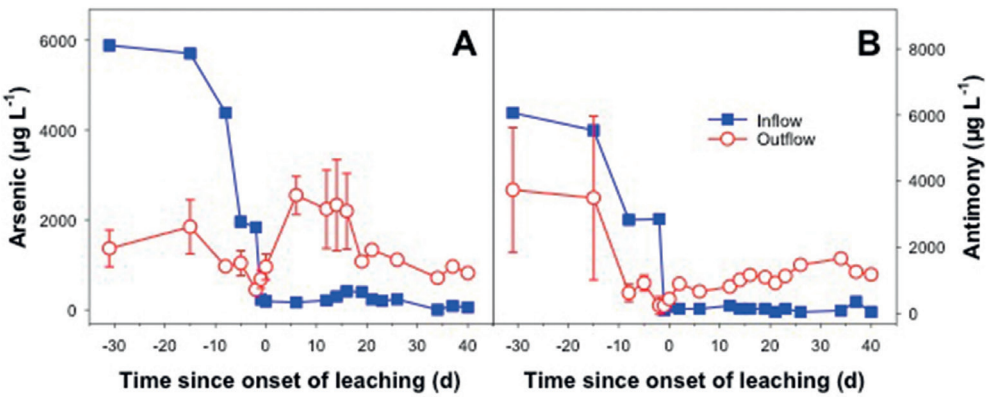

Figure 2 Concentrations of arsenic and antimony in inflow and outflow waters of columns used to test arsenic leaching (A) and antimony leaching (B). Mean values and standard deviations of four columns (until2 days before onset of leaching), three columns (until 6 days since the onset of leaching), two columns (until 16 days since the onset of leaching) and one column (until 40 days since the onset of leaching) are displayed.

been demonstrated previously that antimony is more readily leached than arsenic from peat (Khan *et al.*, 2019). However, since higher amounts of arsenic were removed than antimony in this experiment (Fig. 3), a higher concentration gradient between peat and water was created for arsenic. This gradient may have led to the observed peak in arsenic leaching. After this initial peak in leaching passed, arsenic and antimony both behaved very similarly as the concentration gradient became more comparable. Both contaminants are removed in peatlands through very similar mechanisms e.g., binding to natural organic matter (Besold *et al.*, 2018; 2019).

Columns were sacrificed during the loading phase (antimony only), at the end of the loading phase and at different timepoints during the leaching phase. At the end of the loading phase, highest concentrations of both arsenic and antimony were observed in the first 10 cm from the column inflow (Fig. 3). In the column loaded with arsenic, peak concentrations were close to 600 mg kg_{DW}^{-1} and there was a sharp drop in concentration towards the end of the column, with concentrations near the outflow of less than 50 mg kg_{DW}^{-1} (Fig. 3A). In the column loaded with antimony, peak concentrations were substantially lower, amounting to only 150 mg kg_{DW}^{-1} (Fig. 3B). Concentrations were likewise lower near the end of the column, but overall, the distribution of antimony was more even than the distribution of arsenic. In contrast to this a column sacrificed in an earlier stage of loading showed overall lower antimony concentrations and very low concentrations near the end of the column (Fig. 3B), indicating that the capacity for antimony retention in peat might be lower than for arsenic retention, leading to more antimony bound farther away from the inlet in the later loading phase after retention capacity near the inlet was exhausted. The peak concentration of antimony in peat observed in this experiment is in line with the long-term measurements made in the mining-affected treatment peatland in Kittilä where concentration in peat stabilized around 150-200 mg kg_{DW}^{-1} after 5 years of loading (Khan *et al.*, 2020). In addition, a decline in antimony peat concentration was observed in one of the peatlands after inflow water quality improved due to additional water treatment. Results of this study show that it is more likely that the full-scale peatland is still undergoing redistribution/homogenization of contaminants and substantial leaching to the outflow may be expected in the future.

After eight days under leaching conditions, arsenic was distributed more evenly in the column: While concentrations directly at the inflow were still high (310 mg kg_{DW}^{-1}), the highest concentration of 340 mg kgD_{DW}^{-1} was observed 14 cm from column inflow (Fig. 3A). Concentrations close to the outflow were substantially higher than after loading. After

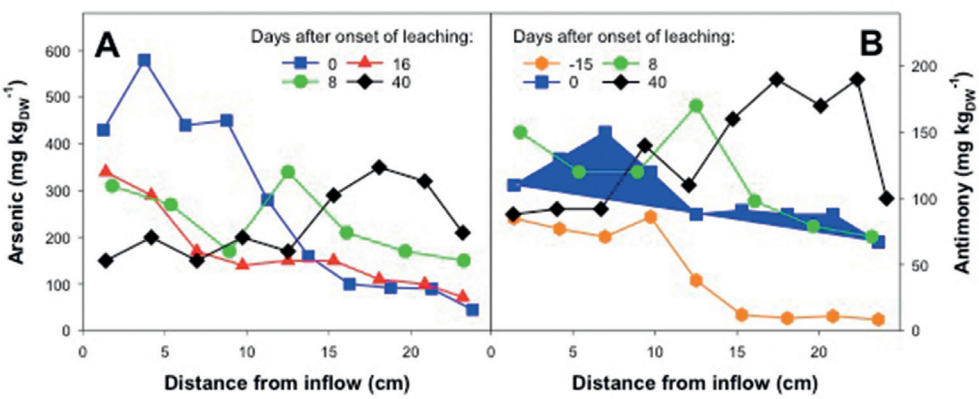

Figure 3 *Effect of artificial mining water with low arsenic/antimony concentrations on the distribution of arsenic and antimony along peat columns. Inflow water was changed from water with high arsenic/antimony concentrations to water with low arsenic/antimony concentrations at day 0. Since columns were destroyed for measurement of concentrations in peat, only unicate measurements were available for each timepoint.*

40 days under leaching conditions, arsenic concentrations near the inflow had decreased to approximately 150 mg kg_{DW}^{-1}, and a concentration peak was observed close to the column outflow (Fig. 3A).

Peak antimony concentrations likewise moved closer to the column outflow with increasing time under leaching conditions (Fig. 3B). Based on this progression, it can be concluded with a fair amount of confidence that the entire amount of accumulated arsenic and antimony will have eventually leached out to the outflow with longer exposure. However, experiments with longer leaching phase should be carried out to say this with certainty.

Conclusion

A flow-through column experiment was run to study leaching of arsenic and antimony from mining-affected water treatment peatlands. Peat columns were first loaded with high concentration artificial mining-affected water and then low concentration water was passed to induce leaching. The results showed that both arsenic and antimony were efficiently retained in the column during the loading phase with removal efficiencies reaching around 90% although arsenic retention capacity of peat was observed to be substantially higher than antimony retention capacity. Reducing inflow arsenic and antimony concentrations led to leaching of the retained arsenic and antimony with outflow concentrations constantly higher than the inflow concentrations till the end of the experiment. Measurement of concentrations in peat revealed that peak concentration of both arsenic and antimony moved farther away from the inlet as leaching phase progressed. This study raises serious questions about the long-term use of natural peatlands for mining-affected water treatment and the fate of metals and metalloids in peatlands currently under use.

References

Abernathy, C. O., Liu, Y. P., Longfellow, D., Aposhian, H. V, Beck, B., Fowler, B., Goyer, R., Menzer, R., Rossman, T., Thompson, C., Waalkes, M. (1999). Arsenic: health effects, mechanisms of actions, and research issues. Environmental Health Perspectives, 107(7), 593–597. https://doi.org/10.1289/ehp.99107593

Arai, Y. (2010). Arsenic and Antimony. In P. S. Hooda (Ed.), Trace elements in soil (pp. 383–407). Blackwell Publishing Ltd.

Besold, J., Eberle, A., Noël, V., Kujala, K., Kumar, N., Scheinost, A. C., Pacheco, J.L., Fendorf, S., Planer-Friedrich, B. (2019). Antimonite Binding to Natural Organic Matter: Spectroscopic Evidence from a Mine Water Impacted Peatland. Environmental Science & Technology, 53(18):10792–10802. https://doi.org/10.1021/acs.est.9b03924

Besold, J., Biswas, A., Suess, E., Scheinost, A. C., Rossberg, A., Mikutta, C., Kretzschmar, R., Gustafsson, J.P., Planer-Friedrich, B. (2018). Monothioarsenate Transformation Kinetics Determining Arsenic Sequestration by Sulfhydryl Groups of Peat. Environmental Science & Technology, 52(13):7317–7326. https://doi.org/10.1021/acs.est.8b01542

Brown, P. A., Gill, S. A., & Allen, S. J. (2000). Metal removal from wastewater using peat. Water Research, 34(16):3907–3916. https://doi.org/10.1016/S0043-1354(00)00152-4

Cooper, R. G., & Harrison, A. P. (2009). The exposure to and health effects of antimony. Indian Journal of Occupational and Environmental Medicine, 13(1):3–10. https://doi.org/10.4103/0019-5278.50716

Dhar, RK, Zheng, Y, Rubenstone J, van Geen, A (2004) A rapid colorimetric method for measuring arsenic concentrations in groundwater. Anal Chim Acta 526:203-209. https://doi.org/10.1016/j.aca.2004.09.045

Dovick, M. A., Kulp, T. R., Arkle, R. S., & Pilliod, D. S. (2016). Bioaccumulation trends of arsenic and antimony in a freshwater ecosystem affected by mine drainage. Environmental Chemistry, 13(1):149–159. https://doi.org/10.1071/EN15046

Gammons, C. H., & Frandsen, A. K. (2001). Fate and transport of metals in H2S-rich waters at a treatment wetland. Geochemical Transactions, 2(1). https://doi.org/10.1186/1467-4866-2-1

Khan, U. A., Kujala, K., Planer-Friedrich, B., Räisänen, M. L., & Ronkanen, A.-K. (2020). Long-term data reveals the importance of hydraulic load and inflow water quality for Sb removal in boreal treatment peatlands. Ecological Engineering, 148, 105785. https://doi.org/10.1016/J.ECOLENG.2020.105785

Kujala, K., Karlsson, T., Nieminen, S., & Ronkanen, A.-K. (2019). Design parameters for nitrogen removal by constructed wetlands treating mine

waters and municipal wastewater under Nordic conditions. Science of The Total Environment, 662, 559–570. https://doi.org/10.1016/J.SCITOTENV.2019.01.124

Liu, Z. rong, Zhou, L. min, Wei, P., Zeng, K., Wen, C. xi, & Lan, H. hua. (2008). Competitive adsorption of heavy metal ions on peat. Journal of China University of Mining and Technology, 18(2):255–260. https://doi.org/10.1016/S1006-1266(08)60054-1

Palmer, K., Ronkanen, A.-K., & Kløve, B. (2015). Efficient removal of arsenic, antimony and nickel from mine wastewaters in Northern treatment peatlands and potential risks in their long-term use. Ecological Engineering, 75(0), 350–364. https://doi.org/10.1016/j.ecoleng.2014.11.045

Tighe, M, Edwards, MM, Cluley, G, Lisle, L, Wilson, SC (2018) Colorimetrically determining total antimony in contaminated waters and screening for antimony speciation. J Hydrol 563:84-91. https://doi.org/10.1016/j.jhydrol.2018.05.056

Characterization of Arsenical Mud from Effluent Treatment of Au Concentration Plants, Minas Gerais – Brazil

Mariana Lemos[1,2], Teresa Valente[1], Paula Marinho[1], Rita Fonseca[3], José Gregório Filho[2], José Augusto Dumont[2], Juliana Ventura[2], Itamar Delben[4]

[1]*Institute of Earth Sciences, Pole of University of Minho, University of Minho, Campus de Gualtar, 4710-057 Braga, Portugal*

[2]*Anglogold Ashanti, Mining & Technical, COO International, 34000-000, Nova Lima, Brazil*

[3]*Institute of Earth Sciences, Pole of University of Évora, University of Évora, 7000 Évora, Portugal*

[4]*Microscopy Center, Universidade Federal de Minas Gerais, 31270-013, Belo Horizonte, Brazil*

Abstract

The determination of the general properties of arsenical mud was carried out in effluent treatment plant of an Au metallurgical facility, located in Nova Lima, Minas Gerais, Brazil. This effluent, which comes from the calcination stage, is treated via Fe-coprecipitation / lime-neutralization and thus mud with high As concentration is generated. Instrumental methods were applied to investigate physical-chemical characteristics, such as pH, in addition to the forms of occurrence of As and its associations. The results indicated that the mud has an alkaline pH (≈ 8.5), particles with grain size below 20 μm, and As, Fe, S and Al concentrations above 5%. The element As is essentially associated with Fe, Ca, S, and Al, forming phases with wide compositional variation as major and minor constituents generically classified as "complex sulfates" and "compounds with S". The obtained results could assist optimization of the treatment routes in the plant and even to consider the potential reuse of this arsenic mud as a potential valuable product.

Keywords: Geochemistry and Environmental Mineralogy, Tailings Dam, Arsenic

Introduction

Arsenic (As) is a common deleterious element in gold (Au) deposits (Jacob-Tatapu 2018). Materials with elevated As concentration are difficult to process without the associated environmental risks. Very few facilities in the world are capable of treating material containing high concentration of As. The main sources are sulfides such as arsenopyrite, commonly associated with Au. In the Au metallurgical beneficiation process, stages for treating toxic elements in effluents are essential and corroborate the environmental and social responsibilities of a sustainable mining sector. Due to limited alternatives, the As is often volatilized or left in tailings exposed to lixiviation and are generally arranged in small dams or pits (Deschamps *et al*. 2002; Procópio 2004; Pantuzzo *et al*. 2007a; Bissacot *et al*. 2015; Moura 2015). This fact, coupled with challenges in the mineral industry regarding the sustainability of its resources and the difficulties of obtaining new environmental licenses, made critical the need for detailed characterization studies in search of new alternatives and improvements for disposal of residues rich in As (Lemos *et al*. 2021a).

The work was focused on arsenical muds generated from the effluent treatment of an Au concentration plant, located in Nova Lima, Minas Gerais (Fig 1). The ore that feeds the plant comes from mines, located within the Rio das Velhas Greenstone Belt in the Iron Quadrangle region and are mainly composed of sulfides such as pyrite, arsenopyrite, pyrrhotite and rare sulfides, like as gerdosffite, galena, sphalerite (Lobato *et al*. 2001; Moura 2015; Kresse *et al*. 2018).

These sulfides are concentrated by flotation, calcined, and subsequently leached to recover Au, as illustrated in Fig 2 (Moura 2015). The As, originating from the sulfide concentrated, is volatilized in the form of As trioxide in the

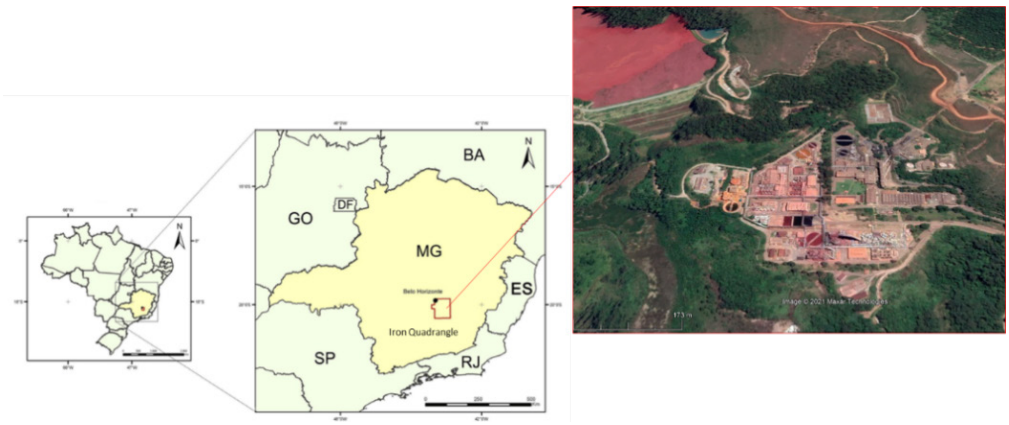

Figure 1 *Study area: a. iron quadrangle map location (modified from Ruchkys U.A 2007) and Nova Lima location and b. Nova Lima Metallurgic plant (SIRGAS2000 – 10-09-2019).*

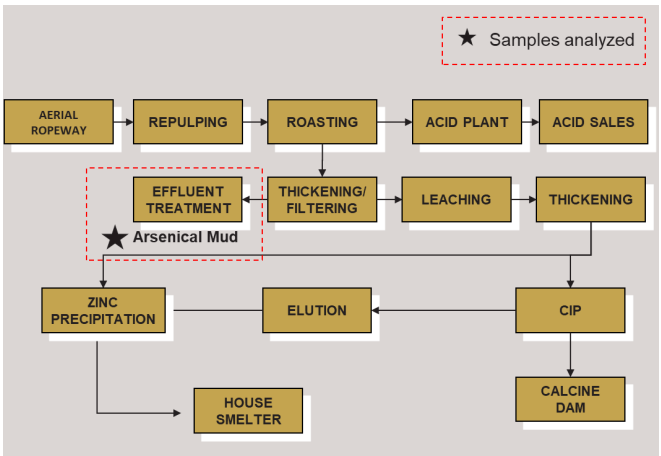

Figure 2 *On-going workflow of Nova Lima´s plant. The yellow stars represent sampling points in Arsenic effluent treatment (modified from Moura 2015).*

roasting stage, absorbed in an aqueous phase in the gas washing towers and finally removed by coprecipitation processes with iron and neutralization with lime (Fig 2). The resulting solid waste (arsenic sludge or mud) is then disposed of in waterproofed ditches (dug into the surface of the land), located in the plant's area of influence (Pantuzzo *et al.* 2007b).

Pantuzzo 2017 refers the presence of As in the waste ditches essentially associated with Fe and to a lesser extent with Ca (probably Ca-arsenates), Al, or even Mn, and Zn, through coprecipitation/adsorption mechanisms. However, it is necessary to detail the sources of As in the waste generated in the plant.

Therefore, the main objective of the present work is the characterization of this current arsenical mud after the neutralization step, mainly the geochemical and mineralogical properties, and identification of the neoformed host phases of As.

Methods

The sampling campaign was performed over twenty-eight days in September 2019 during the production stage, representing a total of 40 samples after neutralization stage from the active plant (Fig 2). All samples were immediately sealed and refrigerated until analysis. Additional material was transferred

to polypropylene bags and frozen until analysis. Refrigerated and frozen samples were packaged and shipped to the chemical laboratory for analysis.

Parameters such as pH of the effluent water samples were obtained using methodologies from the Standard Methods of Water and Wastewater (APHA 2005). Water samples were filtered using a 0.45 μm filter (Sigma Aldrich) and subjected to chemical analysis by inductively coupled plasma mass spectrometry (ICP-MS) at Universidade Federal de Minas Gerais (UFMG) water analysis laboratory.

Chemical analysis of the solid tailings was performed by atomic absorption spectroscopy (AAS using AAS280 FS Varian). Infrared analysis (LECO) was used to obtain analytical S and C data.

The mineralogical study was carried out using polished sections analysed by optical microscopy and scanning electron microscopy (SEM, Field Electron and Ion Company, FEI) at UFMG, Belo Horizonte.

Results and Discussion

This section presents the general properties of the arsenic mud, which in general has particles of fine grain size (P80:15μm).

Geochemistry

The arsenical mud samples are mainly composed of Ca (14.5 - 17.2%), S (13.1 - 13.8%), Fe (6.8 - 8.7%), As (3.6 - 4.2%) and other elements in low concentrations (Tab. 1).

The water has low concentrations of Fe (<2.5 mg /L) and As (1.4 - 5.3 mg/L), which is consistent with the neutralization step in the beneficiation plant. For sulfur, the concentration of 1.0 g/L in the solution of the neutralization step is expected as the pH increases because of the lime addition. The consistency of this information is confirmed, therefore, by the concentration of Fe, As and S found in the solid phase already presented.

Mineralogy

The mineralogical study by SEM revealed the presence of Hematite, Gypsum, Sulfo Arsenical Compounds (CSA), Compounds with S and other elements (Ca, Al, Si, Mg and Fe), Al silicates, Ferrosaponite, Gibbsite and Fe / Al oxides. The types of arsenical sulfo compounds (CSA) were differentiated by their As amount, varying from 3 to 13% (Tab 2; Fig 3). In addition to As and S, they are made up of Fe, Al, Zn, Ca.

The arsenical mud consists essentially of "CSA 1" (38.36% by weight), and "Gypsum Fe" (28.57% by weight). The total percentage of all phases with S (sulfates, "Compounds with S" and "CSA") is 90.63% (Fig 3). Also noteworthy are the low amounts of "Hematite", which make up a total of 1.13% by weight in this sample, as well as quartz and other silicate phases classified as others.

Table 1 Average water pH and concentration of major and trace elements - Solid and Water samples; N – number of samples.

	Solid (N=40)	Residual Water (N=10)
Physical Parameters	Average	Average
pH	-	8.5
Elements	%	mg/L
Fe	8.68	<2.50
As	3.58	5.31
S	13.30	436.39
Si	0.36	-
Ca	14.89	491,01
Al	1.50	<2.50
Mg	0.52	16.58
K	0.02	100.73
Zn	0.43	<0.1
C	0.10	-

Table 2 Mineralogy of Solid samples (average values); N – number of samples.

	Solid (N=40)
Mineral/Composed	Average %
Hematite	1.13
Gypsum (Fe)	28.57
(CSA1 -3%As in composition)	38.36
(CSA2 -13%As in composition)	18.10
(CSA3 -5%As in composition)	11.68
Others	3.03

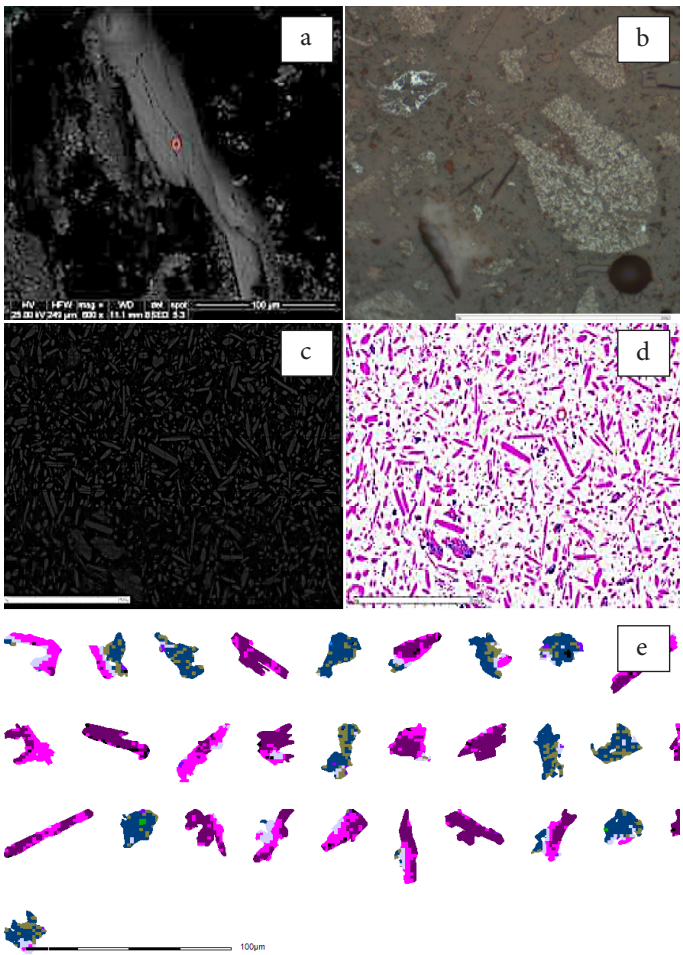

Figure 3 *Backscattered electron image of Sulfo Arsenical Compounds in arsenical mud. a) CSA, b) Reflected light image of porous hematite, c) total sample, d) and e) false image of total samples (pink, purple and blue – Gypsum (pink/purple) and CSA (Blue).*

The predominant presence of calcium and sulfur is consistent with the identification of gypsum indicated by electron microscopy (Fig. 3). On the other hand, the occurrence of Fe and As in relevant quantities is associated with the complex phases that contain variable concentrations of As.

The samples underwent several types of "attacks", from breaking the structure by calcination, followed by complementary chemical processes. This can result in complex phase transformations and, in addition, chemical dissolutions and substitutions in the crystalline structure. As a result, some phases have very complex micro-chemical and textural compositions. These phases with wide compositional variations and made up of several elements as major and minor constituents were generically classified as "Complex Sulfates", "CSA". The rate of this transformation should be directly related to the size of the particles and the availability of the surface for reaction.

In calcination, part of the Fe^{+2} released from the dissolution of the primary minerals (sulfides, oxides, silicates with Fe) is oxidized to Fe^{+3} and precipitated as hematite / oxides, which in turn, may have been attacked chemically generating skeletal and porous hematite, richer in contaminating elements (Fig 3b).

In addition, the breakdown of the structure by calcination may result in ion solubilization,

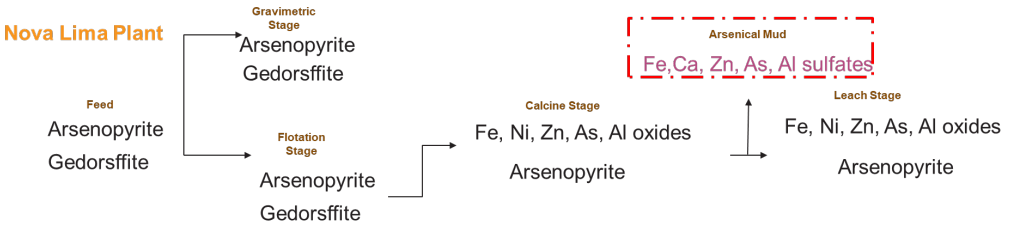

Figure 4 *Transformation path of As sources along Nova Lima Au metallurgical plant until neoformation of arsenic mud.*

such as Ca and Mg, of some silicates (and carbonates) originally present. Also, the leaching of elements by acidic attacks and the addition of lime and precipitating agents may have caused the precipitation of phases, such as gypsum and other sulfates, dissolution and ionic substitutions, partial to total, resulting in the formation of complex phases, with various constituent elements (e.g., Fe, S, Ca, Mg, Al, Si). Fig 4, therefore, illustrates the transformations of As minerals along the process of this metallurgical plant until the generation of the arsenical sludge.

Conclusions

Arsenical sludge is the product of the neutralization stage of the Au treatment of a plant located in Nova Lima, Brazil. An integrated characterization, including geochemistry and mineralogy was performed to evaluate the sources of As and their associations. The predominant presence of Ca and S is consistent with the identification of gypsum. On the other hand, the occurrence of Fe and As in high quantities is mainly associated with the complex phases with variation in the grades of As.

The arsenical mud is mainly composed by Ca (14.5 - 17.2%), S (13.1 - 13.8%), Fe (6.8 -8.7%) and As (3.6 - 4.2%). It is noteworthy that the water has low concentrations of Fe (<2.5 mg/L) and As (1.4 - 5.3 mg/L), which is expected after the neutralization step. The samples analysed underwent several types of "attacks", from breaking the structure by calcination, followed by complementary chemical attacks. This resulted in complex phase transformations and, in addition, chemical dissolutions and substitutions in the crystalline structure. As a result, some phases have very complex micro-chemical and textural compositions. In the analysed samples, these phases with wide compositional variations and made up of several elements as major and minor constituents were generically classified as "Complex Sulfates", "CSA.

From the results of this characterization study, it is possible to propose optimization in the current treatment routes and even propose new alternatives, in addition to initiatives in the reuse of these as a valuable product for As recovery.

Acknowledgements

We thank our colleagues from ICT, microscopy center from Universidade Federal de Minas Gerais (CM-UFMG), and AngloGold Ashanti who provided insight and expertise that greatly assisted the research. This work was funded by FCT—Fundação para a Ciência e a Tecnologia through projects UIDB/04683/2020 and UIDP/04683/2020 and Nano-MINENV 029259 (PTDC/CTA-AMB/29259/2017), and by AngloGold Ashanti Brazil.

References

Bissacot L, Ciminelli V, Logsdon M (2015) Arsenic Mobility under a Neutral Mine Drainage Environment in a Gold-Mine Tailings Dam

Deschamps E, Ciminelli VST, Lange FT, *et al* (2002) Soil and sediment geochemistry of the iron quadrangle, Brazil: The case of Arsenic. Journal of Soils and Sediments 2:216–222. https://doi.org/10.1007/BF02991043

Jacob-Tatapu KJ (2018) Investigating the elevated arsenic concentrations in the Gold Ridge Tailings Storage Facility surface water. School of Civil Engineering

Kresse C, Lobato LM, Hagemann SG, Figueiredo e Silva RC (2018) Sulfur isotope and metal variations in sulfides in the BIF-hosted orogenic Cuiabá gold deposit, Brazil: Implications for the hydrothermal fluid evolution. Ore Geology Reviews 98:1–27. https://doi.org/10.1016/j.oregeorev.2018.05.012

Lemos MG, Valente T, Marinho-Reis AP, *et al* (2021a) Geoenvironmental Study of Gold Mining Tailings in a Circular Economy Context: Santa Barbara, Minas Gerais, Brazil. Mine Water and the Environment 40:257–269. https://doi.org/10.1007/s10230-021-00754-6

Lemos MG, Valente T, Marinho-Reis AP, *et al* (2021b) Geoenvironmental Study of Gold Mining Tailings in a Circular Economy Context: Santa Barbara, Minas Gerais, Brazil. Mine Water and the Environment 40:257–269. https://doi.org/10.1007/s10230-021-00754-6

Lindsay MBJ, Moncur MC, Bain JG, *et al* (2015) Geochemical and mineralogical aspects of sulfide mine tailings. Applied Geochemistry 57:157–177

Lobato LM, Ribeiro-Rodrigues LC, Zucchetti M, *et al* (2001) Brazil's premier gold province. Part I: The tectonic, magmatic and structural setting of the Archean Rio das Velhas greenstones belts, Quadrilátero Ferrífero. Mineralium Deposita 36:228–248. https://doi.org/10.1007/s001260100179

Moura (2015) Lixiviação Queiroz. Thesis

Pantuzzo FL, Cimincllli VS, Braga frany (2007a) Especiação do arsênio em lamas arsenicais

Procópio SO (2004) Caracterização de rejeito de mineração de ouro para avaliação de solubilização de metais pesados e arsênio e revegetação local (1) seção ix-poluição do solo e qualidade ambiental

Ruchkys U.A (2007) Patrimônio Geológico e Geoconservação no Quadrilátero Ferrífero, Minas Gerais: Potencial para a Criação de um Geoparque da UNESCO. Universidade federal de minas gerais instituto de geociências programa de pós-graduação em geologia co-orientação carlos schobbenhaus. Belo horizonte

Application of Anthropogenic Organic Contaminants for the Determination of Water Ingress in the Witwatersrand Goldfields Mine Voids

Lufuno Ligavha-Mbelengwa[1], Godfrey Madzivire[1,2], Pamela Nolakana[1], Tebogo Mello[1], Henk Coetzee[1]

[1]*Council for Geoscience, Water and Environment Unit, 280 Pretoria Street, Silverton, Pretoria, South Africa, lligavhambelengwa@geoscience.org.za*

[2]*University of South Africa, Department of Environmental Science, 28 Pioneer Ave, Roodepoort, South Africa*

Abstract

Historical mining has led to environmental degradation in the Witwatersrand Goldfields ever since mining companies ceased pumping water from the mines. A study of using emerging organic contaminants as tracers to map the sources and pathways of water ingress into the mine voids is underway. Water samples from the surface, boreholes and shafts were collected and analysed. Atrazine and caffeine were the most persistent and displayed average concentrations of 0.176 ng/mL and 0.793 ng/mL in surface water respectively. Bisphenol A showed high concentrations in the subsurface with averages of 0.162 ng/mL and 1.082 ng/mL for wet and dry seasons respectively.

Keywords: Mine Voids, Organic Contaminants, Surface Water, Tracers

Introduction

Contaminants such as manure and biosolid derived reach the groundwater system through surface water-groundwater exchange from run-off (Focazio *et al* 2008). Nevertheless, these pollutants are not contained in high concentrations that are toxic because of natural attenuation and/or dilution (Lapworth *et al* 2012). In cases where contaminants are found in high concentration levels in surface waters, it shows that there could be a direct input from wastewater sources, or the process of attenuation or dilution is less in surface water as compared to groundwater. However, it was further described that karstic and shallow alluvial aquifers are the most vulnerable to contamination due to limited attenuation because of rapid flow during recharge of those aquifers. Thus, the residence time in these systems is short.

The study conducted by Lapworth *et al* (2012) on injecting emerging organic contaminants (EOCs) as tracers in the subsurface showed that as much as natural attenuation is high for most compounds, it is not complete since some compounds still behave in a conservative way during the process. Several researchers have recently written about the use of emerging contaminants as tracers in surface water, groundwater and drinking water. These emerging contaminants comprise compounds such as caffeine, nicotine derivatives, carbamazepine, clofibric acid, benzotriazole, bisphenol, gemfibrozil (Murray, Thomas and Bodour 2010); (Lapworth *et al* 2012). Concentrations of emerging contaminants (pesticides, industrial, pharmaceuticals and personal care products) may be traced in drinking water, surface water, groundwater or in the environmental discharges such as waste water from treatment plants (Murray, Thomas and Bodour 2010).

This study evaluated the application of EOCs to trace water ingress in the Witwatersrand Goldfields. It further utilised eleven compounds commonly found in wastewater discharges. Pearson correlation and Dendrogram analysis were used as complementary methods to display correlation and cluster sites with similarities in terms of organic contaminants found, respectively.

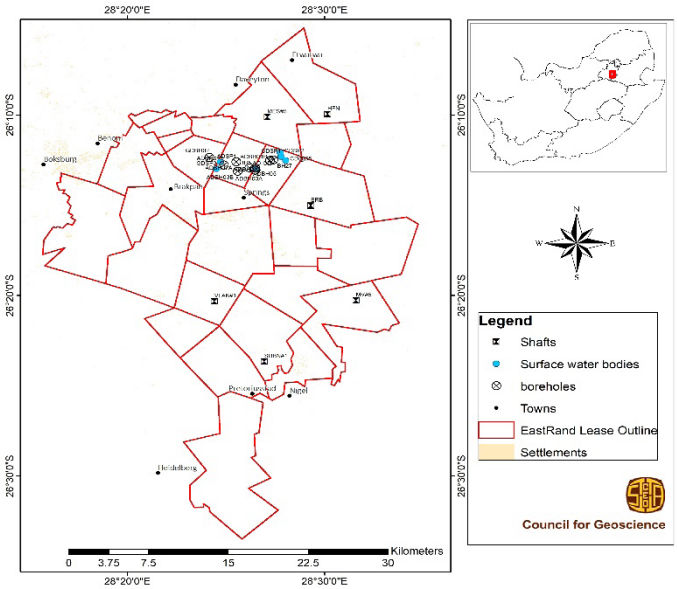

Figure 1 *Locality map of the Eastern Basin.*

Methods

Study area

The study was conducted in the Eastern Basin of the Witwatersrand Goldfields (fig. 1). Surface water bodies, boreholes and shafts were sampled.

Ethical considerations

There were no compounds injected into the environment during this study. Thus, the study is analysing EOCs that are introduced into the aquatic system from point and diffuse sources of contamination. These are compounds used and released into the environment on a daily basis.

Sampling and analytical procedure

Water samples were collected during the wet and dry seasons from shafts, surface water and boreholes for the analyses of EOCs. Seasonal sampling was done to identify seasonal changes in the compounds concentration in the water. Prior collecting groundwater samples, boreholes were purged to remove bore well storage. Plastic bailers were used to acquire samples from boreholes and shafts at the static water level. Water samples from the surface water bodies were collected using the sampling bottles or buckets in areas where water could not be reached easily. A 250 ml glass bottle that was rinsed with water to be sampled was filled at each sampling site for the storage of water for organic contaminants analyses. Samples were stored under cold conditions immediately after sampling and kept for a maximum of 7 days before transported to the laboratory for analyses.

The water was analysed at the Microbial Biochemical and Food Biotechnology Laboratory, University of the Free State.

Samples were processed using solid-phase extraction using Waters Oasis HLB cartridges. Two separate analyses were performed on the eluates:

- Analysis of underivatised samples using targeted MRMs; and
- Analysis of eluates after derivatisation using dansyl chloride. Six labelled internal standards were used to compensate for matrix effects and instrument drift.

Data interpretation

Laboratory data was exported to the Statistical Package for Social Sciences (SPSS) for further statistical evaluation. Statistics tools such as Hierarchical cluster analysis (HCA)

and Pearson correlation plots were done. Furthermore, Microsoft Excel was used to draw graphs that were used for further interpretations.

Results and discussion

Tracers that were analysed in the surface, groundwater and mine voids water for both seasons were metolachlor, caffeine, atrazine, bisphenol A, carbamazepine, diclofenac, estradiol, estrone, ibuprofen, sulfamethoxazole and terbuthylazine. Some of the compounds were either not traced from the water completely, or were below limit of quantification (LOQ).

Occurrence of EOCs in aquatic environments and mine voids

Twenty-two surface water bodies, 28 boreholes and 1 shaft were sampled during the wet season of this study. During the dry season, the same sites were sampled, with five more shafts added to the sampling run making 6 shafts.

Tab.1 displays the average calculated for each compound for the results obtained for the wet and dry seasons in surface water, groundwater and water from the mine voids.

Compounds such as diclofenac, estradiol, estrone and terbuthylazine were either below LOQ or not traced in the mine voids water. Ten orders of magnitude high concentrations were observed for the dry season as opposed to the wet season that displayed low concentrations. This can be explained by the concept of dilution that is assumed to have taken place during the wet season when recharge occurred.

EOCs concentrations in surface water, groundwater and mine voids water

Fig. 2 indicates concentrations variation from surface water bodies to groundwater and then mine voids. Shafts are presented by sites VLAK#1 to ERB, surface bodies by GDSP3 to CDSP2 and boreholes by GDBH02 to BH33. Atrazine and caffeine appear to be found in almost all sites. This could be explained by the persistent behaviour (Schwab, Splichal and Banks 2006) and high usage (Sui *et al* 2015) of these compounds respectively. Bisphenol A also appears to be occurring in all sites, but with high concentrations displayed in water samples collected from boreholes and shafts as opposed to those taken from the surface water bodies. Lapworth *et al* 2015 explained that bisphenol A is more persistent under anaerobic conditions, which explains this observation. Terbuthylazine was traced in all surface water bodies and almost all boreholes, but not in any of the mine voids. Carbamazepine was also traced in all surface water, some boreholes and mine voids. Metolachlor was detected in almost all sites except few boreholes, whilst sulfamethoxazole was mostly traced in surface water and some shafts, but not in groundwater.

Table 1 *EOCs average seasonal variations.*

		Average (Wet season)			Average (Dry season)			
Compounds (ng/mL)	**Purpose**	**SW**	**GW**	**MV**	**SW**	**GW**	**MV**	**LOQ**
Atrazine	Herbicide	0.097	0.024	0.023	0.255	0.036	0.026	0.001
Bisphenol A	Industrial compound	0.052	0.162	0.055	0.272	1.082	1.041	0.01
Caffeine	Psychoactive drug	0.096	0.030	0.036	1.489	0.091	0.329	0.001
Carbamazepine	Pharmaceutical	0.117	0.027	0.019	0.469	0.060	0.064	0.01
Diclofenac	Pharmaceutical	0.017	0.002	0.001	0.059	0.001	0.001	0.001
Estradiol	Sex hormone	0.01	0.01	0.01	0.01	0.01	0.01	0.01
Estrone	Sex hormone	0.1	0.1	0. 1	1.459	1.896	0.1	0.1
Ibuprofen	Pharmaceutical	0.148	0.002	0.001	0.327	0.001	0.013	0.001
Metolachlor	Herbicide	0.034	0.001	0.001	0.053	0.003	0.040	0.001
Sulfamethoxazole	Pharmaceutical	0.036	0.01	0.01	0.470	0.019	0.012	0.01
Terbuthylazine	Herbicide	0.087	0.005	0.002	0.122	0.008	0.001	0.001

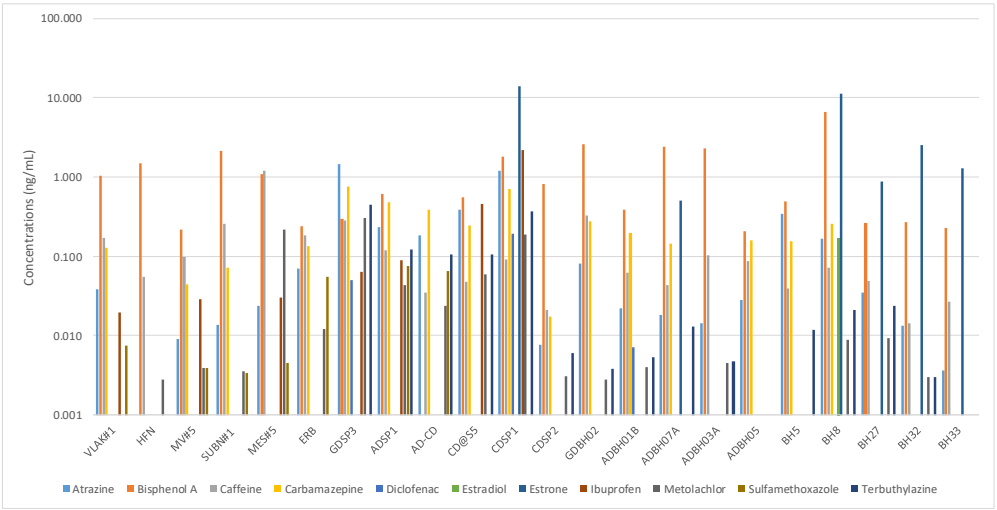

Figure 2 *EOCs concentration variations from surface bodies, boreholes and shafts.*

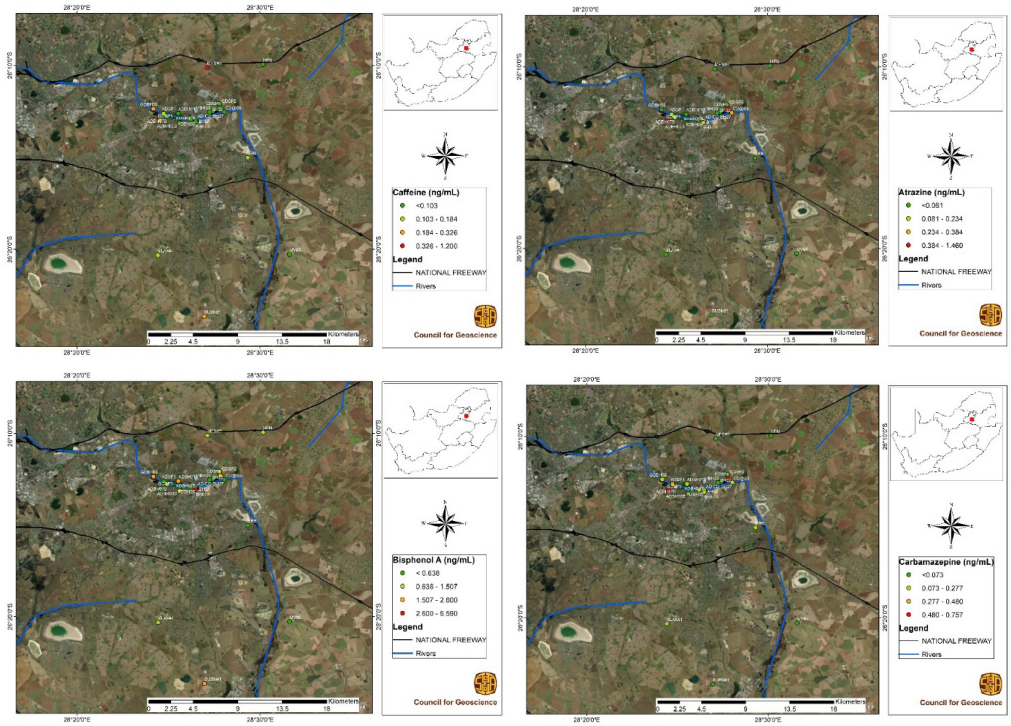

Figure 3 *Compound concentration maps for caffeine, atrazine, bisphenol A and carbamazepine.*

EOCs concentration maps

Compounds maps for caffeine, carbamazepine, bisphenol A and atrazine (fig. 3) were done to display the changes of concentrations from surface water to groundwater and mine voids water. The findings indicated the exchange between these waters. Atrazine although traced in all (except HFN) sites because of its persistent capabilities, appeared to be slightly high in surface water as compared to subsurface water. Caffeine did not display any particular pattern of occurrence. It had

concentrations of >0.103 ng/mL in surface water and shafts. Carbamazepine, unlike others was not traced in some boreholes, especially ones surrounding CD and in shafts HFN and MES#5 that are situated upstream. Lastly, Bisphenol A displayed high concentrations in subsurface sites than what was observed in the surface water.

Statistical analysis

Hierarchical cluster analysis

The dendrogram was produced using the Ward linkage method where five groups were obtained (fig. 4). Group 1 consists of 2 shafts and groundwater from AD. The second group is represented by shaft SUBN#1 and some boreholes surrounding AD. Group 3 clusters CD boreholes together, but with no surface water. Group 4 is the largest and comprises 3 shafts, 4 boreholes and 4 surface bodies.

The findings from these analysis shows surface water, groundwater and mine voids water interaction. Thus, mine voids are receiving water from both surface and groundwater in the surrounding areas.

Bivariate correlation analysis

Pearson correlation results (Tab. 3) indicated interaction relationship between surface and subsurface water. These were observed from high correlation values between the variables. High positive correlation existed amongst the shafts, except for shaft HFN against MES#5 and ERB that displayed a moderate correlation.

High correlations between Alexander Dam (AD) (ADSP1) and the shafts (except MES#5) were observed. Additionally, high relationships were seen between this site and the surrounding groundwater such as ADBH01B, ADBH07A, ADBH05, indicating an interaction between the water.

Further observations were made for sites surrounding the Cowles Dam (CD). Surface water (AD-CD and CDSP1) that were collected at the entrance and exit points of CD displayed low correlations with all sites, except that CDSP1 had a high correlation with the surrounding groundwater. An interaction between surface and groundwater can be deduced from these findings, although it could be "gaining stream" situation.

CDSP2 displayed a high correlation with almost all sites except shafts MES#5 and ERB that were moderate, and the boreholes surrounding CD. The findings therefore gives an indication of surface water interacting with groundwater and mine voids water.

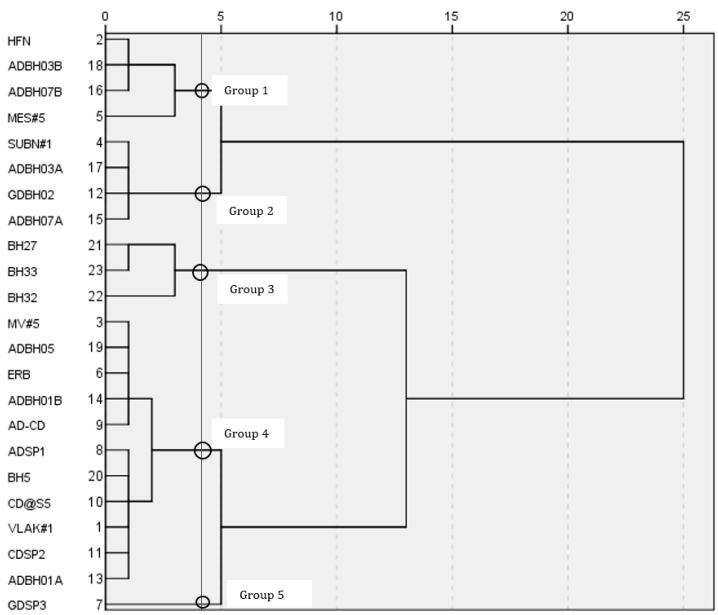

Figure 4 *Dendrogram displaying sites clustering.*

Table 2 Correlation results as obtained from Pearson correlations.

	MV#5	SUBN#1	MES#5	ADSP1	CDSP1	CDSP2	ADBH07A	ADBH05	BH8	BH33
MV#5	**1**									
SUBN#1	**0.939**	**1**								
MES#5	**0.862**	**0.713**	**1**							
ADSP1	**0.772**	**0.748**	.448	**1**						
CDSP1	-.095	-.030	-.141	-.164	**1**					
CDSP2	**0.905**	**0.995**	0.645	**0.746**	-.016	**1**				
ADBH07A	**0.869**	**0.97**	.599	**0.713**	.189	**0.978**	**1**			
ADBH05	**0.864**	**0.773**	0.648	**0.934**	-.126	**0.744**	**0.724**	**1**		
BH8	.304	.413	.174	.156	**0.887**	.425	0.603	.214	**1**	
BH33	-.018	.058	-.045	-.134	**0.983**	.068	.272	-.063	**0.931**	**1**

Conclusions

The application of emerging organic contaminants as tracers in the current study gave an indication of surface-subsurface water interaction. Seasonal sampling results displayed high compound concentrations during the dry season as compared to the wet season. Depending on their behaviour under various conditions, EOCs varied in concentration from surface water, groundwater and mine voids water. Atrazine and caffeine were the most persistent as they were traced in all sites. Bisphenol A was more persistent under anaerobic conditions leading to its high concentration values in subsurface water. The Dendrogram and Pearson correlation results displayed Alexander Dam surrounding sites showing an indication of surface water interacting with subsurface water, whilst, for Cowles Dam, surface water bodies except CDSP1 that had low correlation with shafts did not give an indication of correlation with the surrounding boreholes.

Based on the study findings, it is recommended that a study on understanding precise sources of contamination by EOCs should be considered since this can be utilised in directly identifying some sources of ingress. Additionally, more EOCs that are site specific should be added to the study.

Acknowledgements

The authors would like to send their sincere appreciation to the Department of Mineral Resources and Energy (DMRE) for funding this project. Many thanks goes to the Mine Environment and Water Programme team members, especially those that contributed to this task.

References

Focazio MJ, Kolpin DW, Barnes KK, Furlong ET, Meyer, MT, Zaugg SD, Barber LB, Thurman ME (2008) A national reconnaissance for pharmaceuticals and other organic wastewater contaminants in the United States - II) Untreated drinking water sources, *Science of the Total Environment*. doi: 10.1016/j.scitotenv.2008.02.021.

Lapworth DJ, Baran N, Stuart ME, Ward RS (2012) Emerging organic contaminants in groundwater: A review of sources, fate and occurrence. *Environmental Pollution, 163*, 287–303.

Lapworth DJ, Baran N, Stuart ME, Manamsa K, Talbot J (2015) Persistent and emerging micro-organic contaminants in Chalk groundwater of England and France. *Environmental Pollution, 203*, 214–225. https://doi.org/10.1016/j.envpol.2015.02.030

Murray KE, Thomas SM, Bodour AA (2010) Prioritizing research for trace pollutants and emerging contaminants in the freshwater environment. *Environmental Pollution, 158*(12): 3462–3471. https://doi.org/10.1016/j.envpol.2010.08.009

Schwab AP, Splichal PA, Banks MK (2006) Persistence of atrazine and alachlor in ground water aquifers and soil. *Water, Air, and Soil Pollution*. https://doi.org/10.1007/s11270-005-9037-2

Sui Q, Cao X, Lu S, Zhao W, Qiu Z, Yu G (2015, November) Occurrence, sources and fate of pharmaceuticals and personal care products in the groundwater: A review. *Emerging Contaminants*, 1, 14–24. https://doi.org/10.1016/j.emcon.2015.07.001

Assessment of Ingress Areas/Points in the Witwatersrand Basin using Environmental Isotopes as Tracers

Lufuno Ligavha-Mbelengwa[1], Lerato Mokitlane[1], Godfrey Madzivire[1,2], Humberto Saeze[1], Pamela Nolakana[1], Henk Coetzee[1]

[1]*Council for Geoscience, Water and Environment Unit, 280 Pretoria Street, Silverton, Pretoria, South Africa, lligavhambelengwa@geoscience.org.za*

[2]*University of South Africa, Department of Environmental Science, 28 Pioneer Ave, Roodepoort, South Africa*

Abstract

This study investigated the use of environmental isotopes as tracers to identify sources of water that enters mine voids. Water samples were collected from surface, boreholes and shafts. The findings indicated depleted $\delta^{18}O$ and $\delta^{2}H$ to be related to groundwater and shafts showing recharge by precipitation. Heavy isotopic signature is linked to surface water open to evaporation. Most groundwater and shafts displayed recent recharge by modern rainfall as deduced from tritium, although other sites gave no indication of recent recharge. Findings gave an indication that surface water ingress into the subsurface. Deduced main water types were Na-HCO_3, Mg-Cl-HCO_3 and Ca-Mg-SO_4.

Keywords: Groundwater, Water Interaction, Isotopes, Mine Water, Surface Water, Water Types

Introduction

Jasechko (2019) describes isotope hydrogeology as the measuring of stable or radioactive isotope compositions of river, spring and groundwater, then interpreting the isotopic measurements to quantify or conceptualise groundwater flow paths, velocities and biochemical. The most widely used isotopes in hydrogeology are of hydrogen (^{1}H, ^{2}H and ^{3}H), oxygen (^{16}O, ^{17}O and ^{18}O) and carbon (^{12}C, ^{13}C and ^{14}C). There are a number of uses of groundwater isotopes; among others is the identification of recharge areas and quantifying the recharge rates, which in turn can be used as input for water budget analysis. Isotopes can also be used for dating groundwater.

Stable isotopes of oxygen (^{16}O and ^{18}O) and hydrogen (^{1}H and ^{2}H or deuterium - D) are used to determine whether groundwater is derived from precipitation or local meteoric waters. Stable isotopes undergo fractionation, kinetic and equilibrium fractionation. Meteoric water lines (MWL) which are linear regressions describe the variations of $\delta^{18}O$ and $\delta^{2}H$. Global meteoric water lines (GMWLs) are widely used to describe $\delta^{18}O$ and $\delta^{2}H$ relationship; although at a regional scale a local meteoric water line (LMWL) can be used. The comparison of stable isotopes has been applied to identify whether aquifer systems are recharged by overlying water bodies. The similarities of the values between groundwater and that of the river water is indicative of the river replenishing the local aquifer.

Environmental tritium (^{3}H) is also widely applied as a useful tracer in the hydrological studies. It is a radioactive isotope that decays through low energy beta ray emission and has a half-life of 12.43 years (Abiye 2013). Tritium can be used to measure the age of groundwater regarded as modern groundwater. This is often encountered in shallow groundwater and are more likely to contain anthropogenic contaminants than older waters. The concentration of tritium in the rainwater varies with geographical location, however, these goes up to 5.0 tritium units (TU) (Abiye 2013).

This study assessed the use of environmental isotopes as tracers to map ingress areas in the Witwatersrand Goldfields. Piper diagrams were done to determine the water types from various sources. Stable and

radioactive isotopes were used to determine the origin of the water and to measure its age respectively.

Methods

Study area

The study was conducted in the Witwatersrand Goldfields, Eastern Basin as depicted by fig.1.

Sample collection and preparation

Water samples were collected from surface water bodies, boreholes and shafts for the analyses of stable (oxygen and hydrogen) and tritium isotopes and water chemistry. Prior collecting groundwater samples, boreholes were purged to remove the stagnant water in the borehole with the aim of introducing fresh water from the aquifer into the borehole for representative sample.

Stable and radioactive isotopes

A 1 L polyethylene bottle was filled at each sampling site and used to contain the collected sample for both stable (^{2}H and ^{18}O) and radioactive (^{3}H) analyses. Water analyses were done at the Environmental Isotope Laboratory (EIL) of iThemba LABS, Johannesburg.

The equipment used for stable isotope analysis consists of a Los Gatos Research (LGR) Liquid Water Isotope Analyser. Laboratory standards, calibrated against international reference materials, are analysed with each batch of samples. The analytical precision is estimated at 0.5‰ for O and 1.5‰ for H. Analytical results are presented in the common delta-notation:

$$\delta^{18}O(‰) = \left[\frac{(^{18}O/_{16}O)_{sample}}{(^{18}O/_{16}O)_{standard}} - 1\right] \times 100 \qquad 1$$

which applies to D/H ($^{2}H/^{1}H$), accordingly (Butler *et al* 2020). These delta values are expressed as per mil deviation relative to a known standard, in this case standard mean ocean water (SMOW) for $\delta^{18}O$ and δD (Eddy-Miller and Wheeler 2010).

The tritium samples were distilled and subsequently enriched by electrolysis. Samples of standard known tritium concentration are run in one cell of each batch to check on the

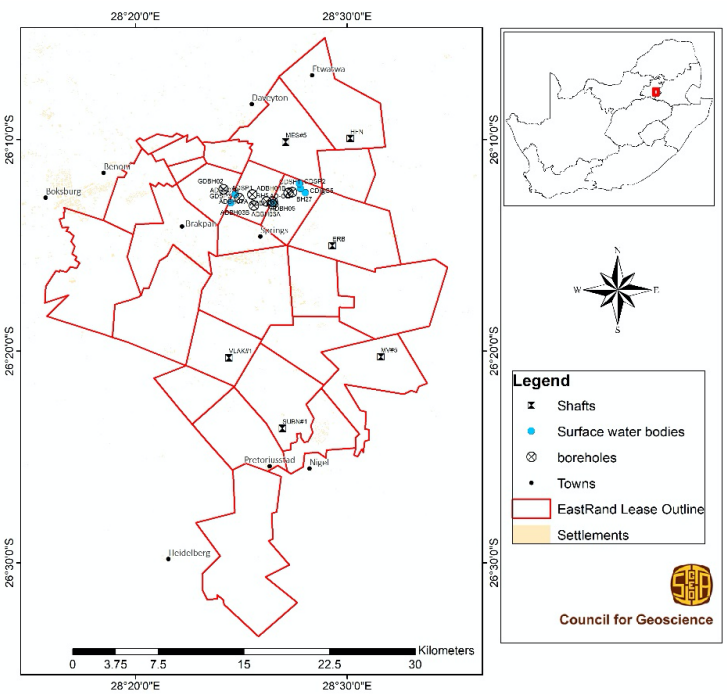

Figure 1 *Locality map displaying surface water, boreholes and shafts of the Eastern Basin.*

enrichment attained. Detection limits are 0.2 TU for enriched samples (Butler *et al* 2020).

Water chemistry

Samples to be analysed for metals/metalloids were preserved by adding 3 drops of concentrated HNO_3, whilst an unpreserved sample was collected for analyses of anions. Polyethylene bottles (100 mL and 250 mL) were used to store samples for metals/metalloids and anions analyses. These were then analysed using inductively coupled plasma mass spectrometry (ICP-MS) and ion chromatography (IC) respectively.

Data interpretation

Stable isotopes

Interpretation of the results that were obtained from the laboratory was done using the Global Meteoric Water Line (GMWL) developed by (Craig 1961) and the long-term measurements of precipitation at Pretoria station (1961-2018) from the International Atomic Energy Agency's Global Network of Isotopes in Precipitation (GNP) program as Local Meteoric Water Line (PMWL) using equation 2 and 3 respectively. The lines were then plotted on the meteoric water plot that displays ^{18}O on the x-axis, whilst ^{2}H plots on the y-axis. This data is then interpreted with reference to the MWL.

$$\delta D = 8 \times \delta^{18}O + 10 \quad (2)$$

$$\delta D = 6.7126 \times \delta^{18}O + 7.175 \quad (3)$$

Radioactive isotopes (^{3}H)

Tritium results are presented as tritium units (TU). South African rainwater has natural tritium of about 3.0 TU, thus determination of recharge by recent water can be done with reference to that of present-day rainfall. Zero tritium is an indication of low to no recharge, whilst measurable tritium will indicate recharge in that particular source (Abiye 2013).

Hydrogeochemical analysis

Results were processed using AquaChem 3.70 and are interpreted using Piper diagrams where various water types are categorised.

Results and discussion

Water types

Chemistry data was plotted on the Piper diagram (fig.2) to determine various water types in the area. The findings from these assisted in the selection of sites to be analysed

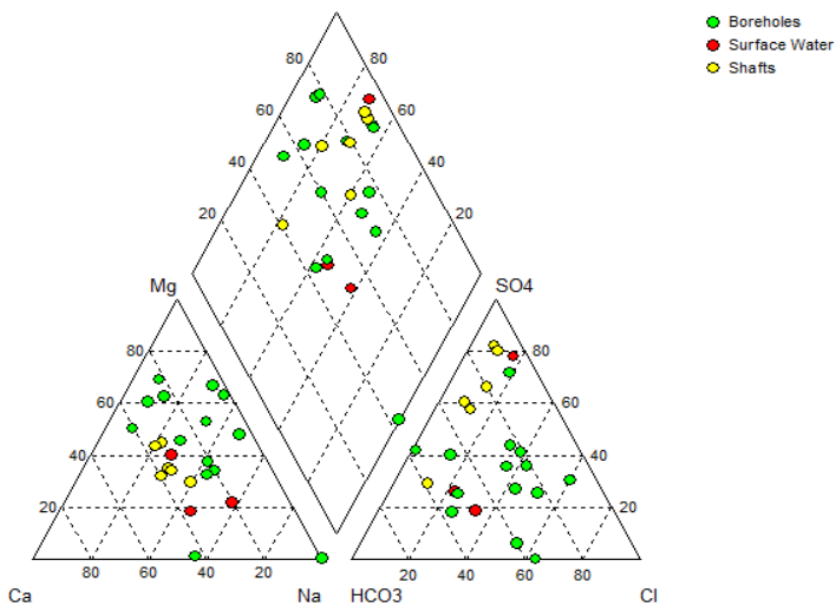

Figure 2 *Piper diagram displaying sampled sites.*

for isotopic composition, especially for sites that are situated in the same vicinity.

Application of hydrochemistry simultaneously as other tracer methods may give an indication of surface water-groundwater interaction. The diagram (fig.2) was plotted using surface, boreholes and shaft water samples. The water types that were deduced from the Piper plot are Na-HCO_3, Mg-Cl-HCO_3, Na-SO_4, Mg-HCO_3, Ca-Mg-SO_4 and mixed type (no dominant ions). In the cation triangle, water from the boreholes show a trend from a more Mg-rich content, presumably due to interaction with the dolomitic aquifer in the area, to a mixed water and to Na-rich (Mg-Cl-HCO_3, Mg-SO_4, Mg-HCO_3, Na-HCO_3 types). In the anion triangle, the trend is from HCO_3-rich content, to Cl and SO_4-rich water.

Shafts display a Ca-Mg-SO_4 water type, except for HFN that displays water that is mostly enriched in HCO_3. Surface and borehole water from CDSP2 and ADBH03A respectively, matches that of shafts with high dominance in Mg and SO_4. ADBH03A has a water signature that differs from that of other boreholes in the same vicinity. CDSP1 on the one hand plots with borehole BH8 and BH32 in the same vicinity. Furthermore, surface water ADSP1 plotted along with ADBH01A, ADBH07A, GDB02 at close proximity as well as shaft HFN, all displaying a more Na-HCO_3/Na-SO_4 water type. The Na-HCO_3 is dominant in surface water and borehole BH8, BH15 and BH32. All the boreholes around Cowles Dam proximity except BH32, BH1, BH15 and BH19 displayed Mg-Cl-SO_4/HCO_3 water type. The variation could be due to water-rock interaction leading to mineral dissolution and water quality evolution. Some boreholes showed water with high concentrations of Na than Ca and vise versa giving an indication of ion exchange.

Deductions from the water types indicate that the Eastern Basin mine voids (shafts) water represents a mixture of water from various sources, with geological influence on the water chemistry.

Meteoric water plots

All surface water samples plotted along the evaporation zone because they are exposed to the atmosphere displaying enrichment in $\delta^{18}O$ and $\delta^{2}H$ isotopes.

Shafts SUBN#1, ERB and MV#5 also plotted along the evaporation line. All these shafts are situated in the southern part of the study site and could be receiving recharge from both precipitation and surface evaporated water (fig.3 and fig.4), indicating the possibility of surface water ingress into the subsurface. All the shafts that are situated

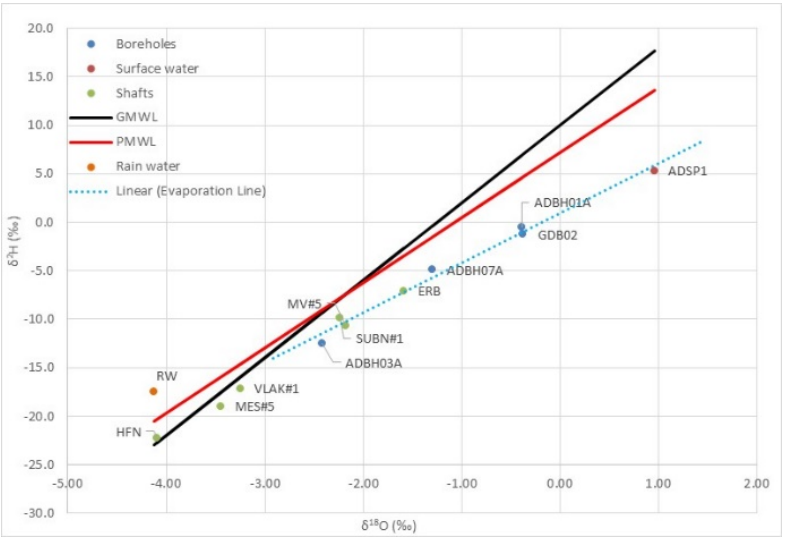

Figure 3 *Meteoric water plot for surface water, boreholes (Alexander Dam) and shafts.*

in the north of Blesbokspruit (MES#5 and HFN) plotted along the meteoric water line showing a possibility of recharge by surface or groundwater that was not prone to evaporation (depletion in $\delta^{18}O$ and $\delta^{2}H$ isotopes). Thus, these shafts might not be linked to surface water bodies that were sampled in this study since they all plotted along the evaporation line.

The meteoric water plot shows groundwater around Alexander Dam plotting along the evaporation line together with shafts SUBN#1, MV#5 and ERB and surface water ADSP1 (fig.3). These sites may be receiving their water from precipitation and evaporated water. Unlike the rest of the boreholes water, ADBH03A is more depleted in $\delta^{18}O$ and $\delta^{2}H$ isotopes.

All surface water (CDSP1 and CDSP2) plot along the evaporation line (fig.4), although CDSP1 is more enriched in $\delta^{18}O$ and $\delta^{2}H$. This could be because of the distance this water travels from CDSP2 where it becomes prone to evaporation. CDSP1 and CDSP2 further plots close to BH32 and BH33 respectively. CDSP2 could be receiving recharge from both surface and groundwater. Whereas, BH33 and BH32 could be receiving recharge from water that underwent a high degree of evaporation as opposed to water from precipitation. BH1, BH27, BH4, BH15, BH19 and BH18 (fig.4) show recharge by precipitation or water that did not undergo long period of evaporation and plots along the meteoric water line. These sites are situated in the same vicinity.

Tritium dating

Tritium was measured in TU with the water signatures ranging between 0.2 – 5.2 TU. According to Murray *et al* (2015), this is an indication of old water (<1.0 TU) that was recharged before 1960, recent water (1.0 – 4.0 TU) and possibly waste contaminated water (>4.0 TU). It is explained that South African rain water have a natural tritium concentration of about 3 TU, as also observed on the acquired tritium results in tab.1 (rainwater sample). Almost all the water sampled from surface, boreholes and shaft appeared to be of recent recharge period because of tritium content that matches one of present-day rainfall. Measurable tritium concentration in these sites gives an indication of surface water-groundwater interaction confirming the ingress of surface water to groundwater and mine voids. However, other sites displayed tritium concentration of less than 1.0 TU. These are shafts MES#5 and HFN and groundwater from ADBH03A, BH33, BH19, BH4 and BH18. Lastly, surface water from CDSP1 displayed tritium amount of 5.2 TU.

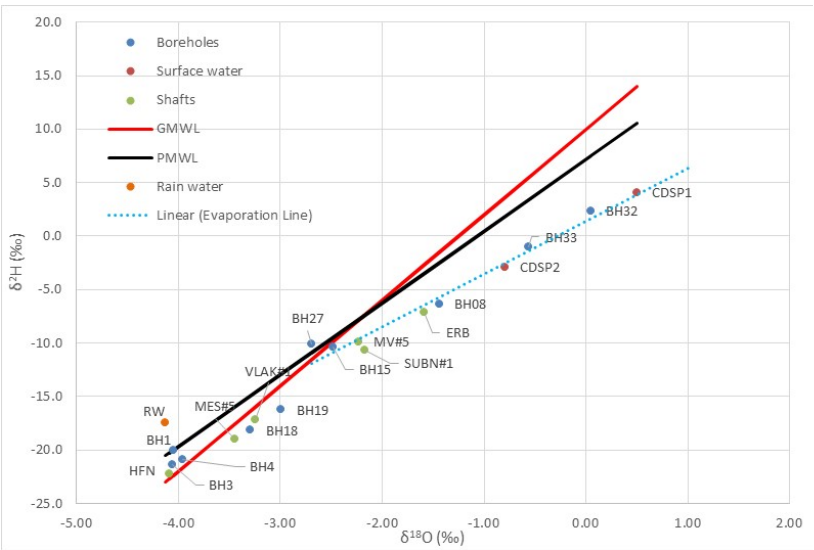

Figure 4 *Meteoric water plot for surface water, boreholes (Cowles Dam) and shafts.*

Table 1 Tritium results for surface water, groundwater, shafts and rainwater in the Eastern Basin.

Sample ID	Tritium (T.U.)			Sample ID	Tritium (T.U.)		
ERB	1.0	±	0.3	BH33	0.7	±	0.3
VLAK#1	1.3	±	0.3	BH27	1.8	±	0.3
MES#5	0.9	±	0.3	BH32	1.1	±	0.3
HFN	0.2	±	0.2	BH08	3.2	±	0.4
SUBN#1	2.0	±	0.3	BH19	0.9	±	0.3
MV#5	1.5	±	0.3	BH3	1.2	±	0.3
ADSP1	2.4	±	0.4	BH1	1.1	±	0.3
CDSP1	5.2	±	0.4	BH4	0.7	±	0.3
CDSP2	1.9	±	0.3	BH18	0.3	±	0.3
ADBH07A	2.5	±	0.3	BH15	2.6	±	0.4
ADBH01A	2.9	±	0.3	GDB02	2.9	±	0.4
ADBH03A	0.7	±	0.3	Rain Water	3.3	±	0.4

Conclusions

Water types as deduced from the Piper plot are; Na-HCO_3, Mg-Cl-HCO_3, Na-SO_4, Mg-HCO_3 and Ca-Mg-SO_4. The findings indicated that groundwater displayed Na-SO_4 and Mg-Cl-SO_4/HCO_3 water types, whereas mine voids water showed Ca-Mg-SO_4 water type. The water compositions are assumed to be influenced by both geological and anthropogenic activities.

The application of environmental isotopes is useful in tracing the source and pathway of the water. Further, to measure the age of modern water. The application of environmental isotopes in this study gave an indication that surface water ingress the subsurface. This was experimented at Alexander and Cowles Dam where groundwater and shafts were showing recharge by meteoric water and water that has undergone evaporation. Additionally, as obtained from tritium results, most shafts and groundwater appeared to be receiving modern recharge with reference to the modern rainfall in South Africa.

However, shafts MES#5 and HFN that displayed different water type and plotted along the meteoric water line apart from other shafts displayed tritium concentration of less than 1.0 TU, which is an indication of old water in these sites. Moreover, most boreholes that plotted along the meteoric water line also displayed water of less than 1.0 TU.

Acknowledgements

The authors would like to send their sincere appreciation to the Department of Mineral Resources and Energy (DMRE) for funding this project. Many thanks goes to the Mine Environment and Water Programme team members, especially those that contributed to this task.

References

Abiye T (2013) The use of isotope hydrology to characterize and assess water resources in South(ern) Africa, WRC Project No. K5/1907.

Butler MJ, Malinga OHT, Mabitsela M (2020) Environmental isotope analysis on water samples. Laboratory report, reference CGS023.

Craig H (1961) Isotopic Variations in Meteoric Waters D STOR ®. In *New Series* (Vol. 133). Retrieved from http:Jninks.jstor.org/sici?sici=0036-8075%2819610526%293%3A133%3A3465%3C1702%3AIVIMW%3E2.0.C0%3B2-J

Eddy-Miller CA, Wheeler JD (2010) *Data Series 518 Chloride Concentrations and Stable Isotopes of Hydrogen and Oxygen in Surface Water and Groundwater in and near Fish Creek, Teton County, Wyoming, 2005-06.*

Jasechko S (2019) Global Isotope Hydrogeology–Review. *Reviews of Geophysics, 57*(3), 835–965. https://doi.org/10.1029/2018RG000627

Murray R, Swana K, Miller J, Talma S, Tredoux G, Vengosh A, Darrah T (2015) The use of Chemistry, Isotopes and Gases as Indicators of Deeper Circulating Groundwater in the Main Karoo Basin, WRC Report No. 2254/1/15.

Groundwater Source Determination of an Underground Diamond Mine Utilizing Water Chemistry and Stable Isotope Analysis

Paul Lourens[1], Adriaan Pretorius[1], Danie Vermeulen[2]

[1]*Institute for Groundwater Studies, Faculty of Natural and Agricultural Sciences, University of the Free State, 205 Nelson Mandela Drive, Bloemfontein, 9300, South Africa, lourenspjh@ufs.ac.za,*

[2]*Faculty of Natural and Agricultural Sciences, University of the Free State, 205 Nelson Mandela Drive, Bloemfontein, 9300, South Africa, vermeulend@ufs.ac.za*

Abstract

An underground diamond mine historically experienced periodic groundwater inflow into the underground workings of the mine, resulting in unsafe working conditions. A conceptual model was developed to better the understanding of the groundwater situation at the mine. Water samples were collected at various points. The samples were analysed for major and minor chemical constituents and the stable isotopes of hydrogen and oxygen. Three sources of groundwater inflow into the mine workings were identified. The investigation illustrates that water chemistry signatures and stable isotope signatures can successfully identify different sources of water that flows into the workings of an underground mine.

Keywords: Groundwater, Inflow, Source, Chemistry, Stable Isotopes

Introduction

The Institute for Groundwater Studies at the University of the Free State was appointed by a mining company to investigate the source/s of groundwater inflow into the underground mine workings. Periodic groundwater inflow into the underground workings result in unsafe and undesirable working conditions.

Diamond (ore) extraction was initially from the open pit and later transitioned into underground mining (block cave method). The current depth of mining ranges between 700 and 800 m below surface. The layout of the mine is presented on the map shown in Figure 1.

Materials and methods

Desktop Study

The desktop study involved the examination of available data, aerial-and satellite maps to better understand the area of investigation and to construct a conceptual model of the area. Additional information acquired from the mining company for the desktop study included, groundwater monitoring data (quantity & quality), geological maps, rainfall data, mine layout plans and previous investigations.

Water Sample Collection

Water samples were collected over a three-month period, which include various points in the underground mine workings, existing groundwater monitoring boreholes and surficial water bodies. The samples were analysed for major and minor chemical constituents (tab. 1) and the stable isotopes of hydrogen (2H & 1H) and oxygen (18O & 16O).

Data Presentation and Interpretation

The chemistry data was graphically interpreted using Piper and Stiff diagrams to identify different water types and waters from different environments. Thus, waters with the same chemical signatures can be grouped together.

Piper diagrams are trilinear representations of cation, anion, and combined cation and anion proportions (Eby 2004), whereas Stiff diagrams show the concentrations of the major cations and anions in milli-equivalents as a shape that

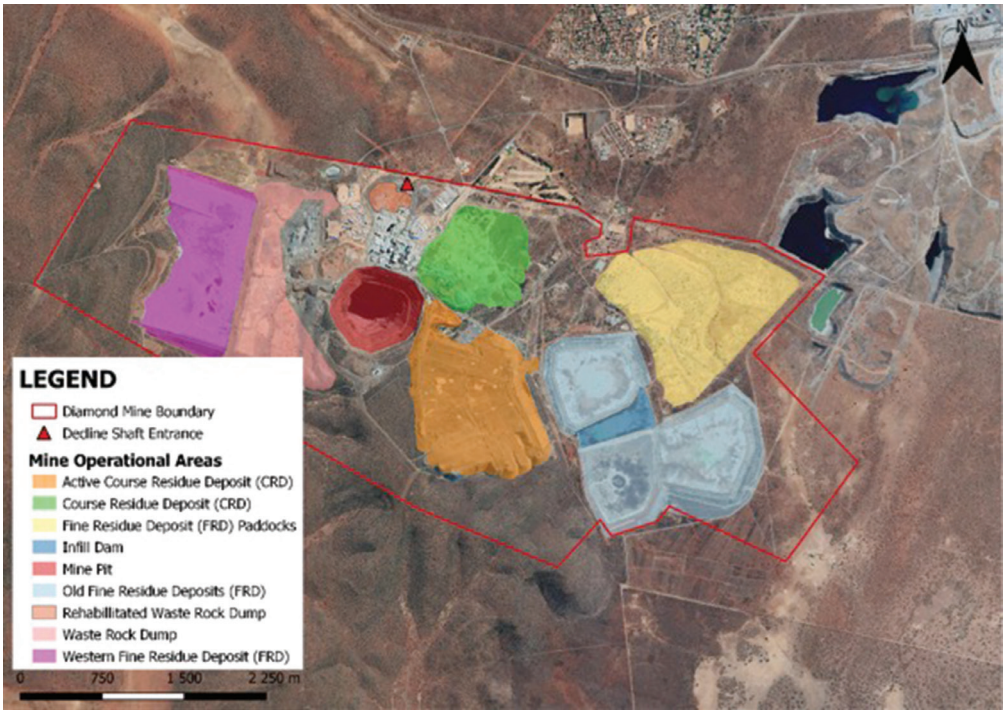

Figure 1 *Mine layout map.*

gives both the relative abundance of the various species and the total abundance (Eby 2004).

The atomic ratios of the hydrogen and oxygen isotope was plotted against the Global Meteoric Water Line (GMWL). Oxygen ($^{18}O/^{16}O$) and hydrogen ($^{2}H/^{1}H$) are constituents of water molecules and can act as conservative tracers and therefore mainly applied in geohydrology to determine the source and mixing of groundwater (Mook and Geyh 2000). The natural atomic ratios are expressed as delta values ($\delta^{18}O$ & $\delta^{2}H$). Most groundwater resources are of meteoric origin and therefor the strong relationship between the $\delta^{18}O$ and $\delta^{2}H$ values of precipitation in the Meteoric Water Line (MWL) (Mook and Geyh 2000).

Site Description

Topography and Rainfall

The regional surface elevation ranges between 1406 mamsl and 1694 mamsl. The mining area of the diamond mine is situated on a topographic high, thus the surface elevation slopes mostly away from the mine. The topographic low of the mining and the lime mining quarries of the neighbouring lime mine (northeast of the diamond mine) are clearly visible on the surface elevation map shown in Figure 2.

The annual rainfall (MAP) between 1967 and 2020 is 388.8 mm. The area received three exceptional high rainfall events over the past 53 years. These rains were received over the summer seasons of 1975, 1988 and 2012.

Table 1 *Major and minor chemical constituents analysed.*

Major and Minor Chemical Constituents
EC, pH, Alkalinity, Ca, K, Mg, Na, Br, Cl, F, NO_3(N), NO_2(N), PO_4, SO_4, Al, As, B, Ba, Cd, Co, Cr (Total), Cu, Fe (Total), Hg, Mn, Mo, Ni, Pb, Sb, Se, Si, Sr, U, V, Zn

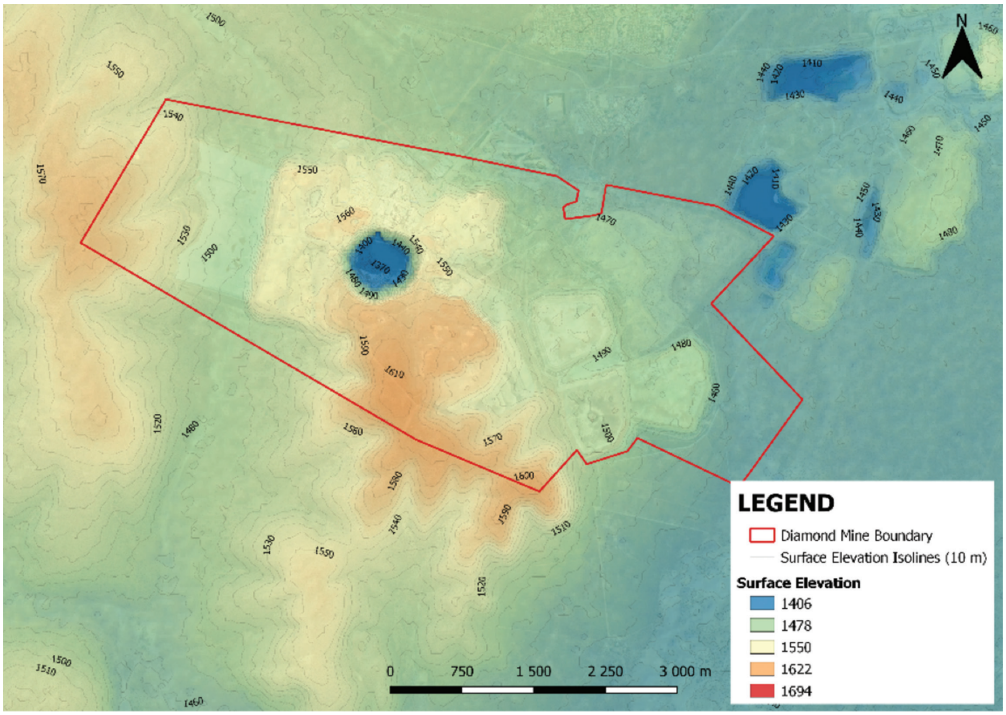

Figure 2 *Surface elevation (mamsl) map.*

The Mean Annual Evaporation (MAE) for the area ranges between 2200 and 2600 mm and the mean annual runoff (MAR) is 8 mm (Midgley *et al*. 1994).

Geology

The diamond mine consists of an 17.9 ha, 118±2.8 Ma old kimberlite pipe (Smith *et al*. 1985) which intruded through a thick sequence of Proterozoic, Griqualand West sequence of sedimentary rocks comprising of dolomites, banded iron formation and shales. There is numerous lineaments of different strike orientations, which represent structural discontinuities, such as faults and fracture zones, and are variably intruded by dykes of different composition and age (fig. 3). The area have the following primary sets off faults and fracture zones:

- NNW-SSE to N-S striking major fault zones
- NE-SW to ENE-WSW striking fault/ fracture zones, commonly intruded by kimberlite precursor dykes
- WNW-ESE striking fault/fracture zones

Hydrogeology

The groundwater of the area constitutes a shallow aquifer within the weathered zone and a deeper aquifer in the fractured and karstic dolomites. The hydrogeological setting consists of partly karstic dolomites and complex zones with linear structures which create a highly interconnected fracture network. The aquifer is further compartmentalised by various dykes which impact on the groundwater regime. These structures act as conduits allowing rainfall to recharge the deeper fractured aquifer network. According to Friese and Terbrugge (2003) karst and fissure formation within the carbonaceous rocks of the Campbellrand Subgroup have been known to develop along structural discontinuities. Faults and dykes can act as either barriers of conduits to groundwater flow, and they often act as both depending on the degree of fracturing and infilling.

Dolomites are subject to solution weathering by percolating water which forms a weak carbonic acid that slowly dissolves the dolomites from the sides of

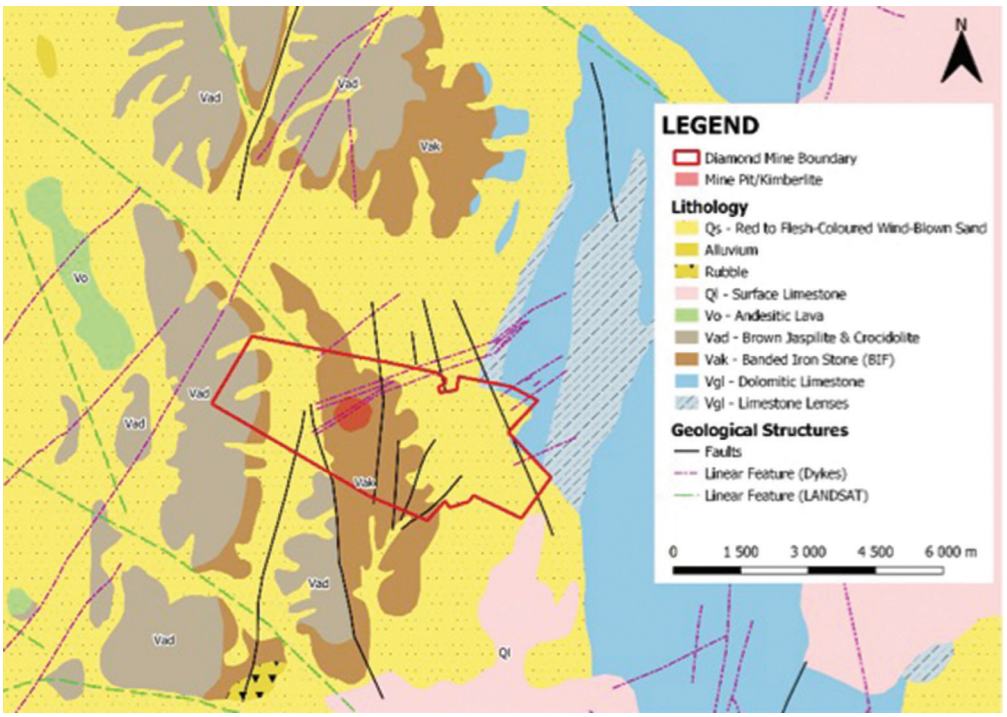

Figure 3 Regional geology map.

geological structures. Dolomite aquifers thus consist of a series of solution cavities. Banded ironstones contain voids created by fracture networks in the ironstones. Groundwater flow is controlled by the width, extent and the degree of interconnectedness of the fractures.

Results and Discussion

The water quality results are plotted on the Piper Diagram in Figure 4. Three water types can be identified from the Piper Diagram, namely:

- Type 1: Calcium-Magnesium-Bicarbonate type – observed for boreholes and underground sampling points
- Type 2: Calcium-Magnesium-Sulfate type – observed for boreholes, surface water bodies and underground sampling points
- Type 3: Sodium-Sulfate type – observed for surface water bodies and underground sampling points

The stable isotope results are represented in Figure 5, showing the results of δ18O versus δ2H relative to the Global Meteoric Water Line (Craig 1961). Three groups can be identified:

- Group 1: Water samples which correspond well with the GMWL, thus indicating water of meteoric origin
- Group 2: Water samples which do not correspond well with the GMWL but fall along a mixing line with water of an evaporated signature
- Group 3: Water samples which do no correspond with the GMWL but fall along the defined evaporation line

The evaporative signatures of the sampling points on 63 Level and the boreholes suggest that these sampling locations receives water inflow from surface water sources. The water quality of sampling point 63/34 on 63 Level is similar to that of the Western FRD (fig. 6). The similar water qualities and the similar isotope signature of the Western FRD and the sampling point 63/34 suggest that seepage from the Western FRD is entering the mine workings on 63 Level.

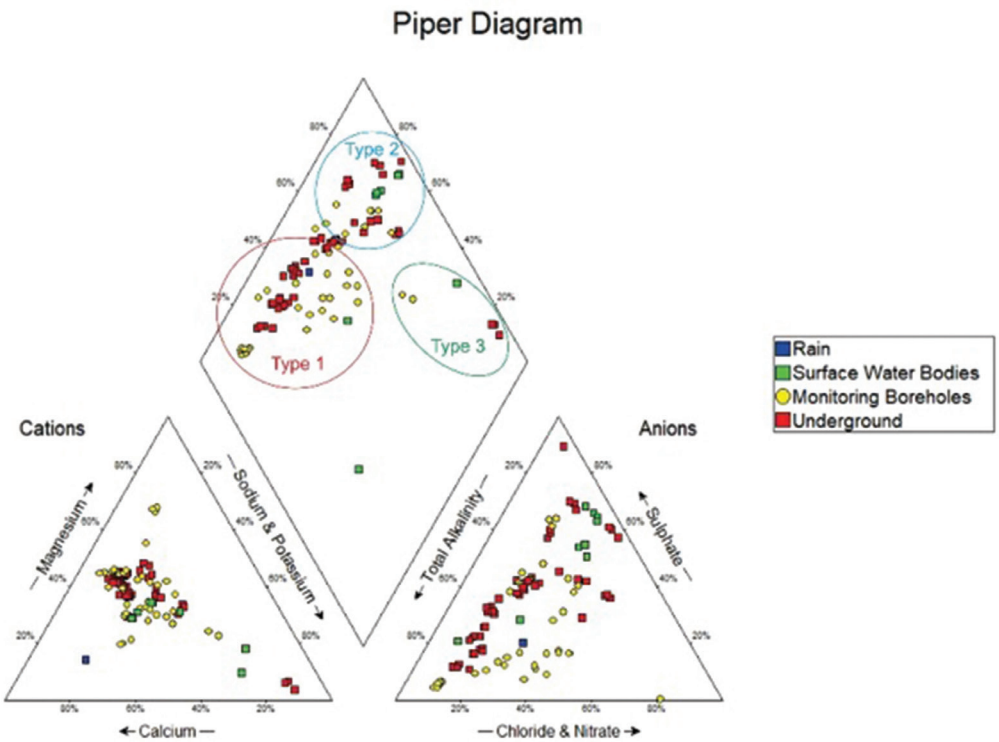

Figure 4 Piper diagram of the samples collected.

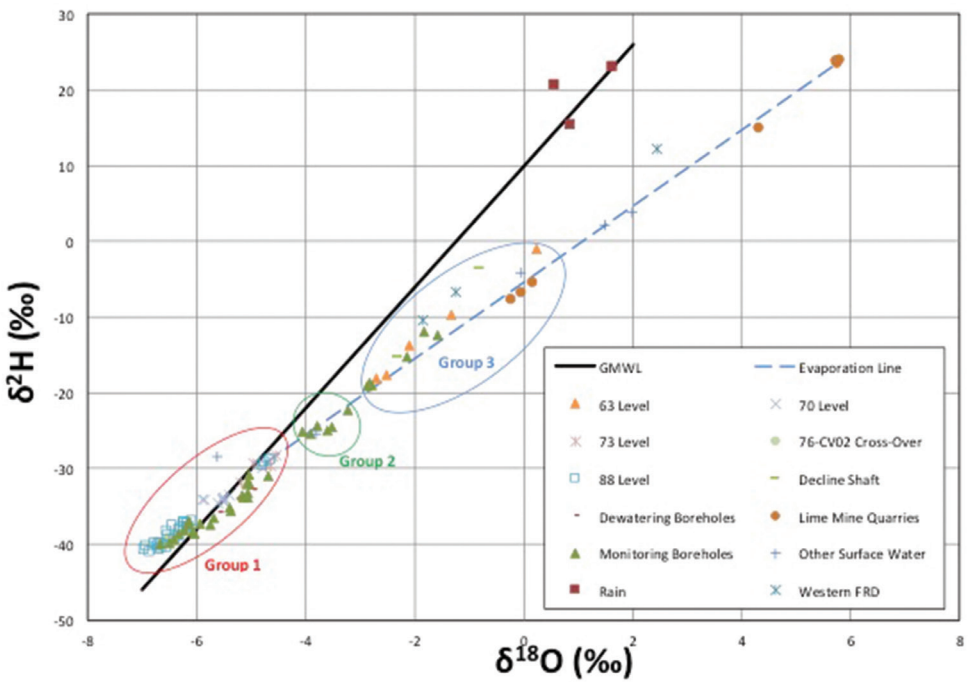

Figure 5 Plot of stable isotope $\delta^{18}O$ versus $\delta^{2}H$ relative to the global meteoric water line (GMWL).

The evaporative signatures of the sampling points in the decline shaft suggest that these sampling locations receive water inflow from surface water sources. The Decline Set-1 and Decline Set-2 sampling locations are situated approximately 75 m below ground level of an old waste rock dump that have been rehabilitated. There are areas on the old waste rock dump that is irrigated on a regular basis. The water quality of the samples collected in the decline shaft are similar to that of the Active CRD (fig. 6). Therefore, the calcium-magnesium-sulphate water signature and the evaporative signature of the decline shaft suggest that it is plausible that seepage from the irrigation activities on the rehabilitated waste rock dump enters the decline shaft at the two sampling locations. The calcium-magnesium-sulphate signature is probably the result of the irrigation water that interacts with the waste rock dump as it infiltrates the subsurface.

The underground water sampling points on 70 Level, 76-CV02 Cross-over and 88 Level mainly indicates waters with a calcium-magnesium-bicarbonate signature and the isotope signatures plots on the GMWL, thus suggesting water with a meteoric origin, in this case, groundwater from the dolomitic aquifer.

Conclusions

The investigation illustrates that water chemistry signatures and stable isotope signatures can successfully identify different sources of water that flows into the workings of an underground mine. The identified water sources includes the following:

- The similar water qualities and the similar isotope signature of the Western FRD and the sampling point 63/34 suggest that seepage from the Western FRD enters the mine workings on Level 63.
- The calcium-magnesium-sulphate water signature and the evaporative signature of the decline shaft suggest that it is plausible that seepage from the irrigation activities on the old rehabilitated waste rock dump enters the decline shaft.
- The water quality and isotopic signature of the underground water sampling points on 70 Level, 76-CV02 Cross-over and 88 Level mainly indicates waters originating from the dolomitic aquifer. The faults and shear zones striking NNW to SSE acts as preferential flow paths for the dolomitic water to enter the mine workings on 88 Level.

Based upon the hydrogeological, hydrochemical and stable isotope data a conceptual model was constructed (fig. 7). It is conceptualised that water from the Western-FRD infiltrates and mixes with the shallow groundwater in the banded ironstone and Passage Beds and is further transported east toward the mine pit where it infiltrates into the underground mine workings on 63 Level. The faults and shear zones striking NNW to SSE acts as preferential flow paths for the dolomitic water to enter the mine workings on 88 Level.

References

Craig H (1961) Isotopic Variations in Meteoric Waters. Science 133(3465): 1702-1703, doi: 10.1126/science.133.3465.1702

Eby GN 2004 Principles of Environmental Geochemistry. California: Brooks/Cole-Thomson Learning

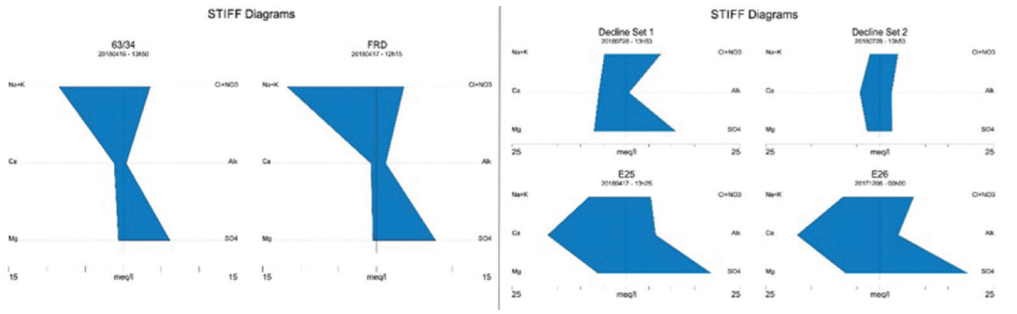

Figure 6 *Stiff Diagrams of the Western-FRD versus 63 Level (left-hand side diagrams) and the Active-CRD versus the decline shaft (right-hand side diagrams).*

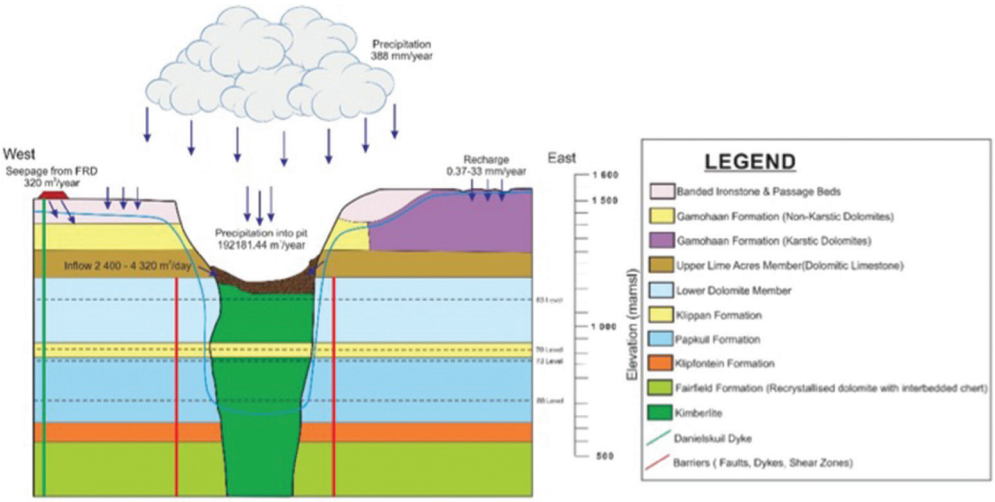

Figure 7 *Conceptual geohydrological model.*

Friese AEW, Terbrugge PJ (2003) The Influence of Block 5 Mining on Existing Surface Infrastructure, SRK Consulting. Unpublished Report

Midgley DC, Pitman WV, Middleton BJ (1994) Surface Water Resources of South Africa 1990, Water Research Commission. WRC Report No 298/1/94

Mook WG, Geyh M (2000) Environmental isotopes in the hydrological cycle, principles and applications. Volume IV: Groundwater. IHP-V, Tech Doc 39:196

Smith CB, Allsopp HL, Kramers JD, *et al* (1985) Emplacement ages of Jurassic-Cretaceous South African kimberlites by the Rb-Sr method on phlogopite and whole-rock samples. Trans Geol Soc South Africa 88: 249-266

Can Saline Pit Lakes Offer Biodiversity Values at Closure?

Mark A. Lund, Melanie L. Blanchette

Mine Water and Environment Research Centre, Edith Cowan University, 270 Joondalup Drive, Joondalup, WA 6027, Australia, m.lund@ecu.edu.au

Abstract

Saline pit lakes are considered to have few prospects upon closure. However, naturally occurring saline lakes may have outstanding biodiversity values. Therefore, we assessed the limnology and biodiversity of four saline pit lakes (≈3.2-10.5 mS cm^{-1}) from Australia's main coal-producing regions. Nutrients, metals, metalloids and major ions were collected as well as physico-chemical profiles throughout the water column. 'Biodiversity values' of lakes were determined via macroinvertebrate, diatom, and plankton assemblages. Lakes were stratified by temperature but not salinity. Salinity did not appear to drive (nor limit) biodiversity in lakes, and relatively neutral pH indicated opportunity to improve existing biodiversity through rehabilitation. We also discuss the risks and opportunities of using saline pit lakes as ecosystems at closure in this brief presentation.

Keywords: Saline Lake, Hunter Valley, Bowen Basin, Mine Rehabilitation, ANZECC/ ARMCANZ

Introduction

Open-cut mining operations create an environmental legacy of large pits throughout the landscape. Many of these open pits are too large or expensive to fill and typically require extensive dewatering operations. Therefore, many of these pits are destined to become large, deep pit lakes. Annual evaporation generally exceeds precipitation in subtropical deserts and semi-desert regions around the Tropics of Cancer and Capricorn. Major mining activities occur within these regions. High evaporation rates within these regions make many pit lakes terminal hydrological sinks. Pit lakes that are terminal sinks are generally predicted via modelling to have increasing salinities over time through evapoconcentration. This salinity may be derived from naturally saline groundwater or surface inflows mobilising salts from overburden, intensified by evapo-concentration.

Australia has a broad range of naturally saline and hyper saline water bodies with unique ecosystems (Timms 2018). We suggest that while high salinity may limit pit lake future uses, saline pit lakes are not necessarily without demonstrable ecological value. Saline mine-pit lakes are unique because they are typically much deeper and may occur in geographical areas that do not naturally have lakes. Unlike naturally occurring saline lakes, little research has been done on the water quality and ecology of saline pit lakes. Further, little is known about rehabilitation of saline pit lakes because most of the research focus worldwide has been devoted to treating acidic pit lakes with high concentrations of metals.

Closure of mines containing pit lakes is problematic because pit lakes are not widely accepted by regulators as a closure option, although this is changing. Therefore, guidance on completion criteria for pit lakes is lacking. Pit lakes may present risks to the wider catchment if they have poor water quality (McCullough and Lund 2006). High salinities are often seen as poor water quality and therefore limits on release of waters from the pit lakes is common, further allowing salinities within the lakes to increase.

Ecological values are the desired measurable attributes of an ecosystem. Measures of community diversity, species abundance, or even the gross attributes of the system itself such as morphology and geographical connectivity could be considered 'ecological values' (Margules and Pressey 2000). There are a range of factors that limit the establishment of

ecological values in pit lakes, such as hydrology and bathymetry, as well as nutrient limitation and poor bankside vegetation development (Lund and McCullough 2011).One of the rare published ecological studies on saline pit lakes examined macroinvertebrates in a series of Queensland pit lakes (Proctor and Grigg 2006). The authors found that although naturally co-occurring water bodies had significantly higher macroinvertebrate species diversity than pit lakes, some of the older and less saline pit lakes were "almost as rich in families" (Proctor and Grigg 2006). This research indicates that saline pit lakes can develop ecosystem values although the body of research is extremely limited.

Biodiversity in pit lakes is typically low, however this appears to be due to limited resources rather than directly due to pH or metal toxicity. Pit lakes that are circumneutral tend to have macroinvertebrate diversity and abundance similar to those found in natural lakes (McCullough and Lund 2008; Proctor and Grigg 2006), although limitations in food and habitat can still curtail development (McCullough *et al*. 2009).

Here we briefly report on a year-long study of the ecology and water quality of pit lakes in the major coal mining regions of Australia in New South Wales and Queensland, across a gradient of salinities and mine water uses. We observed the drivers of algal, zooplankton, diatom and macroinvertebrate communities as indicators of biodiversity values in saline pit lakes.

Methods

Study area

Four pit lakes from Australian former coal mines were selected for this study, two (HL1, HL2) from the Hunter Basin (21,500 km^2) in New South Wales, and two (BL1, BL2) from the Bowen Basin (60,000 km^2) in Queensland (Figure 1)(see Blanchette and Lund 2021, for photos and more research). The Hunter Basin is in Köppen climate type Cfa (humid subtropical, mild with no true dry season and hot summers), with rains typically occurring during summer (Peel *et al*. 2007). The Bowen Basin is within Koppen climate type BSa (arid steppe, with hot summer) with predominantly summer rainfall (Peel *et al*. 2007).

Three of the lakes (HL1, BL1, BL2) had no form of rehabilitation at the time of sampling in 2019, and HL2 was a shallow lake (<5 m), that had been rehabilitated although riparian zone vegetation was largely absent. HL1 was actively used for water storage and the other lakes used occasionally for water management. HL1 was approximately 20 years old at the time of sampling, BL1 was 10 years old and BL2 was still filling.

Instrument chains

An instrument chain was installed in three of the lakes (HL1, BL1 and BL2) for the duration of 2019 (beyond the quarterly sampling timeframe) to investigate stratification in the lakes. Chains were installed in all lakes except HL2, as it was <5 m deep and was therefore

Figure 1 *Morphological diversity extremes of Australian saline pit lakes in study: deep lake, no rehabilitation - HL1 (left), shallow lake, some rehabilitation - HL2 (right).*

unlikely to stratify for substantial periods. The chains were described in Blanchette and Lund (2021).

Water quality measurements

The lakes were sampled quarterly (February, May, August and December (not sampled at HL2)) in 2019 at three sites approximately equidistant across each lake which included the deepest location. On each occasion, an *in situ* physico-chemical profile was collected through the entire water column using a Hydrolab Datasonde DS5 multiparameter instrument (Hach, Austin, USA). Water column profile data were: temperature, pH, dissolved oxygen (mg L^{-1} and % saturation; luminescent), electrical conductivity standardized at 25 °C (EC) and oxidation-reduction potential (ORP, platinum electrode).

Water samples were collected at each site on each occasion for metal/metalloid and nutrient analysis at the surface and bottom (max. 20 m). Bottom samples were collected using a 12 V bilge pump (2088-732-244, Shurflo, Cypress, USA) and a 20 m weighted hose or in HL2 using a Teflon Kemmerer bottle. Water samples were processed in the field and lab according to Blanchette *et al.* (2019). On each occasion, samples from the three sites were composited into a single sample for analysis. An unfiltered aliquot was frozen (-12 °C) for later determination of total N and total P. Another aliquot was filtered (0.5 µm Metrigard GF, Pall, USA) and then frozen (-12 °C) for later determination of Cl^- using ion chromatography (Methrohm, Switzerland), nitrate/nitrite (NOx-N), filterable reactive phosphorous (FRP-P) and ammonia (NH_3-N) on a Lachat autoanalyser (Hach, USA), and DOC (measured as non-purgeable organic C) using a total carbon analyser (Shimadzu, Japan). A second filtered aliquot was acidified with nitric acid to pH <2 then stored at 4 °C for determination of select metals/metalloids and S by ICP-AES/MS. All methods were as per APHA (2017) and were conducted at the Edith Cowan University Analytical Chemistry Facility.

Biota collection

At each site (n=3 per lake) a surface water sample was collected for phytoplankton (*ca.* 0.2 m deep) and treated with Lugol's solution. Phytoplankton were counted and identified to genus level by ALS Ltd. Zooplankton were collected at each site via a vertical tow using an 80-µm mesh (0.2 m dia.) zooplankton net at HL2 or using the bilge pump at the other sites to collect water (≈10 L) from the entire water column to 20 m deep, filtering through the same 80-µm mesh (0.2 m dia.) net. The sample was preserved in >50% ethanol and then species were identified and counted by Australian Waterlife Ltd.

At three approximately equidistant sites around each lake's edge (where safe) macroinvertebrates were collected from a 1 × 0.5 m area parallel to the shore using a 250-µm mesh dip net (triangular (0.3 m sides)). The net was passed vigorously throughout the water column and bounced against the sediment for 20 s. Samples were preserved in >50% ethanol before sorting, identification (to Family) and abundance counts. Identifications were based on Gooderham and Tsyrlin (2002).

At macroinvertebrate collection sites, approximately 50 ml of surface sediment (<20 mm deep) was collected for diatoms within 0.5 m distance of the shoreline. A small amount of ethanol was added to each sample to prevent decomposition. Diatoms were counted and identified to species (where possible) by Dr John Tibby, University of Adelaide.

Results and Discussion

Lakes with instrument chain data demonstrated thermal stratification; HL1 was stratified from October to March and mixed during the rest of the year, BL1 and BL2 were stratified during September to March, briefly mixed and then was weakly stratified until September (see Blanchette and Lund 2021, for details). Large rainfall events (≈100 mm per day) at the Bowen Basin sites resulted in mixing in BL2, however in BL1 while hypolimnion temperature increased following the same rainfall even the lake did not mix until surface temperatures matched the warmer hypolimnion.

Salinity in pit lakes ranged from a low of EC ≈3200 µS cm^{-1} in HL1, to ≈3500 µS cm^{-1} in BL2, ≈6400 µS cm^{-1} at HL2 and ≈10,500 µS cm^{-1} at BL1. There were small differences in conductivity according to lake depth which

likely interacted with thermal stratification and mixing processes (especially during the high rainfall events). However, these small differences in conductivity with depth did not result in a true halocline (data not shown). Stratification resulted in hypoxia in the bottom waters of HL1, and BL1 (the deepest lake at 32 m) demonstrated a reduction in dissolved oxygen concentrations to ≈70% saturation.

In order to investigate pit lakes as ecosystems at closure, water quality results were compared to the ANZECC/ARMCANZ (2018) trigger values for 95% protection of aquatic ecosystems (Table 1) which are typical of most natural aquatic systems in good condition. Guideline values for nutrients were as per 'freshwater South East Lakes and Reservoirs' in ANZECC/ARMCANZ (2018). Freshwater standards were considered more appropriate than marine standards given the relatively low EC compared to marine waters.

During the study, all four lakes exceeded both trigger values and guideline values (Table 1). High levels of NH_3, NOx and Total N were most likely linked to residual from AMFO blasting during mining (Banks *et al.*

Table 1 *Exceedances of ANZECC/ARMCANZ (2018) trigger values for the 95% Protection of Aquatic Ecosystems for metals and metalloids - guidelines for south-east freshwater lakes and reservoirs. Data from sampled pit lakes. Timing and location of exceedance indicated by top (T) and bottom (B) waters.*

Lake		Al	B	Cr (VI)	Co	Cu	Se	U	NH3	FRP	NOx	Total N
	Trigger/Guideline Values (µg L^{-1})	**55**	**370**	**1**	**1.4**	**1.4**	**5**	**0.5**	**10**	**5**	**10**	**350**
BL1	Feb 2019					B	TB	TB			TB	TB
	May 2019					B	TB	TB	B		TB	TB
	Aug 2019				B	T	T	T			TB	TB
	Nov 2019					T	B	B			TB	TB
BL2	Feb 2019					TB		TB	B			
	May 2019					T		TB				
	Aug 2019					T		TB	B		B	
	Nov 2019							T				
HL1	Feb 2019	TB		T	TB	TB		T			TB	
	May 2019				TB	TB			B			
	Aug 2019				TB				TB		TB	
	Nov 2019				TB	B			TB		B	
HL2	Feb 2019	B	B			TB		TB		TB		T
	May 2019		TB					TB	TB			T
	Aug 2019							TB	TB			

Notes:

Al is based on pH>6.5 where it is less toxic

As occurs as both As (III) and As(V) - lowest trigger value is for As(V) about half of As(III)

Cr as measured was not divided into different oxidation states, so exceedances are against the total amount measured versus the trigger value for each oxidation state. The exceedances of trigger values for Cr(VI) therefore represent a worst case scenario, whereas Cr(VI) is generally uncommon in environmental samples.

Mercury due to bioaccumulating - recommended to use guideline value from high level of protection i.e. 99%

Selenium due to bioaccumulating - recommended to use guideline value from high level of protection i.e. 99%

Cadmium, Cr(III), Ni, and Zn trigger values were corrected for hardness as per Warne *et al.* (2018).

Table 2 Measures of biodiversity in Australian pit lakes. Abbreviations are: 'phyto'; phytoplankton, 'TR'; total richness, 'TR-max'; value of sample with highest richness, 'dom.'; dominant, 'Macro.'; macroinvertebrate. Values are for sample months February, May and August 2019 only.

Lake	Phyto. (TR-max)	Phyto (dom. Taxa)	Phyto. (restricted taxa)	Diatoms (TR)	Macro. (TR)	Macro. (abun)
BL1	18 (> 13 all seasons)	Chlorophyta Bacillariophyta and Cyanophyta	n/a	84	6	361
BL2	15	Chlorophyta Bacillariophyta and Cyanophyta	n/a	79	6	791
HL1	18	Chlorophyta Bacillariophyta	Cryptophyta	116	5	269
HL2	18	Chlorophyta Bacillariophyta	Cryptophyta, Euglenophyta	108	10	1064

1997). FRP is often limiting in pit lakes and its presence could be useful in stimulating primary production, although prolonged exceedances would increase the risk of algal blooms (Kumar *et al.* 2016). Local geologies were probably responsible for differences in metals/metalloids of concern to different pit lakes, except at HL1 where regular inflows might also have contributed. Exceedances of Cu and U were up to 20 times the trigger values.

Bacillariophyta, Cyanophyta, Chlorophyta, and Cryptophyta were the most abundant phytoplankton (cells mL^{-1}), and relative dominance of taxa was seasonal. BL2 was dominated completely by Cyanophyta in August, whereas HL2 was co-dominated by all four groups variably throughout the seasons. In August, HL1 was dominated by Bacillariophyta and in November by Chlorophyta. The high abundances of Cyanophyta in BL2 (February to August) was due to *Aphanocapsa* sp. Moderate Al concentrations and low total P are known to favour the growth of *Aphanocapsa* sp over other cyanobacteria (de J. Magalhães *et al.* 2019). As characteristic of cyanobacteria, some strains of *Aphanocapsa* sp may be toxic (Buratti *et al.* 2017).

The most abundant and taxonomically rich zooplankton across lakes were the Cladocera and Copepoda. Large bodied *Daphnia cf. carinata* were most abundant in HL2, although present at low numbers in BL2 and HL1 and absent entirely from BL1. High temperatures and salinities approaching the upper limit of known distributions might exclude *D. cf. carinata* from BL1 (Hall and Burns 2002). Ostracods and Harpacticoid copepods are typically benthic but are routinely collected as part of zooplankton sampling when samples are taken close to the sediments.

Briefly, macroinvertebrate taxa collected were cosmopolitan and pollution-tolerant taxa. The least saline lake had the lowest diversity and abundance of macroinvertebrates and the rehabilitated lake had the highest, suggesting rehabilitation may be more important for macroinvertebrates than salinity, although further analysis is needed.

Conclusions

In this brief presentation of biodiversity in saline coal pit lakes, we found a diverse selection of species from plankton to benthic diatoms and macroinvertebrates. Rehabilitation of the pit lake likely influenced aquatic biodiversity. Salinity did not appear to be the major factor driving biodiversity in these saline pit lakes although further analysis is required. Even without rehabilitation, the saline pit lakes did offer ecosystem values in the form of aquatic biodiversity, although there does appear to be considerable opportunity for improvement through rehabilitation. Some challenges include exceedances of ANZECC/ARMCANZ values and cyanobacteria blooms, although these may be due to natural factors. Comparison to naturally occurring saline lakes would be a useful exercise. Where

miners can demonstrate that pit lakes are well-established ecosystems with a good range of biodiversity, then relinquishment should be more acceptable from community and regulatory standpoints.

Acknowledgements

This research was funded by the Australian Coal Association Research Program and supported by several mining companies and Edith Cowan University. Blanchette and Lund (2021) previously examined the microbial dynamics of study lakes and water quality from this research as cited in text.

References

ANZECC/ARMCANZ (2018) The Australian and New Zealand Guidelines for Fresh and Marine Water Quality. Australian and New Zealand Environment and Conservation Council and the Agriculture and Resource Management Council of Australia and New Zealand. https://www.waterquality.gov.au/anz-guidelines Accessed 17/5/2020

APHA (2017) Standard methods for the examination of water and wastewater. 23rd edn. American Public Health Association, American Water Works Association, Water Environment Federation, Washington DC, USA

Banks D, Younger PL, Arnesen R-T, Iversen ER, Banks SB (1997) Mine-water chemistry: the good, the bad and the ugly. Environmental Geology 32(3):157-174

Blanchette ML, Allcock R, Gonzalez J, Kresoje N, Lund M (2019) Macroinvertebrates and Microbes (Archaea, Bacteria) Offer Complementary Insights into Mine-Pit Lake Ecology. Mine Water and the Environment. https://doi.org/10.1007/s10230-019-00647-9

Blanchette ML, Lund MA (2021) Aquatic Ecosystems of the Anthropocene: Limnology and Microbial Ecology of Mine Pit Lakes. Microorganisms 9(6):1207

Buratti FM, Manganelli M, Vichi S, Stefanelli M, Scardala S, Testai E, Funari E (2017) Cyanotoxins: producing organisms, occurrence, toxicity, mechanism of action and human health toxicological risk evaluation. Archives of Toxicology 91(3):1049-1130. https://doi.org/10.1007/s00204-016-1913-6

de J. Magalhães AA, da Luz LD, de Aguiar Junior TR (2019) Environmental factors driving the dominance of the harmful bloom-forming cyanobacteria Microcystis and Aphanocapsa in a tropical water supply reservoir. Water Environment Research 91(11):1466-1478. https://doi.org/10.1002/wer.1141

Gooderham J, Tsyrlin E (2002) The Waterbug Book. A guide to the freshwater macroinvertebrates of temperate Australia. CSIRO Publishing, Melbourne

Hall CJ, Burns CW (2002) Mortality and growth responses of Daphnia carinata to increases in temperature and salinity. Freshwater Biology 47(3):451-458. https://doi.org/https://doi.org/10.1046/j.1365-2427.2002.00815.x

Kumar RN, McCullough CD, Lund MA, Larranaga SA (2016) Assessment of factors limiting algal growth in acidic pit lakes—a case study from Western Australia, Australia. Environmental Science and Pollution Research 23(6):5915-5924. https://doi.org/10.1007/s11356-015-5829-0

Lund MA, McCullough CD (2011) Meeting environmental goals for pit lake restoration. Factoring in the Biology. In: McCullough CD (ed) Mine Pit Lakes: Closure and Management. Australian Centre for Geomechanics, Perth, p 83-90.

Margules CR, Pressey RL (2000) Systematic conservation planning. Nature 405(6783):243-253. https://doi.org/10.1038/35012251

McCullough CD, Lund MA (2006) Opportunities for sustainable mining pit lakes in Australia. Mine Water and the Environment 25(4):220-226

McCullough CD, Lund MA (2008) Aquatic macroinvertebrates in seasonal and rehabilitated wetlands of the Kemerton Silica Sand Pty Ltd project area (2007), Report №. Edith Cowan University, Perth,

McCullough CD, Steenbergen J, te Beest C, Lund MA More than water quality: environmental limitations to a fishery in acid pit lakes of Collie, south-west Australia. In: International Mine Water Conference, Pretoria, South Africa, 19-23 October 2009. International Mine Water Association, 6 p

Peel MC, Finlayson BL, McMahon TA (2007) Updated world map of the Köppen-Geiger climate classification. Hydrology and earth system sciences discussions 4(2):439-473

Proctor H, Grigg A (2006) Aquatic macro-invertebrates in final void water bodies at an open-cut coal mine in Central Queensland. . Australian Journal of Entomology 45:107-112

Timms BV (2018) On the influence of season and salinity on the phenology of invertebrates in Australian saline lakes, with special reference to those of the Paroo in the semiarid inland. Limnology and Oceanography 36(6):1907-1916

Warne MS, Batley GE, van Dam RA, Chapman JC, Fox DR, Hickey CW, Stauber JL (2018) Revised Method for Deriving Australian and New Zealand Water Quality Guideline Values for Toxicants – update of 2015 version., Report №. Australian and New Zealand Governments and Australian state and territory governments, Canberra, 48 p

Seasonal Geochemical Variation of Sediments in the Sabie River, Mpumalanga, South Africa

Rudzani Lusunzi[1,2], Frans Waanders[2], Tshishonga Robert Khashane Netshitungulwana[1]

[1]*Council for Geoscience, Economic Geology and Geochemistry Unit, 280 Pretoria Road, Silverton, 0184, Pretoria, South Africa, rlusunzi@geoscience.org.za*

[2]*Water Pollution Monitoring and Remediation Initiatives, Research Group (WPMRIRG), School of Chemical and Minerals Engineering, North-West, University, Potchefstroom, South Africa*

Abstract

Water pollution resulting from mining activities has become a major problem in South Africa. In this study, the seasonal variation of geochemical properties of solid wastes and stream sediments in the Sabie River catchment were characterised. There was no significant variation observed in terms of metal (loid) dispersion, namely, Cr, Zn, Cu, Ni, Pb and As during wet and dry seasons respectively. Furthermore, the mineralogy of sediments indicated that acid-producing minerals such as hematite and jarosite, typically found in mine wastes are potential sources of pollution to the Sabie River. In addition, acid-neutralizing mineral dolomite found in the sediments can act as buffers for potential acid. There was no evidence of metal dispersion from the Nestor tailings storage facility to the adjacent water resources, Klein-Sabie and Sabie River respectively.

Keywords: Stream Sediment, Sabie River, Acid-Producing Minerals, Acid-Neutralizing Minerals, Toxicity

Introduction

Together with the Komati and Crocodile basins, the Sabie River basin is part of the Inkomati River basin. Originating at an elevation of 2, 207 m.a.s.l., and the river flows in an easterly direction and passes through the Kruger National Park (KNP) towards the confluence with the Inkomati River in Mozambique. The river flows through commercial forestry plantations (pine trees and eucalyptus), sawmills, trout farms, fishery areas, waste treatment works, defunct mines of the Transvaal Gold Mining Estate (TGME), industrial and agricultural activities which are dominant in its upper reaches. Also located in the upper reaches is the town of Sabie while in the lower reaches of the basin there is the Hazyview town, rural settlement and Kruger National Park (KNP).

Recent studies carried out in the Sabie-Pilgrim's Rest goldfields showed a necessity of studying the geochemical composition of stream sediment along the Sabie River catchment (Novhe *et al*., 2014) (Rudzani *et al*., 2017); (Rudzani *et al*., 2018); (Rudzani, Novhe and Mashalane, 2019). Based on the findings, concentrations of metals such as As, Cr, Cu, Pb, Ni and Zn were elevated on mine wastes. Furthermore, the Nestor tailings storage facility (TSF) had no vegetation cover and susceptible to water and wind erosion which may consequently enrich the surrounding environment with toxic metals. The main aims of this study were to determine the concentration of major, trace and rare earths elements and define anthropogenic versus geogenic distribution in the Sabie River catchment with seasons. The data on the distribution of these metals in sediment near the mine wastes and along the catchment could provide valuable information on risk and exposure assessment of communities near the mine site.

Study Area

The Sabie River system is one of the largest rivers in the Mpumalanga Province, situated within the Inkomati water Management Area and originates at an elevation of 2207 m.a.s.l., and enters the Kruger National Park (KNP) 81.3 km downstream from its source (Figure 1).

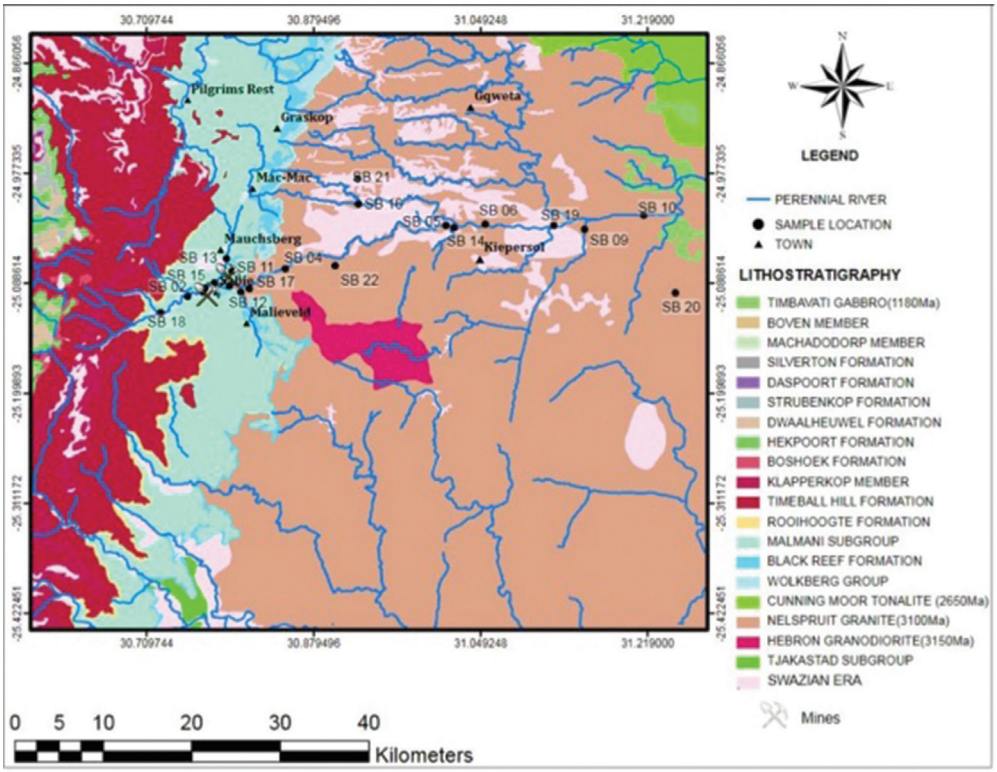

Figure 1 *Location of the Sabie River catchment and sample sites for collection in this project (CGS 1:250 000).*

Geologically, the area comprises of rocks of the Nelspruit Suite ranging from the Swazian era (Nelspruit granite and Hebron granodiorite) and 2800 Ma Cunning Moor Tonalite, Wolkberg Group, Black Reef Formation, Chuniespoort Group (Malmani Subgroup) and Pretoria Group (Rooihoogte, Timeball Hill, Boshoek, Hekpoort, Dwaalheuwel and Strubenkop Formations; Figure 1).

Materials and methods

Sampling and laboratory analyses

Sediments eroded from the Nestor TSF were collected and analysed for the chemical and mineralogical compositions (SB00) and were compared with twenty (20) composite stream sediment samples that were randomly collected to a depth of 15 cm (SB1-21; Figure 1) from Sabie River catchment. Samples were collected at various distances from agricultural areas, industrial areas, mining areas and urban/commercial areas. Sampling was done during November and December 2019, representing a wet season as well as July and August 2020 (dry season). Stream sediment samples were collected in the Sabie basin along the acid mine drainage (upstream, in the middle and downstream) in order to assess their impact on the dispersion of metals on the receiving water. The sediment samples were collected using a shovel with a narrow blade, bucket for homogenization of sediment samples, and plastic bags that were tightened to avoid oxygen penetration and to preserve biological or chemical equilibria. The samples were analysed by X-ray florescence (XRF) spectrometry and X-ray diffraction (XRD) spectrometry.

Data analysis

Assessment of metal pollution in sediment

Results and Discussion

The degree of contamination from the metal species in the Sabie River catchment was evaluated by determining the contamination factor (CF), pollution load index (PLI) and geoaccumulation index (I*geo*).

Enrichment factor (EF)

The enrichment factor (EF) is an index/ indicator used for reflecting the level of environmental contamination. In this study, EF was employed to evaluate possible anthropogenic input of metal species to the Sabie River catchment and was calculated as:

$$EF = (\frac{Cn}{LV})\ sample/(\frac{BB}{LV})\ background$$

where [Cn/LV] sample is the concentration of analysed metal and one of the following metals Fe/Al/Ca/Sc/Ti/Rb and [GB/LV] *background*-reference concentration of analysed metal (Cn) and one of the following elements Fe/Al/Ca/Sc/Ti/Rb (LV). For this study Rb was used as a reference element and SB18 (Mac Mac River) was selected as a background as there are no mining activities and little anthropogenic input. Islam *et al.* (2015c) proposed the ratio of measured concentration to natural abundance as a contamination factor (CF) and classified into four grades for pollution monitoring of a single metal over a period of time: low degree (CF<1), moderate degree (1≤CF<3), considerable degree (3≤CF<6), and very high degree (CF≥6).

Geoaccumulation index (I*geo*)

In order to evaluate the degree of metal pollution of sediment by comparison to the baseline metal concentration of the surrounding area, the geoaccumulation index was used. By definition, the geoaccumulation index is:

$$Geoaccumulation\ index\ (Igeo) = log2\ (\frac{Cn}{1.5Bn})$$

where C*n* is the toxic element concentration in a sample and B*n* is the measured concentration of the element in unpolluted sediments. Other studies had used similar approach to characterize pollution of sediments including (Sarmiento *et al.*, 2011); (Han *et al.*, 2017). Samples were classified as unpolluted (I*geo* < 1) and highly polluted (I*geo* > 5).

Chemical index of alteration (CIA)

The chemical index of alteration (CIA) was used to evaluate the extent of weathering of feldspars relative to unaltered rocks from the Sabie catchment area. Nesbit and Young (1982) defined as:

$$CIA = (Al_2O_3/Al_2O_3+CaO^*+Na_2O+K_2O) \times 100$$

where CaO* is the amount of CaO incorporated in the silicate fraction of rocks. According to Taylor and McLennan (1995), the average upper continental crust denoted a CIA value of 47. This implies that CIA values of between 45 and 55 indicate weak weathering conditions and a value of 100 represent extreme weathering which is supported by the presence of typical weathering minerals such as kaolinite and gibbsite.

Two sediment quality guidelines (SQGs) for metals in freshwater ecosystems described by McDonald *et al.* (2000) were used to describe the possible toxicity levels of metal species in the Sabie River catchment. In SQGs, samples were grouped into two categories: threshold effect levels (TELs) and probable effect concentrations (PECs). The TELs are the concentrations below which harmful effects are unlikely to be observed and the PECs are the concentrations above which harmful effects are likely to be observed (McDonald *et al.*, 2000).

Statistical analysis

The Pearson R correlation analyses were applied to assess elemental associations and origins of analysed elements using software Stata version 13. Critical values of the correlation coefficient (r) 0.81 at p≤ 0.05 were considered highly significant.

Geochemistry of solid wastes and stream sediment

Major elements in mine waste and stream sediments

The results of the XRF analysis of the major elements presented as percentages of the corresponding oxides. The following oxides were observed to be dominant in all sampling sites assessed: SiO_2 (40.24-86.15%), Al_2O_3 (5.67-52.20%), Fe_2O_3 (1.62-11.75%), K_2O (1.02-4.45%), Na_2O (0.08-2.87%), CaO (0.12-1.87), Ti_2O (0.23-1.69%), MgO (0.30-1.63%), MnO (0.018-0.273%), P_2O_5 (0.030-0.270%) and Cr_2O_5 (0.007-0.102%). More than 75% of major elements in all surficial samples were accounted

for Si-Al-Fe component, which is likely reflecting a relatively high quartz, feldspar, clay minerals and mica present in the sediments. The dominant elements such as Si, Al, Fe, Ti and Mn can be potentially toxic to aquatic environment.

According to (Nesbitt and Young, 1982) CIA values of between 45 to 55 indicate that the rocks of the catchment area undergo moderate degree of weathering and value of 100 indicates intense weathering. CIA value for Nestor TSF was 74.04 and varied from 53.19 to 88.58 in wet and dry seasons respectively in the Sabie River (SB01-09). The high CIA values were also observed at Lone Creek (SB10) at 88.46 and 82.33 in wet and dry seasons respectively. This implies that there is wide range of chemical weathering occurring in the Sabie River. However, low CIA values were recorded at sites SB08, SB16, SB17, SB18, SB20 and SB 21, which are underlain by granitic rocks.

Pearson correlation analysis (Table 1) showed the significant positive correlation Ti with both Fe and Al, Cr and Mg, as well as P and Fe. The zero to highly significant correlation between Si and other elements (Ti, Al, Fe, Mn, Mg, Ca K, P, Na, and Cr) suggests their removal from silicate phase during weathering. The highly positive correlation of Al with Ti and Fe, Ca with Mg and Cr with Mg and Ca indicate similar input sources and/or very close mineral association between these groups of elements.

Trace elements concentrations in mine waste and stream sediments

Trace element concentrations (As, Co, Cu, Cr, Ni, Pb, V and Zn) of mine waste (SB00) and surficial sediments (SB01-21) and their mean, minimum, maximum and standard deviation values in the Sabie River catchment gathered in Table 2 were used to evaluate metal their distribution. In addition, the mean upper crust concentrations (UCC- Rudnick and Gao, 2003) and the toxic effect concentrations and probable effect concentrations (MacDonald *et al*., 2000) for freshwater sediments for a selection of trace elements is shown. Analysis revealed that the mean sediment trace element concentration increases in the following order: Pb<Co<Ni<Cu<Zn<As<Cr. Metal species concentrations in mine waste (SB00) were higher than upper crustal crust concentrations (Rudnick and Gao, 2003). However, metal species in mine waste sample are lower than in the stream sediments. The mean concentration of As in sediment was observed 92.7 mg/kg in summer and 80.4 mg/kg in winter respectively which were higher than average upper continental crust. The chromium concentration in the sediment was higher than other metals because of direct discharging untreated wastes from fertilizers (SB01-21). Higher values of Cr recorded during summer season at SB21 (Bega River) indicates its input, which might be originated from residential and industrial wastes.

The concentrations of As, Cr, Cu and Ni in some sediment samples exceeded the consensus-based PEC for freshwater ecosystems, implying probable adverse effect on the ecosystem (Table 2). All mean

Table 1 *Pearson correlation coefficient between major elements.*

	SiO_2	TiO_2	Al_2O_3	Fe_2O_3 (t)	MnO	MgO	CaO	Na_2O	K_2O	P_2O_5	Cr_2O_3
SiO_2	1.00										
TiO_2	-0.93	1.00									
Al_2O_3	-0.90	0.83	1.00								
Fe_2O_3 (t)	-0.87	0.91	0.62	1.00							
MnO	-0.24	0.32	0.07	0.46	1.00						
MgO	-0.47	0.42	0.45	0.41	0.14	1.00					
CaO	-0.17	0.06	0.20	-0.03	-0.08	0.79	1.00				
Na_2O	0.22	-0.33	0.09	-0.60	-0.45	-0.09	0.38	1.00			
K_2O	0.09	-0.20	0.26	-0.46	-0.40	-0.18	0.02	0.75	1.00		
P_2O_5	-0.55	0.45	0.25	0.60	0.16	0.08	-0.04	-0.39	-0.32	1.00	
Cr_2O_3	-0.33	0.31	0.17	0.40	0.38	0.77	0.62	-0.27	-0.47	0.17	1.00

values recorded for As were much higher than consensus based TECs and PECs. This implies a probable adverse effect due to the As-presence in the Sabie River system. A consistent result is also yielded from the calculated geoaccumulation index of As which reached 5.90 and 8.73 in wet and dry seasons respectively (Table 4). There is also probable a Cr and Ni pollution potential in the Bega River (SB21) based on the geoaccumulation index while drainage next to the old Rietfontein Mine (SB15) was observed as a potential Cu-Pb pollutant to the surrounding ecosystem. In addition, geoaccumulation indexes of elements such as Co, Cr, Cu, Pb and Zn showed classes unpolluted to moderately polluted at most sites. This implies that the pollution caused by mine wastes regarding toxic elements may be likely limited to As.

Metal concentrations were high in winter than in summer because of low water flow in winter that can assist toxic metals species to accumulate in sediments.

Pearson correlation matrix showed the following significantly positive correlations during the dry season (shaded): Ni with Co and Cr, Pb with Co and Ni, Zn with Ni and Pb. In wet season, the following correlation was observed (unshaded): Co with Ni and Zn, Cr with Ni, Cu with Pb and Zn with Ni and Pb (Table 3).

The geoaccumulation index of sediments showed that sediment are extremely

Table 2 *Trace elements concentrations and their mean, maximum and standard deviation in the Sabie River catchment compared to threshold effect concentration and probable effect concentration (PEC) (MacDonald* et al.*, 2000).*

Sample	As (ppm)		Co (ppm)		Cr (ppm)		Cu (ppm)		Ni (ppm)		Pb (ppm)		Zn (ppm)	
number	Wet	Dry	Wet	Dry	Wet	Dry	Wet	Dry	Wet	Dry	Wet	Dry	Wet	Dry
SB00	365	_	11	_	135	_	77	_	32	_	38	_	27	_
SB01	23	17	37	38	263	277	86	78	101	103	23	21	89	90
SB02	7.9	15	19	36	214	272	32	65	37	94	17	31	49	73
SB03	382	293	38	36	192	204	79	75	77	82	18	18	135	109
SB04	56	322	15	35	120	155	31	222	25	73	12	24	31	96
SB05	271	277	25	31	110	136	103	159	49	65	16	20	76	93
SB06	186	279	19	17	108	111	52	41	38	38	13	13	55	47
SB07	149	Bdl	17	14	93	89	40	20	33	36	11	16	43	58
SB08	32	13	11	Bdl	69	78	20	6.3	18	7.8	12	5.5	36	9.3
SB09	17	16	7.3	62	81	241	10	68	17	101	7.1	14	15	64
SB10	16	19	33	33	236	268	73	63	83	92	18	20	83	83
SB11	23	18	22	19	253	382	35	27	41	38	27	13	45	25
SB12	170	234	34	43	183	202	67	176	56	107	12	39	85	294
SB13	13	11	61	3.2	211	52	58	7.9	85	15	11	8	55	7.1
SB14	133	186	74	89	162	207	111	147	84	87	27	29	64	49
SB15	90	81	13	18	19	24	420	1180	13	16	52	25	36	41
SB16	Bdl	Bdl	6.1	Bdl	39	24	7.0	4.5	14	10	9.5	9	24	14
SB17	Bdl	Bdl	4.4	11	60	120	6.4	15	18	47	7.7	12	11	39
SB18	13	7.4	21	25	59	81	31	33	28	42	7.5	6.7	26	17
SB19	Bdl	Bdl	6.4	Bdl	38	23	8.4	4.3	9.4	6	4.6	3.2	13	5.4
SB20	Bdl	89	5.1	9.8	35	85	6.8	19	8.8	22	9.2	8.9	14	23
SB21	Bdl	Bdl	38	10	710	240	40	9.7	172	41	16	8.7	80	25
Mean	92.7	80.4	24.3	25.2	159.5	155.8	66.1	115.3	48.8	53.5	17.1	16.4	50.8	80.6
SD	120.5	118.7	18.2	22.0	146.9	100.3	86.9							
UCC	4.8		26.0		92.0		28.0		47.0		17.0		67.0	
TEL	9.79				43.4		31.6		22.7		35.8		121	
PEC	33.0				111		149		48.6		149		459	

Bdl, below detection limit; SD, standard deviation; TEC, toxic effect concentration; PEC, probable effect concentrations UCC: upper continental crust (Rudnick and Gao, 2003).

Table 3 Pearson correlation coefficient between trace elements in the Sabie River.

	As	Co	Cr	Cu	Ni	Pb	Zn
As	1	0.15	-0.08	0.24	0.05	0.34	0.47
Co	0.41	1	0.48	0.14	0.73	0.16	0.64
Cr	0.08	0.56	1	0.48	0.91	0.08	0.53
Cu	0.19	0.12	-0.18	1	0.02	0.82	0.02
Ni	0.37	0.83	0.74	-0.04	1	0.1	0.71
Pb	0.50	0.69	0.48	0.40	0.76	1	0.17
Zn	0.54	0.47	0.37	0.12	0.71	0.79	1

contaminated with As at some sites, especially in winter (dry season) (Table 4).

The calculated enrichment factor values for the Sabie River catchment for trace elements revealed minor to severe enrichment in sediments (Table 5). The values of contamination factor (CF) Co showed moderate contamination (1≤CF<3), whereas all other trace elements (As, Cr, Cu, Ni<Pb and Zn) showed the degree of contamination (CF>6), though values for Cr, Cu, Ni and Pb varied with seasons and were lower than six depending on seasonal change.

Mineralogy of solid wastes and stream sediment

The exposed and underlying lithologies of the Sabie River catchment are dominantly composed of gneiss, granite, quartzite and dolomite. Therefore, surficial sediment samples of mineralogy of the streams closely related to the prevailing rock outcrops. There is great variation in terms of mineralogy of the Nestor TSF sediments and sediments collected from the streams. The mineralogical assemblage of the stream sediment is mostly comprised of quartz (51-87%), followed by feldspars (K-feldspar (1-21%), while phyllosilicate (mica and clay minerals) have concentrations varying from 0 to 15%, and were absent on tailing sediments (Table 6). In addition, dominant on sediments samples is the secondary mineral gibbsite especially on the upper reaches of Sabie River. This is supported by the presence of clay mineral kaolinite. Carbonate mineral dolomite occurred in few locations in the upper part of the catchment at very low concentrations of 0 to 6% (SB02) and near Glynns Lydenburg TSF (SB11). In addition to the minerals detected from stream sediments, the TSF sample contained two acid producing minerals primary mineral hematite (2 wt.%) and secondary mineral jarosite (4 wt.%). Traces of smectite were only found sporadically in the catchment area.

There was significant seasonal variation observed in the predominant pattern of sediment mineralogical composition throughout the catchment area.

Conclusions

There was significant variation in most trace metal concentrations as they were high in winter than summer season. Low concentrations of metal species occurred in

Table 4 Geoaccumulation index of trace metals in sediment of Sabie River catchment.

	Igeo (As)		Igeo (Co)		Igeo (Cr)		Igeo (Cu)		Igeo (Ni)		Igeo (Pb)		Igeo (Zn)	
	Wet	Dry	Wet	Dry	Wet	Dry	Wet	Dry	Wet	Dry	Wet	Dry	Wet	Dry
Min	0.00	0.00	0.04	0	0.04	0.05	0.04	0.00	0.09	0.04	0.12	0.10	0.10	0.08
Max	5.64	8.73	0.71	0.71	2.40	0.90	2.70	0.71	1.23	0.54	1.38	0.93	1.04	1.28

Table 5 Contamination factor of trace metals in the Sabie River catchment.

	CF (As)		CF (Co)		CF (Cr)		CF (Cu)		CF (Ni)		CF (Pb)		CF (Zn)	
	Wet	Dry	Wet	Dry	Wet	Dry	Wet	Dry	Wet	Dry	Wet	Dry	Wet	Dry
Min	0.00	0.00	0.17	0.00	0.09	0.52	0.18	0.08	0.13	0.08	0.90	0.76	0.48	0.34
Max	49.62	48.19	3.05	3.02	12.00	4.93	4.26	7.45	6.19	3.27	5.56	7.22	8.60	22.07

Table 6 Mineralogical composition of tailings and stream sediments in the Sabie River catchment.

Sample	Dolomite		Hematite		K-Feldspar		Quartz		Mica		Kaolinite		Gibbsite		Smectite	
number	Wet	Dry	Wet	Dry	Wet	Dry	Wet	Dry	Wet	Dry	Wet	Dry	Wet	Dry	Wet	Dry
SB00	Bdl	_	2	_	Bdl	_	85	_	9	_	Bdl	_	Bdl	_	Bdl	_
SB01	Bdl	Bdl	Bdl	Bdl	1	1	71	57	7	15	5	15	5	4	6	Bdl
SB02	Bdl	6	Bdl	2	14	1	53	60	5	11	1	11	Bdl	2	Bdl	Bdl
SB03	Bdl	Bdl	Bdl	1	2	9	88	69	4	8	2	8	2	3	Bdl	Bdl
SB04	Bdl	Bdl	Bdl	2	16	17	64	62	3	7	2	7	3	4	Bdl	Bdl
SB05	Bdl	Bdl	Bdl	1	10	5	72	69	3	7	3	11	3	5	Bdl	Bdl
SB06	Bdl	Bdl	Bdl	1	21	7	51	76	3	2	2	3	2	1	Bdl	Bdl
SB07	Bdl	Bdl	Bdl	Bdl	14	9	61	72	Bdl	3	Bdl	3	Bdl	Bdl	Bdl	Bdl
SB08	Bdl	Bdl	Bdl	Bdl	14	7	67	87	Bdl	1	Bdl	Bdl	Bdl	Bdl	Bdl	Bdl
SB09	Bdl	Bdl	Bdl	1	10	1	73	85	1	4	Bdl	2	Bdl	5	Bdl	Bdl
SB10	Bdl	Bdl	Bdl	1	2	Bdl	58	52	11	20	4	17	10	6	4	Bdl
SB11	3	8	Bdl	Bdl	4	4	86	74	Bdl	4	Bdl	3	Bdl	1	Bdl	Bdl
SB12	Bdl	Bdl	Bdl	1	8	1	84	84	4	5	Bdl	4	2	3	Bdl	Bdl
SB13	Bdl	Bdl	Bdl	Bdl	Bdl	21	88	67	Bdl	1	Bdl	1	12	Bdl	Bdl	Bdl
SB14	Bdl	Bdl	Bdl	Bdl	7	4	93	85	Bdl	7	Bdl	3	Bdl	Bdl	Bdl	Bdl
SB15	Bdl	Bdl	Bdl	1	34	21	22	55	10	6	17	4	Bdl	Bdl	Bdl	Bdl
SB16	Bdl	Bdl	Bdl	Bdl	14	11	61	80	Bdl	1	Bdl	1	Bdl	Bdl	4	Bdl
SB17	Bdl	Bdl	Bdl	Bdl	17	7	71	62	Bdl	2	Bdl	5	Bdl	Bdl	Bdl	Bdl
SB18	Bdl	Bdl	Bdl	Bdl	10	6	72	84	1	2	Bdl	1	2	3	Bdl	Bdl
SB19	Bdl	Bdl	Bdl	Bdl	4	3	85	94	Bdl	1	Bdl	1	3	1	Bdl	Bdl
SB20	Bdl	Bdl	Bdl	1	14	17	55	71	1	3	2	2	Bdl	1	Bdl	Bdl
SB21	Bdl	Bdl	Bdl	Bdl	17	7	52	73	9	1	Bdl	Bdl	Bdl	Bdl	Bdl	2
Mean	0.1	0.6	0.1	0.6	10.6	7.6	68.7	72.3	3.2	5.3	1.7	4.9	2.0	1.9	0.6	0.1
SD	0.6	2.1	0.4	0.7	8.6	6.5	16.8	11.7	11.7	5.0	3.7	4.9	3.3	2.0	1.7	0.4

stream sediments compared to mine wastes. The contamination factor, pollution load index and geoaccumulation index showed that sediments were unpolluted to extremely polluted by As. Therefore, sources of contamination to the Sabie River catchment should be closely monitored.

Acknowledgements

The authors would like to acknowledge the Council for Geoscience for financial support. Council for Geoscience colleagues, Mr T. Thiba and Mr D. Nxumalo are acknowledged for their assistance with sampling

References

Han, Y. S. *et al.* (2017) 'Geochemical and eco-toxicological characteristics of stream water and its sediments affected by acid mine drainage', Catena. Elsevier B.V., 148, pp. 52–59. doi: 10.1016/j.catena.2015.11.015

Islam, M.S., Ahmed, M.K., Raknuzzaman, M., Habibullah-AlMamun, M., Islam M.K, 2015c 'Heavy metal pollution in surface water and sediment: a preliminary assessment of an urban river in a developing country. Ecol.Indic.48, 282-291.

MacDonald, D. D., Ingersoll, C. G. and Berger, T. A. (2000) 'Development and evaluation of consensus-based sediment quality guidelines for freshwater ecosystems', Archives of Environmental Contamination and Toxicology, 39(1), pp. 20–31. doi: 10.1007/s002440010075

Nesbitt, W. and Young, G. M. (1982) 'Nesbitt_82 (1). Early Proterozoic climates and plate motions inferred from major elements chemistry of lutites, 299, pp. 715–717.

Novhe NO, Yibas B, Netshitungulwana R, Lusunzi R (2014) Geochemical and Mineralogical Characterization of Mine Residue Deposits in the Komati/Crocodile Catchment, South Africa: an Assessment for Acid/Alkaline Mine Drainage', pp. 978–7

Rudnick, R. L. and Gao, S. (2003) Composition of the Continental Crust. Treatise Geochem 3 :

1-64 Composition of the Continental Crust. 2nd edn, Treatise on Geochemistry. 2nd edn. Elsevier Ltd. doi: 10.1016/B978-0-08-095975-7.00301-6

Rudzani L, Gumbo JR, Yibas B, Novhe NO (2017) 'Geochemical and Mineralogical Characterization of Gold Mine Tailings for the Potential of Acid Mine Drainage in the Sabie-Pilgrim's Rest Goldfields, South Africa', pp. 1381–1388. doi: 10.17758/eares.eap517219

Rudzani L, Gumbo JR, Yibas B, Novhe, NO (2018) 'Acid Base Accounting (ABA) of mine tailings for the Potential of Acid Mine Drainage in the Sabie- Pilgrim ' s Rest Goldfields , South Africa'

Rudzani L, Novhe O, Mashalane T (2019) 'Geochemical and Mineralogical Characterization of Precipitates from Sabie-Pilgrim's Rest Goldfields for the Potential of Acid Mine Drainage', 1, pp. 425–430

SANS (2015) 'South African National Standard (SANS).' Drinking Water for SANS, 241, pp. 1–2. Available at: https://vinlab.com/wp-content/uploads/2016/10/SANS-241-2015.pdf.

Sarmiento, A. M. *et al.* (2011) 'Toxicity and potential risk assessment of a river polluted by acid mine drainage in the Iberian Pyrite Belt (SW Spain)', Science of the Total Environment. Elsevier B.V., 409(22), pp. 4763–4771. doi: 10.1016/j.scitotenv.2011.07.043.

Comparative Life Cycle Assessment for Acid Mine Drainage Management Options in the Central Basin of the Witwatersrand Goldfields

Godfrey Madzivire[1,2], Thakane Ntholi[1], Henk Coetzee[1]

[1]*Council for Geoscience, 280 Pretoria Street, Silverton, Pretoria, 0184, South Africa, gmadzivire@geoscience.org.za*

[2]*Department of Environmental Science, University of South Africa, Roodepoort, Johannesburg, South Africa*

Abstract

Acid mine drainage (AMD) is a product of oxidation of disulfide minerals such as FeS2 in the presence of water and oxygen. The oxidation reaction is catalysed by *Acidithiobacillus sp*. The oxidation results in the formation of sulfuric acid that in turn causes the chemical of weathering of the surrounding rock. AMD management includes treatment or prevention of its formation. The management of AMD is site specific and any management option has to be fine-tuned to meet the volumes and the quality of the water to be treated. In this study life cycle assessment (LCA) was used to evaluate the environmental impacts associated with the prevention of AMD formation through the construction of a canal to prevent ingress of water into the mine voids. This is of importance to avoid burden-shifting in the management of AMD.

LCA is a robust and valuable tool to assess the true environmental impacts of processes in order to enable informed decision-making. The option of canal construction was compared to allowing water to ingress mine voids and subsequent formation of AMD. The functional unit for the research was the evaluation of the environmental impacts per removal (or prevention of the formation of) kilogram of acidity from AMD. The novel of this approach is to identify the environmental impacts.

This study has established that, allowing ingress affects the quality water resources that in turn affecting human health and ecosystem depletion. On the other hand, ingress control has the effects on resource depletion. The effects towards human health and ecosystem depletion due to allowing ingress was because of the formation of AMD. This results in the chemical weathering of the surrounding geology resulting in water containing potentially harmful elements and low pH. This makes the water not suitable for human consumption and causing drastic effects to the flora and fauna. Ingress control depletes natural resources due to the various raw materials that are required for construction of structures to prevent ingress control.

The role of LCA is not to give a directive, but rather to reveal trade-offs for proposed solutions and scenarios. In situations where natural resources are critical, it may be best to allow ingress and follow up with AMD remediation before it affect both ecosystems and human health. In cases where human health is critical, the option may be to implement ingress control.

Keywords: Acid Mine Drainage, Life Cycle Assessment, Functional Unit, Environmental Impacts

Introduction

AMD remains one of the biggest environmental challenges resulting from mining activities. It results from the oxidation of disulfide minerals, particularly pyrite in the presence of water and the reaction continues for as long as the conditions, particularly the availability of (oxygenated) water, remain favourable (e.g. Gray 1998; Blowes *et al.* 2003; Wolkersdorfer 2008; Nordstrom 2011). Ingress of water into the mines occurs through various pathways depending on the structural geology, mine design and surrounding geomorphology and hydrogeology. In active mining areas, the water

is continuously pumped out to enable safe and efficient mining (McCarthy 2011), exposing disulphide minerals to oxidative weathering processes, allowing secondary acid-generating minerals to accumulate in the mine workings. In abandoned/disused mines, these secondary minerals are then dissolved, forming an acidic solution AMD reaction occurs, which fills the mine voids and may finally discharge into the surrounding environment, and contaminating fresh water systems (Younger 1997; McCarthy 2011). Most efforts to deal with AMD have focused on remediation and rehabilitation. Active and passive treatment methods have been developed and some are currently being implemented.

This study focused on alternative approach-ingress control–based on the assumption that identifying and sealing points of water ingress into mine voids decrease the volume of AMD generated, reducing the long term management costs. In this assessment, ingress is compared to a scenario that has not been explored and might be a good baseline for LCA comparison; this is the option to allow ingress followed with no subsequent remediation. Based on field observation and intuition, this should not even be an option but putting this option into the LCA analysis will offer a good baseline of comparison.

Life cycle assessment is a sustainability audit that determines the long-term environmental impact of any process (e.g. Curran, 2006; Lehtinen *et al.*, 2011; Hegen *et al.*, 2014). This is done by considering the environmental impact of producing the individual components that contribute to the process e.g. raw material, equipment, fuel/energy. The assessment can be applied to a whole system i.e. cradle to grave approach or limited to a designated part of the system by setting a system boundary.

With many AMD management solutions to choose from, it is important to have criteria on which to base decisions. In the past, the decisions were based on cost. However, it has since been acknowledged that solutions that are proposed to solve environmental challenges, do themselves lead to a form of environmental impacts such as depletion of natural resources, use of fossil fuels, taking up land space and producing waste.

Methods

In order to determine the holistic environmental impact of all proposed interventions, life cycle assessment (LCA) was performed.

Process descriptions

Two process were compared using a robust LCA to determine the environmental impacts with regard to AMD management in the Witwatersrand gold fields. This processes as shown in Figure 1 are:

i. Allowing water to ingress the mine voids resulting the formation of AMD and
ii. Prevention of ingress of water into the mine voids, thereby avoiding the formation of AMD.

Allowing ingress

This referrers to allowing surface water to flow naturally through the ingress point into the mine voids. It is assumed that for any given volume of water that enters the mine voids, an equivalent volume of AMD is generated. The chemistry of acid mine drainage used for the modelling exercise is given in the Table 1.

Ingress control

This refers to the construction of an ingress control structure. The LCA modeling is based on a site in the Witwatersrand Goldfields (Fig 2a), which was part of the Ingress Control project at the Council for Geoscience. The site was successfully constructed in 2017. The design and construction of the structure was based on the standard design (see Fig 2b).
With this approach, the site was prepared by clearing vegetation cover (see Fig 2), sealing the crack with concrete (or clay where applicable), and backfilling with soil. The top is sealed with alternating geotextile and HDPE layers. Finally, a layer of gravel is placed over the structure.

Life cycle assessment procedure

Life cycle assessment was performed using Simapro 8 software and the EcoInvent life cycle inventory database following the ISO 14040:2006 procedure. The LCA was used to evaluate the environmental impacts resulting from allowing ingress of surface water and eventually generating an equivalent amount

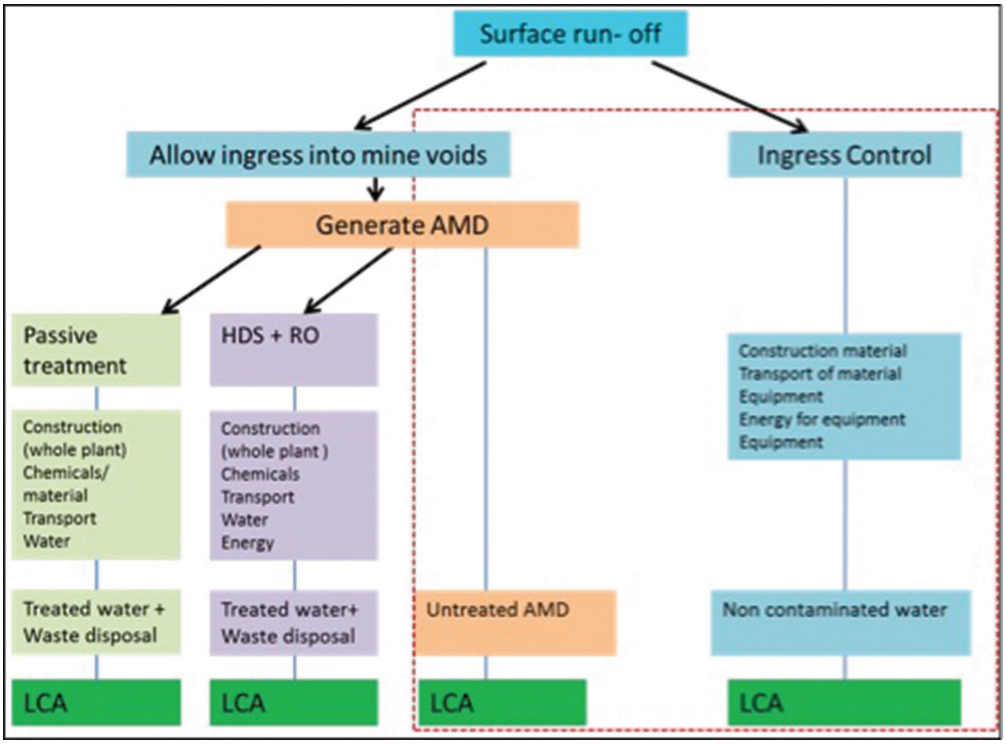

Figure 1 *Flow diagram illustrating the potential fate of water in ingress environment and steps leading to contributing to the LCA.*

Table 1 *Physicochemical parameters of the acid mine water used for LCA modelling.*

ORP	486.2	Ni	4.40
34	2.9	254	5.20
pH	3.36	K	1.56
EC (µS/cm)	7 679	Li	0.68
TDS (mg/L)	4 991	Sr	0.57
acidity calc (mg/L)	2 342.54	Cu	0.18
*SO_4^{2-}	6 686	Be	0.13
Mn	374.70	Rb	0.12
Ca	290.38	Se	0.089
Al	285.34	Cr	0.056
Mg	278.45	As	0.053
Na	53.26	U	0.04
Cl-	24	Cd	0.039
F-	14.94	Ba	0.021
Zn	13.17	Mo	0.0066
Co	9.32	Tl	0.0055
Fe	5.86	V	0.0029
NO_3^-	5.00	Ga	0.0022

*The concentrations of elements are given in mg/L.

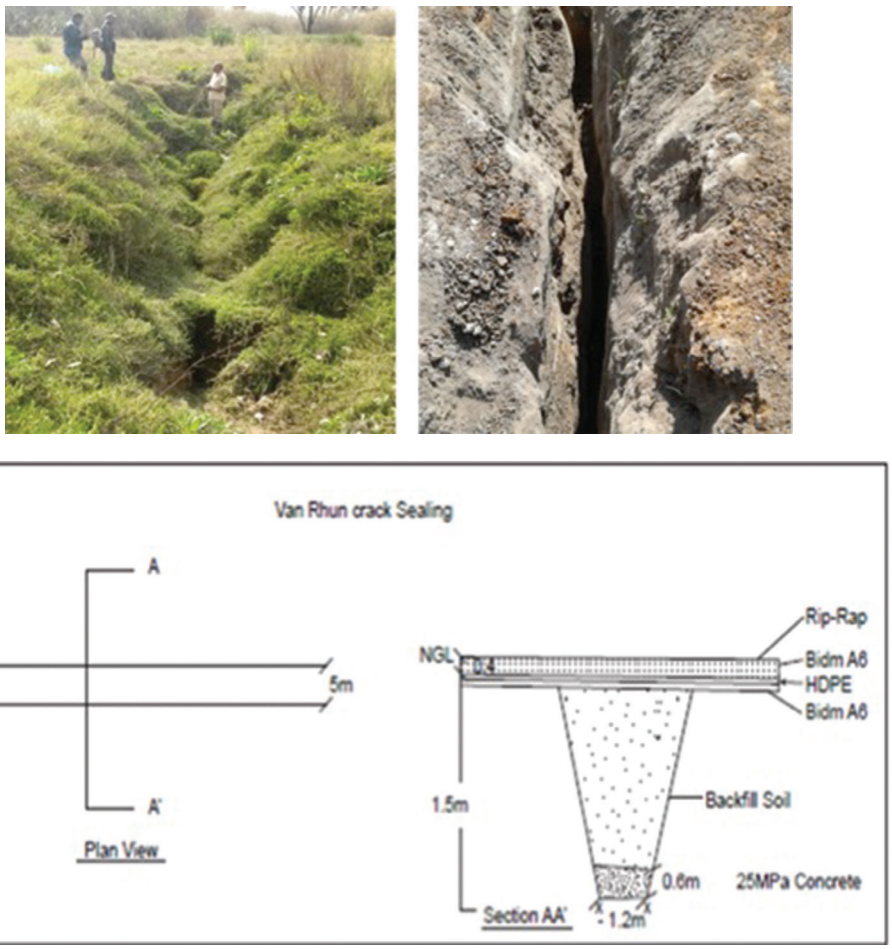

Figure 2 Modderbee ingress point as seen in the field (Source: Tegegn and Coetzee 2017).

of AMD and the impact resulting from preventing ingress by constructing an 'ingress control structure'.

System boundary

The system boundary defines the limits of the system being modelled. The system boundary was set at from the point of potential ingress to the point of release of the resulting water (from either scenario) into the environment.

The system included the raw material extraction, transport of the raw materials, and construction of the ingress control structure.

Functional unit

The functional unit, which is the unit of comparison/normalisation of the systems, was set to be 1 kg of acidity in the resulting water. Therefore, all the environmental impacts were normalised to 1 kg acidity for one year of activity. For every kg of acidity generated through allowing ingress, ingress control prevents a kg of acidity from being generated. Ingress of water on site was measured during different times of the year. In January 2016, the area was flooded and no measurement could be taken. In May 2016, the ingress of water was measured to be 6 L/s and in August the same year the area was dry. For this LCA, a flow rate of 6 L/s was used. Based on the chemistry of the water, a kg of acidity is equivalent to 16 L of AMD.

Materials and transport

There is no material required for allowing ingress. For ingress control, the clay is found on site, the geotextile and HPDE are sourced from a local supplier within 100 km radius from site.

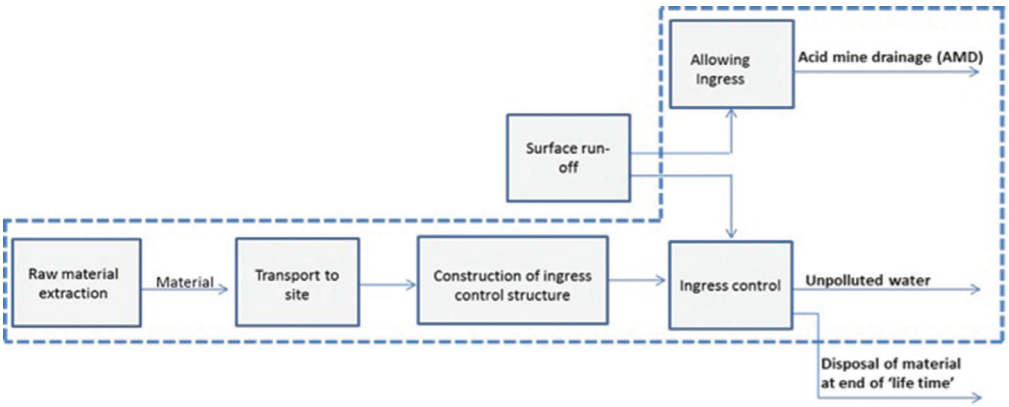

Figure 3 *System boundary for LCA on allowing ingress and ingress control.*

Operation and maintenance

There is no maintenance required for allowing ingress. The ingress control structure requires no maintenance during its prescribed lifespan.

Environmental impact assessment

The environmental impacts that were assessed during this LCA study were: damage to human health, damage to ecosystems and damage to resources.

Results and discussion

The biggest impact of allowing ingress is the generation of acid mine drainage. The acid mine drainage has a negative impact on human health and ecosystems. The natural resources required to generate AMD besides the water itself are negligible as shown in Fig 4(a), while ingress control impacts all three environmental impacts as shown in Fig 4(b).

Allowing ingress impacts on ecosystem occurs when AMD contaminates soil and water bodies on which ecosystems rely. Impact on human health occurs when humans come in contact with AMD, e.g. swimming in affected water bodies, and when they ingest through drinking water or eating crop exposed to AMD. The contamination of soil and water bodies is due to the potentially toxic elements such as As, Pb, U and Cr in AMD as well low pH that is characteristic of AMD.

Human health impacts due to the prevention of ingress of water into the mine voids Figure 4b is predominantly due to transportation of material to site. The manufacturing of polyethylene have the second highest on human health. Concrete has the least effect on human health, this effect results from the manufacturing of the concrete. For ecosystems, transport has the highest impact, followed by concrete and lastly, gravel. The production of polyethylene has the highest impact on natural resources, transport also contributes a substantially.

Transporting the raw materials and HDPE has more environmental impacts as compared to the impacts associated with concrete and gravel. This is because of the use of fossil fuel thereby depleting the natural resource. The burning of these fossil fuels during the transportation of raw materials and making of HDPE produce greenhouse gases such as CO_2 and methane. On the hand the making HDPE requires the mining of fossil fuels such as petroleum products. Gravel has the least impact to the environment because it was collected from site.it

Environmental impacts comparison

The difference in impact between allowing ingress and ingress control is significantly large and explicitly allocated as shown in Figure 5.

Allowing ingress has a significantly higher impact on both human health and ecosystems and a minor impact on resources as compared to ingress control. On the other hand, ingress control has significantly higher impact on resources. It also has an impact on health and ecosystems.

The higher impacts towards human health and ecosystem depletion due to allowing ingress is because of the formation of AMD. This results in the chemical weathering of

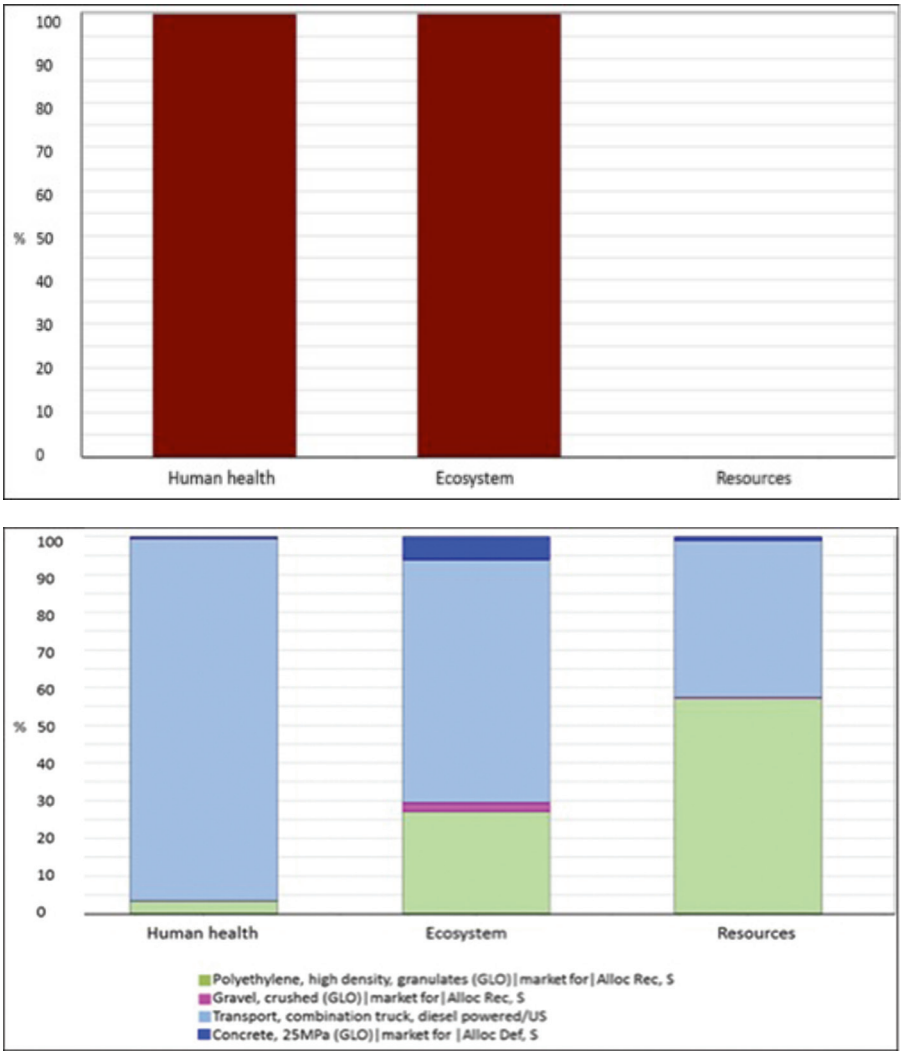

Figure 4 *Environmental impacts associated with allowing ingress (a) and prevention of ingress (b) on surface water and subsequent formation of AMD.*

the surrounding geology resulting in water containing potentially harmful elements and low pH. This makes the water not suitable for human consumption and causing drastic effects to the flora and fauna. Ingress control depletes the resources as shown in Figure 5. This is due to the various raw materials that are required to prevent ingress control. This raw materials are made from the resources that found in the environment.

Conclusions

According to this life cycle assessment, allowing ingress has substantial negative effects on two of the three assessment criteria; human health and ecosystem depletion. Alternatively, ingress control has a greater effect on resource depletion. This information enables decision makers to select a solution based on their preference and needs. In situations where natural resources are critical, it may be best to allow ingress and follow up with AMD remediation before it affect both ecosystems and human health. In cases where human health is critical, the option may be to implement ingress control. LCA is a valuable tool to assess the true environmental impacts of processes in order to enable wise

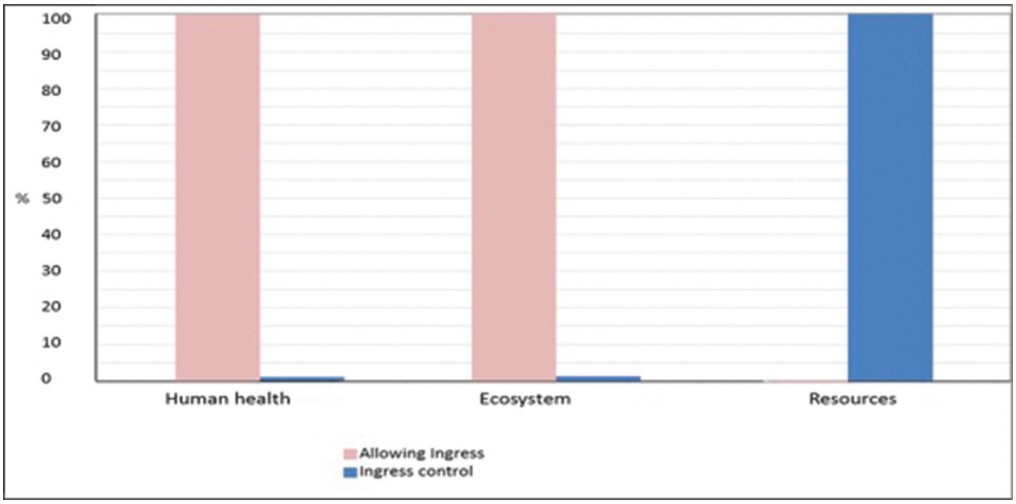

Figure 5 *The comparison of the environmental impacts due to the prevention of ingress and allowing ingress.*

decision making. The role of LCA is not to give a directive, rather, to reveal trade-offs for proposed solutions and scenarios.

Recommendations

It is recommended that LCA be continuously used in other projects to ensure that solutions proposed to stakeholders have been evaluated for environmental impact.

Acknowledgements

Our sincere appreciation goes to the management of Council for Geoscience for the support of the study and the Department of Mineral Resources and Energy for funding of the Mine Water Management project that allowed this study to be undertaken.

References

Blowes, D.W. *et al.*, 2003. The geochemistry of acid mine drainage. In Holland, H.D. & E. G. Turekian, K.K., (Lollar, B.S. (Ed.), eds. Treatise on Geochemistry. Oxford, Elsevier, pp. 149–204.

Curran, M. A., 2006. Life-Cycle Assessment: Principles and Practice. Cincinnati, OH: National Risk Management Research Laboratory, Office of Research and Development, USEPA.

Gray, N.F., 1998. Acid mine drainage composition and the implications for its impact on lotic systems. Water Research, 32(7), pp.2122–2134.

Hengen, Tyler J., Squillace, Maria K., O'Sullivan, Aisling D., Stone, James J., 2014. Life cycle assessment analysis of active and passive acid mine drainage treatment technologies. Resources, Conservation and Recycling. 86. 10.1016/j.resconrec.2014.01.003.

ISO. (2006). 14040: Environmental Management–Life Cycle Assessment–Principles and Framework. London: British Standards Institution.

Lehtinen, H., Saarentaus, A., Rouhiainen, J., Pitts, M., and Azapgic, A., 2011. A Review of LCA Methods and Tools and Their Suitability for SMEs. Manchester, UK: Europe Innova.

McCarthy, T.S., 2011. The impact of acid mine drainage in South Africa. South African Journal of Science, 107(5/6), pp.1–7.

Nordstrom, D.K., 2011. Applied Geochemistry Hydrogeochemical processes governing the origin, transport and fate of major and trace elements from mine wastes and mineralized rock to surface waters. Applied Geochemistry, 26, pp.1777–1791.

Wolkersdorfer, C., 2008. Water Management at Abandoned Flooded Underground Mines: Fundamentals, Tracer Tests, Modelling, Water Treatment. Springer-Verlag, Heidelberg, Berlin.

Younger, P. L., 1997. The longevity of mine water pollution: a basis for decision-making. Science of the Total Environment, 194–195, 457–466.

Gravel Bed Reactors: Semi-Passive Water Treatment Of Metals and Inorganics

Silvia Mancini[1], Rachel James[1], Evan Cox[2], James Rayner[3]

[1]*Geosyntec Consultants Inc., 1243 Islington Ave #1201, Etobicoke, ON M8X 1Y9, Canada, smancini@geosyntec.com, rjames@geosyntec.com*

[2]*Geosyntec Consultants Inc., Accelerator Centre, 295 Hagey Blvd #290, Waterloo, ON N2L 6R5, Canada, ecox@geosyntec.com*

[3]*Geosyntec Consultants Ltd, Unit 2 Aztec Centre, Aztec West, Almondsbury, Bristol BS11 0US, UK, james.rayner@geosyntec.com*

Abstract

Diffuse impacts to surface waters are a critical issue facing mining industries, given rigorous environmental quality standards. Many conventional treatment technologies are expensive and difficult to comply with discharge criteria. Gravel Bed Reactors (GBR™) are a versatile semi-passive treatment technology capable of addressing a variety of water quality issues through altering the geochemistry of extracted mine water. GBRs™ offer simpler, cost-effective alternatives to water treatment facilities, packed or fluidized bed reactors and the possibility to re-use waste rock as packing media. GBRs™ allow installation of smaller systems in remote, challenging environments and the potential to treat mine water at source.

Keywords: Biological Treatment, pH Adjustment, Semi-Passive, GBR™

Introduction

Managing metal and inorganic mass loading in extracted mine water and reducing diffuse impacts to surface water present key challenges to mining globally. The geochemistry of mine water can vary widely including highly acidic or alkaline pH and elevated and variable concentrations of multiple constituents. Metal cations (e.g. cadmium, lead, zinc), transition metals (iron, manganese, copper, chromium, mercury), nonmetals (e.g. sulfur, nitrogen, selenium), metalloids (arsenic, antimony) and actinides (uranium) may be present in mine water. Where these constituents are present in the geological formation of the target resource, they can be mobilized through disturbance of the material and exposure to the atmosphere and/or aerated waters. Nitrogen compounds may also be present associated with degradation products of processing (e.g. gold cyanidation) or residual waste from nitrate- and ammonia-based explosives.

A wide range of commercially available solutions exist for treatment of mine water; however, operational requirements render most conventional technologies expensive and difficult to comply with regulatory constraints, including discharge criteria. Gravel Bed Reactors (GBR™) are a semi-passive water treatment technology capable of addressing the variety of water quality issues typically encountered in mine water. To date, the treatment of metals and inorganics using GBRs™ has focused on inducing microbial and chemical processes to alter mine water geochemistry to degrade and/or immobilize problematic constituents, that have proved to be effective in reducing mass loading in treated discharges to receiving environments/surface waters and the requirement for other treatment technologies to meet discharge criteria.

Methods

A GBR™ consists of an engineered bed of gravel/media within a lined container or cell through which mine impacted water containing constituents of concern is passed and treated through addition of biological and/or chemical amendments. Mine impacted

surface water or groundwater (the influent) are typically diverted through the GBR™ under natural gradients or can be pumped to the GBR™ if necessary. Depending of the contaminants to be treated, amendments such as electron donors (typically carbon substrates), electron acceptors (typically oxygen, nitrate or sulfate) and/or pH buffers (e.g. carbon dioxide) are dosed into the influent within the upgradient portion of the GBR™ to promote the desired biological and/or geochemical reactions prior to discharge of the effluent.

GBRs™ are conceptually simple and very flexible reactors that can be engineered in varying ways to treat a wide variety of contaminants close to the source water, including in remote environments. GBRs™ can be either installed below ground surface within an excavation, onsurface within a natural depression, bunded or constructed cell, or a combination of both, i.e. some portion below ground level surrounded by a bund (Figure 1).

Key components of the GBR™ system typically include (Figure 2):

- A single or composite liner with a cover and insulating layer to hydraulically isolate the gravel bed from the surrounding environment, specifically exchanges with groundwater, precipitation infiltration and/or oxygen diffusion into the GBR™.
- Gravel bed media to support the growth and activity of microbes and biofilms and provide structural integrity of the treatment cell. Engineered material may be used or waste rock crushed to a consistent particle size, where design criteria for long-term geotechnical performance and leaching are met for its re-use in the treatment cell.
- Amendment delivery system(s) comprising storage and mixing tanks, dosing pumps and associated pipework in connection with a manifold header system within the upgradient portion of the GBR™ to deliver amendments uniformly into the saturated gravel bed media.
- Monitoring wells installed in the gravel bed media to permit measurement or sampling to assess water geochemistry and GBR™ performance.
- An upgradient equalization pond, with filtration if required, may be used to dampen fluctuations in influent volumes and water geochemistry entering the GBR™, with a downgradient effluent buffer pond or tank to adjust effluent geochemistry to meet regulatory criteria for discharge to the environment, in particular realignment of dissolved oxygen, pH, suspended solids and/or temperature to ambient conditions.
- In cold climates, heating equipment may be installed to prevent freezing of influent water and amendment delivery systems and/or to enhance sub-optimal reaction rates, with the potential to improve GBR™ operational efficiency and performance in challenging environments.

Operation of the GBR™ consists of monitoring and sampling influent, effluent and GBR™ geochemical conditions (flow

Figure 1 *Example construction of a subsurface GBR™.*

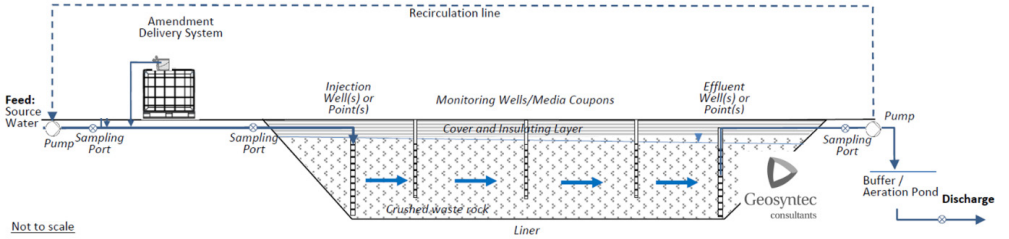

Figure 2 Schematic Cross-Section of a Typical GBR™.

and concentrations) and altering amendment dosing requirements to ensure the treatment remains in compliance with discharge criteria. Experience has shown that real-time measurement and data acquisition instrumentation linked to a programmable logic controller (PLC) with remote access may allow for more efficient GBR™ operation, permitting real-time control and adjustment of the system in response to often dynamic changes in influent conditions.

A wide variety of biological and geochemical processes can be implemented for mine water treatment in the GBR™ (e.g. Rittman & McCarty 2001, Simon *et al.* 2002, Skousen *et al.* 2017):

1. Reductive processes initiated in the presence of electron donors within GBRs™, e.g. natural organic matter, added carbon substrates:

- Biologically mediated degradation of anions (e.g. nitrate, nitrite, phosphate, chlorate, perchlorate and sulfate) to their elemental constituents under anaerobic conditions in the presence of natural or added electron donors, e.g. carbon substrates;
- Redox sensitive metals can be reduced under appropriate redox conditions from soluble forms to insoluble forms that precipitate, e.g. soluble species of hexavalent chromium ($Cr^{VI}_{(aq)}$) and selenite ($Se^{VI}_{(aq)}$) may be reduced to insoluble forms of trivalent chromium ($Cr^{III}_{(s)}$) and elemental selenium ($Se^{0}_{(s)}$);
- Transition metals (e.g. iron, manganese, copper, chromium, mercury) and divalent cations (e.g. cadmium, lead, zinc) can be precipitated as metals sulfides by inducing microbial sulfate reduction to sulfide, where sulfate is present or added in addition to electron donors.

2. Adjusting the pH of the influent water:

- Metalloids present as oxyanions (e.g. arsenate, AsO_4^{3-}) can be immobilized through shifting pH to the acidic range promoting adsorption onto charged mineral surfaces such as iron oxides or clays.
- Metals present as divalent cations (e.g. copper, zinc) can be immobilized by adsorption on mineral surfaces by shifting pH towards neutral or the alkaline range.
- Alkalinity and acid rock drainage-related issues such as acidity, can also generally be adjusted in GBRs™ through addition of various buffers and reactants.

3. Other treatment reactions:

- Phosphate induced stabilization of lead, uranium, plutonium, zinc and cadmium using Apatite II is capable of binding metals within insoluble new minerals.
- Organic constituents associated with mine operations (e.g. petroleum hydrocarbons, wastewater effluent) can be degraded with addition of electron acceptors such as oxygen nitrate or sulfate, to reduce biological oxygen demand (BOD) and chemical oxygen demand (COD) to achieve discharge criteria.

The potential to treat multiple contaminants using the same process is a key benefit of GBRs™, e.g.in anaerobic GBR™ fed with electron donors and sulfate, it could be possible to treat anions, certain redox sensitive metals and divalent metals.

The treatability of contaminants is typically determined through performance of bench-scale studies. Once the treatment reactions

have been selected, the GBR™ design is governed by the mass loading of constituents of concern, the target concentrations in the effluent and the rate(s) of treatment. Estimation of the time required to reduce the influent concentrations of constituents to effluent targets at the anticipated flow rate and mass degradation/removal rate inform the hydraulic residence time required to achieve treatment goals (Vasquez *et al.* 2016).

The required amendment concentrations and frequency of dosing depends on the influent conditions, the concentrations of the constituents of interest and co-contaminants that might compete to utilize the amendments. Under-dosing of the amendments can result in incomplete treatment, so it is important to account for uncertainties by applying safety factors to the amount of amendment theoretically required to complete the treatment. However, over-dosing not only incurs unnecessary costs, but can cause undesirable reactions to occur, e.g. with excessive addition of electron donors, it is possible to generate hydrogen sulfide gas and methane. Balancing amendment addition is thus a critical element to the success of a GBR™ design. Reduced scale GBR™ pilot tests provide cost-effective means to refine key design parameters and inform full scale implementation (Figure 3).

GBR™ Applications

GBRs™ have been used to treat industrial effluent and mine water since the late 2000s (Table 1). Pilot tests have been conducted in North America for treatment in GBRs™ of other contaminants including perchlorate.

Case Study 1 – Urban stream, California, USA

A subsurface GBR™ system was designed and implemented to treat selenium in an urban stream. Selenium had been mobilized from anoxic sediments that were exposed to atmosphere during urban development of the area. Laboratory treatability studies were conducted to evaluate potential methods to reduce selenium concentrations to <5 µg/L and reduce nitrogen loading by 50%. Initially mesocosm studies confirmed potential to reduce selenium in sediment mixed with organic material (electron donor). Subsequently, column studies were

Figure 3 *Example of a GBR™ pilot test system.*

Table 1 *Examples of Full-Scale GBR™ Applications.*

Location	Constituents Treated	Influent Conditions	Effluent Conditions	Flow rate	Media Bed Dimensions
				m^3/d	m, L × W × D
Urban stream, California, USA	Selenium Nitrate	20-40 µg/L 5-15 mg/L	2.3-12 µg/L <8 mg/L	730-1,250	12 × 60 × 3
Mine site, West Virginia, USA	Selenium Nitrate	15-25 µg/L 6 mg/L	<5 µg/L <6 mg/L	270 (average)	28 × 8 × 1.5
Cement plant, USA	Arsenic Alkalinity	>300 µg/L pH ≈13.9	5-10 µg/L pH 7-8	Variable (passive)	14 × 26 × 3

performed to confirm selenium reduction in sand and gravel media, which had more predictable flow characteristics and provide GBR™ design and operational information, including electron donor selection and dosing, acceptable oxidation-reduction potential (ORP) ranges, potential for bio-fouling of the bed media, gas generation and selenium remobilization.

The GBR™ was designed as a lined excavated pit underneath the planned location of an athletic fields. The reactor bed was constructed inside a geomembrane lined containment system, overlain by 1 m soil cover. The bed media was 2 cm gravel and the electron donor sodium benzoate. The influent flow was fed by a header pipe and equalized in a distribution reservoir to discharge horizontally through the GBR™ to an outlet where the treated water was collected and then discharged.

The performance of the GBR™ under start-up, steady-state and upset testing conditions was assessed over a 14-month period (Figure 4). Following the performance evaluation, the GBR™ was operated for more than 6 years, achieving the target reductions in selenium and nitrate concentrations during steady state operations.

The GBR™ was considerably smaller than the constructed wetland alternative treatment under consideration (≈2,200 m^3 compared to ≈80,000 m^3) and enabled the overlying land to be redeveloped during treatment. The system installed relied upon regular sampling and analysis of the influent water to determine electron donor dosing, that resulted in periods of under- and over-dosing and suboptimal treatment. With real-time monitoring of the influent geochemistry, it is anticipated that this GBR™ would have consistently achieved non-detect concentrations of selenium and nitrate in the effluent.

Case Study 2 – Mine Site, West Virginia, USA

Surface water affected by selenium in newly exposed rock was treated within a GBR™ constructed beneath a parking lot to minimize disruption of mining operations. The excavation was lined with a geomembrane and gravel placed allowing the parking area to be reinstated above the GBR™. The GBR™ was designed to treat influent flows

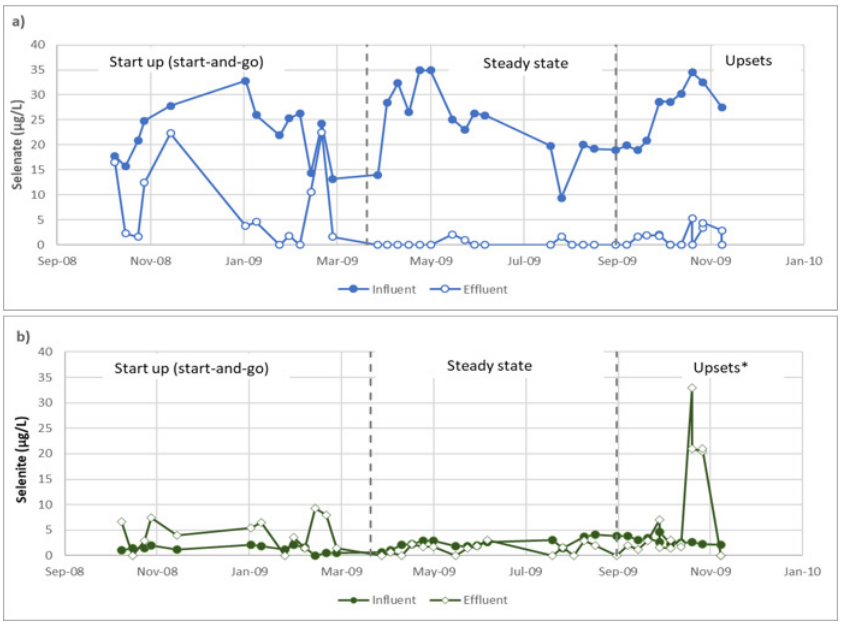

Figure 4 *Performance Evaluation for Selenium treatment in a GBR™. Upset testing involved shocking the system with hydrogen peroxide to oxidize immobilized selenium within the GBR™.*

up to 550 m^3/day, with a hydraulic residence time of 11 hours with the reactor bed. The selenium affected seep water from the newly exposed rock was collected and pumped to the GBR™, where citric acid and acetic acid (electron donors) were added to support bacteria in selenium and nitrate reduction. The GBR™ was operated for 8 months; after a 2-month stabilization period, selenium and nitrate concentrations in the effluent were consistently <5 µg/L and <6 mg/L for the remaining 6 months of operation.

Case Study 3 – Cement Plant, USA

A cement plant operated for more than 80 years in a remote area of the USA. The plant generated cement kiln dust, a fine-grained cement byproduct consisting of highly alkaline material, that was deposited in a nearby ravine. The cement kiln dust caused groundwater to become highly alkaline (pH 13.9) and leaching of metals from native soils, including arsenic, threatening water quality in a nearby pristine mountain stream.

Treatability studies indicated that the arsenic solubility and mobility was linked to the elevated pH and that by reducing pH, arsenic could be immobilized. A field pilot test was conducted to confirm the effectiveness of carbon dioxide (CO_2) diffusion at lowering pH and treating the arsenic in the groundwater.

The GBR™ comprised a 220 m wide funnel-and-gate design to capture the affected groundwater and direct it into the GBR™ under natural flow gradients. The GBR™ comprised soil-cement-bentonite retaining walls enabling the treatment bed to be constructed in place. The treatment bed comprised gravel with baffles to reduce dead flow zones within which silicone membranes were installed to diffuse CO_2 into the groundwater to neutralize the pH and promote immobilization of arsenic, chromium, lead and manganese to achieve compliance with water quality criteria. Given the remote location of this site, the GBR™ was required to be durable, require little maintenance and controllable remotely. The in-situ groundwater remedy produces no waste byproduct and the treated water is discharged directly to surface water without need for further treatment.

Conclusions

GBRs™ have been demonstrated to be capable of treating a wide range of constituents commonly present in mine water, by inducing microbiological and geochemical processes with biological and/or chemical amendments. GBRs™ are simpler, less-engineered solutions, requiring less tankage and equipment, compared water treatment facilities, packed bed bioreactors and fluidized bed reactors, while providing enhanced treatment control and requiring less space than passive treatment options (e.g. engineered wetlands, permeable reactive barriers [PRBs]). Comparatively small GBR™ systems can be installed and operated in remote locations, allowing for mine water treatment at or close to the source, and therefore offer a cost-effective, alternative option for mitigating diffuse impacts of mine water.

References

Rittman BE, McCarty PL (2001) Environmental Biotechnology: Principles and Applications. McGraw-Hill Education

Simon FG, Meggyes T, McDonald C (2002) Advanced Groundwater Remediation: Active and Passive Technologies. Thomas Telford Publishing

Skousen J, Zipper CE, Rose A, Ziemkiewicz PF, Nairn R, McDonald LM, Kleinmann RL (2017) Review of Passive Systems for Acid Mine Drainage Treatment. Mine Water and the Environment 36:133—153. https://doi.org/10.1007/s10230-016-0417-1

Vasquez Y, Escobar MC, Neculita CM, Arbeli Z, Roldan F (2016) Biochemical passive reactors for treatment of acid mine drainage: Effect of hydraulic retention time on changes in efficiency, composition of reactive mixture, and microbial activity. Chemosphere 153:244–253. https://doi.org/10.1016/j.chemosphere.2016.03.052

Performance of the Hybrid Linear Flow Channel Reactor: Effect of Reactors in Series for Enhanced Biological Sulfate Reduction and Sulfur Recovery

Tynan Steven Marais[1], Rob John Huddy[1], Rob Paul van Hille[1,2], Susan Therese Largier Harrison[1]

[1]*University of Cape Town, 21 Lameer Street, 7550 Cape Town, South Africa, mrstyn001@myuct.ac.za*

[2]*Moss Group, 13 Bell Crescent, Westlake Business Park, 7945 Cape Town, South Africa*

Abstract

Acid rock drainage (ARD) is a global crisis that will have long-lasting environmental consequences. The application of semi-passive biological sulfate reduction (BSR) is a potential solution for the remediation of persistent low volume ARD effluents. However, major challenges of BSR, including slow reaction kinetics and management of the generated sulfide, still need to be addressed. The development of a hybrid Linear Flow Channel Reactor (LFCR) has shown promise for remediation of sulfate-rich effluents. In this study, the operation of two hybrid LFCRs connected as a dual reactor system was assessed for the improved removal of residual sulfide and COD.

Keywords: Semi-Passive Bioprocess, Biological Sulphate Reduction, Partial Sulphide Oxidation, Sulphur Recovery

Introduction

The generation and discharge of acid rock drainage (ARD) as a result of mining activities in regions rich in sulfidic minerals has significant implications on the receiving ecosystems (McCarthy, 2011). ARD is generally characterised as acidic water containing high concentrations of sulfate, metals and semi-metals. The long term environmental and socio-economic effects has necessitated the need for the development of ARD treatment technologies.

The semi-passive hybrid LFCR process incorporating both biological sulfate reduction and partial sulfide oxidation has shown potential for application as part of a wastewater treatment to address persistent low volume ARD characterised by high sulfate concentrations (Marais *et al*., 2020a). The process facilitates the formation of an anaerobic zone, within the bulk volume, and an aerobic zone at the air-liquid interface. Sulfide generated within the anaerobic zone by SRB is subsequently oxidised to elemental sulfur by sulfur oxidising bacteria (SOB) near the liquid interface, resulting in the formation of a floating sulfur-rich biofilm (FSB). The FSB is intermittently recovered and serves as a value end product that can be applied in agriculture as a fertiliser.

Biological treatment of sulfate-rich waste streams is dependent on the initial feed sulfate concentration as well as its loading rate. In these processes the sulfate loading rate can be mediated by dilution rate (HRT) or feed sulfate concentration. During wastewater treatment, initial sulfate concentrations can vary based on environmental parameters and source of the waste stream. Sulfate-rich contaminated wastewater can range between 1 - 10 g/L and can impact the performance of an applied treatment (Brahmacharimayum *et al*., 2019). Several studies have evaluated the effects of feed sulfate concentrations on BSR under different reactor configurations and operating parameters (Erasmus, 2000; Moosa *et al*., 2002; Al-zuhair *et al*., 2008; Oyekola *et al*., 2010). These studies highlighted that the sulfate reduction rate increases as feed sulfate concentration increases. However, a decline in overall sulfate conversion efficiency has been attributed to the limitation of SRB to adequately reduce sulfate at high loading rates that exceed its metabolic potential. In addition, several studies reported a decline in BSR performance due to sulfide

inhibition. Previous studies have evaluated the effects of hydraulic residence time on the performance of the hybrid LFCR at laboratory scale treating synthetic sulfate-rich wastewater (Marais *et al*., 2020b). From these investigations, some limitations of the process were identified which included the sulfur recovery inefficiency associated with the management of the FSB as well as the untreated residual sulfide and COD released in the final effluent.

The effects of feed sulfate concentration have yet to be evaluated within the hybrid LFCR system. Therefore, an investigation into the effects of feed sulfate concentration on the performance of the hybrid LFCR is critical to further characterise the process. In this study, the operation of two hybrid LFCR units connected in series was assessed for the improved removal of residual sulfide and COD. The aim of the study was to minimise secondary pollution (residual COD, sulfate and sulfide) and increase overall sulfur recovery.

Methods and Materials

Microbial culture and system operation

The SRB culture has been maintained at the University of Cape Town (UCT) on modified Postgate B medium (Marais *et al*., 2020a). The SOB culture was developed from the SRB culture and has been maintained as floating sulfur biofilms in LFCRs (van Hille *et al*., 2015). An 8 L LFCR was operated continuously at a 4 day hydraulic residence time (HRT) with a feed sulfate concentration of 1000 mg/L and supplemented with of 60% (v/v) sodium lactate solution. This provided a chemical oxygen demand (COD) to sulfate ratio of 0.7.

Dual hybrid linear flow channel reactor system

A detailed description of the reactor design and laboratory demonstration of the 8 L hybrid LFCR have been described in a previous investigation (Marais *et al*., 2020b). Key features of the hybrid LFCR (Fig. 1) includes carbon micro fibres as support matrices for enhanced biomass retention, a heat exchanger for temperature control, sampling ports positioned along the length of the reactor and a mesh-screen positioned just below the air-liquid interface for harvesting the FSB. A second LFCR unit was connected downstream of an 8 L LFCR that had been operational for over 488 days (Marais *et al*., 2020b). An image of the laboratory set-up

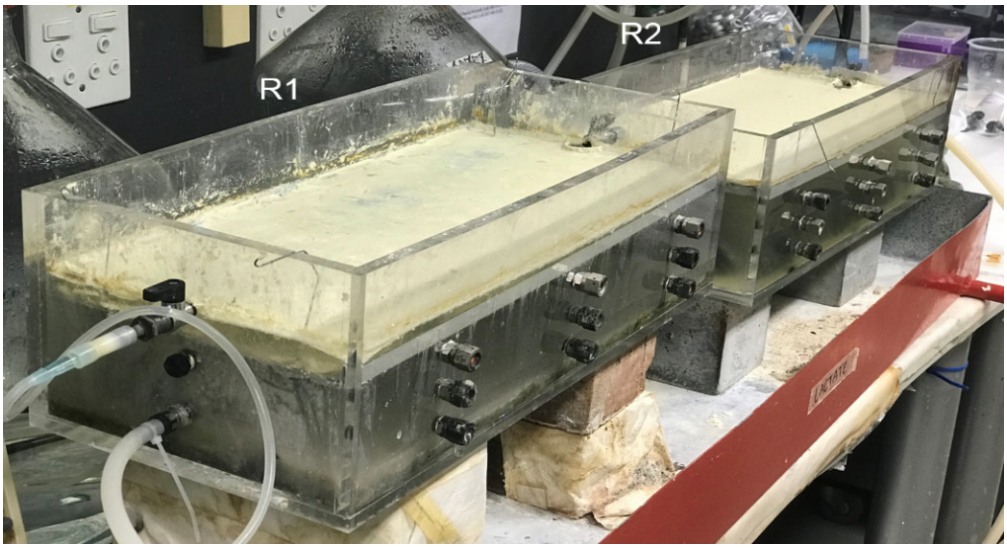

Fig.1 *Dual reactor laboratory set-up showing the two identical 8 L LFCR units connected in series, the primary reactor (R1) was elevated to ensure passive gravitational flow into the secondary reactor (R2). The photograph was taken 21 days after biofilm disruption showing a matured FSB at the surface of both reactors.*

of the dual reactor system is shown in Fig. 1. The secondary reactor was inoculated by overflow collected from the primary reactor. Disruption and harvesting of the FSB were performed intermittently in both reactors. An additional biofilm disruption in the secondary reactor was only performed independently of the primary reactor during operation at 5 and 10 g/L feed sulfate concentrations. The objective was to demonstrate the effect of regulating the frequency of biofilm disruption on sulfide conversion and sulfur recovery.

Analytical techniques

Dissolved sulfide was quantified using the colorimetric N,N-dimethyl-p-phenylenediamine method (APHA, 2012). Residual sulfate concentrations were measured by the barium sulfate method (APHA, 2012). Volatile fatty acid (VFA) analysis was determined using HPLC on a Waters Breeze 2 HPLC system (van Hille *et al.*, 2015). Redox potential and pH were measured on a Metrohm pH lab 827 redox meter relative to a Ag/AgCl reference electrode and a Cyberscan 2500 micro pH meter, respectively. Elemental composition analysis was performed through a CHNOS Elementar Vario EL Cube Elemental Analyser.

Effect of feed sulfate concentration on process performance

Process performance was evaluated across feed sulfate concentrations of 1, 2.5, 5, and 10 g/L. The feed COD/SO_4 ratio was maintained at 0.7 over the range of feed sulfate concentrations to ensure sufficient electron donor for complete sulfate reduction. The FSB was disrupted intermittently where the biofilm is physically fragmented and allowed to settle onto the mesh screen just below the liquid surface. During harvesting of the FSB the mesh screen is completely removed from the reactor and the sulfur-rich biofilm material is collected. At the end of each experimental run, between adjusting feed sulfate concentrations, a biofilm harvest was performed. The harvested FSB was dried at 80 °C and stored for elemental analysis.

Results and discussion

The residual sulfate concentration profile across the dual reactor system is shown in Fig.2a. During operation at 1 g/L feed sulfate concentration, the residual sulfate concentration was relatively stable across both reactors, suggesting little sulfate reduction occurred within the secondary reactor. Once operated at 2.5, 5 and 10 g/L feed sulfate concentration, there was a slight reduction in sulfate within the secondary reactor. However, this was not comparable to the performance achieved in the primary reactor despite there being sufficient residual VFA (not shown) and sulfate available to favour BSR activity. Volumetric sulfate reduction rate (VSRR) increased (0.046 to 0.200 mmol/L.h) as feed sulfate concentration was increased from 1 to 5 g/L in the primary reactor before decreasing to 0.110 mmol/L.h at 10 g/L feed sulfate concentration. The sulfate conversion efficiency decreased from 42 to 10% as the feed sulfate concentrations increased from 1 and 10 g/L, respectively.

Effective removal of residual sulfide was achieved in the secondary reactor. Sulfide concentration rapidly decreased after every biofilm disruption (Fig. 2b). As the biofilm regenerated, sulfide concentration increased nearing the expected theoretical sulfide based on sulfate conversion. This was consistent with previous findings, where the FSB forms a barrier that impedes oxygen mass transfer across the air-liquid interface. As the biofilm matures oxygen transfer declines, eventually inhibiting sulfide oxidation. Through controlled intermittent disruption of the FSB, oxygen ingress into the sulfide-rich reactor volume is significantly increased allowing sulfide oxidation to proceed. In the hybrid LFCR the steep oxygen and sulfide concentration gradients that form across the air-liquid interface provide the ideal redox and pH conditions to favour partial sulfide oxidation to elemental sulfur. In this study, the residual sulfate data confirmed that complete sulfide oxidation to sulfate was negligible in both reactors, a strong indication that elemental sulfur production was favoured throughout the study. This was further supported by the consistent elevated pH seen within the secondary reactor which was expected due to the production of hydroxyl ions as a by-product of partial sulfide oxidation.

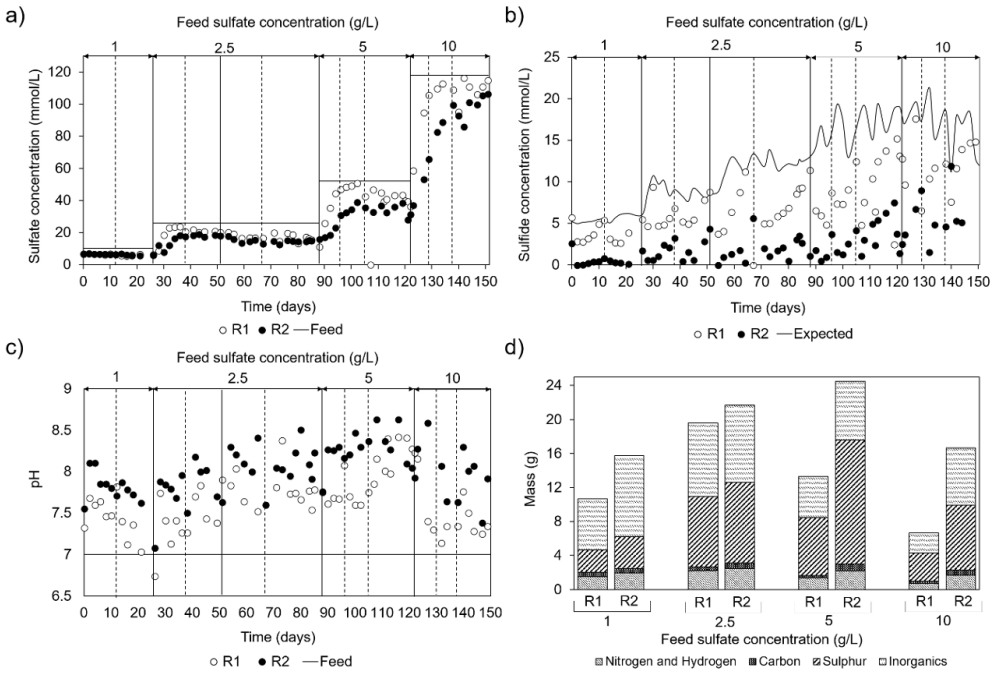

Fig. 2 *Effect of feed sulfate concentration on performance of the dual hybrid LFCR system. The a) residual and feed sulfate concentration, b) measured and expected sulfide concentration and c) pH profile over time as well as d) the FSB harvested in the primary and secondary reactors shown. Vertical dotted and solid lines represent biofilm disruption and harvesting events.*

A marked decrease in pH occurred within the primary reactor during operation at 10 g/L feed sulfate concentration, which ranged between 7.1 and 7.3 (Fig. 2c). These results coincided with the notable decrease in sulfate conversion. In sulphidogenic reactors the pH plays a critical role in the inhibition of sulfide to SRB activity (Moosa *et al*., 2006; van den Brand *et al*., 2016). Undissociated $H_2S_{(g)}$ has the strongest inhibitory effect due to its ability to permeate the cell membrane and resulting in denaturation of enzymes. The quantity of $H_2S_{(g)}$ is largely determined by the pH where hydrogen sulfide exists as a mixture of $H_2S_{(g)}$ and HS^- between pH 6 to 8 (Moosa & Harrison, 2006). Below pH 6, undissociated $H_2S_{(g)}$ dominates while at a pH >7.5, the $H_2S_{(g)}$ fraction of the total sulfide in solution is minimal (van den Brand *et al*., 2016). Therefore, the observed decline in SRB acidity is most likely a consequence of sulfide inhibition due to high sulfide concentrations (> 14.9 mmol/L) concomitant with the decrease in pH below 7.5 (Fig.2b and c).

VFA concentration analysis (not shown) confirmed lactate metabolism in the dual reactor system occurred predominantly via the incomplete oxidation pathway coupled to sulfate reduction. As feed sulfate concentration increased there was a decrease in lactate conversion from 100 to 18% in the primary reactor, at 1 and 10 g/L feed concentration, respectively (Table 1). Lactate conversion increased at every feed concentration with the addition of the secondary reactor. The presence of residual propionate concentrations throughout the study indicated that lactate fermentation occurred. The incomplete oxidation of lactate led to an accumulation of predominantly acetate in the overflow released into the secondary reactor. Since acetate was the most abundant carbon source, the activity

Table 1 Effect of feed sulfate concentration on overall process performance of the hybrid LFCR comparing single and dual reactor operation.

	Single reactor					Dual reactor system			
Sulfate concentration (g/L)	VSRR (mmol/L.h)	Lactate conversion (%)	Sulfate conversion (%)	Sulfide conversion[a] (%)	Sulfur Recovery[b] (%)	Lactate conversion (%)	Sulfate conversion (%)	Sulfide conversion[a] (%)	Sulfur Recovery[b] (%)
1	0.046	100	42	38	85	100	42	85	93
2.5	0.119	77	44	52	54	100	49	79	68
5	0.200	36	34	39	41	53	36	68	71
10	0.110	18	10	31	51	36	10	61	85

[a] Cumulative sulfide conversion based on the expected theoretical sulfide concentration and final effluent sulfide concentration over the duration of each experimental run

[b] Elemental sulfur recovery from harvested FSB calculated based on sulfide conversion

of acetate utilising bacteria was favoured. However, a decrease in acetate concentration in the secondary reactor was not coupled to biological sulfate reduction which strongly indicated the lack of active acetate utilising SRB within the system. Although there was slight fluctuation in propionate concentration between feed sulfate concentrations, little difference between the primary and secondary reactors was observed over the duration of the study. This suggested that minimal lactate fermentation to propionate occurred within the secondary reactor. Furthermore, residual propionate was not utilised as an alternative carbon source within the secondary reactor.

Given that the secondary reactor relied solely on microbial colonisation via the overflow received from the primary reactor where incomplete lactate oxidation occurred, the inoculum may not have selected for a complete oxidising SRB community that can utilise acetate as a carbon source. Furthermore, the secondary reactor may have required a longer acclimatisation period between inoculation and the start of the study to allow the SRB community to establish and for biomass to accumulate in the reactor. Incomplete substrate utilisation and accumulation of acetate in BSR systems is a major drawback of the process and is well documented. To overcome the low sulfate conversion and acetate utilisation, the secondary reactor could be pre-colonised separately with an active acetate-utilising SRB culture prior to dual operation.

The amount of FSB harvested, and elemental composition analysis is shown in Fig.2d. Recovery in the primary reactor increase from 1 to 2.5 g/L and then decreased during operation at 5 and 10 g/L feed sulfate concentration. Although the amount of biofilm recovered from the secondary reactor was slightly higher compared to the primary reactor, during operation at 1 and 2.5 g/L, the marked increase in FSB recovered during operation at 5 and 10 g/L was a consequence of the additional biofilm disruption events that were performed. This allowed the biofilm to regenerate, outside of the biofilm disruption regime applied to the primary reactor. The results demonstrated that an increase in the frequency of biofilm disruption in the secondary reactor can increase the overall sulfide conversion and sulfur recovery within the hybrid LFCR (Table 1). A comparison of the elemental composition revealed that the FSB recovered from both reactors at each feed sulfate concentration, on average, exhibited a similar composition. However, there was an increasing trend in the proportion of elemental sulfur content (24±0.5 to 56±5.8%; mean±s.d) within the biofilm as the feed sulfate concentration increased from 1 to 5 g/L. This coincided with the observed increase in VSRR as the feed sulfate concentration increased.

Conclusion

The key objective of the study was to evaluate the effect of feed sulfate concentration, minimise secondary pollution (residual COD, sulfide) and increase overall sulfur recovery. The highest VSRR was achieved at a 5 g/L feed sulfate concentration. Although there was decrease in sulfate conversion as sulfate loading increased, the system was able to maintain sulfate reduction at the highest feed sulfate concentration of 10 g/L. Conversion of untreated lactate occurred within the secondary reactor however, there was an accumulation of acetate (residual COD) within the system that was not effectively removed. The addition of the secondary reactor enhanced overall sulfide oxidation efficiency (85%) and sulfur recovery (93%), significantly increasing the overall performance of the hybrid LFCR when compared to single unit operation. In addition, the study demonstrated that the frequency of disrupting the biofilm in the secondary reactor is an important parameter to achieve maximum sulfur recovery through the FSB. Efforts to increase sulfate reduction and COD removal across the dual reactor system could be achieved by separately establishing the secondary reactor on an acetate based feed to select for an active SRB community capable of acetate metabolism.

Acknowledgements

The authors acknowledge the Water Research Commission (K5/2393), the Department of Science and Technology (DST), and the National Research Foundation (NRF) of South Africa for funding. STLH holds the South African Research Chair in Bioprocess Engineering (UID64778). TM acknowledges Post-doctoral fellowship support from the NRF (UID 116722).

References

Al-zuhair, S., El-naas, M. H., Al-hassani, H. 2008. Sulfate inhibition effect on sulfate reducing bacteria. Journal of Biochemestry Technology. 1:39–44.

APHA, 2012. Standard methods for the examination of water and wastewater, 22nd edition. E. W. Rice, R. B. Baird, A. D. Eaton and L. S. Clesceri, Eds. American Public Health Association (APHA), American Water Works Association (AWWA) and Water Environment Federation (WEF). USA: Washington, D.C.

Brahmacharimayum, B., Mohanty, M.P., Ghosh, P.K. 2019. Theoretical and practical aspects of biological sulfate reduction: a review. Global NEST Journal. 21(2):222-224.

Erasmus, C.L. 2000. A preliminary investigation of the kinetics of biological sulfate reduction using ethanol as a carbon source and electron donor. MSc (Eng) dissertation. University of Cape Town, South Africa.

Marais, T.S., Huddy, R.J., Harrison, S.T.L. van Hille, R.P. (2020a) Demonstration of simultaneous biological sulfate reduction and partial sulfide oxidation in a hybrid linear flow channel reactor. Journal of Water Process Engineering.

Marais, T.S., Huddy, R.J., van Hille, R.P., Harrison, S.T.L. (2020b) Effects of reactor geometry and electron donor on performance of the hybrid linear flow channel reactor. Hydrometallurgy.

McCarthy, T.S. 2011. The impact of acid mine drainage in South Africa. South African Journal of Science. 107(5/6):1–7.

Moosa, S., Harrison, S.T.L. 2006. Product inhibition by sulfide species on biological sulfate reduction for the treatment of acid mine drainage. Hydrometallurgy. 83:214- 222.

Moosa, S., Nemati, M., Harrison, S.T.L. 2002. A kinetic study on anaerobic reduction of sulfate, Part I : Effect of sulfate concentration. Chemical Engineering Science. 57:2773–2780.

Oyekola, O.O., van Hille, R.P., Harrison, S.T.L. 2010. Kinetic analysis of biological sulfate reduction using lactate as carbon source and electron donor: Effect of sulfate concentration. Chemical Engineering Science. 65(16):4771–4781.

van den Brand, T.P.H., Roest, K., Chen, G.H., Brdjanovic, D., van Loosdrecht, M.C.M. 2016. Adaptation of Sulfate-Reducing Bacteria to Sulfide Exposure. Environmental Engineering Science. 33:242–249.

van Hille, R.P., Marais T.S., Harrison, S.T.L. 2015. Biomass Retention and Recycling to Enhance Sulfate Reduction Kinetics. Proceedings of the 10th ICARD & IMWA Annual Conference on Agreeing on Solutions for More Sustainable Mine Water Management. 21-24 April 2015. Santiago, Chile. 250-275.

Site Specific Optimisation Assessment

James Marsden[1], Steven Pearce[1], Tim Sambrook[1], Julia Dent[2], Andrew Barnes[3]

[1]*Cambrian Environmental Technologies Ltd., 1a Gower Street, Cardiff, Wales, CF24 4PA, United Kingdom, jmarsden@maelgwyn.com*

[2]*Mine Environment Management Ltd., 3a Vale Street, Denbigh, Wales, LL16 3AD, United Kingdom, spearce@memconsultants.co.uk, jdent@memconsultants.co.uk*

[3]*Geochemic Ltd., Lower Race, Pontypool, Wales, NP4 5UH, United Kingdom, abarnes@geochemic.co.uk*

Abstract

A large amount of mine sites globally are recognised to generate discharges in the circum-neutral range, and in recent times regulatory and social pressures have resulted in an increased focus on improving discharge quality for these sites. Because treatment of circum-neutral drainage depends on site specific conditions, and is very sensitive to water quality targets, an assessment methodology based around a treatability curve approach has been developed. This allows generation of a cost-treatability curve that can be based on site specific factors or "levers" that drive water treatment efficiency and cost.

Keywords: Circum-neutral, Water Treatment, Cost-treatability Curve, Zinc.

Introduction

There has been considerable research into mine water treatment, and numerous well developed technologies are commercially available. The majority of research and available technologies are predominantly targeted to acidic mine drainage (AMD) environments. Circum-neutral mine water tends to have low acidity and a circum-neutral pH, with low concentrations of iron. Metal species, such as zinc, are often still found at higher concentrations. Circum-neutral mine waters can be produced if there is little or no pyrite available to oxidise and produce acid, or there is carbonate host rock or gangue producing an acid buffing effect (Warrander and Pearce 2007). Treatment of low Fe circum-neutral mine waters is more challenging because of the lack of Fe and therefore reduced production of Fe(III) that can be used as a sorbent for other metal cations (Gooyong *et al.* 2018). In general the key "levers" for the removal of metal cations are;

- pH
- Oxidation for example Fe(II) to Fe(III)
- Sorption onto suitable media such as iron (hydr)oxide surfaces.
- Reduction potential to sulfides.

In this study we have reviewed the effect of these "levers" as applied to circumneutral drainage based on a literature study complimented by a program of laboratory testing to demonstrate how varying key "levers" will impact on water treatment outcomes. In brief beaker trials were carried out on low iron circum-neutral mine water from Nant-y-Mwyn lead mine, UK (Chemical properties for Nant-y-Mwyn mine drainage used in test work are shown in the Appendix) to explore the effect of:

- pH using a range of pH amendment products (lime, sodium hydroxide and sodium carbonate)
- sorption (using media such as iron oxide powder)
- Aeration (using air sparging)

In general an increase in pH causes metal removal from the soluble phase due to precipitation (hydrolysis) and increase in cation adsorption. The process of adsorption can happen from nearly 0% to 100% in a range of 1 or 2 pH units known as the 'adsorption edge' (Smith *et al.* 1999). Different types of adsorbent have been studied, whilst very few have been brought to commercial viability. For high Fe mine waters the "choice" of sorbent is simple, precipitation of Fe(III) oxides from the minewater itself creates a catalyst for further oxidation of Fe(II) and promotes sorption onto the Fe oxides with no requirement to add additional sorbents (Younger 2000). This

makes high Fe waters theoretically amenable to passive treatment options.

For low Fe mine waters (common for circumneutral drainage) however to achieve sorption as metal removal pathway, an external product is likely to be required as there is no natural sorbent that can be formed from within the minewater (unless the water is heavily reduced in which case it may carry elevated dissolved iron). Standard practice is to buy in produced sorbents such as activated carbon or aqueous ferric oxide, these are effective but can be expensive and in the case of aqueous ferric oxide makes the removal from water more complex (Chaudrhy *et al*. 2016). INAP (2009) recognises this factor and as such recommends that the generic passive treatment category for treatment of water with elevated circumneutral metals such as Zn are systems that aim to reduce dissolved metal species to soluble sulfides. Examples being anaerobic systems such as vertical flow ponds (VFPs) that utilise organic matter as a substrate (which acts as both a sorbent and a reducing agent). This is likely due to limestone treatment-based systems not generating high enough pH conditions to enable hydrolysis of such metals (i.e. minimum solubility for Zn occurs at pH>8) and because of the lack of dissolved iron in the mine water to effect sorption. Examples of passive treatment for metals such as zinc using VFP have been noted (Force Crag UK) as possible reference sites.

Aeration has been long recognised as a key feature in mine water treatment due to the effect of oxidation state on metal mobility, and also the effect of dissolved gases such as CO2 on the carbonate system and ultimately solution pH. Underground mine drainage waters are often depleted in oxygen and may be reducing, and also may be supersaturated with carbon dioxide due to a reaction with limestone or oxidation of organic carbon (Geroni *et al*. 2012). Given many circum-neutral mine waters are sourced from carbonate rich host rock or gangue (Warrender and Pierce 2007), circum-neutral mine waters may be affected by increased dissolved carbon dioxide. Previous studies on the introduction of aeration steps into mine drainage treatment systems have shown a profound affect on water chemistry with an increase in dissolved oxygen (DO) and driving off dissolved carbon dioxide, increasing pH and the oxidation potential of Fe(II), allowing increased precipitation (Kirby *et al*, 2009).

The Cost of Traditional High Density Sludge (HDS) Treatment

As would be anticipated based on an understanding of the key "levers" of water treatment described above the most common form of active mine drainage treatment is oxidation and chemical precipitation (metal hydrolysis). In this technology alkali reagents are added to mine water to increase the pH and promote metal precipitation (hydrolysis). HDS was developed as a more efficient form of oxidation and chemical precipitation to reduce the volume of sludge produced, from a maximum of 5% solids (w/w) in conventional systems to between 15% and 35% solids (w/w) for HDS (Bullen 2006). Chemical precipitation plants are used because they are effective at contaminant removal, allow precise process control which gives the ability to adapt to variable influent and effluent standards and are inherently scalable which means they can take up smaller land area than alternatives including passive treatments, particularly for higher treatment volumes (Trumm 2010).

Estimates of typical HDS costs can vary through a range (Table 1). Given these indicative unit costs are for general chemical precipitation treatment, and CAPEX for HDS is generally higher than for conventional systems, the maximum CAPEX value calculated here is likely to be closest to the actual cost of an HDS system. Further to this, when compared with the actual cost of Wheal Jane, UK phase 1 plant (treating 1240m^3/hr) of around US$4.7 million (Coulton *et al*. 2003) and estimated cost of an HDS treatment plant at Force Crag, UK (treating 22m^3/hr) of US$2.3 million (Bailey *et al*. 2016) this may be an underestimate. OPEX for HDS systems are usually lower than for conventional systems due to the reduced sludge production, leading to lower storage and disposal costs (Bullen 2006).

URS (2014) gives a breakdown of annual OPEX for water treatment facilities, reagent costs are the largest constituent of OPEX at 31.8%. For active treatments such as HDS the largest amount of reagent used is lime to

Table 1 Minimum and maximum CAPEX and OPEX estimates for a chemical precipitation plant treating 72m³/hr mine drainage.

		Minimum		Maximum
Indicative CAPEX per m³/day treated	$	300.00	$	1,250.00
Indicative OPEX per m³/day treated	$	0.20	$	1.50
CAPEX estimate	$	518,400.00	$	2,160,000.00
OPEX estimate per day	$	345.60	$	2,592.00
Annual OPEX estimate	$	123,033.60	$	922,752.00

increase the pH high enough for precipitation. These costs were used for a cost-treatability curve (Figure 1) based on preliminary titrations of samples of mine drainage from the study site.

Metal Hydroxide Precipitation vs Cation Adsorption

Water treatment by pH amendment is generally through addition of a chemical to increase mine water pH to promote precipitation of metal species. Metals are most commonly precipitated as hydroxides, the pH of hydrolysis for each metal cation is different. However it should be noted that during the process of raising pH and precipitation of iron and aluminium, that many other metals are removed from solution by sorption onto newly formed secondary iron minerals and not by precipitation. The relative proportion of metals removed by precipitation and sorption is not typically recorded as part of water treatment system design (sludge composition is not typically a design parameter) and is an inherently site specific function, as such the relative importance of sorption in systems like HDS is a relative unknown factor.

For metals of concern (Zn, Pb and Cd) in low Fe circum-neutral mine drainage, precipitation is most likely to occur between pH 9 and 11. This leads to some chemical precipitation treatment to amend mine water pH to at least 9.5–10 (Bullen 2006; Aubé 1999). Even from circum-neutral pH this can require a large amount of alkali reagent, this is due to pH being a logarithmic function and supersaturation of mine water with CO_2, found in some cases to be at levels 100 times greater than at atmospheric conditions (Jarvis 2006). Before treated water can be discharged the pH generally needs to be reduced to pH 8–9 in line with discharge requirements.

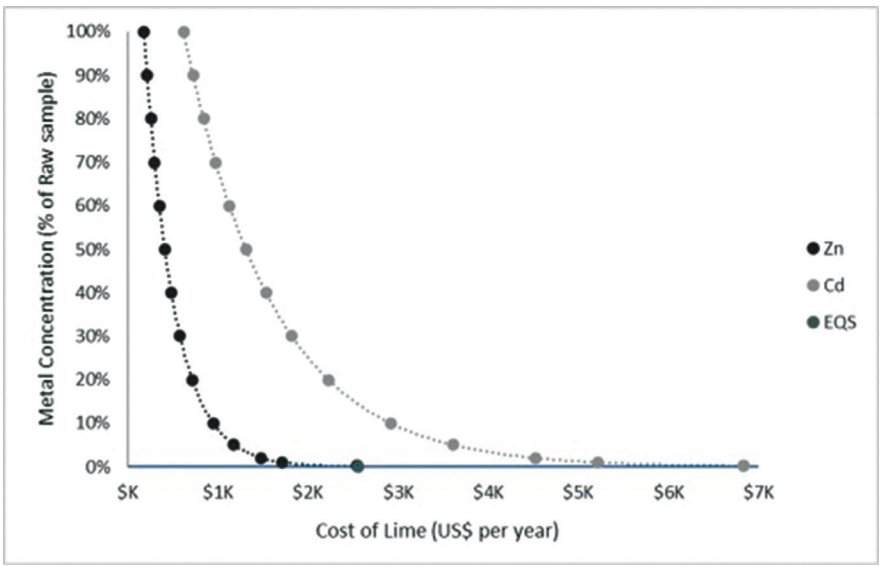

Figure 1 Cost Treatability curve showing lime costs against metal concentration for Zn and Cd.

As part of beaker trials (Figure 2) it has been demonstrated that the addition of Ferric Oxide (FeOx) at a rate of 5 g/L (over a 1 hour period) while raising the pH of water from Nant-y-Mwyn can change the primary treatment driver from precipitation as hydoxides to adsorption onto FeOx. Thus, metal removal occurs at much lower pH than by precipitation alone. Zinc concentration reduction (Figure 2) very clearly occurs at a much lower pH following the addition of FeOx.

Reducing the Cost and Increasing the Sustainability of Active Treatment

Although active treatment such as HDS can be considered "efficient" on the basis of typical cost effectiveness the consideration of sustainability and "green credentials" is becoming increasingly more important with an industry focus on environment and social governance (ESG) and decarbonisation. As such "passive" treatment systems have attracted much interest and investment/research as they are considered to be more aligned with sustainability/ESG/decarbonisation metrics. However, for many sites active treatment is likely to be continued to be required for a number of practical reasons and as such if true life cycle sustainability is to be assessed then a more holistic view is required to be taken. As such we consider an alternative approach termed Sustainable Active Treatment (SAT) that applies a more holistic and whole life cycle methodology to consideration of active treatment technology. This approach deals with the main drivers of cost for active treatment such as reagent use and sludge transport and disposal, as well as consideration of the nature of the sludge, and factors such as energy usage produced by applying sustainable solutions. In the first instance the largest component of OPEX cost is reagents, particularly chemicals to increase pH (Table 2). As such an obvious consideration is to look at the potential for reduction of reagent use which would be both more sustainable and would reduce OPEX costs. To demonstrate this, we performed beaker trial degassing experiments by sparging air through a sample of the mine water from the study site and recording pH at tie intervals (Figure 3). It is noted that the pH increased from 6.53 to >7.6 within ≈ 10 minutes without the use of any reagents (due to degassing of CO_2).

Another major OPEX cost is sludge transportation and disposal. As described herein sludge is produced if precipitation by pH increase is being used as the main means of metal removal, however our experiments show that sorption is an alternative means to remove metals that does not produce sludge. Addition of suitable sorption media for example allows

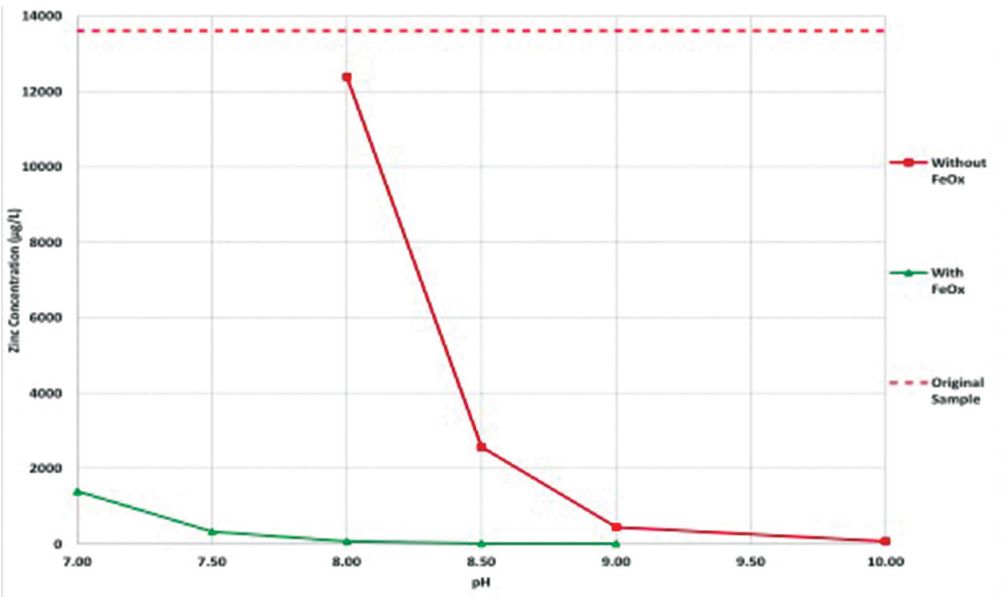

Figure 2 *Zn concentration (dissolved) as a function of pH, with and without FeOx addition.*

the metal cations to adsorb to media surfaces in a manner that does not generate sludge and is geochemically reversable. As reported by URS (2014), 40% of CAPEX costs are for sludge management infrastructure, clarification, sludge thickening and effluent polishing suggesting that avoiding sludge may allow important gains for life cycle sustainability and cost reduction. This approach also opens the possibility for recovery of metals that have been "reversibly" adsorbed if 'stripping' of the sorbed metals is carried out. Selective stripping of metals may be possible to produce relatively "pure" products (or concentrates) which may increase the economic value of this process. In addition, the use of industry by products as sorption media can be explored to further enhance sustainability gains. Iron ochre from coal mine drainage treatment facilities for example has been studied by Mayes *et al.* (2009) and Sapsford *et al.* (2015) as a potential sustainable FeOx media. Further because energy is one of the other major OPEX costs and has major influence on carbon footprint then using systems that have reduced energy demand opens up the possibility of using sustainable renewable sources of energy, such as photovoltaic cells and wind turbines. These would assist with both decarbonisation and OPEX reduction.

Conclusions

Based on our work we consider that consideration of a holistic approach to water treatment when considering active system provides may opportunities to reduce cost and improve sustainability metrics. For circum neutral sites adoption of a cost curve based assessment and the SAT approach will facilitate increased focus on both cost reduction and an increase in sustainability (this may be particularly so for legacy sites). This holistic approach further opens the possibility to look at water treatment as a 'Whole Catchment Approach' whereby consideration of treatment of multiple discharges are considered together rather than focusing on achieving very high removal rates from single point source discharges.

Acknowledgements

We would like to thank National Resources Wales for permission to perform test work on Nant-y-Mwyn mine drainage water and present the results here.

References

Aubé BC (1999) Innovative modifications to high density sludge process. Proceedings for Sudbury '99, Mining and the Environment II. September 13-17, 1999. Sudbury, Canada.

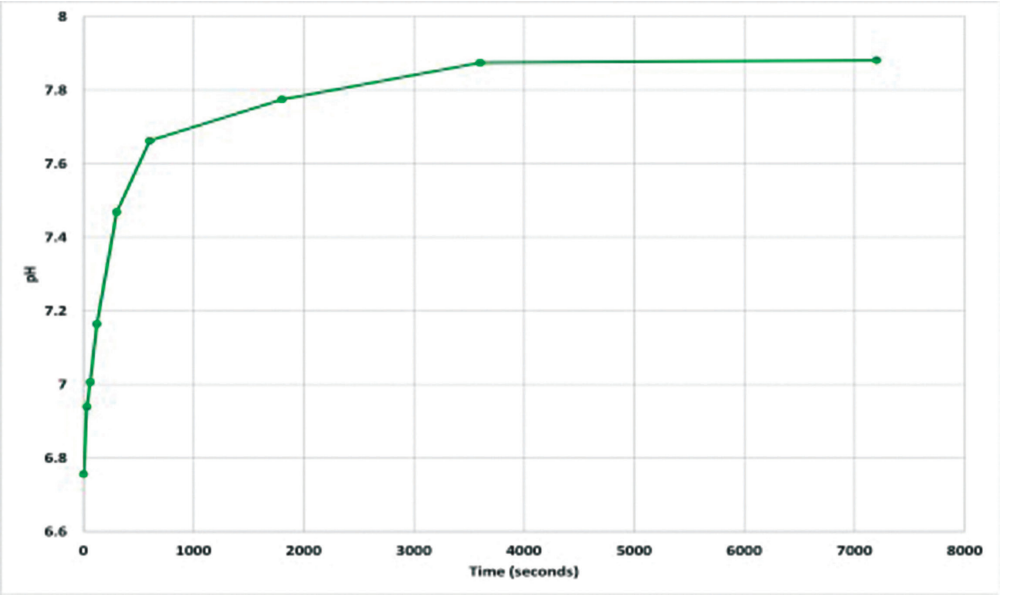

Figure 3 *Results of degassing experiment, change in pH with time.*

Bailey MT, Gandy CJ, Jarvis AP (2016) Reducing life-cycle costs of passive mine water treatment by recovery of metals from treatment wastes. Proceedings IMWA 2016, Freiburg, Germany.

Bekényiová A, Štyriaková I, Danková Z (2015) Sorption of Copper and Zinc by Goethite and Hematite. Archives for Technical Sciences 2015, 12(1), 59-66, doi:10.7251/afts.2015.0712.059B.

Bullen CJ (2006) An investigation into the mechanics controlling the formation of high density sludge. Thesis submitted to the University of Wales for the Doctor of Philosophy. School of Engineering University of Wales, Cardiff, United Kingdom.

Chaudhry SA, Khan TA, Ali I (2016) Adsorptive removal of Pb(II) and Zn(II) from water onto manganese oxide-coated sand: Isotherm, thermodynamic and kinetic studies. Egyptian Journal of Basic and Applied Sciences 3 (2016) 287-300.

Coulton R, Bullen C, Dolan J, Hallett C, Wright J, Marsden C (2003) Wheal Jane mine water active treatment plant – design, construction and operation. Land Contamination & Reclamation, 11 (2), 2003, doi:10.2462/09670513.821.

Florence K (2014) Mechanisms of the removal of metals from acid and neutral mine water under varying redox systems. Thesis submitted for the Degree of Doctor of Philosophy, School of Engineering, Cardiff University, United Kingdom.

Geroni JN, Sapsford DJ, Florence K (2011) Degassing CO_2 from mine water: implications for treatment of circumneutral drainage. Proceeding IMWA 2011, Aachen, Germany.

Geroni JN, Cravotta III CA, Sapsford DJ (2012) Evolution of the chemistry of Fe bearing waters during CO_2 degassing. Applied Geochemistry 27 (2012) 2335-2347.

Gooyong L, Cui M, Yoon Y, Khim J, Jang M (2018) Passive treatment of arsenic and heavy metals contaminated circumneutral mine drainage using granular polyurethane impregnated by coal mine drainage sludge. Journal of Cleaner Production 186 (2018) 282-292.

Jarvis AP (2006) The role of dissolved carbon dioxide in governing deep coal mine water quality and determining treatment process selection. Proceedings of the 7th International Conference on Acid Rock Drainage (ICARD), March 26-30, 2006, St. Louis, MO, USA.

Kirby CS, Dennis A, Kahler A (2009) Aeration to degas CO_2 increase pH, and increase iron oxidation rates for efficient treatment of net alkaline mine drainage. Applied Geochemistry 24 (2009) 1175-1184.

Mayes WM, Potter HAB, Jarvis AP (2008) Novel approach to zinc removal from circum-neutral mine waters using pelletised recovered hydrous ferric oxide. Journal of Hazardous Materials 162 (2209) 512-520.

Sapsford D, Santonastaso M, Thorn P, Kershaw S (2015) Conversion of coal mine drainage ochre to water treatment reagent: Production, characterisation and application for P and Zn removal. Journal of Environmental Management 160 (2015) 7-15.

Smith KS (1999) Metal sorption on mineral surfaces: An overview with examples relating to mineral deposits. In: Reviews in Economic Geology, Volumes 6A and 6B, The Environmental Geochemistry of Mineral Deposits, Chapter 7. Published by the Society of Economic Geologists, Inc. (SEG) 1999.

Trivedi P, Axe L, Dyer J (2001) Adsorption of metal ions onto goethite: single-adsorbate and competitive systems. Colloids and Surfaces, A: Physicochemical and Engineering Aspects 191 (2001) 107-121.

Trumm D (2010) Selection of active and passive treatment systems for AMD – flow charts for New Zealand conditions. New Zealand Journal of Geology and Geophysics, 53:2-3, 195-210, doi: 10.1080/00288306.2010.500715.

URS (2014) Metal Mine Water Treatment Review. Prepared for: The Coal Authority, United Kingdom.

Younger PL (2000) The adoption and adaptation of passive treatment technologies for mine waters in the United Kingdom. Mine Water and the Environment (2000) 19: 84-97.

Warrander R, Pearce NJG (2007) Remediation of circum-neutral, low-iron waters by permeable reactive media. IMWA Symposium 2007: Water in Mining Environments, 27-31 May, 2007, Cagliari, Italy.

Appendix

Chemical properties of Nant-y-Mwyn raw water sample.

	pH	Ca	K	Mg	Na	As	Ba	Cd	Co	Cu	Mn	Mo	Ni	Pb	Sb	Se	Sr	Ti	Tl	Zn
Unit		ppm	ppm	ppm	ppm	ppb	ppb	ppb	ppb	ppb	ppb	ppb	ppb	ppb	ppb	ppb	ppb	ppb	ppb	ppb
Conc.	6.756	23.47	0.941	8.223	7.84	0.549	14.98	40.31	24.69	26.09	13.52	0.119	41.76	137.4	0.258	0.258	51.34	10.74	0.11	13610

Passive Solar Photocatalytic Treatment in Mining Process-affected Water

Jeffrey Martin[1], Tim Leshuk[1,2], Brad Wilson[1,3], Zac Young[1], Frank Gu[1,2]

[1]*H2nanO Inc., 151 Charles St. W., Suite 299, Kitchener, ON, Canada, jeff@h2nano.ca*

[2]*University of Toronto, Department of Chemical Engineering and Applied Chemistry, 200 College St., Toronto, ON, Canada, f.gu@utoronto.ca*

[3]*Stantec, 100-300 Hagey Boulevard, Waterloo, ON, Canada, Brad.Wilson2@stantec.com*

Abstract

H2nanO Inc. has developed SolarPass, a floating reactive barrier comprised of buoyant photocatalyst beads that provides a passive, light-activated treatment process for target contaminants, while simultaneously blocking volatile emissions. Recently, H2nanO validated the efficacy of SolarPass for in-situ treatment of mining tailings water through an outdoor pilot-scale system in Alberta, Canada. Under natural sunlight illumination, target contaminants were degraded, including volatile sulfurous compounds and organics, while simultaneously reducing emissions by >70%. These results demonstrate that the novel SolarPass process can address diverse challenges with mining-influenced waters and provides an effective solution for passive tailings and process water management and remediation.

Keywords: Photocatalysis, Passive Treatment, Tailings, Sulfur, Organics

Introduction

Globally, vast amounts of mining process-affected water are accumulated in tailings ponds which may have an impact on the local environment, community health, and mine water resources. Typically, treatment of contaminants in mining effluents requires chemical additives or capital-intensive separation technologies. These methods are often operationally complex, energy-intensive, and require a high degree of maintenance oversight to operate successfully. Additionally, fugitive volatile emissions and odours can be released from surface of tailings ponds, affecting the local air quality. Due to the scale of these tailings ponds, the elimination of these emissions and odours is a challenge that is not effectively addressed by conventional technologies.

To this end, H2nanO Inc. has developed SolarPass, a novel self-assembling floating reactive barrier (FRB) comprised of buoyant photocatalyst ceramic beads similar to those studied in Leshuk *et al*., 2018. SolarPass provides a passive sunlight-activated treatment process to degrade target contaminants while simultaneously acting as a barrier towards volatile emissions from the mining process-affected water (Figure 1). This in-situ photocatalytic barrier can be deployed and collected in new or existing ponds for continuous oxidative treatment of persistent mining contaminants without the need for chemical or electrical inputs. Furthermore, as the photocatalyst beads are not consumed, they may be recovered from the pond once treatment is complete, for potential re-use elsewhere. This in-pond retrofit provides the ability to quickly and directly intercept and treat volatiles and contaminants without additional land, energy, or operational resources.

Previous work has validated the efficacy of using floating photocatalysts for the treatment of environmentally persistent naphthenic acids in mining process-affected water using natural sunlight UV-radiation at the bench-scale (Leshuk *et al*. 2018). Additionally, literature studies have demonstrated the widespread applicability of photocatalysis to treat mining-related wastewater and tailings including but not limited to the removal of cyanide (Augugliaro *et al*. 1999), arsenic (Lu *et al*. 2019), and selenium (Holmes and Gu

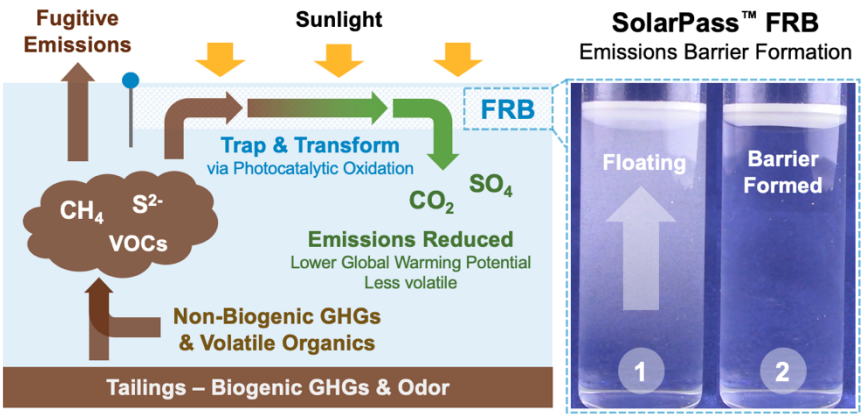

Figure 1 *SolarPass™ FRB floats to form a layer at the water surface, blocks emissions and passively transforms compounds by oxidation photocatalytically using sunlight.*

2016). Expanding on this prior work, H2nanO recently validated the efficacy of the SolarPass system for in-situ treatment of mining tailings through an outdoor pilot-scale system in Alberta, Canada (June to September, 2020). Under natural sunlight illumination, the efficacy of the SolarPass FRB was investigated for the simultaneous treatment and capture of volatile organic compounds (VOC) and reduced sulfur compounds (RSC). Toluene was investigated as a representative VOC using bench-scale experiments to validate the reaction products, and an open-tank pilot-scale experiment to demonstrate its retention via the SolarPass barrier. Reduced sulfur compound treatment was investigated at the pilot-scale using a closed-cell reactor for accurate quantification of the emission retention efficiency for hydrogen sulfide (H_2S) gas. Additional experiments were performed and are detailed in forthcoming publications.

Methods

A preliminary investigation of toluene treatment via the SolarPass FRB process was performed at the bench-scale using the apparatus illustrated in Figure 2. A solution of 1.5 L of 3.5 mg/L toluene in DI water and premeasured amount of catalyst were added to a glass closed-cell reactor (2.5 L total volume). To control the extent of UV exposure, the sides of the reactor were covered with aluminum foil such that the only opening for UV light was a round quartz glass window (8.7 cm diameter) in the stainless-steel reactor lid. Prior to treatment the catalyst beads coalesced for 3h, forming a floating layer at the water surface (0.2-1 cm thick), after which the headspace volume was purged tenfold with compressed air. Pre-treatment of the purge gas was performed using a drying trap to remove moisture (the activated carbon trap is sensitive to humidity), an activated carbon trap to remove trace hydrocarbons, and a 1% w./v. sodium hydroxide scrubber to re-humidify the air while simultaneously removing any carbon dioxide (CO_2). Initial and final samples of the headspace were taken using a thermal decomposition tube (ATD tube) and foil gas bag (1 L). Initial and final liquid samples of 110 mL were also taken. Aqueous samples were analysed for toluene and alkalinity (bicarbonate as $CaCO_3$) and the headspace samples were analysed for toluene and CO_2 (gas). Analysis was performed by ALS Environmental (Waterloo, ON), a CALA certified laboratory.

An open tank reactor (30 m^2 open surface area) with direct exposure to the local environmental conditions was used to obtain the pilot-scale toluene treatment results (Figure 3). A solution of 15 m^3 of tailings pond water (water depth of 60 cm) dosed with 750 mL of toluene was added to the reactor and SolarPass catalyst was added to achieve an FRB layer thickness of 0.2-1 cm. The toluene flux was determined by the concentration in the beam length using open

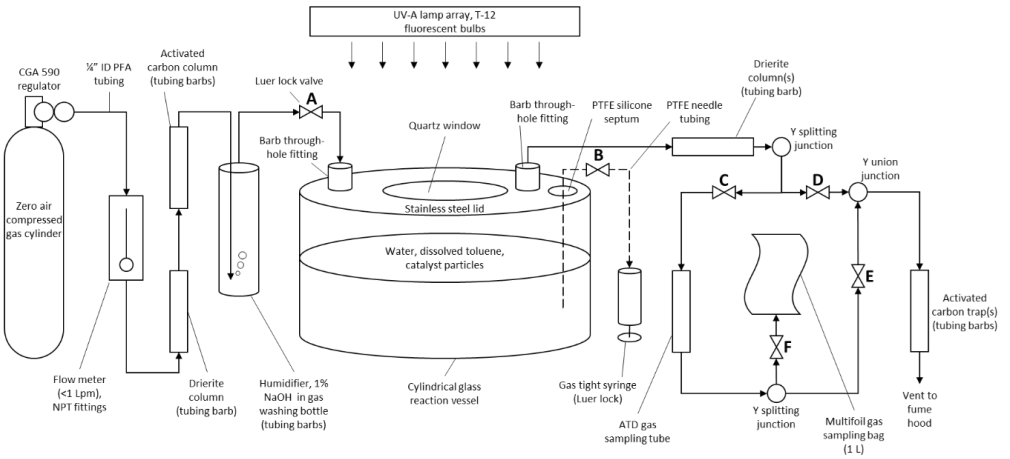

Figure 2 *Bench-scale apparatus for preliminary toluene treatment study.*

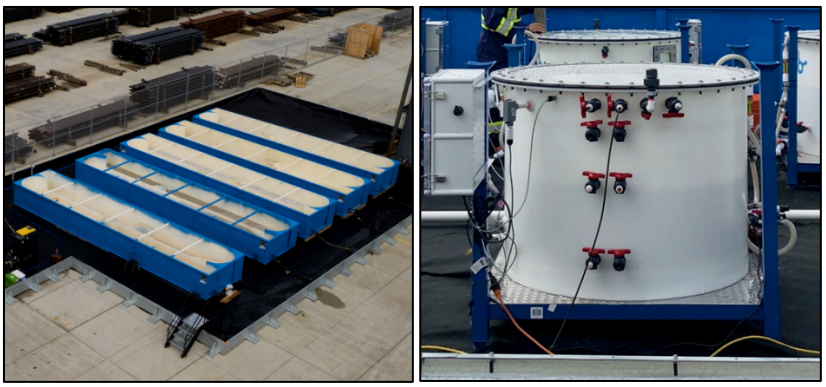

Figure 3 *Open tank (left) and closed reactor (right) used for the pilot-scale treatability studies of toluene and sulfur compounds.*

path Fourier transform infrared (OP-FTIR) spectrometry and applied to the open surface area of the reactors.

For the pilot-scale volatile sulfur compound experiments, a polypropylene closed-cell reactor (650 L total volume), equipped with a UV-transparent acrylic lid (Figure 3), was filled with 530 L of tailings pond water (water depth of 60 cm) and dosed with sodium sulfide (Na_2S) to achieve an initial sulfide concentration 84-130 mg/L sulfide (S^{2-}). The initial pH of the solution was adjusted to 8.5-9 an initial H_2S signal of 500 ppmv would be present in the reactor headspace. A SolarPass catalyst loading was used to obtain a layer of 0.2-1 cm thick. Headspace H_2S concentrations were measured using a Ventis MX4 handheld gas meter. Aqueous sulfide concentrations were analysed according to the standard method for total dissolved sulfides (SM 4500D). Aqueous sulfite was measured according to a colorimetric test referenced from established protocols in literature (Dasgupta *et al.* 1980). Sulfate was analysed using the standard turbidimetric method (SM 4500E). Total sulfur was determined using a two-part analysis following pre-treatment with 0.1 mL of 1 M zinc acetate solution and centrifugation (5 min at 15,000 rpm) to separate the sulfide species (as zinc sulfide precipitate) from the remaining aqueous sulfur. The precipitated zinc sulfide was quantified using the SM 4500D method, and the total sulfur content of the supernatant

(excluding sulfide) was analysed using inductively coupled plasma optical emission spectrometry (ICP-OES) (Whaley-Martin *et al.* 2020).

Results

Prior to quantifying the emission mitigation efficacy of the SolarPass FRB for volatile organic carbon species, bench-scale experiments were performed to validate the photocatalytic treatment of toluene and determine the oxidation reaction products. At the lab-scale, aqueous toluene (3120 ± 13 µg/L) was passively oxidized via photocatalysis to below detection limits (<0.5 µg/L) after 2 weeks of UVA exposure (simulated sunlight). Notably, there was no statistically significant change in the gas-phase toluene concentration (13.7 ± 3.8 µg/m^3 initial and 22 ± 7.4 µg/m^3 final) and >99.9% of the toluene remained in the aqueous phase, demonstrating at a lab-scale the VOC emission retention efficacy of the SolarPass FRB. Of the toluene that remained in the aqueous phase, >50% was fully oxidized to HCO_3^- and CO_2, illustrated below in Figure 4. Any unaccounted-for carbon is assumed to be a non-CO_2 organic oxidation intermediate that remained in the aqueous phase.

Following the validation of the SolarPass FRB for VOC emission retention and treatment at the bench-scale, a pilot-scale study was performed to validate the emission blocking efficacy in an open-tank system under natural sunlight and weather conditions. At elevated aqueous toluene levels 100-450x (to enable detection using the OP-FTIR apparatus), the SolarPass FRB decreased the toluene gas flux by 72% (Figure 5) when compared to a catalyst-free control. These results, combined with the lab-scale treatment study, demonstrate that the SolarPass FRB is a suitable solution for passive VOC emission containment and treatment in tailings ponds.

In addition to VOC's, the efficacy of the SolarPass technology was demonstrated for the retention and treatment of odorous sulfur compound emissions from tailings ponds. At the pilot-scale, Na_2S was added to the closed reactor (84-130 mg/L S^{2-}) and the pH was adjusted to 8.5-9 such that the amount of sulfate expected to be produced by the treatment would be distinguishable above the background sulfate levels naturally already present in the water. Figure 6 highlights the sulfur balances during the photocatalytic process using the SolarPass FRB (left) and a photolysis control (solar illumination without catalyst). Within the timeframe of the experiment, the photocatalytic oxidation process converted 76% of the aqueous sulfide to non-volatile sulfate. Sulfite was also

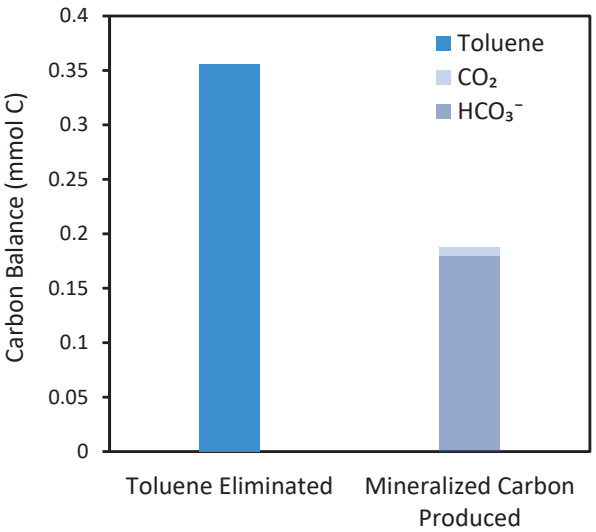

Figure 4 *Carbon balance for the photocatalytic oxidation of toluene via the SolarPass FRB.*

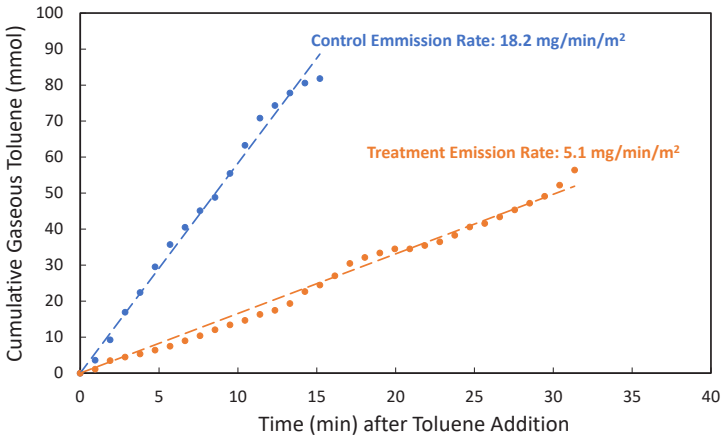

Figure 5 *Emission mitigation efficacy of the SolarPass FRB for toluene.*

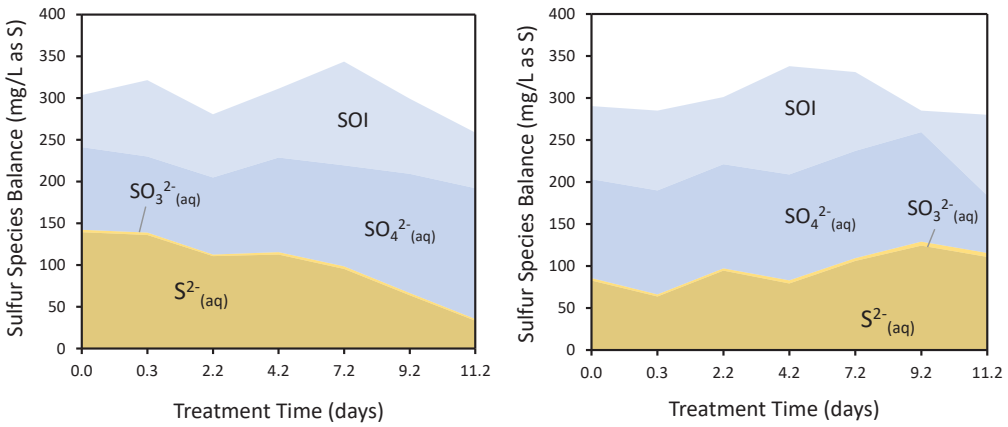

Figure 6 *Sulfur balance comparison between the photocatalytic oxidation of aqueous sulfide via the SolarPass FRB (left) and a photolysis control (right). S^{2-} represents the total dissolved sulfide concentration including S^{2-}, HS^-, and $H_2S_{(aq)}$.*

present as an oxidation reaction intermediate and the concentration decreased throughout treatment. Due to the complexity of aqueous sulfur chemistry, the unaccounted for sulfur was proposed to be a mixture of uncharacterized sulfur oxidation intermediates (SOI) (Whaley-Martin *et al.* 2020). Negligible sulfur losses from the aqueous phase were observed as the total sulfur remained constant at 320 ± 25 mg/L, indicating a closed mass balance.

Comparing the headspace H_2S concentration in both the SolarPass treatment reactor and the photolysis control, there was an average decrease in H_2S emissions of 88% when using the SolarPass FRB (Figure 7). Notably, there is a substantial decrease in the H_2S headspace concentration for both the control and the treatment reactor by 263 h. This is likely due to the added oxygen from sampling and humid environment in the closed headspace resulting in some gas-phase oxidation of H_2S or H_2S re-absorption by condensation droplets formed inside the reactor slow release of the H_2S through the lid-sealing interfaces. Coupled with the aqueous sulfide treatment results above, simultaneous photocatalytic treatment and emissions containment of volatile reduced sulfur compounds for tailings ponds was achieved at the pilot-scale.

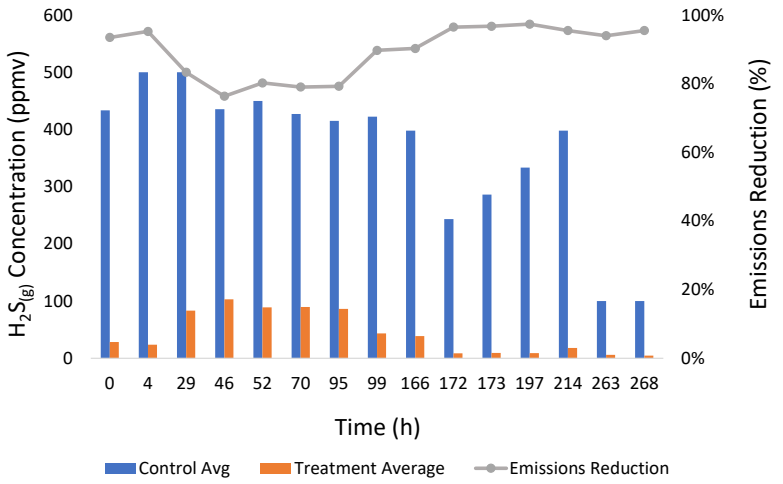

***Figure 7** Emission Mitigation Efficacy of the SolarPass FRB for H_2S Compared to a Photolysis Control.*

Conclusions

As a standalone process or part of a larger treatment system, SolarPass shows promise as a low-cost platform for photocatalytic treatment of mine water contaminants. Using toluene as a representative VOC, >99.9% was oxidized using SolarPass at the bench-scale (>50% mineralization) and the gas flux was reduced by >70% in an open-tank pilot study. Additionally, using SolarPass at the pilot-scale, >75% of aqueous sulfide was oxidized while on average 88% of H_2S emissions were prevented. The results of this work, and those of literature, demonstrate that the novel SolarPass process can address diverse challenges related to mining impacted waters and provides an effective solution for overall remediation, tailings water emissions reduction, and passive tailings management.

Acknowledgements

The authors would like to thank our service providers: AECOM for OP-FTIR equipment and operation, and ALS Environmental for their analytical services. In addition, the authors thank InnoTech Alberta for hosting the pilot-scale study and the H2nanO personnel involved with this study.

References

Augugliaro V, Blanco Gálvez J, Cáceres Vázquez J, *et al* (1999) Photocatalytic oxidation of cyanide in aqueous TiO2 suspensions irradiated by sunlight in mild and strong oxidant conditions. Catal Today 54:245–253. https://doi.org/10.1016/S0920-5861(99)00186-8

Dasgupta PK, DeCesare K, Ullrey JC (1980) Determination of atmospheric sulfur dioxide without tetrachloromercurate(II) and the mechanism of the Schiff reaction. Anal Chem. https://doi.org/10.1021/ac50062a031

Holmes AB, Gu FX (2016) Emerging nanomaterials for the application of selenium removal for wastewater treatment. Environ Sci Nano 3:982–996. https://doi.org/10.1039/c6en00144k

Leshuk T, Krishnakumar H, De Oliveira Livera D, Gu F (2018) Floating Photocatalysts for Passive Solar Degradation of Naphthenic Acids in Oil Sands Process-Affected Water. Water 10:. https://doi.org/10.3390/w10020202

Lu H, Liu X, Liu F, *et al* (2019) Visible-light photocatalysis accelerates As(III) release and oxidation from arsenic-containing sludge. Appl Catal B Environ 250:1–9. https://doi.org/10.1016/j.apcatb.2019.03.020

Whaley-Martin K, Marshall S, Nelson TEC, *et al* (2020) A Mass-Balance Tool for Monitoring Potential Dissolved Sulfur Oxidation Risks in Mining Impacted Waters. Mine Water Environ. https://doi.org/10.1007/s10230-020-00671-0

4500-S^{2-} SULFIDE (2017). In: Standard Methods For the Examination of Water and Wastewater

4500-SO_4^{2-} SULFATE. In: Standard Methods For the Examination of Water and Wastewater

Rehabilitaion of Lake Kepwari: a Previously Acidic Mine Lake in Western Australia

Cherie D. McCullough

Mine Lakes Consulting, PO Box 744, Joondalup DC, WA 6005, Australia, cmccullough@minelakes.com

Abstract

Mine pit lakes typically present significant mine closure liabilities in perpetuity though large volumes of contaminated waters. Lake Kepwari represents a significant achievement in mine closure planning as thefirst successfully rehabilitated and relinquished pit lake in Western Australia.

Lake Kepwari uses seasonal flow to remediate water quality and provide ecological connectivity to the broader catchment. State government endorsed the approach with a formal opening in December 2020 with significant infrastructure developments. Lake Kepwari demonstrates pit lake planning that presents a significant local opportunity for the mining town with regional benefits to state tourism and recreational opportunities too.

Keywords: Pit Lake, Flow-through, End Uses, Australia, Mine Closure

Introduction

The Collie Coal Basin is the centre of the coal mining industry in Western Australia and is located approximately 160 km south south-east of Perth. Waterways in southwestern Western Australia, including the Collie River, play an important role in the lives of First Nations Noongar people; their connection to the Collie River is reflected in their spiritual beliefs and its role as a source of food, water and recreation.

Mining began in the Lake Kepwari (WO5B) pit with diversion of the Collie River South Branch (CRSB) around the western void margin (Figure 1). Rehabilitation works on Lake Kepwari initially started in the 1980s in parallel with open-cut mining operations. When mining ceased in 1997, most reactive overburden dumps and exposed coal seams were covered with waste rock to cover PAF sources. At completion of the mining activities, the WO5B mine void edges were backfilled and graded to 10° to 5 m below water level to form beaches and an island with more than 2 Mm^3 of soil moved. The catchment was then revegetated by direct seeding with more than 60 species of native vegetation. The diversion channel was maintained to permanently divert the CRSB around the pit void to meet requirements of the 1997 Western Australian State agreement mine closure plan for Lake Kepwari as a "closed catchment lake".

To accelerate filling of the pit, additional water was provided through saline first flushes from the seasonal CRSB under a surface water license (Salmon *et al*., 2017). CRSB water quality is typically brackish and highly tannin stained, with moderate eutrophication. The lake was rapid-filled by these winter diversions between 2002–2008 through a valve-regulated offtake when river flow was sufficiently high. The lake reached its capacity volume, as limited by overflow culverts, in 2004. The final volume of Lake Kepwari is around 32×10^6 m^3, with a maximum depth of around 65 m, perimeter of 5.4 km and surface area of 1.0 km^2 (Lund *et al*., 2012).

Although the input of CRSB water initially raised the pH to above pH 7, the pH then fell below 4 once river inflows ceased. This low pH and associated elevated concentrations of some metals and metalloids reduced water quality values and restricted end use opportunities. However, the lake remained visually spectacular with extremely high transparency due to an absence of phytoplankton, restricted by low phosphorus due to AMD (Kumar *et al*., 2016).

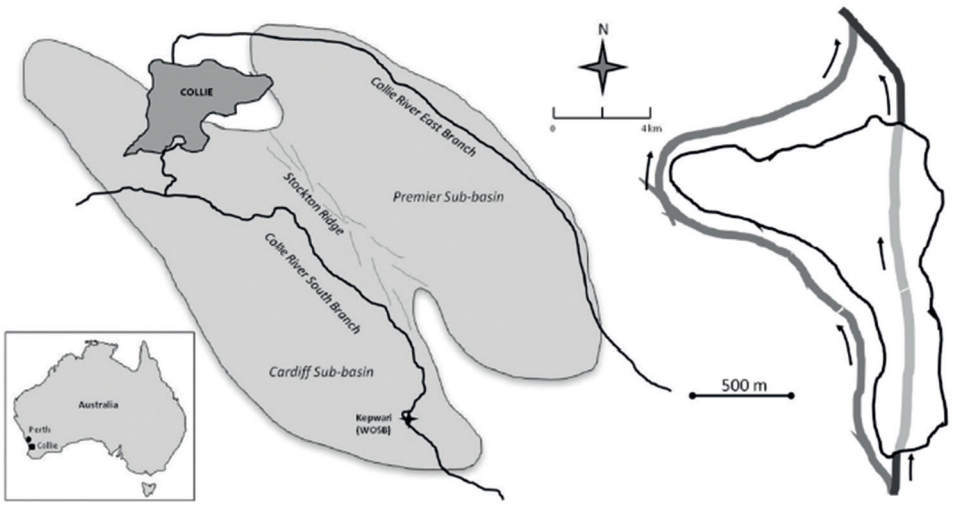

Figure 1 *Location of Lake Kepwari in Western Australia (left) and conceptual model of Lake Kepwari flowthrough design (right) showing historical CRSB channel in black, previous river diversion in dark grey and flow through lake in light grey (DIIS, 2016).*

Closure strategy trial

Heavy rainfall in August 2011 led to the CRSB overtopping the embankment separating it from Lake Kepwari. Approximately 30 m of ground failed and 2 GL of CRSB water flowed through Lake Kepwari, discharging through culverts in the NE and NW sides of the Lake (McCullough *et al*., 2013). This flow substantially improved lake water quality and ecosystem values (McCullough *et al*., 2012), indicating that maintaining the lake as a seasonal flow through system would provide a leading practice closure strategy for the lake. The flow-through event did not significantly impact upstream downstream CRSB values (McCullough *et al*., 2013).

A literature review, coupled with engagement, provided confidence to stakeholders that the approach was good international practice. Following this engagement, including community presentations, a flow-through trial was initiated to assess the benefits of this leading practice management option. The trial was run between 2012 and 2014 with over two years of diverted main-flow and one year of no flow (due to low rainfall). Regular quarterly assessment of biota and chemistry of both Lake Kepwari and the CRSB, and annual reporting of the findings to regulators and community were key components of the trial (McCullough & Harkin, 2015).

Premier Coal obtained approval to permanently divert the Collie River back to its original path through the mine void in November 2018. Recent rehabilitation activities to facilitate ongoing flow through included: widening the Collie River inlet and outlets to allow total flow-through the lake; rehabilitating the breach; and backfilling the diversion channel adjacent to the Lake surrender area. Premier Coal engaged local businesses that employed local people to do this work and civil works enabling the

Table 1 *Inlet and outlet water quality on 8/11/2018. All values filtered as mg/L unless otherwise stated.*

Site	pH @ 25C	EC (µS/cm)	Oxygen	Suspended Solids	Al	As	Fe	Mn	Ni	Zn
Inlet	6.7	4,970	9.1	13.0	0.01	0.001	0.36	2.2	0.060	0.03
Outlet	7.6	2,390	8.1	1.0	0.04	0.001	0.13	0.0	0.007	0.04

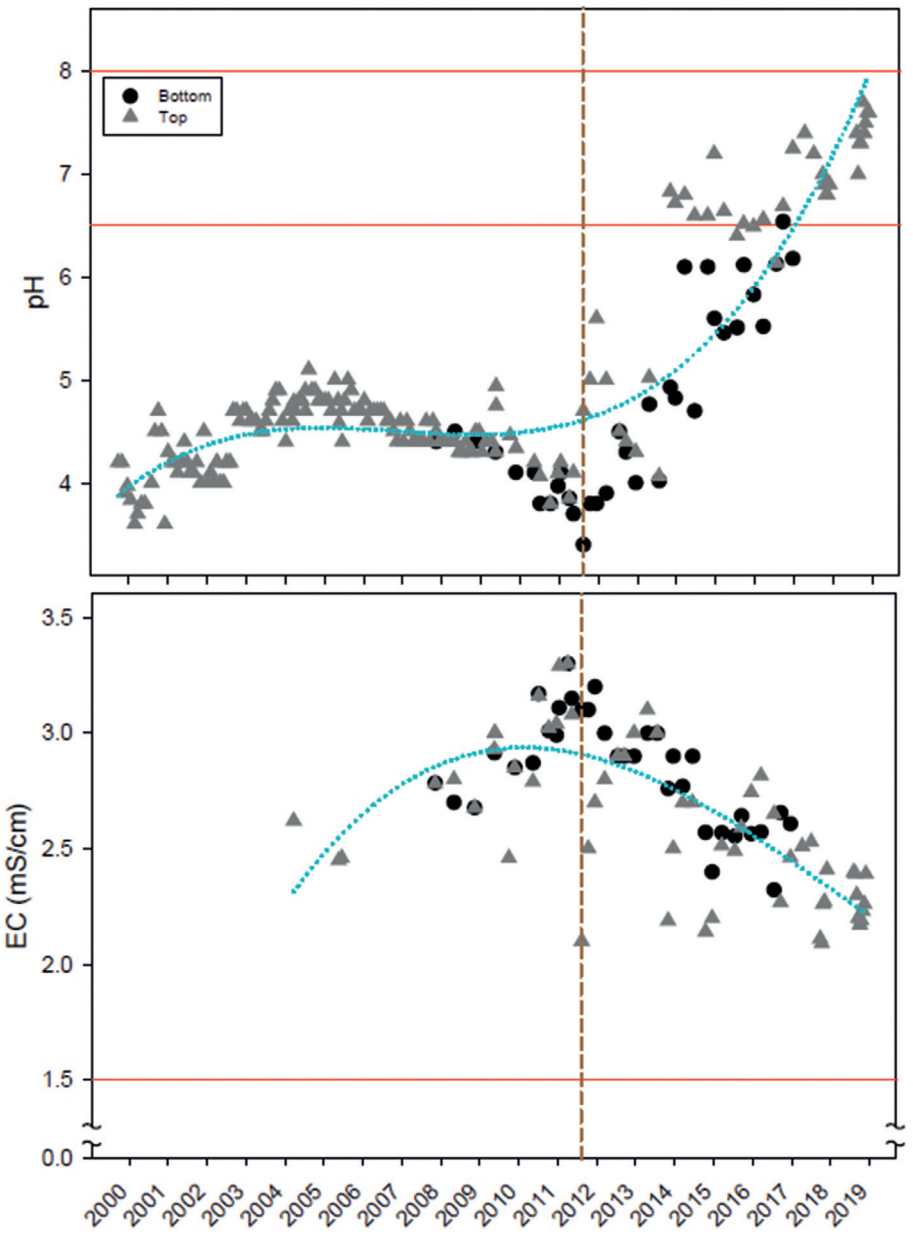

Figure 2 *Time-series graph of Lake Kepwari pH and EC historically, during and after flow-through began (after McCullough et al., 2010; McCullough et al., 2012; McCullough, 2015). Dotted teal regression line indicates pit lake pH and EC trends over time. Dashed brown line indicates date of breach.*

Table 2 *Lake Kepwari discharge water quality on 17 October 2018 (dissolved as µg/L).*

	Al	Cd	Cr	Cu	Mn	Ni	Pb	Se	Zn
Kepwari	0.05	0.00002	0.00043	0.012	0.026	0.007	0.00068	0.00015	0.053
Void	**83**	**0.005**	<0.002	**0.11**	0.1	**0.548**	–	–	3.37

Bold font indicates ANZG (2018) guidelines meet for freshwater aquatic ecosystem protection., – = No data, *As total.

flow-through were completed in June 2019. Yancoal surrendered the Lake Kepwari area from its mining tenement in August 2020.

Closure monitoring

Monitoring results showed downstream river water quality and availability was not significantly degraded by flow-through when discharge occurred during high CRSB flow with concomitant high lake water dilution in the downstream CRSB reaches (McCullough & Schultze, 2015). Furthermore, relative to upstream, downstream river water quality may be improved through trapping suspended solids including particulate forms of nutrients to the lake benthos and removal of soluble forms of phosphorus by co-precipitation with dissolved aluminium and iron from internally-generated lake AMD (McCullough & Schultze, 2018).

Recent monitoring of Lake Kepwari and a similarly large and age pit lake from the lease indicates that a trend of water quality improvement has occurred since implementation of innovative flowthrough. Lake pH is higher than historic and even previously reported levels, and importantly, on an upward trend from acidic to circum-neutral levels (Figure 2, top). Similarly, EC continues to decline from brackish to fresh salinities (Figure 2, bottom). Lake Kepwari discharge water quality also meets default national guideline values for typical mining related contaminants of potential concern (COPC) (ANZG, 2018) for aquatic protection (Table 2).

Regional benefits

Kepwari is a word in the indigenous Wilman language meaning "playing in water", and a range of water sports may be enjoyed at Lake Kepwari. Closure aims of the lake have provided a potential recreation resource for water skiing, diving and other aquatic recreational pursuits.

Collie is a town that has traditionally been reliant on mining and power generation to employ community members and support local businesses. Tourism is also becoming an important driver of a more diversified economy for Collie. The enhancement of nature-based tourism has potential to contribute to economic growth and diversification, supporting a more sustainable post-mining regional community. Transformation of Lake Kepwari into a recreation hub for water sports is expected to attract many tourists and visitors, which will provide a boost for businesses around Collie. Early estimates anticipate that after three years, Lake Kepwari is expected to attract overnight stays and day trip visitors, contributing significantly to the local economy.

State Government identified Lake Kepwari as a key development project in the South West region and committed $5.7

Figure 3 *Water-based recreation is a planned end use of Lake Kepwari.*

million to realising this vision. Recent works commissioned by government to develop the Lake into a recreation hub included a swim beach, picnic areas, campground, toilets, dual lane boat ramp and jetty, parking bays for 85 boat trailers and 65 cars. Upgrades to the entrance road, a new bridge over the Collie River and signage throughout the area has turned the area into a watersports landmark.

Conclusions

Over 100 years of coal mining in Collie resulted in many pit lakes as a lake district (sensu McCullough & Van Etten, 2011). Pit lakes in Collie to date, and also with current closure planning, are isolated from regional surface waters using closure approaches largely unchanged since open cut mining began (Lund *et al*., 2012).With the exception of Lake Kepwari, all are acidic due to AMD production from oxidation of regional low sulfide lithologies (McCullough *et al*., 2010).

The Lake Kepwari catchment-based flow-through closure strategy challenges these practices by using natural catchment attenuation and dilution processes to remediate water quality over a long-term as a passive treatment (McCullough & Schultze, 2018). AMD produced in the backfilled waste rock and pit shell is neutralised by net alkaline river water by regular seasonal flowthrough. Further alkalinity is generated by biological processes (Lund & McCullough, 2009) and mineral acidity is precipitated to lake sediments (Neil *et al*., 2009) e.g., through absorption onto dissolved organic matter (DOM). The net result yields a seasonal thermally stratified freshwater lake of circum-neutral pH (Kumar *et al*., 2013). Lake Kepwari is now part of the Collie River Waugal Aboriginal Heritage Site, which includes the Collie River system. Lake Kepwari will be an important landmark for the mining industry as a good example of how rehabilitating a mine site requires addressing more than just terrestrial landforms.

Acknowledgements

Many thanks to the previous and current Premier Coal and DWIR staff and CDM's consulting and research colleagues and students for collecting monitoring data.

References

ANZG (2018). Australian and New Zealand Guidelines for Fresh and Marine Water Quality. Australian and New Zealand Governments and Australian state and territory governments (ANZG), Canberra ACT, Australia. Available at www.waterquality.gov.au/anz-guidelines.

Figure 4 *The lake is expected to attract visitors to the region.*

DIIS (2016). Leading Practice Sustainable Development Program for the Mining Industry - Preventing Acid and Metalliferous Drainage Handbook. Department of Industry, Innovation and Science (DIIS), Canberra, Australia. 221p.

Kumar, N. R.; McCullough, C. D. & Lund, M. A. (2013). Pit lakes in Australia. In, Acidic pit lakes – the legacy of coal and metal surface mines, Geller, W.; Schultze, M.; Kleinmann, R. & Wolkersdorfer, C. Springer, Heidelberg, Germany, 342-361pp.

Kumar, R. N.; McCullough, C. D.; Lund, M. A. & Larranãga, S. (2016). Assessment of factors limiting algal growth in acidic pit lakes—a case study from Western Australia, Australia. Environmental Science and Pollution Research. 23: 5915–5924.

Lund, M. A. & McCullough, C. D. (2009). Biological remediation of low sulphate acidic pit lake waters with limestone pH neutralisation and amended nutrients Proceedings of the International Mine Water Conference. Pretoria, South Africa. International Mine Water Association, 519-525pp.

Lund, M. A.; McCullough, C. D. & Kumar, N. R. (2012). The Collie Pit Lake District, Western Australia: an overview. Proceedings of the International Mine Water Association (IMWA) Congress. Bunbury, Australia. International Mine Water Association (IMWA), 287-294pp.

McCullough, C. D. (2015). Consequences and opportunities of river breach and decant from an acidic mine pit lake. Ecological Engineering. 85: 328-338.

McCullough, C. D.; Ballot, E. & Short, D. (2013). Breach and decant of an acid mine lake by a eutrophic river: river water quality and limitations of use. Proceedings of the Mine Water Solutions 2013 Congress. Lima, Peru. Infomine Inc., 317-327pp.

McCullough, C. D. & Harkin, C. (2015). Engineered flow-through closure of an acid pit lake; a case study. Proceedings of the International Mine Closure 2015 Congress. Vancouver, Canada. Infomine, 1-10pp.

McCullough, C. D.; Kumar, N. R.; Lund, M. A.; Newport, M.; Ballot, E. & Short, D. (2012). Riverine breach and subsequent decant of an acidic pit lake: evaluating the effects of riverine flow-through on lake stratification and chemistry. Proceedings of the International Mine Water Association (IMWA) Congress. Bunbury, Australia. 533-540pp.

McCullough, C. D.; Lund, M. A. & Zhao, L. Y. L. (2010). Mine Voids Management Strategy (I): Pit lake resources of the Collie Basin. Department of Water Project Report MiWER/ Centre for Ecosystem Management Report 2009-14, Edith Cowan University, Perth, Australia. Unpublished report to Department of Water, Government of Western Australia. 250p.

McCullough, C. D. & Schultze, M. (2015). Riverine flow-through of mine pit lakes: improving both mine pit lake and river water quality values? Proceedings of the joint International Conference on Acid Rock Drainage ICARD/ International Mine Water Association (IMWA) Congress. Santiago, Chile. 1903- 1912pp.

McCullough, C. D. & Schultze, M. (2018). Engineered river flow-through to improve mine pit lake and river water values. Science of the Total Environment. 640-641: 217-231.

McCullough, C. D. & Van Etten, E. J. B. (2011). Ecological restoration of novel lake districts: new approaches for new landscapes. Mine Water and the Environment. 30: 312-319.

Neil, L. L.; McCullough, C. D.; Lund, M. A.; Tsvetnenko, Y. & Evans, L. (2009). Toxicity of acid mine pit lake water remediated with limestone and phosphorus. Ecotoxicology and Environmental Safety. 72: 2,046-2,057.

Salmon, S. U.; Hipsey, M. R.; Wake, G. W.; Ivey, G. N. & Oldham, C. E. (2017). Quantifying lake water quality evolution: coupled geochemistry, hydrodynamics, and

Full-Scale Reducing and Alkalinity Producing System (RAPS) for the Passive Remediation of Polluted Mine Water from a Flooded Abandoned Underground Coal Mine, Carolina, South Africa

Gloria M Dube[1], Tebogo Mello[1], Viswanath Vadapalli[1], Henk Coetzee[1], Kefyalew Tegegn[1], Rudzani Lusunzi[1], Shadung Moja[1], Mafeto Malatji[1], Munyadziwa Ethel Sinthumule[2], Rudzani Ramatsekisa[2]

[1]*Council for Geoscience, Water and Environment Unit, 280 Pretoria Street, Silverton, Pretoria, South Africa, gdube@geoscience.org.za, tmello@geoscience.org.za*

[2]*Department of Mineral Resources and Energy, 70 Meintjies street, Travenna campus, Sunnyside, Pretoria, South Africa, ethel.sinthumule@dmr.gov.za*

Abstract

This paper documents the application of a reducing and alkalinity producing system (RAPS) named CaroRap implemented for coal mine water remediation in South Africa. RAPS combines the mechanisms of anaerobic treatment wetlands and anoxic limestone drains. These systems improve water quality by processes, amongst others, of calcite dissolution and sulfate reduction through sulfate-reducing bacteria (SRB). Results from the system, which became operational in January 2021, show an increase in pH from an average of 2.9 to that of 5.6 coupled with an increase by 35.8 mg/L in alkalinity.

Keywords: Reducing and Alkalinity Producing System, Sulfate-reducing Bacteria, Limestone, Alkalinity.

Introduction

For over 140 years, the mining industry has played a major role in the economic advancement of South Africa, making it the most industrialised country on the African continent (Minerals Council South Africa 2021). However, all this came at a cost as the environment is continuously being affected by polluted mine water. Mine influenced water, mainly Acid mine drainage (AMD), has turned out to be a grave environmental concern in the country, particularly for sustainability of the country's freshwater supply (McCarthy and Humphries 2013). Before the three statutes, i.e. National Water Act 36 of 1998 (NWA), the National Environmental Management Act 107 of 1998 (NEMA) and the Mineral and Petroleum Resources Development Act 28 of 2002 (MPRDA) were enacted, mining practices and their effects thereof on the immediate environment were not adequately regulated in South Africa (Humby 2013). As a consequence, mining companies disregarded environmentally friendly practices and found ways to circumvent environmental liabilities. This then resulted in mines being abandoned without appropriate rehabilitation and the South African government has since inherited environmental liabilities of most of the abandoned mine sites (Novhe *et al*. 2016). Presently, legislation and regulatory frameworks related to mine water management put pollution prevention as a priority, however, in cases where pollution is inevitable, treatment becomes a necessity. Therefore, the work conducted in this study contributes to the bigger basket of mine water management strategies, particularly the passive treatment technologies which have not been thoroughly studied or applied in South Africa.

Despite the quest for a just energy transition and the declining demand from its main export destinations, South Africa is still in the top ten class of large coal producers and exporters (Nicholas and Buckley 2019). In addition, coal plays an essential domestic role in the supply of energy as 93% of the country's electricity is produced by coal-fired

stations (McCarthy and Humphries 2013). Mpumalanga Province is inundated with coal mines and produces over 80% of the country's coal. It is no surprise that this province is the 15th and 2nd largest emitter of carbon dioxide (CO_2) and sulfur dioxide (SO_2), respectively on a global scale (McCarthy and Humphries 2013; Evans 2019). Moreover, the most severe direct environmental concern is that of mine influenced water. Witkranz discharge site in Carolina is an ideal case in point. Acidic mine water with pH of 2.9 is constantly discharged into the environment, feeding a nearby stream, Boesmanspruit, which then confluences with other streams to feed into the Boesmanspruit Dam. Until 2012, this dam was used to supply the town of Carolina with portable water. Unfortunately, following a severe rainstorm event, the water quality in this dam rapidly deteriorated. There was a sudden drop in pH to 3.7 (from 7.4) and contaminants such as iron (Fe), aluminium (Al), manganese(Mn) and sulfate (SO4) were found in elevated levels, ultimately rendering the water toxic and unsuitable for human consumption and use (McCarthy and Humphries 2013). With the financial support of the Department of Mineral Resources and Energy (DMRE), the Council for Geoscience (CGS) stepped in and conducted pilot studies which ultimately led to the implementation of an up-scaled passive treatment system for AMD treatment at a legacy coal mining area, referred to as the Witkranz discharge site. The system, named CaroRap, comprises of a Reducing and Alkalinity Producing System (RAPS) that has been in operation from the 17th of January 2021 and has yielded desirable results.

Objectives

This study was undertaken with an aim to contribute to sustainable mine water management solutions in South Africa by focussing on exploration and, as far as possible, implementation of sustainable solutions to the remediation of mine water discharge. The remediation component is achieved by developing optimised passive treatment units for long-term remediation of polluted mine water, based on results, observations, and lessons learned from previous pilot scale studies that were carried out by CGS.

Study Area

CaroRap system is located on farm Witkranz 53 IT, portion 11, approximately 10 km south of Carolina Town in Mpumalanga (Figure 1). The area forms part of the Ermelo coalfield and all coal seams in this area occur within the Vryheid Formation of the Ecca Group, Karoo Supergroup. This formation is characterized by sandstones with subordinate shales (Bell *et al*. 2002). Although information about the mining history of the area cannot be sourced at this stage, historical imagery as well as an old georeferenced mine plan show mining activities in a portion of land to the east of the discharge point. Both underground and open-cast mining methods seem to have been used in this area. There appears to have been some degree of rehabilitation and a pond was constructed at the discharge point. This is the pond which was later used as a "RAPS 1" unit. Notwithstanding the rehabilitation attempts, the adjacent environment has received noticeable pollution as the nearby Boesmanspruit which is fed by the discharged water has succumbed to a deterioration in water quality (McCarthy and Humphries 2013)

Methods

The selection of an appropriate treatment technique was, in the main, guided by site-specific conditions, chemistry of the water, the flow rate and locally available material. Passive treatment emerged as a winner because (1) it is relatively cheaper to implement in contrast to active treatment, (2) the area under study is in a remote location with adequate land space, (3) the flow rate (which is <50 L/s) can be managed by a passive system and (4) active treatment is generally applied at active mines while passive treatment is usually considered for abandoned or closed mines. The Witkranz discharge site is regarded as an abandoned site, therefore, the application of a passive treatment technique was befitting. Furthermore, previous pilot experiments by Novhe *et al*. (2016) highlighted the feasibility of passively treating the water discharging in the study area with a subsurface flow biogeochemical system containing compost and limestone. The baseline information

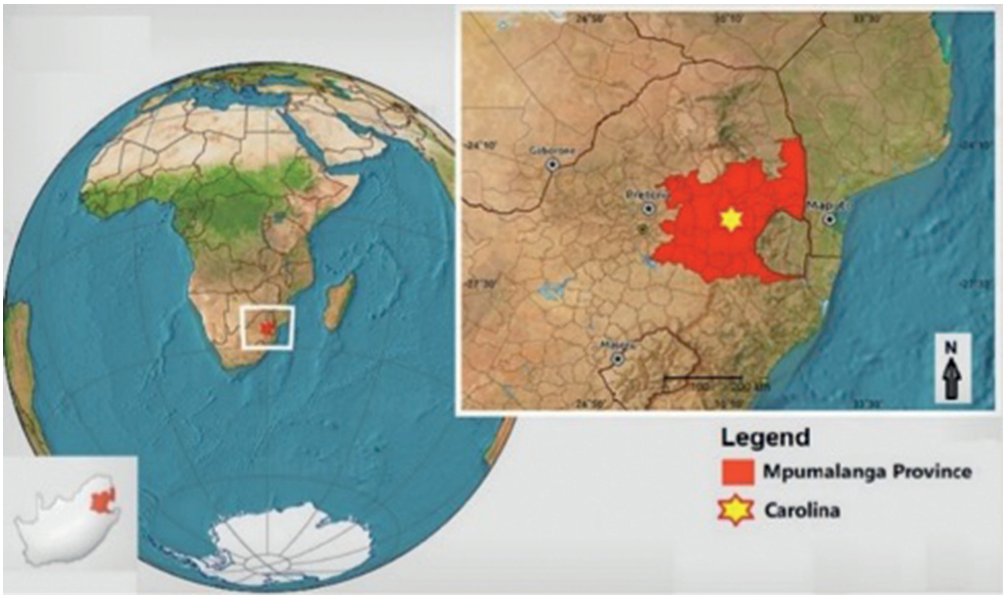

Figure 1 *Map showing the location of Carolina, Mpumalanga Province (image: modified from Maphill 2011).*

collected by the aforementioned authors is summarized in Table 1 below.

Further selection of the appropriate passive treatment technique was done in accordance with the flow chart compiled by Hedin *et al*. (1994). Other factors which were taken into consideration when selecting the suitable passive treatment technique are (1) potential applicability, effectiveness, and performance of the passive treatment in a South African context; (2) effectiveness and consumption rates of locally available reagents and, hence, the lifespan of the passive treatment system; (3) the feasibility and cost benefits of the implementation of the passive treatment system.

Taking into consideration all the aforementioned factors, RAPS was selected as the ideal passive treatment system for the site. A typical RAPS consists of a cell of vertical flow pond or a reducing alkalinity-producing system (RAPS) (as developed by Kepler and McCleary, 1994) and a settling pond. This kind combines the mechanisms of anaerobic treatment wetlands and anoxic limestone drains (ALDs) and has the potential to neutralize acid water and reduce sulfate while concomitantly precipitating elements such as Fe, Zn, As, and Al. For CaroRAP, RAPS system in pond 1 of the system, was constructed in an existing collection pond which required, *inter alia*, emptying of mine water, deepening by removing sediments, strengthening of the embankment walls, lining with a high density poly HDPE liner, construction of a berm and piping. Another pond, referred to as Pond 2, was proposed for a "RAPS 2" unit for further treatment of the water. However, this pond is currently being used as a receiving pond, accepting water from RAPS 1. The use of two RAPS systems in series is advantageous as it increases contaminant removal and further improves water quality. The ponds were designed to have an equal area of 900 m^3 (height = 1 m, length = 50 m and width = 18 m). Approximately 160 tons of limestone

Table 1 *Baseline information for Carolina mine impacted water.*

Flow (ℓ/min)	pH	EC (mS/m)	Dissolved oxygen (mg/ℓ)	Calculated acidity	Fe (mg/ℓ)	Al (mg/ℓ)	Mn (mg/ℓ)	Mg (mg/ℓ)	SO_4 (mg/ℓ)
34	2.9	254	5.20	967.77	331.56	40.62	20.3	61.25	2524.77

with $CaCO_3$ content of 85% was mixed with nearly 270 tons of spent mushroom compost (an organic carbon source) in RAPS 1.

This approach of mixing the limestone and manure was adopted from Younger *et al.* (2004). This method differs from the original RAPS design (depicted in Figure 2A) of Kepler and McCleary (1994), in which a distinct layer of limestone gravel underlies a layer of compost (as shown in Figure 2A). Mixing the two materials, as depicted in Figure 2B, reduces compaction and facilitates greater permeability of the substrate. A layer of water is maintained above the mixed limestone and manure substrate to encourage vertical downward flow. The calculated residence time is expected to be six days before the water is released from RAPS 1 unit. Depending on the efficiency of RAPS 1 with time, it will be decided whether to leave the second unit as an oxidation pond or to create a RAPS 2 with a similar design as RAPS 1. If RAPS 2 is considered, a relatively shallow and wide settling/oxidation pond is proposed for collection of treated water from the RAPS system. This pond will allow Fe, Al, Zn, and other precipitates to settle before the treated water is released to the receiving stream. The proposed settling pond ought to be sized to allow a primary retention time of approximately 12 h. Currently, RAPS 1 is operational and guidelines which were developed prior to the construction of the system are being used to continuously assess the efficacy of the system.

Results and Discussion

In four weeks of operation, the system (Figure 4), which is currently reliant on only RAPS 1 and an oxidation pond, has managed to raise the pH to an average of 5.6 from an average of 2.9 as shown in the left graph of Figure 5. There was also an increase in alkalinity in the ranges of about 35.8 mg/L. The increase in pH and alkalinity is attributed to bicarbonate ions released from the dissolution of limestone. In terms of metal and sulfate removal rates, the system managed to reduce total iron (Fe)

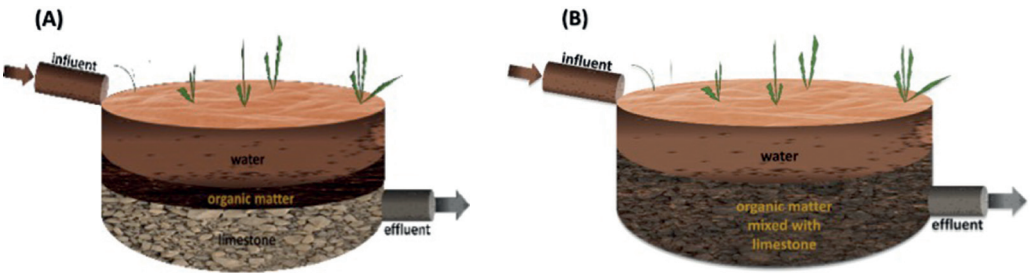

Figure 2 *A typical diagrammatic representation of a RAPS setup (A) and a modified setup (B) currently used to treat mine water from the Witkranz discharge site.*

Figure 3 *Refurbishment of the first pond (RAPS 1) (left) and compost mixed with limestone in RAPS 1 (right).*

Figure 4 An overview of RAPS 1 showing channeled inlet water, ponded mine water under treatment and a berm in the center (for increasing retention time).

by 92% and Al by 58.8%. The graph on the righthand side of Figure 5 shows a substantial decrease in Fe content in the system. On the other hand, the system managed minimal removal rates in terms of Mn and SO4 (shown on the right graph of Figure 6), which were reduced by 22.8% and 19%, respectively. The minimal removal of Mn as shown on the left graph of Figure 6, is attributed to the presence of Fe in the system which tends to compete for oxygen consumption. There was an increase in the Ca^{2+} concentration in the system as a result of calcite dissolution. This rise, from the average of about 38.8 mg/L to 108.5 mg/L, was expected as Ca^{2+} ions are released into the solution when limestone reacts with mine water.

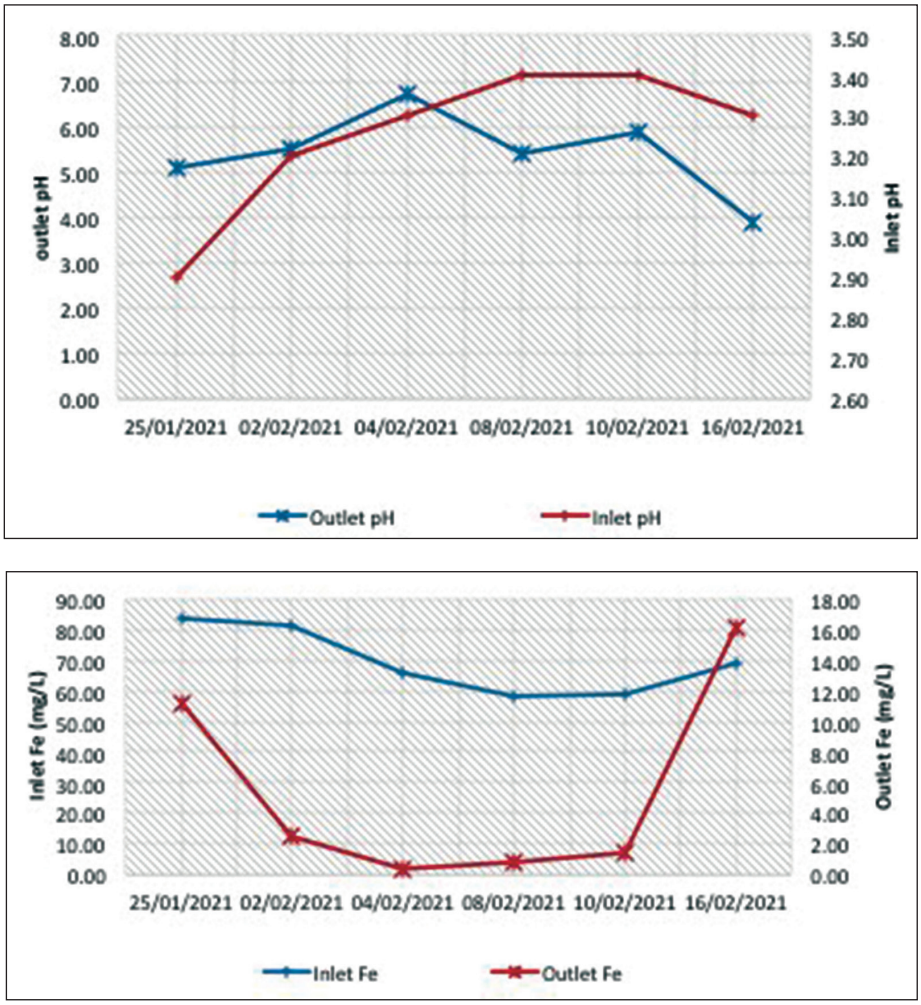

Figure 5 Graphs showing an increase in pH (left) and a decrease in Fe (right) in the treated water from RAPS 1.

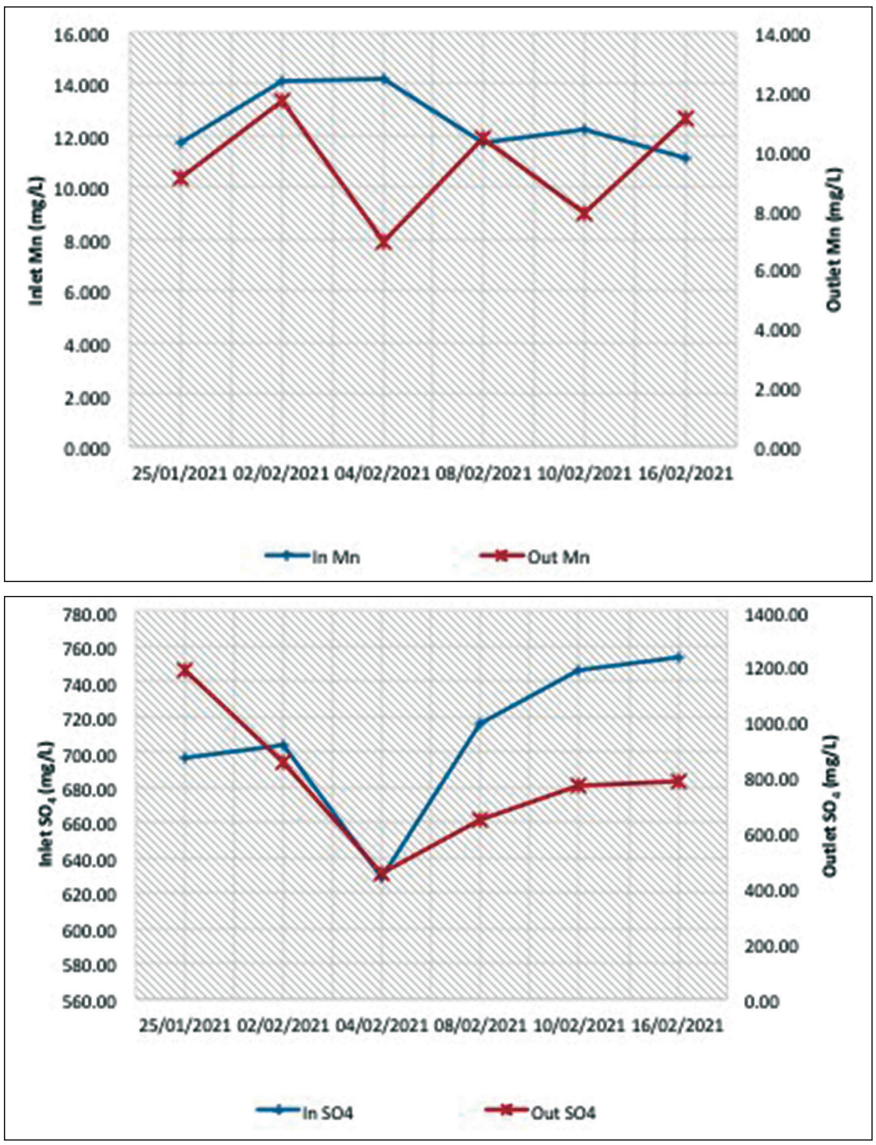

Figure 6 *Graphs showing limited reduction of Mn (left) and SO_4 content (right) in RAPS 1.*

Conclusion

Although the CaroRAP system was recently implemented and is currently reliant on one RAPS unit, results indicate that the discharged water is being successfully neutralised. There are limitations with regards to adequate removal of Mn and SO_4 and measures for optimisation of such will be explored further. SO_4 reduction is dependent on microbial activities, as such, factors such as a suitable organic substrate, pH and contact time, to name a few, will be looked into in the quest to improve the efficiency of the system. Although not currently in the plan, Mn removal can be optimised by incorporating a Mn removal bed in the system. Metals precipitating as sulfides, oxides or hydroxides in the aerobic units, tend to accumulate in passive treatment units, presenting an opportune situation for the recovery of valuable products that can compensate for remediation costs. The efficiency of the system was affected by heavy rains. Passive treatment systems

typically tend to underperform in high flow conditions. Going forward, the CaroRAP system will be monitored continuously to observe its efficiency and identify methods for optimisation in differing seasons. A better understanding of the interaction of surface water and groundwater in the area will also be sought in order to gain a pertinent knowledge of the overall hydrological and hydrogeological dynamics. Moreover, the environmental impact of the system will be studied and documented.

Acknowledgements

The authors would like to convey words of gratitude to the Department of Mineral Resources and Energy for the provision of financial support. Furthermore, Council for Geosciences workforce is acknowledged for their scientific, technical and pragmatic contributions to this project.

References

Bell FG, Hälbich TFJ, Bullock SET (2002) The effects of acid mine drainage from an old mine in the Witbank Coalfield, South Africa. Q J Eng Geol Hydrogeol 35:265–278. https://doi.org/10.1144/1470-9236/00121

Evans S (2019) Area in Mpumalanga is second highest SO2 emissions hotspot in the world - new study | News24. In: News24. https://www.news24.com/news24/SouthAfrica/News/area-in-mpumalanga-is-second-highest-so2-emissions-hotspot-in-the-world-new-study-20190819. Accessed 6 May 2021

Hedin RS, Nairn RW, Kleinmann RLP (1994) Information Circular 9389 : Passive treatment of coal mine drainage. 1–44

Humby T-L (2013) The Spectre of Perpetuity Liability for Treating Acid Water on South Africa's Goldfields: Decision in Harmony II. J Energy Nat Resour Law 31:453–466. https://doi.org/10.1080/02646811.2013.11435343

Kepler DA, McCleary EC (1994) Successive alkalinity producing system (SAPS) for the treatment of acidic mine drainage. In: Proceedings of the international land reclamation and mine drainage conference and the 3rd international conference on abatement of acidic drainage. Pittsburgh, PA, pp 195–205

Maphill (2011) Free Satellite Location Map of Mpumalanga. http://www.maphill.com/south-africa/mpumalanga/location-maps/satellite-map/free/. Accessed 6 May 2021

McCarthy TS, Humphries MS (2013) Contamination of the water supply to the town of Carolina, Mpumalanga, January 2012. SciELO South Africa 109:

Minerals Council South Africa (2021) Transformation. https://www.mineralscouncil.org.za/work/transformation. Accessed 6 May 2021

Nicholas S, Buckley T (2019) South African coal exports outlook: Approaching long-term decline - EE Publishers. https://www.ee.co.za/article/south-african-coal-exports-outlook-approaching-long-term-decline.html. Accessed 6 May 2021

Novhe O, Yibas B, Coetzee H, *et al* (2016) Long-Term Remediation of Acid Mine Drainage from Abandoned Coal Mine Using Integrated (Anaerobic and Aerobic) Passive Treatment System, in South Africa: A Pilot Study. In: IMWA 2016 : Mining Meets Water - Conflicts and Solutions. pp 668–675

Trumm D (2010) Selection of active and passive treatment systems for AMD - Flow charts for New Zealand conditions. New Zeal J Geol Geophys. https://doi.org/10.1080/00288306.2010.500715

Younger PL (2016) A simple, low-cost approach to predicting the hydrogeological consequences of coalfield closure as a basis for best practice in long-term management. Int J Coal Geol 164:25–34. https://doi.org/10.1016/j.coal.2016.06.002

The Influence of Mine Water Rebound on Methane Degassing in Abandoned Coal Mines

Stefan Möllerherm, Christian Melchers

Research Center of Post-Mining at the Technische Hochschule Georg Agricola University, Herner Straße 45, 44787 Bochum, Germany, Stefan.moellerherm@thga.de

Abstract

Hard coal mining is one of the major source for anthropogenic methane emissions. Even after mine closure, methane is still released over a longer period. Experts assume that methane degassing will gradually drop due to the water rising because hydrostatical pressure will reduce the desorption from the seams. However, some scientists have already proved that mine water can contain methane-producing bacteria. This secondary methane geneses potential has not been analysed since then. The authors postulate that bacteria can generate recent methane even in mine water rebound processes. In this paper, they describe their approach to support this thesis.

Keywords: Methane Emission, Abandonment Mines, EU Methane Strategy, Bacteria

EU legislative background

Methane is a powerful greenhouse gas, second only to carbon dioxide in its overall contribution to climate change. On a molecular level, methane is more powerful than carbon dioxide. Although it remains for a shorter time in the atmosphere, it has a significant effect on the climate. Reducing methane emissions therefore contributes to slowing down climate change. The EU Regulation on the Governance of the Energy Union and Climate Action [(EU) 2018/1999)] calls on the Commission to deliver a strategic plan for reducing methane emissions. Furthermore, in the European Green Deal Communication, the Commission indicated that energy-related methane emissions needed to be addressed as part of the commitment to reach climate neutrality by 2050. In this way, policy action to reduce methane emissions will contribute to both the EU's decarbonisation efforts towards the 2030 Climate Target Plan and the EU's zero-pollution ambition for a toxic-free environment [(EU) COM(2019) 640 final].

The EU has reduction targets for 2030 for all greenhouse gases, with anthropogenic methane emissions covered by binding national emission reduction targets under the Effort Sharing Regulation (ESR) [(EU) 2018/842]. However, there is currently no policy dedicated to the reduction of anthropogenic methane emissions. 59% are anthropogenic, of which the largest sources are agriculture (40-53%) – in particular linked to intensive production, fossil fuel production and use (19-30%), and waste (20-26%). In the EU, 53% of anthropogenic methane emissions come from agriculture, 26% from waste and 19% from energy [European Environment Agency (EEA), 2018].

In October 2020, the EU communicated a strategy on reducing methane emissions [(EU) COM(2020) 663 final]. It outlines a comprehensive policy framework combining concrete cross-sectoral and sector-specific actions within the EU, as well as promoting similar action internationally. While in the short-term, the strategy encourages global level voluntary and business-led initiatives to immediately close the gap in terms of emissions monitoring, verification and reporting, as well as reduce methane emissions in all sectors, it foresees EU level legislative proposals in 2021 to ensure widespread and timely contributions towards the aforementioned EU objectives. Now, the Commission is undertaking an open stakeholder consultation process to incorporate the different views and opinions of these parties. The new regulation on methane emissions shall be adopted by end of 2021.

Methane emissions from active and abandoned coal mines

The metamorphosis of terrestrial organic material like peat to coal and anthracite results in the release of water, carbon dioxide, hydrocarbons and nitrogen. Main component of the hydrocarbons is methane. Roundabout 150 – 200 m^3/t of the original organic material originated in the Carboniferous and Permian Age (Gaschnitz 2000). The gas was or is partially absorbed at the coal surface. This methane (also known as mine gas) was generated during the formation of the coal around 300 Mio years ago. Although a huge amount of methane has escaped during millions of years, still significant quantities of methane are stored in the coal deposit.

In active coal mines, methane which is absorbed in the seam and in the strata is released due to the coal extraction process such as longwall mining or room and pillar. The methane is then diluted by fresh air down to a maximum threshold of 1 Vol-% of CH_4 and sucked out of the underground mine by the ventilation air system. In those cases where it is technically not more feasible to dilute the methane to the threshold, the gas is directly drained from the seam or from the strata. The mining company drills boreholes into the strata, sucks the gas and transports it via underground gas pipelines to cogeneration plants on the surface. In these cogeneration plants, the methane is used as a fuel to produce electricity and heat. In the mining business, this type of gas is called Coal Mine Methane (CMM).

While closing a coal mine the release of mine methane will not stop in the underground. Huge amount of gas remains in the strata, in the non-mined areas of the seams and in the over- and underlying seams. Over many years, even decades after mining cessation the coal deposit releases gas into the remaining void, which consists of former galleries and mining-induced excavation-damaged zones. In the sealed areas of the mine, the present air is displaced and the oxygen content is reduced due to oxidation processes. Waterless voids of former coal mining galleries are filled up with oxygen-deficient gas mixtures of methane, nitrogen and carbon dioxide. In general, the content of methane and carbon dioxide will increase after termination of the galleries while at the same time the oxygen content decreases. The gas composition within a closed mine will balance in the long term due to different effects like natural draft or diffusion. Besides the former shafts cracks and fissures in the Coal Formation and in the strata provides another pathway for methane emissions (figure 1). These pathways were created by the

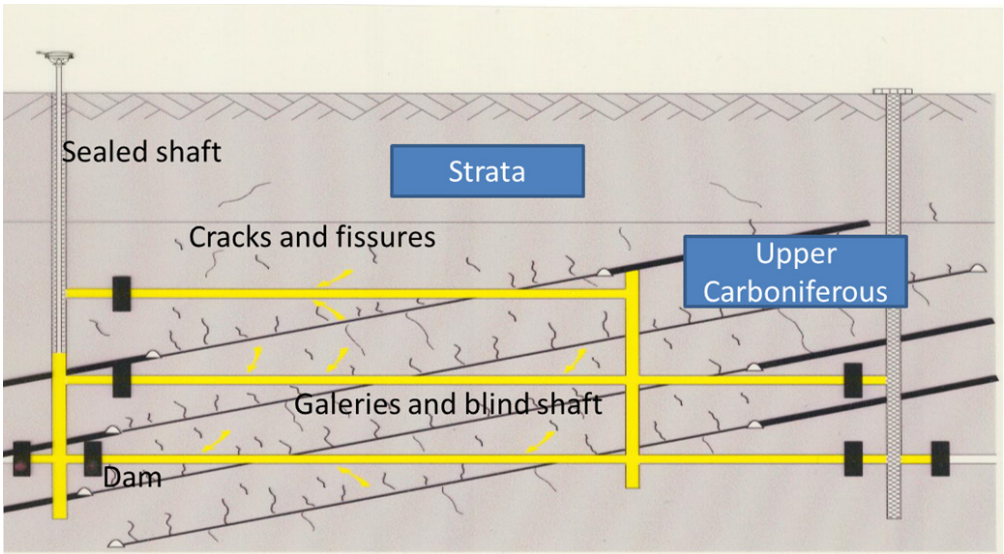

Figure 1 *Schematic methane pathways to the surface (FZN).*

coal extraction and the related deconstruction of the strata due to the ground subsidence.

Therefore, the mining companies at the Ruhr and Saar area are still able to drain methane from this reservoir and utilises the gas in the existing cogeneration plants. Experts call this type of methane Abandoned Mine Methane (AMM). According to the mine authority in North Rhine-Westphalia, roundabout 100 cogeneration plants were running on closed mines in 2020. With an installed electrical capacity of 168 MW 544 Mio kWh of electricity and 108 Mio kWh of thermal heat were produced last year (Wissen 2021).

(Kholod *et al.* 2020) have modelled the global methane emissions from abandoned coal mines. They conclude that the gas from these mines will continue to increase within the next decades even though coal mines will close in the future. Their model estimated global AMM emissions to be 22 bcm in 2010 and forecasts AMM emissions to increase to 75 bcm in 2050 and 162 bcm per year in 2100.

Evolution of the mine degassing process in abandoned coal mines

Several scientists act on the assumption that the methane generation and release process will come to end with flooding the mine (Kholod *et al.* 2020, Imgrund 2020). The mine water rebound will lead to a gradual reduction of the methane release from the strata into the galleries because desorption from the seams will decrease due to the opposing hydrostatical pressure. They assume that the process stops as soon as the hydrostatical pressure exceeds the gas pressure, which correlates with the respective residual gas content of the coal. Furthermore, the water rebound can flood pathways in the galleries and hence interrupt them. This is in particular true for galleries, which were developed on deeper levels to connect different mines. Consequently, these connections between different parts of mines to degassing units or to the cogeneration plants will be inapplicable and hence cannot be degassed or drained any longer. In the course of the water rebound, the gas composition in the void can change too, because the water increase push away methane rich gas mixtures in other voids either in horizontal or vertical directions. This may lead to the fact that the methane content in voids in areas of low or gas free seams will increase. The barometric gas exchange between void and atmosphere will only terminate in case of complete flooding of the mine. Kholod *et al* assume that the gas release process will terminate approximately 6 to 7 years after flooding the mine (figure 2) (Kholod *et al.* 2020).

The diagenesis of coal is not the only source of methane generation. In many coal mining areas one can find evidence for recent methane genesis, which is not of geochemical origin (Rice 1993, Berner & Faber 1996, Zazzeri *et al.* 2016). Bacteria can generate CH_4 out of coal and water under anaerobe conditions. This process has

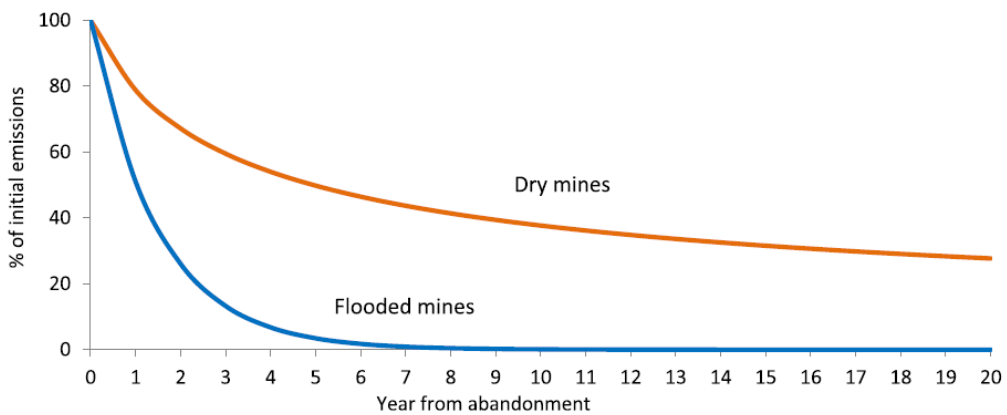

Figure 2 *Assumed AMM emission reductions over time from dry and flooded mines (Kholod et al. 2020).*

taken place also in the Ruhr area and in the Saar area (Thielemann *et al*. 2004, Krüger *et al*. 2008). Thielemann conducted first trials to demonstrate the microbial methane production in the Ruhr area (Thielemann *et al*. 2004). He took samples from 13 sites within 14 months and analysed the components and the isotopes. According to the isotope data, he showed that the methane gas was a mixture of thermogene and by CO_2 reduction generated microbial gas. (Krüger *et al*. 2008) found in mine water samples living methanogens archaea i.e. methane generating bacteria and proved the recent methane gas genesis in abandoned coal mines in the Ruhr area. Despite the indications on secondary genesis of methane, this assumption have not been investigated more in detail in science yet. In addition, a quantitative estimation of a bacterial source term has not been undertaken yet as well. Of particular interest would also be if the mine water rise would lead to an increase of recent methane genesis. Against this background, scientists at the Research Center of Post-Mining in Bochum have initiated the research project "The influence of mine water rebound on methane degassing in abandoned coal mines". The project is conducted in collaboration with the coal mining company RAG, the utility company STEAG and the Federal Geological Survey of Germany (BGR). STEAG is operating cogeneration plants in the former coal mining areas at Ruhr and Saar.

First research results

In 2019 and 2020, the scientists undertook gas-sampling campaigns at the cogeneration plants in the Saar and Ruhr area. The gas from the underground pipeline to the cogeneration plant was sucked via a small injection needle into a vial. At each site, two samples were taken in order to minimize measurement errors. In the Saar area two measurement campaigns at 13 sites have been undertaken, one in 2019 and another one in 2020. At the Ruhr at 29 locations samples have been taken in 2020. Due to the pandemic situation, it was not possible to carry out more campaigns.

Afterwards BGR performed an isotope composition analyses and determined carbon and hydrogen isotopes. The following

Table 1 *Measurement results from the Saar area.*

Site	$\partial_{13}C\ CH_4$ [‰ PDB]	microbial $\delta^{13}C\text{-}CH_4$ -80	thermogen $\delta^{13}C\text{-}CH_4$ -25	CH_4 (%) 2019	Volume flow (m^3) 2019
Allenfeld	-42,5	44%	56%	75,68	3.789.260
	-43,3	46%	54%		
Altenkessel	-46,4	54%	46%	26,10	1.586.552
	-46,7	54%	46%		
Reden	-41,9	42%	58%	25,52	21.763.508
	-41,9	42%	58%		

Table 2 *Measurement results from the Ruhr area.*

Site	$\partial_{13}C\ CH_4$ [‰ PDB]	microbial $\delta^{13}C\text{-}CH_4$ -80	thermogen $\delta^{13}C\text{-}CH_4$ -25	CH_4 (%) 2018	Volume flow (m^3) 2018
Blumenthal 3/4	-52,5	69%	31%	15,6	28.301.287
	-52,6	69%	31%		
Hugo 2/5/8	-56,0	78%	22%	18,8	28.463.241
	-54,5	74%	26%		
Minister Stein 4	-54,5	74%	26%	43,5	10.251.754
	-54,4	74%	26%		

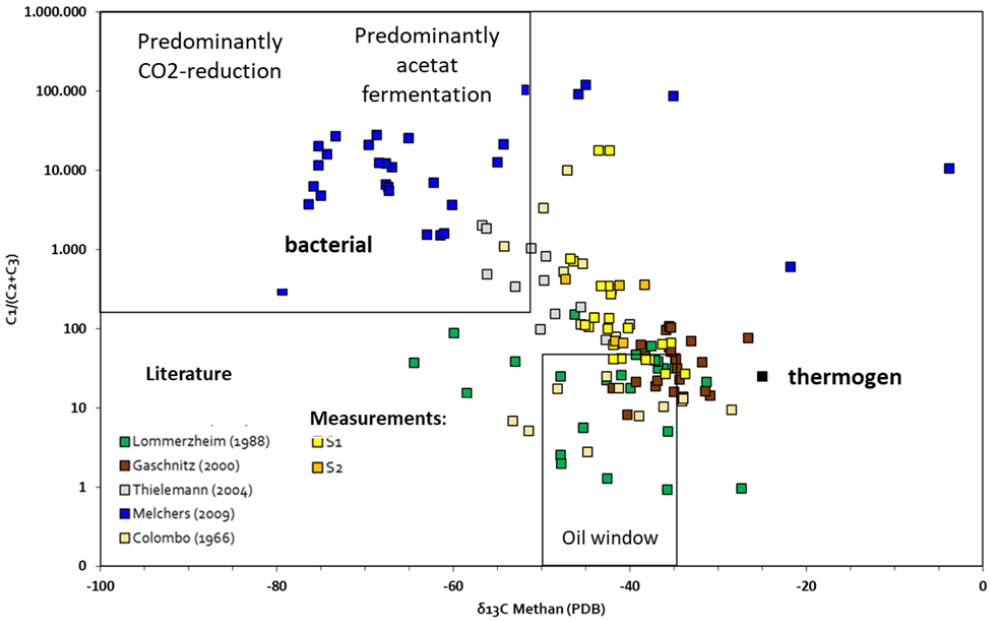

Figure 3 *Plot of the measurement results for the Saar area (FZN).*

tables shows the results for the Saar and for the Ruhr area. (–80) is the end link of the bacterial isotopes and (–25) is the end link of thermogeneous isotopes. It can be seen that the part of microbial isotopes is slightly increasing which is an evidence that bacteria are generating recent methane, in particular in the Ruhr area. Here the percentage of microbial isotope is much higher compared to the Saar.

Afterwards the results were plotted and compared with values taken from literature. Figure 3 shows the results for the Saar area. The x-axis in the chart indicates the $\partial_{13}C$ in methane and the y-axis the ratio of C_1 (methane) to C_2 +C_3 (ethane and other hydrocarbons). Thermogeneous methane was generated in the carboniferous era as coal gas. On the other hand bacterial origin refers to the fact that the gas is generated by bacteria which then can continue to exist. The yellow and green dots in the plot represent the respective measurements of the first two campaigns (S1 and S2) in the Saar region. Thermogeneous origin of methane is dominating in the Saar area, however the main number of analyses are close to the transitional phase.

Summary and outlook

The results of the first isotope analyses underpins the assumption that bacteria can generate recent methane in abandoned coal mines. This can be seen in the Ruhr area, where the portion of microbial methane is higher than the portion of thermogen methane. On the other hand, due to pandemic it was not possible to carry out more sampling campaigns. Another one is currently performed at the Ruhr area. Although the contribution to the overall methane degassing from closed mines is relatively low, however, it cannot be neglected and it will continue to be a source of methane in dry mines. More data are required and additional research is needed to quantify the amount of recent methane generation.

Acknowledgement

The authors want to thank RAG-Stiftung for the financial contribution and the partners RAG, STEAG and BGR for their collaboration.

References:

Berner U, Faber E 1996: Empirical carbon isotope/maturity relationships for gases from algal kerogens and terrigenous organic matter, based on dry, open-system pyrolysis. In: Organic Geochemistry 24 (10-11), S. 947–955. DOI: 10.1016/S0146-6380(96)00090-3

(EU) 2018/1999: REGULATION (EU) 2018/1999 OF THE EUROPEAN PARLIAMENT AND OF THE COUNCIL of 11 December 2018 on the Governance of the Energy Union and Climate Action, amending Regulations (EC) No 663/2009 and (EC) No 715/2009 of the European Parliament and of the Council, Directives 94/22/EC, 98/70/EC, 2009/31/EC, 2009/73/EC, 2010/31/EU, 2012/27/EU and 2013/30/EU of the European Parliament and of the Council, Council Directives 2009/119/EC and (EU) 2015/652 and repealing Regulation (EU) No 525/2013 of the European Parliament and of the Council

(EU) COM(2019) 640 final: COMMUNICATION FROM THE COMMISSION The European Green Deal

(EU) 2018/842: REGULATION OF THE EUROPEAN PARLIAMENT AND OF THE COUNCIL of 30 May 2018 on binding annual greenhouse gas emission reductions by Member States from 2021 to 2030 contributing to climate action to meet commitments under the Paris Agreement and amending Regulation (EU) No 525/2013

European Environment Agency (EEA), (2018). EEA greenhouse gas - data viewer. https://www.eea.europa.eu/ds_resolveuid/f4269fac-662f-4ba0-a416-c25373823292

(EU) COM(2020) 663 final: COMMUNICATION FROM THE COMMISSION TO THE EUROPEAN PARLIAMENT, THE COUNCIL, THE EUROPEAN ECONOMIC AND SOCIAL COMMITTEE AND THE COMMITTEE OF THE REGIONS on an EU strategy to reduce methane emissions

Gaschnitz R 2000: Gasgenese und Gasspeicherung im flözflihrenden Oberkarbon des Ruhr-Beckens. Dissertation RWTH Aachen

Imgrund T, Orzol R 2020: Gutachten zur Grubengasgewinnung in Nordrhein-Westfalen. PFG-Nr. 352019 https://www.wirtschaft.nrw/sites/default/files/asset/document/2020-06-0029877.pdf

Kholod N, Evans M, Pilcher Rc, Roshchanka V, Ruiz F, Cote M and Collings R.: Global methane emissions from coal mining to continue growing even with declining coal production, Journal of Cleaner Production (2020), doi:https://doi.org/10.1016/j.jclepro.2020.120489.

Krüger M, Beckmann S, Engelen B, Thielemann T, Cramer B, Schippers A, Cypionka H 2008: Microbial Methane Formation from Hard Coal and Timber in an Abandoned Coal Mine. In: Geomicrobiology Journal 25 (6), S. 315–321. DOI: 10.1080/01490450802258402.

Lommerzheim, A. (1988): Die Genese und Migration von Kohlenwasserstoffen im Münsterländer Becken. – 260 S + 112 S Anh.; 129 Abb., 28 Tab., 50 Taf.; 6 Karten; Münster. [Dissertation]

Melchers, CH. 2009: Methan im südlichen Münsterland – Genese, Migration, Gefahrenpotential. – XVI + 154 S., 62 Abb., 16 Tab., 12 Anh.; Münster. - [Dissertation]

Rice, D D 1993: Composition and origins of coalbed gas. In: Hydrocarbons from coal: AAPG Studies in Geology 38 (1), S. 159–184.

Thielemann T, Cramer B and Schippers A 2004: KOHLEFLÖZGAS IM RUHR-BECKEN: FOSSIL ODER ERNEUERBAR? DGMK-Frühjahrstagung 2004, Fachbereich Aufsuchung und Gewinnung, Celle DGMK-Tagungsbericht 2004-2, ISBN 3-936418-17-9, Seiten 449 bis 459

Wissen M 2021: EU-Methane-Strategy Measures to reduce emissions from abandoned coal mines. Presentation at the EU stakeholder workshop 15. March 2021

Zazzeri G, Lowry D, Fisher R E, France J L, Lanoisellé M, Kelly B 2016: Carbon isotopic signature of coal-derived methane emissions to the atmosphere: from coalification to alteration. In: Atmos. Chem. Phys. 16 (21), S. 13669–13680. DOI: 10.5194/acp-16-13669-2016

Application of Artificial Intelligence Systems in Mine Water Management – An Introduction to two Effective Predictive Models

Kagiso S. More[1], Christian Wolkersdorfer[2]

Department of Environmental, Water and Earth Sciences, Tshwane University of Technology, Private Bag X680, Pretoria, 0001, South Africa, [1]210042091@tut4life.ac.za, [2]christian@wolkersdorfer.info; [1]ORCID: 0000-0003-2803-7983, [2]ORCID: 0000-0003-2035-1863

Abstract

This work presents a summary of machine learning techniques that are effective in predicting acid mine drainage (AMD). Machine learning can be divided into different categories such as supervised, unsupervised and reinforcement learning. In this study, a supervised learning method will be explored. In this technique, a model has input variables and an output value, and uses an algorithm to learn the mapping function from the input to the output. Predictive analysis is the key focus in this study. Therefore, regression supervised learning techniques will be investigated, and this includes artificial neural networks (ANN) and random forest.

Keywords: Artificial Intelligence, Machine Learning, Supervised Learning, Artificial Neural Networks, Random Forest

Introduction

Artificial intelligence (AI) includes using computers to perform functions that normally requires human intervention. This implies developing calculations or algorithms to characterise, analyse and make decisions from data (Russell and Norvig 2002). Additionally, it involves performing functions on given data, learning from new data and sometimes improves it over time. Unlike many other programs that characterise every conceivable situation and only operate within those characterised situations, AI trains a program for a particular task and allows it to explore and improves on its own (Negnevitsky 2005). These systems operate on large data, so they can learn from it, improve scenarios and make better decisions. AI has multiple branches, and this includes machine learning, expert systems, speech, and robotics, to name a few. This study will investigate machine learning methodologies.

AI systems in mine water treatment plants are designed for the purpose of predicting future mine water quality. Therefore, recommended machine learning model type is the supervised learning with focus on regression. The main aim is on accuracy of the results; therefore, algorithms that can be explored include artificial neural networks (ANN) and random forest.

Artificial Neural Networks

Neural networks are data-driven and work with known input data without any assumptions. They can conclude on meaningful and workable data relationship that can be utilised to give output data when only input data are presented (e.g. Maier *et al*. 2004). The "neural" part of their name implies that they are brain-inspired systems designed to perform what humans can do as elaborated by Russell and Norvig (2002). ANNs are made up of an input layer, where data are initially presented to the model and computation is performed, a hidden layer, where the data are processed and an output layer, where the results are produced (Fig. 1; Wolfgang 2011). Each layer in the ANN structure consists of at least one basic element which can be referred to as a neuron, a non-linear algebraic function. This technique is a mathematical model that operates on three set of rules, i.e. multiplication, summation and activation as explained by Krenker *et al.* (2011).

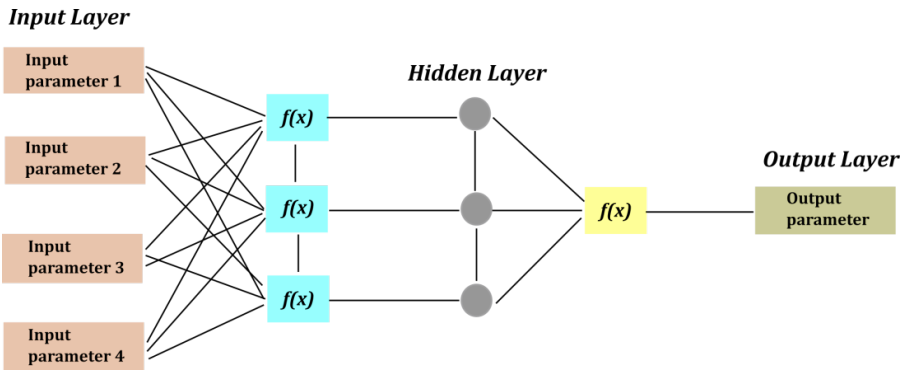

Figure 1 ANN structure.

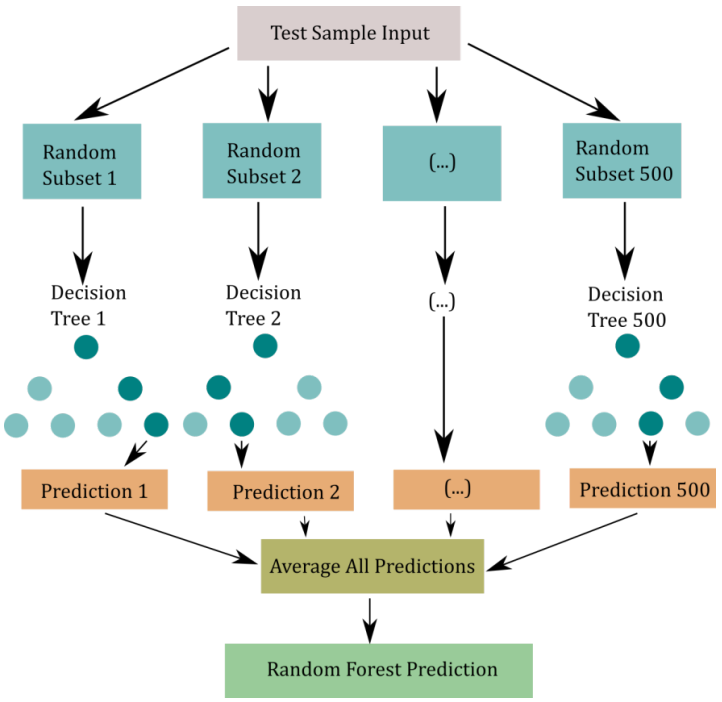

Figure 2 Random forest architecture.

Random Forest

Random forest is one of the supervised machine learning algorithms which uses ensemble learning to perform either classification or regression tasks. They are built on the concept of decision trees algorithm (Fig. 2; Singh *et al.* 2017). Decision trees are machine learning algorithms where the data are repeatedly split according to a certain parameter. The tree consists of a decision node where the data are split and the leaves where the final outcomes and decisions are made. Random forest regressor, which is investigated in this study, builds a "forest", which is an ensemble of decision trees trained using the "bagging" method. Bagging enables random forest to make decision trees run independently and ultimately sums up the outputs to give the final output without preferring one model over the other.

Conclusions

Machine learning modelling goal is to make a machine understand the developed algorithms so it can work as an autonomous system without an expert's intervention. Random forest and ANN are effective in finding the correlation between the input and output variables, the strength of predictions and for forecasting an effect and trend. They perform well on large data sets, are accurate and show less overfitting compared to other AI methods.

References

Krenker A, Bester J, Kos A (2011) Introduction to the artificial neural networks. In: Suzuki K (ed) Artificial neural networks – methodological advances and biomedical applications. InTech, Rijeka

Maier HR, Morgan N, Chow CWK (2004) Use of artificial neural networks for predicting optimal alum doses and treated water quality parameters. Environ Modell Softw 19(5):485-494. https://doi.org/10.1016/S1364-8152(03)00163-4

Negnevitsky M (2005) Artificial intelligence: a guide to intelligent systems. Pearson Education, Edinburgh

Russell S, Norvig P (2002) Artificial intelligence: a modern approach. Prentice Hall, New Jersey

Singh B, Sihag P, Singh K (2017) Modelling of impact of water quality on infiltration rate of soil by random forest regression. Model Earth Syst Environ 3(3):999-1004. https://doi.org/10.1007/s40808-017-0347-3

Wolfgang E (2011) Introduction to artificial intelligence. Springer, Cham

The Use of Industrial Alkaline Wastes to Neutralise Acid Drain Water from Waste Rock Piles

Nikolay Maksimovich, Vadim Khmurchik, Olga Meshcheriakova, Artem Demenev, Olga Berezina

Natural Science Institute of Perm State University, Genkel Street 4, Perm, Russian Federation, khmurchik.vadim@mail.ru

Abstract

Coal mining always results the formation of large volumes of rock wastes, which can be stacked in piles. Around 100 piles of various sizes are located in the Kizel coal basin, Western Urals, Russian Federation; some of these piles are burned nowadays. Rock piles drainage water have pH – 1,8-6,3, Fe – 0,2-28050 mg L^{-1}, Al – 0,5-3550 mg L^{-1}, Mn – 0,13-88 mg L^{-1}, and total mineralization – up to 50000 mg L^{-1}. A lot of metals and metalloids are transported with drain water from waste piles to soil, groundwater and the nearest river systems and pollute them.

We studied the capability of industrial alkaline wastes, covered waste rock piles, to neutralise drain water, formed during rainfalls. Preliminary laboratory experiments showed high efficiency of acid mine water treatment with lime-containing metallurgical slag, alkaline soda plant's waste and limestone mining waste. The last two substances were used as reagents in the burned and unburned waste rock piles treatment experiment. Two solutions were separately used as leaching agents – distilled water to mimic rainfalls, and solution of organic substances (glucose and sodium acetate, 0.5 g L^{-1} each) to mimic rainfalls, drained plant vegetation.

The most effective alkaline reagent for drain water neutralization was soda plant's waste. The investigation revealed that organic substances addition increased the efficiency of waste rock piles treatment with alkaline wastes used. Mathematical calculations showed that covering of waste pile with 0.3 m thick layer of soda plant's waste could be enough for long term neutralization of drain water, being formed during rainfalls.

The using of alkaline industrial byproducts and wastes to cover waste rock piles could be economically appropriated treatment method in the Kizel coal basin because such wastes are located in transport accessibility with the basin. The efficiency of alkaline reagents using could be improved by organic matter addition.

Keywords: Waste Rock Pile, Acid Rock Drainage, Industrial Alkaline Wastes, Column Leaching Experiment

Introduction

Mining industry is associated with the production of large quantities of waste, which potentially may cause environmental problems over very long periods of time. The primary process that causes problems is the oxidation of the sulfide minerals in the waste, which are deposited as waste piles or tailings.

Mining in the Kizel coal basin had been carried out for more than 200 years. Mines were closured in the 1990s. Over 35 million m^3 of waste rocks had been accumulated in more than 100 piles, composed of fragments of argillite, sandstone, and limestone with inclusions of coal; the content of pyrite in piles reaches 4%. Processes of physical weathering, oxidation, hydrolysis, hydration, and metasomatism occur within piles. The oxidation of pyrite releases sulfur acid and is accompanied with heat production. So, self-ignition and burning of piles, roasting and melting of their rocks, and fumarole processes within piles were detected. Rainfalls, drained piles, are enriched in soluble compounds and pollute soils, groundwaters and rivers (Khayrulina *et al*. 2016).

To prevent the pollution and acidification of natural waters from mining waste leachates, it is necessary to minimize sulfide oxidation and/or water infiltration in the waste deposit. The installation of unpermeable or semi-permeable covers, the growth of vegetation, the addition of acid-buffering materials are used to prevent formation of acid rock drainage. As the pH of the leachate is of critical importance for the discharge of contaminants, because the solubility and mobility of metals and semi-metals critically depend on their speciation, the use of carbonate minerals and carbonate-containing waste as the cover to waste pile could be an appropriate measure to prevent environment pollution.

The aim of this study is to investigate the capability of carbonate-containing wastes to neutralize the leachate of waste rock piles in small-scale column experiment.

Materials and Methods

Site Description and Sampling

The Kizel coal basin (the Western Urals, Russia) occupies area of 200 km^2 and is located within West Urals folding zone adjacent to the pre-Ural boundary deflection. Rocks of Palaeozoic (Middle Devonian – Late Permian) age are developed in the area and represented by sandstones, mudstones, siltstones, shales, limestones, dolomites, marls, coals, and others. Carbonate rocks are intensely karsted, especially in the upper part of geologic column. Quaternary deposits are mainly represented by sands, loams, and clays and have often a high content of gravel and pebbles (Khayrulina *et al.* 2016). Coal of the basin exhibits elevated content of sulfur (mainly as a pyrite) – 5.8% (Kler 1988). Annual average regional precipitation is 800-900 mm/a, and the annual average of air temperature is 0-2 °C, with 160-170 days with an average air temperature below 0 °C (Maksimovich, Pyankov 2018).

Samples of burned and unburned waste rocks were taken from the partially burned pile of "Severnaya" mine. About 10 kg of rocks were separately sampled at burned and unburned parts of the pile from the depth of 0.5 m below pile surface. The moisture content of burned waste rock was 18%, pH of water suspension was 3.8. The moisture content of unburned waste rock was 14%, pH of water suspension was 2.8. Samples were sieved and the fraction of less than 1 mm in dimensions was used in column leaching experiment.

Alkaline Wastes

Carbonate-containing wastes of two industrial enterprises, soda plant in Berezniki town and limestone mining quarry at Chusovoy town, were used as alkaline reagents in experiment. These enterprises are located in the transport accessibility with the Kizel coal basin – 20 km for limestone quarry, and 120 km for soda plant.

Soda plant's waste was sampled from the tailing dump. It comprised the water suspension of various minerals with liquid:solid ratio of 85:15 and pH 9.5. Total mineralization of liquid phase was about 180 g L^{-1} (Maksimovich, Pyankov 2018). To determine the water content, the subsample was weighted before and after drying for 2 days at 60 °C. Water content of soda plant's waste was 88%. Mineral composition of the solid phase is presented in tab. 1.

Sample of crushing waste was taken from limestone mining quarry and sieved. The fraction of less than 1 mm in dimensions was used in column leaching experiment. To determine the water content, the subsample was weighted before and after drying for 2 days at 60 °C. Bulk density of the sample was 1.53 kg m^{-3}, water content – 2%. Mineral composition of the sample is presented in tab. 1.

Table 1 *Mineral characteristics of alkaline wastes, %.*

Mineral	Soda plant's waste	Limestone mining waste
Calcite	90.6	88.7
Dolomite	0.6	2.4
Quartz	0	8.9
Cristobalite	0.4	0
Gypsum	4.3	0
Halite	4.1	0
Total	100	100

Table 2 The numeration of columns in the leaching experiment.

Alkaline reagent	Soda plant's waste			Limestone mining waste			No reagents	
Amount of alkaline reagent, %	1	5		1	5			
Leaching solution [a]	W	W	S	W	W	S	W	S
Burned waste rock pile	2, 3	5, 6	4	8, 9	11, 12	10	7	1
Unburned waste rock pile	14, 15	17, 18	16	20, 21	23, 24	22	19	13

[a] W – distilled water, S – solution of glucose and sodium acetate, 0.5 g L^{-1} each.

Column Leaching Experiment

Inverted bottom-cutted 0.5 L bottles made of high density polyethylene (HDPE) were used as cylindrical columns with tapered lower part. The dimensions of cylindrical part were 0.09 m in height and 0.06 m in diameter. The height of conical part was 0.12 m, diameters of conical part were 0.06 and 0.025 m. The lower end of inverted bottle (bottle neck) was sealed with the cap with glued rubber tube (0.2 m in length, 0.005 m inner diameter). HDPE grid (average pore size of 0,5 mm) and filter paper were placed inside the cap to hold sample and prevent finer sample particles escaping from column. Assembled columns were acid washed, triple rinsed with deionised water, and air-dried before use.

250-270 g of waste rock sample was placed into the column and covered evenly with an alkaline reagent, then 50-70 ml of a leaching solution was carefully added to the top of the column to avoid the erosion of cover layer. After percolation of the solution through the column, formed leachate was collected in glass jars and its pH was estimated. The addition of the solution was once a day, the channeling and preferential routs were not observed in the columns during experiment. Columns leaching experiment was performed at room temperature (22.5 ± 2.5 °C), the evolution of the leachate's pH was examined.

Different amounts of alkaline reagents were used to cover waste rock samples, 1 and 5% wet weight of waste rock wet weight. Control columns did not contain alkaline reagents.

Two solutions were separately used as leaching agents – distilled water to mimic rainfalls, and solution of organic substances (glucose and sodium acetate, 0.5 g L^{-1} each) to mimic rainfalls, drained plant vegetation. The matter is, the most of piles are covered with vegetation, so percolating rainfalls are enriched in organic matter originated from root exudates and decomposed plant residues. As a removal of vegetation before the alkaline treatment of piles could be costly and technically difficult, it was the reason to use the solution of organic substances in the experiment. The experiment's scheme is presented in tab. 2.

Results and Discussion

Results of the column experiment with different leaching solutions are presented in fig. 1. Initial pH of water suspensions of burned and unburned waste rock samples were 3.8 and 2.8, correspondingly. pH of distilled water, percolated through the columns, had a tendency to rise gradually and reached 4.4 and 3.5 at 84th day of the experiment. This effect could be attributed to the presence of such alkaline-generating minerals in waste rock piles, as limestone. The presence of this mineral in waste rock piles was observed (Khayrulina *et al*. 2016).

Addition of organic substances to water, percolated through the columns, induced more substantial rise of pH: *approx*. 5.1 to both burned and unburned waste rock samples at 44th day of the experiment, and *approx*. 6.1 and 5.4 at 84th day, correspondingly. These organic substances, glucose and sodium acetate, are readily used by bacteria, inhabiting pile's rocks and producing CO_2 as an end-product in metabolic processes. We supposed, the implementation of plants vegetation on the pile's surface could to some extent be an acid drainage prevention

a)

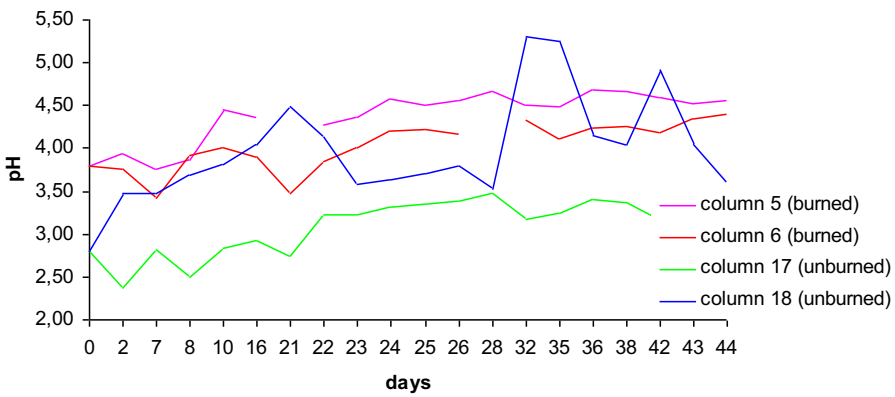

b)

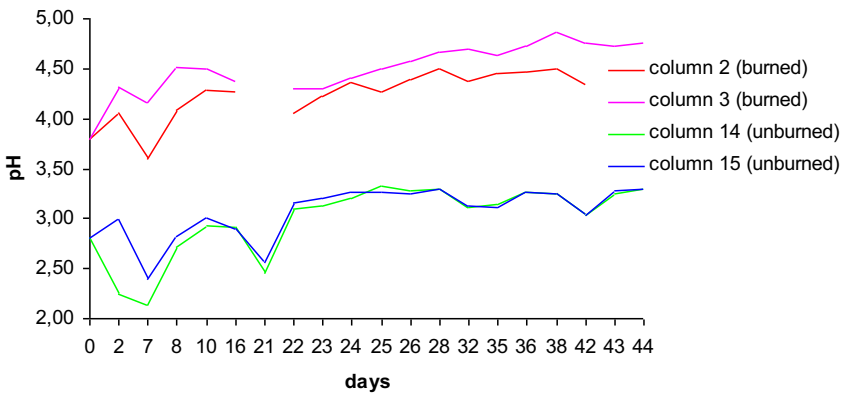

c)

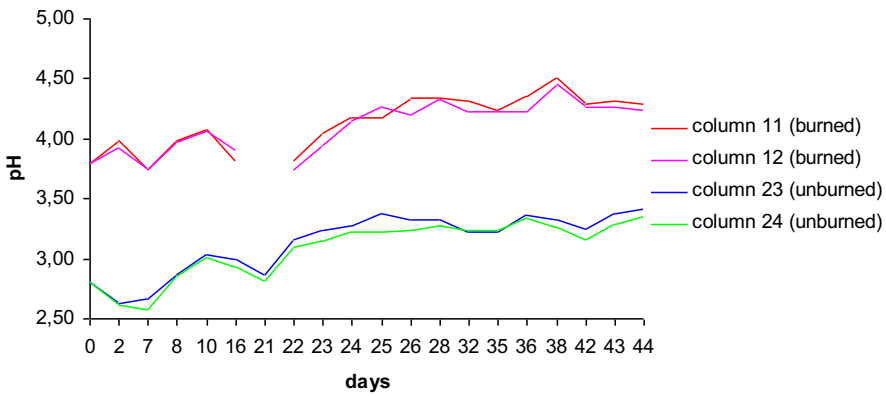

Figure 1 *The evolution of the leachate's pH during experiment.*
a) burned and unburned waste rock + soda plant's waste, 5% + water;
b) burned and unburned waste rock + soda plant's waste, 1% + water;
c) burned and unburned waste rock + limestone mining waste, 5% + water;

d)

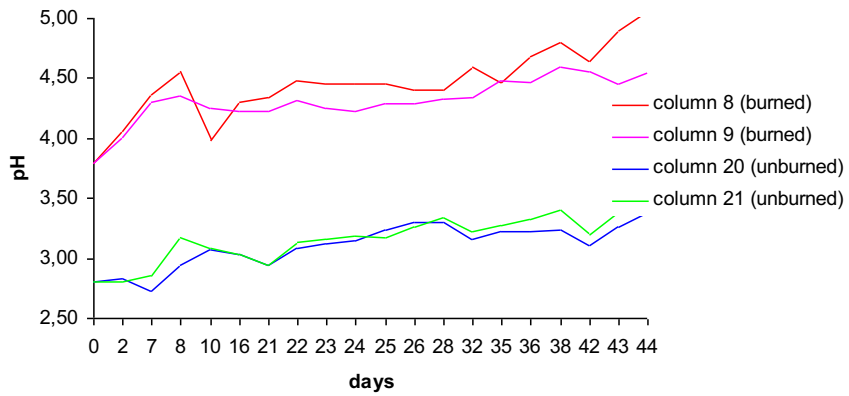

e)

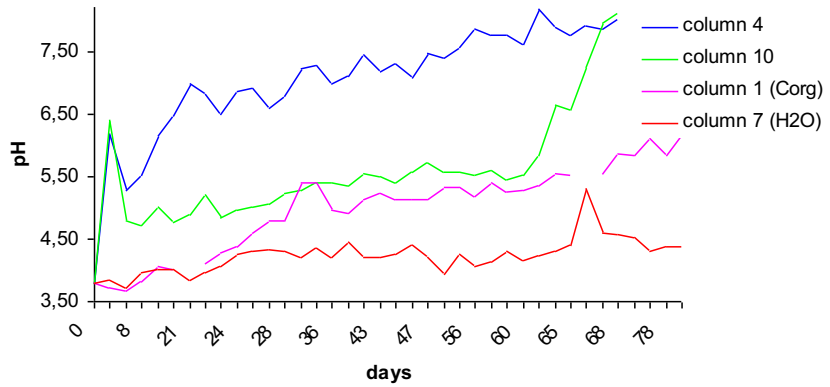

f)

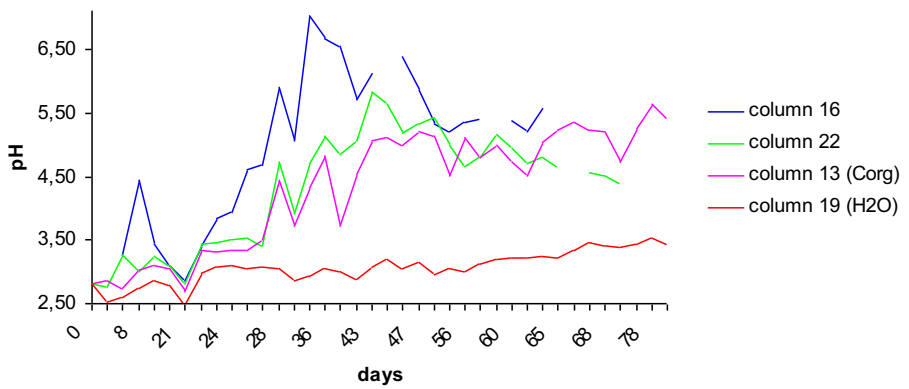

d) burned and unburned waste rock + limestone mining waste, 1% + water;

e) burned waste rock: column 4: + soda plant's waste, 5% + Corg solution; column 10: + limestone mining waste, 5% + Corg solution; column 1: + Corg solution; column 7: + water;

f) unburned waste rock: column 16: + soda plant's waste, 5% + Corg solution; column 22: + limestone mining waste, 5% + Corg solution; column 13: + Corg solution; column 19: + water.

measure due to enhanced water transpiration by plants, decreasing the amount of drained water, and addition of organic substances, originating from living and dead plants and inducing both bacterial metabolism and formation of CO_2 in piles.

The covering of waste rock samples with alkaline reagents rose pH of leaching solutions. The effect of soda plant's waste addition did not substantially differ from limestone mining waste addition, as it can be seen in fig. 1. However, the water content was 88% in soda plant's waste, whereas it was 2% only in limestone mining waste. So, soda plant's waste was the most effective alkaline reagent in the experiment, based on dry weight calculation.

The highest pH values were observed in columns covered with alkaline reagent and drained with solution of organic substances.

Mathematical calculations showed that covering of waste pile with 0.3 m thick layer of soda plant's waste could be enough for long term neutralization of drain water, being formed during rainfalls.

Conclusions

The using of alkaline industrial byproducts and wastes to cover waste rock piles could be economically appropriated treatment method in the Kizel coal basin because such wastes are located in transport accessibility with the basin. The efficiency of alkaline reagents using could be improved by organic matter addition.

Acknowledgements

The reported study was funded by RFBR, project number 19-05-50073.

References

Khayrulina EA, Khmurchik VT, Maksimovich NG (2016) The Kizel coal basin (The Western Urals, Russia): Environmental problems and solutions. In: Drebenstedt C, Paul M (eds) Proc, IMWA 2016 Ann Conf. Freiberg/Germany (TU Bergakademie Freiberg), p. 766–771

Kler VR (1988) Metallogeny and geochemistry of coal-bearing and slate series in USSR, Nauka (in Russian)

Maksimovich NG, Pyankov SV (2018) The Kizel Coal Basin: Environmental Problems and Answers. Perm State University, Perm. 288 p. (in Russian)

Geochemical Sources and Long-Term Implications of Mine Waste Weathering, Cwmystwyth Mine, Wales

Yulieth Marquinez[1,2], Rob J Bowell[2,3], Tim Jones[2], Peter Braham[2]

[1]*Palatine House, Sigford Rd, Marsh Barton, Exeter EX2 8NL, Wales, YuliethM@cgl-uk.com*

[2]*School of Earth and Environmental Sciences, Cardiff University, Park Place, Cardiff, Wales, JonesTP@cardiff.ac.uk; Brabham@cardiff.ac.uk*

[3]*SRK Consulting, Cardiff, Wales, rbowell@srk.co.uk*

Abstract

Evaluation of the distribution and leaching potential of lead, cadmium, and zinc from the Cwmystwyth Mine has been undertaken along with surface grab sample mineralogy. Metal concentrations and pH were evaluated respectively, in which a general weak association between these two factors was found. Using these two parameters, a Ficklin diagram was created to assess the type of drainage being produced at the Cwmystwyth Mine, which indicated that metal leaching neutral mine drainage is being generated.

Discharge water from mine workings, waste materials and outcrop generated some variations in terms of pH and metal concentration, with most samples showing alkaline results but higher metals from water that flows through the mine (Nant y Gwaith).

Given the extensive mining history at Cwmystwyth, it is no wonder that metals are finding their way through the environment, heavily exceeding the EQS set out by the European Commission. Lead concentrations in all samples but one exceeded the EQS range, and dissolved metal concentrations in the water samples significantly increased downstream. Zinc concentrations are uniformly high, reflecting the higher mobility of zinc over lead and secondary zinc minerals are much rarer than lead sulfate or lead carbonate phases. Cadmium geochemistry appears controlled by zinc mobility and secondary phases.

In summary, the mine is heavily contaminating the Ystwyth catchment, with high levels of Pb, Zn, Cd, and other transition metal(loids) are contributing to this contamination such as Mn and As. As proved to be leaching, but it still meets the EQS. Contamination in the river is attributed to the water discharge and perhaps seepage from different mine tailings, adits and underground workings.

It is very unlikely that the site will be remediated by cover or removal of mine waste or by using passive treatment due to its topographical complexity, and the sensitive nature of the site, being within a protected Site of Special Scientific Interest (SSSI). Moreover, the data suggests that there have not been any improvements in terms of dissolved metals in the water when data was compared to historic values; hence the mine remains a potential source of metals to the catchment.

Keywords: Mine Waste Geochemistry, Reclamation

Introduction

The Cwmystwyth mine in central Wales has been exploited for a period of over 2000 years through to final abandonment in the early 1950s chiefly for lead and silver but in later years from the 1880s onwards for zinc as well (Bick, 1993; Meek, 2014). The mine occupies a precarious location on steep slopes and the formally glaciated valley falls sharply to the Ystwyth River with little or no flat ground between the mine workings and the river, indeed the lowest adit occurs at river level (Fig.1).

The presence of transition metals in the mine waste and soils has resulted in significant impacts to the Ystwyth catchment particularly with release of cadmium and zinc but also copper and lead (Jones & Erichsen 1958; Fuge *et al*. 1993; Mighall *et al*., 2002; Edwards & Williams, 2016). This has led to studies evaluating metal removal from water and attenuation mechanisms in the

impacted soils in the area. Cwmystwyth is a hydrologically complex site, with mining activity having had a significant impact on the natural regime. The River Ystwyth receives all surface and sub-surface drainage from the mine, causing it to fail European Water Framework Directive (WFD) standards for zinc, lead, and cadmium. The subsurface workings are drained via Pugh's, Gill's Lower and Kingside adits. Pugh's Adit is the largest point source of metals from the site, whilst Gill's Lower and Kingside are collapsed and emerge as small upwellings. There are also numerous other minor upwellings of contaminated groundwater.

In addition, a number of streams draining the plateau high above Cwmystwyth flow down through the site, eroding and mobilising sulfate and metals from the extensive waste tips and are then lost to ground as they pass over the site through mine waste or through the workings. Mine drainage is also influenced by the large Ystwyth Fault (fig.1) which runs in a northeast to southwest trend, bisecting the River Ystwyth. It is thought that contaminated groundwater from the sub-surface workings discharges directly into the river through this fault zone.

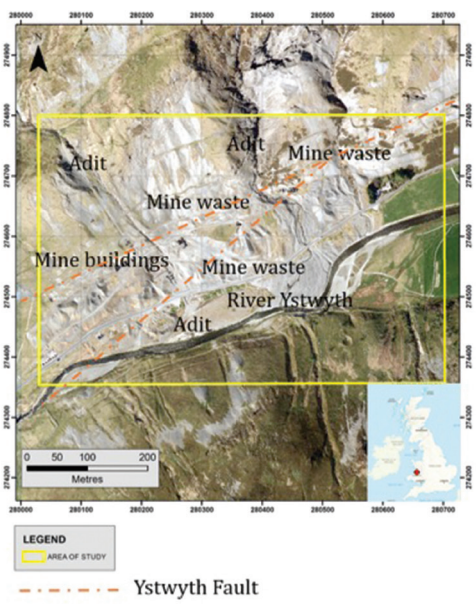

Figure 1 *Study area and main mine facilities at the Cwmystwyth Mine. Insert shows location with respect to the British Isles (Digimap and ArcMap).*

Methodology

The sampling strategy used in the site aimed to characterise areas where waste dump was deposited, and the potential pathway of the transition metals reaching the waters of the River Ystwyth, based on factors discussed in the literature review (Marquinez, 2019). This strategy could provide evidence to determine the mobility of metals in the ground and how its concentration changes downslope. A summary of methods employed is provided in Table 1. Water samples were collected from the Ystwyth River and other local streams and drainage running through the Cwmystwyth Mine. The sampling strategy was based on gathering samples from the confluent and effluents of the streams in the area to visualise changes as the water flows downstream and through the mine. A carbonate rating test was carried out with the purpose of finding out the percentage of carbonate in each sample, which will be subsequently used in a Neutralisation Potential test. Dump waste material was crushed to 4mm chips according to BS EN 12457.

These results have been mapped and compared to in-situ pH data collected in the field from these dump materials. For the purpose of this paper only lead, cadmium, manganese, arsenic, and zinc are described in detail. The heat maps showing metal distribution for these elements and paste pH are provided in Figure 3.

The maps illustrate that high metal bearing material is present at the lower adit adjacent to Ystwyth river as reflected in the hot spots for lead and arsenic at the lower Gill adit (fig.3). By comparison zinc is most anomalous in the wash-out sediment from the Hugh adit and the higher elevation workings where it appears to have been transported (fig.3). Apart from the Pugh adit

Table 1 *Summary of samples collected on site.*

Sample type	Number of samples	Testwork Undertaken
Water samples	7	ICP-MS for dissolved metals/pH
Solid Waste samples	20	XRF/XRD/Leaching test/Carbonate rating/ Neutralisation Potential/pH

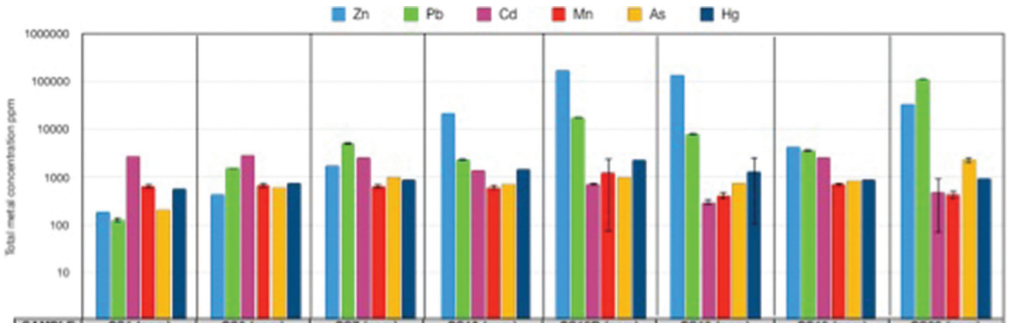

SAMPLE	CS1 (ppm)	CS3 (ppm)	CS7 (ppm)	CS10 (ppm)	CS15B (ppm)	CS18 (ppm)	CS19 (ppm)	CS20 (ppm)
Pb	125.5	1532.5	5006	2293	17558	7869.5	3605	111400
Zn	188	422	1702	21080	171400	140750	4146	33750
Cd	2800	2900	2600	1362.5	709	296.5	2600	493.5
Mn	642.5	662.5	633	596	1249	413.5	694.5	420
As	204	607	987.5	693	972	750.5	859	2274
Hg	568.5	732.5	887.5	1461.5	2300	1346.5	910.5	931.5

Figure 2 *XRF results for selected sites to illustrate range of concentrations in mine waste.*

mouth arsenic shows elevation in more acidic soils and is antipathetic to cadmium and manganese which show a visual correlation to high pH.

Assessment of Carbonate Buffering

The carbonate test results have proved a small, insignificant amount on carbonate in each sample with typically less than 1% total carbonate and only a few samples reported any calcite present, and this is reflected in the widely acidic pH of surface soils on site and reflects the local geology that is comprised of arenite and argillite host rocks (Mason, 1994).

Leached Metals

Using the results of the BS EN 12457 testwork, interpolated heat maps were derived to analyse the spatial distribution of the soluble metals that have potential to leach into the environment and cause serious harm (fig 4). These results portray the potential labile nature of the metals from surface material. Cadmium and manganese show similar trends and are most labile in the area of Gill's lower adit in the south west of the map. Lead and zinc are most labile in the sediments associated with Hugh adit whilst arsenic shows a hot spot on the side of the hill where

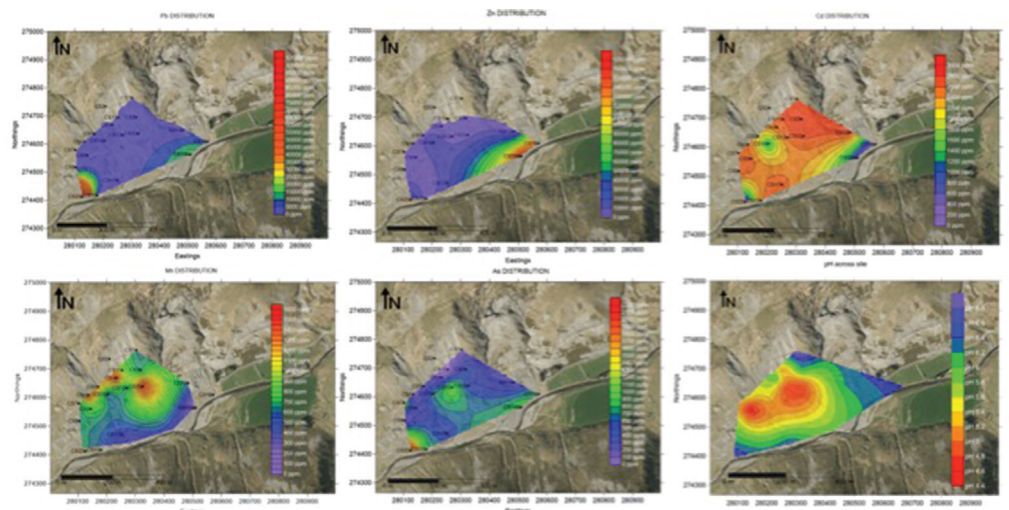

Figure 3 *Heat maps showing total element distribution for Pb, Zn, Cd, Mn, & As as well as paste pH for the area of study shown in Figure 1.*

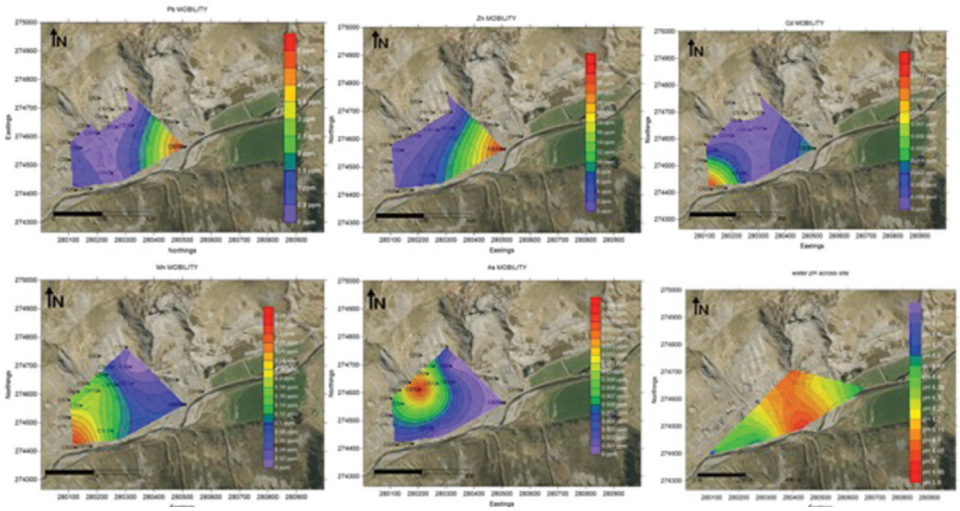

Figure 4 Heat maps for leachable metals in EN12457 leachate and site water map.

pH is neutral and from other data total iron content is low.

In the pH map of the River Ystwyth upstream and downstream from the mine, where acidic to neutral waters can be observed (fig.4). This indicates most of the acidic waters are coming from the Nant Y Gwaith which travels through the mine and waste dump located closer to the Ystwyth river. Regression analysis on water chemistry indicated that lead and zinc have an antipathetic relationship to pH whilst arsenic is positively correlated. Manganese and cadmium show a stronger relationship to alkalinity than pH.

Discussion

A useful visualization for mine water chemistry-pH interactions is the Ficklin diagram (Ficklin *et al.*, 1992). The plot defines fields of different water chemistry based on concentration of divalent cations and pH. The results in the Cwmystwyth mine are plotted in Figure 5, where it can be inferred that Neutral Mine Drainage (NMD) could be taking place, as most samples lie within the near-neutral/high-metal and near-neutral/low-metal zones. However, this diagram is not yet used as a formal guideline to define AMD or NMD, and due to the small number of samples this could be rather inconclusive. However, if more samples had been collected similar results could be expected.

Neutral pH in the mine could be attributed to the lack of pyrite as evidenced by the XRD results, where only sample CS10 contained less than 1% pyrite. The majority of sulfides comprise, galena and sphalerite that are both non-acid generating. According to the XRD and Carbonate Rating test, buffering is coming from silicate minerals rather than calcite, such as Albite ($NaAlSi_3O_8$) and Muscovite ($KA_{l2}(AlSi_3O_{10})(OH)_2$). Carbonate minerals generate significantly more neutralisation potential than silicate minerals, which means that the extremely low concentration of carbonate in the sample after the carbonate test indicates that there is no neutralisation potential for the studied samples, as this is directly related to the abundance of non-Fe/Mn carbonate minerals. This can be compared to a study by Jambor (2003) where it is stated that certain silicate minerals are known to buffer mine effluents at a neutral pH.

A site conceptual model of the Cwmystwyth mine (fig.6) has been developed using literature resources from a desk study and field observations. The conceptual model aims to identify and highlight the environmental linkage for the studied transition metals, which are causing the River Ystwyth to be severely contaminated.

A few sources were identified such as the mine tailings (diffuse pollution) and waste dump located near the river itself. These material dump sites are exposed to weather

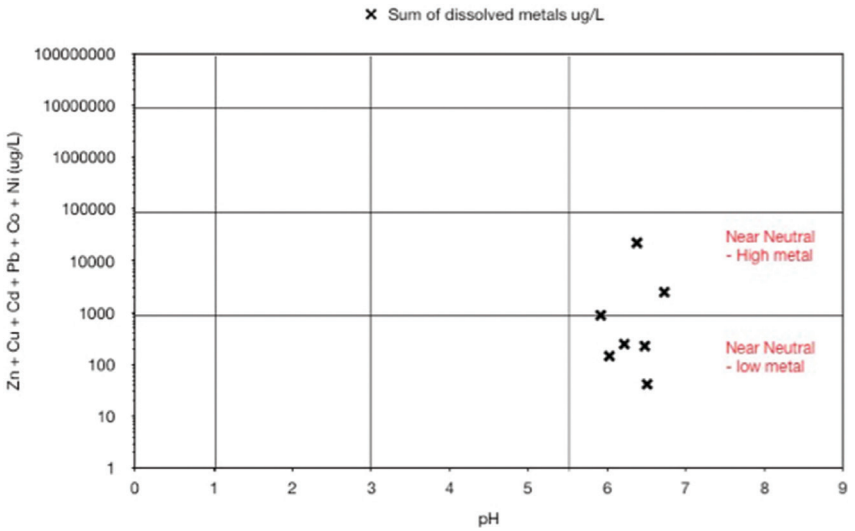

Figure 5 *Ficklin plot, Cwmstwyth mine waters.*

conditions and precipitation. Hydrological processes are a key element in this investigation, as it is expected that rainfall will infiltrate these tailings, weathering and leaching transition metals from ore deposits or mine spoil, which will consecutively seepage into the fractured bedrock reaching the water table and flowing along its direction into the receptor. The mineral lodes containing Pb and Zn underground may be a great source of contamination as the ore is being exposed to water.

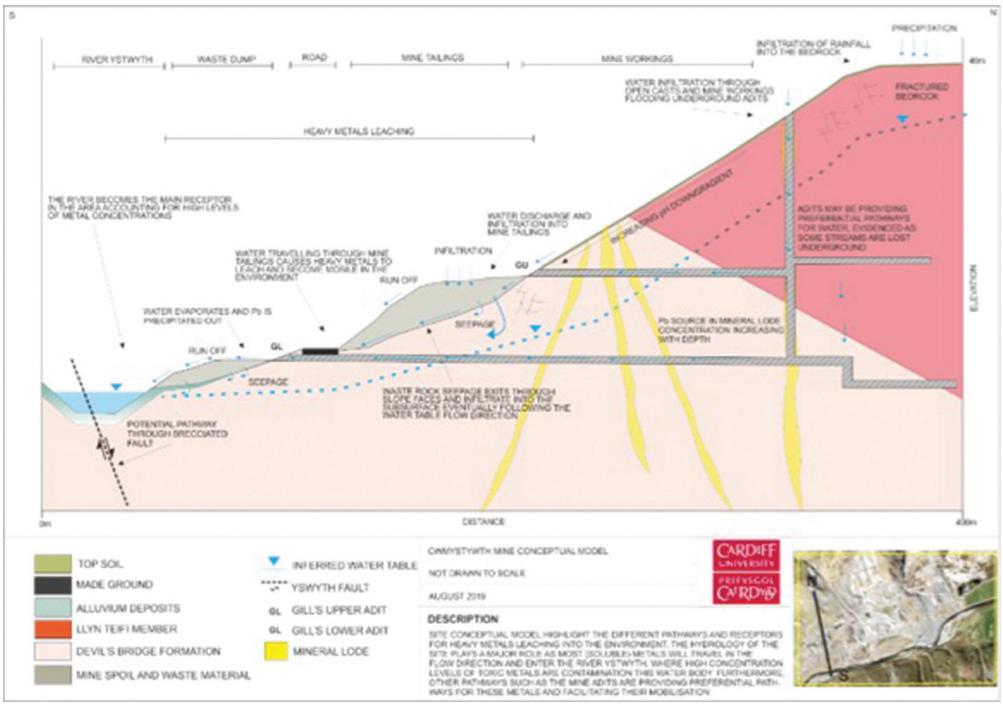

Figure 6 *Conceptual model, Cwmstwyth mine waters.*

The regulation of mine waste in the UK is managed by the Coal Authority in collaboration with the Environment Agency and Natural Resources Wales (Environment Agency, 2016). However, due to the diverse opinions of stake holders to the site and its designation as a Site of Special Scientific Interest it is highly unlikely to be remediated in the near future.

Conclusions

The aim of this research entailed the evaluation of the distribution and leaching potential of transition metals in the Cwmystwyth Mine. Along with this, mineralogy was investigated to determine whether pyromorphite could have an influence in the natural attenuation of lead to prevent its mobility in the environment.

Metal concentrations and pH were evaluated respectively, in which a general weak association between these two factors was found. Using these two parameters, a Ficklin diagram was created to assess the type of drainage being produced at the Cwmystwyth Mine, which indicated that neutral mine drainage is taking place due to the low to high metal concentration and the near-neutral pH linked with the site.

In summary, the mine is heavily contaminating the Ystwyth catchment, with high levels of Pb, Zn, Cd, and other transition metals are contributing to this contamination such as Mn and Ni. As proved to be leaching, but it still meets the EQS. Contamination in the river is attributed to the water discharge and perhaps seepage from different mine tailings, adits and underground workings. The metals leaching are found in favourable conditions which are facilitating their migration into the River Ystwyth such as topography, high rainfall, high exposure to air and water etc. increasing its potential to oxidise and become mobile. Collecting field data during different seasons throughout the year could potentially show a variation in results in terms of dissolved metals being loaded into the catchment.

Reference

Atkins (2008) Metal Mine Monitoring Project 2006/07 Cwmystwyth Mine Site Monitoring Summary Report. Prepared for Environmental Agency Wales

Bick, D.E, (1993) The Old Metal Mines of Wales, Parts 1-6. Pound House, Newent.

Edwards P, Williams T (2016) Abandoned Mine Case Study: Cwmystwyth Lead Mine. June 2016, 2p. Natural Resources Wales.

Ficklin WH, Plumlee GS, Smith KS, McHugh JB (1992) Geochemical classification of mines drainages and natural drainages in mineralized areas. Proc 7th International Symposium on Water-Rock Interaction, Park City, 13-18 July 1992 V1, P381-384. Rotterdam: A A Balkema, 1992

Fuge R, Pearce FM, Pearce NJ, Perkins WT (1993) The geochemistry of cadmium in the secondary environment near abandoned metalliferous mines, Wales. Applied Geochemistry 2: 29-35.

Jambor, J.L., (2003) Mine-Waste Mineralogy and Mineralogical Perspectives of Acid-Base Accounting. In: J.L. Jambor, D.W. Blowes and A.I.M. Ritchie (Eds.), Environmental Aspects of Mine Wastes, Short Course Series Vol. 31, Mineralogical Association of Canada, 117-146.

Jones, J.R. Erichsen (1958). "A Further Study of the Zinc-Polluted River Ystwyth". Journal of Animal Ecology. 27 (1): 1–14.

Mason, J.S. (1994) A regional paragenesis for the Central Wales Orefield. Unpublished M.Sc. thesis, University of Wales.

Mighall TM, Abrahams PW, Grattan JP, Hayes D, Timberlake S, Forsyth S (202) Geochemical evidence for atmospheric pollution, Cwmstwyth, mid-Wales. Science of the Total Environment, 292:69-80.

Meek, J. (2014). Cwmystwyth Mines, Ceredigion: Management and Protection Plan. Dyfed Archaeological Trust.

Warrender R, Pearce NJ, Perkins WT, Florence KM, Brown AR, Sapsford DJ, Bowell RJ, Dey BM (2011). Field trails of low cost Reactive Media for Passive Treatment of Circum-neutral Metal Mine Drainage in Mid-Wales, UK. Mine Water & Environment 30:82-89

Effects of vegetation on erosion in technosols produced from coal waste

Daniel Campos Moro, Jéssica Weiler, Ivo André Homrich Schneider

Universidade Federal do Rio Grande do Sul - UFRGS, Departamento de Engenharia de Minas, Laboratório de Tecnologia Mineral e Ambiental, Porto Alegre – Rio Grande do Sul – Brasil, daniel.campos@ufrgs.br, jessica.weiler18@gmail.com, ivo.andre@ufrgs.br

Abstract

The aim of this study was to evaluate soil loss by water erosion considering different technosols configurations produced from fine and coarse coal waste and an agricultural soil. All substrates were amended with sewage sludge to obtain 3% organic matter. The study considered two precipitation levels and the presence, or not, of the *Medicago sativa* (alfalfa) and grass. Calculations were carried using the Revised Universal Soil Loss Equation. In terms of erosion control, the best configuration was attained with the mixture of coarse and fine waste. The presence of vegetation reduces in almost 100 times soil loss due rainfall.

Keywords: Mining Waste, Technosols, PlantGrowth, Soil Erosion, Rehabilitation

Introduction

Mining sites should be properly managed. Environmental control is essential in the contemporaneous mining as well as in environmental liabilities eventually left by past mineral exploration activities. In this multivariable system, the control of topsoil erosion is one of the important issues to be considered (Yellishetty *et al*, 2013; Zhang *et al*, 2015).

In coal processing plants, coarse and/or fine wastes are produced from parallel circuits (Leonard, 1991; Riazi and Grupta, 2015). Among the main impacts of mining waste disposal are changes in the physical and chemical conditions of the soil, which hinders plant growth (Ghose, 2005; Daniels and Stewart, 2010; Sheoran *et al*., 2010; Kossoff *et al*, 2014). The most common strategy to land rehabilitation is to cover coal waste with the native topsoil removed and stored from the beginning of the mining activity and/or with natural soil from borrow areas (Daniels and Zipper, 2010).

The presence of vegetation is very important to prevent particles transportation by wind or water (Ghose, 2005; Brotons *et al*, 2010; Sheoran *et al*., 2010; Zhang *et al*., 2013; Ghose, 2005; Zhang *et al*., 2015). Soil erosion can generate several negative impacts, including the transport of sediments to water bodies. Thus, it is important to consider strategies of progressive rehabilitation of coal waste deposits, such as the establishment of technosols - artificial soils derived from anthropic materials – which can speed up the revegetation. Recent studies have demonstrated success in plant growth of substrates produced from coal mine wastes amended with organic and alkaline materials (Firpo *et al*., 2015, 2020; Weiler *et al*., 2018, 2020).

The aim of this study was to evaluate soil loss by water erosion considering different technosols configurations produced from fine and coarse coal waste and an agricultural soil. The study also considered the effect of the cultivar Medicago sativa (alfalfa) and grass on the erosion process.

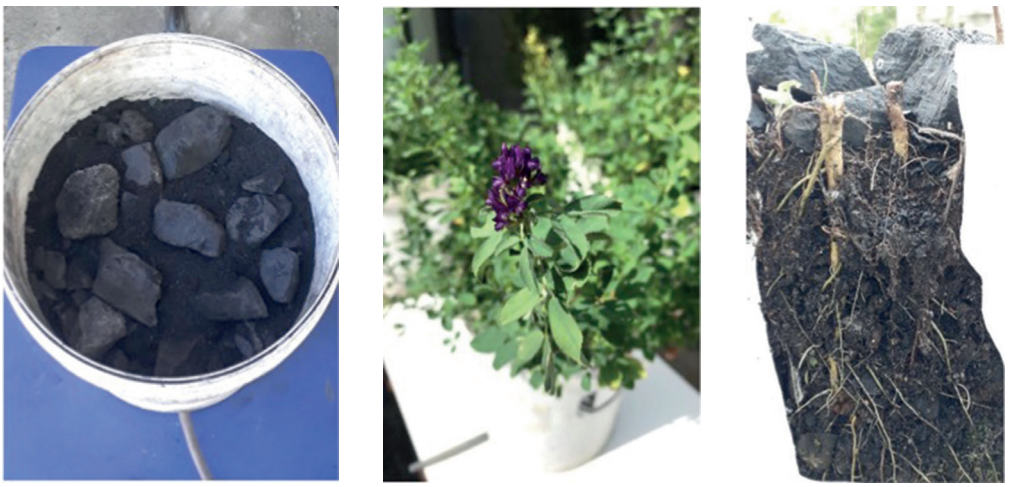

Preparation of technsols | Alfalfa and grass growth | Root system

Figure 1 *Alfalfa and grass growth in technosol experiment.*

Methodology

The study is part of a current experiment in Brazil (started in Dec. 2018), at the Federal University of Rio Grande do Sul. A mixture of mineral (fine and coarse coal waste) and organic (sewage sludge) material to produce technosols was performed in 25 L vessels (Figure 1). The mineral matrix was obtained from the Moatize Mine in Mozambique, one of the largest coal deposits in Africa. In relation to generation of coarse and fine wastes, the beneficiation of coarse ROM particles is performed by dense medium cyclones (1 mm < d < 50 mm) while the fine ROM particles, by spirals or elutriation (fraction 0.25 < d < 1 mm) and by flotation (fractions d < 0.25 mm). The sludge came from a municipal sewage treatment plant.

Fine and coarse coal waste were analyzed by granular and mineral properties. Granular properties of samples were evaluated by particle size distribution, particle density, bulk density, and porosity. Particle size distribution was performed using a Tyler standard screen series. Particle density was determined gravimetrically by pycnometry. Bulk density (or apparent density) and porosity, which were carried out following ASTM D167 (ASTM, 2012a). Mineralogical analysis was carried out by X-ray diffraction (XRD) in a Siemens (Bruker AXS, United States) X-ray diffractometer.

Six technosols using different layer configurations of materials were evaluated, all of them with sewage sludge to obtain 3% organic matter: 1. Fine coal waste (FCW); 2. FCW + Coarse coal waste (CCW) – composing two seams; 3. FCW + CCW – as a mixture; 4. Agricultural soil (AS) + FCW + CCW – composing three seams; 5. AS + mixture of FCW + CCW – composing two seams; 6. AS + FCW + CCW – as a mixture. The last one, numbered as 7 and used as control, was composed just by agricultural soil. The technosols layers are presented in Figure 2. Plant growth have been simulated with *Medicago sativa*, one of the cultivars that present successful growth is such tecnosols (Weiler *et al*, 2020).

The Revised Universal Soil Loss Equation (RUSLE) was used to estimate to estimate the annual soil loss from different soil configurations. The formula of the RUSLE is as follows (equation 1):

$$A = R.K.(L.S).(C.P) \quad (1)$$

where A is the predicted soil loss on the average unit area (t ha^{-1} y^{-1}); R is the rainfall erosivity factor (MJ mm ha^{-1} h^{-1} y^{-1}); K is the soil erodibility factor (dimensionless); LS is the terrain factor – surface length and slope (dimensionless); C is the cover management factor (dimensionless); and P is the conservation practice factor (dimensionless).

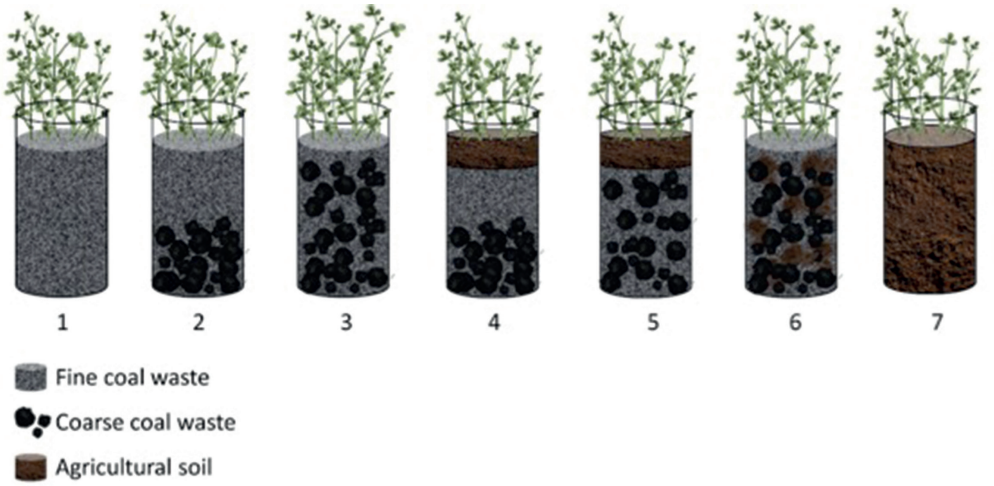

Figure 2 Technosols produced with fine and coarse coal waste and agricultural soil in different layers.

The parameters were adapted according to the geographic region of the coal wastes (Tete Province, Mozambique). It was considered a trapezoidal shape common format of the modules used for the disposal of mineral tailings with a surface inclination of 3°. To calculate the erosivity factor (R), the annual rainfall values of the studied region were considered, with minimum values of 532 mm year^{-1} and maximum values of 1028 mm year^{-1}, according to equation 2 (Roose, 1996):

$$R = a.0.8+0{,}05 \quad (2)$$

where a (mm y^{-1}) is the annual rainfall.

The soil erodibility factor (K) was defined from the EPIC-K equation, where it is necessary to know the organic composition of the soil and its particle size distribution. The formula is (equation 3): (3)
where: SAN, SIL and CLA is % of sand, silt and clay in the particle composition, respectively; C' is % of organic carbon in the soil;

$$SN_1 = 1 - \frac{SAN}{100}.$$

The topographic factors, referring to the length and slope of the studied surface, were obtained from the adaptation of the equations provided by the LS-TOOL Software (Zhang *et al.*, 2013), described below:

$$L = \left(\frac{\lambda}{22.13}\right)^m \quad (4)$$

$$m = \frac{\beta}{(1+\beta)} \quad (5)$$

$$\beta = \frac{sen\theta}{[3\times(sen\theta)^{0.8}+0.56]} \quad (6)$$

$$S = 10.8\times sen\theta + 0.03 \text{ se } \theta < 9\% \quad (7)$$

$$S = 16.8\times sen\theta - 0.5 \text{ se } \theta \geq 9\% \quad (8)$$

where: λ = surface length (m); m = exponent of length-slope variation; β = declivity factor; θ = surface inclination. Based on McCool *et al.* (1989)

The conservation practices factor (P) was considered 1.0, referring to the hillside vegetation management. This is due to the size of the waste disposal modules, which are not long enough to carry out practices such as contour lines and terracing, which would reduce the P factor to 0.5 and 0.1, respectively (Carvalho, 1994). Finally, the soil use and management factor (C) refers to the type of planting established on the analysis surface, considering Alfalfa and grass scenarios which correspond a C factor of 0,0134 (Schmidt *et al.*, 2017).

$$K = \left(0.2 + 0.3e^{\left[-0.0256SAN\left(1-\frac{SIL}{100}\right)\right]}\right) \times \left(\frac{SIL}{CLA+SIL}\right)^{0.3} \times \left[1 - \frac{0.25C'}{C'+e^{(3.72-2.95C')}}\right] \times \left[1 - \frac{0.7SN_1}{SN_1+e^{(22.9SN_1-5.51)}}\right]$$

Equation 3

Table 1 Crystalline components and particle analysis of the components of technosols.

	Fine waste	Coarse waste	Agricultural Soil
Crystalline components			
Major	Quartz	Quartz	Quartz, kaolinite
Minor	Calcite, hematite	Calcite, hematite	Hematite
Particle analysis			
Sand (%)	96.6	8.95	41.75
Silt (%)	3.4	0.22	35.55
Clay (%)	0	0	22.7
Particle size (mm)	0.1 – 1.0	0.5 – 50.0	< 2.0
Density (g cm-3)	1.79	2.21	1,55
Apparent density (g cm-3)	1.09	1.18	1,05
Porosity (%)	46.5	39.5	10

Results

Properties of the materials used to construct the technosols are depicted in Table 1. Regarding the crystalline composition, coal wastes are mainly composed of quartz, calcite and hematite while the agricultural soil by kaolinite and quartz. The particle size distribution varies from 0.1 to 1 mm for fine waste, from 0.5 to 50 mm coarse waste and less than 2 mm for agricultural soil. This assessment was carried out in a previous study by Weiler *et al.* (2020).

The results of soil loss using the RUSLE equation for the technosols configurations, for two precipitation conditions (532 and 1078 mm y^{-1}) and with alfalfa and grass planting, are shown in Table 2. Soil 3 has the lowest soil loss compared to the others, with a loss of 0.13 t ha^{-1} y^{-1} considering a precipitation of 532 mm y^{-1} and 0.27 t ha^{-1} y-1 considering a precipitation of 1078 mm y^{-1}. Soils 4, 5 and 7, which contain agricultural soil on the surface, had higher soil loss. This is due to the fact that the particle size of the agricultural soil is lower than that of the tailings, reducing the soil erodibility factor (K) in the RUSLE equation.

The results presented in Figure 3 were obtained considering the best technosol configuration and the agricultural soil with and without vegetation (alfalfa and grass). They clearly indicate the importance of the vegetation to the erosion control. For a precipitation of 532 mm y^{-1}, the soil loss would increase from 0.13 to 10.03 t ha^{-1} y^{-1} for Technosol 3 and from 0.17 to 13.02 t ha^{-1} y^{-1} for agricultural soil. So, provide a proper condition for plant growth is an essential step in the process of ecological restoration in mining areas.

Table 2 Soil loss in technsols with a vegetation coverage compose by alfalfa and grass considering two precipitation levels and seven soil configurations.

Precipitation mm y^{-1}	Soil Configuration	Soil loss t ha^{-1} y^{-1}
532	1	0.16
	2	0.16
	3	0.13
	4	0.17
	5	0.17
	6	0.17
	7	0.17
1078	1	0.31
	2	0.31
	3	0.27
	4	0.35
	5	0.34
	6	0.34
	7	0.35

Results attained in this work are consistent with some others encountered in the literature. Yellishetty *et al.* (2013) also estimated the soil erosion from mine waste rock dumps using the RUSLE model, finding values between 5 and 25 t ha^{-1} y^{-1} dependent on the slope angle and slope length. These values are similar to those found for soils without plants presented in this work (10,03 and 13,02 t ha^{-1} y^{-1}). Zhang *et al.* (2015) investigated the effects of vegetation on erosion with a field experiment in coal-mine dumps: considering the local rainy season (331 mm), the soil loss was approximately 5 t ha^{-1} for a soil with vegetation and 25 ha^{-1} for soil without vegetation. The values found

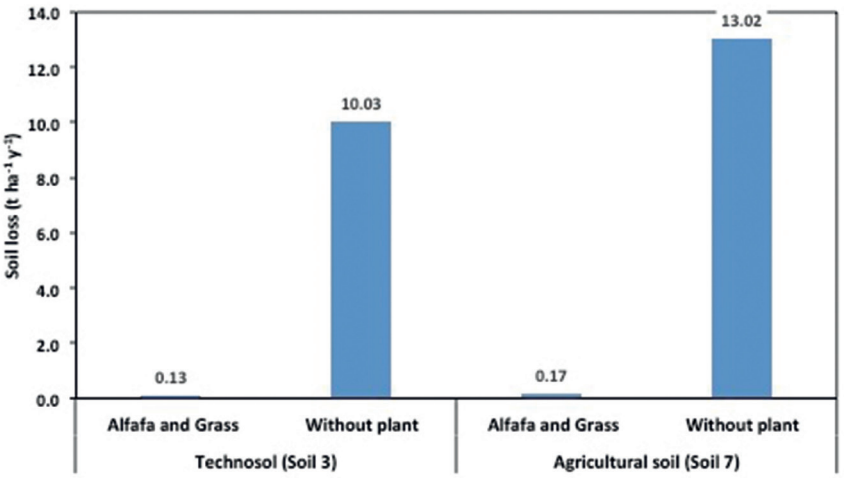

Figure 3 *Soil loss on a technosol and agricultural soil with and without plant coverage considering an annual precipitation of 532 mm.*

considering the use of alfalfa in the present study were lower, but both studies present a great difference in terms of erosion between the soil with and without vegetation. These results confirm that vegetation is fundamental in the conservation of water and soil as well as in the ecology restoration in mined areas.

Conclusion

This study confirms that technosols produced from coal waste can be a successful strategy to the rehabilitation process, allowing plant growth and erosion control. Best configuration for erosion control was attained with the mixture of fine and coarse coal waste in one single layer. The presence of vegetation reduces in almost 100 times soil loss due rainfall. Considering the calculations, soil loss in Moçambique coal deposits the order of 10 t ha^{-1} y^{-1} can be reduced to 0.1 t ha^{-1} y^{-1} as long as is suitable conditions for plant growth. Field observation should be carry out to confirm these results.

Acknowledgements

The authors are grateful for the financial support extended by Conselho Nacional de Desenvolvimento Científico e Tecnológico (CNPq) and Coordenação de Aperfeiçoamento de Pessoal de Nível Superior (CAPES) for this research.

References

Brotons, J.M., Díaz, A.R., Sarría, F.A., Serrato, F.B., 2010. Wind erosion on mining waste in southeast Spain. L. Degrad. Dev. 21, 196–209.

Carvalho, N.O. (1994). Hidrossedimentologia Prática. Rio de Janeiro: CPRM, 372 p.

Daniels, W.L., and Stewart, B., 2010. Reclamation of Coal Refuse Disposal Areas. VCE publication 460-131.

Daniels, W.L., and Zipper, C.E., 2010. Creation and Management of Productive Mine Soils. VCE publication 460-121.

Firpo, B.A., Amaral Filho, J.R., Schneider, I.A.H., 2015. A brief procedure to fabricate soils from coal mine wastes based on mineral processing, agricultural, and environmental concepts. Min. Eng. 76, 81–86.

Firpo, B.A., Weiler, J., Schneider, I.A.H., 2021. Technosol made from coal waste as a strategy to plant growth and environmental control. Energy Geoscience 2, 160-166.

Ghose, M.K. 2005. Soil conservation for rehabilitation and revegetation of mine-degraded land. TIDEE – TERI Information Digest on Energy and Environment 4(2), 137-150.

Kossoff, D.; Dubbin, W.E.; Alfredsson, M.; Edwards, S.J.; Macklin, M.G.; Hudson-Edwards, K.A. Mine tailings dams: Characteristics, failure, environmental impacts, and remediation.

Applied Geochemistry, v. 51, p. 229–245, 2014.

Lima, P.L.T., M.L.N. Silva, N. Curi and J. Quinton. 2014. Soil Loss by Water Erosion in Areas Under Maize and Jack Beans Intercropped and Monocultures. Ciênc Agrotec 38: 129-139.

McCool, D.K.; Foster, G.R.; Mutchler, C.K. & Meyer, L.D. 1989. Revised slope length factor for the universal soil loss equation. Transactions of the American Society of Agricultural Engineers, 32(5): 1571-1576.

Roose E. 1996. Land husbandry: components and strategy. Rome: Food and Agriculture Organization of the United Nations.

Schmidt, M.R. 2017; Fatores erosividade das chuvas de Augusto Pestana (RS), cobertura e manejo do solo e erodibilidade de Latossolo vermelho para uso na equação universal de perdas de solo. Disssertação. Agronomia, PPG Ciências do Solo, UFRGS.

Sheoran, V.; Sheoran, A.S.; Poonia, P. Soil reclamation of abandoned mine land by revegetation: a review. The International Journal of Soil, Sediment and Water: Documenting the Cutting Edge of Environmental Stewardship, v.3, p.1-20, 2010.

Weiler, J., Firpo, B.A., Schneider, I.A.H., 2018. Coal waste derived soil-like substrate: An opportunity for coal waste in a sustainable mineral scenario. Journal of Cleaner Production 174, 739-745

Weiler, J., Firpo, B.A., Schneider, I.A.H., 2020. Technosol as an integrated management tool for turning urban and coal mining waste into a resource. Minerals Engineering 147, 106179.

Yellishetty, M., Mudd, G.M., Shukla, R. 2013. Prediction of soil erosion from waste dumps of opencast mines and evaluation of their impacts on the environment. International Journal of Mining, Reclamation and Environment 27(2), 88-102.

Zhang, H.: Yang, Q; Li, R.; Liu, Q.; Moore, D; He, P.; Ritmsema, C.J. & Geissen, V. 2013. Extension of a GIS procedure for calculating the RUSLE equation LS factor. Computers & Geosciences, 52; 177-188.

Zhang, L., Wang, J., Bai, Z., Lv, C., 2015. Effects of vegetation on runoff and soil erosion on reclaimed land in an opencast coal-mine dump in a loess area. Catena 128, 44–53.

The Use of Mineral Exploration Drilling to Kickstart Hydrogeology Data Collection for Pre-Feasibility Mining Studies and Beyond

Kym L Morton

KLM Consulting Services Pty Ltd, PO Box 119, Lanseria, 1748, South Africa, kmorton@klmcs.co.za, tel.: +27 83 653 1758, ORCID 0000-0002-5865-1979

Abstract

Valuable groundwater information becomes available as soon as drilling starts, particularly during early mineral exploration campaigns. Often the information is not collected as the value does not become evident until the exploration sites become a mine. This paper describes what information can be collected very inexpensively during exploration drilling and how drill holes can be used to create an early monitoring network for the collection of water levels across the site. Examples of logging sheets, daily drill records and construction designs for monitoring boreholes are provided.

During drilling and logging of exploration coreholes the emphasis is all on characterising the orebody. Drilling methods include rotary, air percussion and core drilling. All encounter water and, with very little effort, the information on water intersections, drilling fluid circulation losses, basic water chemistry and rest water levels can be collected by the drilling contractor and the site geologist, under direction from the project managers.

If the basic information is captured, then this significantly reduces the cost of the initial hydrogeological study for the pre-feasibility reports. Some of the holes can be equipped for use as water level monitoring boreholes or preserved for use at a later stage. Old core holes that are not sealed can create conduits for underground inflows when the mine is developed. Decision criteria are provided for the use of the hole after drilling to optimise information from all drillholes and reduce risk when mining commences.

Keywords: Water, Mine Design, Inflow, Flood, Precipitation, PFS

Introduction

Valuable groundwater information becomes available as soon as drilling starts, particularly during early mineral exploration campaigns. Often the information is not collected because the value of groundwater information does not become evident until the exploration sites become under scrutiny for development as a mine.

This paper describes what information can be collected very inexpensively during drilling and how drill holes can be used to create an early monitoring network for the collection of water levels across the site. Examples of logging sheets, daily drill records and construction designs for monitoring boreholes are provided.

During drilling and logging of exploration coreholes emphasis is on characterising the orebody, sometimes even the overburden (future waste-stripping) is not logged. Drilling methods include rotary, air percussion and core drilling. If the basic information is captured, then this significantly reduces the cost of the initial hydrogeological study for the pre -feasibility reports. The information can be valuable at Pre-feasibility, Bankable feasibility, Full feasibility, during construction, during mining and at closure and beyond. Economic sustainability of the mine site can depend on the availability of groundwater, therefore the greater the coverage and longer the record of water levels and groundwater occurrence the better for design, operation and closure.

All holes usually encounter water ranging from damp to undrillable, with very little effort the information on water intersections, drilling fluid circulation losses, basic water chemistry and rest water levels can be collected by the

drilling contractor, the site geologist under direction of the project managers.

Some of the holes can be equipped for use as water level monitoring boreholes or preserved for use at a later stage. Before drilling a hole, it is important to envisage all future uses, risks and impacts, old core holes that are not sealed can create conduits for underground inflows when the mine is developed thus creating unnecessary hazards. Decision criteria are needed prior to drilling for the use of the hole after drilling and should be used to optimise information from all drillholes and reduce risk when mining commences.

Exploration drilling can provide a wealth of information on groundwater that is very valuable for Pre- Feasibility Studies (PFS) and beyond. Each drill hole is capable of being used to determine the depth of the water table, if aquifers are confined or unconfined and then used for water level monitoring, water chemistry information and a long-term record of water level movement prior to mining. The exploration drillholes provide baseline data on the groundwater for very little additional cost or effort. Drillers record a lot of information on water strikes, water levels and drilling fluid loss circulation records which give important information on zone(s) of high permeability. All this information is significant for early mine planning and can reduce the cost of the design of water supply, dewatering and environmental studies. The use of the exploration drill holes as long-term monitoring sites can provide an early monitoring network which will add value to the mine design and planning as well as provide background information critical to the success of the mine.

Often a planned mine area has a very high density of drillholes used for exploration but if these holes have not been used to measure water levels, then additional new holes will have to be drilled at Pre-feasibility stage thus creating an additional high cost to the PFS. During exploration drilling the knowledge and experience of the driller and site geologist should be used to collect the easily available groundwater information and store ready for PFS and beyond.

Figure 1 shows an example of drillhole density for a project in plan.

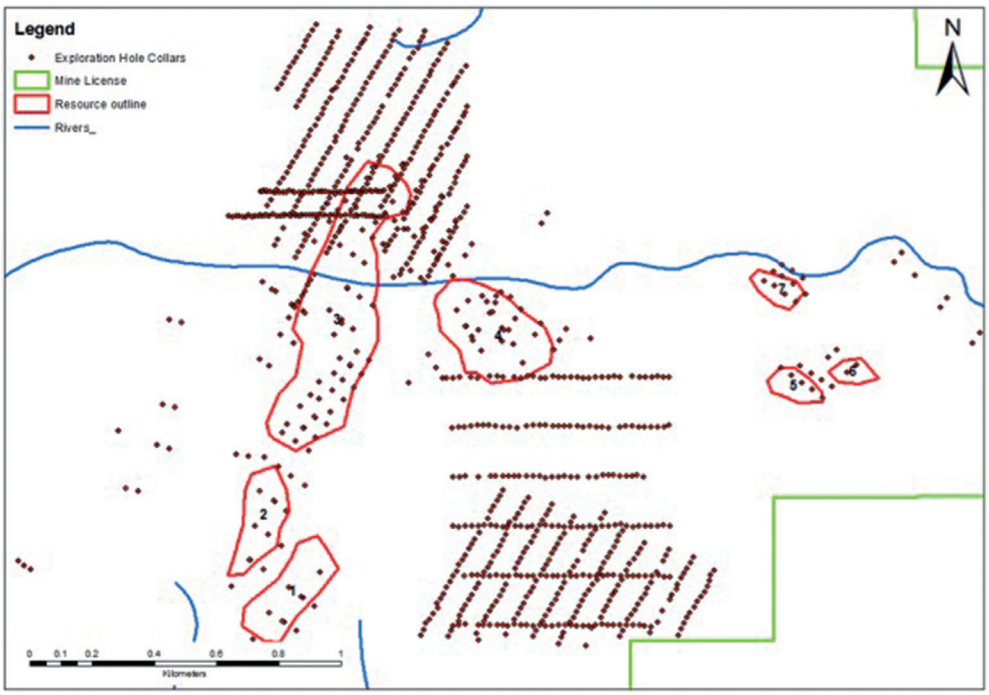

Figure 1 *Typical exploration drilling density in plan and isometric.*

Drill holes are expensive, therefore it is important to extract as much groundwater information from them to enable decisions on sealing (to protect the future mine) or converted to monitoring holes as contribution to a better understanding of the future mine hydrology.

Best practice is to seal drillholes so that they cannot become conduits for flow into mine workings but where possible the drillholes should be sealed using cemented-in vibrating wire piezometers (VWP) to provide 3D monitoring of the ground water prior to and during mining. Modern automation techniques can be used to collect long term water level records which will be of vital interest to PFS groundwater studies and, for very little additional cost, reduce the water risk to the planned and operational mine.

Advantages for ground water can be obtained at all stages of exploration drilling. This valuable information can be used in dewatering design, water supply, water balance reporting, environmental impact studies, closure design and post closure planning.

Drilling stage

Exploration drillholes usually comprise core drilling and sometimes, if there is about 20m+ of weathered material the core holes are usually collared using air percussion or rotary percussion drilling. Reverse Circulation drilling (RC) is also extensively used in exploration, and often the progress of drilling is impacted by the presence of groundwater. The exploration geologist is primarily interested in the ore body and hanging and footwall however it is very important to log the depth of weathering as this can be a significant aquifer or water susceptible zone when the mine is designed. Geotechnical engineers are also interested in the depth and types of weathering. These can be recorded on the standard drilling and geological logs.

During core drilling the driller monitors a minimum of three gauges on a drill rig: water pressure, feed pressure and torque pressure. They are integrated onto the control panel. When the water table is encountered the driller notices that water pressure will start to increase. Also, when lowering the overshot to lift the core tube there will be slack in the line, this is also the sign of a water table in front of the core bit. The web site http://drilling.fordia.com/essential-guide-to-drilling-parameters describes all the parameters monitored by a driller and their use in recording the water encountered in the formation.

During drilling by any method, the depth of the first water strike should be recorded by the driller on daily drill logs and the drill sheets. Most drill sheets are primarily focussed on details for invoicing the client however it can be specified in the drilling contract that all water strikes, water losses and water levels must also be recorded and shared with the site geologist.

Normally all drill hole collars are surveyed within 0.5 cm accuracy for x,y,z. The z needs to be specified for water level measurement which, although measured in metres below ground (or drillhole collar), should be reported in metres above mean sea level (mamsl) as the hydrogeologist is primarily interested in head measurements and groundwater gradient to plot flow lines.

During drilling, the driller can see, very easily, the depth at which water is encountered thus giving a plot of the water table for the area. Water strikes and the subsequent measurement of water levels can indicate the presence of confined aquifers. When encountered in confined aquifers the resultant water level is the phreatic or pressure surface for the area. Both measurements; of water strike and of water level are very important for the understanding of the groundwater conditions and possible impact on the proposed mine.

Figure 2 shows water level intersection of an unconfined aquifer and of a confined aquifer.

Air percussion and rotary drilling can be used to measure the yield of a water strike in litres per second (L/sec) or metres cubed per hour (m^3/hr). Core drilling does not enable the measurement of yield, however, if a permeable zone (possibly an aquifer or water bearing fracture) is intercepted the driller will note circulation losses and need to top up the corehole with water and drilling fluids. The more water and fluid used indicates the greater the permeability. This provides a guide for the possible groundwater characteristics and pumping yields at the corehole location.

Heinz, in his Diamond drilling handbook (1989) describes all the formations that can be noted from circulation losses including:

- Sands and gravels
- Cavernous or vugular limestone and dolomite
- Naturally fractured/fissured rocks
- Induced fractures in solid rocks

It is very valuable to have a record of the drilling circulation losses. Appendix A is a recommended daily drill log. It is important to state in the drilling contract that the information on water strikes, circulation losses and water levels and must be collected.

During core drilling the level of drilling fluid in the core hole represents the hydraulic pressure being maintained by the driller to keep the hole open, the bit lubricated and optimise the efficiency of the drilling. If the drilling is stopped for any reason (e.g., a drillers' break weekend or at the end of the hole) the fluid level will equilibrate to the actual groundwater level. This is essential information and should be recorded with a hole depth and date. As the drill hole deepens different aquifers, with different groundwater pressures may be encountered therefore the level of fluid in the corehole should be measured after any cessation of drilling over 24 hours. It is possible that artesian conditions, where the fluid flows out of the core hole, may be encountered and these too should be noted on the drilling log with date and corehole depth.

During drilling the pH and the electrical conductivity of the water encountered may change indicating interception of different aquifers. Some drilling companies such as Geomechanics (Pty) Ltd ("Geomechanics") offer automated logs of drilling information. Figure 2 is an example of a log created by Geomechanics.

When plotted with the geological log the information can highlight more permeable zones and give guidance to the next stage of hydrogeological investigation.

Down-the-hole geophysics

On completion of a drillhole, exploration coreholes are often surveyed using down-the-hole (dth) geophysical probes to record information on the ore body. The dth logging probes can also provide information on the aquifers encountered in the corehole (Bouw and Morton 1987). At the very least the probes will record when water is entered and thus provide a record of the water level in the corehole on a specific date. Gamma-gamma and resistivity probes can record information on porosity and permeability. Temperature and electrical conductivity probes indicate zones of water flow or different aquifers. Groundwater geophysical logging can be piggybacked on the mineral exploration dth logging and requires discussion with the dth

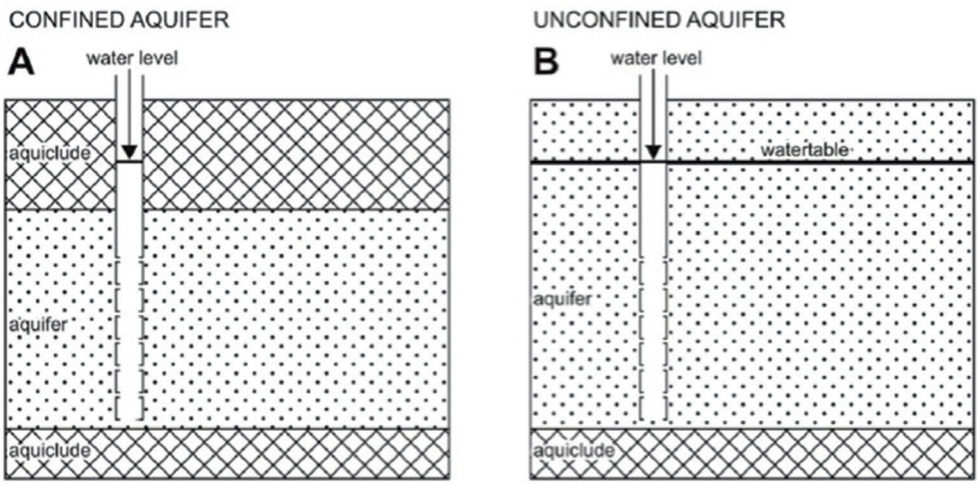

Figure 2 *Water level intersection of an unconfined aquifer and of a confined aquifer.*

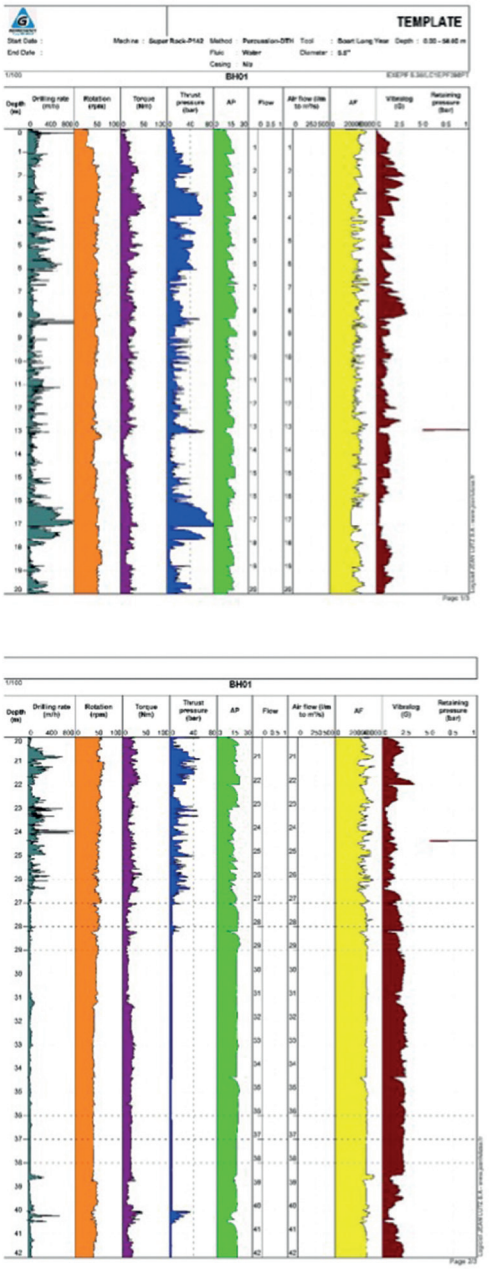

Figure 3 Example of automated drilling log (Geomechanics).

contractors and hydrogeologist to choose the most suitable probes.

Drill hole closure

Following drilling, the hole is often contaminated with mud, grease, and oil. This needs to be cleaned out to unclog the side walls and enable the hole to be used for monitoring either as a temporary (it will collapse if not kept open) open hole or as a permanent water level monitoring hole. A hole can be kept open using plastic conduit or more robust casing. Often both are easily available. It is important the conduit/casing is slotted (can be hand slotted), capped at the bottom and protected at surface. Figure 4 shows a recommended design for an open hole – often called a piezometer.

When water strikes or multiple aquifers have been encountered during drilling then multi-stage open piezometers can be installed. Figure 5 shows a multi open hole piezometer constructed in one hole or using several holes.

If open pit mine or underground mine dewatering is anticipated, then sealed vibrating wire piezometers (VWP) are recommended as these measure groundwater pressure for known depths. A network of VWP's will give the distribution of pressure and plot flowlines in 3D providing valuable

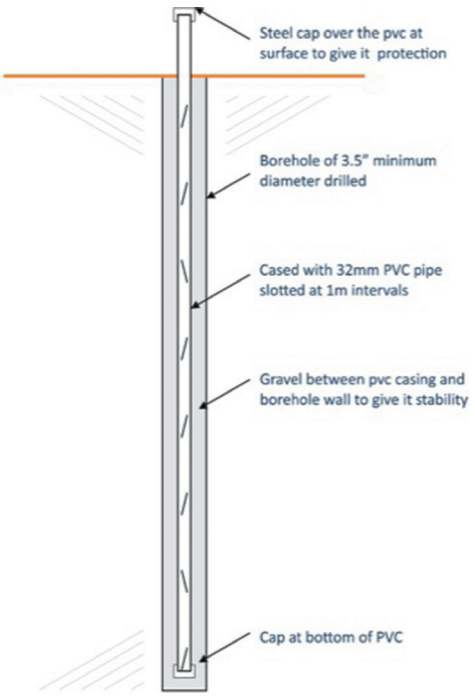

Figure 4 Simple open hole piezometer construction to create a monitoring borehole.

information for the interception of mine water and accurate dewatering design. Figure 5 shows the construction of a vibrating wire type point piezometer and data logger sealed into the backfilled core hole using a tremie pipe.

Appendix B holds an example of a drilling sign-off log. This was developed at De Beers Group for use prior to the drilling of all holes. The document shows the layout and length of the planned hole, its construction and planned use. Then the design is shared with all interested parties such as Geology, Geotechnical, Engineering, Mining and Environmental department heads for sign off before the hole is drilled. This ensure all stakeholders are informed of any new hole and get the opportunity to use the hole for their investigations.

Post exploration

Once exploration is complete, or at least the first phase, the project is evaluated at either Pre-feasibility (PF) or Feasibility levels to obtain funding for either further exploration to improve confidence or to design and open the mine. There is now opportunity to use the initial monitoring network and some of the cleaned out coreholes to collect monthly groundwater levels. This valuable information adds confidence to the studies needed for environmental permitting, water supply and mine dewatering designs. For very little expenditure the monthly plotting of groundwater level fluctuations significantly increase the understanding of the groundwater regime and provide essential data for use in modelling and calibration of the water flow for the planned mine.

As the mine project advances and new exploration holes are added, then the monitoring network can be expanded, and data collection frequency increased. The more hydrological seasons that are covered by monitoring the higher the confidence in the conceptual hydrogeological model and therefore the improved confidence in numerical modelling and the initial water control, water supply and dewatering designs.

Data management

During exploration and PF levels a lot of information is collected by a variety of site staff. It is important that the groundwater information is filed in a dedicated data base for use later in the project development.

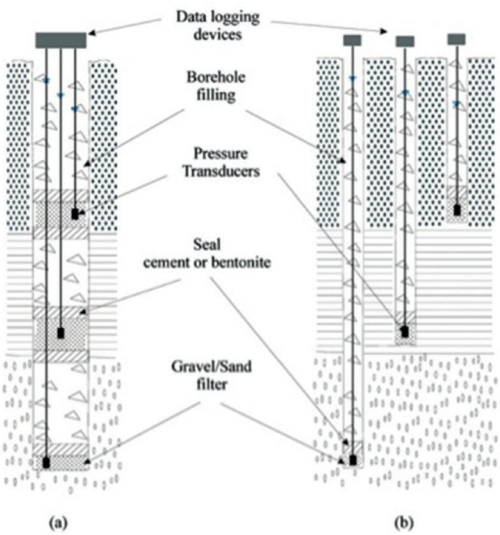

Figure 5 *Multistage open hole piezometers in one or multiple boreholes.*

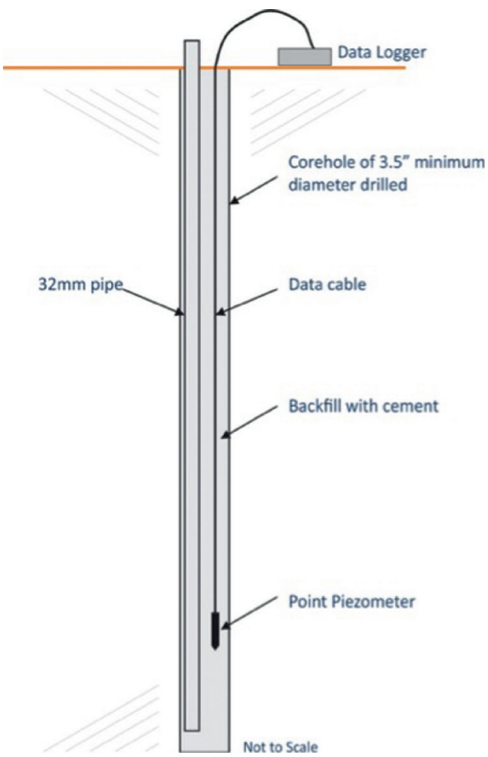

Figure 6 *Vibrating wire piezometer in a corehole backfilled with Cement.*

AcQuire® and QuickLog® are two of the geological logging programmes that can also store water level and water strike information. Other water data packages can be used and can include water chemistry information. It is vital that a chronology of data collection is maintained and back up of data supported.

The data needs to be easily accessible and attached to the dates measured for use in the conceptual and numerical modelling.

Conclusions

Exploration drilling programmes can be used, at very little extra cost, to collect information on groundwater including water strikes, possible zones of increased permeability and water levels. The drill holes can be used to create an initial monitoring network for the collection of water levels. The longer the monitoring record the greater the confidence in the conceptual and numerical models needed to design the water management strategy and obtain permissions for mining. Ground water data can be obtained at all stages of drilling and provides valuable information for project water supply, mine dewatering design, water balance reporting, mine water management, environmental impact studies and ongoing monitoring for eventual closure design and post closure planning.

Acknowledgements

The assistance of Geomechanics Drilling, Grant Rijsmus (the Geo-group) is gratefully acknowledged. Dr Steve Westhead of AIMC and Dr Matthew Field of Mining Plus are thanked for their comments.

References

Bouw, P C and MORTON K L, (1987). "The importance of geophysical logging of boreholes". Borehole water Journal Vol 6. South Africa

Heinz WF 1989 Diamond drilling handbook Johannesburg, South Africa ISBN 0-620-13785-1

Appendices

Appendix A "Drilling log for core holes which include capture of circulation losses" and Appendix B "Sign-off document for all new core and drill holes" can be requested from the authors.

Dewatering, Flooding and Stratification of the Nikolaus-Bader small-scale Gold Mining Shaft in Austria

Elke Mugova[1], Christian Wolkersdorfer[2]

[1]*Technische Hochschule Georg Agricola, University (THGA), Research Center of Post-Mining, Herner Straße 45, 44787 Bochum, Deutschland, elke.mugova@thga.de, ORCID: 0000-0001-6019-9945*

[2]*Department of Environmental, Water and Earth Sciences, Tshwane University of Technology, Private Bag X680, Pretoria, 0001, South Africa, christian@wolkersdorfer.info, ORCID: 0000-0003-2035-1863*

Abstract

To investigate density stratification in flooded underground mines, the 10 m deep Nikolaus-Bader shaft in Biberwier/Tyrol, Austria was pumped out and the subsequent flooding process was observed. After a short time, a density stratification developed, which collapsed in late autumn and built up again in spring. By means of data loggers, measuring pressure, temperature, and electrical conductivity in four different depths of the flooded shaft, a long-term monitoring of the water body is possible, from which conclusions can be drawn about temporal factors for the formation and collapse of density stratification.

Keywords: Underground Mine, Stratification, Flooding

Introduction

In the 1920s to 1940s, while searching for gold within moraine material deposited by the Fernpass mountain slide, Nikolaus Bader of Lermoos, a village in Tyrol, Austria sank a 10 m deep shaft near the Loisach springs. As profitable gold mining never took place, the shaft was forgotten and only rediscovered in a flooded state in 1999 (Wolkersdorfer *et al.* 2007). Since 2004, regular examinations of the water quality and depth profile measurements have been carried out in the shaft. It has been shown that the occurrence and breakdown of stratification occurs at different depths. Stratification of mine water is of relevance pertaining to mine flooding events worldwide, as stable stratification can reduce the need for extensive mine water treatment (Wolkersdorfer 2008; 2017). Highly mineralised and consequently mostly more contaminated mine water usually remains in deeper areas of the mine pools, while relatively less mineralised mine water discharges near the surface (Mugova and Wolkersdorfer 2019). Due to the nature of occurrence, as well as the long-term stability and breakdown of stratification, it is very difficult to monitor the processes in a mine several hundred to a thousand metres deep, hence the 10 m deep Nikolaus-Bader-shaft was selected in 2019 as an investigation shaft for long-term observation.

Investigation

Description of the shaft and previous research

Named after the local pharmacist, miner and businessman Nikolaus Bader, the 2 × 2 m wide and 10 m deep shaft has been flooded since the 1930s. It is located near the Loisach springs close to the village Biberwier in the district of Reutte (Außerfern, Tyrol, Austria). There is no discharge at the shafts surface, so it can be assumed that the shaft water mainly interacts with the groundwater body. In the area of Biberwier, the mesozoic rocks of the Fernpass syncline are covered by material from the Fernpass mountain slide and moraines (till). These moraines belonged to a glacier whose origin is located in vicinity of the Swiss Alps, which explains the gold bearing till (Eichhorn *et al.* 2017). Mining with these low gold concentrations was however ultimately not feasible. Due to its greater residence and contact time with the debris of the toma hills and the till (Table 1), the water from the Nikolaus-Bader-shaft is slightly more mineralised than that from the Loisach river. This is particularly noticeable in the case of calcium and hydrogen carbonate.

Table 1 Water analyses from the Nikolaus-Bader-shaft, the river Loisach and the drinking water well (2005 – 2020); EC: electrical conductivity; Redox: redox potential corrected to standard hydrogen electrode.

Parameter	Outflow drinking water supply Biberwier	Nikolaus-Bader-shaft	River Loisach approx. 300 m downstream of the shaft
pH, –	7.3 – 8.3	7.1 – 7.2	7.7 – 7.9
Redox, mV	62 – 436	64 – 383	62 – 426
EC, µS/cm	365 – 406	381 – 477	367 – 401
Temp, °C	7.5 – 8.7	5.7 – 9.2	7.6 – 9.1
Ca, mg/L	33 – 49	64 – 68	47
Mg, mg/L	23	16	24
Na, mg/L	0.6 – 1.3	0.4	1.3
K, mg/L	0.5	0.7	< 1
Cl, mg/L	4.7 – 7.4	1.1 – 3.9	7.4
HCO_3, mg/L	174 – 210	240 – 255	220
SO_4, mg/L	25 – 29	17 – 22	30
NO_3, mg/L	1.2 – 1.4	1.0	1.2
U, µg/L	5.8 – 6.4	0.2 – 2.2	5.9

Potentially toxic metals are not present in elevated concentrations in the shaft water; interestingly, a water sample from the deepest part of the shaft showed gold concentrations above the detection limit.

Depth measurements of electrical conductivity and temperature, conducted mainly between 2004 and 2006 at various depths in the shaft, showed a density stratification that is linked to seasonal changes and in some cases disappears altogether (Fig. 1). In May 2019, immediately before the start of the experiment, existing stratification in the shaft could be confirmed.

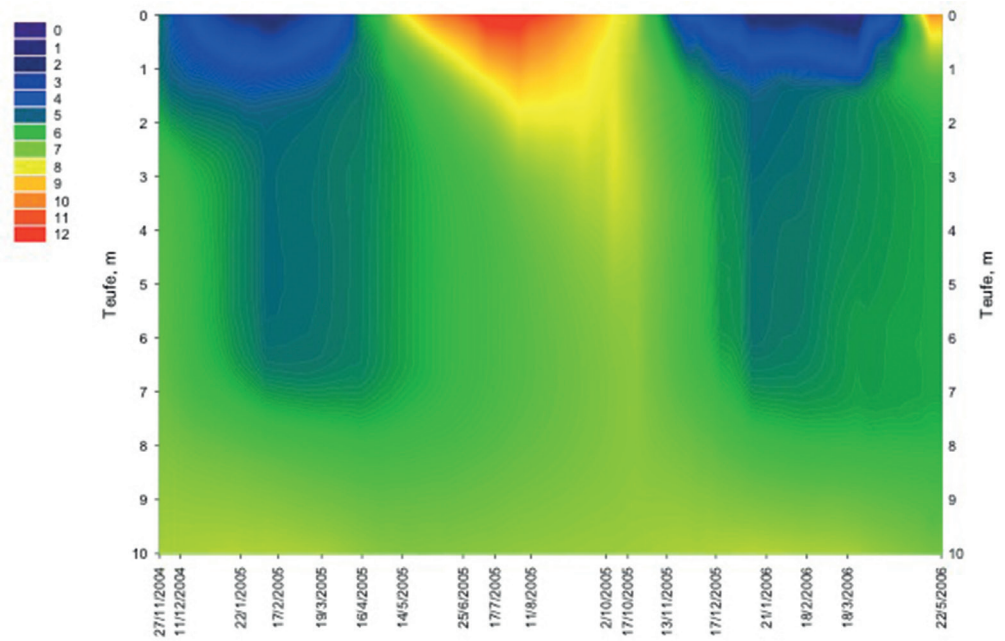

Figure 1 Temperature-depth diagram of the Nikolaus-Bader-shaft with 18 depth-dependent measurements between November 2004 and May 2006.

Objective and implementation of the experiment

To understand the occurrence, breakdown and, most importantly, the long-term stability of stratification in flooded mine shafts, an ongoing monitoring of the shaft water body was begun in June 2019. With aid of a submersible pump, the shaft was dewatered almost empty within a time frame less than 3 hours, and the displaced shaft water was discharged into the nearby Loisach river. As it turned out, the water preserved the original shaft lining, which was in very good condition. A visual inspection and a drive-through with a camera was possible. Water inrush into the shaft from the upper shaft walls could not be observed, leading to the conclusion that interaction with the groundwater body only takes place in the lower area without shaft lining. Before pumping, CTD-Diver data loggers (Van Essen Instruments) were inserted at four different depths (0.8 m, 2.5 m, 7 m and 8 m). These were the approximate depths of the previously observed stratification withing the shaft water body. The data logger at 8 m deep was temporarily lowered to a depth of 9.4 m, just below the surface of the remaining shaft water, to monitor the rebound rate. Values of electrical conductivity, water temperature and pressure are recorded in 15-minute intervals and made available by remote data transmission. In addition, hourly data from the semi-automatic weather recording system (TAWES) in Ehrwald, about 5 km away, is also considered for evaluation.

Results and Discussion

After the pumps were switched off, immediate flooding of the shaft began, primarily through influxes of groundwater in the deepest part of the shaft. By extrapolating the flooding process, the total depth of the shaft could be estimated to be between 9.6 and 9.7 metres. From the first data logger, which was initially installed at a depth of 9.4 m, to the near-surface data logger at a depth of 0.8 m, natural flooding continued for about 25 days. Mine water rebound rates of 0.4 m/d (assuming rise from 9.4 m to 0.8 m) were calculated, which is consistent with visual observations at the onset of flooding. Rebound rates correlated to depth, with greater velocities of up to 0.9 m/d being observed in deeper areas of the shaft, which decreased to less than 0.1 m/d near the surface of the shaft. A possible explanation for these differences is evident in the flooding process itself. There is an increased inflow of water between depths of 9.0 m and 8.0 m, which feeds the rising water. Up to a depth of approximately 2 m the water column builds up steadily, and thus the elevated pressure of the water column prevents a further rapid rise of water within the shaft. Close to the surface, precipitation or infiltration water enters laterally into the shaft at much lower velocities, hence the rebound rates are lower in the upper shaft area. Based on the calculated rebound velocities, kf-values around $1 \cdot 10^{-7}$ m/s were determined for the inflow area by kf-value determination for transient pumping tests, with slightly permeable material (silt to silty sand) around the shaft. This confirms that the area of the inflowing groundwater is moraine material, which is consistent with the historical information provided by Nikolaus Bader to the mining authorities, and with information mentioned in a hydrogeological report by Schuch (1981).

The objective of the pumping experiment and observations following flooding is to verify whether the stratification between different water bodies at 0.8 m, 2.5 m, 7.0 m and 8.0 m encountered in earlier investigations would occur again and if it would remain stable. Values for temperature and electrical conductivity at different depths over time (Fig. 2, Fig. 3) show a horizontal curve, especially at 7.0 m and 8.0 m depths. These 2 curves show convergence about 73 days after the start of flooding. For 16 weeks, the stratification was stable and indicates the formation of a homogeneous water body in the area between 7.0 and 8.0 m, and probably above and below. Fluctuations in temperature and electrical conductivity are more evident in the water body closer to the surface (data logger at 0.8 m), as the curve is more uniform at 2.5 m, 7.0 m and 8.0 m. On 2019-10-12, the upper stratification collapses, and about one month later, as of 2019-11-10, there is no more stratification detectable in the

shaft. Only one homogeneous water body with the same temperature and electrical conductivity exists. From mid-May 2020, the redevelopment of an upper, separated water body is visible in the temperature and less evidently in the electrical conductivity curve. Around the data logger at 2.5 m deep, another water body develops again beginning of July 2020. Due to stratification two separated waterbodies redeveloped over summer 2020, until stratification completely collapsed again end November 2020. Thus, the occurrence and breakdown of stratification observed since 2004 can be confirmed, a repeating annual pattern is evident.

According to the TAWES weather data in Ehrwald, it appears that there is a connection between the beginning of frost and the breakdown of the stratification. At the beginning of November 2019, the upper stratification collapsed after several hours of continuous sub-zero temperatures. Mixing of the entire water body took place after further persistent frost in December. A possible explanation is that due to low air temperatures, the surface water infiltrating and flowing into the shaft has low temperatures and the density differences in the shaft are so small that a stable stratification cannot be maintained. The collapse of the stratification in 2020 is also related to a longer period of frost. To make more precise statements about water pathways in the bedrock, geophysical measurements are to be carried out in the vicinity of the shaft.

Conclusion

Findings deducted from long-term investigations concerning the occurrence and breakdown of stratification, such as that transpiring at Nikolaus-Bader-shaft, should be investigated in detail and ought to be used as an in-situ mitigation measure for future mines, abandoned mines or mines that have already been flooded. After pumping out the 10 m deep Nikolaus-Bader-shaft near Biberwier, complete flooding took place within just one month, and two months later stratification had re-occurred. A general trend can be seen; at the beginning of the frost period inflow of water with low temperatures into the shaft, probably causes the complete collapse of the stratification, and during the spring and summer months stratification re-develops again. These initial results of the long-term observation suggest that findings could be applicable to deeper mines with near surface inflow.

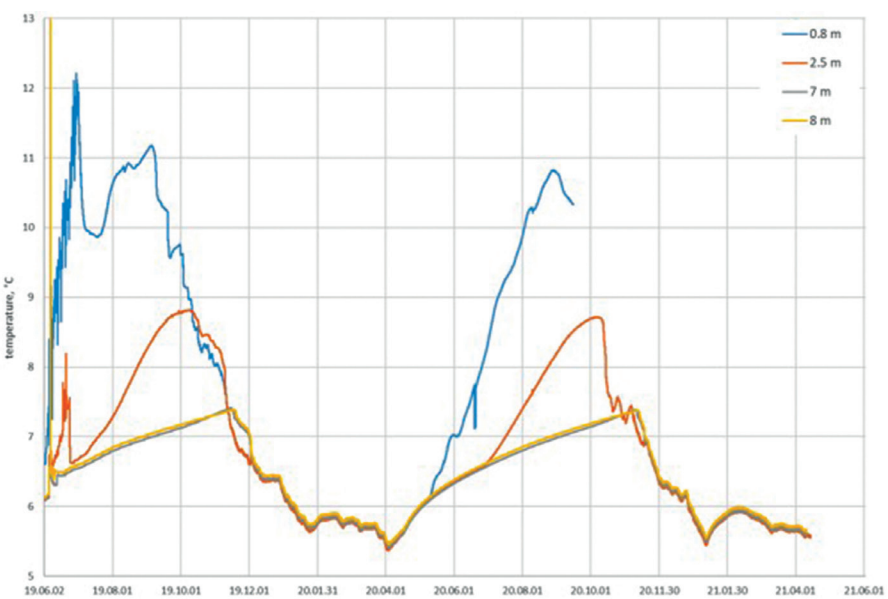

Figure 2 Time dependent temperature log at Nikolaus-Bader-shaft in 0.8 m, 2.5 m, 7.0 m and 8.0 m depth (deflection at 2020-06-20 is due to a modification on the data logger).

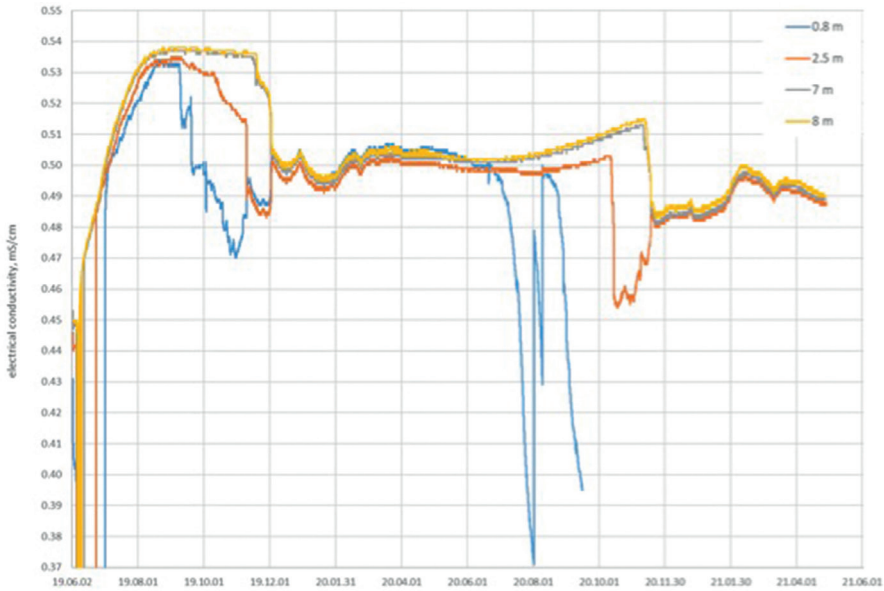

Figure 3 *Time depended electrical conductivity log at Nikolaus-Bader-shaft in 0.8 m, 2.5 m, 7.0 m and 8.0 m depth.*

Acknowledgements

We would like to thank our research institutions, especially "Forum Bergbau und Wasser", for their financial support. Furthermore, great thanks go to Armin Hanneberg, Jana Göbel, Werner Luttinger, Sabine Luttinger, Ulrike Wolkersdorfer, Erich Müller, Andreas Wolkersdorfer, Karoline Wolkersdorfer, Franziska Wolkersdorfer, Jochen Wolkersdorfer, Katrin Wolkersdorfer, Christian Eichinger, Marlen Scheibe, Christiane Neumann, Ellimaria Huusari, Petra Müller, Ana-Sophie Hensler, Daniela Riepl, Andreas Simmerl, Daniel Schreil, Daniel Bischof, Hendrik Klar, Christine Böhmer, Florian Heimann, Fabian Henkel, Constanze Putz and Felice Vogdt, who have contributed to the knowledge gained at the Nikolaus-Bader-shaft over the years. We would like to thank the local authorities and the mayors of Biberwier for their support over many years and the fast approval of the experiment in a drinking water protection area and the two anonymous reviewers for helpful comments. This paper has been published in modified form in German in the Geoforum Umhausen 2020 proceedings.

References

Eichhorn R, Lehrberger G, Loth G, Loth R, Plass D, Pürner T, Rohrmüller J (2017) Auf den Spuren des bayerischen Goldes – 20 Goldene Geotope. Bayerisches Landesamt für Umwelt, München

Mugova E, Wolkersdorfer C (2019) Stratification in Flooded Underground Mines – State of Knowledge and Further Research Ideas. Paper presented at the Mine Water – Technological and Ecological Challenges (IMWA 2019), Perm, Russia:40–44.

Schuch MF (1981) Bericht über die Ergebnisse der Hydrogeologischen Untersuchungen im Bereiche des Weißen-, Mitter- u. Finstersees. Michael F. Schuch, Innsbruck, p 14

Wolkersdorfer C (2008) Water Management at Abandoned Flooded Underground Mines – Fundamentals, Tracer Tests, Modelling, Water Treatment. Springer, Heidelberg

Wolkersdorfer C (2017) Mine Water Hydrodynamics, Stratification and Geochemistry for Mine Closure – The Metsämonttu Zn-Cu-Pb-Au-Ag-Mine, Finland. In: Wolkersdorfer C, Sartz L, Sillanpää M, Häkkinen A (eds) IMWA 2017 – Mine Water & Circular Economy. vol I. Lappeenranta University of Technology, Lappeenranta, p 132-139

Wolkersdorfer C, Göbel J, Hasche-Berger A, Hanneberg A (2007) Führer zum Montan-Wanderweg Silberleithe (Guide to Mining Trail Silberleithe). Bergwerksverein Silberleithe Tirol, Biberwier

Innovative Adaptation of Mining Hydrogeology Practices during a Pandemic

Sofia Nazaruk[1], Grace Yungwirth[2], Jessica Nicholls[3], Gareth Digges La Touche[2]

[1]*Golder Associates, Attenborough House, Browns Lane, Stanton-on-the-Wolds, NG12 5BL, UK, snazaruk@golder.com*

[2]*Golder Associates, 20 Eastbourne Terrace, London, W2 6LG, UK, gyungwirth@golder.com, GDLTouche@golder.com*

[3]*Golder Associates, Cavendish House, Bourne End Business Park, Bourne End, SL8 5AS, UK, jess__nicholls@hotmail.co.uk*

Abstract

Traditional mining hydrogeology practices during site characterisation programmes have relied heavily on the availability of experienced practitioners to travel to mine sites. This was not possible during the COVID-19 pandemic and adaptations of previously established workflows were required. This paper aims to outline an approach for the remote oversight of field programmes by experienced practitioners and outlines the relative risks, rewards and key limitations to the approach developed.

Keywords: Site Characterisation, Data Collection, Remote Support, Mining Hydrogeology Practises, COVID-19 pandemic

Introduction

Global working practices, including overseas travel and fieldwork at mine sites, were heavily disrupted by the COVID-19 pandemic. Adapting working practices in a dynamic environment became a necessity for many mining projects to progress critical studies and design work to support their operations or advancement of new projects. The development of remote oversight and supervision procedures for hydrogeological site investigations are an example of adapting industry practices to meet these challenges.

The remote support workflow developed for the supervision of site characterisation programmes can allow experienced mining hydrogeologists to provide fully remote support to mine-based staff undertaking ground characterisation programmes. Where appropriate, the adaption of mining hydrogeology practices to allow the option of fully remote oversight of site characterisation programmes can be taken forward beyond the pandemic epoch, however this approach should be weighed against the limitations and is not expected to replace the need for experienced practitioners to attend site on occasion.

Traditional Mining Hydrogeology Practices

Site characterisation activities typically progress with the support of in-person oversight or quality assurance/quality control (QA/QC) from experienced practitioners. Traditionally this has involved the travel of experienced specialist staff to mine sites where they would work closely alongside local site-based staff for large proportions of the site characterisation programme. Experienced mining hydrogeologists may typically design, supervise, carry out or record the following as part of hydrogeological site investigations:

- drilling and hydrogeological, geological, or geotechnical logging of investigation boreholes;
- installation of abstraction, dewatering or groundwater monitoring boreholes;
- instrumentation of boreholes to measure groundwater quality/chemistry, groundwater level, pit wall depressurisation, etc.;
- testing of boreholes to estimate yield or hydraulic parameters;
- implementation of groundwater management strategies; and

- identification and measurement of groundwater inflows to adits, open pits, or other infrastructure.

Many of these activities were traditionally considered to require on-site supervision by experienced practitioners in order to be implemented correctly and to ensure QA/QC criteria are met. However, adaptation of the traditional approach to undertaking these tasks has been required during the pandemic period.

Adaptations During the Pandemic

As it was not possible for experienced mining hydrogeologists to travel to mine sites, an adapted approach was developed to allow remotely supported mining hydrogeology site investigations to progress during the global pandemic (fig. 1). The adapted approach focuses on: structured project planning; transfer of knowledge and training to local or site-based staff; streamlined data sharing; effective and frequent communication; and remote data processing and analysis.

Structured Project Planning

The successful planning of a remotely supervised hydrogeological site investigation is dependent on:

- adequate (longer) time allowed for the planning period within the project schedule; and
- early and direct engagement with contractors and the site team executing the work.

Whilst structured planning has always been essential to hydrogeological site investigations, traditionally this process may have been time constrained and cut short to allow for travel of remotely or internationally based practitioners to the mine site, the focus being on "getting there and kicking off the work". This practice meant that planning may have remained at a high level until experienced practitioners arrived at the mine site to discuss practical and logistical details with local and site-based staff. Where time constraints were in place, detailed planning may have previously run concurrently with the commencement of fieldwork, however this was not possible during the pandemic, so it is essential that adequate time for planning be incorporated into the project schedule.

Detailed planning and design during the pandemic required the early engagement of locally based staff and contractors. Previously practitioners may have only spoken to the mine staff (who often directly select and engage contractors) prior to arrival at site and the first engagement with contractor staff and detailed review of the available equipment took place after arrival on site. Early and direct engagement with contractors and site-based staff allowed understanding of the availability of equipment or materials which facilitated early identification of site-specific or practical limitations and revision of detailed designs (fig. 2). This was aided by review of technical specifications of the equipment, photographs and videos of the equipment condition, and

Figure 1 *Adapted Workflow for Remote oversight during the Pandemic (images: Golder).*

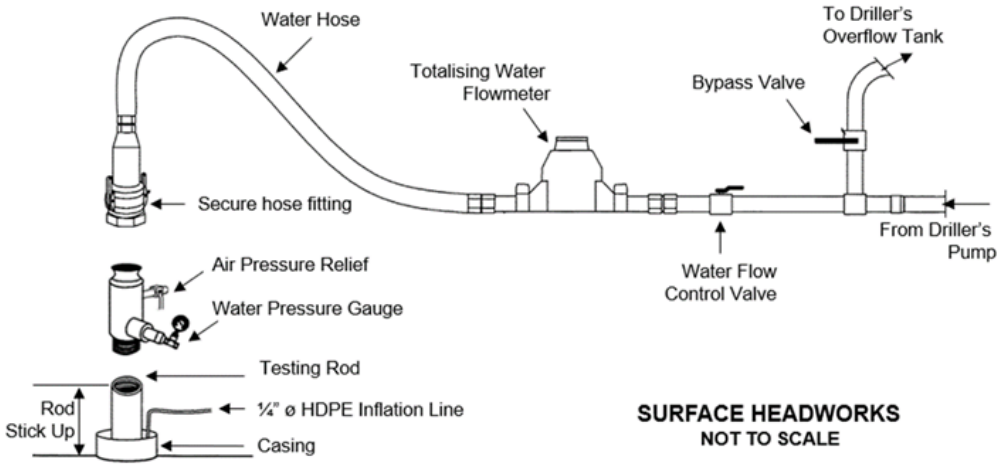

Figure 2 *Example of Design Drawings Used to Demonstrate Requirements to Local Staff (images: Golder).*

iterative test runs of equipment assembly and operation. The process for example, identified unsuitable pressure monitoring equipment and allowed for appropriate equipment to be sourced prior to the commencement of testing. Allowing time in the schedule to iteratively test and refine planning and designs are important during this stage.

Transfer of Knowledge and Training to Local or Site-Based Staff

Remote training and knowledge transfer to local and site-based staff was made successful by:

- early assessment of site staff skillset including recruitment of local support from other disciplines or academia;
- production of detailed training materials supported by site specific visual aids including drawings and photo/videos; and
- active and iterative review of test runs of field procedures.

Remote training of local or site-based staff enabled the successful implementation of the remote oversight workflow and the execution of the programme to an acceptable standard. Understanding the skillsets and experience of the local workforce is crucial to the planning process and dictates the level of detail required within the remote training process. Many mine sites were noted to employ local staff with a geological background, which proved useful to effectively implement early stages of the of the investigations, such as borehole siting and drilling. Collaboration of the mine sites with local universities were also sometimes used to supplement the local workforce and, with remote support from experienced practitioners, students were able to fulfil such roles as the installation of flow monitoring equipment or monitoring of groundwater level and chemistry.

Remote training during the pandemic was supported by the production of extensive visual aids including detailed drawings (fig. 2) supported by photos (fig. 3), site-specific field procedure manuals (Golder, 2020) and blank proforma templates for field record sheets to ensure the recording of full technical field data during the field campaign. Where possible, test runs of the field procedures and the QA/QC of practice data (such as the review of geotechnical or geological logs produced using old core) allowed local staff the opportunity to ask questions and improve their understanding of the data requirements prior to the commencement of the actual site characterisation programme.

Streamlined Data Sharing

Data sharing made use of multiple types of digital technology and multiple communication media as follows:

- regular and frequent real time visual communication directly from the field;

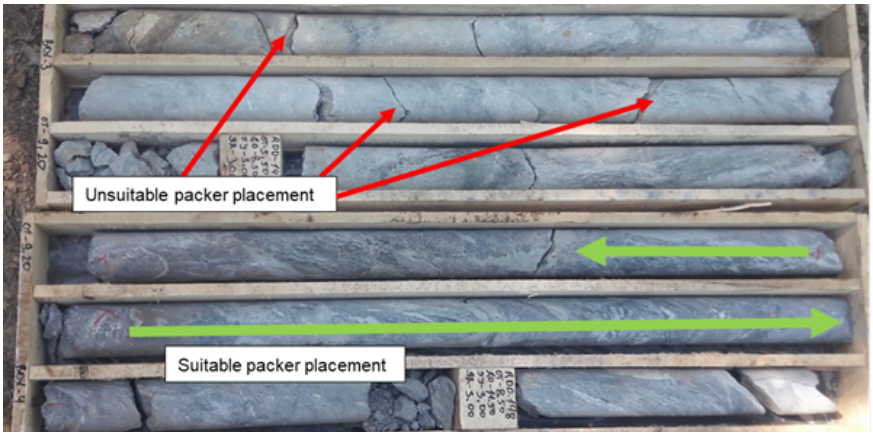

Figure 3 *Examples of Experienced Practitioner Review of Field Images (images: Golder).*

- the use of annotated photographs and recorded video from the field where communication infrastructure was not sufficient for real time communication;
- other types of digital data collection such as drone photography or video footage in lieu of site walkover; and
- a reliable and expert supported shared dataroom for efficient and regular data transfer.

The use of digital technology was used to supplement the transfer of knowledge to local staff and allow for rapid information sharing or QA/QC review. Where sufficient infrastructure exists, the use of video calling using mobile telephones or laptops was found to be highly effective in clearly communicating issues from staff in the field to the remote supervision staff. Where access to internet was poor or limited to certain work areas at the site, the use of annotated photography (fig. 3) and recorded video transmitted as soon as field staff could move to an area with digital signal was also found to be an effective tool. All sites that were remotely supported during the pandemic were found to have sufficient infrastructure to allow for these types of communication.

Other types of digital data, such as drone photography or video footage, were used in lieu of traditional site-walkover methodologies. For example, major geological features or zones of groundwater seepage (fig. 4) were identified from digital data and used to enhance the understanding of the site conceptual model. With the provision of detailed guidance, suitable drone footage was often able to be recorded by site-based staff or locally based contractors. Additionally, the remotely supported installation of automated equipment and, where practicable, telemetry systems can help to minimise the amount of data handling, and potential for data loss, by locally based staff.

Establishing a shared dataroom (such as a Microsoft SharePoint site) for uploading daily logs, risk registers and field data was crucial during the remote oversight process. This improved transparency of the investigation progress, clarity during discussions and enabled prompt review of collected data. Issues sometimes arose, such as lack of access or loss of data, when the site-based teams hosted the shared space. Benefit and security were found when experienced practitioners managed directly managed the dataroom.

Effective and Frequent Communication

Effective and frequent communication is required between remotely based supervisors and site staff making use of the following:

- a multi-tiered communication approach to support oversight and QA/QC process; and
- regular and ongoing review of collected site data as it is produced to allow for iterative correction or adjustment of procedures and data collection methodologies.

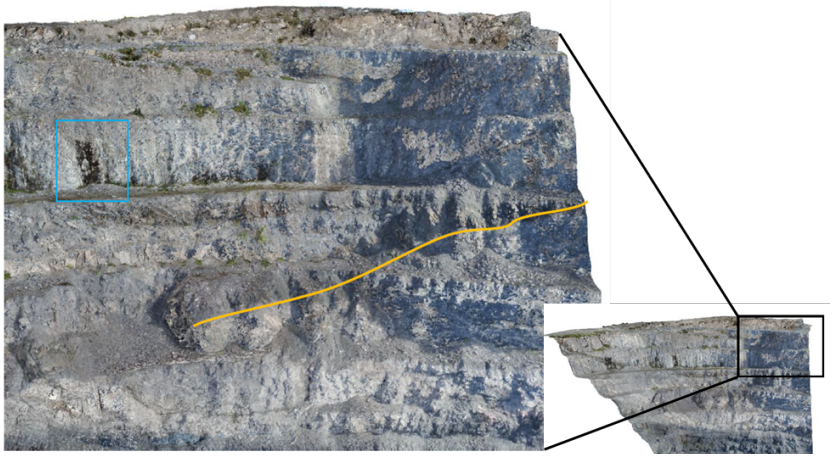

Figure 4 *Example of How Drone Footage Can be Used to Remotely Identify Geotechnical or Hydrogeological Features. Blue = Seepage Zone, Yellow = Geological Contact (images: Land and Minerals Consulting, 2018).*

A multi-tiered communication approach was utilised to support the remote oversight and QA/QC process. In addition to the initial information sharing and kick-off calls during planning stages, daily calls were arranged between the local staff and remote experienced practitioners to discuss the detailed designs, field procedures and daily site activities. The use of instant messaging applications also provided support on an ad-hoc basis and allowed for live communication while staff were at workfaces such as drilling, testing or monitoring locations. This process replaced the conversations which may have traditionally occurred organically while experienced practitioners were in the field. It also allowed for the identification and swift resolution of technical issues.

To ensure the quality of the field programme, daily or weekly QA/QC reviews of the data collected were required to be carried out by experienced practitioners and were completed entirely remotely and in discussion with the on-site overseeing engineers. Due to the fast-paced and multifaceted nature of site characterisation programmes, site-based QA/QC reviews of data by experienced practitioners may have been conducted at less frequent intervals previously. There can therefore be inherent benefits in the requirement for more frequent review when operating remotely, such as early adaptations to data collection methodologies.

Remote Data Processing and Analysis

All data processing and analysis was completed remotely by experienced practitioners to inform the interpretative phase of the investigation. This stage of the site characterisation process remained largely unchanged from pre-pandemic practices however, as described in the previous section, were conducted as the study progressed to iteratively inform subsequent phases of the investigation.

Risks, Rewards and Limitations of Approach

As with all approaches, consideration should be given to the relative risk versus reward and the practical limitations of the remote oversight approach. As there are many parties involved in hydrogeological field programmes (for example, the mine staff, local communities, financial investors, consultants, contractors and local students or academics), these considerations may vary for each stakeholder.

Benefits of the above outlined remote oversight approach can include:

1. Reduced travel time for experienced practitioners and reduced travel costs to the mine.
2. Reduced environmental footprint and increased environmental sustainability due to a lower number of flights and shorter travel distances when utilising local staff.

3. Reduced rotation of overseas based staff and increased consistency of experienced practitioner involvement throughout the field programme.
4. Once field materials and procedures have been established, set-up time for subsequent studies at the mine site may be reduced.
5. Increased frequency in data QA/QC review can identify and allow for rectification of data collection inadequacies early on in the field programme.
6. Increased transfer of knowledge and upskilling of site-based staff and increased opportunities for local student internships.
7. Many mines are under pressure from local communities or financial investors to utilise the local workforce and this approach can help ease this pressure and improve relationships with local communities.
8. Consolidation of experienced practitioner effort from a full day on site to a few hours a day can again reduce costs to the mine and free up experienced practitioners time to provide remote support to multiple projects simultaneously. This may prove to vital to progressing multiple studies during upturns in the mining market.

Risks and limitations of the remote oversight approach can include:

1. Early time constraints can lead to deficiencies during the initial project planning and structuring phase. These may then permeate through to the data collection and interpretation phases. It is essential to allow enough time and resource for planning activities.
2. The approach can only be effective where local staff and contractors are suitably skilled to uptake the required remote training.
3. Limited experience with the equipment can lead to an increase in both technical risks (for example loss or damage of boreholes, data, or testing equipment) and health and safety risks (for example risks to operators when using pressurised equipment).
4. Language barriers, lacking communication skills, and time in the programme for increased remote communication, can be a challenge and a risk to investigations. Investigations where pressure to advance does not allow for regular communications to remote supervision staff or utilisation of either local staff or experienced practitioners who are not suited for this type of remote oversight and communication will lead to poor data collection.
5. The approach may not be suitable where additional communication challenges are faced, such as a large time difference, limited overlap in working hours or inability to access the internet or other communication mechanisms at regular or semi-regular intervals throughout the field programme.
6. Effective implementation relies on the depth of practitioner's experiences and possessing a suitable archive of photographs, field demonstration videos and diagrams.
7. There is need for close supervision and thorough QA/QC checks to ensure data quality is not compromised. This ongoing activity should always be prioritised over progression of the programme.
8. Remote supervision may not be a suitable substitute for site visits required by Competent Persons for financial market reporting.

Conclusions

The remote oversight approach outlined in this paper can allow data collection to progress at locations where travel or access may be restricted. The fully remote oversight approach presented does not, and should not, fully replace the need for traditional supervision or QA/QC on mining hydrogeology characterisation programmes, which must be implemented as soon as practicable or at an appropriate stage in the mining study.

The approach can be used to reduce a project's travel related carbon footprint, allow the mine sites to realise time and cost savings on their programmes while also upskilling site-based or local staff. There are inherent risks to be considered with the remote oversight approach related to the potential for loss or damage of boreholes, data or testing equipment and the potential for reduced quality of data collection when

compared with a traditionally supervised investigation. The approach can however add value to mining projects where other factors may restrict a traditional approach. The relative risk and reward should be assessed on a project specific basis.

References

Golder Associates (UK) Limited (2020) Hydrogeological Monitoring Well Installation Guide. Document reference 19131151.103/B.0.

Land and Minerals Consulting (2018) Bjornvatn North, Major Structures Summary. Produced for Golder Associates (UK) Limited.

Passive Treatment of Acid Mine Drainage at Parys Mountain (Wales): Column Experiment Results

Jose Miguel Nieto[1], Tobias Rötting[2], Peter Stanley[3], Louise Siddorn[3], Francisco Macías[1], José María Fuentes[1], Rafael León[1], Ricardo Millán[1]

[1]*Department of Earth Sciences & Research Center on Natural Resources, Health and the Environment (RENSMA), University of Huelva, Avda. Tres de Marzo s/n, Huelva, Spain, jmnieto@uhu.es, francisco.macias@dgeo.uhu.es, jose.fuentes@dct.uhu.es, rafael.leon@dct.uhu.es, ricardo.millan@dct.uhu.es*

[2]*Golder Associates (UK) Ltd, Bourne End SL8, UK, troetting@gmail.com*

[3]*Natural Resources Wales, Tŷ Cambria, 29 Newport Rd., Cardiff, CF24 0TP, UK, geowyddor@cyfoethnaturiolcymru.gov.uk*

Abstract

Parys Mountain deposit in Anglesey (northwestern Wales) is a volcanic-hosted massive sulphide deposit consisting of lenses of massive Zn-Pb-Cu sulfides at and near the contact between Ordovician shales and overlying Lower Silurian rhyolites. Historical mining activities at Parys Mountain has resulted in extensive workings and the deposition of an important amount of metalliferous mine wastes with a high Acid Mine Drainage (AMD) generation capacity. The highly acidic, metal polluted run-off from Parys Mountain enters the freshwater rivers of the Afon Goch Amlwch and Dulas prior to reaching the Irish Sea, representing a significant outflow of Fe, Cu, Cd and Zn.

As a first step for the design of a full-scale passive treatment plant based on the Dispersed Alkaline System (DAS) technology for the AMDs originating at Parys Mountain, we have run column tests. The experimental arrangement consists of two suites of reactive-sections (DAS-columns) each having 1130 cm^3 capacity. Three columns were used in each arrangement, each one filled with 20 cm DAS reactive material comprising (80% (v/v) wood chips and 20% (v/v) alkaline reagent), including a drainpipe and a 3 cm basal layer of glass pearls, creating a water drainage layer that increases the porosity and permeability of the column. A 25 L tank was used as an AMD-water source and as an iron oxidation/precipitation step prior to the reactive columns. In addition, a decantation vessel of 445 cm^3 was connected to each column in order to reach chemical equilibrium between the treated water and atmospheric conditions, enhancing mineral precipitation. AMD-water was pumped from the 25 L tank into two different DAS-systems: System-A and System-B.

After 5 weeks of test runs, System-A (limestone+MgO DAS) promote total metal removal of Fe, Al, Zn, Cu and Mn. Trace elements (As, Cd, Co, Cr and Ni) were also removed by adsorption/coprecipitation processes. Sulfate removal was, however, not significant. System-B (limestone+$BaCO_3$ DAS) promote total metal removal of Fe, Al, Zn and Cu, and high retention / removal of Mn, As, Cd, Co, Cr and Ni by adsorption/coprecipitation processes. Sulfate removal was highly efficient in this set-up. From the incoming 2340 mg/L of sulfate, the output solution concentration was 543 mg/L. No loss of permeability has been observed during the experiments, which indicate that the pore space occupied by the precipitating metals is compensated by the dissolution of reactive grains.

Keywords: Passive Treatment of Acid Mine Drainage; Dispersed Alkaline System; Parys Mountain; Wales

Full Paper

A full paper on the results of this study will be published in an upcoming issue of the "Mine Water and the Environment" journal. If you have further interest or questions in the meantime, please contact the authors.

Solvent Extraction to Recover Copper from Extreme Acid Mine Drainage

Amir Nobahar[1,2], Alemu Bejiga Melka[2], Jorge Dias Carlier[1], Maria Clara Costa[1,2],

[1]*Centre of Marine Sciences (CCMAR), University of the Algarve, Gambelas Campus, 8005-139 Faro, Portugal, mcorada@ualg.pt*

[2]*Faculty of Sciences and Technology, University of the Algarve, Gambelas Campus, 8005 139 Faro, Portugal*

Abstract

This study evaluated the application of a solvent extraction process from an extreme Acid Mine Drainage (AMD) (with 5.3 ± 0.3 g/L Cu). The extractant Acorga M5640 showed high copper selectivity and 30% (v/v) of this extractant, extracted ≈96% of this metal with a maximum loading capacity of ≈16 g/L in the organic phase. Then, 2M sulfuric acid solution stripped ≈99% of copper and through successive striping steps the concentration of copper was raised up to ≈46 g/L, which is suitable for the electrowinning process. Recyclability of the organic phase was also confirmed in five successive extraction and stripping cycles.

Keywords: Acid Mine Drainage, Solvent Extraction, Copper, Metal Recovery

Introduction

Most strategic metal are obtained through mining from primary sources that are finite and rapidly decreasing as a result of population explosion and modern industrialization (Arndt *et al*., 2017; Segura-Salazar & Tavares, 2018). Some estimates indicate that in the next 2–3 decades different industrial sectors will struggle to maintain their demand for several metals (Elshkaki *et al*. 2016; Frenzel *et al*. 2015; European Commission 2014). Based on world annual data of mining (for year 2018), 20 474 372 metric tons of copper are obtained per year (Reichl & Schatz, 2020) and according to the International Copper Study Group (2019), global consumption of this metal will continuously increase due to population growth, product innovation and economic development. In a recent study, Schipper *et al*. (2018) estimated the copper demand for the year 2100 to be in a range of 3 to 21 times the current demand. Thus, a combined production from mining of primary raw materials and from recycling and recovering from secondary sources is required.

In general, metals' recycling rates from secondary sources are still low and there is significant potential to increase the recovery from such sources (Schäfer & Schmidt, 2019). In the case of copper, the recycling rates continuously decreased from 2011 to 2016 (from 36% to 29%) while the secondary refined production was quite stable over the same period (ICSG, 2018).

Solvent extraction (SX) is a method of separation used in the hydrometallurgical industry to separate and recover metals from aqueous leachates obtained from ores and secondary materials such as slags or tailings (Hedrich *et al*., 2018). In these processes, organic phases of extractants diluted in solvents are used to separate target metal ions (e.g. Cu^{2+}) from multimetallic leaching solutions, which are then stripped from the organic phase to aqueous pure solutions (Davis-Belmar *et al*. 2012; Ruiz *et al*. 2019).

Copper is present in high concentrations in the Acid Mine Drainage (AMD) generated at many mining sites such as São Domingos mining area in Portugal (Álvarez-Valero *et al*., 2008). In this study a solvent extraction process using Acorga M5640 as extractant, like processes in place in the hydrometallurgical industry to separate copper from leaching solutions, was investigated for the separation of this metal but from an extreme AMD collected at Mina de São Domingos.

Materials and methods

Extreme AMD

The extreme AMD sample used in this work was collected at the São Domingos mine, Portugal, from a pond near the sulphur factory ruins, and was transported in the same day to the laboratory for characterization and copper SX tests. The pond is surrounded by roasted pyrite ores (sulphur factories ashes), iron oxides (hematite roasted pyrite) and leached materials in seasonal flooded areas (Álvarez-Valero *et al*., 2008).

SX experiments

SX was carried out by mixing the extreme AMD (aqueous phase (A)) with 30% (v/v) Acorga M5640 diluted in a kerosene-like solvent called Shell GTL with 2.5% (v/v) octanol (organic phase (O)) in 100 mL round bottom flasks, using a A:O ratio of 1:1 and contact with magnetic stirring during 30 minutes at room temperature (25 ± 3 ºC). Initial ($[M_{aq}]_i$) and final ($[M_{aq}]_f$) concentrations of metals in the aqueous phase, measured before and after SX, were used to calculate concentrations in the final organic phase ($[M_{org}]_f$); then, metals' extractions efficiencies were determined through: (%) Extraction percentages = 100 × $[M_{org}]_f$ / $[M_{aq}]_i$ and (D) Distribution ratios = $[M_{org}]_f$ / $[M_{aq}]_f$. Loading capacity of copper in the organic phase was determined by performing a cumulative copper extraction in consecutive SX cycles directly using the same organic phase, but new extreme AMD in each cycle.

Stripping of copper from the loaded organic phase was done by mixing it with 2M H_2SO_4 in 100 mL round bottom flasks, using a A:O ratio of 1:1 and contact with magnetic stirring during 60 minutes at room temperature (25 ± 3 ºC). Cumulative copper stripping cycles were carried out using the same 2M H_2SO_4 solution but different loaded organic phases, to verify the feasibility of raising copper concentration to values suitable for the electrowinning process.

Analytical methods

The pH was measured using a pH/E Meter GLP 21 (Crison) with a glass pH electrode (VWR, SJ 223). The sulphate concentration was determined with a UV-visible spectrometer DR2800 (Hach-Lange) using the sulfaVer4 (Method 8051, Hach-Lange) procedure at 450 nm. The concentrations of iron, zinc, copper and manganese were determined through flame atomic absorption spectroscopy with a novAA 350 system (Analytik Jena), and the concentration of aluminium was measured by microwave plasma atomic emission spectrometry with a 4200 MP-AES (Agilent). Calibration curves were built using standards prepared from metals stock solutions of 1000 mg/L metal in 0.5 M nitric acid: iron, zinc and copper (Merck Certipur, Germany), manganese and aluminium (Panreac AA, Spain). Several samples' dilutions were prepared in 1% nitric acid (0.224 M), and the lowest dilutions fitting in the linear calibration curves were chosen.

Results and Discussion

Extreme AMD

The acidity and concentrations of main pollutants in the AMD sample collected from the pond near the sulphur factory ruins at São Domingos mine (Table 1) are much higher than in the flowing water streams affected by AMD at mining site: pH ≈ 2 to 3, sulphate ≈ 1000 to 5000 mg/L, aluminium ≈ 100 to 500 mg/L, iron ≈ 50 to 500 mg/L, zinc ≈ 20 to 150 mg/L, copper ≈ 20 to 100 mg/L and manganese ≈ 5 to 20 mg/L (e.g. Costa and Duarte 2005; Costa *et al*. 2008).

SX experiments

The extraction from extreme AMD using 30% (v/v) Acorga M5640 in Shell GTL with 2.5% (v/v) octanol was highly selective for copper (with a D value for this metal of 23 ± 2 and D values below 0.1 for the other metals) and allowed to extract of 96 ± 1% of this metal (Table 2). This makes approximately a ratio of Acorga M5640's active compounds (5-nonyl-2-hydroxy-benzaldoxime) to copper ions ($Cu2^+$) of 8, which can be considered a good result. It is only four times higher than the theoretical ratio of 2 for this extractant, and for example the results reported by Agarwal, *et al*. (2010) when using 20% (v/v) Acorga M5640 correspond approximately to a ratio of 24.

Table 1 *Brief characterization of extreme AMD sample collected for this work at the São Domingos mine.*

pH	1.19	Standard unit (s.u.)
$[SO_4^{2-}]$*	142 ± 15	g/L
[Fe]*	63 ± 6	
[Al]*	6.4 ± 0.2	
[Cu]*	5.3 ± 03	
[Zn]*	1.9 ± 0.5	
[Mn]*	0.131 ± 0.002	

*Averages and standard deviations of five analysis using independent dilutions.

Table 2 *Extraction efficiencies* in percentages and distribution ratios (D) of metals analysed in the SX studies (with 30% (v/v) Acorga M5640 in Shell GTL with 2.5% octanol).*

Metals	%	D
Fe	8 ± 5	0.08 ± 0.06
Al	2 ± 3	0.02 ± 0.03
Cu	96 ± 1	23 ± 2
Zn	0 ± 3	0.04 ± 0.03
Mn	0 ± 2	0.01 ± 0.02

*Averages and standard deviations of three SX replicates.

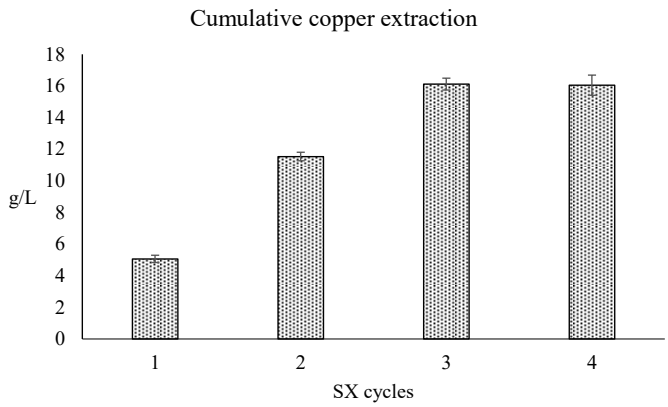

Figure 1 *Copper concentrations in the organic phase after consecutive cycles of extraction using directly the same organic phase (30% (v/v) Acorga M5640 in Shell GTL with 2.5% octanol) and new extreme AMD in each cycle. Results are averages of triplicates ± standard deviations.*

The cumulative copper extraction cycles revealed that after the third cycle, when the tested organic phase was loaded with 16.1 ± 0.4 g/L of copper, it was no longer able to extract this metal from the extreme ADM in the fourth cycle, indicating this is the maximum loading capacity of the tested SX process (Figure 1). This value goes in line with results obtained for the same type of organic phase, but with lower concentrations of extractant: 4.8 g/L and 10g/L, respectively for 10% and 20% Acorga M5640 in ShellSol D70 + 5% isotridecanol (Agrawal & Sahu, 2010).

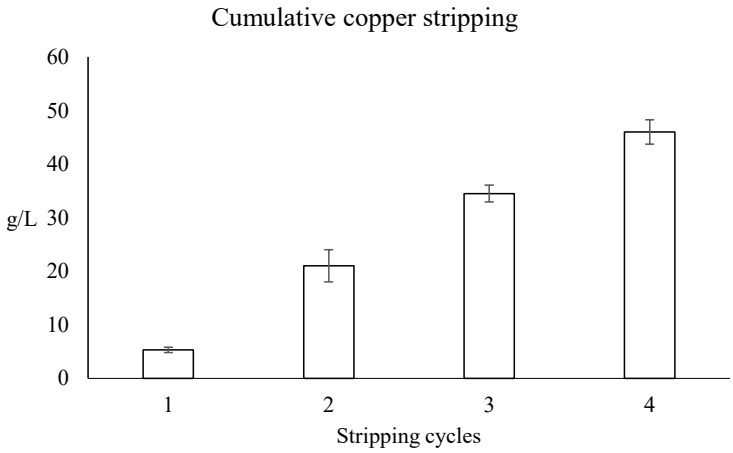

Figure 2 *Copper concentrations in the stripping solution after consecutive cycles of stripping directly using the same stripping solution (2M H_2SO_4) and new organic phases loaded with copper in each cycle (5.56, 16.11, 13.8 and 15 g/L of copper, respectively for cycles 1, 2, 3 and 4). Results are averages of triplicates ± standard deviations.*

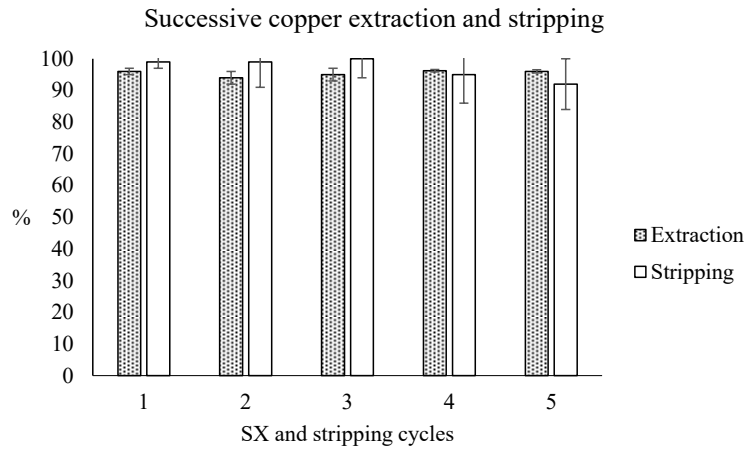

Figure 3 *Copper extraction and stripping efficiencies in five consecutive cycles from extreme AMD using the same organic phase (30% (v/v) Acorga M5640 in Shell GTL with 2.5% octanol) and stripping solution (2M H_2SO_4). Results are averages of triplicates ± standard deviations.*

The fourth cumulative copper stripping cycles revealed that it is possible to achieve at least 46 ± 2 g/L Cu in the tested stripping solution (Figure 2). This value is in the range of concentrations (≈30 to 50 g/L of copper) of typical aqueous stripping solutions exiting the SX operation and entering the electrowinning operation in the hydrometallurgical extraction of copper from slags or tailings (Aksamitowski *et al.*, 2018; Jose Alguacil & Regel-Rosocka, 2018; Schlesinger *et al.*, 2011).

During the five successive cycles of extraction and stripping with the organic phase and the stripping solution under study, the efficiency remained very high in both processes: 95.4 ± 0.9% for copper extraction and 97 ± 3% for copper stripping (Figure 3). These results are promising regarding the development of copper recovery processes from extreme AMDs, since the reusability of the organic phase is crucial for an environmentally and economically viable operation.

Acknowledgments

This work was supported by (1) the Portuguese Foundation for Science and Technology (FCT) through the projects UIDB/04326/2020 and UIDB/00100/2020; and (2) national funds from FCT co-financed by the Algarve´s Regional Operational Program (CRESC Algarve 2020) through Portugal 2020 and European Regional Development Fund (FEDER), under the project METALCHEMBIO (no. 29251).

References

Agarwal, S., Ferreira, A. E., Santos, S. M. C., Reis, M. T. A., Ismael, M. R. C., Correia, M. J. N., & Carvalho, J. M. R. (2010). Separation and recovery of copper from zinc leach liquor by solvent extraction using Acorga M5640. *International Journal of Mineral Processing, 97*(1–4), 85–91. https://doi.org/10.1016/j.minpro.2010.08.009

Agrawal, A., & Sahu, K. K. (2010). Treatment of Chloride Waste Pickle Liquor by Solvent Extraction for the Recovery of Iron. *Mineral Processing and Extractive Metallurgy Review, 31*(3), 121–134. https://doi.org/10.1080/08827501003727006

Aksamitowski, P., Wieszczycka, K., & Wojciechowska, I. (2018). Selective copper extraction from sulfate media with N,N-dihexyl-N´-hydroxypyridine-carboximidamides as extractants. *Separation and Purification Technology, 201,* 186–192. https://doi.org/10.1016/j.seppur.2018.02.051

Álvarez-Valero, A. M., Pérez-López, R., Matos, J., Capitán, M. A., Nieto, J. M., Sáez, R., Delgado, J., & Caraballo, M. (2008). Potential environmental impact at São Domingos mining district (Iberian Pyrite Belt, SW Iberian Peninsula): Evidence from a chemical and mineralogical characterization. *Environmental Geology, 55*(8), 1797–1809. https://doi.org/10.1007/s00254-007-1131-x

Arndt, N. T., Fontboté, L., Hedenquist, J. W., Kesler, S. E., Thompson, J. F. H., & Wood, D. G. (2017). Future Global Mineral Resources. *Geochemical Perspectives*, 1–171. https://doi.org/10.7185/geochempersp.6.1

Costa, M. C., & Duarte, J. C. (2005). Bioremediation of Acid Mine Drainage Using Acidic Soil and Organic Wastes for Promoting Sulphate-Reducing Bacteria Activity on a Column Reactor. *Water, Air, and Soil Pollution*, 165(1–4), 325–345. https://doi.org/10.1007/s11270-005-6914-7

Costa, M. C., Martins, M., Jesus, C., & Duarte, J. C. (2008). Treatment of Acid Mine Drainage by Sulphate-reducing Bacteria Using Low Cost Matrices. *Water, Air, and Soil Pollution, 189*(1–4), 149–162. https://doi.org/10.1007/s11270-007-9563-1

Davis-Belmar, C. S., Gallardo, I., Demergasso, C., & Rautenbach, G. (2012). Effect of organic extractant LIX 84IC, pH and temperature changes on bioleaching microorganisms during SX treatment. *Hydrometallurgy, 129–130*, 135–139. https://doi.org/10.1016/j.hydromet.2012.09.004

Elshkaki, A., Graedel, T. E., Ciacci, L., & Reck, B. K. (2016). Copper demand, supply, and associated energy use to 2050. *Global Environmental Change, 39*, 305–315. https://doi.org/10.1016/j.gloenvcha.2016.06.006

European Commission. (2014). *Report on Critical Raw Materials for the EU*.

Frenzel, M., Tolosana-Delgado, R., & Gutzmer, J. (2015). Assessing the supply potential of high-tech metals – A general method. *Resources Policy, 46*, 45–58. https://doi.org/10.1016/j.resourpol.2015.08.002

Hedrich, S., Kermer, R., Aubel, T., Martin, M., Schippers, A., Johnson, D. B., & Janneck, E. (2018). Implementation of biological and chemical techniques to recover metals from copper-rich leach solutions. *Hydrometallurgy, 179*, 274–281. https://doi.org/10.1016/j.hydromet.2018.06.012

ICSG. (2018). *The World Copper Factbook* (pp. 1–66). Tech. rep.. International Copper Study Group. http://www.icsg.org/index.php/component/jdownloads/finish/170/2876

International Copper Study Group. (2019). *The World Copper Fact Book*.

Jose Alguacil, F., & Regel-Rosocka, M. (2018). Hydrometallurgical treatment of hazardous copper Cottrell dusts to recover copper [PDF]. *Physicochemical Problems of Mineral Processing; ISSN 2084-4735*. https://doi.org/10.5277/PPMP1880

Reichl, C., & Schatz, M. (2020). *World mining data* (Vienna). Minerals Production.

Ruiz, M. C., González, I., Rodriguez, V., & Padilla, R. (2019). Solvent Extraction of Copper from Sulfate–Chloride Solutions Using LIX 84-IC and LIX 860-IC. *Mineral Processing and Extractive Metallurgy Review*, 1–8. https://doi.org/10.1080/08827508.2019.1647839

Schäfer, P., & Schmidt, M. (2019). Discrete-Point Analysis of the Energy Demand of Primary versus Secondary Metal Production. *Environmental Science & Technology*, acs.est.9b05101. https://doi.org/10.1021/acs.est.9b05101

Schipper, B. W., Lin, H.-C., Meloni, M. A., Wansleeben, K., Heijungs, R., & van der Voet, E. (2018). Estimating global copper demand until 2100 with regression and stock dynamics. *Resources, Conservation and Recycling, 132*, 28–36. https://doi.org/10.1016/j.resconrec.2018.01.004

Schlesinger, M. E., King, M. J., Sole, K. C., & Davenport, W. G. (2011). Electrowinning. In *Extractive Metallurgy of Copper* (pp. 349–372). Elsevier. https://doi.org/10.1016/B978-0-08-096789-9.10017-4

Segura-Salazar, J., & Tavares, L. (2018). Sustainability in the Minerals Industry: Seeking a Consensus on Its Meaning. *Sustainability, 10*(5), 1429. https://doi.org/10.3390/su10051429

Evaluating Circum-neutral Mine Drainage: Case Studies of Advanced Testing Methods Generating Representative Empirical Data

Steven Pearce[1], Andrew Barnes[2], Seth Mueller[3], Diana Brookshaw[1]

[1]*Mine Environment Management, 3 Vale Street, Denbigh LL16 3AD, Wales, spearce@memconsultants.co.uk*

[2]*Geochemic Ltd, 3 Coghill Research Laboratories, Lower Race, Pontypool, PN4 5UH, Wales, abarnes@geochemic.co.uk*

[3]*Boliden Mineral AB, Boliden, Sweden, seth.mueller@boliden.com*

Abstract

Standard acid mine drainage (AMD) characterisation testing methods focus on acidity and can underestimate risks posed by circum-neutral mine drainage. For circum-neutral sites, amended testing methods are required to provide representative empirical data. Case studies of where such amended testing methods have been used to refine assessments of discharge quality from circum-neutral drainage sites are discussed.

Keywords: Modified Columns, Circum-neutral Drainage, Modified NAG Test

Introduction

The geochemical testing of mine waste materials aims to characterise their properties to allow prediction of their behaviour longer term under a range of conditions, such as when subjected to different oxygen levels or leached due to rainfall. Since the mine wastes from many sites generate acidity upon oxidation, and the mobility of most metals is enhanced in acidic solutes (e.g. Krol *et al.* 2020), the standardised testing methods are centred around determining the relative acidity of the drainage (for example acid-base accounting (ABA) testing, including net acid generation (NAG) tests and acid-neutralisation capacity (ANC) tests).

Typically, acidity causes mineral dissolution, releasing the components of those minerals, and desorption of metals due to competition with H+ ions. Both of these processes, therefore, can contribute to increase in metal loading of the solute with decreasing pH.

However, many metals released through sulfide oxidation, such as cobalt and nickel, are mobile in circum-neutral pH environment, with order of magnitude difference in solute concentrations occurring over the pH range of 6-8. In environments where sufficient buffering is present to buffer the generated acidity, correct estimation of pore water pH, and changes in metal behaviour at relatively small changes in pH are critical for rock drainage metal leaching assessments.

The behaviour of waste rock materials is characterised through a combination of static and kinetic tests. Static tests reflect 'snapshots' of the behaviour under specific conditions, for example pH-dependent leach test, or under full oxidation, with the net acid generation (NAG) tests. Kinetic tests track the evolution of the solute in response to flushing. In both cases selecting the correct conditions is key to achieving representative results. Standard kinetic tests such as humidity cells, for example, have very high flushing rates, and as such are not likely to capture the slow drain-down processes occurring at low liquid-to-solid (L:S) ratios in waste rock dumps or tailings storage facilities. Using the outputs of such standard kinetic tests to assess drainage risk from circum-neutral sites can result in underestimation of flush-out times for residual sulfate loads from processing, inaccurate simulation of pore water pH conditions and overestimation of metal release rates.

To improve prediction of water quality from circum-neutral sites, a suite of novel or adapted testing methods is needed to target the contaminant release mechanisms that dominate in those conditions such as mineral

dissolution/precipitation reactions and sorption processes. The research discussed here describes a set of tests which have been used to generate robust empirical data as part of metalliferous drainage assessment at active mine sites in Scandinavia (nickel mine in Finland, and a copper mine in Sweden). Materials analysed included samples of partially weathered waste rock material collected from waste rock storage facilities (as part of a sonic drilling program of work), in general material <22mm in size were analysed and for leach testing material <2.36mm was analysed.

Methods

Amended NAG test

To understand the interplay between oxidation, sorption and metal release, and provide additional data in the circum-neutral to slightly-acidic pH range, conditional NAG test leaching was performed with AMIRA P387A-Appendix D as a guideline, with modifications applied to the described method. The amount of solid and 15% H_2O_2 reagent were doubled relative to the standard method, to provide sufficient sample while maintaining the liquid to solid ratio (L:S ratio). After H_2O_2 addition, the test was run for 24 h and monitored. No boiling step was performed, since this was demonstrated to report unrepresentative pH and leachate quality (see Barnes *et al*. 2021) because of the material type (ultramafic mineralogy with carbonates). The NAG pH, EC and temperature were measured and 50 mL aliquot collected, filtered through 0.45 µm polyethersulfone (PES) filter into bottles and preserved with 0.57 mL 40% nitric acid for analysis by ICP. The pH of the NAG liquor solution was then adjusted via titration and samples were taken for analysis at various pH steps including pH 5, 6, 7, 7.5 and 8.

Amended pH dependent leach test and sorption-desorption assessment

The effect of pH on the release of metals and sulfur/sulfate from the partially weathered samples was tested through a series of pH controlled or amended tests. A set of samples of <2.36mm material were equilibrated with deionised water through bubbling with nitrogen during overhead stirring, and in the absence of CO_2. If the starting 'rest' pH after this equilibration was below 8, this was corrected by addition of 100 µL aliquots of 1 M KOH until the rest pH was above 8. The sample solutions were then sparged with CO_2 to achieve precise amendment of the pH to pH 8, 7.5, 7 and 6. Allowing equilibration at each step for 30 minutes before recovering liquid sample aliquot for analysis. This method of controlling pH allows better control to ensure the correct pH is achieved at each step. It also decreases the effect of addition of competing cations to amend pH, which may compound sorption processes.

Mixed leach test

A mixed leach test was designed to better understand the role of the solids (i.e. presence of fine grained mineral particles) in controlling solution chemistry. Initially two DI leaches were performed on <2.36 mm size fraction of higher risk and lower risk waste samples, both at 2:1 L:S ratio, performed for 24 h while mixing by end-over-end tumbling. After the mixing period, equal amounts of each leachate were recovered and filtered with 0.45 µm PES filter, and mixed by end-over-end tumbling for 24 h. An aliquot of the higher risk waste leachate was used as a leachant for a leach test on a new <2.36mm size fraction sample of the lower risk waste sample in a 2:1 L:S ratio. The leachate and waste rock were contacted for 24 h and mixed by end-over-end tumbling.

Amended leach columns testing

The mineral precipitation/dissolution dynamics and their effect on drainage evolution over time were investigated using kinetic columns. The standard method defined in EN 14405:2017 explores solution chemistry at liquid:solid ratios of 0.25 to 10.

Customised column tests were prepared, with bespoke amendments to the standard method to capture specific aspects to provide representative results in a practical timescale (Table 1). Liquid samples were recovered from the seepage from each column and analysed for a suite of physical and chemical parameters including pH, sulfur and metals of interest.

Table 1 Comparisons of amended vs standard upflow column test method.

Test	Flow rate mL/h	Cumulative L:S ratio in first six steps	Temp °C	Atmosphere
Standard upflow test		0.25, 0.5, 1, 2, 4, 8		
	10	24 hours to L:S ratio of 0.5	25	N_2
Small column (start)		0.25, 0.38, 0.51, 0.65, 0.8, 0.9		
	0.95	14 days to L:S ratio of 0.5	8	Air
Small column (long term)		0.25, 0.38, 0.51, 0.65, 0.8, 0.9		
	0.22	14 days to L:S ratio of 0.5	8	Air
Large column (start)		0.25, 0.27, 0.29, 0.31, 0.34, 0.36		
	0.95	98 days to L:S ratio of 0.5	8	Air
Large column (long term)		0.25, 0.27, 0.29, 0.31, 0.34, 0.36		
	0.22	98 days to L:S ratio of 0.5	8	Air

Results

Metal release rates

The standardised NAG testing reported generally NAG pH values above 8 for the nickel mine waste samples (and up to pH 10), with a cluster of results at pH<4, and limited results in the range 8-4. The standardised testing results indicated that at this site NAG pH tests produced results that are spuriously high and are not likely representative of field pore water conditions. This has been confirmed by other studies (Barnes *et al* 2021). The leachate results are considered as a ratio of metal to sulfate concentration to focus on the release mechanisms without bias due to elemental composition of the samples. Based on the leachate quality from this testing, an exponential Ni/S relationship to pH is estimated (Figure 1).

The pH-dependent leach testing provided more detailed results between pH 8 and 4, predicting an exponential relationship between Ni/S ratio and pH. The pH-dependent leach results predicted higher Ni concentrations relative to sulfur for the same pH compared to the standardised NAG leach test. This difference arises because of test conditions and solubility constraints with mineral dissolution at circum neutral pH where gypsum is likely the main sulfate mineral precipitated, but at lower pH conditions sulfates such as jarosite may form. When pH is varied in a sample that has been subject to sulfide oxidation at circum neutral pH the concentration of nickel changes but the concentration of sulfate does not as gypsum is not sensitive to pH but nickel is. In

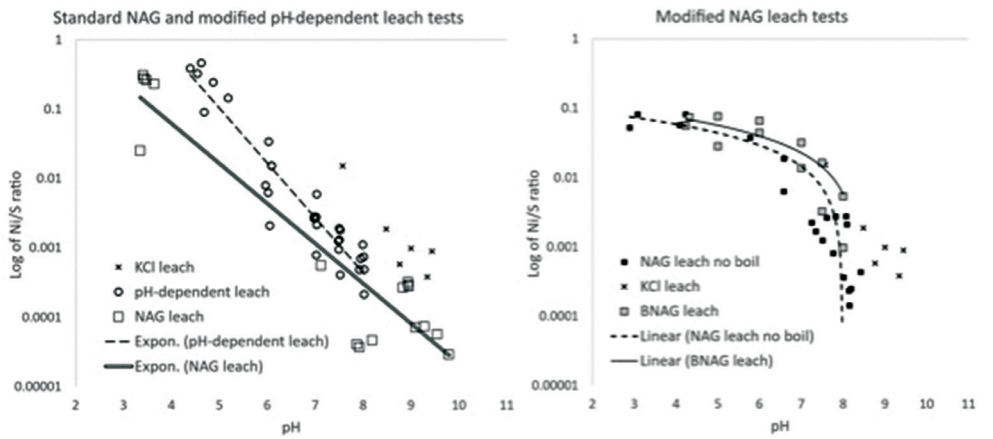

Figure 1 Scatter plots of the nickel to sulfur ratio in leachates of different pH values generated by the tested analytical method. Left: standard NAG leach tests and modified pH-dependent leach test. Right: Modified NAG tests. Potassium chloride (KCl) leach test results are included in both graphs for comparison.

the NAG test high dilution rates of ≈50-100:1 liquid to solid mean that sulfate is not likely limited by solublity constraints, however in test with lower liquid solid ratios sulfate may be solubility constrained. Further where a sample has been subject to sulfide oxidation at lower pH values (<pH 4.5) other sulfate minerals such as jarosite may form which in turn effects the release of nickel. As such the ratios of nickel to sulfate in the NAG test are not likely to accurately represent field conditions when dealing with circum neutral sites, and in particular where they are subject to pH changes over time. This observation is important when considering field conditions where liquid solid ratios in pore water are significantly lower (generally <0.5) and where pore water pH may change over time (for example a decrease over time from ≈8 to ≈5).

When NAG testing was carried out without the boiling step, NAG pH values were typically between 6.5 and 8.5. The available data shows a relationship with pH interpreted as linear (seen curved on a log y axis scale, Figure 1). This was also the case for results where the NAG solution was back-titrated to specific pH steps, with a hysteresis relative to the NAG leach (no boil) results. For both of these tests the Ni/S ratio was higher than the pH-dependent leach, reflecting the effect of oxidative Ni release on the leachate quality (Table 2). The difference in the Ni/S ratio between the results of the no-boil NAG leach test and the BNAG test suggests that less sorption is available in this test (e.g. due to loss of sorption sites relative to material exposed to solute of the same pH where the pH did not decrease further).

The results suggest that the method of assessment to estimate metal/sulfate release and relative solute concentrations has a significant effect on results and as such assumptions that may be used for modelling. For circumneutral sites very careful method design and selection is required. Reliance on standard test methods therefore carries a high degree of risk.

Sorption

Leach test results from low-risk and high-risk solids (standard 2:1 L:S ratio DI method) had similar pH (6.21 and 6.18 respectively), but had very different concentrations of cobalt, nickel and manganese, reflecting the source metal abundance-associated circum-neutral metal leaching potential of the waste rock materials at this site. Copper mobility is highly pH sensitive, reflected in the very similar copper concentrations reported in the 2:1 L:S ratio leachate.

For all metals, mixing the supernatants at 1:1 ratio, resulted in leachate quality approximately equal to the average of the concentrations of the metals in the constituent leachates (Table 2), which given the pH was similar this results is not surprising. When however the same experiment is carried out but in the presence of the low risk solid, the concentrations of all metals except Cu decreased by an order of magnitude, indicating that the presence of solids has a material effect on solute concentration. The results confirm that at circum-neutral pH, sorption processes are a very significant control metal mobility, and that testing method can significantly effect solute concentrations and implied metal mobility. The results are particularly relevant when leaching test results of different materials are assessed in combination (for example taking averages of leach test results for example).

Kinetic solute evolution

Results of the upflow test (Figure 2) show that flushing of the soluble salts occurred within the first 24 hours (or when 1:1 L:S ratio was

Table 2 *Leachate quality in mixed leachate tests.*

Metal/Sample	Co mg/kg	Cu mg/kg	Mn mg/kg	Ni mg/kg
Low-risk solids leach	0.00224	0.00842	0.033	0.0612
High-risk solids leach	1.24	0.01968	21.4	14.84
Composite supernatant mix	0.626	0.01084	10.68	7.56
Low-risk solids leach with high-risk sample leachate	0.01492	0.01542	1.052	0.496

reached). Typically, most parameters had relatively constant concentrations at L:S ratios of over 1, indicating that the majority of soluble salts had been flushed out.

The pH remained above 7.5 in all tests, indicating circum-neutral conditions (Figure 2) however pH was lower in the upflow tests indicating that the faster flushing rate in this test materially influenced pore water pH conditions. The pH results in the small and large column mirrored one another in time, although this was reflective of a different L:S ratio. The results therefore indicate that pH may be controlled by residence time, and therefore related to the kinetics of dissolution of mineral phases rather than the amount of percolation.

In the amended columns, sulfur concentrations had lower initial concentrations and decreased at a slower rate when compared to the upflow test relative to L:S ratio. The greater contact time within these columns was a likely significant influence on sulfate mineral dissolution kinetics and also potentially indicative of greater dissolution of less labile sulfur-containing minerals. These effects likely contributed to a longer time frame to flush out sulfate minerals in the amended relative to the upflow test and are critical to consider when scaling results to field interpretations of timeframes for removal of sulfate minerals from mine waste facilities.

The concentrations of nickel and manganese had a different pattern to sulfate, correlating to time since start of the experiment to a greater extent than L:S ratio, and are significantly lower in the upflow test. These results suggest that nickel and manganese solute concentrations are controlled by pore water residence time to a great extent. Over the initial period of the test to L:S ratio of ≈0.5 sulfate concentrations were higher in the large column for example but nickel concentrations were lower.

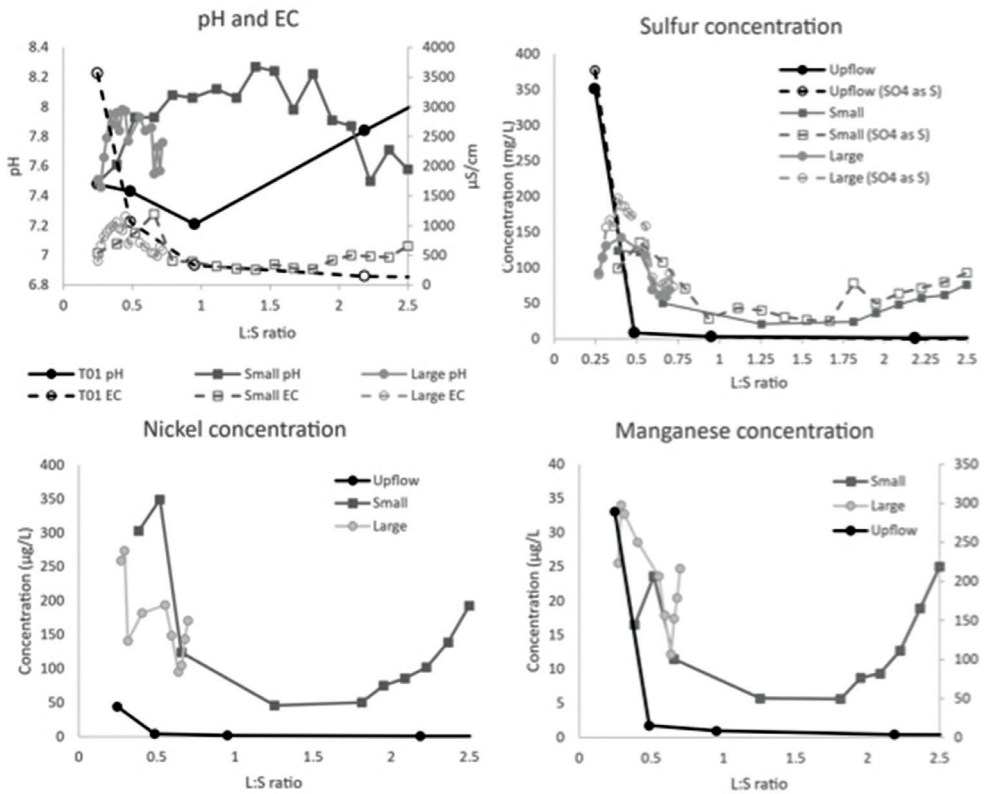

Figure 2 *Scatter plots of results of amended columns of tailings relative to standard upflow test results: Top Left: the pH and EC; Top Right: sulfur and sulfate concentrations; Bottom Left: nickel concentrations; Bottom Right: Mn concentrations.*

The longer-term testing shows that after approximately 150 days sulfate, nickel and manganese concentrations are increasing but this is related to the effects of sulfide oxidation presenting in the seepages and interpretation of this data is beyond the scope of this brief paper.

Conclusions

The use of modified geochemical testing methods to better understand and predict the behaviour of waste materials under circum neutral conditions has been evaluated.

Standard methods like the NAG test have been proven to produce spurious results when considering "real" field conditions with regards to solute pH, and as such modifications are suggested to improve the "representativeness" of this test as applied to the types of materials investigated (ultramafic carbonate containing mineralogy).

The main source of sulfate and metal release from waste materials tested was found to be the dissolution of secondary sulfate (gypsum and epsonite) mineral products that contain free base metals. NAG liquor analysis indicates that these sulfate minerals are formed as a direct result of the oxidation of iron sulfides (pyrrhotite/pyrite) and base metal sulfides (pentlandite and chalcopyrite) and subsequent dissolution/buffering with the magnesium/calcium carbonates dolomite and calcite. The mechanism of dissolution of these sulfate minerals and associated metals within pore water was interpreted from site specific and modified testing to be limited by pH mediated sorption and solubility constrains (in particular gypsum). These processes control the both the rate of dissolution and absolute pore water concentrations of sulfate and key metals such as nickel and as such understanding them is key for making accurate predictions of future water quality.

The key mechanisms for the control of solute metal concentration appears to be related to pH dependant sorption, and the form of the dominant sulfate mineral phase (which is controlled by the ph at which sulfate mineral formation occurs). Based on assessment of testing data, a strong case can be made for adoption of site specific modified testing methods to establish likely metal mobility.

The results of the column testing show that where circum-neutral drainage condition prevail, understanding of kinetic mineral dissolution rates and metal mobility under site specific flushing rates is likely key to be able to predict likely long term pore water concentrations. The results of the testing carried out indicate the high value of empirical data to achieve a thorough understanding of these site specific factors.

In general the results indicate that while the standardised tests play a role in determining the context within which the materials should be considered, where waste materials are likely to generate circum-neutral drainage, standardised tests need to be supplemented with further analysis aimed at providing empirical data that can be used to inform predictive modelling.

References

Krol A, Mizerna K, Bozym M (2020) An assessment of pH-dependent release and mobility of heavy metals from metallurgical slag. J Hazardous Materials 348: 1-9, doi:10.1016/j.jhazmar.2019.121502

Barnes A, Sapsford DJ, Bowell RJ, Dey M (2013) An assessment of rapid turnaround tests for ARD prediction. Presentation at 23rd World Mining Congress, August 11-15th, 2013, Montreal, Canada

Karlsson t, Raisanen ML, Lehtonen M, Alakangas L (2018) Comparison of static and mineralogical ARD prediction methods in the Nordic Environment. Env Mon Assess 190(719), doi:10.1007/s10661-018-7096-2

Application of Detailed Interval Flow Data Measured in Drillholes with PFL Tool in Hydrogeological Conceptualization and Numerical Flow Modelling for Mine Feasibility Scoping

Elias Pentti, Eero Heikkinen, Tiina Vaittinen

AFRY Finland Oy, P.O. Box 4, FI-01621 Vantaa, Finland, Elias.Pentti@afry.com

Abstract

Hydraulic drillhole measurements with the Posiva Flow Logging method have been performed at a planned open pit mining site in Northern Finland to acquire input data for numerical groundwater modelling. The high spatial resolution and low detection limit of the method enabled determining the hydraulic conductivity of bedrock, its depth dependence, and differences between two pit locations on a level sufficient for the numerical modelling. Separate FEFLOW models for two planned open pits were compiled and used to calculate groundwater inflow into the pits and effects on the water table in projected mining phases.

Keywords: Flow Logging, Hydraulic Conductivity, Groundwater Modelling

Introduction

In the Suhanko area in Ranua, Northern Finland, a few open pit mines are being planned for the exploitation of deposits of platinum-group metals in an Archaean mafic layered intrusion. We report hydrogeological field measurements and numerical groundwater modelling of two planned open pit locations at Ahmavaara and Konttijärvi. The goal of the measurements was to acquire hydraulic conductivity data of the bedrock that could then be used as an input in the modelling phase. The main aim of the modelling was to estimate the inflow rate of groundwater into the planned open pits in several stages.

Hydrogeological measurements

Prior to the reported study, data concerning the hydraulic conductivity of bedrock in the pit locations was only available from a few 24-hour crosshole pumping tests. Therefore, a better coverage was required before numerical modelling could be carried out. Downhole wireline hydrogeological measurement using Posiva Flow Logging (PFL) was chosen for data acquisition (Komulainen 2017) based on earlier good experiences elsewhere (Picken *et al*. 2017) and in the Suhanko area. Hundreds of exploratory and inventory drillholes were available for measurements. Information on fracturing and lithology in them was reviewed to define the most interesting locations for measurements, both within and outside of the planned pit shells, and two or three candidate drillholes from each location were selected. Some new holes were also drilled. In the selection of measured drillholes, the aim was to find ones extending below the bottom level of the pit, and to include intersections with modelled fault structures, the ore-hosting formation, the hanging wall, and the foot wall lithologies. A steep inclination was necessary to ensure smooth probe movement. Measurements in the field consisted of 20 drillholes during a time of two months. The flow logging of one 200–300 m long drillhole was typically performed overnight in 10–15 hours.

The PFL method is based on pumping a stable drawdown in an open drillhole, starting several hours before measurement, and running a flow logging with dense depth steps while continuously pumping. Elastic flow guides isolate the measurement section from the rest of the drillhole, so that the measured flow represents groundwater flow from the rock into the measurement section only. From the drawdown and flow, transmissivity associated with the measurement section can be calculated. The method is more sensitive to low transmissivities than spinner or thermal

pulse in-line measurements, usually detecting dozens of flow locations in a drillhole with transmissivities ranging from 10^{-9} to 10^{-5} m²/s, whereas spinner could typically indicate 3 to 5 flow locations with higher than 10^{-6} m²/s transmissivity (Figure 1). The low background transmissivities are necessary in determining the hydraulic conductivity of the rock mass.

Compared with packer measurements, the measurable transmissivity range is similar, but PFL is quicker to implement, does not require a drill rig nor the expansion and deflation of packers, and yields a much denser set of observations along a drillhole in a shorter measurement time. Moreover, there is no need to decide beforehand which sections of the drillhole to test. The radius of influence in PFL is larger than in a packer survey due to typically longer pumping time, which leads to a lower interpreted transmissivity for a given fracture (Aalto *et al.* 2019).

Results

Interval transmissivity was calculated from the measurement data at a dense spacing along each drillhole. Each value represents a single hydraulically conductive fracture or a set of closely located fractures. Figure 2 presents the acquired results in the Ahmavaara pit location as disks along the studied drillholes, coloured according to the transmissivity value. Fractures with the largest hydraulic transmissivities are more abundant in the upper part of the bedrock to the depth of about 100–150 m.

Using the hydrogeological data as an input to numerical modelling required generalization of the results (Komulainen *et al.* 2018). The obtained transmissivities were examined with respect to their spatial distribution, lithology, depth, and coincidence with interpreted interceptions of faults and their zones of influence, as well as to fracturing indicators in drill core data (RQD, fracture frequency, breccia, faults, and core loss). For each drillhole interval in a

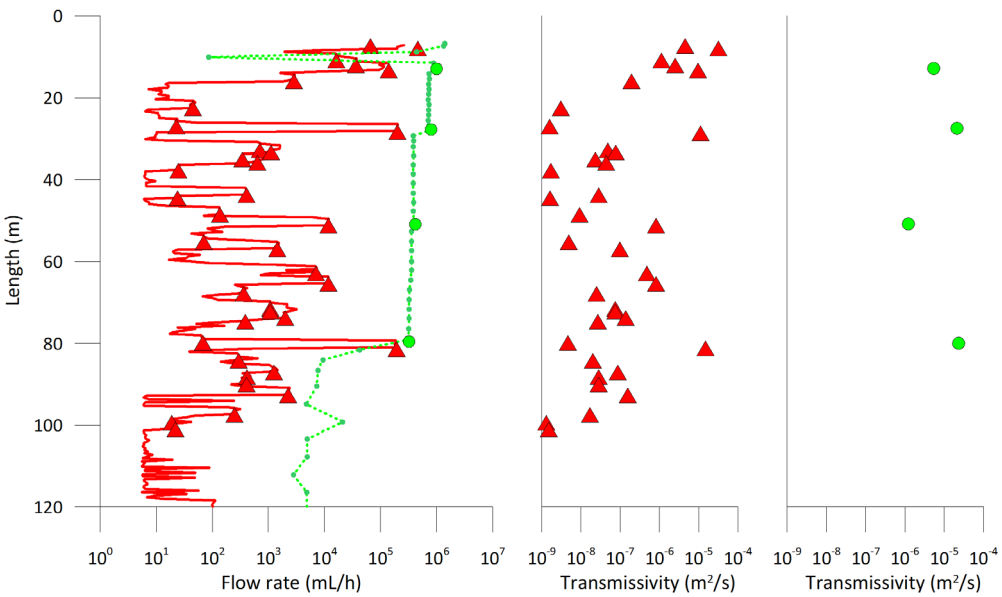

Figure 1 *Measurement data at the upper 120 m part of drillhole AHM-41 in Ahmavaara. Measurement continues to 267 m. In the graph on the left, the red line presents PFL flow data at 0.4 m intervals, red triangles the measured fracture flows (stepwise change in the flow data), the green line flow along the drillhole at 0.5 m to 5 m steps (spinner-type), and the green circles the detected fracture flows. The graph in the middle presents the transmissivities interpreted from the PFL data, and the graph on the right transmissivities interpreted from the flow along the hole. Both measurements were made with the PFL tool, on different runs and settings.*

certain geology, transmissivities were summed and divided by length. The obtained hydraulic conductivity was plotted versus the elevation of the interval centre (Figure 3). Practically impermeable intervals occurred also, shown using a hydraulic conductivity value of 10–11 m/s in the graph. Variability is high, and rock mass heterogeneous. There is no reliable indication of hydraulic conductivity difference between lithological domains. Hanging wall

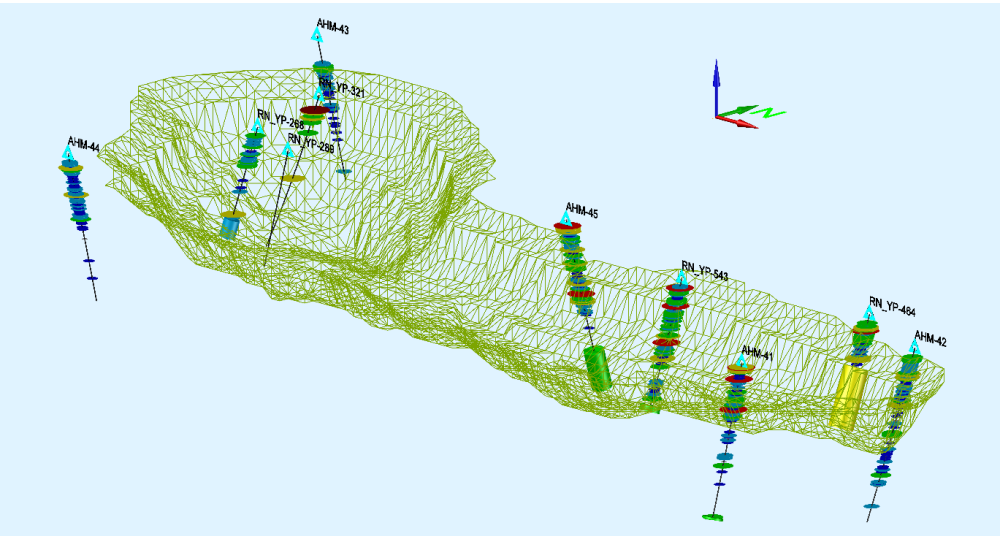

Figure 2 Measurement data from Ahmavaara shown in 3D view, with the planned open pit shell, and results along drillholes. Size and colour of each disk depends on transmissivity (larger and red for greater values, small and blue for lower).

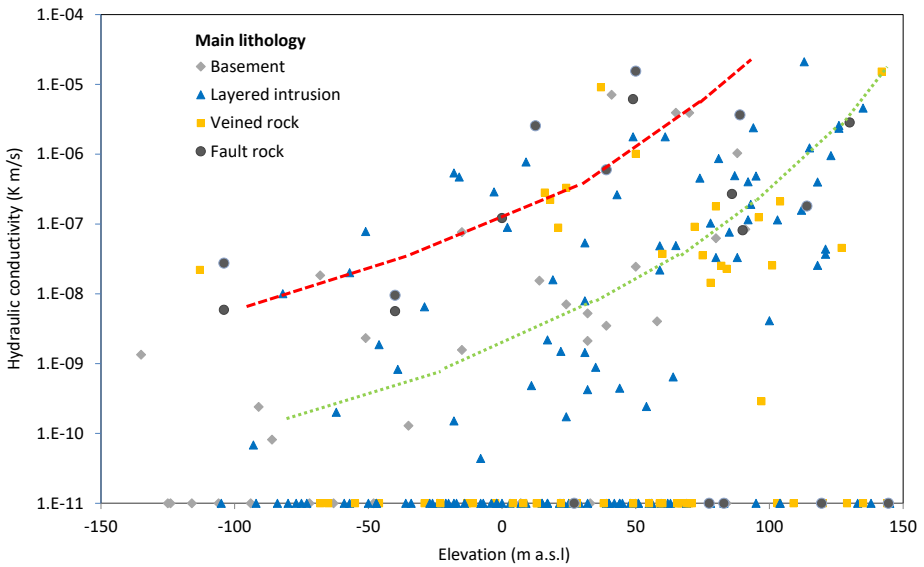

Figure 3 Hydraulic conductivity versus elevation in Ahmavaara according to main lithological and fault interception intervals. Depth trends are sketched by the broken lines. Lower background conductivity (green) applies to average rock, and the scattered elevated values (red) about one order of magnitude higher to faults and fracturing intervals, which occupy a small fraction of total rock volume.

is closer to surface, and it may indicate higher conductivity than the marginal series, which consisted of less fractured rock mass.

For modelling, transmissivities were converted to hydraulic conductivities of 10-metre elevation intervals, including also the contribution of fault interceptions. A distinct depth trend of lowering hydraulic conductivity was observed (Figure 4). There is a difference between the hydraulic conductivity depth distribution between Ahmavaara and Konttijärvi open pit locations.

Data from Konttijärvi shows a lower hydraulic conductivity in comparison with Ahmavaara. Lateral hydraulic conductivity differences between drillholes within the pit areas were negligible. The hydraulic conductivity was generalized to a depth trend, separately for each pit. Fault conductivities are heterogeneous in drillhole interceptions, typically one order of magnitude greater than for average rock and indicating depth dependence. According to the results, both pit locations represent typical Finnish bedrock.

Groundwater modelling

Separate groundwater flow models of the two open pits were made with FEFLOW. Ground topography was obtained from National Land Survey of Finland databases. Figure 5 presents the modelling approach for the pit models on a conceptual level. In general, the overburden in the area consists of two layers, glacial till directly on top of the bedrock and above that, a peat layer. According to weight sounding and GPR, the average peat layer is 1 m, and up to 6–7 m thick in the lower mire areas and almost absent on the surrounding hills. Bedrock topography was obtained from drilling close to the planned pits and supplemented with geophysical data. The till cover is typically 0–30 metres thick. Bedrock outcrops are scarce. Hydraulic conductivity of the peat layer is based on composition studies in laboratory and corresponding values from literature. Hydraulic conductivity of the till layer was obtained from slug tests in observation wells.

In the bedrock, the hanging wall volumes of the intrusion were modelled separately from the rest of the rock volume because of the conductivity differences indicated by the measurements. In all the bedrock, conductivity was assumed to decrease with depth. Vertical or dipping fault zones were included as discrete planar features with additional hydraulic conductivity. Their locations and extensions were interpreted from existing geological and geophysical information. As various waste rock dumps, temporary storage piles, water basins, and tailings areas are planned to be constructed

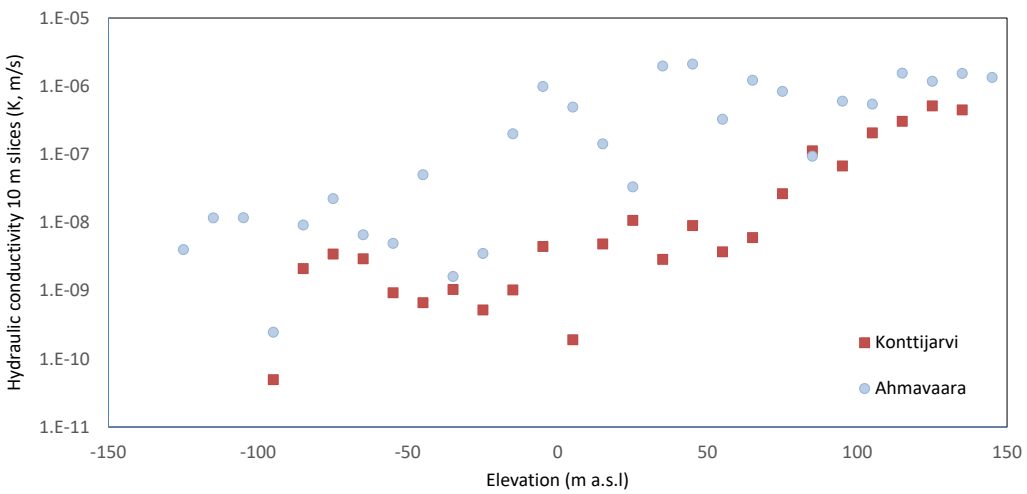

Figure 4 *Measured transmissivities converted to hydraulic conductivity in 10-metre elevation intervals, plotted separately for the two studied pit locations. Konttijärvi appears less permeable.*

close to the pits, they were included in the models. On the surface, natural rivers and brooks as well as artificial ditches were modelled using boundary conditions allowing the removal of groundwater from the model if hydraulic head of groundwater is higher that the assumed level of the body of surface water. Groundwater recharge on the top surface, or infiltration, adds groundwater to the budget of the model. On the sides of the modelled volume, a constant-head boundary condition was set, based on the assumption that the drawdown effect from the open pit will not extend to the model boundary, but head will remain at the value obtained from a regional MODFLOW model compiled earlier.

Figure 6 shows a three-dimensional view of the model geometry for the Ahmavaara open pit in its largest modelled extent. The highest surface elevations, presented in red, are waste rock dumps around the pit. A sector has been cut away from the modelled volume for better visibility of the open pit in the middle.

Modelling results

The main result of the groundwater modelling was the inflow of groundwater into the planned open pit mines. Figure 7 presents a

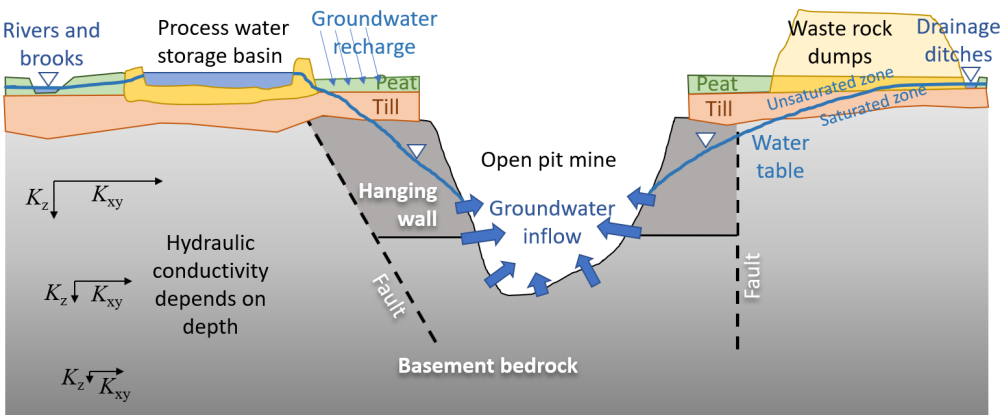

Figure 5 The conceptualization of the modelled open pit mines.

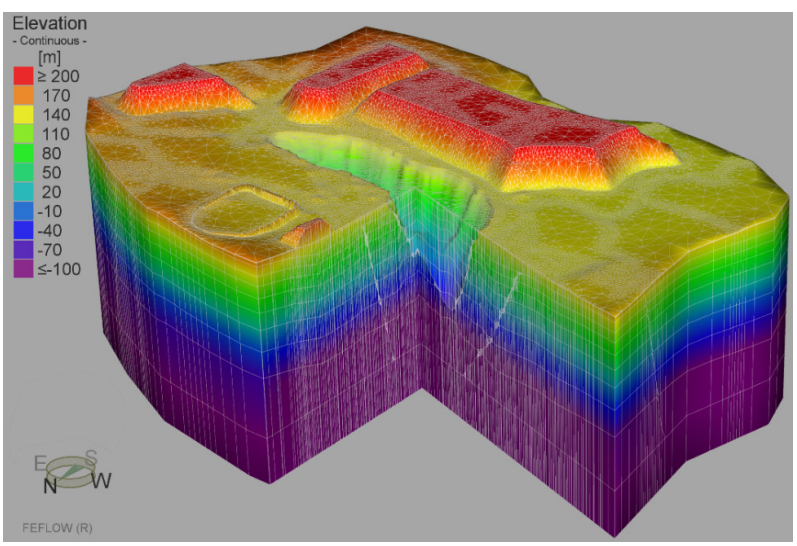

***Figure 6** 3D view of the model of the Ahmavaara open pit in the final mining phase. A sector in the foreground has been cut away to show a cross section of the pit. Vertical dimension exaggerated 3-fold.*

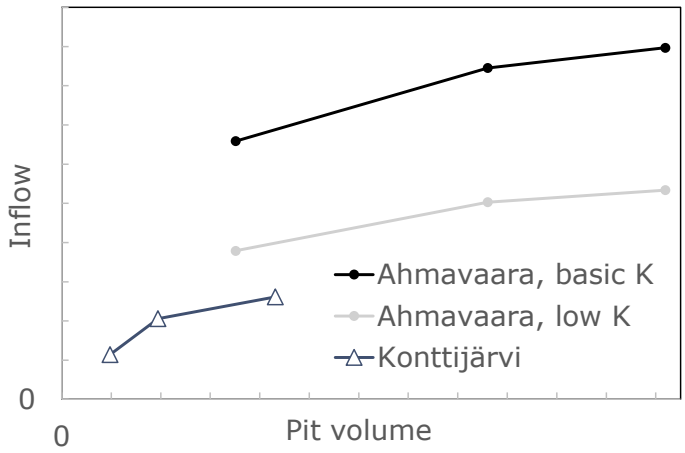

Figure 7 *Relative comparison of calculated groundwater inflow in three mining phases of the planned open pit mines, presented as a function of the volume.*

plot of the relative difference of the calculated inflows as a function of excavated pit volume. For the larger Ahmavaara pit, there are two curves, one for the basic assumption on the hydraulic conductivity of bedrock and the other for low conductivity (one-third of the basic values) calculated for sensitivity analysis. The comparison clearly shows the consequence of the observed difference in the hydraulic conductivities of bedrock in the two pit sites: even with the lower conductivity assumption for Ahmavaara, a larger inflow can be expected for about the same pit size. Especially in the case of the Ahmavaara pit, the increase of inflow as a function of pit volume is rather gentle. This results from the decrease of hydraulic conductivity of bedrock with depth.

Besides the inflow into the pits, the groundwater models yielded estimates of the drawdown of water table and hydraulic head. According to the results, the effect of the pits on the water table will be tolerable, extending mainly to areas around them that will also be altered by surface construction and other activities related to the mining. The models are expected to be useful in future modelling tasks, e.g., for the assessment of environmental effects after mine closure.

Conclusions

Hydrogeological measurements in the field with the PFL method, and generalization of the results for the numerical groundwater flow modelling proved to be a fruitful approach for the task of estimating the groundwater effects of planned open pit mining. The spatial and depth coverage of the measurements was sufficient to obtain the necessary hydraulic conductivity input for the numerical model. A decreasing trend of hydraulic conductivity as a function of depth was confirmed and found to differ in the two studied pit locations, and an increased conductivity related to the known faults was indicated.

The reported investigation was part of preliminary and detailed feasibility studies for the mine project, but it is likely that the obtained conductivity data and the compiled models are also useful in the future for e.g., the assessment of post-closure environmental impact.

Acknowledgements

The authors thank Suhanko Arctic Platinum for permission to use their material in this presentation.

References

Aalto P, Ahokas H, Hurmerinta E, Komulainen J, Pentti E, Tammisto E, Vaittinen T (2019) Quality Assessment of Transmissivity Data Acquired Over Time in Surface Drillholes at the Olkiluoto Site. Posiva Working Report 2018-29. Eurajoki, Finland: Posiva Oy. 434 p.

Komulainen J (2017) Posiva Flow Log (PFL), tool for detection of groundwater flows in bedrock. In: Wolkersdorfer C, Sartz L, Sillanpää M, Häkkinen A: Mine Water & Circular Economy (Vol I) p 556– 563; Lappeenranta, Finland (Lappeenranta University of Technology).

Komulainen J, Vaittinen T, Picken P, Heikkinen E (2018) Hydrogeological Bedrock Characterisation Based on Posiva Flow Log Measurement Data. In: Wolkersdorfer C, Sartz L, Weber A, Burgess J, Tremblay G. 11th ICARD/IMWA/MWD. IMWA 2018 Annual Conference. Risk to opportunity. Vol 1 & 2. Pretoria, South Africa, September 10–14. p 654–659.

Picken P, Karvonen T, Heikkinen E, Vaittinen T, Seppä V-M, Saukkoriipi J (2017) Kittilä Gold Mine dewatering assessment: benefits of a new approach. In: Wolkersdorfer C, Sartz L, Sillanpää M, Häkkinen A: Mine Water & Circular Economy (Vol I). p 540–547; Lappeenranta, Finland (Lappeenranta University of Technology).

A Strategy to Simulate Indigenous Bacterial Communities to Effectively Remediate Mine Drainages

Gerhard Potgieter[1], Errol Cason[2], Mary DeFlaun[3], Esta van Heerden[4]

[1]*iWater (Pty Ltd), 5 Walter Sisulu, Park West, Bloemfontein, South Africa, tech3@iwatersolutions.co.za; Department of Microbiology, Stellenbosch University, Stellenbosch, South Africa*

[2]*Department of Animal Science, University of the Free State, Park West, Bloemfontein, South Africa, CasonED@ufs.ac.za*

[3]*Geosyntec Consultants, 1750 American Blvd Suite 200, Pennington, New Jersey, USA, MDeFlaun@Geosyntec.com*

[4]*iWater (Pty Ltd), Centre for Water Sciences Management, 5 Walter Sisulu, Park West, Bloemfontein, South Africa, esta@iwatersolutions.co.za*

Abstract

Drainages from mining operations frequently contain elevated levels of contaminants of concern (CoC) . Indigenous adapted bacterial communities are characterized and their ability to reduce many CoC are showcased. Each contaminated site consists of a distinct prokaryotic community that in turn requires a specific C:N:P balanced environments to contribute to site remediation. This balanced bioremedial strategy is managed both for in situ or fix-filmed bioreactors, using electron donor selection and ratios, redox potential, and hydraulic retention times. These communities can effectively treat elevated levels of hexavalent chromium (10 mg/L), nitrate (110 mg/L), and sulfate (1 250 mg/L) in a one-pot balanced system.

Keywords: Bacterial Diversity, C:N:P Stoichiometric Balance, In Situ Treatment, Fixed-Film Bioreactors, Redox Ladder

Introduction

Mining operations in South Africa demand a high volume of water usage during operations and tailing deposits. These water volumes often leach or drain causing the mobilisation of elevated contaminants of concern (CoC), including dissolved metals, metalloids, nitrate, and sulfate compounds. In most mine drainages, these CoC are primarily in reducing chemical forms and act as essential oxidants for organic carbon and other reducing chemicals (Fowler *et al.* 2013), where oxidation states are more toxic to the environment and human end receptors.

In recent years in South Africa, concerns have developed around poor managing practices in disposing of CoC. A mirid of treatment options is deployed that include filtration, absorption, and chemical reduction. Each treatment has specific benefits, but often capital and operating costs are high, and many could produce additional, often still hazardous, by-products. Biological reduction of CoC using indigenous bacteria can be an environmentally sound alternative technology that lowers operational costs with less or no hazardous by-products. Bacteria metabolic reactions often use CoC as a terminal electron acceptor, ultimately precipitating compounds as insoluble hydroxides or metal-sulfides (Cason *et al.* 2017; Peng and Zhu 2006).

A better understanding of the biochemical cycles of contaminates, including carbon utilisation, can identify cooperative metabolic functioning within bacterial communities. This metabolic functioning and bacterial community compositions can hold the key to developing more sustainable and advanced biological treatment systems. Using the knowledge and characterization of strategic management practices, each specific environments' indigenous microbes can become powerful bioremediation tools (Lau *et al.* 2016).

This paper deals with the management and stimulation of high metabolic rates of biomes by creating C:N:P stoichiometrically balanced environments, while dominance within species can naturally attenuate in these circumstances. This is demonstrated both, in situ and in fixed-film bioreactors, to treat contaminated mine drainages on-sites. These remedial strategies can remove several contaminants, including hexavalent chromium (Cr_{6+}), nitrate, and sulfate while improving the overall water quality. Using targeted metagenomics, the microbial community and unique biogeochemical cycles are characterised to balance the C, N and P cycles to environmental geochemical conditions.

Methods

Water quality analysis and site selection

Two sites with different concentrations of the selected CoC were sampled. Analyses were conducted at accredited laboratories, using anion analysers, ICP-MS/OES, and auto-titration methods, including benchtop physicochemical analysis. The study source sites are in the KwaZulu Natal (Site A) and North West (Site B) provinces of South Africa. Site A is a chromium process facility that mainly operates leather tanning, while Site B is a chromium smelter that actively mines and processes chrome ore. Activities on both sites resulted in ground and surface water contamination with Cr_{6+} and nitrate.

Microbial diversity and metabolic capabilities

Extracted and purified DNA (Lau *et al*. 2014) was analysed using 16S targeted metagenomic sequencing on an Illumina MiSeq system. Sequence reads were analysed using QIIME 2 (https://qiime2.org) (Bolyen *et al*. 2018). Taxonomy was assigned to amplicon sequence variants (ASVs) against the SILVA 132 99% OTUs reference sequences (SILVA) (Quast *et al*. 2013; Yilmaz *et al*. 2014). The functional potential was predicted using FAPROTAX.

Microcosm studies

Using the data from section 2.1 the N (Potassium Nitrate) and P (Di-Potassium Hydro-orthophosphate) supplementation were balanced. The optimal assimilation and utilisation of electron donors, simple - and complex carbon sources, were assessed for the indigenous bacterial communities. These rates and geochemical data sets are used to calculate the specific C:N:P ratio, while balancing metabolic function to sustain a chosen redox condition for treatment by calculated molar ratios (Appendix – Table 1 & 2). For excess and balanced ratios, the stoichiometrically balanced mixtures were inoculated into site water samples and incubated in 250 mL Scott bottles, at 25 °C, for five days and 20 days. The depletion in dissolved oxygen (DO) concentrations were measured for each incubation period. Refinement of concentration was done with continuous flow measuring reduction of CoC while optimising donor versus acceptor rations.

In situ design

The treatment system for site A was implemented directly at the site of the contaminant (*in situ*) (Appendix – Figure 1). Injection – and extraction boreholes, which is 100 meters apart, were used as the treatment site. Initially, crucial information of the heterogeneous matrix between the selected boreholes was studied for the treatment implementation design and selection. An EC profile of the injection borehole was created to determine the primary fracture depth. At this depth, a stoichiometrically balanced electron donor (Emulsified vegetable Oil – EVO) mixed with groundwater, was injected. This amended groundwater made a final solution containing 2% by volume. A subsurface groundwater pull was created, by withdrawing groundwater from the bottom extraction boreholes, to control the treatment hydraulic retention time (HRT).

iWater treatability plant

A pump-and-treat semi-active strategy was implemented at site B (Appendix – Figure 2). iWaters' proprietary treatability plant design consists of modular fix-filmed bioreactors (5 000 L, each) and treats 80 000 L per day. Inlet site water was continuously dosed with a balanced electron donor (sodium acetate) mixture. All operations, in terms of electron donor dosing concentrations,

redox conditions, and HRT were controlled remotely with a Program Logic Controller (PLC). The PLC also allowed for individual parameters (e.g., EC, flow rate and quantity, pH, and ORP) monitoring and recording. Once reducing conditions were established within the bioreactors, the electron donor was incrementally lowered until the minimum donor requirement was determined empirically. The final treatment stage involved removing any residual organic carbon through various filtration methods (activated carbon) and sterilisation techniques (chlorination).

Results and Discussions

Site selections

It is crucial to understand each contaminated site geochemistry data to design an effective tailored bioremedial strategy (Williams *et al.* 2014). The treatment focuses on creating an optimal environment for the indigenous bacteria to select and stimulate selected community members to reduce site pollutants. Due to the repeated processes of soaking raw hides and wringing them out during the leather tanning process, large amounts of wastewater is created. If this wastewater is not properly managed is often leads to surface and groundwater contamination. Site A contained fluctuating contamination levels of Cr_{6+} and nitrate of around 10 mg/L, and 35 mg/L, respectively. Site B contained similar concentrations of Cr_{6+} (8 mg/L) levels, but with additionally elevated concentrations of nitrate (110 mg/L) and sulfate (1 250 mg/L). The solid products obtained from the smelting of ferrochrome are metal, slag, and dust. This slag by-product is often disposed of as tailings storage facilities (TSF). Slag is regarded as harmless, as the chromium is predominantly present as trivalent chromium (Cr_{3+}). However, there exists a great deal of controversy regarding the possibility of oxidation of Cr_{3+} to Cr_{6+}. Thus, if the TSF is not properly manage or lined it often result in Cr_{6+} leachate into the surface and underground water. In addition, a great environmental risk also lies in the sludge from the gas cleaning system. This is particularly the case for open-top furnaces where chromium is readily oxidised to Cr_{6+} in the off-gas dust. The remaining parameters, of both sites, does not raise any concerns (Appendix – Table 5 & 6).

Microcosm studies

It is essential to understand the indigenous bacterial community's optimum electron donor type and concentration demand using a microcosm study (Lau *et al.* 2016). To determine this balance one can ensure that enough free energy is available for the desirable reductive metabolisms to functions. Site A's indigenous bacterial community is more selective towards a complex long-chain carbon source, with minimum phosphate supplementation required, while site B's community prefers a simple carbon source, also with minimum phosphate supplementation (Appendix – Table 3 & 4). Both indigenous bacterial consortia require similar electron donor concentrations to reduce Cr6+ and nitrate. Site B's consortia interestingly can also reach sulfate reduction if the donor concentration is increased, as it can improve this site's water treatment.

On-site treatment and bacterial composition

Treatment strategies of both sites were implemented as described in sections 2.4 and 2.5. Before and during the treatments, the

Table 1 *Geochemical dataset of inorganic parameters during in situ treatment on site A.*

Elemental concentration of heavy metals (μgL^{-1})					
Determinants	Units	Initial	Injection borehole	Extraction borehole	Extraction borehole
Total alkalinity as $CaCO_3$	mg/L	254	472	198	452
pH		7.04	7.66	8.29	7.05
ORP	mV	+148	-10	-68	-15
Chromium as Cr_{6+}	mg/L	9.87	< 0.02	1.23	< 0.02
Nitrate as N	mg/L	35	< 0.35	< 0.35	< 0.35
Sulfate as SO_4^{2-}	mg/L	120	129	133	38.7

change in bacterial diversity was analyzed and their metabolic functionality could be correlated to the water chemistry changes. At site A, the optimum redox conditions for nitrate, and consequently Cr_{6+}, reduction was reached after 30 days of treatment implementation. Due to the created stoichiometrically balanced environment, the indigenous bacteria were able to reduce both Cr_{6+} and nitrate by 99.9% even after one year of treatment (table 1). By using the groundwater pull-push method, the electron donor was effectively migrated through the entire treatment site. In the initial phase of treatment, the extraction borehole showed delayed Cr_{6+} reduction due to the slower migration of electron donor, illustrate the importance of an engendered balance environment. A major advantage of bacterial metabolic activity is the creation of water alkalinity, in the form of calcium carbonate ($CaCO_3$), that improves the overall buffering capability of a water source.

Before and after one year, the bacterial composition, up to the genus level, was evaluated between the different boreholes. All boreholes were initially dominated by Acinetobacter (39%), Rhodobacter (11%), Prosthecobacter (8%), Acidovorax (8%) and other minor representative groups (MRC) (fig. 1). Figure 1 shows shifts in bacterial communities throughout the treatment site over the course of a one-year treatment. The treatment site is now mainly dominated by (i) Legionella (25% – Pathogenic), Pseudarthrobacter (16%) and (ii) Novosphingobium (56% – aromatic compound degradation) between the injection, and extraction boreholes, respectively. What is of note is that both the injection and extraction boreholes had a dramatic increase in minor representative groups (54% and 30%, respectively). The data also shows that none of the genera co-exists between the different boreholes, suggesting no flow-through of the dominant bacteria through the site, however, Cr_{6+} and nitrate reduction is still evident in all the boreholes.

Interestingly, even though the communities of the separate boreholes are different after treatment, the functional annotation is more closely related, compared to the initial functionality of the communities. Nevertheless, after one year of treatment, the nitrate reduction metabolism functionality seems to be present in all the boreholes (>5%).

At site B, optimum operations and CoC reduction were reached at an HRT of 8 h at 80 000 L per day treated. Using sodium acetate continued dosing, effective Cr_{6+} and nitrate reduction were achieved, with a 99%

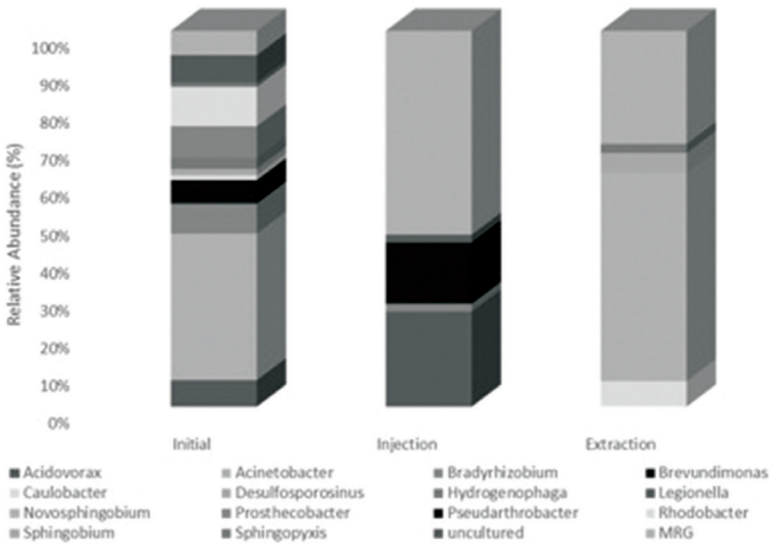

Figure 1 *Taxonomic information (genus level) based on 16S rRNA gene sequences of the indigenous bacteria during Site A's treatment.*

Table 2 Geochemical dataset of inorganic parameters during a pump-and-treat plant treatment on site B. The data represents the final parameters after one year of treatment.

			Nitrate reduction strategy	Sulfate reduction strategy
Determinants	Units	Plant inlet	Final sample	Final sample
Total alkalinity as $CaCO_3$	mg/L	229	692	1425
pH		7.85	7.95	7.36
ORP	mV	+87	-73	-325
Chromium as Cr_{6+}	mg/L	8.19	0.42	< 0.02
Nitrate as N	mg/L	110	0.61	< 0.35
Sulfate as SO_4^{2-}	mg/L	1244	1013	66

reduction of both parameters. The water quality dataset (table 2) represents the final analysis perform one year after treatment implementation. Note that only specific redox metabolism is active at this balanced electron donor mixture, for example, nitrate respiration and denitrification.

In contrast, electron acceptors like sulfate are not metabolised. As an additional, to showcase the treatment strategy capability, the HRT tempo was lowered, and the electron donor ratio changed to achieve a 95% sulfate reduction from 1 244 mg/L (table 2). During this treatment strategy, the overall balance of the water chemistry was improved where alkalinity was increased, and parameters such as total hardness, iron, potassium, and zinc were decreased.

Bacterial compositions of the treatment plant inlet water (In) and within the reactors (Out) was studied at a genus level. The inlet dominance of Pseudomonas (53%), Exiguobacteria (15%), Rhizobium (8%), Stenotrophomona (6%) change to Pseudomonas (65%), Stenotrophomona (3%), Exiguobacteria (2%), and interesting minor representative groups (13%), within the bioreactors (Fig. 2). It is interesting to note that even though Site A and B's indigenous communities are similar, at the phylum level, it demands different electron donor composition. This indicates the importance of the microcosm study to define treatment strategies for each site.

The functional annotation analysis shows that the inlet water's bacterial community

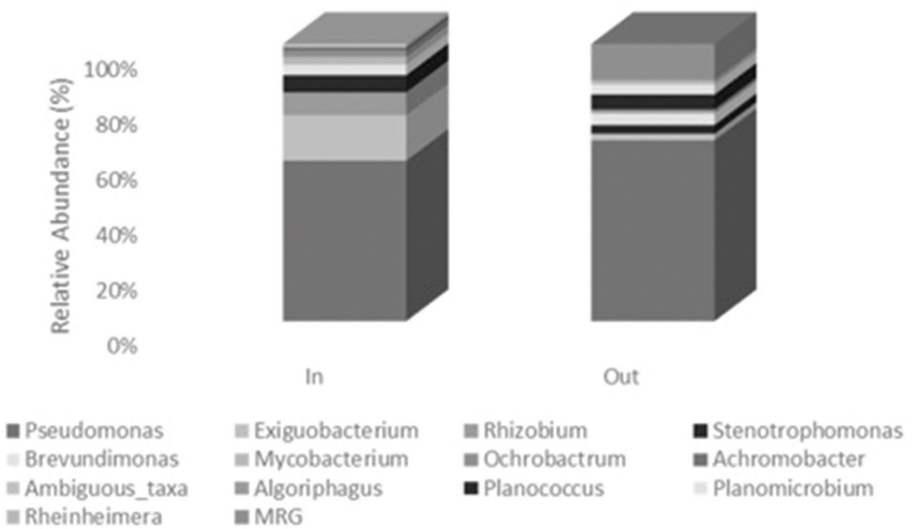

Figure 2 Taxonomic information (genus level) based on 16S rRNA gene sequences of the indigenous bacteria during Site B's treatment.

and those within the bioreactor are specialised for nitrate metabolic potentials (Appendix – Figure 3). The fact that this functional annotation is accelerated within the bioreactors illustrate the importance of a balanced energy flux and that natural attenuation will struggle without supplementation.

At Site A, there appears to be a flow-through of the minor representative groups, causing a specialised functionality towards nitrate, and consequently Cr_{6+}, reduction towards boreholes further away from the injection site. Whereas for site B, the data shows that minor representative groups are only present in the bioreactors. It is essential to mention that several studies confirmed that less dominant bacterial groups support the major communities (Hemme *et al*. 2010; Hugenholtz *et al*. 1998; Tanner *et al*. 1998; Wang *et al*. 2013) and that they are essential for successful reduction of CoC. This means the minor representative groups, present at both sites A and B, should not be eliminated from the indigenous community composition and should be carefully managed.

Conclusions

Anthropogenic activities on both sites have led to groundwater contamination with COC, mainly Cr_{6+}, nitrate, and sulfate. The data sets generated in this paper shows that even if bacterial community compositions are similar, indigenous bacteria from separates environments have different metabolic capabilities and electron donor requirements. This illustrates the importance of understanding the geochemical data and correlating it to the C:N:P ratios of the environment. Through creating a stoichiometrically balanced environment, that is correlated to the free energy flux requirements of the indigenous bacterial communities, dominant bacterial species was allowed to naturally attenuate. Interesting minor representative groups showed an important functionality to unsure that these dominant communities can successfully reduce CoC. This paper illustrates that adapted bacteria acclimate to every change in chemical composition. Thus, it is essential to identify all the informational gaps of each site to tailor the remediation strategy since no aspect from geochemistry, bacterial composition, and their metabolic capacities stand alone. All the generated knowledge will optimise bioremediation strategies to extend to treatment implementation beyond the CoC levels illustrated in this paper.

Acknowledgement

The authors thank all co-organisers for hosting the IMWA2021 Conference. Rita Botha for assisting in the geochemistry analysis and Mosidi Mojaki for assisting in the initial data generation of both sites.

Reference

Bolyen E, Rideout JR, Dillon, MR, Bokulich NA, Abnet C, Al-Ghalith GA, Alexander H, Alm EJ, Arumugam M, Asnicar F and Bai Y (2018) QIIME 2: Reproducible, interactive, scalable, and extensible microbiome data science. PeerJ Preprints (No. e27295v1).

Cason ED, Williams PJ, Ojo E, Castillo J, DeFlaun MF and van Heerden E (2017). Hexavalent chromium bioreduction and chemical precipitation of sulphate as a treatment of site-specific fly ash leachates. World Journal of Microbiology and Biotechnology, 33(5), p.88.

Fowler D, Coyle M, Skiba U, Sutton MA, Cape JN, Reis S, Sheppard LJ, Jenkins A, Grizzetti B, Galloway JN, Vitousek P (2013) The global nitrogen cycle in the twenty-first century. Philosophical Transactions of the Royal Society B: Biological Sciences, 368(1621), p.20130164.

Hemme CL, Tu Q, Shi Z, Qin Y, Gao W, Deng Y, Nostrand JDV, Wu L, He Z, Chain PS and Tringe SG (2015) Comparative metagenomics reveals impact of contaminants on groundwater microbiomes. Frontiers in microbiology, 6, p.1205.

Hugenholtz P, Goebel BM and Pace NR (1998) Impact of culture-independent studies on the emerging phylogenetic view of bacterial diversity. Journal of bacteriology, 180(18), pp.4765-4774.

Lau MC, Cameron C, Magnabosco C, Brown CT, Schilkey F, Grim S, Hendrickson S, Pullin M, Sherwood Lollar B, van Heerden E and Kieft TL (2014) Phylogeny and phylogeography of functional genes shared among seven terrestrial subsurface metagenomes reveal N-cycling and microbial evolutionary relationships. Frontiers in microbiology,5, p.531.

Lau MC, Kieft TL, Kuloyo O, Linage-Alvarez B, Van Heerden E, Lindsay MR, Magnabosco C, Wang W, Wiggins JB, Guo L and Perlman DH (2016) An oligotrophic deep-subsurface community dependent on syntrophy is dominated by sulfur-driven autotrophic denitrifiers. Proceedings of the National Academy of Sciences, 113(49), E7927-E7936.

Peng Y and Zhu G (2006) Biological nitrogen removal with nitrification and denitrification via nitrite pathway. Applied microbiology and biotechnology, 73(1), pp.15-26.

Quast C, Pruesse E, Yilmaz P, Gerken J, Schweer T, Yarza P and Peplies J (2013) The SILVA ribosomal RNA gene database project: Improved data processing and web-based tools". Nucleic Acids Research, 41, D590–596.

Tanner CC, Sukias JP and Upsdell MP (1998) Organic matter accumulation during maturation of gravel-bed constructed wetlands treating farm dairy wastewaters. Water Research, 32(10), pp.3046-3054.

Appendixes

Table 1 *Calculated molar ratios of stoichiometric electron donor demand for redox reactions of anaerobic metabolic electron acceptors, using acetate.*

Electron acceptor	Balanced reaction	Molar ratio
Oxygen	$CH_3COOH + 2O_2 \rightarrow 2CO_2 + 2H_2O$	½
Nitrate	$5CH_3COOH + 8NO_3^- + 8H^+ \rightarrow 10CO_2 + 4N_2 + 14H_2O$	5/8
Chromate	$3CH_3COOH + 8CrO_4^{2-} + 40H^+ \rightarrow 6CO_2 + 8Cr^{3+} + 26H_2O$	3/8
Sulfate	$CH_3COOH + SO_4^{2-} + 2H^+ \rightarrow 2CO_2 + H_2S + 2H_2O$	1/1

Table 2 *Calculated molar ratios of stoichiometric electron donor demand for redox reactions of anaerobic metabolic electron acceptors, using emulsified vegetable oil – EVO.*

Electron acceptor	Balanced reaction	Molar ratio
Oxygen	$C_{57}H_{98}O_{12} + 75.5O_2 \rightarrow 57CO_2 + 49H_2O$	1/77
Nitrate	$C_{57}H_{98}O_{12} + 50.34NO_3^- \rightarrow 57CO_2 + 25.17N_2 + 49H_2O$	1/50
Chromate	$3C_{57}H_{98}O_{12} + 25.75SO42- \rightarrow 57CO_2 + 25.75H_2S + H_2O + 44.5H$	3/77
Sulfate	$C_{57}H_{98}O_{12} + 37.75CrO42- \rightarrow 57CO_2 + 37.75Cr^{3+}\ 49H_2O$	2/77

Table 3 *Microcosm study results of site A's indigenous bacteria oxygen demand from different electron donors.*

Electron donor	DO_0 (mg/L)	DO_5 (mg/L)	DO_{20} (mg/L)	Oxygen demand value
Control	3.40	3.34	-	0
Sodium acetate	3.37	0.99	-	0.48
Sodium acetate + Phosphate	3.48	3.23	-	0.19
EVO	3.48	-	0.08	0.75
EVO + Phosphate	3.45	-	0.23	0.68

Table 4 *Microcosm study results of site B's indigenous bacteria oxygen demand from different electron donors.*

Electron donor	DO_0 (mg/L)	DO_5 (mg/L)	Oxygen demand value
Control	5.12	5.08	0
Sodium acetate	5.22	3.28	0.39
Sodium acetate + Phosphate	5.19	3.35	0.29
Glucose	5.17	4.14	0.17
Glycerol	5.17	4.68	0.08

Table 5 Geochemical dataset of inorganic parameters during in situ treatment on site A.

			30 days after injection		1 year after injection
Determinants	Units	Initial	Injection borehole	Extraction borehole	Extraction borehole
Total alkalinity as $CaCO_3$	mg/L	254	472	198	452
Total dissolved solids	mg/L	595	624	366	600
Total hardness	mg $CaCO_3$/L	171	286	114	314
pH		7.04	7.66	8.29	7.05
ORP	mV	+148	-10	-68	-15
Chromium as Cr^{6+}	mg/L	9.87	< 0.02	1.23	< 0.02
Nitrate as N	mg/L	35	< 0.35	< 0.35	< 0.35
Otrhophosphate	mg/L	4.0	< 0.03	< 0.03	< 0.03
Sulfate as SO_4^{2-}	mg/L	120	129	133	38.7

***Table 6** Hydrochemical dataset of inorganic parameters during a pump-and-treat plant treatment on site B. The data represents the final parameters after one year of treatment.*

			Nitrate reduction strategy	Sulfate reduction strategy
Determinants	Units	Plant inlet	Final sample	Final sample
Total alkalinity as $CaCO_3$	mg/L	229	692	1425
pH		7.85	7.95	7.36
Total dissolved solids	mg/L	3406	2798	3486
Total hardness	mg/L	1690	1480	257
ORP	mV	+87	-73	-325
Chromium as Cr^{6+}	mg/L	8.19	0.42	< 0.02
Nitrate as N	mg/L	110	0.61	< 0.35
Otrhophosphate	mg/L	0.61	5.92	2.26
Sulfate as SO_4^{2-}	mg/L	1244	1013	66
Iron – total	mg/L	2.40	< 0.01	< 0.01
Potassium	mg/L	23	3.91	4.3
Zinc	mg/L	4.12	0.2	< 0.01

Figure 1 *In situ treatment implemented at site A, located in the KwaZulu Natal province of South Africa.*

Figure 2 *Semi-active pump and treat plant implemented at site B, located in the North West province of South Africa.*

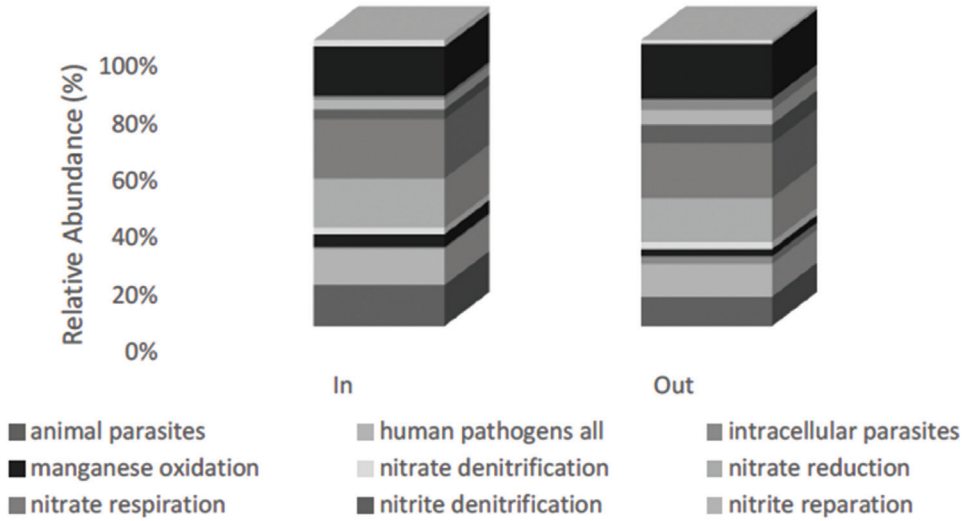

Figure 3 *Functionality assignments of the indigenous bacteria during Site B's treatment.*

Modelling the Geochemical Behaviour of Desulfurized Tailings as a Moisture-Retaining Layer in Insulation Covers with Capillary Barrier Effects using MIN3P-THCm

Asif Qureshi, Bruno Bussière

Institut de Recherche en Mines et en Environnement, Université du Québec en Abitibi-Témiscamingue, Rouyn-Noranda, Québec, Canada, Asif.Qureshi@uqat.ca, Bruno.Bussiere@uqat.ca

Abstract

A column laboratory experiment was performed to assess the hydrogeological, thermal, and geochemical behaviour of an insulation cover with capillary barrier effects (ICCBE) made of desulfurized tailings as the moisture-retaining layer and non-acid generating crushed rocks as the protective and the capillary break layer. The ICCBE was represented in a numerical model developed using MIN3P-THCm. The model simulated the thermal-hydrogeological-geochemical behaviour of the tested ICCBE. The laboratory tests and short-term modelling showed that the tested desulfurized tailings do not generate contaminants at a concentration higher than the regulatory limits and that they can be used as cover material in a typical arctic climate. The preliminary long-term modelling results also suggest that the column will not generate acidity and maintain a leachate quality below the regulatory limits.

Keywords: Insulation Cover With Capillary Barrier Effect (Iccbe), Desulfurized Tailings, Acid Mine Drainage, Freeze And Thaw Cycles, Reactive Transport Modelling

Introduction

Mining wastes produced during mining operations are sometimes sensitive to surface atmospheric conditions and prone to producing contaminant laden leachates that are classified according to their quality and nature as acid mine (or rock) drainage (AMD or ARD), contaminated neutral drainage (CND) or alkaline drainage (AD) (INAP, 2009; Plante *et al*., 2020). The main minerals that influence the quality and the nature of the drainage are sulfide and carbonate minerals. The former generates acidity while the latter creates alkalinity that consumes the produced acidity (entirely or partly) (Bussière and Guittonny, 2020; INAP, 2014; Lottermoser, 2007).

In most cases, the problems associated with the mine drainage can be remediated through appropriate reclamation techniques. For mines operating under Arctic conditions, factors such as climate change, the presence of permafrost, remoteness, the availability of materials, and harsh climatic conditions can make the design and construction of reclamation scenarios more difficult and expensive than for mines in temperate climates (Bussière and Hayley, 2010). While some methods are only a transfer from those used in the South, one technique called insulation covers was explicitly proposed for Arctic conditions. The technique aims at maintaining the mine tailings frozen and below a target temperature to prevent sulfide mineral reactivity and water movement (Boulanger-Martel *et al*., 2020a; Kyhn and Elberling, 2001; Lessard *et al*., 2018; Meldrum *et al*., 2001). To reduce the risk of losing performance in the long term, Boulanger-Martel *et al*. (2016) proposed to add an oxygen barrier into the insulation cover (ICCBE) that would simultaneously control both parameters (temperature and oxygen flux). The moisture-retaining layer (MRL) is the main component of such a cover system that maintains a high degree of saturation (Sr) and significantly restricts oxygen flux from reaching the acid-generating tailings. The MRL is usually made of fine-grained silty materials (Bussière, 2007; Bussière *et al*., 2007). Recent works performed in the laboratory suggest that low sulfide or desulfurized tailings could be used as MRL in an ICCBE to control oxygen migration

(Lessard *et al.* 2018; Qureshi *et al.* 2021). However, questions remain on the potential of these low sulfide or desulfurized tailings to generate contaminants when placed in an ICCBE in the long term (Qureshi *et al.*, 2021a).

Different laboratory experiments are performed on the mining wastes to determine the expected quality and nature of the drainage upon exposure to stimulating environmental conditions (Demers *et al.*, 2008; Hamberg *et al.*, 2018; Kalonji-Kabambi *et al.*, 2020a; Larochelle *et al.*, 2019; Nyström *et al.*, 2019; Pabst *et al.*, 2014; Plante *et al.*, 2014; Qureshi *et al.*, 2019). However, most of the laboratory experiments are time-constrained and are, therefore, primarily representative of the short-term response of mining waste materials under laboratory conditions. Consequently, performing in-situ test cell experiments to produce field representative results is advocated (Bussière *et al.* 2007; Boulanger-Martel *et al.*, 2020b; Qureshi *et al.*, 2016). However, the results generated from such experiments are also relatively short-term (typically 3–5 years). Therefore, reactive transport modelling has gained the interest of many researchers (Molson *et al.*, 2008; Craig *et al.*, 2021; Demers *et al.*, 2013; Kalonji-Kabambi *et al.*, 2020b; Muniruzzaman *et al.*, 2020; Wilson *et al.*, 2018) to predict the long-term behaviour of mining waste materials using multicomponent reactive transport numerical models.

The overall objective of the study is to validate the hypothesis that desulfurized tailings are a viable material for the MRL in ICCBEs by assessing the thermal-hydrogeochemical behaviour of the ICCBEs in the short and long term. The results on the hydrogeological behaviour (Lessard *et al.*, 2018) and the geochemical evolution (Qureshi *et al.*, 2021a) of the column are used here for the numerical modelling part of the study. The specific objectives of this article consist of i) Calibrating a conceptual multicomponent reactive transport model in MIN3P-THCm using column leaching experiments results of insulation covers with capillary barrier effect (ICCBE) utilizing desulfurized tailings (DSTs) as a moisture-retaining layer (MRL), and ii) predicting the long-term (200 years) hydrogeochemical behaviour of the ICCBE column.

Methods

Material characterization

A tailings sample was desulfurized to a residual sulfide content of 0.4 wt% in the laboratory using the froth flotation process by Benzaazoua *et al.* (2017). Mineralogical characterization was performed using optical microscopy first and then by both scanning electron microscopy (SEM; Hitachi S-3500 N, Japan) coupled with Energy Dispersive Spectrometry (EDS; Silicon Drift Detector X-Max 20 mm^2 from Oxford, UK) microanalysis, and X-ray diffraction (XRD; Bruker AXS Advance D8, Billerica, MA, USA; XRD precision ±1%; (Bouzahzah, 2013)). The inductively coupled plasma atomic emission spectroscopy (ICP-AES; Perkin Elmer 3000 DV, Überlingen, Germany) for trace metal in particular and fusion, whole-rock analyses by borate fused disc, were used to determine the major and minor elemental composition of the desulfurized tailings. Analyses of total inorganic carbon (C) and sulfur (S) concentrations were also carried out using an induction furnace equipped with a dedicated infrared (IR) analyzer (Eltra CS 2000, Haan, Germany) with a ±0.05 to 0.1 wt% precision (CEAEQ, 2013).

Column experiment

An ICCBE was simulated in a column constructed from high-density polyethylene (HDPE) with an internal diameter of 0.14 m, a wall thickness of ≈0.022 m, and a height of 2.20 m. The column was filled with a coarse-grained non-acid generating crushed WR to a height of 1.0 m as a capillary break layer (CBL), followed by a 0.7 m moisture-retaining layer (MRL) made of desulfurized tailings and finally a 0.4m thick protective layer (PL) made of the same material from the CBL. The MRL was compacted to a porosity (n) of 0.36–0.40, and the CBL and PL layers to n=0.25. The initial unfrozen volumetric water content (θu) was 0.36 in the MRL, which corresponds to a degree of saturation (Sr) between 90–100%.

The ICCBE column was exposed to a 5 °C controlled temperature environment for 27 days, beginning with a 7-day rinse with two volumes of 1.6 L of deionized water each at 24 h intervals. At the end of

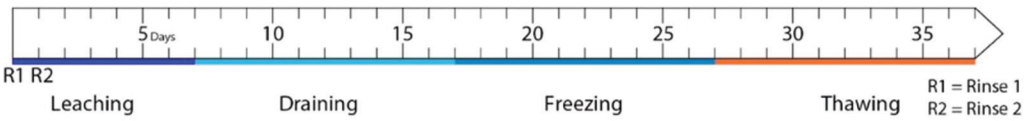

Figure 1 *A typical testing cycle.*

the rinse period, the collected leachates were analyzed for pH, Eh, EC, acidity, and alkalinity before chemical characterization using ICP, following the methods and protocols mentioned above. Following the flushing, the column was exposed to a 5 °C temperature for another 10 days before subjecting them to the F–T cycle of 20 days (10-day freezing and 10-day thawing). A typical cycle is presented in Figure 1. The F–T cycles were performed by exposing the column to temperature conditions inspired by those observed in the Canadian Arctic. A proportional-integral-derivative (PID) controlled industrial grade freezer was used to maintain the temperatures at -13 °C (for freezing) and 5 °C (for thawing), as applied by Boulanger-Martel *et al.* (2016, 2015) before. A total of eight such leachings and F–T cycles were performed over a period of a year.

Conceptual model

A 1-D conceptual RTM was created in MIN3P-THCm using the physical and hydrogeological parameters shown in Figure 2. The model domain was discretized in 100 (CBL), 75 (MRL), and 25 (PL) control volumes. MIN3P-THCm is a multicomponent reactive transport code that is used for simulating thermo-hydro-chemical and mechanical (THCm) processes in variably saturated porous media (Mayer *et al.*, 2002). Some salient features of the code are density dependant flow and solute transport, heat and gas transport, biogeochemical reactions, and one-dimensional hydromechanical coupling (Bea *et al.*, 2012; Henderson *et al.*, 2009; Mayer *et al.*, 2002; Su *et al.*, 2020, 2017). The code includes databases from MINTEQA2 (Allison *et al.*, 1991) and WATEQf4 (Ball and Nordstrom, 1991).

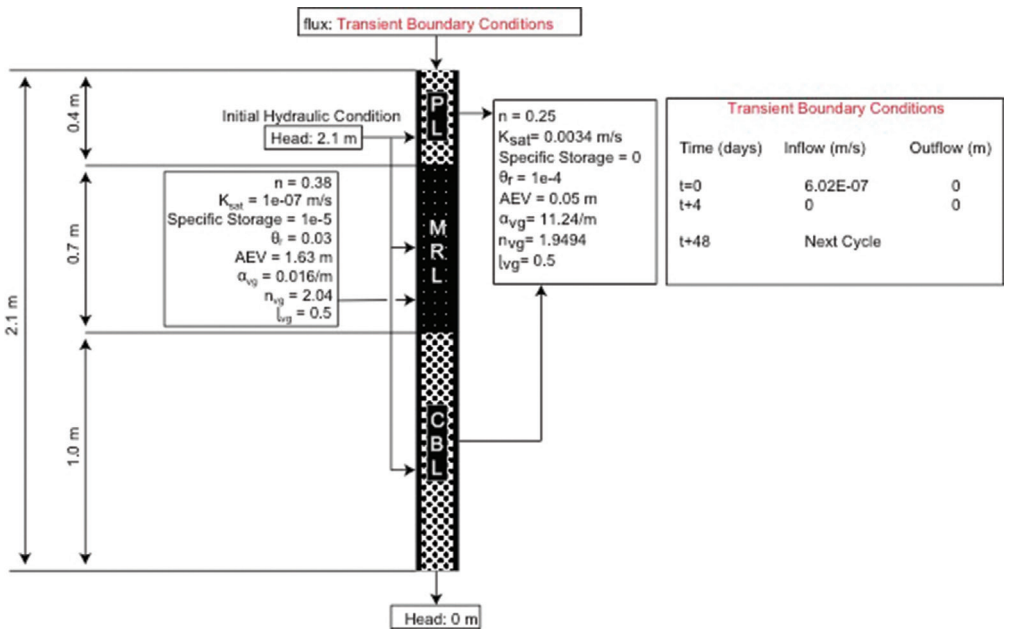

Figure 2 *Illustration of the conceptual model.*

Model parameters

The mineral reactivity in MIN3P-THCm can be set to remain constant or as a time-dependant mineral volume fraction (Mayer *et al*., 2002). For sulfide minerals, however, a shrinking-core model (SCM; assuming a spherical mineral grain) which simulates O2 diffusion-controlled sulfide mineral oxidation can also be applied (Davis and Ritchie, 1986; Mayer *et al*., 2002). In the present research, the non-sulfide minerals that were already present in the tailings have been simulated using surface-controlled reactions, sulfide minerals using SCM and the secondary minerals are allowed to precipitate using constant reactivity (dependant upon the physicochemical changes within the system).

A total of 17 minerals were included in the simulations (Table 1), based on the mineralogical characterization of the materials, and including the secondary minerals suggested by PHREEQC (Parkhurst and Appelo, 2013) batch simulations. An initial grain radius of 9.5×10-7 m was used for all sulfide minerals for the SCM. The minerals' rate expressions (Table S1) and reaction rate coefficients (Table S2) for the simulations are provided in the supplementary material. The model was calibrated using reaction rate coefficients in MIN3P-THCm to simulate the laboratory observed chemical concentrations. However, the simulations were not targeted to achieve exact chemical concentration, instead to produce numerical results within the same range of the measured concentrations that represent the trends for the most important elements or components.

The porewater quality measurements for the first flushing cycle were used as the initial chemical conditions in the model, and the recharge water composition was typical of the tap water used in column experiments (Ouangrawa *et al*., 2009) (Table 2).

Assumptions and simplifications

Some assumptions and simplifications were made to the conceptual model for its calibration. Transient inflow boundary conditions were applied to simulate the temperature effect on infiltration (assuming that no infiltration occurs under freezing conditions; Figure 2). Furthermore, these infiltration conditions were considered to repeat for 200 years in long-term simulations. However, the effect of temperature on reactive transport modelling was applied by utilizing the "define temperature field" option of MIN3P-THCm by using the laboratory observed temperature data (see Lessard *et al*. (2018) and Qureshi *et al*. (2021a) for more details). The WR in PL and CBL was assumed to be non-reactive (except for anorthite (Table 1)).

Results

Results from the reactive transport modelling of the ICCBE system were similar to the laboratory results. They showed that despite the low residual sulfur content after the desulfurization of the tailings, the column produced non-negligible concentrations of SO4-2, Ni and Zn (Qureshi *et al*., 2021). Therefore, pH and these three parameters are considered elements of concern, and their

Table 1 *Minerals' weight percentages and volume fractions1 based on mineral characterization.*

Mineral	MRL		CBL, PL		Mineral	MRL		CBL, PL	
	wt%	Vf [1]	wt%	Vf [1]		wt%	Vf [1]	wt%	Vf [1]
Pyrrhotite	0.64	0.0038	n.d.	n.d.	K-Jarosite	n.d.	n.d.	n.d.	n.d.
Pentlantite	0.29	0.0017	n.d.	n.d.	Lizardite	31.81	0.3392	n.d.	n.d.
Chalcopyrite	0.25	0.0017	n.d.	n.d.	Magnetite	2.56	0.0137	n.d.	n.d.
Actinolite	29.75	0.2660	33.6	Excluded	Melanterite	2.91	0.0425	n.d.	n.d.
Anorthite	n.d.	n.d.	11.2	0.1196	Na-Jarosite	n.d.	n.d.	n.d.	n.d.
Calcite	2.17	0.0222	n.d.	n.d.	Ni-Sulfate	0.087	0.0012	n.d.	n.d.
Clinochlore	26.48	0.2770	14.7	Excluded	Thenardite	2.91	0.0304	n.d.	n.d.
Ferrihydrite	n.d.	n.d.	n.d.	n.d.	Zn-Sulfate	0.087	0.0006	n.d.	n.d.
Gypsum	n.d.	n.d.	n.d.	n.d.					

[1]Volume fraction (m^3 (mineral) m^{-3} (bulk)) = Mineral wt% × (density of rock material ÷ density of mineral) × (1 – porosity) ÷ bulk reservoir volume

n.d. = not detected

Table 2 Initial porewater and recharge water composition.

Initial porewater		Recharge water	
Element	Concentration	Element	Concentration
Ca^{+2} (mol L^{-1})	1.36E-02	Ca^{+2} (mol L^{-1})	2.20E-05
K^{+1} (mol L^{-1})	1.16E-04	K^{+1} (mol L^{-1})	2.00E-05
H_4SiO_4 (mol L^{-1})	1.86E-03	H_4SiO_4 (mol L^{-1})	1.00E-20
Al^{+3} (mol L^{-1})	1.59E-06	Al^{+3} (mol L^{-1})	1.00E-20
CO_3^{-2} (mol L^{-1})	1.00E-13	CO_3^{-2} (mol L^{-1})	0.000317
Fe^{+2} (mol L^{-1})	7.16E-07	Fe^{+2} (mol L^{-1})	1.00E-10
SO_4^{-2} (mol L^{-1})	2.58E-02	SO_4^{-2} (mol L^{-1})	1.00E-05
Fe^{+3} (mol L^{-1})	1.00E-10	Fe^{+3} (mol L^{-1})	2.00E-05
Ni^{+2} (mol L^{-1})	1.72E-06	Ni^{+2} (mol L^{-1})	1.00E-10
Cu^{+2} (mol L^{-1})	1.57E-07	Cu^{+2} (mol L^{-1})	1.00E-10
Mg^{+2} (mol L^{-1})	1.03E-02	Mg^{+2} (mol L^{-1})	8.20E-07
Zn^{+2} (mol L^{-1})	4.07E-06	Zn^{+2} (mol L^{-1})	1.00E-10
Na^{+1} (mol L^{-1})	2.26E-03	Na^{+1} (mol L^{-1})	2.00E-05
HS^{-1} (mol L^{-1})	1.00E-10	HS^{-1} (mol L^{-1})	1.00E-12
pH (-)	7.89	pH (-)	7.0
O_2 (pe)	8.55	O_2 (pO_2)*	0.21

* pO_2 and pCO_2 are atmospheric O_2 and CO_2 concentrations, respectively.

simulated hydrogeochemical behavior is reported in the following sections.

Model calibration

The calibration results of the model for pH, SO_4^{-2}, Ni and Zn are in good agreement with the observed laboratory values (Figure 3). The calibrated model almost accurately reproduced the pH. Similarly, sulfate concentrations were also well reproduced by the model. However, some noticeable differences are present in Ni and Zn; Ni was under-estimated between 50 and 100 days and over-estimated between 200 and 259 days. Similarly, Zn was over-estimated between 25 and 75 days. Other researchers have also observed these differences while performing reactive transport modelling (Demers *et al.*, 2013; Kalonji-Kabambi *et al.*, 2020b; Wilson *et al.*, 2018). Since the objective of the calibration was to produce trends in the same concentration ranges rather than reproducing the absolute values, the model duration was extended to 200 years for long-term predictions.

Long-term predictions

As shown in Figure 4, the long-term simulations are encouraging for the use of desulfurized tailings in the tested ICCBE. They indicate that most of the leachate quality concerns are relatively short-term. The simulations show that the pH spikes above 7.5 after about 30 years, followed by a constant declining trend, which finally stabilizes after 100 years to circumneutral values. Sulfate was one of the most critical concerns from the laboratory experiments, but the simulation shows that, although the sulfate concentrations could remain relatively high initially, they will stabilize to a few mg L^{-1} after four years. This is because of the slow reaction of sulfide minerals and the depletion of thenardite ($Na_2SO_4^{-2}$), which seems to be the main contributor towards the sulfate leaching in the column (see Figure S1 in supplementary material). Sulfide minerals' reactivity appeared negligible, as shown by the sulfide minerals' mineral volume fraction (Figure S2 in supplementary material), probably due to the high degree of saturation maintained by the capillary barrier effects (which restricts oxygen supply) and the low-temperature conditions to which the column was exposed (Lessard *et al.*, 2018; Qureshi *et al.*, 2021). Nickel and Zn concentrations, on the other hand, remain present for a longer duration, but the predicted concentrations shall not be higher than the provincial allowed effluent concentrations for mining operations in Québec (0.5 mg L^{-1} for both Ni and Zn in Directive 019). More specifically, Ni shall stabilize with a maximum concentration of 1.50 × 10-06 mol L^{-1} (or 0.09 mg L^{-1}) after

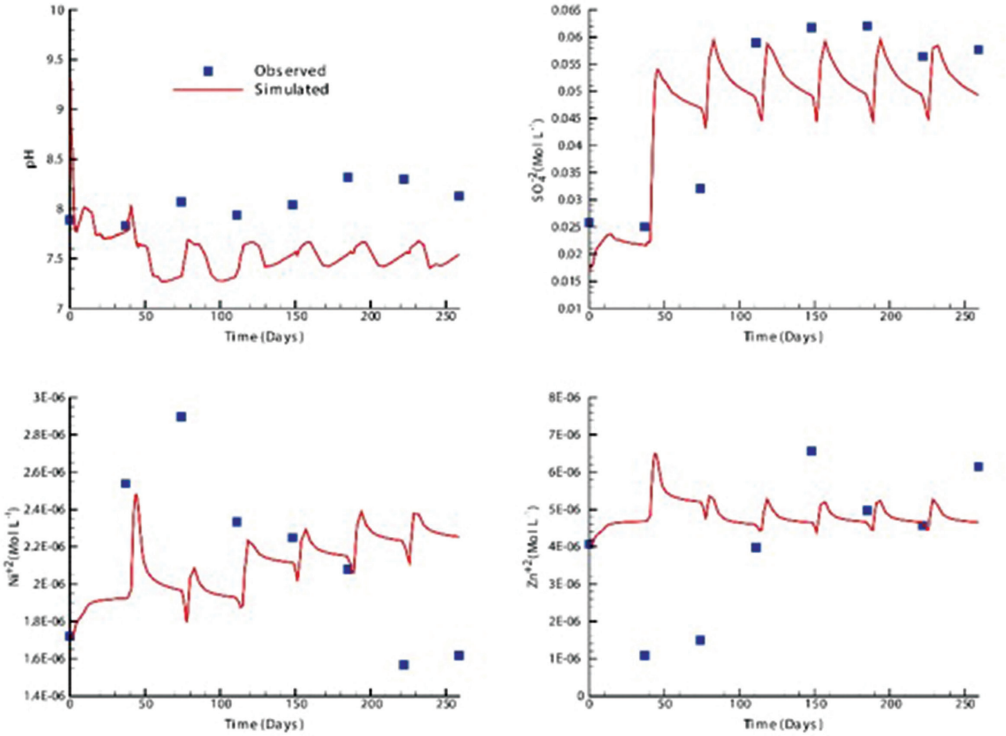

Figure 3 Calibration of the RTM with the laboratory observations.

≈50 years. Similarly, Zn will be leached with a maximum concentration of 3.5 × 10-06 mol L^{-1} (or 0.2 mg L^{-1}) after ≈50 years and shall finally become stable at 4.0 × 10-09 (or 0.00026 mg L^{-1}) after ≈145 years.

Conclusions

A conceptual multicomponent reactive transport model was created to predict the long-term behaviour of an ICCBE system utilizing desulfurized tailings as an MRL and non-acid generating crushed WR as PL and CBL. The model was first calibrated with the laboratory observed concentrations of the main elements of concern (Zn, Ni, SO_4^{-2}, and pH). The calibrated model was then used to perform long-term simulations that show that the ICCBE system can maintain a circumneutral pH for 200 years. The sulfate concentrations shall drop to a few mg L^{-1}, with Ni and Zn concentrations maintained below provincial allowable concentration in Québec for 200 years. These results confirm a low risk of contamination from the MRL made of desulfurized tailings and that this material could be used to build an ICCBE in cold climatic conditions. However, a sensitivity analysis is underway to assess the robustness of the calibrated conceptual model further.

Acknowledgements

The authors wish to thank the NSERC Industrial Chair on Mine Site Reclamation (Grant number: IRCPJ 252714–18) and NSERC Strategic Partnership Grants for Networks "NSERC toward Environmentally Responsible Resource Extraction" (NSERC-TERRE-NET; Grant number: NETGP 479708–15) for funding this research.

References

Allison, J.D., Brown, D.S., Novo-Gradac, K.J., 1991. MINTEQA2/PRODEFA2, A Geochemical Assessment Model for Environmental Systems: Version 3.0 User's Manual, United States Environmental Protection Agency, Office of Research and Development, Washington, DC,.

Aubertin, M., Aachib, M., Monzon, M., Joanes, A.M., Bussière, B., Chapuis, R.P., 1997. Étude de laboratoire sur l'efficacité des barrières de recouvrement construites à partir de résidus

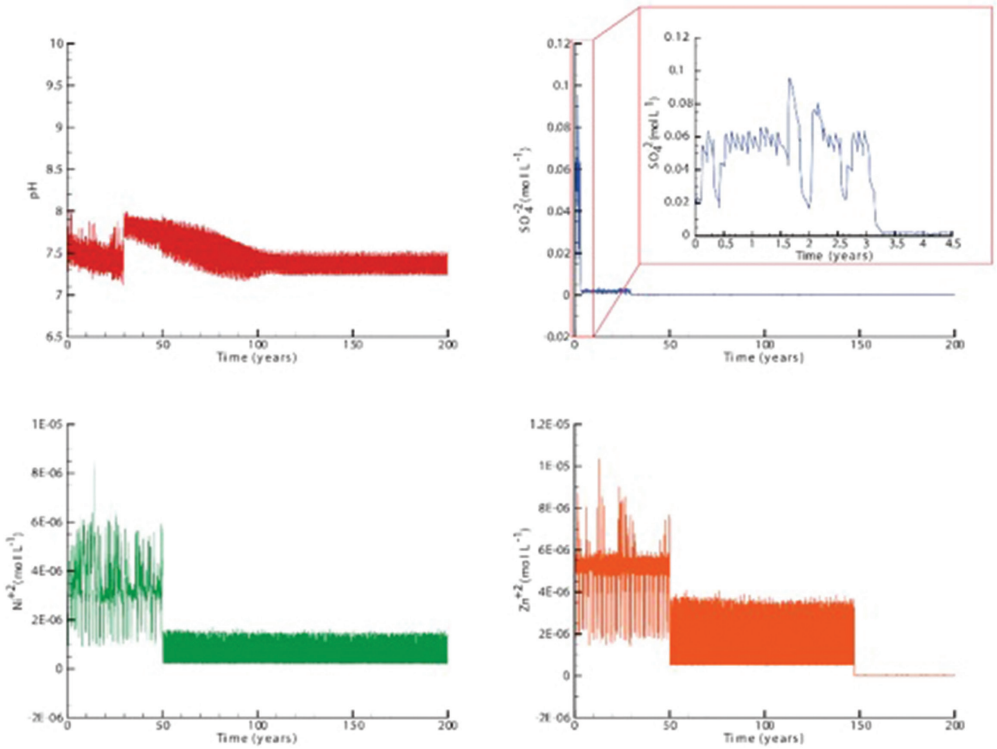

Figure 4 *Long-term predictions for the conceptual ICCBE model.*

miniers, Mine Environment Neutral Drainage (MEND) Report 2.22.2b.

Aubertin, M., Bussière, B., Pabst, T., James, M., Mbonimpa, M., 2016. Review of the Reclamation Techniques for Acid-Generating Mine Wastes upon Closure of Disposal Sites, in: Geo-Chicago 2016. American Society of Civil Engineers, Reston, VA, pp. 343–358. https://doi.org/10.1061/9780784480137.034

Ball, J.W., Nordstrom, D.K., 1991. User's manual for WATEQ4F, with revised thermodynamic data base and test cases for calculating speciation of major, trace, and redox elements in natural waters. Menlo Park, California.

Bea, S.A., Wilson, S.A., Mayer, K.U., Dipple, G.M., Power, I.M., Gamazo, P., 2012. Reactive Transport Modeling of Natural Carbon Sequestration in Ultramafic Mine Tailings. Vadose Zo. J. 11, vzj2011.0053. https://doi.org/10.2136/vzj2011.0053

Benzaazoua, M., Bouzahzah, H., Taha, Y., Kormos, L., Kabombo, D., Lessard, F., Bussière, B., Demers, I., Kongolo, M., 2017. Integrated environmental management of pyrrhotite tailings at Raglan Mine: Part 1 challenges of desulphurization process and reactivity prediction. J. Clean. Prod. 162, 86–95. https://doi.org/10.1016/j.jclepro.2017.05.161

Boulanger-Martel, V., Bussière, B., Côté, J., 2020a. Thermal behaviour and performance of two field experimental insulation covers to control sulfide oxidation at Meadowbank mine, Nunavut. Can. Geotech. J. cgj-2019-0616. https://doi.org/10.1139/cgj-2019-0616

Boulanger-Martel, V., Bussière, B., Côté, J., 2020b. Insulation Covers, in: Bussière, B., Guittonny, M. (Eds.), Hard Rock Mine Reclamation: From Prediction to Management of Acid Mine. CRC Press, Boca Raton, USA.

Boulanger-Martel, V., Bussière, B., Côté, J., Mbonimpa, M., 2016. Influence of freeze–thaw cycles on the performance of covers with capillary barrier effects made of crushed rock–bentonite mixtures to control oxygen migration. Can. Geotech. J. 53, 753–764. https://doi.org/10.1139/cgj-2015-0155

Boulanger-Martel, V., Bussière, B., Côté, J., Mbonimpa, M., 2015. Laboratory column experiment to evaluate oxygen diffusion through covers with capillary barrier effects subjected to

freeze-thaw cycles, in: Proceedings of the 16th International Conference on Cold Regions Engineering, Salt Lake City, Utah. Paper.

Bouzahzah, H., 2013. Modification et amélioration des tests statiques et cinétiques pour une prédiction fiable du drainage minier acide. PhD Thesis. Université du Québec en Abitibi-Témiscamingue (UQAT), Rouyn-Noranda, Québec, Canada.

Bussière, B., 2007. Colloquium 2004: Hydrogeotechnical properties of hard rock tailings from metal mines and emerging geoenvironmental disposal approaches. Can. Geotech. J. 44, 1019–1052. https://doi.org/10.1139/T07-040

Bussière, B., Aubertin, M., Mbonimpa, M., Molson, J.W., Chapuis, R.P., 2007. Field experimental cells to evaluate the hydrogeological behaviour of oxygen barriers made of silty materials. Can. Geotech. J. 44, 245–265. https://doi.org/10.1139/t06-120

Bussière, B., Benzaazoua, M., Aubertin, M., Mbonimpa, M., 2004. A laboratory study of covers made of low-sulphide tailings to prevent acid mine drainage. Environ. Geol. 45, 609–622. https://doi.org/10.1007/s00254-003-0919-6

Bussière, B., Guittonny, M., 2020. Hard rock mine reclamation: from prediction to management of acid mine drainage. CRC Press, Boca Raton, USA.

Bussière, B., Hayley, D., 2010. Effects of Climate Change on Mine Waste Disposal in the Arctic. Geo-Strata —Geo Inst. ASCE 14, 42,44-46.

CEAEQ, C.D. en A.E. du Q., 2013. Determination du carbone et du soufre : methode par combustion et dosage par spectrophotometrie infrarouge. MA. 310 e CS 1.0, Rev. 3. In: Ministere du Developpement durable, de l'Environnement, de la Faune et des Parcs du Quebec, 8.

Craig, A.T., Shkarupin, A., Amos, R.T., Lindsay, M.B.J., Blowes, D.W., Ptacek, C.J., 2021. Reactive transport modelling of porewater geochemistry and sulfur isotope fractionation in organic carbon amended mine tailings. Appl. Geochemistry 104904. https://doi.org/10.1016/j.apgeochem.2021.104904

Davis, G.B., Ritchie, A.I.M., 1986. A model of oxidation in pyritic mine wastes: part 1 equations and approximate solution. Appl. Math. Model. 10, 314–322. https://doi.org/10.1016/0307-904X(86)90090-9

Demers, I., Bussière, B., Benzaazoua, M., Mbonimpa, M., Blier, A., 2008. Column test investigation on the performance of monolayer covers made of desulphurized tailings to prevent acid mine drainage. Miner. Eng. 21, 317–329. https://doi.org/10.1016/j.mineng.2007.11.006

Demers, I., Molson, J., Bussière, B., Laflamme, D., 2013. Numerical modeling of contaminated neutral drainage from a waste-rock field test cell. Appl. Geochemistry 33, 346–356. https://doi.org/10.1016/j.apgeochem.2013.02.025

Hamberg, R., Maurice, C., Alakangas, L., 2018. The formation of unsaturated zones within cemented paste backfill mixtures—effects on the release of copper, nickel, and zinc. Environ. Sci. Pollut. Res. 25, 20809–20822. https://doi.org/10.1007/s11356-018-2222-9

Henderson, T.H., Mayer, K.U., Parker, B.L., Al, T.A., 2009. Three-dimensional density-dependent flow and multicomponent reactive transport modeling of chlorinated solvent oxidation by potassium permanganate. J. Contam. Hydrol. 106, 195–211. https://doi.org/10.1016/j.jconhyd.2009.02.009

INAP, 2014. International Network for Acid Prevention (INAP) Global acid rock drainage (GARD) guide, International Network for Acid Prevention.

INAP, 2009. Global acid rock drainage guide (GARD Guide), http://www.gardguide.com/, International Network for Acid Prevention. The International Network for Acid Prevention (INAP).

Kalonji-Kabambi, A., Bussière, B., Demers, I., 2020a. Hydrogeochemical Behavior of Reclaimed Highly Reactive Tailings, Part 2: Laboratory and Field Results of Covers Made with Mine Waste Materials. Minerals 10, 589. https://doi.org/10.3390/min10070589

Kalonji-Kabambi, A., Demers, I., Bussière, B., 2020b. Reactive transport modeling of the geochemical behavior of highly reactive tailings in different environmental conditions. Appl. Geochemistry 122, 104761. https://doi.org/10.1016/j.apgeochem.2020.104761

Kyhn, C., Elberling, B., 2001. Frozen cover actions limiting AMD from mine waste deposited on land in Arctic Canada. Cold Reg. Sci. Technol. 32, 133–142. https://doi.org/10.1016/S0165-232X(00)00024-0

Larochelle, C.G., Bussière, B., Pabst, T., 2019. Acid-Generating Waste Rocks as Capillary Break Layers in Covers with Capillary Barrier Effects for Mine Site Reclamation. Water, Air, Soil Pollut. 230, 57. https://doi.org/10.1007/s11270-019-4114-0

Lessard, F., Bussière, B., Côté, J., Benzaazoua, M., Boulanger-Martel, V., Marcoux, L., 2018. Integrated environmental management of pyrrhotite tailings at Raglan Mine: Part 2 desulphurized tailings as cover material. J. Clean. Prod. 186, 883–893. https://doi.org/10.1016/J.JCLEPRO.2018.03.132

Lottermoser, B., 2007. Mine wastes: characterization, treatment and environmental impacts. Springer Publisher, Heidelberg.

Mayer, K.U., Frind, E.O., Blowes, D.W., 2002. Multicomponent reactive transport modeling in variably saturated porous media using a generalized formulation for kinetically controlled reactions. Water Resour. Res. 38, 13-1-13–21. https://doi.org/10.1029/2001WR000862

Meldrum, J.L.L., Jamieson, H.E.E., Dyke, L.D.D., 2001. Oxidation of mine tailings from Rankin Inlet, Nunavut, at subzero temperatures. Can. Geotech. J. 38, 957–966.

Muniruzzaman, M., Karlsson, T., Ahmadi, N., Rolle, M., 2020. Multiphase and multicomponent simulation of acid mine drainage in unsaturated mine waste: Modeling approach, benchmarks and application examples. Appl. Geochemistry 120, 104677. https://doi.org/10.1016/j.apgeochem.2020.104677

Nadeif, A., Taha, Y., Bouzahzah, H., Hakkou, R., Benzaazoua, M., 2019. Desulfurization of the Old Tailings at the Au-Ag-Cu Tiouit Mine (Anti-Atlas Morocco). Minerals 9, 401. https://doi.org/10.3390/min9070401

Neculita, C.M., Zagury, G.J., Bussière, B., 2020. Passive Treatment of Acid Mine Drainage at the Reclamation Stage, in: Hard Rock Mine Reclamation. CRC Press, pp. 271–296. https://doi.org/10.1201/9781315166698/-11

Nyström, E., Kaasalainen, H., Alakangas, L., 2019. Prevention of sulfide oxidation in waste rock by the addition of lime kiln dust. Environ. Sci. Pollut. Res. 26, 25945–25957. https://doi.org/10.1007/s11356-019-05846-z

Ouangrawa, M., Molson, J., Aubertin, M., Bussière, B., Zagury, G.J., 2009. Reactive transport modelling of mine tailings columns with capillarity-induced high water saturation for preventing sulfide oxidation. Appl. Geochemistry 24, 1312–1323. https://doi.org/10.1016/j.apgeochem.2009.04.005

Pabst, T., Aubertin, M., Bussière, B., Molson, J., 2014. Column tests to characterise the hydrogeochemical response of pre-oxidised acid-generating tailings with a monolayer cover. Water. Air. Soil Pollut. 225. https://doi.org/10.1007/s11270-013-1841-5

Parkhurst, D.L., Appelo, C.A.J., 2013. Description of Input and Examples for PHREEQC Version 3—A Computer Program for Speciation, Batch-Reaction, One-Dimensional Transport, and Inverse Geochemical Calculations, in: Book 6, Modeling Techniques. U.S. Geological Survey, United States of America.

Plante, B., Bussière, B., Benzaazoua, M., 2014. Lab to field scale effects on contaminated neutral drainage prediction from the Tio mine waste rocks. J. Geochemical Explor. 137, 37–47. https://doi.org/10.1016/j.gexplo.2013.11.004

Plante, B., Schudel, G., Benzaazoua, M., 2020. Prediction of Acid Mine Drainage, in: Bussière, B., Guittonny, M. (Eds.), Hard Rock Mine Reclamation. CRC Press, Boca Raton, pp. 21–46. https://doi.org/10.1201/9781315166698/-2

Qureshi, A., Bussière, B., Benzaazoua, M., Lessard, F., Boulanger-Martel, V., 2021. Geochemical Assessment of Desulphurized Tailings as Cover Material in Cold Climates. Minerals 11, 280. https://doi.org/10.3390/min11030280

Qureshi, A., Maurice, C., Öhlander, B., 2019. Effects of the co-disposal of lignite fly ash and coal mine waste rocks on AMD and leachate quality. Environ. Sci. Pollut. Res. 26, 4104–4115. https://doi.org/10.1007/s11356-018-3896-8

Qureshi, A., Maurice, C., Öhlander, B., 2016. Potential of coal mine waste rock for generating acid mine drainage. J. Geochemical Explor. 160, 44–54. https://doi.org/10.1016/j.gexplo.2015.10.014

Su, D., Mayer, K.U., MacQuarrie, K.T.B., 2020. Numerical investigation of flow instabilities using fully unstructured discretization for variably saturated flow problems. Adv. Water Resour. 143, 103673. https://doi.org/10.1016/j.advwatres.2020.103673

Su, D., Ulrich Mayer, K., MacQuarrie, K.T.B., 2017. Parallelization of MIN3P-THCm: A high performance computational framework for subsurface flow and reactive transport simulation. Environ. Model. Softw. 95, 271–289.

https://doi.org/10.1016/j.envsoft.2017.06.008

Wilson, D., Amos, R.T., Blowes, D.W., Langman, J.B., Ptacek, C.J., Smith, L., Sego, D.C., 2018. Diavik waste rock project: A conceptual model for temperature and sulfide-content dependent geochemical evolution of waste rock – Laboratory scale. Appl. Geochemistry 89, 160–172. https://doi.org/10.1016/j.apgeochem.2017.12.007

Supplementary Material

Table S1 Minerals' rate expressions

Mineral	Rate expression	Mineral	Rate expression
Pyrrhotite	SCM	K-Jarosite	$R = -K^{eff}_{K-Jarosite}\left[1-\frac{IAP}{10^{9.21}}\right]$
Pentlantite	SCM	Lizardite[1]	$R = -K^{eff}_{Lizardite}$
Chalcopyrite	SCM	Magnetite	$R = -K^{eff}_{Magnetite}\left[1-\frac{IAP}{10^{-3.737}}\right]$
Actinolite[1]	$R = -K^{eff}_{Actinolite}$	Melanterite	$R = -K^{eff}_{Melanterite}\left[1-\frac{IAP}{10^{-2.209}}\right]$
Anorthite[1]	$R = -K^{eff}_{Anorthite}$	Na-Jarosite	$R = -K^{eff}_{Na-Jarosite}\left[1-\frac{IAP}{10^{5.28}}\right]$
Calcite	$R = -K^{eff}_{Calcite}\left[1-\frac{IAP}{10^{-8.475}}\right]$	Ni-Sulfate	$R = -K^{eff}_{Ni-Sulfate}\left[1-\frac{IAP}{10^{-2.33}}\right]$
Clinochlore[1]	$R = -K^{eff}_{Clinochlore}$	Thenardite	$R = -K^{eff}_{Thenardite}\left[1-\frac{IAP}{10^{-0.179}}\right]$
Ferrihydrite	$R = -K^{eff}_{Ferrihydrite}\left[1-\frac{IAP}{10^{-3.191}}\right]$	Zn-Sulfate	$R = -K^{eff}_{Zn-Sulfate}\left[1-\frac{IAP}{10^{-1.8683}}\right]$
Gypsum	$R = -K^{eff}_{Gypsum}\left[1-\frac{IAP}{10^{4.58}}\right]$		

[1] Irreversible dissolution

Table S2 Minerals' reaction rate coefficients used for simulations in MIN3P-THCm

Mineral	Rate coefficient			Mineral	Rate coefficient		
	MRL	CBL	PL		MRL	CBL	PL
Lizardite	1E-12	1E-50	1E-50	Ni-Sulfate	4.5E-15	1E-13	1E-10
Actinolite	1E-12	6E-11	1E-50	Thenardite	6E-09	1E-10	1E-10
Clinochlore	1.5E-10	5E-10	1E-50	Melanterite	2.2E-10	1E-10	1E-10
Calcite	7E-11	1E-25	1E-50	Anorthite	1E-25	1E-09	1E-50
Magnetite	1E-07	1E-10	1E-50	Ferrihydrite	1E-10	1E-10	1E-50
Pyrrhotite	3E-12	1E-12	1E-10	Na-Jarosite	1E-10	1E-10	1E-50
Pentlandite	1E-12	3.5E-12	1E-10	K-Jarosite	1E-10	1E-10	1E-50
Chalcopyrite	5E-10	1E-10	1E-10	Gypsum	1E-10	1E-25	1E-50
Zn-Sulfate	4.5E-13	4.5E-13	4.5E-13				

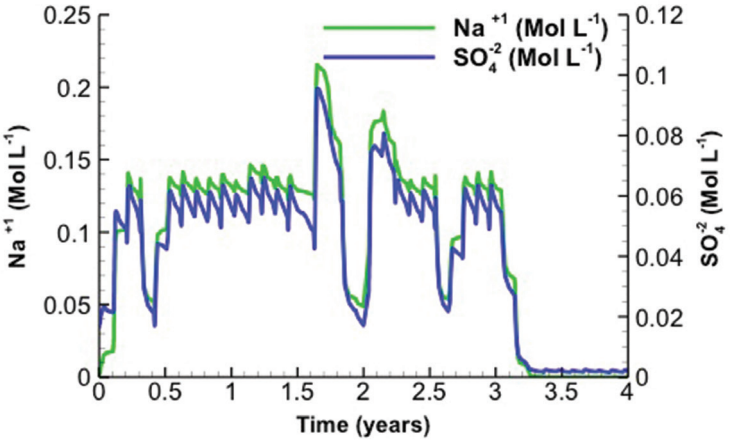

Figure S1 Leaching of sodium and sulfate

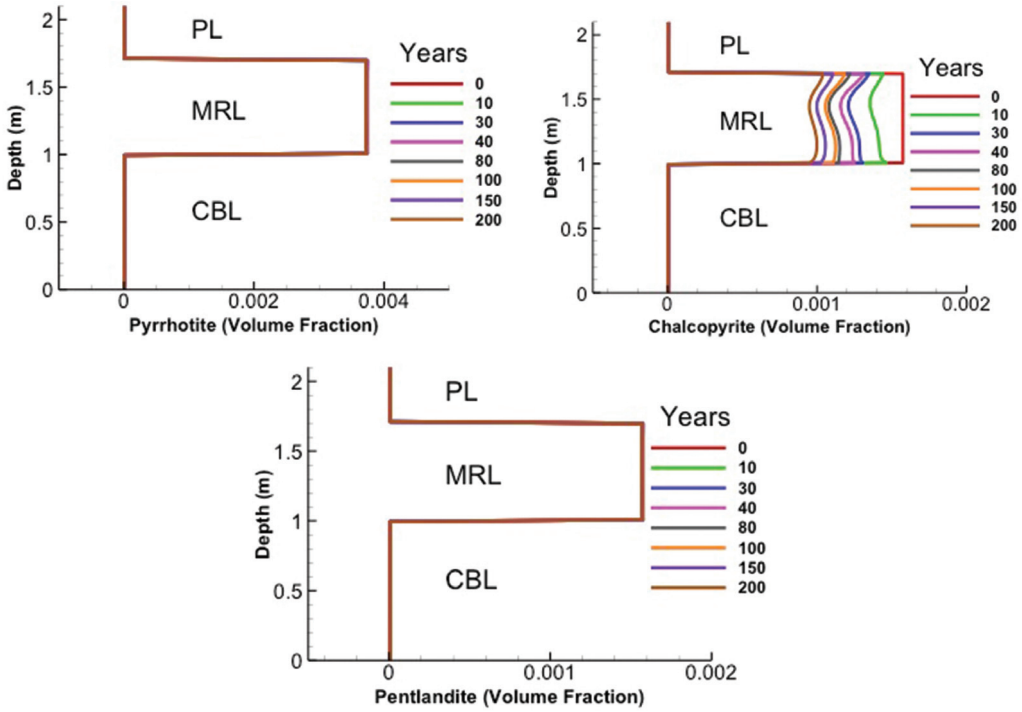

Figure S2 Change in sulfide minerals' volume fractions over time

Design, Operation, and Preliminary Findings from a Field Acid Rock Drainage (ARD) Study at the Bagdad Copper Mine in Arizona

Madhumitha Raghav[1], Jessica Szaro[1], Trika Graham[2], Brent Callen[2]

[1]*Freeport-McMoRan, Inc., 800 E. Pima Mine Road, Sahuarita, Arizona 85629, United States of America, mraghav@fmi.com*

[2]*Freeport-McMoRan Bagdad, Inc., PO Box 245, 100 Lower Main Street, Bagdad, Arizona 86321, United States of America*

Abstract

A field test pad study is ongoing at the Bagdad mine in Arizona to understand acid rock drainage (ARD) and metal leaching (ML) potential of development rock and leached ore stockpiles under field conditions. Seepage oxidation-reduction potential (ORP) and dissolved oxygen (DO) data indicate test pads conditions are not oxygen limited and hence, are likely to promote sulfide oxidation. Seepage pH has remained in the circumneutral range for development rock pads. Seepage flow response suggests development of preferential flow paths within the pads. Study results will be used to support on-going mine planning and permitting processes at the Bagdad mine.

Keywords: Acid Rock Drainage, Metal Leaching, Mine Water Quality, Field Study

Introduction

Characterization of ARD and ML potential through standard lab predictive tests is critical to assessing the future seepage water quality from mined/processed materials. These tests are typically required as part of environmental permitting document submittals. Wide variations in mineralogy and particle sizes of materials create a need for a multi-faceted approach when evaluating ARD and ML potential. Major differences exist between lab testing and field parameters, such as temperature, particle size distribution (PSD), microbial activity, air and water flow mechanisms, which influence the evolution and propagation of ARD and ML processes (Kempton 2012, Pearce et al. 2015). Due to the small sample number and weight tested in standard lab tests and inherent heterogeneities present under field conditions, there is limited representation and prediction of ARD/ML potential through lab testing. Therefore, field testing using constructed test pads provides a more representative demonstration of ARD and ML generation from mine stockpiles under field conditions.

Study Site

The Bagdad mine is an open-pit copper and by-product molybdenum mine operated by Freeport-McMoRan Bagdad Inc., a subsidiary of Freeport-McMoRan Inc. (FCX) located in Yavapai County approximately 130 miles northeast of Phoenix in Arizona, USA (Figure 1a). Average annual precipitation rate at the site is approximately 380 mm/year (WRRC 2016). Average summer high temperature approaches 36 degrees Celsius (°C) in July, and the average winter low is just above 0 °C in January. A field study to understand ARD and ML potential of development rock and leached ore stockpiles under field conditions is ongoing at the mine. A total of six test pads - five development rock (TP3-TP7) and one previously acid leached ore material (TP8), were constructed on the South Waste Rock Stockpile (SWRS) in August-November 2018. This study will provide predictions for the following development rock types - Porphyry Quartz Monzonite, Quartz Monzonite, and Precambrian Undifferentiated. These rock types were selected based on their substantial contribution to total material tonnage in the mine

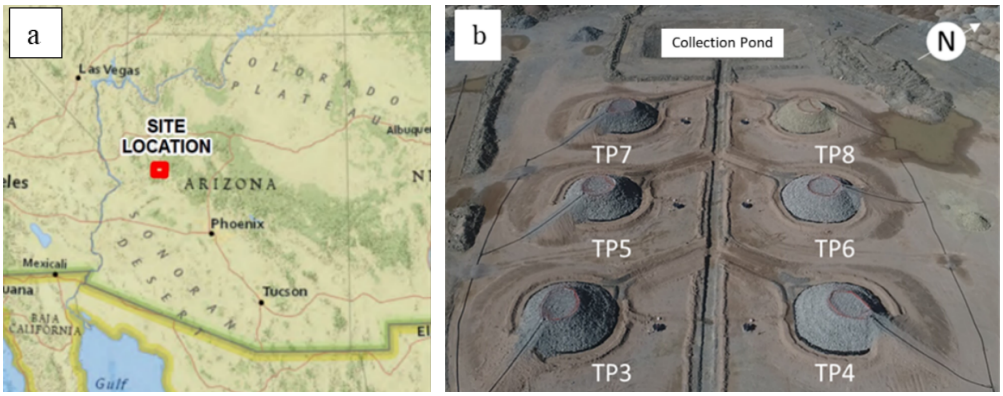

Figure 1 *(a) Bagdad mine location map and (b.) aerial drone image of the study site showing the constructed test pads, outlet/collection channels, and collection pond. Note: TP3 and TP4 - Quartz Monzonite; TP5 and TP6 - Porphyry Quartz Monzonite; TP7 - Precambrian Undifferentiated; TP8 - material from Mineral Creek leach pile.*

plan as well as uncertain classification of ARD potential based on lab testing. Due to semi-arid conditions on site, supplemental drip-line water application is used to augment water received by the pads via natural precipitation. Supplemental water application is expected to accelerate natural mineral-water interactions and facilitate a future water quality evaluation within the relatively short study duration of 2-3 years.

Methods

Construction Activities – Construction activities started in August 2018 on the upper level of the SWRS at the Bagdad mine. A collection pond was constructed to store stormwater run-off and seepage conveyed via test pad outlet channels and a main collection channel. For each pad, the subgrade was sloped at approximately 6 percent towards the center of the test pad to promote seepage collection into a perforated high-density polyethylene (HDPE) collection pipe installed along the center of the pad. The pipe was installed on top of an impermeable HDPE liner to prevent infiltration of seepage into the subgrade. Seepage from each test pad is gravity fed to a 300-L closed cylindrical polyethylene seepage collection tank buried in between the main collection channel and the front of the pad.

Optimum rock size for the test pad materials was selected as 0.3 m minus to eliminate coarse particles that are likely to have a negligible contribution to ARD generation from sulfide oxidation, while achieving a broad PSD within the pads. Test pad materials were placed in 0.5 m to 1.2 m lifts to allow for easy equipment maneuvering and to minimize compaction of materials. A total of nine EC-5 and GS3 sensors from METER Group, Inc. were installed within each test pad during lift construction to measure volumetric water content (VWC), temperature and bulk electrical conductivity (EC) data. The sensors were installed in custom-built boxes containing washed sand placed at 1.2 m and 2.1 m heights within the pads. A drip-line system from Netafim™ was installed on the top surface and upper slopes of pads to augment water received via natural precipitation. Water is conveyed to the dripline system from a 33,000-L storage tank via a 0.1 m HDPE water supply pipeline installed along the perimeter and up the side-slopes of the test pads. A HOBO® weather station from Onset® was installed in the study site to record precipitation received by the pads. The final dimensions (plan view) for all pads are approximately 9 m × 9 m top, 21 m × 21 m bottom, 5 m height from center of the stockpile, and side slopes of 1.5H:1V. Figure 1b shows an aerial drone

image of the pads, along with outlet and main collection channels, and collection pond. Figures 2a-d show the components of the seepage collection, water supply, and water application systems.

Material Collection and Analyses – Before construction, five to eight 210-L barrels of representative materials were collected and shipped to the FCX Technology Center in Sanchez, Arizona for PSD analysis and further material processing. For each test pad, materials in the barrels were blended and a representative sample was screened into finer size fractions for Acid-Base Accounting (ABA), Net Acid Generation (NAG), Synthetic Precipitation Leaching Procedure (SPLP), and total elemental analysis at SVL Analytical, Inc. (SVL), Idaho. Samples were also sent to the Mineralogy lab in the FCX Technology Center in Tucson, Arizona for X-ray Diffraction (XRD) analysis.

System Operation – System operation began in August 2019 and is planned to continue for 2 to 3 years. Potable water is filled in the storage tank and dechlorinated using a Rainfresh® Granular Activated Carbon (GAC) filter system before water application. Dechlorination treatment is expected to prevent any inadvertent effects of residual chlorine on microbial populations within the test pads. Microbial activity is known to accelerate ARD and ML generation from oxidation of sulfide minerals (Nordstrom et al. 2015, Percak-Dennett et al. 2017). A target water application rate of 3,800 L per week per test pad is used to accelerate natural mineral-water interactions as well as promote adequate seepage generation for water quality analyses. This target application volume is approximately three times the annual precipitation volume at Bagdad. Water is applied over a 3-to-4-hour period on the same day every week and actual volumes of water applied on each test pad are recorded by Netafim™ ultrasonic flow meters.

Sampling and Monitoring – A 19-L sampling container placed on a bracketed shelf installed in the seepage collection tank holds the most recent seepage for sample collection and analysis. Test pad seepage, water applied, field blank and duplicate samples are collected for analyses on a monthly/bimonthly basis. Aqueous chemistry analysis at SVL includes major cations and anions, selected trace elements, acidity/alkalinity, and total dissolved solids (TDS).

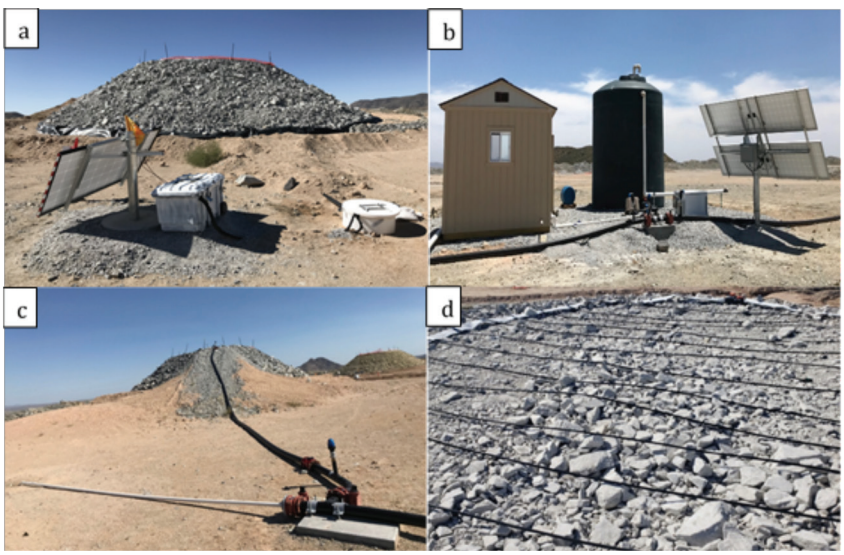

Figure 2 *Bagdad ARD test pad study components – (a) Test pad, seepage collection tank, sampling equipment box, and solar array; (b) water storage tank, solar array, pump, and Tuff Shed® housing Granular Activated Carbon (GAC) units; (c) water supply line installed along the perimeter and side slopes of test pads to supply water to the dripline system; and (d) drip-line system installed on top surface of the test pads.*

Additionally, field parameters - pH, EC, ORP, DO, and temperature are measured during and in between sampling events. A tipping bucket (Hydrological Services America, Model TB6/40) was placed on the shelf for continuous measurement of the seepage flow rate. A Mini Log Model ML1A data logger used to log the tip frequency data was housed in an insulated box next to the tank. Within a few weeks of installation, all ML1A data loggers stopped logging data possibly due to corrosion of reed switch contacts noted during visual inspection. These reed switches were replaced with custom silicone-potted ones prior to system start-up in August 2019. However, only the logger corresponding to TP6 logged data consistently before failing in January 2020. Starting mid-January 2020, two to three manual flow measurements are collected per week and distributed across the weekly water application cycle to include peak and low seepage flow periods. For each pad, a monthly average of manual flow measurements is likely to provide a reasonable estimation of seepage volumes for solute loading calculations. Moisture content data measured by the sensors are recorded by a ProCheck handheld meter during sampling events. In addition, sensors on the 1.2 m level are connected to an Em50 logger set to log data every 12 hours. The HOBO® U30 logger records weather data every hour.

Results and Discussion

This paper will focus on results from the development rock test pads (TP3-TP7). The objective of TP8 is to evaluate rinsing and drain-down of previously leached materials. Results from TP8 are being evaluated separate from the development rock pads and are not discussed in this paper.

Selected pre-study material characterization results – Based on XRD results, chalcopyrite and pyrite were identified as the two sulphide minerals present that, upon oxidation, are most likely to release acidity, sulphate and metals into seepage. No sulphate minerals were detected in the development rock materials. Calcite, biotite, and chlorite are the minerals most likely to provide short- to medium-term neutralization capacity. Based on Net Neutralization Potential (NNP) and Neutralization Potential Ratio (NPR) criteria (ADEQ 2004), most development rock samples are classified as having an uncertain ARD potential, with the rest classified as non-acid generating. Acid Neutralization Potential (ANP) from lab titration is higher than ANP estimated from total carbon content for all samples suggesting that silicate minerals such as biotite and chlorite provide acid neutralization capacity in addition to carbonate minerals. Samples from all the development rock test pads were determined to be non-acid forming based on NAG testing (NAG pH > 4.5).

Flow mechanisms and progression of wetting-fronts – The overall water balance in a rock pile, internal moisture content and flow regimes influence the evolution of long-term seepage chemistry (Lefebvre et al. 2001, Wels et al. 2003). Spatial variability in PSD, abundance of macropores, and high rainfall intensity are factors that promote the development of preferential flow in rock piles (Momeyer 2014, Fretz 2013). Due to different water retention characteristics of sand packed in the moisture sensor boxes (100% of material < 2 mm) and the coarser test pad materials (79-93% of materials > 13 mm), VWC values recorded by the sensors do not represent actual moisture content levels within the pads. However, VWC measured by the sensors are reasonably indicative of wetting front arrival times at different test pad depths. Following the high-intensity precipitation event in January 2019 which resulted in the initial 'wetting-up' of test pads, VWC recorded by one or more sensors on the 1.2 m level are observed to be higher than those recorded by the 2.1 m level sensors for all pads. This suggests that preferential flow paths may have developed following this precipitation event. Other studies have reported similar findings (Momeyer 2014). For this study, it is assumed that a high-intensity precipitation event occurs when precipitation comparable to twice the weekly water application volume (7,600 L) or greater is received in less than a week. Following high-intensity precipitation, seepage flow consistently reached peak levels within a few hours as opposed to 3-4 days observed after weekly water applications. Additionally, the magnitude of peak

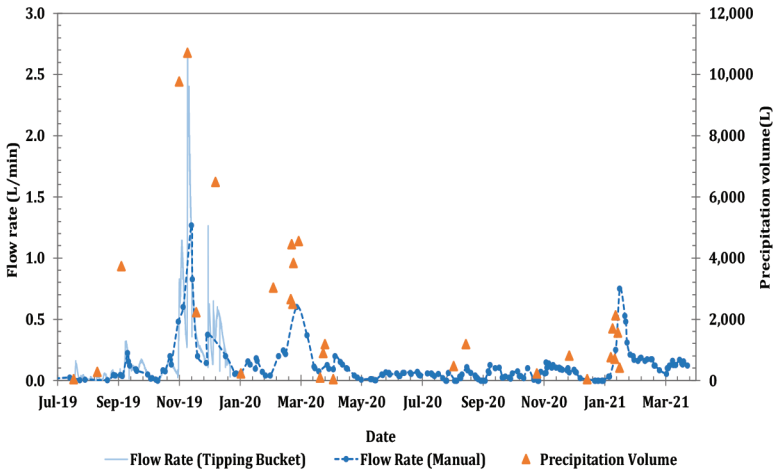

Figure 3 *Test pad TP6 tipping bucket and manual seepage flow rate measurements. Note: Precipitation volumes calculated from weather station data are plotted on the secondary y-axis.*

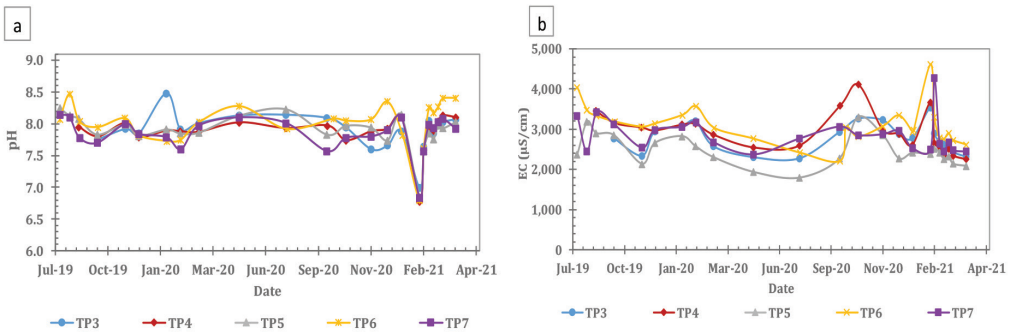

Figure 4 *Test pad seepage field parameters - (a) pH and (b) EC values.*

seepage flow rates following high-intensity precipitation events in November/December 2019, March 2020, and January 2021 were consistently higher than those measured after typical water applications. This is illustrated in Figure 3 using TP6 tipping bucket and manual seepage flow data plotted along with precipitation volumes calculated from weather station data. Manual seepage flow measured for TP6 and the other test pads are not as complete as continuous tipping bucket data. They do not always capture the actual value of peak flow following high-intensity precipitation, especially if safe site access is not available. Nevertheless, the overall findings are applicable for all test pads and consistent with development of preferential flow, which is likely to commence earlier and at greater intensities with increasing rainfall rates (Fretz 2013, Stewart 2019).

Test pad conditions and seepage chemistry – Test pad seepage pH and EC values have remained relatively constant throughout the study at 7.5-8.5 and 2,000-4,000 µS/cm, respectively (Figure 4a and b). Seepage pH values measured a few days after the high-intensity precipitation event in late January 2021 were substantially lower (pH = 6.7-7.0) but increased to the typical range within a week. These observations are consistent with fluctuations in carbon dioxide (CO_2) concentrations within the pads. Periods of higher water content are characterized by higher internal CO_2 levels resulting in

decreased pore water pH. Drain down of the test pads promotes an increase in CO_2 degassing to the atmosphere and subsequently an increase in pore water pH (Peterson 2014).

Degree of water saturation and flushing frequency can influence sulphide oxidation rates and solute loading in seepage (Herasymuik et al. 2006, Hollings et al. 2001). Water application was paused during periods of high-intensity precipitation to prevent constant flooding of pore spaces with water, which could slow down sulphide oxidation by limiting oxygen supply. Conditions within the test pads are not oxygen limited based on consistently positive ORP data and moderate-high DO measurements (DO ≈ 5-10 mg/L; typical DO percent saturation of 50-80%). Additionally, seepage sulfate concentrations have typically remained in the 1,000-2,000 mg/L range. Hence, the volume and frequency of water application are generally appropriate to promote sulphide oxidation by flushing out built-up oxidation products and exposing fresh mineral surfaces for further oxidation.

Preliminary Conclusions

For all development rock test pads, seepage flow response and moisture content data are consistent with the development of preferential flow paths. Based on ORP, DO, and sulfate loading in seepage, conditions within the test pads are typically not oxygen limited. Hence, the volume and frequency of water application are appropriate to promote sulfide oxidation, other mineral-water interactions and meet the objectives of this study. For the development rock test pads, seepage pH values have remained relatively constant in the circumneutral range and EC values have remained in the 2,000-4,000 µS/ cm range. Mineral reaction rates (sulfide oxidation and dissolution of calcite, biotite and chlorite) and solute release rates will be calculated to estimate the future ARD potential and seepage water quality from these materials. The findings from this study will be utilized in support of on-going mine planning, permitting, and closure planning activities at Bagdad.

Acknowledgments

The authors would like to acknowledge Emilio Delgado and Elizabeth Slade, Environmental Technicians with Freeport-McMoRan in Bagdad, Arizona, for their efforts on operation, monitoring, and maintenance activities.

References

ADEQ, 2004. Arizona Mining Guidance Manual BADCT. Aquifer Protection Program. Publication # TB-04-01. Phoenix, Arizona: Arizona Department of Environmental Quality.

Fretz, N. M., 2013. Multi-year hydrologic response of experimental waste-rock piles in a cold climate: Active-zone development, net infiltration, and fluid flow. Master's Thesis. The University of British Columbia, Vancouver.

Herasymuik, G., Azam, S., Wilson, G.W., Barbour, L. S., Nichol, C., 2006. Hydrological Characterization of an Unsaturated Waste Rock Dump. Sea to Sky Geotechnique; 751-757.

Hollings, P., Hendry, M. J., Nicholson, R. V., and Kirkland, R. A., 2001. Quantification of oxygen consumption and sulfate release rates for waste rock piles using kinetic cells: Cluff Lake Uranium Mine, Northern Saskatchewan, Canada. Applied Geochemistry, 16 (9–10), 1215–1230.

Kempton, H., 2012. A Review of Scale Factors for Estimating Waste Rock Weathering from Laboratory Tests. In: Price WA, Hogan C, and Tremblay G editors. ICARD 2012. Proceedings of the 9th International Conference on Acid Rock Drainage (Vol 1); Ottawa, Canada: 1026-1037.

Lefebvre, R., Hockley, D., Smolensky, J., Gélinas, P., 2001. Multiphase transfer processes in waste rock piles producing acid mine drainage: 1: Conceptual model and system characterization. Journal of Contaminate Hydrology. 52, 137–164.

Momeyer, S.A., 2014. Hydrologic Processes in unsaturated waste rock piles in the Canadian subarctic. Master's Thesis. The University of British Columbia, Vancouver.

Nordstrom, D.K., Blowes, D.W., Ptacek, C.J., 2015. Hydrogeochemistry and microbiology of mine drainage: an update. Applied Geochemistry 57:3–16.

Pearce, S., Scott, P., Webber, P., 2015. Waste rock dump geochemical evolution: matching lab data, models and predictions with reality. In Proceedings of the 10th International Conference on Acid Rock Drainage and IMWA 2015; Santiago, Chile.

Percak-Dennett, E., He, S., Converse, B., Konishi, H., Xu, H., Corcoran, A., Noguera, D., Chan, C., Bhayyacharyya, A., Borch, T., Boyd, E., Roden, E.E., 2017. Microbial acceleration of aerobic pyrite oxidation at circumneutral pH. Geobiology 15(5):690-703.

Peterson, H. E., 2014. Unsaturated hydrology, evaporation, and geochemistry of neutral and acid rock drainage in highly heterogeneous mine waste rock at the Antamina mine, Peru. Doctoral Thesis. The University of British Columbia, Vancouver.

Stewart, R.D., 2019. A generalized analytical solution for preferential infiltration and wetting. Vadose Zone J. 18 (1): 1-10.

Wels, C., Lefebvre, R., & Robertson, A. M., 2003. An overview of prediction and control of air flow in acid-generating waste rock dumps. Proceedings of the 6th International Conference on Acid Rock Drainage (ICARD), pp. 639-650.

Western Regional Climate Center (WRCC), 2016. Period of Record Monthly Climate Summary, Period of Record: 5/ 1/1925 to 6/10/2016. Accessed on 4/7/2021, from Bagdad, Arizona (020586): http://www.wrcc.dri.edu/cgi-bin/cliMAIN.pl?az0586

Incorporating 2D Analytical Results into 3D Graphical and Multidisciplinary Mining Models

Hannah Redfern, James Catley, Grace Yungwirth

Golder Associates (UK) Ltd., Suite 9.10, 20 Eastbourne Terrace, London, W2 6LG, UK, hredfern@golder.com, jcatley@golder.com, gyungwirth@golder.com

Abstract

Front end mining studies inform the project development process by assessing key risks and developing an increased understanding of the available site data. 2D analytical models can be appropriate to support hydrogeological assessments during early studies given the level of data available, and the level of confidence required. Incorporating these results into a 3D model can transform a simple methodology into a visual representation which can be integrated with other aspects of multi-disciplinary studies. This methodology incorporates groundwater flow analyses into a 3D surface within standard industry software, Leapfrog Works™, to support an assessment for a proposed open pit mine.

Keywords: Mine water, Pit Inflows, Groundwater, Geotechnical, 3D Visualisation

Introduction

To support Pre-feasibility Studies (PFS) for open pit mining projects, simplified 2D analytical groundwater flow analyses are often used to estimate the potential seepage into the pit, as well as the extent of the cone of depression of the phreatic surface around the pit which is used to inform the understanding of water management measures needed during mining. The results may be incorporated into preliminary geotechnical slope designs as well as used to indicate the likely water management measures needed to stabilise pit slopes. During a recent Golder project, a simple analytical solution, developed by Marinelli and Niccoli (2000), was used to calculate pit inflows and steady state drawdown at representative sections around a proposed open pit. A workflow was created to incorporate these 2D results into a 3D surface for use in the project's Leapfrog model (Seequent Limited 2021), to show the mined out phreatic levels in relation to the topography and pit shell, allowing a cost-effective and visual approach with an appropriate degree of certainty to support the PFS. It is important to note that the appropriateness of this methodology should be assessed on an individual basis dependent on the site condition, hydrogeologic complexity, and level of risk related to groundwater control at the site.

Methodology

The following steps present the high-level methodology created to incorporate 2D analytical results from representative hydrogeological sections, into a 3D surface showing the expected phreatic surface based on pit shells provided by the client.

1. Select representative cross sections around the pit in each of the key domains and to allow appropriate spatial coverage. Multiple conceptual pit geometries may be required due to the site-specific conditions.
2. Calculate the pit inflow and pore pressure profiles for each of the identified cross sections through the conceptual pit geometries using the Marinelli and Niccoli's solution.
3. Using a drafting software, from the calculated drawdown profiles for each conceptual pit or domain, produce a series of circles using the calculated radii and water level elevation to produce a 3D representation of the drawdown profile around each conceptual pit or domain.

4. Export the representative profiles as .dwg files and import them into Leapfrog as polylines.
5. Created a triangulated mesh from each profile, to generate a cone for each domain.
6. Translate the cones so that they lined up with the toe of the pit in the relevant domains.
7. Extract a set of vertices from each cone and filter for the proportion of the cone required to build the final surface.
8. Within Leapfrog create a new surface showing the pre-mining phreatic level, extending to a reasonable distance away from the pit.
9. Added the filtered pointsets into the surface created in Step 8.

Application of the 2D Analytical Solution

The Marinelli & Niccoli (2000) solution is a closed form solution which assumes simplified steady-state 2D flow conditions, **Figure 1**. The solution also assumes a generalised and uniform circular pit geometry, in order to represent a planned pit with an irregular shape and spatially variable hydrogeological and geotechnical conditions the method was modified to consider several representative sections of the planned pit.

Where W is the distributed recharge flux, K_{h1} is the horizontal hydraulic conductivity in Zone 1, K_{h2} is the horizontal hydraulic conductivity in Zone 2, K_{v2} is the vertical hydraulic conductivity in Zone 2, h_o is the initial (pre-mining) saturated thickness above Zone 1, h_p saturated thickness at the pit wall, r_p is the effective pit radius and d is the depth of the pit lake.

For the purpose of the inflow analysis for this project, the pit geometry was generalised to be represented as three circular conceptual pit - 'east', 'west' and 'satellite'. These were chosen following analysis of the geotechnical and hydrogeological data collected during Golder's site investigation and discussed with the geotechnical engineers. The representation of the west pit geometry was further divided to account for the large variation in pre-mining water levels around the pit as these have a significant impact on the inflow calculations (see Figure 2 for pit geometry conceptualisation).

From the hydrogeological conditions for the site, the total pit inflows and radii of influence were calculated for each of the generalised pit approximations (see Figure 3 for example radii of influence). Each pit conceptualisation was weighted to reflect the proportion of inflow the actual pit geometry would receive from each of the approximated circular pits, given in Table 1.

Converting the data into Leapfrog

From the calculated drawdown profiles, a series of 16 circles were produced in AutoCAD for each of the conceptual pits. Each circle had a calculated radius and elevation to represent increasing distances from the pit to provide a visual representation of the drawdown profile. These were exported as .dwg files and imported into Leapfrog as polylines. From the polylines a triangulated mesh was created to generate a cone for each domain, an example is provided in Figure 4. Each of the cones were

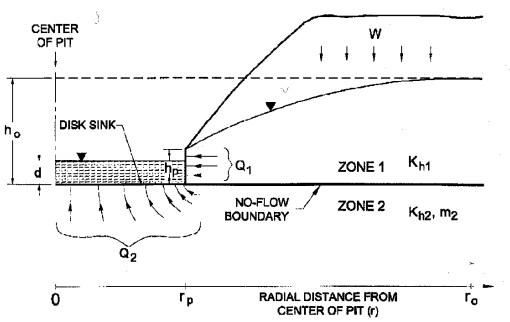

$$h_o = \sqrt{h_p^{\,2} + \frac{W}{K_{h1}}\left[r_o^2 \ln\left(\frac{r_o}{r_p}\right) - \frac{\left(r_o^2 - r_p^2\right)}{2}\right]},$$

$$Q_1 = W\pi\left(r_o^2 - r_p^2\right),$$

$$Q_2 = 4r_p\left(\frac{K_{h2}}{m_2}\right)\left(h_0 - d\right),$$

$$m_2 = \sqrt{\frac{K_{h2}}{K_{v2}}}$$

Figure 1 Pit Inflow Analytical Model (from Marinelli & Niccoli 2000).

Table 1 Percentage weighting of calculation totals.

Pit Geometry	West Pit (A)	West Pit (B)	West Pit (C)	East Pit	Satellite Pit
Percentage of pit geometry contributing inflows	25%	25%	25%	60%	100%

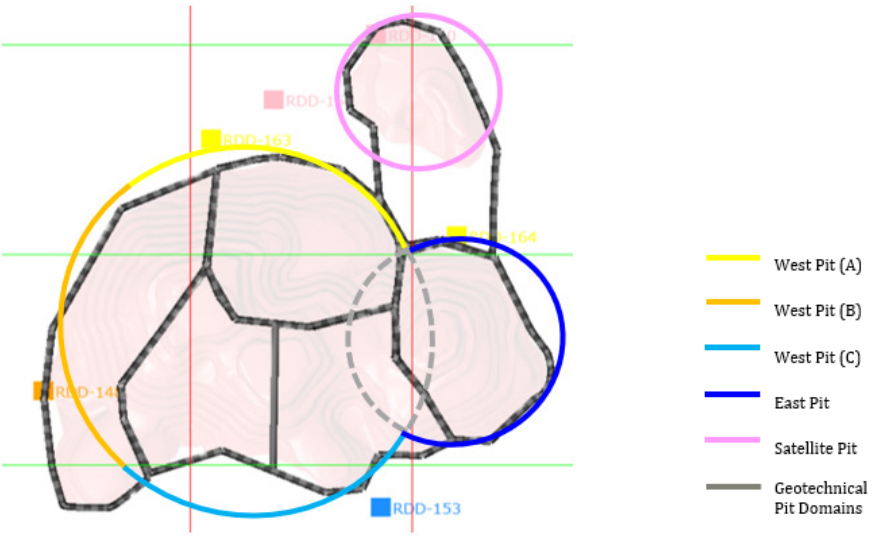

Figure 2 Conceptualised Pit Geometries.

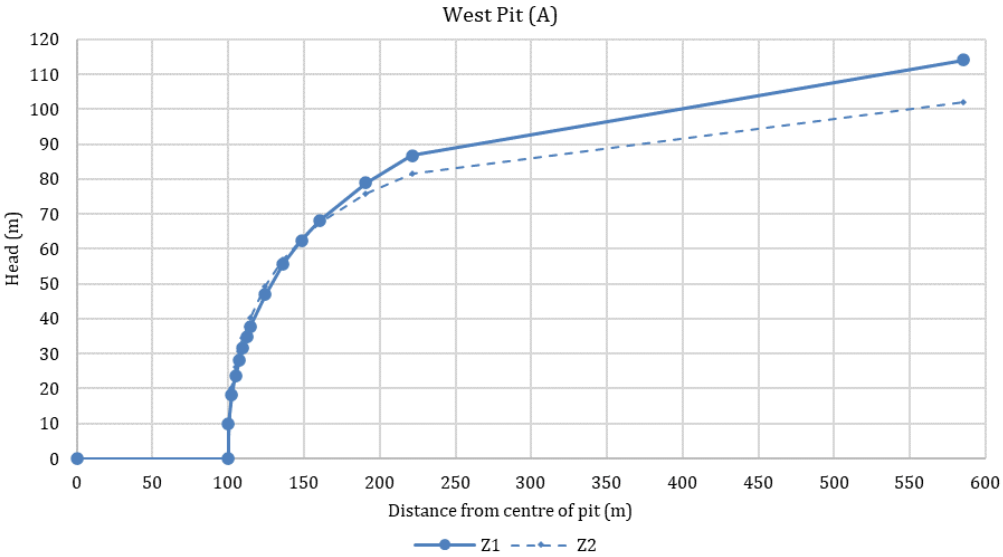

Figure 3 Example calculated drawdown profile.

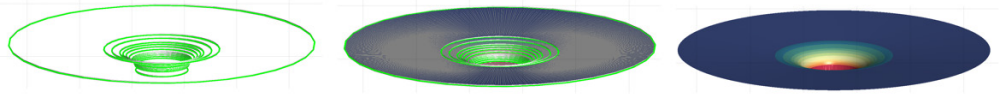

Figure 4 Imported polylines and triangulated mesh Leapfrog surface created for one of the conceptual pits.

manually translated to ensure they line up with the toe of the pit in the relevant domains by visually comparing them to the pit shell within the Leapfrog model.

Recombining the Conceptual Pits

For each of the cones created above, a set of vertices were extracted and each point "categorised" within Leapfrog to reflect the conceptual pit they represent. The "query" filter within Leapfrog was used to choose which points were required in the final surface to reflect the planned pit geometry, the points chosen were consistent with the conceptualisation shown in Figure 2.

A pre-mining phreatic surface was created from existing site water levels, extending to a reasonable distance away from the pit to be outside the radius of influence. The mining induced phreatic levels will be cut into this surface, by adding in the pointsets created above.

The project used for this example was located within a mountainous region with steeply dipping topography around the pit. Adding the mining induced water levels into the pre-mining phreatic surface allowed the final surface to be aligns with the cone segments in each domain whilst reflecting the topography at the extents of the surface away from the pit area (Figure 5).

Integration with Geotechnical Slope Design

Being able to incorporate the post mining phreatic surface into the Leapfrog model allowed geotechnical engineers to visualise and assess the expected pore pressures against other key surfaces (Figure 6). The geotechnical slope stability analysis incorporated the expected pore pressure to determine the design slope angle.

Conclusions and Application

For front end mining studies, the level of data available is often not sufficient to support development of complex 3D hydrogeological models. The results provided by 2D analytical calculations provide a cost-effective solution and often produce suitable results to support

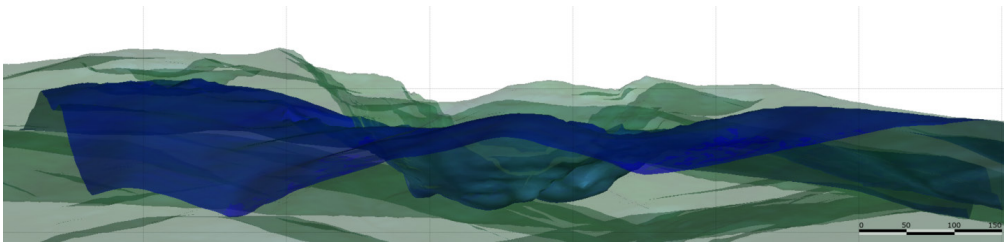

Figure 5 Topography showing mined out pit shell (Green) & Mined out phreatic surface (Blue).

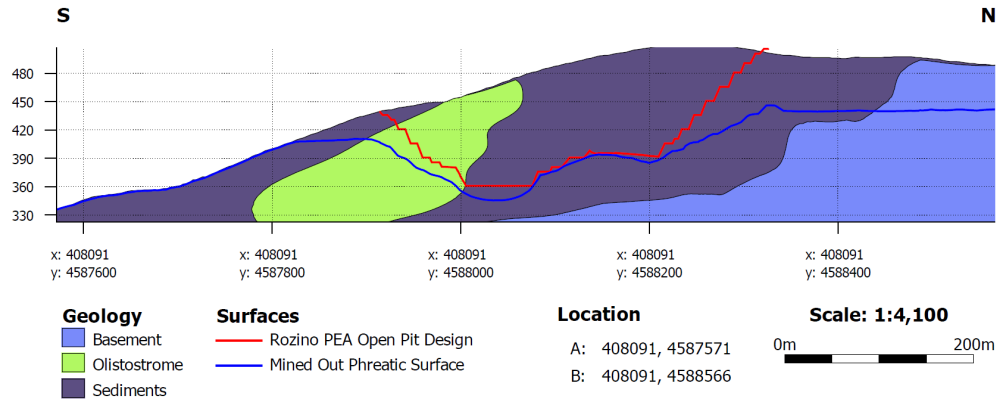

Figure 6 Section showing the geology, pit shell and mined out phreatic surface.

the level of study required, dependent on-site condition and level of risk related to groundwater control at the site. This example used Marinelli & Niccoli's solution however the methodology could be applied to the results of other 2D analyses. As Marinelli & Niccoli's calculations assume a generalised and uniform pit geometry. The calculations can be undertaken for several sections or domains to represent changes in pit geometry, domaining, and hydrogeological conditions.

Transferring the results of the 2D hydrogeologic study into 3D Leapfrog software allows greater collaboration between study disciplines and provides a valuable visual representation of the study results, such as the effect of pit dewatering and geotechnical slope stability considerations to be more easily calculated and visualised by the client and stakeholders. As the project progresses, a more comprehensive hydrogeological modelling should be undertaken once such sufficient data and hydrogeologic understanding is developed.

This workflow was created and executed collaboratively by hydrogeologists, geotechnical engineers, geologists, and technicians within Golder's UK based mining team. It is recognised that this process could be streamlined and assisted by more comprehensive templates and CAD documents.

References

Marinelli, F., and Niccoli, W.L. (2000). Simple Analytical Equations for Estimating Ground Water Inflow to a Mine Pit. Ground Water 38 (2), pp. 311-314.

Seequent Limited. (2021). Leapfrog Works (3.0.1). [Software]. [Accessed 10 October 2019].

A GIS-Based Prioritisation of Coastal Legacy Mine Spoil Deposits in England and Wales for Effective Future Management

Alex L. Riley[1], Patrizia Onnis[2], Elin Jennings[2], Richard A. Crane[2], Karen A. Hudson-Edwards[2], Sean D.W. Comber[3], Ian T. Burke[4], Patrick Byrne[5], Catherine J. Gandy[6], Adam P. Jarvis[6], William M. Mayes[1]

[1]*Department of Geography, Geology and Environment, University of Hull, Hull, HU6 7RX, UK, a.l.riley@hull.ac.uk*

[2]*Environment & Sustainability Institute and Camborne School of Mines, University of Exeter, Penryn, TR10 9DF, UK*

[3]*School of Geography, Earth and Environmental Sciences, Plymouth University, Plymouth, PL4 8AA, UK*

[4]*School of Earth and Environment, University of Leeds, Leeds, LS2 9JT, UK*

[5]*School of Biological and Environmental Sciences, Liverpool John Moores University, Liverpool, L3 3AF, UK*

[6]*School of Engineering, Newcastle University, Newcastle upon Tyne, NE1 7RU, UK*

Abstract

Increases in coastal flooding and erosion due to climate change threaten many coastal mine waste deposits in the UK. As such, a robust approach to prioritising sites for management is required. A spatial dataset of 9094 mine spoil deposits in England and Wales was analysed against coastal erosion and flood projections to identify deposits most at-risk. Of these, 58 were at risk of tidal flooding and 33 of coastal erosion over the coming century. Within the 10 highest-priority deposits, 426,283 m^3 of spoil was at risk of release by erosion, with Blackhall Colliery (County Durham) being the largest predicted contributor.

Keywords: GIS, Climate Change, Coastal Erosion, Tidal Flooding, Mine Spoil

Introduction

The long history of mining in the UK has resulted in a substantial legacy of mine wastes within the environment (Johnston *et al*. 2008). As the deposition of many of these wastes predated our contemporary waste management principles, adverse effects are persistent within the environment through the release and transport of metals and mineral fines from spoil heaps. These effects are of particular concern in coastal environments, which have seen extensive deposition of mining wastes in coastal metal ore- and coal-fields in many jurisdictions (Castilla 1996; Dold 2007; Kwong *et al*. 2019). Increases in the likelihood and severity of flooding and erosion due to climate change (Burningham and French 2017) further threaten coastal waste deposits. A robust approach to prioritising such deposits based on environmental risk is required to aid future management, as limited public funds are available to manage and mitigate impacts at these sites.

Given the abundance and widespread distribution of mine waste sites across the UK (Environment Agency, 2008), a case-by-case field-based risk assessment of each individual spoil deposit may become practically and financially unfeasible. National scale GIS-based prioritisation exercises offer a potentially powerful tool to address this issue, and in particular, have previously been used to screen for, and rank, legacy mine sites in terms of their likely negative environmental impact (Mayes *et al*. 2009). In coastal settings, similar approaches have been used for assessing environmental risks posed by a range of former municipal and industrial waste sites (Le Cozanett *et al*. 2013, Irfan *et al*. 2019). By prioritising sites using

this approach, which can be readily adapted to suit different requirements, a shortlist of sites may be produced and used as an initial guide to better-direct resources for intensive field-based investigations.

Methods

A spatial dataset of metal and coal spoil areas in England and Wales, originating from digitised historical OS maps (previously collated in Mayes *et al.* (2009)), was analysed against predictive datasets of tidal flood risk and future coastal erosion; key factors which may exacerbate pollutant release. To specify spoil type within this dataset, a spatial join was performed in ArcMap 10.7.1 GIS software, using the British Geological Survey Britpits dataset as reference for historically-mined commodities (Crane *et al.* 2017). A spatial screening was also used to identify spoil deposits which physically intersected areas of predicted coastal erosion over 20, 50, and 100-year timescales (from 2018, the baseline for erosion estimates within the dataset), and high-risk tidal flood zones.

A multicriteria decision analysis (MCDA) approach was applied to prioritise spoil areas based on their environmental risk, specifically in terms of coastal processes likely to be exacerbated by climate change. Adapted from a similar study of historical landfills by Irfan *et al.* (2019), Table 1 details the datasets and data processing techniques used to generate values for MCDA for the following criteria; a) the proximity of sites to the current coastline, b) proximity of sites to sensitive receptors (in this case Sites of Special Scientific Interest (SSSIs)), c) area of spoil at risk of coastal erosion at 20, 50, and 100-year intervals, and d) the area of spoil at risk of tidal flooding.

Due to differences in the distributions and units of values generated (Tab. 1), data were normalised and scaled using the Score Range Procedure such that all values ranged from 0 to 1 (Malczewski 1999). Criteria were then ranked based on their relative importance and weighted using the Rank Sum method (Malcewski 1999). The rank assigned to each criterion was based on the combined expertise of the authors, with the rationale for this, and the normalised weights, presented in Table 2. Following weighting, scaled values for each criterion were multiplied by the respective criterion weight, and summed to produce an overall risk score for each spoil area in the database. This was repeated for each of the three timescales of erosion projections, and used to generate ranked lists of mine spoil deposits.

For sites identified as being higher-priority, estimates were made of the volumes of material at risk of being liberated by coastal erosion processes over the next 100 years. Using a combination of high-resolution LiDAR data, historical maps, and erosion buffer zones (Tab. 1), the volume of mine spoil at risk of erosion within the 10 highest-scoring sites was calculated, as per the methods detailed in Riley *et al.* (2020).

Table 1 *Spatial datasets and data processing methods used in the MCDA prioritisation (Specific ArcMap tool names are written in italics). EA = Environment Agency, NRW = Natural Resources Wales.*

Criteria	Origin Database	Source	Data Processing
Distance from coastline (m)	National Coastal Erosion Risk Management (NCERM)	EA, NRW	Datasets merged to single shapefile, *'Near'* analysis.
Proximity to SSSIs (m)	SSSI designation shapefiles	Natural England, NRW	*'Near'* analysis.
Area at risk of coastal erosion (m^2)	NCERM	EA, NRW	Datasets merged, *'Buffer'* generated for shoreline management plan projections (20, 50, and 100-year, 95% CI), *'Intersect'* analysis on overlapping spoil.
Area at high risk of tidal flooding (m^2)	Flood Map for Planning (Zone 3)	EA, NRW	Datasets merged, and filtered by Tidal Model type to remove fluvial flood risk areas. *'Intersect'* analysis on overlapping spoil.

Table 2 Ranking and normalised weights of each criterion used in the MCDA prioritisation process (Rank 1 = highest importance).

Criteria	Rank	Rationale	Weight
Area at risk of coastal erosion	1	Coastal erosion and subsequent transport of spoil fines is considered the primary pollutant release pathway in the coastal zone.	0.4
Area in tidal Flood Zone 3	2	Tidal floods inundate spoil with saline waters and may instigate pollutant release and affect spoil heap integrity, leading to release. Zone 3 has > 1-in-200 annual probability of tidal flooding.	0.3
Proximity to SSSIs	3	SSSIs represent sensitive receptors in the environment, where pollutants will have highest impact.	0.2
Distance from coastline	4	Spoil closer to the coastline typically has greater likelihood of affecting coastal zone than those further inland.	0.1

Results and Discussion

Mine Spoil Database Screening

The mine spoil database contained a total of 9094 spoil areas, accounting for over 528 million m^2 of spoil distributed across England and Wales. Intersect analysis indicated that of these spoil areas, 58 were at a high risk of tidal flooding, and 33 were at risk of coastal erosion over the next 100 years. A summary of the area of *coastal* mine spoil deposits (defined here as those within 2 km of the current coastline) is shown in Figure 1, which reveals the largest areas to be located in the South West River Basin District (RBD; approximately 9 million m^2); a major centre of historical copper and tin mining (Jordan *et al.* 2020). Substantial deposits were also identified in Northumbria (predominantly coal) and Western Wales (lead / zinc mining wastes), with approximately 6 million m^2 and 4 million m^2, respectively. Other key regions of interest include North West England, a centre for historical coal and iron mining, and the Dee on the border of England and North Wales (primarily coal and Pb). Modest areas

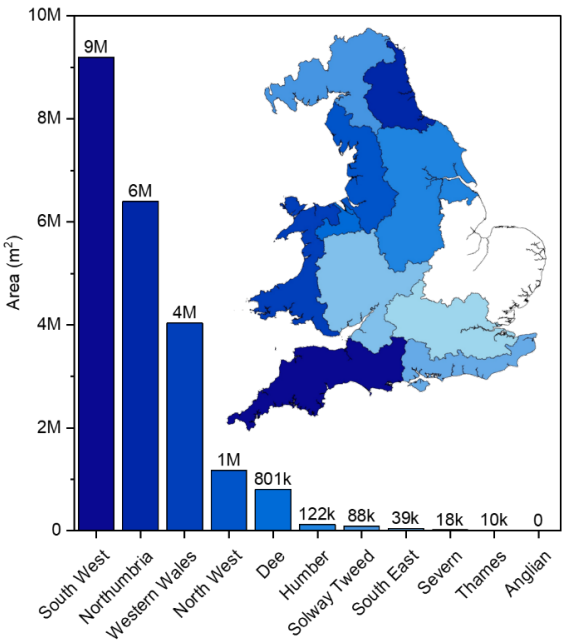

Figure 1 Calculated areas (m^2) of mine spoil within 2 km of the coastline, summarised by RBD.

of coastal spoil were present in the Humber (primarily ironstone), Solway Tweed (coal and iron), the Thames (coal), Severn (coal), and South East (coal) RBDs.

Site Prioritisation Analysis

During the MCDA, each of the 9094 spoil areas were assigned three risk scores, related to the short, medium, and long-term risks, using the criteria in Table 2. Sorting spoil areas by these scores provides an indication of the sites which present a greater risk to the coastal environment, and is useful for determining higher-priority sites at national and regional scales. Although subtle changes in rank positions were observed when assessing sites over different temporal scales for predicted erosion, Dawdon Blast Beach, an area of extensive historical dumping of coal spoil on the Northumberland coastline, was consistently of highest priority (Tab. 3). All sites within the top 10 rank positions were comprised of coal spoil, which may be expected given extensive coastal coal mining legacies in both Wales and northern England (Johnston *et al*. 2008). Sites in the South West, despite having the highest areal extent (Fig. 1) were generally of lower-risk in this analysis, likely due to clifftop locations of many historical Cu-Sn spoil deposits in the area (Rainbow 2020), and the protection from flooding offered by elevated settings.

Coastal Mine Spoil Volume Estimation

Assessments of spoil volume at priority sites offered more insight into potential erosive losses and subsequent environmental risk than areal estimates alone. Of the 10 highest-priority spoil deposits, intersect analysis indicated that four of these sites were predicted to be affected by coastal erosion in modelled future scenarios. Of these sites, Blackhall Colliery in County Durham (ranked 2nd for medium-term risk; Tab.3), was the largest spoil deposit in terms of total volume (>4.3 million m^3; Tab. 4). Interestingly, despite consistently ranking in the highest position, Dawdon Blast Beach contained substantially less waste than other sites within Table 4. This could possibly be linked to major waste removal operations at the site during the 1990s (Heritage Coast 2021) which may not be accurately captured in shapefile data. Furthermore, this suggests that future prioritisation analyses should employ the waste *volume* at risk of erosion as a criterion, as opposed to waste *area*, where feasible to calculate.

Coastal erosion projections coupled with volume estimates indicated that in addition to being the largest deposit, wastes at Blackhall Colliery were also most susceptible to coastal erosion, with over 358,000 m^3 of spoil predicted to be liberated over the next 100 years based on current shoreline

Table 3 *The 'top 10' legacy mine spoil deposits identified as being most at-risk in England and Wales within short-term (S: 20-year), medium-term (M: 50-year), and long-term (L: 100-year) timescales.*

Rank			Site Location	RBD	British National Grid Reference	Waste Type
S	M	L				
1	1	1	Dawdon Blast Beach, Seaham	Northumbria	NZ 43556 47893	Coal Spoil
2	3	2	Gas Terminal, Talacre	Dee	SJ 12630 83697	Coal Spoil
3	2	3	Blackhall Colliery, County Durham	Northumbria	NZ 46125 39734	Coal Spoil
4	5	5	Dee Bank, Bagillt	Dee	SJ 21596 75960	Coal Spoil
5	4	4	Wind Farm, Workington	North West	NX 99590 30795	Coal Spoil
6	6	6	Loughor Foreshore, Gorseinon	Western Wales	SS 57087 98795	Coal Spoil
7	8	7	Coast Road, Mostyn	Dee	SJ 16355 80311	Coal Spoil
8	9	8	Jackson Dock, Hartlepool	Northumbria	NZ 51574 32890	Coal Spoil
9	10	9	Port of Blyth, Blyth	Northumbria	NZ 30418 82324	Coal Spoil
10	-	10	Mostyn Road, Greenfield	Dee	SJ 19143 78025	Coal Spoil

Table 4 Volume estimates of high priority spoil areas which intersect coastal erosion risk zones, and cumulative volumes of spoil predicted to be eroded at each timescale.

Site Name	Total Volume	20-year Erosion Projection	50-year Erosion Projection	100-year Erosion Projection
	m^3	m^3	m^3	m^3
Blackhall Colliery, County Durham	4,319,910	97,754	193,182	358,863
Wind Farm, Workington	874,051	0	4,603	35,751
Dawdon Blast Beach, Seaham	301,898	2,108	4,456	26,667
Loughor Foreshore, Gorseinon	188,535	0	971	5,002

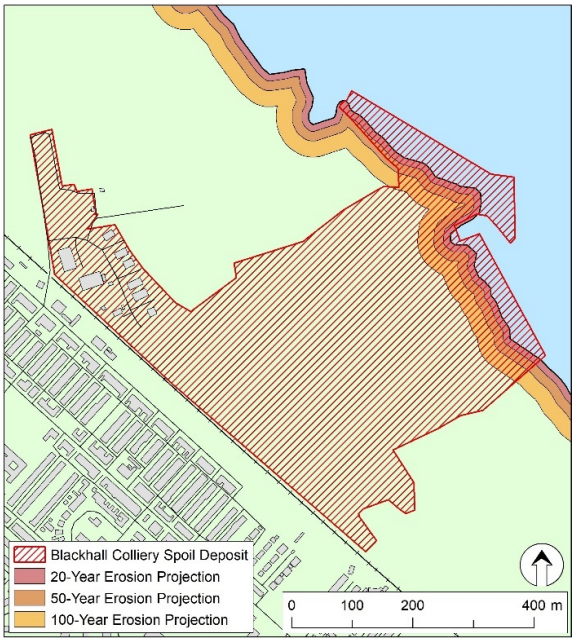

Figure 2 Blackhall Colliery waste deposit in relation to projected 20-, 50-, and 100-year extents of coastal erosion (buffer zones generated using NCERM dataset (Tab. 1) then used in volume estimation as per Riley et al. 2020).

management plans (Tab. 4; Guthrie and Lane 2007). The spatial extent of erosion predicted at Blackhall Colliery is shown in Figure 2, where estimates indicate a coastal retreat of approximately 50 m in the next 100 years. The seaward extension of the spoil deposit boundary is representative of the area of spoil already released via coastal processes.

Both of the Northumbrian sites in Table 4 were predicted to release substantial waste volumes within the next 20 years. The remaining sites, at Workington and Gorseinon, were not predicted to be at risk of coastal erosion in the short-term, but moderate volumes of spoil were deemed at risk over longer timescales, which can also be observed by changes in rank over time, particularly for Workington (Tab. 3). The potential erosive losses identified illustrate the urgent need for risk assessments to inform coastal management practices at these locations.

Conclusions

Legacy mine spoil wastes are present across all regions of the UK and are particularly related to historical coal extraction. The largest areas of coastal spoil were present within the South West, although most regions

contained coastal mine spoil deposits. A GIS-based approach to prioritise these deposits in relation to risks posed to the coastal zone was completed, based on several criteria related to physical coastal processes and proximity to sensitive environmental receptors.

Multicriteria decision analysis allowed for ranking of sites, and indicated that coal spoil deposits posed the greatest risk to the coastal environment, predominantly within the Northumbria and Dee RBDs. Despite their abundance, the flood defence offered by clifftop settings of wastes in the South West RBD resulted in lower risk scores. Within the 10 most at-risk sites, 99,862 m^3 of spoil was at risk of erosion within 20 years, rising to 203,212 m^3 and 426,283 m^3 over the next 50 and 100 years, respectively. Of particular importance were Dawdon Blast Beach, the highest-ranked site, and Blackhall Colliery, the site with potential to release the highest volume of waste (358,863 m^3). This work represents the first UK national prioritisation method for screening coastal mine spoil sites in response to projected climate change effects. Such analysis is crucial for ensuring that resources are best allocated for future management of coastal legacy wastes, and is a method that can be readily expanded to cover additional risk factors, and applied elsewhere to a wide range of nationally-important legacy waste stockpiles from other sources.

Acknowledgements

The authors thank the organisers and hosts of the IMWA2021 Conference, in addition to the anonymous reviewers of this manuscript, whose comments have been valuable during the peer-review process. Thanks to Dr Hugh Potter (Environment Agency) for provision of some of the mine-related spatial data that were used here. This work was funded by the Natural Environment Research Council (NERC) under grant number NE/T003022/1 (Legacy wastes in the coastal zone: Environmental risks and management futures).

References

Castilla JC (1996) Copper mine tailing disposal in northern Chile rocky shores: Enteromorpha compressa (Chlorophyta) as a sentinel species. Environ Monit Asess 40:171-184

Dold (2007) Biogechemical Processes in Mine Tailings with Special Focus on Marine Shore Tailings Deposits and their Remediation. Adv Mat Res 20-21:177-185

Burningham H, French J (2017) Understanding coastal change using shoreline trend analysis supported by cluster-based segmentation. Geomorphology 282:131-149

Crane RA, Sinnett DE, Cleall PJ, Sapsford DJ (2017) Physicochemical composition of wastes and co-located environmental designations at legacy mine sites in the south west of England and Wales: Implications for their resource potential. Resour Conserv Recy 123:117-134

Gandy CJ, Younger PL (2007) Predicting Groundwater Rebound in the South Yorkshire Coalfield, UK. Mine Water Environ 26:70-78

Guthrie G, Lane N (2007) Shoreline Management Plan 2: River Tyne to Flamborough Head. Royal Haskoning Ltd, Peterborough, United Kingdom https://northeastcoastalobservatory.org.uk/data/reports/ [Accessed 19/04/21]

Heritage Coast (2021) Turning the tide. Heritage Coast https://durhamheritagecoast.org/our-story/history/turning-the-tide/ Accessed 19/04/21

Irfan M, Houdayer B, Shah H, Koj A, Thomas H (2019) GIS-based investigation of historic landfill sites in the coastal zones of Wales (UK). Euro-Mediterranean Journal for Environmental Integration 4(1):26

Johnston D, Potter H, Jones C, Rolley S, Watson I, Pritchard J (2008) Abandoned mines and the water environment. Science Project SC030136-41. Environment Agency, Bristol.

Jordan A, Hill R, Turner A, Roberts T, Comber S (2020) Assessing Options for Remediation of Contaminated Mine Site Drainage Entering River Teign, Southwest England. Minerals 10(8):721

Kwong YTJ, Apte SC, Asmund G, Haywood MDE, Morello EB (2019) Comparison of Environmental Impacts of Deep-sea Tailings Placement Versus On-land Disposal. Water Air Soil Poll 230:287.

Le Cozanett G, Garcin M, Mirgon C, Yates ML, Méndez M, Baills A, Idier D, Oliveros C (2013) An AHP-derived method for mapping the physical vulnerability of coastal areas at regional scales. Nat Hazards Earth Syst Sci 13:1209-1227

Malczewski, J (1999) GIS and multicriteria decision analysis. Wiley, New Jersey

Mayes WM, Johnston D, Potter HAB, Jarvis AP (2009) A national strategy for identification, prioritisation and management of pollution from abandoned non-coal mine sites in England and Wales. I.: Methodology development and initial results. Sci Total Environ 407(21):5435-5447

Rainbow PS (2020) Mining-contaminated estuaries of Cornwall – field research laboratories for trace metal ecotoxicology. J Mar Biol Assoc UK 100:195-210

Riley AL, MacDonald JM, Burke IT, Renforth P, Jarvis AP, Hudson-Edwards KA, McKie J, Mayes WM (2020) Legacy iron and steel wastes in the UK: Extent, resource potential, and management futures. J Geochem Explor 219:106630

Tracing the Water – Rock Interaction in the Ibbenbüren Mine - Towards a Reactive Transport Model for Coal Mine Drainage

Thomas Rinder[1], Diego Bedoya Gonzalez[1,2], Sylke Hilberg[1]

[1]*University of Salzburg, Department of Geography and Geology, Hellbrunner Str. 34, 5020 Salzburg, Austria*

[2]*University of Greifswald, Institute for Geography and Geology, Friedrich-Ludwig-Jahn Str. 17a, 17487 Greifswald, Germany*

Abstract

Traces of water-rock interaction in two drill cores from the West field of the former Ibbenbüren anthracite coal were related to both diagenesis and relatively recent weathering processes along open fractures. The coupled appearance of kaolinite-dickite-illite minerals in weathered and unweathered rock sections was clearly connected to the burial history of the Carboniferous sequence. In contrast, the formation of iron (oxide-) hydroxides together with the presence of oxidized pyrite in weathering profiles along both sides of the fractures was positively related to the geochemical footprint of the coal mine drainage.

Keywords: Coal Mine Drainage; Pyrite Oxidation; Water-Rock Interaction

Introduction

Coal mine drainage may often be characterized by poor water quality (Kessler *et al.* 2020). High salinity may become an environmental issue (Timpano *et al.* 2015), as it may cause toxicity to freshwater communities (Elphick *et al.* 2011). Sulfide mineral weathering can lead to the formation of acid mine drainage solutions (Galán *et al.* 2003; Neal *et al.* 2005; Nieto *et al.* 2007) in which case low pH (Simate and Ndlovu 2014) and relatively high sulfate concentrations (Wang *et al.* 2016) may have adverse toxicological effects on the receiving communities. In particular, clogging of the riverbed by the formation of hydrous ferric oxides has a negative effect on the flora and fauna of the affected rivers (McKnight and Feder 1984). In addition coal mine drainage may also carry relevant levels of toxic metals, often related to pyrite oxidation (Cravotta and Brady 2015; Gombert *et al.* 2018).

In the former anthracite coal mine in Ibbenbüren highly saline brines are present in the former East field (Rinder *et al.* 2020), whereas iron and sulfate rich solution are dominant in the former West field (see table 1).

Geological framework

The coalfield, known as the "Ibbenbürener Karbonscholle", is a horst structure of Carboniferous origin, uplifted to the surface in the Cretaceous. As a result, the coalfield is separated from the surrounding area with an offset of up to 2000 m. It consists of two hills (Schafberg and Dickenberg) divided by a NNE-SSW striking graben structure known as the Bockradener Graben (see Figure 1). The hill chain is surrounded by Triassic, Jurassic, and, to a lesser extent, Permian rock formations in the direct vicinity of the fault structure, surrounding the block. The chain reaches a maximum height of 176 m above

Table 1 *Chemical composition of mine drainage from the West- and Eastfield.*

	Temp [°C]	pH	conductivity [µS/cm]	Na^+	Ca^{2+}	K^+	Mg^{2+}	Cl^- [mg/l]	SO_4^{2-}	HCO_3^-	Fe	Ni
West field	23	3.6	3230	232	312	11	131	171	1688	37	99	0.21
East field	43	6.0	225000	77315	1193	445	464	109805	2150	100	34	< 0.05

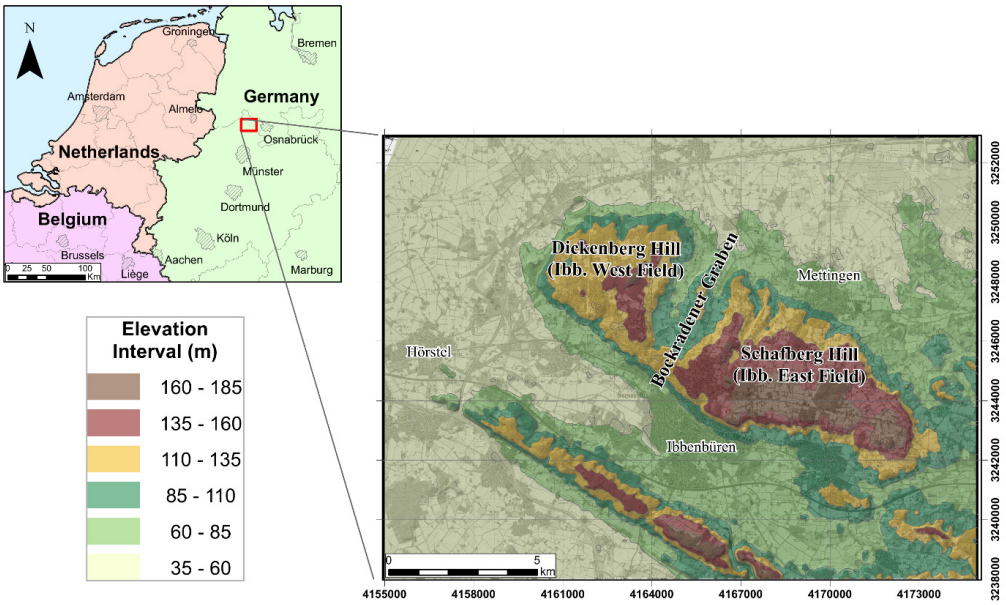

Figure 1 The Ibbenbüren coalfield; modified after (Bedoya-Gonzalez et al. 2021).

sea level, with a length of 14 km and a width of 4 to 5 km (Bässler 1970). During mining operations, the Schafberg and Dickenberg were named "East field" and "West field", respectively.

Origin of mine drainage

In an earlier study, the salinity in the deep Na-Cl brines of the East field was assigned to halite dissolution through Na/Cl and Br/Cl ratios. Within the context of the local geological situation, the origin of these brines from outside of the coalfield was suggested by $\delta^{34}S_{SO4}$ values typical for the dissolution of Mesozoic evaporites that surround the coalfield (Rinder *et al.* 2020). In addition ongoing water-rock interaction of those brines with the siliciclastic rocks of the Carboniferous host rock was indicated by radiogenic strontium. Additionally, $^{87}Sr/^{86}Sr$, $\delta^{2}H_{H2O}$, $\delta^{18}O_{H2O}$, K^{+} and Li^{+} signatures of the mine fluids indicated the presence of formation waters within the sandstones, contributing to the water chemistry (see figure 2).

In contrast, in shallow mine waters down to the third level ≈-270 m below surface showed a $\delta^{34}S_{SO4}$ composition typical for the oxidation of sulfides. No influence of halite, gypsum, or anhydrite dissolution was found in those waters. A similar situation is assumed for the West field. It represents an isolated mountain range, topographically elevated with respect to the foreland. Since flooding of the mine it discharges through the Dickenberg adit, which his elevated above the surrounding Mesozoic sediments. Accordingly, it has been hypothesized that the actual chemical signature of the drainage is influenced by the interaction of percolating rainwater with sulfur-bearing rock layers above the adit (Rudakov, Dmitry V.; Coldewey, Wilhelm G.; Goerke-Mallet 2014). Yet the chemical composition of the mine drainage changes over time, also because sulfide related acidity can be vestigial or juvenile (Younger 1997). Accordingly, the prediction of the long term chemical evolution warrants a closer investigation on possible sulfur sources.

Methodology

We investigated evidences of rock alteration in two drill cores pierced through the rock sequence above the Dickenberg adit. Drill cores were examined through a combined mineralogical and elemental analysis on thin sections using a petrographic microscope, Scanning Electron Microscope (SEM), X-ray diffraction microscope (XRD) and XRF spectroscopy. Special focus was given on signs of water – rock interaction.

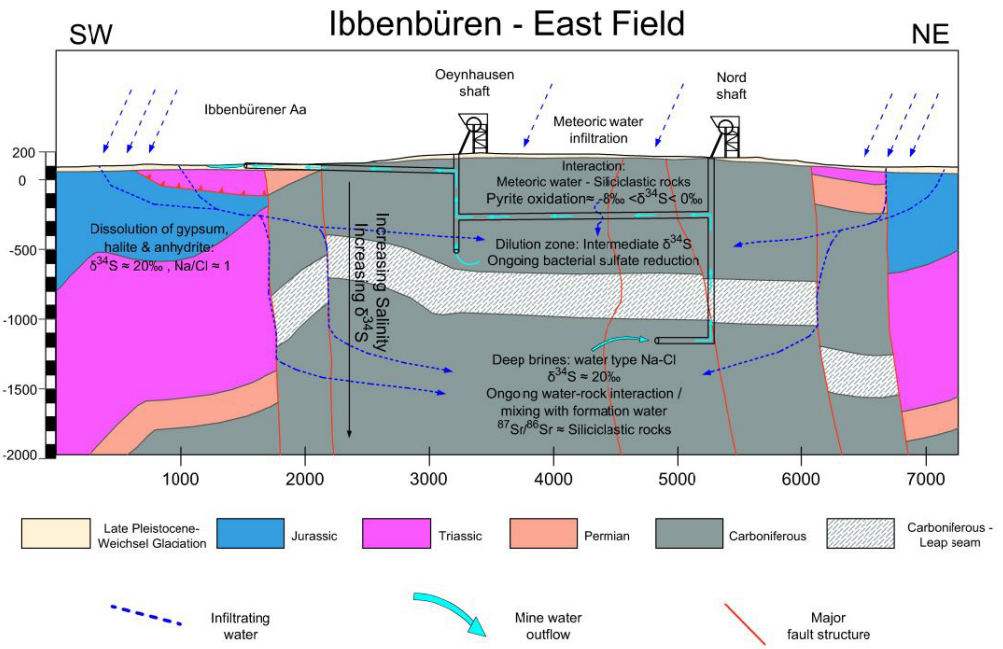

Figure 2 *Schematic cross section through the Ibbenbüren Eastfield including a conceptual hydrogeochemical model, depicting the origin and evolution of mine drainage, groundwater, and brines in the mine; taken from (Rinder et al. 2020); cross section modified after (Drozdzewski 1985).*

Results

The sandstones display high proportions of detrital quartz, with few evidences of overgrowth or sutured contacts. Most of the lithic fragments correspond to chert and ductile mudstones with sericite (Figure 3a). Additionally, several layers contain high proportions of lenses and coal fragments as frame components, some of which exhibit oxidation signs on the surrounding matrix (Figure 3b). Muscovite is detrital and together with the ductile lithics is commonly affected by compaction, being incorporated into the primary pore spaces as pseudomatrix (Figure 3a). Pyrite occurs as clusters of very fine sand and silt crystals (microcrystalline pyrite) usually associated with sedimentary lithic fragments and rarely as frame macrocrystals (Figure 3c). Finally, iron (oxide-) hydroxides were found on lithoclasts surfaces and coating the framework grains of the core intervals crossed by fractures (Figure 3d). SEM and EDX images reveal trace quantities of barite and heavy clay-size particles, enriched in strontium, lead, and Rare Earth Elements (Lanthanum, Cerium and Neodymium). These are encountered in the primary porosity of the rock, alongside the clayey matrix (Figure 3f).

Traces of water–rock interaction were assigned to two different categories. Illite, kaolinite and dickite are evenly distributed among the matrix of the weathered and unweathered rock zones and are related to the diagenesis history of the area. On the other hand, the presence of iron (oxide-) hydroxides along the fractures is linked to the dissolution of pyrite and some influence of juvenile acidity would be suggested from the geological situation. However, relatively high iron contents in the weathered zone face relatively low pyrite contents in the unweathered rocks. For instance, preliminary batch experiments on the investigated unweathered sandstones did not generate high iron or sulfate contents. The low porosity and permeability of the analyzed samples exclude deep percolation of infiltrated rainwater into the rocks. Thus, open fractures, possibly originated from mining activities, may play a significant role

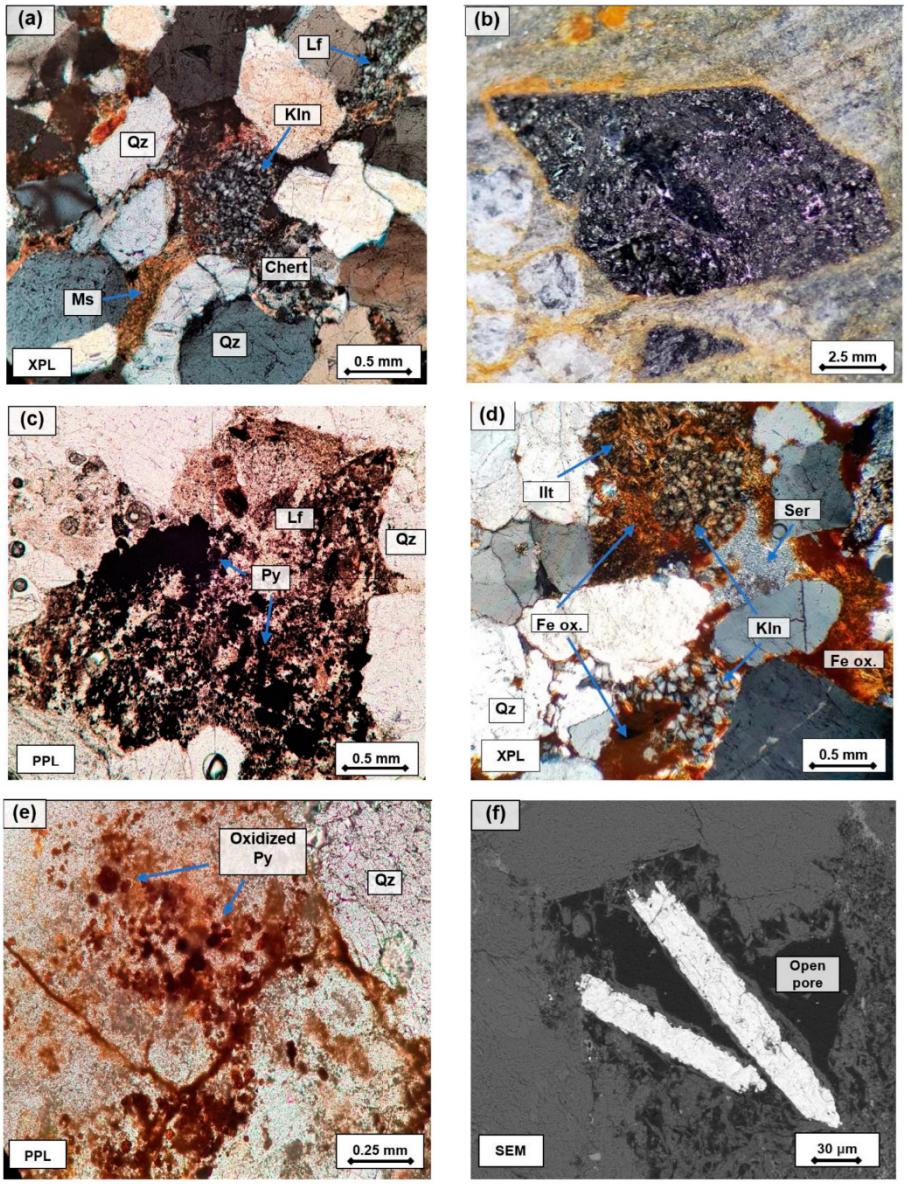

Figure 3 *Photomicrographs of the main components found in the rock sequence. Lf = lithic fragment, Ms = muscovite, Kln = kaolinite-group minerals, Qz = quartz, Py = pyrite, Ilt = illite, Ser = sericite, Fe ox. = iron (oxide-) hydroxides, PPL = plane polarized light, XPL = cross polarized light, SEM = scanning electron microscope; taken from (Bedoya-Gonzalez et al. 2021).*

in the drainage chemistry. The high contents of iron (oxide-) hydroxides could also be the result of outflowing formation water, within a relatively short timespan after the opening of the fractures. Such an explanation however, is at odds with a relatively constant and high sulfate content in the mine drainage during the last decades. Alternatively, pyrite dissolution from outside of the analyzed core samples is also possible. This points to the heterogeneity, observed within the sedimentary sequence and the challenge of upscaling observations from drill cores to complete rock sequences. The setup of a reactive transport model in the

future will hopefully provide more insights into the conditions necessary to generate the observed sulfate contents.

Acknowledgements

This work was supported by the Forum Bergbau und Wasser. Bastian Nippert (from Spang Ingenieurgesellschaft für Bauwesen, Geologie und Umwelttechnik mbH) is thanked for providing the core samples for the studied area. Natasa Ostermann is thanked for her help in the preparation of the thin sections. The authors would also like to acknowledge the facilities and the scientific assistance of the staff at the Department of Chemistry and Physics of Materials at the University of Salzburg, especially David Schiller and Fritz Finger for RFA Analyses and Gregor Zickler for his help with the SEM. We thank everybody from RAG Anthrazit Ibbenbüren for facilitating sampling and providing important insights into mine details.

References

Bässler R (1970) Hydrogeologische, chemische und Isotopen-Untersuchungen der Grubenwässer des Ibbenbürener Steinkohlenreviers. Zeitschrift der Dtsch Geol Gesellschaft 209–286

Bedoya-Gonzalez D, Hilberg S, Redhammer G, Rinder T (2021) A Petrographic Investigation of the Carboniferous Sequence from the Ibbenbüren Mine: Tracing the Origin of the Coal Mine Drainage. Miner. 11. https://doi.org/10.3390/min11050483

Cravotta CA, Brady KBC (2015) Priority pollutants and associated constituents in untreated and treated discharges from coal mining or processing facilities in Pennsylvania, USA. Appl Geochemistry 62:108–130. https://doi.org/10.1016/J.APGEOCHEM.2015.03.001

Drozdzewski G (1985) Tiefentektonik der Ibbenbürener Karbonscholle. In: Beiträge zur Tiefentektonik westdeutscher Steinkohlelagerstätten. Geologisches Landesamt Nordrhein-Westfalen, pp 189–216

Elphick JRF, Bergh KD, Bailey HC (2011) Chronic toxicity of chloride to freshwater species: Effects of hardness and implications for water quality guidelines. Environ Toxicol Chem 30:239–246. https://doi.org/10.1002/etc.365

Galán E, Gómez-Ariza J., González I, *et al* (2003) Heavy metal partitioning in river sediments severely polluted by acid mine drainage in the Iberian Pyrite Belt. Appl Geochemistry 18:409–421. https://doi.org/10.1016/S0883-2927(02)00092-6

Gombert P, Sracek O, Koukouzas N, *et al* (2018) An Overview of Priority Pollutants in Selected Coal Mine Discharges in Europe. Mine Water Environ 1–8. https://doi.org/10.1007/s10230-018-0547-8

Kessler T, Mugova E, Jasnowski-Peters H, *et al* (2020) Grundwasser in ehemaligen deutschen Steinkohlenrevieren – ein wissenschaftlicher Blickwinkel auf Grubenflutungen. Grundwasser 25:259–272. https://doi.org/10.1007/s00767-020-00460-0

McKnight DM, Feder GL (1984) The ecological effect of acid conditions and precipitation of hydrous metal oxides in a Rocky Mountain stream. Hydrobiologia 119:129–138. https://doi.org/10.1007/BF00011952

Neal C, Whitehead PG, Jeffery H, Neal M (2005) The water quality of the River Carnon, west Cornwall, November 1992 to March 1994: the impacts of Wheal Jane discharges. Sci Total Environ 338:23–39. https://doi.org/10.1016/J.SCITOTENV.2004.09.003

Nieto JM, Sarmiento AM, Olías M, *et al* (2007) Acid mine drainage pollution in the Tinto and Odiel rivers (Iberian Pyrite Belt, SW Spain) and bioavailability of the transported metals to the Huelva Estuary. Environ Int 33:445–455. https://doi.org/10.1016/J.ENVINT.2006.11.010

Rinder T, Dietzel M, Stammeier JA, *et al* (2020) Geochemistry of coal mine drainage, groundwater, and brines from the Ibbenbüren mine, Germany: A coupled elemental-isotopic approach. Appl Geochemistry 121:104693. https://doi.org/https://doi.org/10.1016/j.apgeochem.2020.104693

Rudakov, Dmitry V.; Coldewey, Wilhelm G.; Goerke-Mallet P (2014) Modeling the Inflow and Discharge from Underground Structures within the Abandoned Hardcoal Mining Area of West Field (Ibbenbüren). –. In: Sui, Wanghua; Sun, Yajun; Wang C (ed) An Interdisciplinary Response to Mine Water Challenges. 12th International Mine Water Association Congress (IMWA 2014). Xuzhou, China (China University of Mining and Technology)., pp 699 – 705

Simate GS, Ndlovu S (2014) Acid mine drainage: Challenges and opportunities. J Environ Chem Eng 2:1785–1803. https://doi.org/10.1016/J.JECE.2014.07.021

Timpano AJ, Schoenholtz SH, Soucek DJ, Zipper CE (2015) Salinity as a Limiting Factor for Biological Condition in Mining-Influenced Central Appalachian Headwater Streams. JAWRA J Am Water Resour Assoc 51:240–250. https://doi.org/10.1111/jawr.12247

Wang N, Dorman RA, Ingersoll CG, *et al* (2016) Acute and chronic toxicity of sodium sulfate to four freshwater organisms in water-only exposures. Environ Toxicol Chem 35:115–127. https://doi.org/10.1002/etc.3148

Younger PL (1997) The longevity of minewater pollution: a basis for decision-making. Sci Total Environ 194–195:457–466. https://doi.org/10.1016/s0048-9697(96)05383-1

Recovery of Cobalt and Copper from Tailings Through Enhanced Oxidation and Selective Precipitation

Mark Roberts, Nina Swain, Andrew Barnes

Geochemic Ltd, Pontypool, Wales, UK, NP45UH

Abstract

The oxidation of high sulfide tailings by ozone coupled with selective precipitation was investigated as a technique for the recovery of cobalt and copper. Iron was selectively removed from solution as precipitated oxides, with only minor loss of cobalt and copper. The remnant cobalt and copper were then precipitated out of solution forming a concentrate with 8.15% Co and 8.73% Cu with recovery rates of approximately 0.175 kg/tonne achieved. This technique, though in its early stages of development, demonstrates considerable promise as a waste valorisation system which is also capable of reducing latent acidity potential in the waste stream.

Keywords: Tailings, Valorisation, Selective Precipitation, Ozone

Introduction

The large-scale production and storage of tailings from the processing of sulfidic ore bodies continues to be one of the most enduring issues in modern mining. With numerous tailings dam failures and resulting environmental incidents this issue is increasingly entering the consciousness of the non-mining community. This coupled with both industry and governments looking to reduce the environmental impact of mining, and the world moving towards a circular economy, has meant stockpiled tailings are now being looked upon as a potential source for a number of critical metals and becoming targets for potential re-processing. The mine waste hierarchy defines prevention and re-use as the most favourable options for mine waste reduction with a reduction in both scale of waste production and the amount of potentially hazardous substances held within said wastes (Lottermoser, 2011). Up until now recovery of metals of economic interest and the remediation of tailings have been considered distinct from each other with little consideration given to a combined mutually beneficial approach.

With the ongoing shift towards green technologies and a digital economy there is an increasing need for metals required for wiring and battery / fuel cell technologies such as copper and cobalt. The future need for cobalt is such that the European Union has listed cobalt as a critical raw material at moderate supply risk. They estimate that by 2030 the demand for cobalt will have increased 5-fold, while by 2050 the demand is predicted to have increased nearly 15 times relative to 2020 demand levels (EC, 2020). There is significant concern over cobalt supply owing to a number of factors ranging from acquisition to socio-political. The nation with the largest known reserves of Co is the Democratic Republic of Congo (DRC), who's unstable political history gives rise to more supply concerns. Additionally, there is a history of human rights violations and child labour in the country bringing into question the ethics of Co sourced from DRC (Alves Diaz *et al*. 2018). Most Co is mined as a co- or by-product of copper or nickel making Co supply highly dependent on healthy markets for these other metals. This has had the side-effect that throughout history large quantities of cobalt have been lost to mine waste and tailings due to it not being the primary resource during operations. Whilst concentrations of metals of economic interest are typically low in waste residues, the vast quantities of such wastes make them potential targets for reprocessing, concentrating and recovery operations. The use of selective precipitation (SP) in place of traditional liming to remove solubilised metals from acid

mine drainage (AMD) allows for valorisation of the waste and the potential recovery of elements of economic interest (Park *et al.* 2015, Oh *et al.* 2016, Vecino *et al.* 2021), whilst remediating waste streams to meet waste/ emission standards. The generation of a revenue stream from waste treatment also opens the possibility for cost offsetting of treatment, even if the revenue stream is itself is not directly profitable. While sulfidic mine wastes will themselves, when exposed to oxygen, generate AMD and therefor mobilise metals for potential recovery, the rate and extent of oxidation may not be conducive to a practical valorisation methodology. In this paper we explore the potential for a valorisation system combining enhanced oxidation of sulfidic tailings through application of ozone (Pedrosa *et al.* 2012) with selective precipitation via the addition of sodium hydroxide (Vecino *et al.* 2021).

Methods and Materials

Testing was performed on a sample of sulfidic tailings from an iron- copper mine in Finland. The elemental composition of the tailings is displayed in Table 1. The high iron and sulfur content of the sample is reflected in the abundance of the pyrite (FeS_2) (32.8 wt.%) and pyrrhotite (FeS) (7.8 wt.%). The elevated copper is reflected in the presence of chalcopyrite ($CuFeS_2$) albeit at a lower abundance (0.6 wt. %). Deportment analysis suggests that approximately 85% of copper is present in the chalcopyrite phase (Data not shown). Acid base accounting for the sample found the waste to be potentially acid forming (PAF) with the calculated acid potential many magnitudes in excess of the negligible neutralisation potential.

Oxidation of the sample was achieved through the introduction of ozone (O_3) enriched oxygen at a rate of 2 L/min. Ozone was generated by an ENALY HG-1500 ozone generator fed with O_2 produced by a Philips Respironics EverFlo Oxygen Concentrator. The rated O_3 delivery rate was 1250 mg/hour which is equivalent to 10.4 mg (O_3) / L (O_2)). Oxidation and leaching of the tailings were performed in an adapted ASTM D 5744-18 Perspex humidity cell loaded with 2 kg (dry equivalent) of tailings sample. The base of the cell consisted of a perforated base lined with a polypropylene felt filter. Beneath this was a plenum to facilitate both draining and up flow of ozone. Ozone was continually passed, vertically, through the waste sample from below with the exception of leaching periods when the gas flow was stopped. To leach the oxidised tailings 500 mL of 18.2MΩ ultrapure deionised water was introduced to the cell via a separatory funnel. This was left to equilibrate with the sample for 2 hours before being drained under gravity into the plenum and collection vessel. This leaching procedure was conducted three times a week (Mon, Wed & Fri) for a total of 7 weeks with the resultant effluents combined to make one working composite sample. This composite sample was then bubbled with ozone for 2 hours at a rate of 2 L/min to ensure any remnant Fe^{2+} was oxidised to Fe^{3+}.

SP titrations were performed via the addition of 1M NaOH (Fisher Scientific - AR Grade) with a Metrohm 809 Titrando,

Table 1 *Elemental composition of high sulfide tailings sample.*

Analyte	Unit	ADL	Tailings Sample
SiO_2	%	0.01	30.5
Al_2O_3	%	0.01	6.54
Fe_2O_3	%	0.01	31.5
CaO	%	0.01	9.89
MgO	%	0.01	4.00
Na_2O	%	0.01	1.63
K_2O	%	0.01	0.29
Total S	%	-	16.2
Sulfide S	%	-	13.0
As	ppm	0.1	8.80
Co	ppm	0.1	1060
Cu	ppm	0.2	2530
Mo	ppm	0.05	12.9
Ni	ppm	0.2	193
Se	ppm	0.2	16.0
U	ppm	0.05	7.14

Metrohm 800 Dosino dosing device and Metrohm Unitrode Pt1000 pH probe. Each titration was performed in triplicate with 500 mL of composite effluent, stirred with a magnetic stirrer and PTFE stirrer bar. A range of target pHs were utilised between pH 3 and 8. Once achieved, the target pH was maintained for 1 hour before the precipitate was removed via vacuum filtration through 0.45 µm cellulose nitrate filters before being dried at 40 °C for 48 hours. Elemental composition of the precipitates was measured by Panalytical Minipal 4 DY683 ED-XRF with TF-240 4µm gauge polypropylene x-ray film. An aliquot of filtrate was preserved with NHO_3^- for subsequent ICP-MS analysis at an ISO 17025 accredited laboratory (ALS Environmental, Hawarden, UK). The remnant filtrate was then, if necessary, subjected to further pH adjustment as described above.

Results

Analysis of the ozone generated effluent (Table 1) showed a pH of 2.13, conductivity ≈9 mS/cm and elevated concentrations a wide range of elements. Iron and sulfur are by far the most abundant with concentrations of 5210 mg/L and 4190 mg/L respectively due to the oxidation of iron sulfides by ozone. Amongst the very high metal load of the effluent, aluminium (118000 µg/L), cobalt (26600 µg/L) and copper (36900 µg/L) are particularly notable from both a resource recovery and environmental risk viewpoint. Previously conducted net acid generation (NAG) testing showed maximum releases of 453 mg/kg and 2630 mg/kg of Co and Cu, respectively, from the tailings. Oxidation with ozone achieved recoveries of 133 mg/kg and 185 mg/kg Co and Cu, respectively suggesting preferential release of Co and that

Table 2 *Elemental composition of tailings effluent generated by ozone oxidation and post SP effluents.*

ID	Unit	Threshold value	Tailings Effluent	pH 3.5	pH 4.0	pH 4.5	pH 8.0
Aluminium	µg/L	200	118000	92800	93400	82400	139
Arsenic	µg/L	5	79.8	9.9	8.25	8.13	<5
Cadmium	µg/L	0.4	1.16	1.24	0.944	<0.8	<0.8
Chromium	µg/L	10	1060	385	361	357	337
Cobalt	µg/L	2	26600	21100	21400	21600	3650
Copper	µg/L	20	36900	27100	27600	27700	31
Lead	µg/L	10	<2	4.12	<2	<2	<2
Manganese	µg/L	50	1770	237	188	185	155
Mercury	µg/L	0.06	0.0168	0.0226	0.0158	0.0142	0.0117
Nickel	µg/L	10	4390	4000	3780	3700	246
Phosphorus	µg/L	-	16600	<100	<100	<100	<100
Selenium	µg/L	10	209	131	127	126	129
Uranium	µg/L	-	120	107	98.4	98.1	<5
Vanadium	µg/L	-	86.9	<10	<10	<10	<10
Zinc	µg/L	-	691	654	603	599	12.3
Calcium	mg/L	-	85.4	83.1	77.5	77	78.6
Iron	mg/L	0.2	5210	22.6	1.12	0.284	<0.2
Magnesium	mg/L	-	25.4	26.2	24	23.7	23.7
Sulfur	mg/L	-	4190	2910	2920	2870	2250

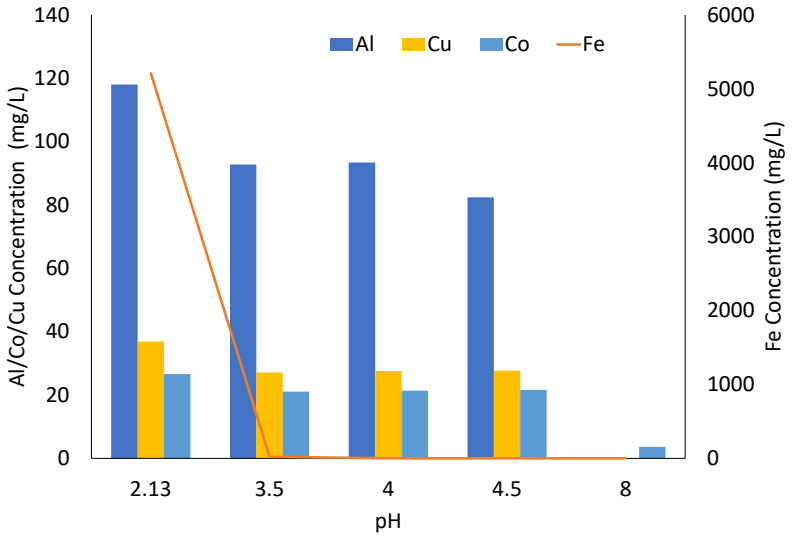

Figure 1 *Mass of iron, aluminium, copper and cobalt within aqueous phase at given pH.*

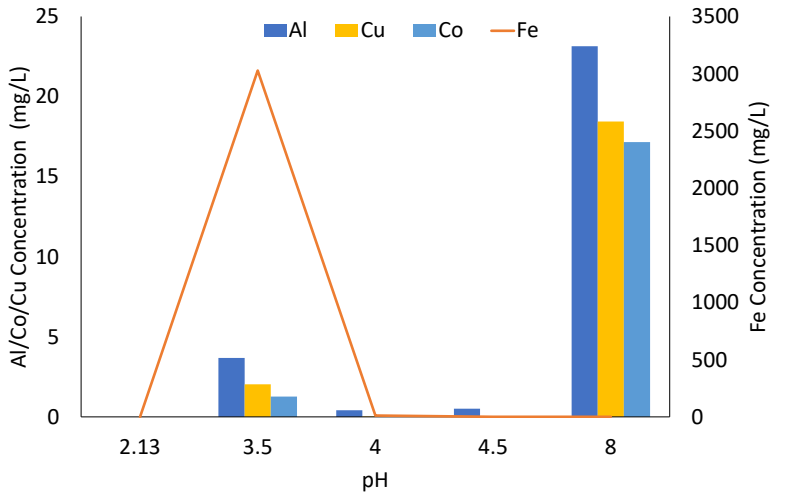

Figure 2 *Mass of iron, aluminium, copper and cobalt within precipitate at given pH.*

chalcopyrite oxidation is far from complete during ozonation. It is likely that this is partly due to gas transfer processes in the tailings column rather than purely due to the action of ozone, offering potential avenues for method refinement and increase efficiency.

SP of iron was achieved by adjustment of solution pH to 3.5 which significantly reduced the dissolved iron concentration of the effluent via the precipitation of ferric iron oxides (Table 1). Relative to the initial concentrations, iron within both the aqueous and solid phases was negligible from pH 3.5 upwards. Discrepancies between the total mass of elements present is as a result of analytical error from two separate analytical techniques coupled with the very high concentrations within the effluent requiring extensive dilutions and therefor introducing more error. Aluminium, cobalt and copper all exhibited slight decreases in aqueous concentration between the initial pH 2.13

and pH 3.5 (Figure 1). Coprecipitation or adsorption of aluminium, cobalt and copper to precipitated iron oxides has resulted in these minor losses (Figure 2). After removal of the iron oxide precipitate there was negligible loss of either cobalt or copper from the aqueous phase at either pH 4 or 4.5. Previous testing, where precipitate was not removed after each titration step, showed significant loss of copper and cobalt during these steps due to adsorption to both iron and aluminium precipitates, with a significant loss of aluminium observed at pH 4 also due to adsorption to precipitated iron oxide (Data not shown).

The final step of increasing the solution pH to 8.0 resulted in the precipitation of the majority of cobalt and copper from the solution. This generated a light blue precipitate consisting of 11.16% Al, 8.15% Co and 8.73% Cu. This equates to an approximate recovery rate of 0.175 kg/tonne for both cobalt and copper collectively. Initial estimates predict approximately 11 Mt of tailings being produced over the life of mine which translates to potential Co and Cu recoveries of ≈930 and 996 tonnes which equates to a potential value of ≈US$43M and US$10M respectively. Note that this only represents 10% metal recovery from the tailings source and potential is much greater. Further additional value may be feasibly recoverable via the isolation of aluminium hydroxide from the solution, which is predicted to precipitate from solution at approximately pH 5. However, this would require further experimentation as the effect the presence of aluminium has on the precipitation of Co and Cu is unknown. If aluminium were to be isolated, then it would remove a large surface area for the adsorption of Co/Cu and therefor potentially reduce recovery rates at pH 8 and/or require additional pH manipulation to higher pH's to achieve comparable results.

Analysis of the remnant effluent after the SP methodology found a solution with a significantly lower metal load relative to the untreated effluent. Iron has decreased to below limit of detection and therefore the investigation threshold value set out in Annex 3 of the EU Groundwater Directive 2006/118/EC (EU, 2006). Other metals to have dropped below the groundwater directive threshold values include aluminium, arsenic and cadmium. Copper recovery has dropped the remnant concentration to near the threshold

Table 3 *Elemental composition of precipitates after SP stages.*

Element	Unit	pH 3.5	pH 4.0	pH 4.5	pH 8.0
Al	%	0.0	0.6	0.0	11.0
Ca	%	0.0	0.0	0.0	0.2
Fe	%	47.8	43.3	0.4	0.1
Mg	%	0.1	0.1	0.0	0.1
S	%	8.2	6.5	1.3	6.5
As	ppm	0.0	0.0	2.5	7.1
Cd	ppm	0.0	1.3	0.0	5.6
Co	ppm	0.0	0.0	54.9	81580
Cr	ppm	383	301	0.0	282.3
Cu	ppm	321	918	59.6	87698
Mn	ppm	372	357	6.4	44.4
Ni	ppm	75.2	39.4	0.0	11562
P	ppm	1535	686	218	141
Pb	ppm	27.9	0.0	0.0	0.0
Se	ppm	38.6	13.2	0.9	10.6
V	ppm	424	191	77.0	88.8
Zn	ppm	14.8	15.4	8.0	1643

value limit, while cobalt remains in excess of its threshold value. However, there is potentially enough cobalt still held in solution to investigate further recovery attempts such as the use of ion exchange resins. Chromium and selenium remain in excess of their threshold values, though this is expected given their increased mobility under mildly alkaline conditions. This also suggests that chromium is present as Cr (VI), which would require subsequent treatment to reduce to Cr (III). While the groundwater directive does not outline a threshold value for sulfur, it does set a value for sulfate of 150 mg/L. The sulfur in the effluent is largely present as sulfate and therefor is likely in excess also, though this is a near ubiquitous issue at mines with sulfides present with a number of potential treatments available for trial.

Conclusions and Further Work

Oxidation of metalliferous, high-sulfide tailings, with ozone, generated a low pH, high conductivity solution to facilitate metal mobility. Removal of iron with minimal loss of target elements was achieved with a Co/Cu concentrate produced. While the production of this concentrate is of itself a noteworthy outcome, it is worth bearing in mind that the initial mobilisation rates of the target elements was only ≈10% and with methodology refinement there is likely to be substantial growth potential with regards to the efficacy of the method for resource recovery. Enhanced oxidation also serves to reduce the AP of the tailings and therefor render them more chemically stable and mitigate against acid generation during storage. The test work has resulted in there being a large reduction in the amount of metal with potential to be released to the environment local to the mine site and the generation of a much chemically stable waste stream with specific elements of economic interest substantially reduced.

With the next phase of investigation for this study further treatment of the post SP effluent is envisaged to ensure compliance with directive for groundwater quality. Potential techniques to be investigated include traditional liming of the effluent to remove both remnant metals and sulfate. Reintroduction of the iron oxides removed after the first SP step could be a promising avenue to remove the residual metals whilst acting to consolidate what would be two waste steams into a singular stream. Also, to be investigated are the potential for implementing electrowinning as a potential recovery technique for solubilised copper and the introduction of a stirred tank reactor to potentially increase the rate and extent of oxidation of sulfides in the tailings and increase the copper mobilisation and recovery.

References

Alves Dias P., Blagoeva D., Pavel C., Arvanitidis N., 2018. Cobalt: demand-supply balances in the transition to electric mobility, EUR 29381 EN, Publications Office of the European Union, Luxembourg, ISBN 978-92-79-94311-9, doi:10.2760/97710, JRC112285.

European Union (EU), 2006. DIRECTIVE 2006/118/EC OF THE EUROPEAN PARLIAMENT AND OF THE COUNCIL of 12 December 2006 on the protection of groundwater against pollution and deterioration: Annex III.

European Commission (EC), 2020. Critical materials for strategic technologies and sectors in the EU - a foresight study. doi: 10.2873/58081 ET-04-20-034-EN-N

Lottermoser, B. 2011. Recycling, reuse and rehabilitation of mine wastes. Elements 7 (6), 405-410. doi: 10.2113/gselements.7.6.405

Oh, C., Han, Y.S., Park, J.H., Bok, S., Cheong, Y., Yim, G. and Ji, S. 2016. Field application of selective precipitation for recovering Cu and Zn in drainage discharged from an operating mine. Science of the Total Environment 557–558, pp. 212–220. doi: 10.1016/j.scitotenv.2016.02.209

Park, S.M., Yoo, J.C., Ji, S.W., Yang, J.S. and Baek, K. 2015. Selective recovery of dissolved Fe, Al, Cu, and Zn in acid mine drainage based on modeling to predict precipitation pH. Environmental Science and Pollution Research 22(4), pp. 3013–3022. doi: 10.1007/s11356-014-3536-x.

Vecino, X., Reig, M., Lopez, J., Valderrama, C. and Cortina, J.L. 2021. Valorisation options for Zn and Cu recovery from metal influenced acid mine waters through selective precipitation and ion-exchange processes: promotion of on-site/off-site management options. Journal of Environmental Management. 283. doi: 10.1016/j.jenvman.2021.112004

Successful Passive Treatment of Sulfate Rich Water

Jamie Robinson[1], Jason Dodd[2], Ian Andrews[3], Jim Gusek[4], Lee Josslyn[5] and Eric Clarke[6]

[1]*CSLR Consulting, Treenwood House, Rowden Lane, Bradford On Avon BA15 jrobinson@slrconsulting.com*

[2]*SLR Consulting, Treenwood House, Rowden Lane, Bradford On Avon BA15 2AU jdodd@slrconsulting.com*

[3]*SLR Consulting, Unit 2, Newton Business Centre Thorncliffe Park Estate, Newton Chambers Rd, Chapeltown, Sheffield S35 2PH. iandrews@slrconsulting.com*

[4,5]*Linkan Engineering, 651 Corporate Circle, Suite 102,Golden, Colorado 80401, jim.gusek@linkan.biz*

[6]*Saint-Gobain Construction Products Limited (trading as British Gypsum), Robertsbridge, E Sussex. Eric. Clark@saint-gabain.com*

Abstract

A passive sulfate reduction system with iron scrubbers was identified as the most viable option for treatment of elevated sulfate within leachate from an old landfill and bench scale trials were established in 2019 at the site to test the theory. This included the use of Biochemical Reactor (BCR) with different proportions of wood chips, straw, manure, limestone, and biochar to culture sulfate reducing bacteria. In addition the concept of 'bugs on booze' was trialled, using Fix Bed Anaerobic Bioreactor (FBAR), where alcohol added to enhance the sulfate reducer activity. In total three BCRs and two FBARs were set up for this stage of the assessment. The resulting treated leachate was then passed through different iron media types (haematite, magnetite and iron filings) to remove sulfide generated by the bacteria, with an aerobic wetland used to polish the effluent. The success of the bench scale project led to a pilot scale system being constructed and monitored in Spring 2020, the results of which confirm the success of the bench scale testing and provides useful insights into management of the system particular in winter months. The COVID crises has had its impact but the system has operated continuously and will run through 2021.

Keywords: Passive Treatment, Sulfate Reduction, Biochemical Reactor, Wetland, Pilot Plant

Introduction

SLR Consulting (SLR) was appointed by British Gypsum (Saint-Gobain Construction Products UK Ltd trading as British Gypsum) to investigate options for the treatment of leachate emanating from an old landfill disposal site at their property in East Sussex. The options analysis undertaken by SLR highlighted a passive treatment option for the removal of the sulfate, to below discharge standards, was a potential option but that it required treatability/ feasibility testing. The concept involved the use of naturally occurring material containing sulfate reducing bacteria to remove the sulfate with the resulting dissolved sulfide in the water being 'scrubbed' by an iron oxide filter. An aerobic wetland would then be used to polish any final effluent before it is discharged. The design of the system was undertaken with Linkan Engineering who also supervised the construction and commissioning of the system with support from SLR.

The Treatment Process

When the design of a treatment system is necessary, its design would be based on the results of a "staged process" of bench and pilot-scale testing. Typically flow rates of c.5 to 10 mL/min or less are termed "bench-scale" with "pilot scale" test as one that would treat about 4 L/min or more.

Bench scale testing is an effective way to advance a project toward to full scale implementation while gaining useful knowledge about appropriate media, reaction rates, and functionality that increase confidence and overall effectiveness. The overall footprint may be reduced from outline

design stage, which leads to lower capital costs and maintenance. The typical passive biological treatment process for sulfate reduction utilizes an anaerobic Biochemical Reactor or BCR. While BCRs receiving Mining Impacted Water (MIW) may be configured as "up-flow" or "down-flow", experience has shown that up-flow BCRs are better than down-flow BCR in treating sulfate rich and metal poor leachates. The system is required for such a water which is being generated by a closed landfill.

The organic substrate comprises hard wood chips, limestone, straw and biochar in varying proportions. 0.1% animal manure is added to provide the naturally occurring sulfate reducing bacteria. The sulfate in the influent leachate is then consumed by the bacteria and produces sulfide:

$$SO_4^{2-} + 2\ CH_2O = H_2S + 2\ HCO_3^-$$

Usually when such systems are used the dissolved metal ions in the mine water react with the sulfide to precipitate insoluble metal sulfides in the wetland/BCR substrate. The lack of suitable metals in the British Gypsum discharge requires a metal ion was needed to be added passively to sequester the sulfide generated through the sulfate reduction process. The dissolved sulfide will precipitate as an insoluble metal sulfide or potentially as free sulfur. For example, at the British Gypsum site, iron was added at bench scale via a treatment substrate such that the following reaction (through precipitation of dissolved iron or on metal iron surfaces), in the substrate will occur, shown simplistically below:

$$Fe^{2+} + S^{2-} \rightarrow FeS$$

Sulfur sequestration is the primary problem with a sulfate-only BCR. While minor amounts of native sulfur will accumulate on the surface of an up-flow BCR, experience has shown that the BCR effluent, bearing dissolved sulfide ion (HS-), needs to be scrubbed with an inexpensive sacrificial metal. This metal can be either in the zero-valent state such as scrap iron, or as an oxide. However, care in media selection is warranted. An Aerobic Polishing Wetland (APW) is also a lined shallow pond filled with soil and locally harvested or cultivated

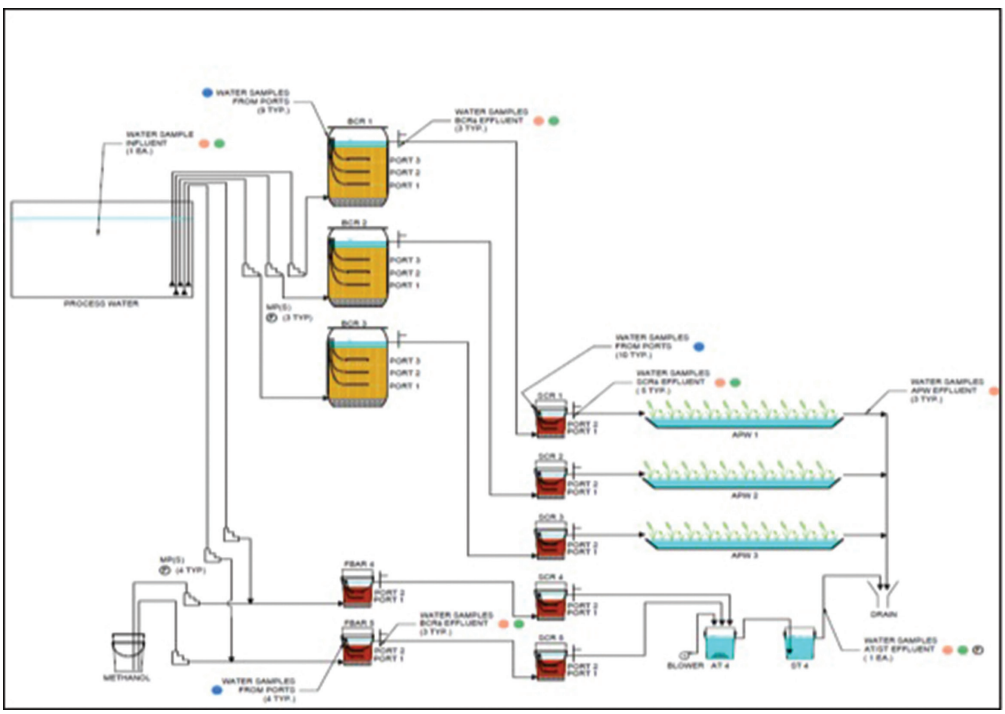

Figure 1 *Bench Scale Test Flow Diagram.*

vegetation (if available). The purpose of this process feature is to re-aerate the anoxic effluent from the BCR.

Bench Scale Set Up

To test the theory of a passive wetland treatment solution, a bench scale system was set up at the site to run for 20 weeks. The bench scale system comprised:

- 3 No. Biochemical Reactors (BCRs) – pump fed, each filled with a different test mixture comprising different proportions of manure, wood chips, hay, limestone, and biochar.
- 3 No. Sulfide Scrubbers (SCR), each filled with a different test mixture comprising magnetite, hematite, and iron filings.
- 3 No. Aerobic Polishing Wetland (APW) cells planted with wetland plants from the site; and
- 2 No. Fixed Bed Anaerobic Bioreactors (FBAR) with 2 No. Sulfide Scrubbers, Aeration Tub and Settlement Tub.

A conceptual layout of the process units used in the bench scale test layout is provided in Figure 1. As part of the treatability, it was also decided to consider the use of a hybrid-passive approach which involves the additional of a soluble form of hydrocarbon such that the bacteria would react more quickly that the less soluble forms held in natural organic matter such as sawdust/manure. In this Fixed Bed Anaerobic Reactor (FBAR) small quantities of ethanol is added to a small system to provide a food source for the bacteria. The reasoning being that with a more soluble food source the bacteria will consume more of the sulfate and hence less area will be needed for the treatment at pilot and full-scale. This also has an active aeration and settling tank in replacement of the aerobic wetland system to act as a comparison.

Monitoring and Results

The system was monitored for a variety of analytes along with the flows throughout the system, Weekly field-based monitoring of pH, redox and conductivity was undertaken along with sulfate, sulfide, nitrate, calcium and magnesium. At monthly intervals, phosphate, alkalinity, hardness, iron, nickel, zinc and total organic carbon (TOC) was analysed. The flows through the reactor were typically 6 L/d for the BCRs and 25 L/d for the FBARs. The latter was also reduced at the end of the treatment to be closer to the BCR flow rate to act as a comparison. The process flow diagram for the system is shown above in Figure 1 and this shows not only the flow process for each of the treatability tests – but also the location and frequency of the sampling of the various parts of the system to assess the treatment progress over time. The monitoring of the system was undertaken at weekly intervals where the redox and pH of the various components coupled with the flow rates were taken. The sulfate and other components were analysed at an offsite UKAS accredited laboratory. The results of the treatability study are shown in Figures 3– 6.

The bench scale test results indicated that both BCRs and FBAR treatment will produce an effluent that would meet a 250 mg/L sulfate limit. In mine water treatment systems sulfate reduction rates typically range form 0.1 – 0.3 moles/m3 substrate/ day. The rates for this study are shown to be at the upper end of this range. In addition, the FBAR rate of sulfate reduction was c.15 times that of the BCR reduction rate. Consequently, the media volume required to accomplish this with a

Figure 2 *Bench Scale Test Set Up.*

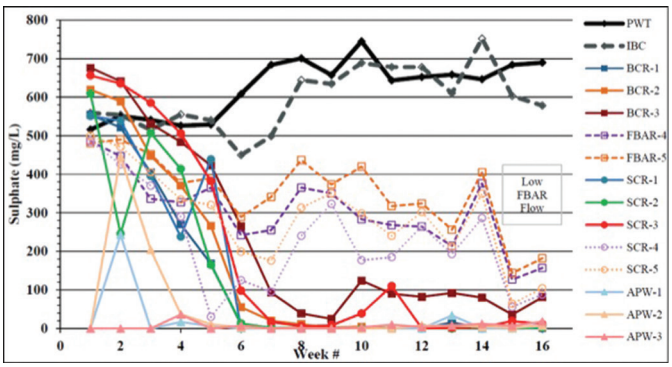

Figure 3 Sulfate Concentrations.

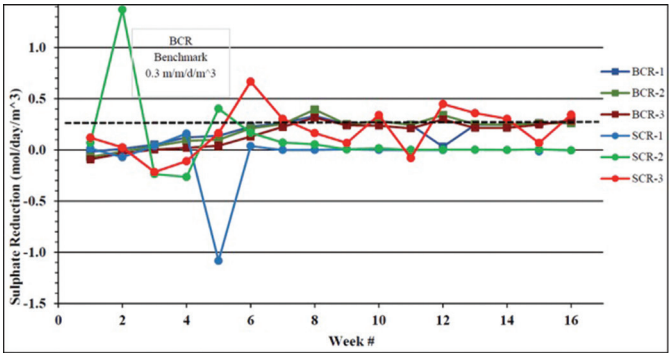

Figure 4 BCR Sulfate Reduction Rate.

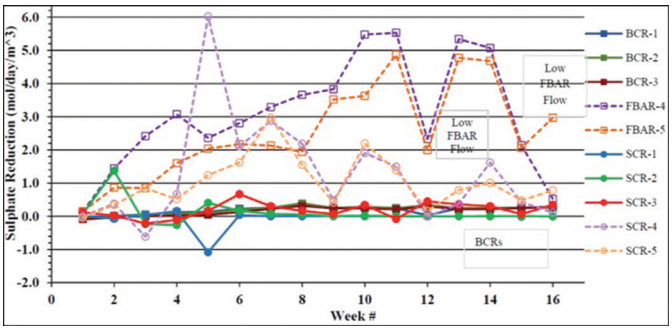

Figure 5 FBAR and BCR Sulfate Reduction Rate.

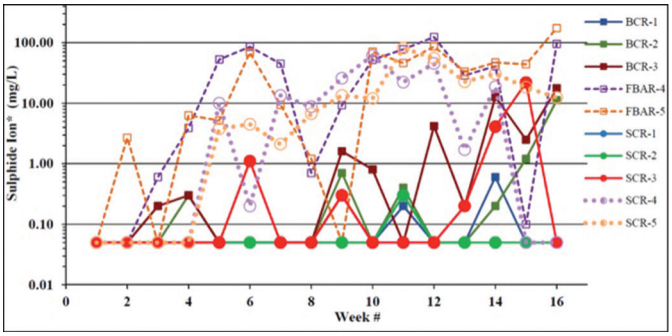

Figure 6 Sulfide Concentrations.

BCR will be c.15 times greater than for the media volume for an FBAR with an identical treatment capacity. The land area footprint required for an FBAR treatment unit would therefore also be 15 times smaller than that required for a BCR. However, the FBAR process will require the delivery of a steady and reliable supply of alcohol as a microbial nutrient.

The BCR process does not require addition of nutrient, as alcohol, and therefore is seen as more passive aside from pumps to move the leachate to the treatment system. The scrubbers sequestered sulfide ion present in the BCR and FBAR effluents. However, the bench scrubbers that received the FBAR effluents, proved to be undersized. The aerobic wetland system was effective in removing the iron leached from the scrubbers and did have a positive impact on the organic carbon which came through the system. The results of the bench scale testing were very encouraging. This has led to the design and development of a pilot scale system at the site.

Pilot Scale Testing

The success of the bench scale trials led to the design and installation of a pilot scale system in Spring 2020 on the site. The purpose of the system was to confirm the success of the bench scale study by using the sulfate removal coefficients and preferred media option. The latter comprised mixing of wood chips, biochar, limestone, wheat straw, bench scale organic material and goat manure inoculum. The desired flow being introduced into the system was 0.5 L/min and above and there was no additional of alcohol as nutrient. The bench scale testing showed that free sulfur was generated in the BCRs and FBRs and hence the scrubbers were not required. However, the pilot scale system allowed addition if the system required additional sulfide removal. Conceptually the pilot scale system had the original orientation of sequential treatment, although three biochemical reactors were established such that variety in flow rate and other parameters can be used to test the system. To construct the pilot plant, available

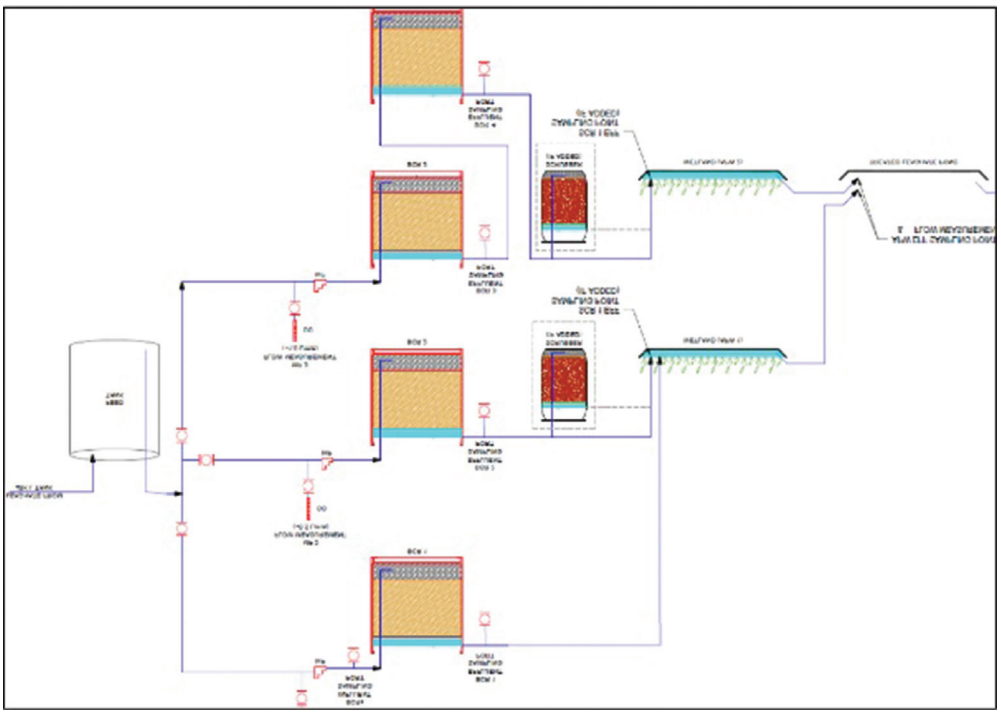

Figure 7 Pilot Plant Layout and Monitoring.

Figure 8 *Passive Treatment Pilot Plant from right to left (Feed Tank; BCR1, 2, 3, 4; Reed bed (APW) 1, 2, discharge holding pond showing purple/white bacteria).*

infrastructure was used. Cargo containers were used for the three BCRs. These were waterproofed and lined with insulation on the base and sides and reinforced such that they could hold the substrate and the water. Sampling ports were established such that different horizons in the units could be analyzed if required. The aerobic polishing reed beds was designed with baffles to lengthen the flow length in the wetland and was designed for the removal of BOD/TOC. Facility was also made to add on the iron-based sulfide sequestering unit should monitoring indicate that sulfide is leaving the system at concentrations which were unsustainable from an environmental perspective.

The pilot system became live through a commissioning phase in Spring 2020 before the COVID emergency, and monitoring was undertaken by a skeleton staff on site since. A number of sampling points were included in the system including redox zone depth measurement in the anaerobic material, along with the treatment zones at various locations along the system.

The results of the ongoing monitoring have indicated good sulfate removal with no sulfide detectable in the effluent. Free sulfur has been identified in the system which has the potential to oxidise and release stored sulfur as sulfate, although during the summer/spring there was no evidence this has occurred. Elemental sulfur may be the primary product of sulfate reduction in the BCRs. Evidence includes the white cloudiness in the BCR effluents, white deposits in the wetland influent zones, and the purple tinge (likely the bacteria Chromatium sp. and Chlorobium sp.) in the final pond influent zone (Figure 8). Purple sulfur bacteria produce elemental sulfur as part of their life cycle. Thus far the pilot cell is confirming the results of the bench scale testing with latest influent sulfate of c.800 mg/L being reduced to c.100 mg/L in the effluent, thus providing robust design data for the full-scale system. The first seven months of sulfate removal are shown in figure 10. In the winter months the treatment efficiency decreased believed to be temperature reduction and potential free sulfur oxidation. This temperature dependency is a relatively well-known phenomenon with passive systems, with sulfate reduction rates improving in spring and some months. This aspect of the pilot scheme has been very useful in guiding potential management changes which may need to be included in winter months to maintain the same reduction in sulfate. The sulfide remained non detected in the discharge and the BOD/TOC, after an initial stabilisation period, was recorded as c.10 mg/L. A full scale aerobic wetland will remove the BOD/TOC with greater efficiency. Notwithstanding the performance of the BCRs was reduced over winter months and this was investigated. The monitoring showed some interesting changes in redox and TOC in the leachate entering the treatment system.

Landfills are large anaerobic digesters, and this can result in inconsistent performance (effluent) from the treatment system. Influent TOC 'food' (that is' digestible' for the pilot BCR organisms - like a 'bugs on booze' system) sustain the BCR well. When this food is reduced quickly in the leachate, the

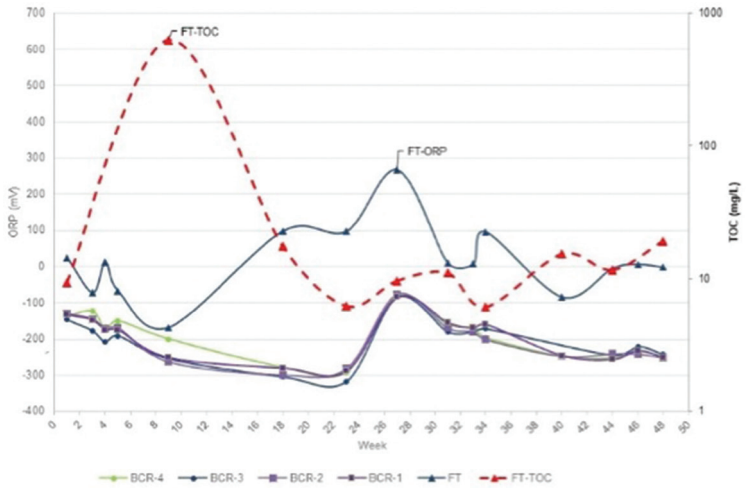

Figure 9 *Results of TOC and ORP.*

whole biosystem in the BCRs is essentially put on starvation mode with knock on lower sulfate reduction rates. The TOC levels are reinforced with the redox reading in the influent water as shown in Figure 9. This is very useful information as it might suggest soluble organic matter amendment (as used in the bench scale testing) may be required during the winter months if the sulfate treatment is shown to fall below established permit conditions.

The pilot system is still in operation (March 2021) and the intention is to operate the system through the summer and winter of 2021 with results reported by the end of 2021. Notwithstanding additional data will be produced as the COVID emergency and lock down is lifted.

Acknowledgements

SLR Consulting Limited would like to thank St Gobain for giving permission to prepare this paper and embracing an innovative technology for sulfate treatment. Lee Josselyn and Jim Gusek at Linkan Engineering are thanked for their continued support on the project, along with the dedicated project team from St Gobain and SLR.

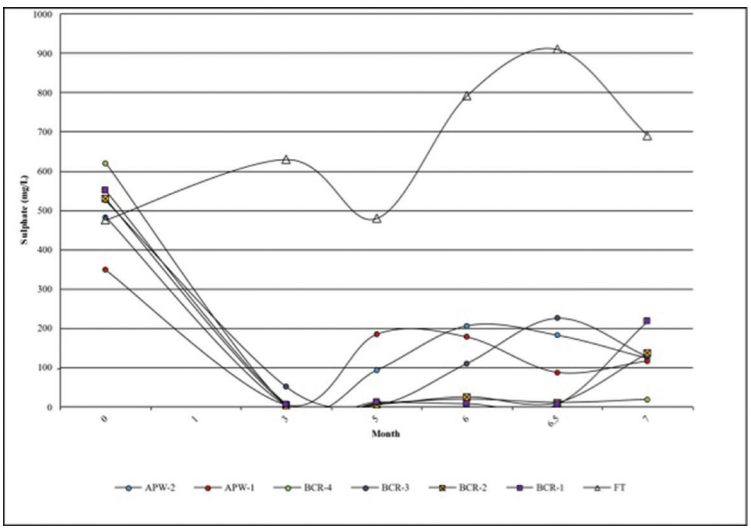

Figure 10 *Results of Sulfate Analysis for First 7 months of pilot plant operation.*

Passive Mine Water Treatment Trials of Dispersed Alkaline Substrate at Two Emblematic Mine Sites in Wales

Tobias Stefan Roetting[1], Gareth Digges La Touche[1], Iain Hall[2], Louise Siddorn[3], Peter Clive Stanley[3], José Miguel Nieto[4], Francisco Macías Suárez[4], Alba Gómez Arias[5,6], Julio Castillo[6]

[1]*Golder Associates UK Ltd, 20 Eastbourne Terrace, London, W2 6LG, UK, TRoetting@golder.com, GDLTouche@golder.com*

[2]*Golder Associates UK Ltd, Citibase Edinburgh Gyleview, Gyleview House, 3 Redheughs Rigg, Edinburgh West Office Park, South Gyle, EH12 9DQ, UK, IHall@golder.com*

[3]*Natural Resources Wales, 29 Newport Road, Cardiff CF24 0TP, Wales, geowyddor@cyfoethnaturiolcymru.gov.uk*

[4]*Department of Earth Sciences & Research Center on Natural Resources, Health and the Environment (RENSMA), University of Huelva, Avenida Tres de Marzo s/n, 21071 Huelva, Spain, jmnieto@uhu.es, francisco.macias@dgeo.uhu.es*

[5]*Office for Research Commercialisation, University of the Free State, PO Box 339, Bloemfontein 9300, Republic of South Africa, gomezariasa@ufs.ac.za*

[6]*Department of Microbiology and Biochemistry, University of the Free State, PO Box 339, Bloemfontein 9300, Republic of South Africa, castillohernandezj@ufs.ac.za*

Abstract

Mine drainage from abandoned mines is a serious environmental legacy in Wales. Passive treatment is an attractive remediation strategy, but it has often failed due to premature clogging or passivation of the systems.

The Dispersed Alkaline Substrate (DAS) treatment system, based on a fine-grained alkaline reagent mixed with wood chips to enhance the porosity, was developed to overcome these problems and is successfully deployed full-scale at two sites in SW Spain. In Wales, where the climate is more maritime, the system is being tested at two emblematic metal mine sites, Parys Mountain and Cwm Rheidol, which are two of the top five most polluting mines in Wales.

Field and laboratory trials started in late 2020/early 2021. The preliminary results from the trial at Cwm Rheidol and initial results from the column tests completed on Parys Mountain mine water at the University of Huelva are presented here. Calcite-DAS combined with MgO-DAS remove Fe, Al and divalent metals to low levels, while calcite-DAS combined with $BaCO_3$-DAS additionally also decreases sulphate concentrations and calcium (hardness).

Keywords: Passive Treatment, Divalent Metals, Sulphate Removal, Clogging, Passivation

Introduction

Wales has a long history of metal mining, dating back to the Bronze Age. By the 1920s most mining of metals had ceased, however drainage from in excess of 1,300 abandoned metal mines continues to impact over 700 km of river reaches today. Passive treatment systems, which only require naturally available energy sources and infrequent maintenance, can be an economical and sustainable option to decontaminate these mine waters. Nevertheless, they are prone to clogging and passivation (loss of permeability or reactivity) when used to treat mine water with high metal concentrations or high acidity loads.

To overcome these constraints, the Dispersed Alkaline Substrate (DAS) was developed (Roetting *et al.*, 2008a, 2008b, 2008c, Torres *et al.*, 2018), which consists of a fine-grained alkaline reagent (e.g., calcite [$CaCO_3$], caustic

magnesia [MgO] or witherite [$BaCO_3$]) mixed with a coarse inert matrix (wood chips). DAS had been tested previously at laboratory column, then field pilot scale and is currently successfully deployed full scale at two abandoned mines in SW Spain. In 2020, Natural Resources Wales (NRW) commissioned field pilot trials at Cwm Rheidol mine (Aberystwyth, Mid Wales) and Parys Mountain (Anglesey, North Wales) to test if this technology can be used to remediate acid mine waters at remote sites in a wet temperate maritime climate. These are two of the top five most polluting mines in Wales.

Cwm Rheidol discharges 9 T/yr of metals at a flow of 9 L/sec that enters the Afon Rheidol then Cardigan Bay. The main contaminants (by decreasing total concentration) are SO_4 (216 mg/L), Zn (20.3 mg/L), Fe (17.8 mg/L), Al (5.5 mg/L), Mn (0.95 mg/L), Pb (0.62 mg/L), Ni (0.38 mg/L), Cu (50 µg/L), Cd (40 µg/L), at pH 4.1.

Parys Mountain discharges 231 T/yr from the Dyffryn Adda adit at a flow of 12 L/sec that enter the Afon Goch Amlwch, which enters the Irish Sea. The main contaminants are SO_4 (2263 mg/L), Fe (646 mg/L), Zn (78 mg/L), Al (73 mg/L), Cu (42 mg/L), Mn (16 mg/L), As (0.67 mg/L), Co (0.42 mg/L), Ni (160 µg/L), Cd (150 µg/L), Pb (20 µg/L), at pH 2.5.

The field trial at Cwm Rheidol has been operating since December 2020. For Parys Mountain, column trials have been carried out at the University of Huelva (Spain) in early 2021 to test the treatment train configuration at laboratory scale, the field trial commences in May 2021. This contribution presents initial results from the trials.

Methods

Dispersed Alkaline Substrate (DAS) is a passive treatment system for ARD (Acid Rock Drainage) with high metal concentrations, which was developed more than a decade ago to overcome clogging and passivation problems experienced with many other passive treatment systems for ARD. The fine-grained alkaline reagent (e.g., calcite [$CaCO_3$], caustic magnesia [MgO] or witherite [$BaCO_3$]) in DAS provides a high specific surface area to increase dissolution rates and minimise passivation problems, while the coarse high surface matrix (e.g., wood chips) provides large pores where secondary minerals can precipitate without compromising substrate permeability, thus reducing clogging.

Calcite-DAS removes Al, Fe(III), Cu and Pb, while MgO-DAS removes divalent metals. Barium cations released by $BaCO_3$ dissolution react with dissolved sulphate

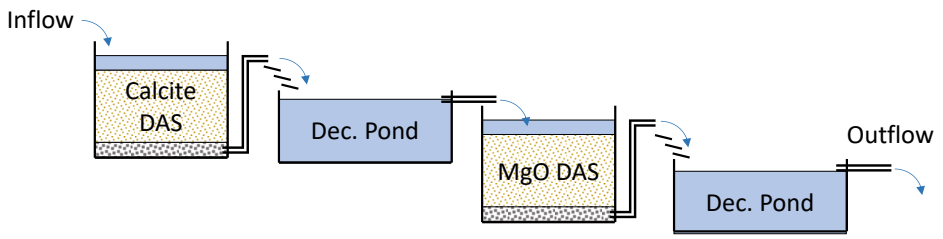

Figure 1 *Schematic setup of the calcite-DAS + MgO-DAS reactors of the field trial at Cwm Rheidol.*

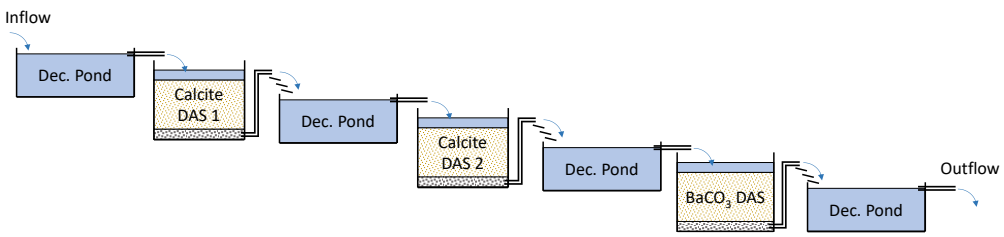

Figure 2 *Schematic setup of the calcite-DAS + $BaCO_3$-DAS laboratory columns for Parys Mountain.*

to precipitate as $BaSO_4$, which has a very low solubility. The increase of alkalinity (release of carbonate anions) may also induce precipitation of Ca and/or Mg as carbonates or hydroxides, thereby reducing the hardness of the treated water.

At both mine sites, combinations of calcite-DAS with either MgO-DAS or $BaCO_3$-DAS are being tested to determine which one performs best under site conditions. In this contribution, for conciseness we only present field results of calcite-DAS + MgO-DAS at Cwm Rheidol and laboratory results for calcite-DAS + $BaCO_3$-DAS for Parys Mountain.

The treatment train of the Cwm Rheidol field trial presented here (Fig. 1) consists of a calcite-DAS tank, a first decantation pond to oxidise and precipitate iron, an MgO-DAS tank and a final decantation pond to stabilise outflow pH due to CO_2 uptake from the atmosphere. The hydraulic residence time is about two days in each DAS tank and about three days in each decantation pond during the initial trial period reported here. Flow rates will be increased and hydraulic residence times decreased at later trial stages to optimise treatment performance and minimise space requirements for full-scale application.

The laboratory treatment train for Parys Mountain presented here (Fig. 2) contains two sets of calcite-DAS columns with decantation vessels to gradually remove the much higher iron concentrations, combined with a $BaCO_3$-DAS column and a final decantation vessel. The hydraulic residence times are similar to the Cwm Rheidol trial.

Results

Cwm Rheidol field trial

Results from the initial five months of field trial operation are presented below for pH, total Fe, Al and Zn.

The pH values (Fig. 3, left) increase from around pH 3.5 at the inflow of the calcite DAS tank to between pH 6.4 and pH 8.9 at the outflow of the calcite-DAS tank 3. The pH increases further to about pH 10.8 at the outflow of the MgO-DAS tank and then decline to about pH 9.6 at the outflow of the final decantation pond.

Influent total iron concentrations (Fig. 3, right) typically range between 5 mg/L and 25 mg/L. On 15th of March 2021, a very high total concentration of 130 mg/L was measured due to high particulate iron of 120 mg/L. Total iron concentration at the outlet of the calcite DAS tank decreases to an average value of 0.07 mg/L, about 0.03 mg/L at the outlet of the MgO-DAS tank and to below the detection limit of 0.03 mg/L at the outflow of the final decantation pond.

Total aluminium concentrations (Fig. 4, left) decrease from between 1.8 mg/L and 12.4 mg/L at the inflow to around 0.04 mg/L at the outlet of the calcite-DAS tank. Concentrations around the detection limit of 0.01 mg/L are observed at the outflow of the final decantation pond.

Total zinc (Fig. 4, right) is partially removed in the calcite-DAS tank, from inflow values between 9 mg/L and 40 mg/L to an average of 8.5 mg/L at the outlet of the tank. MgO-DAS removes virtually all remaining Zn, with concentrations at the outflow of the final decantation pond of around 0.18 mg/L.

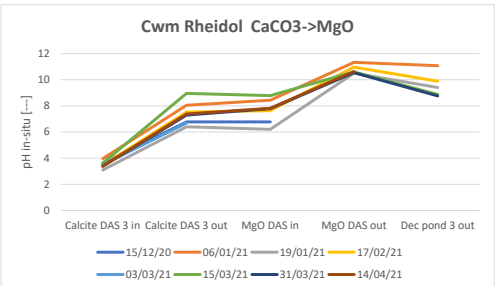

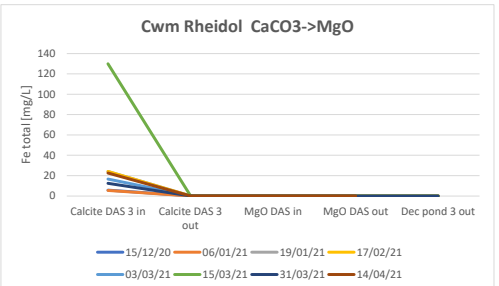

Figure 3 *Evolution of pH (left) and total iron concentrations (right) along the Cwm Rheidol treatment train.*

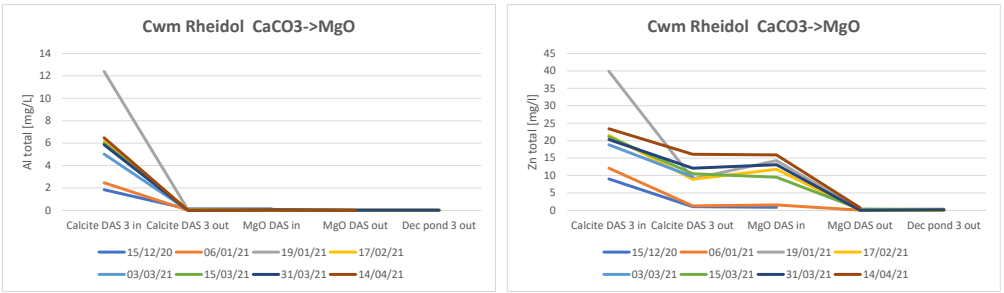

Figure 4 *Evolution of total Al (left) and Zn concentrations (right) along the Cwm Rheidol treatment train.*

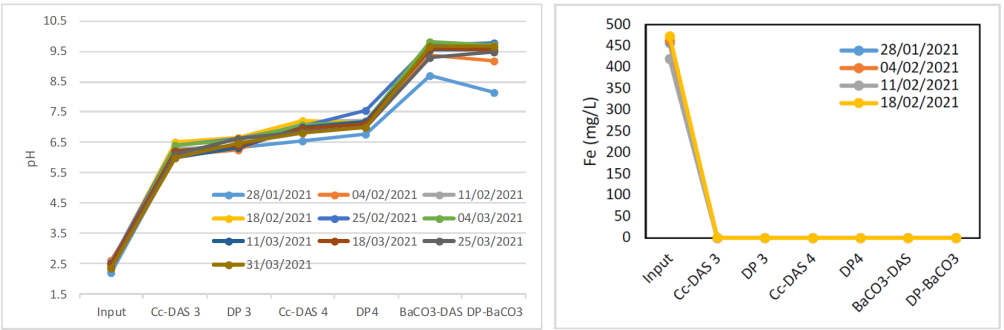

Figure 5 *Evolution of pH (left) and total iron concentrations (right) along the Parys Mountain laboratory columns.*

Parys Mountain column trial

Results from the initial two months of laboratory trial operation are presented below for pH, total Fe, Al and Zn.

Inflow pH is around pH 2.4 throughout the trial (Fig. 5, left). At the outflow of the first calcite-DAS column, it increases to around pH 6.4, to around pH 6.7 at the outflow of the second calcite-DAS column and to around pH 9.5 at the outflow of the $BaCO_3$-DAS column.

Influent total Fe concentration (Fig. 5, right) was around 450 mg/L, and decreased to less than 0.1 mg/L at the outflow of the first calcite-DAS column.

Similar to iron, Al (inflow concentration arounf 60 mg/L; Fig. 6, left) was completely removed in the first calcite-DAS column. Zn (Fig. 6, right) had an inflow concentration of arounf 55 mg/L, with little removal in the first calcite-DAS column. Some Zn (with decreasing efficiency) was retained in calcite-DAS column 2 and decantation pond 2, but throughout the trial all remaining Zn was retained in the $BaCO_3$-DAS tank.

Sulphate concentrations (Fig. 7, left) in the inflow were around 2300 mg/L, and they decreased to around 2100 mg/L in the outflow of the first calcite-DAS column. They remained approximately constant in the first decantation pond, second calcite-DAS column and second decantation pond for all sampling rounds except the first round in January 2021. Sulphate concentrations decreased considerably to between 100 mg/L and 500 mg/L at the outflow of the $BaCO_3$-DAS column, with a decreasing trend in sulphate removal efficiency. Sulphate removal was likely due to precipitation of gypsum ($CaSO_4{\cdot}2H_2O$) in the first calcite-DAS column, and due to barite ($BaSO_4$) precipitation in the $BaCO_3$-DAS column.

Ca concentrations (Fig. 7, right) increased from about 50 mg/L at the system inflow to around 370 mg/L at the outflow of the first calcite-DAS column, indicating that the removal of metals and acidity was driven by calcite dissolution. Ca decreased only marginally in the first decantation pond, second calcite-DAS column and second

decantation pond, but dropped dramatically to between 10 mg/L and 40 mg/L at the outflow of the $BaCO_3$-DAS column, demonstrating that $BaCO_3$-DAS is also capable of removing again the hardness that was added due to calcite dissolution in the previous treatment steps. Ca removal in the $BaCO_3$-DAS column is likely due to alkalinity release from $BaCO_3$ dissolution and subsequent calcite precipitation. The performance of calcite + $BaCO_3$-DAS system is consistent with results obtained previously in column trials treating acid mine drainage from Spain (Torres *et al.*, 2018).

Conclusions

The results to date obtained from the field and laboratory trials are promising and indicate that remediation of both mine discharges is possible using DAS technology. If successful, this passive treatment system will provide a proven cost-effective option to treat differing maritime metal mine waters from different geological sources of the massive sulphide deposit at Parys Mountain to warm brine epigenetic vein type lead zinc deposits of the Mid Wales Orefield. This new treatment tool can be applied in optioneering to reduce the pollutant load, develop resilience, reverse the derogation of Water Framework Directive (WFD) failing waterbodies and restore river health. This is especially relevant at remote maritime sites where other treatment systems cannot be applied either due to excessive treatment costs or land requirements.

Acknowledgements

This study is funded by the joint Metal (Non-Coal) Mine Programme of NRW and The Coal Authority under contract reference number 45374. This contribution has been reviewed and approved by Dr Nina Menichino, Team Leader, Evidence

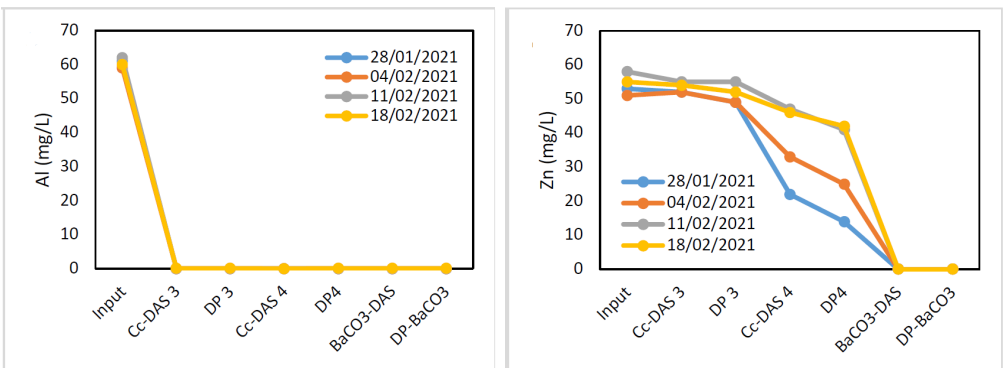

Figure 6 *Evolution of total Al (left) and Zn concentrations (right) along the Parys Mountain laboratory columns.*

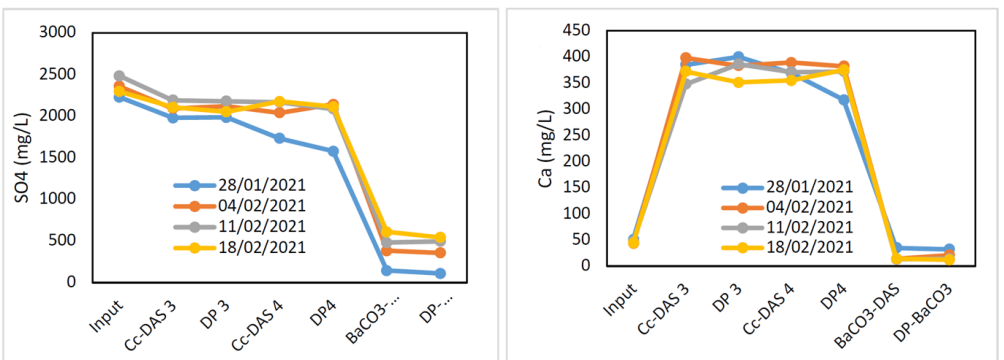

Figure 7 *Evolution of total sulphate (left) and Ca concentrations (right) along the Parys Mountain laboratory columns.*

Portfolio, Programmes and Processes at NRW. The authors acknowledge the laboratory personnel at NRW and Huelva University for their support in analysing the water samples. The authors also thank two anonymous reviewers whose comments helped to improve the manuscript.

References

Roetting, T.S.; Thomas, R.C.; Ayora, C.; Carrera, J. (2008a): "Passive treatment of acid mine drainage with high metal concentrations using Dispersed Alkaline Substrate". Journal of Environmental Quality, 37 (5), 1741-1751. DOI: 10.2134/jeq2007.0517.

Roetting, T.S.; Caraballo, M.A.; Serrano, J.A.; Ayora, C.; Carrera, J. (2008b): "Field application of calcite Dispersed Alkaline Substrate (calcite-DAS) for passive treatment of acid mine drainage". Applied Geochemistry, 23 (6), 1660-1674. DOI: 10.1016/j.apgeochem.2008.02.023

Roetting, T.S.; Ayora, C.; Carrera, J. (2008c): "Improved passive treatment of high Zn and Mn concentrations using Caustic Magnesia (MgO): Particle size effects". Environmental Science & Technology, 24 (42), 9370–9377. DOI: 10.1021/es801761a.

Torres, E.; Lozano Letellier, A.; Macías, F.; Gómez Arias, A.; Castillo, J.; Ayora, C. (2018). Passive elimination of sulfate and metals from acid mine drainage using combined limestone and barium carbonate systems. Journal of Cleaner Production, 182. 10.1016/j.jclepro.2018.01.224.

Monitoring of Water-Bearing Adits – Current Results and Perspectives

Tobias Rudolph, Christian Melchers, Peter Goerke-Mallet, Detlef Engel

Technische Hochschule Georg Agricola Bochum University, Research Center of Post-Mining, Herner Str. 45, 44787 Bochum, Germany, tobias.rudolph@thga.de, christian.melchers@thga.de, peter.goerke-mallet@thga.de, dudo.engel@gmail.com

Abstract

Water-bearing adits represent underground drainage and outflow systems whose functionality is of considerable importance in many mining areas all over the world with regard to safety issues at the surface. In the sense of a perpetual task, stable hydraulic, geotechnical and rock mechanical conditions must be guaranteed in the water-bearing adits. A variety of monitoring methods have to be used to analyse and document the functioning of water-bearing adits and the interconnected mine workings. Water-bearing adits are technical structures that have often been in place for several centuries. In most cases, accessibility is no longer granted directly behind the adit entrance.

situation of a large number of galleries in the southern Ruhr area/Germany. Hydrochemical parameters have been investigated, the rate of discharge and precipitation compared and infiltration tests undertaken. An essential step forward is the evaluation of available mine survey maps of the water-bearing adits and the hydraulically connected mine workings. These prerequisites are needed in order to determine, if possible, the catchment area of a water-bearing adit.

The aim of the work is to gradually better understand the functioning of the water-bearing adits. This is one part of the perpetual obligations of the former mining industry. The essential goal is to predict the mode of operation of the water-bearing or drainage adits and to implement this knowledge in a risk management system. This approach, that uses the over 100 galleries in the southern Ruhr area as an example, has a holistic character. Our innovative research approach combines the fusion of extensive sensor data with in-situ expertise.

The investigations and analyses show that, in order to achieve a reliable process understanding of the water-bearing adits, it is necessary to conduct and evaluate comprehensive geomonitoring.

Keywords: Water Bearing Adits, Monitoring, Perpetual Tasks, Risk Management, Hydro Chemical Parameter

Introduction

In many mining districts around the world, adits were and are still being built today for the purposes of providing access to the deposit, serving as transport pathways and mine ventilation and, in particular, ensuring mine water drainage. In this case the galleries slope upwards. In conjunction with the connected mine workings, these galleries form an underground drainage and outflow system whose functionality extends far beyond the actual operating period (Goerke-Mallet *et al*. 2016). When mine operation is being abandoned the consequence is usually the closure of the access to the gallery system from the surface. The drainage effect of the mine workings remains however completely unaffected and will continue, invisibly, for an unknown time period. It is therefore justified to speak of a mode of action that is designed for eternity.

When a (water-discharging) adit enters into the post-mining phase, it is usually associated with a loss of observation, since ventilation and stability of the mine workings is lost over time (Fig. 1). In the case of water-

Figure 1 Water-bearing adit in the southern Ruhr area (image: THGA).

bearing adits, information on the discharge rate per time unit as well as data on the hydrochemistry of the mine water can only be accessed at the portal. It is impossible to obtain results from 'visual inspection' about the processes taking place underground. These processes include local loosening of the rock and cave-in areas within the mine workings. As a result, obstacles can form that affect the orderly flow of water down the adit. This can lead to temporary or permanent complete blockage of the outflow and to the formation of a water accumulation or stagnant water in the mine workings and the rock mass. As the stowage height so the water pressure increases, the risk of spontaneous failure of the blockage rises. As a consequence, a sudden outburst of water may occur at the portal. The impact of a water outburst and flooding has a considerable impact on the safety of the public and on the ground surface, as events in various mining districts have repeatedly shown.

An adapted risk management system is therefore required, in which particular attention is paid to the occurrence of abrupt water discharges. In addition, the uncontrolled formation of water accumulation in the mine workings can be associated with the risk of sink holes occurring at old shafts and above mining areas close to the surface. Furthermore, the changing level of the water table provokes spatially unexpected leaks of the mine water at the surface. This can happen at natural hydraulic connections (e.g., tectonic faults) or at to date dry and possibly unknown adits.

These explanations are intended to illustrate the complexity of risk management of water bearing-adits. The reliability of the assessments and statements depends to a large extent on the available information and the monitoring methods used. Furthermore, a proper handling of the risks requires a careful consideration of the relevance and resilience of the statements.

The investigations carried out by the Research Center for Post-Mining pursue the objective of improving the process understanding of the principle of operation of water-bearing adits and of developing adapted monitoring measures. As a result, reliable information will be generated to enable the long-term safe and economically feasible management of individual water-bearing adits. The results from risk management also serve as a credible and binding communication with essential stakeholders and with the public. For the organization responsible for the water-bearing adits, it is also a matter of reputation, so to speak the 'social license'.

Methods

TThe methodology to evaluate old and abandoned mine objects like water-bearing adits integrates the available historic information, data and knowledge and combines them with current information and data as well as with the gathered data from the evaluation. Only the full integration of all available information will enable a sustainable analysis and interpretation in the sense of a risk assessment.

Analysis of the mine maps

An essential step in the analysis of the functionality of a water-bearing adit consists in the systematic, three-dimensional evaluation of available mine maps and plans of the requested object and of other mine workings that are hydraulically connected with the gallery (Fig. 2). The documents, based on mine survey work, were created during the drivage of the adit and in the phase of its operational use. Their reliable evaluation requires technical expertise, which is already required for the georeferencing of maps that are often based on historical coordinate systems. The symbols used and the representation of tectonic elements

must be interpreted correctly. Elevation information is often missing. In order to obtain a sufficiently accurate picture of the original subsurface conditions, the interpretation of the old mine maps must be based on expertise in mine surveying, mining and geology. Understanding the functionality of water-bearing adits is the prerequisite for the risk management of the respective object.

In this context, for example, the spatial location of coal seams, tectonic elements, natural and anthropogenic created flow paths and hydraulic connections must be considered. Thus, the Ruhr Carboniferous structure has to be considered as a fissure aquifer. In the following, the water (seeped rainwater, infiltration of waterbodies, anthropogenic sources) and mine water pathways, feeding the drainage adits, have to be identified. If the hydraulic connections or even the adit itself are restricted in terms of hydraulic capacity in the course of caves, stagnant water accumulations occur in the mine workings. In this case, the amount of mine water discharged at the portal can temporarily drop to zero.

As part of risk management, it is necessary to analyse the effects that the formation of water accumulations can have on water seepage at the surface. For example, spontaneous water outbursts may occur at the portal if the rock mass in the caved area is pushed away by the water pressure. However, unexpected water outburst at the surface is also possible if the level of water accumulation overtopped higher hydraulic connections. The forming of a stagnant water can also pose significant risks to neighboring mines if mine water was to flow into these mines through hydraulic connections.

Risk management also includes investigating the risk of sink holes occurring above old shafts, mine workings and the gallery itself. The type of land use at the surface and its distance from mining features must be included in the analysis.

The explanations illustrate the scope and importance of the systematic analysis of the information available in old mine maps and plans about water-bearing adits for risk management. Practical experience not only in the Ruhr area has shown that a wide range of findings can be obtained on this base. However, the recording of the current development in the system of a water-bearing adit requires more far-reaching concepts for monitoring (Goerke-Mallet *et al.* 2016). This means that exploration methods from the air (e.g., satellite remote sensing, copter flights), from the day surface (e.g., perpetrations) and in the subsurface (e.g., boreholes, seismic, gravimetry) can be considered. The integrated application of such methods is also necessary, in particular, if no or only little information from mine maps is available about the adit.

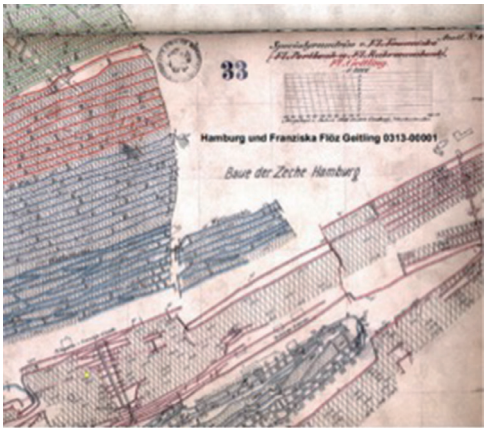

Figure 2 *Exemplary mine map of seam "Geitling" in the area of the mine "Hamburg und Franziska" and the dewatering system of "Franziska" (1888).*

The exploration can also provide a basis for long-term monitoring of the adit. In this way, boreholes can be developed into measuring points for the mine water level and used within the framework of spatial models of the hydraulic pathways. In this context, DMT GmbH has shaped the term 'box model (box = hydraulically active area of an underground mine)'. In these models, the levels of potential water discharge points at the surface or even in the mine workings are also shown in the direction of the catchment area of a neighbouring adit.

The aim of the analyses and evaluations described above is to develop a reliable monitoring concept that adequately reflects the risk parameters determined. The Research Center of Post-Mining is therefore working intensively on converting the mine maps available for individual tunnels into 3D systems. This will allow to make the expertise of the analysts transparent and use it for the development of integrated risk management,

monitoring and communication/science transfer with stakeholders (Goerke-Mallet *et al.* 2018 & 2020). Currently, the extent to which geometric engineering planning and evaluation systems can be used in analysing the functionality of water-bearing adits to create a spatial understanding is being examined (Rudolph *et al.* 2020). For example, the PETREL reservoir tool has already been successfully used to visualize the surface and underground situation. The DUDE (Digital underground and deposit) platform, which RAG AG has already used in the production phase of its mines to edit the mine maps, offers considerable potential that will be investigated in greater detail in the near future.

Analysis of existing historic mine structures

Wherever it is possible, existing mine structures, like shafts, should be incorporated into geomonitoring analysis (Rudolph *et al.* 2020). These shafts are one entry point to the subsurface and provide important information on the hydrology, hydrogeology, and hydrochemistry.

As a showcase, a former mine shaft in a city in the southern Ruhr area was logged with a combined temperature, conductivity and pH sensor (Fig. 3).

The depth profile shows a stratification of water with a slightly elevated temperature T of T = 16 °C above cooler water with a temperature T of T = 15 °C down to a depth $h$of h = -70 m NHN (Fig. 3). These temperatures do not show a full geothermal depth gradient, as this is a mining influenced rock with e.g. induced fractures.

The conductivity and the pH value do not increase with depth and thus do not indicate an increase in the mineralization of the water. The pH value of pH = 7 is considered normal. The conductivity L of L = 1.2 mS/cm indicates normally mineralized waters. The very slight changes in conductivity at depth h of h = 0 m NHN and h = -70 m NHN could indicate slight mine water stratification.

In principle, however, the results are to be interpreted in such a way that within the open shaft column a full convection of the water takes place. Whereby in the top of the shaft surface water probably flows in, as it was also documented in other technical reports. The low mineralized water at the greater depth of the shaft column indicates that there is likely to be inflow and outflow, although this cannot be shown over the entire mining levels.

In summary, the results show that no highly mineralized waters of the Carboniferous were detected, as it is normal

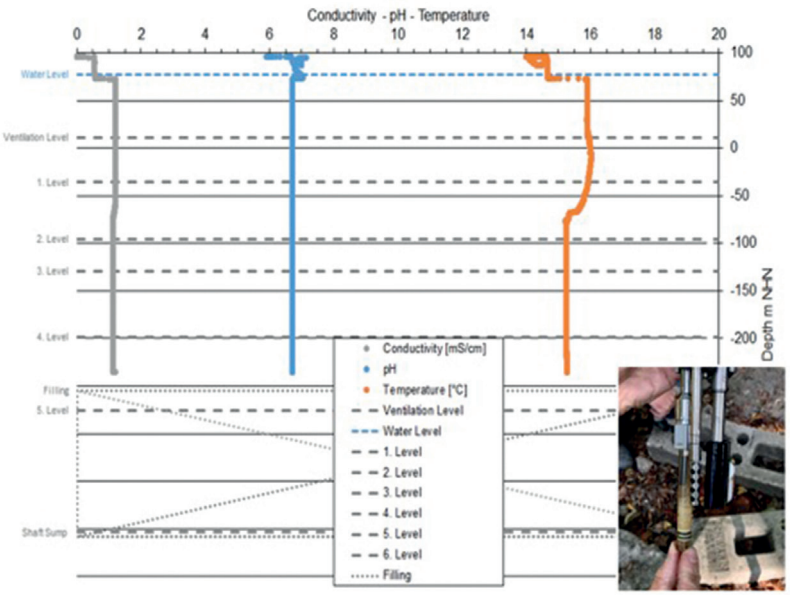

Figure 3 *Results of the trip-out-run with the multi-parameter sensor (inlay: Multiparameter sensor).*

for the Ruhr-area, in the open part of the shaft. There was also no typical stratification of the mine water. This indicates that there must probably be a hydraulic connection with other hydraulic systems.

Assessment of the hydrology and hydrogeology

During the mapping of the vicinity of water bearing adits it is important to understand the local hydrological and hydrogeological situation to build up a complete process understanding. In one particular case the mapping showed that a small river was crossing one part of the water bearing adits and there was the indication that the river could infiltrate via the Carboniferous sandstone beds directly into the adit (Fig. 4 A).

The modern discharge measurements of the river have shown that there is potentially a volume gap between the measurement before and after the crossing of the adit. This was supported by the analysis of the former mine documentation, which reported an increased water inflow during the operation of the mine. Therefore, during summer and at a low discharge an infiltration test with fully saturated brine was conducted to determine the infiltration rate into the underlying mine structure (Fig. 4, B).

The brine infiltrated had a conductivity L of L = 203,000 µS/cm. The conductivity normally measured at the mouth of the drainage adit is between about L = 1,300 µS/cm and L = 1,400 µS/cm, so that changes could still be detected, even with a strong dilution.

Figure 4 *A: Photo of the fractured carboniferous sandstone layers in the river bed above the water bearing adit (December discharge); B: Infiltration test (image: THGA).*

The Infiltration rate I of about I = 1 L/m²min-1 at the two test points was very slow and did not indicate increased permeabilities ("swallow horizons") at the Carboniferous sandstone beds. The externally provided hydrochemical data of the real-time measurements at the adit mouth showed unfortunately no increased conductivity and the data was later interpreted as not properly working measurement devices. The further analysis of the data showed in addition that the bandwidth of data fluctuations of the measured conductivity was about L = 400 µS/cm.

In summary, although infiltration of river water was initially considered very plausible, the infiltration test with the very low infiltration rates did not provide a direct indication of the actual infiltration of the river water.

Hydrochemistry of the Franziska Erbstollen

The mine water hydrochemistry of the Franziska Erbstollen (drainage adit) was investigated over three sampling series in the period from 2015 to 2016. The main cations and anions of the mine water were analysed. In addition, an ion balance was generated from the water analyses and the groundwater type was determined. The results of the analyses are shown in the following table.

The mine water is a $Na\text{-}Ca\text{-}HCO_3\text{-}SO_4$-type showing a comparable water chemistry over the whole sampling period. The main constituents are in the same order of magnitude and largely stable.

The iron and sulfate content in the mine water is related to pyrite oxidation. The sodium content is geogenic and corresponds to the local groundwater conditions of the Carboniferous and the deposit. The same applies to the chloride content and the proportions of strontium and barium. The calcium and hydrogen carbonate contents in the mine water cause natural buffering and lead to the largely neutral pH values in the mine water. The direct influence from near-surface inflow and groundwater recharge has to be regarded as low, as evidenced by the nitrate content. The total mineralization expressed as specific electrical conductivity is comparatively low for mine water. In comparison with the local groundwater situation, it is clearly increased.

In summary, the quality of mine water can be regarded as comparatively harmless. The water-rock interactions are largely constant. The hydrochemistry of the mine water will therefore not be subject to any significant change processes in the future under stable mine conditions and flow paths. This conclusion will be tested by a long-term monitoring program.

Summary

Water bearing adits, drainage adits and galleries are till nowadays an important part for the former mine infrastructure because of their drainage function. As these systems are no longer directly accessible risk managements systems have to be developed and integrated analysis various (sensor-) datasets need to be conducted. The spatiotemporal analysis is the enabler for the verification of the operational functionality.

References

Goerke-Mallet P, Mersmann F, Beermann T, Stöttner, M (2016): Optimizing long-term mine water management of mining sites with the help of directional drilling and liner technology. Mining report 152(2), 171–177

Goerke-Mallet P, Melchers C, Müterthies A (2016): Innovative monitoring measures in the phase of post-mining. – In: Drebenstedt C, Paul M (Eds.): Mining meets water – conflicts and solutions: proceedings. – IMWA 2016, Leipzig, Germany, July 11-15 2016. Freiberg: TU Bergakademie Freiberg, Institute of Mining and Special Civil Engineering, S. 570–577 (DVD-ROM). URL: https://www.imwa.info/docs/imwa_2016/IMWA2016_Goerke-Mallet_201.pdf (accessed 04.05.2021)

Goerke-Mallet P, Müterthies A, Melchers, C (2018): The development of a "Mine Life Cycle Information System". In: Drebenstedt C, von Bismarck F, Fourie A, Tibbet M (Eds): Mine Closure 2018. Proceedings of the 12th International Conference on Mine Closure, 3.-7. September 2018, Leipzig, Germany. – Freiberg: Technical University Bergakademie Freiberg, Institute of Mining and Special Civil Engineering, 99–106

Goerke-Mallet P, Rudolph T, Kretschmann J, Brune JF (2020): The Importance of „Social Licence to Operate" for the Mining Life Cycle. Mining Report 156(4), 323–332

Rudolph T, Goerke-Mallet P, Janzen A, Müterthies A, Pakzad K, Spreckels V, Teuwsen S, Vehling L, Yang C-H (2020): Monitoring measures in the southern Ruhr area. In: Tagung GeoMonitoring 2020. 12.-13. März 2020 in Braunschweig. Hannover: Institutionelles Repositorium der Leibniz Universität Hannover, 163–177 (In German: Bergbaumonitoring im südlichen Ruhrgebiet.)

Rudolph T, Melchers C, Goerke-Mallet P, Müterthies A (2020): 4D Geomonitoring für die E&P Industrie. 1 p. (DGMK/ÖGEW Frühjahrstagung 2020).

Table 1 *Mine water analyses of the Franziska Erbstollen.*

Sample ID	MW 16.1	MW 16.2	MW 16.3
Date	16/6/2015	5/4/2016	26/8/2016
Temperature, °C	14.7	15.1	16.2
Conductivity, µS/cm	1,400	1,420	1,400
pH, 1	7.1	7.1	7.3
Watertype	$\underline{Na}\text{-}Ca\text{-}\underline{HCO_3}\text{-}SO_4$	$Na\text{-}Ca\text{-}\underline{HCO_3}\text{-}SO_4$	$\underline{Na}\text{-}Ca\text{-}\underline{HCO_3}\text{-}SO_4$
Cations			
Ca^{2+}	91	77	88
Mg^{2+}	35	29	32
Na^{+}	182	169	181
K^{+}	14	11	13
Fe^{2+}	3.4	3.4	3.7
Mn^{2+}	0.61	0.56	0.61
Sr^{2+}	1.1	0.99	1.1
Ba^{2+}	0.028	0.011	0.028
Anions			
HCO_{3}^{-}	570	560	570
Cl^{-}	52.8	63	64.2
SO_4^{2-}	202	223	219
NO_{3}^{-}	1	1	1

Integration of Regional and Site Scale Models for an Open-Pit Mine

John Rupp[1], Geoff Beale[2], Kevin Howerton[3], Max Allen[4]

[1]*Senior Hydrogeologist, Piteau Associates, 9090 Double Diamond Parkway, Unit 1, Reno, Nevada, USA, 89521, jrupp@piteau.com*

[2]*Principal, Piteau Associates, 9090 Double Diamond Parkway, Unit 1, Reno, Nevada, USA, 89521, gbeale@piteau.com*

[3]*Principal Hydrogeologist, Round Mountain Gold Corporation, 1 Smoky Valley Mine Road, Round Mountain, Nevada, USA, 89045, kevin.howerton@kinross.com*

[4]*Junior Hydrogeologist, Piteau Associates, 9090 Double Diamond Parkway, Unit 1, Reno, Nevada, USA, 89521, mallen@piteau.com*

Abstract

Numerical groundwater modeling has progressively become the standard industry tool to evaluate and predict hydrogeologic responses to mine dewatering. Experience has shown that most mine sites require at least two numerical models, each at distinctly different scales, to answer key water management questions. This paper draws on over 30 years of dewatering data from an open pit mine in Nevada, USA to illustrate the importance of scale selection on model development. It uses the experience gained from a 3-D regional-scale model and a 2-D pit-scale model to highlight how both are needed to adequately assess the mine's water management system.

Keywords: Numerical, Model, Open-Pit, Mining, Dewatering

Modeling Background

Numerical models are used to support all phases of mine water management evaluations from initial scoping to mine closure. Key mine site numerical modeling needs include: (i) defining potential impacts from mining activities on the regional groundwater system, (ii) demonstrating the environmental performance of a mine, during operations and/or closure, and (iii) developing and managing the mine dewatering or pit slope depressurisation programs.

A few basic issues need to be addressed before mine-specific numerical models are developed:

1. What questions does the model need to answer?
2. What decisions need to be made using the results?
3. At what scale do these questions need to be answered?
4. How do those scales relate to the physical hydrogeologic processes that will drive the answers?

Experience has shown it is usually more efficient and effective to use at least two independently scaled groundwater models than to develop one model to address all study needs. For example, mine environmental departments most often need regional-scale models to support permitting and closure. These studies usually require regular (1 to 5 year) updates with a high level of modeling effort over a period of months or even years. In contrast, the mine engineering or operations departments typically need models to answer sector-specific mine dewatering and/or pit slope design questions to support monthly or quarterly water management decisions. Trying to use one model to address both efforts would sacrifice operational flexibility and overwhelm longer-term regional evaluations with unnecessary detail.

The two most common model scales for mine water management studies are Regional-Scale Numerical Models (RSNMs) and Mine-Scale Numerical Models (MSNMs). The following two sections highlight the key

differences and uses of these two types of groundwater models.

Regional-Scale Numerical Models

First and foremost, a RSNM defines the hydrogeological interaction between the mine site and the surrounding regional groundwater system. RSNMs are used to define the potential for future impacts from (i) proposed mine dewatering programmes, and (ii) new facility development (such as tailing, water, and/or waste rock storage), as well as to better understand current or past effects from mining on the regional groundwater system. RSNMs are also used to evaluate mine water supply feasibility. Since RSNMs are based on hydrogeologically significant basin-scale boundaries, they can also be used to define internal boundary conditions for site-scale or facility-specific models.

A RSNM encompasses hydrogeologically significant boundary conditions such as basin divides, rivers, lakes, or groundwater discharge zones. Depending on the setting and mining operation scale, a RSNM may extend for tens of kilometres beyond the mine property boundaries, potentially across administrative boundaries or international borders.

Basin fill groundwater systems are often represented as lumped hydrogeological units even though systems may be highly layered with variable hydraulic properties. Key regional-scale geology and structures may be incorporated from water-supply and geologic investigations, but the available information is typically not as detailed as the data-rich open pit area. Lumping of geologic and hydraulic parameters to fit typical RSNM grid scales often 'smears out' smaller-scale (slope-scale) geological or hydrogeological details in the pit area that may be important for operational considerations but does not adversely affect the regional-scale evaluation.

A key limitation for RSNMs are computational and data management requirements. Computational requirements are driven by the number of cells (or elements) and layers selected. Grid telescoping, including quadtree grid refinement, is almost always useful to optimize the higher-resolution data in the pit area and the lower-resolution data in outlying areas. However, RSNMs with hundreds of thousands to millions of cells are cumbersome compared to the smaller MSNMs. RSNMs usually require hundreds of man-hours to calibrate even with the assistance of numerical optimization and require substantial time and effort to manage the associated massive quantity of input and output data.

Mine-Scale Numerical Models

A Mine-Scale Numerical Model (MSNM) normally includes part or all of the open pit and/or key project facilities. The purpose of the MSNM is to incorporate geological and hydrogeological details related to fine-scale facility-specific processes that cannot be captured adequately or efficiently with the RSNM.

A MSNM most often provides a groundwater head and gradient distribution in the immediate mine vicinity for operational or mine design analysis. These models also predict the potential range of groundwater inflow rates, based on sectorspecific geology and hydrogeological conditions. MSNMs can assist in planning and design of the general mine dewatering system, the pumped water discharge system, and sensitivity of alternative mine plans to dewatering requirements and sequencing. A MSNM can also be fundamental to understanding the uncertainty in the local hydrogeological system variables, including geology, rock mass hydraulic parameters, the characteristics of known structures, or the variability in local recharge conditions.

A MSNM normally requires local areas of increased data intensity, facilitating identification and characterisation of geological and hydrogeological features that are important to open-pit or facility performance. Geological units surrounding an open pit or facility that are 'lumped' for the RSNMs may need to be sub-divided in an MSNM based on lithology, alteration type or structural domain, and assigned distinct hydraulic properties. The MSNM grid spacing is fine compared to a RSNM, normally on the order of a few tens of meters or less. The MSNM simulates a substantially smaller area compare to a RSNM, because the study area is focused on pit-scale processes.

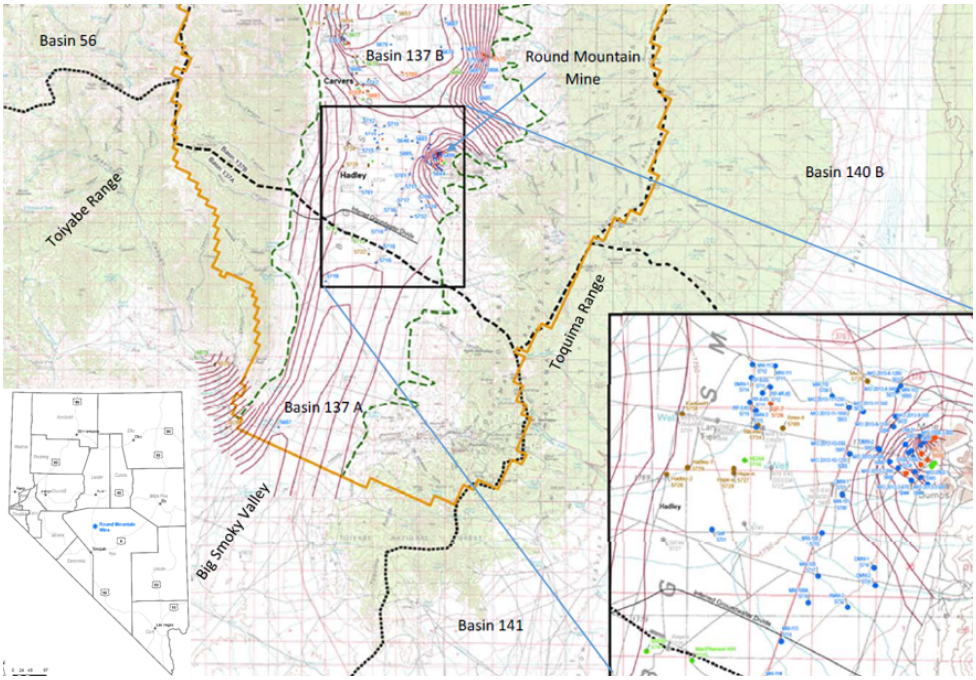

Figure 1 Round Mountain Mine and Big Smoky Valley Location Map, Nevada, USA.

Case Study Example: Round Mountain Mine RSNM and MSNM

The following case study is focused on the open pit Round Mountain Mine, near Hadley, Nevada (Figure 1). The Round Mountain Mining District has been active since the 1800's. Modern mine dewatering commenced in the early 1990's followed by several mine expansions over the years. Numerical modeling commenced at Round Mountain in the late 1980's, providing 30-plus years of hydrogeologic data. Round Mountain Gold Corporation (RMGC) recently completed a feasibility study to evaluate the hydrogeologic effects from mining a six-year push back in the south-eastern part of the existing pit.

The Round Mountain Mine is located Nye County, Nevada, at the southern end Big Smoky Valley, within the Great Basin subprovince of the Basin-and-Range Physiographic Province. The principal hydrogeologic units in Big Smoky Valley are typical of the Nevada Basin-and-Range Physiographic Province:

- **Basin Fill:** This unit is comprised mostly of alluvium with playa and channel deposits. The most significant water-bearing strata in the area are in the coarser gravel and cobble-rich channel and alluvial deposits.
- **Bedrock:** This unit includes volcanic tuffs of Oligocene to Miocene age which were erupted from a group of several calderas in the southern Toquima Range, metasedimentary rocks of Cambrian to Ordovician age, and granitic plutons of Cretaceous age.

In addition to these principal units, the Stebbins Hill Formation, which is a mix of lacustrine clay and volcanic bedrock, forms a hydrogeologically significant aquitard at the western edge of the Round Mountain Pit.

Round Mountain RSNM

The current iteration of the 3-D finite difference Round Mountain RSNM was originally developed in the early 2000's using MODFLOW-SURFACT (Hydrogeologic 2021). The key RSNM model goals are to (i) confirm analytically-estimated dewatering rates and potential drawdowns in the basin-fill and bedrock groundwater systems, (ii) to provide

inputs for the water quantity impacts analysis, and to (iii) simulate the pit lake recovery rate and water balance in permanent closure.

Figure 2 shows the RSNM domain and boundaries. The model domain is large enough to reasonably simulate the 3-meter drawdown isopleths from pumping at Round Mountain without being constrained artificially by distal boundaries. The RSNM grid includes variable-mesh refinement, to reduce cell size in areas of key interest around the open pit. The model grid includes 198 rows, 147 columns and 11 layers, with a total of 320,166 cells. The smallest grid cells (91.4 m by 91.4 m) were specified near the Round Mountain Pit, where simulated pumping rates and drawdowns were the greatest. Progressively larger cells up to 732 m by 823 m were specified towards the model margins.

The RSNM domain shown in Figure 2 includes the entire area with potential for dewatering impacts from the Round Mountain Pit dewatering. The eastern and western boundaries are the surface topographic divides that form the hydrographic basin boundaries (Rush and Schroer 1970; Handman and Kilroy 1997). The northern boundary coincides with springs along the edge of the central-basin playa. The southern boundary is distant enough to avoid the constraint of model-simulated drawdowns from pumping. Groundwater flow out of this boundary is to the south.

The initial calibration process included three key periods: steady state calibration, transient calibration and transient verification. The RSNM currently requires 10 hours to run the entire calibration, predictive dewatering, and mine closure modeling sequence, generates roughly 200 MB of data per model run sequence, and requires 16 to 20 months to complete a bi-decadal level model update, including reporting.

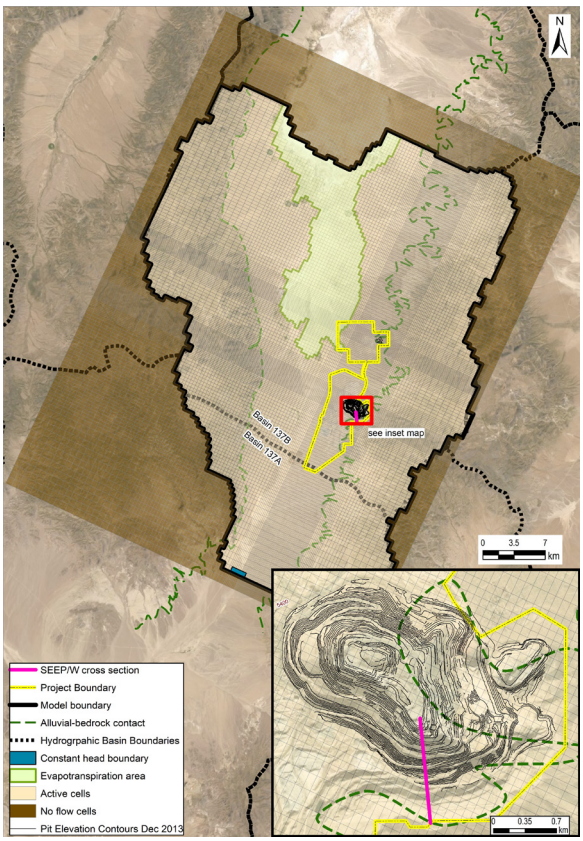

Figure 2 *RSNM boundary conditions, grid, 2-D cross section location, and conceptual model.*

Key model output from the RSNM include pit filling hydrographs and predicted drawdown isopleths. The stabilized pit lake levels are primarily a balance between groundwater inflow and pit lake evaporation. Groundwater-driven inflows are primarily derived from the alluvial groundwater system. Although results show that peak dewatering rates approach 631 L/s and infilling from the alluvium to the pit lake could exceed 189 L/s, the potential impacts to the surrounding groundwater system are manageable.

Two independent validations were completed on the RMGC RSNM (Piteau 2021). The model validations confirm the RMGC RSNM performs well for the regional-scale impacts analysis. However, as noted above, (i) it requires too much time and effort to update the model for operational studies and (ii) the grid spacing is 91.4 m^2 in the pit area, which is too large to meet the needs of the finer pit-scale evaluations.

Round Mountain MSNM

A MSNM was needed to support: (i) the year-by-year dewatering plan for a mine expansion, and (ii) geotechnical stability analysis. Pore pressure was seen to significantly decrease the effective stress of the slope materials, so the input to the geotechnical analysis required a high degree of discretization and accuracy.

The 2-D finite element MSNM was constructed using SEEP/W (Geostudio 2021) (Figure 3). The model cross section corresponds to the key geotechnical design section in the west wall of the Round Mountain Pit (inset on Figure 2). The finite element mesh was defined to correspond with stratigraphic and structural features known to control the pit-scale pore pressure distribution. Mesh refinement ranged from 5 m around the pit slope and structures to 15 m at the more distant model boundary (Figure 3). Because of its simple geometry and limited complexity, the 2-D MSNM can be updated, calibrated, and run in approximately 7 to 10 days. Subsequent predictive scenarios can be run on a calibrated model within 1 to 2 days.

The MSNM Boundary conditions are shown in Figure 3. The MSNM boundary conditions correspond to internal boundaries derived from (i) the RSNM and (ii) the open pit. The lateral model boundary opposite the pit slope was assigned transient heads based on the RSNM simulation. The open pit was represented with a 'seepage' numerical

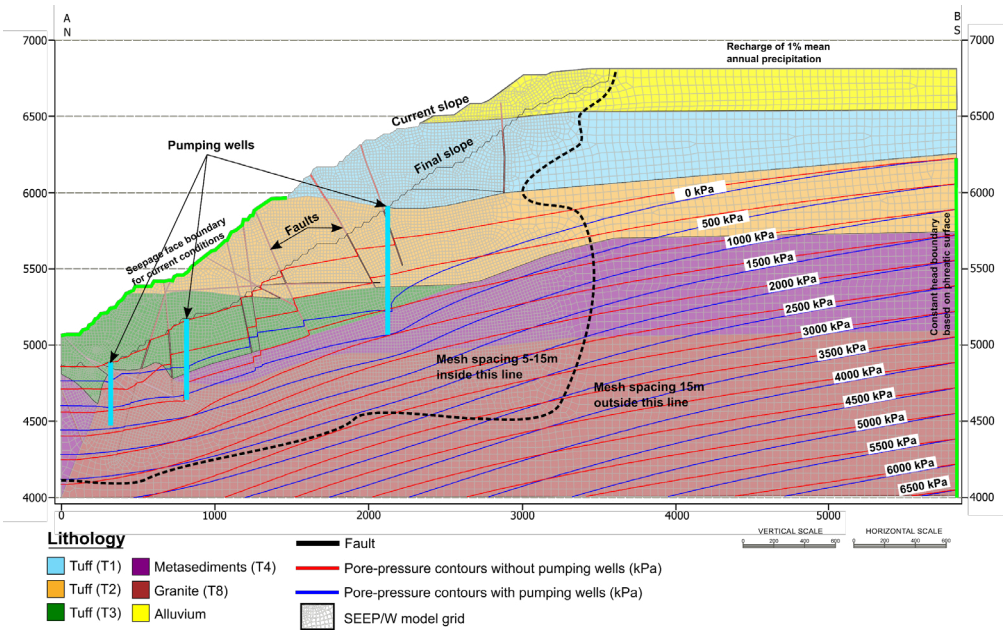

Figure 3 MSNM 2D cross section with boundary conditions, model grid spacing, and pore pressure results with and without pumping wells.

boundary condition. This boundary allows a seepage face to develop in areas where positive pore pressures occur at the pit wall.

The MSNM simulations predicted the pore pressure distribution with and without active depressurisation by dewatering wells and horizontal drain holes (HDHs). The model results support the current pit slope design and demonstrate that the dewatering program can address key issues identified in the slope design process, including the pore pressures associated with individual structures. These results provided key input to the geotechnical pit slope stability analysis that would not otherwise be obtainable from the RSNM.

Conclusions

The results of the study have demonstrated the following:

- Experience has shown it is usually more efficient and effective to construct at least two groundwater models for a given site at different scales.
- RSNMs are used to define the potential for future impacts from (i) proposed mine dewatering programmes, and (ii) new facility development, as well as to better understand current or past effects from mining on the regional groundwater system.
- A key limitation for RSNMs are computational and data management study requirements that can take months or even years to complete.
- A MSNM provides a finer-scale groundwater head and gradient distribution in the immediate mine vicinity for operational or mine design analyses.
- Two independent validations confirm the RSNM performs well for the regional-scale impacts analysis. However, the RSNM requires substantial effort on the order of 16 to 20 months to complete and does not provide finer-scale resolution required for operational dewatering analyses.
- The MSNM model results support the current pit slope design and demonstrate that the dewatering program can address key issues identified in the slope design process, including the pore pressures associated with individual structures. These results were obtained quickly and efficiently because the MSNM is substantially smaller and required less effort.
- Although RSNMs and MSNMs are usually developed independently, added value can be achieved between them by (i) assigning consistent boundaries / hydraulic properties and (ii) adopting similar assumptions to represent key conceptual hydrogeologic processes and (iii) incorporating a "feedback loop" of learnings gained through iterative repeated studies.

Acknowledgements

The authors thank Round Mountain Gold Corporation for their participation and support for this study and the IMWA for review and comments on the paper. We also thank Brian Giroux for his editorial review.

References

Rush, F. E and C. V. Schroer (1970) Water Resources of Big Smoky Valley, Lander, Nye and Esmerelda Counties, Nevada. Nevada Division of Water Resources Bulletin 41.

GeoSlope (2021) SEEP/W overview. Available: https://www.geoslope.com.

Handman, E.H. and K. C. Kilroy (1997) Groundwater Resources of Northern Big Smoky Valley, Lander and Nye Counties, Central Nevada. U.S. Geological Survey Water-Resources Investigations Report 96-4311.

Hydrogeologic (2021) MODFLOW-SURFACT overview. Available: https://www.hgl.com.

Piteau (2021) Groundwater Quantity Impacts Assessment. January.

Carbonation of Magnesium Silicate Minerals in Mine Waste: Practical Laboratory Testing Methods to Assess the Dual Opportunity for Carbon Capture and AMD Mitigation

Rhys John Savage[1,2], Malvina Chmielarski[2], Andrew Barnes[1], Steven Pearce[3], Mark Roberts[1], Phil Renforth[4], Seth Mueller[5], Devin Sapsford[2]

[1]*Geochemic Ltd, Lower Race, Pontypool, NP4 5UH, Wales, United Kingdom, rsavage@geochemic.co.uk, abarnes@geochemic.co.uk*

[2]*Cardiff University, Queen's Building, Cardiff, CF24 3AA, Wales, United Kingdom, sapsforddj@cardiff.ac.uk*

[3]*Mine Environmental Management Ltd, Vale Street, Denbigh, Denbighshire, LL16 3AD, Wales, United Kingdom, spearce@memconsultants.co.uk*

[4]*Heriot-Watt University, Riccarton, Edinburgh, EH14 4AS, Scotland, United Kingdom, P.Renforth@hw.ac.uk*

[5]*Boliden AB, Sweden, seth.mueller@boliden.com*

Abstract

Mineral carbonation has been widely recognised as an important mechanism in the sequestering of CO_2 into mining wastes and by-products. The generation of fast-reacting carbonates in the carbonation process may also have important implications for the mitigation and prevention of acid mine drainage (AMD). Laboratory-scale methods have been developed to assess carbonation potential in mine by-products from an active nickel mine site in Finland. Utilized methods allow assessment of key parameters controlling the carbonation process. It has been demonstrated that the methods can influence waste pore water chemistry and geochemistry as a result of the carbonation process.

Keywords: Carbon Sequestration, Acid Mine Drainage, Geochemistry, Carbonation, Mine Drainage

Introduction

This paper presents the findings of the effects of mineral carbonation on mine waste rock acid neutralising capacity following short-term carbonation experiments.

The primary aim of the research was to improve the understanding of the carbon capture potential (CCP) of mafic and ultramafic waste rock materials excavated from Boliden AB's Kevitsa Ni-Cu-PGE mine in northern Finland. The secondary aim of the study was to verify and further test a number of novel experimental procedures devised by the research group for the determination of CCP from mining waste as a whole. We have attempted to assess the influence of carbon capture on the geochemical properties of mining waste and the ability of treated mining waste to neutralize acidity generated from sulfide oxidation.

It is well understood that Mg and Ca silicate-rich materials have the potential to sequester atmospheric carbon dioxide through the dissolution of minerals such as forsterite (Mg2SiO4) and anorthite ($CaAlSiO_4$) together with subsequent precipitation of stable carbonate minerals or through fixing CO_2 in the dissolved phase where mineral saturation does not occur (Li *et al*., 2018, Wilson *et al*., 2009, Harrison, Power and Dipple, 2013 and Renforth 2019). Previous studies (i.e. Declercq *et al*., 2020) have shown that mineralogical changes occurring in ultramafic mining waste, have potential to increase the carbonate NP and overall acid neutralising potential determined through standard test methods (e.g. EN15875:2011).

A preliminary study undertaken by this research group identified the potential of two relatively low-cost, rapid methods to

assess carbon capture potential in mine waste rock. These methods include manometric determination of CO_2 sequestration rate and carbonation columns (Savage *et al*., 2019). This study extends the work to examine the effects of temperature, particle size distribution (PSD), moisture content and CO_2 concentration on the relative rates of carbonation.

Within this paper the effect of carbonation on acid neutralisation is discussed with a view to potential benefits to mine drainage mitigation.

Methods

Sample Preparation

All testing was undertaken at the Geochemic Ltd laboratory facility located in Wales, UK. Testing was undertaken on composites of individual discrete waste rock samples obtained through screening of 100 mm diameter sonic drill core intervals to 22 mm. The sonic drilling program was undertaken on the existing Kevitsa waste rock dumps and therefore represented material of variable age of atmospheric exposure and states of weathering. As part of the study, each discrete pre-screened (sub-22 mm) core interval sample was further screened through dry sieving into <2.36 mm ('fines') and 2.36 mm to 22 mm ('coarse') size fractions. From the discrete size fractions two composites samples, 'Fine composite' (<2.3 mm) and Sample 'Coarse composite' (2.33 mm to 22-mm), were compiled. The two size fraction composites allowed the testing of the CCP of the two size fractions relatively from the Kevitsa waste rock dump.

Basic Characterisation of Samples

A series of basic geochemical characterisation tests were undertaken on the composite samples both pre and post CO_2 treatments. The tests included the following:

- Elemental composition through Energy Dispersive X-Ray Florescence (ED-XRF) (Panalytical MiniPal-4)
- Total C and S determined through high temperature combustion (Perkin Elmer 2400)
- Determination of water-soluble components 2:1 Liquid to Solid ratio 24-hour deionised water leach, with ICP-OES analysis of leachates – EN 12457-1:2002
- Net Acid Generation (NAG) testing and NAG liquor analysis by ICP-OES – EGI (2002)
- Acid Neutralising Capacity (ANC) in accordance with EN 15875:2011
- Acid Buffering Characterisation Curve (ABCC) AMIRA 2002
- Automated modal mineralogy through SEM-EDX mapping
- Mineral phase identification through fine powder X-Ray Diffraction (XRD)

Due to limitations of the current paper, only results for core tests are given .

CO_2 Treatment Tests

In order to test the validity and variability of two CCP testing procedures devised during the previous research phase (Savage *et al*., 2019), an experimental program was devised to look at variability of the particular testing protocols to changing experimental conditions (Table 1).

Results

Mineralogical Characterisation

SEM-EDX analysis carried out on the coarse (Sample C) and fine (Sample F) composites showed that sample mineralogy was dominated by silicate mineral groups, with magnesium silicate phases identified. Sample C was predominately composed of clinopyroxene (53.5%) and amphibole (17.0%), with lesser phases of serpentine (6.0%) and forsterite (4.4%). Sample F showed similar mineral abundances; clinopyroxene (53.1%), amphibole (15.4%), serpentine (5.9%) and olivine (4.2%).

Elemental Characterisation

Elemental analysis carried out using ED-XRF showed similar elemental contents between the 2 sample sets. The S contents were measured at 0.38% and 0.59% for sample F and sample C, respectively. The major deviations that was noted between the

Table 1 *CO_2 treatment tests and condensed test information.*

Treatment Method	Test Information	Varied Test Parameters
Carbonation rate reactor vessels	The WTW Oxitop-C® measuring heads used in this study are designed to determine aerobic respiration rates using the Warburg constant volume respirometer method in accordance with ISO 16072. It does this through measuring the pressure changes within a closed system such as a jar or bottle. Using this concept but applying CO_2 (or a mixture of **CO_2** and N_2 **rather** than oxygen as the initial gas, it is now measuring the pressure change corresponding to CO_2 consumption rate.	CO_2 Concentration – 100%, 60% (40% N_2), 30% (70% N_2) and 10% (90% N_2) Temperature – 25 °C and 10 °C Particle Size – coarse and fine waste rock[A] Moisture Content (wt%) – 5% and 10%
Short term (62 day) exposure CO_2 reactor columns	This experiment was designed to determine the carbonate formation potential of a variety of materials exposed to pure CO_2 marginally above atmospheric pressure All the columns were set-up and run at room temperature (20°C) with 10% moisture content. The columns ran for two months (62 days).	CO_2 Concentration– 100%, 60% (40% N_2) and 30% (70% N_2) Particle Size – coarse and fine waste rock[A]

[A]Particle size ranges: Coarse – (2.3mm to 22mm) and Fine – (<2.3mm)

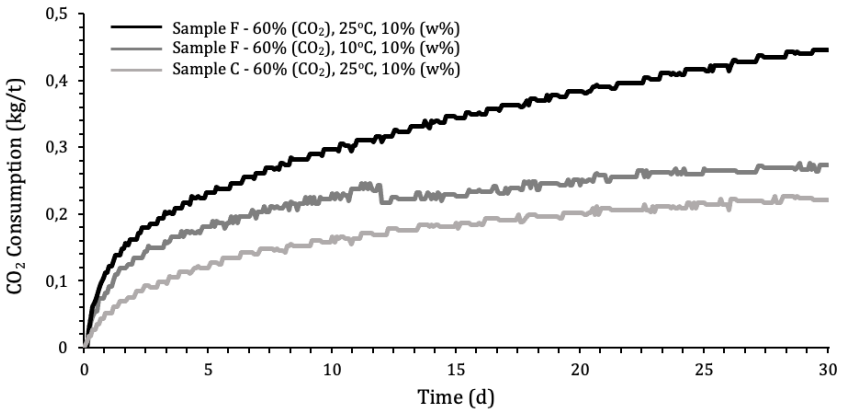

Figure 1 *Sample C (Coarse composite) and F (fine composite) carbonation rate reactor vessel outputs with varied temperature and 60% CO_2 in N_2 gas concentrations.*

sample composites were for Si and Mg. The fine sample fraction measured a Mg and Si content of 4.3% and 11.72%, while the course fraction showed higher levels of Mg and Si with readings of 12.59% and 21.66%.

Carbonation Rate Reactor Vessels

Figure 1 shows the results obtained from CO_2 consumption tests carried out on coarse composite and fine composite samples with variable temperatures (°C) with the same CO_2 concentration (60%), over a 30-day test period. CO_2 consumption was shown to be lower within vessels held at 10 °C compared to 25 °C. With the same test parameters fine samples (<2.3 mm) were shown to have faster consumption rates compared to coarse (2.3 mm to 22 mm). Results obtained from other consumption tests with varied test parameters are shown in table 2. The fastest consumption rate was measured at 6.06 kg(CO_2)/tonne/year for the fine waste rock material, exposed to 100% CO_2 at 25 °C, with a 10% moisture content (wt%).

Table 2 *CO_2 consumption vessel test parameters and measured consumption rates.*

Material	CO_2 (% by volume)	Temperature (OC)	W%	CO_2 Consumption rate[1] ($kg(CO_2)$ /tonne/year)
Coarse Composite	100	25	10	3.8
		25	5	5.0
	60	25	10	2.69
		10	10	2.99
		25	5	3.85
		10	5	1.99
	30	10	10	1.32
		10	5	1.10
Fine Composite	100	25	10	6.06
	60	25	10	5.43
		10	10	3.32
	10	10	10	1.43

[1]Initial rate determined during first 5% of CO_2 consumption.

Implications of Carbonation on Acid Neutralisation Potential

Acid neutralising capacity (ANC) tests carried out on sample residues post CO_2 exposure showed consistent increases in neutralising potential (NP) with both particle size and CO_2 concentration. Pre-treatment ANC NP results for coarse composite and fine composite samples were 27.06 (kg $CaCO_3$ eq./t) and 26.50 (kg $CaCO_3$ eq./t), respectively. This value increased to 32.54 (kg $CaCO_3$ eq./t) within the fine composite exposed to 100% CO_2 gas mix while the coarse composite rose to 30.79 (kg $CaCO_3$ eq./t) at the same CO_2 concentration.

ANC tests on column material post treatment period showed changes in neutralising potential in all samples treated with CO_2. Figure 2 (1) shows ANC results from all coarse composite and fine composite columns. Initial baseline neutralising potential (NP) results from coarse and fine composite samples were 27.06 and 26.50 (kg $CaCO_3$ eq/t) respectively. Post treatment this increased to a maximum of 33.77 (kg $CaCO_3$ eq/t) within the coarse composite column exposed to 60% (by volume) CO_2 gas mix. The fine composite showed a greater increase in neutralizing potential (NP) post treatment with the column exposed to 100% CO_2 giving an ANC of 39.28 (kg $CaCO_3$ eq/t). Dissolved inorganic carbon (DIC), determined with Sievers 820 TOC analyser, carried out on 24 hours 2:1 deionised water leach test leachates before and after treatment showed consistent increases with increased CO_2 concentration. It can be seen in figure 2 (2) that within the coarse composite DIC increases from 7.73 mg/L pre-treatment to 11.60 mg/L within samples exposed to 100% CO_2.

Key Observations

Adaptation of Warburg type constant volume respirometers, such as the WTW Oxitops used in this study, for the purpose of determination of CO_2 consumption is a rapid and cost-effective method for determination of initial carbonation rates of waste materials. The method has allowed determination of material response to variation in experimental conditions such as moisture content, temperature and CO_2 concentration. Due to the relative simplicity and low cost of the testing procedure, the method potentially has wider applicability to other sites and waste material types.

The CO_2 consumption vessel experiments have demonstrated that CO_2 uptake increased

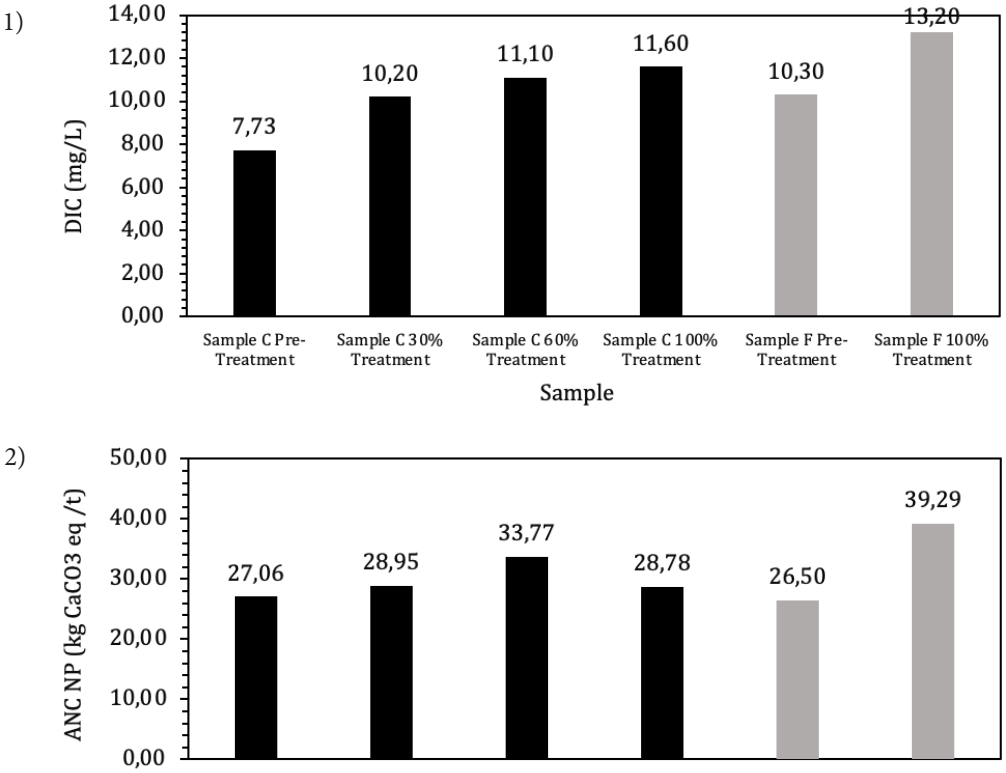

Figure 2 *(1) Reactor column ANC results including pre and post treatment samples (% are % vol CO_2 in reaction vessel). (2) Reactor column dissolved inorganic carbon (DIC) in post-test leachate results including pre and post-treatment samples. Coarse composite sample are indicated as sample C, while fine composite samples are indicated as sample F.*

in finer materials exposed to higher CO_2 concentrations. Within test runs, vessels containing the same material type with varied CO_2 concentrations those with 100% CO_2 showed consistently higher consumption rates over 30-day experiment periods. It has been demonstrated that, although the Mg and Si contents of the fine waste materials was lower than its coarse counterpart the finer waste rock fraction still showed the highest CO_2 consumption rates.

Increased consumption rates were consistently correlated with higher post experiment ANC NP. This suggests materials can yield a greater neutralising potential after only 30 days of exposure to increased CO_2, although more test work is required to confirm these findings. Temperature exerted a strong negative effect on the rate of CO_2 uptake, with the low temperature experiments demonstrating the lowest overall CO_2 consumption rates, regardless of moisture content.

Short-term reactor column experiments showed similar trends to those observed within consumption vessel tests. Over the 62-day test period, with consistent gas throughflow and varied CO_2 concentration, column residues showed increasing ANC NP and DIC with increased CO_2 concentration. Columns containing finer waste rock material (<2.3 mm) showed the greatest increase in ANC NP. In both sets of tests, it has been demonstrated that sample F (<2.3 mm) yielded both increased consumption rates of CO_2 as well as consistently higher ANC NP and DIC post treatment. The test results indicate that the method can determine changes to pore water chemistry and geochemical properties that occur as a result of the carbonation process.

These findings support those reported in previous studies (Declercq *et al.*, 2020) in which ANC was seen to increase in long term weathering tests under ambient CO_2 conditions.

As a result of the demonstrated differences in post treatment geochemical characteristics in both materials in carbonation vessels and short-term reactor columns it can be concluded that the influence of short-term exposure to CO_2 does influence waste material drainage geochemistry. Further testing is planned to further assess the impact of moisture content on rates of carbonation as well as modelling test outputs over extended timescales to assess the implications for mine drainage systems over and beyond the life of the mine.

Current research is being undertaken by the authors is looking at long term impacts of CO_2 on kinetic weathering tests as part of a PhD program.

References

Declercq, J., Bowell, R., Brough, C., Barnes, A. and Griffiths, R. (2020). CO2 storage by mining waste; dream or reality?. *Economic Geology*, (In Press).

Harrison, A., Power, I. and Dipple, G. (2012). Accelerated Carbonation of Brucite in Mine Tailings for Carbon Sequestration. *Environmental Science & Technology*, 47(1), pp.126-134.

Li, J., Hitch, M., Power, I. and Pan, Y. (2018). Integrated Mineral Carbonation of Ultramafic Mine Deposits—A Review. *Minerals*, 8(4), p.147.

Renforth, P. (2019). The negative emission potential of alkaline materials. *Nature Communications*, 10(1).

Savage, R., Pearce, S., Mueller, S., Barnes, A., Renforth, P. and Sapsford, D. (2019). Methods for assessing acid and metalliferous drainage mitigation and carbon sequestration in mine waste: a case study from Kevitsa mine, Finland. *Proceedings of the 13th International Conference on Mine Closure*.

Wilson, S., Dipple, G., Power, I., Thom, J., Anderson, R., Raudsepp, M., Gabites, J. and Southam, G. (2009). Carbon Dioxide Fixation within Mine Wastes of Ultramafic-Hosted Ore Deposits: Examples from the Clinton Creek and Cassiar Chrysotile Deposits, Canada. *Economic Geology*, 104(1), pp.95-112.

Wilson, S., Harrison, A., Dipple, G., Power, I., Barker, S., Ulrich Mayer, K., Fallon, S., Raudsepp, M. and Southam, G. (2014). Offsetting of CO2 emissions by air capture in mine tailings at the Mount Keith Nickel Mine, Western Australia: Rates, controls and prospects for carbon neutral mining. International Journal of Greenhouse Gas Control, 25, pp.121-140.

Planning and implementation of environment-friendly phasing out of German hard coal mining under consideration of water-hazardous organic substances

Christoph Schabronath[1], Christoph Klinger[2], Joachim Löchte[3]

[1]*RAG Aktiengesellschaft, Central Division Health Safety and Environment, Im Welterbe 10, 44151 Essen, Germany, Christoph.Schabronath@rag.de*

[2]*DMT GmbH & Co. KG, Am Technologiepark 1, 45307 Essen Germany Christoph.Klinger@dmt-group.com*

[3]*RAG Aktiengesellschaft, Central Division Health Safety and Environment, Im Welterbe 10, 44151 Essen, Germany, Joachim.Loechte@rag.de*

Abstract

Two hundred years of hard coal mining in Germany ended in 2018. The last two active collieries of RAG Aktiengesellschaft stopped producing hard coal. During the phasing out process one of many challenges will be the reduction of the environmental impact of organic substances. To run the infrastructure fuels e.g. diesel and hydraulic liquids are indispensable. Many of them are water-hazardous but in secure use. Furthermore there are operating fluids which had to be used in the past for safety reasons (e.g. non-inflammable hydraulic liquids containing polychlorinated biphenyls (PCB)) which are now known as toxic. All these fluids can leak and accumulate in the gallery floors of the mine building.

During the process of mine flooding, water can get in contact with those substances and partly mobilize or dissolve them (Denneborg 2018). This is a potential risk for people and the environment. With regard to the Water Framework Directive and the resulting German surface water regulation, the quality of surface water needs to be improved. Hence, the minimization of such substances in mine water discharges and thereby of the environmental impact is an essential part of RAG closedown strategy. RAG addresses this task by deriving a multi-lane concept in cooperation with DMT and the water authorities.

Keywords: Mine Flooding, Remediation, PCB, Organic compounds, Water Framework Directive, Phasing Out, Water-hazardous Substances

Introduction

In mining water-hazardous substances have been used. To avoid environmental impact during phasing out, these substances need to be dealt with according to regulations (Bez. - Reg. 2015). Generally, waste arising underground was collected in designated and labelled containers, transported to specially prepared supply sites above ground and disposed properly (Bundesministerium 1995). In some cases, however, such substances were also subject to losses due to leaks or accidents and, in the case of hydraulic fluids, additional releases due to safety valves.

During and after mine flooding, such anthropogenic water-hazardous substances can be carried along with the rising mine water and discharged to receiving waters. As with PCB, poorly soluble or particle-absorbing substances (e.g. multi-ring PAHs) can predominantly only be transported bound in particulate form. The release and transport processes then behave analogously to PCB and are thus clearly different from the water-soluble compounds.

In addition to mineral oil products and aliphatic compounds, the group of water-hazardous substances also includes monoaromatic (BTEX), polycyclic aromatic hydrocarbons (PAH) and Organochlorine compounds (LHKWs) in the form of e.g. cleaning agents and additives. The vast

majority of lubricants were used in closed systems. However, dripping and handling losses are probable. In particular, high-molecular compounds such as 4- to 6-ring PAHs and PCB have a specific binding tendency on particle surfaces in particular to organic substances. This is described by high sorption coefficients and leads to low proportions dissolved in water. PCB are thus predominantly transported bound to particles in water. In contrast to soluble substances, the solids are swirled up in turbulent water flows and sedimented again at low flow velocities.

The processes around turbidity are complex and are strongly dominated by local and variable processes. These are mining activity, type of lithology, sump management etc. in the active mine. For PCB mobilisation it is required that PCB-containing particles get into the mine water. Such erosion processes (turbulences) are a function of the flow velocity and thus of the local site conditions.

Thus PCB release can only take place in unflooded galleries in which either turbulent flow of water or mining activity cause dispersion. Such erosion channels can be seen everywhere in the mines after water enters inclined sections. Once a mine area has been flooded, turbulences and mining interventions in the floors are absent.

Basic concept

A concept to evaluate the extent of underground contamination and its risk on surface water was required. Such a concept was developed by RAG in cooperation with DMT. It is based on the regulatory requirements of water legislation concerning water-hazardous substances e.g. operating fluids. The flowchart presented in figure 1 is the basic tool to fulfil those requirements. In a systematic analysis it is relevant whether and where such operating fluids were used in the mines. Furthermore the possibility to create a hazardous potential during mine flooding is important. According to the risk of contamination and substance properties, different approaches were defined considering mining-specific conditions.

The basic assumption is that all locations, where water-hazardous substances were utilized, bear a potential risk during the flooding process. Accordingly, defined areas

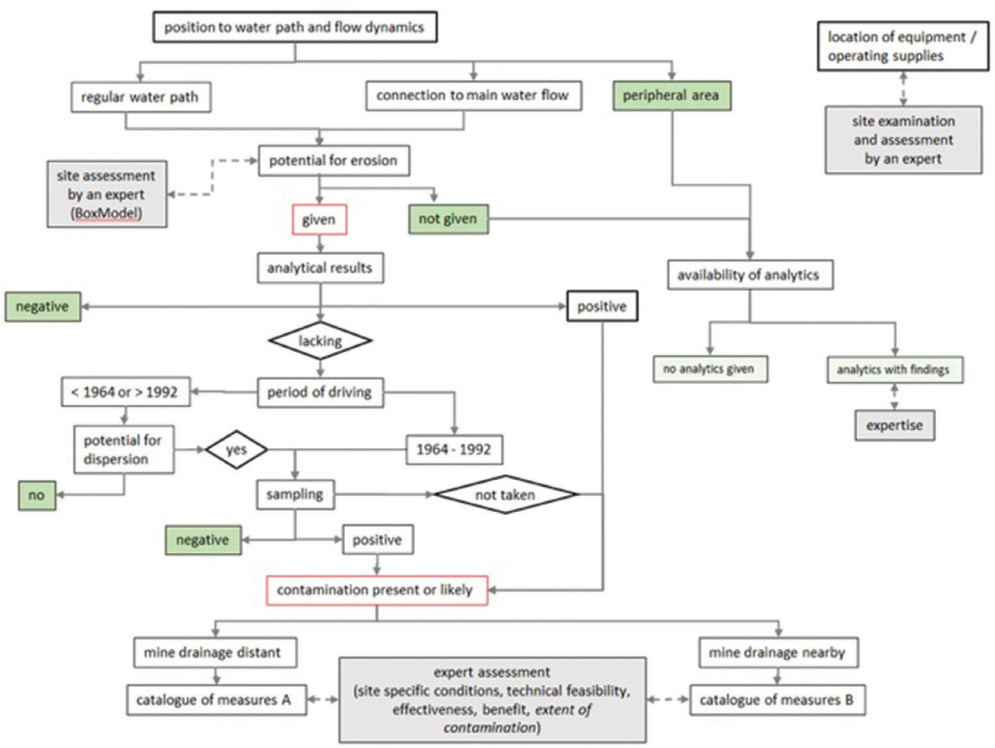

Figure 1 *Concept of phasing out under consideration of surface water-hazardous substances.*

of concern which surround former and active machine locations are actively checked for contamination. Such controls and resulting rehabilitation measures (covering and/or excavation of areas holding loaded matter) are limited to galleries still accessible. The flowchart guides the evaluator through several steps considering gallery location relative to water paths, erosive potential, period of driving, taking samples and dealing with analytic findings.

Based on this assessment, galleries can be declared as hazard-free or treated according to a defined catalogues of measures. The focus here is on facilities which are operated in accordance with the *Ordinance on Facilities for Handling Substances Hazardous to Water* (AwSV) and other areas in which substances hazardous to water (liquids containing mineral oil, resins, etc.) were handled during the operating phase (Bundesregierung 2017).

When leaks or releases through safety valves have occurred in the past, they were in most cases not locally limited or their distribution was unknown. Furthermore it can be assumed that materials and substances could be distributed by water and by coal during the transport over railway systems. It is therefore necessary to identify and characterise such sites or areas, taking into account the materials, substances and groups of substances used underground. Depending on this assessment, measures must then be derived to control, eliminate or minimise impacts on the water path before it gets dammed. After a final examination, to control the measure, the site can be classified as hazard-free.

Identification of facilities or sites

Today, facility locations are being examined, when withdrawing from the still open mine. This applies to both current and former facility locations. Individual sites with a high risk of contamination by water-hazardous substances are investigated and evaluated by an expert individually. Systems that have been in operation for more than 10 years require special care, as the susceptibility to malfunctions increases with time. However, the practice of site inspections showed that the operating time is not always decisive for relevant emissions. Even in the case of shorter operating periods, relevant

Figure 2 *Example for the examination of the gallery floor around a former winder site.*

contamination of the gallery floor can occur. As a result, all accessible facilities are now being inspected, irrespective if still in use or not. The condition of such sites is very different and varies. As the period of decommissioning increases, the probability of locating the former plant site and finding residues, decreases. The range of the sites being considered can be taken from table 1. These site categories are checked and, if necessary, adapted according to the special features of the machinery used in the various mines. Figure 2 gives an example for the inspection of the gallery soil around a former winder location (red ellipsis). Furthermore it shows an already completed measure to cover the contaminated soil with concrete (green ellipsis).

Particular attention is paid to locations for which there are indications, that equipment containing PCB has been used:

– Facilities which operated with PCB-containing liquids e.g. winders and various hydraulic machines
– Assembly/disassembly areas of full-cut machines during the period of use of oils containing PCB.

These facility locations are evaluated for operating time, substances used and properties of the respective system. With that knowledge the type of loads and possible discharge points of operating materials can be identified. If the installations are still present at the site, leaks are often noticed directly. Furthermore site location relative to future main waterways and with respect to flow dynamics e.g. potential of erosion are taken into account (see figure 1). If necessary, locally limited measures are then derived to eliminate, control or minimise the contamination risk.

Such measures are coordinated with the district government are based on site inspections. The implementation or completeness of these measures is checked and approved either by the Environmental Engineer of RAG or by an independent expert.

The process is documented and based on a list of system types. This list is agreed with the Arnsberg district government. The location, type of system, used substances and the inspection by an independent expert or the environmental engineer of the mine are recorded. Furthermore the results of the assessment as well as the implementation of the required measures are documented (see figure 1). This is supplemented by individual expert reports for the system locations, describing the respective situation and the measures to be carried out. Examination practice of past years has shown that more than half of the investigated sites were contaminated and required remedial

Table 1 *Types of facilities operated with water-hazardous substances and evaluation of contaminations during the first inspection.*

Facility / Site	Water- hazardous substances used investigated	Not yet investigated	Contamination			
			no	low	high	Total
Belt conveyor drives	Gear oil	18	32	22	4	76
Other drives	Gear oil	0	2	6	0	8
Shaft cellar	HFC/Gear oil	6	0	4	0	10
Shaft swamps	Divers	3	0	1	0	4
Pumping stations	Diverse oils	5	0	0	0	5
Electric control rooms	Switchgear oil	0	0	1	1	2
Intensive traffic areas	Diesel/HFC/Mineral oil	4	0	0	1	5
Train stations	Diverse oils, Diesel	11	0	5	2	18
Refuelling station	Diesel	2	2	3	3	10
Locomotive mainten.	Diesel/Used mineral oil	5	0	1	1	7
Cleaning station	Oil-bearing water	3	1	1	0	5
Workshops	Diesel/HFC/Mineral oil	0	1	2	0	3
HD pumping stations	HFA/Mineral oil	2	0	1	1	4
Winder locations	Hydraulic oil	6	2	5	1	14
Resin mixing stations	2-component resin	4	0	0	1	5
Total		64	40	52	15	171

measures (see table 1). Hence these areas were declared as hazard-free afterwards.

Diffuse loads of organic matter

Due to intensive transport and material relocation processes (conveyor systems, means of transport, water and weather flows), parts of a mine that are far away from site locations can be affected. Such contaminations are therefore difficult to localise and isolate. Due to mostly low concentrations these diffuse substance contents do not influence mine water quality significantly. The composition of the gallery ground material with high clay contents, organic substance contents and small grain sizes can sorptively bind such substances and reduce the mobilisation.

Nevertheless such low concentrations become recognisable and relevant when sufficiently strong analytical methods are used e.g. analytics of PCB. The analytical findings in the µg/kg range show that low loads are present at many points of a mine. The focus of the examination distributed across the mine is on the period in which PCB were used in underground hard coal mining from. From 1964 up to the 1980s PCB was a component of hydraulic fluids. Subsequently, PCDM-containing replacement fluids were used until approximately 1992. These fluids do not differ significantly in their environmental relevance from PCB. In the following period neither PCB nor PCDM were used. The presence of PCB in the concerned mine can therefore have various causes:

- The coal fields were excavated during the period of use of PCB/PCDM-containing equipment (conventional road header, full-cut machine).
- The coal fields are within the sphere of influence (main haulage routes, waste weather, mine water) of mining areas in which work was carried out with PCB/PCDM-containing equipment.

The assessment of the mobilization and discharge of diffuse material loads is highly related to the later mine-flooding. Therefore specific measures are considered and documented in special reports.

General evaluation and measures

After localisation of contaminated sites specific measures are carried out. These are damming, removal, remediation or covering, e.g. either with gravel (flexible in relation to bottom lifts) or concrete (partly with

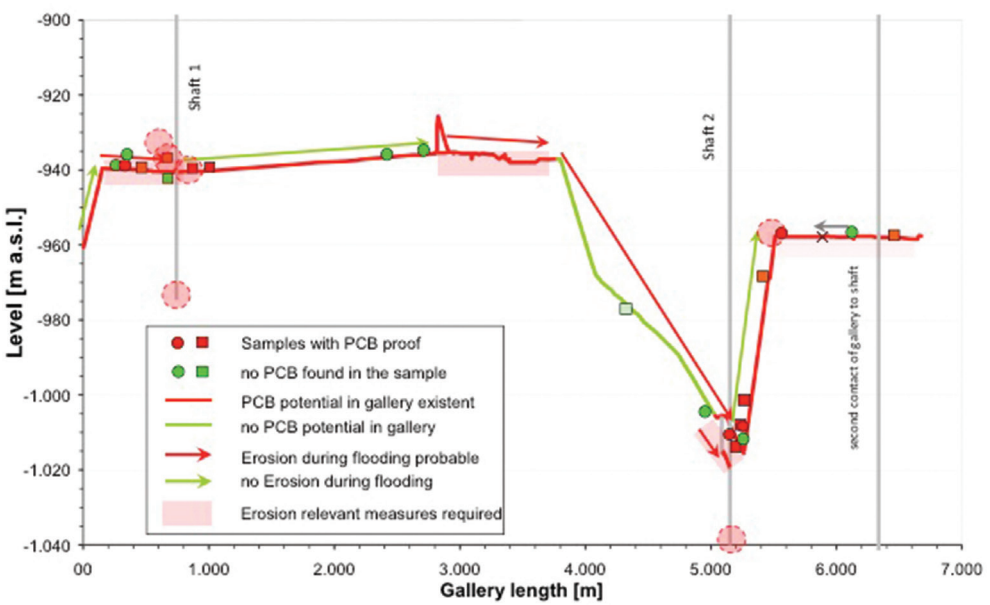

Figure 3 *Example for analysis of PCB contamination and erosion potential in galleries around a mine water pumping station to be abandoned.*

steel reinforcement The specific approach for the evaluation of potential or verified PCB contamination considers mobilisation processes during the flooding process (see figure 3). To prevent or minimize possible turbulent water run-off and erosion of the roadbeds large-scale effective measures can be taken. Figure 3 shows an exemplary site examination of mine workings in the surrounding of two still open shafts. Often the construction of weirs and pipelines, that bypass the sensitive sections of the gallery, is a viable and effective measure. Covering the long routes, with several kilometres of length, was a non-practicable approach.

It can be stated, that mine water from flooded mining areas has only a low content of dissolved water-hazardous substances. This manifests it the low contents of mineral oil hydrocarbons (MFCs usually < 0.1 mg/L) in mine water which came from already dammed mine fields. This was surveyed by a regular monitoring since 2008. Accordingly this value meets the requirements of the *Ordinance on Mining Water* of 0.1 mg/L (test value) or 0.2 mg/L (percolate water). These low test values can be explained by the fact, that MFCS are well bound to the fine-grained and organic substances, contained in the materials of the gallery basis. These are therefore only available to a limited extent for dissolving processes.

Conclusion

For the planned phasing out process from the mine building and the drainage sites, the methodology described here is intended to contribute to the identification of contamination hot spots. If necessary, it helps to derive measures for the elimination, control or minimisation of environmental impacts to receiving waters. The described catalogue of measures is intended to avoid an impairment of mine water quality with water-hazardous substances. It is important that neither locally limited nor diffuse contaminations in the mine, affect surface water negatively by discharge of mine water.

At the sites investigated so far, operating substances hazardous to water were found to varying degrees. These are diesel oil, lubricating oils, hydraulic oils and greases. A contamination with these substances would be reflected by the water monitoring parameters hydrocarbon index and PCB / PCDM.

If a contamination is locally distinct, contaminated materials are largely removed and disposed of (remediation). In case of unfavourable site conditions, which prevent the complete removal of the substance or where localisation/confinement is difficult, safety measures are carried out. Measures like steering water flows and controlling mine flooding are suitable to prevent particle leaching. The Measures are proposed by an expert, realized by the company RAG, checked and documented by an expert and finally approved by the district government. The basic concept presented here enables the mine operator to systematically address the extent of underground contamination by water-hazardous substances. Thereby the risk of surface water contamination is reduced significantly.

Acknowledgements

We thank all people involved in this concept at RAG, DMT and the authorities helping to reduce the environmental impact. Furthermore we thank Dr. Claudia Karus for writing assistance and proof reading.

References

Bez.-Reg. Arnsberg (2015) Regelung zum Umgang mit Sachen und betrieblichen Einrichtungen beim Rückzug aus dem Grubengebäude" (§22a ABBergV)

Bundesministerium der Justiz und Verbraucherschutz (1995) Bergverordnung für alle bergbaulichen Bereiche (Allgemeine Bundesbergverordnung – ABBergV) § 22a Anforderungen an die Entsorgung von bergbaulichen Abfällen

Bundesregierung (2017) Verordnung über Anlagen zum Umgang mit wassergefährdenden Stoffen (AwSV) vom 18. April 2017. – Bundesgesetzblatt Jahrgang 2017 Teil I Nr. 22, ausgegeben zu Bonn am 21. April 2017, p. 905–955

Denneborg, M (2018) Mögliche Umweltauswirkungen von Abfall- und Reststoffen in Steinkohlenbergwerken in Nordrhein-Westfalen.- Grundwasser im Umfeld von Bergbau, Energie und urbanen Räumen, 26. Tagung der Fachsektion Hydrogeologie e. V. in der DGGV e.V., Ruhr-Universität Bochum, 21. - 24. März 2018

Process for the Subsoil Treatment of Acidified Groundwater through Microbial Sulfate Reduction

Ralph Schöpke[1], Manja Walko[2], Konrad Thürmer[3]

[1]*BTU Cottbus-Senftenberg, Germany schoepke@b-tu.de*

[2]*Lausitzer und Mitteldeutsche Bergbau-Verwaltungsgesellschaft mbH, Manja.Walko@lmbv.de*

[3]*Institut für Wasserwirtschaft, Siedlungswasserbau und Ökologie (IWSÖ GmbH), konrad.thuermer@iwsoe.de*

Abstract

Sulphate and the acidity formed mainly from ferrous iron ions are the main contaminants of groundwater affected by mining. The Chair of Wassertechnik & Siedlungswasserbau at BTU Cottbus-Senftenberg has developed a subsurface rehabilitation method using microbial sulfate reduction over the past twenty years. The basis for dimensioning this technology is now available after a successful demonstration test at the Ruhlmühle in the Lusatian mining district. The used substrate guarantees complete implementation and does not trigger any further damaging effects. Nutritional supplements (N, P) are kept to a minimum. The concentration of hydrogen sulfide in equilibrium with the precipitated iron sulfides limits the treatment effect in the incorporation phase.

Keywords: Technology, Reclamation, Dimensioning, Modelling

Introduction

Iron sulfides are oxidized in the ventilated areas of the lowering funnel and the dump during open-cast mining operations. Their acidic reaction products are dissolved by seepage water or rising groundwater and form the amd. The acid mine drainages flows into the acidic pit lake that is being formed during the filling of the remaining open pit. In anoxic groundwater, the acidity (-NP) is presented as dissolved ferrous iron.

$$NP \approx K_{S4,3} - 3c_{Al3+} - 2c_{Fe2+} - 2c_{Mn2+} \quad (1)$$

After the groundwater flow conditions have been restored before mining, the groundwater enriched with pyrite weathering products flows into adjacent surface waters. Rivers such as the Spree in Germany buffer the acidity that has been introduced. The iron carried along affects the waters as brown turbidity. The drinking water supply sometimes can also be impaired by exceeding the sulphate limit values.

Table 1 *Analysis of groundwater inflow in beginning, end and the best effect.*

Parameter	Dimension	start	end	best effect
Temp	°C	11	11	11
pH	1	4,02	4,45	5,3
LF	µS/cm	1919	1295	700
NP	mmol/L	-18,0	-10,6	+1
Fe	mg/L	437	291	50
SO4	mg/L	1240	812	< 100
NH4-N	mg/L	2,6	2,5	0,2*)
PO4	mg/L	0,59	0,47	0,2*)

*) with nutritional supplements

Aims

The aim of the subsoil treatment is to bind ferrous iron as iron sulfide by reducing the sulfate to sulfide sulfur, eq. 2. This lowers the acidity, the iron and sulphate concentration.

$$Fe^{2+} + SO_4^{2-} + \frac{4}{7}C_3H_8O_3 \rightarrow FeS\downarrow + \frac{12}{7}CO_2 + \frac{16}{7}H_2O \quad (2)$$

This process can be done on the path through the aquifer or in the source of contamination.

The process was developed for the treatment of a groundwater flow but can also be used on tip aquifers with an almost dormant solution phase. The general requirements for the rehabilitation process are compiled in a checklist as criteria ok1 to ok6:

ok1 Proof of the intended effect.
ok2 No eutrophication effect of the treated water.
ok3 No higher oxygen consumption in surface waters.
ok4 No acute toxicity of the treated water.
ok5 Limitation of potentially bioaccumula ting substances.
ok6 Limitation of inert substances.

The use of drinking water after conventional treatment of the treated groundwater flow will be guaranteed.

Technology

The substrate is mixed into the groundwater flow intermittently using infiltration lances or equivalent methods. For treatment, the substrate required for sulphate reduction must be added to the groundwater flow and allowed to react on the further course of the flow.

The simplest substrate dosage would be by pump and addition. Then you could leave out the further treatment in the aquifer. So only an intermittent injection with substrate-enriched groundwater is possible. The distribution of the substrate takes place on the further flow path by dispersion processes. The substrate must be entered into the entire flow cross-section.

- Low AMD currents are already treated through passive reactive walls. Various solid substrates are used there, mostly for sulfidic heavy metal binding. The requirements placed on the treated water cannot be met with this.
- The combination of infiltration and injection wells creates a gradient across the direction of the groundwater flow, via which the enriched water reaches the flow area between the wells.
- Another possibility is the ADAG system, in which the groundwater is collected via the collector well and then redistributed via the distributor.
- In the demonstration experiment, lances at different depths were charged with substrate-enriched groundwater. The costly infiltration wells are replaced by infiltration lances.

The sulphate conversion depends on the microbiological activity, the amd quality, the substrate concentration, the available nutrients and possible inhibitors. The mortality rate must also be taken into account. Orientation reaction parameters are available for the kinetics. They must be specified at each location. The pore structure of the aquifer has a very large reactive surface. This also triggers various chromatography effects.

$$c_{Substrat} = \nu_{O2} \cdot \Delta c_{O2} + \nu_{Fe3} \cdot \Delta c_{Fe3} + \nu_{Fe2} \cdot \Delta c_{Fe2} + \nu_{H2S} \cdot \Delta c_{H2S} \quad (3)$$

Tab. 1 *Stoichiometric coefficients for the conversion of oxygen, ferrous and ferric iron, as well as conversion factors for the specification as BOD (Schöpke et al. 2017).*

Substrat		Faktor for BOD	M	stoichiometric coefficients			
		mol/mol	g/mol	nO2	nFe3	nFe2	nH2S
Carbonhydrate	$\{CH_2O\}$	1,00	30	1,00	2,25	2,00	
Methanol	CH_3OH	1,50	32	0,67	1,50	1,33	1,66
Glycerol	**$C_3H_8O_3$**	**3,50**	**92**	**3,5**	**0,64**	**0,57**	**0,71**
Ethanol	C_2H_5OH	3,00	46	3,00	0,75	0,67	
Acetic acid	CH_3COOH	2,00	60	2,00	1,13	1,00	
calculated BOD	O_2		32	1	2,25	2	

Exploration and rehabilitation test

The last demonstration test proceeded over 31 months (2014-2019) with a groundwater treatment of around 6 m^3/h over a width of 100 m and a follow-up observation over 30 months. The effect is monitored and controlled by a monitoring program.

The groundwater flow field is determined through geological exploration. The sulphate conversion depends on the microbiological activity, the amd quality, the substrate concentration, the available nutrients and possible inhibitors. The sulfate reducing bacteria must be grown slowly at first. Fig. 1 shows the course of the sulphate concentration after 900-day remediation operation. During the start-up phase, substoichiometric substrate is added in order to grow the sulphate reducers. In the following time the sulphate concentration decreases. After completion of the measure, it rises again to the inflow concentration. The sulphate concentration at inflow slightly decreases during the remediation operation (Table 1).

The maximum sulfate degradation is limited by the substrate dose. The increase after the addition of the substrate corresponds to that of a conservative tracer. The ferrous concentration will be delayed. During the incorporation of the underground reactor,

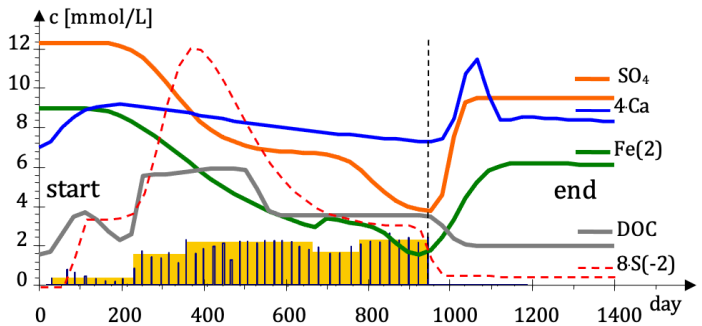

Fig. 1 *Concentration curves of process-characterizing ingredients during the remediation attempt after a 25.5 m flow path through the aquifer. The substrate additions are marked as bars, not to scale.*

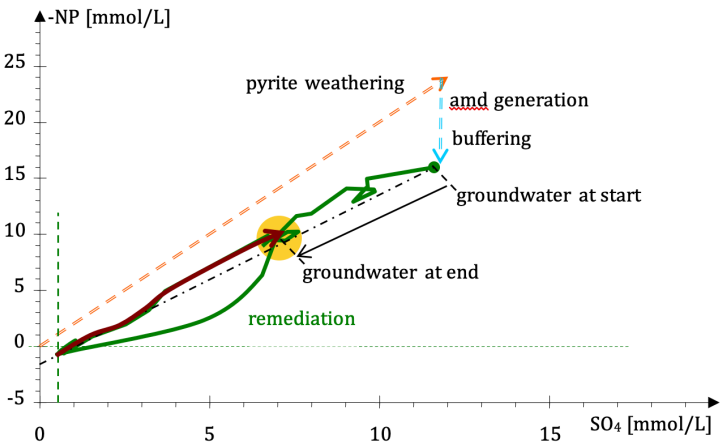

Fig. 2 *Acidity (-NP) -sulphate diagram of amd formation through pyrite weathering and buffering in the aquifer (dashed) and its remediation process through microbial sulphate reduction. The reaction (green) runs along its line of action up to* ***best effect*** *(Table 1). The deviations are caused by various side reactions. After the addition of the substrate, the condition of the inflow is restored (brown). The inflow condition changes during operation (groundwater at end).*

ferrous iron on the solid matrix is exchanged for other cations. These cations are displaced again by the inflowing ferrous iron after the renovation is completed. These cations are displaced again by the inflowing ferrous iron after the renovation is completed. The added substrate is only used incompletely in the beginning. Therefore, the substrate dose should be increased slowly up to the desired maximum dose. The slowly rising pH values can mobilize humic substances that are fixed in the subsoil.

The beginning of the sulphate reduction immediately increases the hydrogen sulphide concentration. Hydrogen sulphide concentration decreases again with the slowly increasing pH value and the aging of the precipitated products. A low sulphide concentration remains after the renovation has been completed. The aging behavior of the sulphide precipitated products is currently insufficiently known. The predicted hydrogen sulfide concentration at the end of the flow section represents, in addition to the remaining substrate concentration, an important control variable for process control. Due to the increasing pH value during the treatment, humic substances can also be mobilized from the subsoil and simulate substrate residues via the DOC. The remaining hydrogen sulfide concentration is in equilibrium with ferrous iron, the pH value and aging iron sulfide phases.

The fluctuations in the nature of the intermittent mode of operation are largely compensated for on the flow path by dispersion processes. The particular solution of the one-dimensional general balance equation describes a jump in concentration. EXCEL offers a function for this purpose. A summary of jump functions are sufficient to smooth the sulfate concentration curve. The material balance is obtained by integrating the material flows of the inflow minus that of the rehabilitated groundwater flow. The jump functions have the property that they can be transformed into rectangular functions of equal area. That makes the balance calculation easier.

The flow resistance will be increased by the reaction products iron sulfide and biomass. Iron sulfide particles from the treatment could not yet be determined using an electron microscope. Iron sulfides can also be deposited on existing pyrite concretions. The diameter of their crystals are from 10 µm. The hydraulic effects resulting from the deposition of reaction products can be calculated with the Kozeny-Carmann equation known from water treatment. All effects has been prognosted using PHREEQC with a mixed cell flow path in Schöpke *et al.* (2020).

Model

A PHREEQC mixed cell model was adapted to the measured concentration curves in the downstream flow of the substrate addition, especially for dimensioning and operational management. This also included adsorption processes on the solid matrix and the hydraulic effect of separated reaction products and possible gas excretions in addition to the biochemical reactions. Gas excretions could be excluded in the previously treated groundwater lamellae. An impairment of the

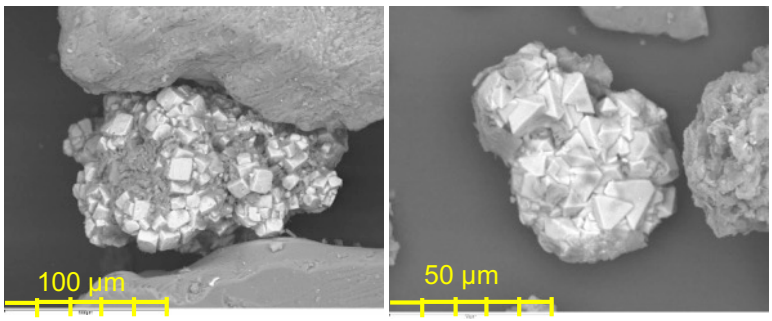

Fig. 4 *Pyrite crystals in pore system.*

$$\frac{\partial c_{Su}}{\partial t} = \mu_0 \cdot c_{Biomasse} \cdot f(Temp) \cdot f(pH) \cdot f_{Su}(c_{Su}) \cdot f_{SO4}(c_{SO4}) \cdot f_N(c_N) \cdot f_P(c_P) \cdot f_I(c_I) \quad (4)$$

permeability (k_f) has not yet been proven, which the flow route model also predicts for the next two decades.

The underground reactor will be represented by a few characteristic flow tubes. Each flow tube is described using a mixed cell model. The infiltration facilities and measuring points are determined on model basis. The exploration is made more precise with the construction of the infiltration and monitoring systems. The operating regime is then determined by PHREEQC modeling. The microbial sulphate reaction describe eq. 4.

The mortality rate must also be taken into account. A large number of side reactions also must be taken into account. The pore structure of the aquifer has a very large reactive surface. This triggers various chromatographic effects. The reaction products deposited in the pore system can be predicted. Orientation reaction parameters are available for the kinetics and surface complexation (Schöpke *et al.* 2016). They must be specified at each location.

Dimensioning

The methodological bases of the dimensioning of an underground reactor is created:

- A thorough exploration is required at first.
- The dimensioning takes place by means of hydrogeological modelling and the use of the flow route model.
- This can be used to construct statistical distributions over the properties of the aquifer about the heterogenity of the groundwater flow and the properties of the sediment matrix. Tracer tests can also be used.
- It will be parameterized a mixed cell model in PHREEQC for the operating regime.
- The renovation operation itself is optimally designed through the combination of monitoring and modelling.
- The profitability can only be calculated on the property.

Recommendations for approval and exploration are available for the preparation of underground reactors (Schöpke *et al.* 2020).

Acknowledgements

The process development was funded by the Lausitzer und Mitteldeutsche Bergbau-Verwaltungsgesellschaft mbH (LMBV) through several projects. We thank you for the financial and technical support.

References

Parkhurst, D. L., Appelo, C.A.J. (2013): Description of Input and Examples for PHREEQC Version 3—A Computer Program for Speciation, Batch-Reaction, One-Dimensional Transport and Inverse Geochemical Calculations. U.S. Geological Survey, Denver, Colorado, Chapter 43 of Section A, Groundwater Book 6, Modeling Techniques

Schöpke, R.; Preuß, V.; Zahn, L.; Thürmer, K. (2016): Modelling the changes in water quality of AMD along the flow path. In: Drebenstedt, C.; Paul, M. (Hg.): Mining Meets Water - Conflicts and Solutions; IMWA Leipzig; Proceedings, IMWA 2016 in Leipzig, Germany, July 11-15

Schöpke, R.; Preuß, V.; Thürmer, K.; Zahn, L.; Walko, M.; Totsche, O. (2017): Control of the remediation of anoxic AMD groundwater by sulphate reduction in a subsoil reactor. In: Wolkersdorfer, C.; Sartz, L.; Sillanpää, M. & Häkkinen, A.: Mine Water & Circular Economy (Vol I). – p. 502 – 510; Lappeenranta, Finland (Lappeenranta University of Technology).

Schöpke, R.; Walko, M.; Regel, R.; Thürmer, K. (2020): Bemessung der mikrobiellen Sulfatreduktion zur Behandlung von pyritverwitterungsbeeinträchtigten Grundwasserströmen – Ergebnis eines Demonstrationsversuches am Standort Ruhlmühle; Schriftenreihe Siedlungswasserwirtschaft und Umwelt, Bd.27; https://www-docs.b-tu.de/fg-wassertechnik/public/Publikationen/Schriftenreihe/Heft27.pdf

Recharge-driven Underground Dewatering and Post-Closure Groundwater Recovery

Simon Sholl[1], Stephen Wheston[2], Geoff Beale[1]

[1]*Piteau Associates, Canon Court West, Abbey Lawn, Shrewsbury SY5 8AN, United Kingdom, ssholl@piteau.com, gbeale@piteau.com*

[2]*Tembusu Ltd, 1 Killastafford Cross, Cashel, Co Tipperary, Ireland, stephenwheston@gmail.com*

Abstract

Lisheen Mine, located in Tipperary, Ireland, was operational between 1999 and 2015. Through most of mine life, dewatering rates were typically within a seasonal range of 60 to 90 MLD (60,000 to 90,000 m^3/d) , and rapidly changed with precipitation, which reflected the low storage of the limestone bedrock. After closure, groundwater levels in the mine workings rose over 120 m in the first three months, further demonstrating the low storage of the bedrock. Full recovery of the workings was confirmed in early 2018, 2 years after closure, when the natural seasonal variation in groundwater levels had re-established.

Keywords: IMWA2021, Ireland, Limestone, Recharge, Underground, Porosity, Storage, Closure

Introduction

Lisheen Mine, located in Tipperary, Ireland, produced around 6,000 tonnes per day of zinc and lead ore between 1999 and 2015. The mine exploited a 'Mississippi valley'-type ore deposit hosted in the Waulsortian (reef) Formation, Carboniferous limestone.

Ore was extracted from four underground mining zones: Main Zone, Derryville, Bog Zone and Derryville Island (Figure 1). During operations, groundwater inflows to the mine typically varied from less than 60 MLD (60,000 m^3/d) during prolonged periods of dry weather to over 90 MLD (90,000 m^3/d) following wet periods. Initially, the groundwater inflow was predominantly derived from local groundwater storage in the weathered Waulsortian limestone and was less sensitive to rainfall patterns.

As mining ended, the underground workings were cleared of all potentially hazardous material and the mine was allowed to flood by stopping all dewatering pumps on 31st December 2015. Bulkheads and three low pressure barricades were built underground to provide a restriction to groundwater flow within the workings post-closure. The objective was to limit the potential for equilibration of heads across the mined out area. Ventilation shafts were backfilled with coarse inert rock, concrete and capped with a reinforced concrete lintel. On commencement of rewatering, the groundwater levels in the mine workings rose over 120 m within the first three months, and full recovery confirmed within 2 years.

Geology

The bedrock throughout the entire Lisheen district consists of Early Mississippian, Carboniferous limestone. Waulsortian Formation limestone is the most dominant unit locally and the unit in which virtually all the production mining occurred. Typically, the Waulsortian in the area of Lisheen has a zone of epikarst extending to about 30 to 50 m below ground level. This zone usually includes more weathered, fractured and cavernous rock. Under natural conditions, most groundwater flow occurs in this upper epikarst zone. The intensity of fracturing below 50 m is observed to decrease significantly. This is typical of Irish limestones where, generally, a more permeable and productive zone extends to a depth of around 30 m, below which isolated faults and fissures form the only permeability to a depth of 150 or 200 m Drew (2018).

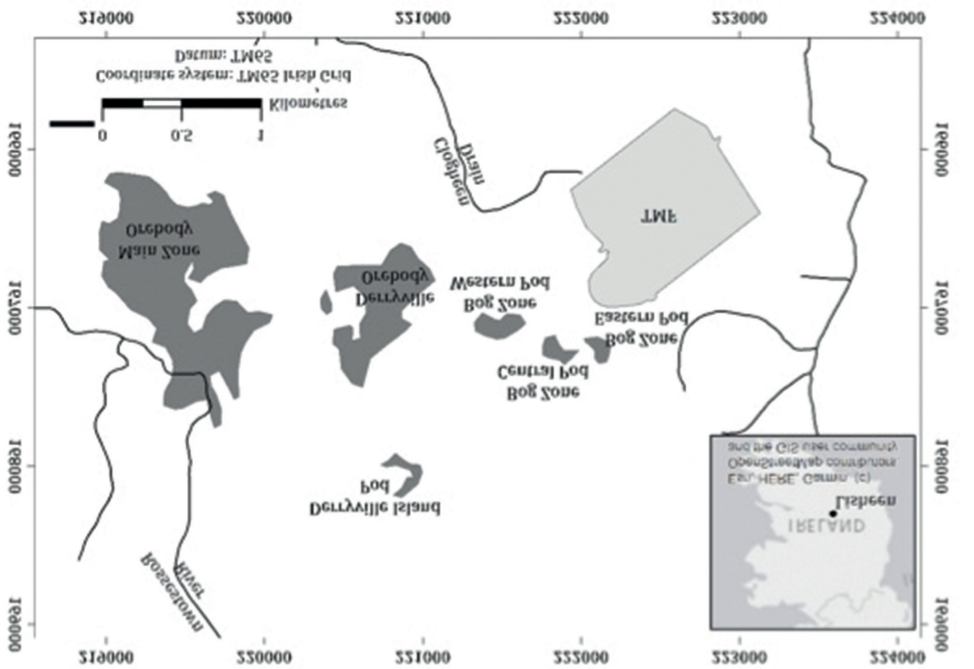

Figure 1 *Plan of Lisheen infrastructure, orebodies and mineral lenses.*

Argillaceous Bioclastic Limestone (ABL) dominates the areas to the northwest and northeast of Lisheen. The ABL is a massive limestone and is generally unfractured. Typically, it does not yield any groundwater and forms a flow barrier between the overlying Waulsortian and the interbedded Lisduff Oolite Member (oolite). The main decline was driven through the ABL.

Locally, little is known about the hydrogeology of the oolite which occurs stratigraphically within the ABL. It is evident from the available data at Lisheen that it provided the main conduit for the inflows to the F2/F3 zone in the decline. F2/F3 defines two major fault zones intercepted during decline development. The oolite is known to be fractured and to yield groundwater in the vicinity of the main geological structures. However, away from the main structures, the degree of fracturing and its potential to transmit groundwater in the area south of Lisheen is uncertain. In the most southerly production areas, mining into the oolite encountered no major groundwater inflows.

In general, the regional geology strikes in a northeast-southwest direction along the axis of the Rathdowney Trend. The two dominant structural orientations are as follows.

- **North northwest-south southeast** structural set forms the dominant local structural trend. The F2/F3 feature, together with most of the main faulting in the vicinity of the orebodies, is aligned along this trend.
- **East northeast-west southwest** structural set associated with the regional Rathdowney Trend is evident in the immediate mine area.

Early mine life

The decline was constructed in ABL to allow advanced dewatering of the orebody (in more permeable Waulsortian) while the decline was being advanced. A major groundwater inflow was encountered as the decline was driven through the NNW-SSE trending F2 and F3 fault zones. The water was derived from the oolite, which had a contact with the ABL, 5 to 12 m below the floor of the

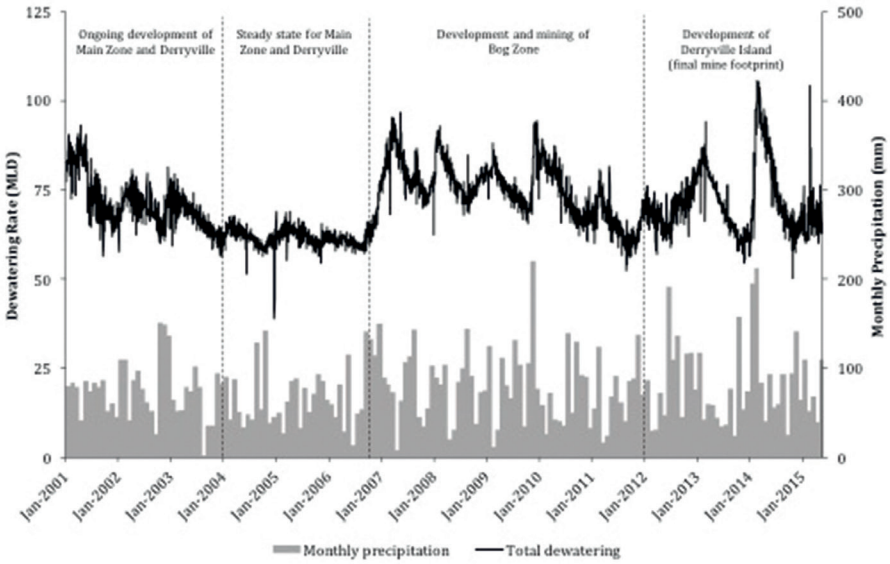

Figure 2 *Dewatering rates from 2001 to 2015.*

decline. The fault-controlled upthrown block of led to sustained inflow from the F2/F3 feature throughout the entire period of mine operations. All other inflows to the mine were from the Waulsortian Formation.

Since the decline was designed to enter the orebody at about 170 m depth, advanced dewatering of the Waulsortian was required (using surface wells) during the time the decline was being advanced. Surface drilling was difficult because of the cavernous nature of the formation (particularly above the Main Zone ore) but sufficient drawdown was achieved to allow depressurization of the initial production workings. Once underground mining was established, sub-horizontal dewatering holes were installed from the workings so the surface wellfield became under-drained and redundant.

Early in mine life, total dewatering reached a peak of 93 MLD in the April 2001 (Figure 2) reducing to around 60 MLD by mid-2006 when it was considered that the hydrogeological system was almost in steady state for the mine workings developed at that time. Virtually all of the groundwater storage removal had taken place, and the dewatering rate was sustained by regional groundwater recharge over the area of drawdown. Water levels in the footprint area of the mine were drawn down to close to the top of the workings.

Operational dewatering

Initially, mining was limited to two primary ore bodies Main Zone and Derryville (Figure 1). It was a number of years before the full footprint of these working areas was developed. Therefore, during the early years of mining, Lisheen was not just managing recharge water but also continued to intercept stored water as new mining areas were developed. It was not until around 2004 that the full extent to the two main orebodies were developed and the mine entered a relatively steady state for a few years until new ore bodies were developed.

From 2007 onwards, the additional mining areas were opened up (Bog Zone and Derryville Island, Figure 1). These mining zones added inflows from groundwater storage during their development as well as increasing the overall area of drawdown around the mine. This led to an increased inflow from recharge.

Over the life of the mine there were periods of high winter rainfall together with a number of very dry summers. These factors caused a both seasonal and inter-annual fluctuations in the mine inflow rate. From late 2008 to the end of mine life (December 2015), groundwater storage removal was a minor contributor to dewatering, with almost

all inflow due to groundwater recharge over the area of drawdown. This was demonstrated in the winter of 2013/14. The mine pumping rate in November 2013 was at an all-time low of 55 MLD (Figure 2) as a result of the very dry summer and autumn. Between 28th December and 19th February, the rate increased from 56 MLD to an all-time high of 106 MLD following exceptionally high rainfall in January and February 2014.

The rapid recharge to the underground workings is, in part, due to the low storage of the limestone bedrock. At its maximum extent, the estimated area of drawdown (in the Waulsortian) was between 90 and 95 km². This area represents a 'zone of capture' for recharge to the mine workings, with a (strongly seasonal) recharge rate typically between 200 and 350 mm/yr, around 15 to 30% of the mean annual precipitation.

Throughout the period of mine dewatering, the near-surface glacial deposits that overlie the Waulsortian showed no measurable drawdown in shallow piezometers. The near-surface water balance was not materially affected by dewatering of the underlying limestone bedrock. Strong vertical hydraulic gradients developed throughout the area of dewatering influence.

Mine closure

Prior to closure, a predictive numerical groundwater model was used to produce an envelope of likely groundwater rebound curves (Figure 3). The model distinguished between the shallow epikarst (typically 30 m thick in the model) and deeper competent bedrock. The epikarst was assumed to have a specific yield of 3% and the deep bedrock 1%. Literature values of porosity for limestones tend to be in the range of 1 to 20% and specific yields between 0.5 and 15%, (Misstear *et al*. 2006).

Volumetrically, by the end of mining, the volume of groundwater removed from storage was estimated to be around 10 million m³ from the epikarst and around 4 million m³ from the competent bedrock. A further 1 million m³ of void space also remained within the mine workings, a small proportion of the total mined volume because most of the workings were backfilled with cemented paste.

Dewatering ended at Lisheen when the dewatering pumps were switched off on 31st December 2015. Groundwater levels in the mine workings rose over 120 m in the first three months. In one monitoring well, water levels rose from -63.8 mOD on 22nd December 2015 to 66.3 mOD on 23rd March 2016. This is an increase of 130.1 m in 92 days; an average of 1.4 m/d.

This initial response to dewatering was faster than predicted (Figure 3), so the rebound prediction was revisited and calibrated to the first three months of monitoring data. The analysis showed that, to calibrate the recovery curve, only the mine workings void space was required. The groundwater storage component of the competent bedrock, therefore, had to be close to zero. Regardless of the actual porosity of the bedrock, this suggests that the specific yield of the competent Waulsortian is significantly lower than 0.5%. The discrepancy between literature and 'calibrated' bedrock specific yield was a key learning from the closure programme. When water levels rebounded, most of the void space being replenished (re-watered) was within the workings themselves. The surrounding Waulsortian bedrock required little additional water to achieve full recovery.

Following the calibration, the monitored groundwater levels remained within the predicted recovery envelope (Figure 3), fluctuating seasonally between being above the 'base case' to below it. The seasonal variation in recovery rates further demonstrates the dominant control that recharge, over storage, has on the groundwater system.

Influence of larger epikarst dewatered volume can be seen once groundwater levels reach around 40 to 50 m below ground level (Figure 3). The rate of recovery reduces significantly from around 1.3 m/d in the deep, low porosity bedrock, to around 0.09 m/d – a 15-fold reduction in rate. However, not all of the reduction can be attributed to specific yield, reduced hydraulic gradients and seasonal recharge variations are also key controls.

The mine achieved full recovery by the summer of 2017, when water levels reached typical summer (seasonal low)

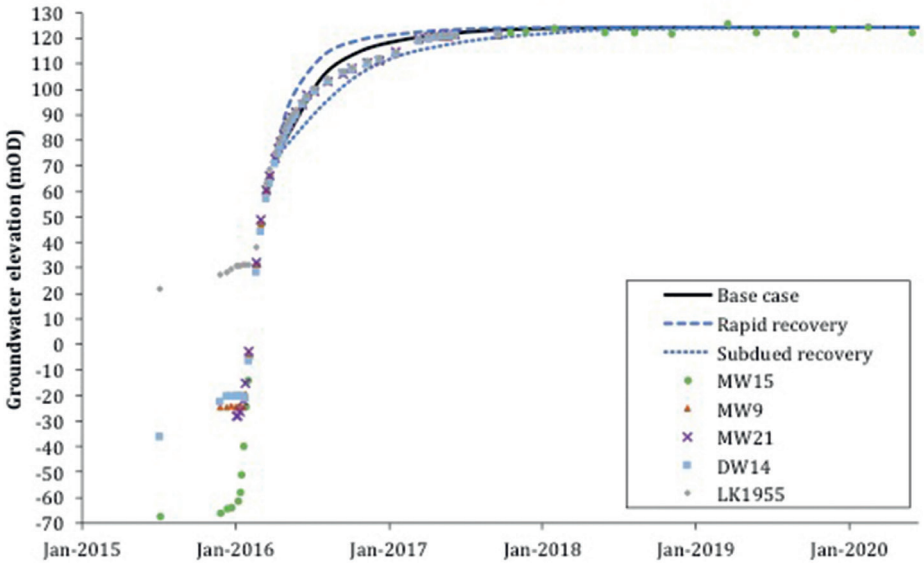

Figure 3 *Groundwater recovery predictions and monitoring data.*

elevations. Full recovery of the workings was confirmed in early 2018 (2 years after closure) when the groundwater level reached between 123.6 and 125.3 mOD, compared with a pre-mining elevation of about 125 mOD. Following that time, a slight seasonal reduction in groundwater levels was observed, indicating that the natural seasonal variation in groundwater levels had become re-established.

Conclusion

Mining at Lisheen required complete lowering of the bedrock groundwater table to the level of the underground workings because of the vertically interconnected nature of the Waulsortian limestone in the immediate area above the orebody. Initial dewatering was carried out using surface wells that were installed concurrently with driving the access decline in low permeability (tight) ABL. The goal of the surface wells was to achieve advanced depressurization of the initial ore zones prior to the decline reaching the Waulsortian. As soon as underground mining in the Waulsortian was established, all dewatering was carried out using underground wells and drill holes, and the surface wellfield became under-drained and redundant.

Groundwater storage removal at Lisheen was primarily associated with the dewatering of the shallow, relatively high storage, higher permeability epikarst. Successive expansions at Lisheen led to short-term increases in storage pumping but also step-change increases in recharge pumping as the area of drawdown progressively increased with each expansion. Once all expansions were complete, the area of drawdown remained relatively constant and so changes in dewatering rate reflected the seasonal and inter-annual variations in recharge only.

For much of the mine life, dewatering rates at Lisheen were typically within a seasonal range of 60 to 90 MLD, but strongly influenced by season and periods of wet weather. This reflects the rapid infiltration rates and limited groundwater storage to 'buffer' recharge before entering the mine workings.

Mine closure provided further evidence of the very low storage conditions at depth. While literature estimates suggest limestone specific yield are within the range 0.5 to 15%, the groundwater rebound analysis at Lisheen suggests that the actual value is significantly lower than 0.5%.

While the specific yield typically describes laboratory-defined drainable portion of a core sample, for 'real-world' dewatering and

closure predictions, the specific yield must be defined by both the drainable portion and the ability for it to be drained at the scale of the mine. The presence or absence of regional permeability, or permeable structures, connecting the country rock to the mine workings has a very significant impact.

This work demonstrates the importance of understanding both the bedrock storage and the seasonal variation in recharge when planning underground dewatering operations and predicting groundwater rebound.

Acknowledgements

The authors would like to thank Vedanta Zinc International for allowing access to information used to generate this paper.

References

Drew D (2018). Karst of Ireland: Landscape Hydrogeology Methods. Geological Survey Ireland, Dublin.

Misstear B, Banks D and Clark L (2006.) Water Wells and Boreholes. Wiley & Sons Ltd.

History of Passive Treatment Technology Development in the United States

Jeff Skousen[1], Bob Kleinmann, Tom Wildeman, Bob Hedin, Bob Nairn, Jim Gusek

[1]*West Virginia University, Morgantown, WV USA, jskousen@wvu.eduo.uk*

Abstract

The concept of passive treatment of acid mine drainage (AMD) was conceived in the early 1980's based on the observations of scientists in Ohio and West Virginia. They noted that the quality of AMD was improved after passing through a natural aerobic wetland and they postulated that oxidation reactions, filtering, and settling of sludge particles caused the improvement. Among the first to construct and report on constructed wetlands were researchers at the US Bureau of Mines (Kleinmann, Hedin, Nairn, and Watzlaf) but many others reported designs and results. By 1989, more than 150 wetlands had been constructed for mine drainage treatment in OH, PA, VA, and WV.

Coating of limestone particles renders limestone ineffective for dissolution and alkalinity generation. Researchers found that AMD passing through limestone in an anoxic state did not coat the limestone with iron oxides and the concept of anoxic limestone drains (ALD) was born.

To extend the use of limestone treatment of oxidized mine-influenced waters (MIW), an idea was developed to pre-treat MIW with organic matter to decrease oxygen in the water before introducing the water into an ALD. Successive Alkalinity-Producing Systems (SAPS) was the original term for these systems, but they are now called vertical flow wetlands (VFW).

Treatment with armored limestone soon was discovered to be an effective, albeit inefficient method. Coated limestone dissolution was 60 to 80% less than fresh limestone dissolution. Open limestone channels (OLC) were developed to treat MIW but require longer contact times.

By 1995, these five technologies (aerobic and anaerobic "compost" wetlands, ALDs, SAPS, and OLCs) formed the basis for construction of thousands of passive treatment systems throughout the world. Further discoveries and refinements include VFWs, slag/limestone leach beds, flushable limestone beds, bioreactors, low-pH Fe-oxidation channels, and hybrid systems that incorporate several types in series for treating acid drainage on a site.

Keywords: Historical Perspective, Wetlands, Anoxic Limestone Drains, Limestone Beds

Bibliography

Skousen, J., C. Zipper, A. Rose, P. Ziemkiewicz, R. Nairn, L.M. McDonald, and R.L. Kleinmann. 2017. Review of passive systems for acid mine drainage treatment. Mine Water Environ. 36: 133-153. DOI 10.1007/s10230-016-0417-1

Full Paper

A full paper on the results of this study will be published in an upcoming issue of the "Mine Water and the Environment" journal. If you have further interest or questions in the meantime, please contact the authors.

Utilisation of Mine Water from Abandoned Mines – Example "Anthracite Mine Ibbenbüren", Germany

Marion Stemke, Georg Wieber

Johannes Gutenberg-Universität Mainz, Johann-Joachim-Becher-Weg 21, 55128 Mainz, Germany, mstemke@uni-mainz.de
wieber@uni-mainz.de

Abstract

Sustainable and environmentally friendly energetic and non-energetic raw material extraction plays an increasingly important role in security of supply. The European Union compiles a list of critical raw materials at regular intervals. On this basis, mine water from the Ibbenbüren coal mine were examined. The results show that critical elements occur in the mine water. The concentration increases with depth. For the flooded Westfeld, the elements Al, B, Co, Li, Mg, Sr and Zn could be determined in the outflow and the loads determined. The calculation of the geothermal potential shows that about 900 single-family homes could be supplied with heat from the freely discharge mine water.

Keywords: Mine Water, Critical Raw Materials, Anthracite Coal Mine, Rare Earth Elements (Ree), Geothermal Use

Introduction

Every 3 years, the EU compiles a list of economically most important raw materials with a high supply risk called critical raw materials. Access to resources is of strategic importance to Europe's goal of achieving climate neutrality, which could lead to a shift from the current dependence on fossil fuels to raw materials that are largely sourced abroad and for which global competition is increasingly fierce (EU 2020). Because of this, other sources of raw materials are also increasingly coming into focus. These include in particular mine water from both closed and operating mines. Many of the substances listed as critical raw materials also occur in traces in the mine water of mining operations. Many of the substances listed (Table 1) as critical raw materials occur in traces in mine water and could be recovered before discharge into surface water.

Based on this list, the mine water of the Ibbenbüren anthracite mine were analysed for critical raw materials.

The Ibbenbüren hard coal mine, which was closed in 2018 as part of the energy transition, is located in north-western Germany. Mining took place in the East (closed in 2018) and West (closed in 1978) fields. The Ibbenbüren coalfield consists of Carboniferous strata that clearly protrude from the surrounding area as a ridge, north of the town of Ibbenbüren. The entire structure has a length of around 15 km and a width of 5 km and towers over the surrounding terrain by up to 100 metres. In relation to the Mesozoic hinterland, the Carboniferous horst structure is bounded by two NW – SE trending fault systems – the

Table 1 *2020 Critical Raw Materials (from EU 2020).*

Antimony	Cobalt	Hafnium	Natural Graphite	Phosphorus	Vanadium
Baryte	Coking Coal	Heavy REE	Natural Rubber	Scandium	Bauxite
Beryllium	Fluorspar	Light REE	Niobium	Silicon metal	Lithium
Bismuth	Gallium	Indium	Platinum Group Metals	Tantalum	Titanium
Borate	Germanium	Magnesium	Phosphate rock	Tungsten	Strontium

northern and southern Carboniferous margin faults (Melchers *et al.* 2019). In addition, the Carboniferous horst structure is divided into several smaller blocks by numerous transverse faults. Due to the fault zones, the area can be morphologically divided into three areas, the western part (Dickenberg), the eastern part (Schafberg) and the rift structure (Bockradener Graben) in between (Fig. 1). The terrain drops steeply south of the ridge into the valley of the Ibbenbürener Aa (Münsterland basin) (Goerke-Mallet 2000). The north-eastern slope of the Ibbenbürener Hochplateau is less steep than the south-western one and merges into the North German Lowlands (Lower Saxony Basin) (Busch 2016).

In the west field, mining ended at the level of -500 mNHN, while in the east field it took place to a depth of 1430 mNHN.

In its undisturbed condition, the coal bedrock represented a fissure aquifer with moderate yield. With the advance of mining into the depths, the rock was loosened and cavities created. With the advance of mining into the depths, the rock was loosened, cavities were created and thus the fissuring was increased. These loosenings cause increased infiltration rates of precipitation water. In the East Field and Bockradener Graben, infiltration is restricted by the Quaternary deposits, which are up to 30 m thick. In contrast, the western field has only a slight weathering cover, which leads to a higher proportion of precipitation in the mine water. While the mine water from the West field flows out of the Dickenberger adit without pressure, the East field is currently being flooded. Previously, the mine water was lifted here and piped to the Püsselbüren wastewater treatment plant (Domalski, 1988).

Methodology

A total of 305 water analyses from various sources from a period of 1957 to 2018 were collected. These come from data from Lotze *et al.*1962, Bässler 1970, Domalski 1988, DMT 2019, Rinder 2020 as well as from the mine operator (RAG AG), the Arnsberg district government (https://www.elwasweb.nrw.de) and own analyses. Of these, 128 are from the West Field, and 177 from the East Field. All analytical values below the detection limit were considered in the evaluation with half of the concentration level.

Results

Some critical raw materials were detected in the mine water. For most critical elements, there is either no sufficient data basis or the measurement data are below or in the range of the detection limit. Figure 2 shows the elements Al, B, Li, Mg, Sr and Zn as a function of depth for the East Field. Except for the elements B, Mg and Sr the concentration level of the individual substances increases with depth. The deeper mine water in the East field are no longer accessible due to mine closure. As a result, the extraction of raw materials from these depths would not be economically viable, as the recoverable quantities would be offset by the additional costs of drilling and pumping.

At present, only the mine water from the Dickenberger adit (West field), which flows out without pressure, is available for raw

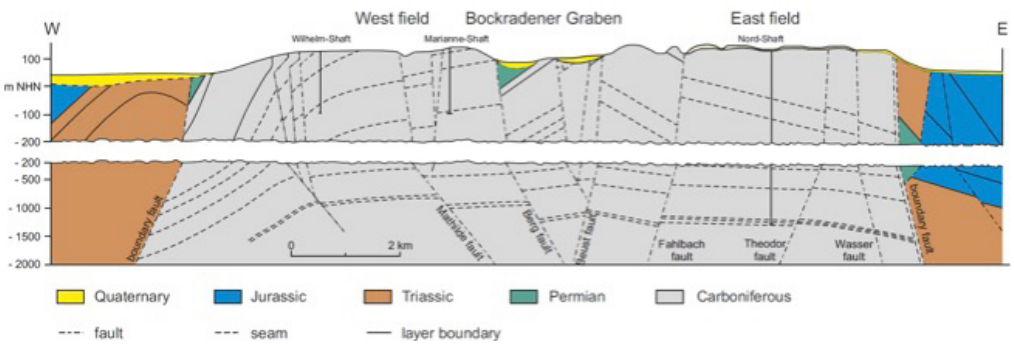

Figure 1 *Geological section through the Ibbenbüren coalfield (modified after Domalski 1988).*

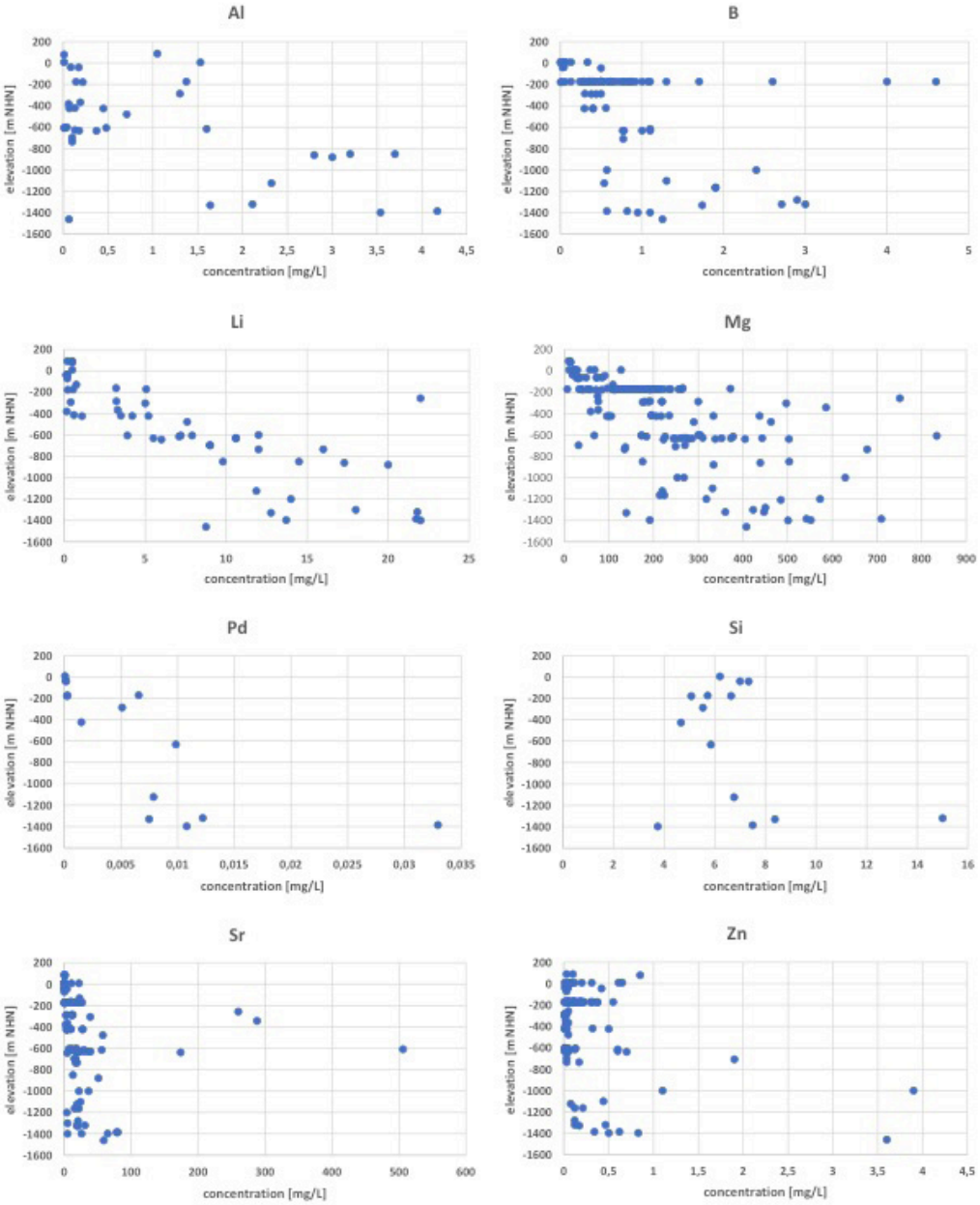

Figure 2 Concentrations as a function of depth in the east field.

material extraction. In the long-term average, 8.1 m³/min flow out here (DMT 2019). 39 water analyses could be assigned to the Dickenberger adit and the concentration level of the critical elements calculated. According to DMT forecasts (2019), the mine water after flooding of the East Field will correspond to those of the West Field. The discharge rate in the east field is expected to be 4.46 m³/min. Table 2 shows the resulting annual loads based on these data and forecasts.

In addition, it would also be possible to extract energy from the Dickenberg adit. Heat can be conducted both over solid rock as the conductive part (heat conduction) of the heat flow and as mass-supported transport

Table 2 Mine water loads Dickenberger adit (West field) and loads predict East field.

Element	Quantity	West field Dickenberger adit	Mine water loads	East field loads (predict)	Total loads
		mg/L	kg/a	kg/a	kg/a
Al	5	0.47	2,001	1,102	3,103
B	39	0.12	511	281	792
Co	5	0.12	511	281	792
Li	5	0.65	2,767	1,524	4,291
Mg	39	136	579,000	318,808	897,808
Sr	39	0.95	4,044	2,227	6,271
Zn	39	0.62	2,640	1,453	4,093

in and over liquids as the convective part (convection) of the heat flow (Kaltschmitt *et al.* 1999). According to Baehr & Stephan (2006), heat conduction represents a transport of energy between neighbouring molecules due to a temperature difference present in the material. In solids, heat conduction is the only energy transport, while convection and heat radiation can still occur in gases and liquids (Baehr & Stephan 2006).

The terrestrial heat flux density is composed of a conductive and a convective part of the heat flux as well as the heat production summed up along the depth. In the continental crust, the conductive part of the heat flux density dominates (Kaltschmitt *et al.* 1999, Clauser 2009, Wieber 2014) and results from the following equation:

$$q_{kond} = -\lambda \cdot \frac{\Delta T}{\Delta z}$$

With: q_{kond} = conductive part of the heat flow [W/m²], λ = thermal conductivity [W/mK], ΔT = temperature gradient [K], Δz = layer thickness [m].

Energy can be transported through the macroscopic movement of fluids. Due to a temperature gradient, heat and energy flow as enthalpy and kinetic energy of the fluid and flow through an (imaginary) surface. This process is called convection and can be described according to Fourier's law for the boundary transition between wall and fluid.

As already mentioned, the Dickenberg gallery drains the groundwater of the flooded west field in free fall with an average discharge of 8.1 L/min corresponding to approximately 135 L/s and a temperature of approximately 12 °C. After flooding, the east field should have a discharge of approximately 4.46 m³/min (corresponding to 74.3 L/sec) with comparable physico-chemical conditions. In total, this corresponds to an average discharge of approx. 200 L/sec, whereby there are strong fluctuations in the discharge, especially in the West Field.

The existing temperatures are not sufficient for direct use for heating purposes. However, they can be raised to a higher temperature level with the help of heat pump technology. Compression heat pumps are predominantly used here, whereby a working fluid is compressed and thus heated. The heat medium changes its aggregate state (liquid/gaseous) when absorbing or releasing heat energy. The energy obtained with this technology (evaporator power) consists of the geoenergy "mine water" as well as the drive energy of the heat pump. The mine water of the anthracite mines in Ibbenbüren offer ideal conditions for geothermal utilisation, as the temperature of continuously 12 °C enables an effective yield, as the mine water are captured and permanently discharged through the galleries.

Two basic options can be distinguished for the geothermal use of mine water for heat pump systems:

- Utilisation of the freely leaking mine water in the deep gallery and/or
- Use of the thermal energy in the flooded mine workings (e.g. shafts).

Heat pump systems require a water quantity of 0.25 to 0.3 m³/h for 1 kW evaporator capacity at a temperature difference of 3K. This corresponds to a water volume of 0.228 L/s at a temperature difference of 1K. The extractable heat/evaporator capacity ($W_{thermal}$) can be calculated for the heat capacity of water

(4200 J/L/K) for a freely discharging water quantity (Q) of 200 L/s and a temperature drop from 12 °C to 2 °C (ΔT: 2 °C):

Extractable heat = heat capacity * ΔT * Q

The geothermal potential of the freely leaking water amounts to around 8,800 kW under the above-mentioned boundary conditions. This geothermal energy corresponds to the heat demand of about 900 modern single-family homes, with the geothermal energy being supplied from the mine at a free gradient. Electrical energy (about one fifth of the energy yield) is only needed to operate the heat pump. There are no changes in the "mine" system due to the use of the leaking water.

Multiple geothermal energy is stored in the rocks of the mine than in the leaking groundwater. In the case of a more extensive use, however, the energy would have to be technically extracted by pumping out or cooling the impounded mine water/rock body. This in turn requires greater technical effort and energy consumption.

Conclusions

The measured data show that critical raw materials are present in the mine water of the Ibbenbüren mine. For most critical elements, however, there is either insufficient data for a reliable assessment of the concentration level or the analyses are only in the range of the detection limit. In the outlet of the Dickenberg adit, the elements Al, B, Co, Li, Mg, Sr and Zn occur in higher concentrations. However, economic extraction is not possible at present. However, boundary conditions may change as the state of the art advances. After the flooding of the East Field and the completion of the newly planned "mine water channel", long-term measurements for critical elements in the mine water would be useful. Especially with the development of technical innovations, the extraction of critical elements from the Ibbenbüren mine water could be ecologically and economically profitable.

Calculations of the geothermal potential from the mine water also show that up to 900 single-family homes could be supplied with heat. Further investigations using the mine rocks to increase the energy yield should be considered.

Acknowledgements

The authors thank all co-organisers for hosting the IMWA2021 Conference. Amy Kokoska, Hetta Pieterse as well as Glenn MacLeod provided critical comments on earlier versions of this text. This work was made possible within the framework of the "Forum Bergbau Wasser" Foundation, which is hereby thanked for the support provided. We owe special thanks to Dr. Rinder for providing his reserve samples.

Reference

Baehr HD, Stephan K (2006) Wärme- und Stoffübertragung. – 757 S.; Berlin – Heidelberg – New York (Springer)

Bässler R (1970) Hydrogeologische, chemische und Isotopen-Untersuchungen der Grubenwässer des Ibbenbürener Steinkohlenreviers. – Z.deutsch. geol. Ges., Sonderh. Hydrogeol. Hydrogeochem. 209-286

Busch W, Walter D, Xi F, Yin X, Coldewey WG, Wesche D, Hejmanowski R, Malinowska A, Kwinta A, Witkowski WT (2016) Bergwerk Ibbenbüren der RAG AG. Analyse von Senkungserscheinungen außerhalb des prognostizierten Einwirkungsbereiches, Gutachten TU Clausthal im Auftrag der Bezirksregierung Arnsberg Abteilung Bergbau und Energie in NRW

Clauser C (2009) Heat Transport Processes in the Earth's Crust. – Surveys in Geophysics, 30: S. 163-191; Berlin – Heidelberg – New York (Springer)

Domalski RF (1988) Bergmännische Wasserwirtschaft der Steinkohlenbergwerke Preussag AG Kohle/Ibbenbüren und Gewerkschaft Sophia-Jacoba/Hückelhoven Ein Vergleich. Mitt. Westfälische Berggewerkschaftskasse, H. 60, 174 S.; Bochum

DMT GmbH (2019) Abschlussbetriebsplan des Steinkohlenbergwerks Ibbenbüren Anlage 17 Prognose zur optimierten Wasserannahme nach Stilllegung des Steinkohlenbergwerkes Ibbenbüren (Ostfeld). https://www.rag-anthrazit-ibbenbueren.de/grubenwasserhaltung/wie-laeuft-das-genehmigungsverfahren-ab/abschlussbetriebsplan/

European Union (2020) Critical Raw Materials Resilience: Charting a Path towards greater Security and Sustainability. https://eur-lex.europa.eu/legal-content/DE/TXT/

?uri=CELEX%3A52014DC0297

Kaltschmitt M, Huenges E, Wolff H (Hrsg.) (1999) Energie aus Erdwärme – Geologie, Technik und Energiewirtschaft. - 265 S.; Stuttgart (Deutscher Verlag für Grundstoffindustrie)

Lotze F, Semmler W, Kötter K, Mausolf F (1962) Hydrogeologie des Westteils der Ibbenbürener Karbonscholle. – Forschungsberichte des Landes Nordrhein-Westfalen, Nr. 999: 113 S., 45 Abb., 8 Tab.; Köln und Opladen (Westdeutscher Verlag)

Melchers C, Westermann S, Reker B (2019) Evaluierung von Grubenwasseranstiegs-prozessen. – Techn. Hochschule Agricola [Hrsg.]: Berichte zum Nachbergbau, H. 1:130 S., Bochum.

Rinder T, Dietzel M, Stammeier J A, Leis A, Bedoya-González D, Hilberg S (2020). Geochemistry of coal mine drainage, groundwater, and brines from the Ibbenbüren mine, Germany: A coupled elemental-isotopic approach. Applied Geochemistry, 104693

Wieber G (2014) Hydrogeologie und Wärmefluss de gefluteten Grube Mercur in Bad Ems, Rheinisches Schiefergebirge. – In: Jber. Mitt. Oberrhein. Geol. Ver., N. F. 96: 361-377, 8 Abb., 3 Tab., Stuttgart

Forecasting Evolution of Sulfide Mineral Oxidation Rates Over Decadal Time Scales

John B. Swenson[1,2], Tamara R. Diedrich[1]

[1]*MineraLogic LLC, 306 W Superior St, Duluth, MN, 55802, USA, jswenson@mnlogic.com, tdiedrich@mnlogic.com*

[2]*Department of Earth and Environmental Sciences, University of Minnesota Duluth, 1114 Kirby Dr, Duluth, MN, 55812, USA, jswenso2@d.umn.edu, ORCID 0000-0002-4238-8395*

Abstract

Leachate from 26 decadal-duration laboratory tests on tailings isolated the time-dependence of sulfide mineral oxidation from field scale sources of variability. Time series from *all* tests show a three-phase evolution, with an **order-of-magnitude decrease in sulfate release rate** during the second phase. The first phase is relatively short (0.7-yr avg.), with large, quasi-steady release rates. In the second phase – of two- to six-years duration – release rates show a power-law dependence on time. Third-phase release rates are near detection limits and quasi-steady or slowly decaying. We attribute the second evolutionary phase to an accumulation of weathering products that hinders sulfide oxidation.

Keywords: Sulfide Minerals, Pyrrhotite, Oxidation Rates, Forecasting

Introduction

Characterizations of long-term (decadal scale or longer) oxidation rates of sulfide minerals in mine waste is directly significant to forecasting contact-water chemistry over the life of mine and post-closure. Incorporating potential time dependence into the oxidation rate characterization—and, therefore, water chemistry forecasts—presents an opportunity to refine the basis for more effectively designed mine waste management systems and closure planning.

Theoretical models of time-dependent sulfide-mineral apparent reactivity have been established for mining and other applications, e.g. Wunderly *et al.* (1996). These models have been successfully applied to describe water chemistry observations across a range of mine sites. However, logistical constraints and complexities inherent of full-scale field systems, such as site-specific seasonality and stochastic fluctuations in temperature and hydrology, limit the ability to isolate the effect of time-dependent oxidation rates from other factors. Laboratory-scale experiments, while introducing uncertainty associated with upscaling results in space and time, would have the potential to eliminate much of the variability in environmental forcing. However, there have been exceedingly few opportunities to test directly these model predictions against observations from well-controlled laboratory experiments conducted over relevant (decadal) timescales.

Here we present data from a unique, industry-supported, laboratory-scale experiment of tailings oxidation. We analyzed leachate from 26 humidity-cell tests (HCTs) of exceptionally long duration (more than a decade). The time series from all HCTs show an order-of-magnitude decrease in sulfate release rates over timescales of less than a decade.

Experimental Methods

Mine waste materials analyzed here are tailings derived from a pilot-plant test program that processed 1.1 Ga, mafic (troctolitic), magmatic Cu-Ni sulfide ore from a mining project in development at the time. The dominant sulfide mineral is pyrrhotite; the tailings are characterized by relatively low overall sulfur content (< 0.15 weight percent S, as sulfide). Based on grain size (d), tailings collected at various stations in the ore-processing flow were subdivided into four classes—fine (d < 75 μm), medium (75 μm < d < 150 μm), coarse (d > 150 μm), and whole

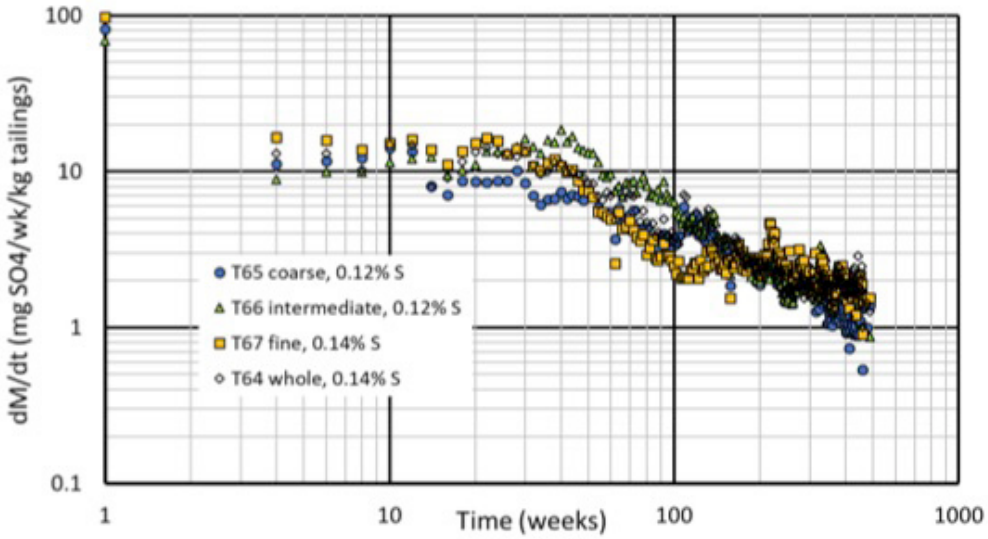

Figure 1 Times series of sulfate-release rates for HCTs T64 – T67; behavior shown here is representative of that observed in all 26 samples.

(unsorted). The 26 samples were given unique identifiers T8 – T13 and T52 – T71 (Table 1), placed in standard humidity cells, and allowed to weather under steady, controlled-climate laboratory conditions. Following ASTM (2013) standards, sample size was 1 kg of tailings, which was rinsed weekly with 500 ml of water. Collected leachate was analyzed for a suite of constituents. The duration of the weathering experiments exceeded ten years, thus providing exceptionally long time series of sulfate release rates under uniform environmental conditions, thereby eliminating the complexity of climate and seasonality that typically plagues field-based studies. Individual samples (HCTs) varied in grain size, sulfur content, but had consistent gangue mineral composition.

Experimental Results and Empirical Model

Each of the 26 sulfate-release time series, when plotted in log-log space, displays a clear break in scaling near a time t_{brk}, where t_{brk} is typically a few tens of weeks. Prior to t_{brk}, i.e. at 'early' times, the SO_4 release rate is relatively steady and large. Importantly, for $t > t_{brk}$, the release rate decays quasi-linearly in log-log space, characteristic of a power-law dependence on time. Figure 1 shows the time series of sulfate release for HCTs T64 – T67, which vary in grain size and sulfur content. The behavior shown in these four release-rate time series is representative of that in *all* 26 HCTs.

Figure 1 isolates and annotates the time series of sulfate release for HCT T67 (fine-grained, 0.14% S). Note the break in scaling at approximately 30 weeks of exposure. Based on observations common to all HCT time series, we established an empirical model of sulfate release through time:

$$\dot{M} = \begin{cases} \dot{M}_o & , \quad t_{min} < t < t_{brk} \\ C_1 t^{-\alpha} & , \quad t_{brk} < t \\ \dot{M}_\infty & , \quad C_1 t^{-\alpha} < \dot{M}_\infty \end{cases} \qquad (1)$$

where $\dot{M}$ is the time-dependent sulfate release rate (mg $SO_4 \cdot kg^{-1} \cdot wk^{-1}$); $\dot{M}_o$, C_1, and α are parameters determined from graphical analysis of each time series; and t_{min} and t_{brk} are, respectively, the time of the first observed release rate to be used in the empirical model (five weeks, per regulatory guidelines) and the end of the first model phase, which is characterized by a nearly steady release rate ($\dot{M}_o$). Parameters α and C_1 represent, respectively, the scaling exponent in a power-law relationship and the *one-week* sulfate release rate.

At very large times, e.g. $t > 200$ weeks, sulfate-release rates again break scaling, departing from the power-law relationship in Eq. 1. In general, the release rates decrease to

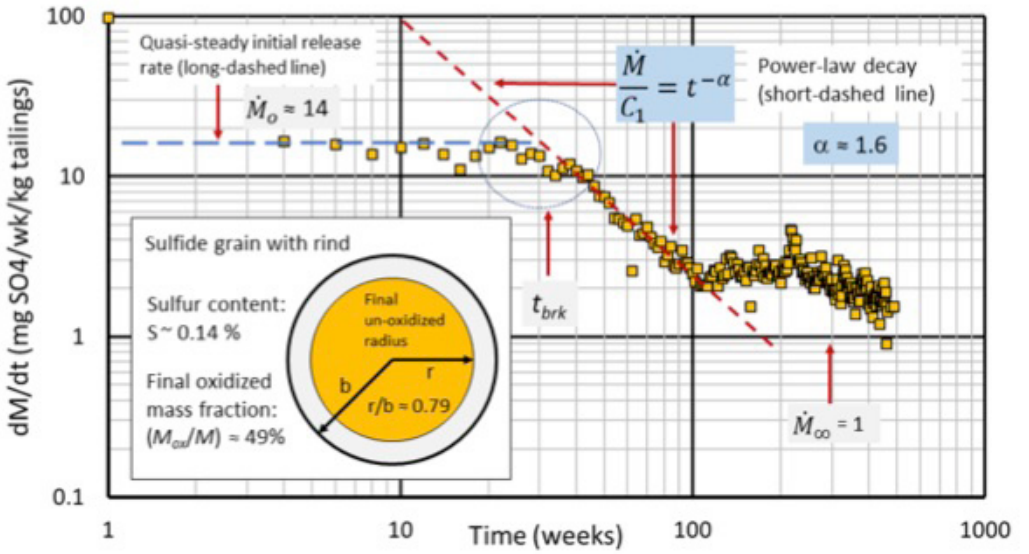

Figure 2 Annotated time series of sulfate release rate for HCT T67; inset cartoon depicts development of weathering rind.

values near 1 – 2 mg $SO_4 \cdot kg^{-1} \cdot wk^{-1}$—hovering slightly above detection limits—and show no consistent trend across the full set of time series. Pending further analysis of these large-time data, we adopt a conservative empirical modeling approach, in which the release rate is set to a constant 'floor' value ($\dot{M}_\infty$) of 1 mg $SO_4 \cdot kg^{-1} \cdot wk^{-1}$ (Eq. 1). Note that this floor applies only to the sulfate release rate model and does not imply that sulfate release continues indefinitely, as ultimately the sulfur source will be exhausted.

Table 1 provides a summary of the observed empirical model parameters, i.e. $\dot{M}_o$, C_1, and α. Tracking sulfur release through time allows straightforward computation of the mass fraction of sulfur oxidized during the experiments, M_{ox}/M, where M is the original mass of sulfur as sulfide. On average, the duration of the HCTs was sufficient to allow oxidization of approximately 50% of the original sulfur (as sulfide) mass. Assuming spherical sulfide grains, the average un-oxidized radius fraction, *r/b*, at experiment completion was 0.79 (Table 1), suggesting the development of a weathering rind in the outer 20% of the original sulfide-grain radius (Fig. 2).

The most important observational aspect of the HCT time series is the **order-of-magnitude decay** in SO_4 release rate in the two- to six-year timeframe of *all* 26 HCTs. In the following section, we present a plausible explanation for this observed decay.

Two-Phase Mathematical Model of Sulfide Oxidation

In many natural systems, a break in scaling—such as that shown in Figs. 1 and 2—commonly reflects a 'handoff' between two competing physical, chemical, or biological processes. A putative explanation of the handoff in sulfate-release rate near t_{brk} is the accumulation of oxidation products—the development of a weathering rind, in effect, composed of iron hydroxides or oxyhydroxides—on the sulfide grain of sufficient thickness to affect the rate of sulfide oxidation (Fig. 3c). Diffusion of dissolved oxygen (inbound) and SO_4 anions (outbound) across this rind is relatively inefficient and thus slows the SO_4 release rate. Continued thickening of the rind with time results in a monotonic decay in sulfate release rates, *sensu* the well-established 'shrinking core' model (Davis and Ritchie 1986). Prior to the accumulation of an appreciable thickness of oxidation byproducts, the SO_4 release rate per unit of reactive area is approximately constant, and any decay in overall sulfate release rate is driven by physical shrinking of the grain, i.e. the so-called 'shrinking

Table 1 HCT sample characteristics and best-fit model parameters.

ID	d (µm)	S %	$\dot{M}_o$	C_1	α	M_{ox}/M	r/b	t_{brk}	j_o	D
T8	>150	0.11	6	2000	1.3	0.48	0.78	90	$5.0{\cdot}10^{-10}$	$2.0{\cdot}10^{-17}$
T9	75 – 150	0.10	8	10000	1.6	0.53	0.81	70	$7.0{\cdot}10^{-10}$	$3.6{\cdot}10^{-17}$
T10	< 75	0.09	18	150	0.9	0.51	0.80	20	$1.5{\cdot}10^{-9}$	$3.1{\cdot}10^{-17}$
T11	> 150	0.11	7	2500	1.3	0.45	0.76	80	$6.0{\cdot}10^{-10}$	$1.8{\cdot}10^{-17}$
T12	75 – 150	0.14	12	7100	1.5	0.51	0.80	81	$7.0{\cdot}10^{-10}$	$1.0{\cdot}10^{-17}$
T13	< 75	0.14	20	300	0.9	0.49	0.79	20	$1.7{\cdot}10^{-9}$	$2.4{\cdot}10^{-17}$
T52	whole	0.09	9	11000	1.5	0.54	0.81	70	$8.0{\cdot}10^{-10}$	$1.3{\cdot}10^{-17}$
T53	> 150	0.10	15	200	1.1	0.48	0.78	20	$8.0{\cdot}10^{-10}$	$3.2{\cdot}10^{-17}$
T54	75 – 150	0.08	10	300	1.0	0.57	0.83	25	$1.0{\cdot}10^{-9}$	$4.0{\cdot}10^{-17}$
T55	< 75	0.10	18	400	1.1	0.55	0.82	30	$1.2{\cdot}10^{-9}$	$2.5{\cdot}10^{-17}$
T56	whole	0.10	9	300	1.0	0.47	0.78	30	$1.0{\cdot}10^{-9}$	$1.8{\cdot}10^{-17}$
T57	> 150	0.11	8	250	1.0	0.42	0.75	30	$8.0{\cdot}10^{-10}$	$1.5{\cdot}10^{-17}$
T58	75 – 150	0.08	8	300	1.0	0.53	0.81	40	$1.0{\cdot}10^{-9}$	$3.1{\cdot}10^{-17}$
T59	< 75	0.11	11	300	1.0	0.46	0.77	20	$1.3{\cdot}10^{-9}$	$2.7{\cdot}10^{-17}$
T60	whole	0.11	10	700	1.2	0.46	0.77	25	$1.0{\cdot}10^{-9}$	$2.7{\cdot}10^{-17}$
T61	> 150	0.11	8	240	1.0	0.42	0.75	20	$1.0{\cdot}10^{-9}$	$2.7{\cdot}10^{-17}$
T62	75 – 150	0.10	9	300	1.0	0.49	0.79	30	$9.0{\cdot}10^{-10}$	$2.4{\cdot}10^{-17}$
T63	< 75	0.12	14	230	1.1	0.40	0.74	20	$1.2{\cdot}10^{-9}$	$1.5{\cdot}10^{-17}$
T64	whole	0.14	13	920	1.2	0.51	0.80	30	$8.0{\cdot}10^{-10}$	$2.5{\cdot}10^{-17}$
T65	> 150	0.12	10	300	1.0	0.49	0.79	20	$8.0{\cdot}10^{-10}$	$2.5{\cdot}10^{-17}$
T66	75 – 150	0.12	13	1400	1.2	0.62	0.85	40	$1.2{\cdot}10^{-9}$	$3.7{\cdot}10^{-17}$
T67	< 75	0.14	14	1600	1.4	0.49	0.79	30	$8.5{\cdot}10^{-10}$	$1.7{\cdot}10^{-17}$
T68	whole	0.12	13	600	1.2	0.46	0.77	30	$9.0{\cdot}10^{-10}$	$1.8{\cdot}10^{-17}$
T69	> 150	0.11	8	240	1.0	0.46	0.77	20	$9.0{\cdot}10^{-10}$	$2.8{\cdot}10^{-17}$
T70	75 – 150	0.11	10	800	1.1	0.51	0.80	35	$1.0{\cdot}10^{-9}$	$3.1{\cdot}10^{-17}$
T71	< 75	0.14	12	520	1.1	0.41	0.74	20	$1.0{\cdot}10^{-9}$	$2.0{\cdot}10^{-17}$
arithmetic mean		0.11	11		1.1	0.49	0.79	36	$9.7{\cdot}10^{-10}$	$2.4{\cdot}10^{-17}$

Note on units: $\dot{M}_o$ and C1 in mg $SO_4{\cdot}kg^{-1}{\cdot}wk^{-1}$; t_{brk} in weeks; j_o in $mols{\cdot}m^{-2}{\cdot}s^{-1}$; and D in $m^2{\cdot}s^{-1}$.

particle' model (e.g., Bilenker *et al.* 2016). We developed a *hybrid* model—summarized below—for sulfate release from an idealized abstraction of an HCT that combines the shrinking-particle and shrinking-core theoretical frameworks.

In our hybrid model, the shrinking-particle framework applies early in the oxidation process, during what we term a 'tarnishing' phase (Fig. 3c). The basic assumptions underpinning the tarnishing model are 1) a constant oxidation rate per unit area of reactive surface on the sulfide grain and 2) insufficient accumulation of oxidation products, e.g. FeO(OH) minerals, to affect the oxidation rate. The constant oxidation rate is embodied in a dissolution flux (j_o; $mols{\cdot}m^{-2}{\cdot}s^{-1}$) of sulfate anions leaving the reactive surface of the sulfide grain. With no accumulation of oxidation products, the diameter of the reactive surface and, by extension, the grain itself must decrease with time, hence the 'shrinking particle' nomenclature (Fig. 3c). HCT data suggest that the size of the sulfide grain at the end of the tarnishing phase (b) has decreased only slightly from its initial size (b_o), i.e. $b_o \approx b$ (Fig. 3c).

The dissolution flux (j_o) depends on the detailed geochemistry of the pore fluid coating the sulfide grain and thus varies with the mineralogy of the parent rock (dominantly troctolite, in this case). While the literature provides broad and useful constraints on jo for pyrrhotite, e.g. Rimstidt (2014) and Bilenker *et al.* (2016), no independent study has constrained the kinetics underpinning j_o for the proprietary tailings we analyzed here. Given this knowledge gap, j_o is treated as a tuned parameter.

The dissolution flux (j_o) depends on the detailed geochemistry of the pore fluid coating the sulfide grain and thus varies with the mineralogy of the parent rock (dominantly troctolite, in this case). While the literature provides broad and useful constraints on

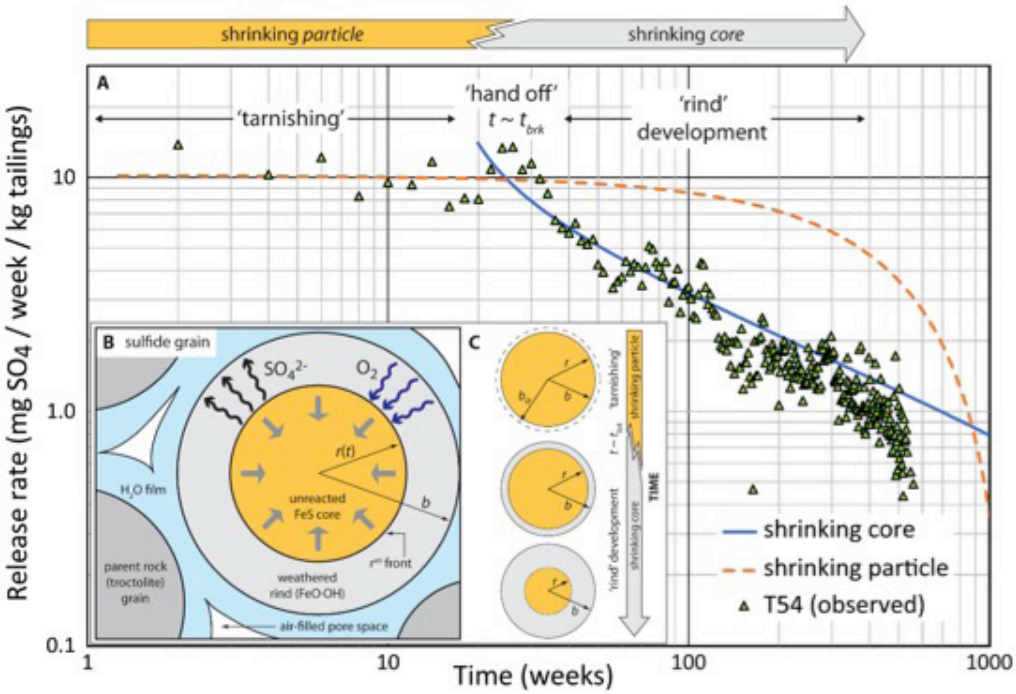

Figure 3 *(a) Observed time series of SO4 release rate for HCT T54, with best-fit shrinking-particle (orange) and shrinking-core (blue) predictions overlaid; (b) conceptual sketch of sulfide-grain weathering; and (c) cartoon illustrating transition from tarnishing phase to rind-development phase in hybrid model.*

j_o for pyrrhotite, e.g. Rimstidt (2014) and Bilenker *et al*. (2016), no independent study has constrained the kinetics underpinning j_o for the proprietary tailings we analyzed here. Given this knowledge gap, j_o is treated as a tuned parameter.

In our model, as the exposure time nears t_{brk}, the 'tarnishing' phase transitions to the 'rind development' phase, thus signifying the handoff from shrinking-particle to shrinking-core framework (Fig. 3). The primary differentiating feature of the latter is its treatment of the Fe-bearing oxidation byproducts, which are assumed to *remain attached* to the grain in the form of an FeO(OH) mineral rind, through which oxygen must diffuse to reach the reactive surface of the shrinking 'core' of unreacted FeS, *sensu* Davis and Ritchie (1986) and Wunderly *et al*. (1996). Likewise, sulfate must diffuse outward through the rind to reach the water film coating the sulfide grain. Throughout this model phase, the overall radius (b) of the affected grain remains steady, but the radius of the unreacted FeS core, r(t), decays with time, while, by extension, the thickness of the rind, b-r, increases with time. Diffusion of oxygen through the rind is slow relative to oxidation of pyrrhotite at the reactive outer surface of the core, which is treated as a 'sharp' front; there is no O_2 consumption in the FeO(OH) rind, i.e. oxidation is complete, and diffusion proceeds in a quasi-steady manner, characterized by a constant and uniform diffusivity D ($m^2 \cdot s^{-1}$). The shrinking-core model, as developed here, contains a pair of tuned parameters: The onset of diffusion-controlled oxidation (t_{brk}) and the diffusivity D of the weathering rind. Both parameters are determined by subjective 'best fits' to the observed SO_4 release-rate time series from HCTs.

Our hybrid model does not address the observed second break in scaling at very large times, as this behavior is beyond project scope. Multiple plausible explanations exist for this apparent handoff to a third set of processes: A likely candidate is pore-scale 'poisoning' of the system via incomplete removal of weathering byproducts and/or precipitation of secondary minerals.

Model Results and Interpretation

Application of our hybrid model to the observed HCT time series is relatively straightforward. The model framework described above applies to an individual sulfide grain. Upscaling to the overall sulfate release rate from an HCT—and its ensemble of sulfide grains—involves determination of the number of sulfide grains based on bulk sulfur content and sulfide grain size. Consider the observed sulfate-release rates from HCT T54 shown in Figure 3a. By inspection, the break in scaling occurs approximately 20 – 30 weeks into the experiment. With 0.08% S and an assumed sulfide particle size of 20 μm, a dissolution flux (j_o) of $1 \cdot 10^{-9}$ mol·m^{-2}·s^{-1} yields a reasonable fit (dashed curve in Fig. 3a) to the observed data from the 'tarnishing' phase of the experiment. This estimate of j_o is similar to that reported by Bilenker *et al.* (2016) for pyrrhotite in slightly acidic waters (jo = $1.5 \cdot 10^{-9}$ mol·m^{-2}·s^{-1}; pH = 6). With jo constrained from the tarnishing-phase data, simultaneous adjustment of t_{brk} (i.e., 'fine tuning' relative to the initial visual estimate of 20 – 30 weeks) and diffusivity, D, gives a subjective best fit (solid curve in Fig. 3a) to the HCT data for parameter values t_{brk} = 25 weeks and D = $2 \cdot 10^{-17}$ m^2·s^{-1}. This diffusivity is consistent with values reported in the literature (e.g. Wunderly *et al.* 1996). Table 1 contains the values of j_o, D, and t_{brk} obtained by repeating this fitting exercise for the remaining 25 HCT time series.

Discussion and Conclusions

By minimizing environmental variability, the long-duration HCT data we present here provide important insight about the time dependence of *grain-scale* oxidation processes. All sulfate-release-rate time series we analyzed share a common and critically important attribute—an order-of-magnitude decrease in SO_4 release rate on decadal timescales, preceded by a relatively short interval of nearly steady release. The ubiquity of this two-phase behavior motivated our development of a *grain-scale* hybrid model that provides a putative explanation for the onset of decay in release rate.

When nested within a site-specific, vadose-zone hydrologic model, our hybrid oxidation model may improve ability to forecast mine water quality over multi-decadal time scales, with attendant implications for mine permitting. While upscaling experimental insight to the mine scale poses well-recognized challenges, utilization of a simple intermittency factor—to reflect seasonality in cool, temperate climates—suggests that the order-of-magnitude decrease in sulfate release rate would be realized within a few decades of mine closure; warmer climates with less seasonality may realize this decrease earlier.

Acknowledgements

We gratefully acknowledge Stephen Day and others at SRK for their contributions to design and oversight of the kinetic test program utilized here.

References

ASTM (2013) Standard Test Method for Laboratory Weathering of Solid Materials Using a Humidity Cell. D5744-13

Bilenker LD, Romano GY, McKibben MA (2016) Kinetics of sulfide mineral oxidation in seawater: Implications for acid generation during in situ mining of seafloor hydrothermal vent deposits. Applied Geochemistry, 75, doi: 10.1016/j.apgeochem.2016.10.010

Davis G, Ritchie A (1986) A model of oxidation in pyritic mine wastes: part 1, equations and approximate solution. Applied Mathematical Modelling, 10(5): 314 – 322

Rimstidt JD (2014) Geochemical Rate Models: An Introduction to Geochemical Kinetics. Cambridge University Press. DOI:https://doi.org/10.1017/CBO9781139342773

Wunderly M, Blowes DW, Frind EO, Ptacek CJ (1996) Sulfide mineral oxidation and subsequent reactive transport of oxidation products in mine tailings impoundments: A numerical model. Water Resources Research, 32(10)

Prevention of Siltation in Artisanal Small-scale Mining

E. Takaluoma[1], T. Samarina[1], A. Peronius[2]

[1]*Kajaani University of Applied Sciences, Ketunpolku 1, FI-87100 Kajaani, Finland,*
esther.takaluoma@kamk.fi

[2]*Hangasojan Kulta Oy, Consulting company, Ylä-Mulkujärventie 123, 99800 Inari, Finland*

Abstract

Silting of waterbodies caused by sluicing in artisanal small-scale mining is a consquence of sluicing directly into receiving waterbodies. Silting lowers the acceptancy of mining activities by locals. Utilizing flocculants and/or coagulants in circulation ponds quickly reduces the amount of silt and colloids in the water. The flocculant can be applied with low-cost methods and the overall process is economical. The process has been tested in a 3–4 m^3/h pilot in the Finnish Lapland.

Keywords: ASM, Gold Mining, Siltation, Prevention

Introduction

Artisanal small-scale gold mining (ASM) is a livelihood for over 40 million people in 80 countries (Weldegiorgis 2018), and rising gold prices increase ASM attractiveness. While many countries are starting the process of formalizing ASM, several social and environmental problems need to be resolved (Singo 2018). Many researchers focus on the mercury pollution from ASM. However, with the correct techniques suitable to the targeted ore applied, the use of mercury can either be circumvented completely with little to no loss of yield, or the mercury can be safely retorted.

Sluicing of alluvial gold containing ore involves the gravimetric separation of gold particles along a slight decline with the help of large quantities of waters, often several hundred liters to cubic liters per minute. Gold particles are separated at the bottom of the sluice by rifles, with profile, spacing, and height according to the ore being processed. Grizzlies or drum screens help to remove overlarge rocks. Thus, sluicing washes the non-gold material into the receiving waterbody. Larger particles quickly settle to the ground, while small and colloid particles can remain flowing for days and months.

Gold mining in the Finnish Lapland underlies strict regulation and environmental protection laws. Despite high levels of regulation, the Lapland Goldminer's Association currently has around 4100 members. Each claim is subjected to individual rules, imposed by mining authorities and based on the Environmental Protection Act, which forbid the contamination of nature and the reduction of recreational value of nature. These laws are subject to interpretation.

With respect to the sluicing process, the biggest concern is the emission of fine particles downstream. Sludge formation can destroy spawning areas and affect developing hatchlings. Therefore, silting of waterbodies and the increase of turbidity is prohibited (Kerr 1995). All gold mining practices must utilize circulating water with settling pond sizes of at least two hours of pump use. All rainwater and surface runoff water have to be guided into the water circulation. Water purged from the circulation is to be absorped by a leaching field.

The law also requires actors to actively anticipate and prevent emissions. In case of disturbances, this can, however, be difficult, particularly in times of rainstorm or at the beginning and preparing of a new area. Therefore, techniques to quickly settle colloids and floating particles could be beneficial in silting reduction from gold mining.

In this article, the results of a low-cost, low-tech method to introduce coagulant/flocculant into circulating water was tested and piloted at a 3–4 m^3/h scale in a working gold mine are discussed.

Samples:
Samples were taken in July 2018 from five different gold mines with three different bed rock areas. The samples also differed in the

life-of-mine stage of the gold mine, ranging from a recently started mine to a tens of years old mature mine. Four mines were processed by excavator and one gold digging place was processed using shovel-operated methods. Coordinates and physical parameters of the samples is gathered in Table 1. Sample Pusku is from a mature settling pond, containing small, plate like colloids, with a particle size of 0.5-2 µm.

Methods

Initially, flocculant testing was performed in the laboratory utilizing JAR-tester and standard methods. The coagulants tested were PIX 105 (Kemira) and PAX XL 100 (Kemira) and they were used as they were received. Flocculants, SA1, Praestol 2500 TR and Drewfloc 270 (Solenis Sweden AB), were prepared as a 0.25% solution 18 h prior to use. The best coagulant/flocculant mixtures were used to test low-cost flocculant addition under field conditions.

Lab test conclusions

All samples could be clarified by a suitable coagulant/flocculant mixture. Because silt particles are usually negatively charged, cationic coagulants and flocculants were used. PIX was favored over PAX because of potentially problematic aluminium concentrations in mine effluent. As such, over dosage of iron-based coagulant would result in natural precipitation of iron oxide hydrates and would, therefore, be environmental benign. The dosage depended on the type of particles in question and on the amount fines in the water. For the samples tested, suitable dosages ranged from 50 mL PIX per m^3 and 2 L polymer to 60 mL PIX and 10 L polymer. To keep treatment costs low, it was preferred that the polymer was increased over an increase of PIX dosage.

It also needed to be taken into account that the dosage was based on the rapid formation of thick flock, which settles fast, to allow quick removal of clarified water. A thick flock was also preferred due to the possibility of strong currents in the clarification ponds, as the gold washing process might be in progress.

Scheme for field tests

The goal of field testing was the proof of concept for a low-cost low-tech-method for silt removal in ASM. The developed method would not require slow-mixing and utilized simple technology, so that could it could easily be copied by miners around the globe. Due to the strict environmental laws, no chemicals or flocculants were allowed to enter the surrounding nature, and the tests were conducted with a side stream-utilizing international bulk container (IBC). Formed sludge was removed from the IBC and disposed of later. according to permissions. The overall concept is depicted in Figure 1 and the implementation in a field test can be seen in Figure 2. The tests were performed at claim "Rinnekulta" while sluicing was in progress during the period of 27.8.-31.8.2018.

Calculation of coagulant and flocculant dosage was based on laboratory tests. An average solid particle content in a circular pond in a running mine is about 10 %. However, the distances from the sluice and the feed, as well as particle size distribution, may vary greatly and only an estimation can be given. Flocculant was administered in a 0.1% solution.

The settling speed of particles was determined in a 500 ml volumetric flask, and the speed of clarification for optimized runs is shown in Figure 3. Utilizing PAC instead of PIX increased the speed of clarification,

Table 1 *Sampling parameters of for water sampling.*

Name	Coordinates		Altitude m a.s.l.	pH	TDS mg/L	Conductivity µS
Palsin tulli	N 68,4577	E 26,9571	254	7.52	20	45.5
Rinnekulta	N 68,45566	E 26,93117	275	6.92	9	20.8
Vehviläinen	N 68,4555	E 26,9309	245	7.38	22	48.7
Mäkärä	N 68,1482	E 26,9791	247	6.81	12	26.6
Roivainen	N 68,0453	E 27,1112	275	6.59	10	19.9
Pusku	N 68,64141	E 25,70372	-	6.64	14	30.7

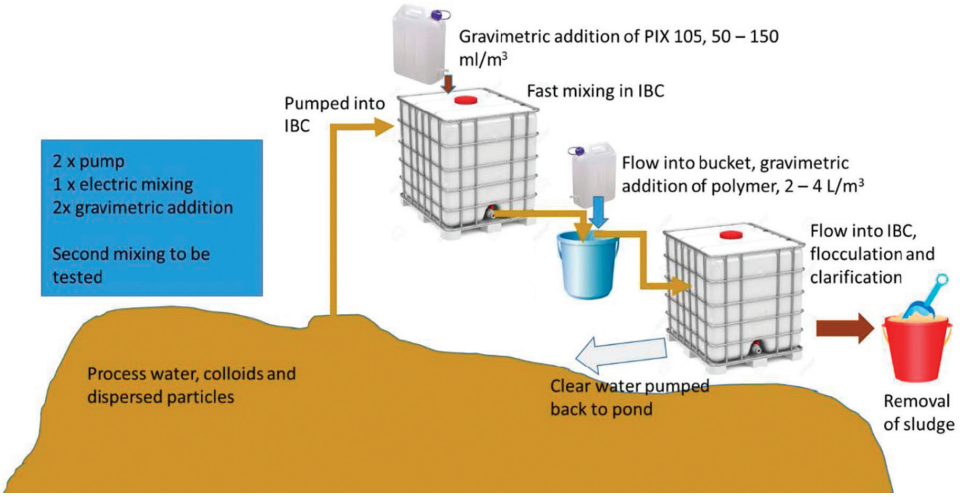

Figure 1 *Scheme for the field tests with equipment used.*

and a larger amount of coagulant (10 mL/min vs 8 mL/min) produced a thicker, heavier flock, that formed a denser sludge. Positively charged coagulant was necessary to neutralize the negatively charged silt particles. PIX, being iron-based, is environmentally more benign. Accidently release of PAC, an aluminium-based coagulant, can affect fish population.

Based on these results, the application of coagulant/flocculant with low-tech gravimetric dosage could be applied to remove colloid particles from ore processing of alluvial gold mining. The dosage of

Figure 2 *Ongoing field tests, left IBC on damn of circulation pond. (photo: E. Takaluoma).*

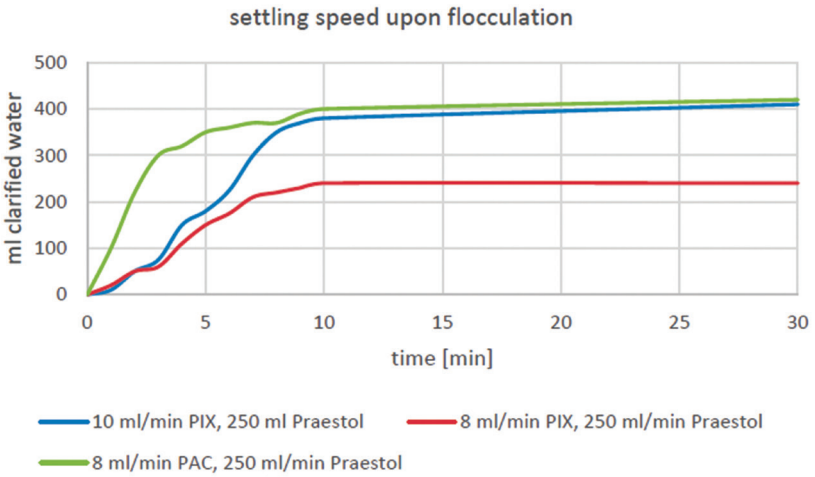

Figure 3 *Settling speed upon flocculation, for three different coagulant/flocculant doses.*

coagulant can be adjusted with respect to environmental discharge permits. A combination of coagulant and flocculant resulted into a thick flock that rapidly settles to the bottom of the pond. After five minutes, the clear water on the surface can be discharged into a receiving water body. This makes the method of coagulation/flocculation a valuable tool for goldminers in the case of sudden failure of pump, flooding, or increase in rain fall. If the goal is purely to utilize the method in the case of emergency, overdosing is not considered a problem.

During the tests, the dosage of coagulant and flocculant was varied. A higher dosage resulted into better flock formation. However, this, in turn, increased the costs. Therefore, the dosage, cost, and desired result before purging in the environment will need to be weighted carefully against each other. It is possible that a smaller amount of coagulant can be sufficient, and the reached flocculation will be within the amounts specified in environmental permits, which varies by claim and area. This will also depend on the flow of the receiving water.

When questioned, Finnish gold miners responded positively towards the water purification methods. There was little concern about the additional workload of mixing and preparing the flocculant/coagulant solution. However, concern over prices was expressed, citing that the use of coagulants should not exceed the pumping costs of the leaching field.

Both PIX and PAC were used as coagulants. Using PIX might be easier to dose, as it does not increase the aluminium concentration, as with PAC. However, liquid PIX is ferrisulfate in sulfuric acid and the pH of the solution is below pH 0. Handling of highly acidic liquids requires trained personal. With PIX, the clarified water had a pH of 4. When PAC was used, the pH of the clarified water remained circumneutral.

In an upcoming project, the formation of flock in pond system will need to be investigated. It can be expected that the wall and bottom structures of the pond, as well as the changes of laminar and turbulent flow, has an effect on the flock formation. The future project will explore this further. It will also be necessary to test the pumpability of formed sludge. In the project, the use of 3D printed mixing tube will be investigated, as an alternative to fast mixing that further eliminates the use of electricity in the concept.

Conclusions

Goldmining in Finnish Lapland can serve as an example for best practices in ASM. The study demonstrated the facile and low-tech method of silt removal from ASM, without the need of slow mixing for flock formation. Coagulation/flocculation can settle the colloids and dispersed particles in circulation and in settling ponds within minutes and remove the need to purge silted water into the receiving body. These results can readily be applied in training for miners and be employed to decrease the environmental impact of ASM. The method can prevent silting of water bodies, which may potentially be drinking water bodies, and therefore greatly increase the social acceptance of mining activities.

References

Weldegiorgis F, Fritz M, McQuilken J,Collins N (2018) Global Trends in Artisanal and Small-Scale Mining (ASM): A Review of Key Numbers and Issues, igfmining.

Singo P, Seguin K (2018) Best Practices: Formalization and Due Diligence in Artisanal and Small-Scale Mining, ISBN: 978-1-897320-39-6.

Kerr, S J (1995) Silt, turbidity and suspended sediments in the aquatic environment: an annotated bibliography and literature review. Ontario Ministry of Natural Resources, Southern Region Science & Technology Transfer Unit Technical Report TR-008.

Effects of pH on arsenic mineralogy and stability in Poldice Valley, Cornwall, United Kingdom

Julian Tang[1], Eric Oelkers[2], Julien Declercq[1], Rob Bowell[1]

[1]*SRK Consulting, 17 Churchill Way, Cardiff, CF10 2HH, UK, jtang@srk.co.uk, jdeclercq@srk.co.uk, rbowell@srk.co.uk*

[2]*University College London, Gower Street, London, WC1E 6BT, UK, e.oelkers@ucl.ac.uk*

Abstract

Many abandoned mine sites in Cornwall, UK, are characterised by elevated concentrations of arsenic (As), which can cause contamination of surrounding soil and water resources. These sites have important historical value that requires access to be maintained, despite exposure of humans to toxins that may lead to health issues including hyperpigmentation keratosis (including skin cancers) and liver fibrosis. The abandoned mine tailings at Wheal Maid has been assessed for As-bearing mineralogy and stability taking into account the public footpaths made by the local council to areas of potential contamination.

Keywords: Arsenic, Mining, Weathering, Scorodite, Thermodynamic, Mineralogy, Environmental Contamination, Oxygenated

Introduction

Human exposure to high arsenic (As) levels can lead to numerous health issues. These include hyperpigmentation keratosis (including skin cancers) and liver fibrosis (ATSDR, 2013). Arsenic may form toxic dust that can rest on garden soils and footpaths that young children may ingest via hand to mouth (Bowell *et al*., 2013). Arsenic is a known toxin (Pascoe *et al*., 1994) and numerous studies have demonstrated higher As uptake in children (Eligali, 1994). However, a preliminary study of inorganic As and methylated metabolites in urine from adults and children in Cornish mining villages showed elevated urinary As contents (Farmer & Johnson, 1990). High As concentrations are commonly found associated with the desired ore products during the mining process and are typically discarded with the rest of the mine wastes (Craw & Bowell, 2014).

Mining for copper and tin in Cornwall began at least by the early eighteenth century (Hunt & Howard, 1994). Towards the end of the nineteenth century, Cornwall dominated copper, tin and arsenic production globally (Buckley, 2005). Prolonged periods of mining without environmental regulations have had a significant impact to the surroundings (Bowell *et al*., 2013). One such mine, the Wheal Maid is located in the Poldice Valley in central Cornwall (Figure 1). This site is of particular interest due to its popularity for outdoor recreation, the lack in reclamation of mine dumps, and its prominence in the production of As. Mine waste and derelict As kilns are still present at the site (Camm *et al*., 2004). Runoff from the workings flow through tributaries approximately 2 km before entering the Carnon River to the southeast. The objective this study are to: (1) identify all potentially harmful contaminants and As-bearing minerals present at the site, (2) assess and evaluate the most common As-bearing minerals in an oxygenated mine tailings dam, (3) collect and analyse water, rock and soil samples from Wheal Maid and along the Carnon River, and (4) determine the minerals controlling As mobility and the effects of varying pH conditions. Thermodynamic and crystallographic data collected in (2), combined into an internally consistent thermodynamic database, can help to predict and explain the occurrence and assemblages of arsenates and associated minerals.

A conceptual model for the Wheal Maid mine tailings facility (Figure 2) was developed from observation of the general topography and the following assumptions are made through discussions during work onsite. These assumptions are made purely in a look-see basis so may not be representative for the study area. The assumptions are as follow:

1. Water falls onto the tailings facility from rainfall
2. Water from rainfall enters the Carnon River through surface runoff and infiltration of the tailings facility
3. Water flows downstream moving from tailings pond 1 to tailings pond 3 and enters the Carnon River through a controlled water barrier
4. Water in the tailings pond infiltrates only a minor amount of water into the deep "Great Adit" groundwater system and mixes with the tailings water leaving the facility at the controlled water barrier
5. Surface runoff is neglected in the model as it is not quantified, and the amount is deemed negligible compared to the flows from the tailings ponds and the "Great Adit" system.

Methods

World Health Organisation Guideline

Water samples representative of the mine tailings and the Carnon River were collected, and characterised following guidelines (Table 1) where available of the World Health Organization's Guidelines for Drinking-water Quality (WHO, 2011).

Field Methods

Water sampling

Water samples were collected in June 2018 at each of the three tailings ponds and 400 m along the Carnon River (Figure 1). Sampling teflon vials were prepared in the lab using ultra-pure deionised and distilled water (to 18.2 MΩ cm resistivity at +25 °C) produced by the VWR Ultrapure water system, P series, to prevent contamination from bacterial growth. Each vial was filled with ultra-pure water that was removed before sampling. The VWR water system is built following Standard Operating Procedures, and a Certificate of Calibration for the temperature and resistivity meters built into the system (VWR, 2019) At each sampling location, samples were taken using a Whatman syringe filter and two drops of 2% aqueous nitric acid (HNO^3) were added (dwi, 2005). The location the pH was measured on site while collecting each sample using a Mettler Toledo 5-easy plus pH probe. The pH probe is calibrated on-site using three buffer solutions, pH 4.0, pH 7.0 and pH 9.21. Detection limit is not applicable. This process was replicated at least three times at each site.

Rock/Soil sampling

Rocks and soils were samples June 2018 at five sites from high to low topography to determine the leachability of material from these solids. The top 10 to 20 cm of the surface material was removed prior to collecting these samples. This method was adopted to avoid solids may have been affected by surface chemical weathering. Samples were then retrieved and stored in separate labelled transparent sample bags (dimensions: 76 × 83 mm). Sampled sediments greater than 6 cm is size were considered as rocks, and those less than 0.5 cm as soil.

Sample Analysis

Water sample analysis

The collected water samples were stored in a refrigerator prior to analysis. Each was analysed by inductively coupled plasma optical emission spectroscopy (ICP-OES) and the inductively coupled plasma mass spectroscopy (ICP-MS) for the major and minor elements respectively. The analysis was completed on a Varian 720 ICP-AES (axial configuration) equipped with autosampler and a Bruker M90 ICP-MS equipped with autosampler. In each analysis, 5 known and 5 blank samples were analysed simultaneously. The detection limits of all elements are all below 0.0001 mg/L which have been removed from the later calculations. ICP-analyses were run together with certified reference material TMDA-70 (fortified lake water) during each analysis session. The known and blank samples with the TMDA-70 were used to calculate the uncertainties of each analysis and check accuracy and reproducibility. The uncertainty of all elemental analyses were found to be less than +/- 10% when evaluated with TMDA-70.

X-ray diffraction

Samples for diffraction analysis were prepared by side-filling the powder, against a ground-glass surface, into a 1.5 mm wide sample holder and consolidating it by gentle tapping. X-ray powder diffraction data were then collected with Cobalt (Co) Potassium (K) alpha (α) radiation, using a PANalytical X'Pert Pro diffractometer, with Bragg-Brentano para-focusing reflection geometry. The X-ray peaks produced are evaluated using the database provided by the PANalytical HighScore Plus software with the ICDD (International Centre for Diffraction Data) database. The minimum tip width for the searched peaks is 0.01, which corresponded to a relative error of 1%, the counting statistical error.

Geochemical Calculations

Thermodynamic calculations in this study were computed with PHREEQC (version 3.5.0.14000) together with a modified version of the WATEQ4F.v4 database (Parkhurst & Appelo, 2013). This database was selected for this study because it includes the all of elements considered for this study of water quality in a mine tailings environment. The solubility constant of scorodite in the database was changed from $10^{-20.25}$ to $10^{-24.5}$. This scorodite solubility constant value is different from that published in literature (Zhu *et al*., 2019), as pure scorodite does not occur in the natural environment. Thus, the modified value for the scorodite + goethite system is more fitting for an acid mine drainage environment.

Additions to PHREEQC database

Nordstrom *et al*., 2014 described the PHREEQC thermodynamic database as an over-determined network in a theoretical sense, but also contains large uncertainties. This inconsistency led to the idea of evaluating previous literature on how solubility measurements were made, in return to limit the use of solubility products measured where large impurities were present. Wagman *et al*., 1982 pointed out that typically two methods have been used to evaluate thermodynamic data, the sequential method, and the simultaneous fit method. In this study, a mixture of both techniques have been used and the solubility products added to the PHREEQC input is shown in Table 2.

Results

Mineralogy of the Mine Site

Mineralogical samples collected from the Wheal Maid were found to be similar in composition confirming a similar style of mineralisation. Whole-sample XRD demonstrated that the predominant mineralogy for sand, silt and clay fractions are quartz, muscovite and chlorite. Cassiterite, dickite, lizardite ($Mg_3(Si_2O_5)(OH)_4$), and tourmaline are also present. These occurrences depend on local geology and weathering of nearby outcrops. Of the samples taken, the products identified by XRD include jarosite), goethite and pyrite (FeS_2). Minor rutile (TiO_2), arsenopyrite (FeAsS), arsenian pyrite (Fe(As,S) S), löllingite ($FeAs_2$), tennantite-tetrahedrite ($Cu_{10}(Zn,Ag,Fe)_2(As,Sb)_4S_{13}$) have previously been reported at these sites, but were not observed in this study (Bowell, *et al*., 2013).

Bulk Geochemistry

Hydrogeochemistry in the vicinity of the mine site

To assess background levels of As in surface water, three tailings ponds and five river water samples were collected. The concentrations are compared with the WHO drinking water guideline values. Figure 3 delineates the As chemistry in each of the monitoring points. Other metal concentrations are presented in the appendix. The accumulation of metals in the tailings ponds results in highly acidic waters (pH 2-3) with As concentrations 2 orders of magnitude above the WHO drinking water guideline value (0.01 mg/L). Other elements with concentrations exceeding the WHO drinking water guideline values are Cd, Cr, Cu, Ni and Pb.

In the Carnon River, arsenic concentrations were 1 – 2 orders of magnitude above the 0.01 mg/L WHO water quality limits despite the pH being circum-neutral (pH 6-7). The pH of the waters was made near to neutral pH by the dilution of tailings pond waters with groundwater. Several elements including Cr, Cu and Ni had concentrations below the WHO limits in the river water, but Cd and

Pb concentrations remained to be above the drinking water guidelines.

Discussion

Mass balance calculation

Taking account of the conceptual model, water flows downstream from the tailings pond and enters the Carnon River through a controlled water barrier. The flow rate of the waters from the tailings pond and the underground source were not measure, hence, the mixing ratio of these waters was estimated through onsite observation of the quantity of water flowing from each source entering the river. The estimated mixing ratio of water entering the Carnon River comprises of 15% tailings pond water and 85% subsurface underground adit-water. This mixing ratio is understood to be representative as the majority of water entering the main river was observed to be from the underground source.

Geochemical Calculations

The water chemistry at the monitoring points delineated in the previous section was used as inputs to the PHREEQC geochemical model and the saturation index (SI) of minerals was calculated. The SI of a mineral indicates the "tendency" of the water to want to precipitate the mineral, if the SI is at or above 0 (the solubility equilibrium, it indicates that the water wants to precipitate the mineral. The SI of the mine runoff waters before and after dilution with respect to scorodite is shown in Figure 4A which indicates that the SI ranges from -2.75 to +2.5. Scorodite is supersaturated in the second tailings pond water and in the marshland of the river which suggests that precipitation of the mineral is likely and can be a factor controlling As mobility in the waters.

Using the provided mixing ratios described, the water chemistry at the monitoring points were mass balanced and used as inputs to the PHREEQC geochemical model to produce the SI of scorodite downstream of the mixing zone (Figure 4B). The four orange bars represent the four monitoring points where predictions are made. Three out of four predictions are noticeably similar to the site measurement (blue bars). The constrains placed on the water calculations involved changing pH (+/- 2 from pH 7) shown in Figure 4C. The bar charts suggest that changing pH alters the saturation index of scorodite significantly in the waters. With an increase of pH units (more alkaline), the water becomes heavily under-saturated in terms of the As-bearing mineral. However, in a more acidic environment (lower pH) the solubility of As is little affected.

The result of the mass balance indicate that an increase of pH leads to the waters becoming increasingly undersaturated with respect to scorodite. The SI of other As minerals have been studied but all minerals are shown to be heavily undersaturated in the waters, hence, scorodite is the most likely mineral to be controlling As concentration in the water. Thus, it may be expected that increasing the pH could lead to the enhanced concentration and mobility of As in the water. Due to the decades of infiltration of mine tailing water into the groundwater system, the dilution mechanism used previously does not prove to be effective as the water chemistry from the groundwater outlet is very similar to those found in pond C of the mine tailings.

Conclusion

Wheal Maid mine tailings is integrated along a wider mining network known as 'the Great County Adit' that contains elevated concentrations of numerous potentially toxic metal(loid)s. The source of these metal(loid)s is related to past mine waste and disturbance of clay-rich country rocks leading to faster weathering rates from placing waste products in mine tailings sites. Arsenic concentrations in waters along the tailings dam and Carnon River range up to 3.6 mg/L which is more than 2 orders of magnitude above the WHO guideline value of 0.01 mg/L for drinking water.

This study indicated that the soil and water of mine tailings at Wheal Maid has the potential of releasing As and precipitating As-bearing minerals. The sampling programme captures information for the site during a relatively the summer period but could be improved by monthly sampling to monitor seasonal fluctuations in one year. The SI of scorodite was near to equilibrium indicating precipitation of the mineral is

likely, however, it doesn't conclude that it is the sole mineral controlling As concentrations. This study highlights the need to better understand As-bearing minerals and slight environmental changes such as increase alkalinity in waters may cause serious consequences in an industrial setting.

Figures

Figure 1 *Map of St Day, Cornwall, South-west England and the location of Wheal Maid.*

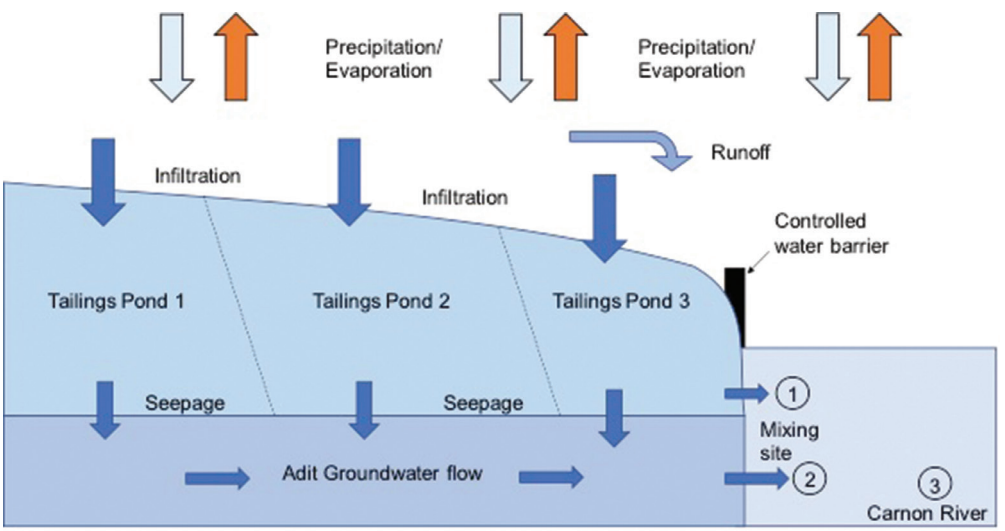

Figure 2 *Conceptual model for the flow of water through the tailings to the Carnon River.*

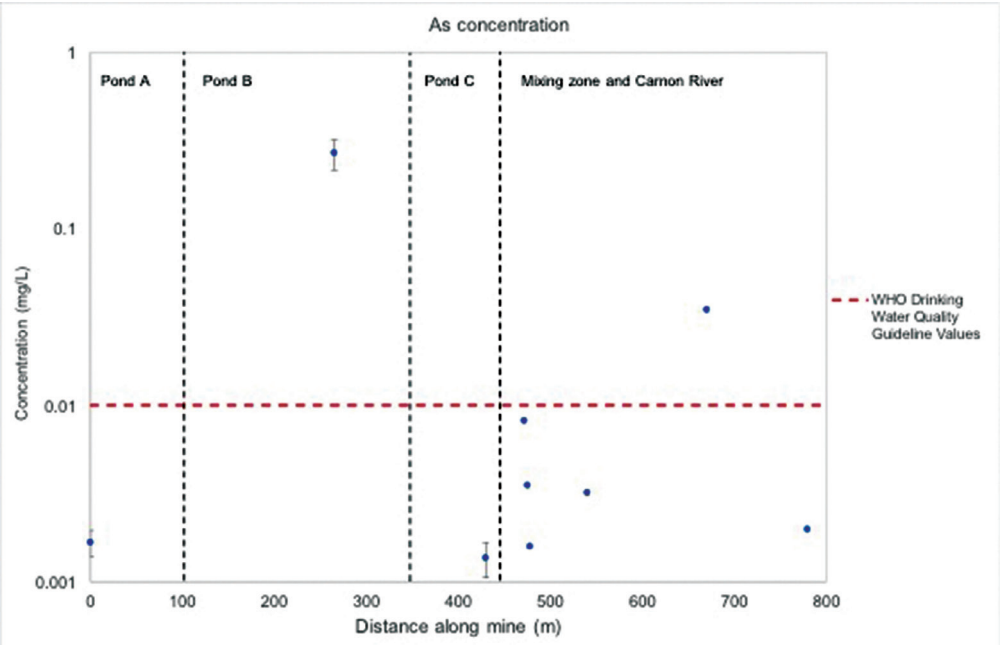

Figure 3 *Arsenic concentration in the water compared to WHO guidelines (WHO, 2011). The location names are as follow: (A) Tailings Pond A; (B) Tailings Pond B; (C) Tailings Pond C; (D) Carnon River.*

Table 1 *WHO Drinking Water Quality Guideline Values (WHO, 2011).*

Element	WHO Drinking Water Quality Guideline Values (mg/L)
As	0.01
B	2.4
Ba	0.7
Cd	0.003
Cr	0.05
Cu	2
Ni	0.07
Pb	0.01

Table 2 *Solubility data updates made to PHREEQC database.*

Additional Phases	Log K	Delta h (kJ/mol)	Reference papers
Arseniosiderite	-21.6	-51.5	Paktunc et al., 2015
Pushcharovskite	-17.2	0	Plumhoff et al., 2020
Geminite	-15.9	0	Plumhoff et al., 2020
Liroconite	-4.92	0	Plumhoff et al., 2020
Zýkaite	-77	0	Majzlan et al., 2015
Haidingerite	-4.79	0	Bothe and Brown (1999b)
Scorodite	-24.5	0	Zhu, et al., 2019

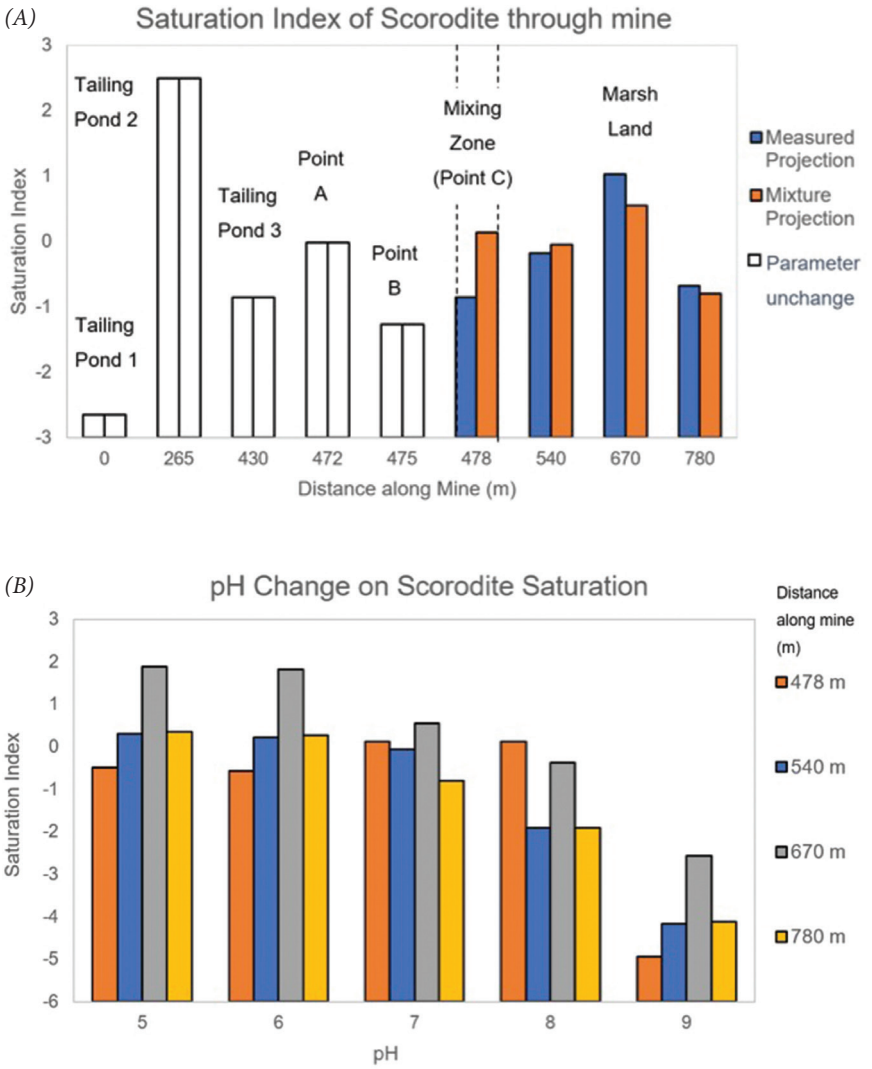

Figure 4 *Saturation index of Scorodite along mine.*
(A) Comparison of measured (blue) and mass balanced (orange).
(B) SI change varying pH +/- 2 from natural conditions of mass balanced values.

References

ATSDR. (2013). What are the Physiologic Effects of Aresnic Exposure? Agency for Toxic Substances and Disease Research.

Bowell, R. J., Rees, S., Barnes, A., Prestia, A., Warrender, R., & Dey, M. (2013). Geochemical assessment of aresnic toxicity in mine site along the proposed Mineral Tramway Project, Camborne, Cornwall. Geochemistry, Exploration, Environment, Analysis, 145-157.

Buckley. (2005). The Story of Mining in Cornwall. Truro, UK: Cornwall Editions Limited.

Camm, G. S., Glass, H. J., Bryce, D. W., & Butcher, A. R. (2004). Characterization of a mining related arsenic contaminated site, Cornwall, UK. Journal of Geochemical Exploration, 1-15.

Craw, D., & Bowell, J. R. (2014). The characterization of Arsenic in Mine Waste. Reviews in Mineralogy and Geochemistry, 79(1), 473-505.

dwi. (2005). Sample preservation and preparation for metal analysis of drinking water. Drinking Water Inspectorate.

Eligali, L. (1994). Evaluation of exposure of young children to arsenic contamination in South West England. University of London.

Farmer, J. G., & Johnson, L. R. (1990). Assessment of occupational exposure to inorganic arsenic based on urinary concentrations and speciation of arsenic. British Journal of Industrial Medicine, 342-348.

Fendolf, S., Eick, M. J., Grossi, P., & Sparks, D. L. (1997). Arsenate and chromate retention mechanisms on goethite. 1. Surface structure. Environ. Sci. Technol, 315-320.

Ford, R. G. (2002). Rates of hydrous ferric oxide crystallization and the influence on coprecipitated arsenate. Environ. Sci. Technol, 2459-2463.

Hunt, L. E., & Howard, A. G. (1994). Arsenic speciation and distribution in the Carnon estuary following the acute discharge of contaminated water from a disused mine. Marine Poluttion Bulletin, 28(1), 33-38.

Li, W., Harrington, R., Tang, Y., Kubicki, J. D., Aryanpour, M., Reeder, R. J., . . . Phillips, B. L. (2011). Differential pair distribution function study of the structure of arsenate adsorbed on nanocrystalline gamma-Alumina. Environ. Sci. Technol, 9687-9692.

Parkhurst, D. L., & Appelo, C. A. (2013). Description of Input and Examples for PHREEQC Version 3 - A Computer Program for Speciation, Batch-Reaction, One-Dimensional Transport, and Inverse Geochemical Calculations. In D. L. Parkhurst, & C. A. Appelo, Groundwater Book 6 (p. Chapter 43 of Section A).

Pascoe, G. A., Blanchet, R. J., & Linder, G. (1994). Bioavailability of metals and arsenic to small mammals at a mining site-contaminated wetland. Journal of Archaeology and Environmental Contamination and Toxiology, 44-50.

VWR. (2019). Instruction Manual. Avantor.

WHO. (2011). Guidelines for drinking-water quality, fourth edition. World Health Organisation.

Zhu, X., Nordstrom, K. D., McCleskey, R. B., Wang, R., Lu, X., Li, S., & Teng, H. H. (2019). On the thermodynamics and kinetics of scorodite dissolution. Geochimica et Cosmochimica, 468-477.

Investigating the Sulfidation and High-Temperature (100 °C – 200 °C) Dissolution of As_2O_3 Stored at the Giant Mine, NWT, Canada

Evelyn Tennant, Tom Al

University of Ottawa, 25 Templeton St, Ottawa ON K1N 7N9, Canada, etenn058@uottawa.ca

Abstract

The former Giant Mine, NWT, generated 237 000 tonnes of As_2O_3-rich dust as a by-product of gold mining. As_2O_3 is a relatively soluble form of As and is currently stored beneath the mine, posing a threat of contamination to the adjacent Great Slave Lake. This research investigates the potential for permanent remediation of the Giant Mine As_2O_3 through sulfidation. This research will contribute to the understanding of As_2O_3 solubility above 100 °C, and it explores the potential for applying high temperature-pressure dissolution as a preliminary step toward sulfidation of the As_2O_3 -rich mine waste.

Keywords: Arsenic, As_2O_3, Contamination, Giant Mine, Sulfidation

Introduction

The Giant Mine is located five kilometers north of Yellowknife, NWT, directly adjacent to Great Slave Lake and near the indigenous communities of Ndilo and Dettah. It produced over seven million troy ounces of gold during its years of operation (1948 – 2004) (Jamieson 2014). The gold-bearing arsenopyrite- and pyrite- rich ore required a roasting step prior to gold recovery using cyanidation. During roasting, arsenic-rich gases were condensed and the arsenic was captured as arsenic trioxide-rich (As_2O_3) dust, 237 000 tonnes of which were stored in mined-out stopes and purpose-built chambers in the mine. If the mine is allowed to flood, the solubility of the waste (≈11 g/L at 10 °C; Dutrizac *et al*. 2000) presents a risk of arsenic contamination to Great Slave Lake. The As_2O_3-rich dust is one of Canada's largest environmental liabilities (Jamieson 2014).

This project explores sulfidation as a path to permanent remediation. The calculated arsenic concentration in anaerobic groundwater at equilibrium with $As_2S_{3(am)}$ (PHREEQC, WATEQ4f database; Parkhurst and Appelo 2013) is on the order of 0.001 g As/L, a factor of ≈11 000 lower than equilibrium with respect to As_2O_3. If the As_2O_3 dust can be converted to As_2S_3, it could be injected deep into the mine, allowing for reflooding without risk of contamination to Great Slave Lake. Sulfidation is being explored with two approaches; the first involves a heterogeneous reaction system whereby sulfide, in the form of H_2S, is added to a slurry of As_2O_3. The second is a two-step method whereby As_2O_3 is first dissolved prior to sulfidation by addition of H_2S to a homogeneous aqueous solution. The rate for reaction of aqueous As(III) with H_2S, forming $As_2S_{3(am)}$ is known to be rapid, but the dissolution rate and the solubility of As_2O_3 are not well known above 100 °C, particularly for the impure As_2O_3 from the Giant Mine. Experiments were designed to define the solubility and dissolution rate for reagent-grade As_2O_3 at temperatures between 100 °C and 200 °C. The results represent a guide for subsequent experiments with the aim of determining the efficiency of aqueous extraction of As_2O_3 from the impure Giant Mine dust at temperatures between 100 °C and 200 °C.

Methods

Heterogeneous Process

Sulfidation of As_2O_3 was first investigated by introducing sulfide (H_2S) to an aqueous slurry of reagent-grade As_2O_3. The experimental setup is displayed in Figure 1. Powdered As_2O_3 was added to 250 mL Pyrex® reaction vessels which were then sealed and purged with N_2. De-aerated distilled water,

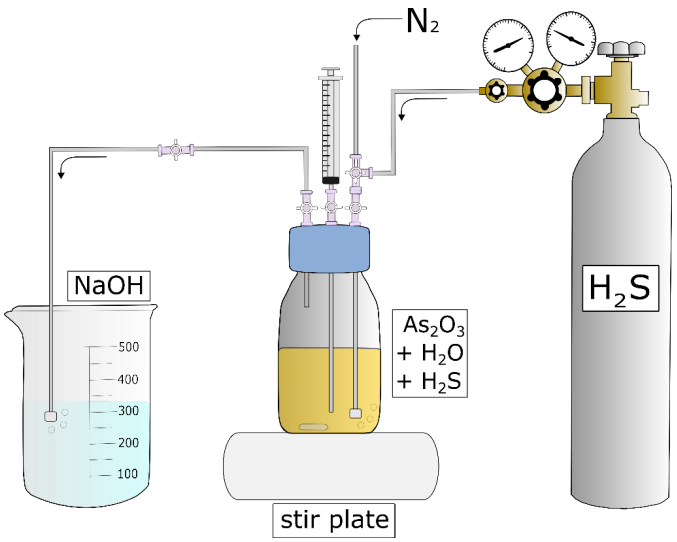

Figure 1 *Experimental setup for sulfidation of an As_2O_3 slurry with H_2S (g).*

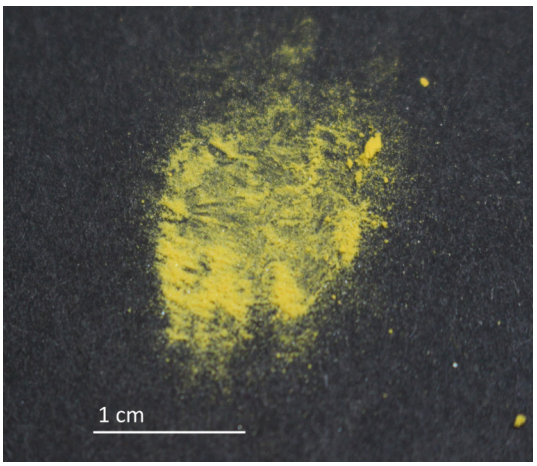

Figure 2 *Reaction product from reaction of an As_2O_3 slurry with H_2S (g).*

acidified to a pH of 4 with HCl, was added to the vessels, as As_2S_3 formation is favourable at a pH of 4 (Eary 1992). H_2S gas was then introduced through a gas dispersion tube for two hours. The solids were then separated by filtration (0.45 µm), dried, and analyzed with X-Ray Diffraction (XRD), Scanning Electron Microscopy (SEM), and Elemental Analysis (EA).

Two-Step Process

The dissolution of the As_2O_3 was initially explored using reagent-grade As_2O_3 to determine the solubility and dissolution rate at elevated temperatures (140 °C, 160 °C, 180 °C, 200 °C) using a CEM Discover® SP microwave. A camera installed in the microwave allowed visual determination of the time to complete dissolution (dissolution rate) for incremental masses of As_2O_3. Similarly, the camera allowed visual determination of the maximum soluble mass (solubility) at any given temperature.

The chemical composition of the Giant Mine dust (archived sample B233-P9) was determined from 10 replicates (each 30 mg) to account for heterogeneity. The replicates were dissolved in concentrated

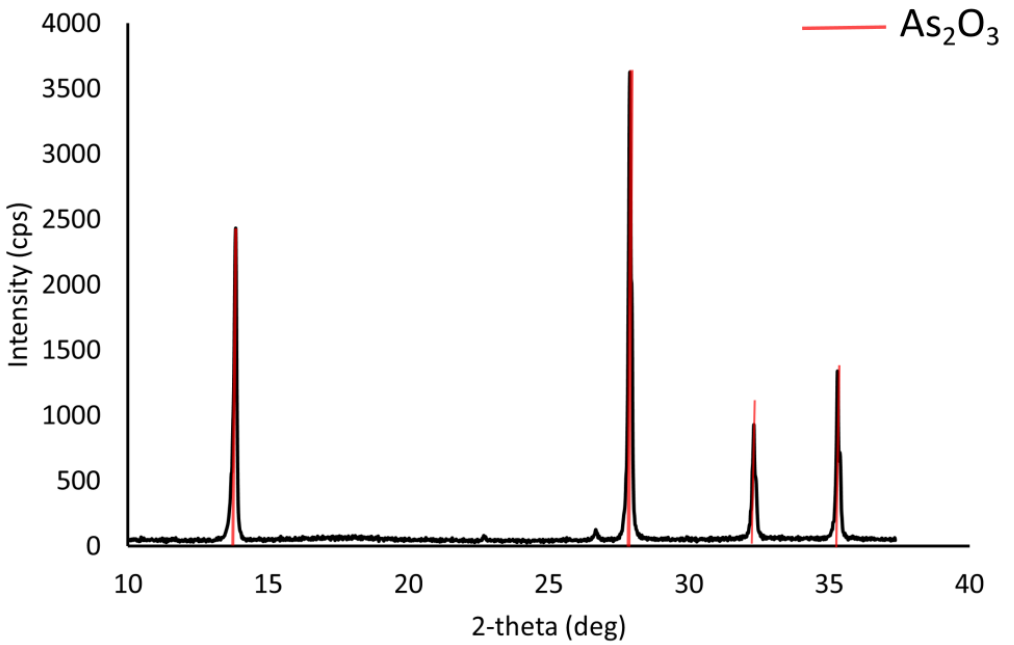

Figure 3 *XRD pattern for the reaction product from heterogeneous H_2S experiments. Minor peaks observed at 22.7 and 26.7 degrees are unidentified, and not associated with As_2S_3.*

aqua regia (90 °C for 24 hours) in a closed Savillex PTFE vial followed by analysis with Inductively Coupled Plasma Atomic Emission Spectroscopy (ICP-OES). The As yield from aqueous extractions of the Giant Mine dust was then tested using 250 mg of dust in 4 mL of distilled water heated to temperatures of 140 °C, 160 °C, 180 °C and 200 °C over duration of 10, 20, and 30 min in a CEM Discover® SP microwave. To allow for calculation of the yield from the aqueous extractions, a fraction of the residual solids was digested as described previously and analyzed with ICP-OES. Another fraction of the residual solids was embedded in epoxy for SEM analysis.

Results

Heterogeneous Process

As the reaction proceeded, the initially white As_2O_3 powder was transformed to a bright yellow colour (fig. 2), suggesting the formation of As_2O_3, however, subsequent XRD analyses displayed peaks of As_2O_3 with no indication of As_2O_3 (fig. 3). Any newly formed As_2O_3 was expected to be amorphous, so the sample was further investigated by SEM/EDS analysis and only traces of sulfur were detected. The EA results indicated that the yellow powder contains approximately 1.1 wt% sulfur, whereas pure As_2S_3 contains 39 wt% sulfur.

Two-Step Process

The experiments are still underway, but the solubility measurement for reagent-grade As_2O_3 at 140 °C is plotted in figure 4a along with the solubility curve below 100 °C from Dutrizac *et al.* (2000). Data for the dissolution rate of reagent-grade As_2O_3 at 140 °C are plotted in figure 4b.

Data from the geochemical characterization of the Giant Mine dust are displayed in Table 1, indicating an As concentration of 40.4 ± 7.4 wt%. Heating the dust in water through a range of temperatures (140 to 200 °C) and over durations of 10 to 30 min yielded residues that amounted to 40.7 ± 1.5 wt% of the original mass. The SEM analyses (fig. 5) for residues obtained at 140 °C indicate the presence of As_2O_3 grains that are surrounded by mixed As, Si, Fe, and Sb phases. Residues

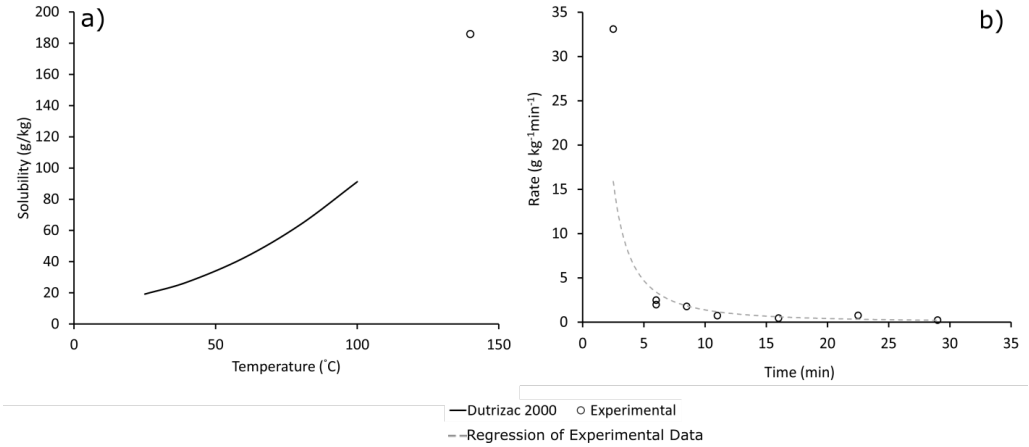

Figure 4 *a) Solubility of reagent-grade As_2O_3 up to 100 °C, determined by Dutrizac et al. (2000), and solubility determined in this study at 140 °C and 50 PSI. b) The dissolution rate of reagent-grade As_2O_3 at 140 °C and 50 PSI over time.*

obtained at 160 °C, 180 °C, and 200 °C were similar to those obtained at 140 °C, but with fewer discrete As_2O_3 grains.

Discussion

Heterogeneous Process

The transformation of the white As_2O_3 powder to bright yellow during sulfidation suggests the formation of As_2O_3. However, the SEM and EA analyses indicate that there is very little sulfur present in the powder, suggesting an incomplete reaction. It was concluded that the reaction did not go to completion because of surface passivation by a thin layer of As_2O_3, creating a limitation on the reaction rate by diffusion through the As_2O_3 layer.

Two-Step Process

The discovery that the heterogeneous reaction approach causes passivation of the As_2O_3 surface necessitated a revised approach with an initial dissolution step prior to precipitation of $As_2S_{3(am)}$ by reaction of the aqueous solution with H_2S. The experiments designed to measure the solubility of reagent-grade As_2O_3 are intended to constrain the dissolution procedure. They are not yet complete, but results to date appear to align with the solubility curve defined by Dutrizac *et al.* (2000) between 25 and 100 °C (fig. 4a). Figure 4b displays the calculated dissolution rates of As_2O_3 at 140 °C between 0 and 30 min, for which a power regression line defines the overall dissolution rate with the expression

$$R=80.21x^{-1.764} \quad (1)$$

where R is the dissolution rate (g $kg^{-1}min^{-1}$) and x is time (min).

Table 1 *B233-P9 Concentrations determined from ten replicates with ICP-OES.*

Element	Mean Concentration	RSD
	mg/kg	%
As (%)	40.4	7.4
Sb	14430	9.8
Fe	90160	5.8
Al	6507	6.0
Ca	9441	8.3
Mg	5464	6.2
K	1151	6.6
Zn	1658	4.9
Na	597	597
Pb	3946	6.0
Cu	641	6.0

The Giant Mine dust that was used for the aqueous extraction experiments (B233-P9) was generated in the early years of the Giant

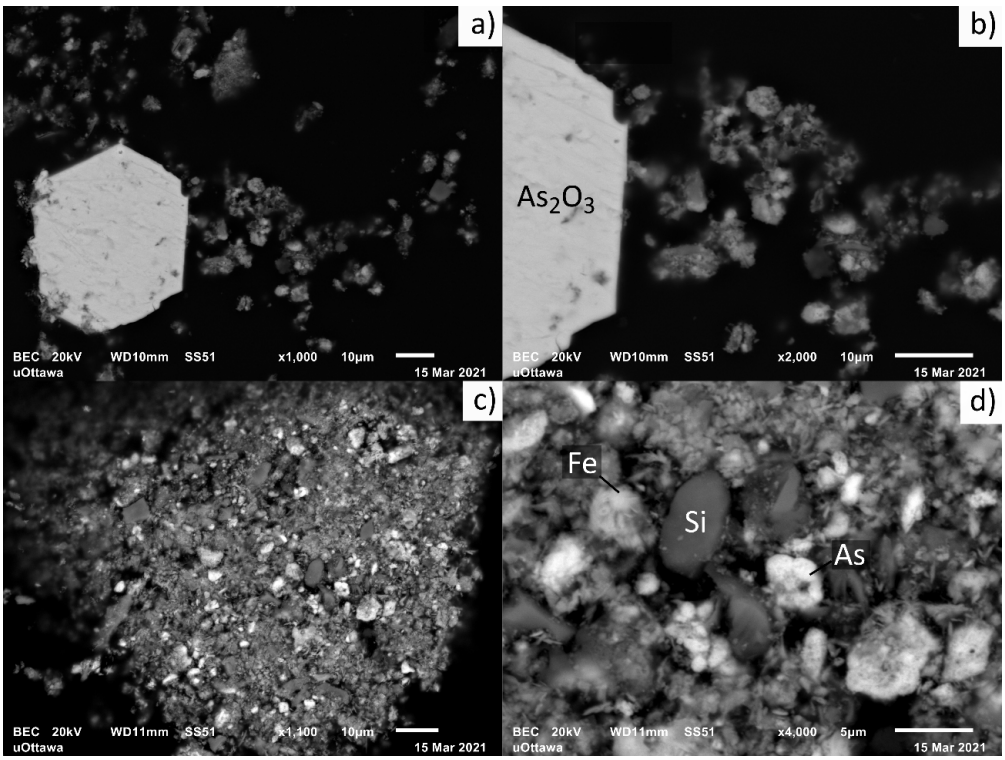

Figure 5 *Sample B233-P9. 1a) Residue remaining after heating to 140 °C and 50 PSI for 30 min. 1b) Higher magnification image of 1a). 2a) Residue remaining after heating to 200 °C and 50 PSI for 30 min. 2b) Higher magnification image of 2a). Labels indicate dominant element, but each grain is a mixed phase consisting of As, Sb, Fe, and Si.*

Mine's operation (1952–1956) when the roasting operation was relatively inefficient. This sample has low As and high Sb content compared to the material generated in the later years of the Mine operation. The chemical composition of the dust determined in this study (Table 1) is consistent with previous analyses by SGS Lakefield Research Ltd (2004). During the aqueous extraction experiments, 59.3% ± 1.5% of the sample mass dissolved, independent of temperature and extraction duration. This suggests that the Giant Mine dust contains a fraction, approximately 60 wt%, which is relatively soluble, with the remainder being recalcitrant. The recalcitrant nature likely relates to the elevated Sb content as Dutrizac *et al.* (2000) noted that the Sb impurity in the As_2O_3 causes a reduction in the solubility. SEM analyses reveal that Sb is ubiquitous in the residual grains. Further research is planned to investigate the characteristics of the residue.

Conclusion

Sulfidation of As_2O_3 has been investigated in i) a heterogeneous reaction system, and ii) a two-step approach with dissolution of the As_2O_3 followed by sulfidation. The research conducted to date leads to the following conclusions.

- In heterogeneous experiments, where $As_2O_{3(s)}$ is reacted with H_2S in aqueous solution, the reaction does not go to completion because of surface passivation by a thin layer of As_2S_3.
- Experiments designed to constrain the dissolution conditions for the As_2O_3 have extended the upper limit of temperature for the solubility curve from 100 °C to 140 °C and have provided data on the dissolution rate at 140 °C (eq 1).

- Aqueous extraction experiments with the Giant Mine dust at temperatures between 100 and 200 °C indicate that the material contains a fraction that is amenable to aqueous extraction (approximately 60 wt%) with the remainder being relatively recalcitrant.
- The recalcitrant fraction contains Sb-rich As_2O_3, and additional work is required to explore methods to stabilize this residue.

References

Eary LE (1992) The solubility of amorphous As_2S_3 from 25 to 90 °C. Geochimica et Cosmochimica Acta 56: 2267-2280

Dutrizac JE, Riveros PA, Chen TT, Dubreuil A (2000) Recovery and purification of arsenic oxide – Giant Mine. Report to Department of Indian Affairs and Northern Development (DIAND) and Royal Oak Mines Inc. (unpublished)

Jamieson HE (2014) The legacy of arsenic contamination from mining and processing refractory gold ore at Giant Mine, Yellowknife, Northwest Territories, Canada. Reviews in Mineralogy & Geochemistry 79: 533-551

Parkhurst DL, Appelo CAJ (2013) Description of input and examples for PHREEQC version 3—A computer program for speciation, batch-reaction, one-dimensional transport, and inverse geochemical calculations: U.S. Geological Survey Techniques and Methods, book 6, chap. A43, 497 p., available only at http://pubs.usgs.gov/tm/06/a43/

SGS Lakefield Research Ltd (2004) The characterization of various arsenic trioxide dust samples from Giant Yellowknife Mine. Report to SRK Consulting Ltd. (unpublished)

On-Site XRF Analysis of Metal Concentrations of Natural Waters

Tommi Tiihonen[1], Tuomo Nissinen[2], Joakim Riikonen[1], Pertti Sarala[3], Vesa-Pekka Lehto[1], Bruno Lemière[4]

[1]*Dept. of Applied Physics, University of Eastern Finland, FI-70210 Kuopio, Finland, joakim.riikonen@uef.fi*

[2]*AWater Oy, FI-70210, Kuopio, Finland, tuomo@3awater.com*

[3]*Geological Survey of Finland, FI-96101 Rovaniemi, Finland, pertti.sarala@gtk.fi*

[4]*BRGM, F-45060, Orléans, France, brunole45@orange.fr, ORCID 0000-0002-8907-1280*

Abstract

Real-time and on-site analysis of metals in waters is not routinely carried out for environmental monitoring. Laboratory analyses are used instead, which require sampling on-site, shipping to a laboratory and analysis making them expensive and slow. A novel analytical technique based on nanotechnology enhanced preconcentration and portable X-ray fluorescence was developed in this study. The analysis system was calibrated for Mn, Ni, Cu and Zn between concentrations of 50 µg/L and 10 mg/L and fast on-site analysis was demonstrated for two mining related sites.

Keywords: On-Site Analysis, Pxrf, Runoff, Hydrogeochemical Exploration, Compliance Analyses

Introduction

Trace element analyses of water are used at all stages of mining projects, for both commodity and environmental purposes. This includes exploration stage (hydrogeochemical exploration, Kidder *et al*. 2020), mine development and exploitation stages (Li *et al*. 2020), ore processing (Ghorbani *et al*. 2017), mine closure stage and modelling (Nordstrom *et al*. 2015; Cánovas *et al*. 2018), as well as post-closure environmental monitoring (Wheeler *et al*. 2021). The analyses are also used in environmental impact assessment and monitoring of any industrial activities or environmental projects.

While metal analyses of solid media are increasingly done on-site (Lemière & Uvarova 2020), allowing sample screening and dynamic sampling plans, most water analyses are still performed in the laboratory. This involves high costs for sample shipping and analyses, and delays for results ranging from days to months depending on site and laboratory location. Most of the time, this precludes any possibility of taking results into account for sample selection, sampling plan adaptation or site management decisions.

Economic reasons may be involved in choosing on-site techniques, by reducing laboratory costs or by increasing the number of analysed samples for a given budget. But the most important expected benefit is to improve the quality of the data set: Better investigations of the anomalies identified on site, a better representativity of samples selected for laboratory analyses, and denser data sets. Denser map grids can be obtained for exploration or impact mapping. Denser time series can be applied for process or runoff monitoring.

Field analysis techniques used for solids, especially portable X-ray fluorescence (pXRF), are not directly usable for water due to the low volumic concentration of analytes. Electrochemical water analysis techniques proved to be more sensitive (Yehia *et al*. 2019) but they require longer operations and highly skilled personnel.

A novel analytical system, Multimetal Water Analysis System (MWAS), developed by 3AWater for sensitive and robust on-site analysis of metal contents of water, without the challenges of electrochemical techniques. The technology is based on concentrating metals from a water sample in a composite filter containing thermally carbonised nanoporous silicon with bisphosphonate functionalised surface (Thapa et el. 2020).

Metals can be concentrated up to 200 times in the filter, which allows analysis with a fast and inexpensive portable X-ray fluorescence spectrometer (pXRF). Empirical calibrations for Mn, Ni, Cu and Zn were used to convert the measured pXRF intensities to the metal concentration of the original water sample.

Experimental

The MWAS system consisting of filter, filter holder, adapter, syringe pump and a pXRF is presented in Figure 1.

The metal collecting composite filters used in the analytical technique were prepared by coating a thin cellulose filter paper with a slurry. The slurry consisted of bisphosphonate functionalised thermally carbonised porous silicon (BP-TCPSi) particles, with median particle size of 15 µm and specific surface area of 230 m^2 g^{-1}, polyacrylic acid (PAA) and carboxymethyl cellulose (CMC) in aqueous solution. The weight ratio of these components in the final slurry was 80% BP-TCPSi, 10% PAA and 10% CMC. To lower the viscosity for easy pipetting of the slurry, 1.9 mL of deionised water and 1 mL of isopropyl alcohol was added per 1 g of BP-TCPSi. 130 µl of the slurry was pipetted on a circular cellulose filter paper with 15 mm diameter. The filters were first dried at RT for 45 min and then in 150 °C vacuum oven for 2 h for the PAA and CMC to form a crosslinked structure binding the BP-TCPSi particles on the filter surface. The mass of the BP-TCPSi was 20 mg per filter.

A specific holder for the filters was designed enabling easy utilization of the method in field conditions. The holder pieces were 3D printed with SLS technique from polyamide 12 and two additional O-rings were used to ensure leak free operation. Schematic design and photographs of the holder with metal collecting filter is presented in Figure 2. A compatible adapter was also designed to be used with Hitachi X-MET8000 pXRF. The adapter was attached on the light radiation shield of the X-MET8000 device, and the holder could be attached there by first removing the top piece from the holder and using the threads of the middle piece to fasten it on the adapter. The size of the holder opening was optimised for the X-ray window geometry of X-MET8000.

The MWAS system was calibrated for four metals Mn, Ni, Cu and Zn. Empirical calibrations were made with water samples prepared by spiking lake water with known amounts of metals. The metal concentrations of the calibration samples varied between 50 µg L^{-1} and 10 mg L^{-1} and the pH was adjusted to 7. 10 mL of the water sample was pumped through the metal collecting filter with flow

Figure 1 *The 3AWater Multimetal Water Analysis System (MWAS, prototype 2.1): A) Battery operated syringe pump, B) consumable filters including a 0.45 µm prefilter and the metal collecting filter inside a filter holder, C) handheld XRF spectrometer, D) adapter on the spectrometer with the filter holder inserted and E) image of the screen of the spectrometer showing results from an on-site analysis (not specific to the present pilots).*

rate of 1 mL min^{-1} and the adsorbed metals were analysed with pXRF. The initial concentrations of the water samples analysed with ICP-MS were plotted with the XRF intensities to create calibration curves optimised for natural water samples with pH close to neutral. Hitachi X-MET8000 Control software (SW version: 4.1.0.222) was utilised to create empirical calibration to X-MET8000 from the data set.

On-site experiments were performed in Finland on two mining sites during spring 2020. The sampling included five groundwater samples from Site 1 and five surface water samples from site 2. pH and electric conductivity (EC) were measured with handheld YSI Professional Plus multimeter on-site in both cases. The MWAS by 3AWater was utilised to analyse dissolved metal concentrations of the samples on-site. Following steps were performed for the MWAS analyses on-site:

1. Approximately 11 mL of water sample was taken into a 20 mL syringe.
2. Battery operated syringe pump was used to pump 10 mL of water sample from syringe through a 0.45 µm prefilter and a metal collecting filter with a 1 mL min-1 flow rate.
3. After the filtration, water was flushed out from the holder by manually pushing air through the holder using a syringe.
4. The filter holder was opened and attached to an adapter on a handheld X-ray fluorescence spectrometer (pXRF, Hitachi X-MET8000 Expert).
5. Metals were analysed from the filter with the pXRF. The metal concentrations in the initial sample were determined using predetermined calibrations. The concentrations were read from the display of the pXRF device.

The pumping took 10 min, flushing and transferring the holder from the pump to the pXRF 1 min and the pXRF analysis 2 min. Therefore, results were obtained within 15 minutes from the sampling.

Reference samples were collected, filtrated through 0.45 µm syringe filter and acidified on-site with ultrapure nitric acid to prevent precipitation and then delivered for ICP-OES analysis to the University of Oulu.

Results

The 3D printed filter holders were designed to protect the filter from mechanical wear and chemical contamination. It allows also easy transfer and attachment of the filter to measurement position of pXRF with the designed adapter. The XRF emission peaks

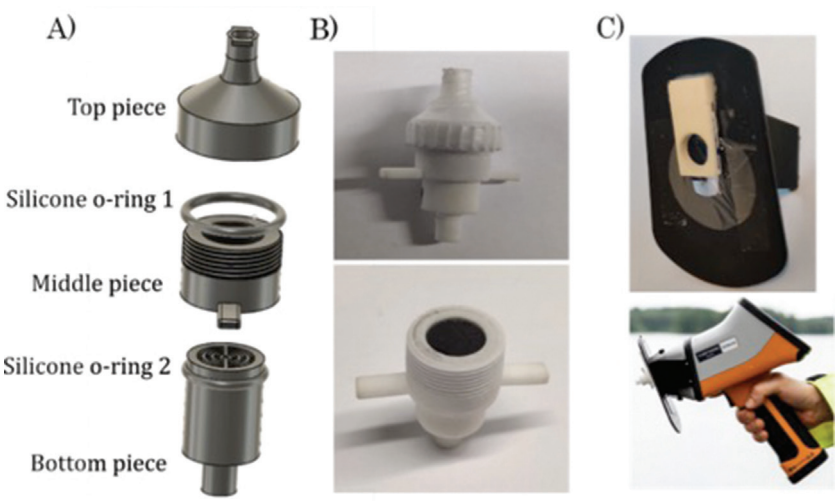

Figure 2 *Filter holder used in the study. A) An exploded view of the design of the 3D printed parts with two additional silicone O-rings. B) Photographs of the holder. The top photograph shows the holder with all parts assembled and the bottom photograph shows the holder with top piece removed showing the surface of the filter, from which metal signals are measured with pXRF. C) Adapter used to attach the filter and holder to pXRF measurement position.*

originating from the metals adsorbed in the metal collecting filter in the calibration experiments correlated well with metal concentrations of the water samples analysed by ICP-MS. A regression analysis was utilised successfully to create metal specific empirical calibration curves (presented in Supplementary Material Figure S1.) for the X-MET8000.

The first site (Site 1) was a mine and analyses were done in environmental monitoring purposes during routine sampling from the groundwater bore holes. The next site (Site 2) was closed mine and sampling was performed on the natural waters surrounding the old tailings pond again on monitoring purposes. The results of the MWAS measurements compared to the laboratory are presented in Table 1 and 2. Among the four metals calibrated in the system, Mn was most often found in the samples, and notable Zn concentration were present in the samples 5 and 8. Notable Ni concentration was also found in the sample 8.

Similar results were obtained from the on-site analyses and the reference ICP-OES analyses for the samples from both sites. Mn results obtained on-site with MWAS follow ICP-OES results accurately in all samples except the Sample 10, showing slightly higher, 36%, difference between the analyses as seen in the Figure 3. The correlation coefficient for the Mn results is 0.83 and if the sample 10 is removed the correlation coefficient is 0.99. The MWAS gave higher concentration for Zn in the Sample 5 compared with ICP-OES with concentration close to the detection limit of the system. Lower concentrations for Ni and Zn were obtained in the Sample 8.

A blank sample for ICP-OES was made by filtrating, acidifying, and storing the DI water similarly as the samples and analysed together with actual samples. The blank sample showed slightly elevated Zn concentration of about 37 µg/l. It seems that small Zn contamination is originated from the bottles or from the acid for reference samples. These higher Zn levels can be seen at least in the ICP-OES analyses of samples 6 – 10. The blank DI water analysis for MWAS did not show any signals from the calibrated metals.

Discussion

Analytical capabilities of the new technology are limited by (a) the analyser and (b) properties of the concentrating media (the filter) (c) the precision of the pXRF and (d) the accuracy of the reference method. Element range of pXRF currently spans from Si to U, excluding light elements and most precious metals, for analyzing solid concentrations between a few mg/kg and a few percents

Table 1 *Results of Site 1 on-site analyses with the MWAS system compared with reference analyses (LAB). Concentrations above the detection limit of the MWAS system (50 µg l-1) are marked with a bold font.*

Sample (Site 1)	pH	Temp (°C)	EC (µS/cm)	Mn (µg l^{-1})		Ni (µg l^{-1})		Cu (µg l^{-1})		Zn (µg l^{-1})	
				MWAS	LAB	MWAS	LAB	MWAS	LAB	MWAS	LAB
Sample 1	5.3	4.4	99	< 50	< 30	< 50	< 20	< 50	41	< 50	16
Sample 2	6.4	4.6	136	**347**	**356**	< 50	36	< 50	< 20	< 50	32
Sample 3	6.0	4.0	101	**348**	**365**	< 50	33	< 50	< 20	< 50	30
Sample 4	6.4	6.4	134	**490**	**479**	< 50	42	< 50	< 20	< 50	27
Sample 5	5.0	4.6	32	< 50	< 30	< 50	< 20	< 50	< 20	**64**	**35**

Table 2 *Results of Site 2 on-site analyses with the MWAS system compared with reference analyses (LAB). Concentrations above the detection limit of the MWAS system (50 µg l^{-1}) are marked with a bold font.*

Sample (Site 2)	pH	Temp (°C)	EC (µS/cm)	Mn (µg l^{-1})		Ni (µg l^{-1})		Cu (µg l^{-1})		Zn (µg l^{-1})	
				MWAS	LAB	MWAS	LAB	MWAS	LAB	MWAS	LAB
Sample 6	5.8	12.9	115	**162**	**153**	< 50	< 20	< 50	< 20	< 50	59
Sample 7	6.3	13.2	138	**376**	**379**	< 50	30	< 50	< 20	< 50	58
Sample 8	6.3	11.8	339	< 50	< 30	**78**	**172**	< 50	< 20	**190**	**326**
Sample 9	6.1	12.8	300	**60**	**79**	< 50	< 20	< 50	< 20	< 50	47
Sample 10	6.5	14.4	479	**291**	**457**	< 50	37	< 50	< 20	< 50	48

(Lemière and Uvarova 2020). Filters are currently able to concentrate cationic species – the metals, sensu stricto. in addition to four metals calibrated, proof of concept study has been performed for U and Pb. These metals already cover the regulatory needs of some mines (coal, iron and transition elements, base metals, phosphate) have been calibrated on the system, but the system's capabilities are not limited to these metals. Additional elements that would not require developments beyond specific calibration include Fe, Co, Ti and Sr. Elements that may be detected if their abundance is high include Cd, Ag, V and Cr.

However, anionic species such as As, Sb or Se cannot be currently analysed. Arsenic is a major issue for mining applications, and a topic of future development. Gold and platinum group elements are beyond the reach of predictable elements and have to be addressed through tracers or proxies. Lithium is also out of reach of pXRF unless indirect approaches are used. Based on the calibration curves MWAS can analyse concentrations ranging about from 50 µg L^{-1} to 10 mg L^{-1} and the range can be sifted to even lower concentrations by utilizing larger volumes for the filtration.

With solid samples, most of the differences between pXRF and laboratory results are systematic biases caused by differences in calibration and on-site samples and a slightly higher dispersion of the on-site analyses compared with the laboratory analyses (Young *et al*. 2016). These can be incorporated in higher reporting uncertainties for safety, but it also is possible to use raw pXRF results reliably for sample ranking and classification purposes (Lemière 2018; Lemière and Uvarova 2020). A bias may also be observed for water analyses between pXRF and laboratory results, but in most cases, there is a good correlation between them for a given matrix type. Samples will therefore be accurately ranked from low to high concentrations for each element, and inter-element ratios will be conserved. Empirical correction factors can be defined for a given matrix type and applied at a given site.

Decisions can therefore be made on-site without waiting for the laboratory results if pXRF results are significantly above or below thresholds or action levels. With the developed system, large gains are possible, in terms of both costs (sampling and analysis) and quality of data sets, because of better sample selection. At the present stage, the results can be used for screening purposes, to detect anomalies, time series variations and therefore efficiently select the samples to be sent to the laboratory. Usability and accuracy of the system are being constantly improved by optimizing the design and calibrations.

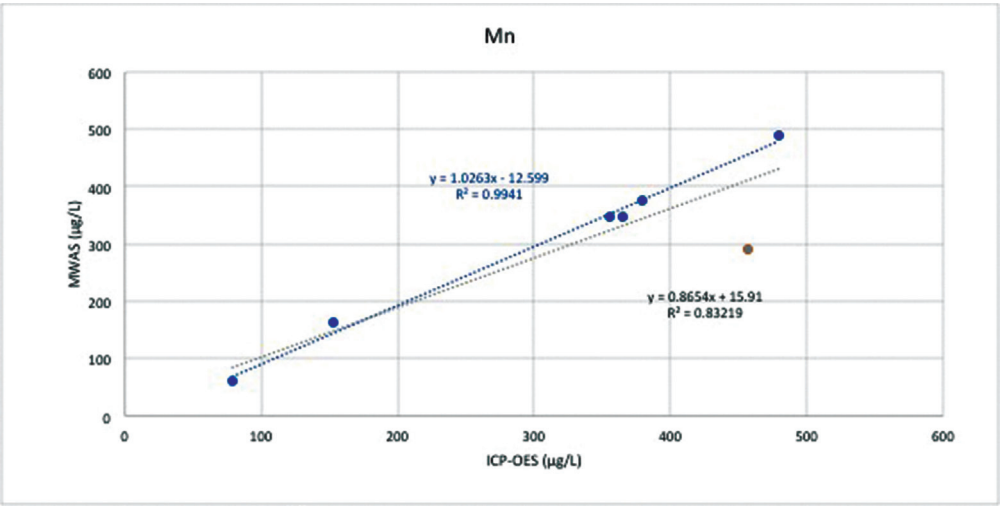

Figure 3 *Correlation between Mn concentrations obtained with laboratory ICP-OES and MWAS on-site analysis system. The grey data point is Sample 10 that differs from the rest of the set. The grey fit line includes the data point and the blue one does not.*

Conclusions

The results show that the current MWAS prototype can be used on-site to screen metal concentrations of environmental waters related to mining. The results correlated especially well with ICP-OES results with Mn. There was more variation between MWAS and ICP-OES results with Zn and Ni. It should be noted that these analyses were the first tests of the prototype and further improvements are being made to improve the precision and accuracy of the system. The results highlight a major advantage of the system. The MWAS on-site analyses do not suffer from possible changes of the sample during storage and transport.

The potential applications of this novel technology are many. At the exploration stage, it would facilitate hydrogeochemical prospecting by allowing on-site analysis, and therefore dynamic sampling. The lower analytical limits may be too high for some elements, but the technique is a simultaneous multielement one. This allows tracking pathfinder elements or favourable matrixes. During mine exploitation and after closure, the technique allows a much more frequent monitoring of discharged water than laboratory analyses. At a processing plant, it allows monitoring the quality of input and output water, and internal loops. It facilitates runoff water reuse and allows immediate operational decisions on water management.

Acknowledgements

This work was supported by the Maj and Tor Nessling Foundation, EIT RawMaterials, Academy of Finland (project no. 292601) and Business Finland (project GWW - Green Sensor for Water and Waste Monitoring). Hitachi High-Tech Analytical Science Oy is acknowledged for providing the pXRF device.

References

Cánovas CR, Macías, F, Olías M (2018) Hydrogeochemical behavior of an anthropogenic mine aquifer: Implications for potential remediation measures. Science of The Total Environment 636:85-93, https://doi.org/10.1016/j.scitotenv.2018.04.270

Ghorbani Y, Fitzpatrick R, Kinchington M, Rollinson G and Hegarty P (2017) A Process Mineralogy Approach to Gravity Concentration of Tantalum Bearing Minerals. Minerals 7:194; doi:10.3390/min7100194

Kidder JA, Leybourne MI, Layton-Matthews D, Bowell RJ, Rissmann CFW (2020) A review of hydrogeochemical mineral exploration in the Atacama Desert, Chile. Ore Geology Reviews 124:103562, https://doi.org/10.1016/j.oregeorev.2020.103562

Lemière, B. (2018) A review of applications of pXRF (field portable X-ray fluorescence) for applied geochemistry. Journal of Geochemical Exploration, 188: 350–363.

Lemière, B. and Uvarova, Y.A. (2020) New developments in field portable geochemical techniques and on-site technologies and their place in mineral exploration. Geochemistry: Exploration, Environment, Analysis. Published Online https://doi.org/10.1144/geochem2019-044.

Li G, Klein B, Sun C, Kou J (2020) Applying Receiver-Operating-Characteristic (ROC) to bulk ore sorting using XRF. Minerals Engineering 146:106117, https://doi.org/10.1016/j.mineng.2019.106117

Nordstrom DK, Blowes DW, Ptacek CJ (2015) Hydrogeochemistry and microbiology of mine drainage: An update. Applied Geochemistry 57:3–16, http://dx.doi.org/10.1016/j.apgeochem.2015.02.008

Rinez Thapa, Tuomo Nissinen, Petri Turhanen, Juha Määttä, Jouko Vepsäläinen, Vesa-Pekka Lehto, Joakim Riikonen, Bisphosphonate modified mesoporous silicon for scandium adsorption, Microporous and Mesoporous Materials 296:109980, https://doi.org/10.1016/j.micromeso.2019.109980

Young, K.E., Evans, C.A., Hodges, K.V., Bleacher, J.E. and Graff, T.G. (2016). A review of the handheld X-ray fluorescence spectrometer as a tool for field geologic investigations on Earth and in planetary surface exploration. Applied Geochemistry, 72: 77-87.

Wheeler S, Henry T, Murray J, McDermott F, Morrison L (2021) Utilising CoDA methods for the spatio-temporal geochemical characterisation of groundwater; a case study from Lisheen Mine, south central Ireland. Applied Geochemistry 127:104912, https://doi.org/10.1016/j.apgeochem.2021.104912

Yehia R, Heberlein DR, Lett RE (2019) Rapid Hydrogeochemistry: A summary of two field studies from central and southern interior British Columbia, Canada using a photometer and voltammeter to measure trace elements in water. Explore 184:1-17.

Supplementary Materials

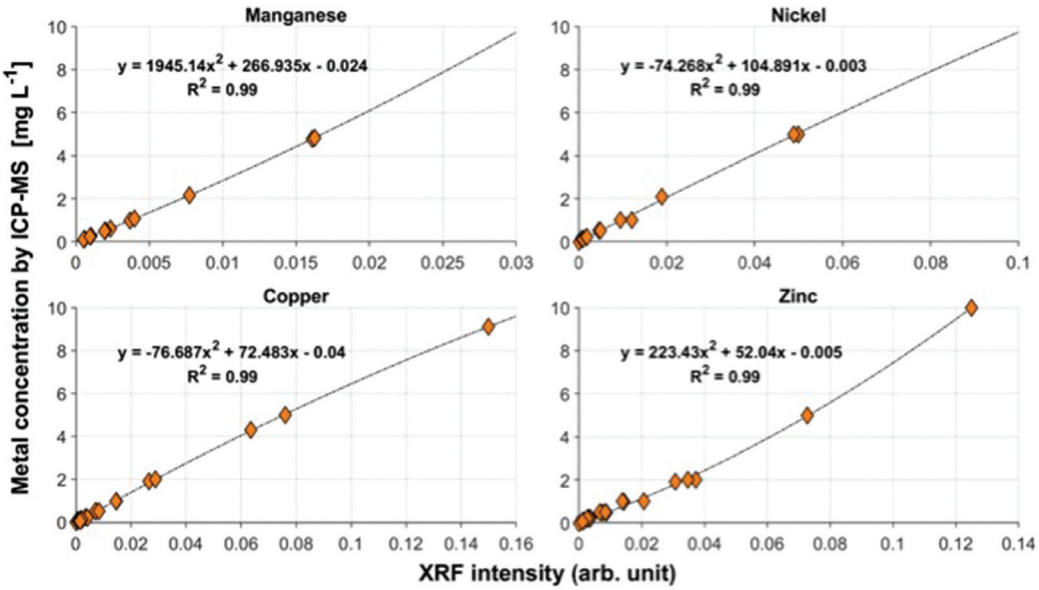

Figure 1 *Empirical calibration curves for Mn, Ni, Cu and Zn created with Hitachi X-MET8000 Control software (SW version: 4.1.0.222) for the X-MET8000 pXRF.*

Source Apportionment of Trace Metals at the Abandoned Nantymwyn Lead-Zinc Mine, Wales

Aaron M.L. Todd[1], Iain Robertson[1], Rory P.D. Walsh[1], Patrick Byrne[2], Paul Edwards[3], Tom Williams[3]

[1]*Department of Geography, Swansea University, Swansea SA2 8PP, UK, 887577@swansea.ac.uk*

[2]*School of Biological and Environmental Sciences, Liverpool John Moores University, Liverpool L3 3AF, UK*

[3]*Natural Resources Wales, Faraday Building, Swansea University, Swansea SA2 8PP, UK*

Abstract

Abandoned metal mines cause longstanding stream pollution problems. The two streams at Nantymywn, Wales, the Nant y Bai and the Nant y Mwyn, cause the River Tywi to fail local standards for Zn for 35 km. In this study NaBr tracer dilution and synoptic water sampling, followed by ICP-MS laboratory analysis, were carried out in baseflow conditions along the Nant y Bai to identify and quantify sources of metals at high spatial resolution. Preliminary results enable Zn sources to be located, including one representing 34% of the stream Zn load, as well as areas of diffuse sources and attenuation.

Keywords: Metal Mine Waste, Synoptic Sampling,Tracer

Introduction

Wales has a long history of mining, more recently for coal, but historically for Pb, Zn, Cu and other base metals (Thornton 1996; Mayes and Jarvis 2012). The age of these mines and haphazard way they were closed or abandoned has left complex hydrochemical problems at many of Wales' 1,300 abandoned metal mines (Environment Agency Wales 2002; Environment Agency 2008). Recent Water Framework Directive (WFD) work has highlighted gaps in knowledge of the fluvial impacts of abandoned metal mines and Natural Resources Wales (NRW) has ranked metal mines' effects in order to remediate those that are most deleterious (Environment Agency Wales 2002; Mayes *et al*. 2009; Mayes and Jarvis 2012; Coal Authority 2016).

Nantymwyn is the largest source of metals to the Tywi, causing its failure of WFD standards for 35 km downstream of the site (Natural Resources Wales 2019). Knowing where to target remediation efforts and achieve the largest improvement in environmental quality possible for the resources available requires data on the location, size, seasonal, and inter annual variation of pollution sources (Byrne *et al*. 2021). This paper reports preliminary results of a programme to identify, quantify and apportion sources of metal pollution from the Nantymwyn mine to the Nant y Bai, a tributary of the River Tywi in central Wales, using a NaBr tracer injection and synoptic sampling approach. Developed by the US Geological Survey, this technique determines pollutant loads at a high spatial resolution that can directly assist with effective remediation (Kimball 1997; Onnis *et al*. 2018; Byrne *et al*. 2021).

Study Area

Nantymwyn mine has been worked sporadically since pre-Roman times until final abandonment in 1932. In the 1700s, Nantymwyn was one of the largest sources of Pb ore in Wales (Hughes 1992; Hall 2011). Located in the upper catchment of the River Tywi, near Llandovery, Carmarthenshire (52°5'12"N; 3°46'20"W), Nantymwyn receives mean annual rainfall of 1,711 mm (National River Flow Archive 2021), and lies on Ordovician bedrock, with a fault NE-SW (Woodcock 1987). The northern side of the steep Nant y Bai catchment terrain is mostly used for rough grazing, with the bare spoil heaps fenced off to animals, and on the southern side there is a coniferous plantation (Figure 1). The underground workings affect

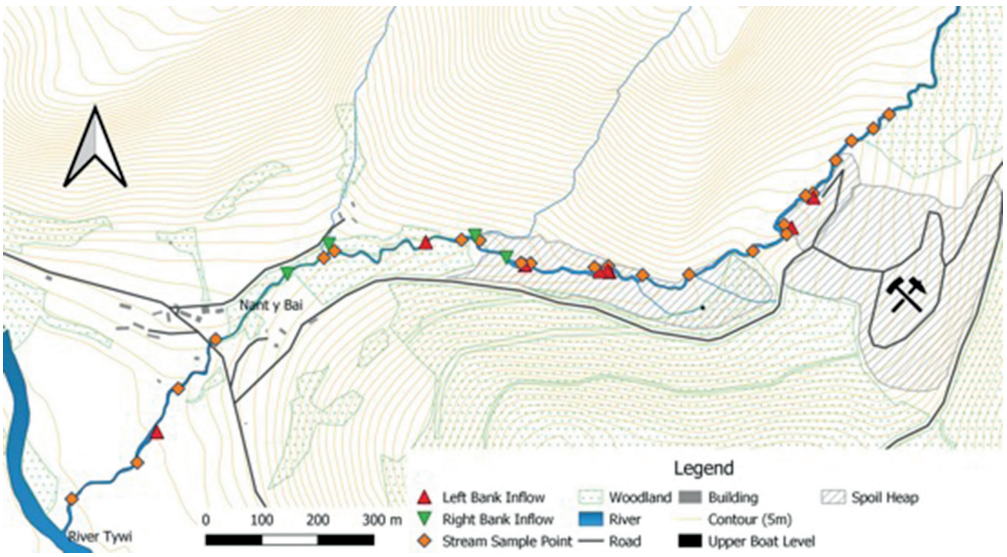

Figure 1 *Map of the study site showing synoptic sampling sites along Nant y Bai. Map created with OS data from Edina DigiMap (Ordnance Survey 2018).*

and drain to two streams, the Nant y Mwyn, and the larger Nant y Bai, with two boat levels (large adits kept flooded, allowing boats to float), and many smaller adits added as the mine expanded (Smith 1792; Roberts 1981; Fellows 2009). Varied levels of ore refinement were carried out on site as technologies progressed, leaving spoil and finings heaps of varying sized particles through which the Nant y Bai flows, as well as the Upper Boat Level's indirect outflow. The Nant y Mwyn receives the Deep Boat Level, the lowest outlet of the subterranean workings. Accumulation of trace metals from the mine in flora, and subsequent deleterious effects to fauna have been recorded (Sartorius 2020).

Methods

In July 2019 the Nant y Bai was injected with a conservative NaBr tracer at a rate of 70 mL min^{-1}, and once a plateau concentration of Br was established, synoptic sampling was carried out at 33 sample points, covering 2 km of the watercourse, following established techniques (Kimball *et al.* 2004; Runkel *et al.* 2013). Samples were collected at 22 stream sites, and the remaining samples were obtained from visible inflows (Figure 1). For the purposes of this study, point sources are those with a visible single inflow into the stream, whereas diffuse sources are those without a visible inflow.

At a temporary field laboratory each sample was split into three vials; one filtered through a 0.45 µm membrane, one filtered and fixed with HNO3, and one fixed but not filtered. Conductivity, pH and water temperature were recorded on site. Trace metals and Br analyses of the samples were carried out at Liverpool John Moores University on an Agilent Technologies ICP MS 7900 Inductively Coupled Plasma Mass Spectrometer (ICP-MS). Flow was calculated at each stream site using the Br concentration compared to the injection rate and concentration (Figure 2), and stream metal loadings were calculated as the products of metal concentrations and calculated flows (Kimball 1997; Kimball *et al.* 2002). The flow percentile during synoptic sampling was estimated at Q82 (lower than or equal to 82% of the historic flows) based on 11 data points from salt dilution flow gauging over 12 months. The nearest comparable NRW flow gauging station, on the Nant y Bustach recorded a flow percentile of Q89. After sampling was completed, two stretches of the Nant y Bai were also flow gauged via salt dilution, with the results corresponding well with the bromide tracer flow calculations.

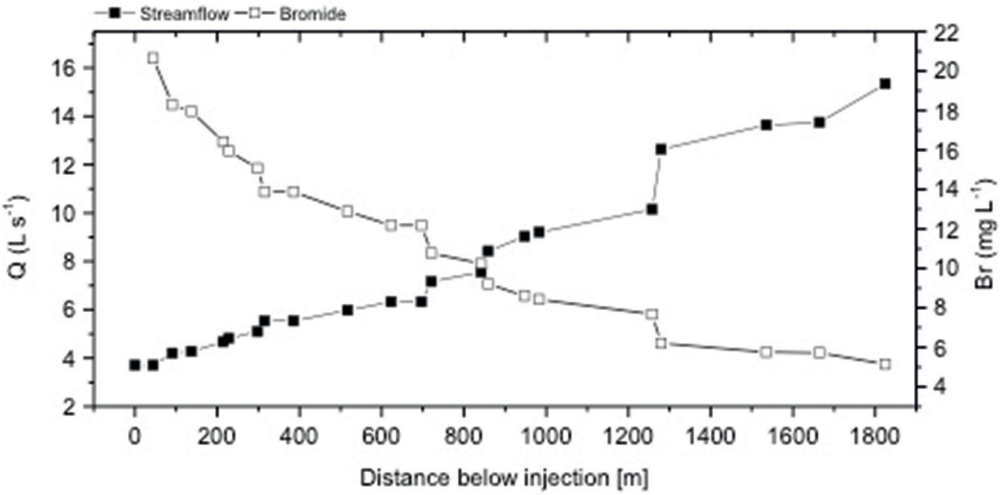

Figure 2 *Br river concentration and river discharge(Q) changes along Nant y Bai.*

Results and Discussion

The Nant y Bai exceeded the WFD long term mean standard for Zn (12.9 µg L^{-1} (dissolved) for the River Tywi) (WFD 2015) for 1600 m of the sampled stretch, peaking at 91 times the standard. Concentrations for the synoptic samplings varied from 5.3 µg L^{-1} (above the mine) to 1,124 µg L^{-1}, with a mean of 503 µg L^{-1}. The annual average environmental quality standard (AA-EQS) for Pb is 1.2 µg L^{-1} (WFD 2015); the Nant y Bai values varied from 6.5 µg L^{-1} to 1083 µg L^{-1}, with a mean of 237 µg L^{-1}. The changes in Zn concentration along the stream are shown in Figure 3

A sharp increase in Zn is shown at 315 m, just after an inflow at 305 m, draining a spoil heap (Figure 3b). This visible inflow had been previously sampled as part of a monitoring regime, but the scale of its contribution to the Zn loading was not clear. It contributes 34% of the total Zn load. Five flow measurements on the inflow at 305 m averaged 3.4 L s^{-1}; the Nant y Bai flow at the nearest point flow gauged regularly (400 m) has an average flow of 100 L s^{-1} from 10 measurements. During high rainfall, surface water flows across the upper tailings which enters the Nant y Bai both at point sources and diffuse processes. The Upper Boat Level adit flows out approximately 600 m below the injection site, with a dissolved Zn concentration of 716 µg L^{-1} on the day of synoptic sampling, but the water is lost to the boggy ground and its influence on the Nant y Bai cannot currently be calculated. Non-mine impacted water joins the Nant y Bai from the Pen y Darren and the Nant y Glo, at 960 m and 1268 m downstream from the injection site respectively and dilutes the metal concentrations in the stream. The Zn load carried by the Nant y Bai only decreases by 1% after the inflow from each stream, suggesting continued Zn input from subterranean sources.

Comparisons of successive calculated instream zinc loads along the Nant y Bai (Figure 4), indicate areas of possible attenuation notably the reduction in dissolved load between the two tailings heaps, as well as load increases that are explained by inflows, such as at 305 m and 847 m. From 1260 m onwards there is an increase in both total and dissolved load, potentially from diffuse subterranean sources. The Nant y Bai erodes through two areas of tailings, the upper (≈140-400 m) having an average Zn concentration of 1,783 mg kg^{-1}, and lower (≈620-950 m) 3,323 mg kg^{-1} (De-Quincey 2020). Dissolved Zn makes up 99% of the total Zn load at the end of the sampled stretch, consistent with regulator monitoring, and with similarly impacted streams (Byrne *et al.* 2013). The Upper Boat Level is likely adding to the Zn load as well. Over the course of the sampled stretch, 44% of the total Zn load was attenuated, compared with just 24% of the dissolved load. As the pH of the stream remains near neutral for the length sampled, the dissolved Zn remains in solution when it enters the Tywi.

Further work will be carried out on the Nant y Bai to confirm the chemical and physical

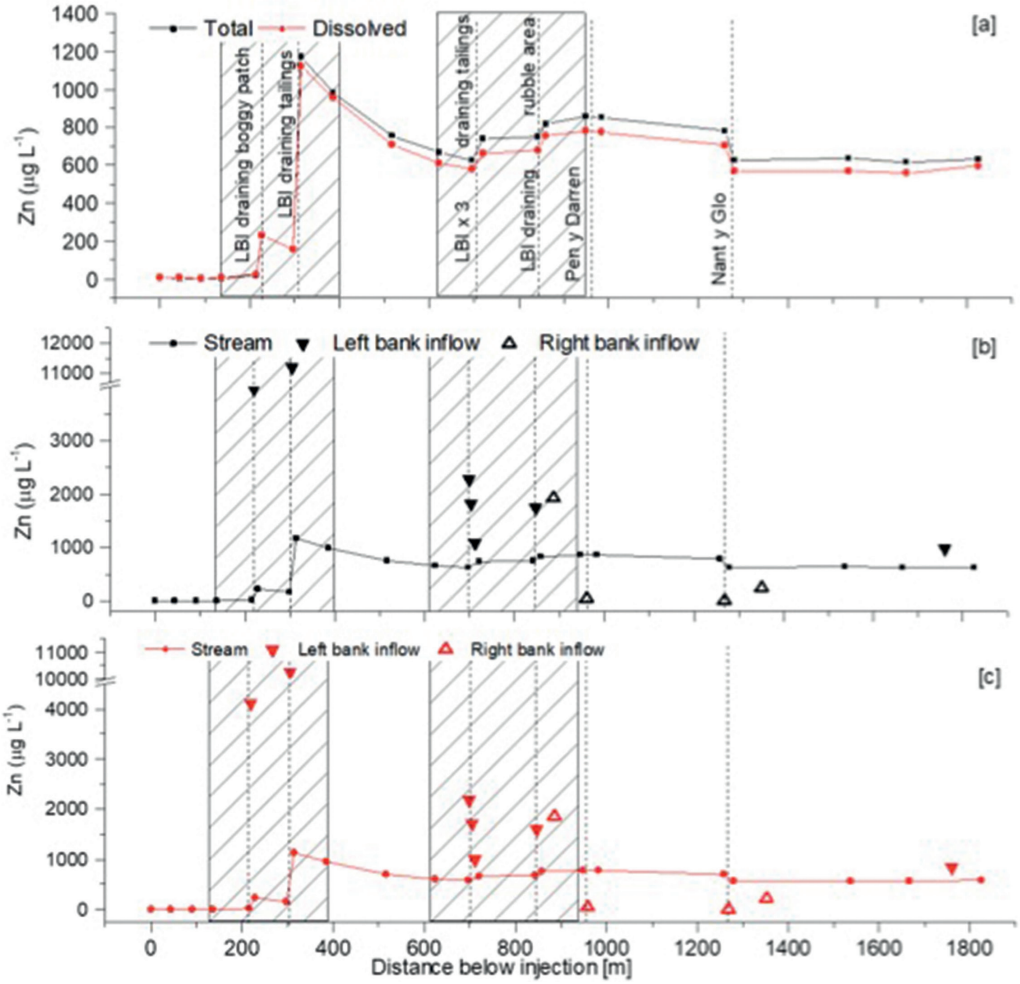

Figure 3 Spatial profiles of stream total and dissolved Zn concentrations [a], total stream and inflow Zn concentrations [b], and dissolved stream and inflow Zn concentrations [c]. Location of major inflows indicated with vertical dashed lines. Shaded areas = upper tailings (≈140-400 m) and lower tailings (≈620-950 m). For locations of sites and inflows see Figure 1.

processes causing the changes in Zn load, both the gradual increase downstream where there are no visible point sources, and the decrease between the two tailings areas. Each stream segment's synoptic sampling data will be assessed for cumulative inflows, revealing areas where unmeasured subterranean inflows are responsible for the increase in stream load. A series of storm surveys are planned to measure the effects of rapid flow increases on metal concentrations and detect any "flush" of pollutants after prolonged dry periods (Byrne *et al.* 2013). A second tracer injection and synoptic sampling experiment at higher flows would improve modelling of varied flow scenarios, and show flow-based changes to the diffuse and point sources identified in this report, as well as potentially identifying sources that were not flowing or underestimated on this low baseflow sampling occasion (Onnis *et al.* 2018).

Conclusion

This purpose of this study was to show variations in metal loadings along the Nant y Bai and identify sources of metals not shown by conventional spot sampling. A continuous tracer injection and synoptic sampling method identified and quantified a previously unknown source at 305 m that contributes 34% of the

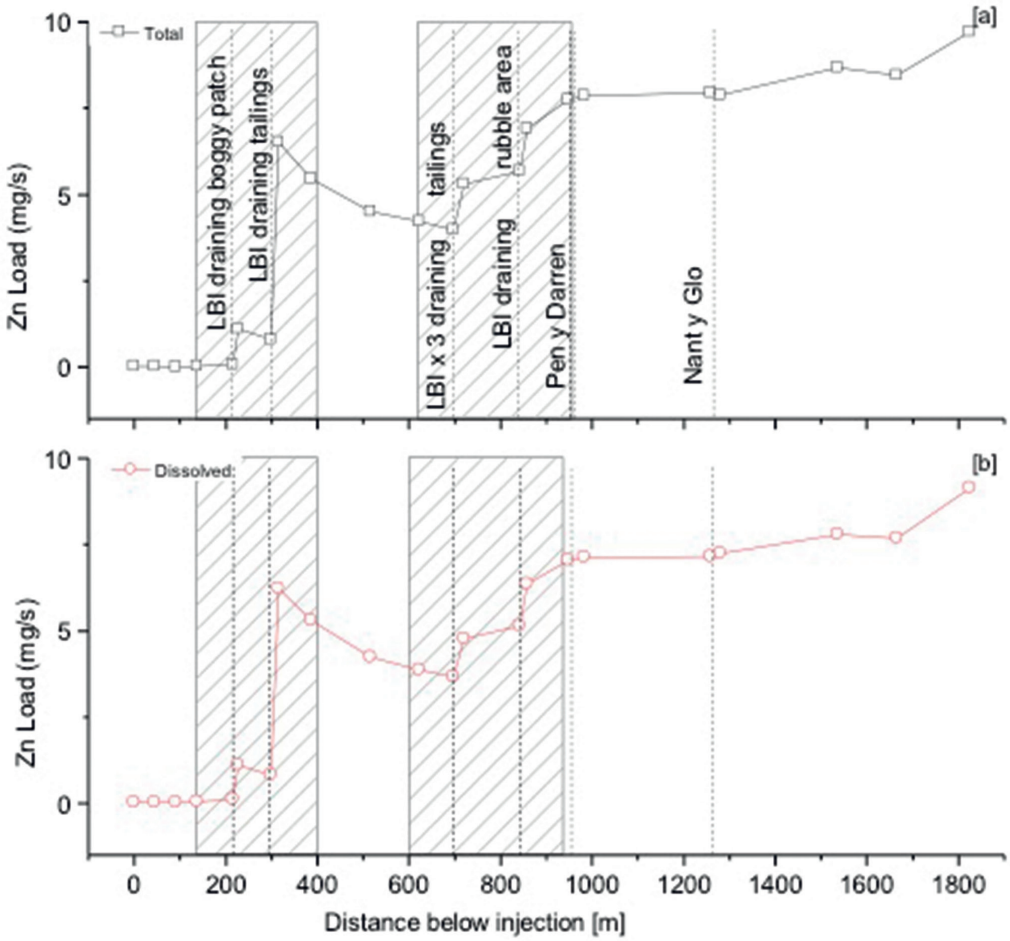

Figure 4 *Spatial profiles of total [a] and dissolved [b] instream Zn loads; total [c] Location of major inflows indicated with vertical dashed lines. Shaded areas = upper tailings (≈140-400 m) and lower tailings (≈620-950 m).*

total Zn load, despite its low flow compared to the river. Areas of diffuse inputs of pollution have been identified and further investigation into these can be planned on the basis of this information. The Nant y Bai fails WFD standards on Zn for the majority of its course.

Spot sampling with flow gauging, while a substantial improvement on just sampling, can easily miss extreme flow events, hence storm flows may not be accounted for in remediation planning. Similarly, sources with a relatively high contribution at low flows may be missed. Using tracer injection and synoptic sampling to provide high spatial resolution data brings clear advantages for regulators for both analysing mine impacts, and for assessing remediation. Further work will be carried out to investigate both sustained high flows and peak flows from storm events, as well as analyses of bed sediment along both streams. Data from the 2019 synoptic sampling will also be used to model flows and possible remediation scenarios.

Acknowledgements

The authors gratefully thank the Knowledge Economy Skills Scholarships (KESS 2) for funding AB's PhD, allowing this research to be undertaken. We also thank Ilaria Frau and NRW staff for their assistance with fieldwork.

References

Byrne P, Reid I, Wood PJ (2013) Stormflow hydrochemistry of a river draining an abandoned metal mine: The Afon Twymyn, central Wales. Environmental Monitoring and

Assessment 185:2817–2832. DOI: 10.1007/s10661-012-2751-5

Byrne P, Yendell A, Frau I, Brown AML (2021) Identification and Prioritisation of Mine Pollution Sources in a Temperate Watershed using Tracer Injection and Synoptic Sampling. Mine Water and the Environment (In press)

Coal Authority (2016) A review of priority metal mine sites in Wales. Coal Authority, Mansfield

De-Quincey H (2020) The development of a surrogate soil to assist the revegetation and stabilisation of metal-mine tailings. PhD Thesis, Swansea University

Environment Agency (2008) Abandoned mines and the water environment - Science project SC030136-41. Environment Agency, Bristol

Environment Agency Wales (2002) Metal Mines Strategy for Wales. Environment Agency Wales, Cardiff

Fellows R (2009) Nantymwyn (Cerrigmwyn) Lead Mine. https://www.aditnow.co.uk/documents/Nantymwyn-Lead-Mine/. Accessed 5 Jun 2020

Hall GW (2011) Nantymwyn Mine. https://www.aditnow.co.uk/Mines/Nantymwyn-Lead-Mine_4295/. Accessed 5 Jun 2020

Hughes SJS (1992) Nant y Mwyn Mine, Llandovery, Dyfed. British Mining 87–110

Kimball BA (1997) Use of tracer injections and synoptic sampling to measure metal loading from acid mine drainage. US Geological Survey Fact Sheet 245-96. USGS

Kimball BA, Runkel RL, Cleasby TE, Nimick DA (2004) Quantification of metal loading by tracer injection and synoptic sampling, 1997-98. US Geological Survey Professional Paper 191–262

Kimball BA, Runkel RL, Walton-Day K, Bencala KE (2002) Assessment of metal loads in watersheds affected by acid mine drainage by using tracer injection and synoptic sampling: Cement Creek, Colorado, USA. Applied Geochemistry 17:1183–1207. DOI: 10.1016/S0883-2927(02)00017-3

Mayes WM, Jarvis AP (2012) Prioritisation of abandoned non-coal mine impacts on the environment. Environment Agency, Bristol

Mayes WM, Johnston D, Potter HAB, Jarvis AP (2009) A national strategy for identification, prioritisation and management of pollution from abandoned non-coal mine sites in England and Wales. I. Methodology development and initial results. Science of the Total Environment 407:5435–5447. DOI: 10.1016/j.scitotenv.2009.06.019

National River Flow Archive (2021) 60007 - Tywi at Dolau Hirion. https://nrfa.ceh.ac.uk/data/station/meanflow/60007. Accessed 1 Feb 2021

Natural Resources Wales (2019) Water Watch Wales. Natural Resources Wales, Cardiff

Onnis P, Byrne P, Hudson-Edwards KA, *et al* (2018) Source Apportionment of Trace Metals Over a Range of Stream Flows Using a Multi-method Tracer Approach Source Apportionment of Trace Metals Over a Range of Stream Flows Using a Multi-method Tracer Approach. In: Wolkersdorfer Ch, Sartz L, Weber A, *et al*. (eds) Mine Water – Risk to Opportunity. Pretoria, South Africa, pp 843 – 849

Ordnance Survey (2018) OS MasterMap® Topography Layer. EDINA Digimap Ordnance Survey Service, Edinburgh

Roberts PK (1981) Boat levels associated with mining: II. metal mining. Industrial Archaeology Review 5:203–216. https://doi.org/10.1179/iar.1981.5.3.203

Runkel RL, Walton-Day K, Kimball BA, *et al* (2013) Estimating instream constituent loads using replicate synoptic sampling, Peru Creek, Colorado. Journal of Hydrology 489:26–41. DOI: 10.1016/j.jhydrol.2013.02.031

Sartorius A (2020) How trace metals distribute throughout ecosystems. University of Nottingham, Poster

Smith JW (1792) Interior of the mining part of Carreg Mowyn where the lead ore is principally carried in boats through narrow level communications branching from the mines: The boats used in this subterraneous navigation are narrow & sharp at each end & of about 5 tons. The National Library of Wales, Painting

Thornton I (1996) Impacts of mining on the environment; some local, regional and global issues. Applied Geochemistry 11:355–361

WFD (2015) The Water Framework Directive (Standards and Classification) Directions (England and Wales) 2015

Woodcock NH (1987) Structural geology of the Llandovery Series in the type area, Dyfed, Wales. Geological Journal 22:199–209. DOI: 10.1002/gj.3350220517

Application of Multivariate Statistical Analysis in Mine Water Hydrogeochemical Studies of the Outcropped Upper Carboniferous, Ruhr Area, Germany

Tuan Quang Tran[1, 2], Andre Banning[1], Stefan Wohnlich[1]

[1]*Hydrogeology Department, Faculty of Geosciences, Ruhr University Bochum, Universitätsstr. 150, 44801 Bochum, Germany, quang.tran@rub.de or tranquangtuan@humg.edu.vn*

[2]*Hydrogeology Department, Faculty of Geosciences and Geoengineering, Hanoi University of Mining and Geology, Hanoi, Vietnam*

Abstract

This study aimed to identify the processes controlling the geochemical characteristics of adit mine waters using correlation analysis and multivariate statistical techniques. The Hierarchical cluster analysis (HCA) classified water samples into 5 geochemically distinct clusters of similar characteristics. HCO_3^- and Ca^{2+} were the dominant ions in the mine water (clusters C1, C2, C3, and C4), indicating the processes of carbonate dissolution, while Na^+ was the most abundant of the cations in cluster C5, suggesting processes of rock weathering. Samples of C2, C4, and C5 were of Ca-Na-HCO_3-SO_4, Ca-Mg-Na-HCO_3-SO_4-Cl, and Na-Ca-HCO_3-SO_4 types, respectively, while those from C1 and C3 were of Ca-Mg-HCO_3-SO_4 type. A total of three principal component analysis (PCA) components accounted for 82.95% of the total variance. PCA 1 accounted for a variance of 58.18%, characterized by high positive loadings for HCO_3^-, SO_4^{2-}, Ca^{2+}, Mg^{2+}, Na^+, K^+, TDS, and EC, suggesting carbonate dissolution, rock weathering, and water salinity. The other components may be related to more local and geological effects. This study demonstrated the usefulness of multivariate statistical analysis in hydrogeochemistry.

Keywords: Multivariate Statistics, Cluster Analysis, Principal Component Analysis, Mine Water

Introduction

The last remaining German active hard coal mine was closed in December 2018. However, after mining, the mine water quality is still one of the concern issues nowadays. The study area is a part of the Ruhr coalfield, where the coal-bearing Upper Carboniferous strata crop out directly on the surface of the Ruhr river valley or underneath very thin overlying sediments of Quaternary age (Frankenhoff *et al*. 2017; Zieger *et al*. 2018), with about 50 km in East-West length and 15 km North-South width (Drozdzewski *et al*. 2008). It covers an area of about 754 km^2 (Fig. 1), spreading over the cities Hattingen, Sprockhövel, Witten, Wetter and Schwerte, and including parts of the cities Essen, Bochum, Dortmund, Holzwickede and Herdecke. The topography of the study area is generally shallow hills and undulating terrain, the elevation ranges between 20 and 333 m above sea level. The highest elevations are in Sprockhövel (about 330 m in Holthausen). The annual average precipitation in the area is 891 mm (DWD 2019). The geology is characterized by Upper Carboniferous cyclothems: sandstone, silt- , mud-, and claystone layers, interspersed with hard coal seams. The layers contain clay minerals and mica (kaolinite, chlorite, biotite), feldspar (albite, anorthite), siderite, dolomite, calcite, quartz, and pyrite (Strehlau 1990; Wisotzky 2017).

It is not easy to identify the processes controlling the geochemical characteristics of mine water, especially in abandoned coal mines, through complex hydrogeochemical data. To protect water resources, it is important to understand processes controlling geochemical variability in such post-mining systems.

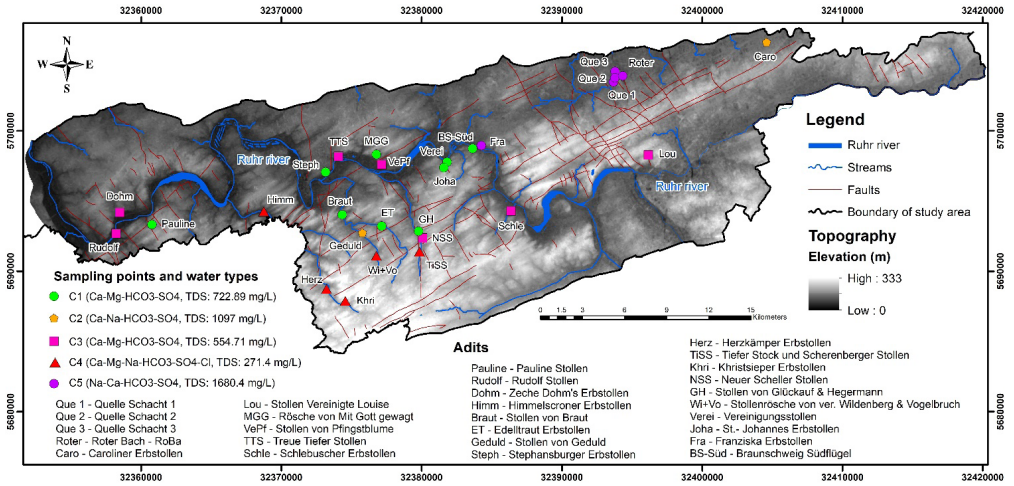

***Fig. 1** Map of the study area, including sampling points and spatial distribution of the mine water types.*

For decades, besides hydrogeochemical and isotopic methods, multivariate analysis techniques have also been used widely in mine water studies (e.g. Li *et al.* 2018). These methods are performed as useful tools to reduce and organize a large hydrogeochemical data set into a small number of factors, grouping samples with similar characteristics (Reghunath *et al.* 2002). Multivariate techniques also were used to study the environmental impacts of medieval mining (Horák and Hejcman 2016) or have been extensively applied to groundwater quality data (Khelif and Boudoukha 2018). Moreover, multivariate analysis has been applied to hydrogeochemical data by many researchers to analyze hydrogeochemical parameters to classify groundwater of varied geochemical features and to identify primary processes controlling groundwater chemical components (e.g. Qian *et al.* 2016).

The purpose of this study was to characterize the chemistry of mine water and to develop hypotheses about processes controlling mine water composition and the origin of the chemical constituents present in mine water of abandoned coal mines in the outcropped Upper Carboniferous of the Ruhr area, Germany. The present study also contributed and demonstrated the usefulness of multivariate statistical analysis in mine water assessment and established a better understanding of hydrogeochemical characteristics of mine water in the study area.

Sample collection and methods

Sampling and analysis

Water samples were collected from the 28 different drainage sites of abandoned coal mines in the study area from January to March 2018. The sampling locations are given in Fig. 1. Physicochemical parameters of water (pH, EC) were measured in situ using portable meters (WTW, Weilheim, Germany). These probes were calibrated using standard solutions, and bottles were washed and rinsed thoroughly with sample water. Samples for cation analysis were acidified using concentrated HNO_3. Samples were stored in the refrigerator at 4 °C until completed analyses. HCO_3^- concentrations were measured using HCl titration. Major anions (SO_4^{2-}, Cl^-, NO_3^-, F^-) were measured using the DIONEX Ion Chromatography System model ICS - 1000, with an AD20 Absorbance Detector system. Major cations (Ca^{2+}, Mg^{2+}, Na^+, and K^+) were analyzed by CD25 Conductivity Detector, IP 20 Isocratic Pump DIONEX.

Multivariate statistical techniques

The correlation matrix, Hierarchical cluster analysis (HCA), and Principal component analysis (PCA) methods were used to evaluate the physicochemical parameters of water samples. Spearman correlation was used to evaluate correlations between different

variables, using the statistical software SPSS 23, combined with the XL-Stat software to check and compare results. These methods were applied to a subgroup of the dataset to evaluate their usefulness for classifying water samples and identifying relevant geochemical processes. The dataset consisted of 28 hydrogeochemical analyses.

The Q-mode HCA technique was performed on the water chemistry data to classify samples into distinct hydrogeochemical groups using values for 12 physicochemical parameters (HCO_3^-, SO_4^{2-}, Cl^-, NO_3^-, F^-, Ca^{2+}, Mg^{2+}, Na^+, K^+, pH, EC, and TDS). The Ward's linkage method with Euclidean distance was used for the measurement of similarity between the water quality variables. The results were represented in a dendrogram. PCA was used to identify major factors governing mine water geochemistry. The varimax rotated factor analyses were carried out for 12 parameters and factor loading was calculated using eigenvalue greater than 1 and sorted by the results having values greater than 0.3. Most mine water physicochemical parameters in this study are non-normally distributed, the Spearman method and Kaiser-Meyer-Olkin (KMO) test were used to indicate the proportion of common variance.

Results and discussion

General hydrogeochemical characteristics

The pH values ranged from 6.39 to 7.65, indicating circum-neutral mine water conditions. EC values were in the range of 202 to 1713 µS cm^{-1} and TDS values ranged between 157 and 1806 mg L^{-1}, which indicates that mine water of several adits is highly mineralized, implying fresh and brackish waters. A Durov diagram (Durov 1948) was plotted for 28 water samples to examine the hydrogeochemical types of mine waters (Fig. 2).

This diagram shows the chemical composition of water in the study area that was formed by the main types: Ca-Mg-HCO_3-SO_4, followed by Na-Ca-HCO_3-SO_4, Ca-Mg-Na-HCO_3-SO_4, and Na-Ca-Mg-HCO_3-SO_4 water types. The average ion concentrations followed the order: $HCO_3^- > SO_4^{2-} > Cl^- > NO_3^- > F^-$ and $Ca^{2+} > Mg^{2+} > Na^+ > K^+$ (% meq L^{-1}). The mine water samples showed the dominance of weak acids (HCO_3^-) over strong acids ($SO_4^{2-} + Cl^-$), and alkaline earths ($Ca^{2+} + Mg^{2+}$) over the alkalies ($Na^+ + K^+$).

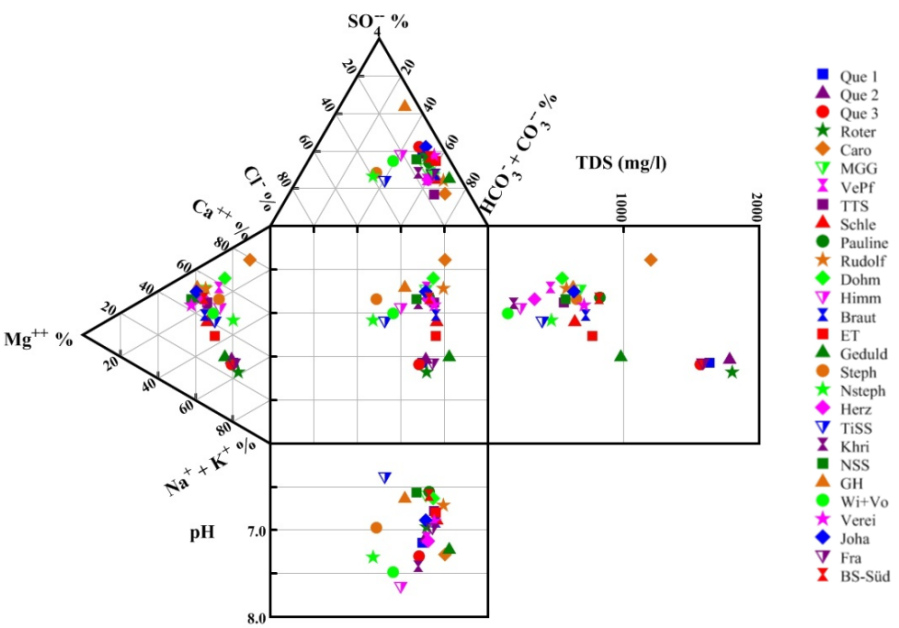

Fig. 2 Durov diagram of mine water hydrogeochemistry in the study area.

Table 1 Spearman correlation matrix of major physicochemical parameters.

	HCO_3^-	SO_4^{2-}	Cl^-	NO_3^-	F^-	Ca^{2+}	Mg^{2+}	Na^+	K^+	pH	EC	TDS
HCO_3^-	1.000	**0.758**	0.436	**-0.728**	0.210	**0.738**	**0.738**	**0.751**	**0.827**	-0.036	**0.877**	**0.936**
SO_4^{2-}		1.000	0.433	**-0.595**	0.319	**0.796**	**0.928**	**0.675**	**0.759**	-0.140	**0.898**	**0.847**
Cl^-			1.000	-0.172	0.114	**0.639**	0.417	**0.659**	0.476	0.014	**0.573**	0.440
NO_3^-				1.000	-0.332	-0.376	**-0.668**	**-0.557**	**-0.677**	0.170	**-0.537**	**-0.602**
F^-					1.000	-0.014	0.231	0.477	0.380	0.185	0.268	0.299
Ca^{2+}						1.000	**0.718**	**0.536**	**0.646**	-0.063	**0.865**	**0.767**
Mg^{2+}							1.000	**0.630**	**0.733**	-0.268	**0.794**	**0.773**
Na^+								1.000	**0.837**	0.099	**0.804**	**0.773**
K^+									1.000	0.029	**0.870**	**0.851**
pH										1.000	0.038	-0.075
EC											1.000	**0.933**
TDS												1.000

Bold indicates correlation is significant at the 0.01 level (2-tailed),
Underlined indicates correlation is significant at the 0.05 level (2-tailed).

Multivariate Statistical Analysis

Correlation matrix

The Spearman correlation coefficients were calculated, the results of the correlation matrix for 12 variables are given in Table 1. The interpretation of the correlation matrix showed that the pH values are not correlated with ions.

TDS values are strongly correlated (r > 0.8) with most of the ions in the water samples, such as TDS - HCO_3^- (r = 0.936) and TDS - SO_4^{2-} (r = 0.847), mostly statistically significant at the 0.01 level ($p < 0.01$), while TDS values show a weaker correlation with Cl- (r = 0.44), significant at the 0.05 level ($p < 0.05$).

Na^+ and K^+ in water samples are correlated positively with Cl^- (r = 0.659, $p < 0.01$) and (r = 0.476, $p < 0.05$), respectively. This may indicate halite/sylvine dissolution influencing mine water chemistry.

Ca^{2+} and Mg^{2+} concentrations are correlated with HCO_3^- with r = 0.738 ($p < 0.01$). This suggests calcite and dolomite dissolution. Ca^{2+} is also correlated significantly with SO_4^{2-} (r = 0.796, ($p < 0.01$)), suggesting possible gypsum dissolution.

Ca^{2+} and Na^+ ions have an average correlation (r = 0.536, $p < 0.01$), indicating that Ca/Na ion exchange also increases the Ca^{2+} concentration in the mine water. EC showed strong to moderate positive and negative correlations with HCO_3^-, SO_4^{2-}, Ca^{2+}, Mg^{2+}, Na^+, K^+, Cl^- and NO_3^-. It reflects the participation of these elements in the brackish mine water environment in the study area.

Hierarchical Cluster Analysis (HCA)

The main result of the HCA performed on the 28 mine water samples is the Dendrogram (Fig. 3). The Q-mode factor analysis, sampling sites with larger similarities are first grouped. Next, groups of samples are joined with a linkage rule and the steps are repeated until all observations have been classified. Based on the desired level of resolution for interpretation and the potential of the data considered, the number of groups is chosen (Ribeiro and Macedo 1995). Ward's method was more successful to form clusters, with the phenomena line of 2.5. Results showed that the HCA classified mine water samples into 5 geochemically distinct clusters (C1-C5) of similar characteristics, represented in Dendrogram to categorize different levels, which the Stiff diagrams show for each group (Fig. 3).

Samples of C2, C4, and C5 are of Ca-Na-HCO_3-SO_4, Ca-Mg-Na-HCO_3-SO_4-Cl, and Na-Ca-HCO_3-SO_4 types, respectively, while those from C1 and C3 are of Ca-Mg-HCO_3-SO_4 type. The C4 cluster accounts for 17.9% of the total samples, including 5 samples, with

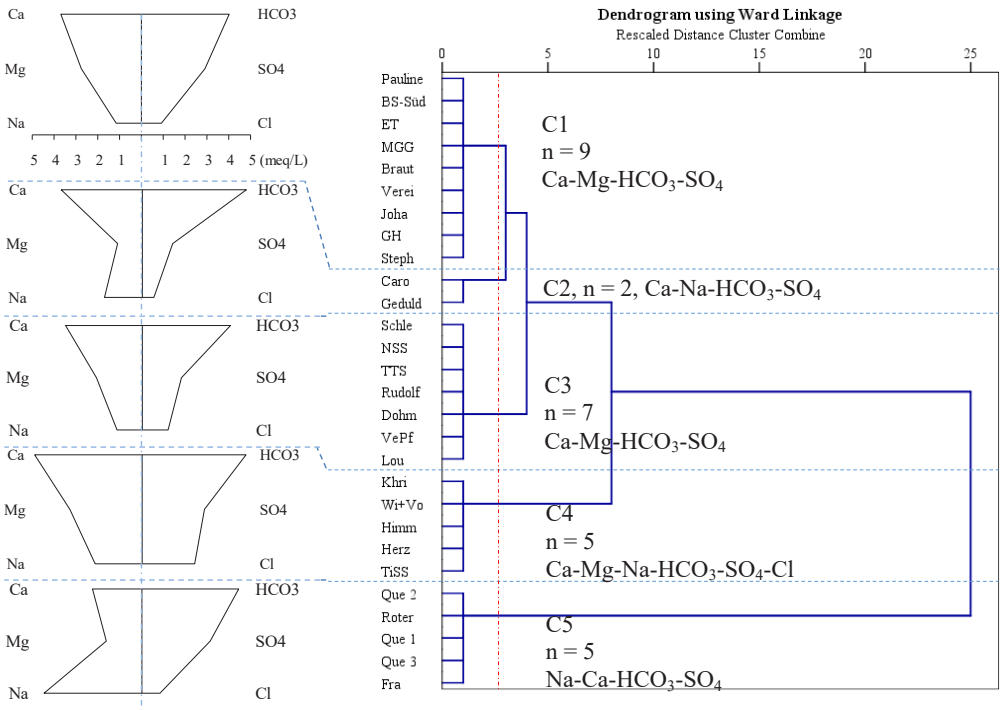

Fig. 3 *Dendrogram of the major ions in mine water and corresponding Stiff diagrams.*

the average EC and TDS values of 301.6 µS cm^{-1} and 271.4 mg L^{-1}, respectively, mostly distributed in the southern part (the highest elevation). C3 consists of 7 samples located at a lower elevation, accounts for 25% of the total samples (average EC: 579.71 µS cm^{-1} and mean TDS: 554.71 mg L^{-1}). The common feature of these water types is low salinity. C1 is composed of 9 samples and represents 32.1% of the total samples. This water type is relatively fresh, with an average EC of 746.89 µS cm^{-1} (mean TDS = 722.89 mg L^{-1}), mostly distributed in the central study area (Fig. 1). C2 included by two water samples (mean EC and TDS values of 897.5 µS cm^{-1} and 1097 mg L^{-1}, respectively), characteristic for mixed water. C5 is represented by 5 samples, with an average EC of 1609.8 µS cm^{-1} (mean TDS = 1680.4 mg L^{-1}), interpreting the character of blended water and characterized by high salinity, mostly distributed in the east-northern part (Fig. 1). HCO_3^- and Ca^{2+} were the dominant ions in the mine water of the study area (clusters C1, C2, C3, and C4), while Na^+ was the most abundant of the cations (cluster C5). The Que 2, Roter, Que 1, Que 3 and Fra water samples presented the highest average values of HCO_3^-, Ca^{2+}, SO_4^{2-} and Na^+ ions.

Principal Component Analysis (PCA)

The PCA was used to identify major factors governing groundwater geochemistry by many researchers (e.g. Qian *et al.* 2016). The value of the KMO test is 0.752 > 0.5, indicating the total number of significant factors. The loadings of different elements, including the total eigenvalues of different factors, the percentage of variances, and the percentage of cumulative variances are summarized in Table 2. A system of orthogonal axes is created, which helped to visualize the projections of the data matrix elements in a plan diagram (Fig. 4).

From the hydrogeochemical data, a total of three PCAs were extracted with total eigenvalues higher than 1 which account for 82.95% of the total variance (Table 2). Three components reflect the major effective factors controlling the mine water chemistry.

The PCA 1 contributed 58.18% of the total variance and is characterized by high positive loadings on HCO_3^-, SO_4^{2-}, Ca^{2+}, and Mg^{2+} (Table 2, Fig. 4). High scores of this component indicate high mineralization of mine water. This suggested that PCA 1 represented the dissolution or precipitation processes of carbonate, such as calcite and dolomite and sulfate minerals (Qian *et al.* 2016). However, PCA 1 had also high positive loadings for Na^+, K^+, TDS, EC, and Cl^- (Table 2, Fig. 4), suggested that it represented rock weathering and water salinity. It is addressed as the highly mineralized factor, because of exhibited high loadings on TDS (0.944), EC (0.974), SO_4^{2-} (0.873), Cl^- (0.65) and Na^+ (0.852). Therefore, mine water is not only contributed by Ca^{2+} and Mg^{2+} but also contributed by Na^+. It implied that it might be represented the ion exchange. The PCA 2 was 14.18% of the total variance in mine water dataset, with mainly consisted of NO_3^- and pH (Table 2, Fig. 4), implied that it might be the consequence of agricultural activities in the study area. The PCA 3 explained 10.59% of the total variation of the matrix data and mainly consisted of F (Table 2, Fig. 4), suggested that it was contributed from the primary geological environment (Teng *et al.* 2018)management, and development. In this survey of a 10-km-wide area along both sides of the Songhua River, northeast China, the hydrogeochemical responses to different SW–GW interactions were studied. Three types of SW–GW interactions were identified—"recharge", "discharge", and "flow-through"—according to the hydraulic connection between the surface water and groundwater. The single factor index, principal component analysis, and hierarchical cluster analysis of the hydrogeochemistry and pollutant data illuminated the hydrogeochemical response to the various SW–GW interactions. Clear SW–GW interactions along the Songhua River were revealed: (1. Moreover, in Table 2, the PCA 3 had also a low positive loading on Na^+ (*0.419*) and a negative one for Ca^{2+} (*-0.397*), implied that ion exchange processes may occur in the mine water environment, as mentioned above.

Table 2 *Loadings of different parameters for the three PCAs following varimax rotation.*

Parameters	Principal Components		
	PCA 1	PCA 2	PCA 3
HCO_3^-	**0.913**	-0.163	0.184
SO_4^{2-}	**0.873**	-0.192	0.249
Cl^-	**0.650**	0.354	-0.230
NO_3^-	-0.275	**0.839**	-0.277
F^-	0.206	0.014	**0.843**
Ca^{2+}	**0.802**	-0.018	***-0.397***
Mg^{2+}	**0.738**	-0.559	0.097
Na^+	**0.852**	0.035	***0.419***
K^+	**0.785**	-0.240	0.197
pH	0.059	**0.801**	0.360
EC	**0.974**	-0.082	0.184
TDS	**0.944**	-0.118	0.193
Total eigenvalue	6.981	1.702	1.271
% of variance	58.18	14.18	10.59
% of cumulative variance	58.18	72.36	82.95

High loading values are highlighted in **bold**

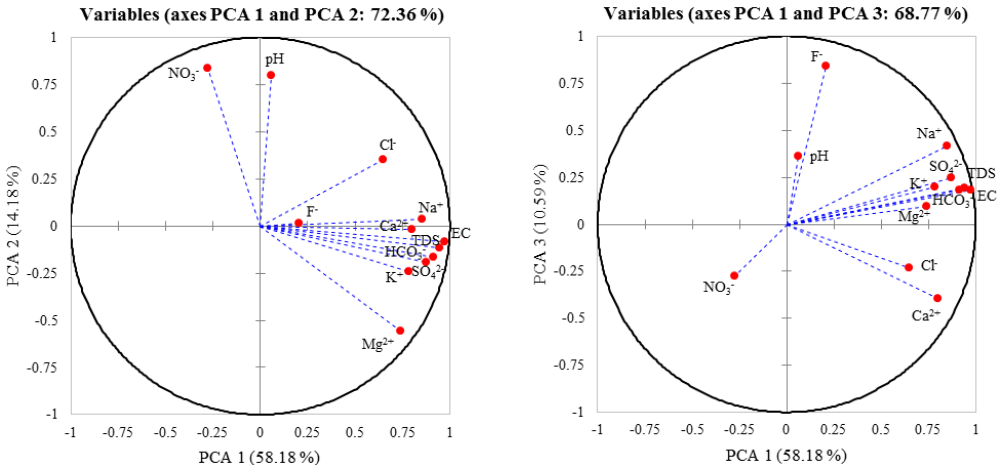

Fig. 4 Representation of the parameters in the factorial plan PCA 1-PCA 2 and PCA 1-PCA 3.

Conclusions

Multivariate statistical methods were used to characterize the origin of the chemical constituents present in mine water of abandoned coal mines in the study area. The correlation of ions in mine water was assessed. The dissolution of carbonate, sulfate, silicate, and chloride minerals are the primary processes controlling mine water chemical composition. The HCA in Q-mode showed 5 statistical groups based on the major distinguishing factors of EC and TDS values. The PCA identified three principal components, which explained 82.95% of the total variance. The first PCA accounted for 58.18% of the total variance and is related to rock weathering, such as dissolution or precipitation of carbonate and sulfate minerals, ion exchange processes, and water salinity, while the other components are controlled primarily by agricultural activities and local geological environment (14.18% and 10.59%, respectively). The results of this study illustrated the usefulness of multivariate statistical analysis in hydrogeochemical studies.

Acknowledgments

This study is financially supported by the 911 Scholarship of the Vietnamese Government and the German Academic Exchange Service (DAAD). Thanks to M.Sc. Sarah Burscheid who helped with sampling in the field, as well as the helping of Mr. N. Richard and Mr. O. Schübbe (Hydrochemistry Laboratory, Institute of Geology, Mineralogy and Geophysics, Ruhr University of Bochum) for the analyzing assistance the mine water hydrogeochemical samples. Last but not least, the hosts who allowed to access their property.

References

Drozdzewski G, Schäfer A, Brix MR (2008) Excursion Guidebook, 26th Regional meeting of the International Association of Sedimentologists

Durov SA (1948) Classification of natural waters and graphic presentation of their composition. Dokl Akad Nauk SSSR 59(1):87-90

DWD (2019) Weather and Climate-German Weather Service (Deutscher Wetterdienst). Online source, https://www.dwd.de/DE/klimaumwelt/cdc/cdc_node.html. Accessed 2019

Frankenhoff H, Balzer I, Witthaus H (2017) Mine water concept in detail - A case study of closing a German coal mine at Ruhr district. pp 175-182

Horák J, Hejcman M (2016) 800 years of mining and smelting in Kutná Hora region (the Czech Republic)-spatial and multivariate meta-analysis of contamination studies. J Soils Sediments 16:1584-1598

Khelif S, Boudoukha A (2018) Multivariate statistical characterization of groundwater quality in Fesdis, East of Algeria. J Water L Dev 37:65-74

Li P, Tian R, Liu R (2018) Solute geochemistry and multivariate analysis of water quality in the Guohua phosphorite mine, Guizhou province, China. Expo Heal 11:81-94

Qian J, Wang L, Ma L, *et al* (2016) Multivariate statistical analysis of water chemistry in evaluating groundwater geochemical evolution and aquifer connectivity near a large coal mine, Anhui, China. Environ Earth Sci 75:1-10

Reghunath R, Murthy TRS, Raghavan BR (2002) The utility of multivariate statistical techniques in hydrogeochemical studies: an example from Karnataka, India. Water Res 36(10):2437-2442

Ribeiro L, Macedo ME (1995) Application of multivariate statistics, trend- and cluster analysis to groundwater quality in the Tejo and Sado aquifer. In: Groundwater Quality: Remediation and Protection. Proc. conference, Prague. pp 39-47

Strehlau K (1990) Facies and genesis of Carboniferous coal seams of Northwest Germany. Int J Coal Geol 15:245-292

Teng Y, Hu B, Zheng J, *et al* (2018) Water quality responses to the interaction between surface water and groundwater along the Songhua River, NE China. Hydrogeol J 26:1591-1607

Wisotzky F (2017) Water chemistry of the "Erbstollen" waters in the southern Ruhr area. In: Korrespondenz Wasserwirtschaft (KW), p 10 (in German)

Zieger L, Littke R, Schwarzbauer J (2018) Chemical and structural changes in vitrinites and megaspores from Carboniferous coals during maturation. Int J Coal Geol 185:91-102

Passive Treatment of AMD Using a Full-Scale Up-Flow Mussel Shell Reactor, Bellvue Coal Mine, New Zealand

Dave Trumm, James Pope, Hana Christenson

Verum Group, 97 Nazareth Avenue, Middleton, Christchurch 8041, d.trumm@verumgroup.co.nz

Abstract

This work presents the results of the first full-scale up-flow mussel shell reactor to treat AMD reported in the literature. In an up-flow configuration, the theory suggests that reducing conditions would be prevalent throughout the reactor, resulting in sulfate reduction and formation of sulfides rather than hydroxides which can reduce permeability with time in downflow reactors. The system raises the pH of the AMD from a median of 2.74 to a median of 6.94 and lowers metal concentrations by 97.2% (Fe), 99.8% (Al), 98.2% (Zn) and 97.0% (Ni). The benefits and challenges of up-flow reactors are discussed.

Keywords: Acid Mine Drainage, Passive Treatment, Mussel Shell Reactor, Bioreactor, Sulfides

Introduction

Incorporation of waste products is used whenever possible in passive treatment systems to minimise the cost of acid mine drainage (AMD) treatment (Gusek 2002, Younger *et al*. 2002, Watzlaf *et al*. 2004). Native to New Zealand, the Greenshell Mussel (*Perna canaliculus*) is the largest seafood export from New Zealand, which produces over 97,000 t per year at a revenue of over $380 m (Aquaculture New Zealand 2020, Stenton-Dozey *et al*. 2020). Much of the export is fully shelled mussels, producing approximately 68,000 t of shell waste annually (approximately 30% of the shellfish weight is meat). Although some of the waste is used as a lime amendment by the agricultural industry, much of it ends up in landfills. Research in New Zealand has shown that this waste product is useful in the treatment of AMD.

Since 2007, waste mussel shells have been used as alkalinity amendments in numerous experiments with bioreactors (McCauley *et al*. 2009, Mackenzie 2010, Mackenzie *et al*. 2011, Uster *et al*. 2015), and were used in full-scale construction of a mussel shell reactor with no organic amendments at the Stockton Coal Mine (Weber *et al*. 2015, Diloreto *et al*. 2016). Two additional full-scale reactors were constructed at other mines in New Zealand (unpublished). All the reactors were constructed with a downflow configuration. Research at the Stockton Coal Mine showed that metals are removed in distinct zones and in distinct forms within the reactor, with the upper layers dominated by Fe hydroxide and Al hydroxide precipitates and the lower regions dominated by Zn and Ni sulfides (Weber 2015, Weisener *et al*. 2015). It was concluded that the waste mussel meat in the shells and other sea life (about 10% by mass) provide organic material for sulfate-reducing bacteria, and lower oxygen concentrations at depth result in the formation of metal sulfides.

The lifespan of mussel shell reactors is likely controlled by reduced permeability as the hydroxides accumulate in the upper layers of the reactor, and it is likely that precipitated sulfides may be oxidised and released as the oxidation front migrates downwards. Trumm *et al*. (2015) used a small-scale trial to show that if these reactors are constructed with an up-flow configuration, the incoming water encounters a highly reduced environment populated with iron reducing and sulfate reducing bacteria (FRB and SRB). The FRB reduce oxidised Fe in the water to reduced Fe and the SRB reduce the sulfate to hydrogen sulphide. The hydrogen sulphide then combines with the divalent metals to form insoluble metal sulfides. Dissolution of the shells results in pH increase and an increase in Ca concentration, which results in removal of Al through the precipitation of Al

hydroxide and some removal of Mn through the precipitation of Mn carbonate. Based on the results of Trumm *et al*. (2015) and Trumm *et al*. (2017), a full-scale up-flow mussel shell reactor was constructed at the abandoned Bellvue Coal Mine in New Zealand.

Methods

The abandoned underground Bellvue Coal Mine is in a relatively remote area of native forest with steep hillsides and deep gullies on the West Coast of New Zealand. The mine adit is on a steep slope (33° angle) approximately 25 m above nearby Cannel Creek. Prior to treatment, AMD discharged from the adit and cascaded down the slope, traversing a platform approximately 25 m by 15 m before joining Cannel Creek. Due to the limited area for a treatment system, it was decided to construct the reactor in tanks. The system consists of five 30,000 L plastic water tanks (3.7 m diameter, 2.5 m high), with associated alkathene piping and plastic valves to convey the AMD from the adit and distribute it equally to the base of each of the five tanks. The water enters each tank through perforated PVC and flows upwards through the treatment media, discharging through perforated PVC at the top of the tank and alkathene piping to Cannel Creek. Each tank is filled with approximately 24 m^3 of fresh mussel shells, broken into pieces approximately 5 cm long. The discharge piping is approximately 22 cm above the top of the shells, thereby maintaining a free water surface above the shells to ensure the reactor remains under reducing conditions.

The tanks were filled with AMD and left static for 10 weeks prior to operation to allow reducing conditions to establish and for FRB and SRB to populate the tanks. After start-up, site visits were conducted on 17 occasions over an 11-month period. During each visit, field parameters were measured, and water samples were collected from the inlet and the outlet of the system and from Cannel Creek upstream and downstream of the confluence with the treated AMD. Field parameters included temperature, pH, dissolved oxygen, conductivity, total dissolved solids, salinity, and oxidation-reduction potential. The water samples were submitted for laboratory analysis of total alkalinity, total ammoniacal nitrogen, nitrite nitrogen, nitrate nitrogen, dissolved reactive phosphorus, sulfate, dissolved organic carbon and dissolved metals (Ca, Fe, Al, Mg, Na, K, Mn, Zn, Sr, Ni, Co, Cr, Ba, Cu, As, Cd, V, Pb, Hg). For the first nine visits, the water samples were submitted from each individual tank; for the last eight visits, a single water sample was composited from the five tanks and submitted to reduce analysis costs.

Results

Mussel shell reactor

The flow rate through the system ranged from 0.16 to 1.23 L/s with an average of 0.62 L/s. The hydraulic residence time (HRT) in the system ranged from 19 to 152 h with an average of 39 h and a median of 34 h. The pH of the inlet water ranged from 2.54 to 2.94, sulfate concentrations ranged from 490 to 740 mg/L, and the average inlet dissolved metal concentrations were 46 mg/L Fe, 27 mg/L Al, 0.28 mg/L Zn, and 0.10 mg/L Ni. The treated water had a pH between 5.30 and 7.23 (median of 6.94) and had an average total alkalinity of 321 mg/L as $CaCO_3$. The treated water average dissolved metal concentrations were 1.5 mg/L Fe, 0.047 mg/L Al, 0.010 mg/L Zn, and 0.0063 mg/L Ni (fig. 1). Regulatory discharge limits in New Zealand are determined on a site-specific basis by risk analysis; they have not been determined for this site. The system removed an average of 97.2% of the Fe, 99.8% of the Al, 98.2% of the Zn, and 97.0% of the Ni and is correlated with HRT (fig. 2). Sulfate concentrations decreased an average of 116 mg/L through the reactor.

Ammonia concentrations in the inlet water ranged from 0.27 to 0.50 mg/L (0.35 mg/L average) and in the outlet ranged from 1.2 to 54 mg/L (10 mg/L average). The highest concentration was detected on the day the system was started and the concentration had declined to 1.25 mg/L seven days later. An unexplained increase in concentration occurred 11 months later (to 32 mg/L). Nitrate plus nitrite concentrations in the inlet water ranged from below detection limits to 0.10 mg/L, and in the outlet water they ranged from below detection limit to

0.30 mg/L. As with the ammonia, the highest concentrations were detected on the day the system was started.

Cannel Creek

The pH of Cannel Creek was raised from a previous median level of 3.1 to a median of 4.8 (ranging from 3.8 to 6.7). Alkalinity in the creek increased from a previous level of below detection limits to 15 mg/L as $CaCO_3$ (upstream alkalinity averages 12 mg/L as $CaCO_3$). Prior to installation of the treatment system the average dissolved metal concentrations in Cannel Creek were 6.98 mg/L Fe, 6.68 mg/L Al, 0.052 mg/L Zn, and 0.028 mg/L Ni (West 2014). After the system was started, the average dissolved metal concentrations in Cannel Creek were 0.82 mg/L Fe, 0.84 mg/L Al, 0.020 mg/L Zn, and 0.012 mg/L Ni. Average dissolved metal concentrations in Cannel Creek upstream of the confluence are 0.39 mg/L Fe, 0.14 mg/L Al, 0.0050 mg/L Zn, and 0.0012 mg/L Ni. Ammonia in Cannel Creek increased from an upstream average concentration of 0.30 mg/L (ranging from 0.010 to 1.0 mg/L) to a

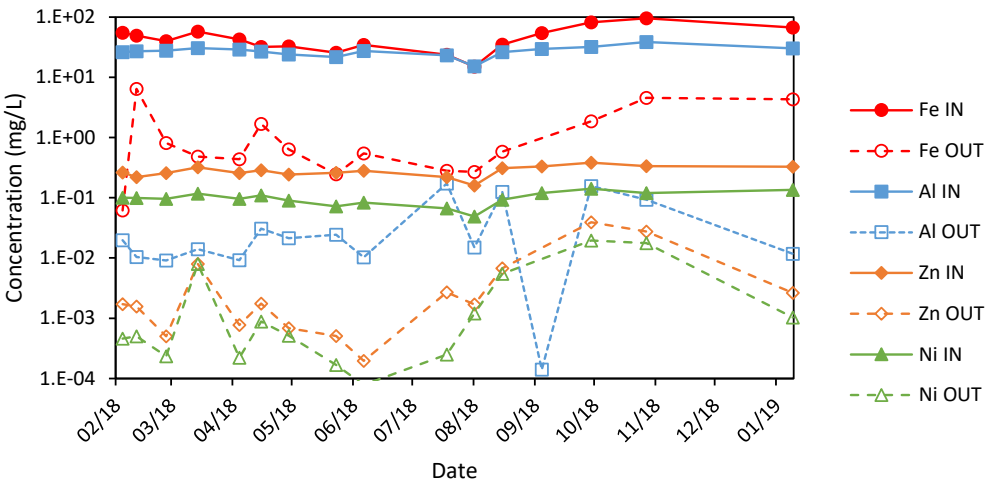

Figure 1 *Dissolved metal concentrations for mussel shell reactor. IN, inlet concentrations; OUT, outlet concentrations.*

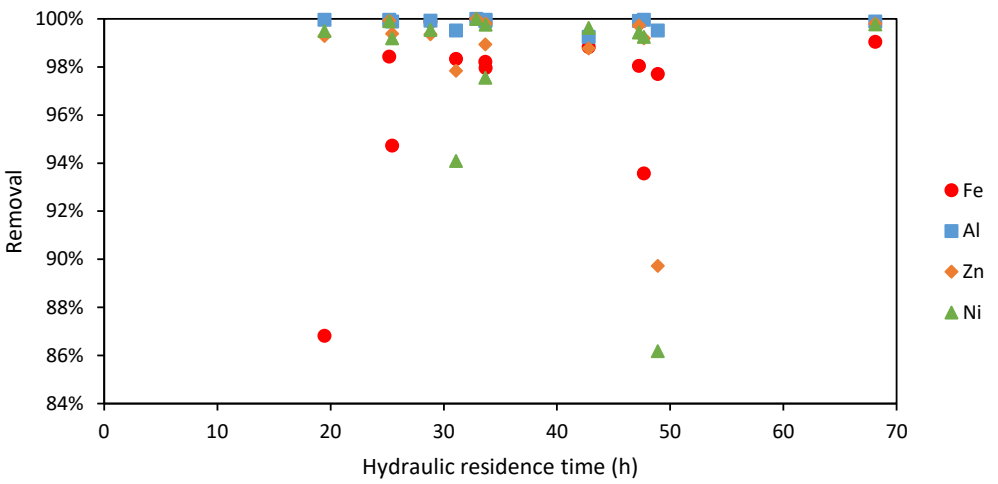

Figure 2 *Percent removal of dissolved metal concentrations in mussel shell reactor.*

downstream average concentration of 0.49 mg/L (ranging from 0.13 to 1.8 mg/L). Nitrate plus nitrite increased from an upstream average concentration of 0.0014 mg/L (ranging from below detection limits to 0.0090 mg/L) to a downstream average concentration of 0.037 mg/L (ranging from below detection limits to 0.16 mg/L).

Discussion

Mussel shell reactor

The treatment system at the Bellvue Coal Mine is the first full-scale up-flow mussel shell reactor in New Zealand (and in the published literature). The results of the Bellvue reactor suggest that an up-flow configuration can be successful at sulfate reduction and removal of metals through the formation of metal sulfides. Treatment effectiveness was similar to the up-flow mussel shell reactor documented for the small-scale trials in Trumm *et al.* (2015). In that system, metal removal percentages, compared to the Bellvue Mine treatment system, were 96-99% Fe (97.2% for Bellvue), >99% Al (99.8% for Bellvue), 98-99% Zn (98.2% for Bellvue) and 95-99% Ni (97.0% for Bellvue). Furthermore, the HRT at Bellvue (19-152 h) was less than that at the other system (40-675 h), suggesting better overall treatment effectiveness at the Bellvue reactor.

Although analysis of metal precipitates has not yet been completed for the reactor, observations during sampling suggest that Fe and divalent trace elements such as Zn and Ni are likely being removed as sulfides. During sampling events, there is a noticeable odour of hydrogen sulfide and a hand-carried hydrogen sulfide gas detector records elevated levels of hydrogen sulfide (often triggering the alarm for dangerously high levels). In addition to this, when drain valves at the base of the reactor tanks are opened briefly, the colour of the water and sediment is black and a noticeable hydrogen sulfide smell is evident. The results of sulfate analyses also support the contention that sulfate reduction is occurring. Future analyses will include XRD and SEM/EDS techniques to determine if sulfides are formed in the reactor.

Aluminium will likely form hydroxides in the reactor, which, along with the accumulation of metal sulfides, may limit permeability with time. The system has been operating for three years as of the date of this publication, and it now requires additional head pressure to maintain flow through the reactor, suggesting that accumulated of precipitate is reducing permeability. Each tank is equipped with a flushing valve at the base. Plans are underway to conduct the first flush of the system through these valves to remove the precipitates.

Cannel Creek

Data show that there has been an improvement in the water chemistry in Cannel Creek since installation of the system. Previously low pH levels, absence of alkalinity, and elevated dissolved metal concentrations are now replaced with pH levels, alkalinity, and dissolved metal concentrations more similar to background levels upstream of the confluence with the AMD. Compared to pre-treatment conditions, the Fe concentration is two times greater than background (previously it was 18 times greater), Al is six times greater (previously it was 48 times greater), Zn is four times greater (previously it was 10 times greater), and Ni is 10 times greater (previously it was 23 times greater).

Although the pH levels ranged from 3.8 to 6.7 in Cannel Creek post treatment, all the low pH levels occurred when flow rate through the system was hampered by build-up of sticks and leaves in the inlet piping. If those data points are removed, the pH level in Cannel Creek ranged from 4.7 to 6.7. Geochemical modelling work by Trumm *et al.* (2017) predicted the pH in Cannel Creek may range from 4.2 to 6.0 post treatment (related to asymmetric response of flow rates in the AMD vs. the creek during precipitation events), which is similar to the documented results to date. Future work to prevent blockages will ensure that pH levels remain elevated in Cannel Creek compared to pre-treatment levels.

Prior to installation of the system, there was concern about potential discharge of ammonia from the system. Since treatment in up-flow mussel shell reactors is primarily through sulfate reduction and formation and sequestration of metal sulfides, the

discharge water from these systems is largely anoxic. During the early stages of operation, significant ammonia may be discharged from the system under these anaerobic conditions. Small-scale up-flow mussel shell reactor trials by West (2014) found initial concentrations of total ammoniacal nitrogen exiting the systems were at concentrations of up to 100 mg/L; however, these concentrations decreased to approximately 50 mg/L within two months of operation and to approximately 5 mg/L three months after start-up. Within four months after start-up, concentrations had decreased to between 1 and 3 mg/L. The New Zealand guidelines for protection of freshwater and marine ecosystems specify ammonia trigger level concentrations according to pH (ANZG 2018). For the expected maximum discharge pH of 7 from the mussel shell reactors, the specified ammonia trigger level for protection of 95% of species of the freshwater ecosystem is 2.18 mg/L. The data for the full-scale Bellvue treatment system shows that although the ammonia concentration in the reactor outlet occasionally exceeds this level, once diluted in Cannel Creek, concentrations are below the threshold. Oxidation of the water occurs as it flows down a channel to Cannel Creek.

As a result of the success of the small-scale trials documented in Trumm *et al*. (2015) and the success of the treatment system at the Bellvue Mine, two additional full-scale up-flow mussel shell reactors have been installed in New Zealand, both at active coal mines. One of the systems is a 1,000 m^3 up-flow reactor and the other is a 3,000 m^3 up-flow reactor. Data to date show both reactors are effectively treating AMD through sulfate reduction and formation of metal sulfides.

Conclusions

The first full-scale mussel shell reactor with an up-flow configuration was installed at the abandoned Bellvue Coal Mine on the West Coast of New Zealand. In an up-flow configuration, the theory suggests that reducing conditions would be prevalent throughout the reactor, resulting in sulfate reduction and formation of Fe sulfides rather than Fe hydroxides which can reduce permeability with time in downflow reactors. Furthermore, the reactors can be constructed with a flushing mechanism so that accumulated Al hydroxides and the metal sulfides can be removed periodically.

The inlet water chemistry to the system had a pH of 2.54 to 2.94, sulfate concentrations of 490 to 740 mg/L (average of 643 mg/L), and average dissolved metal concentrations as follows: Fe (46 mg/L), Al (27 mg/L), Zn (0.28 mg/L), and Ni (0.10 mg/L). Residence time in the system ranged from 19 to 152 h (an average of 39 h). The pH increased through the reactor to a level between 5.30 and 7.23 (median of 6.94) and the alkalinity increased by an average of 321 mg/L as $CaCO_3$. Average metal removal percentages through the reactor were as follows: Fe (97.2%), Al (99.8%), Zn (98.2%), and Ni (97.0%). Sulfate concentrations were reduced by an average of 116 mg/L. Reduction of sulfate concentrations through the reactor, the presence of hydrogen sulfide at the outlet and base of the reactor, and the lack of red iron oxide precipitates in the outlet and base of the reactor suggest that sulfate reduction and metal sulfide precipitation are the dominant treatment mechanisms.

The water chemistry of the receiving stream, Cannel Creek, improved post treatment. A previous median pH of 3.1 was raised to a median of 4.8, alkalinity was increased to an average of 15 mg/L of $CaCO_3$, and dissolved metal concentrations were reduced as follows: Fe (by 88%), Al (by 87%), Zn (by 62%) and Ni (by 52%). Low pH events in the creek correspond to times when the inlet piping to the reactor were blocked by sticks and leaves. Better management of the system is now preventing this occurrence. As a result of the successful system at the Bellvue Coal Mine, two additional full-scale up-flow mussel shell reactors have been constructed at two active coal mines in New Zealand.

Acknowledgements

This research was financed by the Ministry for Business, Innovation and Employment, contract CRLE 1403 and the Coal Association of New Zealand. We thank Ngati Hako, Ngatiwai, Ngai Tahu, West Coast Regional Council (WCRC), Waikato Regional Council, Northland Regional Council, Department of Conservation (DOC),

Straterra, Minerals West Coast, OceanaGold, Solid Energy of New Zealand, Francis Mining Group and Bathurst Resources for their involvement and support for the research programme. We thank the WCRC for the resource consent to install and operate the treatment system, the DOC for the research permit, Geotech Limited for blasting activities for road installation, and the volunteer students and teachers from Tai Poutini Polytechnic (Greymouth) for help with the system installation. Access to the mine sites was provided by MBD Contracting and Solid Energy New Zealand. More information on the Centre for Minerals Environmental Research (CMER), including research currently being undertaken, is available at: https://www.cmer.nz.

References

ANZG 2018. Australian and New Zealand Guidelines for Fresh and Marine Water Quality. Australian and New Zealand Governments and Australian state and territory governments, Canberra ACT, Australia. Available at www.waterquality.gov.au/anz-guidelines.

Aquaculture New Zealand 2020. Aquaculture New Zealand – The World's Best Seafood. https://www.aquaculture.org.nz.

Crombie FM, Weber PA, Lindsay P, Thomas DG, Rutter GA, Shi P, Rossiter P, Pizey MH (2011) Passive treatment of acid mine drainage using waste mussel shell, Stockton Coal Mine, New Zealand. In: Bell LC, Braddock B (Eds), 2011 Proceedings of the Seventh Australian Workshop on Acid and Metalliferous Drainage, Darwin, Northern Territory. 21-24 June 2011, Brisbane, pp. 393-405.

Diloreto Z, Weber P, Olds W, Pope J, Trumm D, Chaganti SR, Heath D, Weisener CG (2016) Novel cost-effective full-scale mussel shell bioreactor for metal removal and acid neutralization. J of Environmental Management 183:601-612.

Gusek J (2002) Sulfate-reducing bioreactor design and operating issues: is this the passive treatment technology for your mine drainage? In: Proceedings of the 2002 National Association of Abandoned Mine Land Programs Annual Conference. Park City, Utah. 15-18 September 2002.

Mackenzie A (2010) Characterization of Drainage Chemistry in Fanny Creek Catchment and Optimal Passive AMD Treatment Options for Fanny Creek, Unpublished M.Sc. thesis, University of Canterbury, Department of Geological Sciences.

Mackenzie A, Pope J, Weber P, Trumm D, Bell D (2011) Characterisation of Fanny Creek catchment acid mine drainage and optimal passive treatment remediation options. In: Proceedings of the 43rd annual conference, New Zealand Branch of the Australasian Institute of Mining and Metallurgy.

McCauley CA, O'Sullivan AD, Milke MW, Weber PA, Trumm DA (2009) Sulfate and metal removal in bioreactors treating acid mine drainage dominated with iron and aluminum. Water Research 43:961–970.

Stenton-Dozey JME, Heath P, Ren JS, Zamora LN (2020) New Zealand aquaculture industry: research, opportunities and constraints for integrative multitrophic farming, New Zealand Journal of Marine and Freshwater Research, DOI: 10.1080/00288330.2020.1752266.

Trumm D, Ball J, Pope J, Weisener C (2015) Passive treatment of ARD using mussel shells – Part III: Technology improvement and future direction. 10th International Conference on Acid Rock Drainage, April 20-25, 2015, Santiago, Chile.

Trumm D, Pope J, West R, Weber P (2017) Downstream geochemistry and proposed treatment – Bellvue Mine AMD, New Zealand. 13th International Mine Water Association Congress, Rauha, Lappeenranta, Finland, 25-30 June 2017, pp 580-587.

Uster B, O'Sullivan AD, Ko SY, Evans A, Pope J, Trumm D, Caruso B (2015) The Use of Mussel Shells in Upward-Flow Sulfate-Reducing Bioreactors Treating Acid Mine Drainage. Mine Water Environ 34:442–454, doi:10.1007/s10230-014-0289-1.

Watzlaf G, Schroeder K, Kleinmann R, Kairies C, Nairn R (2004) The passive treatment of coal mine drainage. Information Circular. National Energy Technology Laboratory, US Department of Energy, 72 p.

Weber P, Weisener C, Diloreto Z, Pizey MH (2015) Passive treatment of ARD using waste mussel shells – Part I: System development and geochemical processes. 10th International Conference on Acid Rock Drainage, April 20-25, 2015, Santiago, Chile, pp 1204 -1213.

Weisener C, Diloreto Z, Trumm D, Pope J, Weber P (2015) ARD passive treatment using waste mussel shells- Part II: System autopsy and biogeochemical investigations. 10th International Conference on Acid Rock Drainage, April 20-25, 2015, Santiago, Chile, pp 1204 -1213.

West R (2014) Trialling small-scale passive systems for treatment of acid mine drainage: A case study from Bellvue Mine, West Coast, New Zealand. Master's Thesis, Department of Geological Sciences, University of Canterbury, Christchurch, New Zealand.

Younger P, Banwart S, Hedin R (2002) Mine water: hydrology, pollution, remediation. Kluwer Academic, London, 442 p.

Assessing heavy elements in tailings water around a Uranium mine in Namibia

Vera Uushona[1,2], Manny Mathuthu[1]

[1]*Center for Applied Radiation Science and Technology (CARST), North-West University (Mafikeng), Cnr Albert Luthuli Road and University Drive, 2735, Mmabatho, South Africa, nvuushona@yahoo.com, Manny.Mathuthu@nwu.ac.za*

[2]*National Radiation Protection Authority of Namibia, Ministry of Health and Social Services, Harvey Street, Namibia*

Abstract

The study investigated the concentration of heavy elements in ground water and process water from the tailings of a uranium mine in Namibia. Inductively Coupled Plasma Mass Spectrometry was used to evaluate the concentration of heavy metals. Tailings water had higher average concentration of elements compared to ground water. The concentration of uranium in the ground water was above 15 µgl-1 and 30 µgl-1 as set by WHO and USEPA This shows that the ground water near the uranium mine is toxicologically not fit for human consumption.

Keywords: Uranium Mine, Tailings Water, Ground Water, Heavy Elements, ICP-MS

Introduction

IMWA2021 Mining and processing of minerals is a key economic activities that contributes to the growth and development of economies of nations. At the same time, mining also produces huge amount of waste that contributes to environmental contamination to the nearby communities by releasing heavy elements to the air, soil and water both surface and ground water (Sracek *et al*., 2012, Olawuyi and Mudashir, 2013, Madzunya *et al*., 2020).

Heavy elements are present in the environment and some are vital for living organisms including human but can be toxic at higher concentrations (Singh *et al*., 2011). Heavy elements are not broken down and thus transferred to humans through food, water, soil or air. The toxicity of the metals is depended on the type of metal, the dose taken and whether the exposure was chronic or acute (CSIR, 2008). Heavy elements such uranium, potassium, strontium, chromium, Manganese and Thorium are geochemically classified as lithophilic metals, while Zinc metal and Arsenic share the Chalcophile/ Lithopilic nature which is signified by their bioaccumulation in the human tissue thus becoming chemo-toxic.

A major concern of mining is acid drainage, that occurs when acids such as sulphuric are added during the mining process and has potential to may pose a long-term devastating impact on rivers, streams and aquatic life. These acids/toxic chemicals are carried through to the tailings dam. When the tailings fail, the seepage can end up in the ground water systems/aquifer to communities in the downstream (Kamunda *et al*., 2016).

The study aimed to measure the concentration levels of heavy elements in tailings process water and ground water. In this study, eight heavy elements, namely Sr, K, U, Mn, Zn, As, Cr and Th were included in the measurement.

Methods

The Study Area

The study area is the Erongo region, situated in Western part of Namibia, arid Namib desert. It lies between -23° 06' 60.00" S latitude and: 14° 51' 59.99" E longitude. The region is rich in various mineralisation such as Gold, Uranium and Lead. Uranium mineralisation was discovered in 1928 (MME, 2010) (MME, 2010). Due to confidentiality agreements signed, the exact location where samples were collected cannot be disclosed. See Figure 1.

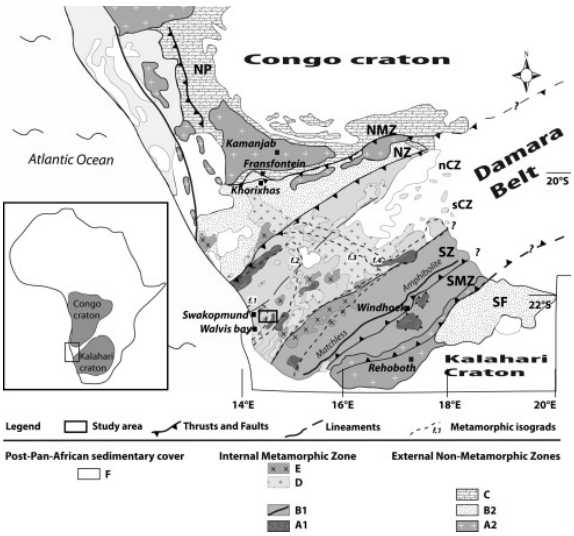

Figure 1 *Location of the Damara orogenic belt between the Congo and Kalahari cratons (Toé et al., 2013).*

Sample collection, preparation and analyses

Twenty samples were collected, 10 ground water and 10 process water from the tailings. The samples were collected in one-litre polyethylene water bottles. The bottles were rinsed with distilled water prior to filling. The samples were treated with 1% Nitric acid. The samples were transported to the Analytical Laboratory at the Centre for Applied Radiation Science and Technology (CARST) for analysis

At the laboratory water samples were filtered utilizing a Whatman No. 41 filter paper to remove any particles. 5 mL of the sample was mixed with 1 mL of 70% of HNO_3 and deionized water was added to fill up to the 10 mL.

The concentrations of uranium and heavy elements were analysed using an Inductively Coupled Plasma Mass Spectrometer (ICP-MS) PerkinElmer NexION 2000, total quant method. The multi-element standard by Perkin Elmer with a concentration of 10 mg/L and elements: Ag, Al, As, Ba, Be, Bi, Ca, Cd, Co, Cr, Cs, Cu, Fe, Ga, In, K, Li, Mg, Mn, Na, Ni, Pb, Rb, Se, Sr, Tl, U, V and Zn was used for calibrating the ICP-MS. The analysis was replicated three times. To check for contamination and drift, the instrument was set to measure blank solution and calibration standard at every 10 set of measurements (Kamunda *et al*., 2016, Madzunya *et al*., 2020). All the chemicals and reagents used were of certified analytical grade and procured from Merck (South Africa).

Results and Discussions

A total of 20 samples analysed for elemental concentration using ICP-MS. The concentrations of heavy metals ground and tailings water (µgL-1) are presented in Tables 1 and 2 respectively.

The average concentrations of heavy elements in the ground water decreased in the order of Sr>K>U>Mn>Zn>As>Cr>Pb>Th. The ranges in µgL-1 were as follow: Sr (2657.06-3216.08), U (121.77-221.26), Zn (6.24-101.02), Mn (29.03-142.46), As (6.43-8.35), Cr (5.26-10.11), Pb (3.35-9.10), Th (0.54-3.98) and K (16916.89-20694.52), respectively. Similarly, the average concentrations of heavy metal in the tailings water decreased in the order of U>Sr>Cr>As>Th. The ranges in µgL-1 were as follow: Sr (8.48-43.66), U (145682.13-239254.77), As (3159.30), Cr (38.27-59.28) and Th (12.40-19.28) respectively.

The results show that mine tailings had generally higher concentrations of of Sr, Cr, U and Th compared to ground water. This may have been caused by acid mine drainage that dissolves heavy metals into the ground

Table 1 Average elemental concentration of heavy metals (µgL-1) in ground water.

	Elemental concentration of heavy metals (µgL^{-1})								
Sample no	**Sr**	**U**	**Zn**	**Mn**	**As**	**Cr**	**Pb**	**Th**	**K**
1	2978.29	134.05	6.5	40.84	6.86	5.34	3.58	1.60	19216.44
2	3013.07	159.66	8.52	40.2	7.18	5.26	4.04	0.63	19436.21
3	3216.08	221.26	17.1	57.2	8.35	6.01	5.58	1.39	20694.52
4	3029.2	197.66	13.52	121.95	7.35	10.11	7.73	3.98	19900.11
5	2657.06	126.5	101.02	56.42	6.64	6.63	3.64	0.54	16916.89
6	2834.3	160.18	39.29	142.46	7.04	7.36	9.1	1.22	18844.53
7	2913.95	137.97	6.24	51.12	7.4	9.06	3.86	1.54	19057.2
8	2898.8	174.19	6.66	86.71	7.16	7.46	7.18	3.39	19028.55
9	2673.32	167.94	8.41	87.96	6.43	5.52	5.59	2.72	16953.45
10	2728.63	121.77	28.74	29.03	6.85	6.24	3.35	1.54	17742.57
Average	**2894.27**	**160.12**	**23.60**	**71.39**	**7.13**	**6.90**	**5.37**	**1.86**	**18779.05**
STDEV	**176.22**	**31.93**	**29.34**	**37.50**	**0.53**	**1.63**	**2.03**	**1.14**	**1227.81**
min	**2657.06**	**121.77**	**6.24**	**29.03**	**6.43**	**5.26**	**3.35**	**0.54**	**16916.89**
max	**3216.08**	**221.26**	**101.02**	**142.46**	**8.35**	**10.11**	**9.10**	**3.98**	**20694.52**

Table 2 The average elemental concentration of heavy metals (µgL-1) in tailings process water.

	Elemental Concentration (µgl^{-1})				
Sample No	**Sr**	**U**	**As**	**Cr**	**Th**
1	8.48	145682.13	3159.3	38.46	12.4
2	12.55	155069.06	3229.62	41.1	13.28
3	29.18	186777.79	3579.92	38.27	15.22
4	36.85	200893.93	4056.96	49.2	16.58
5	40.6	214212.05	4145.88	45.77	17.38
6	40.05	220455.95	4153.35	48.54	17.96
7	41.34	226964.59	4185.37	59.28	18.62
8	42.54	231980.74	3998.59	43.34	18.78
9	43.66	235766.00	3978.21	47.47	19.28
10	41.52	239254.77	3960.11	49.93	19.25
Average	33.68	205705.70	3844.73	46.14	16.88
STDEV	12.90	33349.54	382.99	6.31	2.48
min	8.48	145682.13	3159.30	38.27	12.40
max	43.66	239254.77	4185.37	59.28	19.28

(Madzunya *et al.*, 2020). As heavy metals concentrations in drinking water collected from Municipality water treatment plant did not exceed the stipulated limits by USEPA and DWAF and is toxicologically safe for the members of the public (Madzunya et al., 2020).

The concentration of uranium in the ground water was above 15 µgl-1 and 30 µgl-1 as set by World Health Organization (WHO)

and Unites States Environmental Protection Agency (USEPA) (WHO, 2004, USEPA, 2011), this is attributed to the fact the ground water is in a uranium rich province. Hence, based on the elemental concentration of U, the ground water from the study is not fit for human consumption as it exceeds the recommended limits. Equally, the water from tailings, if they mix with the ground water bodies, can cause significant toxicological to the ground water bodies

Conclusions

The study investigated the concentration of heavy metals in the ground and tailings water from uranium mine. The study concludes that the ground water around the uranium mine is toxicologically not safe for public drinking. The mine operators should ensure that adequate measures are in place to avoid seepage of tailing water into the ground water aquiver of the Erongo region. This can be achieved by ensuring that seepage control mechanism is effectively in place.

Acknowledgements

The authors thank the Technical student (Ms Naomi Dikeledi Mokhine) at the Centre for Applied Radiation Science and Technology, NWU, for assistance in all Analytical Laboratory analysis of samples

References

CSIR 2008. High Confidence Study of Children Potentially Affected by Radionuclide and Heavy Metal Contamination Arising from the Legacy of Mine Water Management Practices on the Far West Rand of South Africa, Project Concept Note. Council for Scientific and Industrial Research. Pretoria.

Kamunda, C., Mathuthu, M. & Madhuku, M. 2016. Health Risk Assessment of Heavy Metals in Soils from Witwatersrand Gold Mining Basin, South Africa. *Int J Environ Res Public Health*, 13.

Madzunya, D., Dudu, V. P., Mathuthu, M. & Manjoro, M. 2020. Radiological health risk assessment of drinking water and soil dust from Gauteng and North West Provinces, in South Africa. *Heliyon*, 6, e03392.

MME 2010. Strategic Environmental Assessment for the central Namib Uranium Rush. Windhoek, Namibia: Ministry of Mine and Energy.

Olawuyi, A. & Mudashir, R. 2013. Environmental and health impact of mining in Abara and Tungar Community of Anka Local Governement Area of Zamfara State, Nigeria. *Congress of Geological Society of Africa*. Addis Ababa, Ethiopia.

Singh, R., Gautam, N., Mishra, A. & Gupta, R. 2011. Heavy metals and living systems: An overview. *Indian journal of pharmacology*, 43, 246-253.

Sracek, O., Kříbek, B., Mihaljevič, M., Majer, V., Veselovský, F., Vencelides, Z. & Nyambe, I. 2012. Mining-related contamination of surface water and sediments of the Kafue River drainage system in the Copperbelt district, Zambia: An example of a high neutralization capacity system. *Journal of Geochemical Exploration*, 112, 174-188.

Toé, W., Vanderhaeghe, O., André-Mayer, A. S., Feybesse, J. L. & Milési, J. P. 2013. From migmatites to granites in the Pan-African Damara orogenic belt, Namibia. *Journal of African Earth Sciences*, 85, 62-74.

USEPA 2011. National Primary Drinking Water Regulations.

WHO 2004. Guideliness for Drinking Water Quality. Geneva: World Health Organization.

Acid Mine Drainage Precipitates at the Nanometric Scale – Properties and Environmental Role

Teresa Valente[1], Ana Barroso[1], Isabel Margarida Antunes[1], Patricia Gomes[1], Rita Fonseca[2], Catarina Pinho[2], Jorge Pamplona[1], Maria Amália Sequeira Braga[1], Juliana P.S. Sousa[3]

[1]*Earth Sciences Institute, Pole of University of Minho, University of Minho, Campus de Gualtar, 4710-057 Braga, Portugal, teresav@dct.uminho.pt*

[2]*Earth Sciences Institute, Pole of University of Évora, University of Évora, Portugal, rfonseca@ueveora.pt*

[3]*International Iberian Nanotechnology Laboratory, Av. Mestre José Veiga s/n 4715-330 Braga, Portugal, juliana.sousa@inl.int*

Abstract

The mineral-water interactions responsible for mobilization of dissolved toxic elements in mine drainage often generate colloids that commonly occur at the nanometric scale. This study presents typical properties of these materials, mostly composed by iron-rich products. The samples were obtained in a variety of contexts, representing mine waters as well as natural acid rock drainage. It concludes by noting the potential influence of the waste and/or the host rocks on the hydrogeochemistry of the systems. Further, the water properties could control the morphology and mineralogy of this very fine material, and consequently its environmental role.

Keywords: Colloids, Nanoparticles, Iron-Rich Precipitates, Morphology, Arsenic

Introduction

The mineral-water interaction processes that generate acid mine drainage (AMD) often contribute to the complete degradation of the ecosystems (Gomes *et al*., 2020). In addition to the classical problems associated with the presence of dissolved potentially toxic elements (PTE), production of colloids (Wolkersdorfer *et al*., 2020), especially in the most iron-rich waters, is a typical aspect in AMD. These colloidal particles, often denominated precipitates of mine drainage, ochre-precipitates or AMD-precipitates (Rait *et al*., 2010), commonly occur at the nanometric scale (Waychunas *et al*., 2005). They represent another important environmental concern as they may be responsible for mobilization of toxic pollutants to long distances from the mining sources. But these micro and nanoprecipitates may also form in neutral and alkaline conditions, affecting the behavior of PTE in the leachates, mining soils and the receiving surface and underground aquatic systems (Vriens *et al*., 2020).

Characterization of these precipitates is a complex task due to aspects like heterogeneity, complexity of assemblages, and small dimensions of the nanoparticles. Therefore, insufficient knowledge about these complex natural mixtures could limit the applicability of first-principles of predictions. Thus, the present study aims to obtain mineralogical identification and detailed properties of nanoparticles resulting from the evolution of acid rock drainage (ARD) and mine waters, including neutral and acid mine drainage. Furthermore, geochemistry and morphology are discussed considering the potential ability to retain or promote the dispersion of contaminants, such as arsenic in the environment. Thus, the obtained results suggest that degree of crystallinity and surface properties associated with morphology may influence the resilience of the affected systems (water or soils) as these precipitates may contribute to the success of natural attenuation processes.

Figure 1 *Images of the sampling sites. a – Receiving stream of AMD from Valdarcas waste-dumps (NW Portugal); b – limestone channel in the passive treatment system of Jales mine (N Portugal); c – discharge of ARD from shallow groundwater in Serro (NW Portugal); d – discharge of AMD from Penedono waste-dumps (NE Portugal); e – stream affected by AMD in Campanario mine (Iberian Pyrite Belt, Spain); f – Receiving stream of AMD from São Domingos mine (Iberian Pyrite Belt, Portugal).*

Methods

Samples of ARD, mine waters, including AMD, and ochre-precipitates resulted from the evolution of these solutions were collected in different contexts. Fig. 1 shows images of the aquatic systems where sampling occurred. The sites were selected to cover a variety of paragenetic, climate, and environmental conditions. Another important idea was to represent sampling locations with a wide range of pH, in order to increase the possibility of distinguish different dominant types of nanoprecipitates. The location of sampling stations took in account the spatial heterogeneity of the AMD systems, defined from previous studies (Valente *et al.*, 2013; Prudêncio *et al.*, 2015; 2019; Valente and Pamplona, 2018; Gomes *et al.*, 2020).

Mine waters and ARD were characterized in the field for pH, electrical conductivity (EC), temperature, and redox potential with portable multiparametric equipment. Laboratory analysis was performed for sulfate by turbidimetry and acidity/alkalinity by volumetric titration. Inductively coupled plasma optical emission spectrometry (ICP-OES) was used for metals and arsenic in samples filtered (<0.45 µm) and acidified with HNO_3 *suprapur* and immediately refrigerated in the field.

The precipitates were collected at the bottom of the streambeds and in artificial structures, like drainage tubes, and limestone channels in passive systems. Fig. 2 shows sampling procedures, such as directly scrapping the substrate and collection the suspended flocculated material. These fluffy

Figure 2 *Sampling of precipitates in Acid Mine Drainage. a) Scrapping the substrate and b) slight agitation of the water for obtaining the flocculated material (fluffy precipitates).*

Table 1 *Properties of mine in consulted at Valente et al (2013)*; Gomes et al (2020) **; Valente et al (2019)#:, and Valente and Pamplona (2018)##.*

Site	pH	CE	SO4	Ac	Alk	As	Fe (mg/L)
Valdarcas (n = 12) V4*	3.15	1664	974	752	-	0.993	178
São Domingos (n = 4) P6**	3.33	1568	687	265	-	0.010	8.16
Campanario (n = 4)	2.74	3245	2320	1138	-	0.168	372
Reboleiro#	6.10	315	2.45	-	nd	64.8	180000
Serro##	3.80	433	179	152	-	0.150	0.140
Jales (n = 4)	6.55	484	42.4	-	146	34.6	143

precipitates were concentrated by centrifugation at 4000 rpm. The other samples were sieved with a 20 μm stainless sieve and washed with MilliQ water. They were dried at room temperature and analyzed by X-ray diffraction (XRD), scanning and transmission electron microscopy (SEM/TEM), and Fourier-transform infrared spectroscopy (FTIR).

Results and discussion

Mine waters and ARD properties

Table 1 shows the main properties of several waters from which nanoprecipitates are formed. They are in the range of pH of 2.74-6.55. The samples from Jales (Au-mine with arsenopyrite in quartz veins) were collected at the end of a limestone channel. Therefore the results reflect neutralization process, revealing alkalinity and high concentration of arsenic in agreement with the ore paragenesis. Reboleiro is mine water collected at the exit of a gallery of an abandoned U-mine. It was not submitted to any treatment, so the near neutral pH is a natural property. Serro is natural acidic shallow groundwater, as the sampled well was built in a sulfide-rich media, representing a case of ARD. All the other samples show typical features of AMD. Valdarcas has a special paragenesis, in which the sulfides coexist with calcite and chalcosilicate minerals from a skarn deposit (Valente *et al.* 2013). Therefore, the effluent should reveal this antagonistic chemistry of the wastes. However it was not enough to assure neutralization. Furthermore, even with addition of limestone along the creek after closure, the creek maintains pH and concentrations of acidity and sulfate in the range of AMD. São Domingos and Campanario are both in the Iberian Pyrite Belt (SW Europe). The low pH and high concentrations of sulfate and acidity are compatible with the abundance of massive sulfides and absence of minerals with neutralization ability.

Nanoprecipitates

The results indicate that precipitates from a variety of sites are oxyhydroxides and hydroxysulfates, mostly with low crystallinity or even amorphous (Fig. 3). XRD revealed the presence of ferrihydrite as the lowest crystalline phase, with two weak and broad bands at 2.56 and 1.47 Å, corresponding to the 11 and 30 *hk* reflections of 2-line ferrihydrite. The combination of methods – XRD, SEM, FTIR and TEM allowed confirming identifications and observing morphological features (Fig. 3).

Goethite, schwertmannite and jarosite were identified in the sites with typical AMD hydrochemical characteristics as already referred by other authors (e.g., Stoffregen *et al.*, 2000). For example, at Valdarcas and Campanario the ochre precipitates are often mixtures of these three minerals, but with dominance of schwertmannite. On the contrary, schwertmannite is rare at São Domingos, where jarosite is the dominant phase. Weakly crystalline goethite was the only ochre-precipitate identified in ARD, also in accordance with the pH <4 (Bigham *et al.*, 1996).

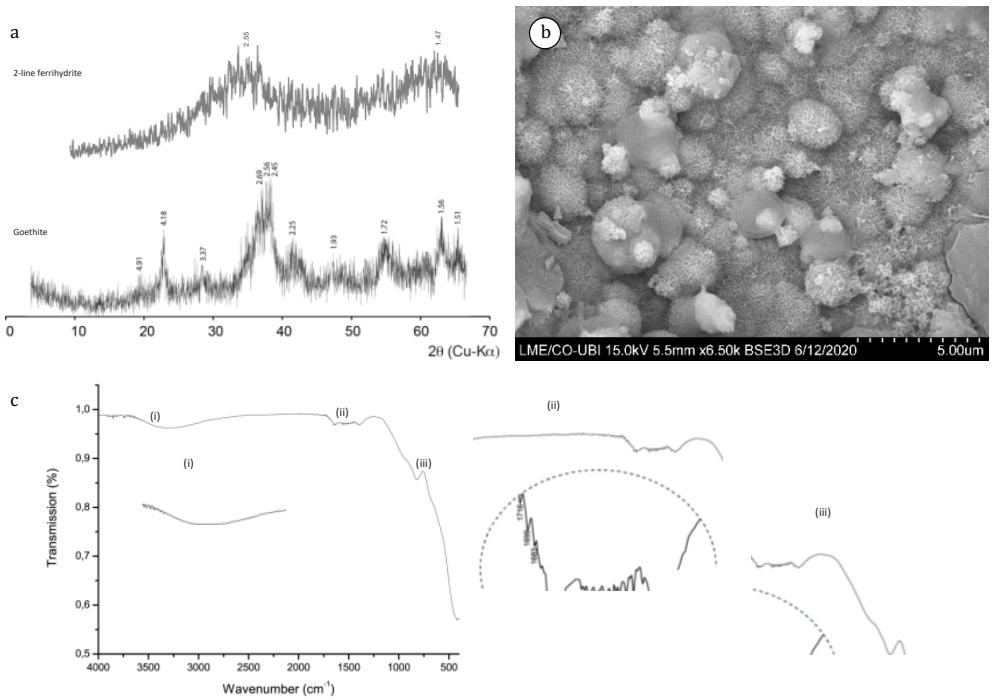

Figure 3 *Examples of identified phases in the ochre precipitates a - XRD analyses revealing patters of weakly crystalline goethite in ARD of Serro and ferrihydrite in Jales; b – typical pin-cushion morphology of schwertmannite in a sample from Campanario (SEM image); c – FTIR, showing the typical bands of ferrihydrite (Fh) in Jales.*

The typical globular aggregates observed in SEM and TEM as well as the analyses of the FTIR spectra (Fig. 3c) confirm the occurrence of ferrihydrite only at Jales and Reboleiro. This result suggests the control of hydrochemistry, and special of the pH, over the mineralogy of the precipitates. In accordance with Bigham *et al.* (1996) ferrihydrite was identified in the sites with higher pH, in the range of 6-7 (Tab. 1). FTIR patterns allowed or confirmed identifications of low crystalline and amorphous compounds, showing the coexistence of different iron-rich minerals in the nanoprecipitates (Gadsen, 1975). The vibration bands centered at 420 and 819 cm^{-1} suggest the presence of arsenic-rich compound (Rout *et al*., 2012), indicating the role of ferrihydrite in retaining As.

Less crystalline or even amorphous compounds were identified by TEM in Penedono samples (Fig. 4). As already referred by Valente *et al.* (2015), iron and arsenic-rich nanoprecipitates appear with spherical shapes, often associated with jarosite and clay minerals. Therefore, these nanoparticles are also fixing the arsenic in the waste dumps, and so limiting the mobilization of this toxic element to the aquatic environment.

Conclusion

Schwertmannite, ferrihydrite, and goethite were the most common identified low-crystallinity minerals. Different morphologies were observed, but there is a predominance of spherical and tubular aspects. The occurrence of these phases, pure or as complex mixtures, depend mainly on the hydrochemistry conditions. FTIR and TEM put in evidence the occurrence of the most weakly and amorphous crystalline phases. Their composition indicates ability to retain arsenic.

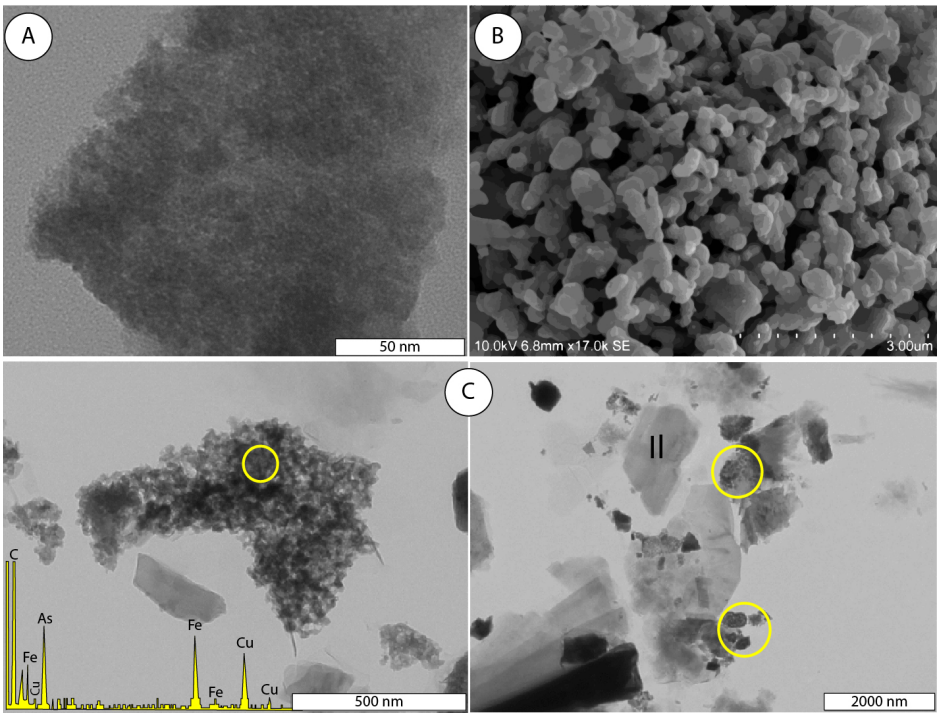

Figure 4 *Images of ochre precipitates A, B – TEM and SEM micrographs of a 2-line ferrihydrite; C – TEM micrographs and EDS spectrum of iron and arsenic-rich nanoprecipitates, showing globular and spherical morphology (marked in yellow) associated with clay minerals; Il - Illite.*

Acknowledgements

This work was funded by FCT—Fundação para a Ciência e a Tecnologia through projects UIDB/04683/2020 and UIDP/04683/2020 and Nano-MINENV 029259 (PTDC/CTA-AMB/29259/2017).

References

Bigham JM, Schwertmann U, Traina, SJ, Winland, RL, Wolf, M (1996) Schwertmannite and the chemical modeling of iron in acid sulfate waters, Geochim. Cosmochim. Acta, 60: 2111–2121

Gadsden JA (1975) The infrared spectra of minerals and related inorganic compounds. London (Butterworths), 277 pp.

Gomes P, Valente T, Geraldo D, Ribeiro C. (2020). Photosynthetic pigments in acid mine drainage: Seasonal patterns and associations with stressful abiotic characteristics, Chemosphere, 239. doi: 10.1016/j.chemosphere.2019.124774

Prudêncio MI, Valente T, Marques R, Sequeira Braga MA, (2015) Geochemistry of rare earth elements in a passive treatment system built for acid mine drainage remediation. Chemosphere 138: 691-700, doi: 10.1016/j.chemosphere.2015.07.064

Rait R, Trumm D, Pope J, Craw D, Newman N, MacKenzie H (2010) Adsorption of arsenic by iron rich precipitates from two coal mine drainage sites on the West Coast of New Zealand, New Zealand Journal of Geology and Geophysics, 53: 177-193, doi: 10.1080/00288306.2010.500320

Rout K, Mohapatra M, Anand S (2012) 2-Line ferrihydrite: synthesis, characterization and its adsorption behaviour for removal of Pb (II), Cd (II), Cu (II) and Zn (II) from aqueous solutions. Dalton transactions, 41: 3302-3312

Stoffregen RE, Alpers CN, Jambor JL (2000) Alunite–jarosite crystallography, thermodynamics, and geochronology. In: Alpers, C.N., Jambor, J.L., Nordstrom, D.K. (Eds.), Sulfate Minerals: Crystallography, Geochemistry, and Environmental Significance. Reviews in

Mineralogy and Geochemistry 40. Mineralogical Society of America,Washington, D.C., pp. 453–479

Valente T, Ferreira MJ, Grande JA, de la Torre, Borrego J (2013) pH, electric conductivity and sulfate as base parameters to estimate the concentration of metals in AMD using a fuzzy inference system. J. Geochem. Explor., 124: 22-28.

Valente T, Gomes P, Sequeira Braga, MA, Dionísio A, Pamplona J, Grande JA (2015) Iron and arsenic-rich nanoprecipitates associated to clay minerals in sulfide-rich waste dumps. Catena, 1-13.

Valente T, Pamplona J (2018) Monitoring of a public water supply system: A case of groundwater contamination by acid rock drainage. 11th ICARD/IMWA – "Risk to Opportunity", (eds. Wolkersdorfer Ch, Sartz L, Weber A, Burgess J, Tremblay G), pp.751-756

Valente TM, Antunes IMHR, Braga MAS, Neiva AMR, Santos ACT, Moreno F. (2019). Mobility Control Of Uranium And Other Potentially Toxic Elements In Mine Waters By Ochre-Precipitates. IMWA2019 (eds. Wolkersdorfer Ch, Khayrulina E, Polyakova S, Bogush A), pp.452-467.

Vriens B, Skierszkan E, St-Arnault, Salzsauler K., Aranda C, Mayer U, Beckie R (2019) Mobilization of Metal(oid) Oxyanions through circumneutral Mine Waste-Rock Drainag. ACS Omega 4: 10205−10215, doi: 10.1021/acsomega.9b01270

Waychunas G, Kim C, Banfield J (2005) Nanoparticulate iron oxide minerals in soils and sediments: unique properties and contaminant scavenging mechanisms. J. Nanoparticle Res. 7: 409–433

Wolkersdorfer C, Nordstrom DK, Beckie RD, Cicerone DS, Elliot T. Edraki M, Valente T, França SC, Kumar P, Oyarzún Lucero RA, Soler i Gil A. (2020) Guidance for the Integrated Use of Hydrological, Geochemical, and Isotopic Tools in Mining Operations. Mine Water Environ 39: 204–228, doi: 10.1007/s10230-020-00666-x

Extension of Measuring Points Network for the Upper Aquifers of RAG Aktiengesellschaft Through the Drilling Pferdekamp

Christine von Kleinsorgen

RAG Aktiengesellschaft, Im Welterbe 10, 45141 Essen, Germany, christine.vonkleinsorgen@rag.de

Abstract

Before the planned rise of mine water, the existing measurement profiles "*Tiefe Pegel Mitte*" and "*Tiefe Pegel Ost*" of RAG Aktiengesellschaft needs to be expanded. Measuring points to monitor the hydrogeological status and the hydrochemistry in different groundwater levels, were created with which the water level before, during and after a rise in the mine water is monitored. For this purpose, the drillings Pferdekamp 1, 2 and 3 with depths of 780 m, 355 m and 90 m respectively were created in Marl, Germany at the former location of the Auguste Victoria mine shaft 8.

Keywords: Groundwater, Hydrochemistry, Hydrogeology, Mine Water

Introduction

The RAG AG mine water concept was design to reduce the locations of the central water management in the Ruhr area with a very high priority to human and environmental protection. The remaining locations are to be converted into well water retention systems. A rise of the mine water level is necessary to enable underground mine waterflow from the individual fields that have been dropped into the central water management system.

The state report on the subject "*Gutachten zur Prüfung möglicher Umweltauswirkungen des Einsatzes von Abfall- und Reststoffen zur Bruch-Hohlraumverfüllung in Steinkohlenbergwerken in Nordrhein-Westfalen, Teil 1*", also supports the evaluation of the RAG experts, that an increase in mine water significantly reduces the PCB emissions. The report deals with the storage of waste in mines under defined conditions. It concludes that waste contact with the increasing water-level, does not cause any detectable increase in substance flow and that a higher mine water level also helps in reducing the substance flow.

The plan is primarily to combine mine water provinces with underground mine water flow with a goal to relieve drainage water, especially the Emscher. The target mine water levels are selected primarily under the premise of maintaining a sufficient safety distance to the usable aquifers. Furthermore, by reducing the number of locations and their new pump levels, energy consumption will be minimized.

To carry out this task, the existing measurement profiles "*Tiefe Pegel Mitte*" and "*Tiefe Pegel Ost*" needs to be expanded. The measuring points are expected to record the hydrogeological situation in the various groundwater aquifers, preferably before, during and after the mine water rises.

Particularly, attention is paid to areas of drinkable water production in the northern part of the Ruhr. *Figure 1* shows the current mine water forecast with increasing water level below the distribution area of the Haltern-Formation. The construction of the new measuring points is planned to be completed in 2025. At that point in time, the mine water level is below the access area of drinkable water production within the Haltern-Formation at about *-800m NN* and in the An der Haard area at *-690 m NN*. Both the planned and existing measuring points should help clarify the question of whether there will be changes in the hydrogeological situation of the various groundwater aquifers during the rise in mine-water level. To do this, the groundwater levels in the respective aquifers must be observed and their chemistry analyzed.

The Pferdekamp boreholes supplements the existing "*Messprofil-Mitte*", which runs in the south-north direction from the

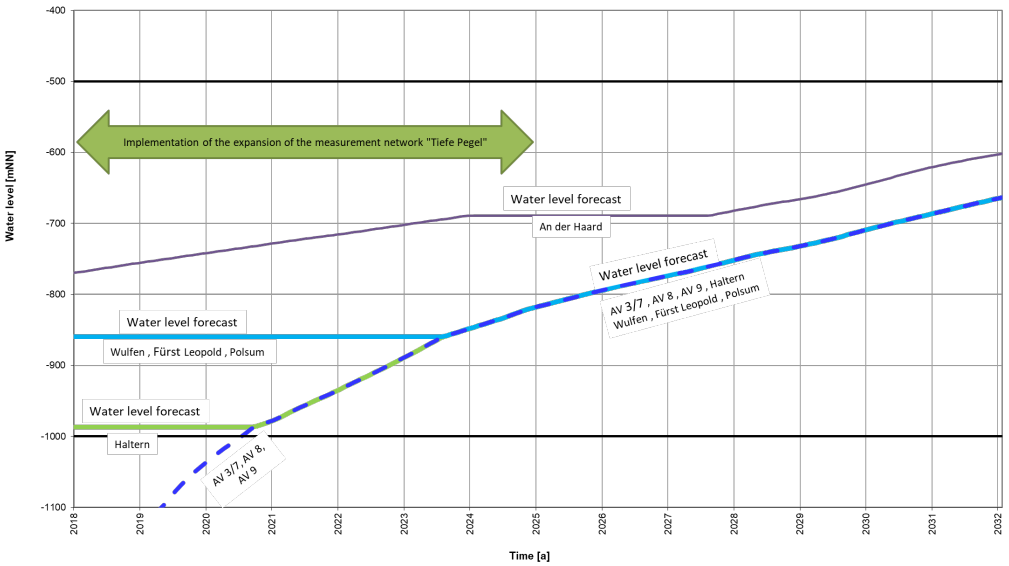

Figure 1 Mine-water level forecast below the distribution area of the Haltern-Formation.

Highway junction BAB A42 and A43 near Herne down to the Herten exit of the A43 Highway near Recklinghausen around the Marl location, in Germany.

Borehole

The boreholes for the groundwater measuring points were made in (Cretaceous-*Marl*) overburden with different depths. The underlying coal-bearing carbon of the hard coal deposit was not drilled as planned. The borehole of ***the groundwater measuring point Pferdekamp 1*** has a depth of 780 m and reaches the layers of the Cenomanium and Turonium of the Upper-Cretaceous (lower groundwater level of the overburden, *Figure 2*).

The borehole of ***the groundwater measuring point Pferdekamp 2*** has a depth of 355 m. The section 170 m to 270 m reaches the lower, fissured area of the aquifer close to the surface within the Recklinghausen-Formation. The groundwater measuring point was deepened to enable hydraulic tests to reach the level of the *Emscher-Marl*, with a non-conductive groundwater characteristic.

The borehole of ***the groundwater measuring point Pferdekamp 3*** has a depth of 90 m and reaches the upper part of the aquifer close to the surface.

To regenerate as much information as possible about the overburden, especially about the Emscher-Formation, while drilling, the *Pferdkamp 1* borehole was cored at a depth of 300 m (start of the Emscher-Formation). The cores are to be examined by the Georg Agricola University of Applied Sciences (THGA) to acquire more information's about the rock properties and permeability. Furthermore, a hydraulic test for horizontal permeability study was carried out in the drilling section of the Emscher-Formation, as well as some geophysical measurements (dual laterolog, electrical resistance, gamma ray, neutron neutron). The results of these measurements shall be linked to the results of the scientific investigations done by Georg Agricola University of Applied Sciences to gain further knowledge about the Emscher-Formation.

Geophysical measurements

The *Pferdkamp 2* bohrhole was drilled to a depth of 355 m. The first section of the drill ended at a depth of 170 m. Since the borehole was not proven stable enough up till this depth, a highly viscous mud with an appropriate density was used throughout the entire drilling operation, which only allows a limited

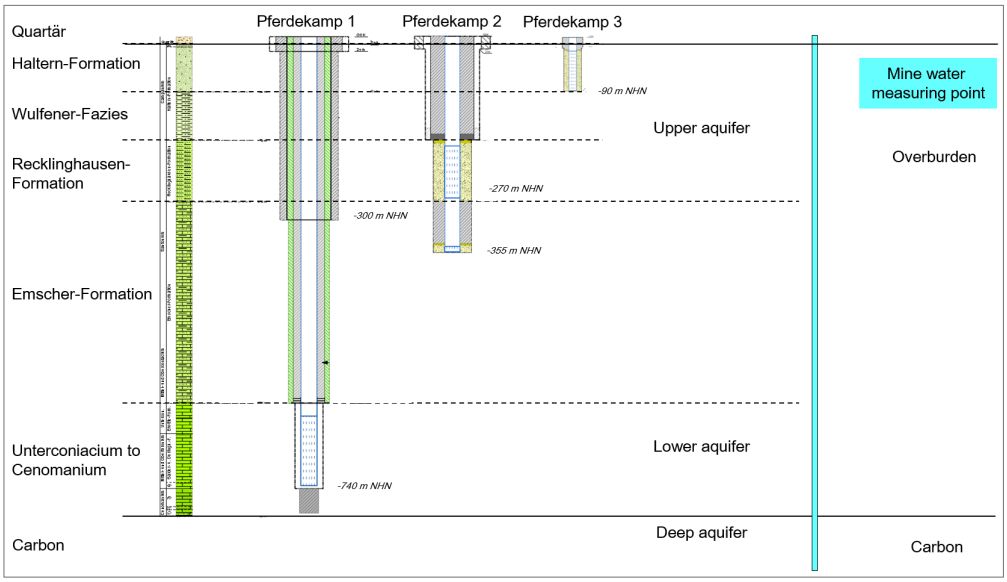

Figure 2 Expansion scheme and depth profile of the boreholes.

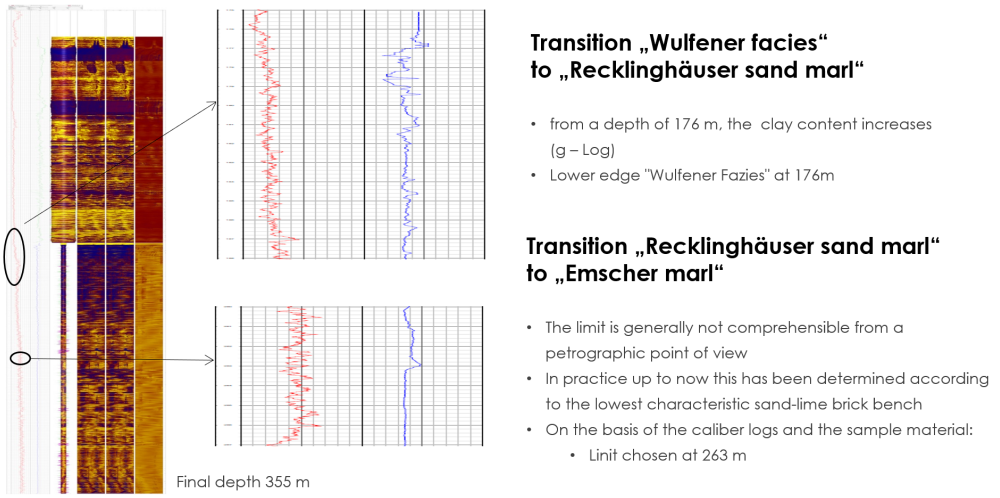

Figure 3 Geophsical result log (GR and ABI) (original LOG DMT, December 2019).

selection of geophysical measurements. To be able to verify the transitions of the different rock packages, the following geophysical measurements were carried out:

- Gamma - Ray - Log (GR)
- Acoustic Televiewer (ABI) with calculated caliber - log (CAL)

After completion of the measuring point, the integrity of the seal in the section 270 m to 340 m (Emscher-Marl section) had to be verified. For this purpose, a Cement Bond - LOG (CBL) was used for the verification in that depth range (270 m – 340 m).

The measurements result shows the following transitions within the rock layers (*see Figure 3*):

- Lower edge “Bottrop marl” at 28.5 m
- Lower edge “Haltern sand” at 98 m
- Lower edge “Wulfener facies” at 176 m
- Lower edge “Recklinghäuser sand marl” selected at 263 m.

The Pferdkamp 1 borehole was cored from *-300 m NHN* to the "*Essener greensand*" at *-780 m NHN* to get a complete overview of the geology at this point and information about the seals of the Emscher-Formation and its barrier effect. The cores were examined lithologically and petrographically and then made available to the Geological Service of North Rhine-Westphalia and THGA for further investigations.

THGA examines the cores with regards to their lithology / sedimentology and petrology. For that purpose, the following geological approaches had to be taken:

- Classical lithological approach
- Sedimentological recording
- Sedigraph / Laser particle sizer (Siliziklastika)
- Petrographic approach

In the petrophysical approach the mineral content, dry density, porosity, and permeability were determined though the results are currently pending.

During the drilling of the *Pferdekamp 1*, the following geophysical measurements were carried out around the Emscher-Formation:

- Dual Laterolog (DLL)
- Electrical resistance (EL-KN / EL-GN)
- Gamma Ray (GR)
- Neutron-Neutron (NN)

The electrical resistance measurements (EL-KN / EL-GN) and the inductive resistances (LLS / LLD) consistently show relatively low resistances of around 6 Ohm/m. The monotonous course of the curve indicates a bit differentiated but homogeneous mountain range. Same phenomenon was observed in the neutron-neutron measurements, which also indicate a homogeneous and monotonous layer sequence. Changes in level in the gamma ray measurements were used to characterize the existing *marl* sequence in detail. Sections were endured, which can be described as much clayey and chalky (*BLM 2020*).

Hydraulic tests

After the geophysical measurements, a single packer test was carried out and evaluated by *Solexperts GmbH* in depth area of about 548 m to 590 m to better describe the hydraulic parameters of the Emscher-Formation in its lower area.

The hydraulic parameters were determined using a multi-phase test procedure. After closing the interval by tensioning the packer, two pulse injection tests were performed. The experimental setup of the test is shown in *Figure 4*.

Cause the results of the evaluated curves vary by two to three orders in magnitude (*Table 1*), an inverse modeling of the measurement data was carried out with a programming tool called n-Sights. The modeling confirms the very low permeability rate of about .

According to *DIN 18130 (1989)*, the layers of the Emscher Marl, between 548 m and 590 m in depth, are classified as very low to almost impermeable. This confirms

Table 1 *Hydraulic test result (from Solexperts, 30.06.2020).*

Test- interval	Depth	Length	Test	T-Value	K-Value	Note
	m bgl	(m)	phase	(m^2/s)	(m/s)	
			PI1	1.1E-08	2.7E-10	A
				8.3E-12	2.0E-13	B
i1	548-590	42	PI2	2.1E-09	5.0E-11	A
				8.3E-12	2.0E-13	B
			n-Sights	**3.1E-11**	**7.4E-13**	-

PK1

Interval i1 => (548.00 -590.10m)

K = 7.4 ⋆10^{-13} ***m/s***

PSR: After installing the test system and including the interval, the pressure rises continuously. An approach to a static pressure level cannot be seen for 3.7 hours.

PI1: After reaching a pseudo-static pressure level after 73 minutes, the interval pressure rises again.

PI2: After approx. 4.3 hours an apparently steady pressure level can be seen again. The interval pressure then rises again continuously overnight, however, without reaching static conditions.

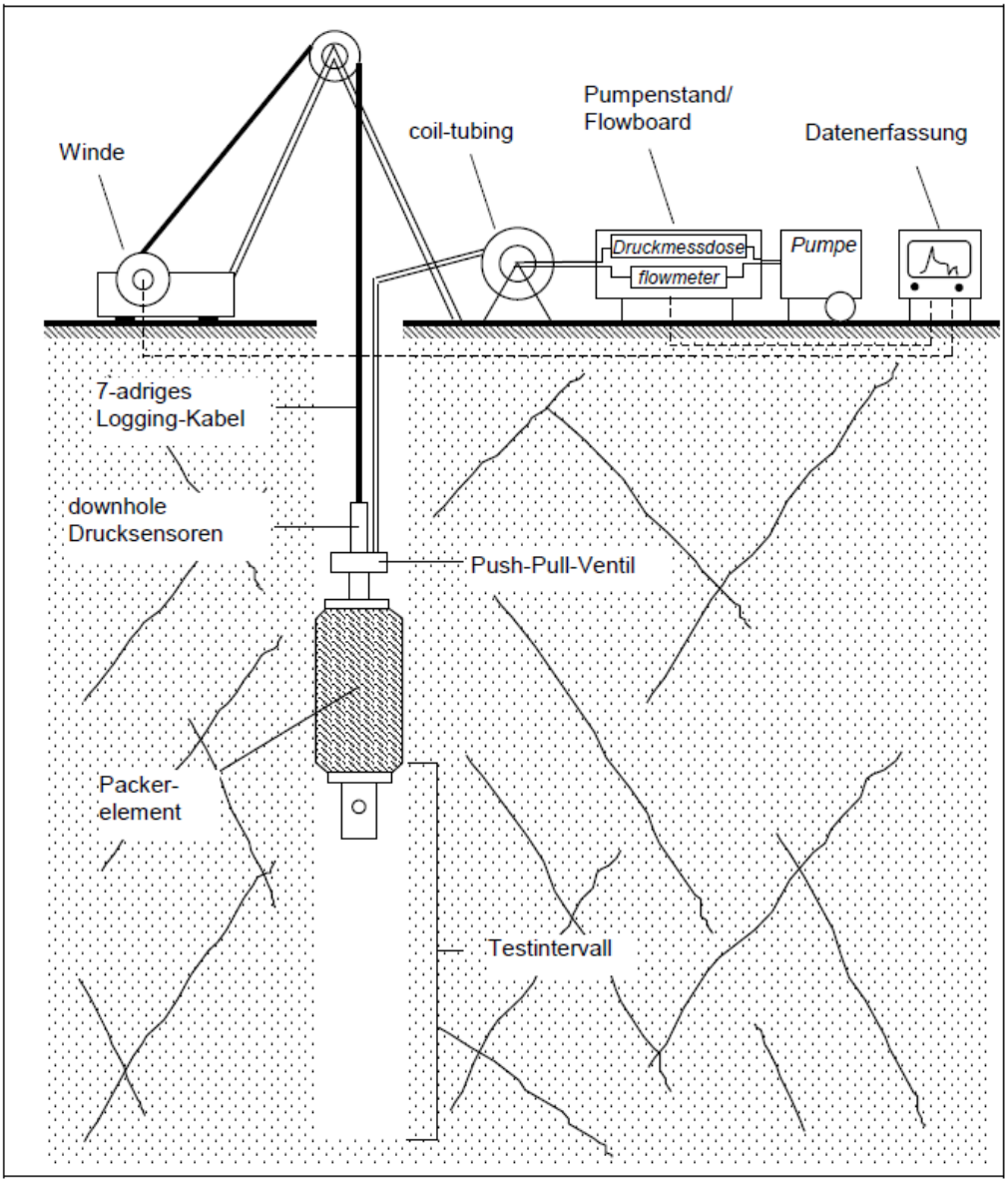

Figure 4 *Experimental setup of the hydraulic test with test equipments (from Solexperts, 06/03/2020).*

the information given in the literature of the Emscher-Formation as a low / non-conductive area.

In the future, a packer test to assess the vertical permeability of the upper section of the *Emscher Marl* is to be carried out at the Pferdekamp 2 measuring point (possibly be done by *Solexperts*, Bochum). For this purpose, in addition to the filter section within 170 m to 270 m depth, the measuring point has been equipped with a further filter section at 340 m to 355 m depth and a circumferential seal between 270 m and 340 m in depth. By placing a single packer at the level of the sealed area, a downward hydraulic gradient can be generated by pumping below the packer.

Based on observation of subsequent time-dependent increase in pressure, taking into consideration the water levels above the packer, a conclusion could be drawn on the vertical water- permeability of *Emscher Marl* in this section.

Conclusion

The Pferdekamp boreholes in Marl, Germany at the former Auguste Victoria Shaft 8 supplements the measuring system of RAG Aktiengesellschaft for observing various aquifers in the overburden, before, during and after the mine water rises. Not only the water level in the respective groundwater aquifers is observed, but also the hydrochemistry.

Furthermore, additional geophysical measurements and a hydraulic test showed that the Emscher formation is a very homogeneous and low to almost non-conductive rock layer.

This result shall be substantiated with a further hydraulic test for the vertical permeability in the upper section of Emscher-Formation and the scientific investigations done by Georg Agricola University of Technology.

References

GEOK GmbH, (2020) Herstellung der hydrogeologischen Bohrung Pferdekamp 1 und 2 zum Zwecke der Nutzung als Grundwassermessstelle für das Monitoring des Grubenwasseranstiegs der RAG Aktiengesellschaft

BLM, Gesellschaft für Bohrlochmessungen mbH, (2020) Dokumentation zu den geophysikalischen Bohrlochmessungen in der Bohrung PK1 in Marl

Solexperts GmbH, (2020) Hydraulische Versuche in der Bohrung Pferdekamp-1 Endbericht

Potash Dump Leachates – Challenges from Environmental Regulatory Requirements and Climate Change

Anne Weber[1], Antje Ulbricht[2], Alexander Müller[3], Astrid Gessert[3], Felix Bilek[2], Thomas Sommer[1]

[1]*Dresden Groundwater Research Centre e.V., Meraner Str. 10, 01217 Dresden, Germany, aweber@dgfz.de, ORCHID 0000-0003-2582-5327 , tsommer@dgfz.de*

[2]*GFI Groundwater Consulting Institute GmbH Dresden, Meraner Str. 10, 01217 Dresden, Germany, aulbricht@gfi-dresden.de, fbilek@gfi-dresden.de*

[3]*Lausitzer und Mitteldeutsche Bergbauverwaltungsgesellschaft mbH, Division Pottash-Spar-Ore, Am Petersenschacht 9, 99706 Sondershausen, Germany, Alexander.Mueller@lmbv.de, Astrid.Gessert@lmbv.de*

Abstract

In a German former potash mining district, highly saline leachates (120 g/L chloride) from three potash dumps are collected in a basin and discharged into the receiving river in a controlled manner. This work illustrates the increasing constraints but also obstacles towards management of saline dump leachate that does not rely on dilution. Besides dump covering, evaporation of leachate is considered the most promising approach to reduce salt load into surface water in the long term and is currently put forward. Here, linking energy and material fluxes on a local basis is pivotal during development of a feasible process.

Keywords: European Water Framework Directive, Germany, Circular Economy, Active Treatment, Evaporation

Introduction

Rich potash salt deposits in the German Southern Harz region have been mined since the 1890s. This contributed to the former German Democratic Republic (GDR) being the third largest potash producer in the world in the 1980s. Mining largely ceased in the wake of German reunification in 1990. Until now, however, deposits at six large potash mining dumps with a total volume of 177 million m^3 are affecting the environment in the Southern Harz region. Their highly saline leachates are characterized by chloride concentrations around 120 g/L and TDS 200 g/L. Since 1992 leachate collected from three of the dumps – Bischofferode, Sollstedt and, if not used for underground backfill, Bleicherode – and local industrial processing wastewater is directed into a basin in Wipperdorf. From there it is discharged into the receiving Wipper River in a controlled manner. In this way about 250.000 m^3 leachate, corresponding to about 30 kt chloride, is annually discharged to the Wipper River without treatment.

Since 1994 state funds have been used to rehabilitate the mining legacies of the former GDR, where Lausitz and Central-German Mining Administration Company (LMBV) is responsible for the potash sites nowadays. According to the European Water Framework Directive (WFD, European Commission 2000) the status of surface and groundwater bodies in the member states must achieve a good chemical and ecological status latest by 2027. The surface water body "Lower Wipper (2)", which belongs to the study area around the Wipperdorf basin, however, is heavily modified with bad ecological potential and a not good chemical status (TMUEN 2016). Main reasons for this are its obstructed water course and the burden from agriculture and potash mining.

Basing on WFD's and further regulations' improvement requirement on the one hand and changing hydrometeorological boundary conditions on the other, the current leachate load control system is increasingly no longer able to comply with regulatory limits. This

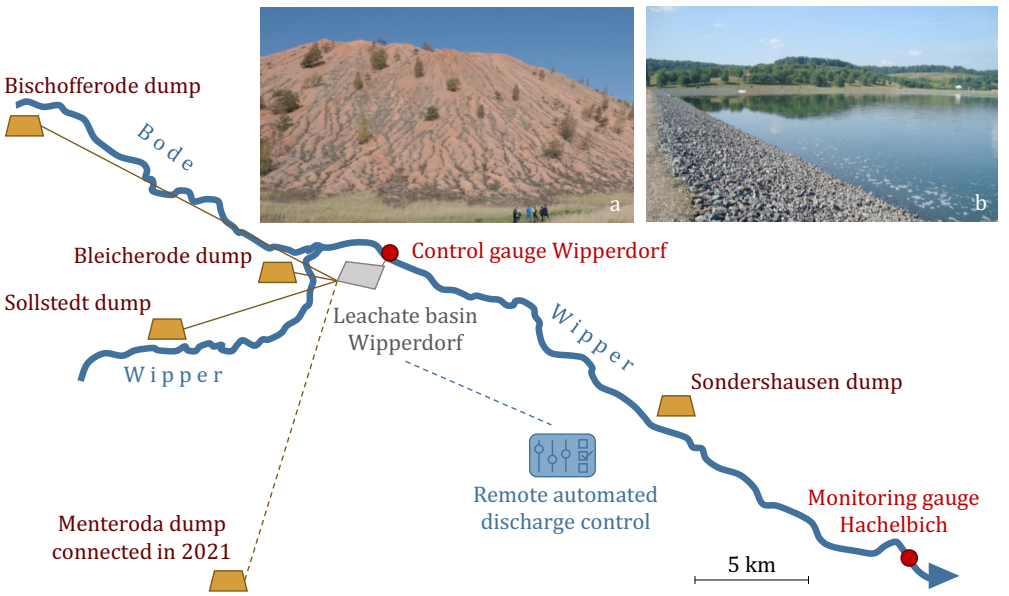

Figure 1 Location of potash dumps, Wipperdorf leachate basin and relevant gauges within the leachate load control system at the Wipper River. a: Bischofferode potash dump, b: Wipperdorf leachate basin.

paper presents the current approach to achieve a load reduction in the Wipper River to address this. In addition, practical experiences from the cooperation with the responsible authorities as well as the causes that led to the implementation of this approach (only) now are shown.

Current state of regulations and measures

In the study area (Fig. 1), environmental pollution from potash mining is reflected in high salt concentrations in groundwater and streams, which is monitored by its key parameter chloride concentration. Right before the point of discharge from the Wipperdorf basin, concentrations around 0.6 g/L Cl are common at mean flow conditions of the Wipper River. About 1 g/L Cl at dry conditions represent the geogenic and mining influenced background concentration that is prevalent in the inflowing groundwater. Directly downstream the potash dumps up to several tens of grams per liter chloride are measured in groundwater monitoring wells. In light of already long-lasting and large-scale salt pollution in the Lower Wipper surface water body it is not seen possible to achieve the chloride concentration limit of 200 mg/L defined in the WFD for a good chemical status by 2027.

Since 2008 a modified official order from the Thuringian State Mining Authority prescribes the conditions for discharge of leachate from the Wipperdorf basin into the Wipper River. Chloride concentration limits for the 27 km downstream gauge Hachelbich set therein take into account the results of comprehensive studies on the possible reduction of the salt load into the river. An annual mean limit value of 1.5 g/L was defined. In addition, a 90th percentile of the 2-hour composite samples of 1.6 g/L was set to reduce concentration fluctuations which would represent an added burden for flora and fauna.

To comply with these limits, the following measures are being implemented which reduce both controllable (discharge from the basin, capture of dump leachate) and uncontrolled (uncaptured dump leachate, geogenic background) chloride loads:

- continued covering of potash dumps,
- safeguarding measures to collect dump surface runoff during heavy precipitation events,

- rehabilitation of Wipperdorf basin, buffer basins, and existing leachate pipelines,
- revision and reconstruction of the existing discharge control system towards an automated discharge control comprising a monitoring system, a database, and a control software.

In addition, representatives of involved authorities, the remediation agency LMBV, and external experts meet twice a year to inform each other and to discuss current issues as well as further measures for the improvement of water quality.

Reasoning and obstacles towards proactive water pollution control

With the above-mentioned measures, the limit values at the Hachelbich gauge have generally been well complied with in recent years. However, with the following, partly new, boundary conditions it has become clear that these measures will not suffice in the future:

- Firstly, relying mainly on dilution to meet regulatory limits is not in agreement with WDF's intention. Consequently current regulations for the site also demand that the salt load to water bodies in the Southern Harz potash district be further reduced.
- As it depends on the water flow in the Wipper River, the current controlled leachate discharge into the Wipper River is limited by hydrometeorological conditions. The last three consecutive dry years 2018 – 2020 have vividly demonstrated the climate prognosis for the region, according to which decreasing precipitation is to be expected throughout the year, especially – as here – in the lee area of mountain ranges. Increase in temperature enhances evaporation towards an even more negative regional water balance.
- Above this, leachate from a further potash dump Menteroda will be directed to the Wipperdorf basin latest in 2022. Subsurface backfill of leachate at this site is to be discontinued with the mining cavities being filled.
- Covering the dumps can effectively slow down the salt load into ground and surface water in the long term. Progress in covering the dumps, however, is limited by the availability of covering material. For the largest dump Bischofferode (53 Mm^3), which is not sealed against the subsoil and the only one not yet being covered, the framework operating plan for covering is currently being drawn up. Though, it will take years until full coverage and a following substantial reduction of salt leaching.
- Every 10 minutes the automated salt load control system calculates the possible discharge from the Wipperdorf basin based on current measurement data. This system is designed to prevent the concentration limit from being *exceeded*. Due to the system-immanent duration of transmission cycles and partly high-frequency flow fluctuations in the Wipper River, there is only minor potential to further optimize the control system towards an increased *utilization* of the approved concentration limit.

Urgency to implement further measures is shown by the fact that hazard prevention measures had to be carried out in the past two winters to prevent the Wipperdorf basin from overflowing. The Thuringian State Office for the Environment, Mining and Nature Conservation (TLUBN) tolerated elevated chloride concentrations of 1.8 g/L at the Hachelbich gauge as long as the water temperature was below 10 °C. As a result, the leachate level in the basin could be substantially reduced and overflow during the dry summer months has been prevented so far.

Various measures are currently being examined that could contribute to an improvement in the ecological state of the surface water body *and* to the safe operation of the Wipperdorf basin. Among them a feasibility study is in progress which evaluates construction and operation of a pipeline from the Wipperdorf basin to a farther downstream river. Considerably higher flow there would allow to discharge captured dump leachate with less effect on salt concentrations. Apart from a not yet clarified feasibility this approach again relies on dilution. Furthermore the project would have high cost expenditures and would have to meet strict formal requirements. Consequently, the most promising approach to

reduce salt load into surface water in the long term is considered evaporation of leachate which is currently put forward and described below. Reasons why this approach is only now being seriously pursued are manifold:

- Even if evaporation seems to be the silver bullet to reduce salt load in the river section of the surface water body Lower Wipper, it is only one of many measures that have been and are being investigated since about 15 years. Other, less costly measures were considered sufficient until the onset of the above mentioned change in boundary conditions.
- Planning and eventual implementation of these initially prioritized measures was very laborious. In conjunction with their regular duration and the iterative procedure a lot of time passed. Furthermore, high formal requirements are connected with the announcement, documentation, and subsequent evaluation of security measures by the responsible authorities. Experience from everyday work shows that compliance with bureaucratic regulations requires a great deal of additional effort, which sometimes stands in the way of efficient implementation of more courageous measures.
- There is no standard technology or process which can guarantee the production of a usable salt from the leachate. Therefore, adaption and optimization to site conditions of this laborious and energy-intensive process requires prior research which further increases the time horizon to implementation as well as the financial expenditures. Especially high operating costs force towards an energy-efficient approach with the target to obtain a marketable product (circular economy).
- Still, the question of proportionality is not raised for the planned evaporation plant. As long as – in this case – the public sector pays for the remediation this seems not to be an argument for water authorities which focus mainly on water quality but less on the total environmental footprint of extensive remediation measures.

Way forward

Alternative strategies for leachate management had to be found in order to prevent overflow of the Wipperdorf basin in the long term and to better comply with the central idea of the WFD. Leachate evaporation with recovery of a usable street salt product is hereby considered as an approach to reduce the total leachate load to the environment. Consideration is also being given to using the leachate as a de-icing agent.

With regard to the processing of leachate into a road salt or a brine as de-icing agent the major challenge is to achieve an appropriate purity and NaCl content of the product. In Germany, requirements regarding the quality of a salt or brine that can be used in winter maintenance are specified in the standards of DIN EN 16811-1. In this context, German standards for the chemical composition of road salts pose a special challenge as they are much stricter than in other European countries. The minimum sodium chloride content of the road salt is 97 wt% in Germany and 90 wt% only in other EU countries. Brine that can be used for winter service must have a sodium chloride content between 18 wt% and 26 wt% in Germany and other European countries.

Figure 2 provides an overview of the possibilities and requirements mentioned related to typical chemical composition for the current leachate and the necessary treatment steps derived from this. In addition, the objectives of past, current and possible future projects are presented.

Currently a pilot plant is in operation where leachate from the Bischofferode potash dump is concentrated to varying degrees by a vacuum evaporator. In further processing steps, the product salt is washed and centrifuged to increase purity and to dry the salt. Because evaporation is very energy consuming, different scenarios for utilizable energy sources have to be assessed (e.g. renewable energy sources, heat extraction of a nearby biomass power plant, use of fossil fuels).

Figure 3 shows the chamber of the vacuum evaporator and a vessel of the produced salt along with the NaCl content achieved in pilot

Leachate (Bischofferode potash dump)

NaCl content of leachate (2012 – 2020): 9 wt% – 24 wt% (mean: 15 wt%)
NaCl content of leachate TDS (2012 – 2020): 81 wt% – 97 wt% (mean: 94 wt%)

	Brine as de-icing agent	**Road salt**
Required NaCl content (DIN EN 16811-1)	18 wt% to 26 wt% NaCl	≥ 97 wt% NaCl
Necessary treatment	Concentration-dependent: thickening of the leachate, filtration to reduce filterable substances	Suitable process for salt separation and achieving the necessary quality
Previous studies and considerations	Analysis of existing data and determination of further relevant data regarding the requirements for winter maintenance products; contacting winter services	Carrying out hydrochemical modelling and laboratory tests (partial evaporation and washing of the salt) to increase the purity of the product salt; tests with the leachate of Wipperdorf basin, which has a lower NaCl content of TDS
Current project		Pilot testing at the Bischofferode dump site: partial evaporation with a vacuum evaporator and washing of the salt
Further project ideas	Cooperation with winter services and first pilot tests	Large-scale plant: depending on the success of the pilot project and the objective
Advantages and disadvantages/ obstacles	+ low treatment effort and energy demand - only useful in winter - cost-neutral/profitable only in the close vicinity → limited utilisable quantity	+ salt production can be carried out all over the year → permanent reduction of the salt discharge - high energy demand, cost-intensive - recovery/disposal of residual/waste products must be clarified

Figure 2 *Requirements and site specific prospects for the utilization of leachate in winter service.*

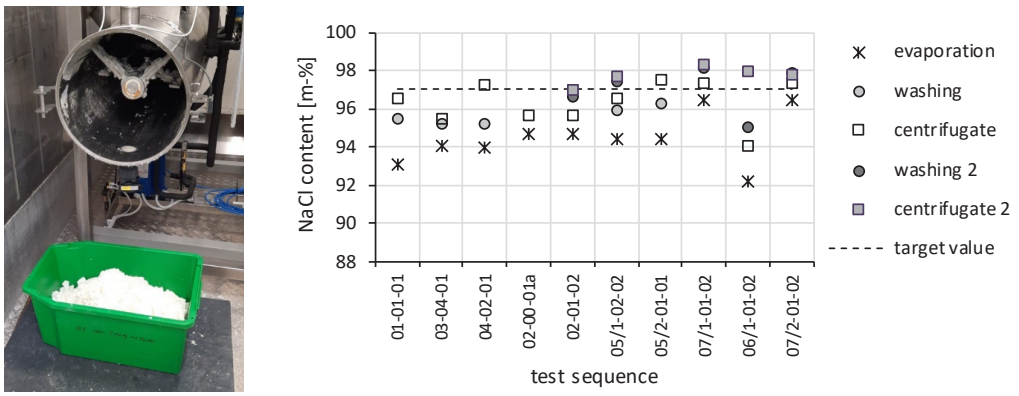

Figure 3 *Chamber of vacuum evaporator and produced salt (left); results of pilot tests: measured NaCl content after each treatment step (right).*

tests. According to this, the required purity of the salt of 97 wt% NaCl can be achieved, when the leachate is only partially evaporated (from the fifth test on). Future tests will show which degree of evaporation and which washing ratio are favorable with regard to achieving the necessary quality and the largest possible product quantity. In future tests, the process will be evaluated with regard to compliance with other quality criteria placed on road salt.

Conclusions

Through LMBV billions of Euros were already spent for rehabilitation of mining legacies on the territory of the former GDR. It can be seen as a lucky circumstance that public funds are provided to this extent. Though, because the use of public funds is strictly regulated, a disadvantage that emerges in the daily remediation business can be seen in a bureaucracy that sometimes hinders swift implementation of measures.

Due to the high costs for treatment of leachates and for other measures to improve water ecology, the responsible mining authority and upper water authority are in a great tension between necessity and appropriateness. Therefore, the **proportionality** of measures must be discussed again and again between all partners involved in the remediation process. Further, the questions "How much remediation can we afford?" or "How much remediation do we want to afford?" will not be answered until ecosystem services of remediated streams can be determined in more detail. Discussion on this issue is just beginning (e.g. Stowasser *et al.* 2021). With the Fauna-Flora-Habitat region "Inland Salt Station at the Ronnenberg Potash Plant", established in 2007, there is a German example of an anthropogenic inland salt site, recently placed under natural protection as valuable habitat (Brock *et al.* 2007). Because this approach may conflict with remediation goals, it remains questionable whether it could be a feasible long-term option for selected locations at the current site.

Above described experiences during implementation of regulatory requirements demonstrate that individual water protection measures must be designed and considered more strongly with respect to economic efficiency and proportionality. Further, site specific linking of energy and material fluxes is pivotal during development of a feasible water treatment process. Thus, the target in the current case should be to gain a marketable product from saline leachate evaporation.

Acknowledgements

This work was carried out within the framework of the German Federal Government and Federal States Administrative Agreement on the Financing of Ecological Contaminated Sites ("Verwaltungsabkommen über die Finanzierung ökologischer Altlasten").

References

Brock J, Aboling S, Stelzer R, Esch E, Papenbrock J (2007) Genetic variation among different populations of Aster tripolium grown on naturally and anthropogenic salt-contaminated habitats: implications for conservation strategies. J Plant Res 120:99—112, doi 10.1007/s10265-006-0030-7

DIN EN 16811-1:2016-10 Winter service equipment and products - De-icing agents – Part 1: Sodium chloride – Requirements and test methods; German version EN 16811-1:2016

European Commission (2000) Directive 2000/60/EC of the European Parliament and of the Council of establishing a framework for Community action in the field of water policy. Official Journal of the European Union (OJ L 327)

Stowasser A, Gerhardt T, Stratmann L (2021) Ermittlung und ökonomische Analyse der Kosten, Nutzen und Erlöse bei der Renaturierung von Gewässern im ländlichen Raum Projekt ElmaR II – Kosten, Nutzen, Erlöse – Abschlussbericht. In LfULG (Ed) Kosten, Nutzen, Erlöse bei der Renaturierung von Gewässern. Schriftenreihe, Heft 2/2021

TMUEN (2016) Thüringer Landesprogramm Gewässerschutz 2016 – 2021. Thüringer Ministerium für Umwelt, Energie und Naturschutz, Erfurt, Germany

Systematic Approach in Environmental Geochemistry as Part of a Mining Project Roadmap

Anneli Wichmann[1], Päivi Picken[2], Eeva-Leena Anttila[3], Kirsi-Marja Haanpää[3], Elin Siggberg[2]

[1]*AFRY Finland Oy, Jaakonkatu 3, 01620 Vantaa, Finland, anneli.wichmann@afry.com*

[2]*AFRY Finland Oy, Koskikatu 27B, 96100 Rovaniemi, Finland, paivi.picken@afry.com, elin.siggberg@afry.com*

[3]*AFRY Finland Oy, Elektroniikkatie 13, FI-90590 Oulu, Finland, eeva-leena.anttila@afry.com, kirsi-marja.haanpaa@afry.com*

Abstract

Geochemistry data gaps often result from insufficient consideration of site-specific circumstances or poor conceptualisation. Whoever plans the first mine site soil sampling or analysis of process trial residues, must understand the many future uses of the data. Misconceptions of other data users´ requirements disable future assessments and cause delays in project schedule. A systematic approach in environmental geochemistry enables better assessments and better environmental risk management. The successful project toolkit includes a combination of tools like conceptualisation, repetitive risk assessment, knowledge base management, gap analysis, roadmap, action plan and sampling and analysis plan.

Keywords: Project Roadmap, Conceptualisation, Gap Analysis, Risk assessment, Geochemistry, Sampling and Analysis Plan

Introduction

At the start of a mining feasibility study or an environmental approval procedure, geochemical gap analysis sometimes leads to rewriting the project schedule. Geochemical sampling, analysis, and testing are very time-consuming processes. Wrong choices made at the early sampling and analysis stages may extend the project schedule by months, potentially even years.

Data gaps result often from insufficient consideration of site-specific circumstances or poor initial conceptualisation. Whoever plans the first mine site soil sampling or programs the analysis of process trial residues, must understand the many future uses of the data, as comprehensively as possible. What kind of primary and supporting data is needed for geochemical modelling? What are all the mine site load details that the aquatic ecologist eventually needs to know, to assess the impacts on the watercourse status? What are the information requirements for selection of correct combination of water treatment technologies? As generation of a geochemical data set can require a long time, misconceptions of other data users' requirements are hazardous for project schedule management.

It may seem obvious that environmental geochemistry work should be systematic. In practice, specialist work is often procured in small pieces. Teams work with cases only over a short period. Projects may also go "hibernating" for a while or projects may simply become so fragmented that no team looks beyond the on-going task. This background forces also geochemists to find tools for better and more long-term management of work.

In addition to enhanced project schedule management, a systematic approach in environmental geochemistry enables better geochemical assessments and better environmental risk management. The successful toolkit includes a combination of tools like conceptualisation, repetitive risk assessment, knowledge base management, gap analysis, roadmap, action plan and sampling and analysis plan.

Challenges Related to Multiple Data Requirements

Factors defining geochemical sampling and analysis requirements vary largely between projects. These factors include, for example, soil and bedrock characteristics, catchment area sensitivities, relevant processing alternatives, mining or waste management options, potential backfill techniques, and data requirements set by modelling techniques (fig. 1).

Requirements for extractive waste characterisation vary largely between different data users. One use of the data is the definition of formal extractive waste and waste facility classification. In Europe, these requirements are derived from European Commission decisions in accordance with EU Extractive Waste Directive 2006/21/EC. Information needs for source term modelling or risk management can be much more complex and they vary between cases and modelling approaches (for example Pierce *et al.* 2016, Charles *et al.* 2016). From this perspective, development of any detailed sampling and analysis plan for a sub-project (e.g. process trial sampling and analysis plan) must be considered also from entire project's data requirement perspective. Another example of data user is water treatment engineering: information requirements do not include just the substances to be removed, but also substances impacting or disturbing the potential water treatment.

Data requirements for aquatic ecology impact assessments can be especially challenging to describe at the early project stages. Load estimate is needed for watercourse modelling and aquatic ecology impact assessment. Load estimate, alone, is usually a result of a chain of models, including hydrogeological models, various source term assessments and site wide water and loading balance model. At worst, the first model in the chain may already disable the last phase. From aquatic ecology perspective, generation of geochemistry work plan should, at least, include the following considerations:

- What are the substances or parameters that may impair different aquatic organisms?
- What are the requirements based on regulation? (In Finland, for example, Government Decree 1308/2015 on priority substances)
- What must be known to assess project compliance with formal objectives? (for example, European River Basin Management Plans and objectives set by the EU Water Framework Directive)
- Are there any other site-specific factors to be taken into consideration in risk management and approval procedures?

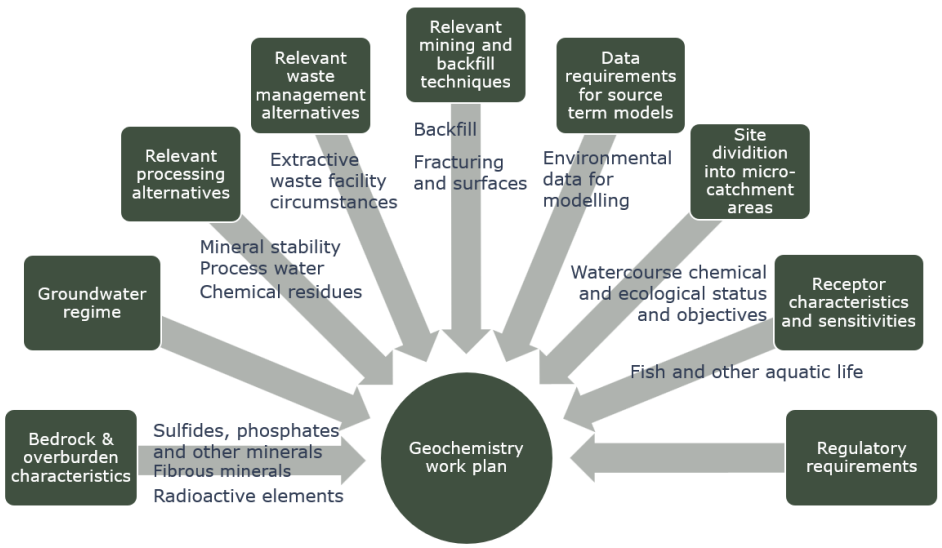

Figure 1 *Factors Defining Sampling and Analysis Requirements.*

In the European Union area, EU Water Framework Directive 2000/60/EC has set a requirement to identify river basin areas and to apply River Basin Management Plans. These plans include watercourse status objectives. Compliance with these status objectives is critical to any mining project and sometimes also one of the most challenging parts of the project. A comprehensive site-specific predictive compliance analysis requires correct choices already at early project stages, like adequate parameter range and detection limits in analytics, or suitable input data coverage over mine construction, operation and closure.

Challenges Related to Data Collection and Timing

Need of data must be recognised well in advance, sometimes years before the data is used. For example, kinetic test-work results that are used as input for source term assessments at feasibility study (FS) phase, must be initiated already during earlier study phases. Sometimes this means that test-work for a technical study should be started before the actual technical study even gets the funding decision.

Number of representing process trials may be few even in a large-scale mining project. Thus, there are not many opportunities to collect and analyse representative process water samples and process trial tailings. In addition, during the actual process trials, the time window for collecting and analysing samples may be narrow. It is important to plan the actual process beneficiation test trials also from water and tailings sample collection perspective, not forgetting sampling of process chemical residues. Persons responsible for project environmental performance and environmental geochemistry should be involved already in trial programming phase. Too narrow parameter range or poor documentation of process trial internal water balance may prevent data usability in necessary future environmental assessments, e.g. tailings water quality source term assessment, site wide loading balance modelling, and both operational phase and post-closure watercourse impact assessments.

Conceptualisation and Risk Assessments as Tools

Conceptual model is an essential basis for numerical modelling work, but it also is a fine tool to support understanding processes inside an individual waste facility (e.g. Lefebvre *et al*. 2001) or site-environment interactions (Enemark *et al*. 2018). First site-wide conceptualisation can be done a lot earlier than in beginning of geochemical or hydrogeological modelling. Early initial conceptualisation helps to identify site-specific data needs, but it also helps to prioritize critical work. While conceptualisation increases understanding on the mine site, also risk assessments are likely to become more comprehensive. Tools applied in risk assessments in mining industry are numerous (Verma and Chaudhari 2016, Tubis *et al*. 2020) and a rather large range of risk identification or risk assessment approaches can help to generate a comprehensive geochemistry work plan. For example, different water risk assessment approaches (Gilsbach *et al*. 2019) can be used in different detail/generalisation levels and in different project phases. Similar approaches can also support planning of geochemistry work. Risk assessment should always be considered as a repetitive process. Each risk assessment round defines and specifies a new or updated risk mitigation plan. Risks deriving from uncertainties in site geochemistry should be assessed as a part of a whole-project risk assessment. For example, extractive waste facility engineering risks cannot be discussed separately from geochemical uncertainties.

Knowledge Base and Gap-Analysis as Tools

Development of site knowledge base (ICMM 2019, 2020) includes a range of aspects from site physical setting and baseline data to operational information, regulation and commitments. Data is collected through all mining project development phases, but also through the years of mine operation and after closure. Site or case knowledge (knowledge base) can be reviewed, for example, before or at start of different study phases. Review also includes identification of gaps and action

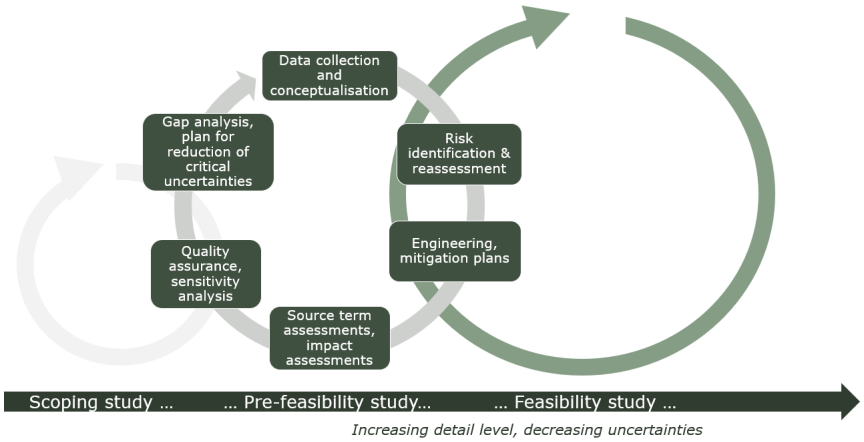

Figure 2 *Illustration of Cyclic Repetitive Work Sequences on a Mining Project Geochemistry Work.*

plan, to fill the critical gaps or to reduce critical uncertainties over the next project phases. At the end of the day, a mining project consists of cyclic repetition of work sequences, reducing uncertainties during every round (fig. 2). These work sequences also include conceptualisation and risk assessments.

According to our experience, data gaps seem to occur even late during the mining project development, especially in situations where environmental impact assessments, permitting, engineering, and economic planning are not genuinely interacting. These processes must be linked to each other at the detail level relevant to the project phase.

Project Roadmap as a Tool

Project roadmap focuses on long-term planning (Albright & Kappel 2016, Phaal *et al.* 2016). It requires defining project goals and understanding project risks. From environmental and social perspective, project roadmap includes identification of site-specific issues and prioritisation of critical issues. Critical issue can be, for example, a sensitive receptor watercourse. In such situation, discharge water quality (or load) can be a major project risk. This means that uncertainties related to water quality and quantity must be reduced as much as possible, as early as possible. This information may be critical even for investment decisions concerning subsequent, more detailed, technical study phases.

Project roadmap organises different study sequences and defines their interdependencies. Scheduling the project requires understanding what inputs each sub-task needs from other sub-tasks. A good roadmap starts from exploration phase and covers a large range of studies and procedures, e.g. different levels of feasibility studies, resource estimates, environmental and social impact assessments, environmental approvals, land-use planning procedures and stakeholder engagement. Roadmap can also be continued over the operational period to closure and post-closure. As the project proceeds and information increases, roadmap must be reviewed and updated time to time.

Integrating geochemistry work plan into the mining project roadmap secures availability of the right information at the right time. Geochemical laboratory testing often takes place between the different technical studies or environmental procedures. From geochemistry perspective, it is always necessary to look beyond the current task. For example, roadmap defines when status of mine planning allows representative waste rock and pit wall sampling. Also, availability of hydrogeological data for geochemical assessments (like pit source term assessments or pit lake models) can be secured by using a roadmap.

Case example: Suhanko PGE-project

Suhanko is a PGE project with a long development history. When a new version of the project plan was on the drawing table, an environmental and social roadmap was

developed to link environmental, social, hydrogeological and geochemical work into approvals procedures and engineering work. Roadmap was based on two initial procedures: risk identification and gap-analysis. Over the last few years, site knowledge base has been complemented to support technical-economic studies, approval procedures and environmental and social risk management. Application of the roadmap has, for example, resulted in a systematic sequence of studies and enabled practical scheduling of complementary geochemical test-work between technical study phases.

Conclusions

Specialist work in a mining project is often rather fragmented and misconceptions of other data users' needs are relatively common. Different teams working with the same project need good quality inputs at the right time. Tools are needed for long-term management of geochemical work. The successful project toolkit includes a combination of tools like **conceptualisation, repetitive risk assessment, knowledge base management, gap analysis, roadmap, action plan and sampling and analysis plan.**

Selecting and using a systematic approach for environmental geochemistry requires multidisciplinary teams and looking beyond the current task. Systematic approach enables better management of environmental risks and project risks. It helps to keep the whole mining project on schedule and budget. Decision makers get the right information at the right time and critical issues are adequately prioritized. Financiers get an understanding on the project´s probable long-term geochemistry work requirements.

Acknowledgements

The authors thank their colleagues at AFRY Finland Oy, Suhanko Arctic Platinum Oy and other companies that have given the opportunity to apply and improve the systematic approach in environmental geochemistry work.

References

Albright R, Kappel T (2016) Roadmapping In the Corporation. Research-Technology Management 46(2):31-40, DOI: 10.1080/08956308.2003.11671552

Charles J, Declercq J, Bowell R, Barnes A & Warrender R (2016) Prediction of Source Term Leachate Quality from Waste Rock Dumps: A Case Study from an Iron Ore Deposit in Northern Sweden. Proceedings IMWA 2016 - Mining Meets Water – Conflicts and Solutions: 1170-1174.

Enemark T, Peeters Lk, Mallants D, Batelaan O (2018) Hydrogeological conceptual model building and testing: A review. Journal of Hydrogeology 569: 310-329.

International Council on Mining and Metals (2019) Integrated Mine Closure: Good Practice Guide, 2nd edition.

International Council on Mining and Metals (2020) Mining Principles, Performance Expectations

Gilsbach L, Schütte, P, Franken G (2019) Applying water risk assessment methods in mining: Current challenges and opportunities Water Resources and Industry, vol 22, 100118

Lefebvre R, Hockley D, Smolensky J, Gélinas P (2001). Multiphase transfer processes in waste rock piles producing acid mine drainage 1: Conceptual model and system characterization. Journal of Contaminant Hydrology 52:137–164

Phaal R, Farrukh C, Probert D (2016) Customizing Roadmapping. Research-Technology Management 47(2):26-37, DOI: 10.1080/08956308.2004.11671616

Pierce J, Weber P, Pierce J, Scott P (2016) Acid and metalliferous drainage contaminant load prediction for operational or legacy mines at closure. Mine Closure 2016: 663-673, DOI:10.36487/ACG_rep/1608_49_Pearce

Tubis A, Werbińska-Wojciechowska S, Wroblewsk A (2020) Risk Assessment Methods in Mining Industry—A Systematic Review. Applied Sciences 10/5172

Verma S, Chaudhari S (2016). Highlights from the literature on risk assessment techniques adopted in the mining industry: A review of past contributions, recent developments and future scope. International Journal of Mining Science and Technology 26: 691–702

Evaluation of a Short-Term Increased Water Influx in a Mine Drainage Facility of a Former Hard Coal Mine

Birgitta Wiesner

RAG Aktiengesellschaft, Im Welterbe 10, 45141 Essen, Germany, Birgitta.Wiesner@rag.de

Abstract

RAG AG currently operates a mine drainage facility at the abandoned coal mine Amalie in the city of Essen, Germany. Throughout April 2020 a short-term increased water influx occurred at this mining site at one dam. To identify on-going processes in the mining plant water chemistry was analysed and investigated. One result of the investigation was, that the break of a dam lead to a new water influx into the water system of the mine. This new water flux resulted in a permanently higher amount of water entering the mine. Chemical analysis of the water also showed a change in composition. The amount of dissolved salts increased significantly. This provides more information on processes in abandoned parts of the mine and helps to improve our predictions of the subsurface water system.

Keywords: Increasing Water Influx, Hydraulic Prospecting, Mine Drainage Facility

Introduction

RAG AG currently operates several mine drainage facilities throughout the former coalmining area Ruhrrevier in western Germany. One drainage facility is located at the abandoned coal mine Amalie in the city of Essen, Germany. The drainage facility at this mining site is in operation to protect further surrounding abandoned mines. Two shafts and about 2 km of drifts are still in use underground. Water is pumped from behind two subsurface dams and collected in a pumping chamber. Water from different parts of the mine mixes in the pumping chamber and is then pumped above ground. One dam, called "W2", is draining the northern part of the former mine. The other dam, called "W1", is draining the southern part of the abandoned mine. In general water volume measurements and samples for chemical analysis are taken above ground from the "mixed" water.

Throughout April 2020 a short-term increased water influx occurred at this mining site at dam W2. The pumped water volume in 2020 is shown in Figure one. The graph shows that within two days in April the pumped water volume increased from 13,500 m^3/d up to 23,000 m^3/d. In the beginning not all the water could be pumped away. A water column built up behind dam W2. To avoid overpressure on the dam an additional pump was activated. This resulted in a maximum pump volume of 27,800 m^3/d. After pumping the water column from behind W2, a water volume of approximately 24,500 m^3/d was pumped for about 4 days. The end of this incident was marked by a decrease in volume within 2 days. Although the decrease wasn't as high as the increase, the main incident was over. The decrease continued slowly until the end of the year.

The main question that presented itself when investigating this incident was if a mine cavity had run empty after a dam breakdown or were there other processes running? To answer this question, it is important to investigate the water volume pumped of the two dams and the water chemistry of dam W1, dam W2 and the mixed water.

Methods

At first, water quality of the total water volume at the surface and dams W1 and W2 was examined by taking samples at the same day. Sampling took place six times from April to November 2020, as indicated with the black circles in Figure one. The major cations (sodium, potassium, calcium and magnesium) and the major anions (chloride, sulphate and hydrogen carbonate) were

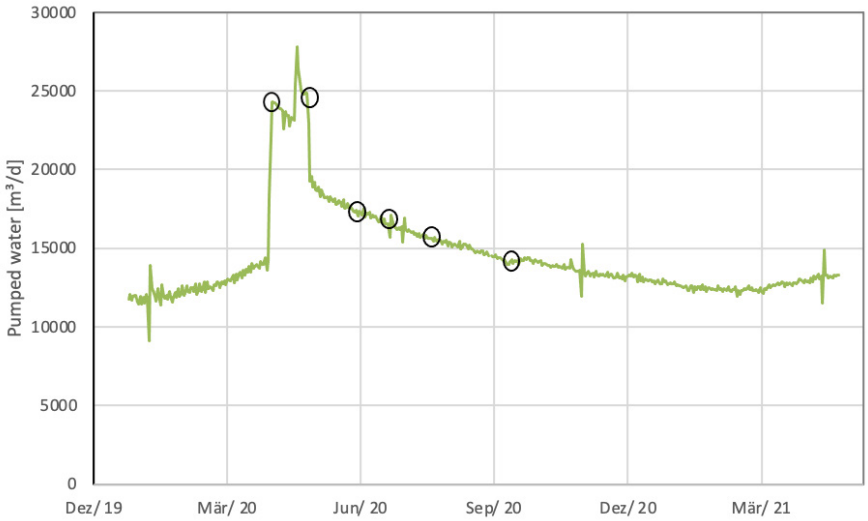

Figure 1 *Daily amount of pumped water of mine drainage facility Amalie in 2020 with dates of sampling in yellow circles.*

Table 1 *Chemistry results of mixed water in the total Water flow of Amalie.*

Amalie – total Water composition							
Date		01.04.2020	29.04.2020	28.05.2020	04.06.2020	09.06.2020	10.11.2020
Electrical conductivity	µS/cm	19100	22500	16300	21100	19100	18800
ph volume	[-]	7	7,1	7,5	7,3	7,2	7,1
Sodium (Na)	mg/l	3880	4570	343	4170	3800	3910
Potassium (K)	mg/l	68	72	54	57	62	65
Calcium (Ca)	mg/l	225	411	302	427	392	417
Magnesium (Mg)	mg/l	76	134	113	131	135	130
Chloride	mg/l	6420	7870	5520	7350	6750	6570
Sulphate (SO4)	mg/l	304	218	256	223	239	210
Hydrogen carbonate (HCO3)	mg/l	1100	780	800	770	780	800

Table 2 *Chemistry results of mixed water in the total Water flow of dam W2.*

Dam W2							
Data		01.04.2020	29.04.2020	28.05.2020	04.06.2020	09.06.2020	10.11.2020
Electrical conductivity	µS/cm	30000	32101	76600	76200	75400	79200
pH value	[-]	6,9	7	6,8	6,7	6,7	6,5
sodium (Na)	mg/l	6440	6623	16400	15900	16600	18900
Potassium (K)	mg/l	88	98	236	178	226	256
Calcium (Ca)	mg/l	347	562	1310	1430	1330	1790
Magnesium (Mg)	mg/l	119	178	392	386	428	508
Chloride	mg/l	10600	11521	31200	30600	30600	33000
Sulphate (SO4)	mg/l	341	150	22,1	16,9	21,5	18
Hydrogen carbonate (HCO3)	mg/l	1200	732	490	480	460	490

Table 3 Chemistry results of mixed water in the total Water flow of dam W1.

		Dam W1					
Date		01.04.2020	29.04.2020	28.05.2020	04.06.2020	09.06.2020	10.11.2020
electrical conductivity	µS/cm	2830	4670	3180	3160	3090	3540
pH Value	[-]	7	7	7,3	7,1	7,2	7
Sodium (Na)	mg/l	468	757	483	513	509	625
Potassium (K)	mg/l	22	24	21	19	22	23
Calcium (Ca)	mg/l	111	131	118	116	112	122
Magnesium (Mg)	mg/l	46	53	48	47	51	51
Chloride	mg/l	374	1090	419	463	451	588
Sulphate (SO4)	mg/l	264	344	262	284	268	263
Hydrogen carbonate (HCO3)	mg/l	870	870	860	860	860	890

Table 4 Results – Calculation water amount provided by dam W2.

Percentage of W2 water [%]	**9%**	**55%**	**15%**	**25 %**	**20%**
Amount of W2 water [m³/min]	1 m³/min	8,437	1,8	3,05	2,34
Total Amount of water	11 m³/min	15,3 m³/min	12,0 m³/min	12,2 m³/min	11,7 m³/min
Date	01.02.2020	01.04.2020	28.05.2020	04.06.2020	09.06.2020

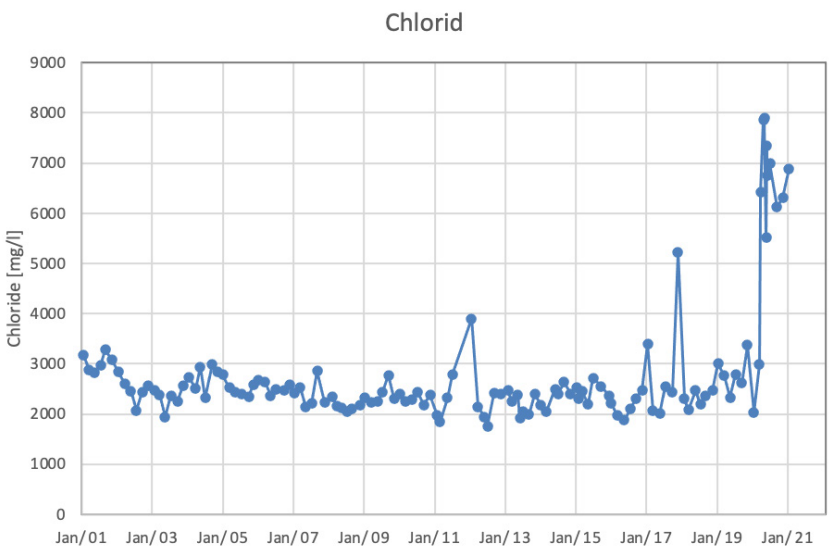

Figure 2 Chloride concentration in the mixed water at the mine drainage facility Amalie of the last 20 years in mg/l.

determined. Results are presented in Table 1 to 3 sorted according to the sampling sites.

We calculate the ratio of water pumped from the dam W1, W2 and the mixed water. We did this by making a mixture calculation based on the chloride content of three water types (dam W1, dam W2 and mixed water). The results are shown in Table 4. Here you can see an estimated amount of 9% W2-Water before the incident. Throughout the incident the water volume increases up to 55% of the total water volume. Afterwards an average

of 15 to 20% of the total water amount is provided by dam W2.

The chemical composition changed completely during this incident as well. As an example, chloride is shown in Figure two. It's obvious that higher chloride values are detected during the incident and afterwards. The high amounts of chloride remain constant until January 2021, also the water volume decreases. Therefore, it is important to look at the development of chloride at the dams in relation to the total chloride concentration. This is shown in Figure 3.

The graphs of dam W1 and of total water amount stay on the same level over time. Major changes of chloride are detected of the dam W2 during decrease of the water volume. Like chloride the other ions change as well. Mainly effects are seen within the sulphate results. This is shown in Graph 4. These lower sulphate results need to be related to higher Strontium and Barium values. Additional

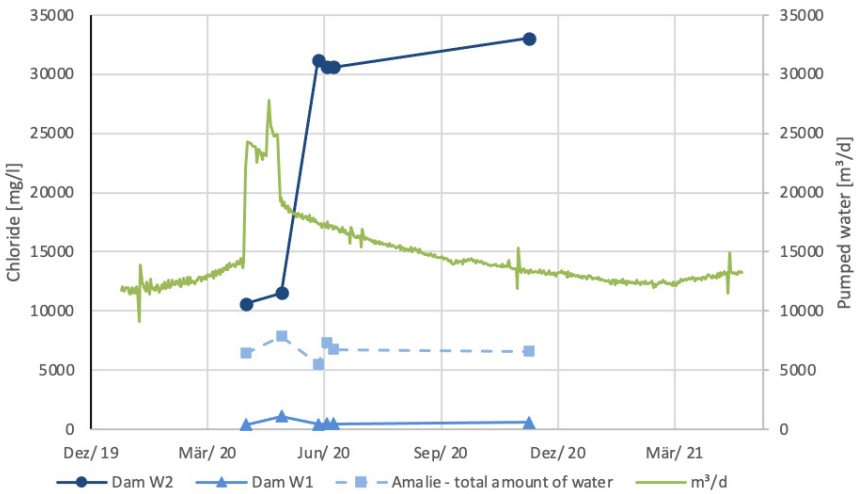

Figure 3 *Chloride concentration in 2020 split on the three sampling points in blue, the total amount of pumped water in with the green graph.*

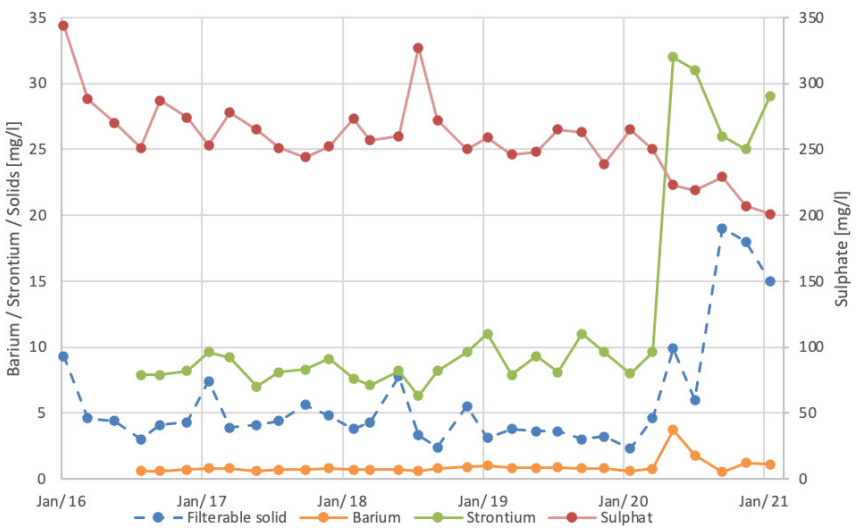

Figure 4 *Impact of barium influence with the new influx in mg/l.*

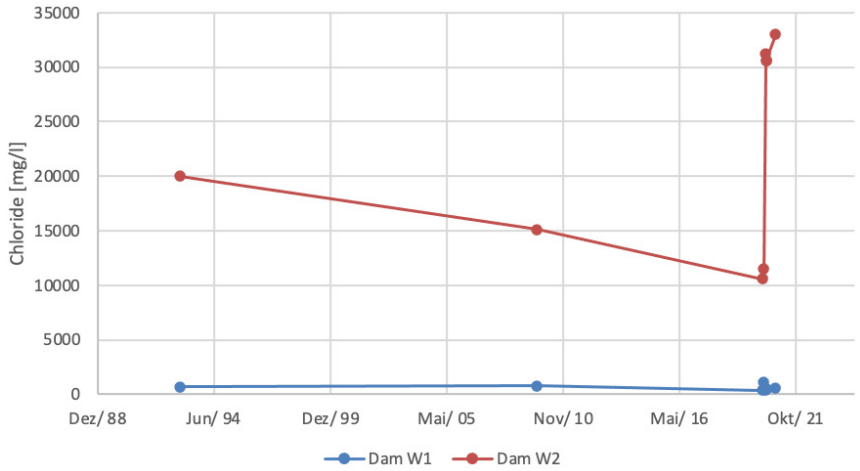

Figure 5 *Development of chloride [mg/l] at the dam W1 and W2 over the last 30 years.*

chemistry data were researched. At least 2 datasets where found from 2009 and 1992 (Wedewardt), which both show values below the ones of the incident. The Graph 5 shows the chloride data.

Conclusions

Chemistry data and calculations paint a clear picture. The mixing calculations indicate a draining of a mining cavity at first. It can be seen by the high percentage of over 50% of W2-dam water volume in the mixed water. High chloride concentration in the mixed water is a result of the main influence of W1-water at first. As the cavity is drained, it's obvious, that the breakdown of a dam lead to new influxes from this part of the mine with dramatic increase of dissolved substances. Taking older data into account a different picture can be painted. As the Figure 5 shows the chloride concentrations decrease over the last thirty years and increases within two months. One explanation might be that a part of the mine develops on its own. Therefore, a water column forms there. Influxes out of deeper parts of the mine are blocked out. The water content of the dam W2 decreases therefore over the years. With the breakdown of a dam water empties out the mining cavity. This leads to influxes out of deeper parts of the mine which now have become part of the water system again. This is indicated by a fundamental change in chemical composition after the decrease of water influx. The new influx shows higher dissolved substances and a new barium dominance as well. Barium sulphate precipitation corresponds to higher suspended solids and sedimentary deposits in water pipelines. A slightly higher percentage of the W2 water within the mixed water also indicates this.

This new information gives us a better understanding of underground processes, which affect not just the small area of the mine drainage facility Amalie, but also allows us to upscale to larger areas and time spans.

References

Wedewardt, M. (1995); Hydrochemie und Genese der Tiefenwässer im Ruhr-Revier, DMT-Berichte aus Forschung und Entwicklung, A-34 pp.

Treatability Trials to remove Zinc from Abbey Consols Mine Water, Wales, UK

Tom Williams[1], Julia Dent[2], Thomas Eckhardt[2], Matt Riding[2], Devin Sapsford[3]

[1]*Natural Resources Wales, Swansea University, Swansea, SA2 8PP, UK, tom.williams@naturalresourceswales.gov.uk*

[2]*WSP Ltd, Willow House, Bristol, BS32 4QW, UK, julia.dent@wsp.com, thomas.eckhardt@wsp.com, matt.riding@wsp.com*

[3]*School of Engineering, Cardiff University, Cardiff, CF24 3AA, UK, sapsforddj@cardiff.ac.uk*

Abstract

Abandoned metal mines are a principal cause of European Union Water Framework Directive (WFD) standards failures in Wales, with 1,300 mines affecting over 700 km of rivers. Abbey Consols lead-zinc mine discharges ≈3 kg day^{-1} of zinc to the River Teifi, causing WFD failures for at least 14 km. This paper presents results of laboratory and field trials to identify an effective method to remove zinc from Abbey Consols mine water. Sodium carbonate (Na_2CO_3) dosing to raise pH and facilitate precipitation is shown to offer an efficient and cost-effective treatment solution, achieving >90% reduction in dissolved zinc concentrations.

Keywords: Metal Mine Remediation, Water Framework Directive, Field Trial, Sodium Carbonate Dosing

Introduction

The abandoned Abbey Consols mine, near Strata Florida Abbey, Mid Wales, has been identified as the primary source of zinc to the River Teifi Special Area of Conservation (SRK 1997; ExCAL 1999; Environment Agency Wales 2012). Contaminated groundwater emerges from a pipe in the northeast of the site, approximately 30 m downgradient of the buried deep adit. This flows in a channel around the former dressing floors, receiving seepages and run-off from waste tips, before discharging to the River Teifi. An extensive ground investigation was undertaken in 2019 to improve the conceptual site model, and to locate the buried adit and confirm the origin of the groundwater pipe discharge. The adit was not located but a pronounced groundwater flow in its vicinity was. A standpipe was installed, enabling the adit water to be sampled (Table 1) and collected in bulk for treatability trials.

An hydrochemical assessment (WSP 2019) found that the groundwater pipe discharge contains a combination of adit water and cleaner groundwater. Some of the adit discharge was also found to follow a groundwater pathway into the waste tips.

Table 1 *Selected chemistry of Abbey Consols mine water sampled from adit standpipe.*

Total µgL^{-1}	Min	Mean	Max
Alkalinity (as $CaCO_3$)	23,700	28,667	31,500
Sulfate	28,400	34,800	40,600
pH	6.62	6.92	7.11
Zinc	14,700	16,267	17,700
Lead	594	3,688	6,790
Cadmium	36	40	45
Iron	2,210	20,293	50,700

As the adit discharge flows into and interacts with water in the waste tips, and the emerging seepages and run-off from the waste tips flow into the groundwater pipe channel, it is not possible to accurately apportion the metal load from the site between these two main sources. To achieve the WFD zinc (dissolved bioavailable) standard of 13.4 μgL^{-1} in the River Teifi, zinc load from the site as a whole would need to be reduced by at least 70%. The remediation works being designed by WSP aim to achieve this by separation of the adit water from the waste tips and transfer to a mine water treatment system. The waste tips will be hydraulically isolated through capping and drainage. This paper presents results from laboratory and field trials to develop the mine water treatment solution.

Laboratory trials: iron dosing with limestone pre-treatment

A treatment options appraisal (WSP 2018) concluded that removal of zinc from the mine water via coprecipitation and sorption during iron precipitation may be a suitable solution. In the absence of elevated dissolved iron concentrations in the mine water, chemical dosing would be required. To assess the feasibility of iron dosing, establish optimum removal rates and to refine the likely concentrations required, laboratory trials were undertaken in May 2019. A limestone pre-treatment step was included due to concerns of lowering pH associated with iron dosing. The aim was to identify the optimum contact time between mine water and limestone gravel that resulted in the largest increase in pH and alkalinity. Limestone gravel of 10-14 mm from B&Q DIY store was washed with deionised water to remove fines that could artificially skew the pH. Four 12 L buckets were filled with the gravel and 680 mL of mine water was added to each. The buckets were placed on an orbital shaker for 2, 5, 15 or 45 min and water was carefully decanted for analysis at each interval. The 45 min exposure resulted in an increase in pH from 6.85 to 8.33 and in alkalinity from 23 mgL^{-1} to 374 mgL^{-1} (Table 2). There was also a concurrent reduction in dissolved zinc concentrations of up to 94%. Hydrochemical modelling indicated the formation of a zinc carbonate to be the likely precipitation process.

Following the limestone pre-treatment tests the mine water was decanted from the buckets into beakers for the iron dosing tests. The aim was to establish the affect on zinc removal of dosing with different concentrations of iron (II) (ferrous) sulfate and iron (III) (ferric) sulfate hydrate. At the time of testing the zinc removal results of the limestone pre-treatment tests were unknown, therefore the dosing tests generally produced unrepresentative results as much of the zinc had already precipitated. It is not known how much the test results were affected by iron precipitation; enabling removal of zinc but potentially also enabling zinc carbonates to re-dissolve with the lowering of pH. These first laboratory trials offered a new opportunity for simplifying the mine water treatment solution relative to the original iron dosing and precipitation approach. It was decided further testing should focus on removal of zinc as a zinc carbonate.

Laboratory trials: carbonate sources and multiple contact cycles

A second set of laboratory trials were undertaken in August 2019 to test a range of limestone sources, repeat contact of mine

Table 2 *Results of different exposure times of mine water to B&Q limestone gravel.*

Contact time	Zinc diss. (μgL^{-1})	Zinc diss. (% removal)	pH	Alkalinity, Tot. as $CaCO_3$ (mgL^{-1})
Raw mine water	15,900	-	6.85	22.8
2 min	9,590	40	6.94	65.0
5 min	6,530	59	7.36	262
15 min	2,940	82	7.77	120
45 min	922	94	8.33	374

water with the limestone and dosing with carbonate-containing reagents as a substitute for limestone. Chalk (20 mm grain size) and two different types of limestone gravel with grain sizes of 16-32 mm (Abergele) and 20 mm (Penderyn) were tested. The chalk and limestone gravels were pre-washed with tap water in a sieve for 5 min, then rinsed with deionised water to remove fines that could misrepresent the long-term behaviour of the limestone and lead to only temporary effects on pH and alkalinity or produce suspended solids which did not arise from the reaction with mine water. A total volume of 0.0048 m^3 of the chalk and two limestone gravels were each placed in 12 L buckets with a 10 mm hole drilled in the bottom and a bung in place. Mine water (750 mL) was added and left undisturbed for either 15 min, 45 min or 2 h. After each exposure period the water was rapidly drained from the bucket into a glass beaker to ensure all suspended solids, as far as possible, were decanted. To measure settlement rates samples of the decanted solution were gathered 1 cm from the surface 15 min, 45 min and 2 h following decanting. Once the contact and settlement time had lapsed the liquid was drained through a glass microfiber filter and dried overnight to determine the quantity of precipitate. Samples of the filtered water were collected for laboratory analysis (Table 3).

The 2 h exposure to chalk resulted in the largest reduction in zinc concentrations relative to the Abergele and Penderyn gravels, as well as the largest quantity of precipitate. Penderyn gravel resulted in equal alkalinity to chalk over the 2 h exposure period, but a lower pH and more limited zinc precipitation. The B&Q gravel used in the May 2019 laboratory tests resulted in greater alkalinity and zinc removal than any of the three gravel sources used here. Overall, high zinc removal rates (>90%) seem to be achievable within a pH range of 8-8.5, but the mass of precipitate formed may be a concern for a full-size system due to disposal costs.

Chalk gravel was selected to test whether zinc removal efficacy is maintained following multiple cycles of contact between mine water and gravel. Fresh chalk was washed with deionised water to remove fines and was placed into a 12 L bucket with a 10 mm hole drilled in the bottom and a bung in place. Mine water (750 mL) was added and left undisturbed for 45 min, after which the water was drained. The process was repeated a total of ten times with fresh mine water on each occasion. Following the first, third, fifth, seventh and tenth exposures precipitate was measured using glass microfiber filters and the filtered liquid was sent for laboratory analysis (Table 4). The repeat exposure of the chalk to fresh mine water resulted in a steady decline in zinc removal rate from 84% to 61%. pH declined from 8.08 to 7.77 and the quantity of precipitate declined from 0.500 g to 0.295 g. This suggests that the efficacy of limestone gravel treatment may diminish over time, however, the test would need to be carried out for longer to establish if the removal rates stabilise or continue to reduce.
The final laboratory tests investigated the efficacy of sodium carbonate (Na_2CO_3)

Table 3 *Selected results following 45 min and 2 h exposure of mine water to different gravel sources, followed by a 2 h settling time and glass microfiber filtration.*

Treatment	Zinc diss. (μgL^{-1})	Zinc diss. (% removal)	pH	Alkalinity, Tot. as $CaCO_3$ (mgL^{-1})	Weight of precipitate (g)
Raw mine water	16,100	-	6.92	32.9	-
Chalk 45 min	5,520	66	7.86	42.5	0.7448
Chalk 2 h	1,080	93	8.10	50.0	0.7366
Abergele 45 min	9,240	43	7.58	35.0	0.1397
Abergele 2 h	4,280	73	7.77	42.4	0.1052
Penderyn 45 min	9,670	40	7.68	46.5	0.1019
Penderyn 2 h	3,810	76	7.85	50.0	0.1238

Table 4 Selected results following repeat contact cycles between chalk gravel and mine water.

Treatment	Zinc diss. (μgL^{-1})	Zinc diss. (% removal)	pH	Alkalinity, Tot. as $CaCO_3$ (mgL^{-1})	Weight of precipitate (g)
Raw mine water	16,100	-	6.92	32.9	-
Cycle 1	2,510	84	8.08	43.5	0.4997
Cycle 3	3,620	78	7.93	40.1	0.3872
Cycle 5	4,450	72	7.97	50.0	0.3696
Cycle 7	4,860	70	7.88	45.0	0.3228
Cycle 10	6,350	61	7.77	43.1	0.2953

Table 5 Selected results following dosing of mine water with Na_2CO_3 and 2 h standing time.

Treatment zinc: Na_2CO_3 ratio	Zinc diss. (μgL^{-1})	Zinc diss. (% removal)	pH	Alkalinity, Tot. as $CaCO_3$ (mgL^{-1})	Weight of precipitate (g)
Raw mine water	16,100	-	6.92	22.8	-
Na_2CO_3 1:1	6,920	57	7.75	38.5	0.0100
Na_2CO_3 1:2	960	94	8.43	55.0	0.0202
Na_2CO_3 1:2.5	123	99	9.27	63.8	0.0225

dosing at different concentrations on the precipitation of zinc and the associated affect on pH. Mine water (1 L) was placed in beakers on a magnetic stirrer and a stock solution of 2.586 g Na_2CO_3 in 1 L of deionised water was made. The Na_2CO_3 solution was then added to the beakers of mine water at zinc:Na_2CO_3 ratios of 1:1 (10 mL), 1:2 (20 mL) and 1:2.5 (25 mL). Following reagent addition samples were taken for laboratory analysis. The turbidity of the water and the rate at which settlement of suspended solids occurred was then recorded by visual observations and a photographic record over 2 h. Once the 2 h had lapsed samples were filtered using glass microfiber filters to quantify the amount of precipitate formed, and the liquid was subject to laboratory analysis (Table 5). Standing time during the experiment appeared to have minor beneficial influence on the results and only those following the 2 h period are presented.

Sodium carbonate dosing at a ratio of 1:1 and 2 h standing time resulted in an increase in pH to 7.75 and a reduction in dissolved zinc of 57%. This improved with increased Na_2CO_3 dosing rates to a maximum of 99% at a 1:2.5 ratio, although the resulting pH of 9.27 was greater than the target maximum of pH 9. No visible turbidity was apparent in the water following Na_2CO_3 dosing and the precipitate mass was very low.

The laboratory trials indicated that raising the mine water pH to 8-8.5 via provision of a soluble carbonate source and subsequent precipitation of zinc as a carbonate could be an effective treatment solution. The use of limestone gravel may be a higher risk option due to decreased efficacy over time and the amount of precipitate generated. Dosing of mine water with Na_2CO_3 may offer a highly efficient, relatively cheap and non-hazardous treatment solution. A non-hazardous reagent is particularly important for a remote and environmentally sensitive setting as Abbey Consols. The treated water has a reduced zinc concentration and its water type is similar to local surface water, lessening any potential impact from the discharge. Treatment volumes in the laboratory were too low to measure settlement behaviour of the zinc carbonate and there was a risk that precipitate could remain suspended in the treatment effluent. It was decided these factors should be assessed through short-term field trials before finalising the design of a large-scale demonstration system.

Field trials: sodium carbonate dosing

A small-scale field trial was designed to test Na_2CO_3 dosing with a continuous higher volume flow of mine water and investigate the settlement rate and characteristics of the precipitate formed. The aim was to generate 1 kg of precipitate, requiring an estimated 40 m^3 of mine water to be processed. The dosing requirements targeted a pH that would provide a maximum zinc removal rate but remained <pH 9 to allow discharge to the environment. The laboratory trials suggested that a dosing ratio of 1:2 (zinc:Na_2CO_3) would provide a pH of ≈8.4 and remove ≈94% of zinc. The trial commenced on 16th March 2020 but had to be suspended on 24th March due to the implementation of coronavirus restrictions. The trial relied on a simple, temporary facility (Figure 1). Mine water was pumped from the adit standpipe to two intermediate bulk containers (IBCs) to provide the mine water feed. A dosing tank was filled with a 2.6 gL^{-1} solution of Na_2CO_3 made on site by weighing out powdered Na_2CO_3 and mixing with deionised water. The dosing tank and the mine water IBCs were connected to a mixing tank and the flows from each controlled by taps. The mixing tank released the dosed mine water via several outfalls to promote laminar flow into the settling pond (6.6 m × 1.3 m). Treated mine water flowed through the settling pond before draining via an outflow at the far end. The typical volume held in the settling pond during operation was 2.36 m^3 and the typical inflow rate was 0.18 Ls^{-1}, providing a retention time just under 4 hours. The dose of the Na_2CO_3 solution was varied with the tap to maintain the target pH of 8.4 in the settling pond.

Total operation time was 31 h 17 min, treating 19,813 L of mine water with 427 L of Na_2CO_3 dosing solution. The dose equates to between 80 and 100 L day^{-1}, and the ratio of zinc:Na_2CO_3 was on average 1:2.2, but at times reached as high as 1:3.1. Flow measurements were taken from the inflow, dosing tap and outflow using a stopwatch and measuring jug. Water samples were taken from the mine water inflow and the treatment outflow twice per day (Table 6). The zinc removal rate per sample set (one inflow and one outflow taken at the same time) are also presented.

The average mine water inflow pH measured in the field was 7.8, slightly higher than laboratory analyses and also previous field measurements of pH from the adit standpipe (Table 1). The average pH achieved in the settling pond (8.3) was slightly lower than targeted (8.4). This is attributed to the sensitivity of dosing control with the tap installation, including optimisation required following dilution by rainfall. At full-scale the dose control will be finer, managed via an automated system triggered by the settling pond pH. Dissolved zinc removal ranged from 58-91% and total zinc removal ranged from 27-61%, the highest removal rates both coinciding with the highest pH of 9.69. The

Figure 1 *Arrangement of field trial at Abbey Consols. Adit standpipe (A), dosing solution tank (B), mine water IBCs (C), mixing tank (D) and settling pond (E).*

Table 6 Zinc removal rates between inflow and outflow for individual samples.

Sample date/time	Mine water flow (Ls^{-1})	Zinc:Na_2CO_3 ratio	Mine water inflow field pH	Settling pond field pH	Zinc diss. (% removal)	Zinc tot. (% removal)
17/03/2020 12:00	0.167	1:3.1	7.77	8.10	62	32
17/03/2020 16:00	0.167	1:3.1	7.88	8.10	63	27
18/03/2020 11:00	0.163	1:2.1	7.57	9.69	91	61
18/03/2020 15:55	0.163	1:2.1	7.90	8.12	79	35
19/03/2020 11:00	0.181	1:2.2	7.80	8.60	83	42
19/03/2020 14:50	0.181	1:2.2	7.90	8.10	58	31
*19/03/2020 16:20**	-	-	-	*8.30*	*68*	*20*
*20/03/2020 10:00**	-	-	-	*7.90*	*69*	*65*
20/03/2020 11:20	0.165	1:1.4	7.83	8.50	75	49
23/03/2020 16:13	0.206	1:2.1	7.77	8.53	86	36
*24/03/2020 10:00**	-	-	-	*8.16*	*81*	*82*
24/03/2020 10:00	0.190	1:1.8	7.90	8.46	87	54

**settling pond sample.*

difference between dissolved and total zinc removal efficiency indicates the settling pond retention time was too short, with precipitate being lost in the outflow. It is also suspected that wind turbulence may have affected how well the precipitate settled.

Three settling pond samples were taken to investigate if standing time affected zinc removal or precipitation overnight (Table 6). On 19th March the settling pond sample showed a much higher dissolved zinc removal rate than total zinc as it was taken following a day of treatment (i.e. no additional settling time). The settling pond samples taken on 20th and 24th March were at the beginning of the day before the treatment system was restarted, indicating the potential removal rate following over 12 h of additional settling time. Although the dissolved zinc removal rates were similar to the operating conditions, the total zinc removal rates were much higher, essentially matching those of dissolved metals, and for the 24th March reached over 80%. The change in removal rates following a longer retention time within the settling pond indicates that the precipitate settling rate is longer than the 3-4 h of the trial. A white precipitate began to form in the settling pond within 1 m of the inflow by the second day of operation and a sample was collected on 23rd March in anticipation of the trial being suspended the following day. The precipitate was allowed to settle in measuring jugs before being filtered with a sieve and paper towel. It was then sealed in a container for transport to the laboratory.

The wet weight of the sample measured on site was between 800-900 g and moisture content of the precipitate was 95%. The zinc concentration was 46%, however, the total inorganic carbon was only 1.2%, much lower than expected if a pure zinc carbonate was forming. The ratios of zinc to carbon suggest it's more likely to be hydrozincite ($Zn_5(CO_3)_2(OH)_6$), although potentially with some additional metal precipitate. Hydrozincite is less dense than smithsonite and potentially more easily resuspended, which will therefore benefit from optimisation of the settling time.

Conclusion

Treatability trials identified that dosing with Na_2CO_3 as a carbonate source and raising pH to ≈8.5 can successfully remove >80% of dissolved zinc from Abbey Consols mine water in the field. Over 90% zinc removal was also shown to be achievable, but with a corresponding pH considered too high for discharge to the environment. During the field trial total zinc removal was lower during operation than following overnight standing time in the settling pond, indicating a larger surface area of the pond and protection from

turbulence caused by wind are required to settle the precipitate more efficiently for the flow rate treated. The large-scale demonstrator system will target pH 8.5-9 and is being designed to allow comprehensive testing of precipitation and settlement behaviour and to explore the precipitation of hydrozincite versus smithsonite. Mechanisms to reduce the water content of the precipitate will also need to be considered in the design to reduce disposal costs. Although the flow rate from the buried adit is currently unconfirmed, it is considered the mine water treatment, in combination with the mine waste capping works, can achieve the >70% reduction in zinc load required to achieve WFD targets.

Acknowledgements

The Abbey Consols Remediation Project is funded by Welsh Government.

References

Environment Agency Wales (2012) WFD Abandoned Mines Project: Afon Teifi catchment.

ExCAL Ltd. (1999) Metal Mine study: Abbey Consols, Grogwynion and Castell.

SRK (1997) Metal Mines Amelioration Study: Pre-Feasibility Study for the Amelioration of Polluted Drainage Waters from 14 Former Metal Mines in Mid-Wales.

WSP Ltd. (2018) Abbey Consols Treatment Options Appraisal Technical Note.

WSP Ltd. (2019) Detailed Hydrochemical Assessment Technical Note. Appendix E in: Abbey Consols Remediation Study: Ground Investigation Interpretative Report.

Using Geological Analogues and Proxies to Better Determine AMD Risk

Timothy Wright[1], Steven Pearce[1], Latipa Henim[2], Janjan Hertrijana[2], Muhammad Hidayat[2]

[1]*Mine Environmental Management Limited, 3A Vale Street, Denbigh,North Wales, UK, LL16 3AD, spearce@memconsultants.co.uk*

[2]*PT Agincourt Resources Indonesia, Jl. Merdeka Barat km 2,5, Desa Aek Pining Batangtoru, Tapanuli Selatan Sumatera Utara 22738*

Abstract

We present initial results from a combined structural and geochemical assessment designed to improve AMD classification at the Martabe gold mine, Indonesia. Martabe conforms to a classic epithermal acid sulfate model displaying local variations in structure and geochemistry that are difficult to constrain using existing resource models. Fracture-controlled mineralisation and oxidation explains the observed irregular and incomplete "oxidation zones" in which Jarosite, a non-sulfide cause of AMD is found. Supported by outcrop analogues such as the Rodalquilar gold mine in SE Spain, these observations imply detailed grade control drilling is justified to improve model resolution and improve waste rock management efficiency.

Keywords: AMD, Structure, Mineralisation, Jarosite, Mine-Waste Characterisation

Introduction

Situated in Sumatra, Indonesia, the Martabe Mine Cluster (MMC) is an epithermal acid sulfate volcanogenic gold deposit developed using open pit mining. Accurately and efficiently classifying waste rocks to prepare a fit-for-purpose waste management schedule presents a challenge due to the complexity of the geological setting and considerable variation in the AMD characteristics of materials being mined at the MMC (e.g. Fig 1). Therefore, we have sought to investigate ways to increase the effectiveness of geological models, test generalised industry assumptions, and improve waste rock classification and processing streams.

Following initial assessments, waste rocks at the MMC are divided into six different classes of waste based on physical and geochemical characteristics which collectively determine relative and absolute AMD risk. Waste rocks are broadly categorised based

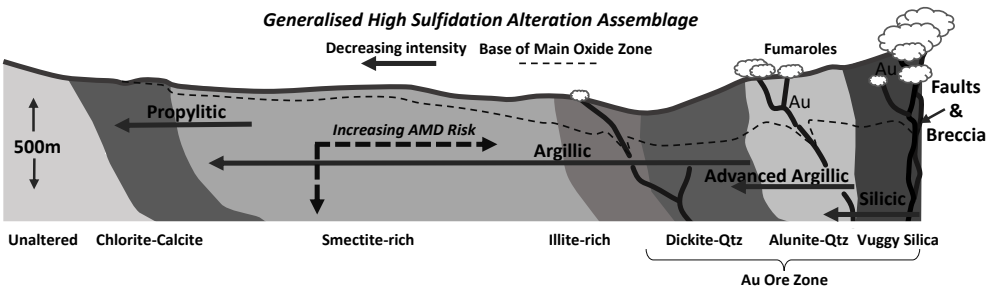

Figure 1 *Generalised high-sulfidation alteration assemblage at the MMC based on the work of Mandradewi et al. 2014 showing a decrease in alteration intensity from a main fractured ore-bearing vent area. The base of a supergene oxide zone is indicated with dashed line along with the approximate extent of alteration assemblages and common indicator minerals. AMD risk is generally assumed to increase towards the ore zone.*

on risk which include higher and lower risk *Potentially Acid-Forming* "PAF" materials, *Non-Acid Forming* (NAF) and material that is PAF but may have a lag time before acid generation occurs. Techniques such as encapsulation of PAF using sealing layers to reduce oxygen ingress are employed at the site to manage AMD generation as part of waste placement in an integrated waste and tailings storage facility. In general, low grade PAF and NAF waste is considered beneficial for use in an outer growth medium zone used to encase the completed integrated waste landform.

To date, waste rocks at the MMC are classified using acid base accounting (ABA) testing based on assay data and laboratory *Net Acid Generation* "NAG" tests undertaken as part of resource development and grade control drilling and sampling. An AMD risk block model based on PT Agincourt's 3D resource development block model is used to map out waste material by waste class and ensure correct identification of materials at an appropriate scale. AMD risk is largely governed by the assumption that sulfide content is the key factor in determining net acidity with buffering provided by carbonates. We investigate whether these simple analytical techniques are sufficient and whether it is appropriate to assume that AMD risk is connected directly to sulfide sulphur (SxS) and the mineralisation system in fig. 1. We seek to investigate scale variance of AMD risk factors and identify more efficient techniques to differentiate classes of waste material using broad proxies and practicable rules or protocols based on quantifiable rock properties in existing resource development models e.g. lithology, alteration type and routine assay metals.

A key area of interest is the possible link between subsurface permeability and oxidation state. We predict permeability and thus AMD risk could be directly linked and influenced by faulting, brecciation and alteration type which are defined in the existing resource development model but are not used directly to model AMD risk. Developing deposit specific AMD models based on a greater understanding of empirical geological and geochemical data can help us design appropriate drilling and laboratory testing strategies e.g. "what is the optimal spacing of grade control drilling?" and "are PAF materials prevalent everywhere or concentrated in certain structural, alteration or mineralogical zones?".

Methods

We used extensive borehole data from the site and analogue deposits to enhance our knowledge of the 3-D geometry and character of alteration zones, faults and mineralisation and determine how PAF materials such as sulfide and the sulfate jarosite are distributed within the MMC. Rodalquilar in SE Spain was identified as our primary geological and geochemical analogue. Rodalquilar was mined using traditional artisanal techniques supplemented by later localised mechanical excavation. In contrast to most modern mines around the world, the original structural fabric of the deposit is largely intact and retains sufficient outcrop to allow a thorough understanding of the 3D distribution and character of faulting and mineralisation. Our descriptions are based on visits to the mine, laboratory analysis and published literature.

To better constrain geochemical data, samples from grade control drilling were assayed and processed to determine sulfide sulfur (SxS) and standard NAG acidity. In addition to repeat QC testing, Paste pH and Rinse pH methods were also used to test whether estimations of net acidity derived from NAG tests require supplemental laboratory test data to define PAF characteristics.

Results

The plots in fig. 2 illustrate varying geochemical characteristics of two boreholes drilled in the Tor Ula Ala site at the MMC. Borehole APSD1879 shown in fig. 2a is drilled over a 130 m section revealing two notable excursions in NAG pH and SxS data indicating locally high-grade waste material. These zones also show elevated Au and Cu. We interpret these zones as being potentially fault controlled ore zones. The concentration of acidity data suggests PAF material might be concentrated in narrow metre or sub-metre scale bands rather than evenly distributed within the rock volume. Such narrow bands could easily be missed with

widely spaced drillhole sampling, therefore the knowledge that such concentrated zones exist has potentially important implications for the resolution of drilling required to identify such features. It is further noted that less PAF waste could be characterised as high risk if the main ore body can be isolated along the fault and treated separately to the bulk waste surrounding it as would be the case in underground or artisanal mining. In fig. 2b borehole APSD2491 is cored over a longer 380 m section and whilst there are fewer obvious narrow excursions, the SxS and NAG pH trends show a marked step at 155 m with the remaining section showing consistently high SxS but rather variable NAG pH suggesting SxS is not directly proportional to NAG pH. Initial testing suggests some of the observed variability is due to calcite which provides a source of acid buffering ANC material, and alunite which returns a false positive from SxS testing.

Assay, XRD, SEM and thin section analysis data shows the main contributions to AMD risk at the MMC are sulfides e.g. pyrite, enargite and covellite. Sulfides are mostly concentrated in Siliceous (Si) and Advanced Argillic (AA) alteration zones, but also occur as patchy concentrations throughout the MMC including within localised pods and veins within the main oxide zone which is contrary to the simple AMD model proposed in fig. 1. This suggests permeability and access to oxygenated water are potentially important factors in determining the levels of sulfide oxidation. On further inspection, our laboratory studies led us to recognise a statistically significant disparity between expected rinse pH and measured sulfide content (SxS) derived from basic NAG testing. Jarosite ($KFe^{3+}_3(SO_4)_2(OH)_6$) has been isolated as the potential cause of the difference and is now recognised as a potential AMD risk factor at Martabe. The distribution and deportment of jarosite is, at present, poorly constrained; however, jarosite usually forms under acidic conditions in the presence of oxygen meaning it could be present wherever partial oxidation has occurred in the presence of acidic leachate

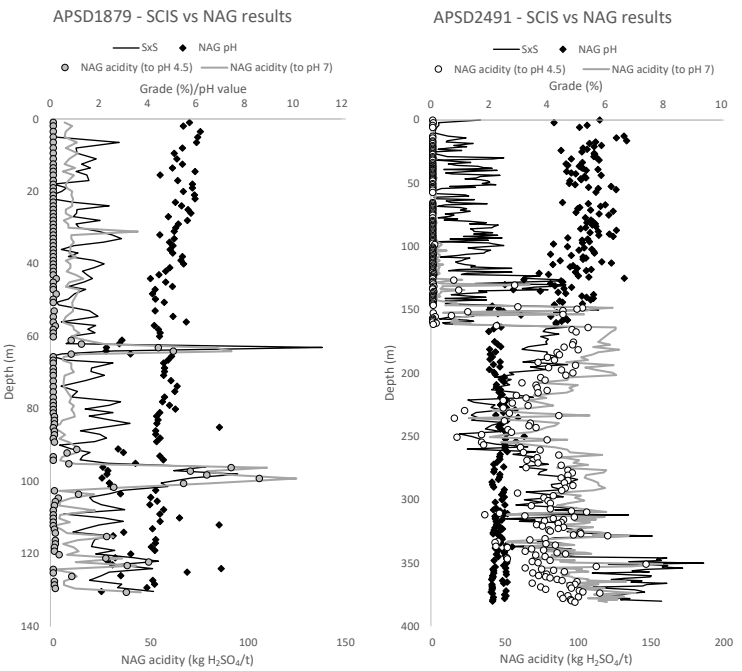

Figure 2a *Plot showing NAG acidity (pH 4.5 and pH 7.0) superimposed with Sulfide Sulfur (SxS) and NAG pH against depth in boreholes APSD1879 and* ***2b*** *APSD2491 at the Tor Ula Ala pit PT Agincourt Resources). Depths are measured depth along borehole.*

(e.g. Cunningham *et al.* 1994). Based on initial cross-plots of Jarosite and SxS, we provisionally conclude transitional SxS grades of 2.0–4.0% could signify higher likelihoods of encountering Jarosite e.g. between 120–140 m in APSD2491. Testing also indicated large concentrations of alunite ($KAl_3(SO_4)_2(OH)_6$) which affects the accuracy and precision of routine SxS readings. Alunite contains bound sulfur which is incorrectly counted as SxS during routine laboratory analysis leading to overestimations of SxS. Rinse pH and NAG pH tests are therefore required to measure jarosite and sulfide grade which are required to reliably calculate AMD risk.

To date, block and wireframe models of PAF material which are the basis for populating the AMD model show limited structural alignment with known ore bodies and suffer as a result of aliasing widely spaced sample points. To enhance the level of geological control, we identified the need to establish reliable rules of thumb and proxies to estimate sulfide and jarosite grade distribution within the MMC. Exploratory drilling suggests the MMC is crosscut by several generations of faulting which may be coeval with acid sulfate mineralisation. The interpreted fault intersections identified in fig. 2a suggest primary structures could be exerting an important influence on the distribution of PAF mineralisation. Field data collected using Analytical Spectral Devices (ASD) also supports a directional component to mineralisation and alteration assemblages at the MMC which appear to be aligned with primary faulting (e.g. Mandradewi *et al.* 2014). Introducing more structural control to the AMD block model using techniques such as Kriging could enhance the accuracy and reliability of the AMD model reducing the need for additional high resolution grade control drilling. Whilst our analysis shows existing modelling is broadly fit for purpose, we are aware of the scale-independent fractal nature of fractures and faults (e.g. Walsh & Watterson 1991) and therefore explored the detailed structural and geochemical character of our chosen analogue acid-sulfate deposit at Rodalquilar, SE Spain.

Rodalquilar is of comparable scale and relief to the MMC and is hosted in similar acid-intermediate host lithologies with a strong structural control on Au grades (e.g. Arribas *et al.* 1995). As with the MMC, Au is late stage at Rodalquilar, focused in quartz-pyrite veins, vuggy cavity filling quartz and complex banded and brecciated veins predominately in silicic and advanced argillic alteration zones (e.g. Saing *et al.* 2015, Rytuba *et al.* 1990, Hedenquist & Lowenstern 1994 and Foley & Hayba 1987). Alteration is observed to be of greatest intensity in highly fractured or brecciated host lithologies suggesting early-stage acid leaching of primary minerals and structural weakness facilitates higher permeability along which later Au and sulfide mineralisation is concentrated. As with the MMC, Rodalquilar displays characteristic decreases in alteration intensity grading outward in a concentric pattern from siliceous and advanced argillic central cores with abundant alunite. Looking in detail at the patterns of excavation artisanal miners have made, ore mineralisation at Rodalquilar is focused along sheet-like silicified faults, narrow silica veins and irregular breccia pipes. Calcite is concentrated in propylitic and unaltered rocks at Rodalquilar. Propylitic zones are comparatively less well developed at the MMT, but calcite appears concentrated in zones away from the more intense alteration zones at both locations. Fig. 3a shows a typical irregular shaped intact siliceous pipe surrounded by various alteration zones and intense localised fracturing. Our observations suggest far more complexity and fractal behaviour between interacting structures and alteration haloes than the generalised model shown in fig. 1 would predict. Complex interactions between irregular sheet and pipe-like 3D features helps to explain the step like behaviour of ore and SxS grades as well as irregular or repeating patterns of alteration mineralogy noted in boreholes at the MMC. Our work suggests routine testing based on widely spaced samples from resource drilling could provide misleading results therefore higher density 1m vertical sampling intervals used in grade control boreholes drilled at ≈10–15 m centres would be necessary to reproduce the types of features shown in fig. 3a in our AMD models at the MMC.

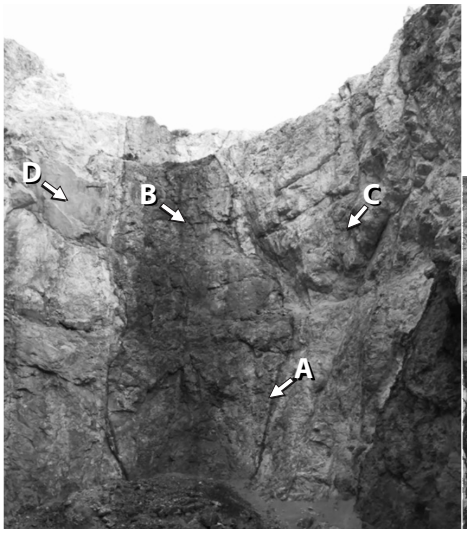

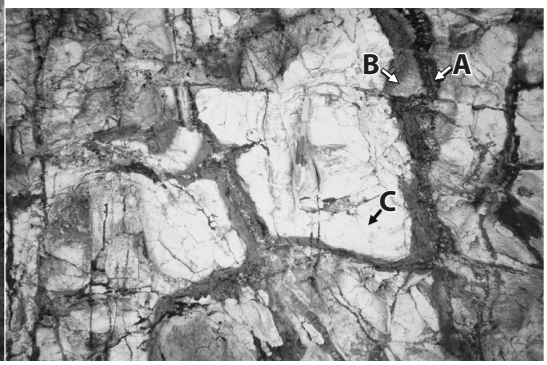

Figure 3a *Excavated gallery at the Rodalquilar gold mine, Almeria, SE Spain showing defined dark alteration margins at "A", a central silica-rich ore zone at "B", advanced argillic alteration rich in alunite at "C" and an isolated intact block of volcanic material at "D" which is relatively unaltered, possibly due to reduced permeability. Field of view is 20m (image: Timothy Wright).* ***Figure 3b*** *Volcanic breccia at the Rodalquilar gold mine, Almeria, SE Spain showing concentrated hematite, jarosite and goethite in the centre of a fracture at "A", with syntaxial development into lower concentrations of iron oxides at "B". Point "C" displays no visible iron oxides but some residual alunite along with kaolinite typical of argillic to advanced argillic alteration. Field of view is 1m wide (image: Timothy Wright).*

Both the MMC and Rodalquilar exhibit marked surface weathering and the development of oxide zones characterised by high concentrations of the stable iron oxides hematite & goethite. Jarosite has been identified together with hematite and goethite in freshly exposed road cut sections at Rodalquilar, e.g. fig. 3b, indicating the presence of iron oxides are on their own not sufficient to determine "low" AMD risk (i.e. absence of sulfides or acid sulfates). Routine testing of the "oxide" zone using the rinse pH analytical technique is advisable to detect jarosite, and sulfide sulfur analysis to detect remnant sulfides. We continue to search for suitable geochemical markers and proxies that can be used to quickly classify waste based on standard assay testing. Initial results indicate Cu and As grades (routine assay data) can be used as potential proxies for estimating SxS and jarosite presence. We also note that sulfide and base metal concentrations are not always directly linked, e.g. Cu and As may be concentrated or depleted in various transitional zones characterised by separate oxidation states to iron sulfides. The regular net-like patterns of concentrated metalliferous mineralisation observed at outcrop scale at Rodalquilar and shown in fig. 3 indicates conventional blasting could also result in preferentially separating and fragmenting higher AMD risk vein material leaving larger pieces of low-risk matrix intact (e.g. Pearce *et al.* 2019). As a result, opportunities are identified for mechanical recovery of resources that would otherwise have been not identified (due to grade weight averaging of "blocks" in modelling) and consequently, the removal of high-risk (high sulfide) material from otherwise inert waste rocks.

Discussion

Our work studying the Rodalquilar deposit has revealed many details of the sinuous, streaky, fracture controlled and brecciated nature of the ore zones and surrounding waste rocks that display fractal behaviour. We have discovered evidence that AMD risk is

generally higher in the most intensely altered siliceous and advanced argillic zones due to a lack of acid buffering calcite, but we also note sulfides are present in lower intensity argillic alteration zones and also more generally defined "oxide" zones. Carbonates do not appear to be present in advanced argillic and siliceous zones, therefore it is true to say low risk material with higher acid buffering potential is more likely to be found in zones of argillic, propylitic and unaltered assemblages (but not assured).

The presence of hematite and goethite in ASD readings is commonly used to define the "oxide zone"; however, in the oxide zones at the MMC and Rodalquilar, there is still abundant sulfide and jarosite so it is incorrect to attribute low AMD risk to all rocks containing common oxide indicators at the MMC. Jarosite appears to be concentrated in zones rich in partially oxidised SxS and therefore might be of greatest concern as a source of acid in advanced argillic and siliceous zones. More research is required to confirm whether this is a quantifiable relationship. Quantitative evaluations indicate faults and breccia zones are generally more prone to hosting high risk material. For example breccia of the type found at the Barani pit in the southern area of the MMC has elevated jarosite suggesting permeability controlled by faulting and fracturing is a key risk factor. We therefore consider whether is it appropriate to abandon a simple oxide zone model and include fault planes and breccia pipes into our AMD model and define a high-risk zone to all material within a given distance of the fault or with potentially elevated permeability. In the case of the "340 vein" at Rodalquilar, anecdotal reports indicate approximately 560 kg of Au was recovered from a planar fracture-hosted zone of silicious material measuring a few metres in width suggesting any associated PAF material would be captured during ore processing with surrounding rocks yielding much lower sulfide grade and lower acidity forming potential. At Martabe (and most modern mines using open pit excavation), such a narrow vein will be treated as "bulk ore" and mined along with lower grade material.

Modern open pit mining is driven by bulk ore grade (using grade weighted averaging and block modelling approaches) negating the need for precision resource modelling and mining technique. Grade weight averaging over 10-20m blocks using single borehole validation will, on average capture sufficient details of the broad mineral system and the resulting resource model will be similar to the generalised model shown in fig. 1. Our research suggests sulfide tends to be focused in localised structurally controlled concentrations therefore small-scale variability could be missed with this block modelling approach which might mean that any given block could register as low-grade AMD risk but contain very high concentrations of AMD material, e.g. along sulfide veins in zones of lower permeability or jarosite pods and streaks in zones of higher permeability that are not intersected by drilling. Failure to consider such features could lead to incorrect classification of waste and deleterious environmental consequences. Anything that can be done within a commercial context to prevent extraction, incorrect classification and disposal of unnecessary material will result in greater efficiency and reduced environmental impact.

Our search for proxies is ongoing with promising indications that As and Cu concentrations could be potential proxies for acid sulfates such as Jarosite at the MMC. We are also considering whether it might be possible to use physical fragmentation characteristics and rock properties of certain classes of material to isolate high-grade waste that could constitute ore and be processed as ore thus reducing the high-grade waste load, or selectively recover higher grade sulfides based on particle size (as vein material tends to act as weak points for fragmentation during blasting).

Conclusions

We have shown that it is helpful to draw on geological analogues when seeking to predict and model AMD risk using integrated resource modelling at the MMC. The fracture- and permeability -controlled nature of oxidation and mineralisation observed in outcrops at Rodalquilar explains the observed irregular and incomplete "oxidation zone" observed at the MMC. We conclude the

MMC AMD model will continue to benefit from enhancements to adequately capture features such as the geochemical excursions noted (e.g. fig. 2a.) Scales of measurement and aliasing are important factors due to the fractal character of pods, streaks and fractures which contain substantial localised concentrations of sulfide and jarosite. We have developed improved modelling strategies which prioritise waste with the greatest AMD risk and reduce the amount of low-grade waste being classified as PAF.

References

Arribas A, Cunningham CG, Rytuba JJ, Rye RO, Kelly WC, Podwysocki MH, McKee EH, Tosdal RM (1995) Geology, geochronology, fluid inclusions, and isotope geochemistry of the Rodalquilar gold alunite deposit, Spain. Economic Geology 90(4):795—822, doi. org/10.2113/gsecongeo.90.4.795

Hedenquist J, & Lowenstern JB (1994) The Role of magmas in the formation of hydrothermal ore deposits. Nature 370: 519-527

Mandradewi W, Khodijah S, Hertrijana J, Hidayat AT & Werror V. (2014) Application of spectral analysis in alteration mapping in Martabe Areas, North Sumatra Indonesia, Palembang (Technical Report)

Pearce S, Brookshaw D, Mueller S and Barnes A (2019) Optimising waste management assessment using fragmentation analysis technology. In: AB Fourie & M Tibbett (eds), Proceedings of the 13th International Conference on Mine Closure, Australian Centre for Geomechanics, Perth, pp. 883-896, https://doi.org/10.36487/ACG_rep/1915_70_Pearce

Rytuba JJ, Arribas A Jr, Cunningham CG, McKee EH, Podwysocki, JG Smith, MH Kelly WC, Arribas A (1990) Mineralized and unmineralized caldera in Spain; Part II, evolution of the Rodalquilar caldera complex and associated gold-alunite deposits. Mineral Depositas 25(Suppl):S29—S35

Saing S, Takahashi R and Imai A (2015) Characteristics of Magmatic Hydrothermal System at Southeastern Martabe High Sulfidation Epithermal Deposit, North Sumatra Province, Indonesia. Thesis Presentation, Graduate School of Engineering and Resource Science, Akita University, Japan

Walsh JJ and Watterson J (1991) Geometric and kinematic coherence and scale effects in normal fault systems. In: Roberts AM, Yielding G and Freeman B (eds) The Geometry of Normal Faults. Geological Society, London, Special Publications 56 193–203, doi.org/10.1144/GSL.SP.1991.056.01.13

Assessment of the Constraints on Sustainable Urban Drainage Systems Due to Rising Mine Water and Mine Water Management

Lee M Wyatt[1], Ian A Watson[1], Sally Gallagher[2], Joanne Grantham[2]

[1]*Coal Authority, 200 Lichfield Lane, Mansfield, NG18 4RG, UK, leewyatt@coal.gov.uk*

[2]*Environment Agency, Tyneside House, Skinnerburn Road, Newcastle upon Tyne, NE4 7AR, UK, sally.gallagher@environment-agency.gov.uk*

Abstract

Many urban areas of the UK have underground mine workings, which were dewatered during mining. Cessation of pumping and resultant rising mine water changes the natural and post mining hydrogeological properties of the subsurface. Sustainable drainages systems are the promoted common approach to manage surface water. Groundwater changes can either be influenced by these systems or their presence can influence effectiveness; leading to an increased flooding risk and contrary to the aims of sustainable drainage. This paper describes a trial screening tool developed to help assess the suitability and site specific design of sustainable drainage now and in the future.

Keywords: Rising Mine Water, Water Management, Sustainable Drainage, Constraints

Introduction – sustainable drainage and planning policies

Within England, the National Planning Policy Framework 2018 requires:

- Local authorities to ensure the flood risk is not increased elsewhere when determining any planning application for major development and where appropriate, application should be supported by a site-specific flood-risk assessment.
- All major developments incorporate sustainable drainage systems unless there is clear evidence that this would be inappropriate. The systems used should take in to account advice from the lead local flood authority (typically councils), and have maintenance arrangements in place for the lifetime of the development (typically in excess of 20 years).

Government policy (25 year plan) – aims to reduce the risks of harm from environmental hazards – people, environment and economy relating to flooding, drought and erosion. This policy includes making sure that decisions on land use including development reflect the level of current and future flood risk.

Introduction – the groundwater problem

The trial of the screening tool was undertaken in the northeast of England, where issues of groundwater flooding have been occurring (Coal Authority, 2018). Here groundwater flooding has been seen in areas where infiltration has been increased due to changes in rainfall patterns, human activity, or where mine water and groundwater levels have recovered.

Large areas of Northeast England (similar to other areas in the UK) have been undermined by coal workings. During mine operation, pumping artificially lowered the groundwater and in many cases, it resulted in significant and long duration changes to natural pathways, through use of mine drainage pathways. Following cessation of pumping mine water and groundwater levels rose and recovered, are still rising or are controlled and managed by pumping to prevent environmental and aquifer pollution. Due to the age of the mine workings in the area (for instance, some started more than 300 years ago), much of the current urbanisation has developed above mine workings, and also

developed when mine water and groundwater levels where artificially lowered by pumping. Fig. 1 shows the area of Newcastle-upon-Tyne and Gateshead and how the urban areas grow along with the extent of underground mine workings.

In some areas, with specific geological, mining and hydrogeological conditions, infiltration based sustainable drainage (SuDS) (or SuDS with an infiltration component or a retention component) may not work at present, or in the future. This could result in groundwater and or surface water flooding risks, in some instances such issues may not occur immediately and develop at a later time.

Where there are mine workings below an area with SuDS, infiltration could be in to the mine workings. Some of these areas have mine water management or controls in place to prevent pollution to surface water courses and the wider environment. Increases or changes in infiltration patterns (due to changes in rainfall patterns) could have adverse impacts on the environment, and potentially on the mine workings.

In many parts of the UK, groundwater flooding often appears to have been overlooked, and has sometimes not been considered an issue. This status is even more pronounced when in areas with ongoing mine water management or mine water rebound. Often, it is assumed the groundwater and infiltration regimes will not change in the future. Fig 3 shows the mine water blocks in the northeast of England and also highlights the areas where mine water level could change in the future (rising mine water or pumping controlled blocks).

Due to the potential risks from changing mine water, the Coal Authority and the Environment Agency undertook a joint project to assess potential risks and develop a

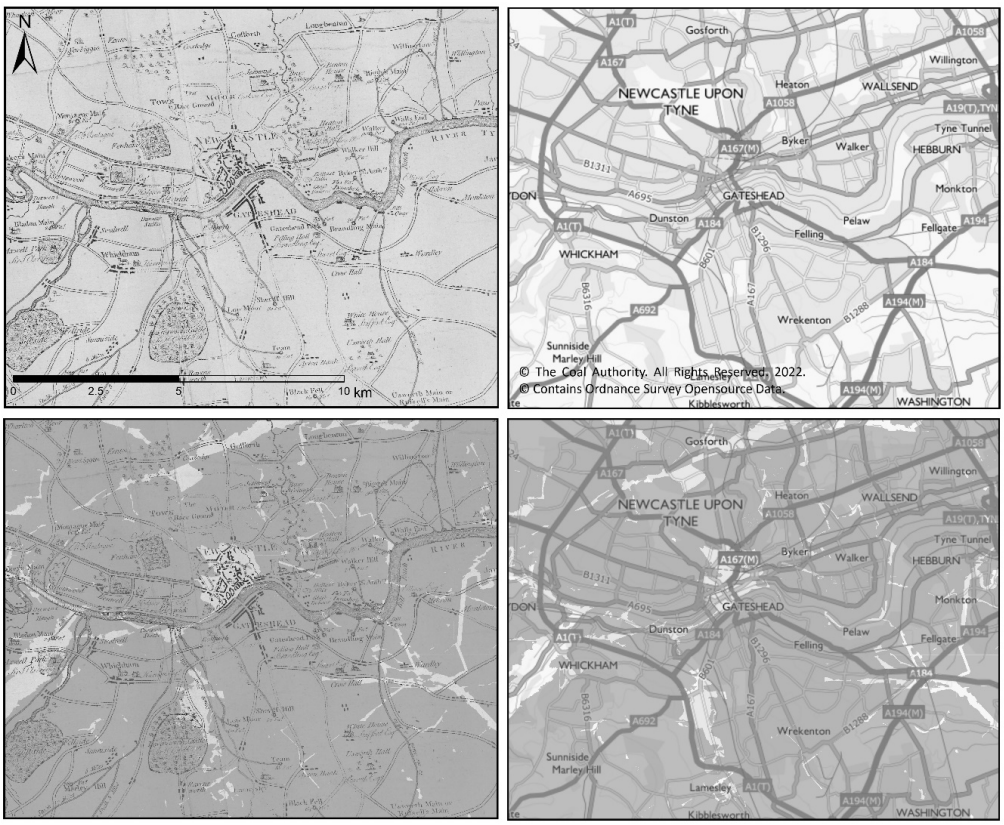

Figure 1 *maps showing urban development between and coal mine workings (top left: map dated 1788; top right map dated 2020; shaded areas on bottom maps are mine workings).*

Figure 2 *groundwater flooding caused by an unplanned reduction in mine water pumping (the pumping station is 7 km from the groundwater issue). Images Coal Authority© and Environment Agency©.*

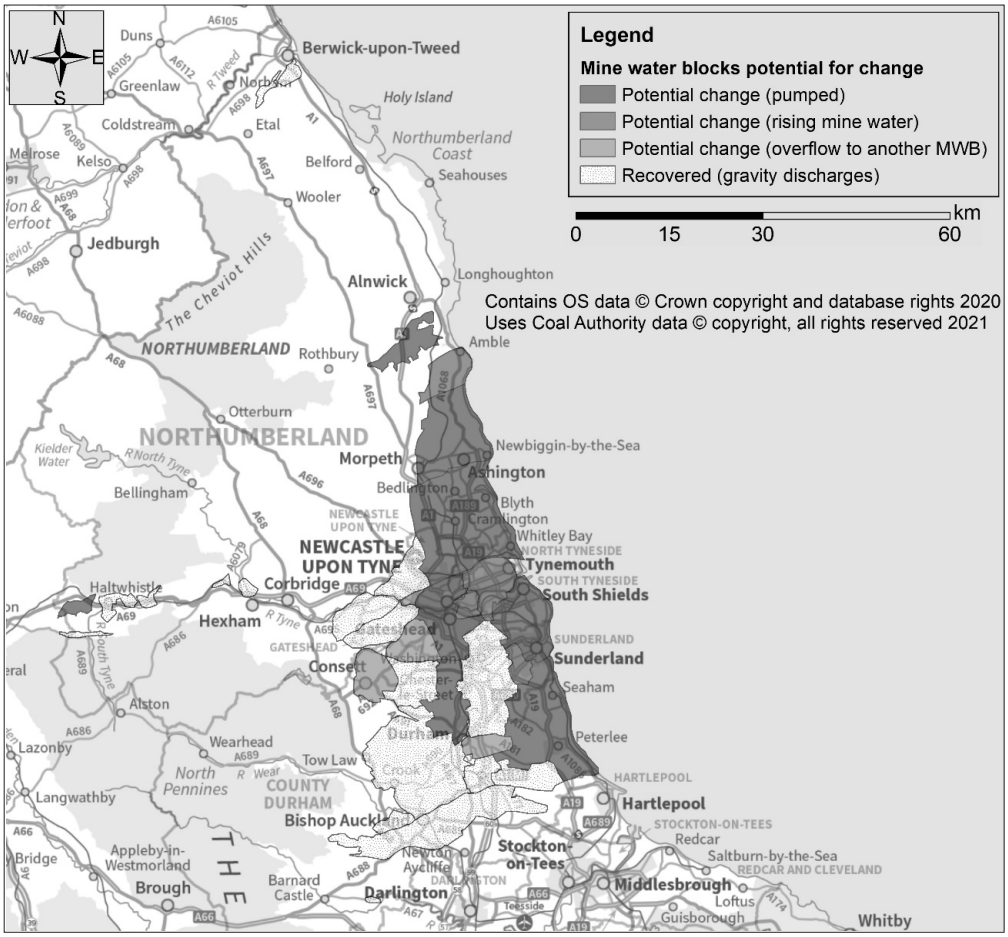

Figure 3 *map of mine water blocks and areas where mine water levels could change.*

screening tool to be used by lead local flood authorities, developers, and consultants.

Screening tool development methodology

The section below describes how different parts of the tool were developed. Essentially, the screening tool was developed using the following key stages.

Stage 1 – assess and appraise potential risks and constraints of SuDS and mine water.

- Set up of an early project group between the Coal Authority, Environment Agency, and 2 of the lead local flood authorities in northeast England.
- Initial ideas were for risk based maps, however, due to the complexity of the potential surface and groundwater interaction, a preferred constraints tool was chosen.
- Standard approach of "source-pathway-receptor" used throughout the development of the tool.

Stage 2 – determine or delineate mine water blocks (hydraulically connected workings) for the northeast of England coalfield.

- Historically the coalfield was divided in to areas, mainly for management during mining, but in some instances these management areas are connected underground.
- Coal Authority mining information and former coalfield reports used along with mine water level data to determine mine water blocks.

Stage 3 – develop a decision process (flowchart) for SuDS constraints category assessment (simplified version in fig. 4).

- Key criteria chosen (with a Yes or No answer) to use for the assessment, following liaison with the project group, these were: major development defined by the Town & Country Planning Act, shallow mine water (<10 m below surface); shallow mine workings (<30 m below surface); and controlling outflow (gravity discharge or pumping station) nearby (<1 km from site).

Stage 4 – produce mine water contours based on 2018 water levels.

- Mine water contours were drawn in ArcMap™ using various contouring techniques such as spline-tension, and spline regularized at different grid spacing settings, these were compared to hand drawn contours, as a reality check. In some instances to help with the automated contouring, dummy points were created.

Stage 5 – determine standard contouring methods to be used for future prediction.

- The methods used for drawing 2018 contours within ArcMap™ for different mine water management scenarios were used to draw future (fully recovered) contours.
- Each block was assessed to determine potential or actual controlling outflow point such as unfilled mine shaft.

Stage 6 – produce predicted mine water contours in a fully recovered situation.

- If the mine water block was fully recovered then the future and current contours were the same.
- In mine water blocks that are pumped or rising, potential controlling outflow points (such as unfilled mine shafts) were identified and determined, based on their surface elevation. Steep conservative mine water gradients of up to 0.002 (1 in 500) and the potential controlling outflow points were used to produce possible future mine water levels.

Stage 7 – write up factsheets for each mine water block.

- Documents for each mine water block (34 in total) were produced that gave a brief summary of the mine water block, its boundaries, the data used for the assessment, and the methodology used for contouring.

Stage 8 – Spatially map the constraints for the full combined extent of the mining blocks.

- The different key criteria layers were mapped in a GIS and analysed using the decision tree, this resulted in a single layer on constraints for use.

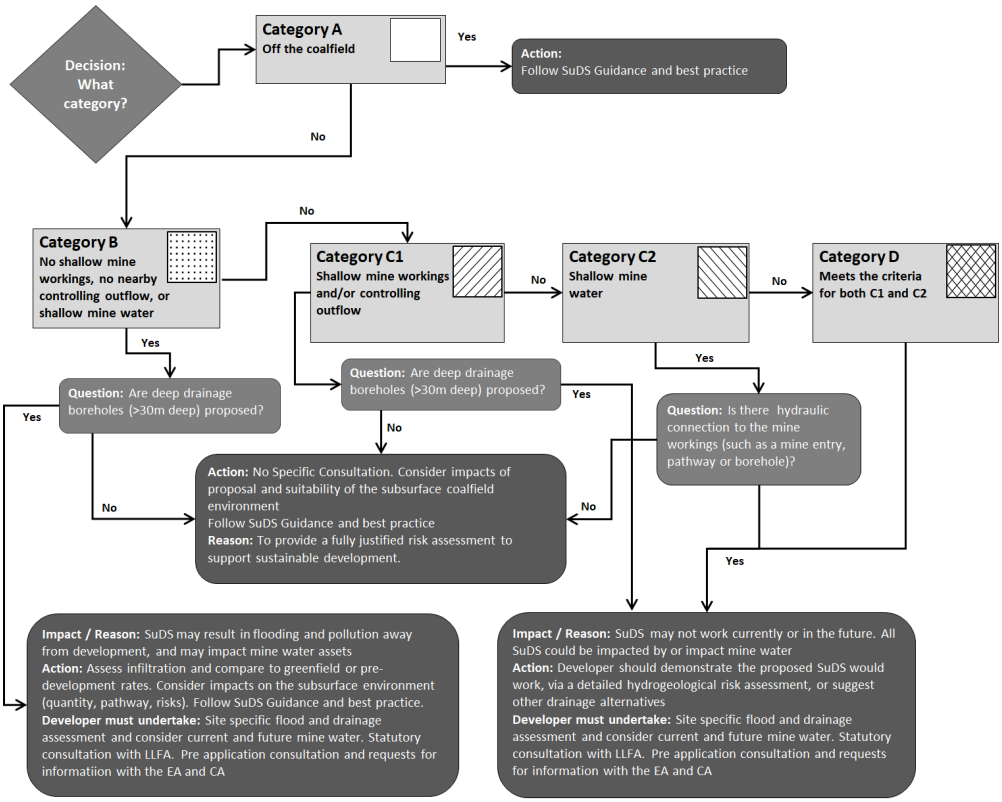

***Figure 4** simplified flow diagram for constraints categories.*

Stage 9 – write the guidance documentation.

Stage 10 – publish the screening tool package and trial for 1 year.

Throughout all the stages, regular stakeholder workshops were held with the key end users of the tool. This was to help make sure that the tool was easy to use, easy to understand, it was beneficial, and it met the needs of the end users.

Screening tool, what is it?

The screening tool incorporates three key components, which include: the 'constraints map', which spatially maps the constraints categories, a guidance document and a supporting document which collates the 34 mine water block factsheets; all of these are EA assets but published and accessed online by the Coal Authority (Coal Authority 2018 and Coal Authority 2021). The reason being because the published constraints map has been developed to be used with other key information which are already available on the Coal Authority Interactive Viewer, such as surface coal mining, mine entries and probable shallow mine workings, and lead local flood authority information. The constraints map available on the Coal Authority Interactive Viewer (fig. 5) has been issued to key end users such as the local planning authorities and the lead local flood authorities.

General comments

Dissemination of the constraints tool on the development of sustainable drainage via the screening has been hugely successful in raising awareness of the associated risks to and from sustainable drainage systems from mine water and groundwater recovery.

Other areas in the UK would benefit from adopting this screening tool approach where the same risks require assessing and mitigating.

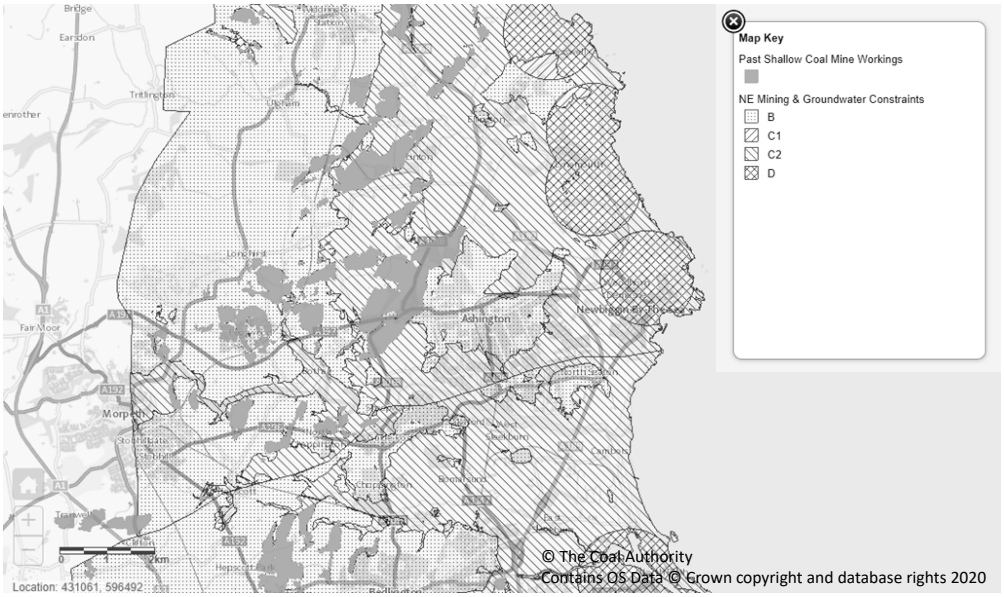

Figure 5 *screenshot of online interactive viewer with the constraints categories and shallow mine workings.*

Use of the screening tool for strategic planning (such as Strategic Flood Risk Assessments, Local Development Frameworks, urban drainage plans); and for assessing development control applications has helped identify the drainage risks and mitigation measures for development. It has also help identify new and additional evidence or data that has both validated and identified where the assessment and screening tool requires improving. This has resulted in updates are planned for 2021-22.

The screening tool has greatly changed and informed the understanding of mine workings hydrogeology. Continuing to use this tool will aim to develop additional supporting assessments and datasets, which can be used to identify critical drainage areas. Expanding partnerships and development of the tool can also be used for the development of fully integrated flood models, planning and management of sustainable urban drainage, and potential development of a predictive and groundwater flood warning system.

Acknowledgements

The authors would like to acknowledge and thank staff at the Environment Agency, Coal Authority, and the lead local flood authorities for their help in producing and testing the tool.

References

Coal Authority (2018) Mining and groundwater constraints for sustainable development and drainage systems (North East England only). Prepared in partnership with the Environment Agency. https://www.gov.uk/guidance/mining-and-groundwater-constraints-for-development

Coal Authority (2021) Interactive map viewer. https://mapapps2.bgs.ac.uk/coalauthority/home.html

Spatial and Temporal Changes of Physio-Chemistry Aspects of Mine Water, Due to Post-Closure Water Management

Lee Wyatt, Jack Cropper

Coal Authority, 200 Lichfield Lane, Mansfield, NG18 4RG, UK, leewyatt@coal.gov.uk

Abstract

Over time and spatially, in dynamic mine systems, the water changes naturally and due to alterations in water management. Understanding the behaviour of water within the mine system, along with how this water changes can be essential. Understanding of the mine system and the water can help with future predictions, and result in most beneficial management options being used.

Part of mine water management includes inspections of the mine shafts; discrete sampling; and electrical conductivity logging of the water in the shafts. These tests are used to confirm or improve the conceptual understanding of the mine system, and often used in mine water prediction and water management planning.

The project focussed on the Dawdon-Horden Coalfield, in northeast England. Shaft logging discrete samples have been taken between 2000 and 2019, from 4 mine shafts. Mine water levels were monitored since 1990s to predict mine water rebound risks. Prior to 2004, the physio-chemistry data taken from the shafts and it was used as part of mine water rebound and risk assessment. Since 2004, pumping of the mine system has been undertaken at Horden and Dawdon mines, to prevent pollution of an overlying aquifer.

The discrete depth samples and electrical conductivity-temperature logs show variations in chemistry and water temperature. These variations are throughout time, and with the water columns in the shafts. Analysis and assessment of data from four shafts in the coalfield has been undertaken. Trends in data have been used to confirm and improve the knowledge of the mine system and how it interacts with the environment. Spatial and temporal trend analysis was undertaken at each shaft, and the assessment of each shaft was input in to the conceptual model to create a temporal-spatial analysis of the mine system.

Changes in the mine water can be used to predict things about the mine system, such as sources of recharge; and predominant flow pathways within the mine system. Such changes not only give confidence in the conceptual understanding, but can also be used to confirm risk, and that best mine water management options are being utilised now and in the future. The data obtained can also be used to help assessment of mine water energy schemes, and how these schemes and water management options may influence the physio-chemistry of the water.

Keywords: Chemistry, Temperature, Post-Closure, Water Management, Stratification

Full Paper

A full paper on the results of this study will be published in an upcoming issue of the "Mine Water and the Environment" journal. If you have further interest or questions in the meantime, please contact the authors.

Emerging Opportunities for Improving Legacy Metal Mine Water Pollution driven by Changing Regulatory Environments and Outputs of Novel Fieldwork in the Southern Uplands of Scotland

Alan Yendell[1], Patrick Byrne[2]

[1]*Scottish Environment Protection Agency, Angus Smith Building, Maxim 6, Parklands Avenue, Eurocentral, Lanarkshire ML1 4WQ, alan.yendell@sepa.org.uk, ORCID 0000-0002-5755-2987*

[2]*School of Biological and Environmental Sciences, Liverpool John Moores University, Liverpool, L3 3AF, UK, p.a.byrne@ljmu.ac.uk, ORCID 0000-0002-2699-052X*

Abstract

The Wanlock Water is polluted by relicts of a former lead mining and processing industry. The problem is well known but it has been difficult to justify funding bids for remediation due to uncertainty about the scale of the water quality improvement remediation works could deliver. Utilising opportunities created by a regulatory shift at SEPA, source apportionment work has been undertaken. Application of tracer injection and synoptic sampling in the Wanlock Water improved the understanding of key sources. Water quality improvements achievable by remediation have been estimated and collaboration towards improvement is progressing in the context of wider political objectives.

Keywords: Regulation, Collaboration, Source Apportionment, Tracer Injection, Synoptic Sampling.

Introduction

Metalliferous deposits in Scotland are generally small scale and scattered throughout the country (EnviroCentre Ltd *et al.* 2015). Accessible and productive galena and sphalerite veins resulted in the villages of Leadhills and Wanlockhead in the Southern Uplands of Scotland being at the centre of lead production for the country, especially in the 19th & 20th century. The Wanlock Water contains elevated concentrations of Cadmium (Cd), Lead (Pb) and Zinc (Zn) associated with former lead mining and production industry in and around the village of Wanlockhead. Evidence of this industrial activity remains prominent in the landscape and there are numerous potential mine pollution sources in the head waters of the Wanlock valley within the River Nith catchment (Figure 1).

The Wanlock Water has a Water Framework Directive (WFD) classification of less than Good due to the pollution caused by the mining that once thrived there (SEPA 2019). The Wanlock Water flows northwest for 8 km to the Crawick Water, where the Pb attenuates and is diluted, but Cd and Zn cause it to be of less than Good status. Cadmium concentrations continue to be elevated in the River Nith with a total of over 50 km of river at less than Good status.

The WFD requires countries to work towards rivers being of Good ecological status or above and required agencies such as SEPA to classify all water bodies. The monitoring of rivers in the areas under the WFD has helped to formalise the scale of the problem of mine water pollution. Yet legislation restricts the liability that can be placed on those who owned and operated mines that were abandoned prior to 1999 (Environment Agency 2008). This, in effect, severely restricts the likelihood of successful enforcement and creates a situation whereby alternative funding models are required to fund remediation. In Scotland, funding routes could be available to help improve the water quality, but the options and opportunities may increase by collaboration with other aims.

The pollution, the regulatory situation, and potential funding opportunities available for remediation gives cause for sufficient understanding of the numerous mine pollution sources that are known to be present. In particular metal loadings from both point

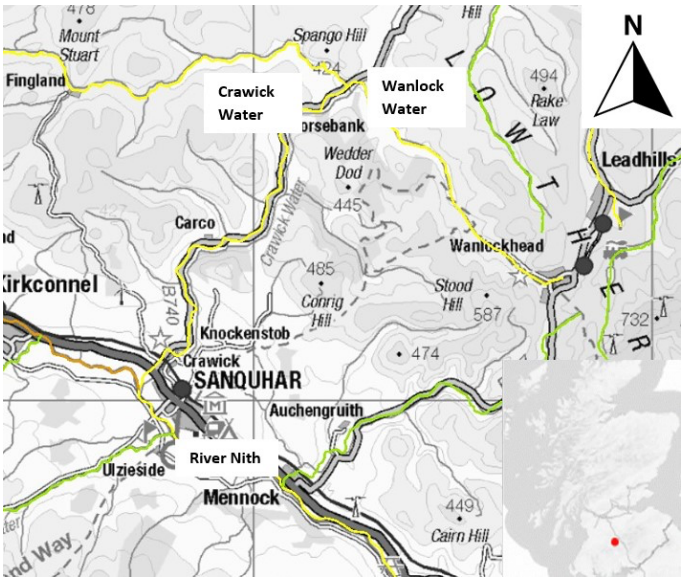

Figure 1 *Wanlock Water and Crawick Water in the River Nith catchment, Scotland.*

and diffuse sources are required to be able to understand the improvements that could be achieved by targeting specific sources and what the scale of any improvement in water quality would be to the wider catchment. This paper discusses the value of a source apportionment study in the Wanlock Water using novel techniques, and the remediation opportunities arising from it, in the context of the Scottish Environment Protection Agency (SEPA) regulatory strategy.

One Planet Prosperity

The Regulatory Reform Act (Scotland) 2014 gave SEPA its current statutory purpose, to protect and improve the environment in ways that, as far as possible, create health and well-being benefits and sustainable economic growth. The organisations' strategy to implement this purpose is called One Planet Prosperity (1PP) which highlights that as a country Scotland overuses it resources and that SEPA should be aiming to improve the environment while helping communities and businesses thrive within the resources of our planet.

While the approach does not alter any of the environmental regulations businesses must adhere to, or how they are enforced, it does change the approach taken to regulation with a push to work with communities and business to go 'beyond compliance' to improve their overall environmental impact in the climate emergency. This enables collaboration in a way that has a benefit to the environment and supports potential innovations in the field of mine water remediation.

In the context of the pollution issues known in the Wanlock Water, instead of just aiming to meet water quality standards, any projects to improve water quality are more likely to succeed if they have multiple aims and benefits. These could include supporting national climate change goals, increasing the amenity value of land to the local community, increasing the value of the industrial heritage or introducing the principals of circular economy into the solution. Using and building in other benefits to mine water remediation projects allows a variety of organisations to become involved to drive the water quality improvements.

A brief history of monitoring in the Wanlock Valley

In the former mining area of Wanlockhead and the adjacent village of Leadhills, knowledge of water pollution from the former mines is longstanding. The Clyde River Purification Board identified trout with blackened

tails, an indicator of chronic Pb poisoning, with analysis of fish tissues revealing elevated Pb concentrations back in the 1980's in the Glengonnar Water flowing from Leadhills (SEPA 2011). In the same valley high levels of Pb have been found in the floodplain sediments (Rowan *et al.* 1995). As mining occurred in the same mineral veins, along with processing and smelting activity in the Wanlock valley similar pollution was anticipated to be present in the Wanlock Water.

Subsequent studies by the Coal Authority identified that there are numerous potential mine pollution sources in the head waters of the Wanlock Valley (Coal Authority 2011; Coal Authority 2014). The work confirmed previous findings that Cd and Zn are found in the river predominantly in dissolved (<0.45 µm) form while Pb is predominantly in particulate form. In total over 20 potential diffuse and point sources were identified, either by sampling run off and discharges or desk study researches, with potential for distinct sources within some of the larger features. Though some calculations were carried out on loadings from particular sources, source apportionment of the many identifiable sources had not been carried out. Some of the key features of interest and potential sources are shown in Figure 2 and Figure 3 which also show the change in the valley over the most industrious period of mining and processing between the mid 1800's and mid 1900's.

Local challenges and the benefits of source apportionment studies

The Environment Agency (EA) in England and Wales, and subsequently Natural Resources Wales (NRW) have both made good progress in securing funding for non-coal mine water contamination remediation. By comparison, Scotland has a smaller scale of problem with metal mine water pollution. Resource constraints can make it challenging to dedicate sufficient effort to gathering concurrent metal concentration and flow data by standard salt slug methodologies on the scale required to understand loadings from numerous mine pollution sources on a 3 km reach of river. Furthermore, in this area of south west Scotland the annual rainfall exceeds 1500 mm/a (Rowan *et al.* 1995). As a result collecting good quality metal loading

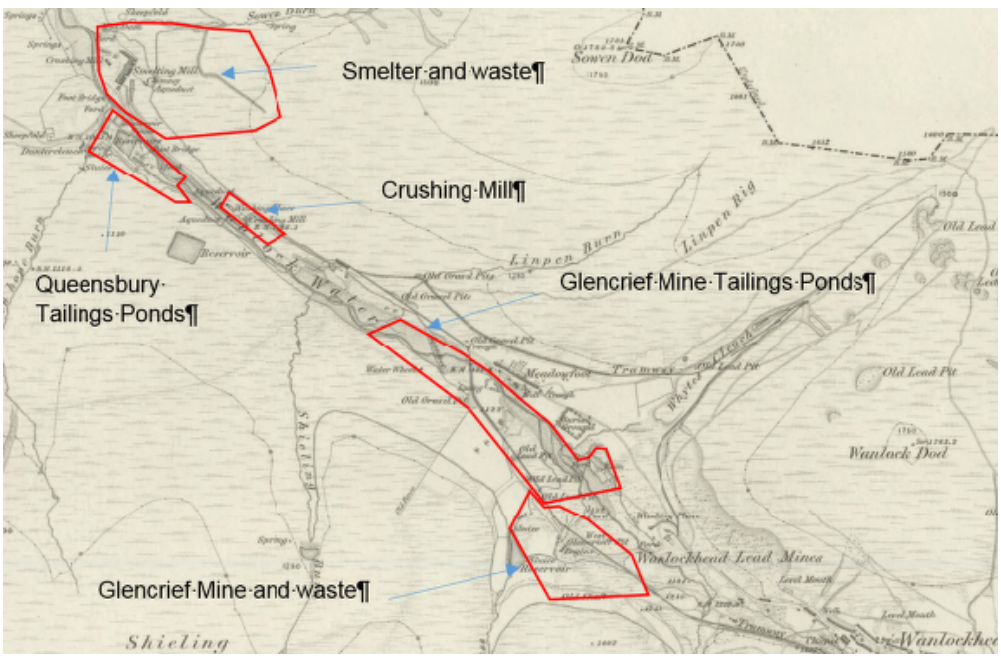

Figure 2 *Potential diffuse sources in the Wanlock Valley on an extract of the Ordnance Survey Map of 1860 (OS 1860).*

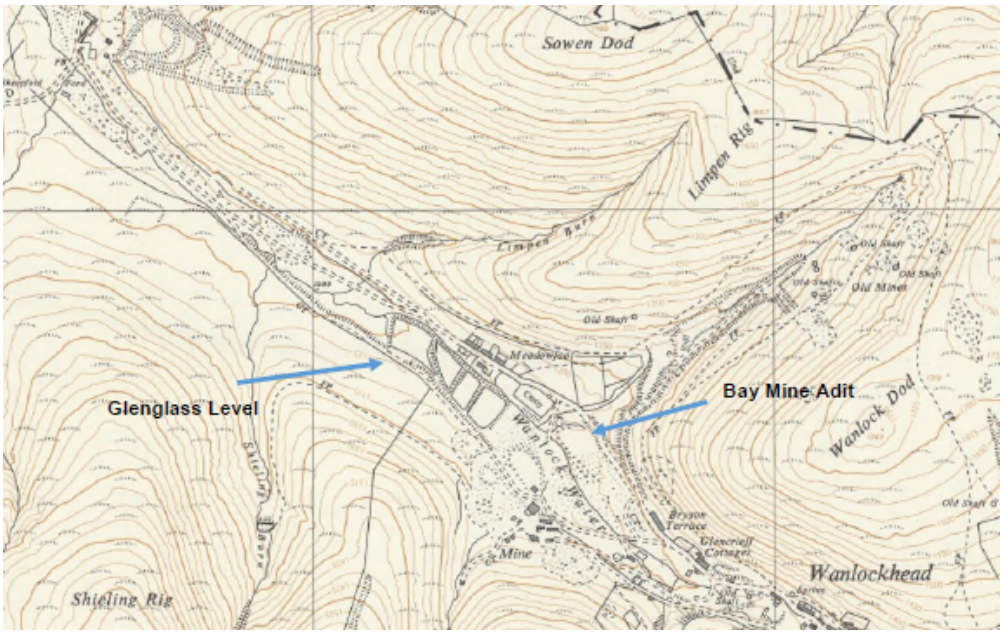

Figure 3 *Potential point sources in the Wanlock Valley on an extract of the Ordnance Survey map of 1962 (OS 1962).*

data at multiple locations and under a specific flow regime can be challenging when the site work required is likely to span a number of days, and the river is known to react rapidly to rainfall. Such work requires a level of reactive sampling that is not practical to deploy.

Knowledge sharing events such as those hosted by NRW in recent years have highlighted the benefit to their mine remediation program of a concurrent flow and water quality sampling method using continuous injection of conservative salt tracers (Byrne *et al.* 2020). The technique developed by the U.S. Geological Survey (USGS) to undertake source apportionment of mine water pollu-tion has since been used successfully to identify discrete pollution sources in rivers affected by mine water pollution (Kimball *et al.* 2002; Runkel *et al.* 2017).

In partnership with Liverpool John Moores University (LJMU), SEPA undertook a source apportionment assessment using a continuous salt tracer injection and synoptic sampling along a 2 km river reach of the Wanlock Water. The work was commissioned due to the potential to drive improvements in the context of the 1PP regulatory strategy.

Source apportionment results

The fieldwork and subsequent sample laboratory work and data analysis was carried out by SEPA and LJMU. The methodology is presented in Byrne *et al.* (accepted). The source apportionment data identified that under Q30 (medium to high) river discharge conditions, three mine water discharges contribute c.60% of dissolved Cd and Zn loading. An area of tailings deposits in the floodplain and a braided section of the river contributed c.60% of dissolved Pb, the tailings were also notable sources of Cd and Zn (Byrne *et al.* accepted). The work also demonstrated that tracer injection and synoptic sampling works well in small temperate rivers at flow rates of around 280 L/s, and could be scaled up further if necessary.

While it is acknowledged that this study was undertaken only on one occasion, when combined with the large amount of historic water quality monitoring data in the wider catchment, it adds substantial new detail to the available evidence. It identifies the largest pollutant loads to be from diffuse mine tailings source (Cd and Pb), a braided wetland section of the river likely affected by sediment

deposition (Pb) and point source mine water discharges (Cd and Zn). The metal loading data provides simple visual tools to convey technical data effectively to stakeholders including government, landowners, local authorities and community groups such as the map and graph presented in Byrne *et al.* (accepted) and reproduced here by way of example in Figure 4.

Emerging opportunities

The outputs from the recent and historic monitoring data set were utilised by SEPA to inform Source Apportionment Geographical Information System (SAGIS) modelling to provide an indication of the metal loading reduction required to achieve status improvements in the wider River Nith catchment downstream from the study area. This indicated that a 20% reduction in Cd and Zn at source in the Wanlock Water could lead to improvement in status of the River Nith.

Potential reductions from five different remediation scenarios based on the pollutant loadings for Cd and Zn as shown in Figure 4[b] were undertaken by Byrne *et al.* (accepted). Given that achieving 100% reductions from a single source location is unrealistic, it is considered that to achieve a 20% reduction in Cd and Zn from more than one source would need to be targeted.

Upon completion of the work the outputs have been utilised to compile an up to date picture of our understanding of the pollutant

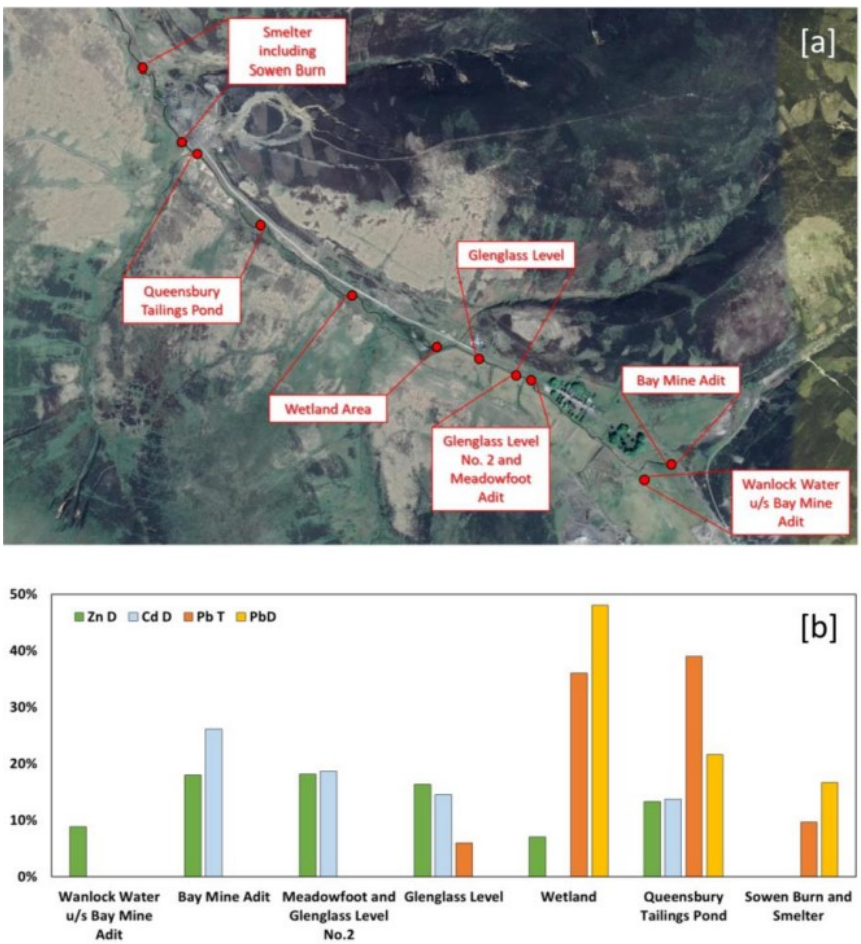

Figure 4 *Locations [a] and percentage loadings [b] over the study reach of Wanlock Water from Byrne et al. (accepted)*

sources in the area. It is clear that at least one of the point sources of mine water discharge needs to be targeted to reduce Cd and Zn, but in order to reduce the Pb loading work will also be required on the diffuse sources of legacy land contamination. One of these features is the un-vegetated former Queensbury tailings pond, located adjacent to the Wanlock Water and is eroding into the river, causing pollutant loading of Cd, Pb and Zn. It is therefore a good feature to consider for remediation, and the source apportionment backs up previous recommendations to remediate this feature by the Coal Authority.

Source apportionment allows us to highlight the important sites to researchers and as the environmental regulator working to the 1PP strategy we can collaborate to support and facilitate research work where appropriate within the bounds of SEPA's remit. Existing connections to academic and research and development projects in the field of remediation and the circular economy have presented opportunities such as an international project to trial planting of biofuel crops on contaminated soils, which could provide a purpose to many vacant and derelict sites to produce more sustainable fuels. It is hoped to use areas of tailings as test sites for this project. Trials are also planned of novel methods of mine water treatment that have potential commercial applications in many other water treatment scenarios. We are now better placed to identify the most appropriate site to trial water treatment techniques in the area.

Other opportunities can come from changing government policy in planning, introducing the concept of placemaking goals being embedded in environmental improvement projects. This could lead to outcomes such as improving tourism facilities, visibility of heritage sites, and amenity land for local people being provided as part of remediation works. Work is underway to bring together a wider stakeholder working group with the ultimate aim of it leading various projects to improve water quality, facilitated but not led by SEPA.

Conclusions

Understanding the significance of mine water pollution in the context of the wider political climate of a country provides a sound base to achieve the goals of watershed management plans. It can be seen how source apportionment work, in combination with existing data and the new regulatory environment is allowing us to highlight the legacy mine water pollution issues to the various stakeholders. This in turn helps promote the potential of remedial projects to deliver environmental improvements, while embedding other socio-economic principals. As action to combat climate change rises higher up the agenda, it will be critical to embed wider sustainability goals into projects to achieve funding. The challenge now in Scotland is to engage and collaborate with the right people and organisations to make that happen and deliver at least some improvement to the water quality in the Nith catchment.

References

EnviroCentre Ltd, Pleydell Smithyman (2015) Inventory of closed mining waste facilities. Scottish Government

Scottish Environment Protection Agency (2019) Classification Hub http://www.sepa.org.uk/data-visualisation/water-classification-hub/

Environment Agency (2008) Abandoned mines and the water environment. SC030136/SR41

Scottish Environment Protection Agency (2011) Review of metal concentrations data held for Glengonnar Water and Wanlock Water, South Central Scotland

The Coal Authority (2011) The impacts of mining on the Glengonnar Water, Leadhills, South Lanarkshire – Scoping Study

The Coal Authority (2014) The impacts of mining on the Wanlock Water, Wanlockhead, Dumfries and Galloway – Scoping Study

Ordnance Survey (1860) Dumfriesshire Sheet VII (1:2500)

Ordnance Survey (1962) Sheet NS81SE (1:10000)

Rowan JS, Barnes SJA, Hetherington SL, Lamber B (1995) Geomorphology and pollution: the environmental impacts of lead mining, Leadhills, Scotland Journal of Geochemical Exploration 52:57-65

Byrne P, Onnis P, Runkel RL, Frau I, Lynch SFL, Edwards P (2020) Critical Shifts in Trace Metal Transport and Remediation Performance under Future Low River Flows Environ. Sci. Technol. 2020, 54, 24, 15742–15750 doi.:10.1021/acs.est.0c04016

Kimball BA, Runkel RL,Walton-Day K, Bencala KE (2002) Assessment of metal loads in watersheds affected by acid mine drainage by using tracer injection and synoptic sampling: Cement Creek, Colorado, USA Applied Geochemistry 17:1183-1207 doi: 10.1016/S0883-2927(02)00017-3

Runkel RL, Kimball BA, Nimick DA, Walton-Day K (2017) Effects of Flow Regime on Metal Concentrations and the Attainment of Water Quality Standards in a Remediated Stream Reach, Butte, Montana Environ Sci Technol 50:12641-12649 doi:10.1021/acs.est.6b03190

Byrne P, Yendell A, Frau I, Brown A (2021) Identification and prioritisation of mine pollution sources in a temperate watershed using tracer injection and synoptic sampling. Accepted for publication in a future edition of Mine Water and the Environment.

Influence of Coal Mining on Water Environment and Ecology in the Yellow River Basin

Fawang Zhang[1], Zhiqiang Zhang[1,2,3]

[1]*Chinese Academy of Geological Sciences, Beijing 100037, China, zzqiang187@163.com*

[2]*Hefei University of Technology, Hefei 230009, China*

[3]*Hebei GEO University, Shijiazhuang 050031, China*

Abstract

The upper and middle reaches of the Yellow River are important coal production bases in China, and the current situation of "more coal and less water" has been the main factor restricting its economic development. In addition, the destruction of water resources caused by coal mining makes the "coal and water contradiction" more prominent and becomes the bottleneck restricting the high-quality development of the Yellow River Basin. Based on the coal resources in the upper and middle reaches of the Yellow River and the history of the Yellow River's dry-up, this article puts forward the main environmental problems faced by the Yellow River; Such as prominent coal-water contradiction and sharp contradiction between water supply and demand; declining natural river runoff and river dry-off; fragile ecological environment and increased soil erosion; serious water pollution and so on. The impact of coal mining on the natural water cycle, water environment, soil erosion, and water-sediment relationship are systematically analyzed, and the following conclusions are drawn: coal mining damages the underlying hydrological surface and changes the transformation relationship between precipitation, surface water and groundwater. Therefore, the natural water cycle process is destroyed; A large amount of mine water, slime water and coal gangue leaching water produced in the process of coal mining are the main pollution sources that cause ammonia nitrogen, permanganate index, BOD5 and other factors in the Yellow River Basin to exceed the standard; The sediment of the Yellow River mainly comes from the gully area of the Loess Plateau between Hekou Town and Longmen. The large-scale mining of coal resources in the basin has aggravated the process of soil erosion of the original landform, changed the natural relationship between water and sand in the basin, and led to the siltation of downstream rivers. In order to effectively and rationally use water resources and realize the coordinated development of ecological protection and social economy in the Yellow River Basin, the coordinated development proposal of "Ecological Environment-Water Resources Protection-Mineral Development" was finally put forward, which provided ideas for solving the problem of "coal-water contradiction" in the Yellow River Basin.

Keywords: Coal and Water Contradiction, Water Resources, Yellow River Basin, Coal Mining

Introduction

The Yellow River basin is an important link connecting the western, central and eastern regions of China. It is also known as China's "energy basin" because it is rich in coal, oil and non-ferrous metals. In recent years, the large-scale mining of mineral resources in the Yellow River basin has not only promoted the economic development of the basin, but also brought about new environmental problems (Zhang *et al*. 2000, 2007). In particular, the mining of coal resources in the upper and middle reaches of the Yellow River has caused a series of ecological and environmental problems, such as soil erosion, land subsidence, water shortage and water pollution and so on.

The key to solve the ecological environment problems in the upper and middle reaches of the Yellow River lies in the coordination of the "coal-water contradiction" and the maximum reduction of the damage of coal mining to water resources (Zhang *et al.* 2001).

It is an important content to protect the ecological environment of the Yellow River Basin, and the key to promote the high-quality development of the Yellow River Basin.

Overview of coal resources in upper and middle reaches of the Yellow River

The upper and middle reaches of the Yellow River are the main coal production bases in China. Seven of the 13 large coal bases in China are located in the upper and middle reaches of the Yellow River, and the total coal resources account for 60.4% of the 13 large coal bases. The basic information of large coal bases in the upper and middle reaches of the Yellow River is shown in Table 1.

The break-off discharge in the Yellow River

The break-off discharge in the Yellow River began in the 1970s (Zhang *et al.* 1998). The break-off discharge in the Yellow River means that the measured runoff at Lijin Hydrological Station, the lowest reaches of the Yellow River, is less than $1m^3/s$. According to statistics, the lower reaches of the Yellow River were break-off discharge for 22 years, from 1972–1999 (Wang 2002; Cao *et al.* 2007). A total of 902 days, 1991 ≈1999. Especially in 1997, the precipitation and runoff in the Yellow River basin were less, and the lower reaches of the Yellow River have been severely break-off discharge in history.

Main environmental problems in the upper and middle reaches of the Yellow River

(1) The contradiction between coal and water is prominent, and the contradiction between supply and demand of water resources is sharp

The middle reaches of the Yellow River are dominated by the coal industry. As a high-water consuming industry, the coal industry consumes a large amount of water resources on the one hand, and on the other hand, it destroys the natural water circulation system and pollutes water resources, which leads to the decrease of available water resources and intensifies the contradiction between supply and demand of water in the basin.

Table 1 *Basic information of large coal bases in the upper and middle reaches of the Yellow River.*

Coal bases	Area km^2	Location	Coal resources	
			Coal resources (10^8t)	Proportion(%)
Shendong	9000	North Shanxi Province and west Inner Mongolia Autonomous Region	1723.59	36.46
Jinbei	6700	North Shanxi	262.89	5.56
Henan	10849	West and East (Middle) of Henan Province	265.89	5.62
Jinzhong	27475	Central Shanxi Province	1098.08	23.23
Huanglong	11084	Central Shaanxi Province and eastern Gansu Province	247.97	5.25
Ningdong	2105	East of Ningxia Hui Autonomous Region	377.70	7.99
Shanbei	18366	Northern Shaanxi Province	751.17	15.89
Total	85579	—	4727.29	100

Table 2 The break-off discharge in the Yellow River over the years.

Years	The average number of days without flow d	The longest number of days without flow in a year d	Maximum channel length without flow in a year km
1972-1979	86	21	316
1980-1989	105	36	662
1990-1999	901	226	704
1972-1999	1092	226	704

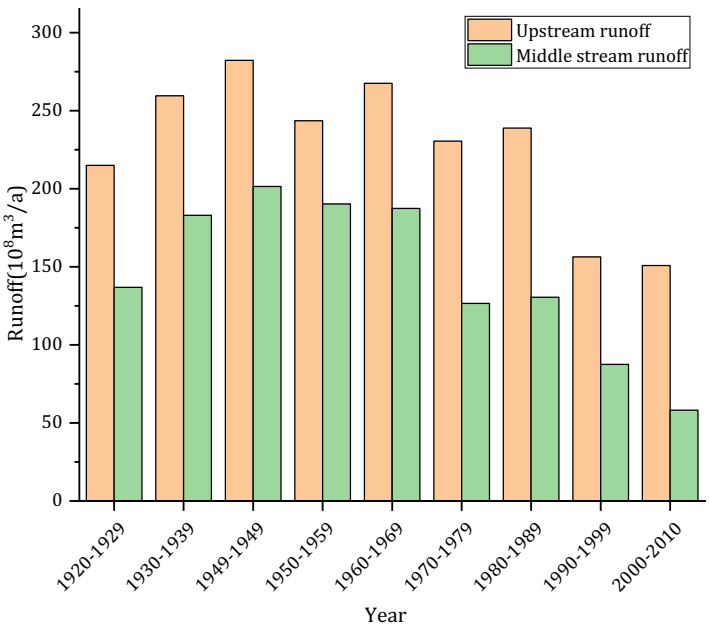

Figure 1 Variation of annual average runoff in the upper and middle reaches of the Yellow River.

The "Impact and Evaluation of Coal Mining on Water Resources in Shanxi Province" shows that every ton of coal mined in Shanxi consumes 2.48 tons of water resources. From 1949–2004, Shanxi mined 7.7 billion tons of coal and lost 19.1 billion tons of water (Niu 2003).

(2) The natural runoff of the river has been sharply reduced, and the problem of river break-off discharge is prominent

The average runoff of the Yellow River decreased from 19.03 billion m^3 in 1950–1959 to 5.82 billion m^3 in 2000–2010 (Li *et al.* 2014; Liu *et al.* 2019). In the 28 years from 1972–1999, the flow of the lower reaches of the Yellow River was break-off discharge for 22 years due to the decrease of inflow and the intensification of water resources and coal resources development.

(3) The ecological environment is fragile and soil erosion is aggravated

The biggest characteristic of the Yellow River is different from other big rivers: less water and more sediment, different sources of water and sediment, resulting in the "over-ground river" of the lower reaches. These characteristics are related to the ecological environment of the Yellow River basin.

Serious soil erosion has brought serious ecological environment problems to the

Loess Plateau, such as the destruction of vegetation and the decline of ecological function, and the deterioration of ecological environment has been aggravated by the unreasonable economic activities of human beings. From 1949–2004, the area of land damaged by coal mining in Shanxi Province was 1151.95 km^2.

(4) Serious pollution of water environment

Along the Yellow River, there are many industrial enterprises with high pollution, such as energy, heavy chemical industry, non-ferrous metal and paper making, and the discharge of wastewater is increasing year by year. Since the 1980s, about 40% of the water quality monitoring sections in the main stream and tributaries of the Yellow River are worse than the third grade water quality in the Chinese Environmental Quality Standards for Surface Water (GB3838-2002), rising to 60% in the late 1990s, and as high as 70–80% in the 21st century (An XD 2007).

The influence of coal mining on the middle reaches of the Yellow River

(1) Destruction of water resources

Coal mining will lead to the destruction of the hydrological underlying surface. Under the influence of the "three zones" (namely caving zone, fracture zone and bending subsidence zone) of the mining overburden, a large amount of surface runoff leaks along the mining-induced fissures, resulting in the decrease of surface water resources.

Influenced by the mining of coal resources, the runoff of Kuye River, the main tributary of the Yellow River, has been sharply reduced in the past 10 years. In addition to climate change and other natural causes, the high intensity coal mining since the 1990s is the main reason for the discharge attenuation and flow interruption of the Kuye River (Fan 2007). From 1997–2005, the contribution rate of coal mining to runoff reduction in Kuye River Basin reached 52.27% (Liu *et al.* 2013)

(2) Polluted water environment

In the process of mining coal resources, a large number of mine wastewater will be produced, such as mine water, coal slime water and coal gangue leachate water, which contains a variety of high-concentration pollutants, such as SS, COD, metals and semi-metals, which will cause water resource pollution if treated improperly.

The discharge of coal mine wastewater in the upper and middle reaches of the Yellow River in China is about 86.17 million t/a, among which the 7 coal mine bases discharge about 81.94 million t/a, accounting for about 95% of the total discharge of coal mine wastewater in the upper and middle reaches of the Yellow River.

As shown in Table 2, the water quality of V and bad grade in the main Yellow River reaches 1761 km, accounting for 48.7% of the evaluated river length. The water quality of V tributaries and inferior parts of the Yellow River reaches 2963 river lengths, accounting for 76.3% of the evaluated river lengths.

(3) Soil and water loss

The Loess Plateau, located in the upper and middle reaches of the Yellow River, is the most serious area of soil and water loss in China. Coal mining will severely disturb the surface, often leading to surface collapse and vegetation destruction. At the same time, soil structure is loosened, soil is more vulnerable to erosion and desertification, which leads to serious soil and water loss. The area in the middle reaches of the Yellow River belongs to the semi-arid continental monsoon climate in the north temperate zone, with low vegetation coverage rate and loess and aeolian sand as the main surface materials. The middle reaches of the Yellow River itself is very easy to produce soil and water loss, and the large-scale mining of coal resources in the basin induces and intensifies the process of soil and water loss of the original landform and intensifies the desertification of the land.

Problems that should be paid attention to in the process of mining coal resources

(1) Explore new development models

Taking "ecological environment, water resources protection and mineral exploitation" and other factors as an organic whole, we should take all factors into consideration to achieve coordinated development.

(2) Control water consumption

We will strengthen the management of red lines for the development and utilization of water resources and strictly control the total amount of water used. The layout and scale of the coal base development in the basin and the coal industry projects are reassessed according to the principle of "depending on water to determine the production", and scientific adjustment is made. Strictly restrict the development of coal mining, coal power generation and coal chemical projects that exceed the carrying capacity of regional water resources and water environment. We will strictly control the increase of coal production capacity, speed up the elimination of outdated coal production capacity, and support the development of renewable energy.

(3) Resource utilization of mine drainage

The mine water should be regarded as mineral resources, and the resource utilization of mine water should be realized, and the comprehensive utilization rate of mine water should be improved, especially the resource utilization of low temperature mine hot water in shallow and middle level.

(4) Prevent and control the damage of aquifer and implement coal mining with water conservation

According to the characteristics of aquifer, impermeable layer and coal seam, the threshold value of groundwater level control is determined to reduce the movement and deformation process and damage degree of mining overburden. To study the evolution process of groundwater, stress, and fissure under mining conditions, and to study the evolution process and mechanism of groundwater level during mining. At the same time, the change process of groundwater level, water quality and water temperature in the process of mining is monitored, and the evolution process of stress field, fracture field and seepage field in the coal face and the affected area is monitored.

(5) Optimize well design to reduce the destruction of water resources

In order to reduce the damage to the aquifer, no well and roadway should be arranged in the aquifer or the engineering across the aquifer should be reduced by optimizing the design of the well and roadway engineering. The exposed aquifer outlet points should be blocked by grouting or chemical plugging in time to reduce groundwater leakage. For the boreholes with water conduction structure and poor sealing, exploration work should be done well, and avoidance measures should be taken in the design to prevent the exposure or conduction of aquifers and water storage structures.

References

An XD (2007) Current status of management and regulation of Yellow River water resources and future prospect. China Water Resources 13:16-19 (In Chinese)

Cao JF, Wang KJ, Jiang JY (2007) Impact of lower Yellow River cutoff on the formation and exploitation of groundwater in alongside areas. Journal of Jilin University (Earth Science Edition) 37(5):937-942 (In Chinese)

Fan LM (2007) Analysis of groundwater leakage caused by coal mining in the northern area of Shaanxi Province and its prevention. Mining Safety & Environmental Protection 34(5):62-64 (In Chinese)

Li EH, Mu XM, Zhao GJ (2014) Temporal changes in annual runoff and influential factors in the upper and middle reaches of Yellow River from 1919-2010. Advances In Water Science 25(2): 155-163 (In Chinese)

Liu CM, Tian W, Liu XM (2019) Analsis and understanding on runoff variation of the Yellow River in recent 100 years. Yellow River 41(10):11-15 (In Chinese)

Liu EJ Zhang XP, Zhang JJ (2013) Variation of annual streamflow and the effect of human activity in the Kuye River during 1956 to 2005. Journal of Natural Resources 28(7):1159-1168 (In Chinese)

Niu RL (2003) Impact and evaluation of coal mining on water resources in Shanxi Province. Science and Technology of China Press, Beijing (In Chinese)

Wang AJ, Zhu C (2002) Response of water break-off in the Yellow River to global climate change. Journal of Natural Disasters 11(2):103-107 (In Chinese)

Zhang FW Hou XW (2000) The influence of coal exploitation on water and soil resources and its protection technology. Hydrogeology & Engineering Geology 2:52-53 (In Chinese)

Zhang Fw Wang GL Hou XW (2001) Environment geology chain due to mine exploitation and methods for control. Earth Science Frontiers 8(1):107-111 (In Chinese)

Zhang FW Zhao HM Song YX Chen L (2007) The effect of coal-mining subsidence on water environment in the Shenfu-Dongsheng mining area. Acta Geoscientica Sinica 28(6):521-527 (In Chinese)

Zhang RY Yang XL (1998) Historical review and analysis of the Yellow River cutoff. Yellow River 20(10):38-40 (In Chinese)

Investigating Potential Subvertical Dewatering Wells at an Open Pit Mine

Patrick Moran, Joe Ross, Rod Williams, Ramsey Way

Iron Ore Company of Canada, 2 Avalon Drive, Labrador City NL, Canada A2V 2G4, patrick.moran@ironore.ca

Abstract

Groundwater poses a risk to mining at the Iron Ore Company of Canada (IOC). Ore bodies being mined are currently dewatered via borefields comprised of vertical wells. While vertical wells are a proven technology, and have enabled mining to progress below water table, they are not an optimal solution for every situation. Subvertical wells are an optimal alternative. Two subvertical pilot holes were recently drilled at IOC. Both intersected strongly weathered low RQD (<50%) aquifer and are therefore interpreted as viable well targets. This paper presents drilling results, in the context of well theory, and advocates for the construction of subvertical wells at IOC.

Keywords: Angled Well Drilling, Anisotropic Aquifers, Mine Dewatering, Iron Ore

Introduction

IOC is a leading North American producer of iron ore products and is jointly owned by Rio Tinto (project manager), Mitsubishi Corporation, and Labrador Iron Ore Royalty Corporation. Mining operations are located in the province of Newfoundland and Labrador, in eastern Canada (Fig 1). Five hydrogeologically complex ore bodies are being mined, near to or below water table, to meet current production targets.

At IOC mining below water table is achieved by dewatering ore bodies, in advance of mining, via borefields comprised of vertical wells. Sustained pumping has enabled mining to progress below the water table in active pits. While vertical wells are a proven technology, they are not a universal solution. Their main limitation is the required alignment between well collars, hydrogeologic features, and stable areas of the pit (i.e., areas not scheduled to be mined within five years).

Identifying long lived vertical wells has become problematic, but not impossible, in IOC's Luce Pit due to hydrogeologic features failing to align vertically with stable areas as the pit deepens. However, extensive hydrogeologic features do exist proximally to stable areas. As a result, subvertical wells represent a potential solution.

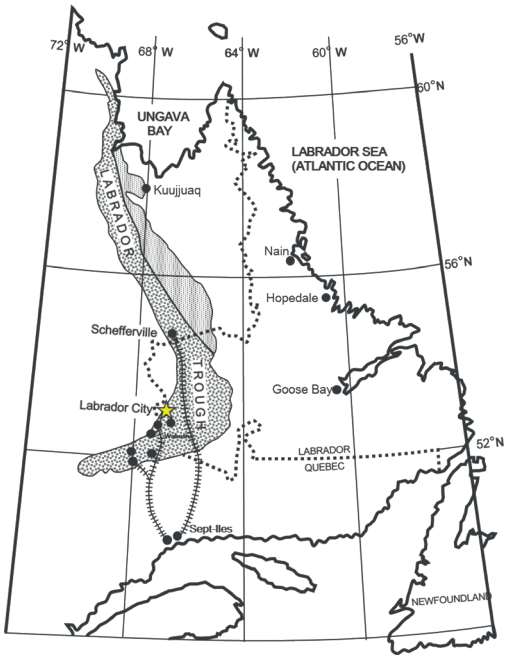

Figure 1 *Geographic map of Labrador. Labrador Trough superimposed for context. Star indicates the location of the mine. Modified after Rivers* et al. *(1978).*

Hydrogeologic Features

Rock comprising the deposit occurs within the 2.17–1.87 Ga aged Sokoman Iron Formation (Wardle *et al*. 2002), which is part

of the larger Labrador Trough (Conliffe 2019) (Fig 1), and has been metamorphosed, folded, and faulted during two orogenies (van Gool *et al*. 2008). The age and tectonic evolution of the deposit gives rise to a variety of complex hydrogeologic features.

These features can be divided into two hydrogeologic domains (Moran 2019). Domain One, representing the majority of the deposit, is comprised of unaltered crystalline metamorphic non-porous and minimally transmissive rock (Brown *et al*. 2019). Domain Two is limited in extent and comprised of limonite alteration (Piteau 1981) associated with shear zones.

Hydraulic conductivity of the altered rock is several orders of magnitude greater than unaltered rock (Gnansounou *et al*. 2015) (Table 1). Domain Two features form distinct aquifers within Domain One. A well intersecting Domain Two features will be productive while a well only intersecting Domain One features will not (Moran *et al*. 2020).

Limonite alteration corresponds to low Rock Quality Designation (RQD) values at IOC (Moran *et al*. 2020). RQD values below 50% signify weathering while RQD values of 100% signify solid rock (Deere *et al*. 1988). Low RQD, limonitic rock, below water table and at depth, is a good indicator of potentially productive hydrogeologic features (Moran *et al*. 2020).

In Luce large low RQD, limonite altered, shear zones exist along the west wall of the pit (Owen *et al*. 2017). These features are proximal to an existing stable pit area, the Luce 470 elevation Dewatering Corridor (Fig 2a) and form the largest aquifer in this pit. The corridor, and the features, are therefore an ideal location for subvertical well placement.

Methodology

Work to identify subvertical well targets, along the Dewatering Corridor, began in 2019. Preliminary work involved reviewing the existing diamond drill core database for continuous intervals of strongly limonite altered low RQD rock. Continuity of the identified zones was confirmed through examination of the geologic, structural, and geotechnical models. Rates of groundwater decline, observed in surrounding piezometers, and the need to replace or augment existing wells were also considerations. Additionally, it was decided that target inclination should not exceed 20°, from vertical, in order to minimize potential complications during future well construction. Two potential targets, LU-20-594 and LU-20-595, met the selection criteria.

LU-20-594 and LU-20-595 were diamond drilled, in HQ diameter (63.5 mm) core size, during October 2020. Diamond drilling was utilized to maximize the amount of information retrieved. Falling head tests were conducted on both holes. Drill core was geologically and geomechanically logged, with particular attention paid to alteration and RQD patterns, and the core assayed at IOC's on site laboratory. Thin sections were made from select samples. 50 mm PVC pipe was installed to full depth and pressure transducers, programmed to collect hourly groundwater level readings deployed.

Results

LU-20-594 Pilot Hole

LU-20-594 is a potential subvertical replacement well for an existing, highly productive, vertical dewatering well (In-Pit 13). LU-20-594 was drilled at a 20° dip and a 183° azimuth to 203 meters. Drilling was stopped short, of a planned 250 meters, due to caving associated with extremely limonite altered low RQD rock. The hole intersected altered rock with RQD values ranging from 0% to <50%, from 110 meters to 203 meters (end of hole) (Fig 2b). Figure 2c shows the

Table 1 *Hydraulic conductivities for select Domain One and Two lithologies (Gnansounou* et al*. 2015).*

Lithology	Hydraulic Conductivity (m/sec)	Geometric Mean(m/sec)
D1 Quartz-Carb (n=8)	5×10^{-11} to 9×10^{-7}	4×10^{-9}
D1 Quartzite (n=6)	2×10^{-10} to 2×10^{-7}	4×10^{-9}
D1 HMO (n=5)	4×10^{-11} to 3×10^{-4}	7×10^{-9}
D2 Limonite (n=4)	3×10^{-8} to 2×10^{-5}	6×10^{-7}

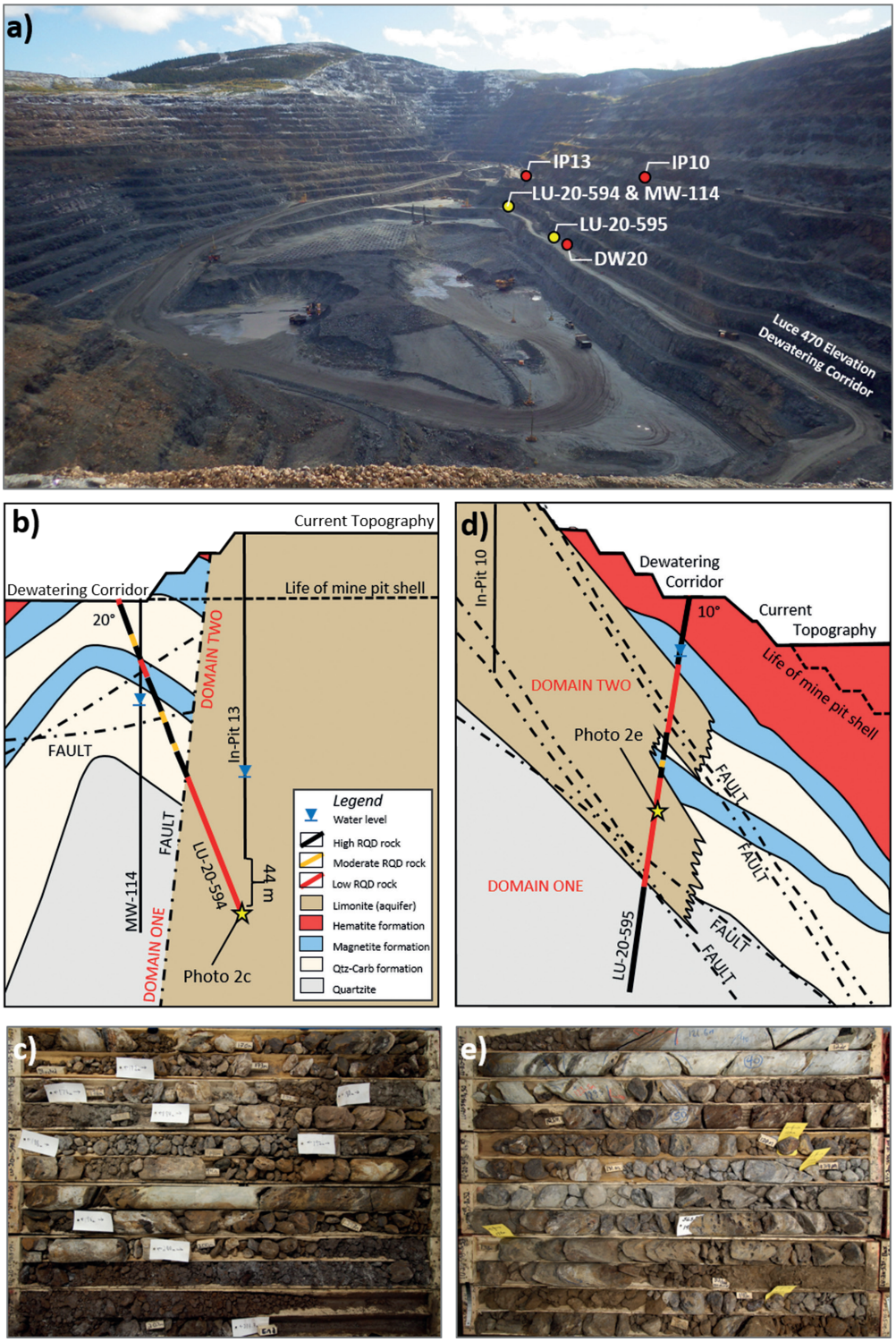

Figure 2 *a) Photograph of Luce Pit, view looking south, showing the location of the Luce 470 elevation Dewatering Corridor, LU-20-594/595, IP13, and DW20 b) cross section showing LU-20-594 drill trace (shear zones modified after Owen* et al. *2017), c) LU-20-594 drill core (169-203 m), d) cross section showing LU-20-595 drill trace (shear zones modified after Owen* et al. *2017), e) LU-20-595 drill core (121-144 m).*

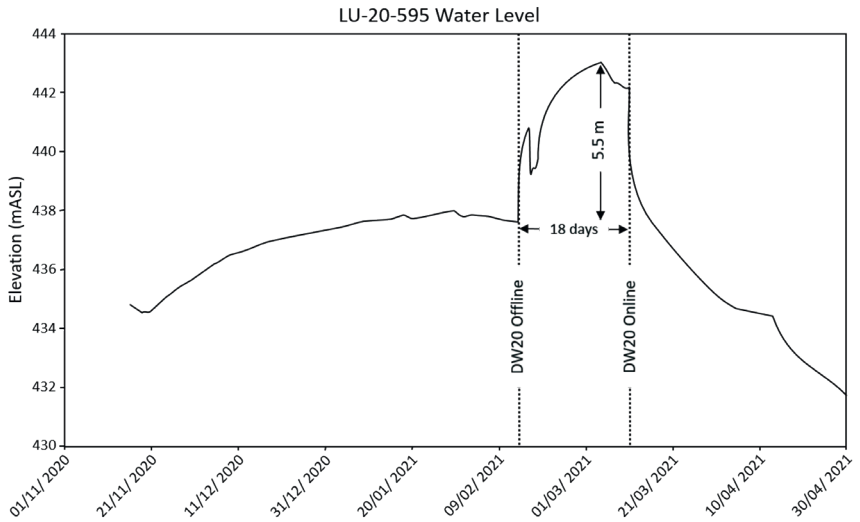

Figure 3 *LU-20-595 hydrograph annotated with DW20 downtime.*

drill core, from the very deepest portion of LU-20-594, altered to the consistency of sand (0% RQD). Thin sections show limonite alteration on the microscopic scale (Wingrove 2020).

The initial groundwater level was 73.2 meters (corrected for dip) below the collar. A falling head test was conducted upon conclusion of drilling. 1,052 litres of water were pumped downhole, over a 31 minute period, increasing the water level in the hole by 0.4 meters. Upon cessation of pumping the water level rapidly decreased.

Based on these results LU-20-594 is considered a viable subvertical well candidate. It is also 77 meters deeper than the bottom of, and in the same hydrogeologic feature as, In-Pit 13.

LU-20-595 Pilot Hole

LU-20-595 is a potential subvertical replacement well for an existing, moderately productive, vertical well (Dewatering Well 20 [DW20]). LU-20-595 was drilled at a 10° dip and a 303° azimuth to 251 meters. Drilling reached target depth. The hole intersected limonite altered low RQD rock, in two distinct intervals: from 44 to 83 meters and 104 meters to 182 meters (Fig 2d). RQD values range from 2% to <60%. Rock below 182 meters is unaltered and high RQD representing non-hydrogeologically productive material. Figure 2e shows the low RQD, limonite altered rock, intersected at depth in this hole.

The initial groundwater level was 35.9 meters (corrected for dip) below the collar. A falling head test was conducted upon conclusion of drilling. 1,770 litres of water were pumped downhole, over a 30-minute period, increasing the water level by 14.6 meters. The water level returned to a pre-test level four minutes after cessation of pumping.

Groundwater level increases during periods when DW20, located 60 meters north, is not pumping (Fig 3). This indicates LU-20-595 intersected features connected to the larger hydrogeologic features.

Based on these results LU-20-595 is considered a viable subvertical well candidate. Furthermore, it intersects the same hydrogeologic features at over twice the depth as DW20 (Fig 2d)

Discussion

Subvertical wells are simply vertical wells drilled at a steep angle. Both well types are straight casing completions and therefore share fundamental characteristics. Many vertical wells have been constructed at IOC making subvertical wells a logical progression. The crucial difference between the two well types is that subvertical wells can access a larger area, and more hydrogeologic features, from a single collar location (Short 1993). This concept is demonstrated in Figure

4. This makes subvertical wells especially advantageous in areas with limited space, like the 470 elevation Dewatering Corridor, to collar wells. In comparison, vertical wells are constrained to intersecting water bearing features directly below where the well is collared.

Figure 4 illustrates how a 200 meter long well drilled at progressively shallower angles increases the range of ground accessible from a single collar location. A 200 meter well drilled at 10°, from vertical, covers approximately 3,681 m^2 while the same length of well drilled at 20° covers approximately 14,698 m^2. Increasing the angle by 10° results in a 300% increase in the coverage area!

Increasing the area accessible from a single collar location also potentially increases the number of accessible hydrogeologic features. Hydrogeologic features can be large and continuous, like those intersected in LU-20-594 and LU-20-595, or small and discrete (e.g., faults, joints). The application, and benefit, of subvertical wells is different for different features. For large well-connected features (aquifers), like those proximal to the 470 elevation Dewatering Corridor, the main benefit is the flexibility from which the feature can be accessed (e.g., location of the wellhead). For discrete features, subvertical wells improve productivity because flow into a well is proportional to the amount of a well's surface area in contact with transmissive rock (Short 1993). By orienting a subvertical well, parallel to and down dip, the amount of well surface area in contact with transmissive rock is maximized.

Figure 5 is a hypothetical cross section, not representing any one pit or deposit, illustrating the concept of dewatering well placement. As mining deepens Luce Pit hydrogeologic features and stable areas of the pit are failing to optimally align (5a). Vertical wells can still be constructed but they intersect transmissive rock for only a portion of their length, and it is necessary to construct them in areas of the pit that will be relatively short lived (Fig 5b). Subvertical wells fully or partially resolve these problems. Well collar locations, water bearing features, and pit shells can be uncoupled by collaring at a suitable location and drilling at an angle into hydrogeologic features (Fig 5c). The length of transmissive rock intersected can be maximized by adjusting the subvertical well azimuth and dip (Fig 5d). Subvertical wells even have the potential to be collared outside, and angled under, pit limits (Fig 5e).

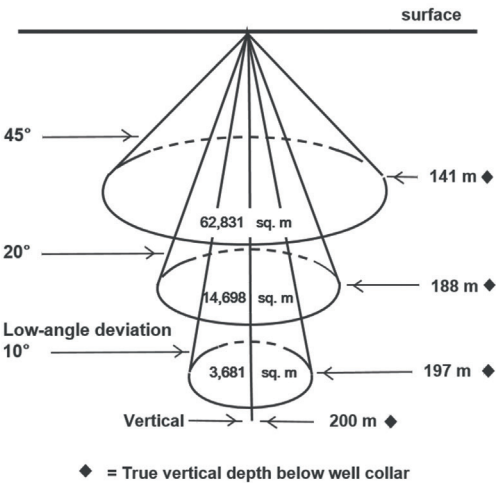

Figure 4 *Subvertical wells increase accessible ground from a single collar location. Figure modified after short (1993).*

Conclusions

Dewatering Luce Pit with subvertical wells is an enhanced alternative over vertical wells. Subvertical wells potentially increase mining flexibility, broaden the range of available targets, result in longer lived wells, and reduce the need for costly pit step outs. They can unlock further value by increasing the type, number, and productivity of water bearing features. Two viable subvertical well targets, LU-20-594 and LU-20-595, have been identified in Luce Pit. They are recommended to be re-drilled as subvertical dewatering wells. Successful implementation of subvertical wells has the potential to unlock substantial value, not only in Luce Pit, but across all pits at IOC.

Acknowledgements

The ideas in this paper were made possible by previous work completed by the IOC Mine Technical Services team. Appreciation is extended to Garrick Field for providing early reference material and feedback. Jason Ross, we are indebted to you for supervising drilling and logging. Dayne Wingrove and Clark Pearce thank you for your help logging and deploying the pressure transducers.

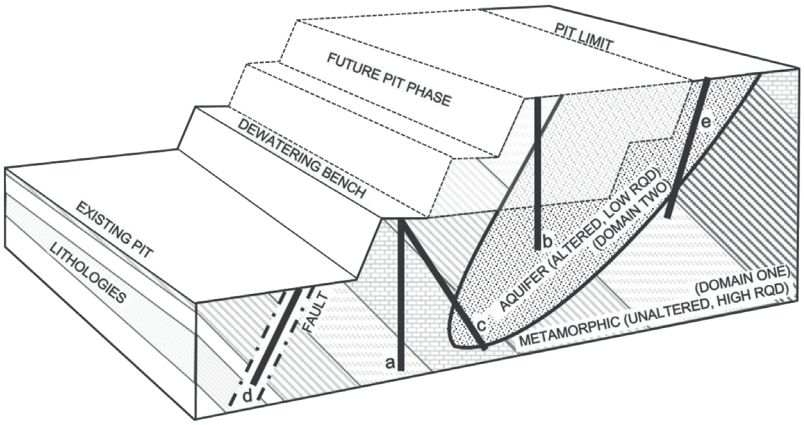

Figure 5 *Hypothetical section demonstrating vertical and subvertical well placement relative to mine design and hydrogeologic features.*

References

Brown Z, Oliver D (2019) IOC hydrogeological conceptual site model update. WSP Inc. report to IOC Mine Technical Services department, Labrador City, Newfoundland and Labrador (unpublished)

Conliffe J (2019) Iron-ore deposits of southwestern Labrador. Newfoundland and Labrador Natural Resources and Mines occasional paper, St. John's NL, p 11-39

Deere DU, and Deere DW (1988) The rock quality designation (RQD) index in practice. In Kirkaldie L ed. Rock classification systems for engineering purposes. Philadelphia, P.A., American Society for Testing and Materials (ASTM) Special Publication 984, p. 91-101.

Moran P (2019) Groundwater occurrence at, and advanced dewatering of, a geologically complex orebody at the Iron Ore Company of Canada open pit mine in subarctic Labrador Canada. In: Proceedings of the Canadian Geotechnical Conference and IAH-CNC conference ("GeoSt. John's 2019"). St. John's, NL

Moran P, Ross J (2020) Mine dewatering wells: reducing economic risk and increasing the probability of success through diamond drilling. In: Proceedings of the Canadian Geotechnical Conference and IAH-CNC conference ("GeoVirtual 2020"). Online

Owen G, Barnett W (2017) Structural model for Luce open pit, IOC, Labrador. SRK Ltd. Report to IOC Mine Technical Services department, Labrador, Newfoundland and Labrador (unpublished)

Piteau DR, Claridge FB, Dakin RA, Stewart AF (1981) Hydrogeology assessment for seepage control in open pit mines. Piteau Associates Inc. report to IOC Mine Technical Services department, Labrador, Newfoundland and Labrador (unpublished)

Gnansounou DR, Holmes AT (2015) Wells In-Pit 8 and In-Pit 9 Assessment, Luce Pit Dewatering. Piteau Associates Inc. report to IOC Mine Technical Services department, Labrador, Newfoundland and Labrador (unpublished)

Rivers T, Wardle RJ (1978) Labrador Trough: 2.3 billion years of history. Report prepared for Mineral Development Division Department of Mines and Energy, St. John's, p 33

Short JAJ (1993) In: Introduction to directional and horizontal drilling. Pennwell Publishing Company, Tulsa, p 4-13

van Gool, Rivers J, Calon T (2008) Grenville Front zone, Gagnon Terrane, southwestern Labrador: configuration of a midcrustal foreland fold-thrust belt. Tectonics 27: 1-13

Wardle RJ, James DT, Scott DJ, Hall J (2002) The southeastern Churchill Province: synthesis of a Paleoproterozoic transpressional orogen: Proterozoic evolution of the northeastern Canadian Shield. Lithoprobe eastern Canadian Shield onshore-offshore transect. Canadian Journal of Earth Sciences 39: 639-663

Wingrove D (2020) Dewatering within the Carol Lake Mine, Labrador City: A Hydrogeological Look at Porosity Within One of the Largest Iron Mines in Canada. Report to IOC Mine Technical Services department, Labrador, Newfoundland and Labrador (unpublished)

Hydrogeochemistry and Mineralogy of a River System in a Mining Region with a Cu-world-class Deposit in Mongolia

Tseren-Ochir Soyol-Erdene[1,2], Teresa Valente[3], Khulan Tsermaa[2,4], Enkhdul Tuuguu[1,5], Munkhzul Davaadorj[2,6,7], Boldbaatar Goosh[2,6,8], Maria Amália Sequeira Braga[3]

[1]*Department of Environmental and Forest Engineering, National University of Mongolia*

[2]*Laboratory of Environmental Chemistry and Geochemistry, National University of Mongolia*

[3]*Institute of Earth Sciences – pole of University of Minho, University of Minho, Braga, Portugal*

[4]*Engineering Faculty, German Mongolian Institute for Resources and Technology, Nalaikh, Mongolia*

[5]*Laboratory of Environmental Engineering and Clean technology, National University of Mongolia*

[6]*Department of Chemical and Biological Engineering, National University of Mongolia*

[7]*Water Agency, Ministry of Environment and Tourism, Mongolia*

[8]*Water Supply and Sewerage Authority, Ulaanbaatar city Governance, Mongolia*

Abstract

The present work is reporting the environmental conditions of a river (Khangal River) under the influence of one of the biggest Cu mines in the world: the Erdenet mine, located in North Central Mongolia. The results show that the Khangal River is suffering the influence of the mining works and waste accumulations of the Erdenet Cu mine. The high proportion of calcite neutralizes the acidity potential of sulfides. However, the potential toxic elements represent high environmental risk. In such alkaline conditions and in the absence of mineralogical control, elements such as Mo and As have high mobility, contaminating the ecosystem and preventing the use of water, either for consumption or for irrigation.

Keywords: Erdenet, Khangal River, Potential Toxic Elements

Introduction

Environmental degradation promoted by mining activities is most commonly associated with acid mine drainage processes. However, contamination also occurs in neutral to alkaline mine waters. Some potentially toxic elements (PTE) could show high mobility in such pH conditions.

The Erdenet is a small industrial city with over 100 thousand population in the North-Central part of Mongolia (Ziadat, Jiries *et al*. 2015) and developed along with exploring porphyry copper-molybdenum (Cu–Mo) deposit since 1974 (Battogtokh *et al*. 2014, Ziadat *et al*. 2015, Solongo *et al*. 2018, LCC Monitoring 2021). The city is located in the forest-steppe zone in the Orkhon-Selenge river basins at an altitude of 1300 m above sea level. It has an extreme continental climate characterized by the cooler in the warm season, relatively warm in the cold season with the increasing wind in the spring and autumn, leading to increased dryness and temperature fluctuations (Ziadat *et al*. 2015, LCC Monitoring 2021). The Erdenet mine (Figure 1) is one of the largest open-pit Cu mines in the world and it has been producing around 580 thousand tons of Cu and 5 thousand tons of Mo concentrates annually since 1978 (LLC, 2021, Battogtokh *et al*. 2014, Ziadat *et al*. 2015, Solongo *et al*. 2018, LCC Monitoring 2021).

Along with the production of ores, around 25 million tons of tailings are produced annually and stored north of the city, becoming sources of various environmental pollution (Ziadat, Jiries *et al*. 2015). Currently, the tailing pond contains about 800 thousand tons of mine tailings including slag and liquid. Therefore, such materials might penetrate the local river, the Kangal (Solongo *et al*. 2018). The Khangal flows from the west along with the tailing ponds and mining sites to the east and is used as a water supply by locals even

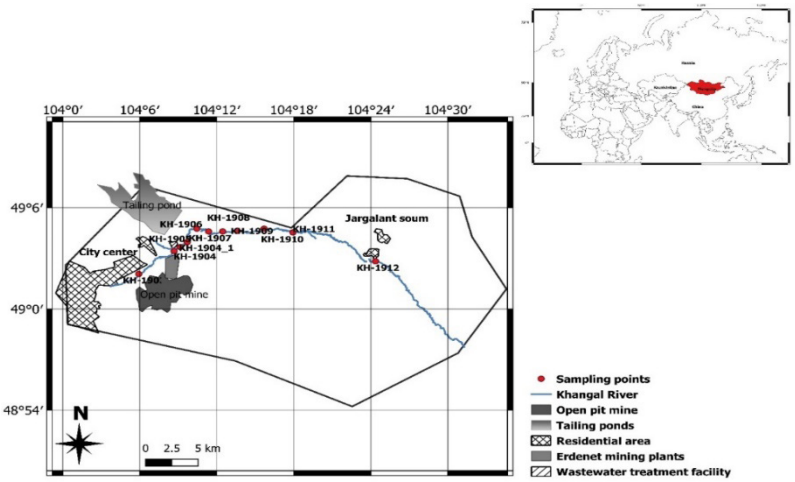

Figure 1 *Sampling points of river and sediments of Khangal River*

though the official drinking water source is the Selenge River (Battogtokh *et al.* 2014, Solongo *et al.* 2018).

Materials and Methods

Eleven sites along the Khangal River were chosen for surface water and sediment sampling (Fig 1). The samples were collected in July 2019 during the warmest season of the year. River water were collected and temperature and pH were measured on-site using a portable multi-parameter meter (Horiba U51), which was calibrated according to the manufacturer's instruction. Water samples were filtered through a 0.45 µm membrane, acidified with HNO_3 and maintained in refrigerated conditions until the further analyses. Sulfate and other major ions for water samples were analysed by ion chromatography (Dionex ICS3000, USA) and metals measured by inductively coupled plasma mass spectrometry (NeXION 300Q, Perkin Elmer, UK). The sediment samples were taken from the uppermost layer of the profile (0–10 cm) using a plastic dipper and a polyethylene bag. Bulk sediment samples were dried at 60 °C, milled, thoroughly homogenized, and two size fractions were obtained: <2 mm and <2 µm. Total concentrations of metals were determined in <2 mm size fractions by inductively coupled plasma mass spectrometry (ICP-MS, NeXION 300Q, Perkin Elmer, UK) and inductively coupled plasma optic emission spectrometry (ICP-OES, Optima 7300DV, Perkin Elmer) at the SGS International Laboratory in Ulaanbaatar, Mongolia. The precision and accuracy of the analyses were checked with the certified reference materials (GBM 901-5, OREAS 501c and NIST2705). The mineralogy of the sediment was studied by X-Ray diffraction in the XRD Lab of University of Minho, Portugal in two size fractions. A mineralogical bulk composition for <2 mm was obtained in the interval 3 to 65 °2θ. The finest fraction (<2 µm) was analysed from oriented aggregates in the interval of 3 to 35 °2θ in order to identify clay and associated minerals.

In order to give proper assessment of the degree of contamination in river sediment, attempts were made to calculate the pollution load indexes (PLI) using the Tomlinson, Wilson *et al.* (1980) approach. The PLI represents the number of times by which the metal concentration in the sediments exceeds the average natural background, and gives a summative indication of the overall level of metal toxicity in a particular sample. We used the average continental crust concentration (Hans and Wedepohl 1995) as a reference background to calculate the PLI as follows:

$$PLI = (CF_1 \times CF_2 \times CF_3 \times \ldots\ldots CF_n)^{1/n} \quad (1)$$

Where, n is the number of metals (n = 12 in this study). PLI<1 implies that the site is free from contamination whilst, PLI = 1 implies to base line level of pollution and PLI> 1 = deterioration of site quality. The CF represents the individual impact of each trace metal on the sediments obtained using the equation:

$$CF = C_n/C_{ref} \quad (2)$$

Where C_n represents metal concentration in the studied environment and C_{ref} being the background concentration in the environment. Then, CF values were interpreted as follows: CF < 1 low contamination, 1 < CF < 3 moderate contamination, 3 < CF < 6 considerable contamination, 6 < CF very high contamination.

Results and Discussion

Khangal river hydrochemical characteristics

The pH of Khangal River's water was neutral to weak alkaline (pH 7.3 - 8.4), which is high compared to other mine area that possibly receive contribution from mining activities. The concentrations of total dissolved solids is high as indicated by electrical conductivity values that range between 2.28 and 10.1 mS/ cm, and hardness are in range of 4.87 - 19.2 mg-Eq/L. The detailed chemical compositions of the Khangal river's samples are presented in Table 1.

Total dissolved solids and hardness were increased by 52% and 35.6%, respectively since 1973 Battogtokh *et al* (2014), suggesting that pollution increased due to the mining activity. The cation composition of all samples was dominated by Na^+, Ca^{2+}, and Mg^{2+}; the anion composition was overall dominated by HCO_3^- and SO_4^{2-}. Almost all parameters, especially SO_4, Ca, Na, K, HCO_3^- Sr, and Ni were higher at the sampling site KH-1904-1. This site represents special conditions, namely it is stagnant water located at the industrial area and near leakage water from the tailings pipe of the Cu processing plant. The upstream characteristics of Khangal River were previously reported as dominated by sulfate ion but it has now changed to bicarbonate and downstream is dominated by sulfate ions. This is maybe due to seasonal variations in input of sulfate ions. The increased concentration of sulfate in downstream could be related with the oxidation of sulfides in the Erdenet Cu-Mo mine tailings.

As presented in Table 2, the concentrations of dissolved metals and As in the Khangal river water are 933 – 1444 µg/L for Sr, 3.23 – 97.6 µg/L for Mn, 0.7 – 2.66 µg/L for Ni, 34.1– 73.3 µg/L for Mo, 7.88–11.1 µg/L for U, 0.52–4.29 µg/L for V, 1.24–3.2 µg/L for As, and 0.07–2.18 µg/L for Pb. While, the concentrations of Cd (<0.13 µg/L) and Sn (<0.03 µg/L) are comparably low. The mean concentrations of dissolved elements in the water samples were

Table 1 *Major ions and selected physical-chemical parameters of the Khangal River samples (mg/L)*

Sample	T (°C)	pH	EC, mS/cm	HCO_3^-	Cl^-	NO_3^-	SO_4^{2-}	Ca^{2+}	Mg^{2+}	Na^+	K^+
KH-1903	10.5	7.53	2.28	279	9.8	16.2	81	48.3	29.9	43.4	1.4
KH-1904	15.9	7.30	2.97	360	19.5	9.1	150	84.2	38.8	49.2	7.2
KH-1904-1	20.3	7.50	10.1	1320	8.2	3.4	450	371	7.8	229	84.9
KH-1905	16.5	7.68	3.00	424	10.0	7.8	78	75.5	37.9	46.4	2.9
KH-1906	15.2	7.65	3.32	409	13.7	8.4	180	106	43.1	47.5	2.5
KH-1907	16.2	7.61	3.25	365	13.6	9.2	187	98.6	42.2	44.7	2.5
KH-1908	16.9	7.86	3.17	354	9.7	6.6	128	75.2	39.3	41.2	2.2
KH-1909	17.8	7.95	3.16	180	20.7	13.9	306	92.6	42.5	45.0	2.5
KH-1910	18.6	8.04	3.08	311	16.1	9.3	206	88.9	41.9	46.8	2.7
KH-1911	18.9	8.05	3.00	262	16.8	13.1	227	85.4	40.8	46.2	2.6
KH-1912	20.6	8.40	2.96	201	21.1	9.5	263	81.0	38.5	51.2	2.9

Table 2 The trace metals concentration of the Khangal River samples (µg/L); bdl – below detection limit.)

Sample	Cu	Mn	Sr	V	Ni	Mo	As	Cd	Sn	Sb	Pb	U
KH-1903	bdl	bdl	933	1.37	bdl	34.1	1.24	0.08	0.01	0.13	0.07	8.27
KH-1904	22.3	97.6	1267	1.55	2.09	73.3	3.20	0.13	0.02	0.39	0.22	7.88
KH-1904(1)	20.9	129	1540	bdl	88.2	0.85	0.06	0.28	0.07	0.03	0.48	0.52
KH-1905	11.3	50.6	1054	1.72	1.27	44.7	1.95	0.08	0.01	0.25	0.05	8.18
KH-1906	4.49	29.3	1444	0.52	2.66	68.5	1.75	0.10	0.003	0.20	0.18	11.1
KH-1907	4.96	10.5	1360	1.92	1.89	60.7	1.83	0.11	0.02	0.18	0.20	10.3
KH-1908	3.19	3.23	1105	0.93	0.77	60.1	2.05	0.10	bdl	0.21	0.50	9.94
KH-1909	2.29	4.17	1290	1.24	2.01	60.4	1.97	0.13	0.03	0.23	0.09	10.7
KH-1910	7.29	5.15	1230	2.68	2.10	61.5	2.30	0.10	0.02	0.24	2.18	10.2
KH-1911	11.7	5.06	1200	1.92	1.78	58.1	2.16	0.11	0.014	0.25	0.13	10.0
KH-1912	3.42	8.53	1286	4.29	1.71	50.9	2.51	0.10	0.016	0.32	0.17	9.80

decreased by following order Sr>Mo>Mn>U >Cu>As>V>Ni>Pb>Sb>Cd>Sn. Increases in concentration of As, Pb and U in the Khangal River were evident along the mining area and further downstream. In contrast, the concentrations of Cu and Mo in the river water decreased from the upstream to downstream, suggesting the possible precipitation into the sediments or other attenuation processes, such as dilution (Santos *et al* 2012). These dissolved elements should be closely related to the mining activities as the mine tailings discharge potentially toxic elements, thus polluting water resources as referred for other mining systems (Guo *et al*. 2013)

Sediment quality and mineralogy: The results of the analyses of potentially toxic elements in surface sediments from the Khangal River is given in Table 3. Concentrations of total elements at sites KH-1904(1) were much higher than other sites as already observed and discussed for water. The increase in Cu and Mo concentration from the second sampling point may be due to the infiltration of water from the tailing pond, which stores Cu concentrate tailings, into the river. Trace elements were arranged in the following order: Cu > V > Zn > As > Pb > Ni > Mo > Co > U > Cd. Cu concentration in sediment was higher than other metals as a consequence of direct activities in this mining area.

The calculated CFs, Cd, and PLI are presented in Table 4. The contamination factor indicates a difference in the contamination levels for some PTE. Except for the KH-1906 and KH-1910 samples, the PLI index is greater than 1, indicating an anthropogenic origin of metal contamination. From the CF values, stream sediments are heavily contaminated with Cu and Mo, the main components of the ore materials from the Erdenet mine. The CF of As in sediments also indicated by high contamination. In other world contexts, high concentrations of As in sediments have been be attributed to anthropogenic activities such as treatment from the fertilizers and arsenical pesticides industries (Fu *et al*. 2014), treating of wood by exhausting copper arsenate and tanning about some chemicals especially arsenic sulfide (Baeyens *et al*. 2007). However, there are practically no such industries in Erdenet. Therefore, such pollution is should be associated with the mining industry. Indeed, As is closely associated with ores containing metals such as Cu and Pb (ATSDR 2007). The contamination factors for all PTE with exception of Cu, Mo, and As indicated low to moderate contamination degree for other sampling points. The C_d and PLI of sediments samples did not vary between samples. The contamination degree of the sampled points varies, but all points except KH-1906 are found to be very highly contaminated. The accumulation of PTE such as Cu, Mo, and As in the Khangal River is directly related to the operation of the Erdenet

Mining Corporation, but this pollution may be transmitted in several ways. In the fall and spring, when precipitation is low, the white dust from ore dumps and tailings is carried away by the wind and could pollute the soil (Banzragch *et al.* 2018, Chonokhuu *et al.* 2019). This further leaches to the surface water by the runoff of rainwater resulting in the increase of the concentrations of elements in sediments.

The other reason for the contamination of sediments is a leakage from the tailing's impoundment and the temporary storage of tailing materials which discharges from the rock piles with subgrade ore materials. The temporary storage area is located outside of the tailing dam, a few tens of meters away from the Khangal River. It is used for holding tailing materials when the water-recirculation system requires maintenance. There is overflow of the discharge water in the storage due to the strong rainfall resulting in the flooding to Khangal River (Battogtokh *et al.* 2014).

The mineralogy is in accordance with the ore deposit paragenesis and with the geology of the region. Therefore, pyrite was identified by XRD in agreement with the volcano-sedimentary nature of the Erdenet mine. Calcite is one of the most abundant

Table 3 *Concentrations of potential toxic elements in surface sediments from the Khangal River, mg/kg*

Sample	Cu	Mn	Sr	V	Ni	Mo	As	Cd	Pb	Zn	Co	U
KH-1903	74.1	649	684	155	30	9.93	53.6	0.16	24.8	72.4	15.9	2.21
KH-1904	254	537	660	125	19.6	15.7	40.5	0.10	21.7	59.5	12.8	1.3
KH-1904(1)	2094	474	353	77.2	13.7	128	62.4	0.54	73.2	227	12.7	1.71
KH-1905	163	711	740	84.7	16.1	56.9	110	0.10	28.2	61.8	13.1	1.14
KH-1906	137	570	590	73	17.3	8.8	0.5	0.091	19.1	54	12	1.16
KH-1907	174	667	715	77.1	17.4	17.9	48.9	0.096	20.3	62.9	13.5	1.32
KH-1908	100	674	701	55.5	13.3	7.7	29.6	0.057	16.9	46.7	10.8	0.94
KH-1909	49	716	679	83.5	13.4	4.51	44.3	0.06	13.8	54	11.5	1.09
KH-1910	27.1	583	568	49.3	13	4.36	42.8	0.05	11.7	37.7	10.2	0.68
KH-1911	187	620	749	89.3	18.7	16.1	40.7	0.12	21.4	69.7	12.3	1.28
KH-1912	62.3	702	864	107	23.8	4.99	45.6	0.092	17.1	66.6	15.4	1.32

Table 4 *Contamination factors (CF and Cd), the pollution load index (PLI) and pollution rate of sediments sample*

Sample	CF												C_d	PLI
	Cu	Mn	Sr	V	Ni	Mo	As	Cd	Pb	Zn	Co	U		
KH-1903	5.2	1.2	2.2	2.9	1.6	7.1	26.8	1.6	1.5	1.4	1.4	0.9	53.7	1.63
KH-1904	17.8	1.0	2.1	2.4	1.1	11.2	20.3	1.0	1.3	1.1	1.1	0.5	60.9	1.48
KH-1904(1)	147.	0.9	1.1	1.5	0.7	91.5	31.2	5.3	4.3	4.4	1.1	0.7	289.6	2.06
KH-1905	11.4	1.4	2.3	1.6	0.9	40.7	55.0	1.0	1.7	1.2	1.1	0.5	118.7	1.56
KH-1906	9.6	1.1	1.9	1.4	0.9	6.3	0.2	0.9	1.1	1.0	1.0	0.5	25.9	0.98
KH-1907	12.2	1.3	2.3	1.5	0.9	12.8	24.5	0.9	1.2	1.2	1.2	0.5	60.5	1.44
KH-1908	7.0	1.3	2.2	1.1	0.7	5.5	14.8	0.6	1.0	0.9	0.9	0.4	36.3	1.12
KH-1909	3.4	1.4	2.2	1.6	0.7	3.2	22.2	0.6	0.8	1.0	1.0	0.4	38.5	1.17
KH-1910	1.9	1.1	1.8	0.9	0.7	3.1	21.4	0.5	0.7	0.7	0.9	0.3	34.0	0.94
KH-1911	13.1	1.2	2.4	1.7	1.0	11.5	20.4	1.1	1.3	1.3	1.1	0.5	56.5	1.53
KH-1912	4.4	1.3	2.7	2.0	1.3	3.6	22.8	0.9	1.0	1.3	1.3	0.5	43.1	1.43

minerals, which reflects the lithology of the Permian Khanui Group volcanics, composed of alkali-rich trachyandesite. The mineralogy of the fine fraction is dominated by calcite, mica and quartz. Among clay minerals there is a 14 Å phase, kaolinite, and traces of smectite. Goethite was detected in trace or small proportions. Therefore, beside traces of goethite, other iron oxyhydroxides and high proportions of clay minerals known by their ability to retain PTE were not detected. Such an absence may contribute to dispersion of contamination along the river.

Conclusion

The Khangal River is suffering the influence of the mining works and waste accumulations of Asia's largest Cu mine. In addition to the beneficiation processes, the high proportion of calcite should contribute to neutralize the acidity potential of sulfides in the ore paragenesis. However, PTE represent high environmental risk. Water pH was in the range of 7.30-8.40. In such alkaline conditions and in the absence of mineralogical control, namely by adsorption at the surface of iron oxyhydroxides and smectite, the elements such as Mo and As have high mobility, contaminating the ecosystem and preventing the use of water, either for consumption or for irrigation.

Acknowledgments

The authors thank all co-organisers for hosting the IMWA2021 Conference. The financial supports were provided by Swiss Cooperation Agency in Ulaanbaatar, Mongolia under a Small Action Project at the National University of Mongolia and by FCT through projects UIDB/04683/2020 and UIDP/04683/2020 and Nano-MINENV (PTDC/CTA-AMB/29259/2017).

References

ATSDR (2007). Agency for Toxic Substances and Disease Registry. P. H. S. U.S. Department of Health and Human Services, Division of Toxicology 1600,. U.S, Atlanta, GA 30333.

Baeyens, W., A. d. Brauwere, N. Brion, M. D. Gieter and M. Leermakers (2007). "Arsenic speciation in the River Zenne, Belgium." *Science of The Total Environment* 384(1): 409-419.

Banzragch, L., C. Sonomdagva, B. Ch and B. Byambaa (2018). "WHITE DUST SIMULATION FOR TAILINGS POND OF ERDENET COPPER MINING USING HYSPLIT." *Proceedings of the Mongolian Academy of Sciences* 57: 24.

Battogtokh, B., J. M. Lee and N. Woo (2014). "Contamination of water and soil by the Erdenet copper–molybdenum mine in Mongolia." *Environmental Earth Sciences* 71.

Chonokhuu, S., C. Batbold, B. Chuluunpurev, E. Battsengel, B. Dorjsuren and B. Byambaa (2019). "Contamination and Health Risk Assessment of Heavy Metals in the Soil of Major Cities in Mongolia." *International journal of environmental research and public health* 16(14): 2552.

Fu, J., C. Zhao, Y. Luo, C. Liu, G. Z. Kyzas, Y. Luo, D. Zhao, S. An and H. Zhu (2014). "Heavy metals in surface sediments of the Jialu River, China: Their relations to environmental factors." *Journal of Hazardous Materials* 270: 102-109.

Hans Wedepohl, K. (1995). "The composition of the continental crust." *Geochimica et Cosmochimica Acta* 59(7): 1217-1232.

Loska, K., J. Cebula, J. Pelczar, D. Wiechuła and J. Kwapuliński (1997). "Use of Enrichment, and Contamination Factors Together with Geoaccumulation Indexes to Evaluate the Content of Cd, Cu, and Ni in the Rybnik Water Reservoir in Poland." *Water, Air, and Soil Pollution* 93(1): 347-365.

Sakan, S. M., D. S. Đorđević, D. D. Manojlović and P. S. Predrag (2009). "Assessment of heavy metal pollutants accumulation in the Tisza river sediments." *Journal of Environmental Management* 90(11): 3382-3390.

Tomlinson, D. L., J. G. Wilson, C. R. Harris and D. W. Jeffrey (1980). "Problems in the assessment of heavy-metal levels in estuaries and the formation of a pollution index." *Helgoländer Meeresuntersuchungen* 33(1): 566-575.

Pueyo, M., J. Mateu, A. Rigol, M. Vidal, J. F. López-Sánchez, and G. Rauret. 2008. "Use of the Modified BCR Three-Step Sequential Extraction Procedure for the Study of Trace Element Dynamics in Contaminated Soils." *Environmental Pollution* 152(2):330–41.

Rauret, G., J. F. López-Sánchez, A. Sahuquillo, R. Rubio, C. Davidson, A. Ure, and Ph. Quevauviller. 1999. "Improvement of the BCR

Three Step Sequential Extraction Procedure Prior to the Certification of New Sediment and Soil Reference Materials." *Journal of Environmental Monitoring* 1(1):57–61.

Guo, Y.-g., P. Huang, W.-g. Zhang, X.-w. Yuan, F.-x. Fan, H.-l. Wang, J.-s. Liu and Z.-h. Wang (2013). "Leaching of heavy metals from Dexing copper mine tailings pond." *Transactions of Nonferrous Metals Society of China* 23(10): 3068-3075.

Santos, J. S. d., M. J. S. d. Santos and M. L. P. d. Santos (2012). "Influence of the rainfall regime on the mobility of zn, cd, ni, cu, mn and fe in the surface sediments of the contas river located in the Brazilian semi-arid region." *Journal of the Brazilian Chemical Society* 23: 718-726.

Battogtokh, B., *et al*. (2014). "Contamination of water and soil by the Erdenet copper–molybdenum mine in Mongolia." *Environmental Earth Sciences* 71(8): 3363-3374.

LLC, Monitoring E. (2021). "Official website of Erdenet LLC." Retrieved April 20, 2021, from https://www.erdenetmc.mn/.

Monitoring, N. A. M. a. t. E. (2021, 2021). "Meteorolgy and Environmental analysis of provinces and capital." Retrieved April 20, 2021, from http://orkhon.tsag-agaar.gov.mn/info/atmosphere.

Solongo, T., *et al.* (2018). "Distribution and Chemical Speciation of Molybdenum in River and Pond Sediments Affected by Mining Activity in Erdenet City, Mongolia." *Minerals* 8: 288.

Ziadat, A., *et al*. (2015). "Bio-monitoring of Heavy Metals in the Vicinity of Copper Mining Site at Erdenet, Mongolia." *Journal of Applied Sciences* 15: 1297-1304.

Author Index

__E

__F

__G

__H

__I

__J

__K

__L

__M

__N

__O

__P

__Q

__R

__S

__T

__U

__V

__W

__Y

__Z

Keyword Index

__D

__E

__F

__G

__H

__I

__J

__L

__M

__N

__O

__P

R

S

T

U